National Library of Canada
Bibliothèque nationale du Canada

Canadian Theses Service
Service des thèses canadiennes

Ottawa, Canada
K1A 0N4

NOTICE

The quality of this microform is heavily dependent upon the quality of the original thesis submitted for microfilming. Every effort has been made to ensure the highest quality of reproduction possible.

If pages are missing, contact the university which granted the degree.

Some pages may have indistinct print especially if the original pages were typed with a poor typewriter ribbon or if the university sent us an inferior photocopy.

Previously copyrighted materials (journal articles, published tests, etc.) are not filmed.

Reproduction in full or in part of this microform is governed by the Canadian Copyright Act, R.S.C. 1970, c. C-30.

AVIS

La qualité de cette microforme dépend grandement de la qualité de la thèse soumise au microfilmage. Nous avons tout fait pour assurer une qualité supérieure de reproduction.

S'il manque des pages, veuillez communiquer avec l'université qui a conféré le grade.

La qualité d'impression de certaines pages peut laisser à désirer, surtout si les pages originales ont été dactylographiées à l'aide d'un ruban usé ou si l'université nous a fait parvenir une photocopie de qualité inférieure.

Les documents qui font déjà l'objet d'un droit d'auteur (articles de revue, tests publiés, etc.) ne sont pas microfilmés.

La reproduction, même partielle, de cette microforme est soumise à la Loi canadienne sur le droit d'auteur, SRC 1970, c. C-30.

NL-339 (r. 88/04)

Canada

THE UNIVERSITY OF ALBERTA

Design of Shallow Tunnels in Soft Ground

by

Arsenio Negro Jr.

Ⓒ

A THESIS
SUBMITTED TO THE FACULTY OF GRADUATE STUDIES AND RESEARCH
IN PARTIAL FULFILMENT OF THE REQUIREMENTS FOR THE DEGREE
OF Doctor of Philosophy

Department of Civil Engineering

EDMONTON, ALBERTA
SPRING 1988

Permission has been granted to the National Library of Canada to microfilm this thesis and to lend or sell copies of the film.

The author (copyright owner) has reserved other publication rights, and neither the thesis nor extensive extracts from it may be printed or otherwise reproduced without his/her written permission.

L'autorisation a été accordée à la Bibliothèque nationale du Canada de microfilmer cette thèse et de prêter ou de vendre des exemplaires du film.

L'auteur (titulaire du droit d'auteur) se réserve les autres droits de publication; ni la thèse ni de longs extraits de celle-ci ne doivent être imprimés ou autrement reproduits sans son autorisation écrite.

ISBN 0-315-42863-5

THE UNIVERSITY OF ALBERTA

RELEASE FORM

NAME OF AUTHOR Arsenio Negro Jr.

TITLE OF THESIS Design of Shallow Tunnels in Soft Ground

DEGREE FOR WHICH THESIS WAS PRESENTED Doctor of Philosophy

YEAR THIS DEGREE GRANTED SPRING 1988

Permission is hereby granted to THE UNIVERSITY OF ALBERTA LIBRARY to reproduce single copies of this thesis and to lend or sell such copies for private, scholarly or scientific research purposes only.

The author reserves other publication rights, and neither the thesis nor extensive extracts from it may be printed or otherwise reproduced without the author's written permission.

(SIGNED) ....

PERMANENT ADDRESS:

Alameda Franca 74 - 83
01422 Sao Paulo (SP)
Brazil

DATED on 8th January 1988

THE UNIVERSITY OF ALBERTA

FACULTY OF GRADUATE STUDIES AND RESEARCH

The undersigned certify that they have read, and recommend to the Faculty of Graduate Studies and Research, for acceptance, a thesis entitled *Design of Shallow Tunnels in Soft Ground* submitted by Arsenio Negro Jr. in partial fulfilment of the requirements for the degree of Doctor of Philosophy.

....

Supervisor

....

....

....

....

....

External Examiner

Date 8th January 1988

DEDICATION

To Dona Nair, Sr. Nene and Te.

You deserve more than just this.

ABSTRACT

This work reviews and discusses the behaviour of shallow tunnels in soil. The most relevant factors controlling the ground behaviour are identified.

A comprehensive review of available design methods is presented. Existing procedures and current design practice are assessed and the deficiences of current approaches to shallow tunnel design are recognized. It is demonstrated that there is a need to improve these routines by coupling ground settlement prediction with lining load estimates. While this can be done using numerical techniques, the practice asks for simpler yet reliable procedures, presently unavailable.

Accordingly, a new design method is developed. It assumed the ground behaviour to be non-linear and time independent, and the tunnel to be shallow, single and circular. The method was developed through generalization of results obtained by two and three-dimensional finite element modelling, after assessing the ability of these techniques to portray tunnelling behaviour.

The two dimensional modelling allows relationships to be established between tunnel closure, ground mass displacements, the amount of ground stress release and the resulting ground stiffness changes. The results of the generalization process are presented in dimensionless form, through equations and charts, which allow the above relationships to be defined for distinct soil strengths, ground stiffnesses, in situ stress conditions and for different tunnel sizes and depths.

The effects of the delayed installation of the lining are accounted for by combining the above results with an estimate for tunnel closure, developed from three-dimensional finite element parametric analyses. The lining-ground interaction is taken into consideration through an analytical closed form solution which includes the effects of the gravitational stress field.

A step by step sequence for the application of the method is presented. The method is validated by applying it to results of three-dimensional finite element analyses, model tests and to a large number of case histories. It is shown that the proposed procedure yields very sensible estimates of the tunnel performance whenever good ground control conditions exist.

ACKNOWLEDGEMENTS

Dr. Z. Eisenstein made this thesis possible and I am grateful for his support.

Financial assistance came from a variety of sources including the Natural Science and Engineering Research Council, the Fundacao de Amparo a Pesquisa do Estado de Sao Paulo (Brazil), the University of Alberta Dissertation Fellowship, the Department of Civil Engineering of the University of Alberta and also from the Fundacao Armando Alvares Penteado (Sao Paulo, Brazil).

During implementation of the 2D Finite Element program I was helped by Dr. L.V. Medeiros, Dr. D.W. Murray and Dr. D. Chan. Part of this work was done at the Pontificia Universidade Catolica do Rio de Janeiro where I was assisted by Jose Napoleao and Celso Romanel. Dr. Jose Brandt contributed tremendously in this phase, but certainly not only here!

The 'soft till' issue involved support from Drs. S. Thomson, F. El-Nahhas and D.C.C. Sego. Gerry Cyre was instrumental in the field and in the laboratory. But without Ralph Wittebolle's cooperation, I wouldn't have achieved anything.

Also, I would have been in trouble with the german literature and with the 3D analyses had Heinrich Heinz been elsewhere!

Dr. N.R. Morgenstern is to be credited for his suggestions and for having raised my interest on the drained

versus undrained issue in soft ground tunnels. I am thankful to Dr. B. Ladanyi for a discussion we had in Winnipeg from which emerged our interest on the 3D ground-lining response to tunnelling and to Dr. J.G. MacGregor for his comments on lining-ground interaction.

Paulo Branco is to be awarded for reading and commenting on the entire handwritten version of this work. Susan Evison bravely edited this tome of a thesis. By enduring my english she learned lots of portuguese!

After typing it Tanya Schulz promised she would never type another thesis in her life. No wonder! Thanks to Donna Salvian for the tables and to Denise Nickels for most of the figures.

Flavio M. Kuwajima cooperated in different ways which included loosing a squash game to me from time to time...

Many people contributed to this work and a complete list may ask for an additional volume. Some of them are those who replied to our questionnaire and are listed in Appendix B.

Once I was told by the late Arthur Casagrande that to do useful and serious research work, firstly, one would have to be sure what one is talking about. Secondly, one would have to conduct the work with integrity and ingenuity (he loved this word!). Thirdly, one would have to present it in its full transparency so it can be assessed and, more importantly, reproduced. I am grateful for his advice.

Table of Contents

Chapter Page

1. INTRODUCTION 1

1.1 Preamble 1

1.2 Aims 7

1.3 Scope and Thesis Organization 10

2. IDEALIZED BEHAVIOUR OF SHALLOW TUNNELS: STRESS AND STRAIN CHANGES 15

2.1 Introduction 15

2.2 Shallow and Deep Tunnels 15

2.3 Soil Response to Tunnelling 26

2.3.1 Foreword 26

2.3.2 Idealized Stress Changes 27

2.3.3 Idealized Strain Changes 34

2.3.4 Stress and Strain Changes Under Less Idealized Conditions 45

2.3.4.1 Stress Paths 45

2.3.4.2 Ground Reaction Curves 53

2.3.4.3 Shear Strain Development 56

2.3.4.4 Volume Changes 75

2.3.5 Idealized Lining Action 86

2.3.5.1 Preamble 86

2.3.5.2 Good Lining Contact in an Ideally Deep Tunnel 89

2.3.5.3 Good Lining Contact in a Shallow Tunnel 97

2.3.5.4 Poor Lining Contact 106

2.3.6 Three Dimensional Response 122

2.3.6.1 Plane Strain Representation and Three Dimensional Response 122

2.3.6.2 Three Dimensional Arching and Ground-Lining Response 127

2.3.6.3 Evidence of Three-dimensional Ground-Lining Response 135

2.3.6.4 Three-dimensional Ground-Lining Responses from Numerical Analyses 148

2.4 Summary and Conclusions 163

3. IDEALIZED BEHAVIOUR OF SHALLOW TUNNELS: STABILITY AND GROUNDWATER 178

3.1 Introduction 178

3.2 Tunnel Stability 178

3.2.1 Foreword 178

3.2.2 Three-Dimensional Stability 180

3.2.3 Two-Dimensional Stability 194

3.3 The Role of Groundwater 210

3.3.1 Foreword 210

3.3.2 Generation of Porewater Pressure Changes .210

3.3.2.1 Idealized Porewater Pressure Changes 210

3.3.2.2 The Effect of Gravity 213

3.3.2.3 Porewater Pressure Changes in Less Idealized Conditions 214

3.3.3 Dissipation of Excess Pore Water Pressures 229

3.3.3.1 Linear Elastic Consolidation 229

3.3.3.2 Non-Linear Consolidation 234

3.3.3.3 Additional Consequences of the Consolidation Process 238

3.3.4 Drained and Undrained Behaviour 246

3.3.4.1 Foreword 246

3.3.4.2 Steady State Seepage 247

3.3.4.3 Total and Effective Stress Paths 255

3.3.4.4 Changes in Stability with Time ..258

3.3.4.5 Drained and Undrained Response Boundaries 264

3.4 Summary and Conclusions 275

4. PRESENT STATE OF THE DESIGN OF SHALLOW TUNNELS 285

4.1 Introduction 285

4.2 Design Requirements 288

4.2.1 Basic Requirements for Lining Design 289

4.2.2 Basic Requirements for Displacement Prediction and Damage Estimate 301

4.2.3 Basic Requirements for Verification of Excavation Stability 321

4.3 Available Design Methods 329

4.3.1 Foreword 329

4.3.2 Prediction of Lining Loads 331

4.3.2.1 Classification of Methods 331

4.3.2.2 Empirical and Semi-Empirical Methods 333

4.3.2.3 Ring and Plate Models 344

4.3.2.4 Ring and Spring Models 361

4.3.2.5 Numerical Methods 378

4.3.2.6 Numerically Derived Methods 379

4.3.2.7 Account for Three-Dimensional Effects in Two-Dimensional Models 389

4.3.3 Prediction of Ground Displacements 402

4.3.4 Ground Stability Verification 416

4.4 Survey of the Current Design Practice 426

4.4.1 Foreword 426

4.4.2 Prediction of Lining Loads 427

4.4.2.1 Survey of Practice 427

4.4.2.2 Results of the Survey 434

4.4.2.3 Final Comments 454

4.4.3 Prediction of Ground Settlements 460

4.4.3.1 Survey of Practice 461

4.4.3.2 Results of the Survey 466

4.4.3.3 Final Comments 480

4.5 Summary and Conclusions 483

5. SHALLOW TUNNEL MODELLING 508

5.1 Introduction 508

5.2 Two-Dimensional Modelling 513

5.2.1 Review of Previous Studies 513

5.2.1.1 Modelling Aspects 514

5.2.1.2 Prediction of Performance by Finite Elements 534

5.2.2 Numerical Simulation Applied 552

5.2.2.1 General Description of the Solution 552

5.2.2.2 Discussion on the Solution Adopted 564

5.2.3 Parametric Studies 576

5.2.4 Analyses of Some Case Histories 577

5.2.4.1 Opening Remarks 577

5.2.4.2 Alto da Boa Vista Tunnel 581

5.2.4.3 Edmonton Light Rail Transit (LRT) Tunnel 613

5.2.4.4 Edmonton Experimental Tunnel 653

5.2.5 Summary and Conclusions 717

5.3 Three-Dimensional Modelling 725

- 5.3.1 Introduction 725
- 5.3.2 Available Solutions for Estimates of Tunnel Convergence 730
- 5.3.3 Review of Three-Dimensional Modelling by the Finite Element Method 737
- 5.3.4 Numerical Solution Adopted 747
- 5.3.5 Parametric Analyses 753
  - 5.3.5.1 Analyses and Results 753
  - 5.3.5.2 Interpretation of the Results ...774
- 5.3.6 Application of the Results 804
  - 5.3.6.1 Tunnel Closure 804
  - 5.3.6.2 Ground Movements Ahead of the Tunnel Face 842
- 5.3.7 Summary and Conclusions 847

5.4 Conclusion 850

6. TWO DIMENSIONAL MODELLING FOR GENERALIZATION 860

6.1 Introduction 860

6.2 Modelling Simplifications and Ranges of Variables 864

- 6.2.1 Foreword 864
- 6.2.2 Cohesionless Soil Model 864
- 6.2.3 Frictionless Soil Model 880
- 6.2.4 Comments on Some Simplifying Assumptions .894
  - 6.2.4.1 The Effect of Janbu's Modulus K .894
  - 6.2.4.2 The Effect of Janbu's Exponent n 895
  - 6.2.4.3 The Effect of the Cohesive Strength Component 911
  - 6.2.4.4 The Effect of Poisson's Ratio ...923

6.2.5 Ranges of Variables for the Parametric Analyses 931

6.3 Parametric Analyses 939

6.3.1 Details of the Analyses 939

6.3.1.1 Number of Unloading Increments ..939

6.3.1.2 Mesh Design and Influence of the Lower Boundary 946

6.3.2 Results of the Analyses 960

6.3.2.1 Frictionless Soil Model Results .962

6.3.2.2 Cohesionless Soil Model Results .975

6.3.2.3 Relationships Between Surface and Crown Settlements 993

6.4 Generalization of the Results 1013

6.4.1 Opening Remarks 1013

6.4.2 Frictionless Soil Model 1014

6.4.3 Cohesionless Soil Model 1035

6.5 Limits of the Generalized Solution 1078

6.5.1 Extrapolation of the Numerical Results ..1078

6.5.2 Assessment of the Two-Dimensional Stability 1085

6.6 Summary and Conclusions 1102

7. DEVELOPMENT AND VALIDATION OF A DESIGN PROCEDURE ..1115

7.1 Introduction 1115

7.2 Soil-Lining Interaction 1117

7.2.1 Choice of the Model: Hartmann Solution ..1117

7.2.2 Soil-Lining Interaction Analysis for Delayed Lining Installation in a Non-Linear Ground Mass 1131

7.2.3 Influence of the Lining Presence on the Ground Settlements 1153

7.3 Guidelines for Using the Proposed Design Procedure 1158

7.4 An Example of the Use of the Proposed Design Procedure 1168

7.5 Validation of the Proposed Method 1196

7.5.1 Verification Against a Tunnel Model Test 1196

7.5.1.1 Model Test Procedures 1196

7.5.1.2 Soil Conditions in the Test 1198

7.5.1.3 Predicted and Measured Ground Responses 1201

7.5.2 Verification Against a Three-Dimensional Finite Element Analysis of a Shallow Tunnel 1207

7.5.3 Verification Against Actual Case Histories 1212

7.5.3.1 Foreword 1212

7.5.3.2 A Large Shielded Tunnel in Marl: The Frankfurt Baulos 23, Domplatz Tunnel 1214

7.5.3.3 Twin NATM Tunnels in Marl: The Frankfurt Baulos 25, Romerberg Tunnel 1224

7.5.3.4 A Small Shielded Tunnel in Till: The Mississauga (Ontario) Tunnel 1234

7.5.3.5 A Large NATM Tunnel in Granular Soil: The Butterberg Tunnel, in Osterode, near Hannover 1246

7.5.3.6 A Large Shield in Till: The Edmonton LRT Tunnel 1257

7.5.3.7 An NATM Tunnel in Marl: The Munich U - Bahn - Line 8/1, Baulos 18.2 1263

7.5.3.8 An NATM Tunnel Built under Compressed Air: The Munich U-Bahn-Line 5/9, Baulos 7 1269

7.5.3.9 An NATM Tunnel Driven Through Heterogeneous Ground: The Bochum Baulos A2 Double Track Subway Tunnel 1279

7.5.3.10 An NATM Tunnel with Staged Installation of the Lining: The Sao Paulo North Extension Double Track Tunnel 1282

7.5.4 Analysis and Interpretation of the Results Obtained 1293

7.6 Summary and Conclusions 1310

8. CONCLUSIONS 1324

REFERENCES 1341

APPENDIX A - RESULTS OF 3-D FINITE ELEMENT ANALYSES 1406

APPENDIX B - LIST OF RESPONDENTS TO THE QUESTIONNAIRE ..1410

APPENDIX C - NORMALIZED GROUND SETTLEMENTS 1415

APPENDIX D - TWICE NORMALIZED GROUND REACTION CURVES ...1453

List of Tables

Table Page

2.1 Assessments of the Effects of the Presence of the Ground Surface and of the Gravitational Stress Gradient in Shallow Tunnels 18

2.2 Shear Strain Distributions Observed in Model Tests and in Actual Tunnels in Drained Conditions 57

2.3 Plane Section Model Tests in Clay and Sand Under Drained Conditions 63

2.4 Plane Section Model Tests in Clay Under Undrained Conditions 68

3.1 Soil Properties in Johnston and Clough (1983) Analyses 219

4.1 Existing Criteria for Damage Assessment of Structures Subjected to Ground Movements 310

4.2 Damage Related to Building Distortion for Brick-Bearing Wall Structures Adjacent to Excavations (modified after Cording et.al., 1976:535) 315

4.3 Reported Ground Control Procedures in Soil Tunnelling 330

4.4 Ground Pressure Theories: A Partial Survey 338

4.5 Recommended Lining Distortion Ratios for Design Verification (after Schmidt, 1984: modified) 341

4.6 Some Review Works on Ring and Plate or Ring and Spring Models for Design of Linings Under Non-Uniform Stress Fields 350

4.7 Assumptions and Features of some Ring and Plate Solutions for Non-Uniform Stress Field 353

4.8 Assumptions and Features of some Ring and Spring Models 364

4.9 Details of Some Numerically Derived Methods for Lining Loads Prediction 382

Table Page

4.10 Account for Three-Dimensional Effects in Two Dimensional Models 394

4.11 Features of some Methods for Ground Displacement Prediction for Shallow Tunnel Design 404

4.12 Features of some Methods for Ground Stability Verification 420

4.13 Envisaged Ground Conditions for Response of Questionnaire on Lining Design (modified after Duddeck, 1982:173) 430

4.14 ITA Questionnaire Response on Lining Design 433

4.15 Questionnaire on Ground Movements Caused by Shallow Tunnels 464

4.16 Questionnaire Response on Ground Movements 465

4.17 Type of Practice of Respondents 467

4.18 Preferred Approaches Indicated by Respondents for Ground Settlement Prediction 471

4.19 Noted Qualities for Different Settlement Prediction Procedures 476

5.1 Some Guidelines for Two-Dimensional Finite Element Mesh Design, Derived from Sensitivity Studies 516

5.2 Excavation Simulation Procedures for Tunnel Modelling with Finite Element Techniques 520

5.3 Numerical Procedures to Account Approximately for Three-Dimensional Effects of a Tunnel Advance in Two-Dimensional Finite Element Analyses 521

5.4 Classification of Prediction According to Lambe (1973) 536

5.5 Review of Some Numerical Predictions of Shallow Tunnel Behaviour Using Two-Dimensional Finite Element Analyses 537

Table Page

5.6 Overall Aspects of Reviewed Numerical Predictions of Shallow Tunnel Performance 543

5.7 Case Histories Selected for Analyses with the Adopted Numerical Solution 579

5.8 Typical Ranges of Properties of ABV Soils 585

5.9 Range of Geotechnical Parameters for the Variegated Soil at the ABV Site 586

5.10 Range of Geotechnical Parameters for the Red Porous Clay at the ABV Site 587

5.11 Parameters Varied in ABV Tunnel Back Analyses 596

5.12 Measured and Calculated Performance of ABV Tunnel 601

5.13 Range of Basic Soil Properties Found Along LRT Tunnel Alignment at Jasper Avenue 618

5.14 Range of Geotechnical Parameters for Edmonton Till at the South LRT Tunnel Line 619

5.15 Range of Geotechnical Parameters for Lake Edmonton Clay at the South LRT Tunnel Line 622

5.16 Range of Geotechnical Parameters for Saskatchewan Sands and Gravels at the South LRT Tunnel Line 623

5.17 Parameters Varied in the LRT Tunnel Back Analysis 635

5.18 Measured and Calculated Average Thrust Forces at Rib Joints in the LRT Tunnel 647

5.19 Measured and Calculated Performance of the LRT Tunnel 648

5.20 Results of Oedometer Consolidation Tests on Till for Edmonton Experimental Tunnel 661

5.21 Parameters of Fitted Hyperbolae for Softer Till 668

Table Page

5.22 Parameters of Hyperbolae Fitted to Stress-Strain Curves of Till, Tested under Distinct Total Stress Paths and Drainage Conditions 681

5.23 Parameters Varied in the Edmonton Experimental Tunnel Back-Analyses 696

5.24 Measured and Calculated Average Thrust Forces at the Lower Lining Joint in the Edmonton Experimental Tunnel 709

5.25 Measured and Calculated Performance of Edmonton Experimental Tunnel 712

5.26 Results of the Numerical Simulations of the Final Tunnel Performance in Three Case Histories 722

5.27 Some Solutions for Tunnel Convergence Estimates under Time-Independent Conditions 732

5.28 Review of Some Three-Dimensional Finite Element Simulations of Tunnel Construction 740

5.29 Cases of Three-Dimensional Analyses 755

5.30 Coefficients of the Adopted U and K Relations for Sections at Different Distances Behind the Face 787

5.31 Predicted and Measured Displacements at the Face and at the Point of Support Activation in Shallow Tunnels for the Crown 809

5.32 Predicted and Measured Displacements at the Face and at the Point of Support Activation in Shallow Tunnels for the Springline 813

5.33 Predicted and Measured Displacements at the Face and at the Point of Support Activation in Shallow Tunnels for the Floor 815

5.34 Calculated and Observed Maximum Horizontal Movements of the Tunnel Face 845

Table Page

5.35 Calculated and Observed Maximum Longitudinal Distortions at the Ground Surface, Ahead of the Tunnel Face 846

6.1 Input Parameters for Finite Element Analyses of Tunnels with the Same H/D and with a Homothetic Hyperbolic Stress-Strain Soil Model with c=0 870

6.2 Invariance of NGRC and Normalized Displacements to Changes in the Unit Weight of the Soil 879

6.3 Input Parameters for Finite Element Analyses of Tunnels with the Same H/D and with Homothetic Hyperbolic Stress-Strain Soil Model with $\phi=0$ 882

6.4 Variation of the Maximum Normalized Surface Settlement with the Exponent n and with the Amount of Stress Release Allowed in the Opening 909

6.5 Ratio of Normalized Crown Displacements for n=0 to n>0, for Different Exponents n and Different Amount of Stress Release at the Opening 910

6.6 Variation of the Maximum Normalized Surface Settlement with the Cohesive Strength of the Soil and with the Amount of Stress Release Allowed 916

6.7 Variation of the Dimensionless Crown Displacement for the Different Strength Assumptions made and for the Different Amounts of Stress Release 924

6.8 Selected Variables for the Parametric Finite Element Analyses 940

6.9 Recorded Final Movements below Actual Tunnels and Tunnel Model Tests 957

6.10 Parameters used and Obtained in the Reduction of the Twice Normalized Ground Reaction Curves for the Frictionless Soil Model, for H/D=3 1016

6.11 Parameters used and Obtained in the Reduction of the Twice Normalized Ground Reaction Curves for the Frictionless Soil Model for H/D=1.5 1022

Table Page

6.12 Parameters Used and Obtained in the Reduction of the Twice Normalized Ground Reaction Curves for the Frictionless Soil Model for H/D=6 1023

6.13 Parameters Obtained in the Reduction of the Twice Normalized Ground Reaction Curves for the Frictionless Soil Model 1024

6.14 Parameters Used and Obtained in the Reduction of the Twice Normalized Ground Reaction Curves of a Tunnel with H/D=3, for the Cohesionless Soil Model with K_o=0.8 1037

6.15 Parameters Used and Obtained in the Reduction of the Twice Normalized Ground Reaction Curves for the Frictionless Soil Model and for K_o=0.6 1045

6.16 Parameters Used and Obtained in the Reduction of the Twice Normalized Ground Reaction Curves for the Frictionless Soil Model and for K_o=0.8 1046

6.17 Parameters Used and Obtained in the Reduction of the Twice Normalized Ground Reaction Curves for the Frictionless Soil Model and for K_o=1.0 1047

7.1 Typical Relative Stiffness Ratios for Common Linings and Soils 1122

7.2 Calculation of the Reduced Unit Weight of the Soil for the Lining-Ground Interaction Analyses 1142

7.3 Calculation of the Reduced Average Ground Stiffness at Lining Installation 1146

7.4 Performance at the ABV Tunnel as Measured and as Calculated by the Proposed Procedure 1191

7.5 Measured and Calculated Ground Response in the Centrifuge Model Test 2DP by Mair (1979) 1204

7.6 Typical Properties of Frankfurt Clay used in the Analysis 1216

Table Page

7.7 Selected Ground Parameters for Drained Analysis of Tunnel in Dense Sand-Clay Till 1237

7.8 Selected Ground Parameters for Analysis of Tunnel in Well-Graded Sandy-Silty Gravel 1249

7.9 Selected Parameters for Munich Marl 1265

7.10 Measured and Calculated Performances at the Munich Line 5/9 Tunnel 1278

7.11 Results of the Application of the Proposed Calculation Procedure to Some Case Histories of Shallow Tunnels 1297

7.12 Calculated and Measured Widths of the Final Surface Settlement Profiles in Some Case Histories 1306

List of Figures

Figure		Page
2.1	Effect of Gravity on the Elastic Stress Paths in a Deep Tunnel	30
2.2	Stress Changes due to the Reduction of the In Situ Stress in a Deep Tunnel	33
2.3	Stress and Strain Changes Around a Tunnel	35
2.4	Stress Paths Around a Shallow Tunnel	48
2.5	Ground Reaction Curves for a Shallow Tunnel	54
2.6	Relationship Between Crown Displacement and Factor of Safety in Drained Model Tests	64
2.7	Relationship Between Crown Displacement and Factor of Safety in Undrained Model Tests	69
2.8	Relationship Between Dimensionless Displacement of the Crown and Factor of Safety Observed in Drained and Undrained Model Tests	74
2.9	Distribution of Volumetric Strains around Shallow Tunnels	77
2.10	Schematic Representation of Specific Volume Changes with Varying Tunnel Depth	84
2.11	In Situ Stresses and Lining Loads on a Rigid Lining for Non-Slip Condition	91
2.12	Normal Stress on a Rigid Lining for Full Slip Condition	91
2.13	Equilibrium Points for Crown and Springline of a Deep Tunnel with Full Slip Interface Between Soil and Lining	96
2.14	In Situ Stresses Around a Shallow Circular Tunnel Profile Prior to Excavation	98
2.15	Stress Distributions Around a Rigid Lining in a "Shallow" Tunnel	100

Figure Page

2.16 Points of Equilibrium of a Ground-Lining Interaction Analyses Using Finite Element Method 104

2.17 Reaction of the Support to External Gravity Loads 119

2.18 Incremental Displacement Field in the Longitudinal Vertical Plane, caused by an Incremental Advance of the Tunnel Face by Heading and Bench Excavation (after Heinz, 1984; modified) 125

2.19 Three-Dimensional Arching near the Face of an Advancing Tunnel (after Eisenstein et.al. 1984: modified) 129

2.20 Ground-Lining Response Concept for the Tunnel Crown (after Eisenstein et.al., 1984: modified) 133

2.21 Vertical Stress and Displacement Measurements at Crown Elevation for Tunnels in Frankfurt (modified after Sauer and Jonuscheit, 1976 and Stroh and Chambosse, 1973) 137

2.22 Radial Stress and Displacement at Springline Elevation for Tunnels in Frankfurt (Modified after Sauer and Jonuscheit, 1976 and Chambosse, 1972) 139

2.23 Measured Footing Pressures in the Upper Shotcrete Arch at the Munich Subway (Baulos 18.2) 143

2.24 Longitudinal Distribution of Thrust Forces at the Tunnel Crown (after Schikora, 1984: modified) 149

2.25 Radial Stresses and Displacements at the Crown Elevation (L/D=2/3) 152

2.26 Radial Stresses and Displacements at the Springline Elevation (L/D=2/3) 153

2.27 Radial Stresses and Displacements at the Floor Elevation (L/D=2/3) 154

2.28 Ground-Lining Response Curves at the Crown 159

Figure Page

2.29 Ground-Lining Response Curves at the Springline 160

2.30 Ground-Lining Response Curves at the Floor 161

3.1 Three-Dimensional Collapse Mechanisms in Shallow Tunnels 181

3.2 Influence of Geometric Conditions on the Undrained Stability of Tunnel Headings in Overconsolidated Kaolin 183

3.3 Undrained Stability of Fully Lined and Fully Unlined Model Test Tunnels in Overconsolidated Kaolin 185

3.4 Distributions of the Longitudinal Distortion Index Along A Stable and an Unstable Tunnel 189

3.5 Longitudinal Distortions above the Crown of a Model Tunnel Test (based on Casarin, 1977) 191

3.6 Stress Paths and Stress Ratio of a Soil Element at the Tunnel Crown 196

3.7 Local Collapse at the Roof of a Deep Tunnel in Dense Sand 197

3.8 Ground Reaction Curve and Stress Ratio Changes in an Element of Soil at the Crown of a Tunnel Approaching Collapse 208

3.9 Short Term Pore Pressure Changes and Total Stress Distributions 217

3.10 Pore Water Pressure Changes in a Soil Element Adjacent to the Opening upon Decrease of Internal Tunnel Pressure 220

3.11 Calculated Contours of Undrained Porewater Pressure Changes Around a Tunnel in Boston Blue Clay for two Overconsolidation Ratios (after Johnston, 1981:133,140 - modified) 224

3.12 Pore Pressure Coefficients for Elastic Consolidation of a Deep Circular Tunnel (modified from Carter and Booker, 1982) 231

Figure Page

3.13 Changes in Lining Bending Moments with Time during Elastic Consolidation (modified from Carter and Booker, 1984:603) 233

3.14 Non-Linear Consolidation of a Thick Cylinder: Evolution of Radial Stress and Pore Pressures at the Rigid Lining-Soil Interface with Time (modified from Gunn and Taylor, 1985) 236

3.15 Distributions of Surface and Subsurface Settlements before and after Consolidation (modified from Johnston, 1981:104) 239

3.16 Schematic Flow Net in the Longitudinal Plane for a Partially Lined Shallow Tunnel during Construction 249

3.17 Steady State Flow Nets Around Shallow Tunnels with Different Lining Permeabilities (from Fitzpatrick et.al., 1981:99 - modified) 252

3.18 Schematic Distribution of Settlements in the Cover of a Shallow Tunnel due to Groundwater Drainage 254

3.19 Idealized Total and Effective Stress Paths Around a Tunnel 257

3.20 Idealized Changes in Shear Stress, Pore Pressure and Factor of Safety during and after Construction of a Plane Strain Shallow Tunnel in Saturated Clay 261

3.21 Degree of Consolidation and Maximum Surface Settlement Evolution in a Shallow Tunnel (modified after Johnston, 1981:106) 266

3.22 Tentative Boundaries for Undrained and Drained Responses Around a Deep, Impermeable Unlined Tunnel in an Elastic Soil 270

3.23 Tentative Boundaries for Undrained and Drained Responses along line AB of the Cover of a Shallow and Permeable Tunnel, resulting solely from Ground Drainage 273

Figure Page

4.1 Displacements and Strains from Finite Element Simulation of a Shallow Tunnel 306

4.2 Classification of Some Typical Examples of Methods for Lining Load Prediction 332

4.3 Maximum Bending Moment Variation with Flexibility Ratio for a Deep Tunnel Liner from Different Ring and Plate Closed Form Solutions 359

4.4 Equivalence between Continuum and Spring Models for an Unlined Circular Opening under a Gravitational Stress Field 375

4.5 Maximum Bending Moment Variation with Flexibility Ratio for a Deep Tunnel Liner from Ring and Spring and Ring and Plate Solutions 377

4.6 Classification of Methods for Ground Settlement Prediction for Shallow Tunnels 407

4.7 Assumed Ratio Horizontal to Vertical In Situ Stresses used for Design of Shielded or Mined Tunnels in Soil 435

4.8 Ground Load Assumption Considered in the Responses for the Design of Shielded and Mined Tunnels 436

4.9 Criteria Indicated in the Responses for Ground Load Reduction both in Shielded and Mined Tunnels 440

4.10 Types of Statical Systems used for Assessment of Lining Loads in Shallow Tunnels 442

4.11 Statical Systems Applied in Shielded and Mined (NATM) Tunnels 443

4.12 Procedures for Evaluation of the Spring Constant to be used in Ring and Spring Models for Lining Design of Shielded or Mined Tunnels 445

4.13 Distribution of Respondents on the Statical System used for the Design of the Primary and Secondary Linings in Mined Tunnels 447

Figure Page

4.14 Obligation to Account for the Non-Linear Behaviour of the Soil or the Support, in the Design of a Shallow Tunnel in Soil 449

4.15 Obligation to Account for Non-Linear Behaviour of the Soil or the Support in Shielded and Mined Tunnels 450

4.16 Consideration of Three-Dimensional Effects in the Lining Design of Shielded and Mined Tunnels 451

4.17 Factors of Safety used in the Design of Shallow Tunnels in Soil 453

4.18 Type of Practice of Respondents 468

4.19 Distribution of Respondents that Normally Perform Quantitative Prediction of Settlements Caused by Shallow Tunnelling 469

4.20 Distribution of most often used Methods for Settlement Prediction among Respondents 472

4.21 Basic Qualities of any Settlement Prediction 474

4.22 Noted Qualities of the "Empirical" and "Numerical" Approaches for Settlement Predictions Routinely Performed by Practitioners 477

4.23 Distribution of Respondents Affirming they Couple Settlement and Lining Load Prediction in their normal Design Practice 479

4.24 Distribution of Approaches Used for Coupling Ground Settlements and Lining Load Predictions 481

5.1 Examples of Stress-Strain Relations for Soil used in Shallow Tunnel Modelling 527

5.2 Triaxial Test Results on a Lightly OC Clay and Predictionsby the Hyperbolic and Jardine et.al. (1986) Models 533

Figure Page

5.3 Stress-Strain Relations for OC London Clay under Unconsolidated Undrained Triaxial Test (after Jardine et.al., 1985:512, modified) 533

5.4 Types of Numerical Prediction of Shallow Tunnel Behaviour made by Two-Dimensional Finite Element Analysis 545

5.5 Performance Aspects Compared in Numerical Predictions of Shallow Tunnel Behaviour by Two-Dimensional Finite Element Analyses 545

5.6 Comparison of Surface Settlements Calculated by Two-Dimensional Finite Element Analyses and Measured Values 546

5.7 Comparison of Subsurface Settlements Calculated by Two-Dimensional Finite Element Analyses and Measured Values 546

5.8 Comparison of Horizontal Displacements Calculated by Two-Dimensional Finite Element Analyses and Measured Values 550

5.9 Comparison of Lining Loads Calculated by Two-Dimensional Finite Element Analyses and Measured Values 550

5.10 Hyperbolic Model Representation 558

5.11 Derivation of the Current Tangent Modulus 559

5.12 Details of the Finite Element Mesh 562

5.13 Longitudinal Profile Along ABV Tunnel 582

5.14 Profile of the In Situ Deformation Modulus at the ABV Site 588

5.15 Construction Details at the ABV Tunnel 590

5.16 Assumptions and Fixed Parameters for ABV Tunnel Back Analyses 594

5.17 Measured and Calculated Surface Settlements at the Face of the ABV Tunnel 598

Figure Page

5.18 Measured and Calculated Subsurface Vertical Displacements at the Face of the ABV Tunnel 599

5.19 Measured and Calculated Final Surface Settlements at the ABV Tunnel 602

5.20 Measured and Calculated Final Subsurface Vertical Displacements at the ABV Tunnel 603

5.21 Measured and Calculated Final Radial Stresses on ABV Tunnel Lining 604

5.22 Calculated Contours of Major and Minor Principal Strains Around the ABV Tunnel 609

5.23 Calculated Principal Strain Differences and Changes in Tangent Modulus Around the ABV Tunnel 610

5.24 Subsurface Profile of Southbound LRT Tunnel along Jasper Avenue (after Branco, 1981:modified) 615

5.25 Profile of In Situ Deformation Modulus at the LRT site 625

5.26 TBM and Lining System used at the Edmonton LRT Tunnel (after Branco, 1981:modified) 627

5.27 Assumptions and Fixed Parameters for the LRT Tunnel Back Analyses 630

5.28 Measured and Calculated Surface Settlements before Lining Activation at the LRT Tunnel 637

5.29 Measured and Calculated Final Surface Settlements at the LRT Tunnel 637

5.30 Measured and Calculated Vertical Displacements Along a Vertical Line 10 m off the Centreline of the LRT Tunnel 638

5.31 Measured and Calculated Vertical Displacements Along a Vertical Line 4 m off the Centreline of the LRT Tunnel 639

5.32 Measured and Calculated Lateral Movements in the Ground beside the LRT Tunnel before Lining Activation 642

Figure Page

5.33 Measured and Calculated Final Lateral Movements in the Ground beside the LRT Tunnel 643

5.34 Measured and Calculated Thrust Forces at Rib Joints in the LRT Tunnel 645

5.35 Calculated Changes in Tangent Modulus around LRT Tunnel 652

5.36 Subsurface Profile of Edmonton Experimental Tunnel along 125 Avenue (Yellowhead Trail) (after El-Nahhas, 1980:modified) 654

5.37 Geotechnical Profile at the Instrumented Section 3 of Edmonton Experimental Tunnel 658

5.38 Grain Size Distributions 659

5.39 Location of Shelby Sampling and Types of Test in Edmonton Experimental Tunnel 662

5.40 Void Ratio - Effective Stress Curves from Oedometer Tests for Edmonton Experimental Tunnel Through Till 663

5.41 Drained Passive Compression Tests in Softer Till (24 - 25 m depth) 669

5.42 Consolidated Undrained Passive Compression Tests in Softer Till (11.5 m depth) 670

5.43 Consolidated Undrained Passive Compression Tests in Softer Till (21.0 m depth) 671

5.44 Consolidated Undrained Passive Compression Tests in Softer Till (28.5 m depth) 672

5.45 Variation of Initial Tangent Modulus with Confining Pressure for Till in Edmonton Experimental Tunnel 674

5.46 Effective Stress Strength Parameters for Till in Edmonton Experimental Tunnel 677

5.47 Total Stress Strength Parameters for Till in Edmonton Experimental Tunnel 677

Figure Page

5.48 Profile of in Situ Deformation Modulus at the Edmonton Experimental Tunnel 678

5.49 Consolidated Undrained Compression Test in Softer Till with Constant Average Stress 682

5.50 Consolidated Undrained Active Compression Test in Softer Till 683

5.51 Stress-Strain Curves of Softer Till Tested under Distinct Total Stress Paths and Distinct Drainage Conditions 684

5.52 Tangent Moduli of Deformation of Till in Edmonton Experimental Tunnel for Distinct Total Stress Paths and Drainage Conditions 685

5.53 Stress Paths of Triaxial Tests on Till in Edmonton Experimental Tunnel 687

5.54 TBM and Lining System used at the Edmonton Experimental Tunnel (after El-Nahhas:1980:modified) 688

5.55 Assumptions and Fixed Parameters for the Edmonton Experimental Tunnel Back Analyses 691

5.56 Measured and Calculated Settlements after Complete Passage of the TBM at the Edmonton Experimental Tunnel 699

5.57 Measured and Calculated Subsurface Vertical Displacements along the Tunnel Centreline, after Complete Passage of the TBM at the Edmonton Experimental Tunnel 702

5.58 Measured and Calculated Subsurface Vertical Displacements along a Vertical Line 2.5 m off the Centreline, after Complete Passage of the TBM at the Edmonton Experimental Tunnel 703

5.59 Measured and Calculated Subsurface Settlements after Complete Passage of the TBM, at the Edmonton Experimental Tunnel 704

Figure Page

5.60 Measured and Calculated Lateral Movements in the Ground beside the Edmonton Experimental Tunnel before Lining Activation 706

5.61 Measured and Calculated Lateral Movements in the Ground beside the Edmonton Experimental Tunnel after Complete Passage of the TBM 707

5.62 Measured and Calculated Thrust Forces at Segment Joints in the Edmonton Experimental Tunnel 710

5.63 Calculated and Measured Zones with Maximum Shear Strain Greater than 1% in the Edmonton Experimental Tunnel 714

5.64 Calculated and Measured Zones with Maximum Shear Strain Greater than 2% in the Edmonton Experimental Tunnel 716

5.65 Conceptual Relations Between the Amount of Stress Release and Loss of Ground in a Two-Dimensional Representation 728

5.66 Radial Displacements of an Unlined Deep Tunnel in Elastic Ground (after Niwa et.al., 1979) 734

5.67 Three-Dimensional Finite Element Mesh and Input Parameters 749

5.68 Dimensionless Radial Displacements at the Crown of a Lined and Unlined Shallow Tunnel (H/D=1.6 and K=0.75) 756

5.69 Dimensionless Radial Displacements at the Springline of a Lined and Unlined Shallow Tunnel (H/D=1.6 and K=0.75) 757

5.70 Dimensionless Radial Displacements at the Floor of a Lined and Unlined Shallow Tunnel (H/D=1.6 and K=0.75) 758

5.71 Dimensionless Radial Displacements at the Crown of a Lined and Unlined Deeper Tunnel (H/D=2.8 and K=0.75) 760

5.72 Dimensionless Radial Displacements at the Springline of a Lined and Unlined Deeper Tunnel (H/D=2.8 and K=0.75) 761

Figure Page

5.73 Dimensionless Radial Displacements at the Floor of a Lined and Unlined Deeper Tunnel (H/D=2.8 and K=0.75) 762

5.74 Closure of an Unlined Tunnel in Elastic Ground Compared to that of Lined Tunnels in Elasto-Plastic Material 765

5.75 Dimensionless Crown Displacements of the Shallower (H/D=1.6) Unlined Tunnel for Different In Situ Stress Ratios K 767

5.76 Dimensionless Crown Displacements of the Deeper (H/D=2.8) Unlined Tunnel for Different Stress Ratios K 768

5.77 Dimensionless Springline Displacements of the Shallower (H/D=1.6) Unlined Tunnel for Different Stress Ratios K 770

5.78 Dimensionless Springline Displacements of the Deeper (H/D=2.8) Unlined Tunnel for Different Stress Ratios K 771

5.79 Dimensionless Floor Displacements of the Shallower (H/D=1.6) Unlined Tunnel for Different Stress Ratios K 772

5.80 Dimensionless Floor Displacements of the Deeper (H/D=2.8) Unlined Tunnel, for Different Stress Ratios K 773

5.81 Comparison of Dimensionless Crown Displacements of the Shallower and Deeper Unlined Tunnels 775

5.82 Comparison of Dimensionless Springline Displacements of the Shallower and Deeper Unlined Tunnels 776

5.83 Comparison of Dimensionless Floor Displacements of the Shallower and Deeper Unlined Tunnels 777

5.84 Ground Movements in the Vertical Longitudinal Plane of the Shallower (H/D=1.6) Unlined Tunnel 778

5.85 Ground Movements in the Vertical Longitudinal Plane of the Deeper (H/D=2.8) Unlined Tunnel 779

Figure Page

5.86 U and K Relationships for the Section at the Face 781

5.87 U and K Relationship for a Section D/4 Behind the Face 782

5.88 U and K Relationship for a Section D/2 Behind the Face 783

5.89 U and K Relationship for a Section 1.D Behind the Face 784

5.90 U and K Relationship for a Section 2.D Behind the Face 785

5.91 U and K Relationships for the Tunnel Crown 789

5.92 U and K Relationships for the Tunnel Springline 790

5.93 U and K Relationships for the Tunnel Floor 791

5.94 Coefficients of the U and K Relationship for the Crown of an Unlined Shallow Tunnel (1.5<H/D<3.0) as a Function of the Distance to the Face 792

5.95 Coefficients of the U and K Relationship for the Springline of an Unlined Shallow Tunnel (1.5<H/D<3.0) as a Function of the Distance to the Face 793

5.96 Coefficients of the U and K Relationship for the Floor of an Unlined Shallow Tunnel (1.5<H/D<3.0) as a Function of the Distance to the Face 794

5.97 Maximum Horizontal Displacement of the Tunnel Face Expressed in Dimensionless Form, as a Function of the Stress Ratio K 795

5.98 Maximum Angular Distortion Along the Tunnel, at Crown Elevation 799

5.99 Maximum Angular Distortion Along the Tunnel, at an Axis 0.3D Above Crown Elevation, as a Function of the Maximum Crown Distortion 801

Figure Page

5.100 Maximum Angular Distortion of the Ground Surface Along the Tunnel Alignment as a Function of the Maximum Crown Distortion 803

5.101 Comparison Between Niwa et.al. (1979) and the Present (Averaged) Tunnel Closure Solution 807

5.102 Predicted and Measured Crown Displacements at the Face for Different Ground Types 823

5.103 Predicted and Measured Springline Displacements at the Face, for Different Ground Types 826

5.104 Predicted and Measured Crown Displacements at the Face for Different Tunnel Construction Methods 827

5.105 Predicted and Measured Springlne Displacements at the Face, for Different Tunnel Construction Methods 829

5.106 Predicted and Measured Crown Displacements at the Section the Support was Installed for Different Ground Types 831

5.107 Predicted and Measured Crown Displacements at the Section the Support was Installed for Different Tunnel Construction Methods 832

5.108 Dimensionless Crown Displacements Observed when the Support was Installed at Different Distances Behind the Tunnel Face 834

5.109 Predicted and Measured Springline Displacements at the Section the Support was Installed, for Different Ground Types 838

5.110 Predicted and Measured Springline Displacements at the Section the Support was Installed for Different Tunnel Construction Methods 839

5.111 Distributions of Measured Crown Displacements after Support Installation 840

Figure Page

5.112 Distributions of Measured Crown Displacements at the Tunnel Face 843

5.113 Evaluation of the Ground Stress Release at the ABV Tunnel for a Two-Dimensional Numerical Simulation 853

5.114 Evaluation of the Ground Stress Release at the LRT Tunnel for a Two-Dimensional Numerical Simulation 856

5.115 Evaluation of the Ground Stress Release of the Edmonton Experimental Tunnel for a Two-Dimensional Simulation 858

6.1 Example of Homothetic Hyperbolae 866

6.2 Uniqueness of the Normalized Homothetic Hyperbolae for c=n=0 867

6.3 Ground Reaction Curves for the Crown of Geometrically Homothetic Tunnels in a Soil with a Homothetic Hyperbolic Stress-Strain Relationship (cohesionless model) 871

6.4 Ground Reaction Curves for the Springline of Geometrically Homothetic Tunnels in a Soil with a Homothetic Hyperbolic Stress-Strain Relationship (cohesionless model) 872

6.5 Ground Reaction Curves for the Floor of Geometrically Homothetic Tunnels in a Soil with a Homothetic Hyperbolic Stress-Strain Relationship (cohesionless model) 873

6.6 Normalized Ground Reaction Curves of Geometrically Homothetic Tunnels in a Soil with a Homothetic Hyperbolic Stress-Strain Relationship (cohesionless model) 874

6.7 Subsurface Settlements along the Cover of Geometrically Homothetic Tunnels in a Soil with a Homothetic Hyperbolic Stress-Strain Relationship (c=0), for Stress Release of 50% 875

Figure Page

6.8 Surface Settlements over Geometrically Homothetic Tunnels in a Soil with a Homothetic Hyperbolic Stress-Strain Relationship (c=0), for Stress Release of 50% 876

6.9 Ground Reaction Curve for the Crown of Geometric Homothetic Tunnels in a Soil with a Homothetic Hyperbolic Stress-Strain Relationship (frictionless model) 884

6.10 Ground Reaction Curve for the Springline of Geometric Homothetic Tunnels in a Soil with a Homothetic Hyperbolic Stress-Strain Relationship (frictionless model) 885

6.11 Ground Reaction Curve for the Floor of Geometric Homothetic Tunnels in a Soil with a Homothetic Hyperbolic Stress-Strain Relationship (frictionless model) 886

6.12 Normalized Ground Reaction Curves of Geometrically Homothetic Tunnels in a Soil with a Homothetic Hyperbolic Stress-Strain Relationship (frictionless model) 887

6.13 Subsurface Settlements along the Cover of Geometrically Homothetic Tunnels in a Soil with a Homothetic Hyperbolic Stress-Strain Relationship ($\phi=0$), for a Stress Release of 50% 888

6.14 Surface Settlements over Geometrically Homothetic Tunnels in a Soil with a Homothetic Hyperbolic Stress-Strain Relationship ($\phi=0$), for a Stress Release of 50% 890

6.15 Influence of Janbu's Modulus K on the Ground Reaction Curve of the Tunnel Crown 896

6.16 Influence of Janbu's Modulus K on the Ground Reaction Curve of the Tunnel Springline 897

6.17 Influence of Janbu's Modulus K on the Ground Reaction Curve of the Tunnel Floor 898

Figure Page

6.18 Variations with Depth of the In Situ Tangent Modulus for Three Values of Janbu's Exponent, n 900

6.19 Normalized Ground Reaction Curves for the Tunnel Crown, Calculated for Different In Situ Tangent Modulus Profiles 901

6.20 Normalized Ground Reaction Curves for the Tunnel Floor, Calculated for Different In Situ Tangent Modulus Profiles 902

6.21 Normalized Ground Reaction Curves for the Tunnel Springline, Calculated for Different In Situ Tangent Modulus Profiles 904

6.22 Ground Reaction Curves for the Crown and Floor, with the Displacements Normalized to the Soil In Situ Stiffnesses at Points Half a Diameter Above and Below the Tunnel Respectively 905

6.23 Normalized Subsurface and Surface Settlements for 50% Ground Stress Release at the Opening, for Different Exponent n Values 907

6.24 Normalized Ground Reaction Curves for the Crown, Calculated for Different Cohesive Strengths of the Soil 913

6.25 Normalized Ground Reaction Curves for the Springline, Calculated for Different Cohesive Strengths of the Soil 914

6.26 Normalized Ground Reaction Curves for the Floor, Calculated for Different Cohesive Strengths of the Soil 917

6.27 Normalized Subsurface and Surface Settlements for 50% Ground Stress Release, Calculated for Different Cohesive Strengths of the Soil 918

6.28 Normalized Ground Reaction Curves for the Crown, Calculated for Different Soil Strengths 921

Figure Page

6.29 Normalized Ground Reaction Curves for the Springline, Calculated for Different Soil Strengths 922

6.30 Normalized Ground Reaction Curves for the Crown, Calculated for Different Poisson's Ratios 926

6.31 Normalized Ground Reaction Curves for the Springline, Calculated for Different Poisson's Ratios 928

6.32 Normalized Ground Reaction Curves for the Floor, Calculated for Different Poisson's Ratios 929

6.33 Normalized Subsurface and Surface Settlements for 50% Ground Stress Release, Calculated for Different Poisson's Ratios 930

6.34 Distributions of Sizes and Depths of Tunnels Reviewed 934

6.35 Distributions of Geotechnical Properties of the Grounds Through Which the Tunnels Reviewed were Driven 935

6.36 Distribution of the In Situ Stress Ratios in the Case Histories Reviewed 937

6.37 Distribution of Construction Methods and Distance of Support Activation in the Tunnels Surveyed 938

6.38 Normalized Ground Reaction Curve for the Springline Calculated for Different Numbers of Unloading Increments 942

6.39 Difference in the Calculated Dimensionless Displacement U for Ten and Twenty Unloading Increments 943

6.40 Differences in the Normalized Ground Settlements for Stress Release of 50%, Calculated for Ten and Twenty Unloading Increments 944

6.41 Normalized Ground Reaction Curves for the Crown, Calculated for Different Positions of the Lower Rigid Boundary 948

Figure Page

6.42 Normalized Ground Reaction Curves for Springline, Calculated for Different Positions of the Lower Rigid Boundary 950

6.43 Normalized Ground Reaction Curves for Floor, Calculated for Different Positions of the Lower Rigid Boundary 951

6.44 Distribution of Subsurface Normalized Settlements for 50% Ground Stress Release, Calculated for Different Positions of the Lower Rigid Boundary 952

6.45 Subsurface Settlement Distribution for 50% Ground Stress Release, Calculated for Different Positions of the Lower Rigid Boundary 954

6.46 Transverse Profiles of Normalized Ground Surface Settlements for 50% Stress Release, Calculated for Different Positions of the Lower Rigid Boundary 955

6.47 Normalized Ground Reaction Curves for H/D=3 and an Undrained Strength Ratio of 1.25 964

6.48 Normalized Subsurface Settlements along Tunnel Axis for H/D=3 and an Undrained Strength Ratio of 1.25, Calculated for Increasing Amount of Stress Release 965

6.49 Normalized Surface Settlements for H/D=3 and Undrained Strength Ratio of 1.25, Calculated for Increasing Amount of Stress Release 966

6.50 Normalized Ground Reaction Curves at the Crown for an Undrained Strength Ratio of 1.25 and Different Tunnel Depths 967

6.51 Normalized Ground Reaction Curves at the Springline for and Undrained Strength Ratio of 1.25 and Different Tunnel Depths 968

6.52 Normalized Ground Reaction Curves at the Floor for an Undrained Strength Ratio of 1.25 and Different Tunnel Depths 969

Figure Page

6.53 Normalized Subsurface and Surface Settlement for an Undrained Strength Ratio of 1.25 and 50% Ground Stress Release, Calculated for Different Tunnel Depths 971

6.54 Normalized Ground Reaction Curves of the Crown for H/D=3 and Different Undrained Strength Ratios 972

6.55 Normalized Ground Reaction Curves of the Springline for H/D=3 and Different Undrained Strength Ratios 973

6.56 Normalized Ground Reaction Curves of the Floor for H/D=3 and Different Undrained Strength Ratios 974

6.57 Normalized Subsurface and Surface Settlements for H/D=3 and 50% Ground Stress Release, Calculated for Different Undrained Strength Ratios 976

6.58 Normalized Ground Reaction Curves for H/D=3, K_o=0.8 and ϕ=30° 978

6.59 Normalized Subsurface Settlements for H/D=3, K_o=0.8 and ϕ=30°, Calculated for Increasing Amount of Stress Release 979

6.60 Normalized Surface Settlements for H/D=3, K_o=0.8 and ϕ=30°, Calculated for Increasing Amount of Stress Release 980

6.61 Normalized Ground Reaction Curves for Different Tunnel Depths, Calculated for ϕ=30° and K_o=0.8 982

6.62 Normalized Subsurface and Surface Settlements for Different Tunnel Depths, Calculated for ϕ=30°, K_o=0.8 and 50% Stress Release 983

6.63 Normalized Ground Reaction Curves of the Crown for H/D=3 and K_o=0.8, Calculated for Different Friction Angles 985

6.64 Normalized Ground Reaction Curves of the Springline for H/D=3 and K_o=0.8, Calculated for Different Friction Angles 986

Figure Page

6.65 Normalized Ground Reaction Curves of the Floor for H/D=3 and K_o=0.8, Calculated for Different Friction Angles 987

6.66 Normalized Subsurface and Surface Settlements for H/D=3, K_o=0.8 and 40% Ground Stress Release, Calculated for Different Friction Angles 988

6.67 Normalized Ground Reaction Curves of the Crown, for H/D=3 and ϕ=30°, Calculated for Different In Situ Stress Ratios 990

6.68 Normalized Ground Reaction Curves of the Springline, for H/D=3 and ϕ=30°, Calculated for Different In Situ Stress Ratios 991

6.69 Normalized Ground Reaction Curves of the Floor, for H/D=3 and ϕ=30°, Calculated for Different In Situ Stress Ratios 992

6.70 Normalized Subsurface and Surface Settlements for H/D=3, ϕ=30° and 50% Ground Stress Release, Calculated for Different In Situ Stress Ratios 994

6.71 Variation of the Maximum Normalized Surface Settlement with the Amount of Stress Release and other Variables, for the Frictionless Soil Model 997

6.72 Variation of the Maximum Normalized Surface Settlement with the Amount of Stress Release and other Variables, for the Cohesionless Soil Model 999

6.73 Relationships between Normalized Maximum Surface Settlement and Relative Depth of Tunnel, Calculated for the Frictionless Soil Model, for 30% Stress Release 1002

6.74 Relationships between Normalized Maximum Surface Settlement and Relative Tunnel Depth, Calculated for the Frictionless Soil Model, for 50% Stress Release 1003

Figure Page

6.75 Normalized Settlement Ratios for ϕ=40° and 30% Stress Release 1004

6.76 Normalized Settlement Ratios for ϕ=40° and 50% Stress Release 1005

6.77 Normalized Settlement Ratios for ϕ=30° and 30% Stress Release 1006

6.78 Normalized Settlement Ratios for ϕ=30° and 50% Stress Release 1007

6.79 Normalized Settlement Ratios for ϕ=20° and 30% Stress Release 1008

6.80 Normalized Settlement Ratios for ϕ=20° and 50% Stress Release 1009

6.81 Normalized Settlement Ratios Observed in some Case Histories 1011

6.82 Twice Normalized Ground Reaction Curve (NNGRC) for the Crown of a Tunnel with H/D=3, for the Frictionless Soil Model 1017

6.83 Twice Normalized Ground Reaction Curves (NNGRC) for the Springline of a Tunnel with H/D=3, for the Frictionless Soil Model 1019

6.84 Twice Normalized Ground Reaction Curves (NNGRC) for the Floor of a Tunnel with H/D=3, for the Frictionless Soil Model 1020

6.85 Variation of the Coefficient A with Relative Tunnel Depth, for the Frictionless Soil Model 1025

6.86 Variation of the Coefficient B, for the Tunnel Crown, with Strength and Depth Ratios, Calculated for the Frictionless Soil Model 1026

6.87 Variation of the Coefficient B for the Tunnel Springline, with Strength and Depth Ratios, Calculated for the Frictionless Soil Model 1027

6.88 Variation of the Coefficient B for the Tunnel Floor, with Strength and Depth Ratios, Calculated for the Frictionless Soil Model 1028

Figure | Page

6.89 Twice Normalized Ground Reaction Curve (NNGRC) for the Crown of a Tunnel with H/D=3, for the Cohesionless Soil Model with K_o=0.8 1038

6.90 Twice Normalized Ground Reaction Curves (NNGRC) for the Springline of a Tunnel with H/D=3, for the Cohesionless Soil Model with K_o=0.8 1040

6.91 Twice Normalized Ground Reaction Curves (NNGRC) for the Floor of a Tunnel with H/D=3, for the Cohesionless Soil Model with K_o=0.8 1041

6.92 Slope of the Arbitrary Axes used to Obtain the NNGRC, Represented as a Function of H/D, for K_o=0.6 1051

6.93 Relationships between a_{ref} and the Friction Angle for K_o=0.6 1052

6.94 Twice Normalized Ground Reaction Curves for Tunnel Crown Calculated for K_o=0.6 1053

6.95 Twice Normalized Ground Reaction Curves for the Tunnel Springline, Calculated for K_o=0.6 1054

6.96 Twice Normalized Ground Reaction Curves for the Tunnel Floor, Calculated for K_o=0.6 1055

6.97 Variations of λ' for the Tunnel Crown, Calculated for K_o=0.6 1056

6.98 Variations of λ' for the Tunnel Springline, Calculated for K_o=0.6 1057

6.99 Variations of λ' for the Tunnel Floor, Calculated for K_o=0.6 1058

6.100 Slopes of the Arbitrary Axes used to Obtain the NNGRC Represented as a Function of H/D, for K_o=0.8 1061

6.101 Relationships between a_{ref} and the Friction Angle of K_o=0.8 1062

6.102 NNGRCs for Tunnel Crown, Calculated for K_o=0.8 1063

Figure Page

6.103 NNGRCs for Tunnel Springline, Calculated for K_o=0.8 ... 1064

6.104 NNGRCs for Tunnel Floor, Calculated for K_o=0.8 ... 1065

6.105 Variations of λ' for the Tunnel Crown, Calculated for K_o=0.8 ... 1066

6.106 Variations of λ' for the Tunnel Springline, Calculated for K_o=0.8 ... 1067

6.107 Variations of λ' for the Tunnel Floor, Calculated for K_o=0.8 ... 1068

6.108 Slopes of the Arbitrary Axes used to Obtain the NNGRC Presented as a Function of H/D, for K_o=1.0 ... 1069

6.109 Relationships between α_{ref} and the Friction Angle for K_o=1.0 ... 1070

6.110 NNGRCs for Tunnel Crown, Calculated for K_o=1.0 ... 1071

6.111 NNGRCs for Tunnel Springline, Calculated for K_o=1.0 ... 1072

6.112 NNGRCs for Tunnel Floor, Calculated for K_o=1.0 ... 1073

6.113 Variations of λ' for the Tunnel Crown, Calculated for K_o=1.0 ... 1074

6.114 Variations of λ' for the Tunnel Springline, Calculated for K_o=1.0 ... 1075

6.115 Variations of λ' for the Tunnel Floor, Calculated for K_o=1.0 ... 1076

6.116 Variations of the Initial Slope of the Twice Normalized Ground Reaction Curves with K_o and H/D ... 1077

6.117 Extension of the NGRCs for H/D=3, K_o=0.8 and ϕ=30° ... 1081

6.118 Extension of the NGRCs for H/D=3 and $c_u/\gamma D$=1.25 ... 1084

Figure Page

6.119 Reference Values used for Normalizing the NGRC of the Tunnel Crown for the Frictionless Soil Model and Components to Define the Limiting U of the Fitted Function 1086

6.120 Reference Values used for Normalizing the NGRC of the Tunnel Springline for the Frictionless Soil Model and Components to Define the Limiting U of the Fitted Function 1087

6.121 Reference Values used for Normalizing the NGRC of the Tunnel Floor for the Frictionless Soil Model and Components to Define the Limiting U of the Fitted Function 1088

6.122 Lower Bound Solution for Tunnel Collapse Pressure in a Frictionless Soil 1095

6.123 Lower and Upper Bound Solutions for Tunnel Collapse Pressure in a Frictional and Cohesive Soil (ϕ=10°) 1097

6.124 Lower and Upper Bound Solutions for Tunnel Collapse Pressure in a Frictional and Cohesive Soil (ϕ=20°) 1098

6.125 Lower and Upper Bound Solutions for Tunnel Collapse Pressure in a Frictional and Cohesive Soil (ϕ=30°) 1099

6.126 Lower and Upper Bound Solutions for Tunnel Collapse Pressure in a Frictional and Cohesive Soil (ϕ=40°) 1100

7.1 Notations and Conventions used in Hartmann's Solution 1124

7.2 Lining Stresses, Displacements and Internal Forces Given by Hartmann's Solution 1125

7.3 Comparison of Lining Responses Calculated for Different Tunnel Depths, with and without Account of the Influence of the Ground Surface 1129

7.4 Equilibrium Points of the Soil-Lining Interaction at Tunnel Crown 1137

Figure Page

7.5 Equilibrium Points of the Soil-Lining Interaction at Tunnel Springline 1138

7.6 Equilibrium Points of the Soil-Lining Interaction at Tunnel Floor 1139

7.7 Distribution of Final Settlements Calculated for a Tunnel Lined after 40% Stress Release, Compared to the Distributions for an Unlined Tunnel Equal Crown Displacement 1155

7.8 Distribution of Final Settlements Calculated for a Tunnel Lined after 80% Stress Release, Compared to the Distributions for an Unlined Tunnel with Equal Crown Displacements 1156

7.9 Suggested Sequence of Steps for Application of the Proposed Procedure for Shallow Tunnel Design 1161

7.10 Calculation Sheet with Geometric Ground Properties Data and Tunnel Closure at Lining Activation 1169

7.11 Calculation Sheet for Estimates of the Stress Release and Ground Stiffness at the Section the Lining is Activated 1170

7.12 Calculation Sheet for 2D Stability Verification and Lining-Ground Interaction Analysis 1171

7.13 Calculation Sheet for Iterative Analysis of the Lining-Ground Interaction 1172

7.14 Calculation Sheet for Subsurface and Surface Settlements 1173

7.15 ABV Tunnel - Input Data and Tunnel Closure at Lining Activation 1176

7.16 ABV Tunnel - Stress Release and Ground Stiffness at Lining Activation 1179

7.17 ABV Tunnel - Two Dimensional Stability Calculation and Lining-Ground Interaction 1182

7.18 ABV Tunnel - Iterative Calculation for the Lining-Ground Interaction 1185

Figure Page

7.19 ABV Tunnel: Subsurface and Surface Settlement Calculations 1187

7.20 Calculated and Measured Final Subsurface Settlements at the ABV Tunnel 1192

7.21 Calculated and Measured Final Surface Settlements at the ABV Tunnel 1193

7.22 Calculated and Measured Radial Stresses on the ABV Tunnel Lining 1194

7.23 Measured and Calculated Ground Response at Tunnel Crown for the Centrifuge Model Test 1205

7.24 Measured and Calculated Surface Settlement Profiles for the Centrifuge Model Test at Two Internal Pressures 1208

7.25 Subsurface Settlement Distributions Calculated in a Three-Dimensional Analysis and by the Proposed Method 1211

7.26 Profile of Surface Settlements Calculated in a Three-Dimensional Analysis and by the Proposed Method 1213

7.27 Measured and Calculated Final Subsurface Settlements over the South Tunnel in the Frankfurt Baulos 23 (Domplatz) Subway 1220

7.28 Measured and Calculated Final Surface Settlements over the South Tunnel in the Frankfurt Baulos 23 (Domplatz) Subway 1221

7.29 Predicted Lining Loads in the South Tunnel (1st driven) Compared to Measurements in the North Tunnel (2nd driven): Frankfurt Baulos 23 (Domplatz) Subway Tunnels 1222

7.30 Measured and Calculated Subsurface Settlements over the Frankfurt Baulos 25 (Romerberg) Subway 1228

7.31 Measured and Calculated Final Surface Settlements at the Frankfurt Baulos 25 (Romerberg) Subway Tunnel 1229

Figure Page

7.32 Measured and Calculated Final Surface Settlements over Twin Tunnels at the Frankfurt Baulos 25 (Romerberg) Subway 1231

7.33 Predicted Lining Radial Stresses for Single Tunnel and Measured Stresses in Twin Tunnels at the Frankfurt Baulos 25 (Romerberg) Subway 1232

7.34 Measured and Calculated Final Subsurface Settlements over the Mississauga Sewer Tunnel 1242

7.35 Measured and Calculated Final Surface Settlements over the Mississauga Sewer Tunnel 1243

7.36 Measured and Predicted Radial Stress Distributions on the Lining of the Mississauga Sewer Tunnel 1245

7.37 Measured and Calculated Final Subsurface Settlements over the Butterberg Tunnel 1253

7.38 Measured and Calculated Final Surface Settlements over the Butterberg Tunnel 1254

7.39 Measured and Predicted Radial Stress Distributions on the Shotcrete Lining of the Butterberg Tunnel 1256

7.40 Measured and Calculated Final Surface Settlements over the Edmonton LRT Tunnel 1261

7.41 Measured and Calculated Thrust Forces on the Edmonton LRT Primary Lining 1262

7.42 Measured and Calculated Final Subsurface Settlements over the Munich Line 8/1 Tunnel 1268

7.43 Calculated and Measured Radial Stress Distributions on the Shotcrete Lining of the Munich Line 8/1 Tunnel 1270

7.44 Measured and Calculated Surface Settlements over the Munich Line 5/9 Tunnel 1275

Figure Page

7.45 Measured and Calculated Final Subsurface Settlements over the Bochum Baulos A2 Tunnel 1283

7.46 Measured and Calculated Final Surface Settlement Profiles over the Bochum Baulos A2 Tunnel 1284

7.47 Calculated and Measured Radial Stress Distributions on the Shotcrete Lining of the Bochum Baulos A2 Tunnel 1285

7.48 Measured and Calculated Final Subsurface Settlements over the Sao Paulo North Extension Tunnel 1290

7.49 Measured and Calculated Final Surface Settlement Profiles over the Sao Paulo North Extension Tunnel 1291

7.50 Calculated Maximum Surface Distortions Compared to the Observed Maxima 1301

7.51 Calculated Tunnelling Performance Compared to Field Observations 1304

A.1 Radial Stresses and Displacements at the Crown Elevation (L/D=1/2) 1407

A.2 Radial Stresses and Displacements at the Springline Elevation (L/D=1/2) 1408

A.3 Radial Stresses and Displacements at the Floor Elevation (L/D=1/2) 1409

C.1 Normalized Settlements: $K_o=1$, $c_u/\gamma D=2.5$, $H/D=1.5$ 1416

C.2 Normalized Settlements: $K_o=1$, $c_u/\gamma D=1.25$, $H/D=1.5$ 1417

C.3 Normalized Settlements: $K_o=1$, $c_u/\gamma D=0.625$, $H/D=1.5$ 1418

C.4 Normalized Settlements: $K_o=1$, $c_u/\gamma D=0.3125$, $H/D=1.5$ 1419

C.5 Normalized Settlements: $K_o=1$, $\phi=20°$, $H/D=1.5$ 1420

C.6 Normalized Settlements: $K_o=1$, $\phi=30°$, $H/D=1.5$ 1421

Figure Page

C.7 Normalized Settlements: $K_o=1$, $\phi=40°$, H/D=1.5 1422

C.8 Normalized Settlements: $K_o=0.8$, $\phi=20°$, H/D=1.5 1423

C.9 Normalized Settlements: $K_o=0.8$, $\phi=30°$, H/D=1.5 1424

C.10 Normalized Settlements: $K_o=0.8$, $\phi=40°$, H/D=1.5 1425

C.11 Normalized Settlements: $K_o=0.6$, $\phi=20°$, H/D=1.5 1426

C.12 Normalized Settlements: $K_o=0.6$, $\phi=30°$, H/D=1.5 1427

C.13 Normalized Settlements: $K_o=0.6$, $\phi=40°$, H/D=1.5 1428

C.14 Normalized Settlements: $K_o=1$, $c_u/\gamma D=2.5$, H/D=3 1429

C.15 Normalized Settlements: $K_o=1$, $c_u/\gamma D=1.25$, H/D=3 1430

C.16 Normalized Settlements: $K_o=1$, $c_u/\gamma D=0.625$, H/D=3 1431

C.17 Normalized Settlements: $K_o=1$, $\phi=20°$, H/D=3 1432

C.18 Normalized Settlements: $K_o=1$, $\phi=30°$, H/D=3 1433

C.19 Normalized Settlements: $K_o=1$, $\phi=40°$, H/D=3 1434

C.20 Normalized Settlements: $K_o=0.8$, $\phi=20°$, H/D=3 1435

C.21 Normalized Settlements: $K_o=0.8$, $\phi=30°$, H/D=3 1436

C.22 Normalized Settlements: $K_o=0.8$, $\phi=40°$, H/D=3 1437

C.23 Normalized Settlements: $K_o=0.6$, $\phi=20°$, H/D=3 1438

C.24 Normalized Settlements: $K_o=0.6$, $\phi=30°$, H/D=3 1439

Figure Page

C.25 Normalized Settlements: K_o=0.6, ϕ=40°, H/D=3 1440

C.26 Normalized Settlements: K_o=1, $c_u/\gamma D$=2.5, H/D=6 1441

C.27 Normalized Settlements: K_o=1, $c_u/\gamma D$=1.25, H/D=6 1442

C.28 Normalized Settlements: K_o=1, $c_u/\gamma D$=0.625, H/D=6 1443

C.29 Normalized Settlements: K_o=1, ϕ=20°, H/D=6 1444

C.30 Normalized Settlements: K_o=1, ϕ=30°, H/D=6 1445

C.31 Normalized Settlements: K_o=1, ϕ=40°, H/D=6 1446

C.32 Normalized Settlements: K_o=0.8, ϕ=20°, H/D=6 1447

C.33 Normalized Settlements: K_o=0.8, ϕ=30°, H/D=6 1448

C.34 Normalized Settlements: K_o=0.8, ϕ=40°, H/D=6 1449

C.35 Normalized Settlements: K_o=0.6, ϕ=20°, H/D=6 1450

C.36 Normalized Settlements: K_o=0.6, ϕ=30°, H/D=6 1451

C.37 Normalized Settlements: K_o=0.6, ϕ=40°, H/D=6 1452

D.1 NNGRC for Crown, K_o= 0.6, H/D=6 1454

D.2 NNGRC for Crown, K_o= 0.6, H/D=3 1455

D.3 NNGRC for Crown, K_o= 0.6, H/D=1.5 1456

D.4 NNGRC for Springline, K_o= 0.6, H/D=6 1457

D.5 NNGRC for Springline, K_o= 0.6, H/D=3 1458

D.6 NNGRC for Springline, K_o= 0.6, H/D=1.5 1459

D.7 NNGRC for Floor, K_o= 0.6, H/D=6 1460

Figure Page

D.8 NNGRC for Floor, K_o= 0.6, H/D=3 1461

D.9 NNGRC for Floor, K_o= 0.6, H/D=1.5 1462

D.10 NNGRC for Crown, K_o= 0.8, H/D=6 1463

D.11 NNGRC for Crown, K_o= 0.8, H/D=3 1464

D.12 NNGRC for Crown, K_o= 0.8, H/D=1.5 1465

D.13 NNGRC for Springline, K_o= 0.8, H/D=6 1466

D.14 NNGRC for Springline, K_o= 0.8, H/D=3 1467

D.15 NNGRC for Springline, K_o= 0.8, H/D=1.5 1468

D.16 NNGRC for Floor, K_o= 0.8, H/D=6 1469

D.17 NNGRC for Floor, K_o= 0.8, H/D=3 1470

D.18 NNGRC for Floor, K_o= 0.8, H/D=1.5 1471

D.19 NNGRC for Crown, K_o= 1.0, H/D=6 1472

D.20 NNGRC for Crown, K_o= 1.0, H/D=3 1473

D.21 NNGRC for Crown, K_o= 1.0, H/D=1.5 1474

D.22 NNGRC for Springline, K_o= 1.0, H/D=6 1475

D.23 NNGRC for Springline, K_o= 1.0, H/D=3 1476

D.24 NNGRC for Springline, K_o= 1.0, H/D=1.5 1477

D.25 NNGRC for Floor, K_o= 1.0, H/D=6 1478

D.26 NNGRC for Floor, K_o= 1.0, H/D=3 1479

D.27 NNGRC for Floor, K_o= 1.0, H/D=1.5 1480

1. INTRODUCTION

1.1 Preamble

The intense urban development observed worldwide in this century has enhanced the requirements for land use and has increased the general concern regarding its impact on the environment. Such factors as increased land costs and community opposition to disruption caused by new public works have forced underground alternative schemes to be contemplated and implemented. Tunnelling schemes, otherwise not considered for economic or purely technical reasons, are being increasingly favoured as solutions to a variety of urban problems. These encompass mass transport, sewerage, drainage, water and energy supply, etc. Also, recent developments in construction technology yield reductions in the costs of tunnelling operations hence construction in difficult ground conditions has become a viable proposition.

Public utilities are usually installed underground at relatively shallow depths, where, more frequently than not, "soft" ground is found. "Soft" ground is defined in this thesis to be: any incompetent, soil-like material, where a tunnelling excavation driven through it, will require some form of virtually continuous support to maintain the stability of the excavation. The underground excavation alternative minimizes social, environmental and economical impacts by reducing disturbances caused by a cut-and-cover operation. However, it can still cause appreciable disruption. This may result from ground deformation induced by tunnelling operations, with potential environmental effects on neighbouring constructions and utilities.

The shallow ground tunnel cover may not be sufficient to attenuate the deformations induced by the underground excavation. This is the case of the system of transit tunnels built in central Germany in the last decade, for instance, the Bochum system in some locations has barely 2 m cover of post war rubble fill. In contrast to this, some tunnels of the London Underground system built late last century have up to 70 m of soil cover, for instance, at Parliament Hill on the Northern Line "tube".

Some points emerge from the preceding discussion. If anyone is aiming to plan, design or build such a structure, he has to answer a few questions beforehand. Will the cavity be stable during construction? What support or lining system should be installed and what loads will it endure during its service lifetime, with what margin of safety? What are the magnitude and distribution of the displacements induced by the tunnelling operation? What is the damage potential of these displacements on existing structures in the vicinity? These questions, although not exhaustive, must have played on the minds of the pioneering tunnel engineers, when faced with the demand of constructing an urban tunnel. As in many occasions in the history of technology, the pressing need of the structure was greater than the intellectual or scientific interest to answer the questions. As a consequence, those questions remained unanswered or poorly answered. But the structure was built, possibly imperfectly in technical terms. Such imperfection may have resulted from the tunnel construction emboding excessive safety and cost or insufficienct safety.

When practical problems are not promptly solved by available theories or when these are not known to the practitioner, solutions are often empirically developed. By observing successful and unsuccessful past experiences, for instance (in mechanical terms, stable or unstable performance) in tunnel construction, it has been possible to develop some observational design rules. These, however, do not generate information about the margin of safety of the structure. Since these rules embody only successful experience, it is recognized that the structure built according to them will have a factor of safety greater than unity. How much greater is not easily to established. Unlike theoretical solutions that can furnish safe or unsafe design, depending on the validity of the assumptions made, empirical solutions generally provide a conservative design. The above discussion is applicable not only to soil tunnelling but to any other field of geotechnical engineering and it may be considered as a truism. However, a review of the state-of-the-art reports prepared on the subject over the last two decades (Peck, 1969, Attewell, 1977, Clough and Schmidt, 1981, Ward and Pender, 1981, to quote few) reveals that an appreciable amount of empiricism still exists as a design basis for soft ground tunnelling. This may be surprising in view of the significant developments in soil mechanics within the same time span, with the introduction of a variety of new modelling techniques for solving increasingly difficult geotechnical problems. Persistence in using empirical or semi-empirical approaches in the practice of urban tunnel design, can be attributed to a number of different causes. One may be that some theories which have been transferred from other engineering fields are unable to fully or properly solve all aspects of shallow tunnelling. The risks in transferring behavioural or conceptual models from one scientific or technical field to a completely different field was addressed by Ladanyi, (1982). During the transfer process, the underlying assumptions of the theory being transferred are not always clearly stated and the validity of the theory may be questionable for a particular practical application. Another reason might be that the theory is too complex for routine use by non-specialized engineers in design practice.

As will be seen in the next two chapters, shallow tunnelling in soft ground involves a number of behavioural features that preclude the use of any simple theoretical model. This and the current impracticality of using more sophisticated modelling tools in routine practice, may explain to some degree, the continued use of empirical approaches. Moreover, the attraction that empiricism holds should not be disregarded, as it enables one to ensure the ultimate performance of the structure. Tunnels being designed using fairly elaborate numerical techniques, frequently have the final design decisions made only after checking the results against known empirical rules. The opposite is also true. Tunnels being designed entirely on the basis of previous experience may only have some numerical modelling conducted, possibly just to satisfy some contractual requirement or to comply with the client's request. It is common then to find the more involved and possibly more adequate design procedures have little or no impact on the major design decisions.

The capability of numerical modelling, frequently treating the problem as two dimensional, is becoming increasingly known within the community of practioners. Their current limitations are being recognized and clients are becoming gradually concerned when their use is not treated with healthy skepticism. "The enormous developments in measurements and computing capabilities over the last two decades have drawn many researchers" - and numerically or computer oriented practitioners - "into a vortex of ever-increasing sophistication and complexity. They have become so intrigued by their ability to solve previously intractable problems that the primary objectives of research" and practice - "have been obscured" (Poulos, 1982).

As will be seen in following chapters, it has been fully recognized by tunnellers that a fairly clear relationship exists between the magnitude of the displacements in the ground mass around the tunnel opening and the magnitude of stress eventually carried by the support system. This dependence between stress and displacements was expressed using ground-support interaction diagrams. Fenner (1938) was the first to define and obtain these diagrams analytically, using an elastic-plastic model. Obviously, the magnitude of the displacement occurring at the tunnel opening dominates the magnitude of settlement at the ground surface. Therefore, the settlement should be related to the magnitude of the stress supported by the lining. Despite this obvious connection between the two quantities, whose assessment represents the key issues of design, it is suprising to find that in practice one tends to ignore the connection (see Chapter 4). It will be noted that lining design is frequently conducted independently of settlement predictions and, in many instances, using conflicting design assumptions that finally lead to overconservative solutions for both the support system and ground control measures. A possible reason for this state of affairs is the persistent empirical approach which treats the two problems separately. Also the behavioural and conceptual models used to treat these problems were transferred from entirely different fields and in some instances, are based on conflicting hypotheses. As an example, lining design evolved predominantly from a continuum mechanics approach, whereas many prevailing methods for settlement estimates were developed from stochastic theories. In contrast with the theories of elasticity or plasticity, the stochastic medium is typically a discontinuous particulate mass, subjected to gravitational body forces, with their movements controlled by probabilistic laws. Putting aside for a moment the discussion of the validity of using either approach (as addressed by de Mello and Sozio, 1983), it should be recognized (Eisenstein, 1982 and Eisenstein and Negro, 1985) that although convenient numerically, the separation of the problem of displacement and the issue of lining pressure predictions is entirely artificial.

It would appear that research directed towards the development of a practical procedure coupling displacement prediction with lining design is needed. It would preclude the dichotomy of surface settlement and lining load treatment. Also, enough room exists to develop a procedure that would lie somewhere between the more elaborate design approach that makes use of numerical techniques and the prevailing empirical approach for the design of shallow tunnels. This is the subject of the next item.

1.2 Aims

In broad terms, and following the reasoning of Poulos (1982), it could be suggested that any applied research to shallow tunnelling in soil, should include attempts to:

a) identify unsolved or partly solved problems that affect existing practices;

b) more adequately appreciate the mechanisms involved in the soil and in the behaviour of the supporting structures, whenever possible identifying the controlling parameters;

c) develop procedures or approaches to solve the above mentioned problems;

d) summarize the results of the research work in a comprehensive manner and in such a way that it may be used by the practitioner;

e) validate the results of the research by applying them to practical problems and to define ranges of validity.

Sometimes, time or resource constraints or even personal preferences may channel the applied research into one or two of the summarized general points. In the present study, an effort is made to balance the importance of each of the above items.

This work attempts to develop a design procedure that simultaneously treats the problems of estimating lining loads and of predicting the ground settlements in shallow tunnels driven in soil. These activities are part of the overall design considerations of a shallow tunnel and will be discussed in Chapter 4.

To achieve this aim, a basic premise was established at the onset of the work: reasonable simplicity. The demand for simple design oriented procedures is evident from a survey carried out and discussed in Chapter 4 of this thesis. This general demand may reflect the known fact that despite how elaborate an analysis might be, "there will always be practical limitations on its ability to model real geotechnical problems" (Poulos, 1982). Such limitations are well known: uncertainties in modelling the geological profile in detail, in assessing the soil parameters, in recognizing the dominant factors that govern the behaviour, etc. These uncertainties result from a variety of reasons, ranging from economic considerations, time availability and also the present difficulties of properly simulating more complex behaviour (eg. instability after excessive straining of a structure).

Although it should be simple, the needed design procedure would have to be based on a consistent theoretical background to avoid the shortcomings of the existing empirical methods. Hence, it would have to encompass a fairly large number of variables or factors known to affect tunnel behaviour. This required that, in its development, use had to be made of fairly involved modelling techniques, (numerical and analytical), and these were selected on the basis of their recognized simplicity and reliability in solving the posed problem. However, to render the problem tractable, a considerable number of simplifying assumptions had to be made and limitations were imposed as will be seen in the following chapters. This was done, however, knowing that the predictive exercises performed to date in geotechnical engineering show differences in results that are more related to differences in judgement between different predictors, than to differences in the methods of analysis used. One may conclude that the success in applying a method to solve a practical problem, depends as much on the qualities of the designer as on the method itself. In other words, experience in using a method is of paramount importance and in this regard it is probably easier to gather experience with a simple procedure than with a complex one (Poulos, Op.cit).

If it were possible to develop such a design oriented method, it would lie between the simpler empirical methods and the more complex numerical solutions. Ideally it would allow the practitioner to evaluate possible ranges of behaviour or responses to tunnelling, to predesign or design the support and to evaluate field data from instrumentation monitoring, as part of an observational approach to tunnel construction which enables feedback for the final design solution.

1.3 Scope and Thesis Organization

To achieve the objectives as previously described, a number of major factors will be explicitly considered in the development of the proposed design procedure. These are to account for the effects of the following:

a) the delayed installation of the lining;

b) the non-uniform state of stress in the soil in situ, represented by the stress gradient generated by gravitational body forces and by a horizontal to vertical stress ratio different from unity;

c) the non-linear response exhibited by most soils in terms of their stress-strain relationships, including dependence on stress level and strength;

d) the stress free boundary represented by the ground surface;

e) the interactive nature of the load transfer process developed between the soil and its support system; and

The reasons for selecting these factors as those to be appraised in the development of the method will emerge from the discussions in the next two chapters and throughout this thesis. To a large extent, the selection criteria relied initially on observations of real tunnels and on conceptual models, which have been confirmed through more elaborate models. No attempt has been made to develop a new numerical technique for the purpose of this study. Existing methods were simply adapted, to develop the proposed design procedure. This and the need to keep the method as simple as possible meant that despite the already appreciable number of variables taken into consideration, a significant number of factors had to be excluded. Hence it was decided to limit the study to single tunnels with a circular profile, driven through isotropic, time-independent continuous media, excavated full-face under free air, and without water seepage effects. Non geostatic loadings produced by a non-uniform surface or subsurface foundation loads were also not considered. No treatment is given to special classes of soils such as those exhibiting strong post peak softening, e.g., sensitive clays.

It will be shown that the proposed procedures will furnish reasonable results whenever, "good ground control" conditions are attained. These can result from favourable ground (firm) conditions or from the use of appropriate construction techniques applied to poorer ground, where otherwise "ravelling" or "running" of the ground would occur [1]. Attempts will be made in this thesis to better define "good ground control conditions" and to quantify the expected behaviour.

The exclusion of some factors from this study should not lead one to surmise that they play a minor role in the behaviour of a tunnel in soft ground. For the sake of completeness, their role is briefly discussed in the following two chapters.

In Chapters 2 and 3 the idealized behaviour of shallow tunnels is presented. The influence of a number of factors affecting the behaviour is briefly discussed, using simple conceptual models whenever possible.

Chapter 4 summarizes the present state of the design of shallow tunnels with the more important available design methods being reviewed. The merits of the more frequently used methods for lining design and settlement prediction are identified and critically assessed. Finally, an evaluation of the present needs and a definition of potential improvements for current practice are attempted.

---

[1] The Wilson tunnel, partly driven though residual soils in the Koolau Range northeast of Honolulu, is an interesting example of the varying response of the same ground to different construction technologies (see Peck, 1981). The ravelling ground response to full face excavation was changed to very favourable and stable conditions, when the tunnel was advanced in small drifts and in short longitudinal sections.

Chapter 5 reviews shallow tunnel modelling using two and three dimensional finite numerical techniques. The capability of two dimensional finite element analyses to portray the behaviour of selected case histories is assessed. The need to estimate the magnitude of tunnel opening displacements prior to lining installation is justified in order to identify the amount of stress release allowed before the support is installed in the two dimensional representation. For this purpose, parametric three dimensional simulations are carried out and an approximate procedure is established to simulate displacement prior to support activation.

Chapter 6 presents numerical modelling and generalizations to be used for the development of the design model. Reduction of parameters and model simplifications are introduced. The two dimensional finite element parametric analyses are carried out from which generalized relations between stress, ground deformation profile and displacements around the opening are obtained for both frictionless and cohesionless soils.

In Chapter 7 a design procedure is developed based on results obtained in Chapters 5 and 6. Assessments of the effect of delayed lining installation and the soil-lining interaction are made. How to obtain the surface and subsurface settlements is explained. Finally a guideline for using the design procedure in practice is established with the underlying assumptions re-stated to define the range of validity for the proposed method.

Also in Chapter 7, the proposed design procedure is compared with a number of well documented case histories and laboratory model tests. Limitations of the method and the approximations introduced for practical use are discussed.

Finally in Chapter 8 a brief summary of the research work and the main conclusions are presented. Also included are suggestions regarding future applied research on the subject.

2. IDEALIZED BEHAVIOUR OF SHALLOW TUNNELS: STRESS AND STRAIN CHANGES

2.1 Introduction

The purpose of this Chapter is to briefly review some of the more important factors affecting shallow tunnel behaviour, integrating the soil and its support system. As much as possible, the discussion will be framed within a soil mechanics background. In contrast to other geotechnical fields, such as the design of slopes, embankments and foundations, the understanding of soil tunnelling is founded predominantly on tradition and empiricism, where the soil mechanics perspective in not always clear. To put the subject in a basic form, use will be made of simple conceptual models, complemented by results from field observations, model tests and numerical analyses. Some factors will be studied separately, although it is recognized that substantial interaction exists between them. Such an approach is artificial but can be justified for a broad overview.

2.2 Shallow and Deep Tunnels

Despite the fact that a really deep tunnel does not exist, the concept of a "deep" tunnel arose for reasons of theoretical convenience. This enables two effects to be neglected in assessing the behaviour of an opening in the ground (at depth): (a) the stress field gradient across the opening becomes negligible; (b) the influence of the stress free boundary surface is minimized.

Under conditions of plane strain and material homogeneity, the symmetry of a deep circular opening enables the pattern to be typified by the study of one quadrant. However, if effects (a) and (b) above were to be included in the analysis, then the cross section is symmetrical about the vertical axis only. Moreover, unsymmetrical patterns develop about the horizontal axis, in terms of (a) stress distributions; (b) displacement distributions; (c) possible modes of failure.

Almost all of the analytical closed form solutions available for the analysis of ground-liner interaction were developed assuming ideally deep tunnels (see Chapter 4). Then, it would be of some use to be able to identify when a tunnel could be considered "deep", but a closer look into this apparently simple question reveals no simple answer. Depending on the parameter being investigated (stress or displacement at a certain location), on the criteria to define whether a tunnel is "deep" or not, and, possibly, on the type of analysis being conducted, the answer may vary considerably. In terms of the judging criteria, two possibilities could be considered: a) negligible effect of the free surface and b) negligible effect of the stress field gradient across the opening.

A number of investigators studied the problem and the result of a brief survey into the subject is summarized in

Table 2.1. The common assumptions used in these studies are indicated in the table. Among others, all analyses considered a linear elastic ground. Mindlin (1938, 1939) was one of the first to address the subject, studying the case of an unlined tunnel. Unlike previous investigators (Schmid, 1926, Yamaguti, 1929), who studied the problem of a mass of indefinite extent, subjected to gravity, Mindlin considered a half space limited by a horizontal stress free surface. Mindlin followed and corrected the approach given by Jeffrey (1920), who studied a similar problem for the case of zero body forces, with a plate subjected to uniform tension, parallel to its straight edge. By describing the system in bipolar co-ordinates Mindlin was able to calculate the stress around the opening, but made no attempt to calculate the corresponding strains. His solution was obtained by making use of an infinite series expansion. By comparing the tangential stress at the tunnel crown for the half space condition with that for the infinite plate under gravity action, Mindlin identified that for cover to diameter (H/D) ratios greater than 0.25, the effect of the free surface becomes negligible, provided the stress field ratio K is equal to unity (K is the ratio of lateral to vertical field stresses).

For a non hydrostatic stress field defined by $K=\nu/(1-\nu)$, Mindlin found that the threshold ratio H/D depends on the Poisson's ratio (ν). For ν of 0.5, the associated threshold is again equal to 0.25, as found in his

Authors	Analyses	Investigated Parameters	Source	Criteria	
				Negligible effect of the free surface at	Negligible effect of of the gravitational stress gradient at
Mindlin (1939)	Closed form solution of unlined tunnel	σ_θ at crown and K = 1	Author's equations 45 and 47 in limit (Fig. 5) compared	H/D > 0.25	Not assessed
		σ_θ at crown and K = v/(1-v) with v = 0.25	Author's equations 57 and 58 (Fig. 6) compared	H/D > 1.5	Not assessed
Ewoldsen (1968)	Mindlin's solution for unlined tunnel	σ_θ above crown (interior points)	Figures 5 and 6 of author's paper	H/D > 4	H/D > 50
Peck et.al. (1972)	Finite element, lined tunnel, non slip, K_0 = 0.5 and 2	Max. thrust, bending moments and diameter changes	Figures 10 and 11 of author's paper	H/D > 1	Not assessed
Ranken (1978)	Finite element, lined tunnel, full and non slip, K_0 = 0.5, fixed lin. stiff.	Thrusts, moments, diameter changes, radial displac. at crown, spring. and floor	Figures 4.2, 4.3, 4.5 and 4.6 of author's thesis	H/D > 1.5	H/D >> 5

Note: In all analyses, linear elastic, homogeneous, isotropic domain subject to gravity, circular opening, horizontal ground surface, plane strain condition and constant in situ K ratio (H = tunnel cover; D = tunnel diameter).

Table 2.1 Assessments of the Effects of the Presence of the Ground Surface and of the Gravitational Stress Gradient in Shallow Tunnels

first analysis. For ν of 0.25 (K=1/3), the analysis indicated that the effect of the free surface becomes imperceptible at H/D slightly greater than 1.5.

In both analyses, Mindlin was solely concerned with the effect of the proximity of the stress free boundary and made no attempt to assess the effect of the gravitational stress gradient.

Table 2.1 shows also the findings of Ewoldsen (1968), who carried out a parametric study by computer, using Mindlin's basic solution. Instead of inspecting only the tangential stress at the crown, as Mindlin did, Ewoldsen examined the stress at interior points within the ground mass above the crown. By removing, in an approximate way, the stress gradient effect from the solution, he showed that the presence of the free boundary surface is still discernible for values of H/D in excess of four. He also showed that the gravitational stress gradient is felt for cover to diameter ratios in the order of 50.

The inclusion of a lining in the opening highlights a special feature of shallow tunnel analysis. This refers to an overall uplift of the opening which is more pronounced when the lining is stiff. This trend to "float" is due to the fact that the resultant force generated by the excavation of the opening in a gravitational medium is vertical and upwards, being equal to $\pi\gamma D^2/4$ per unit length of tunnel. The corresponding upward movement is a consequence of the gravitational stress gradient. However, it depends also on the deformation properties of the ground and lining and it is affected by the presence of the stress free boundary. This feature is evident when performing elastic analyses where the creation of the opening and lining installation occur simultaneously. In real tunnels, this effect is partly or completely suppressed since the liner installation is delayed. The introduction of the lining gives rise to other parameters that can be used in judging criteria for defining shallow and ideally deep tunnels. These are the thrusts and bending moments developed within the liner.

Peck et.al., (1972) reported results of finite element analyses of lined tunnels, for initial stress ratios, K, of 0.5 and 2.0, and for variable H/D ratios. Examining the magnitudes of the maximum thrust in the lining, the bending moments at the springline and the invert, as well as the changes of the horizontal and vertical diameters of the lined opening, these authors suggested that, regardless of the stiffness of the lining with respect to that of the soil, the effect of the free boundary surface becomes negligible for H/D greater than 1.0.

A more detailed study was performed by Ranken (1978), using a similar approach. For a certain relative stiffness, for a lining installed at the moment of creation of the opening, and for K=0.5, Ranken concluded that the effect of the free surface on thrusts, bending moments, diameter changes and radial displacements in the lining, is neglible for all H/D ratios greater than 1.5. He also detected that the influence of the gravitational stress gradient across the opening, is greater than the influence of the ground surface boundary and remains at a significant level to a much greater depth (H/D>>5). Like Ewoldsen (1968), Ranken used an approximate scheme to assess the two effects separately. This was possible after realizing that the liner response at the springlines is less affected by the influence of the stress gradient across the opening (Ranken, 1978:108). Ranken also noticed that the threshold value of H/D depends slightly on the condition of the ground-lining interface, which he represented in his analysis by either full or non-slip.

The results presented so far permit one to conclude that the influence of gravity is not to be disregarded even for tunnels of appreciable depth (H/D>50). However, the effect of the free ground surface on stress, displacements, thrust and bending moments in the liner, can be considered negligible in a linear elastic analysis, for cover to diameter ratios greater than about 1.5. Although this is true when the pertinent parameters are taken at or near the opening perimeter, this conclusion may not be valid in terms of induced displacements away from the opening. Barrat and Tyler (1976) and Eisenstein et.al. (1981) presented case histories of tunnels driven in soil, with cover to diameter ratios of about 8 and 10, respectively. In both cases, appreciable displacements were recorded at the ground surface upon tunnelling, whereas beyond small distances (about 1D) below the invert elevation, no displacements were detected. Hence, even for fairly deep tunnels, the presence of the ground surface and the action of gravity make the displacement distributions above and below the tunnel highly non-symmetrical. Eisenstein et.al., (Op.cit) also showed that an asymmetric development of plastic zones around the opening was inferred from field observations of vertical and horizontal displacements. This again reflects both the influence of the ground surface and the action of gravity. It was not possible to single out the dominant factor that caused these asymmetric responses, but, as far as the displacements are concerned, one is tempted to believe that the proximity of the ground surface may have had a preponderant role.

A deep tunnel is occasionally defined as one in which the cover to the crown is sufficiently thick so that the effect of the displacements occurring at the opening are able to attenuate, making the surface settlements negligible. Although this definition may be correct for a tunnel in a linear elastic ground, it is misleading for real ground conditions, where non-elastic and time-dependent responses may develop. Imperceptible surface settlements could hypothetically be possible in a tunnel of small cover, if the excavation is through a soil with a highly dilatant response which may compensate the inward displacements of the opening. Conversely, it is possible to conceive a tunnel with a fairly thick cover of compressible soil, which is driven in such a way that the short term displacements are insignificant, but where time dependent effects (e.g. consolidation due to drainage towards the permeable opening) may finally induce signigicant surface settlements.

German authors frequently refer to "shallow" and "deep" tunnels. Possibly reflecting current practice in Germany, a design guideline for tunnels was prepared by a working group and was published by Duddeck (1980). A summary of these recommendations is presented by Heinz (1984). The distinction between shallow (H/D smaller than 2) and deep (greater than 3), according to Duddeck (Op.cit), reflects a concern with respect to the effect of the proximity of the ground surface. More than that, it expresses the need to identify the condition where the so called "partial embedding" assumption should be applied. According to this, the interaction between lining and soil in the upper 90° arch of the crown should be disregarded. In other words, the ground above tunnel crown should be taken as a "heavy fluid", able to transmit loads to the support, but unable to withstand any additional shear. As maintained by Duddeck (1980), this assumption would be applicable to shallow tunnels with limited overburden (cover to diameter ratio smaller than 2, according to Duddeck, Op.cit, or smaller than 2.5 according to Duddeck and Erdmann, 1982 and Erdmann and Duddeck, 1984). The German recommendations propose that, for H/D greater than 3 (or 2.5 according to Duddeck and

Erdmann, Op.cit and Erdmann and Duddeck, Op.cit), a complete embedding of the lining by the ground can be assumed, and a continuum model for interaction can be used. Moreover, Duddeck and Erdmann (1982) suggest that, in deeper tunnels, allowance could be make for some reduction of the primary in situ stress, as opposed to in shallow tunnels, where a full overburden condition should be assummed. A discussion of the merits and validity of these assumptions is given in other sections of this thesis. However, it should be anticipated that no field evidence has been found so far, supporting these highly consequential assumptions. The hypothesis of full overburden has the premise of a ground with no shearing resistance, which is clearly highly debatable. The assumption of no embedding in the crown region is also open to discussion. Wong (1986:34) defended it, by accepting the full development of two failure zones running upward from the tunnel, intercepting the ground surface, thus bounding a soil block free to move down, towards the opening. In other words, one would have to admit a complete collapse mechanism of the soil above the tunnel crown, in order to justify the German assumption of no embedding in that region. Although this is a possibility, it normally cannot be accepted in an urban tunnel, and therefore it has to be inspected in the design stage as an extreme condition and its risk of occurrence either minimized or eliminated. Moreover, it should not be taken as a routine hypothesis for engineering design. An involved discussion on the consideration of extreme conditions in geotechnical design is given by de Mello (1977), who also addresses the problem with respect to soil tunnelling practice (de Mello, 1981:212). Moreover, if it is the collapse mechanisms that justify the partial embedding assumption for a shallow tunnel, there is no justification to support the selection of the region where this condition prevails (crown). In fact, the observation of collapse mechanisms for plane-section tunnels in centrifuge tests carried out in Cambridge, U.K. (e.g. Mair, 1979) and plasticity solutions of this very problem (Davis et.al., 1980), demonstrate that depending on the geometry (H/D) and on the relative strength of the material, the critical failure mechanism varies. Accordingly, the partial embedding assumption would have to be extended not only to the crown 90° arch, but also to the springline.

Since a condition of total collapse is difficult to justify as a normal or "average" (de Mello and Sozio, 1983) design hypothesis, the assumption of "embedding absence" should more feasibly be replaced by that of a "weakened" or "softened embedding". Partial or localized failure could then be accounted for, assuming a proportionally reduced deformation modulus for the soil around the tunnel, as a function of the degree of shear strength mobilization. Additional comments on the above subject will be presented later in this Chapter and in Chapter 4.

In summing up, two conclusions emerge from the above discussion, bearing in mind that the underlying assumptions are highly idealized:

a. When studying the behaviour of the ground or lining responses strictly around the opening, the presence of the stress free boundary at the ground surface can be neglected for H/D greater than 1.5, but the influence of the gravitational stress gradient should always be taken into consideration in the design of urban tunnels.

b. When studying the displacement field around an urban tunnel or possible modes of collapse of the ground, the effect of the ground surface as well as the action of gravity should always be considered.

2.3 Soil Response to Tunnelling

2.3.1 Foreword

The following is a qualitative description of the expected response of the soil subjected to the effects of a tunnelling operation. Generally, in simple physical terms, this operation involves a) the removal of the soil within the cut profile, which produces an overall reduction in the stiffness of the ground mass; b) the reduction of the in situ stress around the opening (normal and shear stresses), causing stress changes throughout the ground mass which generate volumetric and shear strains and also pore water pressure changes; c) the change in the hydraulic boundary conditions which affects the dissipation of the excess pore water pressures, and the ground water seepage pattern.

The tunnelling operation also involves the inclusion of a support system, which interacts with the soil, further changing the ground stress and its stiffness. Attention here will be mainly given to the ground response, as the "design of a tunnel lining is not a structural problem but ground/structural problem, with the emphasis on 'ground'" (Kuesel, 1986). It will be assumed in this section that the tunnel is driven above the water table, with fully drained conditions. Later on, in Chapter 3, the role of the water table within the system will be discussed.

The ground reaction to the advance of the tunnel excavation involves stress transfer mechanisms, which are clearly three-dimensional. A two-dimensional representation may be a reasonable approximation at a sufficient distance from the advancing face. To simplify the analysis, a two-dimensional plane strain condition will be adopted initially. The implications associated with relaxing this assumption are discussed later.

2.3.2 Idealized Stress Changes

The stress changes induced by a stress free circular opening, in an infinite plane strain, homogeneous, isotropic elastic plate, subjected to uniform vertical (σ) and horizontal ($K\sigma$) normal external stresses, can be determined through Kirsch's (1898) solution. This is a zero body force solution that corresponds to an ideally deep tunnel. Let us assume that the radial (σ_r) and shear stress ($\tau_{r\theta}$) at all points around the perimeter of the opening, are proportionally reduced to a fixed fraction, Σ, of the original in situ stress (σ_{ro}, $\tau_{r\theta o}$). Hence, at the perimeter:

$$\sigma_r(\theta)= \Sigma\sigma_{ro}(\theta)$$

$$\tau_{r\theta}(\theta)= \Sigma\tau_{r\theta o}(\theta)$$

At the crown (or floor) and springline, the shear stresses are zero, and, therefore, the radial and tangential stresses are principal stresses. For these points, it is possible to show that, after reducing the in situ stresses around the perimeter by a uniform fraction (1-Σ), the principal stresses will be:

$$\sigma_{rc}= \Sigma.\sigma \qquad [2.1]$$

$$\sigma_{\theta c}= K\sigma + (1-\Sigma)(2K-1)\sigma \qquad [2.2]$$

for the crown, and:

$$\sigma_{rs}= \Sigma.K\sigma \qquad [2.3]$$

$$\sigma_{\theta s}= \sigma + (1-\Sigma)(2-K)\sigma \qquad [2.4]$$

for the springline.

If K=1, then:

$$\sigma_{rc}=\sigma_{rs}=\sigma_r=\Sigma\sigma$$

$$\sigma_{\theta c}=\sigma_{\theta s}=\sigma_\theta=2\sigma-\Sigma\sigma$$

The mean normal stress and the maximum shear stress at the crown and springline are:

$$\sigma_m=\sigma$$

$$\tau_{max}=(1-\Sigma)\sigma$$

The stress path corresponding to the reduction of the in situ stress is shown in Figure 2.1 as line 1-1. In this case, the stress changes of any point on the perimeter are described by a unique stress path.

If body forces due to gravity are now included, but still neglecting the effect of the stress free ground surface, the in situ principal stress at crown, springline and floor are:

$$\sigma_{rco}=\sigma_{\theta co}=\sigma-\gamma\frac{D}{2}$$

$$\sigma_{rco}=\sigma_{\theta so}=\sigma$$

$$\sigma_{rFo}=\sigma_{\theta Fo}=\sigma+\gamma\frac{D}{2}$$

respectively, where γ is the specific weight of the elastic material and D is the diameter of the opening. Mindlin's solution for a deep tunnel with gravity can furnish the magnitudes of the tangential stress at those points, for a hydrostatic state of in situ stress, after a complete release of these stresses at the opening (Mindlin, 1939:1132). For a Poisson's ratio of 0.5, the final tangential stresses at the crown, springline and floor, are:

$$\sigma_{\theta c}=2\sigma-\gamma\frac{D}{2} \qquad [2.5]$$

$$\sigma_{\theta s}=2\sigma \qquad [2.6]$$

$$\sigma_{\theta F}=2\sigma+\gamma\frac{D}{2} \qquad [2.7]$$

The final mean normal stresses and maximum shear stresses are:

$$\sigma_{mc}=\tau_{maxc}=\sigma-\gamma\frac{D}{4} \qquad [2.8]$$

$$\sigma_{ms}=\tau_{maxs}=\sigma \qquad [2.9]$$

$$\sigma_{mF}=\tau_{maxF}=\sigma+\gamma\frac{D}{4} \qquad [2.10]$$

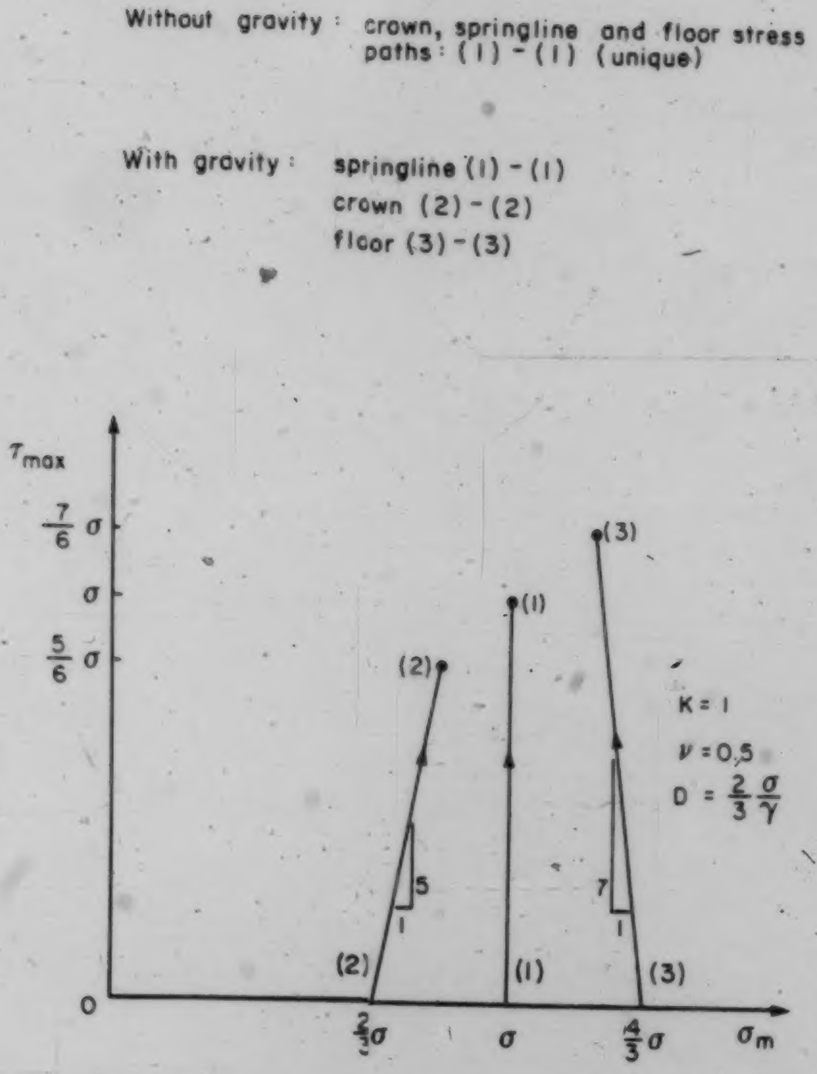

Figure 2.1 Effect of Gravity on the Elastic Stress Paths in a Deep Tunnel

Due to gravity, different elastic stress paths are identified for the crown, springline and floor (Figure 2.1). Gravity does not affect the stress path followed by the springline which exhibits a state of pure shear (no change in mean normal stress). Gravity causes a decrease in the maximum shear stress in the crown and an increase in the floor. With respect to the mean normal stress, an increase is observed in the crown and a decrease in the floor. Elastic volume changes are therefore expected to occur at the crown and floor.

The inclusion of the effect of the ground surface will further alter these stress paths. For K different from unity, some points at the opening will experience rotation of the principal stresses. The increase of shear stress in response to the stress release at the opening may cause yielding of the ground, making the stress path distort towards failure. Local failure of a soil element may eventually occur and, if further reduction of the stress at the opening is imposed, the stress path will travel down the failure line. Figure 2.2(a) illustrates this stress path for an element of soil at the opening springline, while figure 2.2(b) shows schematically the changes in stresses at interior points in the ground. This progressive stress transfer process, where the shear strength of the ground is increasingly mobilized upon the continuous reduction of the internal stresses at the opening, is the "arching" mechanism. Clearly, this mechanism is not confined to a two-dimensional stress redistribution. Upon advance of the tunnel face, a three-dimensional arching process develops, as will be seen later. Tunnelling operations which make use of "good ground control", tend to inhibit soil failure. It will be seen that the portion CD or CE of the stress path shown in Figure 2.2(a) may involve highly detrimental consequences, which are normally not acceptable when tunnelling in urban areas. In such areas, good quality construction will tend to confine the stress path to the portion AC. In practice, the means to ensure this include, for example, the following: (a) the use of "earth pressure balance" techniques, where compressed air or bentonite slurry minimizes the stress release at the opening; (b) the use of favourable sequences of excavation and of support installation (which also controls the amount of stress release at the opening); (c) the use of continuous or discontinuous fore-polings and long spiles (which, again, attempt to reduce the stress release); (d) the practice of promptly filling or grouting the void behind the lining, or of expanding the latter against the excavated profile (to avoid full stress release at the opening or even to increase the stress at the perimeter); (e) the use of ground treatment prior to the excavation (which does not control the stress changes, but favourably changes the failure envelope of the soil).

For conditions different than those which have been asssumed, different stress path responses will be found for

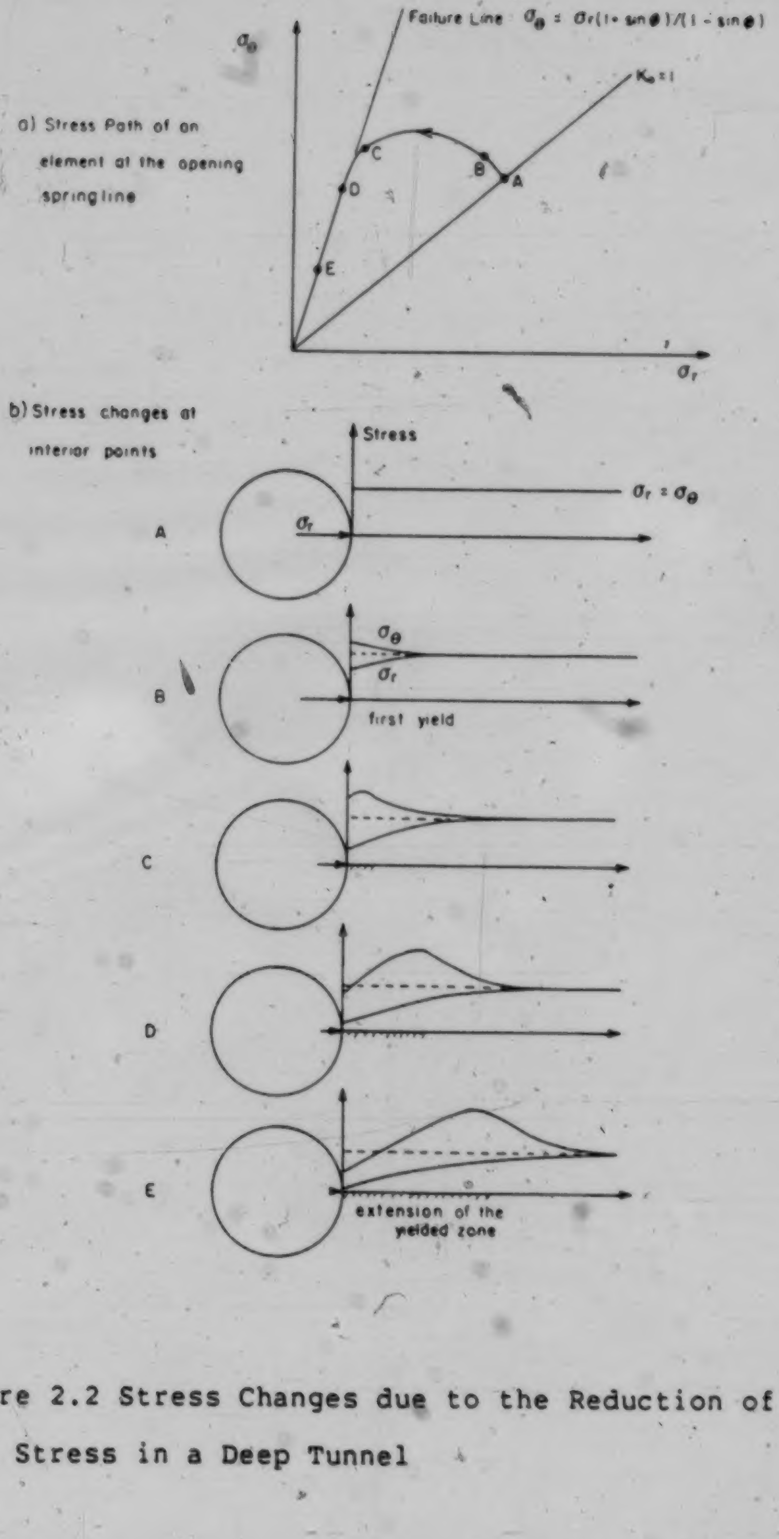
Failure Line $\sigma_\theta = \sigma_r(1+\sin\phi)/(1-\sin\phi)$
σ_θ
$K_o = 1$
a) Stress Path of an element at the opening springline
A
B
C
D
E
σ_r
b) Stress changes at interior points
Stress
$\sigma_r = \sigma_\theta$
σ_r
σ_θ
σ_r
first yield
extension of the yielded zone

Figure 2.2 Stress Changes due to the Reduction of the In Situ Stress in a Deep Tunnel

different points around the opening. It has been shown that gravity as well as the existence of the ground surface affects the stress changes. Moreover, if K is different from unity, some points around the tunnel may reach failure sooner than others.

2.3.3 Idealized Strain Changes

The stress path shown in Figure 2.2 has been replotted in Figure 2.3a. Assume that it represents the response of an ideally deep tunnel operation in a lightly overconsolidated soil, showing negligible cohesive strength under a hydrostatic in situ stress condition. We shall retain the assumption of full drainage occurring as the stresses at the opening are reduced. We shall also admit that this soil, has its "stiffness" (be it a "current" Young's modulus or a shear modulus) dependent on the mean normal stress and on the degree of shear mobilization. Also, we shall admit that upon failure, no appreciable reduction in friction angle is observed. These assumptions were already underlaid but not explicitly formulated, when the changes in stress shown in Figure 2.2 were discussed. The following is a discussion of the strain changes that will likely occur in a soil element P, adjacent to the opening.

As the idealized gradual excavation takes place, the radial stress σ_r is steadily reduced. From A to B, (Figure 2.3a) the ground response is nearly linear elastic and the tangential stress, σ_θ, increases proportionally to

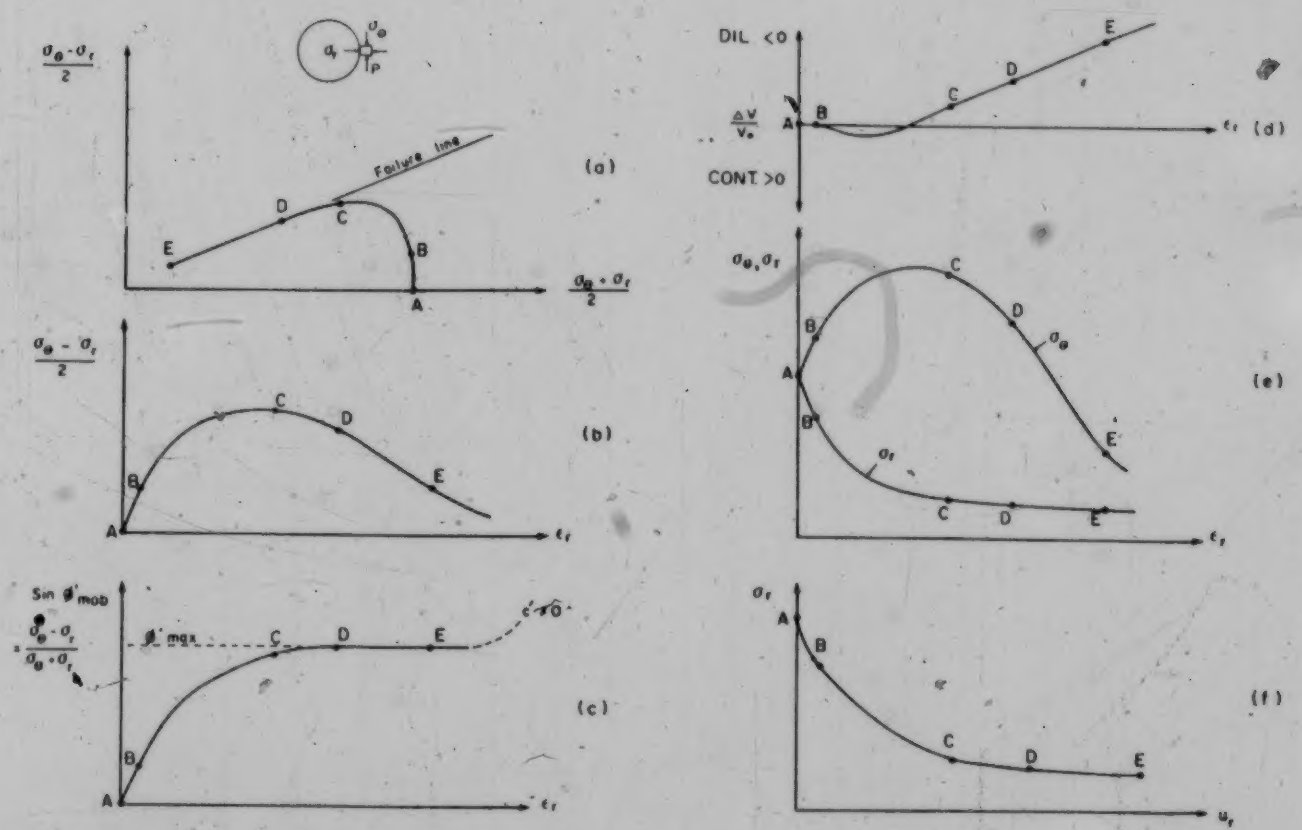
$\frac{\sigma_\theta - \sigma_r}{2}$
σ_r
σ_θ
P
Failure line
E
D
C
B
A
$\frac{\sigma_\theta + \sigma_r}{2}$
(a)
$\frac{\sigma_\theta - \sigma_r}{2}$
A
B
C
D
E
ϵ_r
(b)
Sin ϕ'_{mob}
$= \frac{\sigma_\theta - \sigma_r}{\sigma_\theta + \sigma_r}$
ϕ' max
A
B
C
D
E
$c' \neq 0$
ϵ_r
(c)
DIL <0
$\frac{\Delta V}{V_0}$
CONT >0
A
B
C
D
E
ϵ_r
(d)
σ_θ, σ_r
A
B
C
D
E
σ_θ
σ_r
B
C
D
E
ϵ_r
(e)
σ_r
A
B
C
D
E
u_r
(f)

Figure 2.3 Stress and Strain Changes Around a Tunnel

the decrease in σ_r. The radial strain, ϵ_r, increases almost linearly (Figure 2.3b). At B some yield develops and σ_θ ceases to increase at the same rate as σ_r decreases. The stress path shows a more pronounced non-linear shape as does the stress-strain response (Figure 2.3b). Around point C, the maximum shear stress peaks and failure is attained soon after[2]. Failure is achieved with the mean normal stress reducing faster than the increase in shear. As a result, the maximum shear stress after point C starts to drop. Thereafter, the shear stress-radial strain curve (Figure 2.3b) starts showing a conspicuous downwards trend resembling a "strain-softening" response. A closer inspection, of course, reveals no "actual" strain softening since it is assumed that no reduction in friction angle occurs after failure. In fact, if the stress obliquity (the ratio of maximum shear stress to mean normal stress) is plotted against radial strain (Figure 2.3c), no actual "strain-softening" is revealed as expected. As the stress path travels down along the failure line (portion CDE in Figure 2.3a), the friction angle is fully mobilized and the stress obliquity (Figure 2.3c) remains fairly constant, provided the cohesive component of strength (c') is very small or zero. If this is not the case, the stress obliquity increases rapidly as the radial stress is reduced to zero, with the soil then experiencing a tensile type of failure (dotted line in Figure 2.3c).

---

[2] Clearly, this is a local failure condition of the soil element adjacent to the opening and it does not necessarily mean that the whole structure is at a collapse state. If this element at failure, is part of an overall stable system, then, additional unloading may alter the state of stress in the element and so cause finite increments of strains (Atkinson, 1981:59-61)

The associated specific volume changes experienced by the soil element are shown in Figure 2.3d. Typically, in the nearly elastic portion AB of the loading process, near zero volume changes occur, as pure shear develops. Depending on the type of response of a particular soil upon yielding (stress level and history), it may show a small decrease in volume, which is soon compensated by a more pronounced trend of the soil to swell, associated with the faster reduction in mean normal stress (portion BC in Figure 2.3d). From C to E both shear strains and dilatancy will develop, their magnitudes dependent on a number of factors.

Figure 2.3e gives the relationships between tangential and radial stresses and radial strain in the soil element. While the changes in radial stress and strain display a continuous and monotonic evolution, the tangential stress presents a reverse trend after peaking around point C. In order to comply with the failure criteria, the tangential stress has to be reduced. This stress reduction results in an overall stress redistribution in the soil mass that causes stresses to be transferred to neighbouring soil elements, that may also be brought to failure.

At this point it is worth mentioning the differences between localized failure and tunnel collapse. As already pointed out, around point C in Figure 2.3, the maximum shear stress is peaked and failure is achieved in the soil element under consideration. Provided no mechanism is created, the failed soil element will remain in place. Also by virtue of the previously mentioned stress transfer process, adjoining soil elements will be further sheared and the failure zone will propagate into the ground. Gravity will control this propagation, and it will also be affected by the presence of the ground surface. Eventually, the zones of high shear strain will create a mechanism, and the complete collapse of the ground into the opening will become possible. Tunnels in cohesionless soils such as that depicted in Figure 2.3 would reach a collapse state at points D or E with a non-zero compressive radial stress. For a given soil, the ratio H/D will regulate the distance between local failure and collapse stress states. Shallower tunnels would reach collapse at point D, closer to C and deeper tunnels at E. It is worth stressing that for a number of soils, first yield will occur at B, well before local failure is achieved. It is also important to mention that as the local failure condition is attained, both the local straining and associated displacements of the ground go uncontrolled. The risk of experiencing large settlement at the surface increases. This is why good tunnelling practice should lead to stress changes confined to within zone AC, recognizing, however, that some limited amount of yield will develop.

The radial displacement at a point in the opening, is the result of summing the radial strains from that point to the limits of the ground mass. The displacement then reflects the combined response of points close to the tunnel and away from it. One would end up with a curve like the one shown in Figure 2.3f, that relates the reduction in the radial stress with the development of radial displacement at a particular point of the tunnel wall. In a more general case, shear stresses will also be present at the tunnel wall and the idealized tunnelling operation causes a reduction in these as well. As already assumed earlier in this section, the rate of stress decrease at the tunnel wall, is the same for both radial (or normal) stress and shear stress. The ratio between shear and normal stresses acting on the wall of the plane strain opening will be constant. The magnitude of the ratio will vary from point to point depending on the in situ K_0 value. Therefore, the curve shown in Figure 2.3f will also reflect the shear stress removal upon tunnelling. It should be recalled that this curve has been obtained on the assumption that each point of the opening wall has its in situ stress reduced in decrements to a constant fraction $(1-\Sigma)$ of its original value. This curve has been referred to as a "Ground Reaction Curve", as "Convergence Curve" or a "Characteristic Line". It reveals a fact that has been long recognized: the existence of the interconnection between the magnitude of the convergence of the tunnel walls and the magnitude of the loads ultimately carried by the support system.

So far the action of the support has been intentionally put aside, since it is the topic of discussion later in this chapter. However, its role and effect on the ground response should not be forgotten. Besides restraining the amount of stress release at the opening, it may alter the stress and strain patterns shown in Figure 2.3. In general, the inclusion of an element of a different stiffness will alter the load transfer mechanisms, the development of volumetric and shear strains, as well as the so called ground reaction curve.

The soil behaviour depicted in Figure 2.3 includes a number of features that resemble those of a real soil even though a number of simplifying assumptions had to be made. But even with these simplifications, not much data is available on the behaviour of fully drained soils loaded along the stress path given in Figure 2.3a. Some preliminary test results, using the Bishop and Wesley (1975) stress path apparatus and following a loading sequence similar to that discussed, have been presented by Burland and Fourie (1985). Material tested included undisturbed and reconstituted overconsolidated London Clay, and clay samples from the Claygate Beds in Bell Common, Essex, U.K. (Hubbard et.al., 1984). Their investigation referred to the behaviour of elements of soil located underneath the bottom of an open cut retained excavation, entailing stress release under conditions of limiting passive equilibrium. This stress path - termed "passive stress relief" by the authors - has similarities to that experienced around a tunnel. The results they have obtained confirm to some extent, the overall response that has been speculated here. The special feature presented in Figures 2.3b and c regarding the "softening" behaviour associated with the "unloading" boundary condition, has been recognized by Potts and Burland (1983) while performing a type "A" prediction (Lambe, 1973) of the retained excavation mentioned above. The addition of factors, such as the non-hydrostatic state of in situ stress, the action of gravity and of the free ground surface, the influence of support installation, the nature (and stress history) of the soil, etc. to the conceptual analysis just presented, may make the analysis even more intricate. Evidently, the detailed soil response will differ from what has been shown, but broad behaviour trends can be drawn, adopting the same type of reasoning. When all factors pertaining to a shallow tunnel are at play, two simple facts emerge. Firstly, the ground response will be clearly dissimilar for different points around the opening perimeter. No unique response will be observed at soil elements around the perimeter of a given shallow tunnel. Secondly, an obvious non-linear response will be experienced in terms of the stress-strain behaviour.

Normally consolidated and even lightly overconsolidated soils, as well as most granular non-cohesive soils undergo yielding after relatively small stress changes and their response is typically non-linear. Seneviratne (1979) carried out some plane strain drained model tests of shallow circular tunnels (H/D between 0.5 and 0.95), in normally consolidated spetstone Kaolin. By reducing the internal tunnel pressure and monitoring the ground mass displacements through radiographic techniques, Seneviratne was able to obtain ground reaction curves such as that shown in Figure 2.3f. His results suggest that these curves ceased to show a linear pattern after less than a 10% reduction of the initial tunnel pressure (Seneviratne, Op.cit., Figure 4.10.b). For these tests, it is customary to define a "load factor" (see Atkinson and Potts, 1977). as:

$$LF=\frac{\sigma_o-\sigma_i}{\sigma_o-\sigma_c} \qquad [2.11]$$

where σ_o is the initial vertical stress at the tunnel axis, σ_i is the current tunnel pressure (uniform in a model test), and σ_c is the tunnel pressure at collapse. This factor, as defined, may be understood as the reciprocal of a factor of safety (FS) against global collapse of the structure. Seneviratne's results show departure from a linear response at load factors between 0.4 and 0.5 (i.e. factors of safety between 2 and 2.5). Results from similar tests in overconsolidated kaolin (Cairncross, 1973 and Orr, 1976), as well as in loose and dense sand (Potts, 1976), were conducted in Cambridge and were presented by Atkinson and Potts (1976), Atkinson et.al., (1975) and Orr et.al., (1978). Again, it is revealed that, in terms of the ground reaction curves for the tunnel crown, non-linearity is observed at load factors higher than 0.33 to 0.5 (or factors of safety smaller than 2 to 3).

It is also customary to express a ratio called "overload factor" as:

$$OF=\frac{\sigma_o-\sigma_i}{c_u} \qquad [2.12]$$

where σ_o and σ_i have the same meaning as before and c_u is the undrained shear strength of the soil.

For purely cohesive soils, Davis et.al. (1980), were able to bound fairly closely the exact tunnel collapse pressure (σ_c). This pressure is given by:

$$\sigma_o-\sigma_c=Nc_u \qquad [2.13]$$

where N is the overload factor at collapse (also called the stability ratio). N is a function of the relative tunnel cover (H/D) and of the ratio $\gamma D/c_u$, where γ is the specific weight of the soil and D is the tunnel diameter. For a 4m diameter tunnel, driven 20 m below the surface in a stiff overconsolidated soil (for example, London Clay) with an undrained strength of 200 kPa, the ratio $\gamma D/c_u$ is smaller than 0.4. For all practical purposes, this ratio may be taken as zero. For this condition, Davis et.al., (Op.cit., Figure 13), furnish values for N ranging from 5 to 6 (lower and upper bound), for H/D of 5. Therefore, under these circumstances, the tunnel collapse pressure would be given by:

$$\sigma_o-\sigma_c=(5\text{ to }6).c_u$$

Judging from field observations of tunnels built in London Clay, (approximately 4 m diameter and H approximately 20 m), Ward (1969) noted that, if the overload factor, OF, is less than 2, then the short term ground response is elastic (Ward, Op.cit.:321). This was confirmed by Attewell and Farmer's (1974:391) observations regarding the Green Park tunnel in London Clay. Combining equations 2.11 and 2.13, one finds:-

$$FS=\frac{1}{LF}=\frac{N}{OF} \qquad [2.14]$$

For N = 5 to 6 and OF = 2, the ratio N/OF can be understood as a minimum factor of safety (FS) below which a non linear ground response would predominate. Thus, for London Clay, the factor of safety would range between 2.5 and 3.0. Similar reasoning was used by Morgenstern and Eisenstein (1970) to investigate the limits of applicability of linear elastic theories to open cut excavations. They found a limiting factor of safety against undrained base failure of 1.5 to 2.0, above which a linear response would be expected.

Hence, from model test results and from field observations of shallow tunnels, it could be said that non-linear ground response is to be expected whenever the factor of safety against collapse is less than 2 to 3.

Unlike foundations, which are designed with factors of safety sometimes in excess of 3, shallow tunnels are built with factors of safety much lower than this. It will be seen later in this thesis, that tunnels are built frequently with factors of safety of around 1.5 or less, after equilibrium with the support is achieved. Current construction techniques allow releases exceeding 20 to 30% of the original in situ stress. Tunnelling operations tend to bring about collapse of the ground much sooner than other geotechnical constructions. This is partly due to the stress changes the soil is forced to withstand upon tunnelling. As it was shown, a typical stress path for soil elements around a tunnel combines stress changes of a conventional laboratory extension test (in the radial direction of the opening) with those of a traditional compression test (in the tangential direction). This leads to a shorter path to soil failure. For non-hydrostatic in situ stress conditions, those points around the plane strain tunnel, which do not undergo rotation of principal stresses, exhibit an even faster path to failure (e.g., points located at the springline, for K_o smaller than unity). Soil structures undergoing appreciable yielding or exhibiting low factors of safety show non-linear responses (Morgenstern, 1975). The unavoidable stress release associated with tunnelling operations and the lower factors of safety found for this type of geotechnical structure, lead to conditions where the soil response will be predominantly non-linear.

2.3.4 Stress and Strain Changes Under Less Idealized Conditions

2.3.4.1 Stress Paths

The assumptions of plane strain and fully drained conditions are maintained, but now the effects of gravity, the free ground surface and a non-hydrostatic in situ stress condition are considered. It will be seen that tunnelling operations entailing a proportional and gradual reduction of the in situ stresses at the opening will cause a more complex ground response.

For these conditions and also to account for the non-linear stress-strain behaviour of the soil, one needs a numerical procedure, such as the finite element method, in order to obtain the stress paths of points around the opening. Using the non-linear hyperbolic elastic model described by Eisenstein and Negro (1985), (further discussed in Chapter 5), it was possible to obtain the paths shown in Figure 2.4. Clearly, other constitutive models would provide slightly different pictures but the overall response would be fairly close to that which is shown in the figure. Details of the finite element code employed (using constant strain triangles), as well as the tunnelling simulation procedure will be given elsewhere in this thesis. The plane strain circular opening was subjected to a gradual reduction of the orginal in situ stress, with no support being installed. This was done incrementally, each stress (normal and shear) decrement amounting to 10% of the initial stress magnitude at each point of the tunnel perimeter, through an "incremental stress reversal boundary condition." The tunnel had a diameter of 4 m and a cover to diameter ratio of 1.5. The soil layer was assumed to be isotropic and homogeneous. In situ stresses were calculated for K_o equal to 0.8. The selected soil properties would be typical of a lightly overconsolidated deposit, with zero cohesive strength and a friction angle of 30°. The groundwater level was assumed to lie far below the tunnel floor, so that fully drained conditions prevailed. A constant Poisson's ratio was assigned to the soil and a pair of Janbu's (1963) coefficients, K and n, were selected in such a way that a constant tangent modulus of deformation of about 31 MPa, before tunnel excavation, was obtained. Upon each applied stress decrement, this modulus was updated as a function of the normal stress level (defined in terms of the minimum principal stress in the plane) and of the shear stress level (defined in terms of the maximum principal stress difference in the plane) relative to the shear stress at failure. Certainly, this representation is a rough approximation of the actual soil behaviour, since no account is taken of the real plastic phenomenon associated with yielding (Morgenstern, 1975). The latter is represented here in so far as the non-linear elastic modulus of the soil changes as a function of the normal and shear stress levels. The simplicity of such a numerical model and the fact that it is reported to be used fairly successfully in practice (Christian, 1980), make it attractive for the present purpose. This is so, despite the fact that in its standard formulation the input parameters are obtained from laboratory tests following stress paths that are not related to those actually observed in the soil mass surrounding the opening.

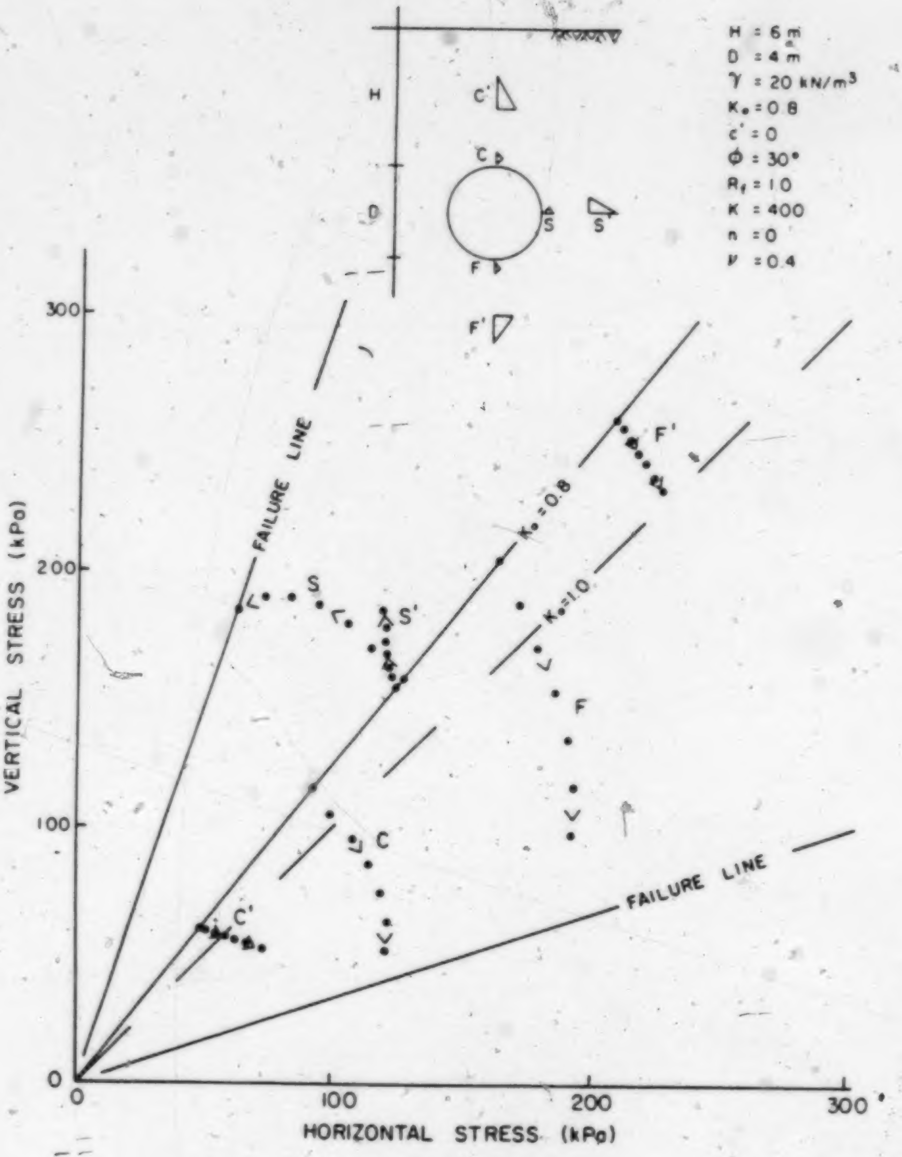

Figure 2.4 Stress Paths Around a Shallow Tunnel

Figure 2.4 shows the stress paths obtained for points C, S and F, at the crown, springline and floor, respectively, (elements located 0.25 m away from the cut profile) and for points C', S' and F', (elements at 3.0 m from tunnel wall at C' and F', and 2.5 m at S'). Although they are not principal stresses (except initially), the vertical and horizontal stresses were plotted in order to make the evaluation easier. Since the selected points are close to either the vertical or horizontal axis through the tunnel centre, both vertical and horizontal stresses have magnitudes very close to maximum and minimum stresses within the plane (less than 5% difference).

Each point of the stress paths represents the state of stress after each decrement of the in situ stress. Point "0" corresponds to the in situ condition and "6" to the final condition, at which a certain element of the finite element mesh reaches local failure. As the numerical model used has not been designed for simulation of failure control conditions, the stress paths shown represent stress changes before failure.

The paths followed at S, C and F are not dissimilar to those depicted in Figures 2.2 and 2.3. It is observed, however, that because K_0 is different from unity, the principal stresses rotate at C and F between the first and second stress decrement, with no rotation observed at S. As a result, S goes faster towards failure, and this is attained after decrement number 6, before any other point fails. Different behaviours would be noted depending on the in situ stress, geometry and ground properties, and different points may reach failure singly or simultaneously. If the soil strength was high and had a large cohesion intercept, the stress paths at C, S and F would end at the zero radial stress level with no failure being observed.

Although the magnitudes of the stress changes for points at farther locations from the opening are much smaller than at points closer to the tunnel, they will experience quite distinctive stress paths. At C', the changes in the vertical stress are smaller than in the horizontal stress. The stress path resembles that of a vertical extension laboratory test, under horizontal passive loading (passive extension test). At S', the stress path is similar to that of a conventional passive compression test, whereas at F', the path is close to that of constant mean normal stress with almost pure shear loading. Certainly, as the tunnel undergoes further unloading, these stress paths may also distort towards failure, in a similar way to C, S and F. However, they may be affected by the development of highly sheared zones or discontinuties in anticipation of the tunnel collapse.

Seneviratne (1979) and Karshenas (1979) carried out similar analyses, in an attempt to identify the drained stress paths at points around plane strain model tests. These were conducted in normally consolidated kaolin and in dense sand. In both cases, modified versions of the Cam-clay model were used. Test simulation included the effects of sample preparation and tunnel cutting. Examining the portions of the stress paths that correspond solely to the tunnel unloading (Seneviratne, Op.cit:Figure 6.12a, Karshenas, Op.cit:Figure 6.19 to 6.21), very similar pictures emerge. Despite the use of different constitutive models, their results agree quite well to what has been described herein. Seneviratne also performed undrained finite element analysis and noted that the total undrained stress paths are similar to the total drained stress paths, even though they pass through different points in the stress space (Seneviratne, Op.cit. Figure 6.12b).

Ng and Lo (1985) were also able to draw effective stress paths from an elastoplastic undrained finite element analysis of a shallow tunnel under plane strain conditions. Details of the finite element formulation, which takes into account an anisotropic elastic behaviour and a non-associated flow rule for plastic response and assumes a Mohr-Coulomb failure criterion, are given by Rowe et.al., (1983) and Ng (1984). Once more the stress paths are found to be very similar to those presented here. Ng and Lo go further in an attempt to identify which standard laboratory tests would better represent the stress paths they obtained numerically. They suggest that for a soil element at the crown, the effective stress path of an undrained or drained anisotropically consolidated extension test with axial stress decreasing would be similar to that obtained in the numerical analysis. This is clearly a simplification and moreover, for other soil elements, no conventional triaxial stress paths are representative of the numerically obtained stress paths. These authors then suggest that "extreme" stress path tests bounding the "real" stress paths, should be conducted to evaluate stress path dependency of the ground.

Capellari and Ottaviani (1982) also used a non-linear elastic hyperbolic formulation to obtain representative plane strain stress paths around a shallow tunnel. They attempted to map the predominant stress paths around the opening. Their results are consistent with what has been shown here, although the division of the surrounding soil into just three stress path areas could be considered as an oversimplification. An accurate mapping would reveal a larger number of typical stress path areas.

Although the development of controlled stress path triaxial testing (Bishop and ~~Wesley~~, 1975), using only servo mechanisms to ensure the follow up of a predefined stress path (Menzies et.al., 1977), enlarged testing capabilities, it seems to be quite an unlikely venture to actually follow all stress path possibilities around a shallow tunnel. Furthermore, the three-dimensional stress changes occurring in the soil, the unavoidable disturbances associated with sampling, the behaviour of soils under small strains, etc, pose additional difficulties which are possibly as relevant as the stress path dependency. So, except in very special cases, a large degree of simplification will have to be taken in approaching a practical tunnelling problem. These factors and points will be further discussed in this thesis.

2.3.4.2 Ground Reaction Curves

The finite element analysis performed to obtain the stress paths depicted in Figure 2.4 can also furnish relationships between the radial stress and displacements, for different points around the tunnel perimeter. Figure 2.5 presents ground reaction curves thus obtained for points at tunnel crown (C), springline (S) and floor (F), which are typical for a shallow tunnel. As noted before, no unique response is observed around the perimeter, even for the case of a hydrostatic in situ stress state (see also Eisenstein, 1982 and Eisenstein and Negro, 1985). This clearly precludes any attempt to use the so called "Convergence Confinement" Method (Gesta et.al., 1980), that in its original formulation is strictly valid for ideally deep tunnels under $K_0=1$ conditions. The original concept of the ground reaction curve has been extended to account for a non-hydrostatic initial stress field for elastoplastic materials with a Mohr-Coulomb yield criteria (Detournay and Fairhurst, 1982), but the account of gravity and of the free ground surface effects have only been incorporated in an approximate form (for example; Daemen, 1975, Hoek and Brown, 1980:252). For a hydrostatic in situ stress condition, Wong (1986) used Daemen's simplified approach to include the gravity within the plastic zone only. He relaxed Daemen's original

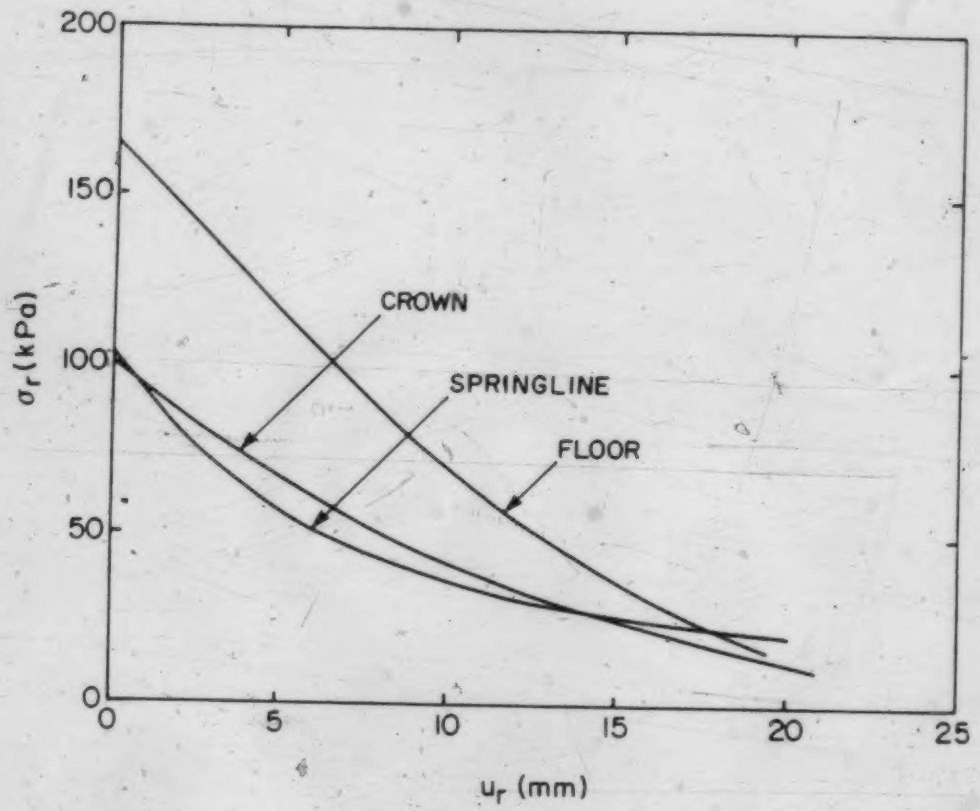

Figure 2.5 Ground Reaction Curves for a Shallow Tunnel

assumption of zero plastic volumetric strain by indroducing Ladanyi's (1974) average plastic volume strain and thereafter followed the approach of the latter author. He claimed (Wong, Op.cit, p.38) to have also included the effect of the free surface, but his derivation shows otherwise since he assumed a plastic zone of constant radius around the circular tunnel (Op.cit, p.39 and 41). This is in conflict with the development of a non-uniform plastic zone which occurs when the effects of gravity and of the free ground surface are correctly taken into consideration. In brief, Wong's formulation for ground reaction curves is another approximate solution, furnishing good results for an ideally deep tunnel, but with limited practical interest for a shallow tunnel, in view of its inherent limitations (Wong, Op.cit, p.41,42).

Numerical techniques seem to be the only effective means currently available to allow representation of stress-displacement relationships for points around shallow tunnels. It seems unlikely that any closed form solution will ever account for the stress and strain changes illustrated in Figure 2.3, and also include other relevant features of a shallow tunnel in soil. Even finite element codes are not always able to treat in a satisfying way, the boundary value problem involving the pseudo strain softening behaviour at decreasing stress levels, as is the case shown in Figure 2.3b. But if interest is limited to pre-failure conditions, the finite element method can be used to extend the original concept of ground reaction curves, as suggested by Lombardi (1980:254), Duddeck (1980:247), Eisenstein (1982) and Eisenstein et.al.,(1984). The stress-displacement curves thus obtained would then be an end result of some ~~fairly~~ realistic stress-strain changes developing in the ground, and would reflect the influence of dominant features controlling the shallow tunnel response under less idealized boundary conditions.

2.3.4.3 Shear Strain Development

The development of shear strains around a plane strain shallow tunnel upon gradual unloading can be examined by numerical techniques, model testing and field observations. Preceding tunnel collapse, the growth of high shear strain zones are frequently observed. The difficulties associated with the numerical simulation of localized deformations are recognized and these are being the subject of ongoing studies. If the evolution of these strains up to tunnel collapse is a matter of interest, then it seems more instructive to examine observations made on models or prototypes.

Table 2.2 summarizes some observations made in plane strain model tests in Cambridge (UK) with soil displacements monitored by means of radiographic or photographic imagery. It also includes data derived from field instrumentation of two tunnels. Despite the fact that shear strain distributions for undrained conditions are very similar to those under drained conditions (Seneviratne, 1979:63), the

Case	Author	Data From	Soil	C_u (kPa)	ϕ' (°)	E_0 (MPa)	K_0	D (mm)	H/D	$\sigma_0^{(1)}$ (kPa)	$\sigma_c^{(2)}$ (kPa)	LF (3) and (FS)	$u^{(4)}$ (mm)	$U^{(5)}$	Max. Shear Strain (%)	Shear Strain Contours (%)
1 (D2)	Seneviratne (1979)	static model	n.c. kaolin	26	20	6	0.64	60	0.67	138	76.1	0.67 (1.49)	1.9	1.38	8	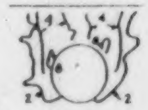
2 (D3)	Seneviratne (1979)	static model	n.c. kaolin	26	20	6	0.64	60	0.95	138	51.7	0.96 (1.04)	5.5	3.99	24	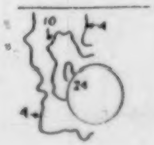
3 (D4)	Cairncross (1973) (quoted by Atkinson, et al, 1975)	static model	o.c. kaolin (OCR = 3.5)	~60 (7)	15.4 (8)	13 (9)	~10	60	1.20	140	0	0.81 (1.24)	2.0 (10)	3.10	4	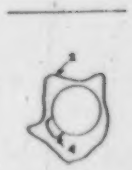
												0.95 (1.05)	0.60 (10)	13.30	20	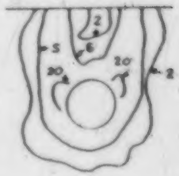

Table 2.2 Shear Strain Distributions Observed in Model Tests and in Actual Tunnels in Drained Conditions

Case	Author	Data From	Soil	c_u (kPa)	ϕ (°)	E_0 (MPa)	K_0	D (mm)	H/D	$\sigma_0^{(1)}$ (kPa)	$\sigma_c^{(2)}$ (kPa)	LF (3) and (FS)	$u^{(4)}$ (mm)	$\Delta U^{(5)}$	Max. Shear Strain (%)	Shear Strain Contours (%)
4	Orr (1976) (quoted by Orr et al 1978)	static model	o.c. kaolin (OCR = 3.9)	~66 (7)	15.4	13 (9)	~1.0	60	0.35	140	67	0.60 (1.67)	0.34 (10)	0.53	2	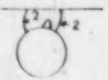
												0.90 (1.11)	1.45 (10)	2.24	4	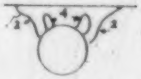
5 (D5)	Potts (1976) (quoted by Karshenas, 1979)	static model	dense sand (e_0 = 0.52)	-	~50	110 (11)	1.0	60	1.0	210	6	~10 (1.0)	0.84	7.33	3	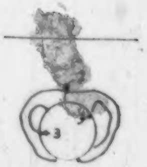
6 (D6)	Potts (1976) (quoted by Karshenas, 1979)	static model	dense sand (e_0 = 0.52)	-	~50	110 (11)	1.0	60	0.5	210	7	~1.0 (1.0)	1.71	14.88	8-10	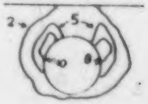
7 (D7)	Atkinson and Potts (1977)	static model (self weight)	dense sand (e_0 = 0.52)	-	~50	-	0.2(?)	60	1.48	2	0.007	0.96 (1.04)	3.0	?	20	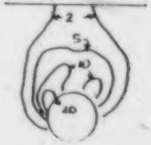

Table 2.2 Continued

Case	Author	Data From	Soil	C_u (kPa)	ϕ' (°)	E_0 (MPa)	K_0	D (mm)	H/D	$\sigma_0^{(1)}$ (kPa)	$\sigma_c^{(2)}$ (kPa)	LF $^{(3)}$ and (FS)	$u^{(4)}$ (mm)	$U^{(5)}$	Max. Shear Strain (%)	Shear Strain Contours (%)
8	Atkinson and Potts (1977) Atkinson, Potts and Schofield (1977)	centrifuge model	dense sand (e_0 = 0.52)	-	~50	-	0.2(7)	60	1.48	~180	-	~1.0 (1.0)	-	-	10	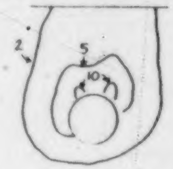
9	Atkinson, Brown and Potts (1977)	static model (self weight)	loose sand (e_0 = 0.69)	-	42°	-	0.3(7)	60	1.48	1.8	0.010	0.91 (1.10)	3.3	-	10	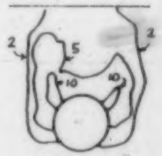
10	Hansmire (1975)	Washington Metro (C-Line)	tunnel mainly in dense sand, cover of stiff to medium clay	-	35°(7)	35(7)	0.5(7)	6,450	1.81	~300	-	-	~330	~7.8	15	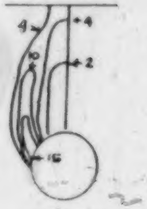
11	El-Nahhas (1980)	Edmonton sewer tunnel	"soft" till	70	16°	15	0.8	2,560	9.3	~480	-	-	~50	~0.6	>2	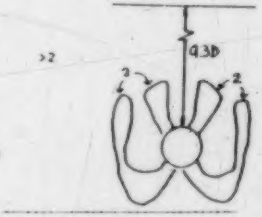

Notes:
(1) Initial vertical stress at tunnel axis
(2) Uniform tunnel pressure at collapse
(3) Load factor and factor of safety
(4) "Crown" settlement at a given LF or FS; in model tests this displacement is taken at a point D/10 above tunnel crown
(5) Dimensionless crown displacement
(6) Maximum Observed
(7) Acc. to Nadarajah (1973) data
(8) Acc. to Sketchley (1973) data
(9) Acc to Orr et al (1978), page 136
(10) Assuming zero displacement at the floor
(11) From Karshenas (1979), p. 168-9

Table 2.2 Continued

table includes only data believed to represent predominantly drained behaviour.

Except for case 8 the tests were performed under static conditions, with the models subjected to uniform vertical surface loads, as well as uniform lateral loads. Shear strain distributions at low load factors (LF smaller than 0.5) or high factors of safety, are difficult to obtain as the observed displacements (from which strains are derived, using approximate techniques) are small. Therefore, the recorded distributions represent mainly pre-collapse conditions (LF greater than 0.6 to 0.7). It is seen that the shear strain distribution under these conditions is mainly controlled by the presence of the free boundary surface. Indeed, in cases 1 to 7, the gravitational stress gradient can be neglected, as the self-weight stress in the model material is negligible in comparison to the imposed stress field.

The shear strain distributions (for lower load factors) are controlled by the initial yielding processes and its propagation. As such, it is mainly determined by the original in situ stress (K_0 value), the geometry (H/D), the strength of the ground mass and the amount of stress release allowed. Wong (1986) proposed a method to assess behavioural modes of yield propagation mainly for cohesionless soils. However, the final shear strain distributions at or around collapse, as shown in Table 2.2 are all very similar, always showing highly strained narrow zones travelling up from the tunnel sides towards the surface. Complete tunnel collapse will occur if these zones reach the ground surface but the actual collapse mechanism will differ for distinct geometric and soil types as will be seen later. However, they encompass an overall similarity. The inclusion of gravity (case 8) through centrifuge testing does affect the shear strain pattern and its magnitude, possibly not as much as by itself but by the larger stress induced. But again, the overall picture is not much changed. In other words, shear strain propagation and collapse mechanism development is mainly controlled by the presence of the free ground surface and by the relative position of the opening.

Most of the tests represent very shallow tunnels (H/D smaller than 1.5). Undrained centrifuge tests with larger covers (H/D equal to 3.1) carried out by Mair (1979), show once more comparable response. Clearly, the high strain zones may not reach the ground surface for stronger soils or deeper tunnels. But even for the latter, the strain pattern is again similar (case 11).

The zones of high shear strain concentration tend to develop and propagate very rapidly upon tunnel unloading. This occurs for factors of safety lower than 1.4 in normally consolidated soft clay and less than 1.05 in dense sands. At this point, however, it seems worth examining the amount of displacements associated with these high strain situations. It is likely that they also will be very high.

Table 2.3 provides details of some plane strain static model tests carried out at Cambridge under drained conditions. In all cases, the field stress was simulated by the application of external loading on to the model. A flexible rubber bag installed in the circular opening allowed a uniform fluid pressure to be applied against the tunnel perimeter. This pressure was gradually reduced and the displacement field around the opening up to tunnel collapse was observed by means of radiography techniques. As the tunnel collapse pressure is known for each test, it is possible to identify the factor of safety (FS) at each stage of the internal pressure release. This factor can be related to the radial displacement (u) of the nearest point to the opening crown (on average, at 0.1 D above crown point, along the vertical axis). Figure 2.6 shows observations between crown displacements (normalized to tunnel diameter) and corresponding factors of safety for different soils and H/D ratios. In all cases, a very pronounced drop in safety is observed in the early stages of testing, which is associated with limited displacements.

The so called "loss of ground", defined as the volume of soil crossing the ideal cutting profile of the tunnel, is sometimes estimated by means of Cording and Hansmire's (1975:575 and 580) approximate rule. This volume is expressed as a percentage of the tunnel volume. If the displacement is measured at a point situated at a distance y=0.1D above the crown, the loss of ground is given by:

Test (1)	Author	Soil$^{(1)}$	$\sigma_0^{(2)}$ (KPa)	$\sigma_c^{(2)}$ (KPa)	H/D
D1	Seneviratne (1976)	n.c. kaolin	138	82.1	0.50
D2	Seneviratne (1976)	n.c. kaolin	138	76.1	0.67
D3	Seneviratne (1976)	n.c. kaolin	138	51.7	0.95
D4	Cairncross (1973)	o.c. kaolin	140	0	1.20
D5	Potts (1976)	dense sand	210	6	1.48
D6	Potts (1976)	dense sand	210	7	1.48

Notes: (1) All static model tests; fully drained condition; tunnel diameter D = 60 mm

(2) For soil properties see Table 2.2

(3) See notes (1) and (2), Table 2.2

Table 2.3 Plane Section Model Tests in Clay and Sand Under Drained Conditions

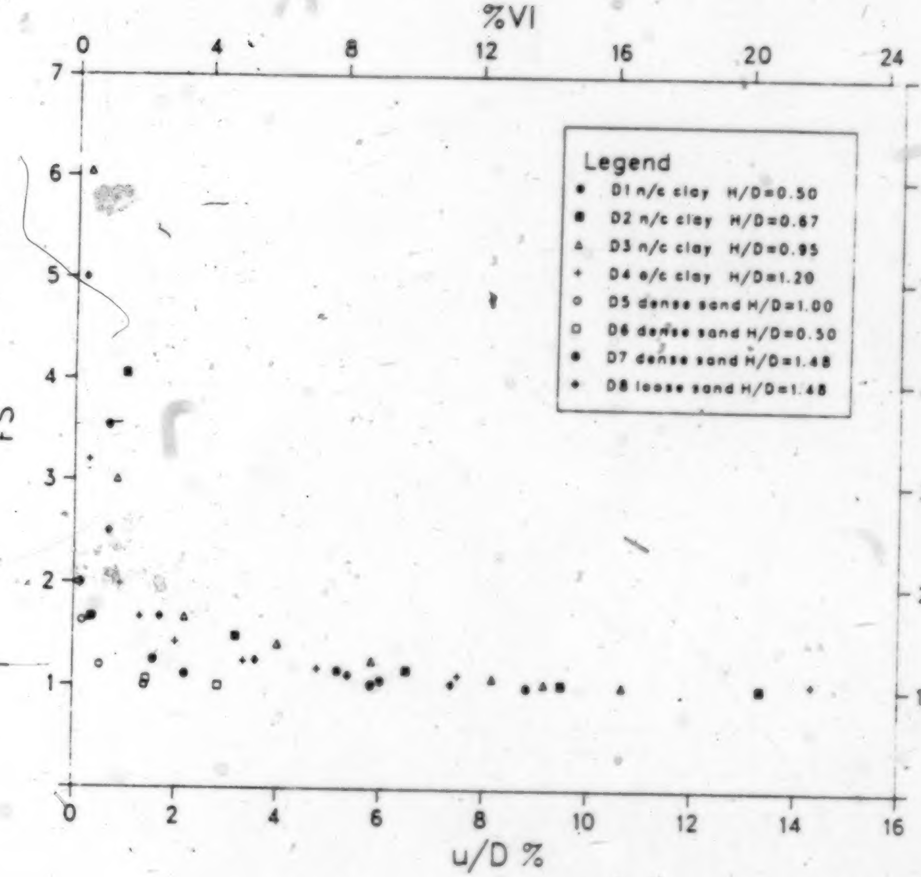

Figure 2.6 Relationship Between Crown Displacement and Factor of Safety in Drained Model Tests

$$\%V_1=\left[2\left(\frac{D}{2}+y\right) u/\pi \frac{D^2}{4}\right] 100 \qquad [2.15]$$

$$= 152.8\ u/D\ (\%)$$

Figure 2.6 also indicates estimated ground losses for a given FS, calculated at a given stage of tunnel pressure reduction. Experience shows that despite the fact that the ground also undergoes considerable volume changes, which might be either predominantly expansive or contractive, the volume of the settlement trough at the surface is directly proportional to the volume of ground lost into the tunnel. Accordingly, as the tunnel seviceability is related to an acceptable ratio u/D, the damage potential and the degree of disruption at the surface is connected to the maximum loss of ground ($\%V_1$) that can be accepted. For most tunnels, seviceability is jeopardized if u/D exceeds 3 to 4%. Before these values are realized, however, the surface settlements are likely to be excessive in an urban environment in most instances. The corresponding limits of loss of ground are 5 to 6%. For an idealized condition of no volume change in the ground, the volume of settlement at the surface would be equal to these values of losses of ground. A "poor construction quality" as defined by Negro (1979), who extended Peck's et.al., (1972) definition of quality of construction as applied to tunnelling, corresponds to settlement volumes greater than 3%. Hence, the 5 to 6% losses of ground would likely be far too excessive. For the normally consolidated and overconsolidated clay samples tested, a factor of safety greater than 1.4 to 1.7 would probably be sufficient to ensure tunnel serviceability by keeping the ground losses and surface settlements within acceptable limits. A lower-limiting factor of safety could be postulated for dense sand, but since this type of material collapse is attained in an appreciably abrupt fashion, a limiting factor of safety for this soil could be taken as 1.2 to 1.3, for most practical purposes.

The concept of a limiting factor of safety based on acceptable deformations in a geotechnical structure is not new. It has long been used in foundation engineering. In embankment dams, it is nowadays customary to refer to a limiting rate of horizontal movements per metre rise of fill, as a controlling parameter, rather than the more traditional factor of safety for collapse (Penman and Charles, 1974 and Penman, 1986). Resendiz and Romo (1972) proposed a theoretical relationship between factors of safety from limit equilibrium analyses and the maximum horizontal displacement at the slope of an embankment, calculated by the finite element method. In tunnels through soil, this concept has not been introduced so far, possibly because it is not as evident as in oth[illegible] types of structures. Clearly, the factor of safety is very much dependent on the stress-strain response of the ground. Soils exhibiting pronounced post-failure stress reduction (e.g., sensitive clays), would possibly require limiting factors of safety different from the above, in order to avoid progressive failure. The soil stress-strain response is very path dependent and it was shown that no unique stress path exists around a shallow tunnel. This makes attempts to define limiting factors of safety for tunnels on the grounds of acceptable deformation, a very complex task. A way out is to rely on model testing, but even here the tunnel simulation is still highly idealized.

Comparing the suggested limiting factors of safety based on an acceptance criteria for deformation in the soil, with those previously identified for the development of high shear strain concentrations, it is seen that the former are higher than the latter. If design and construction ensure good ground control conditions (limited losses of ground and limited tunnel convergences), the development and propagation of the zones of high shear stains is unlikely or limited. Results from undrained model tests on normally and overconsolidated kaolin (Table 2.4 and Figure 2.7) also confirm these findings, suggesting that this conclusion can be fairly generalized, except possibly, for soils exhibiting strong strain softening behaviour.

Referring again to Table 2.2, it is noted that around collapse, the maximum shear strain zones progress from the opening shoulders more or less at a 45° angle between crown and springline, pointing up towards the horizontal surface. The magnitude of the maximum shear strain ranges from 3 to 24% and varies with the soil type and the geometry. Based on the available information, no shear band was identified in any of the cases reported in Table 2.2, except when a full

Test (1)	Author	Test Type	Soil	C_u (kPa)	$E_0^{(2)}$ (MPa)	$K_0^{(3)}$	$\sigma_0^{(4)}$ (kPa)	$\sigma_c^{(5)}$ (kPa)	H/D
U1	Seneviratne (1979)	static	n.c. kaolin	26	6	0.64	138	60.4	1.00
U2	Seneviratne (1979)	static	n.c. kaolin	26	6	0.64	138	46.0	1.45
U3	Mair (1979)	centrifuge (75 g)	o.c. kaolin (OCR = 2.8)	24	3.6	1.0	150	76.0	1.67
U4	Mair (1979)	centrifuge (65 g)	o.c. kaolin (OCR = 1.8)	25	5.2	0.82	249	116	3.11

Notes: (1) Tunnel diameter D = 60 mm in all tests

(2) Undrained "initial tangent modulus"

(3) Ratio between effective horizontal to vertical stress (derived from measurements of negative pore water pressure, at the end of equilibrium stage in Mair's tests)

(4) Total vertical stress at tunnel axis

(5) Uniform tunnel pressure at collapse

Table 2.4 Plane Section Model Tests in Clay Under Undrained Conditions

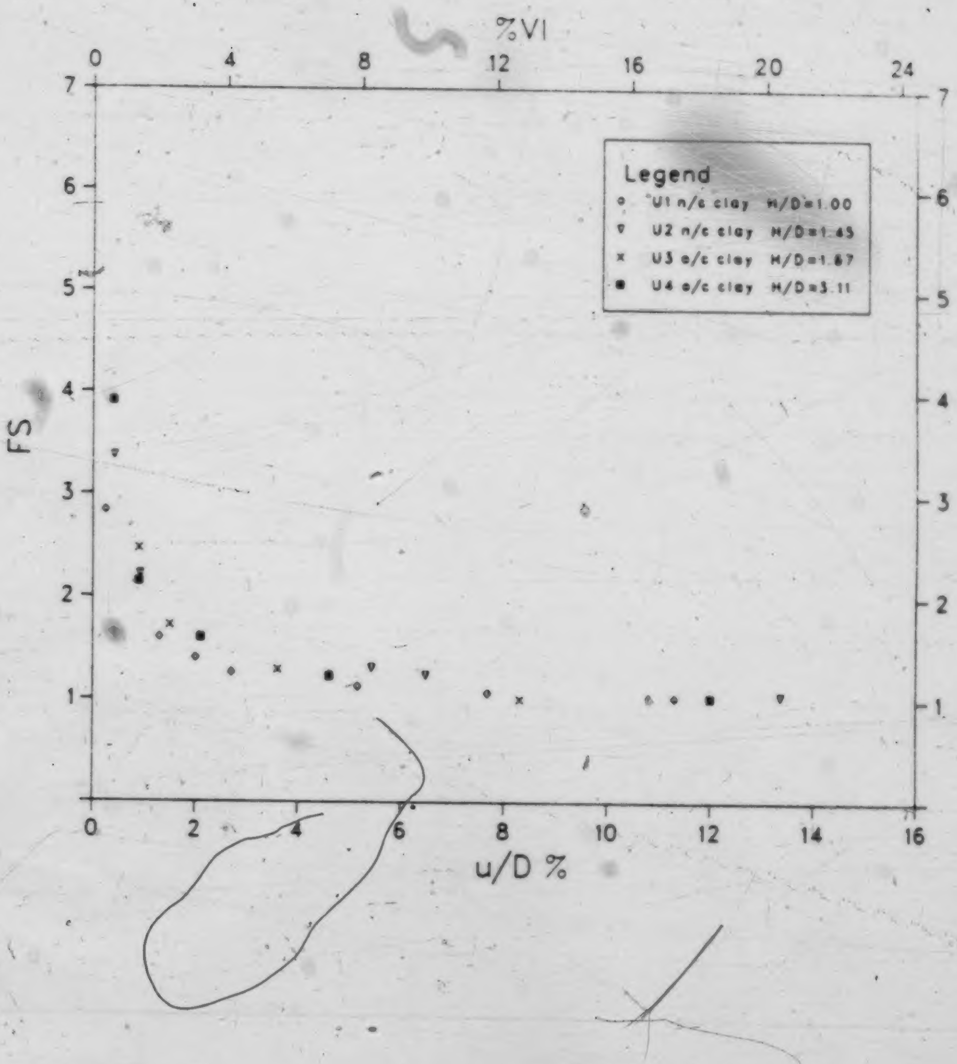

Figure 2.7 Relationship Between Crown Displacement and Factor of Safety in Undrained Model Tests

collapse condition was observed (case 8, FS=1, Atkinson and Potts, 1977:321). However, in some other model tests carried out in Cambridge, thin shear bands were detected in the soil, shortly before collapse. This was the case in some three-dimensional tunnel loading model tests performed by Casarin (1977:46). The soil was an overconsolidated kaolin (OCR=3.5), with K_o close to unity and an undrained cohesion of about 60 kPa. The shear bands appeared ahead of the tunnel face, dipping into it, in two undrained tests, at factors of safety lower than 1.11 (for lining placed one diameter behind the face) and 1.25 (for lining placed at the face). If these discontinuities are not clearly visible in the displacement field, they will hardly be identified through the shear strain contours. These contours are obtained on the assumption of constant (uniform) strains within each triangular element defined by three adjacent lead or silvered markers. Usually Cambridge researchers space the markers 10 mm apart. Casarin (1977) spaced them 5 mm apart, but even with this denser marker grid, his shear strain contours (Casarin, Op.cit, Figures 5.14 and 5.26) fail to identify the shear band, which was visible in his experiments. The reason for this is that the thickness of the shear band is far less than the spacing between markers. Roscoe (1970) proposed that its thickness is about 10 times the average grain size of a granular soil, while Vardoulakis (1986) suggested a factor of 16. However, observations made by Morgenstern and Tchalenko (1967) on shearbands in kaolin samples under direct shear, indicate thicknesses of 0.1 to 0.2 mm (about 50 to 4000 times the size of a kaolin particle). The assumption of constant strain elements and the use of markers spaced at distance one or two orders of magnitude wider than the shear band thickness, allow the discontinuity to go unnoticed by backcalculated shear strain contours. The extension of Casarin's shear bands was of the order of one tunnel radius, and the maximum shear strain was calculated as 30%. Actual shear strain, within the shear band, could well have been one or two orders of magnitude higher. If formation of these thin shear zones is a matter of concern, different modelling techniques and results interpretations should be implemented. However, the subject seems to be of limited practical interest if tunnel construction is undertaken avoiding near collapse conditions. Localized shear band formation may be possibly precluded if the factor of safety against tunnel collapse is higher than about 1.5. More investigations are, however, needed to generalize this statement.

Even when this phenomenon is not present, it is a difficult task to map the shear strength mobilization around the opening, or else to define a "failure zone" from shear strain contours. Failure strains in soils are difficult to be properly assessed from laboratory testing, as they depend on the apparatus boundary conditions, type of equipment, shape and size of the testing sample, etc. Uniform straining at failure is normally not guaranteed. Moreover, the shear strain at failure is very sensitive to the stress path experienced by the soil element before reaching failure. It was shown that the stress path around a plane strain tunnel is not unique and varies considerably from point to point. Furthermore, there is still the additional practical complication that these stress paths may differ appreciably from those normally followed in usual laboratory testing. El-Nahhas (1980) (case 11, Table 2.2) favoured a compromise, choosing a range of maximum shear strains at failure, based on tests run along selected stress paths extremes (active and passive compression tests).

The foregoing discussion showed that there is evidently a correlation between the factor of safety and ground displacements, particularly those at the tunnel crown. These displacements are affected by soil stiffness and strength, the geometry (H/D), the in situ stress condition (K_o). Differences in these parameters may explain the scatter of data shown in Figures 2.6 and 2.7. It seems convenient to introduce a dimensionless displacement defined as :

$$U=\frac{u\ .\ E_o}{D\ .\ \sigma_{ro}} \qquad [2.16]$$

where, u is the radial displacement at a point of the tunnel perimeter (herein, only those at tunnel crown will be referred to), E_o is an initial tangent modulus of elasticity, σ_{ro} is the initial radial stress at this point (the vertical in situ stress at the crown, for instance) and D is the tunnel diameter. In a drained analysis, E_o is taken as a drained modulus and σ_{ro} is an effective stress. In an undrained analysis, E_o would be an undrained modulus and σ_{ro} a total stress.

Having estimated such initial deformation moduli, on the basis of the information provided by the various authors cited in Tables 2.2 and 2.4, it is then possible to calculate the dimensionless displacement of the crown. This displacement is calculated for each decrement of tunnel pressure, for each model test, and is related to the current factor of safety. Figure 2.8 shows this relationship for all model tests discussed, including those performed under drained (series D) and undrained (series U) conditions. The introduction of a parameter related to soil stiffness reduces the test result scatter slightly, as it should. For a typical factor of safety of 1.5, the corresponding range of U would be 0.5 to 1.8, against a u/D range of 0.2 to 3.8%. Regardless of the strengths of the soils tested, U values in excess of 1.8 will generally be near the collapse condition with high shear strain concentration. The so called "good ground control conditions", would correspond to smaller U values, typically 1.0 or less. Consequently under equivalent conditions and for the same factor of safety, a softer soil may experience larger crown displacements than a stiffer soil. Indeed, the model tests show that the final collapse is attained sooner in terms of displacement for stiffer soils.

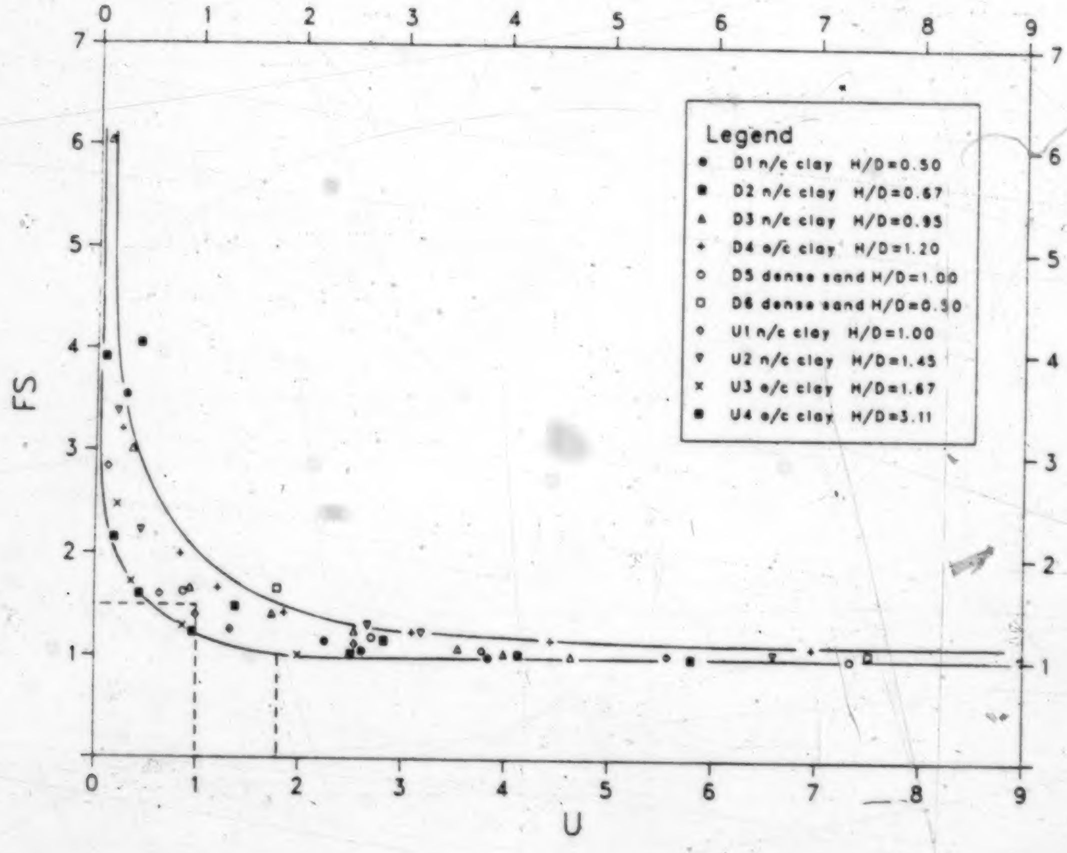

Figure 2.8 Relationship Between Dimensionless Displacement of the Crown and Factor of Safety Observed in Drained and Undrained Model Tests

2.3.4.4 Volume Changes

Unlike the development of shear strains, the time independent volume changes experienced by the soil upon tunnelling may differ from one soil type to another. The magnitudes and distribution of volumetric strains in the ground mass will depend on a number of factors. These include the mean normal stress level, the shear stress level, the stiffness of the surrounding soil (and lining if any), the stress history of the soil, the presence of the stress free ground surface, gravity and others. Volume changes due to pore water pressure changes will only be discussed briefly in this section.

An increase in shear stress may cause either compression or dilation, depending on the nature of the particular soil. A reduction in the mean normal stress will tend to cause swelling. Although the relations between volume changes and stress changes around tunnels are difficult to anticipate, it is tempting to generalize the observations made in model tests, performed under drained conditions.

Figure 2.9 shows the volumetric strains for some of the cases presented in Table 2.2. Magnitudes of strains are shown as a percentage, dilation being indicated as negative, contraction positive. Distributions (a) to (d) were obtained from static model tests, whereas (e) was obtained from centrifuge testing. Distribution (f) refers to the final volume changes derived from field observations made in the first tunnel of Washington Metro (C-line). Most of the diagrams correspond to pre-collapse conditions, where the high degree of shearing above the tunnel may dominate and control the volume changes. Clearly, different pictures would arise for higher factors of safety (or smaller reduction of the tunnel pressure). Nevertheless some conclusions may be attempted.

Volume changes in clays depend significantly on changes of both the mean normal stress and shear stress. Soft, normally consolidated clays (Figure 2.9a and b), will frequently experience volume reduction upon tunnelling under plane strain conditions. For this type of soil, if the ground cover is small and insufficient to attenuate the straining, the tunnel collapse is reached soon after local failure is attained (somewhere around points C and D in Figure 2.3). Under these circumstances, the reduction in mean normal stress is therefore limited and the associated swelling is insufficient to balance the characteristic contraction due to the shearing and yielding observed in this type of soil. Results of tests by Seneviratne (1979), shown in Figures 2.9a and b seem to confirm this reasoning. The test with larger cover exhibits some dilation beneath the tunnel floor, which is unobserved in the shallower tunnel. In both cases, the resulting contractive volumetric strains were equal to or less than 6%, near the collapse condition.

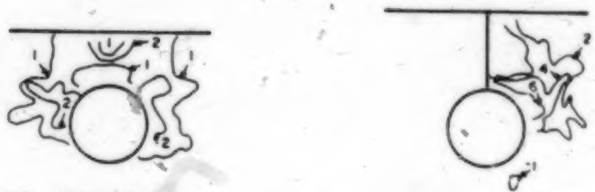

a) N.C. Kaolin (case 1)
FS=1.5, H/D=0.67

b) N.C. kaolin (case 2)
FS=1.04, H/D=0.95

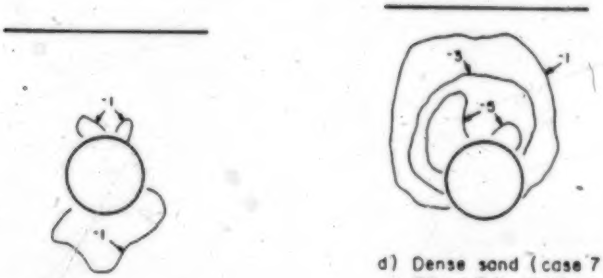

c) O.C. kaolin (case 3)
FS=1.05, H/D=1.20

d) Dense sand (case 7)
FS=1.04, H/D=1.48

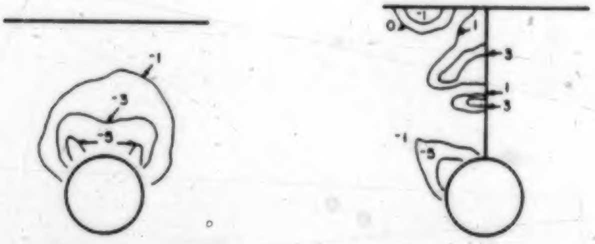

e) Dense sand, centrifuged (case 8)
FS = 1.0, H/D = 1.48

f) Washington Metro (C-Line)
H/D = 1.81

NOTE: See Table 2.2 for details. Dilation with negative sign.
Numbers refer to volumetric strain in %.

Figure 2.9 Distribution of Volumetric Strains around Shallow Tunnels

On the other hand, stiffer overconsolidated clays will generally exhibit volume expansion near tunnel collapse (Figure 2.9c). This class of soil frequently experiences dilation upon shearing, which is further enhanced by the swelling associated with a decrease in mean normal stress. The model tests conducted in Cambridge, using kaolin with an overconsolidation ratio of 3 to 4, show, however, that the magnitudes of the expansive volumetric strains were small (less than 1% as shown in Figure 2.9c, for a near collapse situation).

Volumetric strains in loose or dense sands are mainly controlled by changes in shear stress but changes in mean normal stress also have some influence. Contraction is, therefore, expected in loose deposits and dilation in dense ones. Static and centrifuge model tests carried out in dense sand (Figure 2.9d and e) confirm this. Also known is the fact that in sands, the rate of dilation increases as the magnitude of normal stress decreases. This may explain the differences observed in the distributions of volumetric strains between Figure 2.9d, where the results are from a static test with σ_0 equal to 2 kPa and Figure 2.9e, which are from a centrifuge test with σ_0 equal to 180 kPa (Atkinson and Potts, 1977:321, see Table 2.2). The proximity of the ground surface makes the shear strains concentrate above the tunnel, as shown previously. The lower normal stress level above the tunnel combined with the higher shear straining in this region, cause the higher dilation rates to be above the tunnel, rather than anywhere else (Figures 2.9d and e). The effect of the normal stress level on the rate of dilation suggests that for two tunnels driven in dense sand, with the same ratio H/D, but at different depths, the soil around the deeper one will experience a smaller specific volume increase (total volume change divided by the tunnel volume), all other conditions being equal. Also, as it will be seen later in this chapter, the volume increase above the tunnel can be of such a magnitude that local collapse of the tunnel crown may occur, triggering a progressive mechanism that can lead to a complete collapse of the tunnel.

Figure 2.9f presents volumetric strains calculated from field measurements in the first tunnel of the Washington Metro at Lafayette Park, (Hansmire 1975:77). The tunnel was driven through dense sand and gravel in the upper half of the section and interbedded sands and clay layers in the lower half. Tunnel cover was a stiff to medium silty clay with layers of silty sands. The mixed ground condition and the presence of the lining may explain the more erratic volumetric strain distribution. However, the region above the crown seems to have experienced an overall volume increase, fairly typical for the soil types encountered there. The magnitudes of these strains (1 to 3%) compares well with those measured in model tests in dense sand and in overconsolidated clay.

Departures from the modes of behaviour just described would be expected for some special soils such as very fissured, sensitive and collapsible clays, but no attempt will be made to address them in this general discussion.

The practical significance of the study of volumetric strains in the soil around a shallow tunnel, was briefly addressed in Section 2.2. Ideally, if the ground experiences no volume change upon tunnelling, the volume of the surface settlement troughs (V_s) would equal the volume of ground lost into the tunnel (V_l) as defined previously. Overall volume changes in the soil will make V_s greater or smaller than V_l, according to whether the overall ground response is mainly contractant or dilatant, respectively.

Hansmire (1975:92 and 192) integrated the volumetric strains calculated in the Washington D.C. Metro tunnel through dense sands and was able to identify an overall expansion , despite some significant localized compression in lateral zones adjacent to the tunnel (Figure 2.9f). Cording and Hansmire (1975:395) extended their investigation to other single tunnels, using instead their approximate correlation to estimate the loss of ground (Equation 2.15). They noted that usually in medium to stiff clays, the volume of the settlement troughs was approximately equal to the volume lost into the tunnel. In softer saturated clays, the volumes were equivalent under undrained short term conditions, but a substantial amount of time dependent volume change may occur, leading to V_s greater than V_l. These facts are consistent with observations made in model tests. Those authors pointed out further, that, it is mainly in granular soils that appreciable time independent volume changes may develop. Overall dilation of up to 50% of the volume of lost ground can be observed in dense sands. In loose sands, volume decrease can occur above the tunnel. Negro et.al., (1985:252) estimated a total volume decrease of almost 90% of the total volume loss (calculated as 0.42% of the tunnel volume), in an early section of a large NATM tunnel (D=10 m, H/D=0.65). This tunnel was driven for the Sao Paulo Metro, Brazil, under a loose sand cover (SPT = 1 to 6) interbedded with medium clay lenses. The large volume decrease occurred despite some cement-clay grouting above the crown, undertaken before tunnelling.

Heinz (1984:44) extended Cording and Hansmire's (Op.cit) survey on overall volume changes, by including data from a large number of NATM tunnels. He pointed out that, notwithstanding the possible inaccuracy of Cording and Hansmire's correlation for estimating V_1 (also noted by Attewell, 1977:897), the ground, in most NATM tunnels, exhibits an overall reduction in volume (around 50% of V_1). But in all fifteen NATM cases analysed, the losses of ground were smaller than 1.5% of the tunnel volume. Heinz (Op.cit:45) suggested that tunnels excavated by the NATM method may create displacement fields dissimilar to those observed in shielded tunnels and which ultimately lead to the overall ground contraction which is frequently observed. Negro et.al. (1985:58) also detected volume decreases of up to 30% of V_1 in other sections of the same NATM tunnel for the Sao Paulo Metro, which were in a stiff fissured clay, but this behaviour was attributed to a partial drainage of the saturated clay with its associated volume changes, rather than to a time independent response. It may be argued that some of the tunnels quoted by Heinz may have also undergone a similar history, particularly in cases where dewatering well in advance of construction was not undertaken. Although an attempt is normally made to separate the time dependent from the time independent settlements in tunnels driven below the ground water level, this task is not always simple. This subject will be further addressed later on.

Eisenstein and Negro (1985), reporting three case histories of tunnels driven with different construction technologies, under a lateritic porous clay cover, mentioned the contracting nature of the overall volume change observed in the ground. This could be possibly attributed to the more or less "collapsible" structure of the surficial porous deposits frequently found in tropical environments.

Based on the effect of the mean normal stress level on the rate of dilation of sand as mentioned before, it is possible to speculate how the volume changes will develop above a given tunnel in a deposit of uniform dense sand. The study would be done with varying tunnel depths, for a fixed amount of stress release which would not cause failure. Total volume changes, ΔV, will be scaled to the volume of the tunnel, V_t, to represent a specific volume change, $(\Delta V/V_t)$. Assume initially that the ground zone experiencing expansion above the tunnel is entirely surrounded by non expanding soil (Figure 2.10), or else, that the tunnel is sufficiently deep to have that zone not intercepting the ground surface. The specific volume change will decrease as the tunnel depth increases, as shown schematically by curve 'ab' in Figure 2.10. However, as the tunnel depth reduces, the expansion zone is intercepted by the ground surface and the integration of the volumetric strains that furnishes ΔV, is performed over an increasingly reduced area. A reduced soil cover may not be able to undergo sufficient expansion in order to compensate for the ground lost into the tunnel. Therefore, the specific volume changes should decrease as the tunnel depth decreases, possibly according to curve 'cd' in Figure 2.10. The combined effect of the mean normal stress level and of the ground surface on volume changes with tunnel depth, can possibly be described by the curve 'ef' in that figure. For a given tunnel size, the position of the inflexion point 'f' with respect to the surface, will be a function of the prescribed amount of stress release at the tunnel perimeter or, else, of the magnitude of the established factor of safety.

There is some limited evidence supporting this conceptual model. Hansmire (1975:192), from by his analyses of the behaviour of the Washington, D.C. Metro tunnels, maintains that the response depicted by the line 'cd' is

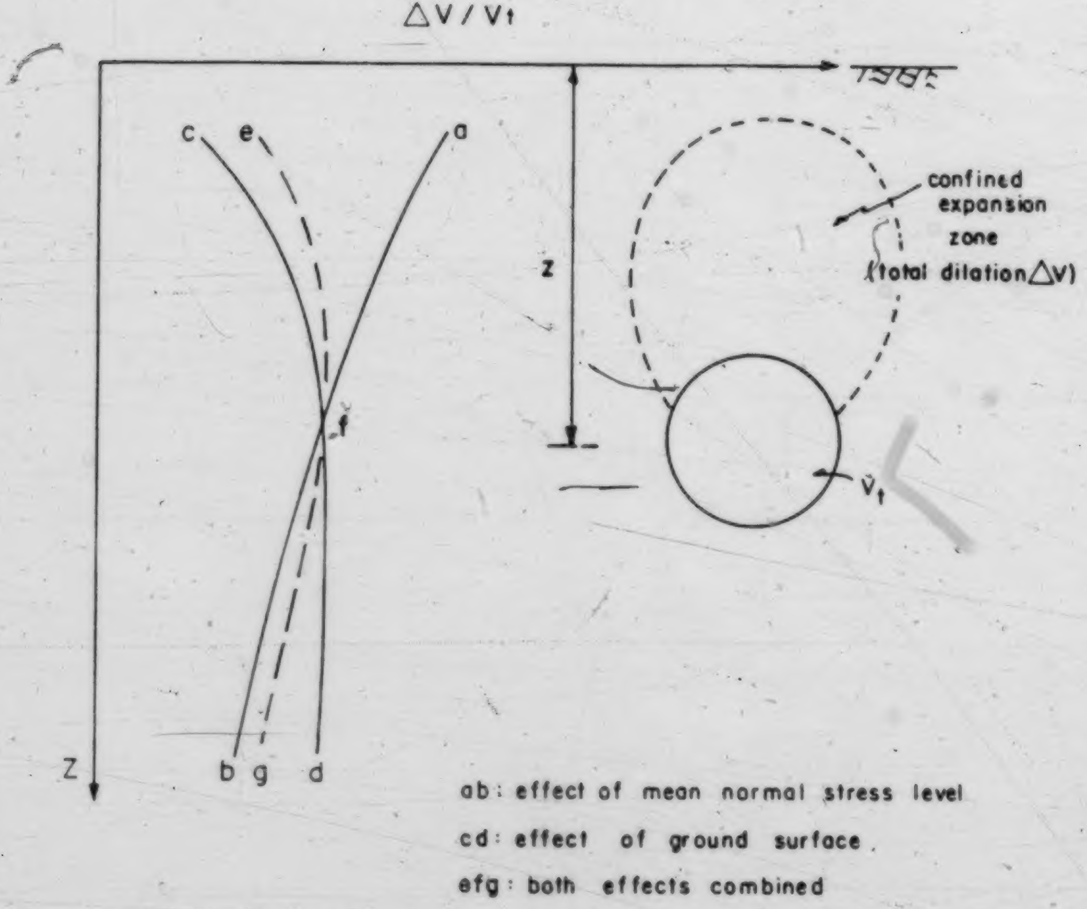
ΔV / Vt
c
e
a
z
f
confined expansion zone (total dilation ΔV)
Vt
Z
b
g
d
ab: effect of mean normal stress level
cd: effect of ground surface
efg: both effects combined

Figure 2.10 Schematic Representation of Specific Volume Changes with Varying Tunnel Depth

correct. The maximum soil cover in this project was equal to 2.5D, and the construction technique used allowed a substantial stress release in the soil. Possibly due to these facts, Hansmire did not record that the volume expansion could not go on increasing with tunnel depth increasing. Poor ground control conditions led to crown settlements in excess of 300 mm and lining load measurements suggest that the in situ stresses were reduced by as much as 80% (Hansmire and Cording, 1985:1317). Localized collapse of the sand at the crown may have occurred and the soil zone undergoing substantial dilation reached the ground surface (Figure 2.9f).

On the other hand, model test results carried out in Cambridge and shown in Figures 2.9d and e, tend to support the behaviour represented by the curve 'ab' in Figure 2.10, or more properly by the portion 'fb', since in these cases the soil zone undergoing significant expansion seems to have been almost fully confined.

If one expects to take advantage of the ground volume expansion to account for the attenuation of ground losses and possible reduction of surface settlements, the model summarized in Figure 2.10 is of some relevance. In practice however, this is a risky venture, since proper assessment of the magnitude of ground expansion is a difficult task, where mixed soil conditions may frequently hinder expected ground dilation. Moreover, large dilations in the soil will be normally induced when substantial stress release is permitted during tunnelling operations. This corresponds to a condition somewhere around points C or D in Figure 2.3. In other words, it is a near collapse situation, and is one that should normally be avoided in an urban tunnel. If these circumstances arise it may lead to the development of "loosening", as will be described later. The ground above the tunnel, which has already experienced considerable expansion, will undergo further volume increase, and the dense sand, in consequence, will become "looser". The term "loosening", frequently used in rock tunnelling (Szechy, 1967:136), is somewhat misleading in soils. A dense sand may remain dense even after the development of expansive volumetric strains as high as 5%. It does not become really loose, but simply less dense.

2.3.5 Idealized Lining Action

2.3.5.1 Preamble

Throughout this section a two dimensional plane strain condition will be assumed. As a rule a tunnel in soil will always require some form of support to keep the opening stable both in the short and long terms. This support is normally provided by some form of lining, which is usually continuous and for the sake of simplicity, will be assumed herein, to be a circular ring behaving as a linear elastic material.

The inclusion of a body with a stiffness different from that of the surrounding medium will change the overall system stiffness. Some form of interaction between the soil and lining will occur, and the stress and strain change mechanisms discussed in the three previous sections, will be affected to a larger or smaller degree, depending on the relative stiffness of the soil to the lining. An early inclusion of a more rigid body within a softer medium, will cause the unbalanced loads generated by the tunnelling operation to be transferred to that body[3]. An equilibrium condition may eventually be reached (otherwise unattainable on the premise of an unstable ground in plane strain conditions).

Some extreme conditions are going to be briefly investigated herein. The first refers to the form of radial contact between the soil and its lining, at the instant the latter is installed. At installation, full radial contact may or may not exist. It is quite clear that a full radial contact (complete embedding by the soil) should always be preferred in practice, in order to prevent any form of load concentration (e.g., "gravity" loading) leading to unnecessary additional bending of the lining. This is more easily achieved with concrete linings cast in place against the cut ground profile (whether pumped or sprayed concrete). But for pre-cast concrete segments, steel sets and wooden lagging, steel or cast iron liner plates, some sort of lack in radial contact may frequently exist, as the cut profile is hardly as regular as the outside profile of the liner. To minimize the voids behind it, prompt grouting or lining expansion is usually specified and undertaken. But, as a rule some space is always left behind the lining. The full radial contact condition, along all points of the soil lining interface will be referred to as "good lining contact". The condition of partial or no radial contact along the tunnel perimeter will be called "poor lining contact".

---

[3] By "softer medium" one should understand the ground and the opening inclusive. Otherwise, the lining is normally "softer" than the ground it replaces, since some sort of deformation is always expected after its installation.

The second extreme condition refers to the form of tangential contact between the soil and lining, with the tacit assumption that a full radial contact exists. Two extreme conditions are now visualized: no slip and full slip between the soil and its support. The first corresponds to an assumption of infinite shear strength at the interface. No relative tangential displacement would then occur between the soil and the lining. This condition could be acceptable in practice, whenever the maximum mobilized shear stress does not exceed the finite shear strength of the interface. The full slip assumption considers that zero shear strength exists along the interface, allowing the soil and lining to move freely relative to each other, in the tangential direction. This condition could approximate in practice the case of a very smooth lining, placed against a very softened, or smeared ground surface. Real slip conditions may lie somewhere between these two extremes, more probably closer to the first. The outer surface of a lining is normally fairly rough and the shear stress mobilization in the interface is likely to be small. The lining is usually installed fairly close behind the tunnel face (one to three radii behind), but still after the soil has experienced a considerable amount of displacement and stress release. As a result, the mobilized shear may be much smaller than the strength. This is further discussed in Section 2.3.5.3.

2.3.5.2 Good Lining Contact in an Ideally Deep Tunnel

As with the ground reaction curve (GRC), a support reaction curve (SRC) is normally formulated. For an ideally deep tunnel under a hydrostatic in situ stress condition (K=1), a unique GRC exists and similarly, a single SRC can represent the lining action, with radial stress and displacements increasing with the load transfer onto the lining. Symmetry implies that zero bending moments exist in the lining. The condition of the tangential contact is irrelevant since the shear stresses are zero at the interface. Equilibrium is, therefore, attained at the intersection of the two reaction curves. For a linear elastic lining, the SRC is a straight line, whose slope can be predicted on the basis of the support properties and geometry (see Hoek and Brown, 1980:252, for a review on the subject). If the lining is installed before any ground displacement occurs and if it is ideally rigid and incompressible, the stress acting on the support will be equal to the field stress.

If K is different from unity, then the in situ stresses are those shown in Figure 2.11. If a rigid lining is installed without allowing any displacement and if a no slip condition is postulated, then these stresses also represent the loads the lining must withstand. If a full slip condition is admitted, with the other assumptions remaining unchanged, the stress distribution on the rigid lining will be different from the in situ stress distribution. The shear stresses at the interface are reduced to zero and, therefore, the radial normal stress will have to change in order to ensure equilibrium (see Figure 2.12). To reduce the shear stress to zero, equal and opposite shear stresses will have to be applied, forcing the soil to displace tangentially, relative to the support. If K<1, this displacement will be from the crown or the invert towards the springline. Since the lining is assumed to be rigid, no radial displacement develops at the interface and for K<1, the radial stress decreases at springline and increases at the crown (and floor), the reverse occurring for K>1. This simple fact, not always clearly understood, was correctly analyzed and interpreted by Ranken (1978:60). Ranken's (Op.cit:407,423) or Einstein and Schwartz's (1979) linear elastic analytical solutions for deep tunnels enables one to assess these effects both for a thick and a thin lining. Ranken (Op.cit:Section 3.3) presents a comprehensive discussion on the effect of the no slip and full slip assumptions on liner thrusts, bending moments and

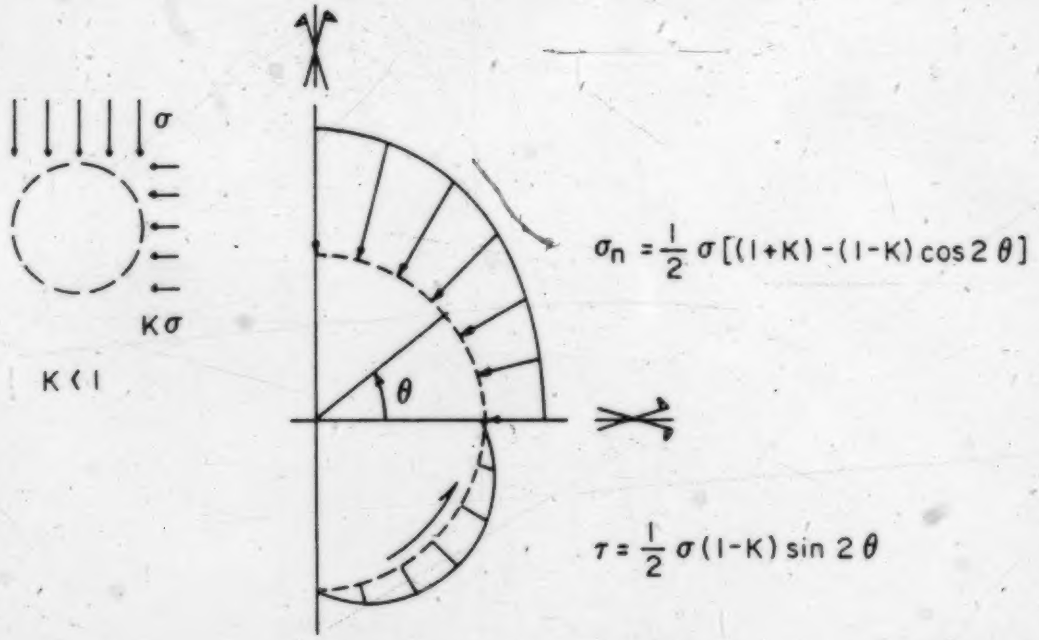
σ
Kσ
K < 1
θ
$\sigma_n = \frac{1}{2}\sigma[(1+K)-(1-K)\cos 2\theta]$
$\tau = \frac{1}{2}\sigma(1-K)\sin 2\theta$

Figure 2.11 In Situ Stresses and Lining Loads on a Rigid Lining for Non-Slip Condition

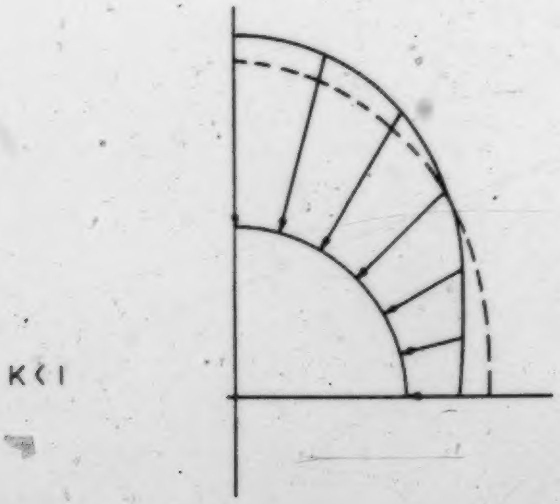

Figure 2.12 Normal Stress on a Rigid Lining for Full Slip Condition

displacements. Briefly, the slip condition does not significantly affect bending moments and lining radial displacements. The full slip assumption furnishes bending moments that are less than 10% larger than those obtained with the non-slip condition (Ranken, Op.cit:73, Einstein and Schwartz, Op.cit:513). Lining thrusts are more affected by the condition of slip. The difference between thrusts in the crown and springline are greatest for the non-slip condition, due to higher shear stresses existing at the interface. With the full slip condition, these differences are much smaller and the thrust magnitudes approach the average of the crown and springline non-slip thrust values. In other words, the greatest and lowest thrusts are always given by the non slip assumption, either at the crown or at the springline, depending on the K value (see Ranken, Op.cit:68,74).

For intermediate conditions between full and non slip, no analytical solution is available and the problem is approached by using numerical methods. This can be done using beam-spring models, with lining-soil contact represented by springs with different stiffnesses in the radial and tangential directions (for example Paul et.al., 1983:70) It can also be done using the finite element method, by including joint or interface elements (Rodriguez Roa, 1981:353, Paul et.al., Op.cit:85).

The interaction that will take place between the soil and lining when a good contact exists, takes the form of a mutual reduction of deformations in the soil and in the lining. The insertion of a stiffer body into the opening (the lining), restrains the ground deformations. On the other hand, the complete confinement of the lining offered by the soil, restrains its deformation. The interaction becomes more complicated when it is recognized that the soil loads being transferred onto the lining depend on the magnitude of the displacements (Section 2.3.3). Additionally, loads may also be transferred from the lining into the soil, altering the so-called arching process (Section 2.3.2) associated with the reduction of the in situ stress. This may also lead to changes in stiffness of the surrounding soil, for instance, by the increase of the mean normal stress in the ground adjacent to an ovally seated lining. Both volume changes and shear strains in the ground are also inhibited by the lining. Consequently, the response of the confined and embedded support will differ from that of an isolated support subjected to external loads. Similarly, the ground response (Figure 2.5) will also be affected. Rigorously, after both elements (lining and soil) are put together, their responses are not unique but interdependent and cannot be anticipated separately, except for the case of K=1 and for an ideally deep tunnel.

Clearly, the stress and displacements found when equilibrium is achieved as a result of the soil-lining interaction process, will depend on the relative stiffnesses between both elements. These are defined in terms of extensional and flexural stiffness ratios of the soil and the support, and are expressed in different ways. They are normally referred to as the compressibility (C) and flexibility (F) ratios. The expressions given by Einstein and Schwartz (1979:501) are preferred to those by Peck et.al. (1972:269) or Ranken (1978:339), as the first authors consider the stiffness of a perforated ground mass, which is more appropriate. They are written as:

$$C = \frac{ER\,(1 - \nu_s^2)}{E_s A_s (1 - \nu^2)} \qquad [2.17]$$

$$F = \frac{ER^3 (1 - \nu_s^2)}{E_s I_s (1 - \nu^2)} \qquad [2.18]$$

in which E, ν and E_s, ν_s are elastic constants for the ground and the support, respectively, A_s and I_s are the cross sectional area and the moment of inertia of the support per unit length of tunnel, and R is the tunnel radius.

To illustrate some of the points just discussed, Figure 2.13 was prepared using Einstein and Schwartz's (1979) elastic solution for a deep tunnel under a full slip condition with $K=0.5$. The vertical stress field is given by σ_v. The points for $C = F = 0$ correspond to a perfectly rigid support, and, as observed, despite a zero radial displacement condition, σ_r increases at the crown and decreases at the springline. The large difference in stress at these two points indicates that considerable bending moments exist in the lining. The points, $C=F=\infty$, represent an unlined opening after full stress release. The two bold lines correspond to the ground reaction curves for the crown and the springline, for a continuous reduction in the in situ stress at the perimeter. The points C=0 and F=∞ represent an ideally flexible tunnel, as defined by Peck (1969:245). The outward movement of the springline is equal to the inward displacement of the crown and floor, and the opening profile becomes approximately an ellipse[4]. The cross-sectional area of the opening does not change and, therefore, the "net" loss of ground is zero.

The radial stress becomes uniform and equal to the mean in situ stress, the bending moments are zero and lining thrusts are uniform and compressive. This is the "ideal" lining that most modern designs try to achieve. If the lining becomes compressible but remains ideally flexible (points C=1, F=∞), the radial stress still remains uniform but less than the original mean in situ stress, and the crown downward displacement is larger than the springline outward movement, resulting in a "net" loss of ground. The points (F=10, C=0) and (F=10, C=1) are shown as representing intermediate behaviours. Most tunnel linings in soil have C

---

[4] Peck (1969:245,246) and Muir Wood (1975:117) refer to the deformed lining profile as an ellipse. Rigorously this profile is not elliptical. If C=0, the lining circumference does not change, but just its shape. The closed form solution for C=0 and full slip interface yields crown and springline displacements of equal magnitude but with opposite sign. If the deformed profile were actually elliptical, for a given crown settlement, the outward displacement of the springline would be slightly less than the former. The difference between the two is actually less than 1% (calculations based on Selby, 1962:13). Obviously, for all practical purposes, the deformed profile can be taken as an ellipse.

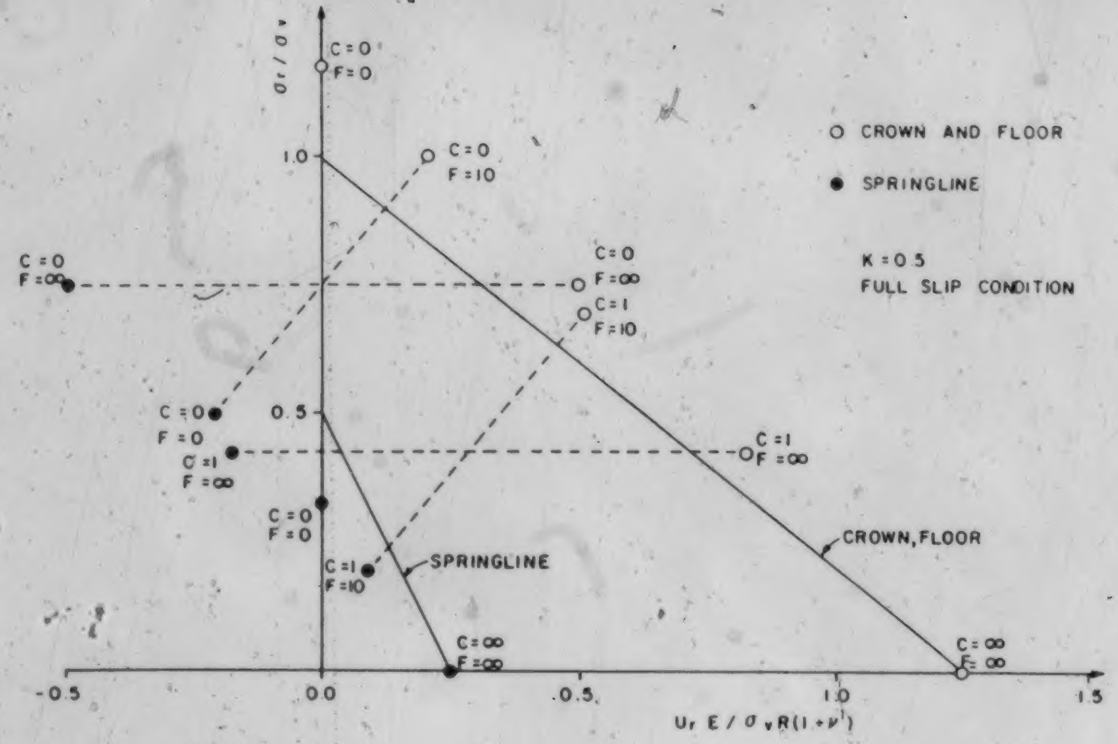

Figure 2.13 Equilibrium Points for Crown and Springline of a Deep Tunnel with Full Slip Interface Between Soil and Lining

values between zero and 2; and F values between 10 and 10,000.

Also worth mentioning is the fact that all the equilibrium points between the lining and soil shown in Figure 2.13, do not lie on the ground reaction curves for the crown or the springline. This point was raised by Pender (1979), who explained it by saying that the stiffness of the soil is not the same for the release of the asymmetric part of the in situ stress and the application of an asymmetric pressure to the tunnel perimeter by the lining. But not only this, since the equilibrium points are also affected by the stiffness of the lining. Only when this asymmetric stress is absent (deep tunnel and K=1) is it possible to review the ground and support responses independently, as is done by the convergence-confinement method.

2.3.5.3 Good Lining Contact in a Shallow Tunnel

If the tunnel is shallow, the gravity action means that symmetry of the in situ stress exists around the vertical axis only, as shown in Figure 2.14. This is given for an H/D ratio equal to 2 and K=0.5. The equation shown is derived from Hartmann (1970:215). If a rigid lining is installed without any prior displacement, and if a non-slip condition is assessed, the normal and shear stress distributions onto this lining will be different from the in situ values shown in Figure 2.14. Using Hartmann's (1972:15) elastic solution for a tunnel under a gravitational stress field, with its centre at a depth z sufficiently far from the stress free

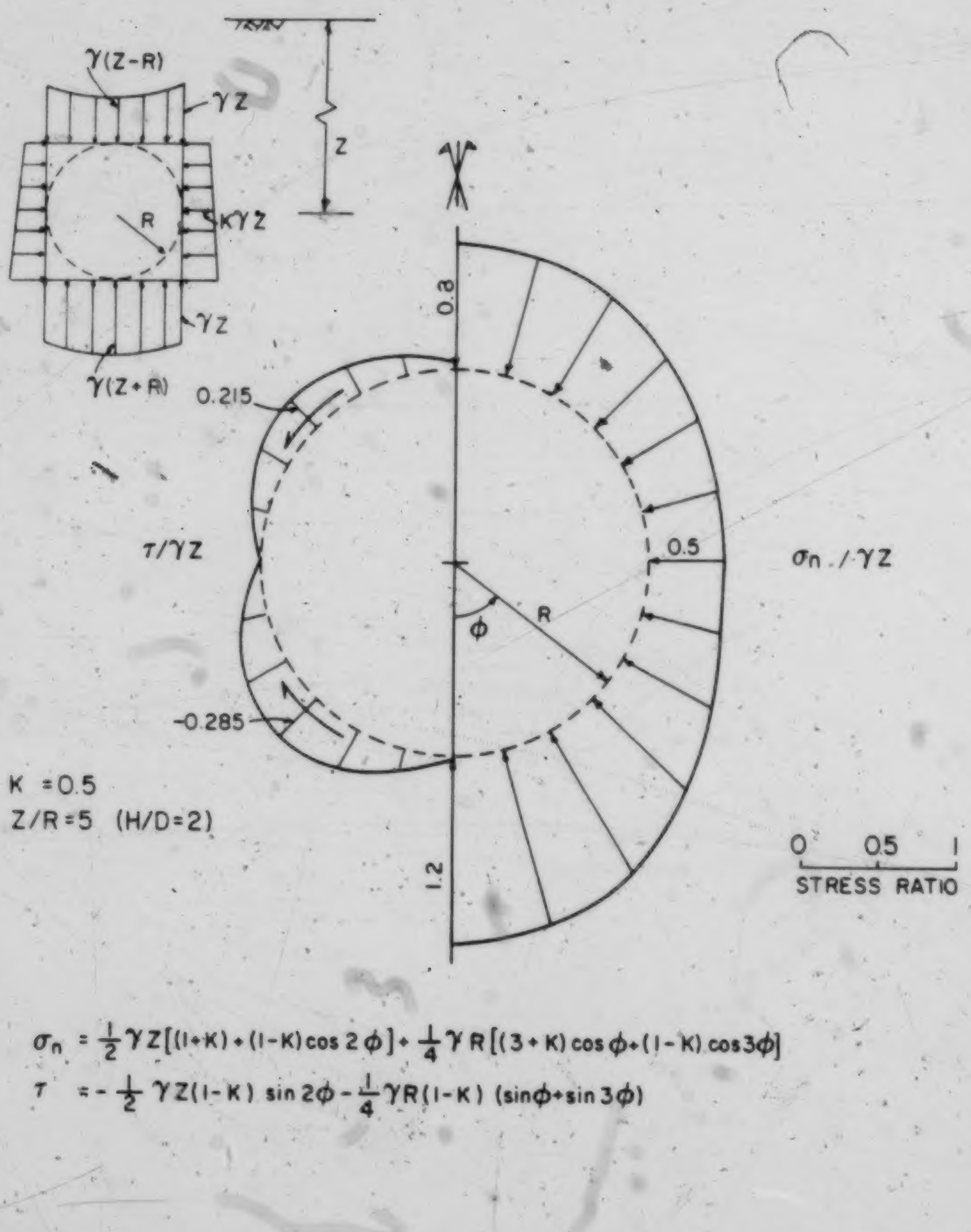
γ(Z−R)
γZ
Z
R
KγZ
γZ
γ(Z+R)
0.8
0.215
τ/γZ
0.5
σn / γZ
φ
R
−0.285
K =0.5
Z/R=5 (H/D=2)
1.2
0 0.5 1
STRESS RATIO

$$\sigma_n = \frac{1}{2}\gamma Z\left[(1+K)+(1-K)\cos 2\phi\right]+\frac{1}{4}\gamma R\left[(3+K)\cos\phi+(1-K)\cos 3\phi\right]$$

$$\tau = -\frac{1}{2}\gamma Z(1-K)\sin 2\phi-\frac{1}{4}\gamma R(1-K)(\sin\phi+\sin 3\phi)$$

Figure 2.14 In Situ Stresses Around a Shallow Circular Tunnel Profile Prior to Excavation

ground surface, one obtains the distributions of normal and shear stresses shown in Figure 2.15, where γ is the unit weight of the soil. Since the crown and floor in situ normal stresses are not equal, the rigid lining tends to "float" upon removal of the soil within the lining. The crown normal stress increases from $\gamma(z-R)$ to $\gamma(z-R/2)$, and the floor normal stress decreases from $\gamma(z+R)$ to $\gamma(z+R/2)$. The buoyant effect also causes changes in the shear stress distribution, increasing the shear in the tunnel shoulders and decreasing it in the haunches. It should be also noted that the normal stress at the springline ceases to be a principal stress as shear develops at this point. Even for $K=1$ there will be positive shear (from crown to floor direction) at the interface, being maximum at the springline and equal to $0.5\gamma R$.

The ratio of mobilized shear stress to acting normal stress at the soil-lining interface is a measure of shear strength mobilization. By inspecting the values shown in Figure 2.15, one notes that the risk of occurrence of a slip at the interface is highest around the tunnel shoulders. For this given geometry, in situ stress condition and support stiffness, the maximum mobilized friction angle at the interface is less than 22°. Thus, if the frictional strength of the soil-lining interface exceeds this value, or if it is smaller but has some cohesive component, appreciable tangential movement between the soil and lining may not be expected. Even if some slip does occur locally around the

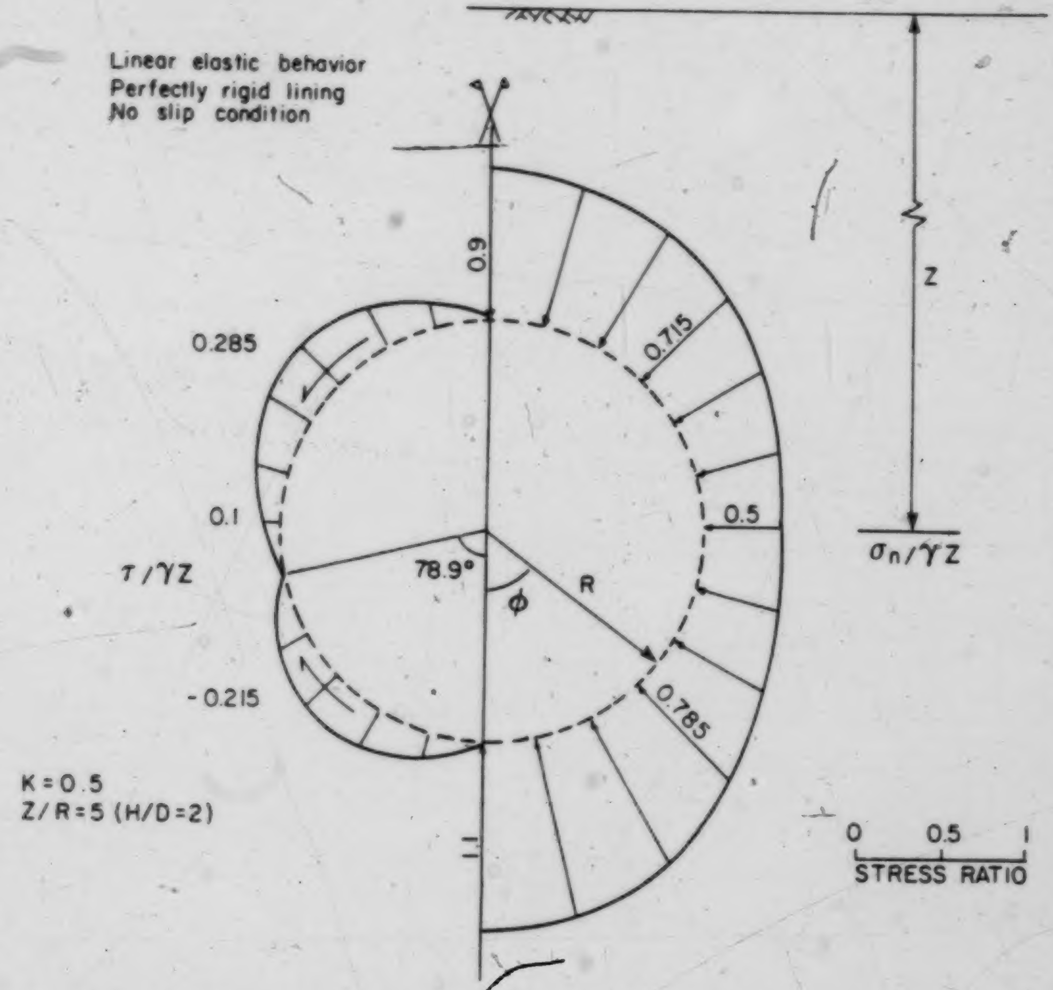
Linear elastic behavior
Perfectly rigid lining
No slip condition
0.9
0.285
0.715
Z
0.1
0.5
σn/γZ
τ/γZ
78.9°
φ
R
-0.215
0.785
K=0.5
Z/R=5 (H/D=2)
0
0.5
1
STRESS RATIO

$$\sigma_n = \frac{1}{2}\gamma Z\ [(1+K)+(1-K)\cos 2\phi] + \frac{1}{4}\gamma R\,[(1+K)\cos\phi + (1-K)\cos 3\phi]$$

$$\tau = -\frac{1}{2}\gamma Z(1-K)\sin 2\phi + \frac{1}{4}\gamma R\,[(1+K)\sin\phi - (1-K)\sin 3\phi]$$

Figure 2.15 Stress Distributions Around a Rigid Lining in a "Shallow" Tunnel

shoulders, resulting in some shear transferred to adjacent points, a full slip condition all around the tunnel profile would not exist. Shear strength mobilization decreases as the tunnel becomes deeper, as K tends towards unity and as the lining becomes more flexible.

The stress changes observed around the tunnel after installing the rigid lining, are given by the differences between the equations shown in Figure 2.14 and 2.15. Thus,

$$\Delta\sigma_n = -1/2\ \gamma R \cos\phi$$

$$\Delta\tau = 1/2\ \gamma R \sin\phi$$

By adding the integrals of these stress changes along the entire tunnel contour, a force equal to $\pi\gamma R^2$ is obtained, which is exactly the weight of the soil removed from the opening, as noted in Section 2.2.

If the circular opening is left unlined, the tangential stress at the crown, springline and floor of the "shallow" tunnel perimeter are, respectively (Hartmann, 1972:15):

$$\sigma_{\theta c}=(3K-1)\ \gamma(z-\frac{R}{2}) \qquad [2.19]$$

$$\sigma_{\theta s}=(3-K)\ \gamma z \qquad [2.20]$$

$$\sigma_{\theta F}=(3K-1)\ \gamma(z+\frac{R}{2}) \qquad [2.21]$$

Equations 2.5 and 2.7 derived from Mindlin's (1939:1132) solution and presented in Section 2.3.2, are particular cases of the above expressions.

Clearly, if the influence of the stress free ground surface is included, the tangential stress will differ from those given above, but the differences should be small for H/D greater than 1.5, as discussed in Section 2.2.

A more general case that includes the effect of the stress free ground surface and, perhaps, the non-linear ground response, would require numerical solution, since no analytical solution is yet available. Furthermore, in the real case, the lining is installed behind the tunnel face, after the projected tunnel profile has undergone some displacement. That could be represented in a plane strain analysis by a certain limited amount of in situ stress release at the tunnel contour.

The finite element model and simulation procedures applied for obtaining the stress paths shown in Figure 2.4 and for the ground reaction curves presented in Figure 2.5, could also be used to approach the solution of the more general case just discussed. Details of this numerical model were summarized in Section 2.3.4 and will be discussed further later in this thesis.

The construction of a tunnel of 4 m diameter with 6.2 m of ground cover was numerically simulated, assuming the following properties for the non-linear elastic hyperbolic model representing the soil:

γ = 16 KN/m^3

K_0 = 0.75

ϕ' = 21°

c' = 39 kPa

R_f = 1

K = 330

n = 0.23

$\nu = 0.3$

The symbols have the meanings explained in Section 2.3.4.1, and c'is the cohesion intercept of the Mohr-Coulomb envelope. A fully drained behaviour was assumed. Since Janbu's exponent, n, is non-zero, the in situ elastic modulus of soil increases with depth, being approximately equal to 24 MPa at the tunnel axis line.

The support was represented by a linear elastic material, with C = 1.8 and F = 86, with respect to the in situ elastic modulus of the soil at the tunnel axis elevation. These values could be typical for a shotcrete lining, with a reduced E value at its early age.

Four analyses were carried out, each one with different uniform amounts of in situ stress release at the opening prior to the lining installation: 0%, 40%, 80% and 100%. The full stress release corresponds to no liner installation, and enabled the construction of the ground reaction curves, in terms of radial stress and displacements, at three points of the tunnel contour: the crown, springline and floor. These are shown in Figure 2.16. The 0% stress release analysis corresponds to the material discussed so far in this section: the lining is installed in such a way that no displacements occur before its activation. This is clearly a crude abstraction of reality, and the analyses corresponding to 40% or 80% of stress release prior to lining installation are more plausible. In these cases, the lining was introduced after the development of some displacements at

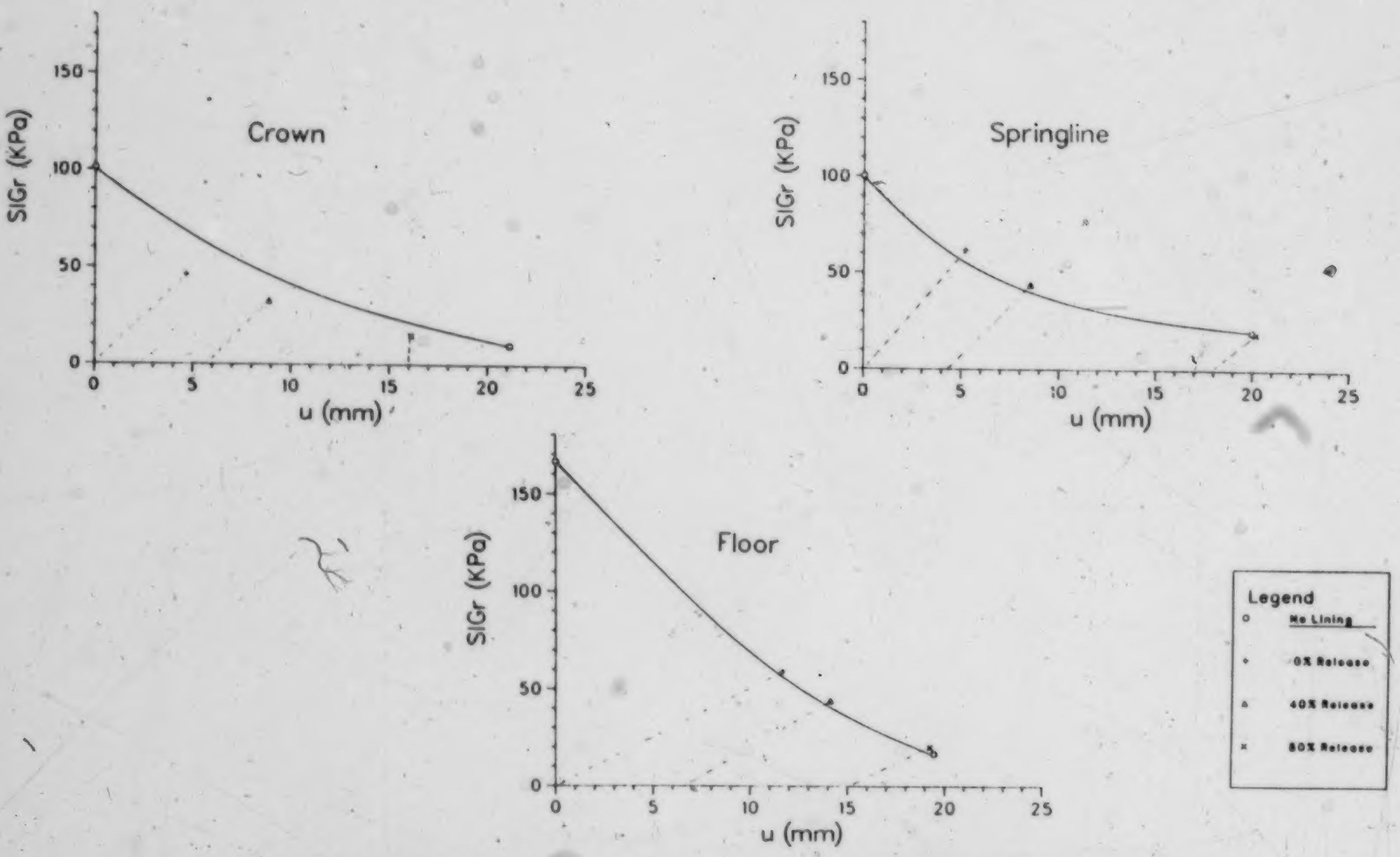

Figure 2.16 Points of Equilibrium of a Ground-Lining Interaction Analyses Using Finite Element Method

the opening. The equilibrium points between the lining and the soil obtained are identified in Figure 2.16. The larger stress release before support installation, obviously leads to smaller equilibrium stress and larger final displacements. The dashed lines linking the equilbrium points to the starting point of lining activation could be interpreted as support reaction curves. Unlike the radial displacements which are calculated at nodal points, it was necessary to extrapolate the calculated element stresses up to the tunnel perimeter in order to obtain the radial stresses at the soil-lining interface. This involves a certain degree of approximation.

As pointed out before, the equilibrium points do not coincide with the non-linear ground reaction curves especially at the crown. Here the ground response curve, which does not take into consideration the interaction with the lining, seems to be an upper bound for the corresponding equilibrium points. It also seems that the effect of this interaction is considerably reduced when the stress release allowed before lining installation increases.

The slopes of the dotted lines shown are measures of the stiffness of the support at each point of the tunnel contour. It is noted that for a single point, these slopes changed with variable amounts of stress release, despite the fact that the nominal values of C and F had been kept constant in all analyses. This is due to the changing value of the elastic modulus of the soil around the tunnel which results from the unloading process. Broadly speaking, an overall reduction in this modulus would be expected and for fixed lining properties, one could envisage a stiffer support response as the amount of in situ stress release increases. This is particularly true for the crown but less evident for the other points considered. Acceptance of this arguement would lessen the impact of the relative stiffness ratios such as C and F, in a non-linear response context. It may possibly be more adequate to define these ratios in terms of a reduced average ground modulus, current with the instant of lining activation.

2.3.5.4 Poor Lining Contact

When using prefabricated lining systems, it is customary to overexcavate the tunnel profile in order to easily accommodate the support. Also, to reduce jacking forces needed to advance a tunnel boring machine, it is usual to cut a profile larger than the TBM shield. This overcut was normally done in the past by a small radial extension called a "bead", 5 to 15 mm in thickness, fixed on the leading edge of the TBM. Modern machinery design, with full face mechanical excavation, allows overcutting by means of variable length teeth, protruding radially from the face cutter. This permits a more efficient control of the excavation, allowing adjustments in the overcutting, without major disruption during tunnel advance. The voids left behind the assembled lining ring are filled with some sort of grout or the lining is expanded against the soil. Details of construction techniques used can be found in Craig and Muir Wood (1978) and in Maidl (1984). In many cases, the voids are left unfilled for a considerable amount of time, when the grouting operation is delayed. In some other cases the grout is insufficient or inefficient (grout losses, grout settling, etc) and a void is left open in the crown region.

Depending of the size of this space behind the support, the ground response may vary. If the space is small,then with the advance of the tunnel face, a soil with sufficient stand up time will come in contact with the lining without the development of local instability or global ground collapse. If the ground has no stand up time, the void will immediately be filled with soil, but as the space size is small, then again, neither local nor global collapse will be observed. The stress changes in the soil element beside the void are clearly three dimensional, and the acting mean normal stress is possibly close to zero. In an equivalent plane strain simulation, the stress state of this element would lie between points B and D in Figure 2.3.

If the void space is sufficiently large, either local instability or global ground collapse may occur. Distinctions will be made between these two mechanisms in following sections. In a dense sand local collapse is associated with the fall of a wedge like portion of the ground from the roof (Atkinson et.al., 1975:84). In fissured, stiff, clayey soils, local collapse may be associated with the fall of blocks bounded by pre-existing discontinuities (Matheson, 1970). To the writer's knowledge no empirical or theoretical guidelines exist presently to limit the maximum amount of overcut space left unfilled, in order to prevent those occurrences. However, it is tempting to make use of the discussion presented on shear strain development in Section 2.3.4, based on the results of plane strain model tunnel tests. It was observed there, that a near complete collapse condition is reached in all soils tested, when the dimensionless displacement at the tunnel crown, U, given by equation 2.16, exceeded 1.8.

Out of this total figure, some displacements will occur ahead of the face and some after the soil comes in full contact with the support and loads it.

As will be seen in Chapter 5, (see also Negro et.al., 1986), the crown displacements occurring ahead of the face of shallow tunnels leads to U of not much more than 0.5, except in very soft clays. Some displacements are also likely to occur once the soil establishes a good contact with the lining. It was seen that these depend on the relative stiffness of the lining and if a very rigid support is present then the increment in U due to lining deformation is negligible. The estimate of an upper bound of the increment in U for a flexible support would preferably be made by some analyses, either as an analytical closed form solution, or numerical, such as those mentioned under the previous heading (and further discussed in following chapters). Perhaps also, it could be bounded from available field data of real tunnel performances. Shielded tunnel cases, making use of prefabricated lining rings, offer little help in this search, as it seems practically unfeasible to identify when the soil came in full contact with the lining. Fortunately, data from NATM cases can provide some assistance, if one accepts that the shotcrete ring is likely to fulfill the requirements of good contact with the ground. In Chapter 5 of this thesis, it is shown that in all NATM cases investigated, the increment of the dimensionless crown displacement U, due to the shotcrete lining deformation after the closure of the support ring invert, is likely to be less than 0.3, with the exception of tunnels departing considerably from a circular profile (e.g., the heading of Sao Paulo Metro North extension, with a temporary heading invert, as described by Negro et.al., 1985 and Eisenstein et.al., 1986, which had a width to height ratio of about 0.5. This value may likely serve as a conservative upper bound. It is not certain how the relative stiffness of a shotcrete lining compares in reality to that of a prefabricated lining system. In both cases, there is quite a degree of uncertainty on the assessment of various parameters, for example the stiffness of segment joints, the deformation modulus of the shotcrete at its early ages, etc. However, the field data from shotcrete lined tunnels may possibly serve as a rough upper bound, since it includes the influence of a reduced deformation modulus of the hardening concrete placed at the floor.

If the crown displacements occurring ahead of the face (corresponding to a maximum U equal to 0.5) are added to those taking place due to lining deformation (which corresponds to U between 0 and 0.3), the limiting dimensionless crown displacement increment for movement into the void space behind the lining which might produce a near collapse condition, will range from 1.0 to 1.3. If some factor of safety is included, the limiting U increment at the crown may vary from 0.5 to 0.65. From this, one could estimate a limiting crown displacement increment, and therefore, a maximum crown overbreak, which should be less than or equal to the limiting value. This approach is unquestionably very approximate and open to discussion. However, since no other guidelines are presently available, it may serve as an interim expedient to treat the problem, until a more adequate solution is formulated. Needless to say that caution should be exercised when applying the above criterion since it was developed from results of tests that made use of "well behaving" soil types under fairly idealized conditions. Minor geological details such as the presence of small sand lenses or pockets, are known to have an important role in localized collapse mechanisms (Matheson, 1970). Stiff, fissured clays, collapsible and sensitive soils may have modes of collapse which are very dissimilar to that observed in the model tests.

Unfortunately, not many documented cases in which local or global instabilities are reported in the literature can offer an opportunity to test the aforementioned criteria. Thus, verification was limited to two cases in which the writer was personally involved. One of them is the Tamanduatei Sewer Tunnel, driven in Sao Paulo, Brazil, reported by Negro (1984). The tunnel was driven with a fully mechanized TBM, with a cutting diameter of 1.79 m, a ground cover of 6.2 m and through a medium to coarse quaternary loose sand with an in situ specific weight of 17 KN/m^3. An in situ elastic modulus of 4.5 MPa was estimated for this sand from static penetration cone tests carried out just above the crown elevation. The ground water level had been lowered to the tunnel haunch elevation, and some capillary rise was detected above it. Water surface tension was expected to have provided some stand up before grouting operations. Overcutting led to a void space of 5 cm behind the 10 cm thick precast segemented concrete lining. Typically, grouting was undertaken 15 hours after ring installation. Before this could take place, local collapse of the soil around the shoulders and crown was detected through six inspection holes left open in the upper segment of each lining ring under observation. Local collapse was also observed through three extensometer points installed above the tunnel crown, at 18, 34 and 48 cm above the excavation contour. The volume of material dislodged was estimated as 0.19 m^3/m, or 7.5% of the tunnel volume. Using the reasoning just presented, the limited overcutting at the crown that would bring about instability would have been 4.2 cm. Indeed, local collapse was observed with an overbreak of 5 cm. The extensometer readings indicated that it had occurred above the 5 m long body of the TBM. The length of the overcutting teeth was subsequently reduced and the overbreak was limited to about 3 cm in the crown region. No ground instability was observed thereafter in other instrumented sections.

The second case referred to is the LRT tunnel built with a TBM along Jasper Avenue in Edmonton, Alberta, reported by Branco (1981:110). Unfortunately, the geological setting of this tunnel is very particular, since the ground mass included a stiff jointed till and some dense and dry sand pockets. It is therefore a typical case where minor geological details may have a dominant role on localized instability, and thus not ideally suited to check the aforementioned approach. A roof failure involving some 1.5 m^3 (5% of the tunnel volume) of material being caved in was detected by a multipoint extensometer (ME17). Instability was limited to a fairly dry sand pocket located at and above the tunnel crown. The sand flowed into the void above the TBM leaving behind an empty cavity bounded by stiff till walls. This type of occurrance seems to have happened on other occasions along this LRT line. An in situ E value of around 50 MPa is estimated for this sand. With an excavated diameter of 6.2 m and a ground cover of 8.9 m, a limiting overbreak of 2.2 cm at the crown would be obtained using the above criteria. The void space at the crown above the TBM body amounted to some 2 cm (Branco, Op.cit:23). Instability was observed in this section, just above the cutting head of the machine. However, no instabilities were detected when the tunnel cross section was fully embedded in till free of sand pockets.

More field evidence is needed to fully validate and perhaps extend this approach which has merit in that it relates a limiting overbreak to the amount of displacement that may trigger an instability process in the ground.

If the overbreak is left unfilled and is large enough that the ground displacements have sufficient magnitudes for instability to occur, the lining will be loaded in a very different fashion to that discussed with respect to good lining contact. While in the latter a continuum mechanics approach may be acceptable, it may not be acceptable if the contact between the lining and the soil is poor or entirely lacking. Fissures in the soil may open, soil blocks may slide or fall down and rest against the poorly confined lining ring. Running or ravelling soils, such as sands, will drop, or literally flow, from the crown and shoulders, filling the space behind the tunnel haunches, from the floor upwards. The lining will gradually be loaded by the accumulation of loosened material against it, and these loads are mainly due to the self weight of such disturbed soil. This mechanism is referred to as "loosening", and is normally associated with large volumetric expansion above the tunnel as described previously. If the tunnel is shallow, this disturbed zone propagates upwards and may reach the ground surface, and complete tunnel collapse is achieved. If the tunnel is deep or if a stronger ground cover exists, an equilibrium situation may be encountered before this zone of disturbance reaches the surface. These ideas have been fairly well established in rock tunnelling practice for quite some time (see, for instance, Ritter, 1879, quoted by Steiner and Einstein, 1980:37). Terzaghi's (1946) rock load theory is based on them. Results of model tunnel tests in dense sands (Atkinson et.al., 1975) suggest that the loosening process is initiated by a wedge like zone experiencing large dilation above the crown. The complete collapse of the tunnel was sudden with very large movements. The ultimate failure mechanism showed two vertical slip surfaces bounding the unstable soil up to the surface, for tests with cover to diameter ratios between 1 and 4. The final loads that the lining will sustain are called "gravity loads" (Mohraz et.al., 1975; Ranken, 1978:50; Paul et.al., 1983:11). Their development will be basically controlled by the quality of the contact between the lining and surrounding soil. As pointed out by O'Rourke et.al., (1984:13), "if there is a close contact between the lining and surrounding soil, loosening may be prevented entirely or confined to a small distance above the tunnel crown".

The connection between the load development due to such a loosening condition and the amount of displacement allowed at the tunnel crown has long been recognized (for instance, Kommerell, 1940 and Terzaghi, 1946, as quoted by Steiner and Einstein, 1980:45 and 63). However, the existence of a critical crown displacement, associated with the instant the loosening processes (and the collapse mechanism) is triggered, is not as clearly recognized. Wong (1986:30 and 35) did recognize it and presented a simplified guideline to obtain the critical displacement. He proposed that at a certain point of the ground reaction curve for the crown (point b in his Figure 2.9), when the continuum mechanics approach fails to provide a solution due to numerical difficulties, a straight line tangent to this point should be used for extrapolation. The critical displacement would be obtained on this extrapolated line, assuming that the corresponding critical pressure is given by Atkinscn et.al. (1975) solution for local roof collapse in sand. Wong (Op.cit:30) claims that this procedure is safe, in as far as the slope of the extrapolated line is steeper than the actual ground reaction curve, which goes undefined beyond his end point b. However, he uses a critical tunnel pressure derived from the upper bound theorem of plasticity (Wong, Op.cit:35), which is an unsafe estimate of the real critical pressure (Davis et.al., 1980:399). Since the slope of this extrapolated line can actually be very flat, despite being steeper than the actual reaction curve, the use of an upper bound tunnel pressure may lead to quite an unsafe estimate of the critical crown displacement. Moreover, the local collapse mechanism at the roof appears to be a sole feature of tunnels in dense sands, and it has not been observed in any of the drained model tests carried out in Cambridge both in normally and overconsolidated clays with cover to diameter ratios smaller than 2. The use of a lower bound solution would have been a wiser choice. But even so, the extrapolation Wong adopted is still open to criticism, mainly because the result it leads to is highly dependent on the definition of the "end point" of the ground reaction curve, as provided by the continuum mechanics approach. Different finite element codes will provide, inevitably, different "end points" in the stress-displacement, even prior to the uncertainty associated with linear extrapolation.

Paul et.al., (1983:11) discusses critically the subject in an intuitive but sensible way, pointing out that for the development of the loosening condition, stiffer soils will require smaller deformations than softer soils. This is properly accounted for by the suggested criteria, as the dimensionless crown displacement (U) is a direct function of the in situ deformation modulus and, therefore, the limiting displacement bringing about instability is inversely related to the modulus. However, Paul et.al., (Op.cit), contemplated that in stiff soils these displacements "are so small", that even when the tunnelling operation is designed to prevent "excessive" ground deformation, the loosening condition may possibly be achieved. If this is the case, it means that the tunnelling operation or even the tunnelling method used was inadequate for that particular situation. Indeed, the term "excessive" should be taken in relative terms. A tolerable deformation for a softer soil may well be unacceptable for a stiffer soil, as it may represent an impending collapse condition in the latter, as shown before.

The magnitude of these gravity loads are frequently related to the weight of a cerain "height" of ground above the tunnel, expressed as nD where n is a constant that is normally empirically defined (Kommerel, 1940; Terzaghi, 1943 arching theory, etc.). The value for n may be established for a particular site, on the basis of monitored performance of tunnels previously built (for instance, El-Nahhas, 1980:189; Branco, 1981:206; Corbett, 1984:185). For design purposes, these loads are supposed to act as external vertical loads (with different distributions) on the lining in the crown region, where embedding is assumed to be lacking. Some approaches assume full embedding for the remaining part of the tunnel contour (e.g., Ranken, 1978:227; Saha, 1981:32 and 34), at points where the loading system does not lead to separation of the lining from the soil (radial tension). Some other approaches also specify lateral external loads (see Szechy, 1967:267, for a review on the subject), either assuming or not assuming the embedding action of the surrounding soil (i.e. interaction is accounted for or not).

If no embedding is assumed, then no interaction develops between the lining and the soil, and the former will be loaded only by the external gravity loads resulting from loosening and the collapse of the ground mass. Assuming that the ultimate loading system is known (magnitude and distribution), it is possible to estimate what the final lining response is likely to be. However, since the process of load build up will presumably be fairly erratic and quite unpredictable, the evolution of the lining response up to the ultimate equilibrium will also be irregular. This fact is illustrated in Figure 2.17 for a linear elastic thin circular lining, submitted to three different loading paths leading to the same final load condition. For the sake of simplicity, uniform vertical and lateral dead loads have been assumed. If the ground does not provide any embeddment, it is simple to show that the change in the vertical diameter is given by:

$$\Delta D_v = \sigma_v R^2 \frac{1 - \nu_s^2}{E_s} \left[\frac{1 + K}{A_s} + \frac{(1 - K) R^2}{6 I_s} \right] \qquad [2.22]$$

where σ_v is the current vertical stress, $K\sigma_v$ is the current lateral stress, and the other symbols have the same meaning as before. Loading path A corresponds to a proportional increase of both the vertical and lateral stresses, similar to that experienced in an ideal excavation loading, when good lining-soil contact is ensured. Loading path B represents a case where gravity loading starts acting initially on the crown, and then lateral external loads

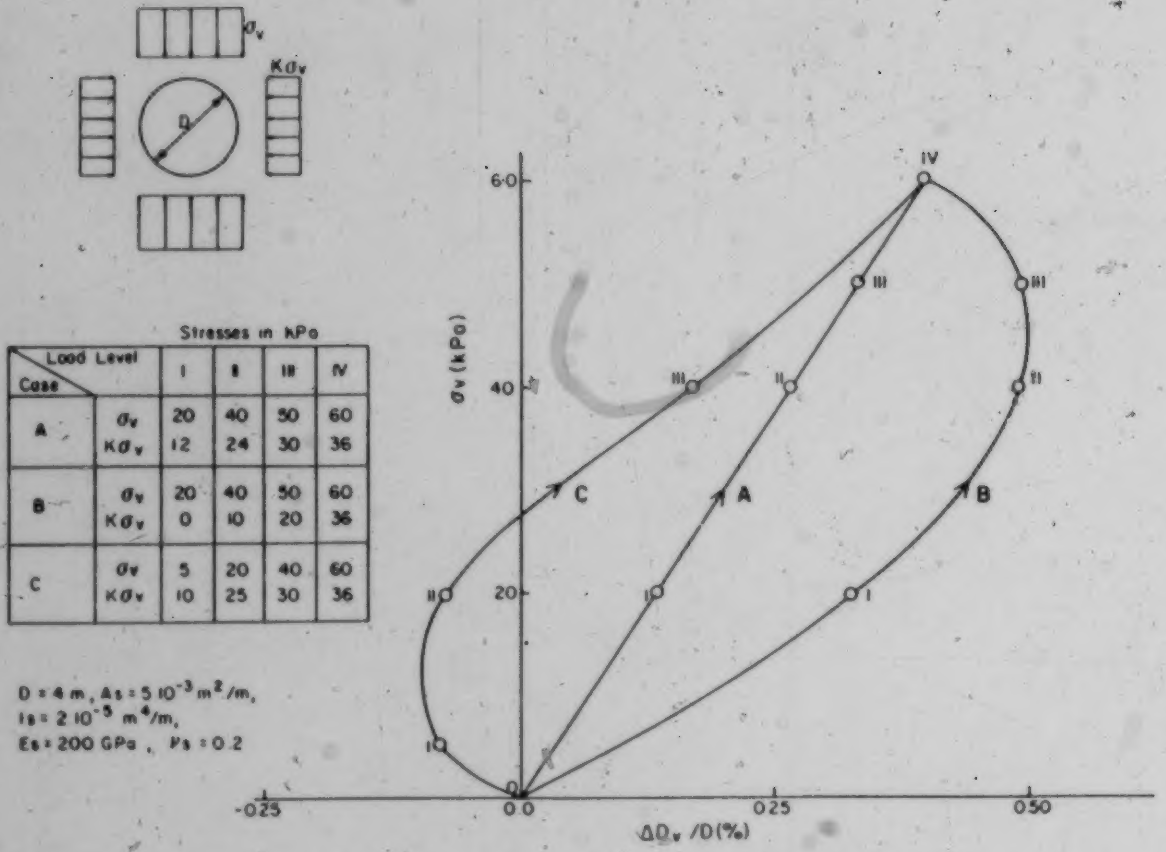

Stresses in kPa

Case \ Load Level		I	II	III	IV
A	σ_v $K\sigma_v$	20 12	40 24	50 30	60 36
B	σ_v $K\sigma_v$	20 0	40 10	50 20	60 36
C	σ_v $K\sigma_v$	5 10	20 25	40 30	60 36

$D = 4$ m, $A_s = 5\ 10^{-3}$ m^2/m,
$I_s = 2\ 10^{-5}$ m^4/m,
$E_s = 200$ GPa , $\nu_s = 0.2$

Figure 2.17 Reaction of the Support to External Gravity Loads

build up. Finally, path C corresponds to a case of initial higher lateral loading, which reverses as the deformation increases.

The lining characteristics are given in Figure 2.17. The non-linear support reactions of an otherwise linear elastic lining, result from the non-proportional increase in external loads in cases B and C, in which the ratio K varied during the load build up. This simple analysis serves to illustrate the fact that the load transfer onto the support during an idealized uncontrolled ground loosening condition, may lead to unpredictable lining responses. This in turn may cause support distortions during load build up, which can be more critical than the final ones. The knowledge of the final gravity loads, in itself difficult to ascertain. does not ensure the prediction of lining behaviour before the equilibrium situation is achieved. Therefore, the so called loosening condition should not only be avoided in practice for its detrimental effect on the ground response (low factor of safety, large losses of ground and large ground deformation), but also for its adverse impact on the lining behaviour. Locally concentrated loads on linings have been observed in soil tunnels. Their existence has been used to contend possible misinterpretation of field measurements (Duddeck and Stading, 1985). Their occurrence in the case of good ground control and good lining contact is questionable, with the possible exception of very heterogeneous ground conditions. The accuracy and representation of the measurements that led to the acceptance of these lining load concentrations (e.g., Kaiser and Barlow, 1986) is open to discussion (e.g. Corbett, 1984:35-198). The separation process of loads that are not related to ground pressures is always very complex, particularly when an expanded lining is used and a good contact is not assured at all points of the tunnel contour. However, from what was shown before, it is clear that higher bending moments can actually develop in linings where poor ground control conditions prevail and loosening or local collapse mechanisms develop. This was the case in the 3.2 m diameter Kenedalle Sewer tunnel in Edmonton, driven in till and sand,(Corbett, 1984), where the final dimensionless crown displacement, U, is estimated to have been greater than 1.5 in all instrumented sections. Therefore, based on the explanation in Section 2.3.4, the chances are that a collapse or near collapse condition was likely reached along this tunnel. If large amounts of overbreak or voids are left unfilled, as they were this in particular case [5], erratic lining loading is indeed to be expected, as well as higher bending moments (and, possibly, smaller thrusts) leading to a critical condition in terms of liner capacity. Unfortunately, attempts to quantify this erratic loading increase, due to poor ground control, are doomed to be sterile. Although it may sound like a truism, the unpredictable is not predictable in soil tunnelling engineering. De Mello (1981:212) poses the problem correctly:

---

[5] A construction void approximately 2 m in height and 3 m width was detected above the tunnel crown at the magnet extensometer No.3, according to Corbett, Op:cit:65)

"Surely, it is accepted that in tunnelling we automatically face a greater proportion of strictly localized conditions of heterogeneity and possible failure (...). Such conditions are those that must either be bearable and borne as unquantifiable risks, or must be resolved in design and construction by a 'change of statistical universe' (...). Our design engineering concern can only be with conditions that permit averaging and quantifications based thereon.(...)"

In this particular case, the "change of statistical universe" can include a large number of provisions, ranging from a reduction in overcutting, drainage and dewatering prior to construction, injection grouting, etc. If these measures do not ensure the aimed goals or are not feasible, one concludes that the tunnelling method in itself is not adequate for the particular site.

2.3.6 Three Dimensional Response

2.3.6.1 Plane Strain Representation and Three Dimensional Response

So far both the ground and lining responses have been analysed in terms of a plane strain representation, which may be reasonable for a tunnel section sufficiently far from the advancing tunnel face. Ranken and Ghaboussi (1975:3-4) using an axisymmetric numerical simulation, say that this is the case for sections at distances greater than one to two tunnel diameters from the face, if the tunnel is unlined and deep, the ground is linear elastic and the in situ stress state is hydrostatic. This suggested distance increases,with increasing amount of plastic yielding in the ground. They go further by saying that if the tunnel is lined near the face (Ranken and Ghaboussi, Op.cit:5-2),and regardless of soil behaviour, the three-dimensional stress-displacement zone extends not more than one diameter behind the leading point of the tunnel liner. Field observations by El-Nahhas (1980:237,241) in the Edmonton Experimental Shielded Tunnel, indicate that the zero longitudinal strain condition is attained somewhere between one to one and a half diameters behind the point of lining activation. This is also confirmed by tunnel heading model tests conducted in Cambridge by Casarin (1977) in overconsolidated kaolin.

The ground displacement induced by a single shift of the face during tunnel advance, resembles a "flow" of soil towards the unsupported excavation (see, for example, Ranken and Ghaboussi, 1975:3-74). Figure 2.18 reproduces the results of a 3D linear elastic analysis carried out by Heinz (1984:171), in terms of incremental displacements in the vertical plane containing the tunnel axis which are caused by an incremental advance of the face. A similar picture is observed in a horizontal plane through the axis. One notes that the longitudinal component of the displacement tends to be larger than the vertical one for points ahead of the face, with this trend being reversed as the tunnel heading region is approached. By adding the displacements of each consecutive step of face advance, it is not difficult to foresee that the total longitudinal displacements at points around and away from the tunnel perimeter, may not end up as zero, as it is normally assumed in a two dimensional representaion of a tunnel. This is confirmed by axisymmetric numerical analyses (e.g. Ranken and Ghaboussi, 1975:3-54), and by three dimensional finite element analysis (e.g. Heinz, 1984:170). As the tunnel advances, the longitudinal component of the displacements around the perimeter (against tunnel advance direction) peaks at the face, and then the soil starts moving back towards its original position. This feature was detected through slope indicator measurements by Branco (1981:112) in the Edmonton LRT tunnel. This rebound is not necessarily complete, especially in linear elastic numerical analyses (see Ranken and Ghaboussi, Op.cit:3-54 and Heinz, Op.cit:170). The practical consequences of these residual longitudinal displacements are uncertain (Heinz, Op.cit:172). If they were negligible, as suggested by the field measurements in Edmonton's LRT tunnel (Eisenstein and Branco, 1985:58), the final longitudinal strains would then be zero, as is the simplifying assumption for a 2D plane strain analyses. But during tunnel advance these strains are not zero, and therefore, the response of a strain path dependent soil would not be fully portrayed in a simplified 2D plane strain representation (Branco, 1981:112).

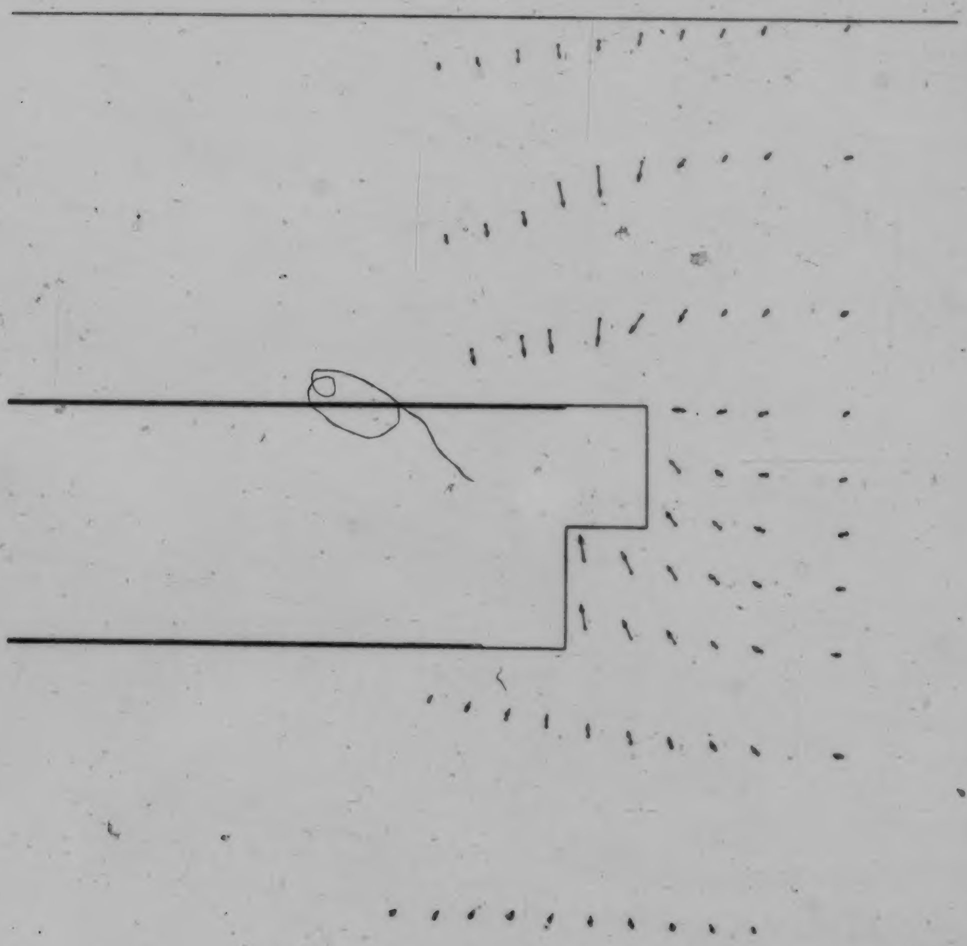

Figure 2.18 Incremental Displacement Field in the Longitudinal Vertical Plane, caused by an Incremental Advance of the Tunnel Face by Heading and Bench Excavation (after Heinz, 1984; modified)

What is important, however, is that, even if some residual longitudinal components of the displacement do remain after the tunnel face moves away, these are much smaller than the components orthogonal to the tunnel. This is particularly true if the lining is installed at a distance greater than half a diameter from the face (Ranken and Ghaboussi, Op.cit:352,354). The two dimensional transverse displacement field will predominate even more if a non-linear constitutive relationship is postulated for the soil. This is apparent from Ranken and Ghaboussi's (Op.cit:3-89, and 3-54) axisymmetric analysis using an elastoplastic cohesive and frictional model, and from a three dimensional finite element analysis using a hyperbolic non-linear elastic model for a shallow tunnel performed by Katzenbach (1981:95). Linear elastic analyses with lining installation close to the face, seem to enhance the residual longitudinal component of the displacements and also the residual longitudinal strain, and may not represent actual field conditions (e.g. Branco, 1981:112). El Nahhas (1980:236,242) derived from field displacements, longitudinal strains during tunnel advance varying from -0.4 to +0.4%, as compared with the horizontal transversel strains ranging from -3 to +3%, approximately. As mentioned before, the former decreased to zero just after the lining was expanded, while the latter remained high. Despite its narrow range of variation, the longitudinal strains may locally dominate the ground response. This is the case around the face and heading region, when they can become the major principal strain. This is tacitly recognized in practice by the usual concern of face or face-heading stability. All these facts are fully confirmed by tunnel heading model tests (e.g., Casarin and Mair, 1981:38,39).

The three-dimensional stress-displacement zone extends also ahead of the advancing face of the tunnel. The distance of influence of this zone increases as the distance between the face and the point of lining installation decreases (Ranken and Ghaboussi, Op.cit), and also, as the soil strength decreases. Numerical analysis, field evidence and laboratory model tests, show that, typically, at distances between one to two diameters ahead of the face, the longitudinal strains are close to zero.

If one assumes that, for most tunnels, the lining is activated one diameter (D) behind the face, the region between 1 to 2D ahead and 2D behind the face is where non-plane strain conditions prevail. Within this region that fully surrounds the unsupported or partly supported excavated cavity, the stress and strain changes are dominantly three dimensional. The ground and lining responses are, therefore, affected by the longitudinal strains which had been neglected in the preceding sections.

2.3.6.2 Three Dimensional Arching and Ground-Lining Response

In a non-pressurized tunnel, over a certain length, the in situ stresses around the contour of the expanded cavity are fully reduced to zero. This happens even in shielded tunnels since, more frequently than not, soil overcutting is always necessary. In the idealized two dimensional plane strain ground response, the face advance was represented by a gradual and continuous reduction of the in situ stress, but they were never reduced to zero since some support was always assumed to be installed at a certain instant. Rotation (or inversion) of the principal stresses occurs not only in the transverse plane, but also in the vertical longitudinal plane through the tunnel axis, and in the horizontal longitudinal plane. Similar to that shown in the two dimensional representation (Sections 2.3.2 and 2.3.3), the shear stress increases in order to maintain equilibrium, after the total reduction of the in situ stress at the cavity wall. Therefore, the real "arching" mechanism is truly three-dimensional as illustrated in Figure 2.19 (Eisenstein et.al., 1984).

In the preceding sections, the existence of the transverse arching has been acknowledged. Terzaghi's (1943) arching theory is one of the existing approaces to study stress transfers associated with this phenomenon. A similar stress transfer mechanism develops in the longitudinal direction of the tunnel, spanning over the unsupported heading between points ahead of the tunnel face and the installed lining. This mechanism is also recognized in tunnelling practice, being referred to as the "doming" effect. Less evident but still present is the horizontal

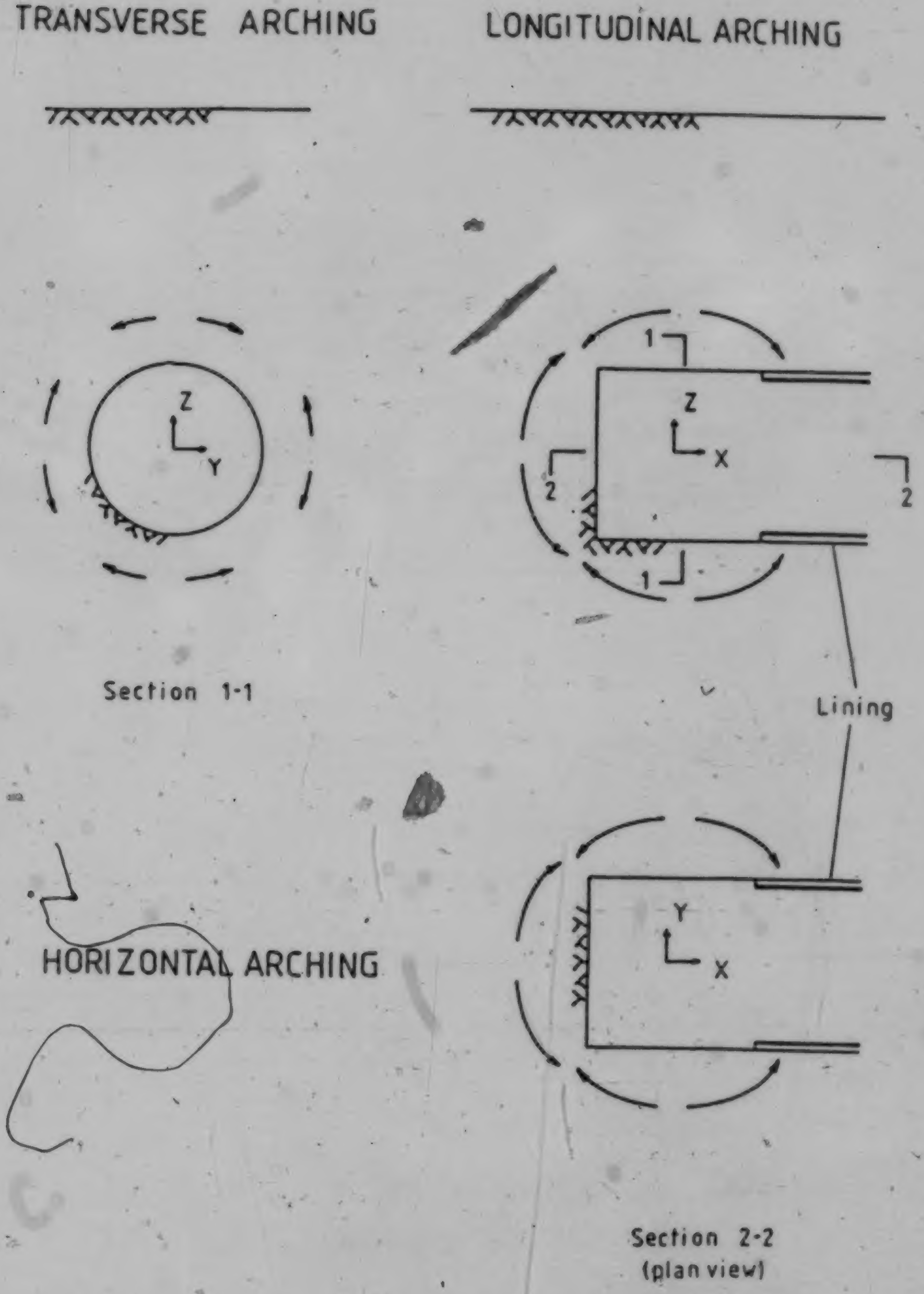
TRANSVERSE ARCHING
LONGITUDINAL ARCHING
Z
Y
1
1
2
2
Z
X
Section 1-1
Lining
HORIZONTAL ARCHING
Y
X
Section 2-2
(plan view)

Figure 2.19 Three-Dimensional Arching near the Face of an Advancing Tunnel (after Eisenstein et.al. 1984: modified)

arching, again in the longitudinal direction, but with stress transfers spanning between the lining side walls and points ahead of the face. The unsupported cavity requires a three-dimensional shear stress mobilization in order to maintain equilibrium.

As the tunnel excavation and lining installation proceed, the unsupported heading moves ahead. Stress changes in the ground are caused by this advancing heading. At some section behind the face, the stress changes stabilize in equilibrium with the lining. Ground response in terms of stress changes and displacements, is therefore related to the advance of the tunnel, even in a ground with time independent behaviour as is assumed herein.

The ground response, relating radial stress and displacements as discussed in preceding sections, fully recognizes the arching occurring transversely to the tunnel, but only that. Various authors have attempted approximate approaches to account for the three dimensional effects around the unsupported heading by incorporating some additional factor into a plane strain analysis. For instance, Lombardi (1972:373, 1973:341), introduced the concept of a core disc reaction which is able to undergo progressive weakening and which generates an internal pressure that acts on the tunnel walls. Daemen and Fairhurst (1972:366), using an axisymetric finite element analysis, introduced a "proportionality factor" obtained from the radial displacement variations along the tunnel, This factor is then used to reduce the support pressure, which is assumed to have a direct relationship with the radial displacements. Amberg and Lombardi (1974:1058) introduced a ficticious body force acting outwardly into the ground. This was to account for the deviation of the longitudinal stress trajectories associated with the longitudinal arching in an axisymmetric configuration. Panet and Guellec (1974:1165) also introduced a fictitious internal pressure but selected it in such a way that the corresponding radial displacements are equal to those experienced at the face (or at the point of lining installation) in an axisymmetric tunnel. Egger (1974:1009, 1980:313) proposed another simplification by approximating the tunnel face by a half sphere. Closed form solutions relating stress and displacements are available for a sphere in a hydrostatic in situ stress state. Egger (Op.cit) combined the latter with that for a cylinder to represent the tunnel and thus approximately account for the face effect.

All methods aforementioned have limitations that are readily identifiable. Lombardi and Amberg's (1974:476) system of loading assumes that the maximum shear planes in the ground are orthogonal to the tunnel heading walls. The arrows shown in Figure 2.19 represent schematically the maximum principal stress trajectories. Hence the maximum shear stress is not always orthogonal to the tunnel walls (Kerisel, 1980:235). The most important limitations, common to all methods, are that they do not include gravity action, or stress conditions which are not axisymmetric.

Following the Lombardi and Amberg (Op.cit) and Kerisel (1980:236) conceptual models, Eisenstein et.al. (1984:111) proposed pictorial distribution of the radial stress, σ_v, and radial displacements, u, along a longitudinal line at the tunnel crown elevation, which is reproduced in Figure 2.20(a). Field evidence in mining operations (for example, Wilson, 1981, quoted by Brady and Brown, 1985:376) suggest that there might be some stress concentration at point B ahead of the tunnel face (certainly not very high in shallow urban tunnels), this being followed by a rapid decrease of the vertical stress to zero at C. The radial stress should be zero along the unsupported heading (points C-D), provided that the lining is installed at a certain distance behind the face and no internal pressure is applied against the heading walls. With the lining installed, there should be an increase of vertical stress and a stable equilibrium situation is eventually attained at point F. Depending on the relative stiffness of the lining and the ground and also depending on the distance between the face and the point of lining installation, one could also expect some sort of stress concentration (point E) near the leading lining edge before final equilibrium is achieved at F.

The vertical displacement distribution is slightly more continuous, but again, some sort of concentration might be suggested, as indicated by the dotted line around point E.

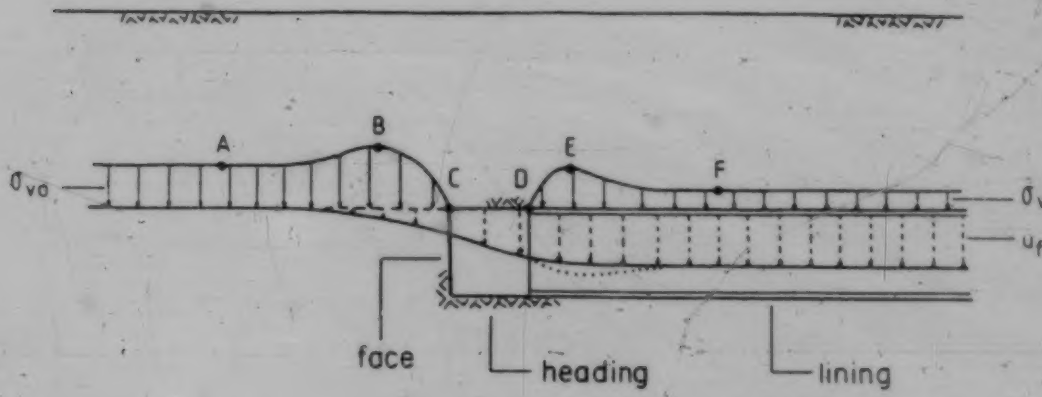
A
B
C
D
E
F
σ_{vo}
σ_{vf}
u_f
face
heading
lining

a) VERTICAL STRESS AND DISPLACEMENT DISTRIBUTION ALONG THE CROWN

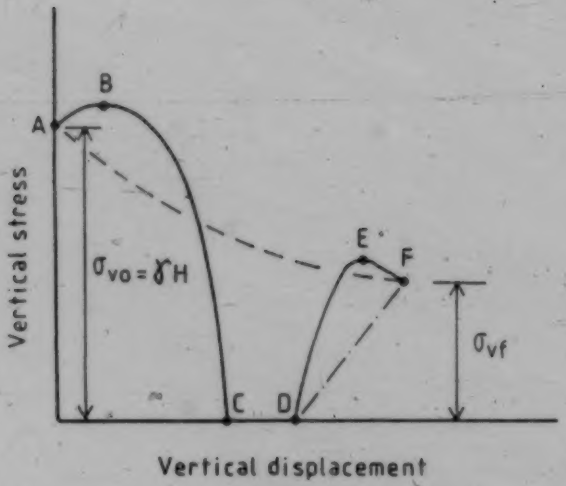

b) GROUND-LINING RESPONSE AT THE CROWN

Figure 2.20 Ground-Lining Response Concept for the Tunnel Crown (after Eisenstein et.al., 1984: modified)

The combination of the stress and displacement distributions shown enables one to draw a response curve of the combined soil and lining system, and this is depicted as the solid line (ABCDEF) in Figure 2.20(b). Although conceptual, this ground-lining response curve has the virtue of incorporating the main features of the actual three-dimensional stress transfer mechanisms. Similar responses would be expected at other points of the tunnel contour.

Departures from this idealized response would be expected in less ideal situations such as those respresented by unstable and sensitive soils, high horizontal in situ stresses, etc. However, in all cases, a drop in radial stress around the unsupported heading would be observed.

It should be stressed that the solid line ABCDEF in Figure 2.20(b), incorporates the response of both ground and lining, including their three-dimensional interaction. The portion ABC would represent mainly the ground response ahead of the face, but it is to some degree affected by the presence of the lining installed at D, by virtue of the longitudinal arching mechanism. Reciprocally, the portion DEF would be dominated mainly by the lining response, but again, it also expresses the interaction process between the support and the soil. The dashed curve, which is shown in the figure, would be an idealized plane strain ground reaction curve, and the chainsdotted one would represent the plane strain support reaction curve. The equilibrium point given by the intersection of these two latter curves, is shown coinciding with the equilbrium point F, but as explained in Section 2.3.5, this should not be the case. It was also suggested in that section that the ground reaction curve can be an envelope of equilibrium points, according to variations in the liner stiffness or in the delay of liner installation.

Some of a number of field observations supporting the concept of the ground-lining response just discussed are presented in the following paragraphs.

2.3.6.3 Evidence of Three-dimensional Ground-Lining Response

The assessment of the stress redistribution around the advancing face of a soft ground tunnel has not beeen fully explored in the field, mainly because stress measurements within a soil mass are difficult to obtain. The inevitable inclusion of a body of different stiffness into the ground, the stress sensor, and the installation effects frequently lead to unreliable results. Sauer and Jonuscheit (1976) reported one attempt to measure stress changes during excavation by the so called NATM. Twin tunnels were driven simultaneously in a fairly stiff tertiary clayey marl, locally known as Frankfurt clay, as part of the Frankfurt Underground Transit System (S-Bahn-Los6). Each tunnel had a circular profile with an excavated diameter of 7.7 m, running parallel at a distance apart of 4.9 m wall to wall, with a ground cover of 14.65 m. Stress measurements around the tunnels, and especially in the 4.9 m ground pillar between the tunnels, were taken by means of several clusters of Gloetzl pressure cell. The cells were installed about three months before tunnel construction, by being carefully packed in clay filled bags which were then lowered into boreholes. The bags in place were surrounded by poured sand and the rest of the hole was filled with clay cuttings. Further details on this instrumentation can be found in Sauer and Sharma (1977). Since disturbance of the in situ stress field is unavoidable in forming the boreholes, the magnitude of the measured stress certainly does not represent their actual values (the initially recorded cell pressures, after equilibrium was attained, varied from one-fifth to one-tenth of the overburden pressure). However, the observed pressure changes are believed to provide some qualitative idea of the relative stress changes associated with the tunnel advance.

Figure 2.21(a) shows the variation of the vertical pressure readings at a point located 0.35 m above the crown of one of the tunnels. The measurements show a stress increase above the initial value as the face approaches the measuring point. A peak is reached about a half diameter ahead of the face. As the tunnel face passes below the instrument, the readings fall fairly sharply down to a minimum which is close to zero. After closure of the shotcrete ring at the invert (at about 2.4 m behind the face), the pressure readings begin to increase, up to a value which is smaller that the observed peak ahead of the

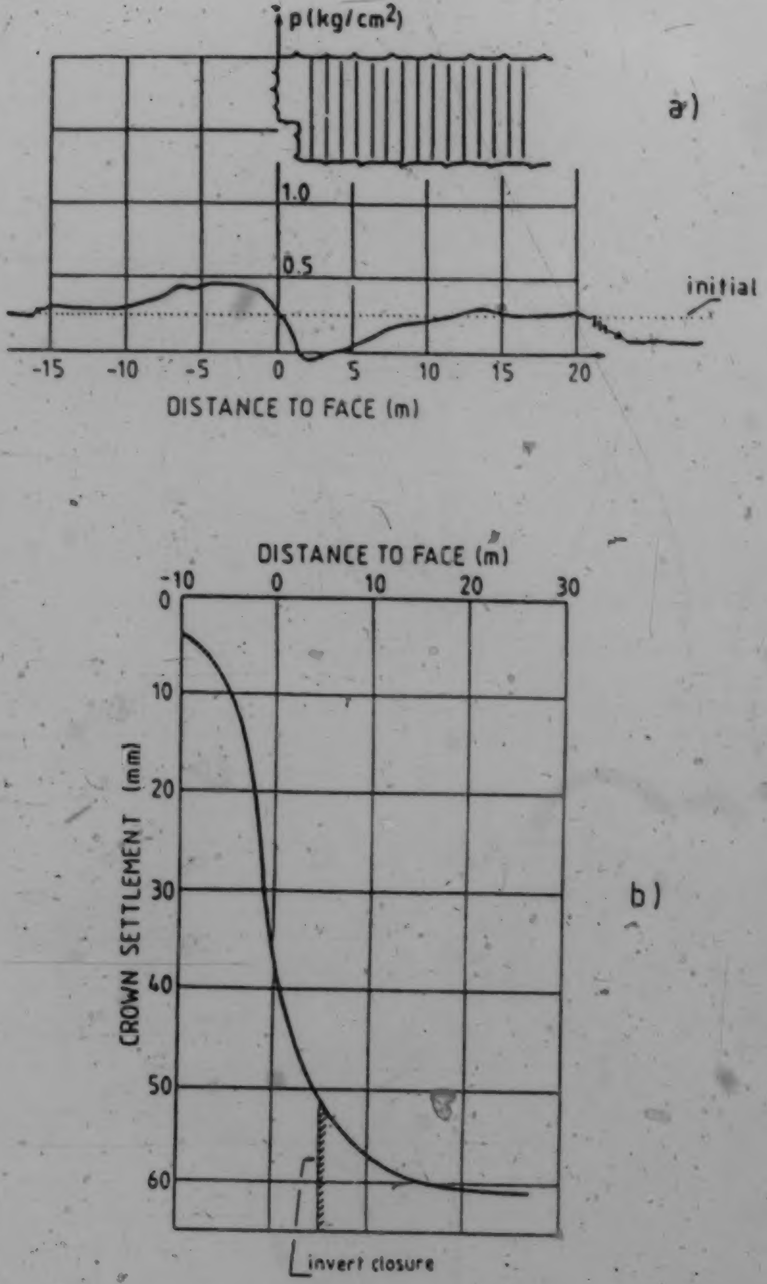

Figure 2.21 Vertical Stress and Displacement Measurements at Crown Elevation for Tunnels in Frankfurt (modified after Sauer and Jonuscheit, 1976 and Stroh and Chambosse, 1973)

face. Continued observations showed that the readings fell to a value below the initial reading after several months.

Unfortunately Sauer and Jonuscheit (1976) did not present measurements of observed ground displacements at this site. To complete the picture, data from another tunnel in Frankfurt (U-Bahnbau-Los25 Romerberg, Stroh and Chambosse, 1973) driven in the Frankfurt clay under similar conditions is presented in Figure 2.21(b). The excavated diameter and the ground cover of this tunnel were slightly less than the former (D=6.5 m and H=11.5 m). Again in this case, two tunnels were driven parallel and simultaneously at a distance of 6.2 m wall to wall. The settlements were measured at a point located 0.5 m above the crown of the north tunnel.

If the data from Figure 2.21(a) and (b) were combined, a picture similar to that shown in Figure 2.20(b) would emerge, thus confirming the three-dimensional ground-lining response concept that was postulated.

Figure 2.22(a) and (b) present similar data for the springline elevation in the ground pillar between the tunnels, as shown schematically. The Gloetzl cell was installed half a metre away from the S-Bahn tunnel wall. The horizontal displacements were observed by Chambosse (1972:Figure 75) in the U-Bahn tunnel by means of a specially designed measuring device installed from the surface, and also located 0.5 m away from the excavated tunnel wall. Unfortunately, the displacements are given as a

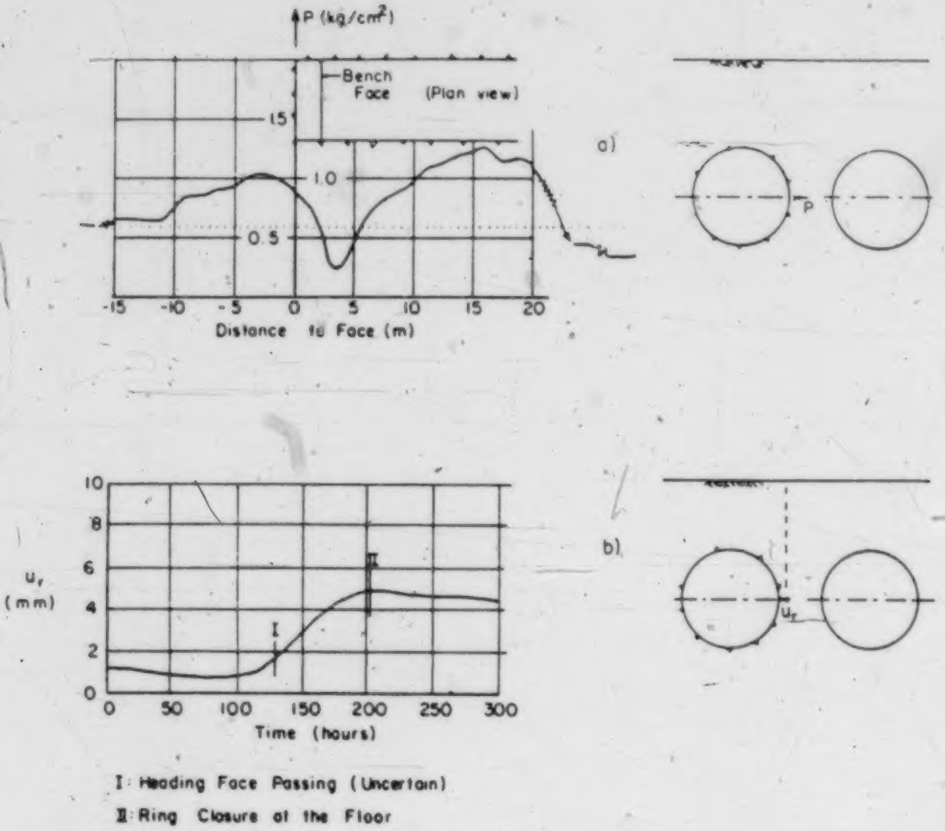

Figure 2.22 Radial Stress and Displacement at Springline Elevation for Tunnels in Frankfurt (Modified after Sauer and Jonuscheit, 1976 and Chambosse, 1972)

function of time, rather than of the distance to the heading face. However, some information is provided regarding the instant the face hits the instrumented section and the invert region being shotcreted, closing the lining ring (at a distance of 5 to 6 m behind the face). The same sort of response is observed at the springline as for the crown. One notes however, a minor outward radial displacement, after the support ring is closed (Figure 2.22(b)). From this data one may conclude that the concept postulated for the crown, is also valid for the springline region, thus confirming the "horizontal" side arching shown in Figure 2.19.

An outward displacement of the crown after lining installation is sometimes observed as was seen for the springline. This was noted during a careful internal levelling of the crown in a shallow tunnel built in Sao Paulo's tertiary soils. This tunnel was built by the NATM and is described in detail by Negro and Eisenstein (1981), Simondi et.al., (1982) and further summarized by Heinz (1984:273). A deep bench mark was installed in the access shaft located about 20 m behind the measuring points. The bench mark anchor was installed some 25 m below the floor elevation. A metallic invar levelling rod and a Wild N3 levelling instrument were used. The zero readings were taken soon after the first shotcrete layer was in place. The evolution of settlements was observed at two points in the lining crown. A minor but distinct crown heave was noted 1.5 to 3 diameters behind the face and it is supposed that this is related to the three-dimensional load transfer mechanism.

A crown heave is sometimes evident in plane strain numerical simulations of shallow tunnels with staged excavation. This was noticed by Heinz (1984:131) and Negro et.al., (1985:25), when a Lambe's (1973) Type A prediction was performed prior to the construction of a large cross section tunnel for Sao Paulo Metro, again using the NATM with shotcrete support. To some extent, a limited crown heave seems to be related to the process of numerically simulating the stages of tunnel construction in a plane strain situation. This heave may develop during invert excavation and immediate lining erection, in the two dimensional representation. In the true three-dimensional situation, the recently applied shotcrete is attached to sections already fully completed further behind, and this may generate some longitudinal bending in the upper arch shell, thus minimizing upward movement at the crown. Not to be disregarded is a possible effect of the shotcrete hardening with time, and this may also act towards reducing this trend. Despite these considerations, field monitoring of this tunnel once built, revealed some crown heave after closure of the shotcrete inverted arch (Kochen et.al., 1985:Figure 6 and Eisenstein et.al., 1986:717). The measured heave was about half of the predicted amount.

Field evidence seems to confirm that longitudinal bending of the upper shell of the open shotcrete ring occurs upon the advance of the heading face in tunnels built by the

NATM, in a heading and bench scheme. Laabmayr and Weber (1978:88) furnish measurements of pressures in the footing of the upper shotcrete arch resting on the heading floor of a Munich Subway tunnel (Baulos, 18.2). These were measured using four contact hydraulic pressure cells installed between the shotcrete and soil. The results obtained are schematically presented in Figure 2.23. The absolute magnitude of the measured contact pressures may be debatable, considering that readings of this kind of cell are very senitive to installation procedures. However, if it is assumed that the same procedure has been used in all cells installed, the results shown can be considered in relative terms: a non-uniform contact pressure distribution prevails and it could possibly be explained by the longitudinal bending of the upper shotcrete shell supporting the heading.

One could possibly argue that the measurements could have been affected by the existence of steel ribs inserted in the shotcrete (TH channel sections were used with 89 to 108 cm height and 16 to 21 kg/m). These steel sets are said to concentrate loads and a non-uniform footing pressure would then be expected with the pressure cell reading varying according to its distance from the steel sets. However, measurements taken in more recent projects in Munich (Baumann, 1985:450), where steel ribs have been replaced by lighter lattice girders, show the same tendency. In this case, thrust forces and transverse bending moments

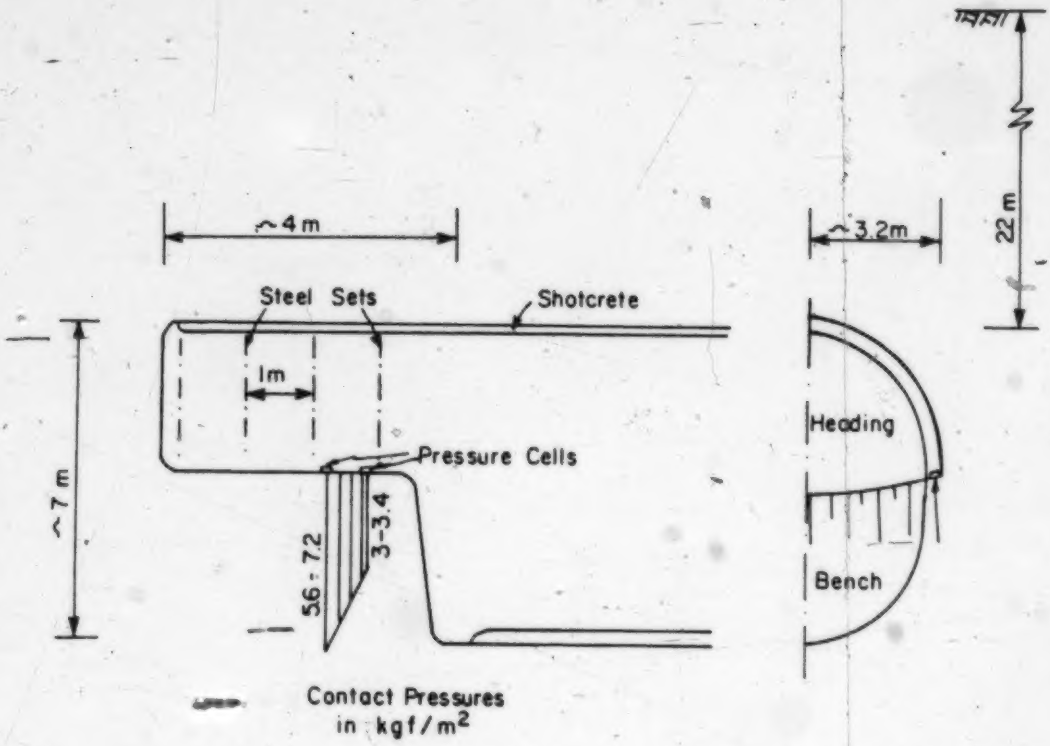
~4 m
~3.2m
22 m
Steel Sets
Shotcrete
1m
~7 m
Pressure Cells
5.6 - 7.2
3-3.4
Heading
Bench
Contact Pressures in kgf/m²

Note: Measurements of four cells, given by Laabmayr & Weber (1978:89) for heading face at Station 85. Not to scale.

Figure 2.23 Measured Footing Pressures in the Upper Shotcrete Arch at the Munich Subway (Baulos 18.2)

were measured directly in the shotcrete lining, using a specially designed embedded gauge. Except for a broad description, no detail is given on this patented equipment. Nevertheless, the measurements indicate a non-uniform thrust force concentration in sections nearer to the advancing face (maximum thrust forces of almost 100% in excess of the average value were recorded about at one diameter behind the face). The reliability of these results have been questioned by some, on the grounds that the way the measuring equipment works was never disclosed (Gais, 1985:201). But they show, once more, that lining load concentrations may be found near the advancing heading and these could be associated with the three-dimensional loading mechanism already discussed.

Load concentrations in support sections near the tunnel face were also detected in deeper rock tunnels. This was the case in the Kielder Experimental Tunnel in mudstone, (Ward 1978:155) in which higher thrusts were measured in the steel lining ring closest to the face. This unit was installed less than 0.1D behind the front and it is suspected that a smaller load concentration would have been detected if its installation had been delayed.

Three-dimensional numerical simulations confirm some of the field evidence just discussed. The axisymmetric finite element analyses by Ranken and Ghaboussi (1975) confirm the existance of a radial stress concentration ahead of the face (Op.cit:3-5,3-69,3-85). It may exceed the in situ stress by as much as 10% depending on the conditions of the analysis.

These authors (Op.cit:3-62,3-80,3-90) also found higher thrusts in the sections of the lining closer to the face. This load concentration decreased as the distance from the face to the front of the lining installation increased. For the usual distances to the point of liner installation which is normally greater than 0.5D in soil tunnels, Schwartz and Einsteins's (1980:71,168) results indicate no load concentration occurs in closed lining rings at all. They suggest that only in cases with stiff supports and short delays of lining installation that this condition is observed. The analyses also show that the lining load concentration tends to be reduced when a non-linear constitutive relationship is postulated for the ground (Schwartz and Einstein, 1980:67,162).

Schikora (1984) presented results of three-dimensional finite element analyses for non-hydrostatic in situ stress conditions, assuming a non-linear elasto-plastic constitutive relationship for the soil and for two different schemes of face advance (full face and heading and bench). Moreover, he took into account the effect of the shotcrete hardening , by assignin increasing Young's moduli to lining rings located at increasing distances from the tunnel face. He found that while no load concentration was detected in the longitudinal distribution of the average thrust forces ther was a significant thrust variation within each lining segment regardless of whether it was a closed ring or not (see Figure 2.24). The average thrust forces steadily increased from close to zero near the face to the final equilibrium value further behind. In each segment, the larger thrust forces occur in the leading edge, closer to the tunnel face, and smaller forces were obtained in the trailing edge. This seems to result from the non-uniform radial displacement distribution of the unsupported heading in the longitudinal direction. Upon further advance of the face, a discrete length of the stiffer support system is installed against the contour which will tend to deform more uniformly than the previously unsupported soil. This leads to higher loads in the leading edge (which potentially tend to displace more) and smaller loads in the trailing edge. The result is a 'saw-tooth' type of thrust force distribution as shown in Figure 2.24. The final thrust force distribution is obtained by superimposing the thrust increments due to a single step of face advance. This is shown as a shaded area in Figure 2.24a. Clearly, a continuous variation of thrust would be observed if both the lining and face continuously and not in finite amounts.

Hutchinson (1982:161) also found similar non-uniform thrust distributions within a liner segment, from an axisymmetric finite element elastic analyses. He pointed out further, that this longitudinal variation in liner thrust is mainly influenced by the delay in liner placement, but is also affected by the extent of the "softened" ground zone ahead and around the tunnel heading. If this type of behaviour is actually representative of that in a prototype, then one would expect different factors of safety against liner failure at different points within the same liner segment (Hutchinson, Op.cit:167).

These numerical results confirm the findings by Laabmayr and Weber (1978) and Baumann (1985) which were discussed previously. The role of increasing stiffness with age of shotcrete lining in this process is not yet very clear. Also to be properly assessed are the global consequences of these findings, particularly for a heading and bench scheme, during the period that the shotcrete ring is not closed at the floor. To the writer's knowledge, just one well documented case history of a shallow tunnel failure is reported in the literature, in which the upper shotcrete shell failed under signifcant longitudinal bending [*]. The 6 m diameter tunnel, with 11 m soil cover was driven through soft and saturated organic clay (MH, with c_u=20 kPa). The tunnel heading was advanced only with a fairly flat temporary invert, and closed some 3 to 4 mbehind the face (protected with a core berm). The accident was described by Cruz et.al., (1982) and was analyzed by Kochen and Negro (1985) and by Kochen et.al., (1987). Lining failure came

---

[*] Muller (1978:31) made reference to the collapse of two tunnels in soil, apparently under similar circumstances. However, the scarcity of data available does not permit any detailed interpretation. Both tunnels were driven in marls, one for a railway scheme near Paris, in 1973 and the other for a subway scheme somewhere in Germany. Similar accidents were detected more frequently in soft rock tunnels. The failures in the Pfaffenstein tunnel in Regensburg, Germany, are an example, reported by Blindow and Wagner (1978) and by Hereth (1979). In all cases collapse seemed to have been associated with excessive drivage of the heading, without closure of the inverted arch.

after very large surface settlements (up to 300 mm) were detected in the soil, above and in front of the heading. The impending ground collapse was brought about by the failure of the lining which had not been designed to withstand large longitudinal bending stresses. Although this may be an extreme case, it seems that there is a need to investigate further the mechanisms of transient lining loading during tunnel advance, both numerically and by specific field instrumentation. The work by Pelli et.al., (1986) is an example of one such attempt, and the results they obtained confirmed to some extent the phenomenon described herein. They show further, that depending on the ground and lining properties, on the round length of the excavation, on the delay of lining installation and on the in situ stress state, tensile thrust forces may develop in the trailing edge of a liner segment. To the writer's knowledge, this has not been observed so far by field monitoring in shallow tunnels, and further investigation of the issue would be of considerable interest bearing in mind its consequential effects.

2.3.6.4 Three-dimensional Ground-Lining Responses from Numerical Analyses

In order to better assess the ground-lining response concept postulated formerly for a shallow tunnel, a three-dimensional finite element analysis was performed using the program ADINA (Bathe, 1978). Details of this study were presented by Eisenstein et.al. (1984) and Heinz

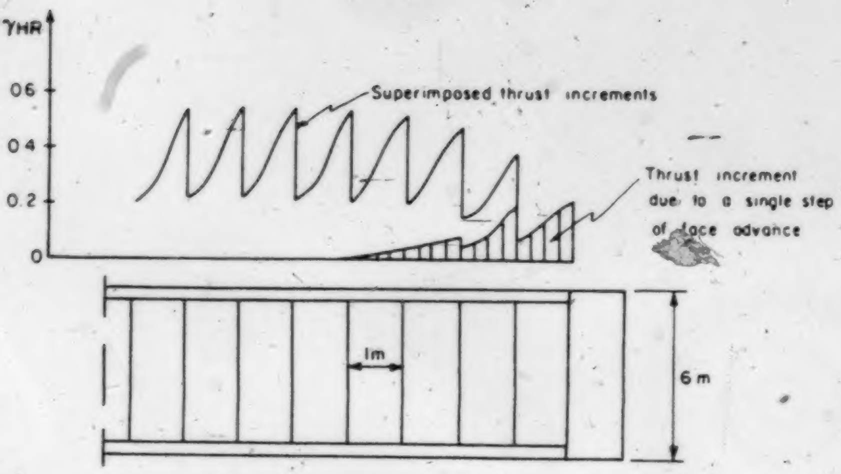

a) Full face advance

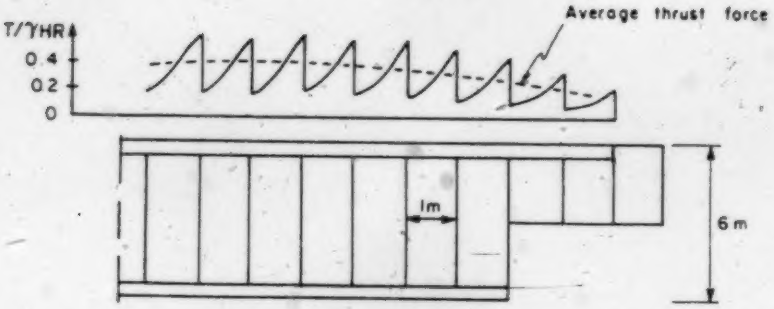

b) Heading and bench advance

Notes: Cover $H = 20$ m ; soil properties: $\gamma = 21$ kN/m^3, $K_o = 0.8$, $E = 100$ MPa, $c = 50$ kPa, $\phi = 20°$; Lining : thickness $= 0.15$ m, $E = 30$ GPa. (final) Results from 3D FE elasto-plastic analyses.

Figure 2.24 Longitudinal Distribution of Thrust Forces at the Tunnel Crown (after Schikora, 1984: modified)

(1984:176). Complementary results will be presented herein. This type of analysis was favoured in order to identify the expected distinct response for different points of the tunnel contour, all of which in an axisymmetric analysis of a deep tunnel would be identical.

Very briefly, the analysis involved the establishment of the initial stress condition by the application of gravity loads, leading to an at-rest coefficient, K_o, equal to 0.75 expressed as a function of Poisson's ratio. Linear elastic behaviour was assumed for both the soil and lining. The former had a Young's modulus increasing with depth and was equal to 13.7 MPa around the tunnel. A Young's modulus of 5 GPa and a Poisson's ratio of 0.25 were selected to represent a shotcrete lining of 15 cm thickness. The tunnel had an excavated diameter of 3.9 m and a ground cover of 6.3 m, rendering a ratio H/D of 1.62. The relative stiffness of the support given by equations 2.17 and 2.18, were C=0.034 and F=64.2. Details of the finite element mesh design and of the boundary conditions used are given by Eisenstein et.al., (Op.cit:115) and Heinz (Op.cit:180). Full face excavation was simulated using the "birth-death" option. All the elements in the region to be excavated are initially active and at the designated step when excavation is to take place, these elements are deactivated. The lining elements, initially active as a soil material are de-activated and later re-activated as concrete. Kochen et.al., (1985) discussed in detail this feature of the ADINA code, comparing it with other numerical procedures. Tunnel advance was conducted in eight steps and two runs were performed: one with the leading lining edge located at a distance L equal to one half of the tunnel diameter behind the face and another with L equal to two-thirds of the diameter.

Figures 2.25 to 2.27 show the longitudinal distributions of the dimensionless radial displacement U, defined by equation 2.16 (normalized to the in situ radial stress), and of the radial stress ratio (current stress divided by the inital stress), for points at the crown, springline and floor for L=2D/3. Displacements were taken from points at the tunnel contour, whereas the stresses correspond to the ground stresses calculated at the Gauss points of the soil elements adjacent to the tunnel perimeter. The stresses were taken from Gauss points giving the lowest stress value and were plotted against the distance between the face and the centre of the soil element.

The mechanism that causes the longitudinal variation of thrusts in the liner, also induces variations in the ground stress and displacements that lead to "wavy" longitudinal distributions, especially behind the face, after the lining is installed (see Hutchinson, 1982:168). This effect was enhanced by the size of the elements used and by the fact that in some initial and final steps, the length of excavation round was larger than that in the central portion

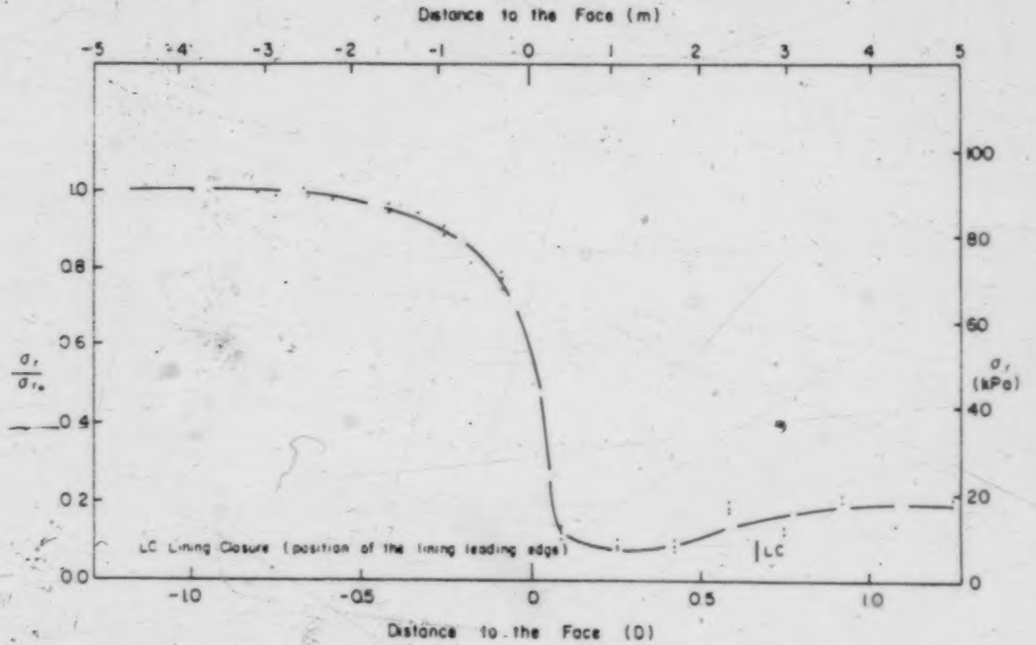

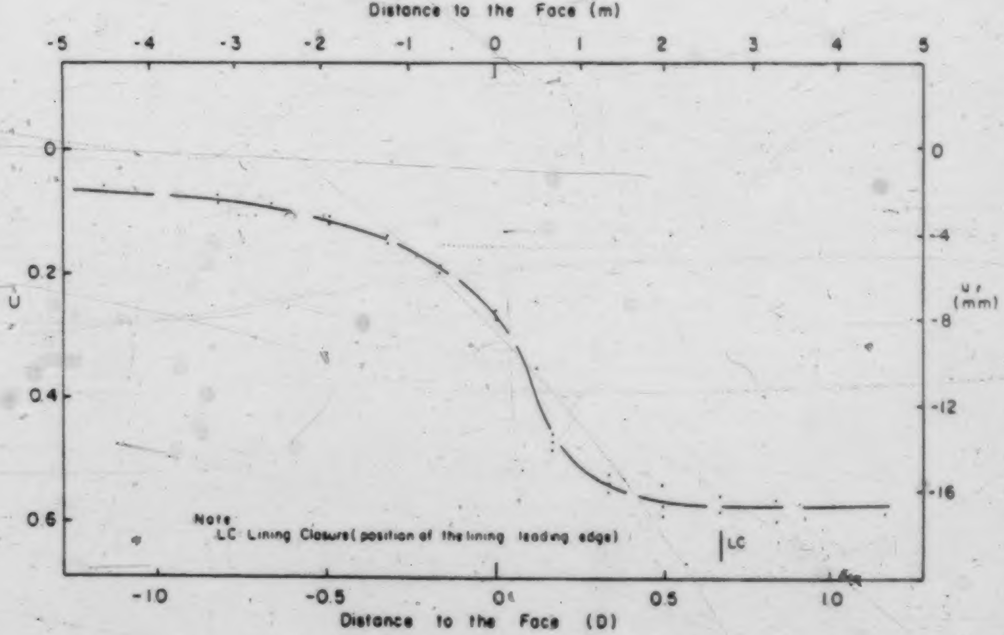

Figure 2.25 Radial Stresses and Displacements at the Crown Elevation (L/D=2/3)

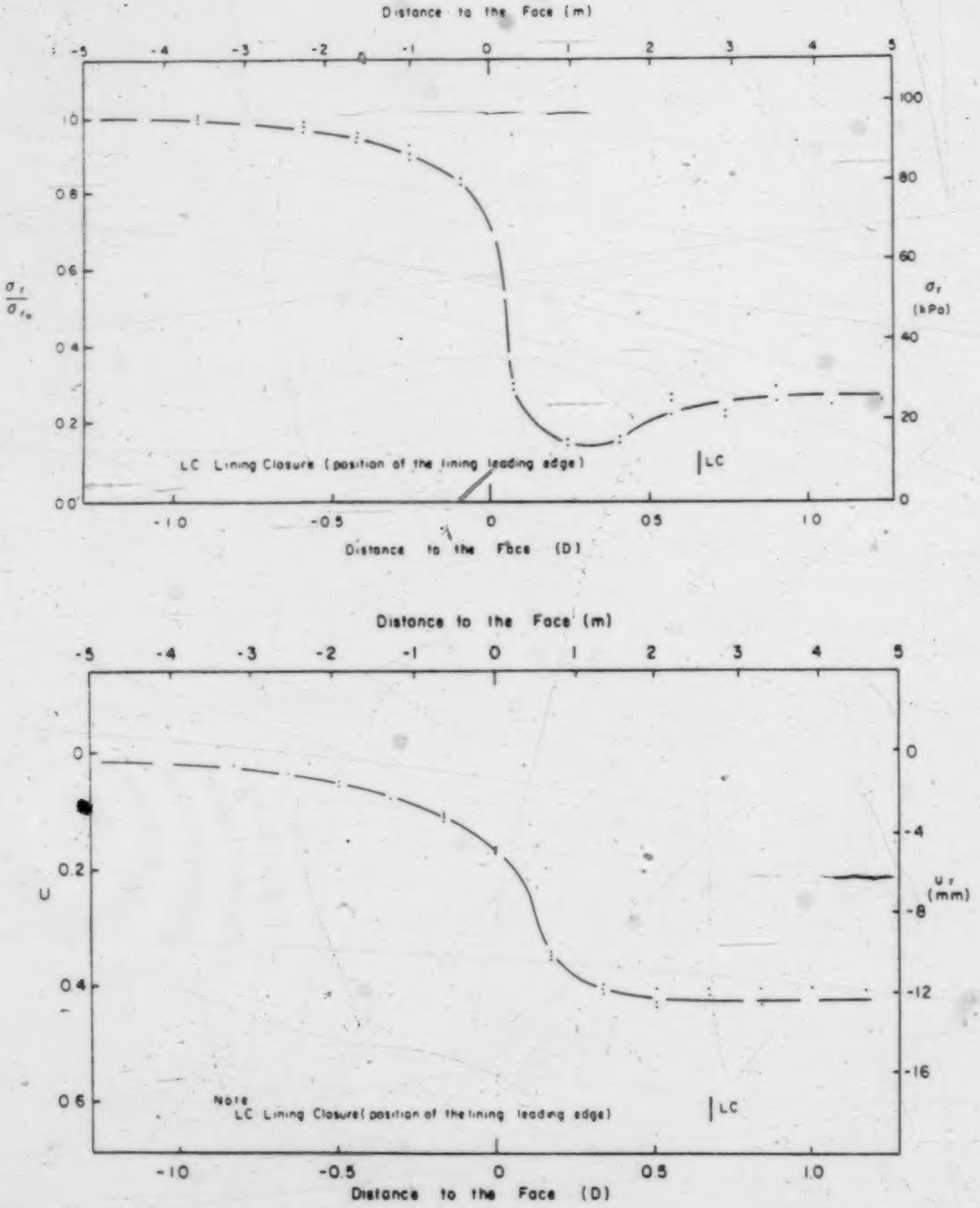

Figure 2.26 Radial Stresses and Displacements at the Springline Elevation (L/D=2/3)

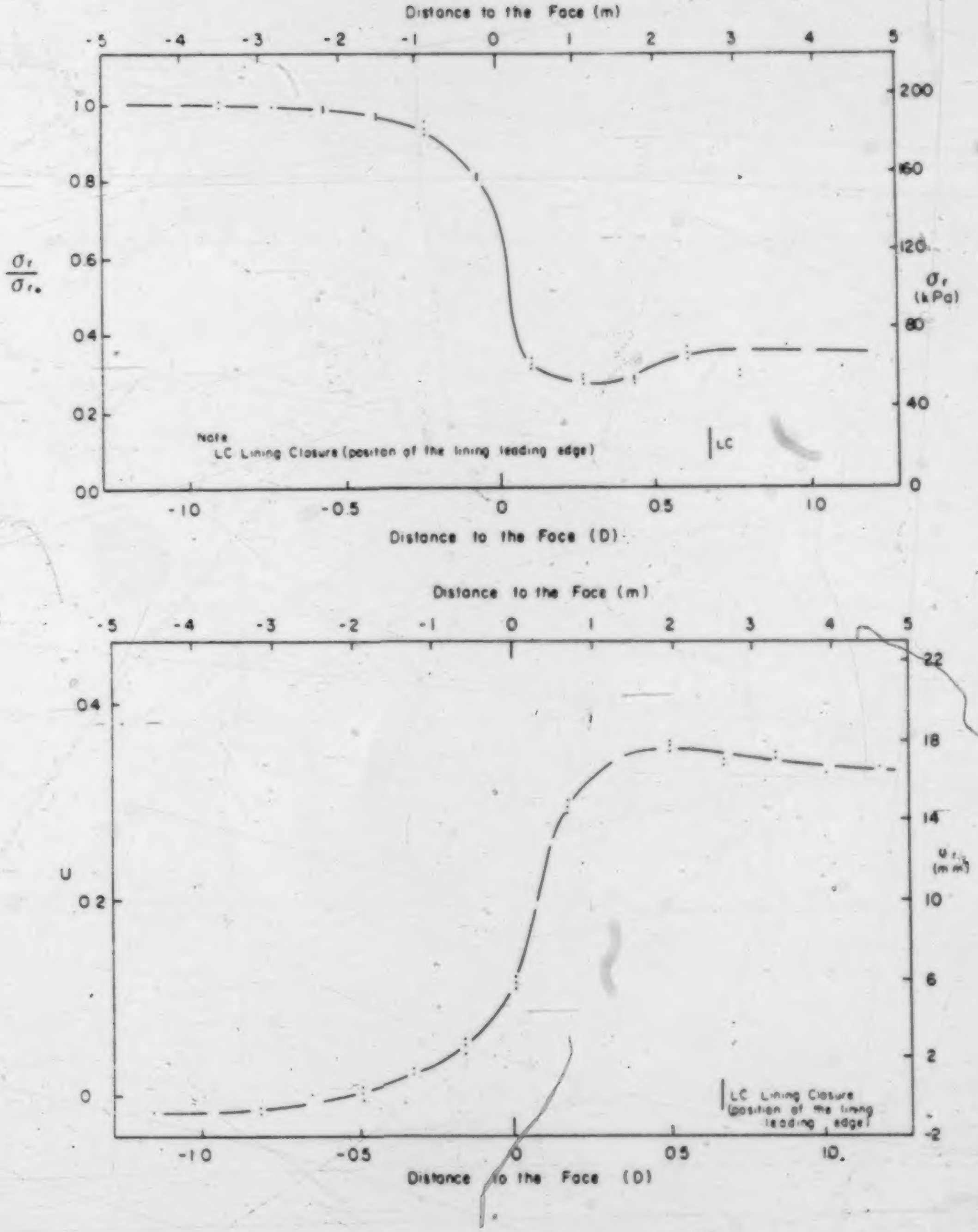

Figure 2.27 Radial Stresses and Displacements at the Floor Elevation (L/D=2/3)

of the finite element mesh. Also known to affect the results is the method used to reduce the stresses in the heading when elements are de-activated. Zones of high stress gradient, such as those found in the vicinity of the advancing heading, require small sized elements, which in turn increases the cost of the analysis considerably. To minimize these effects, only the results of the excavation of the central portion, were considered where the elements were smaller, but even so, some scatter in the stresses and displacements is present. In order to exclude this effect and therefore to obtain a response that would ideally correspond to a continuous advance of the face and a concomitan, continuous lining installation, the stress and displacement distributions were smoothed out through averaged results. This was done by superimposing output stress and displacements from three consecutive steps of the face advance, in the central portion of the mesh. and by making the face portion in these three steps coincide. The same procedure was used for points at the crown, springline and floor, for the run with L=D/2 (Appendix A). The smoothed out stress and displacement distributions found may differ slightly from that shown by Heinz (1984), a different criteria have been adopted herein.

The radial stress distributions did not show any significant concentration at any point of the tunnel contour, either ahead or behind the unsupported heading. However, it can be seen that this stress decreases sharply from its original value for points adjacent to the unsupported heading. They do not drop to zero along the unsupported span, since they refer to points at some small distance away from the excavation contour. As a further consequence of their location, these points start to partly recover stress at some distance ahead of the leading edge of the lining. If the point were directly at the excavation line, it would experience stress increase only after the lining had been placed against it and not before.

The longitudinal gradient of the radial stress and displacement ahead of the advancing heading, show different patterns for the cases studied. The rate of change in stress is clearly greater than that for displacement. Three-dimensional non-linear elastic finite element analysis by Katzenbach (1981:102,114,115) and Hutchinson (1982:564,568) also showed similar results, thus supporting these observations. Also the contrast seen between the measured stress and displacement rates in the Frankfurt tunnels (Figures 2.21 and 2.22) confirm this finding.

The first consequence of this fact is that the ground response, in terms of the stress-displacement relationship for points ahead of the face, is non-linear, even for a linear elastic ground. It results from the continuously changing geometry and boundary conditions of the problem, and is also affected by the presence of the lining further behind. Under these conditions, the principle of superposition is not valid and the problem requires an incremental excavation approach, even when the ground and liner both display linear elastic behaviour. As pointed out by Ranken and Ghaboussi (1975:4-16), the sequential excavation simulation is less significant in 3D analyses of unlined tunnels in linear elastic ground. For this, the simulation of the entire tunnel excavation in just one excavation step gives results nearly identical to those obtained when the full excavation sequence is used.

Another feature observed in Figure 2.25 to 2.27 and in those in Appendix A, is that both the magnitude and distribution of the radial stresses and displacements ahead of the face are only slightly affected by the lining installation distances, for all points in the tunnel contour. This finding was confirmed also by Pelli et.al., (1986), who used a more refined three-dimensional mesh. These authors showed also that the radial displacements are not much affected by variations in the relative stiffness of the support (C from 1.4 to 14 and F from 9 x 10^3 to 2.4 X 10^5). In other words, the soil response ahead of the face is not very much influenced by the presence of the liner. Both the displacement and stress distributions behind the face are much affected by the position of the lining, and as would be expected, an increase in the unsupported heading length, ratio L/D, leads to larger radial displacements and smaller radial stresses. The same thing was noted in a plane strain simulation (Section 2.3.5), where the delay in support installation was represented by an arbitrary reduction of the in situ stress, prior to lining activation.

The ground and lining response, in terms of the relationship between radial stress and displacement, for the three points of the tunnel contour, can be obtained from the curves shown in Figures 2.25 to 2.27 and in Appendix A. The response curves for the two distances to support installation for the crown, springline and floor are shown in Figures 2.28 to 2.30, respectively. They are presented in terms of non-dimensional stress and displacements. The dimensionless radial displacement is taken as an increment, ΔU, since some non-zero residual displacements were found in the boundary of the 3D mesh, ahead of the face. The curves simply confirm what has been described before. They are strongly non-linear and ahead of the face they are similar,(portions AB and AB'), although they do not coincide. The effect of the lining presence is felt slightly more at the tunnel crown, since the distances between curves AB and AB', for different L/D ratios, are larger than for the other points. For each point of the tunnel contour, the major differences in the response curves are seen for the portion BDs and B'D', which are more affected by the variations in size of the unsupported heading span and by the relative stiffness of the lining. Noteworthy, is the fact that the springline curve, for the smaller L/D value, reflects a characteristic outward movement, after the radial stress reaches a mimimum before the support is actually installed, as mentioned previously. A similar response is

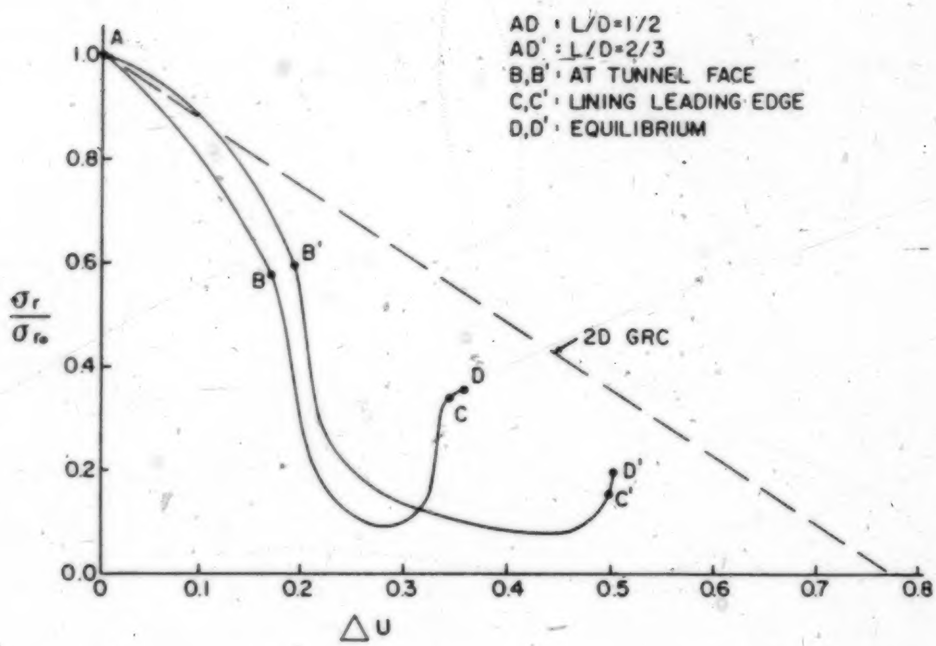

Figure 2.28 Ground-Lining Response Curves at the Crown

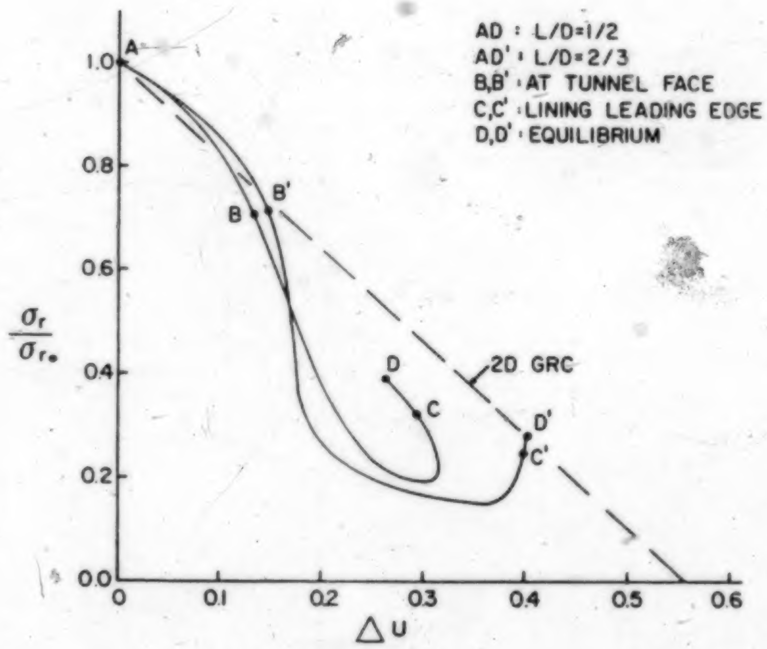

Figure 2.29 Ground-Lining Response Curves at the Springline

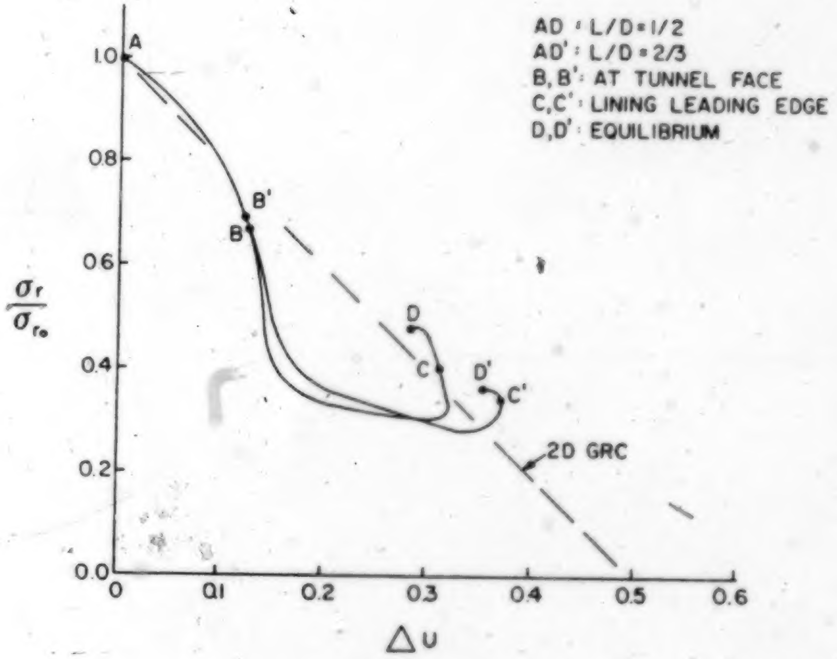

Figure 2.30 Ground-Lining Response Curves at the Floor

noted in the floor, where a small settlement is observed, after the expected heave.

For the sake of comparison, a two-dimensional finite element analysis was also performed, in order to generate the ground reaction curves for the crown, springline and floor. This is also described by Eisenstein et.al., (1984:122) and by Heinz (1984:197). Both mesh and material properties used for this analysis correspond exactly to a transverse plane section of the 3D mesh. A single step excavation was performed and no lining was installed. Stress and displacements were obtained in the same locations as in the three-dimensional analysis. The ground reaction curves thus obtained are shown as dashed lines in Figures 2.28 and 2.30.

It has been shown (Section 2.3.5) that the equilibrium points of the ground and support interaction in a plane strain simulation, do not lie on these lines. that do not account for that interaction. Therefore, it is not surprising that the equilbrium points from the 3D analyses do not coincide with these curves either. However, it seems noteworthy to point out that, with the exception of the tunnel floor point, the two dimensional ground reaction curves seem to operate as an upper bound for the equilibrium stresses and displacements of the 3D analyses. But even for the floor, the 3D equilibrium points are not too far off the 2D reaction line.

2.4 Summary and Conclusions

In this chapter the idealized behaviour of a shallow tunnel under time independent conditions was presented. An attempt was made to identify the differences between shallow and ideally deep tunnels. It was found that, depending on the criteria used, the relative tunnel depth beyond which a tunnel is said to be "deep", may vary considerably. Previous works on the subject were reviewed, and from them, two conclusions could be drawn:

(a) When studying the tunnel lining response or the behaviour of the ground immediately around the opening, the presence of the stress free ground surface can be neglected for relative tunnel depths (H/D) greater than 1.5. However, the influence of the gravitational stress gradient should always be taken into consideration.

(b) When studying the displacement field around a tunnel or the possible modes of collapse of the ground, the effect of the ground surface, as well as the action of gravity should always be considered.

Thus, a 'deep' tunnel, across which the stress field gradient becomes negligible and at which the influence of the stress free boundary surface is minimal, represents an idealization with limited practical value for the study of an urban tunnel.

Stress and Strain Changes in the Ground

The stress changes around an unlined opening in plane strain were investigated. The effects of gravity and of the non-linear ground response were discussed. The associated strain changes were then studied for certain ideal conditions. Some peculiarities of the stress-strain ground response were addressed and explained in terms of the stress changes leading to soil failure around a 'deep' tunnel. Among them are the apparent 'strain-softening' response and combined dilation ('loosening') noted after failure is reached in a frictional material. Soil failure around the tunnel may or may not lead to formation of a collapse mechanism. The results of this conceptual analysis were discussed and were extended to less idealized conditions. The consequences of the non-linear response of the ground were addressed.

Field and tunnel model test results were used to identify when the ground response to shallow tunnelling becomes definitely non-linear. It was shown that if the factor of safety against collapse is greater than 2 or 3, the ground response may be approximated by linear elasticity, but below that, a non-linear response is to be expected. Shallow tunnel construction under "good ground control conditions" involve factors of safety of about 1.5 or even less. Moreover, the path to failure in soil tunnels is short, and the degradation of safety with ground displacements is rapid. Therefore, for usual construction conditions, the soil response to tunnelling, in terms of stress and displacement relationships are typically non-linear.

The stress paths around a plane strain shallow tunnel in a non-linear ground were investigated. The prefailure stress paths were found to vary considerably from point to point around the opening, and to depend on the in situ stress state, on the relative tunnel depth and on the soil strength. If the three-dimensional stress state is taken into account, even more intricate stress paths would be observed. Evidently, it is difficult to anticipate the likely stress path. A large degree of simplification will be required in this regard when approaching a practical tunnelling problem.

The development of shear strains around shallow tunnels was examined using published results of model tests and field measurements. High shear strain concentrations were found around or at the collapse stage, their geometric pattern being mainly controlled by the presence of the ground surface and the relative tunnel depth. Despite this dependence, the shear strain patterns at collapse are all similar. Prior to collapse they are not necessarily so. These zones of high strain concentration tend to develop and propagate rapidly upon tunnel unloading. For normally consolidated soft clays, this development occurs for factors of safety less than 1.4, while for overconsolidated stiff clays and for dense sands the high shear straining becomes apparent for factors of safety less than about 1.1. The model tests indicate that there is a clear relationship between the factor of safety and the tunnel crown displacement. Moreover, they indicate that the deterioration of safety is rapid with increasing crown displacement. To ensure serviceability, these displacements should be usually less than 4% of the tunnel diameter. For this, the model test results indicate that the factors of safety should be higher than the values given above. In other words, the requirement for tunnel serviceability or for limited ground surface settlements usually seems to imply factors of safety higher than those at which formation of high shear straining is observed.

The above analysis was repeated, reinterpreting available model test results in terms of the dimensionless crown displacement, U. This parameter seems to correlate better with the factor of safety. Regardless of the test type (drained or undrained) and the soil type, U values in excess of 1.8 will generally mean a near collapse condition, with high shear strain concentration and small factors of safety. A U value of 1 or less, corresponding to factors of safety of, typically 1.5, would represent tunnelling under 'good ground control conditions' where high ground shearing will usually not be present.

Though presented tentatively, the above criterion has the merit of recognizing the dependence between factors of safety and ground displacements. Moreover, it expresses in quantitative terms, through a limiting crown displacement, the condition at which the ground stability becomes critical. Beyond it, ground control conditions cease to be 'good', as it involves ground collapses and uncontrolled ground deformations. The criterion also indicates that, under equal conditions and for the same factor of safety, a softer soil may experience larger crown displacements than a stiffer soil. Different limiting dimensionless crown displacements may exist for different soil types. The test results available did not allow a clear definition of this aspect, though they seem to suggest a higher limiting dimensionless crown displacement for softer soils.

The proposed criterion is largely empirical. Its use for conditions different from those found in the model tests, therefore, cannot be ensured. For instance, it may not be applicable to soils showing strain softening behaviour. Before further investigations on the subject are undertaken, the criterion may be used tentatively, with due care.

The development of volume changes around shallow tunnels was also examined using published results of model tests and field instrumentation. Volumetric changes in the ground, under time-independent conditions, were found to be a function of many factors, including the mean normal stress level, the shear stress level, the relative tunnel depth, the soil type and its stress history. Typical volume strain distributions around tunnels were examined, and typical responses were identified.

A conceptual model was proposed for tunnels in sand, in which the total volume change scaled to the tunnel volume, was related to the tunnel depth. The model assumes a fixed amount of ground stress release at the opening (a fraction of the in situ stresses) and takes into account the increase of the mean normal stress level with depth and the influence of the ground surface. As the tunnel gets deeper, the overall volume change increases up to a certain depth beyond which the volume changes becomes less affected by the ground surface and more controlled by the mean normal stress level. Thereafter, the overall volume changes decreases. This conceptual model is supported by some field and model test results.

Idealized Lining Action

In previous discussions, the action of the lining was reduced to that of some balancing stresses applied to the opening, in order to keep it stable. The actual lining action was then discussed, assuming a two-dimensional plane strain condition. Some extreme conditions were investigated, regarding the physical contact between the lining and the soil. In the tangential direction, a full and a no slip condition were assumed and the consequences of these assumptions were assessed. In the radial direction, conditions representing a full and an incomplete lining ground contact were investigated and were referred to as 'good' and 'poor' lining contact.

The support and ground responses were then analysed, assuming a good lining contact in an ideally deep tunnel. The lining-ground interaction was examined using available linear elastic analytical solutions. The analysis was then repeated, incorporating the effect of the gravitational stress field present in a shallow tunnel case. It was noted that the shear strength mobilization at the lining-ground interface may not be very high, decreasing as the tunnel gets deeper, as the in situ stress ratio tends towards unity, and as the lining activation inside the tunnel is delayed. The actual slip conditions may lie somewhere between the full-slip and the non-slip condition, possibly closer to the second, particularly if a good lining-ground contact is ensured.

In order to include the effect of the ground surface, of the non-linear soil response and of the delayed lining installation, the results of some finite element analyses were examined. The support response was noted to vary, as the amount of ground stress release before lining activation increased. The ground stiffness reduction associated with the increasing stress release leads to different relative lining stiffnesses and different support-ground interaction, though the same lining was used in all analyses. The compressive and flexural stiffness ratios are better described, for these conditions, in terms of the current ground stiffness.

The consequences of a poor lining-ground contact were then addressed. This condition is represented, for example, by a void left unfilled between the lining and soil at the crown region. If the size of this gap is small, then with the advance of the tunnel face, the soil may come in contact with the lining without a local or global ground collapse being observed. However, if the void space is sufficiently large, either local or global instabilities may develop. In dense sands, a wedge like portion of the roof may collapse. In fissured stiff soils, blocks bounded by pre-existing discontinuities may fall and rest on the lining. Unlike the case of good lining contact, non-uniform and concentrated ground loads may develop on the lining. If the contact between the support and ground at the tunnel walls is also poor, the ground may not offer lateral confinement to the lining.

Under these conditions, the support will be loaded by the accumulation of loosened material against it, and these loads are mainly due to the self weight of the disturbed soil. This mechanism is referred to as 'loosening' and the associated loads are described as 'gravity loads'. The development of this process, which is associated with significant volume expansion above the tunnel, involves large ground movements which may not be acceptable in an urban tunnel. This loading mechanism is associated with ground conditions approaching a collapse state.

The magnitude and distribution of these gravity loads are difficult to predict, as they cannot be estimated by classical continuum mechanics approaches. Moreover, it is also difficult to predict the extent and distribution of the voids left behind the support. Hence, the definition of the extent of the soil embedment for these conditions is uncertain.

A simple model was presented to show that even if the magnitude and distribution of the final gravity loads were known, the lining response during an uncontrolled ground loosening condition is not predictable. The support response during gravity loading depends on how these loads build up to their final values. This uncontrolled loading process can cause lining distortions which are more critical than those calculated for the final gravity loads.

The above conditions are, therefore, critical in terms of the ground response, approaching a collapse state with uncontrolled and possibly excessive movements. They are also critical regarding the lining response, which may involve large distortions or even instabilities (from lack of embedment). Consequently, they represent poor ground control conditions which are not acceptable in urban tunnelling practice. Rather than designing for them, the practitioner should identify the possibility of their development and make design provisions to eliminate them. Many ground control measures are available for that purpose. Some of them are discussed in Chapter 4.

The development of these uncontrolled tunnelling conditions depends, of course, on the soil conditions. However, it equally depends on the size of the void space left behind the support. While the identification of the soil conditions leading to such a development are readily made, the identification of the critical void size that may cause it is not. An approximate solution to this problem can be derived from the limiting dimensionless crown displacement, U, introduced earlier. If the uncontrolled conditions are related to a near ground collapse condition, the dimensionless displacement at the crown should be greater than 1.8. It will be shown in Chapter 5 that the maximum U developing ahead of the face of a shallow tunnel is usually smaller than 0.5 and that the increment of U due to lining deformation is generally smaller than 0.3 (for a good-lining ground contact). Therefore, the limiting dimensionless crown displacement increment for movement into the void space behind the lining, which might produce a near collapse condition, is equal to 1.0. From this, one could estimate a limiting crown displacement increment, and therefore, a maximum crown overcut, which could be less than or equal to the limiting value. Though approximate, this approach may serve as an interim expedient to treat the problem.

Needless to say that caution should be exercised when applying this criterion, which has been developed empirically and based on model test results of laboratory prepared soils. For instance, minor geological details are known to have an important role in localized collapse mechanisms. Despite this, the criterion was tested in two case histories and proved to yield sensible results. More field evidence is needed to further validate this approach, which has merit in that it relates a limiting overbreak to the amount of displacement that may trigger an instability process in the ground.

Three-Dimensional Tunnelling Response

During tunnel advance, the longitudinal displacements in the ground are non-zero and the actual conditions are not plane strain, as assumed so far.

Numerical analyses, field evidence and results from laboratory model tests indicate that a zone in which a fully three-dimensional stress-strain state exists, extends ahead of the advancing tunnel face. The extension of this zone depends on the distance between the face and the section where the lining is installed, and on the soil strength. Typically, at distances of one to two diameters ahead of the face, the longitudinal strains are close to zero.

This three-dimensional zone also extends behind the tunnel face. As the tunnel advances, the longitudinal components of the displacements around the perimeter (opposite to the direction of tunnel advance) peak at the face, and then the soil starts moving towards its original position. This rebound may not be complete, especially in linear elastic numerical simulations. The longitudinal ground displacements may not end up as zero, as is normally assumed in a two-dimensional representation of a tunnel. Non-linear numerical analyses, model test results and field instrumentations indicate, however, that the final longitudinal strains usually result in being very close to zero, as assumed in plane strain analyses. Despite this, during tunnel advance these strains are not zero and consequently, the response of a stress path dependent soil would not be fully portrayed in a simplified two-dimensional plane strain representation.

What is important, however, is that even if some residual longitudinal components of the displacement do remain after the tunnel face moves away, these are much smaller than the displacement components orthogonal to the tunnel. This is particularly true if the lining is installed at a distance greater than half a diameter from the face and if a non-linear constitutive relationship is postulated for the soil. Field and laboratory observations seem to confirm this. In this regard, the two-dimensional plane strain representation of a tunnel section well behind the tunnel face can be said to be valid. However, the longitudinal strains may locally dominate the ground response at sections close to the tunnel face, when they can become major principal strains. This is tacitly recognized in practice by the usual concern with face or face and heading stability.

Based on available evidence, if one assumes that for most tunnels, the lining is activated one diameter (D) behind the face, the region between 1 to 2D ahead and 2D behind the face is where non-plane strain conditions prevail. Within this region, the stress and strain changes are dominantly three dimensional. The ground and lining responses are, therefore, affected by the longitudinal strains which had been neglected in the preceding discussions.

A conceptual model for three-dimensional arching and ground-lining responses around an advancing unsupported tunnel heading was proposed by Eisenstein et.al. (1984). This model was reviewed and revised. Also reviewed were some approximations which were proposed by different authors, to account for the three-dimensional effects in plane strain analyses.

Field evidence supporting the conceptual model of three-dimensional ground response was reported, both for the tunnel crown and springline.

Other field evidence suggested the presence of the three-dimensional stress transfer effects. They refer to lining crown heave after invert closure, to some load concentrations in shotcrete supports near the tunnel face, and to longitudinal bending of the shotcrete shell at the crown before ring closure at the floor. Similar results were also obtained in some three-dimensional numerical simulations reviewed. The role of these effects in controlling the tunnel lining design has not been clearly established. Further investigation of this issue would be of considerable interest, bearing in mind its potential consequences.

The results of the three-dimensional linear elastic finite element analyses presented by Eisenstein et.al. (1984) and Heinz (1984:176) were reviewed and supplemented.

A shallow tunnel construction was simulated with two different distances, L, between the tunnel face and the leading lining edge (L=D/2 and L=2D/3). The radial stress distributions in the longitudinal direction did not show any significant concentration at any point of the tunnel contour, either ahead or behind the unsupported heading. The rate of change in stress was found to be greater than that for the displacement. These results are similar to those obtained in other finite element analyses and to field measurements in some case histories.

Since radial stress and displacement gradients in the longitudinal direction are dissimilar, the ground response in terms of the stress-displacement relationship is non-linear, although linear elastic material properties have been assumed.

Also noted is the fact that both the magnitude and distribution of the radial stresses and displacements ahead of the face are generally unaffected by the lining installation distances, for all points of the tunnel contour. Similar results were reported by Pelli et.al. (1986), who showed also that the radial displacements ahead of the face are not much affected by the relative stiffness of the support. In other words, the soil response ahead of the face is not influenced very much by the presence of the liner.

Ground-support response curves were thus obtained for points at the tunnel crown, springline and floor, in terms of normalized radial stresses and displacements. As noted earlier, the portions of these curves representing the response ahead of the face are not affected much by the lining placement position. However, behind the face, the lining placement position strongly affects the response.

Two-dimensional ground reaction curves were also obtained through a plane strain finite element analysis of the unlined tunnel, using the same material properties and a mesh corresponding exactly to a tranverse plane section of the three-dimensional mesh. It was noted that the equilibrium points obtained in the three-dimensional analysis lay close to the two-dimensional ground reaction curves, which except for the floor, seem to operate as an upper bound for the equilibrium stress and displacements of the three-dimensional analyses.

3. IDEALIZED BEHAVIOUR OF SHALLOW TUNNELS: STABILITY AND GROUNDWATER

3.1 Introduction

The idealized behaviour of shallow tunnels is further discussed herein. Two behavioural aspects, not included or superficially discussed in the previous chapter, are treated in the following sections: the stability of a shallow tunnel in soil and the role of groundwater in the ground response to tunnelling.

The discussion follows the same lines set forth earlier, in that the behaviour is studied through simple conceptual models, supplemented by results of analytical and numerical analyses. As before, the discussions will be framed within basic soil mechanics concepts. Some discussions on certain aspects are presented as mere speculative exercises, deserving further investigations to confirm or reject present interpretations.

3.2 Tunnel Stability

3.2.1 Foreword

The major interest of this study is related to shallow urban tunnels under operational conditions, in which ground displacements are to be minimized. Although this requires collapse to be precluded, the question of stability is of clear concern. It was recognized in the previous chapter that the factor of safety of a tunnel deteriorates very rapidly with increasing ground displacements and, that, despite the specification of good ground control conditions, operational factors of safety are normally low.

Even though relevant, the stability of the tunnel lining will not be addressed here. In many cases, the lack of lining stability has been attributed more to ground instability and construction defects, rather than to the lack of structural capacity.

It was pointed out in Section 2.3.3 that soil elements adjacent to the opening may fail once their strength is fully mobilized but that this does not necessarily mean that the whole ground structure is at a collapse state. Collapse means the creation of a mechanism through which a local or global disintegration of the ground mass is experienced.

Local collapse is observed in some types of soil. When a limited part of the ground mass becomes unstable, without the creation of mechanisms which extend up to the ground surface (Sections 2.3.3 and 2.3.4). This is the case of roof collapse in dense sands and instabilities associated with heterogeneous soils such as fissured stiff clays, residual soils, etc. Such local collapse may or may not trigger a global collapse. The latter is known to occur in incompetent grounds, as all soils are supposed to be, as defined in Section 2.3.5. Zones, or bands, of high shear strain develop up to the surface and a block of the ground cover becomes unstable and slides into the tunnel.

Since in most instances the installed lining has sufficient capacity to inhibit the development of a collapse mechanism in the supported sections of a tunnel, instabilities are mainly a concern in the region of the unsupported heading advance. Except in cases of poor lining contact, global instabilities are limited, in practice, to the tunnel face or to the unsupported or partly supported heading. As a result the mechanisms involved are entirely three-dimensional.

3.2.2 Three-Dimensional Stability

With the exception of soils where local collapse prevails [7], tunnel stability is mainly governed by geometric conditions. These can be defined in terms of the cover to diameter ratio, H/D, and of the unsupported heading length to diameter ratio, L/D. Depending on these ratios, two extreme collapse modes are possible, as shown in Figure 3.1. Mechanism A, corresponding to smaller values of L/D, implicates both face and roof stability. With increasing L/D, the collapse mode gradually changes to that of mechanism B where roof stability dominates. As L/D tends towards infinity (an unsupported tunnel), mechanism B becomes a two-dimensional situation. If L/D tends towards zero (fully supported tunnel except for the face), then tunnel collapse is controlled by the face stability.

---

[7] Atkinson (1976) (quoted by Mair, 1977:8), showed that the differences in behaviour at collapse of 3D tunnel headings and 2D plane section tunnels is not significant for dense sands.

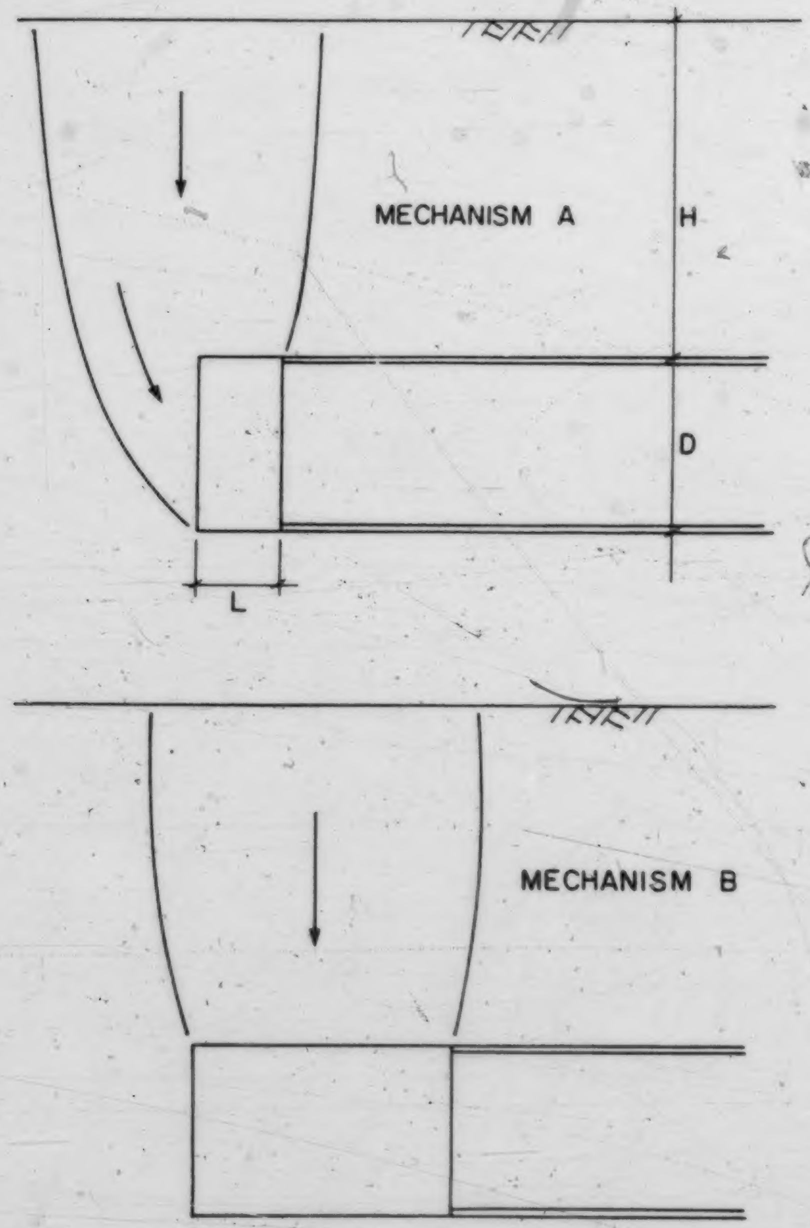
MECHANISM A
H
D
L
MECHANISM B

Figure 3.1 Three-Dimensional Collapse Mechanisms in Shallow Tunnels

The issue of face stability was studied by Broms and Bennermark (1967) who used the closely related solutions of both bearing capacity of piles (e.g. Skempton, 1951) and stability of deep excavations (e.g. Bjerrum and Eide, 1956) to investigate the undrained stability of tunnel faces in saturated clays. These authors used a semi-empirical approach which proposed that the stability ratio that leads to face collapse of a fully lined and deep tunnel is given by:

$$N= \frac{\sigma_o - \sigma_c}{c_u} = 6 \text{ to } 8$$

The symbols have the meanings given in section 2.3.3. They further suggested that the lower value should be taken as a safe reference for face stability evaluation.

Undrained static model tests of 3D tunnel headings (Casarin, 1977:51) and centrifuge experiments (Mair, 1979:116) in overconsolidated kaolin ($K_o \approx 1$) confirmed the collapse mechanisms shown in Figure 3.1. Moreover, these tests showed that there is increasingly more displacement at the crown and less at the face as the ratio L/D increases (Casarin and Mair, 1981:36). These tests, as well as drained tests by Casarin (Op.cit:51), also demonstrated that tunnel stability decreases as the unsupported heading span increases. This is indicated by their results which are gathered together in Figure 3.2. For a given overload factor (i.e., a fixed tunnel depth, a fixed internal pressure and a fixed c_u), the factor of safety against collapse (given by equation 2.14), decreases with N increasing. As depicted in

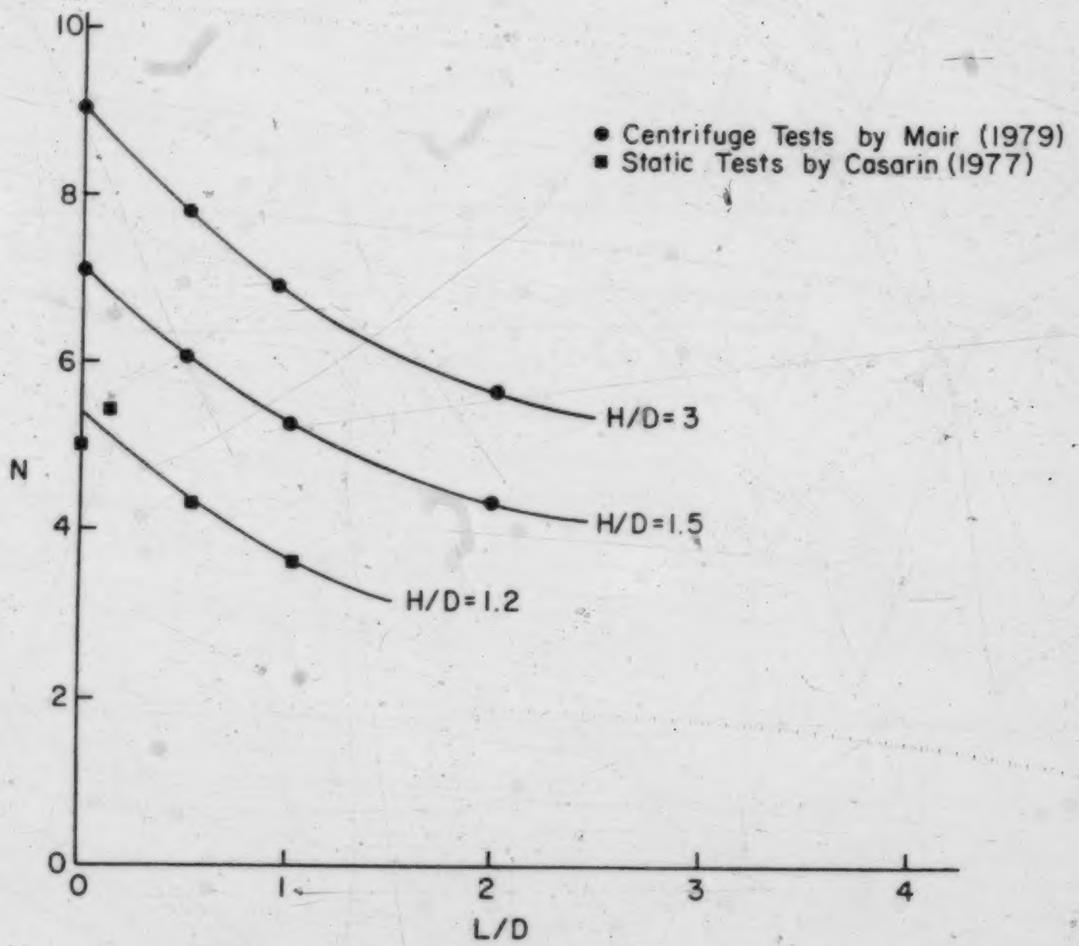

$$N = \frac{\sigma_o - \sigma_i}{Cu} \text{ at collapse}$$

Casarin's soil : OCR = 3.5, Cu ≅ 60 KPa, k_o = 1

Mair's soil : OCR = 2-4, Cu = 20-25KPa, k_o = 1

Figure 3.2 Influence of Geometric Conditions on the Undrained Stability of Tunnel Headings in Overconsolidated Kaolin

Figure 3.2, N is inversely related to L/D and proportionally related to H/D. For L/D tending to infinity, N may be obtained from plane strain model representations and as L/D tends to zero, N will approach the condition analysed by Broms and Bennermark (1967).

Results of some model tests for L/D=0 situations are included in Figure 3.3. It is interesting to note that, as pointed out by Casarin and Mair (1981:40), the stability ratio N for the face of a fully lined tunnel tends towards an approximately constant value at a certain cover ratio. For H/D greater than 1.5, the stability ratio N at collapse is within the range given by the Broms and Bennermark (1967) solution, which had been formulated for an ideally deep tunnel. In other words, a tunnel with a cover to diameter ratio greater than 1.5 can be approximated by a deep tunnel solution.

The theoretical assessment of the three-dimensional stability conditions can be approached by solutions based on the Lower Bound (or Safe) and Upper Bound (or Unsafe) Theorems of Plasticity. Examples of upper bound solutions are presented by Casarin (1975:65-69). For three kinematically admissible mechanisms in a frictionless and cohesionless soil, he produced solutions for both mechanisms A and B with varying degrees of accuracy. Davis et.al., (1980), furnished lower and upper bound 3D solutions for face stabilty (L/D=0) in frictionless soils. Muhlhaus (1985) presented a lower bound 3D solution for stability assessment

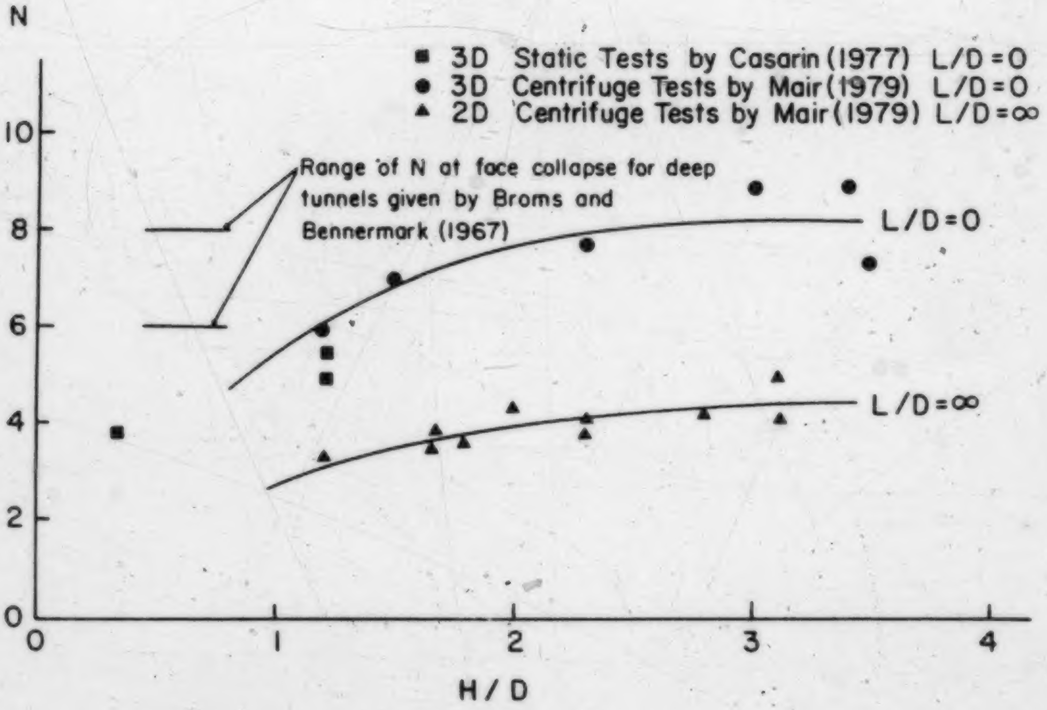

$$N = \frac{\sigma_o - \sigma_i}{C_u} \text{ at collapse}$$

(See preceding figure for soil properties)

Figure 3.3 Undrained Stability of Fully Lined and Fully Unlined Model Test Tunnels in Overconsolidated Kaolin

of the unsupported heading (L/D not equal to 0) for a cohesive, frictional soil. These plasticity solutions appear to reasonably bound the actual collapse conditions seen in a number of model tests and in at least one subway tunnel (Kochen and Negro, 1985), that collapsed according to mechanism A. This case history was briefly mentioned in Section 2.3.6.3.

The assessment of actual stability conditions in the field is not always simple. The critical dimensionless crown displacement, U, of 1.8 suggested in Section 2.3.4.3, could serve as a criterion to identify impending stability problems. However, it has been derived from plane strain model tests and its use requires the knowledge of the in situ deformation modulus of the ground mass, which is not always available. Some prefer to follow the distribution of vertical displacements in the tunnel cover between the crown and the surface, especially in relatively shallow tunnels. A zero or near zero vertical straining condition within the cover depth could represent a collapse or near collapse situation, if the soil cover moves as a rigid block. However, some soils exhibit appreciable volume changes upon shearing, which may lead to misinterpretation of this model. Moreover, possible volume changes due to soil drainage and consolidation of the tunnel cover, may cause a reversal in the distribution normally expected in a homogeneous, time independent material. Resulting surface settlements may end up being larger than the crown settlements without any sign of impending ground collapse. The situations above have been identified in a number of case histories.

Perhaps a promising practical criterion for the detection of instability problems in the field, is that proposed by Negro and Kochen (1985), and consists of inspecting the longitudinal distribution of the settlements at the crown elevation similar to the one given in Figure 2.25. If field measurements allow this curve to be obtained, then it is possible to estimate a longitudinal distortion index given by:

$$\gamma(x)=\mathrm{LDI}(x)=\frac{\delta u(x)}{\delta x}$$

where, u(x) is the displacement at a point x. This ground distortion is a shear strain, which relates to the slope of the settlement trough, and can be interpreted as a measure of the shear strength mobilization of the soil. Therefore, it can be related to the tunnel stability condition, allowing one to identify incipient collapse mechanisms.

Figure 3.4(a) depicts the settlement and distortion distributions for a stable ground condition. The longitudinal distortion distribution resembles a Gaussian normal probability curve. If some instability process is triggered around the tunnel heading and face, a marked change in the shape of this curve is noted, even for a minor change in the shape of the settlement curve (Figure 3.4(b)). The magnitude of the maximum LDI could be taken as an index of ground control during heading advance, by referencing it to some critical shear strain. For saturated clay, the critical shear strain would be $2c_u/E_u$ where E_u is the undrained inital tangent deformation modulus. However this criterion which is similar to that proposed by Sakurai (1981:279) says very little about the overall stability condition of the tunnel, since it may merely give an indication of some localized ground failure. This can occur without necessarily bringing the tunnel to a collapse state.

The distribution of the longitudinal distortions rather than its magnitude, furnishes a clearer indication of the overall stability of the ground cover. A minor instability trend, which otherwise goes undetected, is reflected by appreciable changes in the shape of the distribution: the LDI decreases in some regions, perhaps becoming negative at some points and increasing somewhere else. Such changes in the distribution pattern is a sign that a collapse mechanism is being formed.

The static 3D tunnel heading model tests by Casarin (1977) may be of assistance to check the proposed criterion. Figure 3.5 furnishes details of the test conditions. Variable water pressures were used to simulate a surface load that would give the field stress, σ_o, and provide an internal pressure σ_i, in the tunnel. An overconsolidated kaolin was tested up to undrained failure by increasing the pressure difference $(\sigma_o - \sigma_i)$. Further details of the testing procedures can be found in Casarin (Op.cit) and Casarin and Mair (1981). The longitudinal distortions were calculated from the vertical components of the measured

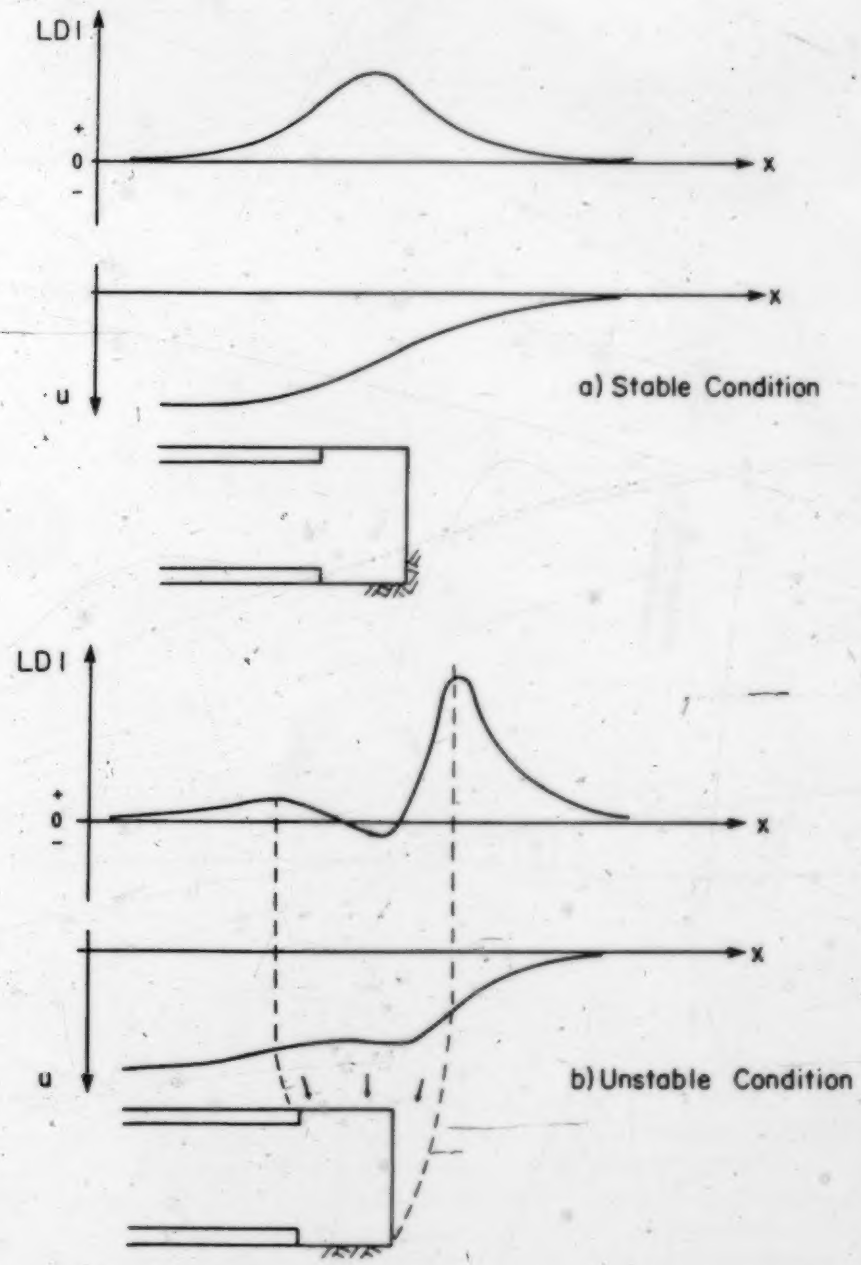
LDI
+
0
-
x
x
u
a) Stable Condition
LDI
+
0
-
x
x
u
b) Unstable Condition

Figure 3.4 Distributions of the Longitudinal Distortion Index Along A Stable and an Unstable Tunnel

displacements from radiographs, along a horizontal line AA situated at a distance of about a half diameter above the crown elevation. The solid line distribution was obtained from the intial displacements measured just after cutting and lining the tunnel. It represents, therefore, the ground response under stable conditions, prior to the loading which lead to failure. The broken lines correspond to the distortions calculated from the additional measured displacements, which occurred after increasing the pressure difference. These are added to the initial displacements caused by the tunnel excavation. They represent the longitudinal distortions at two loading stages, which correspond to factors of safety of 1.30 and 1.09. A very pronounced change in shape of the LDI distribution is noted with decreasing stability. Despite the fact that the model test results are directly related to the stability of a stationary tunnel heading under increasing pressure difference ($\sigma_o - \sigma_i$), it is believed that the overall stability of an advancing heading is fundamentally the same (Casarin and Mair, 1981:43).

The criterion above was also tested by Kocken et.al., (1987) in a subway tunnel in Sao Paulo, which collapsed according to mechanism A (see Section 2.3.6.3). By analysing, after the event, the settlements measured in six surface monuments distributed at approximately one tunnel diameter spacings along the tunnel axis , it was possible to note a change in the longitudinal distortion profile two

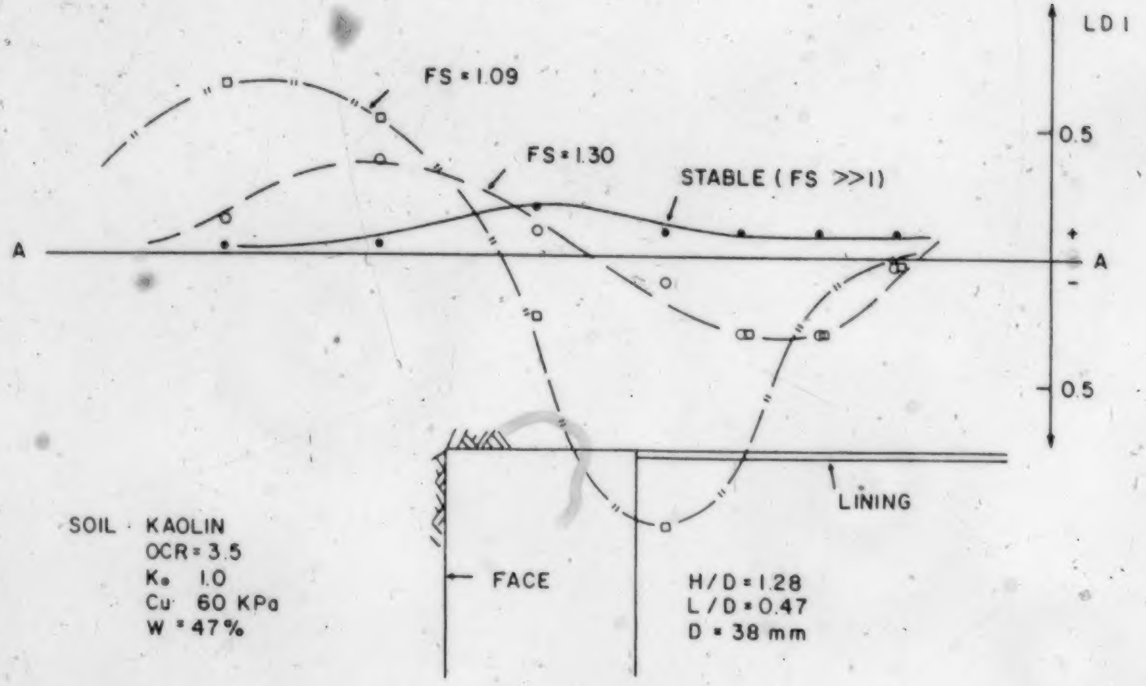

Figure 3.5 Longitudinal Distortions above the Crown of a Model Tunnel Test (based on Casarin, 1977)

days prior to the collapse, at which time the face had advanced an additional 2.4 m. Once the LDI became locally negative, a full collapse condition had already developed. A much clearer picture could have been established if the settlement points had been located closer to the tunnel crown elevation, and not at the surface.

Horiuchi et.al., (1986:756) independently developed a similar approach, using the same longitudinal distortion index. However, they preferred to relate it to some limiting index and proposed that the LDI should be calculated at a fixed point, for different positions of the tunnel face. For the reasons revealed previously this approach may not be as effective and as general as relating to the change of the LDI longitudinal distribution with tunnel advance. However, if properly calibrated for an individual site it can be proved useful as shown by Horiuchi et.al., (Op.cit). They applied their method to a large cross section tunnel built in Tokyo, through fine to medium, uniform, alluvial sand. The ground water table was at or below the springline elevation, creating flowing sand conditions which were ultimately controlled by prompt application of a sprayed chemical coating and shotcrete. The criterion was tested and calibrated against a global collapse situation of the tunnel heading, which had been experienced at the early stages of construction. At the time of collapse, the heading had been advanced with a temporary invert, some 15 m ahead of the lower bench face. The distortion index was calculated from settlements measured through a horizontal inclinometer installed 3 m above the crown. The maximum LDI value found just before the unstable condition occurred, amounted to 1.3% (about 0.7% at ground surface). In the case of the collapsed subway tunnel in Sao Paulo, the maximum LDI found at the surface amounted to 2.5%, just prior to the failure of the organic clay cover.

Horiuchi et.al. (Op.cit:756) also proposed another monitoring index for stability of the ground. This is calculated from the third derivative of the longitudinal settlement profile. If the ground cover can be approximated by an elastic beam with a flexural rigidity, EI, and a sectional area, A, then it is possible to estimate the shear force and shear stress from its deflection curve. However, the evaluation of the third derivative requires the longitudinal deflection curve to be defined from very closely spaced settlement measurements. Also this evaluation cannot be performed if the data is too scattered. This imposes a serious restriction in using standard deep settlement point data for the evaluation of this shear index. Horiuchi et.al. (Op.cit) used data from the horizontal borehole inclinometer and calibrated this new index for the same tunnel site, finding again a good correlation with the ground stability condition. This enabled them to define a limiting shear index. The disadvantages of this approach are clear. Moreover, the need to use a continuous monitoring device for the assessment considerably reduces the practicality of the suggested approach.

3.2.3 Two-Dimensional Stability

In spite of the fact that the actual stability condition of a tunnel exhibits a three-dimensional nature, the study of the collapse mode of a plane strain tunnel does have some practical as well as academic interest.

The theoretical assessment of the two-dimensional stability condition of the ground around a circular opening, can also be approached by plasticity solutions (upper and lower bound theorems). Lower bound solutions are sometimes formulated using the method of characteristics (Davis, 1968:354). Examples of these solutions are those presented by Davis et.al. (1980) for frictionless soils, by Atkinson and Potts (1977) for cohesionless soils, by Caquot and Kerisel (1956), D'Escatha and Mandel (1973) and Muhlhaus (1985) for cohesive and frictional soil, and others. The validity of the assumptions made and the accuracy of the solutions provided are discussed in other sections of this thesis.

The stress changes imposed on an element of soil adjacent to the plane strain circular opening have already been discussed (Sections 2.3.2 and 2.3.4). Figure 3.6(a) illustrates the stress path of a soil element 'P' at the crown of the opening, replotted from Figure 2.3(a), the same assumptions made as before. A non-hydrostatic in situ stress condition (K_o<1) has been assumed, and the soil was assumed to be cohesionless. As before, the initial condition is represented by point A, and local failure is approached at C. If the tunnel is shallow, a collapse mechanism may develop at D, or if the tunnel is deeper the collapse will be nearer point E. Here, the soil deformations are unrestrained and the displacements are very large. The evolution of the ratio K, horizontal to vertical stress at P, is shown in Figure 3.6(b). This ratio increases from K_o<1 at A and K approaches K_p at the onset of a passive type failure. If no support is provided, the stress path travels along the failure line, the ratio K remains constant and equal to K_p. If it is assumed that the tunnel is in a dense sand and is fairly deep so that it collapses at E, there is evidence showing that the collapse is initiated with the failure of a wedge shaped block of soil, sliding from the roof, as illustrated in Figure 3.7 (Atkinson et.al., 1975:84). The internal tunnel pressure at this instant could be approximated by an upper bound solution. The associated flow rule ensures that the dilation angle, ψ, is equal to the friction angle, ϕ, and this allows the wedge block to move downwards, dilating at such a rate that no separation occurs along the sliding surfaces. This is clearly an approximation of point E in Figure 3.6. Actually, the angle of dilation is smaller than the friction angle and the wedge block separates from the rest of the ground mass, and falls down. From point E onwards, the continuum mechanics approach

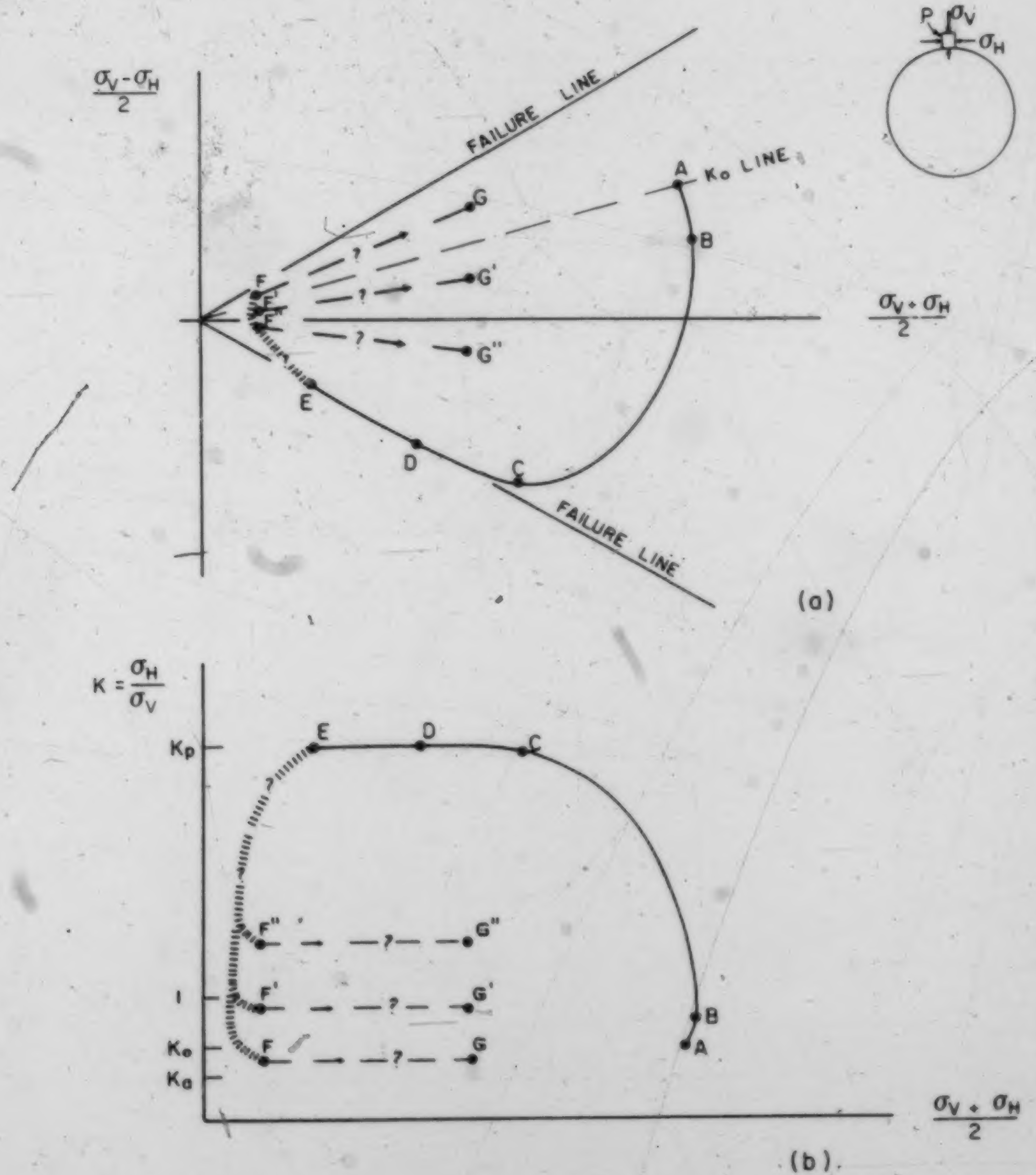

Figure 3.6 Stress Paths and Stress Ratio of a Soil Element at the Tunnel Crown

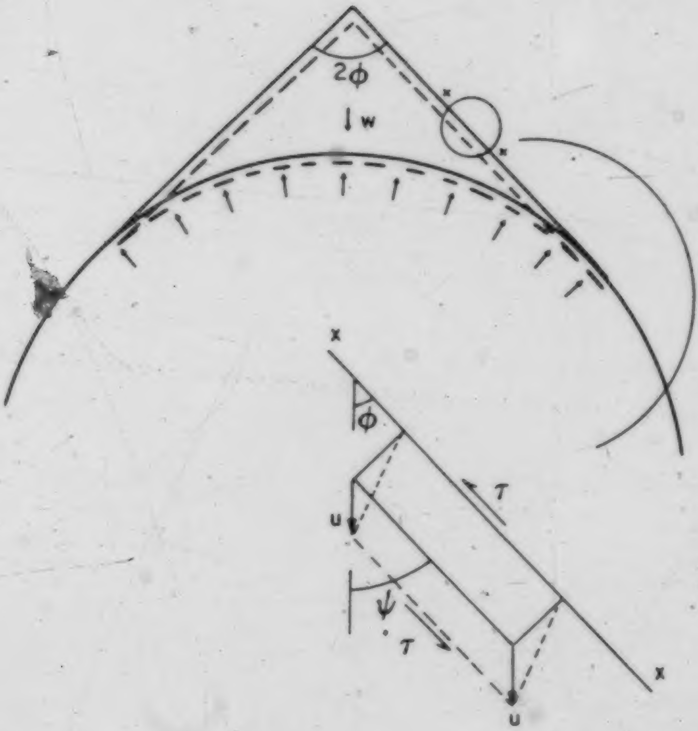
2ϕ
w
x
ϕ
T
u
ψ
T
x
u

Figure 3.7 Local Collapse at the Roof of a Deep Tunnel in Dense Sand

is no longer applicable and the stress changes occurring in the soil cannot be determined. For these reasons, the following discussion should be taken as a mere speculative exercise.

Assume that after the stress release has been applied inside the opening, an ideally stiff lining had been installed. Assume also a that poor lining contact exists all around the tunnel contour, so that, up until point E the soil does not come in contact with the rigid lining anywhere. The falling block of soil at E experiences a sudden displacement, which is equal to the amount of void remaining behind the liner at the crown. The block rests against with the support and a new equilibrium situation due to this is achieved at any of the three F points shown in Figure 3.6(a). Assume now that this local ground collapse triggers a progressive failure above the tunnel crown, so that the expanded soil cover "loosens" and the failed material accumulates on the lining crown. Eventually two approximately vertical slip surfaces are formed upward from the opening, reaching the ground surface and bounding the unstable ground cover. This is observed in some model tests by Atkinson et.al. (1975). The debris accumulation process leads to an increase in the vertical stress at the failed soil element P, and any of the three G points shown in Figure 3.6(a) could represent a final equilibrium condition. The final vertical stress will not be equal to the original in situ vertical stress, as some residual shear stress is likely to be mobilized along the vertical slip surfaces. therefore some stress will be transferred from the unstable ground As a result some stress within the unstable ground mass is transferred to the adjacent more stable ground, by some type of "arching" process.

The arching mechanism that is developed above a yielding trap door mimics the arching process above an actual tunnel in soil, but they are not rigorously alike. Terzaghi's (1936) trap door experimental results suggest that the final equilibrium point is given by G''with K>1 in Figure 3.6(a). So, this measured value of K which was greater than the in situ K_o, would be an indication that the major principal stress trajectory at points above the trap door is a concave downward arch.

Some contend, however, that there will be an inversion of the stress trajectory after roof collapse and the accumulation of loosened soil over the liner is complete. The major principal stress trajectory would again become vertical at the centreline, and the minor principal stress trajectory turns to a concave upwards arch. A marked reduction in K is would be associated with rotation of the principal stresses, from E to F in Figure 3.6(a) and (b). Final equilibrium is reached at G with a higher vertical stress existing at point P. This inverted arching configuration, resembling that taking place behind an active-state translating retaining wall or in a silo under first filling was investigated by Handy (1985) and accepted by Wong (1986:36) for his derivation of the final vertical loading condition over a tunnel lining. Wong's proposal should also be taken as speculative, since no evidence is furnished to support it. It has, possibly the virtue of providing an upper bound value of the vertical stress, since he assumed a very conservative K ratio which was equal to the Rankine active coefficient, K_a (Wong, Op.cit.:36). Although not explicitly, Wong assumed the support to be infinitely rigid, as has been done here so far. If the lining yields under the load of "loosened" soil, the displacements at P will not only depend on the size of the void behind the lining, but also on the rigidity of the lining itself. Upon lining deformation, the vertical stress will decrease, and rotation of principal stresses may occur. The principal stress trajectory may resemble that at the start of emptying a silo filled with granular material, (Blight, 1986:36). In the upper cover portion the major principal stress is vertical and in the lower region, closer to the tunnel, it is horizontal.

It is also possible to speculate on a compromise represented by point G' in Figures 3.6(a) and (b). The fact is, however, that this alternating rotation of principal stresses or inversion of the "ground arch", has not been clearly observed, although they may explain some features detected in both the field and the laboratory. Model tests conducted in Cambridge failed to reveal this phenomenon (for example, Seneviratne, 1979:61), but this may be due to the internal tunnel pressure being applied to the ground through a rubber bag in close contact with the soil. Under these conditions, the development of the proposed collapsed soil mechanism may be prevented. It could perhaps be better approximated by the displacement controlled model testing procedure followed by Cording et.al. (1976:15-2). These authors, however, did not furnish details of the strain or stress trajectories.

The foregoing speculative discussion is an attempt to verify the sometimes disputed assumption that the ground reaction curve of a shallow tunnel in soil, may sweep upward when a loosening state develops. This occurs after a miminum pressure is attained. It is well accepted that the stability of an underground opening is very much dependent on the post-failure behaviour of the ground. Soils exhibiting a rapid loss of strength after some peak is reached will clearly demand increased tunnel support to balance the shear strength loss. Although recent views (Read and Hegemier, 1984) question the strain softening response referred from standard laboratory testing, which is exaggerated by inhomogeneities or localization of deformations, it seems unquestionable that actual strain weakening does exist in certain classes of soils. For these, an upward ground reaction curve may result under certain circumstances. This has been proved by Nguyen Minh and Berest (1977) for a hollow sphere and by Berest and Nguyen (1979) and Nguyen and Berest (1979) for a hollow cylinder. These authors assumed an elastoplastic material with strain softening behaviour, a Mohr-Coulomb failure criterion and a non-associated flow rule. They have shown that, unlike the classic solutions for a perfectly plastic material, this type of ground may show a point of minimum pressure in the ground reaction curve. This inversion of the curve ceases to exist, however, when the external radius of the sphere of the cylinder is large compared to the internal radius of the opening, or, in other words, when the tunnel becomes deep. Since they assumed a non-associated flow rule, their analytical closed form solutions derived for small and large strains, may not be unique (Gunn, 1984:24), as is recognized by Nguyen Minh and Berest (1979b:255). However, there is some experimental and field evidence suggesting that this may also be observed in cohesionless granular soils, which have no significant post peak strength loss.

As mentioned before, although the yielding trap door experiments do not fully correspond to a tunnel simulation because the ground displacement modes are not entirely equal, their results do show an upward trend in the stress-displacement curve after a point of minimum pressure is reached. This was observed by Terzaghi (1936:309) in displacement controlled tests he conducted in dense and loose sand, after imposing displacements of 1.4% and 2.7% of the trap door width. Ladanyi and Hoyaux (1969) also did displacement controlled trap door tests, using instead Schneebeli's (1957) rod material, for simulating a granular ground mass in plane stress condition. Unlike Terzaghi, Ladanyi and Hoyaux performed tests with different depths of trap door burial (H/D from 2 to 5.33). In all cases, an upward trend of the pressure-yield curves was noted, with different minimum pressures for various H/D values. The tests were done for displacements of 8 to 10% of the width of the trap door. The material tested (roughened aluminum rods) had a peak friction angle of 30° and a post peak residual angle of 28°, but this difference does not explain the increase in pressure (Ladanyi and Hoyaux, Op.cit.:12). The authors found that the pressure increase reduced as the ratio of H/D increased. The increase in pressure after a minimum was justified by Ladanyi and Hoyaux (Op.cit.:12), in terms of the enlargement of the effective width of the vertical flowing mass above the yielding door, a different mechanism to that postulated before.

From all stress controlled model tunnel tests carried out in Cambridge, just those reported by Atkinson et.al. (1975) showed an increase in internal tunnel pressure after a minimum was reached. Some eight static tests were carried out in dense sand, with cover to diameter ratio varying from 0.88 to 3.97. As described by those authors (Op.cit:84) : "... radiographs taken prior to tunnel collapse indicate that soil movements are initially restricted to a zone immediately above the crown where relatively large dilation occurs. Consequently, a collapse mechanism like that shown (...) with a wedge (...) moving downwards (...) "develops.

"Collapse of all tunnels was sudden and occurred at a well defined tunnel pressure for each test. Collapse results in sudden large movement of sand into the tunnel causing compression of the air ..." in an air-filled rubber bag simulating the tunnel pressure "... and a consequent increase in tunnel pressure to a new equilibrium value. For each test the collapse pressure and, in most cases, the final equilibrium tunnel pressure were recorded (,..). Inspection of radiographs taken after tunnel collapse suggests an ultimate collapse mechanism (...) where a block of soil descends along two vertical slip surfaces ...".

It appears from this description that, had the air-filled rubber bag been absent, no increase in tunnel pressure would have been observed. This seems to support the behavioural model that had been described before, and appears to be valid only for cohesionless granular soils, as it has not been observed in tests conducted in other types of materials.

The only field evidence alluding to this type of behaviour is that noted in Washington D.C. Metro, reported by Hansmire and Cording (1985:1316). Measurements were taken in twin tunnels driven through sandy river terraces, with two different shields. Better ground control conditions were achieved in the second tunnel construction, which led to an average springline thrust in the steel ribs and wooden lagging of about 25% of the maximum thrust, given by the in situ stress ($\gamma HD/2$). The corresponding crown displacement at equilibrium was about 1.2% of the tunnel diameter. These figures are to be compared to an average thrust of 33% and a total of 5.3% crown displacement measured in the first tunnel, where difficulties in steering the TBM, larger overcut, inadequate rib expansion, etc., were experienced. causing large ground displacements. Hansmire and Cording (op.cit:1318) stated that once sufficient ground yielding had taken place, the load in the lining increased (from 25 to 33%) with increasing ground displacement (from 1.2 to 5.3%).

If loosening is defined as an increase in the internal tunnel pressure at increasing displacement of the tunnel wall, then the preceding descriptions reveal that evidence for the mechanisms is limited. This lack of practical evidence, as opposed to the bulk of data showing otherwise, caused this concept to become a very controversial one. Researchers at MIT (Schwartz, Assouz and Einstein, 1980) contend that not only the factual evidence supporting the concept is meagre, but also that the theoretical possibility of loosening as assessed by some is questionable, even for strain softening materials. They question Daemen's (1975) approximate plane-strain analytical solution which treats loosening as a feature of a strain softening material response. Schwartz et.al., (1980:20) pointed out an inconsistency in Daemen's solution, allegedly resulting from the simplifying assumptions he made. This was that an ideally brittle material, showing the most strain-softening response, does not exhibit any loosening at all. Schwartz et.al., (Op.cit:23) further say that the conceptual models explaining loosening by means of the arching theories are highly speculative and cannot fundamentally explain it. Results of an extensive parametric study using a plane strain analytical solution, in which the ground was represented by a piecewise linear stress-strain relationship (elastic, strain softening and perfectly plastic), are presented by these authors (Op.cit.:41). They conclude that "the often advanced opinion that strain softening ground necessarily leads to loosening is thus incorrect, nevertheless, it still cannot be concluded that strain softening never leads to loosening" (Einstein et.al., 1979:19). Recall that the analytical solutions by Berest and Nguyen (1979) and Nguyen and Berest (1979 appeared conclusive in showing that under certain circumstances loosening does occur. The analytical solution of Schwartz et.al., (1980:41) did not indicate an upward trend of the ground reaction curve simply because they assumed the medium to be infinite, whereas the solutions by the other authors assume it to be finite.

Going back to the speculative model presented before, it is possible, from the ideas presented along with Figure 3.6, to propose a stress-displacement curve as shown in Figure 3.8(a). Upon reduction of the internal stress to reach point E, local collapse develops, and the soil starts to progressively fail and accumulate over the rigid lining.

Conditions change from stress governed conditions, to a displacement controlled situation, in which the magnitude of the additional displacement, Δu, is governed by the size of the void left behind the rigid lining. The vertical stresses referred to are those acting against the lining. An increasing vertical stress is assigned to F'', F' or F, depending on the stress changes assumed at this event (Figure 3.6). As the collapsing soil accumulates over the rigid lining, the vertical stress increases according to a constant K ratio,(eg. F' to G') which is preceded by a rapid drop in K after point E is passed (Figure 3.8(b)). If this interpretive model is proven correct, the portion EFG of the stress-displacement curve would not be solely a "ground" reaction curve, since it is controlled not only by the soil properties (mainly its strength), but also by the size of the gap behind the liner, and by the liner stiffness. Indeed, if the lining were flexible, the FG portion of the curve would no longer be vertical but inclined, according to the rigidity of the support. In a stress controlled condition, not unlike that encountered in the excavation of a tunnel before the support comes in contact with the soil, the stress cannot increase, even though the ground requires it to remain stable. A stress increase will only be detected if conditions are changed to a displacement controlled situation, such as that offered by an installed support, which restrains the displacements according to its relative stiffness. If it is agreed that the final equilibrium

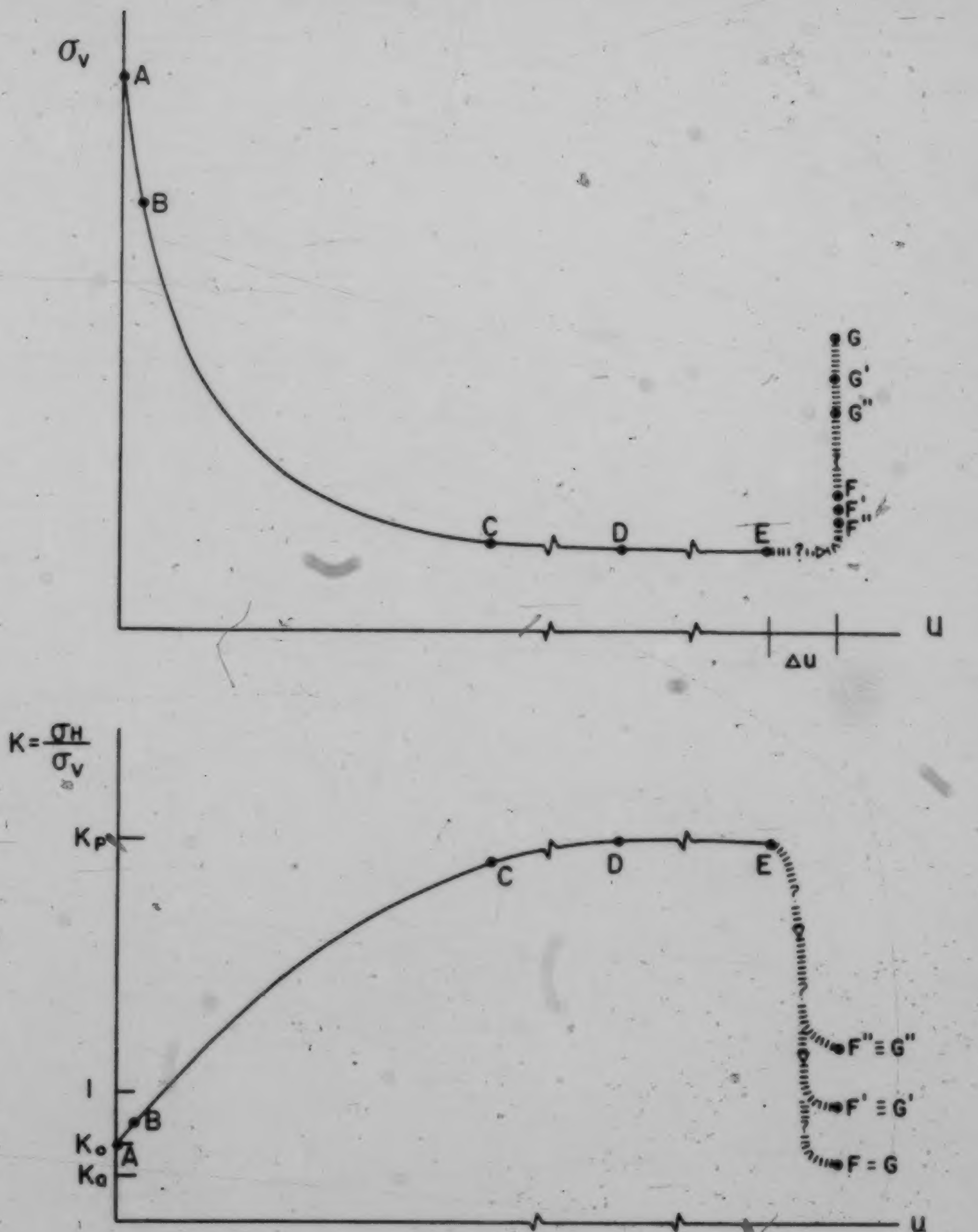

Figure 3.8 Ground Reaction Curve and Stress Ratio Changes in an Element of Soil at the Crown of a Tunnel Approaching Collapse

stress, such as that at G, can be uniquely assessed by some sort of plasticity solution, as a function of the ground properties and conditions, then the slope of the portion FG of the curve can be partly controlled by the support characteristics, being, therefore not unique.

The overall ground response resembles that of a strain softening structure loaded under displacement controlled conditions. It seems valid to relate it to the formation of inhomogeneities in the ground mass, such as the shear bands formed in trap door experiments observed some fifty years ago by Terzaghi and more recently by Vardoulakis et.al., (1981:61). If the post-failure tunnel behaviour is a matter of interest, model testing under displacement controlled conditions seems to be a promising research area. The available numerical modelling tools based on traditional elastic and plastic theoretical formulations currently seem unable to describe this mechanism.

It would be argued that loosening is likely to occur in non-cohesive granular soils at large deformations. Typically, this might include crown displacements of greater than 1 to 2% of the tunnel diameter, and would generally be in excess of those developed in properly constructed urban tunnels. The problem was also addressed in Sections 2.3.4 and 2.3.5 of this thesis, and an expedient criterion was set up ad interim to assess the likelihood of this occurrence.

3.3 The Role of Groundwater

3.3.1 Foreword

In his 'Principles of Tunnel Lining Design', Kuesel (1986) states that if the most important part of the tunnel lining is the ground that surrounds it, the most important component of the ground is the groundwater. Groundwater plays a paramount role not only in the design of the lining but also in the overall tunnel construction and subsequent performance. The presence of water in the ground may govern tunnel heading stability, especially in cohesionless granular soil. Pore water pressure changes may control the magnitude of ground settlements, particularly those due to drainage and consolidation, and these may well exceed those developed under short term conditions. Mechanisms of soil consolidation and swelling are known to be one possible cause of time dependency of the lining loads.

A brief review of the subject is attempted in this section, with emphasis being given to the changes in porewater pressure caused by the tunnelling operation and the consequences in the overall tunnel behaviour.

3.3.2 Generation of Porewater Pressure Changes

3.3.2.1 Idealized Porewater Pressure Changes

It is recognized that even without any total stress change in the ground, the pore water pressures may be changed by a simple alteration of the hydraulic boundary conditions. More often than not, a tunnel acts as a drain, regardless of the attempts to provide an ideal impervious lining (Ward and Pender, 1981:268). It will be assumed however that unless indicated otherwise, the tunnel contour is an impermeable boundary.

The short term, or undrained changes, in pore water pressure in a saturated soil are related to the change in volume of the soil pores. If the ground is depicted by a plane strain plate under a uniform stress field, and if the opening is circular, it can be shown that for an elastic, homogeneous and isotropic soil, the total stress path of a soil element adjacent to the tunnel is one of pure shear. No volume changes are experienced because the total mean normal stress remains constant and shear stress does not cause volumetric strains in an isotropic elastic body. If the in situ stress is non-uniform (K not equal to 1 or a gravitational stress field), then the total stress paths will generate pore pressure changes. It has been shown already that the mean total stress will vary during the reduction of the in situ total stress at the tunnel contour. Moreover, if the ground is anisotropic or inelastic, there will be generation of pore pressure changes with respect to these in situ conditions.

Short term pore pressure changes, in a saturated, homogeneous, isotropic, elastic ground, at points close to a circular opening representing a deep tunnel can be derived from elasticity without major difficulties. The in situ total stress state in terms of polar coordinates (θ is the anticlockwise angle measured from the springline, see Figure 2.11) is;

$$\sigma_r = \frac{1}{2}\sigma\ [(1+K) - (1-K)\cos 2\theta] \qquad [3.1]$$

$$\sigma_\theta = \frac{1}{2}\sigma\ [(1+K) + (1-K)\cos 2\theta] \qquad [3.2]$$

$$\tau = \frac{1}{2}\sigma\ [(1-K)\sin 2\theta] \qquad [3.3]$$

where σ is the total in situ vertical stress. If the initial ground water condition is hydrostatic and the phreatic level coincides with the ground surface, the total stress ratio, K, is given by:

$$K = K_o + (1-K_o)\ \gamma_w/\gamma \qquad [3.4]$$

where K_o is the effective stress ratio and γ_w and γ are the unit weights of water and soil respectively.

If σ_r and τ at the opening are proportionally reduced to a fixed fraction Σ of their original values, only the deviatoric term $\sigma_d=(1-K)\sigma/2$ will generate pore pressure changes. Under the assumed plane strain and fully saturated conditions, (the out of plane stress being equal to the intermediate principal stress, σ_z), it is possible to calculate the pore pressure changes in the soil. Immediately after a partial stress release at the opening, the pore pressure, u, at points adjacent to the unlined and impervious tunnel contour will be given by:

$$u = u_o + (1-K)\ (1-\Sigma)\sigma \cos 2\theta \qquad [3.5]$$

where u_o is the in situ pore pressure.

The pore pressures can be derived either using a coupled or an uncoupled approach with total stress. The first route was followed by Carter and Booker (1982). The second approach makes use of Skempton's (1954) A and B pore pressure coeffiecients which are equal to 0.5 and 1.0, respectively for a saturated soil under plane strain conditions. The excess pore pressure, $u-u_o$, is non-zero if K is different from unity, it increases as the tunnel gets deeper and as the amount of allowed stress release increases. For K <1, the crown (and floor) will show a reduction in pore pressure whereas the springline will experience an increase. The transition point between the zones of potential swelling and consolidation, is at θ=45°, where the excess pore water pressure is zero. For points other than at the tunnel contour, Carter and Booker (1982) furnish initial excess pore pressure distributions, both for an impermeable and permeable opening. To simplify the solution (approached both analytically and numerically), these authors made use of the principle of superposition, by treating the individual components of the complete problem separately (reduction of mean normal stress, of the deviatoric stress, and of the pore pressure).

3.3.2.2 The Effect of Gravity

The body forces due to gravity are now included, still assuming, however, that the opening is not influenced by the stress free ground surface. For K=1, the pore pressure changes at the tunnel perimeter can be calculated from the total stress changes given by Mindlin (1939) or by Hartmann (1972), assuming a full in situ stress release is applied to the impermeable opening (equations 2.5 to 2.7 or 2.19 and 2.21). At the crown, springline and floor, the pore pressures that will result are:

$$u_c = u_{co} + \gamma D/4 \qquad [3.6]$$

$$u_s = u_{so} \qquad [3.7]$$

$$u_f = u_{fo} - \gamma D/4 \qquad [3.8]$$

As expected from the total stress paths shown in Figure 2.1, no pore pressure changes would be observed at the springline, since a pure shear condition prevails here. However, at the crown, there is an increase in pore pressure equal to the increase in the mean total normal stress. On the other hand, a pore pressure reduction is observed in the floor, resulting from a reduction in the mean total normal stress. Similar trends will be observed for K different from unity.

Broadly speaking, the action of gravity in a soil with K less than one, will lead to more pronounced changes in pore pressures at the tunnel floor than at the crown.

3.3.2.3 Porewater Pressure Changes in Less Idealized Conditions

Departure from linear elasticity will lead to generation of pore pressure changes, even for a deep tunnel under a uniform stress field. The likely undrained changes in pore pressure in a lightly overconsolidated soil, can be anticipated from the discussions related to Figures 2.2 and 2.3. Of particular interest are the volume changes shown in Figure 2.3(d), for an element of soil close to the tunnel perimeter. If changes in volume are precluded upon removal of the in situ stresses, the soil will initially experience an increase in pore pressures associated with yielding which is followed by a pressure reduction as it approaches failure and beyond. The later changes are largely controlled by the decrease in the mean normal stress.

The distribution of the pore water pressure changes with distance from the opening wall, can be determined from both coupled and uncoupled approaches. The latter was favoured by Clough and Schmidt (1981:609), who combined the stress distributions furnished by an elasto-plastic closed form solution presented by Deere et.al. (1969) for a frictionless soil, with the Henkel's (1960) pore pressure coefficients. The inconvenience of this approach is that the required parameters for the solution (strength and pore pressure) must be chosen in a consistent manner, as they are not independent variables (an extensive testing program is required).

Ladanyi (1966) followed an ingenious alternative approach, adapting his former work on the expansion of a cavity in saturated clay, to the tunnel problem under a uniform stress field. This is a numerically approximate solution that takes into account the actual stress-strain curve of a soil tested in the laboratory under plane strain conditions. The piecewise integration of the stress-strain curve is done approaching it by discrete linear segments in the larger shear strain region and by fitting a curve in the smaller shear strains region (for instance, by a hyperbola). Ladanyi (Op.cit.) discusses the errors involved in an elastoplastic formulation in which a constant deformation modulus is assigned to the soil before plastic failure, in order to advocate the preference for the curve description model.

Figure 3.9 illustrates schematically the distributions of pore water pressure changes, (Δu), assuming a non-linear stress strain behaviour for the soil and a full stress release at the impermeable opening. They represent typical distributions for a lightly and a heavily overconsolidated soil. Plotted together are the distributions of radial and tangential total stress. As indicated, in a lightly overconsolidated soil, the pore water pressures will decrease in the region closer to the tunnel and increase further away. In a more heavily consolidated clay, the pore pressure will simply decrease. If the in situ stress is only partially released, there will be a reduction in the magnitude of the pore pressure changes, and the zones of suction may practically disappear in both cases. The magnitudes of the pressure changes also depend on the degree of overconsolidation of the clay. All these facts are supported by results of the analytical and numerical analysis presented by Clough and Schmidt (1981) and by Ladanyi (1966). Also supporting this, are the results of undrained centrifuge model tests of tunnels in saturated overconsolidated kaolin, conducted by Mair (1979:108,130).

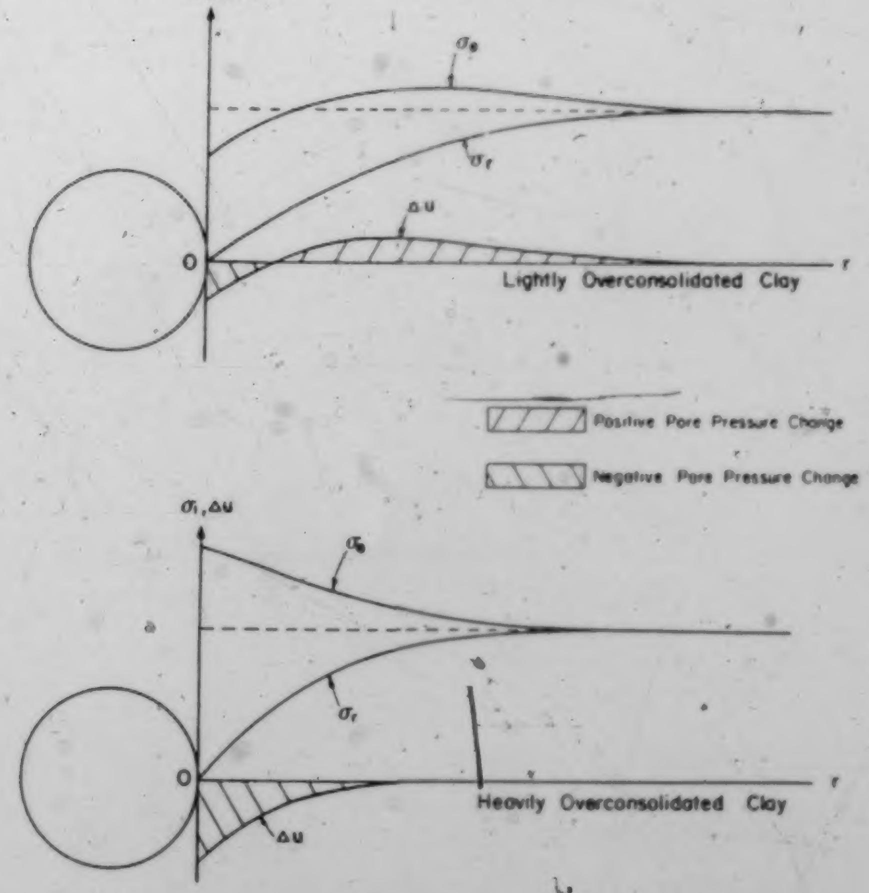
σi, Δu
σθ
σr
Δu
O
r
Lightly Overconsolidated Clay
Positive Pore Pressure Change
Negative Pore Pressure Change
σi, Δu
σθ
σr
O
r
Heavily Overconsolidated Clay
Δu

NOTES: DEEP TUNNEL, K=1, IMPERMEABLE OPENING, UNDRAINED CONDITIONS, HOMOGENEOUS AND ISOTROPIC, NON LINEAR SOIL

Figure 3.9 Short Term Pore Pressure Changes and Total Stress Distributions

From the plots in Figure 3.9 it is also possible to anticipate the likely changes in the effective stress. As pointed out by Ladanyi (1966), the mean effective normal stress will predominantly increase in a more overconsolidated clay and decrease in a less overconsolidated soil. In the former case, even if the opening is stable in the short term, a delayed failure process may develop if the tunnel is left unsupported as pore pressures equalize back to the initial hydrostatic condition.

Figure 3.10 illustrates the pore pressure changes of a soil element at the tunnel contour, as the internal tunnel pressure is decreased. It was obtained using the same reasoning as before, being easily derived from Figure 2.3. The behaviour depicted is confirmed by the quoted numerical solutions and by laboratory model testing (Mair, 1979:108). As noted previously, the negative pore pressure changes can be suppressed if the in situ total stresses are not fully reduced at the opening. Moreover, if the opening contour is impermeable as supposed so far, once the critical state is attained under undrained conditions, the deviator stress, $(\sigma_\theta - \sigma_r)$, remains constant. The pore pressure changes thereafter are equal to the changes in the mean normal stress. The zero volume change condition prevents the effective stress path from travelling down as in Figure 2.3. The effective stresses remain constant, and the pore pressure changes are equal to the changes in the internal

OCR	1 and 2
K_o	0.55 and 0.8
C_u/σ'_v	0.3 and 0.45
γ (kN/m^3)	18.07
λ	0.15
κ	0.03
e_{cs}	1.74
M	1.20$^{(1)}$
G/C_u	74$^{(2)}$
k (m/s)	1.547×10^{-7}

Notes:
(1) Equivalent to $\phi' = 30°$ in compression
(2) Shear modulus to undrained strength ratio in plane strain
(3) Cam-clay parameters taken from Carter et al (1979)

Table 3.1 Soil Properties in Johnston and Clough (1983) Analyses

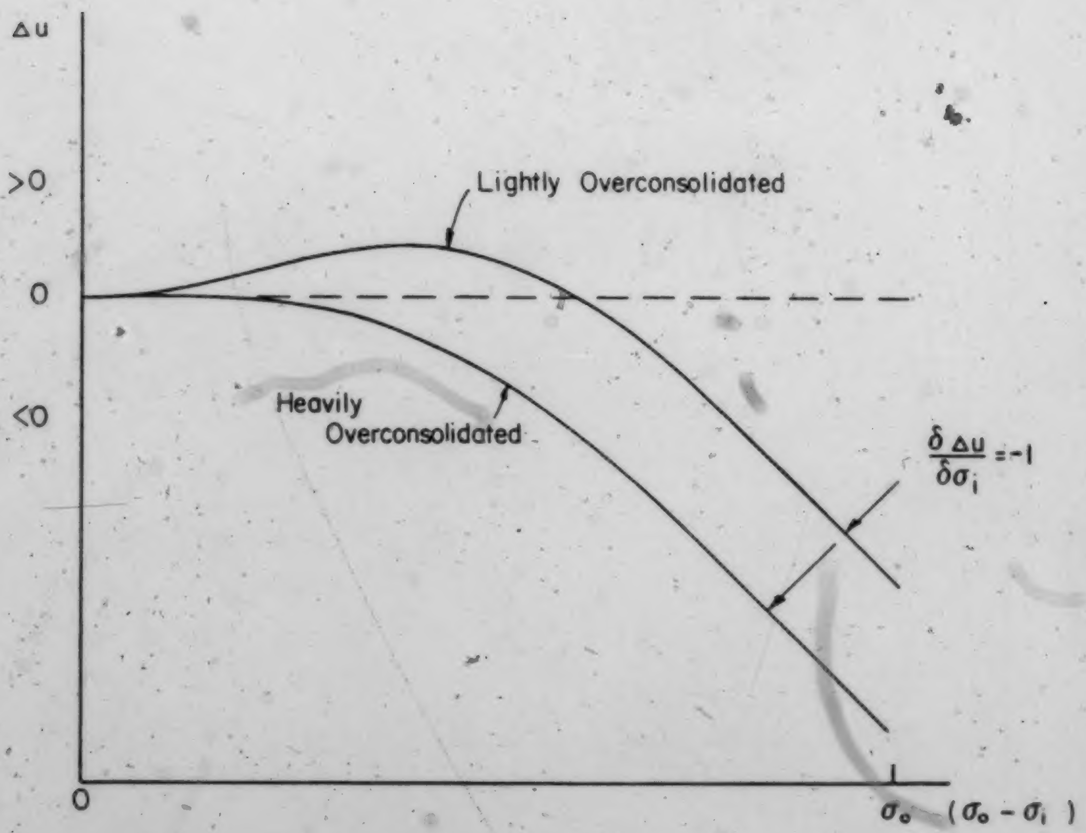

σ_o = uniform in situ stress field

σ_i = uniform tunnel internal pressure

Figure 3.10 Pore Water Pressure Changes in a Soil Element Adjacent to the Opening upon Decrease of Internal Tunnel Pressure

tunnel pressure. The curves shown in Figure 3.10 become straight lines with negative unit gradients.

A more generalized plane strain solution of the pore pressure generation problem for a shallow tunnel, including the effect of the free ground surface, a non-uniform in situ stress field, and the non-linear behaviour of the soil would require numerical techniques such as the finite element method. Examples of these are given by Branco (1987) and Samarasekera (1987). Johnston (1981), and Johnston and Clough (1983), also presented results of some finite element analyses, in which the undrained pore pressures were obtained using a coupled elasto-plastic approach assuming the Cam-clay model to represent the soil behaviour.

They simulated the construction of circular tunnels with an excavated diameter of 7.92 m and with a soil cover of 9.45 m ($H/D \simeq 1.2$). In their analyses, they assumed that the ground water level was at the surface, which was free draining. The rigid base of the compressible stratum located 9.45 m below the tunnel invert was also free draining. Tunnel excavation was simulated by applying the equivalent nodal loads at tunnel boundaries, in increments representing the gradual reduction of the in situ stresses. Small time increments were selected in order to ensure an undrained behaviour and the tunnel contour was assumed to be impermeable. Soil properties adopted are shown in Table 3.1, using Cambridge notation, and were said to represent those of the Boston Blue Clay. The results of two particular analyses are shown as follows. One refers to the response of the soil in a normally consolidated condition (OCR=1 and K_o=0.55) and the other to a lightly overconsolidated condition (OCR=2 and K_o=0.8). The undrained strength of the clay was expected to increase with depth which led to an undrained cohesion at the tunnel axis level of about 34 kPa in the first case and 50 kPa in the second. These values are said to be typical for such soft clay content.

In the analyses, the tunnel perimeter was allowed to deform gradually upon the stress release, up to a pre-determined amount which corresponded to a hypothetical closure of a void left behind the lining. In both cases, this gap closure at the tunnel crown amounted to 50.8 mm and since the soil stiffnesses are not equal in the two analyses, different amounts of stress release at the opening would be expected. A larger reduction of the in situ stress should have occurred in the OCR=2 case.

Figure 3.11 presents contours of the undrained pore pressure changes, at the instant of the hypothetical gap closure. The excess pore pressures are expressed as a fraction of the in situ total vertical stress at the tunnel axis elevation. They correspond to the results shown by Johnston (1981:133,144) and reflect the effect of an increasing overconsolidation ratio for a fixed displacement boundary condition at the opening.

Despite the higher stress release necessary in the OCR=2 case to attain the same opening closure, one notes that the magnitudes of the excess pore pressures generated in this case are much less than that calculated for the normally consolidated condition. This is partly due to the differences in strength and K_o. A maximum increase of about 11% of the hydrostatic in situ pore pressure is noted with OCR=1, against about 4% with OCR=2. Also the suction below the tunnel floor is higher for the normally consolidated case. Furthermore, the shapes of the contours are dissimilar. The zone of positive pore pressure change moved up from the springline region towards the crown as the OCR increased. The increase in the K_o ratio, and also the higher stress release imposed contribute to the difference. It is worth noting that the crown and floor regions tend to show pore pressure changes with opposite signs. This is attributed partly to the effect of the gravitational stress field on the ground stress paths, as explained before.

The inclusion of a support with some finite stiffness will have an effect on the generation of the undrained pore pressure changes, as it affects the stress changes in the soil. Carter and Booker (1984) studied the problem of elastic consolidation around a deep lined circular opening using numerical analyses, and assuming that the tunnel excavation is proceeding with the lining already in place. This hardly to represents reality. Johnston (1981) also included in his elasto-plastic analysis described previously, the effect of a lining installed after closure of the fictitious gap. This more closely represents the

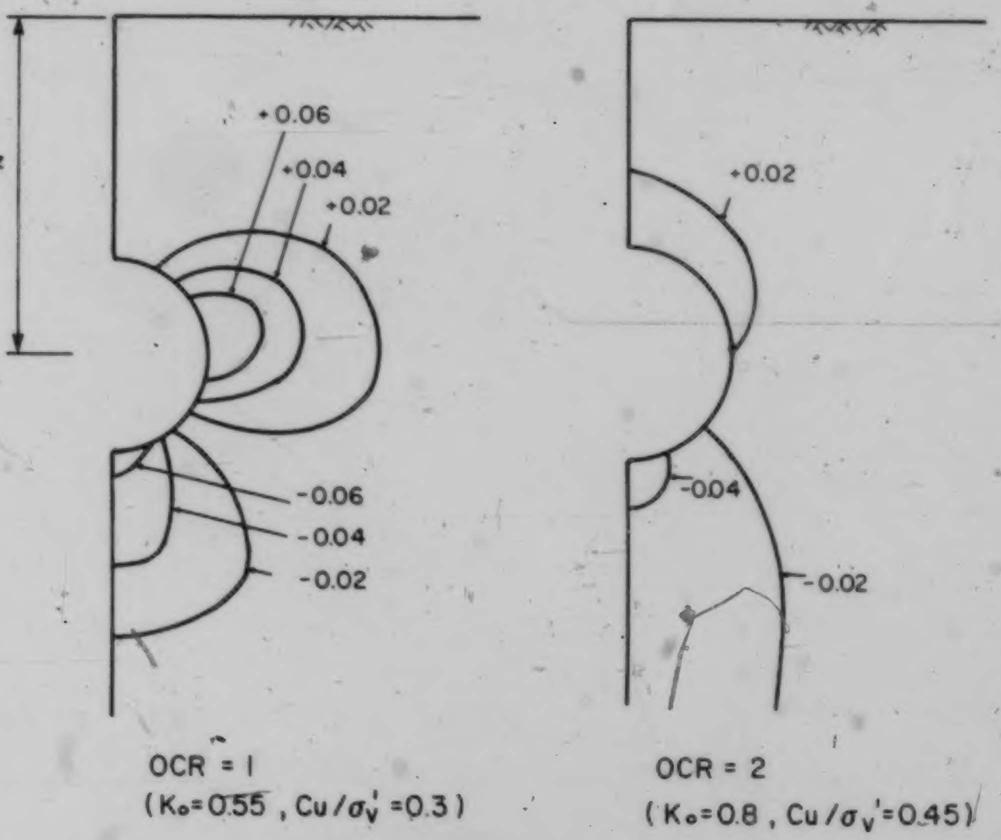
z
+0.06
+0.04
+0.02
-0.06
-0.04
-0.02
OCR = 1
(Ko=0.55 , Cu/σv' =0.3)
+0.02
-0.04
-0.02
OCR = 2
(Ko=0.8 , Cu/σv'=0.45)

NOTE: Values shown are ratios of pore pressure changes to the total vertical stress (γz) at tunnel axis.

Figure 3.11 Calculated Contours of Undrained Porewater Pressure Changes Around a Tunnel in Boston Blue Clay for two Overconsolidation Ratios (after Johnston, 1981:133,140 - modified)

actual behaviour, in which some stress release takes place before support placement. He used the soil properties corresponding to OCR=1 (Table 3.1), but introduced a 0.508 m thick continuous, impervious concrete ring with Young's modulus varying from 0.207 to 2.07 GPa. These lower values were used to account for the presence of bolted joints of a segmented precast lining. It is interesting to compare the calculated undrained excess pore pressures developed in the soil for the two extreme lining stiffnesses (Johnston, 1981:127) with the contours obtained before lining installation (Figure 3.11). The additional deformations resulting from the lining being loaded lead to increases in the excess pore pressure profiles. The pore pressure contours are those after the soil loads are fully transferred to the support and a short term equilibrium is achieved. However, the increased suction below the tunnel is far greater than the increase of the excess pressure at the springline (about 10 times greater). The influence of the underlying rigid base restrains the soil below the tunnel from moving up, thus enhancing the negative water pressure changes (Johnston, Op.cit.:109). So, a tendency towards an increase in suction pressures, perhaps not as much as calculated, is to be expected. It has been shown that after lining activation in a shallow tunnel the support may tend to "float" (Section 2.3.5) regardless of the position of the lower rigid base, which can partly explain the observed response in an undrained analysis.

So far it has been assumed that the tunnel contour is an impervious boundary, both prior to and after lining installation. In reality, once the tunnel heading is excavated, the soil is exposed and the radial total stress drops to zero. Also, zero pore pressures at the tunnel perimeter most likely represent the actual case, provided no supporting fluid such as compressed air, slurry, etc., is used. In any case, the tunnel contour at this instant is better depicted as a free draining hydraulic boundary. A lining with a permeability two to three orders of magnitude less than that of the soil can be assumed as impermeable for all practical purposes (Fitzpatrick et.al., 1981:99). Therefore, if such a lining is installed after the heading excavation, the tunnel contour will again become an impervious boundary. The pore pressures that underwent a substantial decrease next to the unsupported heading, may therefore, experience an increase over time as the consolidation process develops. In summing up it might be said that an undrained excavation of a tunnel in an overconsolidated clay, will induce a pore pressure response at the crown, showing a small pressure increase at points ahead of the face, followed by a pronounced decrease above the unsupported heading. Then, if an "impermeable" lining is installed and soil consolidation develops, the pore pressure will gradually rise, but normally not to its original value, as most tunnels act as drains in the long term (Ward and Pender, 1981:268).

Not much data is available on pore pressure generation in the three-dimensional stress transfer process occurring in the advancing heading of a shallow tunnel. To the writer's knowledge, no 3D results of the consolidation process around a tunnel have been made available yet. However, limited data from field measurements appears to confirm the suggested evolution of pore pressure changes at the crown. Despite the fact that in reality, an undrained response is hard to secure, the rise in water pressure ahead of the face, followed by a reduction above the heading and a partial recovery with time, has been noted near the crown of tunnels in the stiff London Clay (Barrat and Tyler, 1976:8), in a fairly sensitive and lightly overconsolidated soft glacial lacustrine clay (Palmer and Belshaw, 1980:180), in an also sensitive, but stiffer marine clay (Ballivy et.al., 1983:349), in a stiff varved lacustrine clay (Hardy Associates, 1980:18), and in the stiff and extremely sensitive overconsolidated Leda Clay (Eden and Bozozuk, 1969:26). This overall common trend may be altered and even reversed if the heading is supported by some fluid pressure such as compressed air. This was the case in the Willington Quay Tunnel, England, driven through a soft organic alluvial silt with an air pressure of 90 kPa, which was about 40% of the overburden (Sizer, 1976:125).

As mentioned previously, the full reduction of the in situ total stress at the unsupported heading leads to a reduction in the pore pressure in the soil. They may compensate each other, resulting in a positive mean effective stress in the soil close to the opening. This effect is more pronounced in overconsolidated soils and even if its effective cohesion intercept is negligible, the opening may remain temporarily stable despite being unsupported. This is the so called "stand up" phenomenon. With time, as the consolidation process develops, the zone of negative excess pore pressure dissipates causing the soil to swell and the effective stresses to be reduced. This may ultimately result in the initiation of a localized collapse mechanism. The span of time required to initiate the instability process is called "stand-up time", and it is a function of the magnitude and distribution of the negative excess pore pressures (hence the stress history of the soil). and of the consolidation properties of the soil. Assessment of this time is especially important when the tunnel is advanced by mining operations without a shield. The construction sequence of a staged excavation (depth of heading advance, etc.), are strongly dependent on the "stand up time" of the soil. It is therefore somewhat suprising to see this parameter being estimated in practice, on strictly empirical grounds using Terzaghi's (1946) criteria. Some limited research work has been done recently (Taylor, 1979 and Myer et.al., 1981), but the so far results obtained have not been incorporated in to routine practice.

3.3.3 Dissipation of Excess Pore Water Pressures

3.3.3.1 Linear Elastic Consolidation

The dissipation process of the excess pore pressures around a plane strain deep unlined circular tunnel in homogeneous, isotropic and elastic saturated soil, was studied by Carter and Booker (1982). As mentioned, they divided the solution of the problem into separate components which could be assembled together by superposition, to render the complete solution. They analysed the cases of a permeable and of an impermeable tunnel contour. Of relevance to the discussion are the components that lead to time dependent response. These are the removal of the deviatoric stress component, σ_d, for the permeable and impermeable opening and of the reduction of the in situ pore pressure (u_o) for the case of a permeable tunnel. The removal of the mean normal stress does not cause changes in pore pressures. Recall that the deviatoric stress component is given by:

$$\sigma_d = 1/2\ (1-K)\ \sigma \qquad [3.9]$$

The changes caused by the removal of this deviatoric component are given by:

$$\Delta u = (1-K)\ \sigma\ P \cos 2\theta \qquad [3.10]$$

where P is a pore pressure coefficient which is a function of the position of this point with respect to the opening (r/r_o) and of a non-dimensional time factor represented by

$$T = \frac{ct}{r_o{}^2} \qquad [3.11]$$

In this expression, t is the consolidation time, r_o the radius of the opening and c the coefficient of consolidation (equal to that of swelling as linear elasticity was assumed) given by:

$$c = \frac{k}{\gamma_w m_v} \qquad [3.12]$$

where m_v is the coefficient of volume change which is related to the constrained modulus D by:

$$D = \frac{1}{m_v} = \frac{E\ (1-\nu)}{(1+\nu)\ (1-2\nu)} \qquad [3.13]$$

E and ν are the Young's modulus and Poissons's ratio of the soil in drained conditions.

The pore pressure changes caused by the removal of the in situ pore pressure, u_o, is:

$$\Delta u = -P.u_o \qquad [3.14]$$

and, of course, is independent of the angle, θ.

The pore pressure coefficients, P, calculated numerically by Carter and Booker (Op.cit.) are shown in Figure 3.12. These are for a Poissons's ratio of the soil skeleton equal to zero which corresponds to the slowest rate of elastic consolidation possible (minimum c value). The pore pressure changes associated with the removal of u_o in a permeable tunnel, as given in Figure 3.12c, are independent of the Poisson's ratio (Carter and Booker, Op.cit.:1067).

If the tunnel is supported in such a way that the in situ stresses are not disturbed prior to lining installation, the changes in pore water pressures generated by the excavation will vary with time and will affect the interaction process between the soil and support. As a result, the loads onto the lining will vary with time. Provided the lining is impermeable, and despite these local

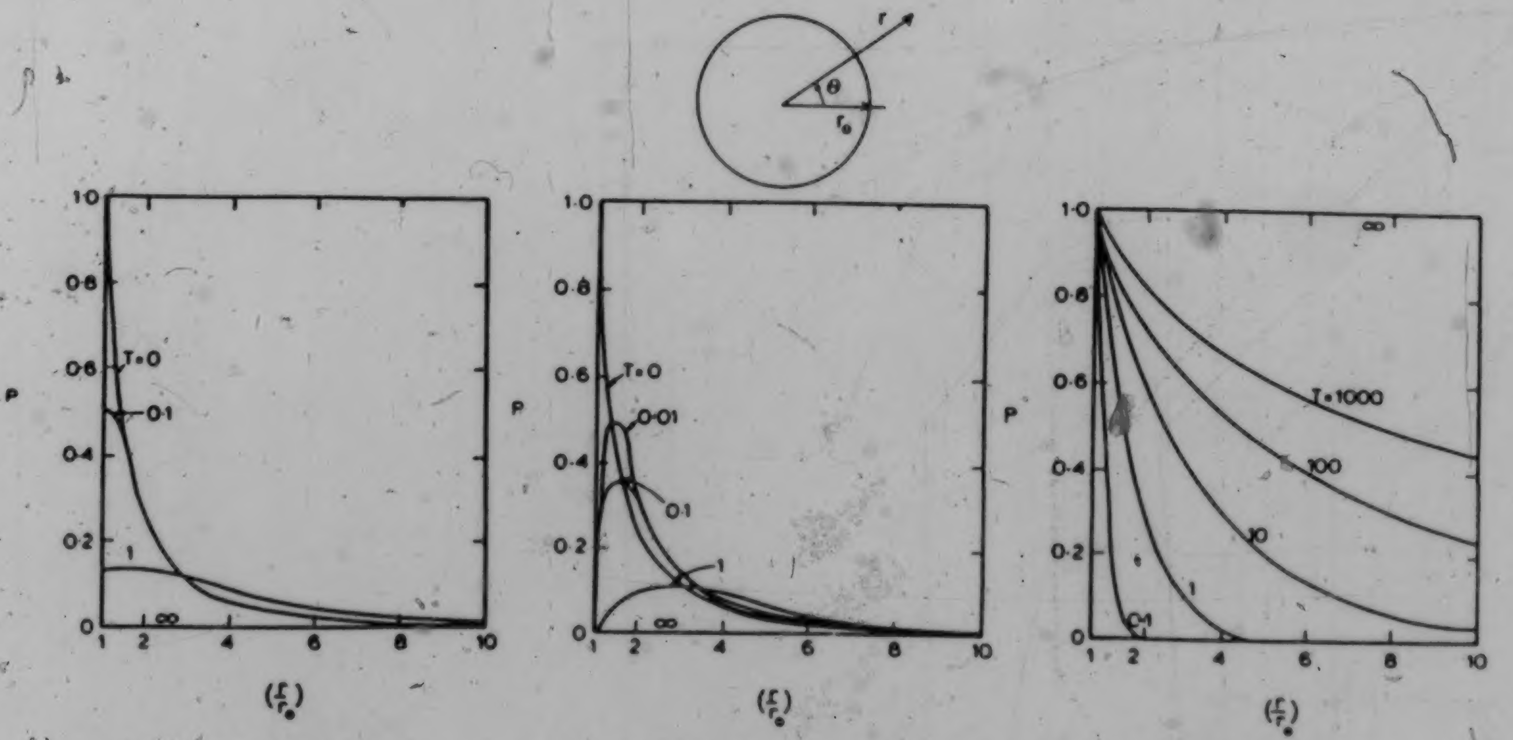

a) Removal of σ_d in an impermeable opening

b) Removal of σ_d in a permeable opening

c) Removal of u_o in a permeable opening

Figure 3.12 Pore Pressure Coefficients for Elastic Consolidation of a Deep Circular Tunnel (modified from Carter and Booker, 1982)

variations in load with time, it should be noted that the average radial and shear stresses at the interface will remain constant. Therefore, the average thrust force is time independent and will remain constant as it is governed by the mean normal stress removal which does not produce changes in pore water pressures. Carter and Booker (1984) studied this problem, extending their solution and by including an impervious elastic lining, and considering two types of interfaces: full and no slip. For the no slip condition, they found that the thrust force may marginally increase or decrease locally with time, (typically ±10% with respect to its short term value), as compared to the local changes in the bending moments, which may vary by as much as 100% (Carter and Booker, Op.cit.:608).

The changes in bending moments with time for the particular condition they investigated, are shown in Figure 3.13, and m is a coefficient, from which the bending moment is calculated as:

$$M = -m \frac{(1-K)}{2} \sigma r_o^2 \cos 2\theta \qquad [3.15]$$

The coefficients, m, shown in Figure 3.13 were calculated assuming a non-slip condition, for a lining with a constant thickness, t, equal to one-tenth of the opening radius, and for a soil with zero Poisson's ratio. Clearly, besides being a function of the time factor, m is also a function of the relative stiffness, RS, of the support to the ground, expressed as:

$$RS = \frac{2 E_s}{(1-\nu_s^2) E} \qquad [3.16]$$

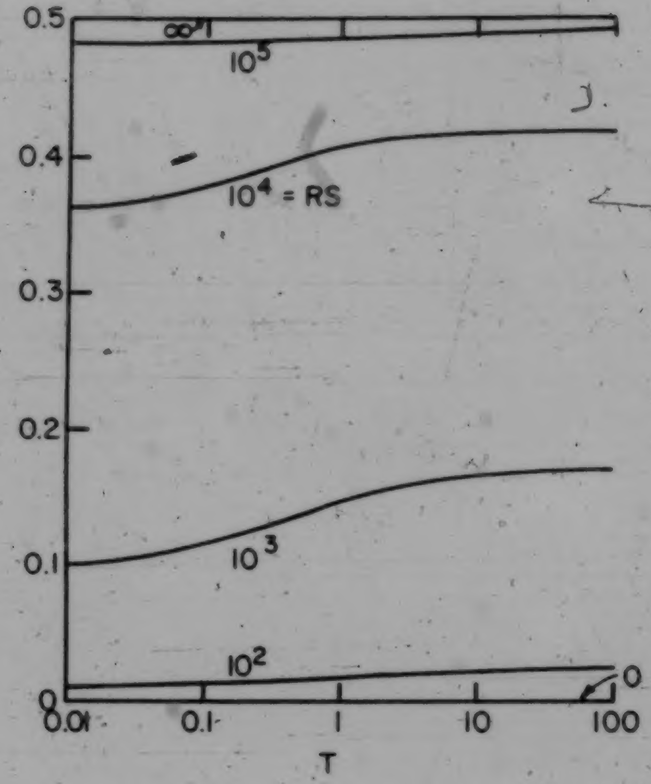

Notes: For non-slip condition, $t/r_o = 0.1$ and $\nu = 0$
$RS = 2\,E_s / E(1-\nu^2)$ .... relative stiffness
$T = ct / r_o^2$ .... time factor
$M = -m \cdot \frac{(1-k)}{2} \cdot \sigma \cdot r_o^2 \cdot \cos 2\theta$ ..... bending moment

Figure 3.13 Changes in Lining Bending Moments with Time during Elastic Consolidation (modified from Carter and Booker, 1984:603)

where E is the drained Young's modulus of the soil.

3.3.3.2 Non-Linear Consolidation

If the soil behaviour becomes non-linear, with yielding developing at some stage of tunnel unloading, pore water pressure changes will develop even for the idealized case of a deep tunnel under a hydrostatic stress field.

The dissipation of the excess pore pressures under such conditions was investigated by Gunn (1984) and Gunn and Taylor (1985), using a finite element program developed by Taylor (1984). Effective stresses were related to soil strains by means of an elasto-plastic relationship, in which the yielding condition was given by the Mohr-Coulomb failure criterion. The tunnel problem was simulated in the analysis by a thick cylinder in plane strain conditions, with an outer radius 9 times greater than the inner radius (equal to 25 mm). The initial stress state was given by a uniform total stress of 200 kPa and a pore pressure of 100 kPa throughout the cylinder. Soil properties are given in Figure 3.14. The stresses acting on the external boundary were kept constant, and tunnel excavation was simulated by a constant rate of reduction of the total stresses to a value of 50 kPa, over a time interval of 10 seconds, during which the soil response was assumed to be undrained. After this partial stress release, the nodal points at the inner boundary were fixed to represent the insertion of a rigid lining. Throughout the analysis, the outer boundary was assumed to be a permeable surface with a constant pore pressure equal to 100 kPa. Two cases were considered with respect to the inner boundary: after "lining" installation, the inner surface was assumed to be impermeable in one case and permeable with pore pressure fixed at zero, in the other. However, before fixing the internal nodal points, the boundary was impervious in both cases.

Figure 3.14 shows the results of the finite element calculations for the two cases considered. Identical responses occurred during the undrained unloading, with the pore pressure at the opening remaining constant while the response is elastic, and decreasing with the total stress reduction after yield. In time, water migrates away from the impermeble lining and an increase in pore pressure is noted until it recovers its initial hydrostatic value of 100 kPa. Similarly, an increase in the total radial stress with time is also observed from the imposed reduced value of 50 kPa to a final lining load of about 110 kPa. The radial effective stress, however, displays a continuous reduction as the swelling process evolves. Once the consolidation process starts around the permeble lining, the pore pressure at the inner surface remains at zero, but the consolidation and drainage at points away from the contour, causes changes in the effective and total stresses. These changes are not large but an increase in both of them is evident as a steady state flow is established (water being supplied at the outer boundary), and radial seepage forces develop increasing the lining load. This increase is, however, smaller than that

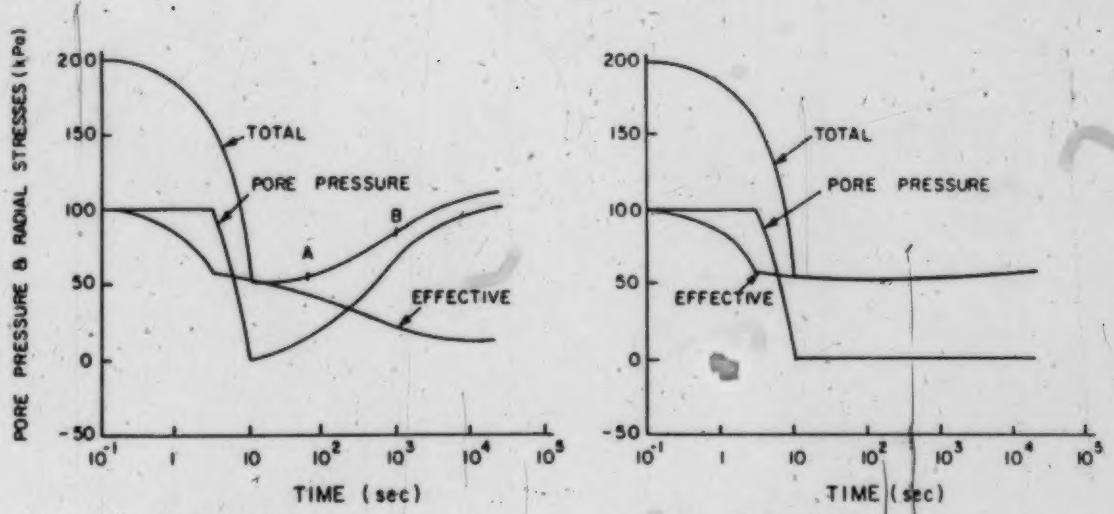

a) Impermeable Lining

b) Permeable Lining

NOTES: 1) Properties of soil skeleton E = 5 MPa, ν = 0.33, Ø = 26°, C' = 0, k = 10^{-7} cm/s, angle of dilation ψ = 0°, γ_w = 10 kN/m^3

2) Up to 10s undrained unloading. Thereafter consolidation.

Figure 3.14 Non-Linear Consolidation of a Thick Cylinder: Evolution of Radial Stress and Pore Pressures at the Rigid Lining-Soil Interface with Time (modified from Gunn and Taylor, 1985)

observed in the impermeable case.

This expected load increase with time in an impermeable lining only occurred because the soil yielded and it would not happen for a linear elastic soil as shown before. The rate of increase in lining load should be a function of the coefficient of consolidation (or swelling), which is equal to about 10^{-2} cm^2/s in this case. Even for a permeable lining some load increase is also expected which results mainly from seepage body forces, but the increase in this case is not very high. However, of considerable interest in both cases, is that the lining loads never recover the original 'in situ' value of 200 kPa. In the first case the final total lining load increased to 55% of the original and in the second to 31%. These increases were from the initial reduction to 25% at the end of the undrained unloading applied in both cases.

Obviously, the results just discussed cannot be fully generalized to actual tunnelling conditions, since a number of simplifications were adopted. One of them is the assumption of zero dilatancy. With respect to this, Gunn (1984) also analysed the impermeable tunnel problem assuming an associated flow rule to the Mohr-Coulomb yield-failure criteria ($\psi=\phi=26°$ in this case). For this case he found smaller displacements if a lining is not installed, than for the $\psi=0$ analysis. Also the rate at which this radial displacement takes place is higher for zero plastic volume change on yielding. Moreover, he noted also that the angle of dilation, ψ, has minimal influence on the total stress distribution within the thick cylinder, but markedly affects the pore pressures and, consequently, the effective stresses. If a rigid and impervious lining is included, Gunn (Op.cit.) noted that the associated flow rule assumption led to an increase in the effective radial stress at the inner boundary resulting from the higher suction under the undrained loading, but a substantial drop in the effective stress occurs with time and re-establishment of the original pore pressure. The assumption of $\psi=\phi$ led to a slightly higher final total lining load of 60% of the total initial stress, compared with the 55% obtained with the $\psi=0$ assumption.

3.3.3.3 Additional Consequences of the Consolidation Process

Some of the consequences of the dissipation of excess pore pressures have already been pointed out in the previous paragraphs. The results of the analyses conducted by Johnston (1981) and described in Section 3.3.2.3 are useful to illustrate some points.

Figure 3.15 presents the distribution of surface and subsurface settlements before and after consolidation for OCR=1. The events occurring prior to the consolidation include undrained excavation, support of the tunnel with a 0.508 m thick impermeable lining (Young's modulus=0.5175 GPa) and closure of a void gap of 91.4 mm behind the lining at the crown. An increase in the settlement due to the

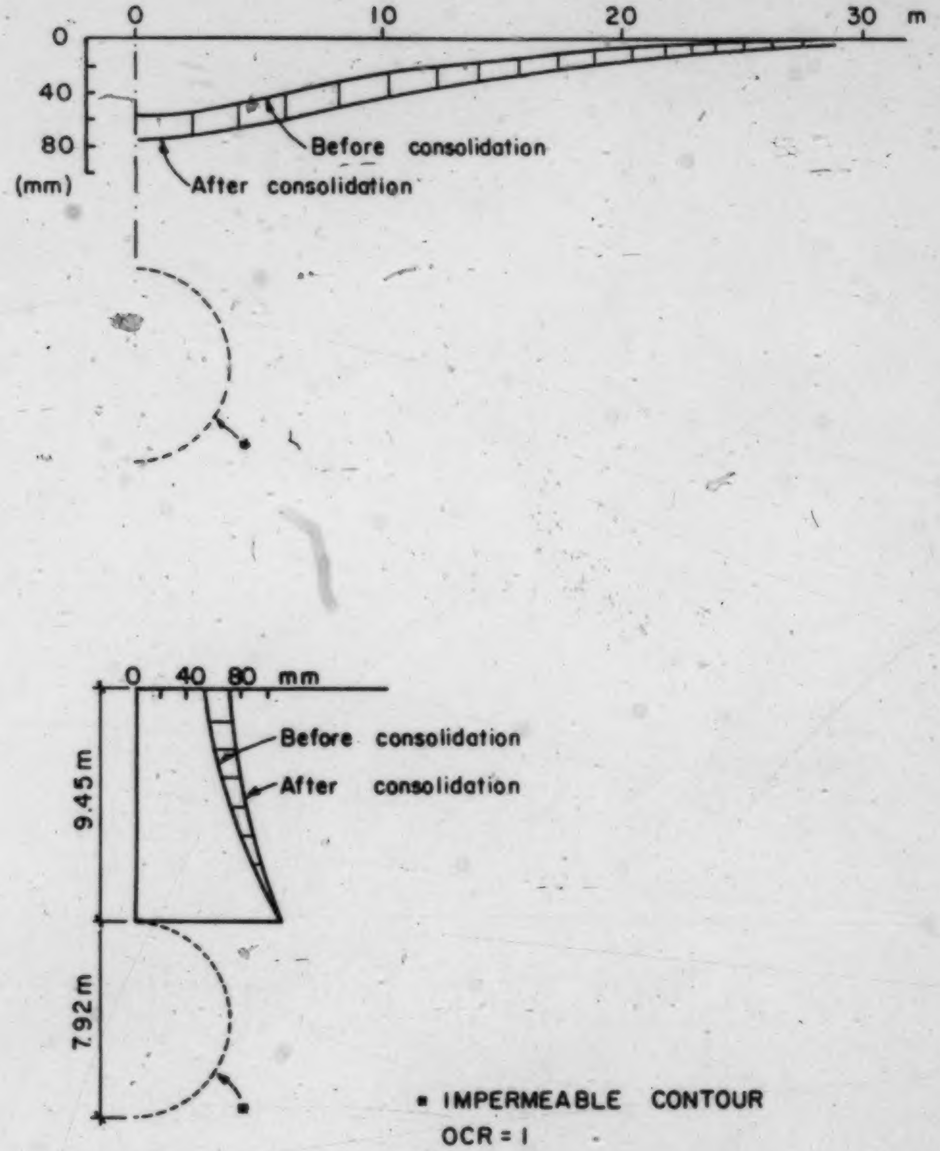

Figure 3.15 Distributions of Surface and Subsurface Settlements before and after Consolidation (modified from Johnston, 1981:104)

consolidation is noted, but this was found to be a function of the void gap size. For an OCR=2, almost no increase in settlement was noted (Johnston, Op.cit.:136) and, actually, they even decreased locally by virtue of the swelling and associated heave developed in the high suction zones below the tunnel. Also when the gap size was reduced to 50.8 mm, for OCR=1, only a marginal increase in surface settlement was noted with time (Johnston, Op.cit.:131).

These results broadly confirm field observations in lightly to heavily overconsolidated clays showing that most of the settlement measured develops within a short term during tunnel excavation, and that those due to time dependent factors account only for a small fraction (if any) of the total displacements observed (see for instance, Barrat and Tyler, 1976:7). If the ground control is efficient (represented by a smaller void gap in the numerical analysis), then the degree of disturbance and remoulding induced in the clay is reduced and the long term fraction of settlement is considerably reduced. For instance, Palmer and Belshaw (1980:179) reported an increase of less than 15% in settlement over sections of the Thunder Bay tunnel one year after the drivage, when good ground control was exerted. This may be compared with an almost 100% increase, also after one year, in a length where poorer ground control prevailed. This occurred in a zone where a slightly more unfavourable stratigraphy existed, due to a slightly thicker clay cover (Belshaw and Palmer, 1978:578, Palmer and Belshaw, 1979:168). Poorer ground control can be understood in terms of higher stress releases in the opening and therefore the associated increase in both shearing and pore pressure changes. Higher long term displacements are observed mainly in very soft to soft, normally to very lightly overconsolidated soils, such as the Mexico City clay (Rodriguez et.al., 1983:432, Schmitter and Moreno, 1983:406), the San Francisco's recent bay mud (Clough et.al., 1983:140), and some alluvial clayey or silty soils in Japan (Hanya, 1977:776), in Newcastle, U.K. (Sizer, 1976:34) and in Ireland (Glossop and Farmer, 1979:70). The length of time required to stablize displacements in these cases, varied from 20 to 300 days. Clearly, if the tunnel acts as a drain, the steady state flow that eventually develops will further increase these settlements.

Another important consequence of the consolidation processes around tunnels in soil, is the change in lining loads that has been referred to before. Peck (1969:250) presented results of long term observations of average all-around soil pressures on tunnel linings in different clayey soils, showing that in some cases they tend to increase at almost linearly with the logarithm of time. Peck also showed similar trends for the relative increase in the tunnel horizontal diameter. Tunnellers use different (and conflicting) jargon when alluding to this phenomenon, calling it 'squeezing' or 'swelling'. Considerable controversy has been raised on the subject. Some authors prefer to treat the problem using the framework of 'classical' soil mechanics, attributing it simply to the 'primary' (non-linear) consolidation of the soil (Atkinson and Mair, 1981:20, Gunn, 1984:21, Gunn and Taylor, 1985:75, and others). If this is so, the rate of increase in lining loads attenuates in a log time plot, as in Figure 3.14. Some of Peck's (1969) data seems to follow this trend. Others contend that the phenomenon is solely controlled by the creep behaviour of the soil medium or to the 'secondary' consolidation of the clay, giving loads which increase at a constant rate in a log time plot. The ground response is interpreted by means of viscoelastic function, in terms of deviatoric creep (e.g. Sakurai and Yamamoto, 1976, Carter and Booker, 1982) and of volumetric creep (Carter and Booker, 1983). Others use viscoelastic - plastic models to represent the time-dependent response (e.g. Sakurai, 1970), or viscoplastic models (Nguyen Minh, 1986).

Despite the considerable computational and modelling efforts undertaken, not much has emerged from these approaches in practical terms, as far as soil tunnelling is concerned. Attempts to simulate observed field responses by the proposed numerical models has largely been avoided. A superficial overview on the subject may possibly suggest that, more often than not, the time dependent lining load response can be explained in terms of the equalization of pore pressures in a "classical" consolidation framework. For the London clay tunnels, most of them driven through the less fissured 'blue' horizon, it is inviting to draw a parallel between observed responses and the long term behaviour of first-time slides in cuttings in London clay. The delayed failures in a number of cuttings in the more fissured upper 'brown' zone, were attributed to the very slow rate of pore pressure stabilization. This process was not very clearly understood prior to research conducted at Imperial College in the early seventies and summarized by Skempton in 1977. Time spans in excess of 40 to 50 years were recognized as being required to equalize the negative pore pressure changes and to recover an equilibrium condition. It would not be surprising to identify similar delayed responses in terms of lining load build up or of diameter change, in tunnels excavated through the less fissured soil. Vaughan and Wallbancke (1973) noted that the back estimated coefficient of swelling in a cut in the Blue London clay, from field measurements of pore pressures, was not dissimilar in magnitude from those obtained from laboratory testing of small undisturbed samples.

All London clay tunnel case histories reported by Peck (1969) involved continued monitoring up to about 10 years or less. The much longer time required to stabilize the ground response could have possibly eluded Peck's scrutiny, since in the sixties this fact was not fully appreciated. The data he reported could well have lain in the early or mid portions of the lining load-log time plot as in the segment AB in Figure 3.14(a). The linear extrapolation of the loads in the log-time plot led him to suggest the use of a design lining load, equal to the fully recovered averaged in situ stress $(1+K)\gamma z/2$ for heavily overconsolidated swelling clays such as the London clay (Peck, Op.cit.:258). However, the rate of load increase may attenuate in the long term and the final lining loads may stabilize at a lower average stress level. If this interpretation of the time-dependent behaviour of tunnels in London clay is correct, then Peck's recommendation regarding the long term loads on a lining can only be accepted as a design hypothesis. Moreover, it is a conservative assumption, as it is equivalent to ignoring the ability of the soil to withstand shear. The long term progressive failures in slopes of cuttings in London clay, revealed that the effective strength parameters of the soil approach, 40 to 50 years after excavation, the "fully softened" or "critical state" condition. These values are lower than the peak strength but higher than its residual values (Skempton, 1977:267). This reduced strength could enable the soil to carry some load caused by the excavation unloading, and allow the lining to achieve final equilibrium under loads smaller than those in situ.

A review of the data quoted by Peck (1969:252) on tunnels in London reveals that in all cases he studied but one, the maximum long term average lining loads ranged between 44 and 83% of the in situ stress. These were calculated using a K_o profile given by the average Skempton (1961) and Bishop et.al. (1965) for London clay. One case lies above that range, showing a local maximum around 98% of the total in situ stress. The final load measurements in this tunnel built in 1942 with a reinforced concrete lining, showed some scatter, and an "average" maximum of 90% could also be interpreted.

Although debatable, Peck's suggestion of a full overburden load for the final tunnel liner design pervaded unchallenged in practice, possibly because it is, in many instances, not a critical design loading. Modern tunnel design calls for flexible linings with low bending moments. The assumption of full overburden, therefore, tends not to aggravate the lining design, since it can be accommodated by a nominal increase in lining thickness at marginal costs. Moreover, prefabricated lining systems have their sections largely controlled by conditions other than ground loads, such as handling, assembling and shield loads.

On the other hand, one could also argue that since soil tunnels are frequently built with fairly low factors of safety, some sort of "drained" creep response under sustained shear stress could possibly be expected. Bishop (1966:124) showed that London clay samples subjected to constant shear stresses around 90% of peak strength, can be brought to failure under drained conditions. He also pointed out that the creep rate does not stay constant at any stage in his tests, which precludes the use of simpler rheological models to solve the problem. Depending on the factor of safety applied to the peak strength, Bishop detected that the creep rate increased or decreased. Although in reality, the shear stress may not remain constant as in Bishop's tests, it is possible to accept that this creep response may not be significant whenever the factor of safety against tunnel collapse is high.

The aforementioned discussion stands on a very speculative basis. 'Primary' consolidation may account for a large portion of the observed time dependent loads but creep or 'secondary consolidation' may well have role in this load build up process. This may be the case in softer, recent organic clay deposits, subjected to a high stress release by the tunnelling operation. There is a clear need of investigations of these phenomena as related to its effect on a soil tunnel response. The comments by Ladanyi (1982:6) regarding the effect of time in rock structures, is equally valid here. Too few cases of long term observations in soil tunnels are available, or if so, the time of observation is generally too short, in order to allow a proper understanding of the effect of time on the soil response.

3.3.4 Drained and Undrained Behaviour

3.3.4.1 Foreword

As any other geotechnical structure, there is a practical need to identify the likely response of the soil around a shallow tunnel, in terms of the of generation and dissipation of excess pore pressures with time. The method of analysis used to anticipate the ground response (eg.

settlement prediction, lining loads, factors of safety, etc.), as well as the selection of the soil input parameters, normally require the identification of the problem within two extremes: a fully drained or a fully undrained condition. The distinction between these two extreme conditions lies in the rate of loading compared to the rate of pore pressure redistribution. The former is connected to the rate of tunnel advance and the latter to the rate the pore pressures equalize towards a steady state condition, which occurs as the excess pore pressures are dissipated and, possibly, as a new hydraulic boundary condition is created.

Recognizing that a tunnel frequently acts as a drain in the long term, it is appropriate to briefly explore how a steady state condition is achieved in a shallow tunnel.

3.3.4.2 Steady State Seepage

If the tunnel is being driven through an ideally incompressible and saturated granular material, and if no fluid pressure is applied to a stable heading (the opening is under atmospheric air pressure), then there will be changes in the hydraulic boundary conditions of the permeable ground domain. As a result, a flow regime will be estabilished with the tunnel heading acting as a drain. If the soil is assumed to be isotropic and homogeneous, and the lining is assumed to be impervious, a seepage flow net can be drawn, for instance for a condition of no depletion of the original groundwater level (permanent water supply to the system). The water flow will obviously be three-dimensional, but its pattern longitudinally to the tunnel will ressemble that shown schematically in Figure 3.16. This approximate flow net has been drawn ignoring all surface tension effects, and assuming that at a distance from the opening, the water regime is hydrostatic and is not affected by the tunnel. The flow channels 1, 2 and 3, receive out of plane water flow contributions (3D flow supply from the upper and sole aquifer, around the sides of the lined impervious tunnel). This makes the flow net slightly different from that given by Glossop (1978) who assumed a plane strain situation, in which the flow at points far behind the face was fully intercepted by the impermeable lining (the water above the tunnel being unable to migrate to points below it). A point such as A (Figure 3.16) will exhibit a near hydrostatic pore pressure. At B, above the permeable heading, the pore pressure will be very small, as the vertical flow towards the crown is nearly uniform and one dimensional, and thus the total hydraulic head is close to the elevation head. At point C, the pore pressures will be higher than at B, but smaller than A. But if C was moved further to the left, its pore pressure would approach the initial hydrostatic value.

For the present conditions and assumptions, if the heading is advanced continuously, a point like A in Figure 3.16 would experience a drop in pore pressure, followed by an increase once the opening below it is lined. The recovery

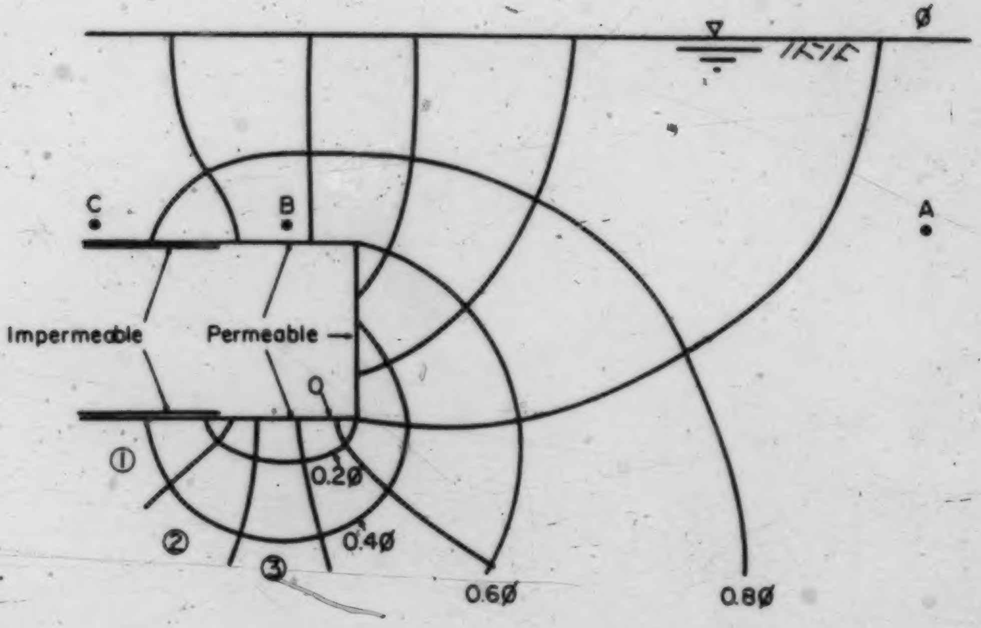
Ø
C
B
A
Impermeable
Permeable
O
①
②
③
0.2Ø
0.4Ø
0.6Ø
0.8Ø

Figure 3.16 Schematic Flow Net in the Longitudinal Plane for a Partially Lined Shallow Tunnel during Construction

in pore pressure may be only partial if the lining has a finite permeability. The transient hydraulic boundary conditions in an advancing heading, may also explain some of the observed changes in pore pressures above tunnels mentioned in Section 3.3.2.3. However, the rate of change in this idealized case will be solely controlled by the rate of tunnel advance and so is time independent.

Once the heading has moved further away, a two-dimensional flow may develop if the lining is permeable. Fitzpatrick et.al. (1981) presented a number of flow nets for different conditions that included the varying geometry (ground cover, diameter and depth to impermeable bedrock), varying the lining permeabilities, non-homogeneities in the ground profile, anisotropic permeability and the effect of compressed air. In all cases, they considered that a strong aquifer recharge is present, so that the water table will not be drawn down by the tunnel drainage. They have shown that this assumption is fairly easily met in practice for relatively impervious soils (k smaller than 10^{-7} cm/s), since, a water recharge corresponding to 2 to 3 cm of rainfall per year will be sufficient to keep the groundwater table at a constant level.

Figure 3.17 shows two flow nets from Fitzpatrick et.al., (Op.cit:99) for a given geometry, but for two distinct ratios of soil to lining permeability (1 and 10). One notes that in the first case (which represents a fully permeable lining condition, whenever its thickness, is small), along the vertical flow line towards the tunnel crown, the total hydraulic heads are nearly equal to the elevation heads. Therefore, the steady state pore pressures along the symmetrical axis above the tunnel are nearly zero. If the lining has a permeability smaller than the soil, the pore pressures above the tunnel are non-zero. In Figure 3.17(b), the pore pressure at the crown is equal to a head of about 4 m of water. Nevertheless, in both cases the pore pressures above the tunnel experienced a reduction with respect to the original in situ condition.

If the soil is compressible, the ground cover will consolidate upon drainage and settlement will develop. Points located below the tunnel will also experience a reduction in pore pressures and will consolidate as well. If the tunnel construction was performed in such a way that the in situ total stress was not altered, and if the lining had a non-zero permeability, then the resulting ground drainage would induce a long term settlement distribution along the cover similar to that shown by the solid line(b) in Figure 3.18(b). Note that at the crown, the settlement due to this process is non-zero as the rigid tunnel lining also settles due to the consolidation of points located below the floor. If one adds this settlement distribution to the immediate displacements induced by the unavoidable changes in the total stress caused by the tunnel construction (dashed curve (a) in Figure 3.18), the resulting settlement distribution could be that given by the dotted-dashed curve (c). This

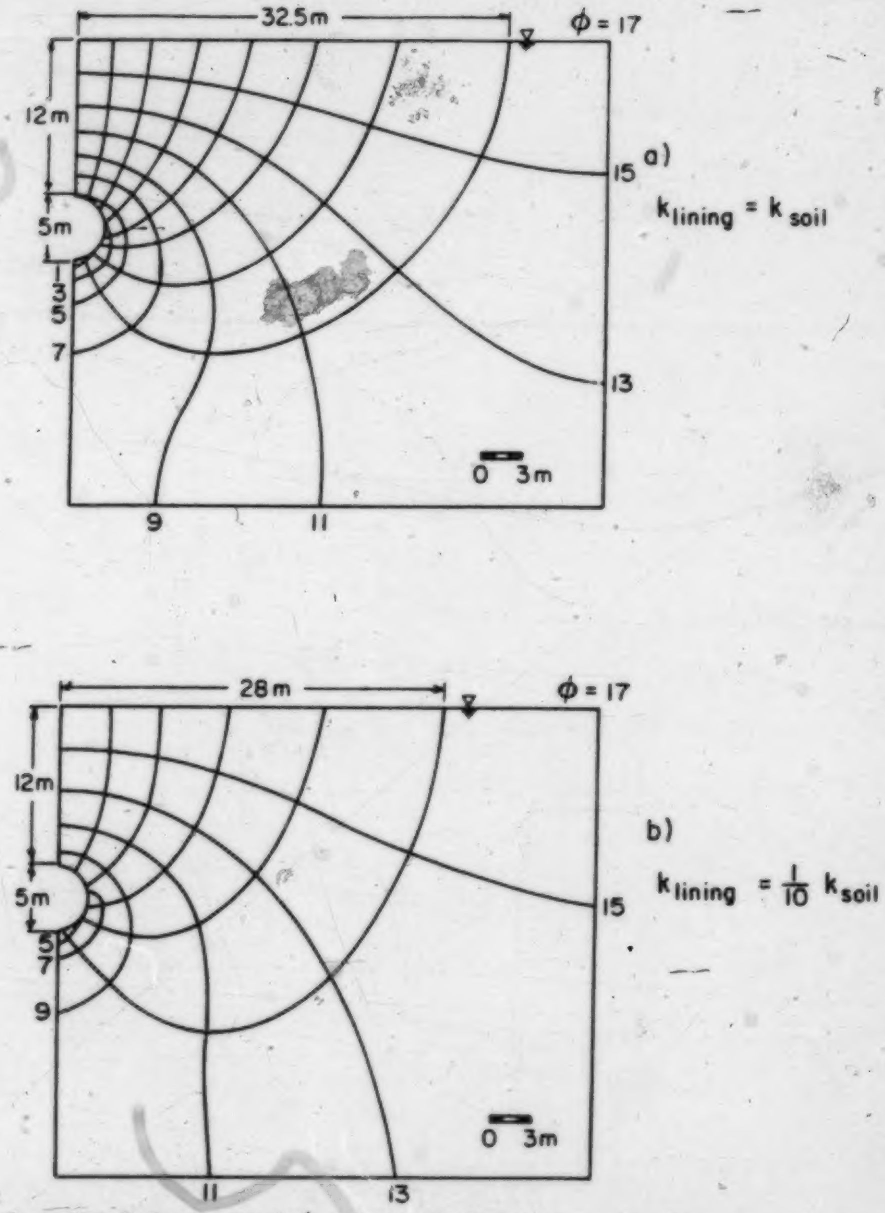
32.5m
φ = 17
12m
5m
1
3
5
7
9
11
13
15
a)
$k_{lining} = k_{soil}$
0 3m
28m
φ = 17
12m
5m
5
7
9
11
13
15
b)
$k_{lining} = \frac{1}{10} k_{soil}$
0 3m

Note: Total equipotential hydraulic head ϕ calculated for a zero elevation head at tunnel floor.

Figure 3.17 Steady State Flow Nets Around Shallow Tunnels with Different Lining Permeabilities (from Fitzpatrick et.al., 1981:99 - modified)

curve is similar to that shown for after consolidation in Figure 3.15, the difference being that the permeable tunnel condition allowed higher long term settlement to develop. A near zero vertical straining condition can therefore result without being associated with a near collapse situation, as pointed out in Section 3.2.2. This feature has been observed in a number of tunnels driven through soft, normally or lightly overconsolidated clays (for example, by Terzaghi, 1942:185 in the Chicago Subway, by Glossop and Farmer, 1979:71 in the Sewer Tunnel at Sydenham, Belfast, etc.). In this type of soil, the settlement associated with the drainage may become significant, and perhaps as large as those developed in the short term by the tunnel excavation. However, if the soil is overconsolidated or if the lining is impermeable, then the long term increase in settlement will be a small fraction of the immediate settlement. An approximate assessment of this long-term settlement was done by Howland (1981) for some of the soft clay cases just referred to. Howland simply used Terzaghi's one-dimensional consolidation theory, only taking into account the changes in pore pressure given by the steady state flow net. Despite the obvious simplification, the calculated surface settlement compared well with that measured at different times after tunnel construction.

The consequences of a steady state flow regime on the loads of a fully permeable lining have not received much attention. One reason for this could be that a lining is

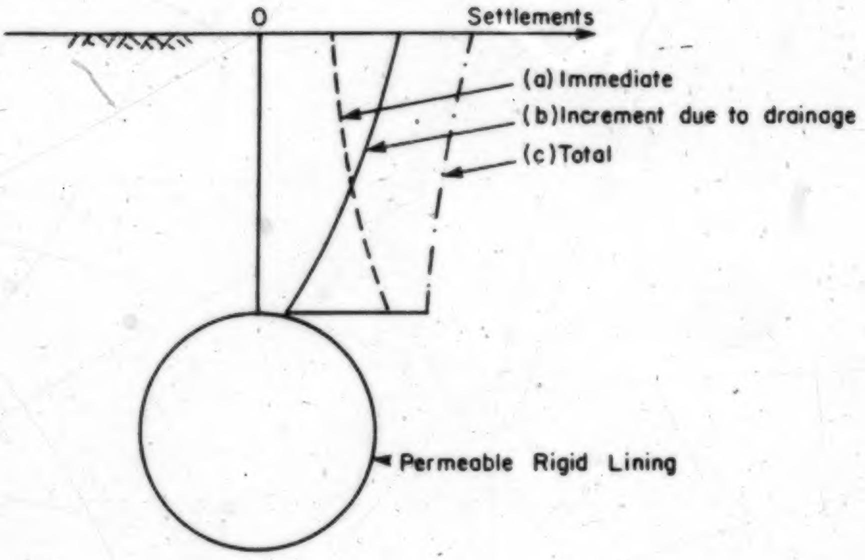
0
Settlements
(a) Immediate
(b) Increment due to drainage
(c) Total
Permeable Rigid Lining

Figure 3.18 Schematic Distribution of Settlements in the Cover of a Shallow Tunnel due to Groundwater Drainage

normally designed to be impermeable and therefore the regime is not established. But if it does, one has to take into account the effect of the steady state pore pressures on the effective stresses, even for a hypothetical case of a lining installed without affecting the in situ stresses. Atkinson and Mair (1983) were one of the first authors to address this problem. They questioned the frequently made assumption, that the total load on a tunnel lining is substantially reduced if the latter is made permeable. For very idealized conditions, (they assumed a deep tunnel, no drawdown, and no soil strains after lining placement), they showed that the long term loads are the same regardless of the lining being permeable or impermeable. Their generalization seems debatable and was questioned by others (Hungr, 1985 and Gunn and Taylor, 1985). The limited numerical evidence shown in Figure 3.14 and discussed previously, does not fully support Atkinson and Mair's statement. The magnitude of the soil strains both before and after lining placement, seems to significantly affect the total lining loads. Nevertheless, their conclusion is possibly a valid one, and further research seems needed to clarify the subject.

3.3.4.3 Total and Effective Stress Paths

A proper assessment of the stress paths around a shallow tunnel is not possible without involved numerical analyses. However, to illustrate a few points, one can follow Atkinson and Mair's (1981:22) simplified reasoning.

The total and effective stress changes in an element of isotropic saturated soil near the contour of a deep tunnel will be considered under plane strain conditions. A uniform in situ stress state is assumed and two types of soil are considered: normally consolidated and overconsolidated. Tunnel excavation and support installation is considered to be performed in an undrained condition, immediately followed by a consolidation stage. The stress changes are assumed not to cause soil failure.

Figure 3.19 shows the total stress path, ABC, this element of soil may experience (assumed to be unique for both soil types). Point A represents the in situ stress state, and u_o the original hydrostatic pore pressure. From A to B, the opening is unloaded and the in situ stress reduces under undrained conditions. An overconsolidated soil (oc) will react developing negative excess pore pressures and at the end of this unloading proces (point B'), the pore pressure will be u_{oc}, smaller than u_o. For the normally consolidated soil (nc), it will be assumed that the partial unloading is such, that a positive excess pore pressure develops, and at the end of construction (B''), the pore pressure is u_{nc}, larger than u_o. Following the construction period, consolidation occurs and is fully completed at the C points. If, for simplicity, the changes in total stresses during this process are ignored, as in Terzaghi's linear consolidation theory, points B and C coincide and no change in the mean total normal stress or shear stress develops. If

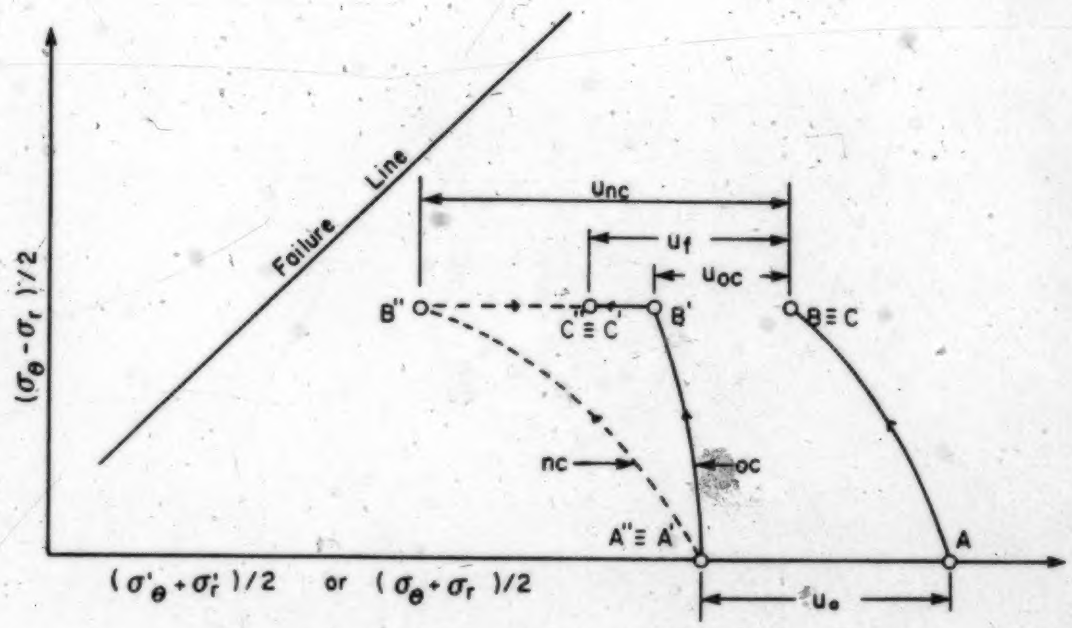
Failure Line
u_{nc}
u_f
u_{oc}
B''
C ≡ C'
B'
B ≡ C
nc
oc
A'' ≡ A'
A
u_e
$(\sigma_\theta - \sigma_r)/2$
$(\sigma'_\theta + \sigma'_r)/2$ or $(\sigma_\theta + \sigma_r)/2$

Figure 3.19 Idealized Total and Effective Stress Paths Around a Tunnel

the lining has some finite permeability, a steady state flow towards the tunnel will finally be established in both cases and a final equilibrium pore pressure u_f, such as those given by the flow nets in Figure 3.17, is attained at C. The overconsolidated soil will swell to C', with the effective stress path moving towards failure. The normally consolidated soil will consolidate towards C'', away from failure, the factor of safety thus increasing. Under the assumed conditions, the paths B'C' or B''C'' lead to pure volumetric straining, whereas along A'B' or A''B'', only shear strains develop.

3.3.4.4 Changes in Stability with Time

One reason to identify what kind of response the soil will exhibit in terms of pore pressure changes, is the assessment of the ground stability. Strictly speaking, the stability to be investigated is that of the ground and lining combined. However, if it is assumed that after heading excavation, the support is installed with good soil contact and with sufficient structural capacity, the concerns are generally limited to the ground stability during the unsupported heading advance, (Section 3.2.1.). Therefore, it is normally assumed that the plane strain stability condition of a tunnel is not critical, if the three dimensional stability of the heading has been ensured. Despite this generally being the case, it is worthwhile to address the plane strain stability problem of a hypothetical tunnel in which the lining action is represented by an internal tunnel pressure and the opening contour is assumed to be partly permeable.

For these idealized conditions it is tempting to draw a parallel between other geotechnical structures and the shallow tunnel problem. Bishop and Bjerrum (1960:469) investigated the changes in the stability conditions of open cuts in clay. They suggested on theoretical grounds that, due to the negative excess pore pressures that are generated in the undrained unloading of an excavation, the reduction in effective stresses with swelling and the establishment of steady seepage leads to a critical long term condition in terms of stability. In an open cut, the in situ stresses at the cutting profile are fully reduced, and therefore the reduction in the mean principal stress tends to dominate the pore pressure changes. Negative pore pressure changes are likely to occur, irrespective of the shear stress changes and possible effects of the rotation of principal stresses.

Under these simplified assumptions, the stability response of a shallow tunnel with time is likely to be distinct from that of an open cut. The reason for this is that the undrained pore pressure response in a tunnel depends on the amount of stress release allowed by the construction. Figure 3.20 depicts the possible changes in the average shear stress, pore pressure and factor of safety for a shallow tunnel in overconsolidated and normally consolidated clays. It has been assumed that tunnel construction is performed in undrained conditions, with pore pressure redistribution occurring thereafter. Also, it has been supposed that the average shear stress along potential slip surfaces above the crown, remains constant during the consolidation process. This may not be correct if a lining is installed which restricts displacements in the opening. Even if the ground is assumed homogeneous, isotropic and elastic, it is known that the total stresses at the beginning and at the end of the consolidation process will not be the same if a displacement boundary condition is introduced (Lambe and Whitman, 1969:417,489). It was also shown (Figure 3.14), that the total stresses change in a consolidation process involving time-dependent plastic behaviour of the ground. Nevertheless, it will be assumed, for discussion purposes, that the shear stresses remain unchanged after construction.

It was shown in Section 3.3.2 (for instance, Figure 3.10), what the likely changes would be in pore pressures of a soil element close to the tunnel, upon a decrease in the tunnel internal pressure. From this, the pore pressure responses during the undrained unloading can be qualitatively estimated. Depending on the amount of in situ stress release, on the degree of overconsolidation of the soil, and on the final pore pressures developed at equilibrium, the pore pressures in an overconsolidated soil may or may not reach a minimum at the end of construction. Consequently the long term stability condition may or may not be a critical one (Figure 3.20a).

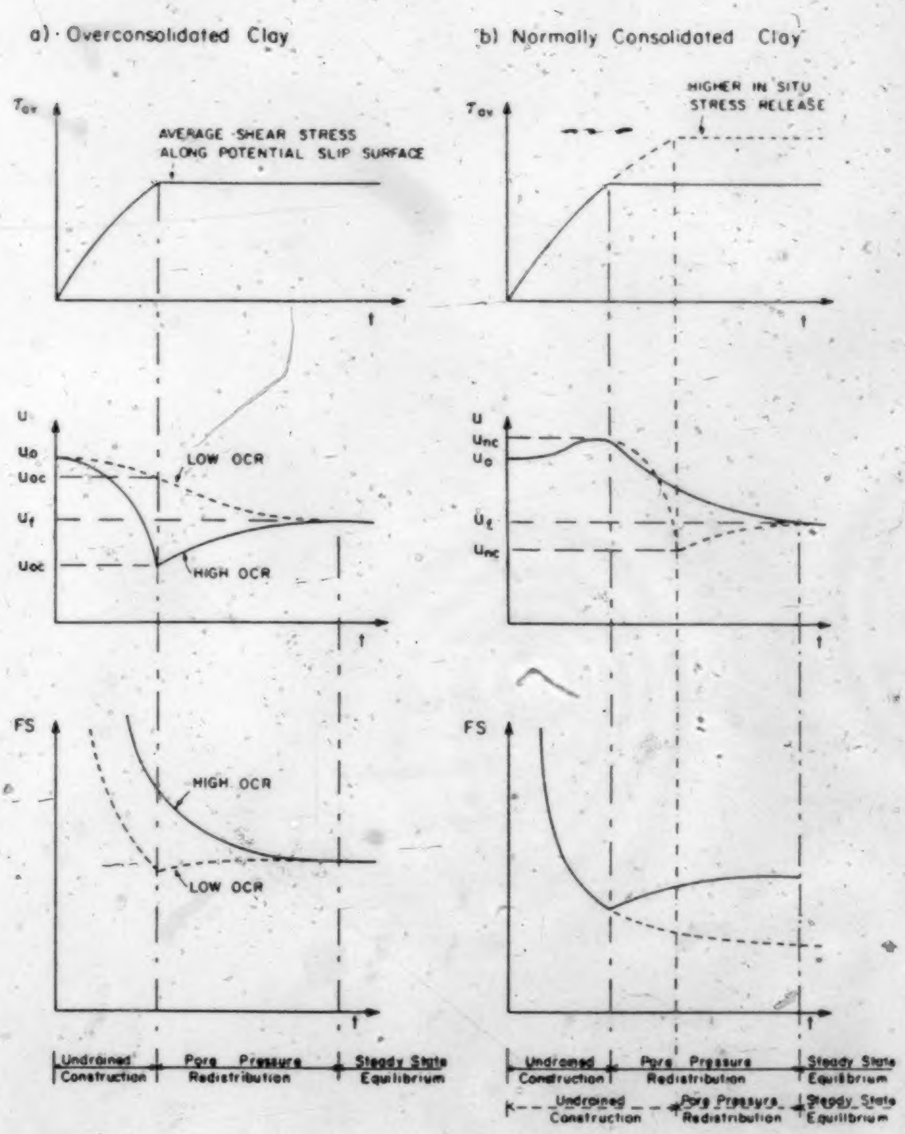

Figure 3.20 Idealized Changes in Shear Stress, Pore Pressure and Factor of Safety during and after Construction of a Plane Strain Shallow Tunnel in Saturated Clay

If the construction induces different degrees of shear stress mobilization in a normally consolidated clay (Figure 3.20b), the pore pressure response may be somewhat dissimilar. For limited in situ stress release corresponding to a good ground control condition, the pore pressures may show an increase by the end of the undrained tunnel construction, followed by a decrease with time. The associated change in the factor of safety will indicate a critical condition in the short term rather than in the long term. However, if the construction technique is poor and allows substantial plastification of the soil around the opening during the undrained unloading process, then the pore pressure changes may become negative close to the tunnel and one could speculate that a critical long term stability condition may develop.

If the tunnel contour is assumed to be fully impervious, so that a hydrostatic condition is re-established with u_f equal to u_o, and if good construction is applied with reduced amount of in situ stress release, then the most likely responses are similar to those shown by the solid lines in Figure 3.20a or b. Hence for the overconsolidated soil, the critical stability situation is in the long term and in the short term for the normally consolidated soil. The limited amount of evidence from theoretical studies, field observations and model testing discussed in Section 3.3.2.3, suggest, however, that for these described conditions (particularly if the ground control is good), the undrained changes in pore pressures in the tunnel cover are likely to be small, compared with those found in other geotechnical structures. In contrast to an open cut excavation, the mean principal stress in the cover of a shallow tunnel does not decrease as much. Thus, the pore pressures may be controlled mainly by the shear stress changes, which are limited if the construction quality is good. Therefore, one might suggest that the changes in the factor of safety after the undrained tunnel construction could be relatively small, whenever the tunnel contour is impermeable.

Unlike Bishop and Bjerrum's (1960) suggestion for slope excavation, which has been proven correct both through numerical simulations and by interpretation of actual cases (see, for example, Kenney and Uddin, 1974 or Eigenbrod, 1975), the discussion with respect to tunnels should be taken as speculative. Finite element simulations for generation and dissipation of pore pressures seem to provide a valid approach to check this conjecture. Static model tests of tunnels in conditions resembling those established here, both for normally and overconsolidated kaolin (Seneviratne 1979:64) appear to confirm what has been suggested: that critical stability is in the short term for OCR=1 and in the long term for OCR>3.

3.3.4.5 Drained and Undrained Response Boundaries

To the writer's knowledge, no quantitative criteria have been made available so far, allowing the classification of a tunnel response as drained or undrained. Legitimate treatment of this problem would require, for instance, an approach similar to that followed by Eigenbrod (1975) for slope excavation, extended to cover an ample range of influencing parameters, and necessarily including the three dimensional nature of the tunnel heading advance.

The definition of the degree of consolidation in a plane strain tunnel problem is not as simple as in a one-dimensional situation. In a shallow tunnel, both positive and negative excess pore pressure dissipation occurs simultaneously and the usual definition of the compression at a certain time, divided by the final compression, may not be satisfactory, as the consolidation swelling process may have a balancing effect. For this reason, Johnston (1981:103) introduced an excess pore pressure constant, U_e, as

$$U_e = \int_A |\Delta u| \, dA \qquad [3.17]$$

and, defined a degree of consolidation as

$$U = 1 - \frac{U_e}{(U_e)_{max}} \qquad [3.18]$$

The non-dimensional time was expressed by Johnston (Op.cit.:105) as:

$$T = \frac{ct}{z^2} \cdot \frac{(1-2\nu)}{2(1-\nu)} \qquad [3.19]$$

where c is the coefficient of consolidation defined in terms of the soil elastic constants at the tunnel axis elevation, and z is the drainage distance, taken as the depth to the tunnel axis. Both the surface and the rigid base at 2z below, were taken as free draining boundaries in his analysis. A plot of the degree of consolidation, U, against T is shown in Figure 3.21(a), using the lining and soil properties (OCR=1) given in Section 3.3.2.3, and assuming a gap closure of 91.4 mm (same conditions that led to the settlements shown in Figure 3.15). One notes that most of the consolidation process has taken place before T=0.1.

For comparison, the maximum surface settlement is shown in Figure 3.21(b). It is expressed as a percentage of the final surface settlement at the tunnel axis, plotted against the non-dimensional time factor. It is noted that most of the settlement takes place before T=1.0. The evolution of the maximum surface settlement lags behind the degree of consolidation. This is caused by the negative excess pore pressures below the tunnel floor (Figure 3.11) that dissipate more rapidly than the positive excess pressures elsewhere. The faster swelling (and heave) associated with the former, initially hinders the overall settlement trend, which is controlled by the consolidation of the positive excess pore pressure area around the springline. This process occurs at a lower rate and has a longer drainage path (Johnston, Op.cit.:105).

Also worth noting in Figure 3.21b is the fact that the time dependent settlement, in this case (normally consolidated clay, impermeable lining and a large void gap

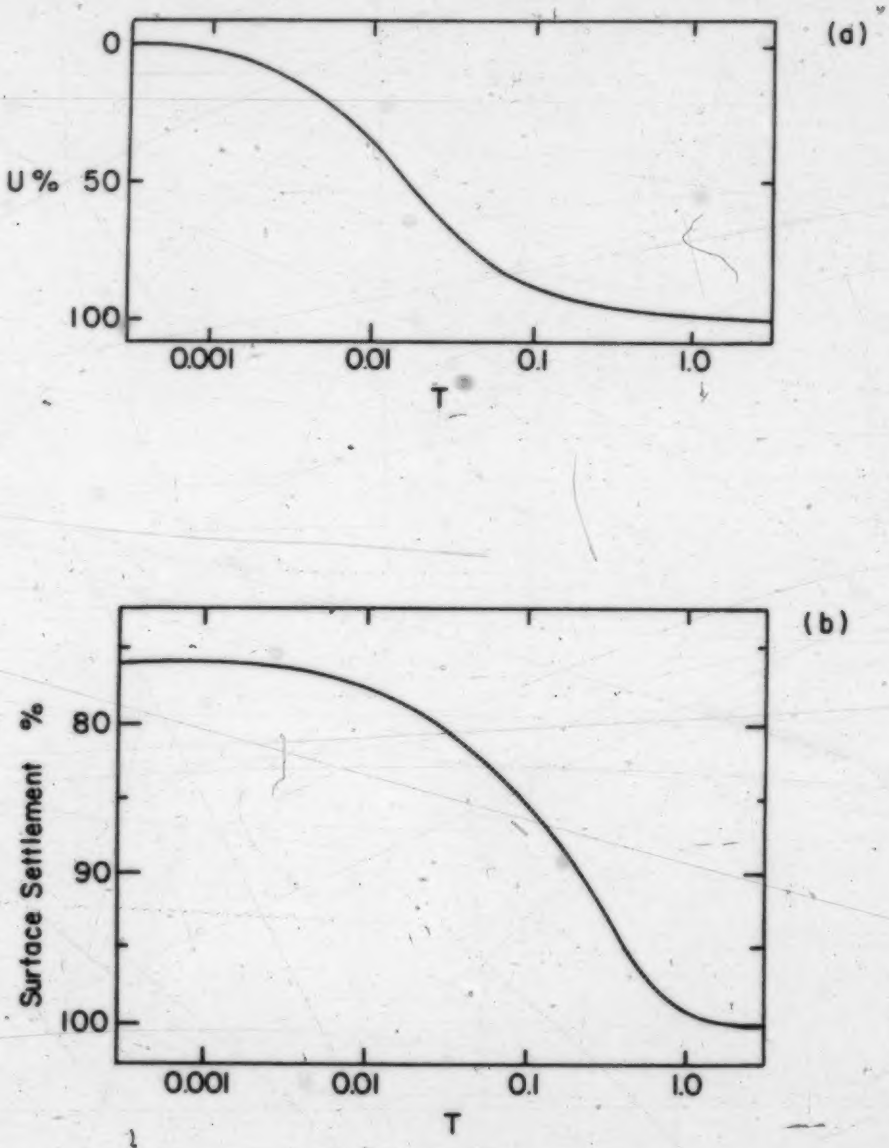

Figure 3.21 Degree of Consolidation and Maximum Surface Settlement Evolution in a Shallow Tunnel (modified after Johnston, 1981:,106)

behind it) is responsible for less than a quarter of the total surface settlement. This fraction is reduced to 14% when the fictitous gap is reduced to 50.8 mm (Johnston, Op.cit.:131) and to 11% for a 50.8 mm gap when the OCR is increased to 2 (Johnston, Op.cit.:136). This confirms that, with good ground control and an impermeable lining, for both lightly and more overconsolidated soils, the time independent settlements are far greater than the time dependent ones. The latter are considered negligible for all practical purposes.

Curves as shown in Figure 3.21 are useful to evaluate the amount of time required for a fully drained response to be achieved. However, they are only applicable to the limited conditions (Johnston, 1981), and therefore it is worth investigating the influence of some extreme conditions.

For a deep unlined tunnel with an impermeable contour, the linear elatic consolidation solution provided by Carter and Booker (1982:1070) can furnish some assistance. Equation 3.10 and Figure 3.12(a) give the pore pressure changes at any point around the tunnel, for some dimensionless time factor, T. Recall that the Poisson's ratio of the soil skeleton is equal to zero, which corresponds to the slowest rate of consolidation (Section 3.3.3.1). By using the same definition of the degree of consolidation introduced by Johnston (1981:103), in terms of the absolute modulus of excess pore pressure over the total area of the soil around the circular opening, it is possible to numerically integrate the curves shown in Figure 3.12(a), for each of the time factors given. One is then able to say that, for T smaller than 0.1, the consolidation process is incomplete, with less than 10% of the consolidation having occurred. On the other hand, it is noted that for T greater than 100, the consolidation process is nearly complete, with more than 90% of the consolidation having occurred. Bearing in mind the definition of the time factor T given by the equation 3.11, one can easily establish practical boundaries for undrained and drained behaviour.

The following points are established for an elastic, isotropic and homogeneous ground. For the consolidation process of the excess pore pressures generated by the shear stress changes around an unlined and impermeable deep circular opening, one can say that:

1. tunnels with diameters D, such that

   $$D>\sqrt{40ct} \qquad [3.20]$$

   will exhibit negligible (U<10%) consolidation over a time interval t, after the full release of the in situ stresses under undrained conditions;

2. tunnels with diameters D, such that

   $$D < 0.02\sqrt{ct} \qquad [3.21]$$

   will exhibit appreciable (U>90%) consolidation over a time interval t, after the full release of the in situ stresses under undrained conditions.

The chart shown in Figure 3.22 is readily obtained following similar reasoning used by Vaughan (1974) for the dissipation of pore pressures in embankment dams. If one takes, as an example, a deep 4 m tunnel in blue London clay, with a consolidation (or swelling) coefficient of about 10^{-4} cm^2/s, one notes that over a time period of one year, the redistribution process of the excess pore pressure can be taken as negligible.

It is possible that the above analysis can provide some insight into a deep tunnel case, but for a shallow tunnel or in the case where the lining is permeable, it may not be adequate. Another extreme situation that could be envisaged, is that of a shallow tunnel built in such a way that the installation of a rigid lining does not disturb the in situ stress condition and in which the pore pressure changes are solely produced by a change in the hydraulic boundary condition at the tunnel contour. If it is assumed that the tunnel lining is fully permeable, a steady state seepage flow net similar to that shown in Figure 3.17 may eventually be formed. If the ratio, H/D, is small, the pore pressures along line AB (inset in Figure 3.23) in the ground cover, will end up being very close to zero. A nearly uniform gravitational flow is established along AB, with an average hydraulic gradient equal to one, since the total hydraulic head losses are approximately equal to the elevation head losses. This is so even for anisotropic flow conditions with horizontal permeability greater that the vertical (see, for

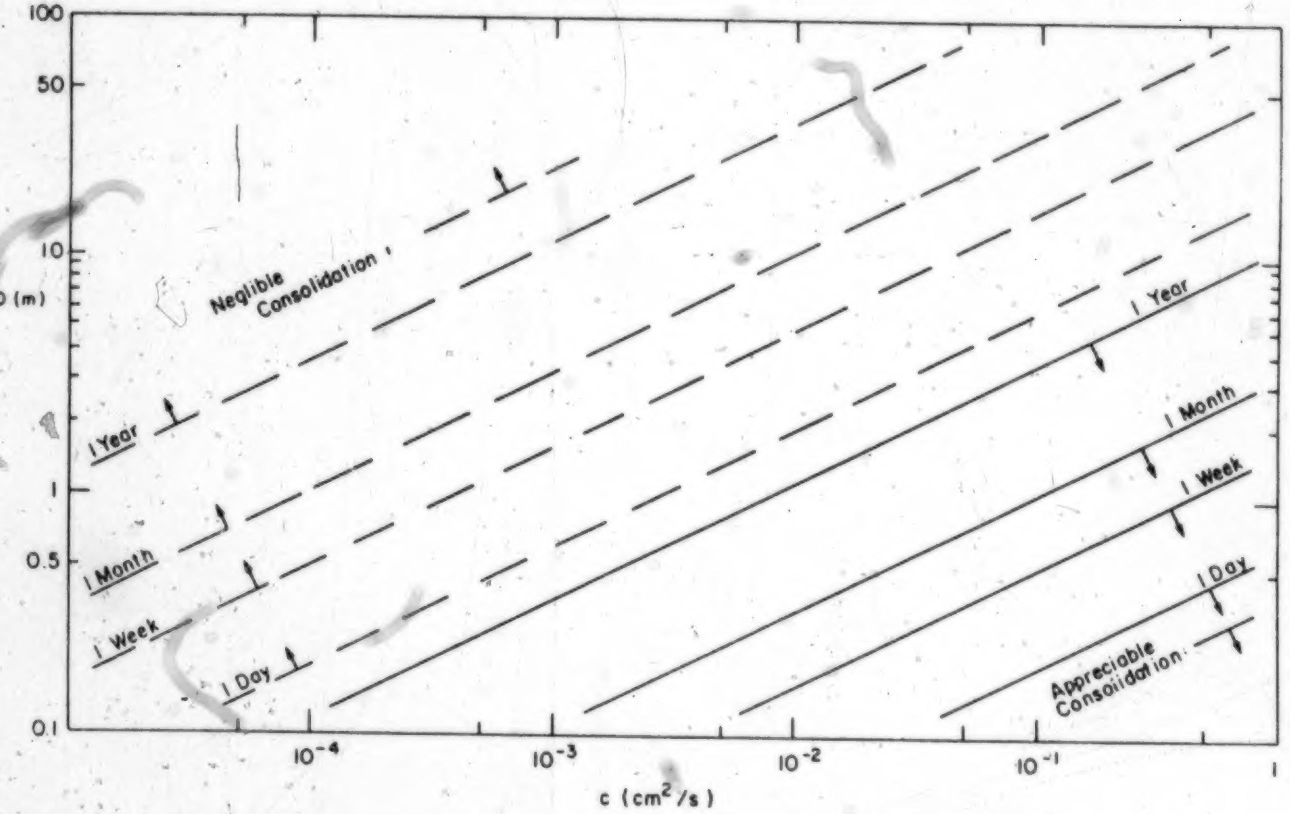

Figure 3.22 Tentative Boundaries for Undrained and Drained Responses Around a Deep, Impermeable Unlined Tunnel in an Elastic Soil

instance, Fitzpatrick et.al, 1981:102).

If one admits that the dissipation process of the nearly triangular excess pore pressure distribution along AB is a unidimensional one, and also ignores possible total stress changes with time, the consolidation of soil elements in the tunnel cover along the symmetry line can be assessed simply by Terzaghi's theory. Therefore, it can be said that for a time factor T smaller than 0.008, the consolidation along AB is incomplete * with less than 10% of the process developing. On the other hand, the consolidation along AB will be nearly completed, with more than 90% of excess pore pressures dissipated, for T greater than 0.848.

For the consolidation process along the line of symmetry, AB, of the tunnel cover due only to excess pore pressures generated by the change in the hydraulic boundary condition at the fully draining tunnel contour, one can say that:

1. tunnels with depth of cover H, such that

   $H > 22.361\sqrt{ct}$ [3.22]

   will exhibit negligible (U<10%) consolidation over a time interval t, after tunnel construction;
2. tunnels with depth of cover H, such that

   $H < 2.172\sqrt{ct}$ [3.23]

   will exhibit appreciable (U>90%) consolidation over a time interval t, after tunnel construction.

---

*, For this particular case $T = 4ct/H^2$, as a double drainage condition was assumed, H being the depth of the cover.

The above boundaries are also approximately valid for tunnels which are partly draining (lining with a finite permeability), provided the initial excess pore pressure distribution along AB is close to linear.

Again, the chart shown in Figure 3.23 can be easily obtained. One may consider, as an example, the large cross section tunnel built for the Sao Paulo Subway system, described by Eisenstein et.al., (1986:713). The tunnel was driven through a stiff, silty-sandy clay layer, with a coefficient of consolidation of about 10^{-3} cm^2/s. The 3 m cover of this soil, underlies a saturated sandy horizon, assumed to be fully draining. Somewhere between one to four weeks, a fully drained condition should have been established. Indeed, the field instrumentation, which included deep settlement points and some hydraulic piezometers, did indicate so (Negro et.al., 1985:58). As another example, one can take the Thunder Bay (Array 2) tunnel, driven through a silty clay-clay layer, to give a cover of 8 m. The material has a c value of about 10^{-3} cm^2/s (Lo and Rowe, 1982:165), and neglecting any other excess pore pressures generated except those due to some drainage, one concludes that only after more than a year could almost full cover consolidation be assumed. If a fully drained condition is set at some sand layer boundary at say 2 to 3 m above the tunnel crown, then, the time required to achieve an appreciable consolidation condition would drop to somewhat less than a year. This is more consistent with the

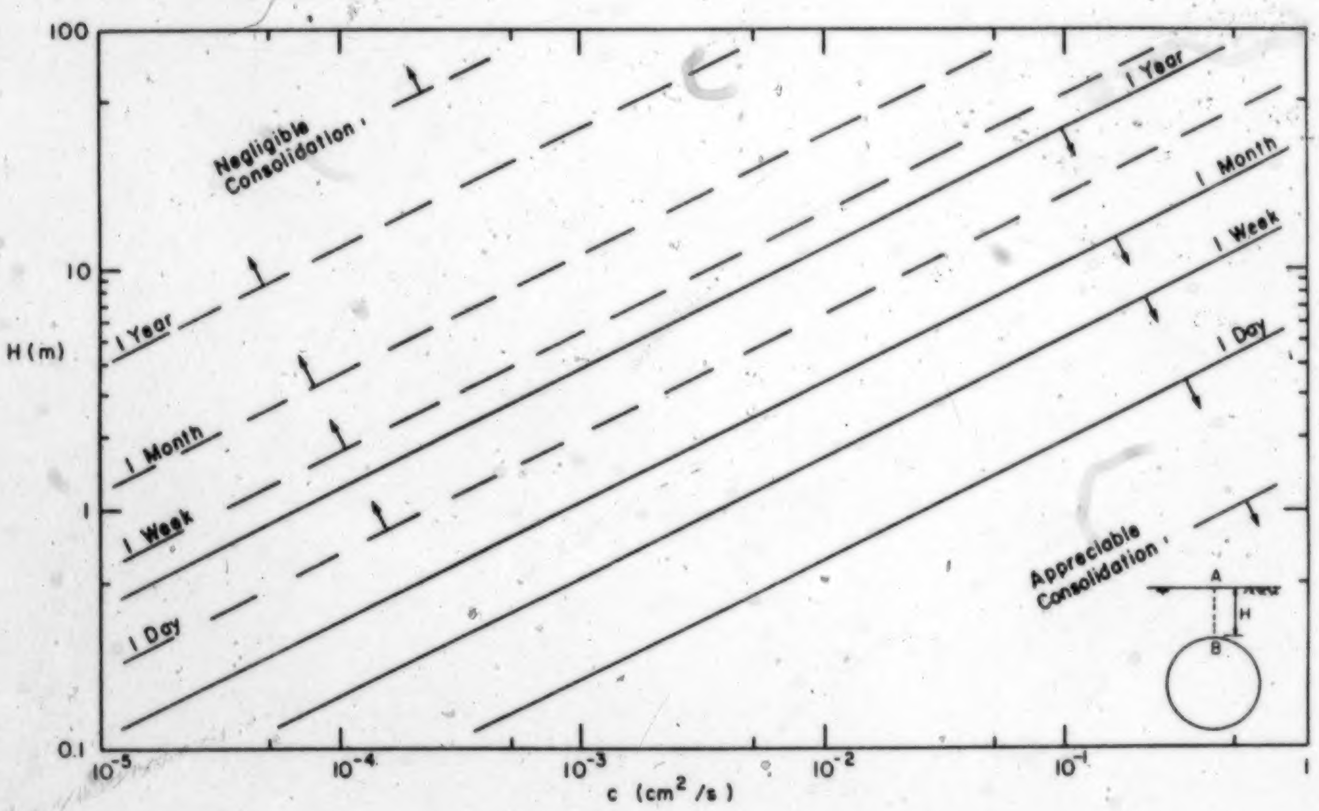

Figure 3.23 Tentative Boundaries for Undrained and Drained Responses along line AB of the Cover of a Shallow and Permeable Tunnel, resulting solely from Ground Drainage

field instrumentation observations made by Palmer and Belshaw (1980:181) who concluded that a near steady state flow condition towards the tunnel existed after a period of one year.

In practical terms, other tentative boundaries could be established to distinguish undrained from drained ground response, by possibly using other less idealized assumptions. The foregoing discussion, perhaps serves more as a simple means of approaching the problem, rather than an attempt to establish general criteria. One feature that should not be overlooked is the different rate of pore pressure equalization and displacements evolution in time, that has been illustrated by a numerical simulation, but is also known to occur in practice. It is believed that even more realistic approaches to the problem will always require some degree of simplification. This will be required on account of the three-dimensional nature of the problem, or on account of stratigraphic singularities frequently found in a site, or on minor hydrogeological details, that have major effects on the rate of pore pressure change with time. A considerable degree of judgement will always be required to accommodate any criteria, simple or otherwise when applied to real situations where such features are normally present. Nevertheless, it would be highly desireable to extend the approach just discussed to more general, but still simplified conditions, such as those that might include the action of gravity, the longitudinal plane strain heading problem, and the axisymmetric heading case. The validity of any criteria emerging from these simplified approaches should ideally be tested against some fully three-dimensional consolidation analyses of a shallow tunnel, that, to the writer's knowledge have not been made available so far.

3.4 Summary and Conclusions

The idealized behaviour of shallow tunnels was further discussed in this chapter. Two behavioural aspects not included or only superficially discussed in the previous chapters were addressed: the stability of a shallow tunnel in soil and the role of groundwater in the ground response.

Tunnel Stability

Though the lining stability can also be a matter of concern, only ground stability problems were addressed in this section. As noted in Chapter 2, even under good ground control conditions, the factors of safety involved in soil tunnelling are usually low and stability deteriorates rapidly with increasing ground displacements. Ground collapse was defined as the creation of a mechanism, through which a local or global disintegration of the ground mass is experienced.

Except for cases of poor lining contact, the ground instabilities are usually restricted to the unsupported length of the tunnel, involving collapses at the face or at the heading. The collapse mechanisms are thus usually three-dimensional.

The groundwater conditions aside, it was shown that the 3D stability of the ground is usually controlled by geometric conditions as well as by the geotechnical parameters (soil strength). An exception to this rule is dense sand, where the stability is less affected by the geometric conditions.

Model test results indicate that the factor of safety decreases as the unsupported heading length increases and as the relative tunnel depth (H/D) decreases. For H/D greater than about 1.5, undrained model tests indicate that the stability ratio or overload factor becomes constant, and the "face only" stability approaches that for a deep tunnel.

Plasticity solutions are useful tools for anticipation of stability problems in a design stage. They may be of little help for the assessment of global stability problems during construction. Different criteria were examined for stability assessment in the field.

The limiting or critical dimensionless crown displacement, U, of 1.8 suggested in Chapter 2, though useful at a design level and of some help for interpretation of field monitoring, may be inconvenient, as it requires the knowledge of the in situ deformation modulus of the ground mass, which is not always available.

The zero vertical straining along the soil cover may not be a reliable criterion for conditions involving appreciable ground volume changes (contraction or dilation).

The use of critical shear strains as a stability index is also of little help, as it may indicate some localized ground failure, that may or may not bring the tunnel to a collapse state. In other words, it may indicate soil failure, but it may not identify the formation of a collapse mechanism.

A perhaps, more promising criterion was suggested. It consists of observing the shape (and sign) of the distribution of longitudinal distortions, calculated from the longitudinal distribution of ground settlements at a certain elevation above the tunnel crown. This criterion was tested against the results of a tunnel heading model test in saturated kaolin and furnished consistent results. Moreover, it was tested in a subway tunnel where a global collapse mechanism was observed. It was shown that the instability experienced could have been identified well before the global collapse occurred.

The idealized stress changes in the crown of a plane strain tunnel, driven through a cohesionless soil approaching collapse, were investigated. The stress changes following ground collapse cannot be determined, so a speculative discussion was undertaken. Possible interpretations were attempted and their consequences analysed.

The relevance of the above discussion is related to the shape of the ground reaction curve of the tunnel crown after collapse stage is reached. There is some evidence that at this stage, the ground reaction curve of a shallow tunnel in soil may sweep upward, when a 'loosening' state develops after a minimum pressure is attained. The ground stress thus, would not be uniquely related to the ground displacements.

The phenomenon can be explained for soils exhibiting loss of strength after a peak strength is mobilized, provided the tunnel is not deep. For other types of soil, no definite explanation was found for the upward trend of the ground reaction curve, inferred from some limited experimental observations in sand.

A speculative model explaining this phenomenon was described. In it, the apparent ground response after collapse is not only a function of ground properties, but is also controlled by the support system. Traditional continuum mechanics approaches may not be adequate to test the validity of this interpretation. A physical or numerical verification of its validity would require simulations under displacement rather than stress controlled conditions.

The relevance of the subject seems to be confined to the post collapse response of a tunnel in non-cohesive granular soils, an area which has not been sufficiently investigated by research in soil tunnelling.

The Role of Groundwater

Though the present research does not involve the study of time dependent ground response due to consolidation, or of other effects related to the presence of water, the subject is important and deserves some consideration.

The presence of water affects the ground stability condition, the settlement magnitude and distribution as well as the lining loads.

The generation of excess pore water pressure was studied through available plane strain analytical and numerical solutions. The development of short term excess pore pressures around an opening is controlled by a number of parameters. The influence of some of these parameters was studied under idealized conditions: the effect of the in situ stress ratio, the effect of gravity, and the effect of the amount of stress release allowed. For less idealized conditions, results of published numerical solutions were interpreted to assess the influence of other factors controlling pore water pressure generation: the influence of non-linear stress-strain properties of the soil, the effect of the overconsolidation ratio, the effect of the ground surface, and the effect of the tunnel lining. In the discussions above, the tunnel contour was assumed to be impervious, an assumption that was later relaxed to assess the likely ground responses for conditions closer to those found in real situations. Results of pore pressure generation analyses, under the three-dimensional tunnelling could not be found. A qualitative assessment of pore pressure changes for these conditions was attempted, taking into account the hydraulic boundary changes associated with the advances of the tunnel heading and lining. Results of some field observations supporting this assessment were discussed.

A full reduction of the in situ stresses may create appreciable negative excess pore pressures around an unsupported heading. This effect is more pronounced in overconsolidated soils, and may explain the ability of some soils to stand up over a certain period of time. The subsequent swelling process will govern the pore pressure equalization and the opening stability, thus controlling what is called the 'stand-up-time'. Though the process governing the phenomenon is fairly well understood, no theoretical criterion has been advanced so far to assess the 'stand-up-time'. Despite being an important parameter which may control contruction sequences, it is presently estimated using purely empirical approaches.

The dissipation of excess pore water pressures around a plane strain tunnel was then studied by means of available analytical and numerical solutions. The linear elastic consolidation around a deep and lined impermeable tunnel, shows that the average support thrust is time-independent, although, thrust forces may vary locally (within±10%) along the tunnel contour. Local changes in bending moments are higher (up to 100% with respect to the short term value).

The above analysis cannot fully explain the increase of lining loads with time in certain tunnels. If the non-linear stress-strain behaviour of the soil is taken into consideration, the results of numerical simulations indicate that an increase in the average thrust value can indeed occur as the pore pressures equalize. The results indicate that the lining loads increase at a non-linear rate with the logarithm of time. Moreover, they show that in the long term, the lining loads stabilize at a higher level than the short term level but lower than that given by a full overburden assumption. Evidence from cuts made in fissured overconsolidated soils such as the 'brown' London clay, suggest that the time required for pore pressure equalization may exceed 40 to 50 years. It would not be surprising to identify similar time dependent responses, in terms of lining load build up, in tunnels excavated through the less fissured 'blue' London Clay.

The above discussion was presented to suggest that the lining load increase with time, observed in some soil tunnels, can be simply explained in terms of non-linear 'primary' consolidation. The linear increase of loads with the logarithm of time suggested by Peck (1969) for tunnels in London Clay, would have resulted from observations gathered over too short a time interval (10 years or less). Had the monitoring been extended to larger time intervals, one might have observed lining load stabilization at levels lower than full overburden, contrary to Peck's interpretation. However, the possibility of 'secondary' consolidation or creep in certain conditions, should not be disregarded. Nevertheless, it can be said that the time dependent ground response will be minimized if provisions are made to restrain the consequences of the non-linear response of the soil. In other words, if higher factors of safety are used, reflecting smaller amounts of ground stress release, prompt lining activation, etc., the time-dependent components of the ground response will be attenuated.

Similar consequences regarding ground settlement development upon pore pressure dissipation were discussed, using available numerical results of 2D non-linear consolidation around shallow tunnels. The time dependent settlements were noted to decrease, as the degree of overconsolidation of the soil increases and as the amount of ground stress release allowed decreases. For good ground control conditions, the short term movements represent the major part of the total ground displacements, unless the lining is permeable and the tunnel acts as a drain. Otherwise, the time dependent components of the movements are small.

The consequences of the development of a steady state seepage into a permeable tunnel were examined, in terms of settlement generation and lining load change. The steady state flow into an unsupported heading in a pervious and incompressible soil was studied. If the tunnel is continuously advanced under these conditions, pore pressure changes will be observed at a point above the tunnel crown. The rate of change in this idealized case will be solely controlled by the rate of tunnel advance, which controls the transient changes in the hydraulic boundary conditions. The observed response is, in this case, totally time independent.

The assessment of the ground stability requires the identification of the ground response, in terms of the generation and dissipation of the excess pore water pressures. The two-dimensional stability of a partly permeable tunnel, supported by internal stresses, was studied in order to illustrate the problem in qualitative terms. Though some parallel could be drawn with the stability of an open cut, the ground response may be dissimilar, as it is affected by the variable amount of stress release allowed in the plane strain model. The porewater pressures may or may not reach a minimum at the end of the undrained reduction of the internal stresses. Depending on the degree of overconsolidation of the soil, on the final steady state pore pressures and on the amount of stress release, the stability of the tunnel for these idealized conditions, can be critical either in the short or the long term.

Tentative criteria were developed in order to identify the likely response of the ground around a tunnel in terms of the consolidation process for certain idealized conditions. The linear elastic consolidation solution by Carter and Booker (1982) was used to identify the amount of pore pressure equalization around a deep, impermeable and unlined tunnel for different coefficients of consolidation, different tunnel sizes, and over different time intervals. A second criterion was developed for another extreme condition, in which the amount of consolidation in the soil cover of a shallow tunnel was investigated. In this criterion, the excess pore pressures were reduced to those resulting from a change in the hydraulic boundary conditions at the tunnel contour, which is assumed to be fully pervious. It would thus represent the equalization process resulting from the drainage of the tunnel cover.

Other similar criteria could have been developed using different approaches. For instance, the consolidation around the unsupported tunnel heading during face advance, could be studied, approximating it by available solutions for the three-dimensional consolidation around a pervious sphere. The foregoing discussions did not attempt a general solution to the problem. Rather, they served as examples of simple lines of approaching it. A more accurate solution would be more complex, and it is believed that a considerable degree of judgement would still be required when applying any criterion of this type to real situations. This judgement will always be needed once it is recognized that minor stratigraphic features or soil heterogeneities, have a major influence on the rate of pore pressures changes with time. Moreover, it was pointed out that the rate of pore pressure equalization may be different from the rate of ground displacement evolution with time.

4. PRESENT STATE OF THE DESIGN OF SHALLOW TUNNELS

4.1 Introduction

This chapter presents discussions on design requirements and on available design methods for single shallow tunnels. Its main purpose however, is to review current design practice and to attempt an identification of the present needs for design method improvements. The discussion will be limited mostly to those design aspects where the geotechnical role is more evident.

The design of soil tunnels involves a number of similarities with respect to the design of other soil structures. At the same time, there are also some peculiarities that make it distinct from the others.

As in foundation design, there is need to satisfy the stability condition of the ground and to anticipate the magnitude of displacements induced by construction. While the total loads in a foundation are more or less readily estimated, since the interaction between super-structure and the ground is routinely ignored, it is not possible in tunnels to disregard the interaction between the support and the ground. Both the magnitude and distribution of these loads are needed for the structural design, particularly for the primary lining.

Also, unlike foundation engineering where there is ample room for manipulating the working loads in the foundation elements by changing the superstructure, the ability to "select" these loads in soil tunnels is rather limited. Lining loads depend predominantly on the soil but also on the construction technology. If the latter is defined by other imposed boundaries, very little room is left to manipulate the working loads on a primary support.

As a direct consequence, while in foundation practice ample factors of safety are normally found, in soil tunnelling, safety factors (of the ground mass) tend to be much smaller, not unlike open cut excavations in soil. Being far from collapse, foundation problems are often successfully treated using linear elasticity, whereas the latter is frequently found to render poorer results in soil tunnelling practice. Also, as pointed out by Gunn (1984:5), it should be noted that in the case of foundations, one of the primary interests is the estimation of displacements at points of the ground where the external load is applied. In contrast, in soil tunnelling one is interested in displacements not only at the tunnel contour where the loads are "applied", but also further away, at the ground surface. The "applied loads", instead of being well defined as they are in the foundation problem, are one of the unknowns. It is, therefore, much easier to find certain elastic constants that would very closely fit an observed response of a foundation, than of a tunnel response. Since it is difficult to obtain a representative Young's modulus from laboratory testing, the use of empirically adjusted elastic parameters confirmed by measured foundation performance became fairly widespread in practice (e.g., Poulos and Davis, 1980:102). This procedure can hardly be used in soil tunnelling, except in some particular cases. The rate of time independent deformation (unrelated to consolidation or creep) of foundation or earth fill structures is generally governed by their construction rate, provided the major part of the loads are of a self-weight type. This rate is measured in the spans of weeks, months or years. By contrast, the rates of advance of a soil tunnel are measured in terms of hours or days. This has a major impact in the potential damage induced in construction adjacent to the tunnel (Cording and Hansmire, 1975:610). The rapidly changing loads and displacements induced by an advancing tunnel, create a situation which is more critical than in other geotechnical structures. Less time is available for existing neighbouring structures or utilities to interact with their foundations and to redistribute the additional loading generated. As discussed previously in this thesis, time dependent deformations normally represent a small fraction of the total deformations in the soil around the tunnel. Exceptions to these rules include the remarkable cases of subway and railway tunnels built in Oslo, Goteborg and Stockholm (Holmsen, 1953, Karlsrud and Sander, 1978, Broms, 1978). The tunnels driven through bedrock (mostly sedimentary rocks in the Oslo area, and granites in the Stockholm region) acted as drains, and caused pore pressure reductions in any deposits of marine clays which overlay the bedrock.

Resulting settlements of more than 100 to 200 mm have been recorded over periods of 3 or more years, in contrast to negligible short term displacements induced in the rock during construction.

4.2 Design Requirements

The requirements for the design of a shallow tunnel may vary according to its proposed use (highway, rail or subway, sewage, water supply with low or high pressure, etc). Different operational criteria may be found with respect to safety, tolerances, maintenance, service life, etc. The establishment of these criteria is discussed in detail by O'Rourke et.al. (1984:4). However, there are some requirements which are common to any situation. They refer to:

1. The stability of the excavation;
2. The integrity of the support, both in the short and long terms;
3. The integrity of existing neighbouring structures, utilities and environment, both in the short and long terms.

There is an overall agreement that these are the basic requirements controlling the design of shallow tunnels through soil in urban areas (for instance, Peck, 1969:226, Clough and Schmidt, 1981:604, Resendiz and Romo, 1981:3, Ward and Pender, 1981:261). Also it is quite clear that these three requirements are largely interrelated. The separation is, nonetheless, convenient for discussion purposes.

For a given site and geometry, requirement (1) is chiefly controlled by the construction technology. Condition (2) is given by the magnitude and distribution of the loads onto the support, mainly with respect to its structural capacity. Long term changes in the overall physical conditions should not be disregarded (bordering new constructions affecting the active loads or lining deterioration processes affecting the structural capacity, for example). Requirement (3) is mainly controlled by the short and long term displacements induced by the tunnel.

Clearly, another requirement which is common to the design of other geotechnical structures, is the assessment of the ground conditions and properties. The subject will not be specifically treated herein as it is beyond the scope of this work. However, a few relevant comments will be made whenever necessary.

Although arbitrary, it is thus convenient to separate the tunnel design, with respect to the geotechnical aspects, into three major activities: i) lining design, ii) prediction of displacements and iii) stability verification.

4.2.1 Basic Requirements for Lining Design

It can be said that the first requirement for lining design is the selection of the lining type. This is a rather important design decision, which is not always simple and has far reaching consequences. The decision depends on a variety of aspects including tunnelling method, costs, schedule, supply availability, local traditions, performance requirements (water proofing, corrosion potential, etc.), maintenance requirements, etc. Despite its relevance, the subject goes beyond the scope of this study. The reader is thus referred to some review works such as those by McBean and Harries (1970) on precast concrete segmented linings; by O.M.T.C. (1976) on lining for transit systems; by Craig and Muir Wood (1978) on lining practice in the United Kingdom; by Maidl (1984) on lining practice in Germany; by Clough (1980) on lining systems in Japan; and O'Rourke et.al. (1984) on lining practice in the U.S.A.

If the support construction of a single tunnel is staged, including primary ("temporary", "immediate" or "initial") and secondary ("permanent" or "final") linings, the design of the former is where the geotechnical component is normally more evident. If the assessment of the support ability to sustain loads is an exercise of confronting predicted loads against the structural capacity of the lining, again, it is in the design of the primary support that the geotechnical role is more apparent.

The operational loads of a primary lining results, among other factors, from the interaction process between the soil and lining. Within the present work, it will be assumed that these loads represent the controlling factor of the lining design. In some instances this is known to be a gross simplification, as can be the case in precast concrete segmented linings, where either handling, transporting, stocking, erecting, shoving, expanding or grouting loads may control the design. The identification of the most critical loading configuration is not always immediate. This was the case in the 1.79 m sewer tunnel built in Sao Paulo, partly described in Section 2.3.5.4. The 100 mm thick unreinforced segmented concrete, with four pieces per ring, showed some longitudinal open cracks in certain location which did not coincide with the existing stress relievers. These were initially attributed to excessive transversel bending and to an alledged inefficiency in design of the stress raisers. It was felt possible that these did not reduce the stress in the concrete section sufficiently to ensure crack localization. After an extensive review program in which all phases of construction were monitored, it was identified that the cracking mechanism was triggered by the shoving forces that the full face TBM applied to the spigot pins, used to interlock the circumferential joints. The pins, made out of a high strength but ductile and light plastic compound, expanded against the mating holes walls, under the axial compression generated during the TBM advance. Tensile stresses, sometimes in excess of 6 MPa were estimated in the concrete due to this effect and exceeded the concrete tensile strength. A minor modification to the spigot pin and hole design eliminated the problem.

Even in the case of cast-in-place shotcrete lining, where pre-construction loads are absent, there are some concerns about transient loading conditions which may be more critical than the final, plane strain operational loading. Some of these conditions were discussed in Section 2.3.6.3, involving three-dimensional loading mechanisms, that depend on the scheme of the excavation (for instance, possible longitudinal bending of the upper shotcrete shell in the heading). The limited available field and numerical simulation results discussed in that section, indicate that such transient conditions may in fact exist. It is, however, uncertain if they are more critical than the final loading of the primary lining, or else, in what conditions they can critically prevail. An obvious and extreme case is that where the heading is advanced with the inverted floor arch lagging well behind. This construction scheme is frequently advocated by contractors for its economics and construction ease, and is appealing, particularly for large cross-section tunnels. Wittke et.al., (1986) studied this problem as applied to rock masses. There is an apparent need to investigate the subject within the soil tunnelling context, where a very limited advance of the heading without ring closure is normally practiced.

Under operational loads, structural failure of a circular tunnel lining which has good contact with the ground, can result from reaching a limiting stress, under the combined action of thrust forces and bending moments.

Shear failure or lining buckling are not normally observed in shallow tunnels of this type (Peck, 1969:255, Deere et.al., 1969:101).'

For these conditions, the basic requirement for lining design involves computations of moment and thrust, and comparing these with limiting moment and thrust combinations causing failure. The moment-thrust interaction curves are helpful tools to assess lining capacity. Their generation and use are not within the scope of the present work. Examples of applications of this approach to the tunnel support design can be found in works by Sgouros (1982), Paul et.al., (1983:70), O'Rourke et.al. (1984:65), Hansmire (1984:40), Kaiser and Barlow (1986).

For concrete linings with good contact against the soil, the assumption of linear lining response furnishes a conservative design, particularly for relatively stiff supports with larger load eccentricities. This is because if the actual non-linear response of the concrete is accounted for when cracks are developed, the eccentricity decreases, and a higher thrust value is permitted for a reduction in moment capacity. As pointed out by O'Rourke et.al. (1984:67), non-linear analysis shows that concrete linings do not fail by excessive moment, but rather by thrust which

---

' If the ground control is good, and for a good lining contact with the soil, the lining of a circular or near-circular tunnel section is not normally provided with shear reinforcement. Rather, the lining thickness is adjusted to resist shear, if this is actually needed. Paul et.al., (1983:136) provides guidelines for shear failure verification in concrete linings.

is affected indirectly by the bending moment. Paul et.al., (1983:144) provides a simple procedure to take into account the positive action of the non-linear behaviour of concrete sections in lining design. However, as most modern lining designs aim for small eccentricities (negligible bending moments), the assumption of a linear response for the lining does not lead to excessively conservative design, and will be taken as a rule in the present work.

Factors of safety applied to the lining design result normally from the combined application of specified capacity reduction factors to the section and of load factors to the design loads. This usually provides factors of safety that are equal to or greater than two. As noted by Paul et.al. (1983:134,136), that while there appears to be little reason to use reduction factors different from that prescribed for other structures in appropriate design codes, the load factors should be distinct especially when ground loads are conservatively estimated. Additional cautions regarding the use of structural codes are discussed by O'Rourke et.al. (1984:22).

Once the lining capacity has been assessed, an additional design requirement for the primary lining is the verification of its deformations or diameter changes, which must be acceptable both terms of capacity and serviceability.

The primary lining is usually designed to withstand all transient loads developed during construction as well as the "short-term" ground loads. The secondary lining is provided to ensure a safe support for the tunnel under possible increased "long-term" ground loads, as well as any other additional loading resulting from future changes in the overall physical conditions. For instance, if the primary lining has been installed in a dewatered ground, it is customary to design the secondary lining to withstand the loads due to water pressures that may eventually be recovered. This is an arbitrary assumption, as it is readily recognized that upon an increase in pore water pressure, the effective stresses will be changed, and possibly the total stresses. Hence, the primary lining loads are likely to be changed as well. If the secondary lining is already in place, the changes in ground stresses and pore pressures will lead to changes in the support loads, that generally will be shared by the combined primary and secondary lining system. To the writer's knowledge, no analysis has been made available so far showing how these load changes will be partitioned between the primary and secondary supports. It deserves a thorough investigation. Peck (1969:247) suggests, however, that the changes in effective stresses will lead to small alterations in the moments and the increase in water pressure will lead to a fairly uniform all-round pressure that also does not induce appreciable bending in a circular lining.

The action of capillary tensions in the water, especially in fine grained soils, should not be overlooked.

Dewatering is generally conducted in such a way that the drawdown phreatic surface is brought below the tunnel floor elevation. Inevitably, a considerable part of the soil lying above this new phreatic surface will remain either saturated or partly saturated, by virtue of surface tension. The soil zone within the capillary head will be subject to negative pore pressures. The extension of this zone and the magnitudes of these pore pressures will depend on the pore size distribution of the soil. For materials finer than a medium sand, this zone may well cover a sizeable amount of the tunnel cross-section. The negative pore pressures will increase the effective stresses which may remain non-zero, even after the tunnel is cut through. This improves tunnel stability and increases the ground stand up time. This effect has been identified in some tunnel cases, one of them being the sewer tunnel built in Sao Paulo, briefly discussed in Section 2.3.5.4. Neither the interaction between this phenomenon and heading stability, nor the mechanisms of stress changes developing upon the phreatic surface raise after the tunnel is built have been subjects of formal investigation.

While it was customary in the recent past to provide a tunnel with distinct primary and secondary support systems, there appears to be a worldwide effort to develop a single lining scheme, fulfilling both short and long term requirements. This trend is represented by precast concrete segmented linings with new waterproof sealing techniques, developed in the U.K., Japan, U.S.A., Germany and Brazil over the last 10 years. Along the same lines, the development of the extruded liner system in the U.S.A., U.S.S.R. and Germany should be referred to, (see, for example, Babendererde 1986). Moreover, recent advances in shotcrete technology indicate that more tunnels are being built with the staged application of a shotcrete support which acts as the sole and final lining. As a result, the once common practice of leaving the primary lining design to the contractor (Peck, 1969:247) is being gradually reviewed and abandoned, notably outside the U.S.A.. The practice is being replaced by the detailed lining design being conducted by the owner or the consultant. It usally provided an opportunity for the contractor to come up with an alternative design, whenever it is felt that some benefit may be gained with this. The once somewhat neglected primary lining design is currently becoming a lively integral part of the tunnel design, notably when shotcrete is used. As a result, the present design trend is to consider the primary lining system (with some allowance for physical deterioration with time, if appropriate) as an integral part of the final support. Consequently, consideration should also be given to the long term creep characteristics of the primary shotcrete lining, which may lead to a portionof the ground loads initially sustained by it, to be shared by the combined primary and secondary lining system.

While the above discussion covers the basic requirments for lining design, it is not uncommon to have the finished tunnel later subjected to other loading conditions such as the construction of a parallel tunnel, an adjacent open cut excavation, etc. These are special problems that require individual analyses. A review on the design of two parallel tunnels was presented by Ranken (1978:161), who also presented the results of a parametric plane strain finite element analyses that can be useful for a preliminary assessment of the problem. By representing the soil behaviour through a linear elastic model (in some selected cases, an elasto-plastic model was also used), Ranken investigated the influence of the distance between the tunnels (pillar width) and the influence of the construction sequence (tunnels built simultaneously or not). His studies were not limited to the effect on lining loads, but also included the effect on ground displacements. The charts and tables presented can be used for preliminary design purposes, bearing in mind, however, the conditions modeled (linear elasticity, K_o equal to 0.5, plane strain representation, tunnel fully lined or unlined). The combined use of these results and of Peck's (1969:255) recommendations based on observed performance of neighbouring tunnels, may serve as an interim design approach, until a more generalized procedure is developed.

As for the effect of open excavations beside an existing tunnel, very little has been done regarding a general design procedure for this class of problem, since Peck's (1969:257) discussion on the subject. Provided the tunnel diameter is small in comparison to the depth of the adjacent open cut (this could be the case of jacked pipe tunnels or "mini-tunnels"), the tunnel could be approximated by a small diameter pipe using some of the design methods recently developed for buried pipelines adjacent to deep trench excavations. The subject has been attracting increasing interest since the late seventies, especially in the U.K. Most of the available methods treat the pipe as an elastic beam embedded in an elastic foundation, but neglect the presence of the pipe when estimating the ground displacements induced by the adjacent excavation, which will cause the pipe to distort. The displacements are estimated on empirical or theoretical grounds. Crofts et.al., (1977) favoured the first treatment, developing an "upper bound" method, which was later criticized for offering too conservative an estimate of the additional pipe straining induced by the adjacent excavation (Symons, 1978:213, O'Rourke, 1978:215). However, Crofts et.al. (1977), possibly concerned with the large horizontal ground movements frequently observed in trench excavations in the overconsolidated London Clay, neglected the vertical component of bending in the buried pipe. The authors presented a revised form of their method (1978:217), and later included the effect of the pipe joints in their approach (Tarzi et.al., 1979). The entire method was finally re-published in 1981 (Crofts et.al., 1981), but still, the effect of the vertical component of ground displacement was never considered. However, this can be estimated using the approach developed by Rumsey and Dorling (1985). They extended the results of parametric plane strain finite element analyses of a linear elastic soil (with constant elastic modulus or linearly increasing with depth) obtained by Kyrou (1980). Rumsey and Dorling (Op.cit.:37) developed also an alternative empirical predictive method, based on the observed performance of pipes in a large number of field experiments. This can be used in an ancillary manner with their numerical approach. They enable the net resultant maximum movement of the pipe to be assessed and, from which, the maximum pipe strain can be conservatively estimated.

Nath (1983:1410) showed that the plane strain approximation of the problem can furnish ground displacements that agree within 10% of the maximum movements calculated at the symmetry transverse plane of a three-dimensional analysis, provided the open cut has a width to depth ratio less than 1/3 and a length to depth ratio greater than 2. Results from 3D analyses (Kyrou and Kalteziotis (1985)) confirm Nath's findings, showing also that the maximum bending moments in the pipe are found near the ends of the open cuts.

While the above methods can provide some guidance to the design check of small diameter tunnels under the effect of a nearby excavation, they cannot be applied to larger tunnels which may entirely disrupt the assumed induced displacement pattern. Moreover, the tunnel approximation by a simple elastic beam may not hold any longer as the resulting transverse bending of the lining may be as large as the longitudinal bending. Presently, there is no simple solution to the problem although it is believed that there is room for its development, following approaches similar to those used for buried pipes. Inevitably, the required analyses will have to be more involved. An example of one of such analysis is given by Medeiros et.al., (1982) , involving an unusual situation where a 6.2 m diameter tunnel was built through the site of an underground subway station, prior to its cut and cover excavation.

4.2.2 Basic Requirements for Displacement Prediction and Damage Estimate

Another requirement for urban tunnel design is the prediction of ground movements due to the tunnel construction and, after that, the evaluation of their effect on neighbouring structures and utilities, or, broadly speaking, on the environment. Conceptually, this requirement is similar to that for the lining design, since it involves an estimate of some quantities (displacements) and an assessment of some capacity (ability of nearby structures to withstand the anticipated movements).

However, unlike the design of the lining, in which the stress and strain interaction between the support and ground is normally taken into account, the interaction between the ground and nearby structures is usually not accounted for. In general practice, footing loads are calculated using a frame analysis in which it is assumed that no foundation displacements occur. Then settlements are estimated as though each footing were not structurally connected to the rest of the frame. In other words, the changes in loads in the structural elements due to the induced movements, or, the change in the ground displacements due to the presence of the structure are normally ignored, or only roughly assessed (de Mello, 1969:121).

A proper analysis for the tunnel problem would demand a coupled solution, in which the nearby structure would be fully portrayed (including its foundation elements) and the tunnel construction adequately simulated. Rigorously, this analysis should be carried out including the structure construction simulation and the interaction of the foundation with the ground. An example of this, is the finite element analysis conducted by Larnack and Wood (1972), who took into consideration both immediate and long term settlements. In such a simulation, the effect of both structure and soil stiffness changes during building construction should not be disregarded (also shown by De Jong and Harris, 1971). After this, the tunnel simulation should be performed, allowing the full interaction between soil, lining and building structure. To the writer's knowledge, results of such numerical exercise have not been made available yet and seem to be too involved for routine application. Despite this, there is a considerable academic and practical interest in conducting some limited parametric studies of this type, representing typical conditions frequently encountered in practice.

A compromise has been favoured in recent studies summarized by Attewell et.al. (1986:237). In these studies, the interaction between the ground and the existing structure at the surface is fully accounted for. The ground surface displacements induced by the tunnel are estimated, the presence of the existing structure is neglected. Equivalent loads applied to the ground surface, causing those estimated displacements, are numerically calculated. These loads are then used as implosed boundary conditions to the combined soil-structure interface . The final foundation settlements are obtained as well as the additional loads induced in the structure, as a result of the tunnel induced movements. Attewell et.al. (Op.cit.:250-277) were able to derive design charts applicable for particular conditions from which the maximum stresses in the structure are determined. These could be compared to stress-based criterion for the onset of damage.

The above method has not been sufficiently tested but it is felt that it has potential for practical use. An important limitation it presents is related to the procedure adopted to define the ground displacements induced by the tunnelling operation. This was done in a semi-emprical way, assuming a fixed volume of settlement at the surface (Attewell et.al., 1986:246) and a settlement distribution profile given by a normal probability curve. The fixed settlement volume assumption is very arbitrary and does not take into account the basic parameters controlling the generation of ground movement. The development of analyses accounting for these effects is yet to be seen.

The absence of such results forced the practitioner to establish empirical rules, derived directly from observations made in prototypes. From practice it was noted that there are two main sources of damage to structures associated with nearby tunnelling activities. They are the specific differential settlements and the specific differential lateral displacements induced in the ground by the tunnel excavation. The first is the difference in settlement between two points at the ground surface, or at the foundation elevation, divided by the original distance between these two points. It is also called angular distortion, or, simply, distortion. The second is the difference in horizontal displacement of the same two points, again divided by the distance between these points. It is also called lateral strain or transverse strain.

Prediction of these displacements or strains can be performed numerically. The finite element analysis described in Section 2.3.4.1, used to obtain the stress paths shown in Figure 2.4, can also be used for this prediction. Figure 4.1 shows the settlements and lateral displacements, obtained through this non-linear elastic analysis. They are calculated at the ground surface, for two degrees of in situ stress release: 30% and 60%. Also readily obtained are the surface distortions and the lateral strains at the surface. The inset shows the distributions of subsurface settlements and of vertical strains along the tunnel cover. Strains and displacements increase with the amount of stress release allowed. Maximum distortion is observed at the inflexion points of the settlement troughs, but the maximum lateral displacements and maximum lateral strains are noted elsewhere. Also noted are zones of lateral compression closer to the tunnel axis and of lateral extension further away, near the edge of the troughs. Both maximum ground shear distortions and maximum lateral strains at the surface have, basically, the same order of magnitude, a fact recognized by Cording et.al., (1976), through field measurements. However, these maxima develop at non-coinciding points.

In the above analysis, no support was installed in the tunnel and the existence of buildings at the surface was also ignored. If the interaction between the ground and any building had been accounted for, the displacements and strain distributions shown in Figure 4.1 would have been different. A structure at the surface normally has sufficient stiffness to flatten out the settlement trough beneath it. Field measurements confirm that this can be taken as a normal rule (see, for example, Breth and

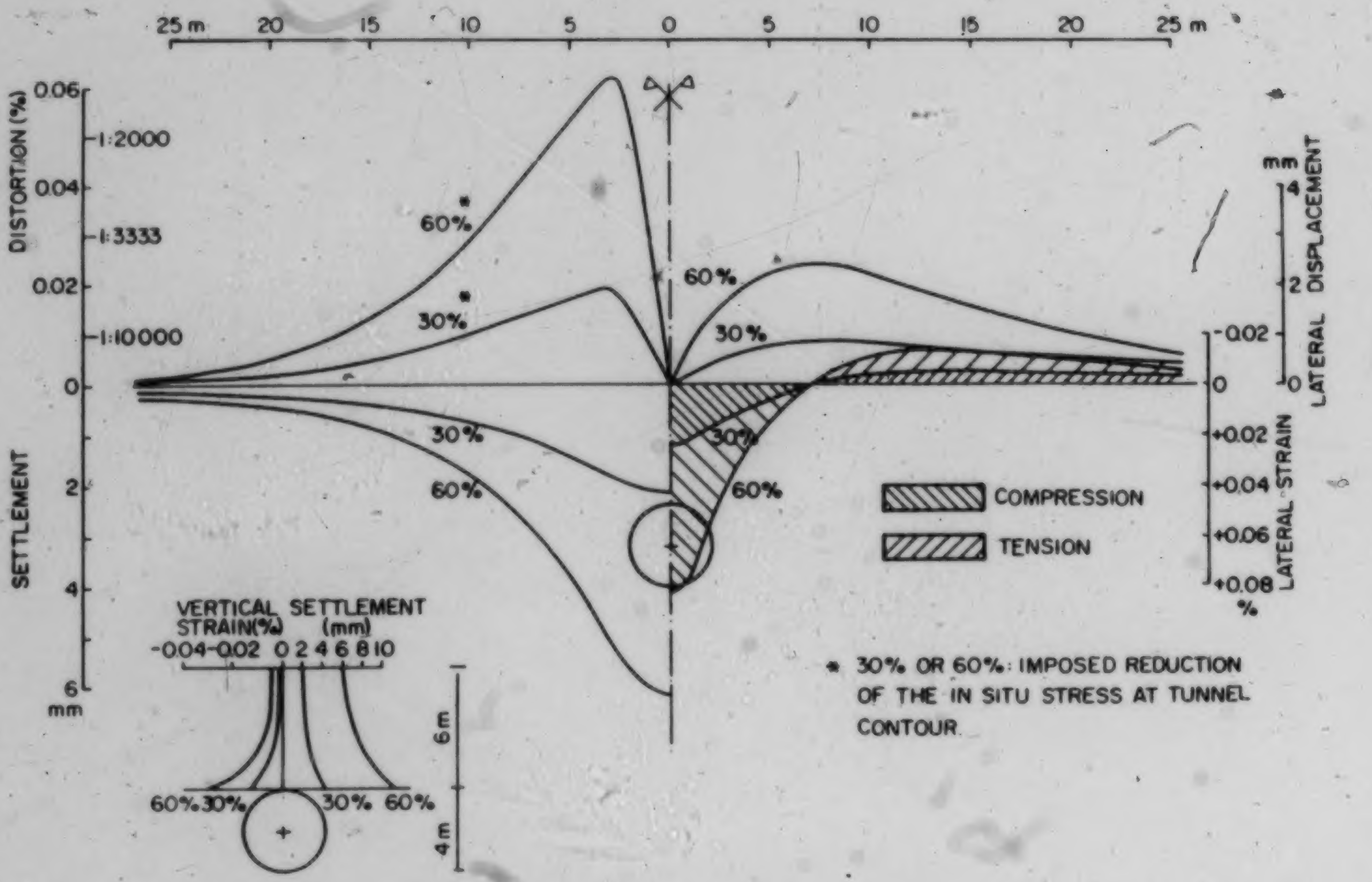

Figure 4.1 Displacements and Strains from Finite Element Simulation of a Shallow Tunnel

Chambosse, 1975:331). Hence, predictions of strains and displacements at the surface, ignoring building-ground interaction, will usually overestimate the magnitude of those variables, by some unknown amount.

Lateral strains seem to control the potential damage to structures located over underground long wall mining. The scale and extent of the induced subsidence under these circumstances are such, that the differential settlements over the limited extent of a typical surface construction are small, despite the magnitude of the settlements being one or two orders greater than that in urban tunnelling. In this latter case, the width of the structure is of the same order as the depth of the tunnel and its diameter. The structure will then be subjected to combinations of both lateral straining and differential settlements and their effects are difficult to separate (Cording et.al., 1976:519). However, from Figure 4.1, it can be anticipated that damage to a building located closer to the centre line is more likely to be associated with the shearing distortion of the ground, whereas for a building closer to the edge of the settlement trough, the damage potential is controlled by the tensile lateral strain that predominates here. Field evidence shown by O'Rourke et.al., (1976) on brick-bearing-wall structures seems to confirm this.

Two damage categories are usually identified (partly following Skempton and MacDonald, 1956:730):

a) Architectural damage: involving initially the appearance of the structure, and is related to cracking and separations in panel walls, floors and finishes; in the extreme it may involve functional damage of building utilities, impairment of services, such as jammed doors, pipe breakage, etc.

b) Structural damage: impairing the stability of the building, which is associated with cracks and distortion of the main support elements, etc.

Experience shows that damage of the first type precedes that of the second for most building structures. Therefore, the structures will normally become unserviceable before any structural instability occurs which would endanger building occupants. This seems to facilitate the definition of a damage criterion as it will be mainly related to architectural or functional aspects. However, this may actually cause the criterion to become fairly subjective, as pointed out by Peck et.al., (1956:778). The degree of damage considered to be evident may vary from observer to observer. Moreover, the tolerance towards these damages will have different thesholds among individuals and from place to place.

It seems acceptable that most damage (prior to collapse) manifests itself as cracking, resulting from tensile strain in a structure (Burland and Wroth, 1975:616). This tensile strain results from differential settlements (inducing bending and/or shearing in the structure) and from lateral strain, caused by tunnel excavation. The tensile strain is not readily predictable from estimated ground movements. Therefore other indices have been introduced to directly correlate damage with displacements. As noted before, since surface lateral strains are of the same order of magnitude as surface distortions, the empirical attempts to define damage criteria mainly made use of the latter. Many authors (see Table 4.1) related the occurrence of damage to the observed maximum distortion between the structure footings, after eliminating the rigid body tilt of the building. Skempton and MacDonald (1956:762) presented examples of the calculation of tilt. Although easy to calculate once the structure settlments are known, the anticipation of building tilt is very difficult as it requires full knowledge of the superstructure details and its interaction with the foundation. Thus, structure distortion is usually conservatively anticipated ignoring the tilt. Attempts to correlate the greatest distortion and the maximum settlement or the maximum differential settlement were criticized (Terzaghi, 1956:775). This type of correlation may hold for specific building types on particular and well defined soil units or for specific geological sites, but it may not be valid in a more generalized way. The relationship between these quantities is strongly dependent on the uniformity of the soil and on the distribution of loads over the structure foundation.

Ward (1956) contended that damage would be better related to the maximum curvature (second derivative) of the

Authors	Movement Cause	Index	Availability of a limiting index criteria for damage
Skempton and MacDonald (1956:731)	A	Maximum angular distortion, with rigid body tilt discounted	Yes
Meyerhof (1956:774)	A	Maximum angular distortion, with rigid body tilt discounted	Yes
Bjerrum (1963)	A	Maximum angular distortion, with rigid body tilt discounted	Yes
Ward (1956:783)	A	Maximum curvature (d^2u/dx^2)	No
Polshin and Tokar (1957:404)	A	Deflection Ratio	Yes
Burland and Wroth (1975:623)	A/B	Deflection Ratio	Yes
Kerisel (1975:463)	B	Radius of curvature	Yes
Cording et al (1976:534) and O'Rourke et al (1980:656)	B	Average angular distortion with rigid body tilt discounted	Yes
Breth and Chambosse (1975:336)	B	Maximum angular distortion, with rigid body tilt included	Yes

Note: A = structure self weight
B = tunnelling or open cut excavation
A/B = structure is weightless

Table 4.1 Existing Criteria for Damage Assessment of Structures Subjected to Ground Movements

deformed structure foundation. Kerisel (1975) advocated in favour of the radius of curvature of the deformed ground profile, particularly in relation to the damage of old structures. In both cases, it is assumed implicitly that the tensile strains causing cracking result mainly from bending (related to the curvature). This may not be the case in some instances, as these strains may also develop diagonally, due to shear deformation of the structure (for example, see Burland and Wroth, 1975:619). In general, as pointed out by Cording et.al., (1976:529), local curvatures of the soil settlement trough induced by a tunnel are not as significant as the distortion, since the structure is able to bridge or level out small local curvatures. Moreover, curvature is difficult to measure with accuracy in practice, as it is very sensitive to data scatter and as it requires very narrow spacing of settlement points across the subsidence trough. For these reasons, Cording and Hansmire (1975:610) preferred to relate damage to the average settlement slope or average distortion.

Burland and Wroth (1975), following the work by Polshin and Tokar (1957), favoured the use of a deflection ratio to assess building damage. This ratio is defined as (Burland and Wroth, Op.cit.:616) the maximum displacement relative to the straight line connecting two reference points a distance L apart, divided by this distance. If L is taken as the transverse length of the structure, the ratio will be related to the average settlement distortion.

Table 4.1 lists some of the existing approaches to evaluate building performance upon settlements. The limiting relative displacement criteria usually distinguishes the structure type (framed, load-bearing walls, etc.), structure width to height ratio, type of damage, etc. Most of the allowable settlement criteria derived from empirical observation of building damages is related to the settlement of its foundation under its self-weight. Therefore, most criteria are not actually applicable when settlements are due to the tunnelling construction. In the latter case, the building already exists with all finishes and plaster in place, and the rate of movements are much higher than that due to the structure weight. Moreover, by the time the tunnelling settlements develop, the structure has already been subjected to movements due to its own weight, and may already sustain strains close to the critical. Minor additional straining might soon bring it to a condition of damage.

It is believed that the criteria by Burland and Wroth (1975) could be adapted for this different condition, as it is, like that by Polshin and Tokar (1957), based on the fundamental causes of building damage and makes use of a plausible behavioural model. The allowable settlements, (expressed as deflection ratios), are defined for different building structures as a function of a critical tensile strain at which cracking of cladding and finishes (and not structural elements) would become visible. According to these authors, this strain varies from 0.03 to 0.1% (the lower portions of the range applying to reinforced concrete and the upper to brick or blockwork with cement mortar) and an average of 0.075% could be taken for most structures. Limiting deflection ratios were calculated for different buildings represented by a weightless rectangular beam of unit thickness, with different length to height ratios, under combined modes of deformation involving bending and shear. Different criteria were established for frame buildings (that tend to flex under shear), for load-bearing walls (that crack under bending) and for masonry buildings undergoing hogging (crack in the upper edge upon bending).

Out of the approaches listed in Table 4.1 only those due to Kerisel (1975:436), Breth and Chambosse (1975:336), Cording et.al., (1976:534) and O'Rourke et.al., (1978:656) are actually related to tunnelling excavation problems. The limitation of Kerisel's approach has been already discussed. The damage criterion by Cording et.al. (Op.cit.) and O'Rourke et.al., (1978) are fully empirical and are derived from field observations made in structures adjacent to tunnels and open cuts recently excavated in the U.S.A.. These authors proposed that the average angular distortion (discounting tilt) causing architectural damage in brick-bearing walls and frame structures adjacent to the excavations, are those exceeding the limits 1:1000 and 1:750 respectively. These distortions are much less than that given by the approaches related to settlement of structures under their own weight. As explained, this is due to the higher rate of movements associated with excavations, to the presence of residual strains in the structure prior to the excavation, and also to the lateral strains that are induced in the ground. Moreover, the aging process in the structure might also have a role in producing these relatively low distortion limits.

Table 4.2 reproduces the description of damages related to the building distortions for brick-bearing wall structures summarized by Cording et.al., (1976:534), and O'Rourke et.al., (1978:656). Needless to say that the table should serve as a broad guideline, and that individual cases will normally require additional judgement. Traditional underpinning methods are known to induce appreciable distortion (values of as much as 1:400 have been reported) which may cause serious cracking in a building (Peck et.al., 1956:779). Hence, considering the low threshold distortion value for architectural damage, it seems unlikely that traditional underpinning methods can be used to prevent this type of damage. Moreover, these methods may ultimately solve problems related to differential settlement, but will hardly avoid the effects of lateral straining. Some more modern techniques, such as inclined jetted piles ("pali-raddice") or jet grouting, seem to show better potential for solving this problem. (see for instance, Guatteri et.al., 1986:190).

If the anticipated ground movements are expected to cause architectural damage, the current attitude is, to

Description of Damage	Associated average ground surface distortion with rigid body tilt discounted *
Threshold of architectural damage	1:1000
Architectural damages, including cracks and separations up to 6 mm wide, sticking doors	1:1000 to 1:300
Functional damages, such as jammed doors and windows, breakage of window panes, restrictions in building services; cracks and separations up to 25 mm wide; lintel instability	1:300 - 1:150
Spalling of stone cladding	1:150 - 1:125

* Angular distortion and lateral strains assumed to be approximately equal.

Table 4.2 Damage Related to Building Distortion for Brick-Bearing Wall Structures Adjacent to Excavations (modified after Cording et.al., 1976:535)

firstly balance the anticipated costs of architectural repair works in the building against the costs of protective or ground controlling procedures. In many cases, the former costs are lower than the latter. If this is not possible or acceptable, the second approach is to improve the tunnel construction quality by selecting the most efficient construction method or sequence in terms of ground control. The third alternative is to condition the soil by using techniques that may improve the ground response. The fourth and last measure (usually the most expensive) is to contemplate modern underpinning techniques that can effectively reduce the risk of damage, without creating transient conditions that might be more critical than those due to the tunnelling process.

The subject, already complex, may become even more intricate, when there is also a need to consider the longitudinal distortion of the ground ahead of the tunnel face. As noted by O'Rourke et.al., (1978:650), upon tunnel advance, a building is subjected to a settlement wave that causes a three-dimensional warping of the structure, even if its final distorted configuration can be approximated by a plane strain representation. This effect can be better understood through the plots shown in Figure 4.1, considering for instance, that the 30% curves correspond to the displacements induced at a transverse plane containing the tunnel face and the 60% curves representing the final plane strain condition. It is readily recognized that both angular distortion and horizontal straining will develop in vertical planes parallel to the tunnel axis during tunnel excavation. This three-dimensional distortional effect in neighbouring structures has not been studied so far, and perhaps, requires further investigation. Less frequently addressed, but certainly not less important, are the concerns regarding the effects of tunnelling induced settlements in neighbouring buried utilities (mains, gas pipes, etc.). Only recently the subject started attracting increasing interest. Howe's (1982) review on damage control for distribution systems, revealed that the major cause of buried pipe fracture is movement induced by open cuts and tunnelling operations. Provided the diameter of a buried pipe is small compared to the tunnel, it is customary to ignore the interaction between the pipe and the soil, as far as ground movements caused by the tunnelling operation are concerned. In other words, the prediction of ground movements is done independently, neglecting the existence of the utility buried in the ground. However, for assessment of the additional straining resulting from tunnelling induced ground movements, the interaction between the pipe and the surrounding soil is taken into consideration in a simplified way.

The evaluation of damage risk in buried pipes can be based on either a breaking strain (or stress), or on a maximum strain (or stress) for unserviceability. Crofts et.al., (1977:174) suggested that if the factor of safety applied to limiting strains is less than 5/3, there will be an unacceptable risk of breakage or unserviceability. For instance, according to Carder et.al., (1985:21), the maximum acceptable ultimate tensile strain for a new cast iron pipe is 0.2%. Strains due to other causes, not directly related to tunnelling induced ground movements, should be added in assessing that factor of safety. These authors further suggested that, if the factor of safety is greater than 4, breakage or damage will be unlikely.

Assessment of additional straining by tunnelling operations is frequently done by assuming the buried pipe is to be represented by an infinite elastic beam embedded in an isotropic elastic foundation, represented by a sub-grade reaction modulus. The ground movements predicted separately are used as an imposed displacement boundary condition, and bending moments, stress or strains can be calculated solving the appropriate differential equation. This approach has been followed by Takagi et.al. (1985) and by Yeates (1985), both works providing design charts resulting from parametric numerical analyses of steel pipes. The first authors study the behaviour of continuous pipes transverse to the tunnel, assuming that they deform according to the normal probability curve as suggested by Peck (1969). To corroborate their method they compared predicted and measured bending stresses in an instrumented test pipe, installed above a large shallow tunnel. The results were encouraging. Yeates (1985) used a similar approach and went further by including the case of a continuous pipeline parallel to the tunnel axis. To do this, he used the expression for the cummulative normal probability curve suggested by Attewell and Woodman (1982) to represent the ground settlements parallel to the tunnel axis. Unlike Takagi et.al., (Op.cit.), who only considered the vertical component of the induced displacements, Yeates (Op.cit.) considered also, but separately, the effect of the horizontal movements parallel to the pipeline axis. Using the treatment by Poulos and Davis (1980:74) for axially loaded piles, Yeates provided elements to estimate the maximum tensile pipe strains at points of maximum hogging, both transversely and parallel to the tunnel. Again, the analysis requires an independent estimate of the horizontal displacement as an input. Throughout his derivation, Yeates made a number of conservative assumptions, which lead him to claim that his predictive method is safe, although comparison with field measurements has not been provided.

Takagi et.al., (1985:107) also studied the influence of mechanical joints in ductile iron pipes, and showed that they have suprisingly little effect in the numerical results obtained. This was attributed to the standard lengths of these pipes (4 to 6 m) as compared to the usually wider transverse widths of settlement troughs of shallow tunnels. Yeates (1985:137) reached a similar conclusion independently.

A comprehensive review of the available methods for assessment of the consequences of tunnelling induced ground movements on buried pipelines was recently published by Attewell et.al. (1986:122). These authors provided a number of solutions for the problem and presented examples of applications for a variety of practical conditions. In these solutions, the ground displacements induced by the tunnel construction are estimated semi-empirically by assuming that their distribution follows a normal probability curve (see Section 4.3.3), and by empirically estimating the volume of ground settlements. An improvement on this fundamental aspect of the solution would be desirable.

Although extremely useful, the above methods need to be properly correlated to actual observed performance in order to be fully validated. Not many case histories are available for this purpose, however. The use of centrifuge modelling (e.g. Kusakabe et.al., 1985) may be helpful in this assignment.

If the size of the buried utility is comparable to that of the tunnel, the simple approach just discussed may not be valid. The induced displacements may be affected by the presence of the utility (an old tunnel, for instance), and in this case, a more complicated numerical analysis will be required, allowing the complete interaction between utility, ground and tunnel to be accounted for. An example of this type of problem and analysis was shown by Hansmire et.al., (1981), and related to a sewer tunnel built with a clearance of just 0.6 m over an old twin subway tunnel in New York City. A simplified two-dimensional plane strain finite element analysis was performed in order to assess the effect of the tunnelling including jacking forces, on the existing tunnels. Details of this study are presented by Ghaboussi et.al., (1983), who also evaluated the action of jacking the TBM in the new tunnel on the old subway lining, by means of a simplified three-dimensional finite element analysis.

As mentioned earlier, whenever it is anticipated that the induced ground displacements will likely cause damage to neighbouring structures or utilities, the tunnel design should call for ground control measures. The design of such measures are currently taken as an intergral part of tunnel design. The subject will be briefly covered in the next section, as it is also closely related to the ground stability control.

4.2.3 Basic Requirements for Verification of Excavation Stability

Lining design requires that the support capacity is sufficient to withstand soil loading conditions so that collapse of the supported opening is precluded.

This, and the assurance that good lining-soil contact exists reduces the verification of the tunnel stability to issue of the heading excavation in terms of local or global ground collapse. As noted in Section 3.2.2, the problem is fully three-dimensional and its complete solution is rather involved. Available methods for stability assessment are applied to very idealized conditions, and the current design approach is to bound the correct solution, using fairly extreme assumptions and a large amount of judgement.

The basic requirement, as in any other stability calculation, involves the evaluation of driving forces and resisting forces, with their comparison allowing the assessment of a factor of safety. This is preferably done through the limit theorems of plasticity (upper and lower bound solutions), which enable the correct factor of safety to be bounded. Except in cases where the collapse mechanism is fairly well defined beforehand, normal design decisions are not solely based on conventional limit equilibrium calculations. These are upper bound solutions formed from the condition that the mechanism is kinematically admissible, and, therefore, they may provide unsafe estimates of the factor of safety.

Available solutions for the stability of tunnel headings are applicable to homogeneous soils, represented either by a frictionless material or by a frictional and cohesive material. The action of pore pressures are not rigorously accounted for. Solutions that assume the soil to be a purely cohesive material could represent the case of a heading excavation in saturated soil under fully undrained conditions. Therefore, at the design stage, it is necessary to identify the pore pressure responses in terms of the rate of dissipation compared to the anticipated rate of tunnel advance. As no general solution has yet been made available for the three-dimensional consolidation process around an advancing heading, the practitioner is compelled to adopt simplified approaches to the problem, as the one presented in Section 3.3.4.5. From these approaches, the most likely response, from fully undrained to fully drained is identified, and the most adequate stability solution is selected for the case under investigation. Usually the lower bound approach of the three-dimensional stability problem of the face or heading will suffice. Being a "safe" solution, fairly low global factors of safety are generally accepted (from 1.1 to 1.3), provided the ground conditions and properties are well known.

If the likely response of a saturated ground during tunnel advance can be assumed to be fully drained, then the stability evaluation of the tunnel face or heading should ideally be performed in terms of effective stresses, with pore pressures obtained from flow nets. However, to the writer's knowledge, no solution to this fairly complex three-dimensional problem including the action of steady state pore pressures, has been developed so far. Upper bound work rate calculations seem to provide an easier path for this development, but they are not available, except for dry soils (for example, Casarin, 1977:65). De Mello and Sozio (1983), proposed a two-dimensional approximation, treating the tunnel face as a long wall mining face and using a limit equilibrium approach. This is obviously an oversimplification that may be accepted only for comparative purposes.

Once the support is installed and an equilibrium is reached, the overall stability of the combined soil-lining system will generally increase, by virtue of the inclusion of the stiffer and stronger support element. This increase in safety is not apparent from the discussion on the idealized changes in stability with time, presented in Section 3.3.4.4 (Figure 3.20), since there, the contribution of the support in the overall safety was intentionally neglected. Actually, the assessment of safety in the combined system is usually not attempted, but rather, factors of safety are separately estimated for the ground and for the lining, in the final, long-term plane strain situation. Different factors of safety are therefore assessed, using the equilibrium loads resulting from the interaction process between the soil and the support, and the acceptance of these factors is analysed independently. There is no pre-established minimum safety factor for the soil under this condition. As noted in Section 2.3.4.3, the minimum acceptable factor is defined in terms of the maximum tolerable ground deformation. The limited amount of tunnel model test data analysed in that section, indicated that a "good ground control" condition would be achieved, whenever the dimensionless crown displacement, U, was smaller than 1, and this would correspond to factors of safety greater than typically 1.5. This value should not be taken as a rigid reference, as different amounts of settlements or losses of ground would be expected for different soil types for the same factor of safety. Hence, values lower than 1.5 may be acceptable for stiffer or denser soils (possibly 1.3 to 1.4), and higher factors may be required for softer or looser soils (e.g., 1.6 to 1.7), for the same amount of acceptable loss of ground or tunnel closure (see Figures 2.6 and 2.7). Summing up, the assessment of the final long-term factor of safety of the ground is generallly not, in itself, a mandatory design requirement. Provided that the stability of the face and heading is fully ensured, that lining capacity is sufficient (both for short and long terms) and that the final ground displacements are acceptable, the assessment of the final factor of safety of the ground is generally an accessory design evaluation. Only in some special conditions this rule may not prevail. Exceptions to it sometimes involve cases where good lining-soil contact is not ensured. This is the case, for example, of tunnels lined with precast support elements and with a delayed application of grout to fill the voids behind them.

Another important requirement for the ground stability evaluation is the adequate assessment of soil strength. This point deserves special consideration particularly when dealing with some stiff fissured soils. The effect of soil fissures on the strength of the soil mass was analysed by Bishop (1966) and Marsland (1972), among others. The controlling role of these fissures in the short term stability of a large cross section tunnel (10 m diameter, approximately) built in São Paulo, Brazil, described by Negro et.al., (1985) and Eisenstein et.al., (1986), was addressed by Negro et.al., (1985:187). The spacial distribution of fissures and other weakness facies, in this stiff sedimentary silty clay, was found to be erratic and the spacing ranging from 5 to 30 cm, or about 1/200 to 1/30 of the tunnel diameter. If the criterion by Deere et.al., (1969:1-15) for jointed rock masses was applicable to this case, it could be said that the ground mass around the tunnel would behave as a fairly homogeneous continuum (average fissure spacing less than 1/50 of the tunnel diameter). The strength of this soil was investigated by means of unconfined compression tests in a number of undisturbed cubic specimens with sides ranging from 4 to 22 cm. It varied from 0.7 MPa for the smallest specimens to 0.05 MPa for the largest. If Bishop's (1966) proposed relationship relating the strength of the intact soil to that of the fissured soil mass expressed as a function of fissure spacing, is accepted, then, the former would be found to be about 1.5 MPa and the latter 0.2 MPa, after a best fit of strength data with sample size is performed. In this particular case, tunnel stability would be better assessed using a strength compatible to the lower figure above, which better represents the strength of the ground mass.

Also not to be overlooked in the design stage is the action of possible water seepage into the heading. Steady state seepage during tunnel advance such as that discussed in Section 3.3.4.2 may generate localized piping mechanisms that may trigger an instability process, particulary in fine draining ground masses. This effect was investigated (Taylor, 1980) by modelling a plane strain tunnel failure in a homogeneous silt in a centrifuge, under the action of ground water seepage. Stratigraphic details and local hydrogeologic features have a major influence in this process and require a great deal of investigation. Proper assessment of potential problems of this nature is rather complex, as it involves three-dimensional transient flow which is highly affected by the above features. However, qualitative evaluation of difficulties can be performed under simplified two-dimensional assumptions, particularly when studying alternative means to control the groundwater flow (see, for instance, De Mello and Sozio, 1983).

Another basic requirement is the selection and design of ground control measures needed to ensure the stability of the excavation, whenever it is assessed that the tunnelling scheme does not present adequate safety. It is not unusual to find designers or owners leaving the design of ground control measures to the discretion of the contractor. This is partly due to legal and contractual dispositions found in some countries or due policies of some authorities. Modern attitudes toward risk sharing contract types are forcing this condition to be changed. Technically speaking, it is highly advisable to include the design of ground control measures as an integral part of the tunnel design. The subject is beyond the scope of the present work, but for the sake of completeness, Table 4.3 has been prepared and summarizes the most common expedients and means to exercise ground control or ground conditioning presently used in soil tunnelling in urban areas. The primary objectives of these processes can be stability control or also reduction in ground displacements. Some processes may have broader actions and functions than indicated, but those shown seem to be sufficient for an initial assessment of their technical virtues. The list of techniques and references included do not intend to be complete, but only illustrative. Also, some processes may be classified in more than one technique group, or they may also be used in a combined way. No attempt has been made to include comments on costs since they may vary considerably, thus not allowing a general assessment to be made. Grouted soil anchors or bolts could be included in group E, combining the actions of processes E2 and E3m when suspension grout is used. Their effectiveness as a ground control technique has, however, been questioned (Laabmayr and Weber, 1978:82, Steiner et.al., 1980:321, for example), and therefore they are not included in the table. When used in stiff, residual soil masses, where the behaviour is controlled by preserved parent rock features, grout bolting can, however, be an effective control measure.

Other techniques that could be potentially considered include electro-osmosis and lime stabilization, but their applications for ground control in soil tunnelling have not been reported to the writer's knowledge.

4.3 Available Design Methods

4.3.1 Foreword

In this section, a survey of existing methods of shallow tunnel design is attempted with attention being paid to their features and limitations. It includes procedures that are highly disseminated among practitioners, as well as others not so well known, despite their merits. No attempt is made to review each method in detail, as this has been done to variable extent by different authors in the recent past. These review works, however, are referred to as additional sources for reference. Although the survey was undertaken in order to be as complete as necessary, to allow a comprehensive classification of existing methods, it is far from exhaustive. This is partly due to the extremely large number of design procedures developed over the last two to three decades in different countries and published in different languages, being therefore, not always accessible. To make the survey simpler, brief and less tedious, the review covers groups of methods rather than individual methods, unless deemed necessary. Attention is given to

Technique Group	Process	Action	Function	Comments	Recent References
A Staged excavation	1 Heading and bench 2 Side drift or galleries 3 Multiple drift method, etc.	Reduces unit size of face excavation, reduces influence of fissures and weakness facies in ground mass stability.	Increase stability of excavation, may reduce settlements also.	Usually not suitable for mechanized excavation schemes; applicable to medium or large size openings; reduction in ground displacement depends on excavation and support schemes.	A1: Negro and Eisenstein (1981); A1 and A2: Eisenstein et al (1986); A3 Vasishth (1986); Parker and Robinson (1983)
B Controlled stress release in excavation or support application.	1 Slurry, bentonite shield or hydroshield 2 Earth pressure balance shield. 3 High density slurry-shield 4 Extruded shield	Allows excavation or support installation under minimized in situ stress release; reduces shear in ground mass.	Reduce ground displacements and increases ground stability.	Presently used in TBM schemes only. Can induce ground heave, including B4.	B1: Watanabe (1984); B2: Clough et al (1983); B3: Sasanabe et al (1986), Matsuzaki et al (1986); B4: Novak (1984), Babendererde (1986).
C Presupport Techniques	1 Continuous steel pipe forepoling 2 Jet grouting forepoling 3 French saw 4 Blade shield 5 Marche-avant	Allows excavation under protection of pre-installed support or lining; may reduce in situ stress release if pre-support is stiff enough.	Improve local ground stability and possibly global stability; ground displacement control may be marginal.	Global stability only with long forepoling.	C1: Nishiwaki (1984); C2: Lunardi et al (1986). C4: Gruner (1978), C5: Lunardi and Louis (1984).
D Groundwater control techniques	1 External or internal dewatering 2 Compressed air 3 Chemical coating	Minimize or eliminate ground water flow, or its consequence, may increase soil strength.	Improve either local or global stability of the ground, reduce risk of piping or 'flowing' ground condition.	May increase ground displacements by drainage and consolidation (D1 and D2); D3 currently used with shotcrete support also.	D1: Kriechke and Weber (1981) D2: Strobl (1986), Yoshida et al (1986); D3: Horiuchi et al (1986)
E Ground Improvement Techniques	1 Permeation grouting 2 Replacement grouting 3 Compaction grouting 4 'Claquage' grouting 5 Freezing	Increase ground mass strength, reduce its deformability, and possibly its permeability.	Improve global and local stability. Reduce settlements. May improve groundwater control.	May induce ground heave; E2 refers to techniques in which soil is mixed in place by hydraulic or mechanical action with suspension grouts; Settlement is balanced by heave in E3, if performed simultaneously to tunnel advance.	E1: Tan and Clough (1980); Guatteri et al (1986), Migliacci et al (1986), E3: Lopez and Baker (1984), Baker et al (1983); E4: Oliveira & Ferreira (1982); E5: Koenz & Garbe (1986), Mettier (1979) Schmid (1981).
F Exclusion Techniques	1 Slurry trench walling 2 Sheet pile walling 3 Tangent pile walling	Confine unstable zone, limiting extension of subsiding ground zone; may reduce hydraulic gradients.	Protect neighbouring structures against excessive vertical movements.	Movements above tunnel not prevented but increased; amount of lateral ground movement will depend on flexural rigidity of wall; it may not be appreciably reduced.	F1 and F2: Hanya (1981).

Table 4.3 Reported Ground Control Procedures in Soil Tunnelling

procedures developed in the recent decades as well as older methods that are often used in present days.

4.3.2 Prediction of Lining Loads

4.3.2.1 Classification of Methods

Once the lining type has been selected and its dimensions preliminarly defined[19], the internal lining forces have to be calculated, in order assess the lining capacity. These loads can be calculated using a variety of methods which can be classified in one of the five main groups shown in Figure 4.2. The terminology adopted is fairly commonly used, but for clarity some explanations will be presented in the following sections.

It is clear from the discussions presented in Chapter 2, particularly in Sections 2.3.5 and 2.3.6, that all models used for predicting lining loads are to some extent an approximation of the prototype. Maffei (1982) thoroughly discussed this aspect and classified the available methods which take into account the ground-lining interaction, into two groups: those in which the ground loads onto the lining are imposed and those in which lining loads result from the stress redistribution upon the stress release representing tunnel excavation. It is believed that this distinction may

---

[19] This is basically done on the basis of functional or construction impositions: minimum clearance of concrete forms for cast-in-place linings, minimum thickness of concrete segments allowing handling and complying joints, design requirements, minimum thickness imposed by standards and code provisions, etc.

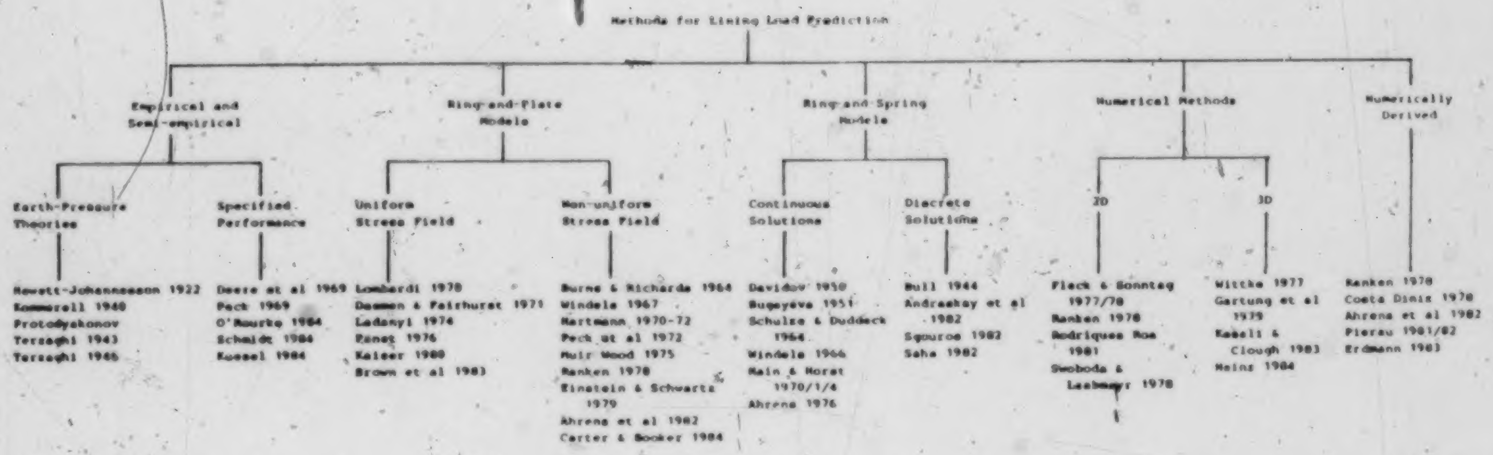
Methods for Lining Load Prediction
Empirical and Semi-empirical
Ring-and-Plate Models
Ring-and-Spring Models
Numerical Methods
Numerically Derived
Earth-Pressure Theories
Specified Performance
Uniform Stress Field
Non-uniform Stress Field
Continuous Solutions
Discrete Solutions
2D
3D
Hewett-Johannesson 1922
Kommerell 1940
Protodyakonov
Terzaghi 1943
Terzaghi 1946
Deere et al 1969
Peck 1969
O'Rourke 1984
Schmidt 1984
Kuesel 1984
Lombardi 1970
Daemen & Fairhurst 1971
Ladanyi 1974
Panet 1976
Kaiser 1980
Brown et al 1983
Burns & Richards 1964
Windels 1967
Hartmann 1970-72
Peck at al 1972
Muir Wood 1975
Ranken 1978
Einstein & Schwartz 1979
Ahrens et al 1982
Carter & Booker 1984
Davidov 1950
Bugayeva 1951
Schulze & Duddeck 1964
Windels 1966
Hain & Horst 1970/1/4
Ahrens 1976
Bull 1944
Andraskay et al 1982
Sgouros 1982
Saha 1982
Fleck & Sonntag 1977/78
Ranken 1978
Rodriques Roe 1981
Swoboda & Laabmayr 1978
Wittke 1977
Gartung et al 1979
Kasali & Clough 1983
Heinz 1984
Ranken 1978
Costa Diniz 1978
Ahrens et al 1982
Pierau 1981/82
Erdmann 1983

Figure 4.2 Classification of Some Typical Examples of Methods for Lining Load Prediction

be too subtle for practical purposes, since a particular method can belong to any of the two classes, depending on the way the structural system is loaded. The purpose of the classification is, therefore, not fulfilled. Moreover, it may be argued that the stress release representing the excavation, as it is performed in a number of numerical simulations, may be understood also as an imposed loading condition. Maffei's classification identifies the types of load onto the lining-ground system (gravity load versus actual excavation loading), but does not classify the methods of calculation according to the grounds on which they are based. The latter approach was favoured by Katzenbach (1981:14) and it is followed here in a different form.

4.3.2.2 Empirical and Semi-Empirical Methods

These are methods based on observations of successfully completed tunnel supports or simply based on past experience. Some of them were developed using less simple theoretical frameworks. Nevertheless, they tend to include a considerable amount of empiricism in their assumptions. As discussed in Section 1.1, these methods include an unknown, but normally wide, margin of safety. Sometimes, if the range of cases or situations used as a basis for its development was limited, or it was developed for a particular site and construction technology, and then applied to a different scenario, it may furnish an unsafe design.

These methods can be divided into two sub-groups: the earth pressure theories and the methods in which the lining performance is determined beforehand.

Earth Pressure Theories

The earth pressure theories normally provide ground pressure envelopes (reduced overburden criteria) to be applied to the lining, from which the internal support forces can be calculated, using known solutions from structural analysis (for a monolithic ring sections, see Szechy (1967:343) for a summary of these solutions). It is a common assumption in almost all these methods that the earth pressure loads are independent of the ground displacements, and that the support is not embedded in the soil. The soil is assumed to be acting only as a source of load. By neglecting the ground-lining interaction, a conservative lining design is attained. However, the displacement independent earth pressure load assumption may or may not lead to a conservative lining design.

It seems that the above assumptions correspond to conditions of poor ground control, represented by a poor lining contact with the soil and by a large degree of "ground loosening". These features were discussed in Section 2.3.5. These conditions are hardly acceptable in normal practice nowadays, but could represent a common situation in the past, when most of these methods were developed. The Hewett-Johannesson (1922) method can be pointed out as a singular departure from this rule, as it suggests that the horizontal earth pressures should be selected appropriately, between the active and passive extreme cases. This is an attempt to define ground loads which are compatible with the deformantion mode of the lining. However, this merit is obliberated by several weak points and inconsistencies (the assumption of a rigid lining as opposed to the acceptance of different modes of lining deformation, is one of them).

Some earth pressure methods are based on soil arching or silo theories, for example Terzaghi (1943). The assumption in shallow tunnels of vertical shear failure planes reaching the ground surface with full shear strength mobilization, reveals, once more, conditions of poor ground control, and large ground displacements.

Newmark (1964:14) studying the design of underground protective construction under the effect of a pressure pulse at surface, suggested that pressure attenuation with depth could be estimated taking into consideration the ground arching effect which may be present if the construction roof yields. He recognized, however, that the degree of arching would vary with the amount of roof deformation. Therefore, he modified Terzaghi's theory in order to include the deformation but neglected the soil self weight.

As an academic exercise, the writer followed the same reasoning for the case of a yielding roof, including the soil self weight and both the cohesive and frictional components of strength. Shear stress along the vertical shear planes was assumed to be linearly proportional to the displacements. The distribution of the vertical displacement of the yielding soil cover was assumed to be a known exponential curve. With these assumptions, Terzaghi's arching theory was re-derived and the solution of the equilibrium differential equation furnished a relationship between the pressure over the support and the displacement profile above it. The rather lengthy expression included terms that required numerical integration. This approach could explain, at least qualitatively, ground pressure development in excess of those provided by Terzaghi's original theory, whenever soil shear strength is only partly mobilized. However, it can not fully explain the development of pressures smaller than Terzaghi's, as noted by Ladanyi and Hoyaux (1969:12) in trap-door experiments, and by Gais et.al., (1986:61) in the Munich Subway. The reason for this lies on the assumptions made. It was accepted that the shear transfer mechanism develops only along the vertical shear planes, which were assumed to be fully developed at the onset before any displacement occurs. The solutions would be correct if these failure planes existed as pre-sheared surfaces. However, this is not true, since they are progressively formed as a result of ground deformations as the soil goes towards collapse. A more likely interpretation of pressure development with soil displacement was presented in Section 3.2.3.

In its original version, Terzaghi's arching theory may be said to approximate a near collapse situation and possibly be represented by point G" in the schematic ground reaction curve shown in Figure 3.8. Therefore, for good control conditions, represented by the portion BC of that curve, (in which the failure planes are not fully developed), Terzaghi's theory would furnish ground loads either above or below the actual equilibrium load. Therefore, it can provide either a safe or unsafe estimate of loads, depending on the magnitude of the displacements occurring in the field. This was also noted by Wong (1986:232).

Table 4.4 presents a brief summary of some earth pressure theories. Some of them were originally developed for rock masses but include soil tunnels as special cases. Other methods were included for their historical significance and some for their popularity among designers. A few illustrative comments are added as well as indications of works where some of these methods were extensively reviewed, notably Szechy (1967), Deere et.al., (1969) and Steiner and Einstein (1980). The use of these earth pressure theories seems to be diminishing in practice, in favour of methods that include the lining-ground interaction and ~~that~~ the acknowledgement that loads are displacement dependent. However, they can still provide useful guidance once they are calibrated with field data from a particular site and for a specific construction technique. Under these

Author	Comments	Review
Ritter (1879)	Only 'gravity' loads, for deep tunnels; first method for lining load assessment	In (1):211 in (2):37
Forchheimer (1882)	Derived from experiments in dry sand	In (1):211
Kommerell (1912, 1940)	Only 'loosening' loads, for shallow tunnels; loads directly related to the amount of crown settlement	In (1):209 and in (2):45
Bierbaumer (1913)	Based on observations in timber supports and in tests on timber blocks; observational approach	In (2):75
Hewett-Johannesson (1922)	Developed for shielded tunnels; first approximate attempt to account for soil-lining interaction	In (1):356 and in (3):34
Protodyakonov	Parabolic shaped dead load over support; deep tunnel assumption; very used in Soviet Union	In (1):213
Terzaghi (1943)	"Rock Load Theory", based on Kommerell's and Bierbaumer's data	In (2):53 and in (3):44
Stini (1950)	Developed for timber supported tunnels; similar to Terzaghi (1946)	In (2):70
Balla (1963)	Actually a method for stability analysis; based on Kotter's differential equation; valid for flat roof	In (1):206 and in (3): IV-17

Reviewers: (1) Szechy (1967); (2) Steiner and Einstein (1980); (3) Deere et al (1969)

Table 4.4 Ground Pressure Theories: A Partial Survey

conditions, they can be used to extrapolate experience within that site and for that particular method of construction, but they may furnish incorrect load predictions if used outside the framework in which they were developed.

Methods that Specify Tunnel Performance

The second subgroup includes methods in which the lining performance is specified beforehand, and they represent an improvement over to the former methods. Here the lining flexibility is taken in consideration, as opposed to using the rigid lining concept suggested by the others. This more recent design approach is based on the concept of the "ideal lining" put forward by many modern tunnelers, notably Peck (1969). The lining is represented by a ring which is very rigid in uniform compression and very flexible upon bending. It is consistent with modern design trends that lead to negligible bending moments under limited ground losses.

Different versions of this design approach have been presented by different American designers, including Deere et.al. (1969:95), Peck (1969:257), Peck et.al. (1972:266), O'Rourke et.al. (1984), Schmidt (1984), and Kuesel (1986), among others. This approach, which in reality is a criterion that goes beyond the prediction of lining loads, can be briefly stated as: "Flexible circular tunnel linings should be designed for a uniform ring compression, corresponding to the overburden pressure at the springline, plus an arbitrary imposed distortion measured as a percentage change in radius" (Kuesel, 1986:6). The full overburden assumption proposed by Peck (1969) resulted from his interpretation of field data and was critically reviewed in Section 3.3.3.3 as generally being a conservative design assumption. Clough and Schmidt (1981:615) contend that it is a fair assumption but they do not provide factual evidence supporting it. Schmidt (1984) extended Peck's recommendation regarding the imposed distortion for design verification, and put forward ultimate lining distortion ranges for different soil types (see Table 4.5). These recommended values were derived from field observations and are to be used for design, although higher distortion values have already been reported under extreme circumstances. For example, Schmitter and Moreno (1983:406) report total diameter changes as much as 6% in the precast segmented lining used in a Mexico City tunnel, without support collapse.

The maximum bending moments resulting from these imposed lining distortions can be calculated from elastic beam theory (Morgan, 1961:41, Deere et.al., 1969:99 or Craig and Muir Wood, 1978:190):

$$M_{max} = 3\ E\ I\ \frac{\Delta R}{R^2}$$

According to this empirical approach, the relevant point is to ensure that the anticipated distortions are acceptable in terms of the serviceability of the lining (offset and water leakage aspects, mainly). This attitude results from the fact that in most soils, if a good

Soil Type	Ultimate Distortion Range ΔR/R (%)
Stiff to hard clay (OF < 2.5 - 3)	0.15 - 0.40
Soft clays or silts (OF > 2.5 - 3)	0.25 - 0.75
Dense or cohesive sands, most residual soils	0.05 - 0.25
Loose sands	0.10 - 0.35

Notes: (1) Add 0.1 - 0.3% for tunnels in compressed air, depending on air pressure.

(2) Add appropriate distortion for external effects such as passing neighbouring tunnels.

(3) Values assume reasonable care in construction, and standard excavation and lining methods.

Table 4.5 Recommended Lining Distortion Ratios for Design Verification (after Schmidt, 1984: modified)

lining-ground contact is ensured, the displacements needed to mobilize appreciable passive resistance in the soil are small compared to the lining's capacity for distortions. Field data reveals that even in soft soils, diameter changes of less than 1% in a flexible lining are entirely resisted by the mobilized shear stress in the soil (O'Rourke et.al., 1984:16).

In addition to the above requirements, the approach requires adequate consideration of the possibility of buckling. Peck et.al. (1972:267) suggested that in soft clays, the overburden stress should be

$$\gamma z < \frac{3E_s I_s}{R^3}$$

for buckling to be prevented.

As noted by Craig and Muir Wood (1978:197), this criterion is more conservative than Morgan's (1961:45) lining collapse pressure, p, given by:

$$p = \frac{3E_s I_s}{R^3} + \frac{E}{1+\nu}$$

where E and ν are the elastic constants of the soil.

Deere et.al., (1969:50) present another simple and partly empirical equation for assessment of the buckling of a thin walled cylinder embedded in soil, represented by a coefficient of radial ground reaction, C. The uniform all-round pressure causing instability is given by:

$$p = 2\sqrt{\frac{C\ E_s\ I_s}{R^3}}$$

All three equations above are conservative for a uniform lining load, but they are not strictly valid for non-uniform loading conditions. They can provide an unsafe estimate of lining buckling if the ground-lining contact is poor (Deere et.al., Op.cit.:51), with local concentrations of ground loads. Otherwise, they show that buckling of usual lining systems due to external pressures is very unlikely for customary tunnel depths and tunnel sizes. Buckling becomes a matter of concern when the lining is very thin or when the external pressures are significant, such as in the case of high water heads in undersea tunnels.

Some weak points are apparent in this empirical approach of lining design. The assumption of uniform ring compression is not consistent with the need to account for distortional bending. Also the full overburden assumption is debatable, particularly when considering that the approach is valid for good lining contact and good ground control conditions. Nevertheless, this empirical method is very useful for a preliminary dimensioning of the lining, which requires a more detailed design analysis afterwards.

Finally, it should be noted that the above empirical methods could be used together with the observational method, as described by Peck (1969). This could form a third empirical group besides these two already described. Steiner and Einstein (1980:311-380) call this group, the "Empirical Observational Methods", and discuss their potential use in rock tunnelling. Their methodology and ideas could be extended specifically for soil tunnelling.

4.3.2.3 Ring and Plate Models

These are mainly analytical models in which the ground is represented by a plate and the support of a circular opening, corresponding to the tunnel excavation, is represented by a continuous ring. Both ring and plate are assumed to be in a state of plane strain, depicting a cross section of the tunnel far from the advancing face and unaffected by the three-dimensional stress transfer process. Solutions developed by these models are based on continuum mechanics approaches and most of them are of the closed form style, therefore very easy to handle. Without any exception, existing solutions assume the plate to be of infinite extent and therefore it is accepted that the presence of a stress free ground surface does not influence the analysis. With respect to the lining and its interaction with the ground, it was shown (Section 2.2) that the presence of the ground surface has negligible influence, if the cover to diameter ratio (H/D) is greater than 1.5. Therefore, the infinite plate is not a restrictive assumption for tunnels with ground cover of not shallower than 1.5 diameters. However, neglecting the gravitational stress gradients, as most models of this group do, is a more restrictive assumption, since most cases encountered in practice present a cover to diameter ratio for which the effect of these gradients is not small.

The ring and plate models are divided into two categories, according to whether the the type of in situ stress field which they assume is uniform or non-uniform. The former subgroup includes mostly analytical models which are axi-symmetrically solved as a result of the geometric, the stress state and the material symmetries. The latter include solutions in which the distortional component of the initial stress state is present or in which stress non-uniformity is simply caused by the action of gravity. Therefore, the solutions take advantage of, at least one plane of symmetry, and usually two.

Uniform Stress Field Solutions

These solutions are collectively included in the so called 'convergence-confinement' models. As explained in Section 2.3.5 they are only applicable to the ideal deep tunnel case with K equal to unity. By virtue of this fact, the equilibrium between the ground and the lining can be assessed by solving a set of two equations. One represents the ground reaction in terms of radial stress and displacement at the tunnel wall and the other represents the support reaction in terms of the same variables. The particular state of stress assumed and the assumption of isotropy ensures that the two functions describing the ground and support reactions can be independently assessed. The evaluation of the interaction process is greatly simplified since no distortion of the lining occurs under these conditions.

The overall simplicity of the problem allowed the introduction of relatively complex constitutive relationships for evaluation of the ground response, including different stress-strain models, yield criteria and volume change hypotheses. An excellent review of the subject was presented by Brown et.al. (1983). As for the support response, available solutions treat it as a linear elastic material, and they are presented by Daemen (1975) and reviewed by Hoek and Brown (1980).

The capability of the available solutions to model complex ground responses, include for instance, elastic-brittle plastic behaviour, non-linearity of stress-strength criteria, accounting for short and long term strength, rate dependent strength and stiffness, and associated and non-associated flow rules for the treatment of volumetric strains. Despite this, the assumption of a uniform stress field seems to be excessively restrictive when one is dealing with shallow tunnel design. If applied to a non-uniform in situ stress condition, the convergence-confinement method will only provide the ground and support responses in terms of average stress and displacement since the distortional component of the stresses are not considered. It will furnish indications of the mean ground pressure or mean lining thrust and mean ground losses at equilibrium, which may be of some help for a qualitative design estimate. However, the impossibility of assessing the development of lining bending is a crucial limitation of this approach. Perhaps this is one of the reasons why practitioners seldom use this method for shallow tunnel design. Past and recent attempts to generalize the model to non-uniform stress field (e.g. Kastner, 1949, or Detournay and Fairhurst, 1982) were limited to the evaluation of the ground response. The interaction with the support system was still neglected.

For a proper assessment of the equilibrium between lining and soil, an independent evaluation of the ground response before lining activation is required. This class of solutions cannot provide the tools for this task.

The applicability of the convergence-confinement method to the design of shallow tunnels was objectively undertaken by Branco and Eisenstein (1985). This was done by comparing predictions by this method with field measurements from two tunnels driven through Edmonton Till, one with H/D equal to 1.4 and the other equal to about 10. In both cases, K was close to unity, and the effect of the gravitational stress gradient was present in both, obviously more so in the shallower case. These authors used Kaiser's (1980) formulation for the ground response. The results they obtained showed poor agreement for the shallower tunnel,and better but not fully satifactory agreement for the deep tunnel, even when the displacements developed before lining installation (as measured in the field) were accounted for. They attributed the discrepancies to the non-axisymmetric mode of deformation noted in both cases prior to lining activation, which was due to the presence of the free ground surface and to the effect of the gravitational stress field.

In both cases, the in situ stress field was non-uniform, despite the stress ratio being close to unity. Available solutions do not account adequately for this stress field non-uniformity and even when the stress and displacement developments prior to lining installation are properly accounted for, the method does not provide satisfactory predictions. These facts, as well as others addressed in the conference "Analysis of Tunnel Stability by Convergence-Confinement Method" of the Association Francaise des Travaux en Souterrain (Paris, 1978) '' make this approach not fully applicable for the design of linings of shallow tunnels. Nevertheless, Figure 4.2 provides references to some representative solutions among this group.

Non-Uniform Stress Field Solutions

These are solutions in which the in situ stress non-uniformity is due to the stress ratio, K, being not equal to unity or due to gravitational stresses. Most of them were surveyed by a number of authors, to variable degrees of detail, and therefore, another review would simply be redundant. A summary of the most representative review works on the subject, presented over the last two decades, is presented in Table 4.6. As indicated, the methods reviewed include not only the ring and plate solutions but also ring and spring models, which will be discussed in the next section. Apart from the reference to

---

'' English translation: In Underground Space, Volume. 4, No. 4, 5 and 6, Pergamon Press, 1980.

the methods reviewed by each review author, the table indicates the availability of comparisons of results provided by those methods. These are provided by some authors in terms of dimensionless moment or thrust coefficients as a function of the lining's flexibility and compressibility ratios. Finally the table has a few comments providing the main issues focussed by each review work.

Among these review works, that by Katzenbach (1981) is referred to as one of the most comprehensive register of methods available. Another notable work is that by Erdmann (1983), who provides one the best assessments of each method reviewed, including the basis of their derivation, assumptions used and furthermore, a detailed comparison of results obtainable by those methods. Part of his original work, written in German, was summarized in English by Duddeck and Erdmann (1982), Erdmann and Duddeck (1983) and Duddeck and Erdmann (1985). Also worth mentioning is the work by Ranken (1978), who provided perhaps the most detailed assessment of the assumptions used for the development of ring in a plate solutions (external and excavation loading, ground-lining interface hypothesis, thin and thick lining assumptions, effect of tunnel depth, etc.).

Despite all these review works, it was decided to prepare a summary table, in which the important assumptions of each ring and plate derivation could be easily assessed and compared. Table 4.7 includes most of the closed form analytical solutions developed over the last quarter

Review Author	Methods Reviewed	Comparison of Results	Comments
1. Szechy (1967)	Zurabov and Bougayeva (1962)^{2}; Bodrov-Gorelik^{2}, Polygonal Method^{2}; Davidov (1950)^{2}; Varga (1961)^{2}; Meissner (1964)^{1}; Orlov (1954)^{1}; Rozsa and Kovacs^{1}	NA	Mostly methods used in eastern countries; worked example provided. Only qualitative comparisons between methods available.
2. Duddeck (1972)	Rozsa (1963)^{2}; Schulze and Duddeck (1964)^{2}; Bougayeva (1951)^{2}; Voellmy (1937)^{1}; Windels (1967)^{1}; Morgan (1961)^{1}, Meissner (1963)^{1}; Durth (1969)^{2}; Windels (1966)^{2}	A	Comparison of ring-spring and ring-plate solutions, assessment of 2nd order effects. Bending moments and thrust forces compared.
3. Duddeck (1973)	Morgan (1961)^{1}; Schulze and Duddeck (1964)^{2}; Windels (1966)^{2}; Windels (1967)^{1}; Hain (1970)^{2}; Hain and Horst (1979)^{2}	A	Comparison of bending moments methods developed mainly by German authors.
4. Mohraz et al (1975)	Burns and Richard (1964)^{1}; Hoeg (1968)^{1}; Peck et al (1972)^{1}	A	Assessment of effects of loading assumptions: external, excavation and gravity loadings. Solution for last two types SAP F.E. program. Methods developed by American authors.
5. Craig & Muir Wood (1978)	Morgan (1961)^{1}; Muir Wood (1975)^{1}; Curtis (1976)^{1}; Schulze and Duddeck (1964)^{2}, Curtis (1974)^{1}	NA	Only qualitative comparison between methods. Emphasis on British methods compared to others.
6. Ebaid & Hammad (1978)	Davidov (1950)^{2}; Engelbreth (1961)^{1}; Zurabov & Bougayeva (1962)^{2}; Peck et al (1972)^{1}; Muir Wood (1975)^{1}; Curtis (1976)^{1}	A	Quantitative comparison of bending moments provided by methods reviewed.
7. Ranken (1978)	Morgan (1961)^{1}; Muir Wood (1975)^{1}; Curtis (1976)^{1}; Burns and Richard (1964)^{1}; Dar and Bates (1974)^{1}; Hoeg (1968)^{1}; Peck et al (1972)^{1}; Ranken (1978)^{1}	A	Quantitative assessment of effects of lining loading assumption. External and excavation loading analytical solutions compared. Comparison with FE solutions. Gravity loading case studied through numerical simulation.
8. Katzenbach (1981)	Voellmy (1937)^{1}; Morgan (1961)^{1}; Engelbreth (1961)^{1}; Meissner (1963)^{1}; Windels (1967)^{1}; Hartmann (1970-1972)^{1}, Schulze and Duddeck (1964)^{2}; Windels (1966)^{2}; Hain (1968)^{2}, Hain and Horst (1970, 1971, 1974)^{2}	NA	Mainly a comprehensive register of methods within a classification system.

Table 4.6 Some Review Works on Ring and Plate or Ring and Spring Models for Design of Linings Under Non-Uniform Stress Fields

Review Author	Methods Reviewed	Comparison of Results	Comments
9. Duddeck & Erdmann (1982)	Schmid (1926)[1]; Voellmy (1937)[1]; Engelbreth (1961)[1]; Morgan (1961)[1]; Schulze and Duddeck (1964)[2]; Windels (1966)[2]; Windels (1967)[1]; Muir Wood (1975)[1]; Curtis (1976)[1], Einstein and Schwartz (1979)[1]; Ahrens et al (1982)[1]	A	Review provides quantitative comparison of results provided by most methods reviewed, in terms of thrust forces and bending moments.
10. Erdmann & Duddeck (1983)	As No. 9	A	A slightly more detailed review than the above, extending the assessment of effects of the no-slip and full-slip assumptions on lining loads.
11. Paul et al (1983)	Ranken et al (1978)[1]; Einstein et al (1980)[1]; Burns and Richards (1964)[1]; Der and Bates (1974)[1]; Hoeg (1968)[1]; Morgan (1961)[1]; Muir Wood (1975)[1]; Curtis (1976)[1]; Peck et al (1972)	NA	A brief review of closed form solutions of 'hole-in-a-plate' type developed in english-speaking countries.
12. Erdmann (1983)	Schmid (1926)[1]; Voellmy (1937)[1]; Ahrens et al (1982)[1]; Schulze and Duddeck (1964)[2]; Windels (1966)[2]; Curtis (1974)[1]; Morgan (1961)[1]; Muir Wood (1975)[1], Windels (1967)[1]; Engelbreth (1961)[1]; Peck et al (1972)[1]; Einstein & Schwartz (1979)[1]; Durth (1969)[2]; Hain & Horst (1970, 1971)[2], Ahrens (1976)[2]	A	Most comprehensive review, including discussion on assumptions of each method, summary of equations and comparison of results given by most methods.
13. O'Rourke (1984)	Peck et al (1972)[1]; Muir Wood (1975)[1]; Ranken et al (1978)[1]; Schwartz & Einstein (1980)[1]; Curtis (1976)[1]; Burns & Richard (1964)[1], Hoeg (1968)[1], Der & Bates (1974)[1]	NA	A brief historical review of some closed form solutions developed in english-speaking countries.
14. Duddeck (1985) & Duddeck & Erdmann (1985)	The same methods reviewed by Duddeck & Erdmann (1982) and and Erdmann and Duddeck (1983)	A	Combine previous reviews by the same authors; discuss effects of non linearities, of hinges in precast linings segments, use of methods reviewed for shield tunnelling and NATM.

Notes:
1: Ring-and-Plate solutions.
2: Ring-and-Spring solutions
A: Available in the review
NA: Not available in the review

Table 4.6 Some Review Works on Ring and Plate or Ring and Spring Models for Design of Linings Under Non-Uniform Stress Fields (Continued).

century. All solutions were derived assuming a plane strain condition and also that the lining is installed in close contact with the surrounding ground prior to any displacement development. Recognizing that this latter assumption can hardly be a reasonable approximation of the reality, some authors put forward approximate correction factors to account for the ground stress release caused by the delayed installation of the lining. Hartmann (1972:43) discusses stress reduction factors that would be pplied either to the specific weight of the ground or to the depth of the tunnel (the distinction between the two approaches is subtle as his solution accounts for gravity). According to this author, these factors would be empirically evaluated from field measurements. Muir Wood (1975:124) proposed an arbritary reduction of 50% of the in situ stresses on account of the delayed lining installation. Schwartz and Einstein (1980:75) suggested correction factors, derived from axisymmetric finite element analyses, to be applied to the calculated thrust or moments. Hutchinson (1982:175) questioned the criteria provided by Schwartz and Einstein, and proposed a reviewed procedure for the factor which is applied to the lining thrust.

Moreover, all solutions included in Table 4.7 assume both lining and ground to be linear elastic, homogeneous and isotropic materials. Most of them consider an "excavation loading" condition as opposed to a few that adopt an "external overpressure loading" condition. The latter

	Author	Year	Loading Condition	In Situ Stress Ratio (K)	Account For Gravity	Lining-Ground Interface	Lining Thickness	Lining Compressibility	Special Features and Comments
1	Morgan	1961	Excavation	Any	No	Full slip	Thin	Incompressible	Assume elliptical mode of deformation. Initial stress distribution incompatible with slippage condition. Only distortional component of stress is considered. Error in plane strain assumption (corrected by M. Wood, 1975).
2	Burns & Richards	1964	External overpressure	v/(1-v)	No	Both no and full slip	Thin	Compressible	Developed for analysis of buried structure subjected to overpressure. Use extensional shell theory to model liner.
3	Windels	1967	Excavation	Any	No	Both no and full slip	Thin	Incompressible	Incldde second order effects (geometrical non-linearity). Approximate account of deviations of lining section from ideal circle during assemblage.
4	Hoeg	1968	External overpressure	Any	No	Both no and full slip	Thin	Compressible	Full slip solution is incorrect (Ranken, 1978:20 and Schwartz and Einstein, 1980:18). Solution was later corrected by Ranken, 1978.
5	Hartmann	1970-72 1985-86	Excavation and external overpressure	Any	Yes	Both no and full slip	Thin	Compressible	Include second order effects (geometrical non-linearily). Uses Flugge cylindrical shell theory to model liner.
6	Peck, Hendron and Mohraz	1972	External overpressure	Any	No	Full slip	Thin	Compressible	Developed from Burns and Richards (1964) solution.
7	Dar and Bates	1974	External overpressure	v/(1-v)	No	No slip	Thick	Compressible	Lining is represented by a thick elastic cylinder.
8	Muir Wood	1975	Excavation	Any	No	Full slip	Thin	Incompressible	Elliptical mode of deformation. Include both uniform and distortional stress components but initial stress distribution not compatible with slippage condition. Approximations for partial slip, for stress release prior to liner installation and for effect of lining joints in flexibility.

Table 4.7 Assumptions and Features of some Ring and Plate Solutions for Non-Uniform Stress Field

	Author	Year	Loading Condition	In Situ Stress Ratio (K)	Account For Gravity	Lining-Ground Interface	Lining Thickness	Lining Compressibility	Special Features and Comments
9	Curtis	1974-76	Excavation	Any	No	Both no and full slip	Thin	Incompressible	Correct account of the distortional in situ stress component for full slip. His solution to be superimposed to Muir Wood's for the uniform component to get complete solution. Approximation for partial slip. Treatment of soil creep through visco-elasticity.
10	Ranken	1978	Excavation and external over-pressure	Any	No	Both no and full slip	Thin and thick	Compressible	Most complete set of solutions for 8 conditions of a deep tunnel, including second order effects.
11	Einstein and Schwartz	1979	Excavation	Any	No	Both no and full slip	Thin	Compressible	Uses Flugge's shell theory to model liner but neglect second order effects.
12	Schwartz and Einstein	1980	Excavation	Any	No	Both no and full slip	Think	Compressible	Same derivation of Einstein and Schwartz, 1979. Include approximate account of delayed lining installation (corrected by Hutchinson, 182:175) and of ground yielding.
13	Ahrens, Lindner and Lux	1982	Excavation	Any	Partly	Both no and full slip	Thin	Compressible	Uses Flugge's Shell Theory to model liner. Parametric analyses presented by Erdmann (1983:78). Include second order effects.
14	Carter and Booker	1984	Excavation	Any	No	Both no and full slip	Thin	Compressible	Uses cylindrical shell theory to model liner. Include coupled analysis of elastic consolidation, assuming imper-meable lining. Solution obtained by numerical integration (not analytical). Results presented in graphs.

Table 4.7 Assumptions and Features of some Ring and Plate Solutions for Non-Uniform Stress Field (Continued).

implies that the opening has been excavated and supported before the stress field is applied to the plate and could represent the case of a backfilled culvert. The lining acts as a "rigid inclusion" in the perforated plate and therefore thrusts, bending moments and lining displacements are overestimated, when compared to the "excavation loading" solutions in which the opening is excavated and supported after the stress field is applied to the plate. This latter condition more approximately represents the real tunnel situation. Differences in thrust and displacement calculated with the two loading assumptions, are more pronounced than the differences in moment or shear, but they tend to decrease as the relative stiffness of the lining to the ground decreases (Mohraz et.al., 1975:137, Einstein and Schwartz, 1979:508).

Most solutions take the field stress ratio is an independent variable but two of them, define it as a function of Poisson's ratio. All solutions, but one, do not account for the gravitational in situ stress field in the infinite plate and so treat the problem as an ideally deep tunnel. As pointed out previously, while the effect of the stress free ground surface can be accepted as negligible for H/D greater than 1.5, the influence of gravity cannot be neglected in the interaction analysis between ground and lining for most shallow tunnels.

The method by Ahrens et.al., (1982:268) is, in essence, a deep tunnel solution, since it neglects the in situ stress gradient across the opening. However, to account partly for the effect of gravity, the uniform vertical stress field is taken as the in situ vertical stress at the crown elevation, γH, and the uniform horizontal stress field is taken as the in situ horizontal stress at the springline elevation, $K_o\gamma(H+R)$. Consequently, the results become dependent not only on the absolute tunnel depth, H, as in other deep tunnel solutions, but also on the relative depth of the tunnel, H/D. Erdmann (1983:78) later explored this method, reducing it to an actual deep tunnel solution by making the ratio H/D equal to infinity. The only method that takes the action of gravity fully into consideration (including the heave caused by the unequal vertical stresses) is that by Hartmann (1970,1972).

The majority of the solutions consider both the case of full and no slip conditions at the ground-liner interface and assume the lining to be a thin membrane whose behaviour is approximated by thin shell theory. Only these solutions by Dar and Bates and by Ranken are entirely based on the theory of elasticity (thick lining solutions). Despite both types of solutions being applicable to linings of any thickness, rigorously only those assuming the lining to be thick, are strictly correct for all lining thicknesses. However, as noted by Ranken, (1978:312), provided the ratio of lining thickness to the mean lining radius is smaller than 0.1, the two solutions furnish essentially the same results. The preference for the thin lining appproach is due to its easier manipulation in practice as opposed to the thick liner solutions which result in cumbersome equations. Some of the solutions assume the liner to be incompressible or inextensible under thrust (compressibility ratio, C, equal to zero), despite being responsive to distortion or bending (finite flexibility ratio, F). All solutions were analytically derived, and except for one, they are presented in closed-form. The exception is the Carter and Booker (1984) method where a numerical integration is required to obtain an explicit solution which is presented in charts. All solutions neglect geometric non-linearity except for those by Windel, Hartmann, Ranken and Ahrens. These four were developed using second order theory and therefore they furnish, for instance, slightly different bending moments. The second order moments arise from differences in the internal and external liner radii, even for a uniform stress field. However, as noted by Schwartz and Einstein (1980:367), these second order terms are of small magnitude for usual lining thicknesses and therefore could be neglected for all practical purposes.

Except for solutions by Morgan (1961) and Muir Wood (1975) (which included some inaccuracies in their derivations, later amended by others, see Table 4.7), the external loading solutions for deep tunnels (solution by Peck et.al. therefore excluded), furnish almost the same values for thrust forces and bending moments. Figure 4.3, which includes part of Erdmann's (1983) data, illustrates this point and shows that bending moments from those solutions essentially coincide within the usual range of relative stiffnesses found in practice. Similar results are found regarding thrust forces (Erdmann, Op.cit.:111,112).

The most complete set of solutions for the deep tunnel situation is that provided by Ranken (1978), who corrected and further developed previous closed-form solutions. The most useful solution regarding the application to the shallow tunnel case, is that by Hartmann, as it fully accounts for the action of gravity. It is very suprising that this solution, which is older than those most frequently used (e.g., Peck et.al., Muir Wood-Curtis, Einstein and Schwartz) is rarely referenced in the literature. Even in West Germany, where his method was published, no reference was made to it except a simple mention in Katzenbach's (1981:122) survey, without any further comments (see Table 4.6). A possible explanation for this solution to have passed unnoticed and not have raised larger interest, is the fact that it has been presented in four separate and lengthy parts between 1970 and 1972, including its very long and complex derivation comprising over three hundred and forty algebraic equations. Notwithstanding this, it is the single most valuable solution of this group for the shallow tunnel problem. The complete solution by Hartmann for the excavation loading will be presented and discussed in other sections of this thesis (Chapter 7).

$$M_{max} = m \left[\frac{1-K}{2} \cdot \sigma_v \cdot R^2 \right]$$

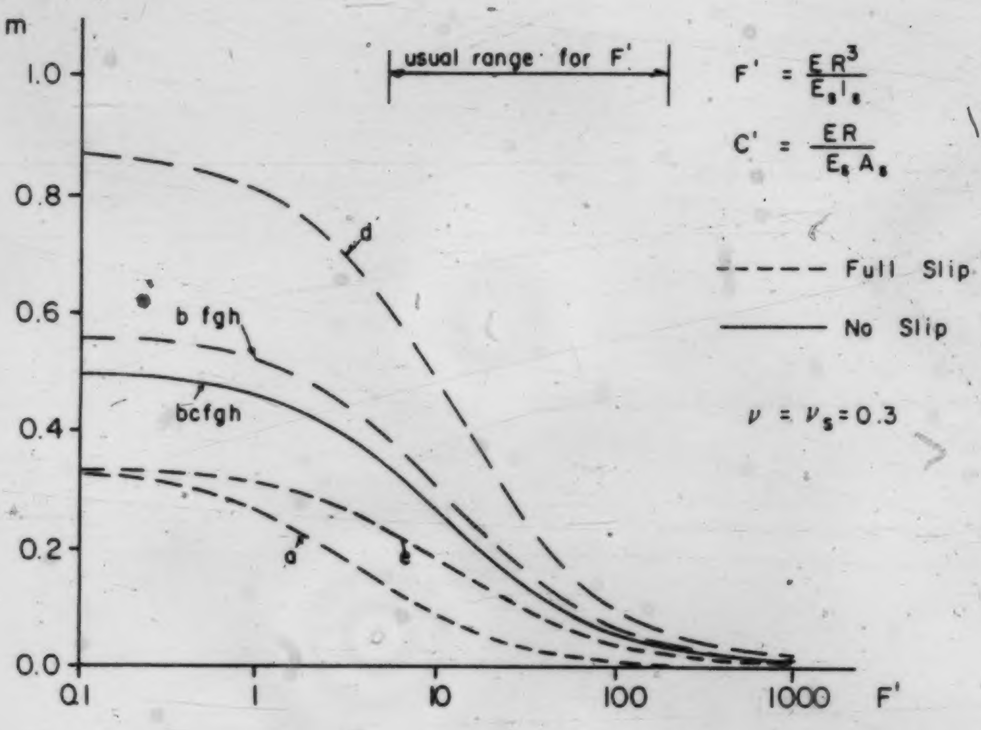

Legend[1]: a. Morgan (1961), b. Windels (1967), c. Hartmann (1970, 1972)[2],
d. Peck et al (1972), e. Muir Wood (1975), f. Curtis - Muir Wood (1976),
g. Einstein and Schwartz (1979), h. Ahrens, Lindner and Lux (1982)

Notes:
1. Solutions a, d, e and f assume C' equal to zero (incompressible lining) The others (b, c, g and h) were calculated for a virtually incompressible lining with C'/F equal to 5×10^{-4}.
2. Hartmann solution has been reduced here to a deep tunnel situation.
3. Maximum bending moment at springline or at crown/floor.

Figure 4.3 Maximum Bending Moment Variation with Flexibility Ratio for a Deep Tunnel Liner from Different Ring and Plate Closed Form Solutions

Broadly speaking, one of the major limitations of these solutions is the assumption of a plane strain condition and therefore the inability to account for the inevitable three-dimensional stress transfer associated with the delayed lining installation. If the lining design is understood as an exercise in behaviour prediction, to which some safety criteria is applied, the unavoidable ground stress relaxation taking place before support application cannot be neglected. Available empirical approaches to account for this effect are too arbitrary to be reliable. Some approximate numerical approaches, that will later be reviewed, are more adequate, but still have limitations, such as ideally deep tunnel assumption.

The assumptions of linear elasticity, homogeneity and isotropy are other shortcomings of these methods. One may concede that if the ground-lining contact is good, and if ground control conditions are also good once the support is fully installed, additional ground or lining deformations are likely to be small compared to the movements of the soil occurring before lining installation. Schmidt (1984) noted total lining closures of less that 0.03 to 0.3% of the tunnel diameter after the support was installed). However, the question regarding the "elastic" modulus of the groundto be used in the analysis remains unanswered. Besides the usual heterogeneities in the ground properties and their variation with depth, the stress paths at points around the opening are different (Section 2.3.4.1), and different stress-strain responses should be anticipated. Even if an initially homogeneous ground condition exists, by the time the support is installed and the interaction with the ground is developed, a non-homogeneous ground condition would have been generated. Prior to lining activation, the soil around the opening would have undergone different degrees of straining, exhibiting stiffnesses which differ from the in situ value (Section 2.3.5.3). It will be seen later in this thesis that the potential of the ring and plate solutions could be improved if an independent procedure is developed to take these effects into consideration.

4.3.2.4 Ring and Spring Models

These are models in which the ground is represented by springs that provide reactions which are displacement dependent (Winkler type of reaction). The lining is depicted by a continuous ring when the ground-spring embedding is also continuous, or by a segmented ring formed by interconnected segments or beams, when the ground-spring embedding is of a discrete type. Accordingly, the solutions are analytically approached by treating the ring as an elastically embedded shell, or numerically approached by treating the liner as a frame which is elastically supported at its nodes. While in the first group, the final solution of the basic differential equation (usually of 4th order on radial displacements) may be obtained either analytically or numerically, the second group requires the solution to be obtained by numerical methods, like finite element analyses.

Figure 4.2 furnishes typical examples of methods of ring and spring type, according to the type of embedding or solution adopted. Like ring and plate solutions, these also assume a plane strain state, and handle non-uniform loading stress conditions.

All methods indicated in Figure 4.2 and others have been surveyed by various authors to a large extent. Therefore, a case by case review of methods will not be attempted herein, but an overall discussion on the assumptions and basic features will be presented. A summary of the most representative review works on the subject is presented in Table 4.6. The table provides an indication of the methods reviewed and the availability of comparisons of results from different approaches which assess the influences of the particular assumptions made. A noteworthy contribution is that by Duddeck and Associates who paid considerable attention to comparative studies between the ring and spring models, mostly developed in West Germany, and ring and plate models, which have been particularly favoured by English speaking authors. Perhaps the most complete review work is that by Erdmann (1983). Besides presenting the bases of the methods they reviewed, a thorough discussion is introduced on the correspondence between ring and spring and ring and plate models (Erdmann Op.cit.:25,90), largely based on the work by Ahrens et.al., (1982).

For the sake of completeness, Table 4.8 has been prepared, with the intent of providing brief indications of the most important assumptions and features of some ring and spring models, which are not always readily recognizable. Although most of the solutions indicated are based on the assumption of continuous subgrade ground reaction and are analytically developed, the discrete ground reaction models using numerical solutions, like the one by Andraskay et.al., (1972), seem to be more popularly used in practice. In the latter, the ground reaction is simulated by beam or spring elements positioned at the nodes of the lining frame. When this simulation is performed and the lining is loaded the liner and springs will deform and both will share parts of the imposed load, according to their relative stiffnesses. Some of the springs will compress, while others will be extended under tension, possibly in the crown region. Some reason that if the latter were to represent the soil, they should not withstand tensile stresses, and therefore they should be removed from the statical system. This arguement is problematical, particularly in the case of a uniformly loaded ring since the same reasoning asks that all springs around it to neglected as they all undergo tension. Some others contend (see Sections 2.2 and 2.3.5.4) that a fully developed failure zone will be generated above the tunnel, confined by two slip surfaces running upwards from the opening and intercepting the ground surface (e.g. Windels, 1966:265). Therefore, the soil above the tunnel crown would

	Author	Year	Ground Reaction	Embeddment	Type of Springs	Loading Condition	Lining Compressibility	Solution Formulation/ Presentation	Special Features and Comments
1	Rull	1944	Discrete	Partial	Radial	Localized (crown)	Compressible	Numerical (programmable)	Iterative solution; computer program developed by Mathis (1974).
2	Davidov (after Szechy, 1967)	1950	Continuous	Complete	Horizontal	Hypothetical all round distribution	Incompressible	Closed form	Deep tunnel loading. Use equivalent elastic subgrade reaction. Elastic embedding correctly fulfilled at springline only.
3	Bugayeva (after Szechy, 1967)	1951	Continuous	Partial (except upper 90°)	Radial	Localized (crown)	Incompressible	Closed form with tabulated coefficient	Compatibility of displacements at springline and floor only. At other points arbitrary ground reaction.
4	Schulze and Duddeck	1964	Continuous	Partial (except upper 100°)	Radial	Approx. in situ stresses (gravity partly accounted)	Incompressible	Numerical (design charts)	May or may not include effect of interface shear stresses. Takes radial in situ stress at springline. Assumes equal radial stresses at crown and floor (approx. equal to overburden stress).
5	Windels	1966	Continuous	Partial (except upper 90°)	Radial	Approx. in situ stresses (gravity partly accounted)	Incompressible	Design charts (iterative procedure)	May or may not include effect of interface shear stresses. Rad. stress at crown and floor equal to overburden. Partial acc. of geom. non linearity (linearized 2nd order effects acc. to Erdmann, 1983:98). Approx. acc. of pre-activation lining deformations.
6	Hain and Horst	1970	Continuous	Partial (variable)	Radial & Tangential	In situ stresses (gravity included)	Compressible	Numerical (programmable)	Tangential springs included only in the basic theory, not in the solution. Include linearized 2nd order effects. Adapted for non circular profiles. Do not account for load changes due to lining heave.

Table 4.8 Assumptions and Features of some Ring and Spring Models

	Author	Year	Ground Reaction	Embedding	Type of Springs	Loading Condition	Lining Compressibility	Solution Formulation/ Presentation	Special Features and Comments
7	Hain and Horst	1971	Continuous	Partial	Radial	In situ stresses (gravity included)	Compressible	Numerical (programmable)	Correct account of load changes due to lining heave. Include geometric non linearity.
8	Hain and Horst	1974	Continuous	Complete	Radial & Tangential	In situ stresses (gravity included with $K = \nu/(1-\nu)$	Compressible	Numerical (programmable)	Correct account of load changes due to lining heave. Include linearized 2nd order effects and account for pre-activation lining deformations.
9	Ahrens (after Erdmann, 1983)	1976	Continuous	Partial	Radial & Tangential	In situ stresses (gravity included)	Compressible	Programmable (iterative procedure)	Tangential springs included in the basic derivation. Full account of geometric non linearity. Lining with time dependent non linear (plastic) constitutive law.
10	Sgouros Saha	1982 1982	Discrete	Partial (no tension radial springs)	Radial & Tangential	Localized (crown)	Compressible	Finite Element	Finite element formulation (three nodes beam element and springs). Lining with non linear piece wise elastic representation
11	Andraskay, Hofmann and Jemelka	1972	Discrete	Partial (except upper 90°)	Radial	Reduced in situ stress	Compressible	Computer Program (STRESS)	Reduced overburden stress by Voellmy (1937) arching theory.

Table 4.8 Assumptions and Features of some Ring and Spring Models (Continued).

not be able to withstand any additional shear, and could not provide an embedment to the support ring in that area. Although this is an actual possibility, particularly if ground control conditions are deficient, it is hardly acceptable in a normal urban tunnelling situation since it implies the existance of an extreme collapse condition as a design hypothesis. As discussed in Chapter 2, the magnitude of ground movements are likely to be large for this condition and probably unacceptable in routine urban tunnelling. When ensuring limited and acceptable ground losses by selecting adequate ground control measures, the dimensionless crown displacement (Section 2.3.4.3) is likely to be smaller than that tentatively established for a near collapse condition. Thus, it would be reasonable that the crown embedment can be accounted for in the lining design. Normally the partial embedment assumption leads to more conservative bending moments and thrust forces in the lining.

Except for Ahrens (1976), who assumed a non-linear (plastic) behaviour for the liner, all other solutions assume linear elasticity, both for the lining and the springs. Duddeck and Erdmann (1985:257) showed results of an analysis in which the non-linear constitutive behaviour of a concrete lining was taken into account. While the thrust forces in this analysis were not much changed, the magnitude of the maximum bending moment decreased by about 33%. A safer estimate of lining loads is usually obtained from the assumption of linear elasticity for the support and this is possibly why this assumption is normally accepted.

This agrees with findings by Paul et.al., (1983:137) who also performed analyses assuming a non-linear behaviour for the concrete lining as discussed earlier. Moreover, these authors showed that, for this sort of lining response, a partial or non-slip condition at the lining-ground interface will furnish lower ultimate (failure) thrust loads than the full slip case (Paul et.al., Op.cit.:87).

Most commonly the embedment is provided for by radial springs only, which would mimic the tangential slip case. Solutions by Schulze and Duddeck (1964) and Windels (1966) may or may not include the shear stresses at the lining-ground interface as active loads into the system. If these stresses are neglected, their solutions correspond to Muir Wood's (1975) original solution (see Table 4.7) and therefore they are formally inaccurate, as they do not take into consideration the deformation components due to the full slippage condition (see Section 2.3.5.2). For a given radial spring constant[13], if tangential springs are also considered in the analysis, a stiffer ground response can be anticipated, which in turn leads to smaller bending moments and thrust forces in the lining. In other words, the assumption of radial springs only, normally leads tc a safer estimate of lining loads (depending on the assumed value for the spring modulus).

---

[13] The spring constant or spring modulus is defined as the stress-displacement ratio at a point of the lining ground interface, in terms of radial or tangential components, with units of force/length^3. This terminology will be preferred to the also used terms "Winkler constant" (or modulus) and "ground-reaction constant" (modulus or coefficient).

Two main groups of ground load assumptions are identified in Table 4.8. The first refers to a localized gravity loading condition in the crown region only, where the lining is not embedded. This would be the case of a tunnel in a fairly self supporting ground, experiencing loosening that results in localized loads. This corresponds to what has been defined in Section 2.3.5.1 as a "poor lining-ground contact", under conditions of poor ground control. The second refers to an in situ stress load condition, assuming that the lining is installed before any ground stress redistribution occurs. In this case, the loads are not localized but distributed all around the lining perimeter. While most solutions within the second group take full account of the action of gravity (gravitational stress gradient all across the tunnel profile), the methods by Schulze and Duddeck (1964) and Windels (1966) account for the effect of gravity only partly. Similar to the ring and plate solution by Ahrens et.al., (1982), they assume equal active stresses at the crown and floor, therefore avoiding the unbalanced vertical force that would heave a shallow tunnel. The active radial stress at the springline is taken as the in situ horizontal stress at the tunnel axis elevation. However, their different assumptions of interface shear stress results in vertical and horizontal active stress distributions, which are non-uniform but are symmetric with respect to the vertical and horizontal axes of the tunnel. The approximate account of gravity makes their solution to be dependent on the relative depth of the tunnel.

As discussed in Section 2.2, the coupled assumption of partial embedding and of in situ ground loads (full overburden) is questionable since they are incompatible. If the lack of embedding in the crown region requires the assumption of complete collapse of the tunnel cover and the development of two shear failure planes, running up to the ground surface, then the full overburden load assumption is in conflict. It implies zero shear strength along the two slip surfaces, which is not acceptable as a design assumption for most soil types. In other words, if lining embedding is taken as partial, then for consistency, the ground loads should be represented by a reduced in situ stress resulting from soil cover arching between the two slip surfaces. This is what Andraskay et.al., (1972) assumed in their solution and it is frequently adopted in practice.

Most of the solutions available are not expressed in closed form or in design charts, therefore requiring a small frame computer to be used. To make the solution simpler, the closed form approaches usually assume the lining to be imcompressible in thrust (compressibilty ratio equal to zero). Some of the existing solutions take into consideration the second order effects of the theory of elasticity. This geometric non-linearity is either accounted for completely (e.g. Ahrens, 1976), including the lining shortening by tangential compression, or partly, when only 2^{nd} order effects due to bending deformation are considered (e.g., Windels, 1966). Schulze and Duddeck's (1964) solution and others disregard these effects, assuming that the lining deformations are small and that equilibrium conditions can be verified in the undeformed lining geometry. However, Duddeck (1973:267) and Duddeck and Erdmann (1985:256), have shown that these assumptions may have some influence on the calculated moments, but have little influence on the thrust forces. In typical subway tunnels (6 m in diameter and steel or cast iron linings) these effects are negligible. However for larger tunnels (10 m in diameter or more), the complete account of geometric non-linearity may increase maximum bending moments by up to 50%, or up to 20% if the lining shortening is neglected.

While most of the solutions available were developed for a circular lining profile, some of them accommodate non-circular cross sections. This is the case in the continuous solution by Hain and Horst (1970), and of the discrete solutions based on finite element formulations, such as that by Andraskay et.al., (1972) or Sgouros (1982). This is, perhaps, one of the features that make these latter solutions very attractive for practical use. This capability is not available in any of the ring and plate solutions discussed in the previous section.

A point that normally raises interest is how a ring and spring solution relates to a ring and plate one. Broadly speaking, the methods in Table 4.7 are unrelated to most methods included in Table 4.8, since they imply different representations for the ground and ground-liner interaction. For instance, the partial embedding frequently assumed in the ring and spring models has no parallel solution in the ring and plate models. Moreover, the former assumes spring constants which are usually arbitrary and non-representative of the continuum solution ground response. For instance, the radial spring constant, K_r, is in many instances, related to the soil's constrained modulus (D).

$$K_r = C\,\frac{D}{R} = C\,\frac{(1-\nu)}{(1-2\nu)}\cdot\frac{1}{(1+\nu)}\,\frac{E}{R}$$

where R is the mean radius and C is an empirical constant. Schulze and Duddeck (1964:107) recommend that C be taken as equal to one. Windels (1966:266,273) suggests C varyies between 2/3 and 3/2.

The German recommendations for lining design (Duddeck, 1980), suggest that C be taken as equal to one. Hence for a Poisson's ratio of 0.3, K_r would be about 0.74E/R. Some other authors (Ebaid and Hammad, 1978:61, Sungur, 1984:21, for instance) suggest that the independent variable K_r be taken as

$$K_r = \frac{1}{1+\nu}\,\frac{E}{R}$$

This expression is obtained from the uniform convergence of a deep tunnel in elastic ground under a uniform stress field. The latter gives, for the same Poisson's ratio, K_r

equal to 0.77E/R. The minor difference in K_r by both approaches did not invite much discussion, but the actual equivalence between the spring models and continuum models remained unsolved.

As noted by Sgouros (1982:32) and Paul et.al., (1983:21), ring and spring discrete solutions normally used do not fully account for the interaction between the lining and ground, which is more properly treated by the continuum (ring and plate) models. This is due to the usual assumptions of partial embedment of the lining, of radial ground action only and of fairly arbitrary discrete spring constants. Nevertheless, the works by Hain and Horst (1974:14), Sonntag and Fleck (1976), Ahrens et.al., (1982:271) and the review work by Erdmann (1983:27,90), have shown that a complete correspondence between ring and spring continuous solutions and ring and plate continuum models is possible. Hence, complete embedment and the introduction of both radial and tangential springs are required for full correspondence between the two types of elastic solutions.

Such a correspondence is fairly easily assessed for an unlined circular tunnel in a gravitational stress field. What is required is the determination of the radial spring constant,

$$K_r = \frac{\partial \sigma_r}{\partial u_r}$$

and of the tangential spring constant

$$K_t = \frac{\partial \tau}{\partial u_t}$$

The radial and tangential stresses, (σ_r, τ), and the displacements, (u_r, u_t), can be obtained, from Hartmann's (1970,1972) solution. By taking into account the effect of tunnel heave under the gravitational stress field, as suggested by Hain and Horst (1974:13), the spring constants can be easily determined from Hartmann's (1972) equations, 178,140 and 180,141. The resulting constants are given in Figure 4.4, which include also their value for the special case of an ideally deep tunnel.

It is worth noting that for a complete correspondence, both K_r and K_t should be expressed as a function of the position angle, ϕ, the in situ stress ratio, K, the position of the stress free boundary, n, and, of course, of the elastic constants, E and ν. If an unique average radial spring constant is to be considered (independent of ϕ), as in many ring and spring models, this value can be derived from the expression for K_r in Figure 4.4. Considering a range of in situ stress ratios between 0.6 and 1.0, of Poisson's ratio of 0.3 to 0.4, for shallow tunnels with cover to diameter ratios between 1.5 and 6 (n=2 to 11), a corresponding range of values for the mean radial spring constant is found:

$$\bar{K}_r = (1.05 \pm 0.06)\, K_{ro}$$

or, approximately

$$\bar{K}_r \approx \frac{1}{1+\nu}\,\frac{E}{R} = K_{ro}$$

The latter can be taken as a reasonable approximation for equivalence between spring and continuum models of an unlined circular tunnel. The lined tunnel case could be approached in a similar manner, again using Hartmann's closed form solution. The resulting expressions for K_r and K_t would, however, result in a more complex form. More importantly, the spring constants become functions of the relative stiffness of the lining (C and F), as pointed out by Hain and Horst (1974:14). For the case of a deep lined tunnel and for a non-slip condition, Erdmann (1983:90) was able to find explicit expressions for the radial and tangential spring constants (for the uniform and the non-uniform in situ stress components), derived from the ring and plate closed form solution by Ahrens et.al., (1982:269). The latter discussed in detail the correspondence between the two types of models for both full and no slip cases. Erdmann (1983:27) reviewed previous works on the subject and summarized the findings of different authors in a comparative form.

For discrete ring and spring solutions, the correspondence with continuum solutions is not as simply found. The numerical approach involves substantial approximations, one of them being the development of some tangential shear even for a uniform loading condition. This results from the usual representation of the springs by bars of finite length, in the radial and tangential directions.

Figure 4.5, that partly reproduces data from Erdmann (1983:117,118), furnishes a comparison between the maximum bending moments (at the lining crown) calculated from Schulze and Duddeck (1964) solution and from the ring and

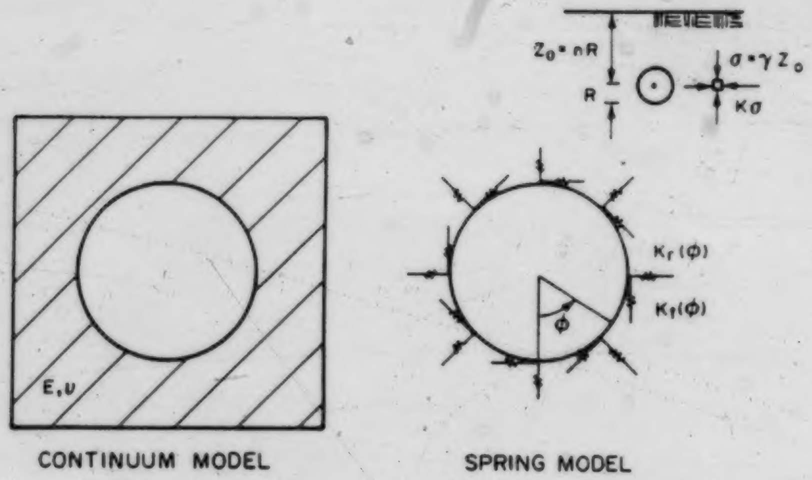

$$K_r = K_{r0}\,\frac{(1+K)\left(1+\frac{1}{2n}\cos\phi\right) + (1-K)\left(\cos 2\phi + \frac{1}{2n}\cos 3\phi\right)}{(1+K)\left(1+\frac{1}{4n}\cos\phi\right) + (3-4v)(1-K)\left(\cos 2\phi+\frac{1}{4n}\cos 3\phi\right)}$$

$$K_t = K_{r0}\,\frac{(1+K)\,\frac{1}{2n}\sin\phi - (1-K)\left(\cancel{\sin 2\phi} + \frac{1}{2n}\sin 3\phi\right)}{\left\{-(1+K)\,\frac{1}{4n}\sin\phi+(1-K)\left[(3-4v)\sin 2\phi + \frac{1}{4n}\sin 3\phi\right]\right\}}$$

with

$$K_{r0} = \frac{1}{1+v}\,\frac{E}{R}, \qquad n = \frac{Z_0}{R}, \qquad K = \frac{\sigma_H}{\sigma_v}$$

Deep tunnel: $n \to \infty$

$$K_r = K_{r0}\,\frac{(1+K) + (1-K)\cos 2\phi}{(1+K) + (3-4v)(1-K)\cos 2\phi}$$

$$K_t = \frac{-K_{r0}}{(3-4v)}$$

Figure 4.4 Equivalence between Continuum and Spring Models for an Unlined Circular Opening under a Gravitational Stress Field

plate model by Ahrens et.al., (1982), both for a deep tunnel situation and for different flexibility ratios. The former solution assumes a constant radial spring modulus equal to the constrained modulus of the soil divided by the tunnel radius. In both cases, Poisson's ratio is equal to 1/3 and the lining is virtually incompressible. Although the solutions do not precisely correspond to each other, since the ring and spring model uses a constant and arbitrary spring modulus, some conclusions can be drawn from the comparison. For a usual range of flexibility ratios, the Schulze and Duddeck solution (which includes the effect of the in situ shear stresses) tends to overpredict the bending moments. For a typical flexibility ratio, F', of 100 (this might represent a shotcrete lining of a subway tunnel in a stiff clay), the Schulze and Duddeck method gives bending moments approximately 100% higher in the no slip condition and 75% higher in the full slip situation when compared with the ring and plate solutions. The conservative estimate of moments results from the assumptions of radial springs only and from the partial embedment hypothesis. For the thrust forces, Erdmann (1983:116) shows similar trends, with the ring and spring solution giving values of 45% to 20% in excess for this typical F' figure.

The ring and spring solutions have limitation very similar to those of the ring and plate models, but have some advantages over the latter. The main limitations for both include the disregard of the ground stress relaxation due to

$$M_{max} = m\left[\frac{1-K}{2}\,\sigma_v\,R^2\right] \quad \text{(at crown)}$$

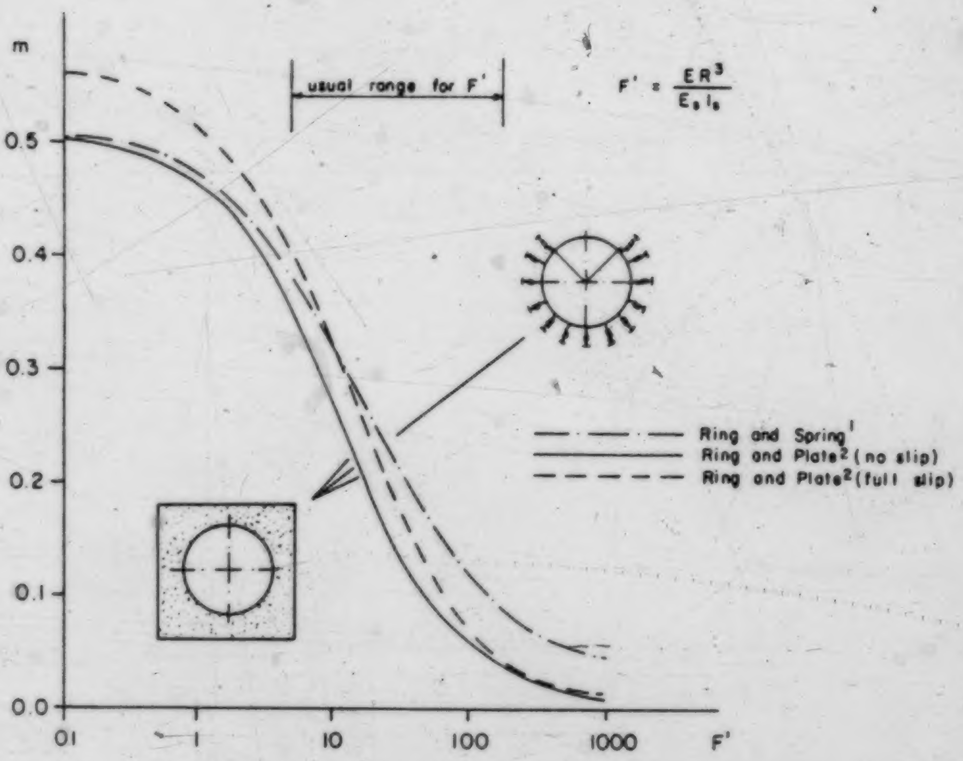

NOTES: 1. Ring and Spring by Schulze and Duddeck (1964) including shear stress load at interface; radial springs with $K_r = \frac{1-\nu}{1-2\nu} \cdot \frac{1}{1+\nu} \cdot \frac{E}{R}$ where $\nu = 1/3$; $C' = 0$ and $H/D = \infty$

2. Ring and plate solution by Ahrens et al (1982), for $H/D = \infty$; $\nu = 1/3$; $F'/C' = 3000$.

Figure 4.5 Maximum Bending Moment Variation with Flexibility Ratio for a Deep Tunnel Liner from Ring and Spring and Ring and Plate Solutions

the three-dimensional stress transfer, and the linear elastic representation of the material properties. The discrete solution group, however, may have some advantage provided a better procedure is developed to estimate more realistic active ground loads and spring constants. These need to account for the different degree of ground straining and softening taking place before lining activation at different points of the tunnel contour. The latter was considered in an analysis performed by Costa Diniz (1978:42), who used a lower spring constant at the crown and floor regions and a higher one at the springlines.

4.3.2.5 Numerical Methods

These are the methods which make use of procedures such as the finite element analysis for prediction of lining loads. Ring-and-spring models, in which a 'discrete' approach is used (see Section 4.3.2.4), also use numerical solutions, which can even be a finite element analysis (for example, Sgouros, 1982). To distinguish from the latter model, those called 'numerical' would be the methods that treat both lining and ground as a continuum.

The present solution has been introduced here only for the sake of completeness. The use of finite element techniques in shallow tunnel design, is treated in detail in other sections of this thesis.

By treating the problem as a continuum, these methods allow lining loads and ground displacements to be obtained simultaneously. This is, perhaps, the most important feature of this group of models.

As indicated in Figure 4.2, the numerical methods are divided into two sub-classes: two-dimensional and three-dimensional analyses. Examples of the first type are reviewed in Section 5.2.1, whereas Section 5.3.3 reviews applications of the second category.

The main difficulty involved in a two-dimensional numerical simulation of a shallow tunnel, is how to account for the actual three-dimensional effects. Since this problem is common to other 2D methods for lining load prediction (ring-and-plate and ring-and-spring models), the subject is treated separately in Section 4.3.2.7.

An assessment of the ability of 2D finite element analyses to predict lining loads in tunnels actually built is made in Section 5.2.1.2. A brief review on the lining representation and lining material modelling is included in Section 5.2.1.1. Further comments on the subject are included in Section 5.2.2.1. Different contributions on the subject are described in those sections. Noteworthy are the works by Fleck and Sonntag (1977,1978) on the influence of lining discretization and on comparisons between solutions where the ground is represented by a continuum and by discrete springs.

4.3.2.6 Numerically Derived Methods

These are methods derived from parametric numerical analyses, (numerical modelling) with results generalized for certain ranges of conditions using dimensional analysis.

Bending moments or thrust forces are thus obtained by means of dimensionless coefficients obtained from sensitivity studies that normally make use of a numerical procedure such as the finite element method.

This type of design method development has become very popular in foundation engineering over the last two decades. The work by Poulos and Davis (1980) is a noteworthy contribution towards a comprehensive treatment of pile foundation design and makes use of elastic-based theory for the analysis of complex ground-pile interaction problems. In soil tunnelling engineering, this approach has not yet become as popular, but a few contributions have been noted already over the last decade. Some of these are included in Table 4.9. All of them are derived from finite element analyses for either plane strain or three-dimensional conditions, and assuming the materials to be homogeneous and isotropic. Other authors presented notable contributions resulting from fully axisymmetric parametric finite element analyses (e.g., Ranken and Ghaboussi, 1978, Schwartz and Einstein, 1980, Hutchinson, 1982). While they are helpful in providing an insight to the behaviour of the lining-ground interaction, they are of restricted practical value whenever the distortional in situ stress component is neglected. Therefore they will be omitted in this brief review.

The solution by Ranken (1978:223) was developed for the special case of a uniform vertical localized gravity pressure load in the crown region, and therefore is only applicable to ground control conditions or lining-ground contact in which this type of loading may develop. The effect of the stress free ground surface was intentionally neglected in his plane strain elastic analysis and the lining-ground interface was represented by a full slip condition. This was numerically simulated by means of an interface element which allowed not only the tangential slippage but also the radial separation of the liner from the ground when locally loaded. This ensured an interaction by compressive radial stresses only (no contact tension). The solution was presented in the form of dimensionless equations for moment and thrust. The coefficients are assessed from tables and diagrams as functions of the position of the localized load and of the flexibility and compressibility ratios. By superimposing the results from two or more uniform loading geometries, it is possible to estimate the lining moments and thrusts for non-uniform localized active loads. However, the superposition method can only be accepted, as an approximation, since the problem is geometrically non-linear with respect to the loading and the resulting interface separation.

Costa Diniz (1978) on the other hand developed a very useful method applicable to tunnel profiles of elliptical shape with a horizontal major axis, as used in some double track subway tunnels. In his plane strain elasto-plastic ground (with fixed strength parameters) and elastic lining representations, he assumed complete support embedment,

	Author	Year	Loading	Analysis Details	Solution Formulation	Comments
1.	Ranken	1978	Localized gravity (uniform and non uniform over variable arc length).	2D, FE plane strain; deep tunnel; full slip; interface element allowing separation between ground and lining (partial embedding at crown); linear elastic behaviour; circular cross sections.	Moments (M) and thrusts (T) from equations, tables and charts, for C between 0.01 and 3 and F from 1 to 1,000(1).	Solution for non uniform localized loads obtained by superposition (thus approximate).
2.	Costa Diniz	1978	Excavation loading (in situ stresses with gravity for $K = \nu/(1-\nu)$).	2D, FE plane strain, shallow tunnel; no slip; complete embeddment; elasto-plastic behaviour ($c = 50$ kPa and $\phi = 30°$, fixed); elliptic cross sections with horizontal major axis.	M and T at crown, springline and floor from equations and charts for Z/B between 1.5 and 8, for A/B between 1 and 2, B/t between 7.5 and 30, E_s/E from 0 to 600, K from 0.33 to 0.67(2).	Approximate equations furnished for quick estimate of moment and thrust at springline.
3.	Ahrens et al	1982	Excavation loading (approx. in situ stresses with gravity partly accounted, for any K).	2D, FE plane strain; shallow tunnel; both no and full slip (with a special interface element); partial embeddment (no cover elements over the 90° arch at crown); linear elastic; circular cross section.	M, T and radial displacement at particular points, from equations and charts, for an incompressible liner with β from 5 to 500(3).	Loading condition not fully compatible with shallow tunnel assumption.

Table 4.9 Details of Some Numerically Derived Methods for Lining Loads Prediction

	Author	Year	Loading	Analysis Details	Solution Formulation	Comments
4.	Pierau	1981 1982	Stepwise excavation simulating actual 3D construction process (in situ stresses with K - v/(1-v).	3D, FE analyses of shallow tunnel; no slip; completed embedding; linear elastic behaviour; double track tunnel, non-circular cross section with 8m height and 10m width; inclined tunnel face (65°).	M and T at particular points, and maximum surface settlement, from charts, for ground covers varying from 5 to 25m, for shotcrete thicknesses from 10 t0 30cm, soil elastic modulus from 10 to 50MPa (v=0.3 to 0.4); constant shotcrete modulus.	
5.	Erdmann Erdmann & Duddeck	1983 1984	Stepwise excavation simulating actual 3D construction process (deep tunnel stress field with any K).	3D axisymmetric FE analyses of deep tunnel, with plane symmetric (non-axisymmetric) stress field; no slip; complete embeddment; linear elastic behaviour; two distances for delayed lining installation; fixed F/C ratio; fixed lining thickness-diameter ratio.	Reduction factors to be applied to thrust, moment and radial displacements, obtained from ring and plate model. Factors given as a function of lining compressibility or flexibility ratios and of the distance from face to lining edge.	Treatment of non symmetric in situ stress field similar to the approach by Hanafy & Emery (1980, 1982).

Notes:

(1) C [illegible] $\frac{(1-v_s^2)}{(1+v)\,(1-2v)}\ \frac{E}{E_s}\ \frac{R}{A_s}\ ;\ F = \frac{(1-v_s^2)}{(1+v)}\ \frac{E}{E_s}\ \frac{R^3}{6I_s}$

(2) A: half of major axis length (horizontal); B: half of minor axis length (vertical); Z: depth to tunnel axis; t: lining thickness

(3) β: flexibility ratio = ER^3/E_sI_s

Table 4.9 Details of Some Numerically Derived Methods for Lining Loads Prediction (Continued).

fully accounting for the effects of the ground surface and gravity. He assumed, however, the stress ratio to be a function of the Poisson's ratio. Bending moments and thrust forces are obtained at three points of the lining contour from an equation whose coefficients are obtained from ingeniously designed diagrams. These coefficients are a function of the tunnel depth ratio, of the cross-section geometry, of the relative thickness of the lining and of the support-soil stiffness ratio. The method was elaborated for use in urban subway tunnels supported with shotcrete lining, and his analysis almost completely covered the normal range of conditions found in large cross section tunnels. No comparison of results between this method and other solutions or field measurements was made available to assess its potential.

Ahrens et.al., (1982) developed a similar method, but assumed linear elastic relationships and a circular tunnel profile. This method was reviewed and summarized by Heinz (1984:306). Furthermore, the lining was assumed to be only partially embedded, as all of the ground cover represented by the prism of elements overlying the upper 90° crown arch was not discretized in their analyses. This would thus represent the conservative assumption of complete soil cover collapse. With respect to the ground loading, Ahrens et.al., (1982) used the same assumption introduced in their analytical solution for the ring and plate model: a deep tunnel stress field, with the vertical stress equal to the overburden stress at the crown elevation and with the horizontal stress equal to the in situ horizontal stress at the springline elevation. The solution that results is dependent on the relative depth, not only due to the loading assumption, but also because in their numerical simulation the ground domain was bounded by a stress free ground surface. Their solution furnishes moment, thrust and radial displacements at particular points of the lining contour. These are obtained from equations and design charts covering a large range of lining flexibilities, but with the conservative assumption that the support is incompressible. This method accounts also for both no and full slip at the lining-ground interface. To represent the slippage condition, Ahrens et.al. (1982:266) introduced an infinitely rigid one-dimensional bar element radially linking the soil to the lining. These elements would thus transmit the axial loads only. This approach was used earlier by Ranken (1978:96) who claimed that, in order to avoid distorting the analysis results, the same elastic properties of the ground should be assigned to the bar elements, with cross sectional areas selected to "fill" the gap behind the support. If lining properties were assigned to the bars (as Ahrens et.al. (1982) apparently did), the results obtained would be equivalent to that of a liner with its thickness increased by an amount equal to the size of the gap.

Pierau (1981,1982) carried out some three-dimensional parametric finite element analyses of a shallow tunnel, in which the actual construction was fully represented, including the stepwise excavation and application of the support. Linear elasticity was assumed and constant elastic properties were assigned to the simulated shotcrete lining. The non-circular tunnel cross section was kept constant in all his analyses (8 m height by 10 m width). The in situ stress ratio was assumed to be a function of Poisson's ratio and a rigid boundary was placed at 0.2 m below the tunnel invert. The results of his parametric studies are presented in terms of bending moments, thrusts and displacements at particular points of the lining contour. They are expressed graphically as a function of the ground cover, lining thickness and the elastic properties of the soil. Although his results are not readily generalized as he did not reduce his data in a dimensionless form, and used some specific and fairly particular assumptions, this was the first attempt to develop a procedure that fully accounts for the three-dimensional nature of the tunnelling construction.

Erdmann (1983) and Erdmann and Duddeck (1984) presented results of a particular type of three-dimensional finite element analyses, in which the problem was represented axisymmetrically, but the stress field was assumed to be non-symmetric. Their approach was similar to that adopted by Hanafy and Emery (1980 and 1982), with, the non-symmetric stresses and displacements expanded into Fourier series (Hanafy and Emery, 1982:205). The actual sequence of construction of a deep tunnel was fully represented by

Erdmann (1983:174), including the stepwise excavation and application of the support. The latter was designed to simulate a shotcrete lining, with three assumptions regarding its stiffness: a constant modulus (of 15 GPa), and two different variable moduli assumption (from a near zero modulus at the lining edge to 15 GPa one diameter behind, in both cases). The parametric study assumed linear elasticity for the ground as well as for the support. Solutions were obtained for two distances between the tunnel vertical face and the leading edge of the liner (a quarter and a half the tunnel diameter, D). Some of their results assume that the ratio between the flexibility and the compressibility ratio is constant (in these analyses, they assumed a uniform lining thickness equal to 0.03D). Correction factors were then obtained by relating the thrusts, moments and displacements calculated in the 3D analyses, with those from the ring and plate solution by Ahrens et.al. (1982). Each of these factors were split into two components, one being applied to the zero term of the Fourier series expansion and the other to the term two. The solution is applicable to any in situ stress ratio, to any tunnel size, for appreciable ranges of soil stiffness, compression and bending stiffnesses of the lining.

From the results provided by Erdmann (1983:193-205) it can be suggested that the influence of the increasing shotcrete stiffness with time (or with distance to the face) on lining displacements, thrust or moments, is nearly equivalent to a net increase in the delay of the application of a constant stiffness lining. Although this point requires further investigation, it is believed that for all practical purposes, this influence can be accounted for in an analysis by using an increased unsupported heading span and a constant stiffness liner. Any simple or general rule to account for the effect in this way cannot be formulated at the moment. A unique rule may not be found as it will depend on the combined rates of shotcrete hardening and lining placement. But as those rates do not vary too widely, it is believed that some criterion may emerge in the future from some combined parametric analyses.

Despite the deep tunnel assumption and other more or less restrictive assumptions, the method developed by Erdmann entails an appreciable generality as compared to Pierau's. It is believed that with a progressive reduction of computing costs and, more importantly, with the development and widespread implementation of user friendly pre and post-processing software, more comprehensive analyses of this type will become available in the future.

This group of methods for lining load estimates are particularly promising for the development of solutions for conditions not covered by the available procedures. An example of such conditions is the non-circular tunnel cross sections built by staged excavation with shotcrete support, like studies by Costa Diniz (1978) or currently by Heinz (1987).

A special procedure that intentionally has not been included in Table 4.9 is the method by Baudendistel (1973). His procedure does not allow the procurement of lining loads, but rather, it gives the minimum required thickness of an unreinforced concrete liner for a circular shallow tunnel, to avoid either compressive or tensile failure (with some safety margin). This method was developed from plane strain, finite element analyses, with the soil represented by an elasto-plastic model, with three pairs of strength and stiffness parameters. Baudendistel's design charts cover tunnels with diameters ranging from 6 to 12 m, and soil covers from 5 to 160 m. He considered also in situ stress ratios ranging from 0.2 and 1.0, and a no slip condition. Unlike other plane strain methods reviewed, Baudendistal (Op.cit.) devised an approximate procedure to account for the stress relaxation prior to lining installation. This procedure will be discussed in the next section. His design method thus defines a minimum concrete thickness for delayed lining installation (support applied at one or one quarter of a diameter behind the face).

4.3.2.7 Account for Three-Dimensional Effects in Two-Dimensional Models

With the exception of those methods for lining load prediction which were numerically derived using three-dimensional finite element analyses, such as that by Pierau (1981) or Erdmann (1983), or those that on a case by case basis, make use of a fully three-dimensional numerical analysis (e.g. Heinz, 1984:141), none of the other methods reviewed in the previous sections, take the actual three-dimensional stress transfer process that occurs with the tunnel advance directly into account.

Most of the methods reviewed approach the tunnel problem as a plane strain situation in a transverse section normal to the tunnel axis. Therefore they are unable to take into consideration the ground displacements and the ground stress changes that take place before the support is installed and the lining-ground interaction starts. In those methods, it is usually assumed that the liner has been installed before excavation started, and consequently, they will normally provide displacements which are smaller and lining loads which are larger than those that should actually be observed.

The greater ease associated with a two-dimensional treatment, compared to the more expensive, involved and time-consuming three-dimensional approach influenced many to introduce approximate methods to account, at least partly, for the actual 3D nature of the problem. Most of these methods have in common, the assumption that the 3D situation can be approximated by a succession of 2D plane strain representations transverse to the tunnel axis. Therefore, the out of plane stresses are principal stresses and the shear stresses acting on these planes are zero. In the 3D case, non-zero shear stresses develop on these planes, as a result of the equilibrium and displacement compatibility.

The tunnel closure in the 3D unsupported heading is thus smaller than the closure in the 2D unstressed opening. In order to make the 2D representation closer to the 3D condition, the opening is never left unsupported. Otherwise, a complete unload of the final opening, in which the stresses around it are reduced to zero, followed by the installation of the lining, would inevitably lead to an unstressed support condition. No ground-lining interaction would take place in a time-independent situation. Unless time dependent responses are expected (consolidation or creep), this simulation would lead to unreliable estimates of ground movements or lining loads.

The effect of the longitudinal stress transfer or arching, is normally incorporated in the 2D representation by the introduction of some balancing internal stresses in the opening, even in sections that represent the unsupported tunnel length. This is achieved by two or three different procedures, which at the end, correspond to smoothing out the longitudinal stress distribution shown in Figure 2.20(a). The extreme stresses at B,C,D and E are not accounted for and the stress state is assumed to gradually change from A to F in a continuous way, not unlike the development of the displacements shown in the same figure. Correspondingly, the ground response result is equally gradual, as shown by the dashed curve in Figure 2.20(b). These different procedures are defined and calibrated in such a way that the final results of the 2D model in terms of displacements or stresses, approximate as closely as possible, those observed in an actual 3D configuration. It should be pointed out that, regardless of how rigorously each of these procedures is incorporated or implemented into the two-dimensional model, they are all not more than a faint approximation of the real phenomenon. Their merit lies in the fact that they attempt to bring the 2D solutions closer to the actual conditions. However, their qualities should not be interpreted in terms of the generality of their assumptions or of the degree of rigour they exhibit. Rather, they should be evaluated in terms of their degree of simplicity for practical use and of their ability to offer results that better approximate the reality.

No attempt will be made herein to assess in depth the virtues of each available procedure to account for 3D effects in 2D models. But, they can be inferred to some extent by comparing the features of these procedures. For this purpose Table 4.10 has been prepared, gathering some representative approaches selected from many of those available.

Most of the procedures focus on estimates of lining loads, but those developed as numerical simulation techniques for two-dimensional finite element analyses, are in principle, also applicable for ground displacement predictions. Actually, some of the latter group were designed basically for the last purpose (Table 4.10, procedures, 9, 15, 16, 17 and 18).

The procedures reviewed were classified according to the models they are to be applied to: convergence-confinement (uniform stress field solutions), ring and plate models with non-uniform stress fields and numerical models (basically, the finite element method).

Table 4.10 presents also the type of approach adopted in each case to simulate the 3D effects. Some of the approaches applied to numerical models were reviewed by different authors (see, for example, Eisenstein, 1982, Katzenbach and Breth, 1983:202, Heinz, 1984:111, Kochen et.al., 1985:205 or Rowe, 1986:98). As mentioned earlier in this section, the 3D effect is usually simulated in the 2D model by introducing some internal balancing stresses to the section of the tunnel to be. This can be performed by a gradual stiffness reduction of the ground material within the tunnel profile (tunnel "core"). However, as noted by Kochen et.al., (1985:205), this may not be enough to cause movements in the soil mass, since for instance in a numerical simulation, the ground mass is in equilibrium with the stress field and the nodal forces may not be altered by a simple change in the ground stiffness. Hence the stiffness reduction is always followed by reducing the ground stress around the contour, which can be partial (as in Swoboda and Laabmayr, 1978 method) or total (as in Schikora, 1982, 1983). The partial reduction involves an additional approximation, as it requires acceptance of the principle of superposition of two different structures (Maffei,

Author	Year	Where Applicable	Approach Type	Type of Development	Assumptions and Comments
1. Lombardi	1972, 1973	Convergence-Confinement	Core stiffness reduction	Analytical	Face effect represented by a core disc in plane strain or stress, progressively weakened (yielding and reduction of disc thickness) generating internal tunnel pressure. Arbitary linear distribution of radial displacement along tunnel.
2. Daemen & Fairhurst	1972	Convergence-Confinement	Ground stress reduction	Numerical	Stress field reduction linearly proportional to the radial displacement variations along unlined tunnel obtained from axisymmetric linear elastic finite element analysis. Neglects ground-liner interaction.
3. Hartmann	1970, 1972	Ring and Plate	Ground stress reduction	Empirical	Stress field reduction back analysed from field instrumentation. Reduction factor to be applied either to the specific weight of soil or to the depth of the tunnel (in solutions accounting for gravity).
4. Baudendistel	1972, 1973	Finite element (non linear)	Progressive core removal	Numerical Simulation	Progressive removal of concentric layers of elements with full stress release within the tunnel section, before lining installation. Extent of removal defined as to cause 25% or 100% of elastic convergence of tunnel contour (empirically related to the lining leading edge position at D/4 and 1D behind the face, respectively).
5. Egger	1974	Convergence-Confinement	Ground stress reduction	Analytical.	Tunnel face approximated by a sphere in uniform stress field. Convergence at face thus obtained for elasto-plastic ground, hence reduced tunnel pressure in the axisymmetric model.
6. Amberg & Lombardi	1974	Convergence-Confinement	Ground stress reduction	Analytical	Convergence curve at tunnel face obtained by introduction of fictitious body forces outwardly oriented, causing the deviation of the longitudinal stress trajectories in an axisymmetric configuration.
7. Panet & Guellec Panet Panet & Guenot	1974 1976 1982	Convergence-Confinement	Ground stress reduction	Numerical	3D effect represented by a fictitious internal pressure selected such a way that the 2D radial displacement is equal to the 3D axisymmetric one, at the section being considered. Linear elastic and elasto plastic axisymmetric FE analyses of unlined tunnel were used to obtain pressure-distance to the face distribution. Good correspondence between perforated 2D and 3D models for distance to the face greater than D/4.

Table 4.10 Account for Three-Dimensional Effects in Two Dimensional Models

Author	Year	Where Applicable	Approach Type	Type of Development	Assumptions and Comments
8. Muir Wood	1975	Ring and Plate	Ground stress reduction	Empirical	Arbitrary reduction of ground stresses by 50% of their in situ values.
9. Wanniner & Breth Wanninger Negro et al Katzenbach Eisenstein et al	1978 1979 1984 1985 1986	Finite element (incremental analysis)	Progressive core removal	Numerical Simulation	Staged excavation of the tunnel face, with progressive removal of elements and full stress release at the zone being excavated. Concurrently, lagged application of the support. Attempt to represent sequential construction as in the NATM.
10. Swoboda & Laabmayr Swoboda	1978 1979	Finite element (incremental analysis)	Stiffness and stress reductions	Numerical empirical	Stiffness of tunnel core reduced by 50%. Ground stress reduction estimated from the evolution of settlement of crown with face advance, as measured in the field. Staged excavation of tunnel face.
11. Baudendistel	1979 1984 1985	Finite element	Ground stress reduction	Numerical	Ground stress reduction factors obtained from 3D FE linear elastic analysis of an unlined deep tunnel, for $K_o = 0.5$ and for a given non circular cross section, with three excavation sequences. Different reduction factors for crown, springline and floor, obtained by relating the longitudinal distribution of radial displacements with a linear relationship between the latter and the radial stress.
12. Van Dillen et al Ohnishi et al	1979 1982	Finite element (incremental analysis)	Core stiffness reduction	Numerical simulation	Tunnel core represented by multiple element layers each with a fraction of the ground stiffness. The sum of the stiffnesses of all layers is equal to the stiffness of the intact ground. 3D analysis of unlined tunnel provide relationship between closure and distance to the face. 2D analyses furnish relation between closure and layer stiffness fraction. Thus a rule is established between cumulative stiffness of layers and distance.
13. Schwartz & Einstein	1980	Ring and Plate	Core stiffness reduction	Analytical and Numerical	Ground-liner closed form solution with a core modulus reduction factor included. Load reduction factors defined as thrust and moment ratios with and without core stiffness reduction. Thrust load factor versus lining-face distance obtained from axisymmetric FE elastic analyses of lined tunnels (relationship corrected by Hutchinson, 1982:175). Thus a relation between stiffness reduction and distance is found (valid for thrust only).

Table 4.10 Account for Three-Dimensional Effects in Two Dimensional Models (Continued).

Author	Year	Where Applicable	Approach Type	Type of Development	Assumptions and Comments
14. Zagottis Rocha Schikora & Fink Baumann et al	1981 1975 1982 1985	Finite element	Ground stress reduction	Numerical simulation	After removal of soil elements within the tunnel, the in situ stresses are reduced arbitrarily, what which represents the stress transfer into the ground. Once the liner is installed, the rest of balancing stresses are released and ground-liner interaction develops.
15. Tan Clough et al	1977 1985	Finite element (incremental analysis)	Ground stress reduction	Numerical simulation	Reduce stiffness of soil elements within the tunnel to near zero and reduce gradually the in situ stresses around tunnel contour. Monitor displacement at crown. Once a predetermined displacement at crown is reached (gap size), activate liner and continue unloading (either uniformly or not) until the balancing stresses are eliminated.
16. Rowe et al Lo and Rowe Rowe et al Rowe and Kack Rowe Ng et al	1981 1982 1983 1983 1986 1986	Finite element (incremental analysis)	Ground stress reduction	Numerical empirical	Approach and assumptions similar to Tan (1977) but using a stress relaxation technique. Moreover, ground-lining interaction starts when any point of excavated profile comes into contact with the lining. Hence, unlike the former, not all points will come onto the liner at the same time. Also, the rate of stress relief is not constant around the contour, being initially greater at the crown than at the floor (Lo and Rowe, 1982:216). Requires empirical estimate of a 'gap' parameter.
17. Schikora Schikora & Fink Schikora Baumann et al	1982 1982 1983 1985	Finite element (incremental analysis)	Stiffness and stress reductions	Numerical empirical	Approach and assumptions similar to Swoboda and and Laabmayr (1978). Core stiffness reduction factor empirically assessed (back analyses). Full stress relief around softened core contour. Also stagged excavation of tunnel face.
18. Ohta et al	1985	Finite element (incremental analysis)	Imposed tunnel convergence	Numerical simulation	Displacement boundary condition at tunnel contour. Rate of displacement imposition given by longitudinal analyses (axisymmetric and plane strain). Magnitude of displacements imposed apparently by trial and error. Non-uniform displacements imposed around contour (maximum at crown).

Table 4.10 Account for Three-Dimensional Effects in Two Dimensional Models (Continued).

1982:162). By reducing the ground stresses around the contour, some ground displacements towards the softened core are induced and the core reacts against them. Thus balancing stresses are generated around the contour of the tunnel to be, which result from the interaction between the softened and the unsoftened ground areas. The analytical approach by Schwartz and Einstein (1980) differs slightly from other core stiffness reduction procedures, as they assumed a softened core inclusion before application of the stress field (subtracting the displacements induced in this phase from the final solution).

Another procedure, which is implemented numerically only, is the progressive core removal (for example, Baudendistel, 1972, Wanninger and Breth, 1978, Negro et.al., 1984). It consists of a complete piecewise removal of portions of the tunnel core, followed by the partial application of the support in these portions, as in a staged excavation of a tunnel. In essence, it also involves a reduction of the central core stiffness, as each part of the ground removed is assigned a zero stiffness (for instance, by deactivating the corresponding elements). It involves as well, an overall reduction of the in situ stress around the opening, as the ground stresses around the partial excavation profile are reduced to zero in each portion that has been removed.

As the support in this procedure is generally activated after the excavation, it is initially unstressed, and will pick up load as the removal procedure is extended throughout the tunnel section. As a consequence, it will normally underestimate the lining loads. The results obtained for a full face one step excavation are obviously meaningless.

Another procedure is the gradual reduction of the in situ stress around the tunnel contour or gradual boundary stress reversal in a fully perforated ground mass (core stiffness previously reduced to zero). The 3D longitudinal arching effect is simply represented here by the gradual reduction of the internal stress initially set equal to the in situ values. The advantage it offers in relation to the core stiffness reduction approach is that it eliminates one fictitously created unknown, namely, the core stiffness, as well as its rate of softening. The disadvantage it contains is that the balancing internal stresses have an undefined distribution around the excavation profile. In the core stiffness reduction, this distribution results automatically from the interaction between the softened and unsoftened ground zones. Some interpretations may indicate that a non-uniform release of the in situ stresses around the tunnel occurs. Stresses at the tunnel crown (in a 2D repesentation) decrease at a faster rate than elsewhere (for K<1), and the ground stress redistribution developing towards a more uniform lining load condition than that given by the in situ stress field ratio (Branco, 1981:201, Branco and Eisenstein, 1985, Lo and Rowe, 1982:216). Most methods of this class assume a uniform rate of stress release for all points around the opening. The latter assumption avoids the inclusion of an unknown and yet arbitrary variable (the non-uniform rate of stress release around the contour). Besides being simpler, it tends to be a safer one with respect to the development of bending moments in the lining at equilibrium.

Swoboda (1985:1653) made reference to the use of non-uniform release of in situ stresses around tunnels in two-dimensional simulations. However, to the writer's knowledge, results of such a simulation have not been made available so far.

An alternative procedure to the imposed boundary stress approach is the displacement imposed boundary condition. This was the approach favoured in some analyses by Negro and Eisenstein (1981), by Resendiz and Romo (1981) and by Ohtea et.al. (1985). This alternative may be attractive when dealing with TBM excavated tunnels, where the size of the void between the outer surface of the liner and excavation walls is relatively well defined. But for other tunnelling procedures (e.g. NATM), it may not be as clearly handled, since a physical gap behind the lining is not present. Although not exactly a displacement boundary method, the approaches by Tan (1977) and Rowe et.al. (1981) combine a ground stress reduction procedure with a following the gap closure around the opening. The lining is activated and interaction is started when the soil comes in contact with the support. Again, this procedure appears to be adequate and relevant for TBM excavated schemes, but less applicable to NATM schemes. Moreover, to account for the displacements developing ahead of the face in the real situation, the gap behind the lining has to be increased by some amount, which can be approximated in the 2D representation by using a slightly larger excavated tunnel diameter (e.g. Rowe and Kack, 1983:300). This approximation requires an independent evaluation, either empirical (from field measurements) or numerical (necessarily three-dimensional).

As indicated in Table 4.10 some of the procedures were developed for generalization, using an analytical framework (e.g. Lombardi, 1972, 1973 and Egger, 1974). Others are based on numerical developments, for instance, Panet and Guellec (1974) using an axisymmetric solution, or Baudendistel (1979) using an actual 3D finite element analysis. The latter assumes along with Daemen and Fairhurst (1972), a linear relationship between radial displacements and stresses, to obtain ground stress reduction factors for different delayed lining distances. The discussions in Chapter 2 demonstrated that generally speaking, this is an oversimplified assumption that should not be accepted, as it tends to underestimate the loads acting on the lining installed some distance behind the tunnel face. The exception is for ground behaviour close to linear elastic, which could be acceptable in some rock tunnels, but not in soils. A more adequate development is that by Panet and Guenot (1982:199) in which the stress reduction factors were derived from non-linear ground reaction curves which accounted for an elasto-plastic behaviour of the soil.

Some other developments are entirely empirical, (Muir Wood, 1975, or Hartmann, 1972), in which suggested reductions in ground stresses are either arbitrary or based on back analysed field performances. A large number of the methods included in Table 4.10 are not formulated in a generalized way, but represent numerical simulation procedures to be applied in finite element analyses. They are usually performed incrementally and on a case by case basis. Such is the case for all methods applicable to finite element analyses (eg. Wanninger and Breth (1978), Swoboda (1979), Van Dillen et.al. (1979) or Rowe et.al. (1983)). Their potential practical use is limited as they require a tunnel design load based on finite element solutions, which may not be available in many routine situations.

Unfortunately, most of these methods that do not require a finite element approach were developed for uniform stress field solutions, therefore being of limited practical value for shallow tunnel design. Only three are set in non-uniform stress field conditions, of which two are empirically developed. The other (Schwartz and Einstein, 1980), although originally formulated for a non-uniform stress field, fails to provide a definite criteria relating the load reduction factor applied to the non-uniform stress component (especially bending moments) to the distance of delayed lining installation. The core stiffness reduction factor they introduced was related to that distance under uniform stress conditions (axisymmetric analyses). They assumed the same relation would be valid under a non-uniform stress state (3D analyses). Moreover, the method is valid only for deep tunnels and does not account for gravity effects. If the deep tunnel problem is of interest, then a better and more accurate approach is that by Erdmann (1983), which is directly derived from three-dimensional parametric analyses and therefore does not involve the inherent approximations of Schwartz and Einstein's (Op.cit.) method.

The present review reveals that, except for some fully empirical procedures, there is not a single solution, not even an approximate one, to account for three-dimensional effects in non-numerical two-dimensional models. applicable to shallow tunnels. Such a model would thus account for the gravitational stress field and for the presence of the stress-free ground surface.

4.3.3 Prediction of Ground Displacements

The number of methods available for the prediction of ground displacements is considerably smaller than those for lining loads. This simplified the survey on the subject, which was still quite extensive but certainly not exhaustive. The review of methods is presented in the same format used for the lining load prediction. Similarly, a classification of methods, according to the type of development on which the method is based, is presented in

Figure 4.6. In the majority of the cases, the prediction is restricted to estimates of vertical displacements in the ground, so that they will be simply referred to as methods for settlement prediction. Other reviews of ground settlement predictions were presented by Schmidt (1969), Szechy (1973;1035), da Fontoura and Barbosa (1985), for example. They included methods that are also applied to mining subsidence, but these will not be covered herein.

Four main groups of methods are identified, as indicated in Figure 4.6, and are discussed in the following. The third group shown, include those methods which are entirely based on the numerical simulation of the problem. They are performed on a case by case basis, using any type of numerical technique, for instance, the finite element method. Examples of applications of this approach to ground settlement predictions are numerous and will not be covered specifically here. References to these applications were made in Section 4.3.2 and they will be extended in Chapter 5, where the subject will be discussed in more detail.

To facilitate the review, Table 4.11 was prepared, including examples of the other three groups of calculation methods. Indications of the underlying assumptions, summaries of the developments, descriptions of the basic requirements for input and the type of output supplied by each method are given, The conditions to be fulfilled for the application of these methods in practice can be gathered from these indications on an individual basis. The

Author/Year	Type of Development	Output of Method	Features and Comments
1. Manya (1977)	Empirical	Transverse settlement profile at surface	Developed for shield driven subway tunnels. Valid only for Japanese conditions and construction procedures. Considers 4 ground conditions and 4 types of shield. Relates maximum surface to overburden and to overload factor.
2. Fujita (1982)	Empirical	Maximum surface settlement	Shielded driven tunnels. Only for Japanese soil conditions as well as construction procedures. Considers 3 types of ground conditions and 4 shield types.
3. Limanov (1957)	Semi-Empirical	Maximum surface settlement	Settlement calculated from linear elastic solution (approximate) of a hole in a semi-infinite plate. Assumes zero body forces and uniform internal pressure reduction in the opening ($K_0 = 1$). Developed from Jeffery (1920) solution for stresses. Suggests that transverse settlement profile at surface can be obtained assuming a normal probability curve.
4. Murayama & Matsuoka (1969) (also see Kawamoto & Okuzono, 1977)	Semi-empirical	Maximum surface settlement and trough width; subsurface settlements along vertical axis	Settlements due to yielding (loosening) of granular soils. Assumes full development of plastic flow. Derived from observations in trap-door experiments. Takes into account dilatancy due to shear (empirically). Requires an independent estimate of crown settlement. Neglects ground movements prior to yielding.
5. Szechy (1973:1048)	Semi-empirical	Transverse settlement profile at surface	Settlements due to yielding (loosening) of granular soils. Postulates plastic flow zones in the ground. Assumes no volume change. Distinguishes losses through the face and through tunnel contour. Approximates settlement trough by straight line segments. Limits of subsiding zone defined from a Rankine active state assumption. Requires independent estimate of crown settlement.
6. Lo et al (1984)	Semi-empirical	Subsurface settlement distribution along vertical axis	Settlements over shielded tunnels driven in saturated clays [illegible] drained condition). Uses elastoplastic solution of hole in infite plate, developed by Ladanyi (1974), for uniform stress field (deep tunnel, $K_0 = 1$). If overcutting is large (large gap), assumes a crown settlemint equal to the unrestricted radial displacement of the deep tunnel solution. If overcutting is small, assumes a crown settlement equal to the physical overcutting gap, plus the radial displacement at face, plus an empirical parameter, related to the construction quality. The face displacement is taken as 1/3 of the total unrestrained plane strain displacement.
7. Herzog (1985)	Semi-empirical	Maximum surface settlement and width of settlement trough	Calculates loss of ground from linear elastic solution of hole in a plate problem (deep tunnel, $K_0 = 1$). Assumes that the volume of settlements at surface is equal to the loss of ground. The width of settlement profile derives from Rankine active state consideration.

Table 4.11 Features of some Methods for Ground Displacement Prediction for Shallow Tunnel Design

Author/Year	Type of Development	Output of Method	Features and Comments
8. Schmidt (1969) Peck (1969)	Semi-empirical	Transverse settlement profile at surface	Derived from earlier applications of stochastic theory to the solution of subsidence problem (works by Litviniszyn in the fifties and sixties). Assumes that the profile is given by a normal probability curve. Shape of the curve (position of inflexion point) defined empirically, as a function of ground conditions and relative tunnel depth. Requires independent estimate of maximum surface settlement. For clays in undrained condition, it can be calculated by making the volume of settlement equal to the loss of ground, estimated from the elasto-plastic solution of hole in infinite plate ($K_0 = 1$). Else, the maximum settlement is estimated empirically from past experience.
9. Cording and Hansmire (1975)	Semi-empirical	Transverse settlement profile at surface	Modified version of Peck-Schmidt method. Requires independent estimate of the surface settlement volume which is equal to the loss of ground plus the overall ground volume change. Presents procedure to estimate the broken down components of the loss of ground. Provides indication for estimating overall ground volume changes in dense sands.
10. Attewell (1977)	Semi-empirical	Transverse settlement profile at surface	Modified version of the former two methods. Provides empirical indications for estimates of the losses of ground and settlement volumes in clay and granular soils, as a function of the overload factor and of the construction quality. The overall volume changes in the ground are also empirically estimated.
11. Yoshikoshi et al (1978)	Semi-empirical	Transverse settlement profile and longitudinal profile along the axis, at surface	Introduces a minor modification into Peck-Schmidt method. Additionally, it proposes that the longitudinal profile of settlements can be approximated by a cumulative probability curve (error function), which is used to fit available data only.
12. Attewell and Woodman (1982) Attewell and Yeates (1984) Attewell et al (1986:53)	Semi-empirical	Complete displacement field above the tunnel	Assumes that the transverse settlement profiles at surface and below surface are approximated by normal probability functions. Like in the previous method, assumes that the longitudinal distribution of settlements (along tunnel axis and parallel to it, both at surface as well as below it) can be pproximated by a cumulative probability curve. The latter is obtained by integration of the subsidence surface generated by a spheric 'point' source of loss. Displacements at directions other than vertical are obtained by integration of strains calculated on the assumption of zero volume changes in the ground. Requires an independent estimate of the final settlement volume, what is done empirically. Requires an estimate of the inflexion distance (empirically done also). Assumes that the settlement at the face is 1/2 of the final settlement. Design charts are provided to facilitate applications.

Table 4.11 Features of some Methods for Ground Displacement Prediction for Shallow Tunnel Design (Continued).

Author/Year	Type of Development	Output of Method	Features and Comments
13. Sagaseta and Oteo (1974) Sagaseta et al (1980) Oteo and Sagaseta (1982)	Numerically derived	Transverse settlement profile at surface and subsurface settlement distribution along along vertical axis. Lateral displacements at surface.	Derived from linear elastic 2D FE analyses of shallow circular unlined tunnel in gravitational stress field with $K_0=\nu/(1-\nu)$ (ν from 0.1 to 0.4, thus K_0 from 0.11 to 0.67). Assumes full in situ stress release at the opening. Settlement distributions are conveniently normalized Introduces an empirical multiplying factor ($\phi < 1$), to correct the calculated displacement on account of construction procedures, lining type and soil conditions. Factor ϕ = 0.4 to 0.5 for soil conditions and construction methods found in Madrid. Solution developed for a rigid boundary located 4D below tunnel floor.
14. Resendiz and Romo (1981) Romo and Resendiz (1982)	Numerically derived	Transverse settlement profiles at any elevation above tunnel	Developed for shielded tunnels (with or without compressed air) in saturated clays (undrained condition). Derived from non linear (hyperbolic) elastic 2D FE analyses of shallow circular tunnel. Apparently in situ ground stiffness assumed independent of K_0. Identifies losses due to (a) stress release at the face, (b) radial closure of tunnel walls. For (a) assumed a 2D longitudinal representation (with rigid lining and face subjected to uniform internal pressure). Transverse displacement profile due to (a) from 2D transversal representation and uniform stress field condition (K_0=1 and no body forces). For (b) assumed also a 2D plane strain representation and displacement boundary condition at the opening (requires independent estimate of a uniform tunnel closure). Requires CU triaxial test results. Final settlements by superposition. Final crown settlement can be smaller than surface settlement due to simulation of ground loss (a).
15. Ito and Hisatake (1982)	Numerically derived	Transverse and longitudinal surface settlement profiles	Derived from linear elastic 3D Boundary Element analyses of unlined shallow circular tunnel in gravitational stress field. Assumes $K_0 = \nu/(1-\nu)$ with ν = 0.45 (K_0 = 0.82), but assess influence of ν (and K_0). Longitudinal and transversal settlement distributions of ground surface presented in conveniently normalized form, for H/D from 0.5 to 2.0. Includes account for ground creep and layered soil conditions.
16. Pierau (1981, 1982)	Numerically derived	Maximum surface settlement	Derived from linear elastic 3D FE analyses of lined shallow tunnel, with larger (non-circular) cross-sectioned area. Assumes $K_0 = \nu/(1-\nu)$ and parametric results cover a limited range of application. The study aconcentrated more on lining (shotcrete) design. See section 4.3.2.6 for further details.

Table 4.11 Features of some Methods for Ground Displacement Prediction for Shallow Tunnel Design (Continued).

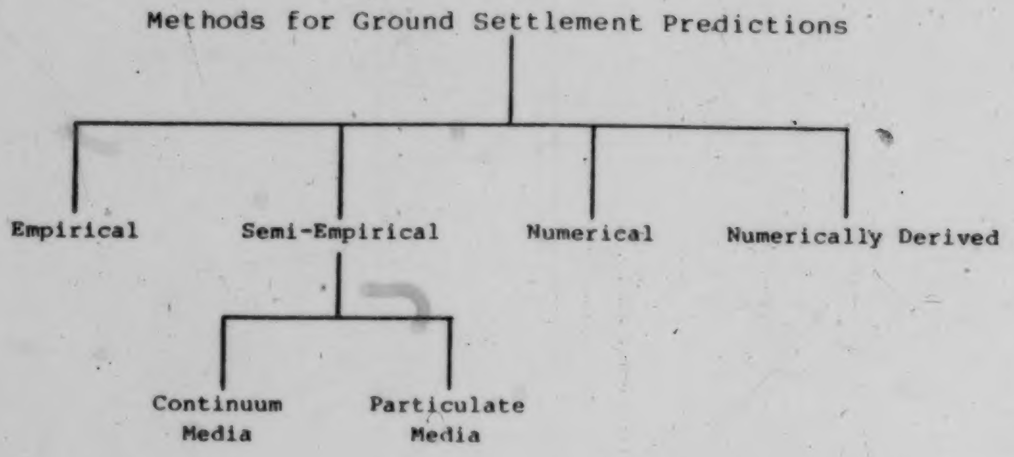
Methods for Ground Settlement Predictions
Empirical
Semi-Empirical
Numerical
Numerically Derived
Continuum Media
Particulate Media

Figure 4.6 Classification of Methods for Ground Settlement Prediction for Shallow Tunnels

limitations of each method can be deduced from the information on their development and on their assumptions. A global evaluation of each group of methods is attempted in the following.

The fully empirical methods are those which were developed from the observation of the performance of tunnels previously built. As noted in Sections 1.1 and 4.3.2.2, they may include an unknown, normally wide safety margin. They are usually developed for applications in a particular site, for a specific set of ground conditions, and for certain types of construction schemes, which formed the data base from which the methods were elaborated. Applications outside these ranges of conditions may not be successful, as the extrapolation of results is not usually based on fundamental properties that control the phenomenon. This is perhaps the most serious limitation of these methods, which otherwise yield effective results when used within their specific range of validity. Only two published examples of methods belonging to this category are included in Table 4.11, but a much larger number should exist, which are mostly unpublished.

The second class includes the semi-empirical methods, which normally make use of some more or less simple theoretical framework to represent the phenomenon. This enables them to take into account some more fundamental variables, but yet, to a large degree, they rely on empirically developed procedures.

This group can be divided into two subclasses depending on whether the assumed type of representation for the ground medium is continuum or particulate. Some methods, in fact, combine theoretical elements derived from these two types of media to reach their goals (e.g., Limanov, 1957 or Schmidt, 1969).

The continuum theories model the ground as an ideally elastic, plastic or elasto-plastic medium. Examples of these are the methods by Limanov (1957), which calculates the maximum elastic surface settlement, by Murayama and Matsuoka (1969), which estimates settlements in granular soils represented by a plastic continuum, and by Lo et.al. (1984) which calculate settlements assuming the ground to be a linear elastic perfectly plastic material. Though these methods address some of the fundamental mechanisms involved in the process of settlement generation, they are formally approximate as they neglect some other aspects or variables of the problem, as well as including factors which were empirically derived. The degree of generality of these approximate solutions are clearly larger than that of a fully empirical method, but they still can be applied only to certain particular conditions.

The second subclass of the semi-empirical group includes those methods based on theories that recognize the discrete nature of the ground. These methods have in common the treatment of the subsidence as a stochastic problem, where the convergent downward particle flow towards an open orifice is viewed as equivalent to a counterflow of voids entering the orifice and migrating upwards (Mullins, 1977:37). The number or volume of particles at a certain point in the ground passing through the orifice (a void space behind the liner, for instance) is a measure of the subsidence at this point. This volume, in turn is related to the probability of a particle located at that point to move down, as a result of the creation of an orifice (Schmidt, 1969;32). It follows that the ground surface subsidence can be approximated by a normal or Gaussian probability function.

The use of this theoretical framework was criticized by de Mello (1981) and de Mello and Sozio (1983). The criticism derived from the fact that under good ground control conditions, the basic nature of the physical phenomenon involved in the settlement generation is not addressed by the Stochastic Theory. The response of the ground mass upon the stress release induced by the construction of the tunnel is closely approximated by a continuum mechanics approach, and the fundamental soil behaviour involved is not probabilistic, unless localized collapses of the unsupported ground are the issues under investigation (de Mello and Sozio, 1983:18).

For good construction conditions, the normal probability function could be understood as being a simple curve-fitting tool to adjust measured settlement profiles. According to this view, this class of calculation methods would be better defined as fully empirical, since they do not address any fundamental aspect of the ground behaviour. It is not debatable, however, that the normal probability curve does fit the observed settlement troughs well, unless the displacements are very large and the resulting trough is narrower than that predicted by Peck's boundaries (Cording and Hansmire, 1975:607). It is with interest that one notes, as indicated by Attewell (1977:935), that for these conditions, high shear strain concentration tends to develop and the settlement profile ceases to follow a normal probability curve. In other words, for poor ground control conditions, this approach would also not be suitable.

In all methods within this category (8 to 12 in Table 4.11), an independent estimate of the total volume of settlement is required. In this regard, an important contribution was made by Cording and Hansmire (1975). The settlement volume was defined by the sum of the volume of the soil lost into the tunnel plus the overall volume changes in the ground. The authors extended Schmidt's (1969:55) qualitative assessment of the sources of lost ground, and proposed a quantitative criterion, that allowed the identification of individual sources. For this, they assumed a two-dimensional approximation and neglected possible interactions between the different types of losses. This criterion, further extended by Attewell (1977), facilitates the estimate of the total volume of ground lost, but the volume of settlements remains undefined, as the overall ground volume change is not readily determined.

A simpler alternative for settlement volume estimates was suggested by Negro (1979, 1983), who recognized that both the loss of ground and the volume changes are directly related to the quality of construction. By extending suggestions made by Peck et.al. (1972), Negro (Op.cit.) proposed four levels of construction quality, to which total volumes of surface settlements, V_s, are directly associated. These are defined as a percentage of the tunnel volume, V_t:

a. High construction quality: V_s=0.5% V_t

b. Normal construction quality: V_s=1.0% V_t

c. Poor construction quality: V_s=3.0% V_t

d. Failure condition: V_s=40% V_t

Though entirely empirical and involving rather subjective qualifications of the contruction operation, this criterion was able to explain improved ground responses noted in tunnels built in Sao Paulo and in Frankfurt over an extended period of time (see Heinz, 1984:32). The experience gained in applying particular construction methods to specific ground conditions, led to increasingly smaller ground settlement volumes reflecting a better quality of construction.

Interesting contributions were made by Yoshikoshi et.al. (1978) and Attewell and co-workers (Table 4.11, item 12). These authors extended the assumption of normal probability for the transverse settlement to the distribution in the longitudinal direction, which should result in a cumulative probability curve. This is because it reflects the summation of the subsidence surface generated by a 'point' source of loss, caused by the tunnel face advance. With this assumption, Attewell and co-workers were able to derive a curve fitting technique that seemed to adjust the complete displacement field above a tunnel. To achieve that, some additional simplifying assumptions had to be introduced, one of them being that the soil does not undergo volume changes. Applications of this technique to granular soils would, therefore, be less appropriate, though the probability approach was originally developed for this class of materials. This fact enhances the empirical nature of the method. The method requires an independent estimate of the loss of ground (equal to the volume of settlements), which is done empirically. Moreover, it assumes that the settlement of a point, when the tunnel face passes under it, is equal to 50% of the final settlement of this point.

The last group of methods to be discussed are those derived numerically. As explained in Section 4.3.2.6, these methods result from parametric numerical analyses, whose results are generalized through a normalized form using non-dimensional variables for certain ranges of conditions. Unlike other types of approach reviewed in the present section, these methods were developed from theoretical frameworks that take into account the fundamental aspects of the phenomenon. Their generality is controlled by the validity of their built-in assumptions, and by the range of conditions covered in their development. As they were derived from basic mechanism representations, they tend to present broader ranges of application which allows an extrapolation of results which is not always possible by empirical methods. Some examples of those methods are given in Table 4.11.

The method by Sagaseta and co-workers was one of the first developed along these lines, using the finite element method as a modelling tool. The linear elastic behaviour it assumes for the soil is a fairly restrictive hypothesis, also shared by others (methods 15 and 16, Table 4.11). In their analyses, Sagaseta and co-workers overemphasized the role of Poisson's ratio on the ground response. In fact, the noted influence of Poisson's ratio, reflects more the effect of the in situ stress ratio, defined as a function of the former. In the development, they assumed a full stress release at the opening. To adjust this assumption to actual conditions, where a partial stress release occurs, the authors introduced an empirical multiplication factor smaller than unity, to be applied to the calculated settlements.

Resendiz and Romo (1981) went further and considered the non-linear, yet elastic, behaviour of the ground. They assumed a hyperbolic stress-strain relation for the soil, treated as a non-frictional material, and followed a development similar to one of those presented in Chapter 6. Thus, the application of the method is restricted to saturated clay soils in undrained conditions. Further details of their method is given in Table 4.11. The account of the ground settlements induced by the stress release at the face, was approximated by a two-dimensional representation of the shallow tunnel in the longitudinal direction, in which the finite element nodes at the tunnel crown and floor were fixed (rigid lining). The resulting settlements caused by the stress release at the face tend to be excessive as a result of this assumption. Moreover, for certain conditions, the method tends to furnish final settlements at the tunnel crown which are smaller than those at the surface, a result which seems inconsistent with the expected ground response, under the assumptions made. It appears that this result again, is a reflection of the representation adopted for the evaluation of the settlements induced by the stress release at the face. The method requires an independent estimate of a uniform tunnel closure, to represent the loss of ground through the opening contour, which is an additional limitation of the method. These problems and limitations are solved however, if the tunnel closure solution derived in Section 5.3 of this thesis is used to evaluate, not only the losses through the tunnel contour, but also those occurring ahead of the tunnel face. The combination of these two procedures seems to yield more sensible results.

The last two methods included in Table 4.11 present some of the limitations of the method by Sagaseta and co-workers. However, they take into account the three-dimensional nature of the problem. While the method by Pierau (1981, 1982) used a finite element formulation in its development and considered the tunnel to be lined, the one by Ito and Hisatake (1982), was based on a 3D boundary element analysis of unlined tunnels. As noted in Table 4.11, despite the account of 3D effects, both methods included other assumptions and features that largely restrict their practical application.

With the exception of the method by Pierau (Op.cit.), the other methods were developed in such a way that the prediction of ground settlements is dissociated from the prediction of lining loads. This is one of the most critical limitations of the methods reviewed in the present section.

4.3.4 Ground Stability Verification

The basic aspects of the ground stability problems involved in soil tunnelling were presented in other parts of this thesis, particularly in Section 3.2. It was shown there that tunnel stability is mainly governed by geometric conditions, defined by the cover to diameter ratio, H/D, and by the unsupported heading length to diameter, L/D.

On the other hand, the basic requirements for excavation stability assessment were presented in Section 4.2.3. It was discussed then, that conventional limit equilibrium calculations may not be recommended for stability assessment in practice, as they can provide unsafe estimates of the factor of safety. The stability verification is preferably performed by traditional plasticity solutions, such as those derived from the Lower Bound Theorem, which in theory, furnishes safe estimates of the collapse loads.

A fairly large number of plasticity solutions appeared over the last decade, most of them resulting from research work conducted in Cambridge, U.K. These solutions have been mainly tested through physical modelling, where they showed considerable potential for practical application. Notwithstanding this, their use in practice is conditional on the validity of the assumptions made in their development. A more detailed discussion on some of these assumptions is presented in Section 6.5.2, where these solutions are used to assess the limiting conditions for the application of a design procedure whose development is presently projected.

Briefly, in the application of the Lower and Upper Bound Theorems of Plasticity (see Calladine, 1969) to the shallow tunnel problem, it is customary to introduce the following assumptions:

a) the soil is homogeneous;
b) the problem is time independent;
c) the collapse load is unique;
d) the soil has an associated flow rule;
e) the soil has a perfectly plastic behaviour.

There are solutions that relax some of these assumptions. For example, Gunn (1984:13), developed a lower bound solution for a frictionless heterogeneous soil with an undrained strength increasing linearly with depth. Also, there are solutions that introduce other simplifying assumptions, such as a soil with zero body forces (the driving force being a surcharge at the surface), a uniform internal tunnel pressure, etc.

The solutions available do not recognize time dependent effects resulting from changes in pore pressures and effective stresses, as they operate in terms of total stress changes. A rather simplified assessment of this problem was made in Section 3.3.4.4, where it was analysed in mere qualitative terms. Some of the problems related to assumptions (c) and (d) are discussed in Section 6.5.2.

It appears that very little has been investigated regarding the consequences of assumption (e). Muhlhaus (1983) was one of the few who attempted to study the effect of the soil deformations prior to collapse of the shallow tunnel. A specially designed finite element code was developed to study the problem, which seems to have avoided numerical difficulties normally encountered as the collapse condition is approached. He presented results suggesting that collapse loads assessed by the method of characteristics (a lower bound solution) may be larger, thus less safe, than those calculated including the effect of ground displacements prior to collapse. Muhlhaus (Op.cit.)

used a non-linear elastic homogeneous material to represent the soil. He noted that a better agreement between the plasticity solution collapse load and that given by his solution is found as the soil becomes stiffer, and therefore closer to the rigid-plastic assumption.

These limitations indicate that the use of the plasticity solutions in practice should be undertaken with due care and be understood as an approximation, which is not unlike many other similar procedures normally used.

In the present section, an attempt is made to survey the available shallow tunnel plasticity solutions. No attempt is made here to review in detail or to apply the existing methods to practical situations. A more detailed description, as well as examples of applications of some of these solutions are presented in Chapters 6 and 7.

Accordingly, Table 4.12 was prepared to summarize the survey undertaken. In it, each method of shallow tunnel stability assessment is identified by its author. The types of stability problems addressed were classified into five groups, following the more important instability mechanisms discussed in Section 3.2:

a) face instability;

b) face and heading instability;

c) heading instability;

d) plane strain (P.S.) tunnel instability;

e) local instabilities.

	Author/Year	Stability Problem	Type of Solution	Soil Self-Weight	Strength Condition	Geometric Approach	Solution Presentation	Comments
1.	Casarin (1977:67), Mair (1979:134)	Face	UB	No	U	3D	Equation	Circular shaft failure
2.	Davis et al (1980:409)	Face	UB	Yes	U	3D	Chart	Elliptical and inclined shaft failure
3.	Davis et al (1980:408, 409)	Face	UB	Yes	U	2D	Equation	Long wall face; liner roughness does not affect
4.	Britto and Kusakabe (1985)	Face	UB	No	U	3D	Chart	Composed circular shaft failure
5.	Davis et al (1980:407, 409)	Face	LB	Yes	U	2D	Equation	Smooth lining
6.	Davis et al (1980:409)	Face	LB	No	U	3D	Equation	Thick cylinder approximation
7.	Davis et al (1980:409)	Face	LB	No	U	3D	Equation	Thick sphere approximation
8.	Casarin and Mair (1981)	Face	LB	No	U	2D	Chart	Long wall face; stress characteristics solution
9.	Casarin (1977:68)	Face and Heading	UB	No	U	3D	Chart	Square tunnel
10.	Muhlhaus (1985:50)	Face and Heading	LB	No	D	3D	Equation	Thick sphere approximation; zero tunnel pressure
11.	Casarin (1977:66)	Heading	UB	Yes	U/D(c=0)	3D	Equation	Approximate solution
12.	Caquot and Kerisel (1956:470)	P.S. Tunnel	LB	Yes	U/D	2D	Equation	Consider internal fluid pressure
13.	O'Reacatha and Mandel (1974)	[illegible] Tunnel	LB	Yes	U/D	2D	Charts	With and without fluid pressure; stress characteristics
14.	Seneviratne (1979:76)	P.S. Tunnel	LB	No	D(c=0)	2D	Equation	Corrected Atkinson and Cairncross (1973:203); solution not complete
15.	Muhlhaus (1985:44)	P.S. Tunnel	LB	Yes	U/D	2D	Equation	Uniform internal pressure

Table 4.12 Features of some Methods for Ground Stability Verification

	Author/Year	Stability Problem	Type of Solution	Soil Self-Weight	Strength Condition	Geometric Approach	Solution Presentation	Comments
16.	Atkinson and Potts (1977:210)	P.S. Tunnel	LB	No	D(c=0)	2D	Equation	Complete solution
17.	Atkinson and Potts (1977:211)	P.S. Tunnel	LB	Yes	D(c=0)	2D	Equation	Complete solution
18.	Seneviratne (1979:75)	P.S. Tunnel	UB	No	D(c=0)	2D	Equation	Correction of Atkinson and Cairncross (1973:204) solution
19.	Atkinson and Cairncross (1973:203)	P.S. Tunnel	LB	No	U	2D	Equation	Also at Davis et al (1980:400)
20.	Seneviratne (1979:79)	P.S. Tunnel	LB	Yes	U	2D	Chart	Stress characteristics; also at Davis et al (1980)
21.	Gunn (1984:12)	P.S. Tunnel	LB	No	U	2D	Equation	Retangular tunnel
22.	Gunn (1984:13)	P.S. Tunnel	LB	No	U(C_ufZ))	2D	Equation	C_u varying linearly with depth
23.	Mair (1979:119)	P.S. Tunnel	UB	Yes	U	2D	Chart	Solution independent of self-weight; 4 mechanisms
24.	Atkinson et al (1975:84)	Local collapse-roof	UB	Yes	D(c=0)	2D	Equation	Wedge failure; also at Atkinson and Potts (1977:212)
25.	Davis et al (1980:411)	Local collapse-face	UB	Yes	U	2D	Equation	Long wall face
26.	Davis et al (1980:411)	Local collapse-face	UB	Yes	U	3D	Equation	Circular tunnel face
27.	Davis et al (1980:412)	Local collapse-face	LB	Yes	U	2D	Equation	Solution is depth independent; long wall face
28.	Davis et al (1980:411)	Local collapse-P.S.	UB	Yes	U	2D	Equation	
29.	Davis et al (1980:411)	Local collapse-P.S.	LB	Yes	U	2D	Equation	Solution depends on relative tunnel depth

Table 4.12 Features of some Methods for Ground Stability Verification (Continued).

For the face stability assessment, it is always assumed that the tunnel contour is entirely lined, up to the plane vertical tunnel face. All solutions in this group assume the tunnel to be full face excavated and that the lining is perfectly rigid. Some of them assume the lining-soil interface to be 'smooth', but most assume it to be 'rough'. They all furnish a critical internal tunnel pressure (for example, a fluid pressure), uniformly applied to the face, in problems where the driving forces are represented by surface surcharge loads and/or the ground self-weight. A discussion on the effect of the uniformly applied internal pressure at tunnel face is presented by Davis et.al. (1980:413).

The second group treats the combined stability of the face and of the unlined heading zone and the third focuses only the stability of this unlined zone. In all case, once more, the rest of the tunnel is supposed to be fully supported by some stiff lining. The solutions assume that an internal tunnel pressure acts against the unlined heading, except in that by Muhlhaus (1985:50), which assumes this pressure to be zero. The latter furnishes the critical unsupported heading length causing ground collapse.

The fourth group treats the case of the two dimensional stability of an unlined tunnel in plane strain condition, and furnishes the value of the internal tunnel pressure causing collapse.

While the former solutions postulate a complete collapse of the ground mass, the fifth group addresses the problem of localized instabilities, which may occur even though the overall stability of the ground mass is secured. Three sub-classes are assigned within this group according to the place where this instability process is identified: at the tunnel face, tunnel roof and tunnel walls in a plane strain condition. In undrained conditions, local instabilities may develop regardless of the value of the uniform tunnel pressure, and in some cases, regardless of the relative tunnel depth. Local collapses in these conditions, are found to be mainly dependent on the undrained strength ratio, $c_u/\gamma D$. The size, D, of the excavated opening is controlled by local collapse conditions.

Table 4.12 also identifies the type of plastic solution used in each method. Typically, two classes of solutions are included: lower bound (LB) and upper bound (UB). These solutions are sometimes derived analytically when they are presented explicitly through an equation, or numerically when they are defined for certain ranges of variables and are usually presented in charts. For simpler situations, stress fields can be postulated and explicit lower bound solutions can be found. Complex cases, for instance when the soil body forces are taken into account, require numerical approaches, usually implementing the method of stress characteristics. Upper bound solutions always require a critical tunnel pressure to be found, associated with a certain collapse mechanism. This is achieved after maximizing the value of the tunnel pressure with respect to the variation of a dimension or an angle that geometrically defines the mechanism. This optimization process can be done either analytically or numerically, depending on the complexity of the problem.

Two classes of geometric approximations are involved in the solutions included in Table 4.12. For instance, the face stabiliity problem can be approached three-dimensionally, as it should, or a two dimensional approximation may be considered. If this is the case, the actual 3D problem is reduced to that of the stability of a long wall mining face.

Two types of ground strength conditions are usually considered: undrained (U) or drained (D). In the first case, the soil is assumed to be frictionless with its strength defined by its undrained cohesion. In the second case, the soil is assumed to be frictional and the cohesive strength component (c) may or may not be considered.

In most cases, the tunnel cross section is assumed to be circular, though some solutions assume other tunnel shapes (square, rectangular, long wall).

None of the above methods yield the correct collapse conditions, which is theoretically approximated by maximizing the upper bound tunnel pressure and by minimizing the lower bound solution.

A definition of the factor of safety was introduced in Chapter 2 and its calculation, using the above methods is exemplified in Section 6.5.2.

This survey indicates that though a large number of solutions is available for a variety of stability problems, some important conditions are not covered by these existing methods. For instance, there are no upper or lower bound solutions for the 3D face stability problem under drained conditions (i.e. for a frictional and cohesive soil). This particular situation could be approximated by the stress field solutions put forward by Mandel and Halphen (1974) (not included in Table 4.12). By this approach, the tunnel face would be approximated by a spheric cavity in a plastic domain with drained or undrained strengths, under the action of gravity that these authors considered.

Among those that treat the two dimensional tunnel stability problem (P.S. tunnel), the solution by D'Escatha and Mandel (1974) is the most general. It considers both drained and undrained strength conditions as well as the soil self weight. For this reason, this particular solution will be presented later in this thesis (Chapters 6 and 7). As it derives from the method of stress characteristics, it is a lower bound, and therefore 'safe' solution.

A serious limitation of all these solutions is the fact that they are unable to consider the effect of pore pressures in the ground stability problem. Under certain circumstances, it is known that the stability of the ground is totally controlled by the groundwater condition. Seepage action may have a controlling role in the three dimensional tunnel face and heading stability. This class of problem is usually treated in practice, using simplified limit equilibrium analyses, with pore pressure calculated from flow nets (see Sections 3.3.4.2 and 4.2.3).

4.4 Survey of the Current Design Practice

4.4.1 Foreword

In this section an attempt is made to analyse some aspects of the current practice in geotechnical design of shallow tunnels. Two of the three major design activities (see Section 4.2) are reviewed herein: the prediction of lining loads and the prediction of ground displacements. The third activity, the ground stability verification, is not covered by the present survey. This exclusion reflects a decision to focus on topics directly related to the aims of the present research, and should not be understood as a disregard of this equally important design activity.

For the first design aspect, the review of the current practice on lining load prediction was based on a survey carried out earlier by the International Tunnel Association. A similar survey was conducted by Sgouros (1982:36). The results of this study, however, were of limited value as they represented only the design practice in the United States. In addition, this survey was largely based on personal interviews, which did not seem to have been arranged in a format that would allow comparative or statistical analyses of the results.

For the second design aspect, a specific inquiry was organized to cover the current practice on ground settlement prediction, in a large segment of the international designer's community.

The following sections present the details on how the inquiries were undertaken, the results of the surveys and, finally, their interpretations.

4.4.2 Prediction of Lining Loads

4.4.2.1 Survey of Practice

The lining design practice as it stood in the late seventies and early eighties was surveyed by a working group on structural design models for tunnelling, set up by the International Tunnelling Association (ITA). This was done by means of a questionnaire sent to ITA member nations in December 1978. The questionnaire focussed not only on shallow tunnels in soil, but also cut and cover tunnels and deep tunnels in moderately hard rock. The results of the survey, including the questions formulated, a summary of the answers, and the list of the respondents were presented in a report by Duddeck (1982). He was the co-ordinater of the working group, "Views on Structural Design Models for Tunnelling: Synopsis of Answers to a Questionnaire, May, 1981 " (published in "Advances in Tunnelling Technology and

Subsurface Use", Vol. 2, no. 3, 1982, Pergamon Press).

This section will review and re-interpret some of the results of this survey solely on what is pertinant to the practice related to soil tunnelling. It should be pointed out that the analyses and subsequent syntheses to be presented in the next items, resulted from the writer's interpretation of the responses to the ITA questionnaire as they appeared in descriptive form, (Duddeck (Op.cit)). This, in turn, is a condensed form of the original replies as prepared by the ITA working group. Although it had been submitted and proofed by the original respondents in August, 1980, (Duddeck, Op.cit.:161), it may include some interpretation by the working group members who prepared the condensation. Despite all attempts made by the writer and most likely by those who prepared the condensation, to depict an unbiased and faithful picture of the original responses, some inaccuracy might have been introduced in the condensation process. It is believed however, that, if any inaccuracy exists at all, it should not affect the main conclusions or the broad statistical trends that will be discussed.

The questionnaire was preceded by a statement on general motivations, and to get replies as specific as possible, the respondents were invited to answer the questions twice, for two ideal tunnelling situations. The first situation referred to a 6 m diameter tunnel with 8 m of ground cover, driven by a shield machine in a soil with properties shown in Table 4.13. This could represent a subway tunnel driven through a fairly cohesive soil, with a strength and stiffness greater than those of the overconsolidated Frankfurt clay. The second situation referred to a tunnel mined through a stronger and stiffer soil, with identical geometry. The stiffness of this soil is not dissimilar to that observed in the clay marl layers of Munich Tertiary Sediments, however at a higher depth. The strength properties, though, are appreciably higher than Munich "Flinzmergel", particularly regarding the cohesive component. Also dissimilar to Munich's condition is the absence of ground water. Tunnel construction in this second condition was done using shotcrete and steel arches for support, as in the NATM.

Only 47% of the respondents answered the questionnaire for the two situations envisaged. The remaining 53% provided answers to either one or other condition. Hence, differences in the answers to each question, as applied to the shielded or mined tunnel, may reflect different views in treating the design of tunnels built by distinct construction methods, as well as different design attitudes for distinct ground conditions. It may also be a reflection of different personal views, as distinct individuals replied to the questions associated with each tunnelling situation. To some extent this was an unfortunate circumstance regarding the survey preparation and results. It partly impaired a definite identification of distinct design attitudes (if

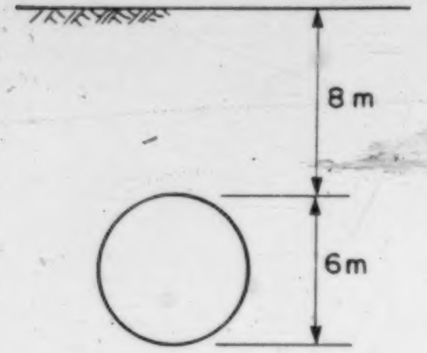

Ground Conditions and Properties	Shielded Tunnel Situation	Mined Tunnel Situation
Friction Angle	25°-30°	30° - 35°
Cohesion (kPa)	100-200	300-400
Modulus of Soil Stiffness (MPa)	30-40	100 - 200
Density (KN / m^3)	20	20
Groundwater Level	2-15 m below surface	no groundwater (only small amounts of seeping water)

Table 4.13 Envisaged Ground Conditions for Response of Questionnaire on Lining Design (modified after Duddeck, 1982:173)

any) regarding distinct construction techniques. These facts should be borne in mind when analysing the results that follow. It could be said that in both cases, the tunnelling conditions are very favourable. Both grounds show high cohesive strength which reduces the risk of stability problems during excavation, and high stiffness whicha allow one to anticipate relatively small ground displacements upon standard tunnelling construction.

The questionnaire was prepared, including motivation and explanations, with 25 questions. Most of these demanded descriptive answers. but 4 questions were prepared in a multiple choice form, allowing the respondents to mark more than one answer per question. These questions were reproduced by Duddeck (1982:163) and will not be included here. Only those questions deemed relevant to the present work will be discussed. These refer mainly to the procedures for lining load prediction, including the statical system used for calculation and the ground loads. Questions related to other types of loads, site investigations, structural safety of the support and field monitoring will not be addressed here. Their answers can be found in Duddeck (Op.cit.)

The questionnaire was replied to by 19 respondents from 12 countries. The return rate is not known, as the number of questionnaires sent was not disclosed. Nine of the total number of respondents answered the questionnaire for both types of tunnelling situation. Five of them replied to the questions as it applied to shielded tunnels and another five answered the questionnaire for mined tunnels. Table 4.14 lists the number of respondents and responses for both tunnel situations and shows the representation of each country and region in the survey conducted. As it is seen the survey on lining design for shielded tunnels represents mainly the European practice (57%). On an individual country basis, the answers coming from the U.S.A comprise 21% of the total responses, followed by the United Kingdom and West Germany, each contributing 14%. Regarding the lining design for mined tunnels, the results of the survey represent, again, mostly the European practice (71%) and the two countries that mainly contributed with answers were West Germany (21%) and the United Kingdom (14%).

As noted by Duddeck (1982:165), the questionnaire was intended to be answered by "those engineers who prepare tenders and who actually design tunnels, not from scientists who may tend to say what ought to be done". However, it was not possible to assess with accuracy the actual type of practice of the respondents, since their technical background was not clearly identified, from the information made available. Nevertheless, it is believed that more than half of the responses reflect the intended view of consultants and contractors (in more or less equal parts).

		Shielded Tunnels		Mined Tunnels	
Region/Country	No. of Respondents	No. of Responses	% of Total	No. of Responses	% of Total
Europe					
Austria	1	1	7	1	7
Belgium	1	1	7	-	-
France	1	1	7	1	7
W. Germany	4	2	14	3	21
Poland	1	-	-	1	7
Spain	1	1	7	1	7
Switzerland	1	-	-	1	7
United Kingdom	2	2	14	2	14
	12	8	57	10	71
North America					
U.S.A.	3	3	21	1	7
Australasia					
Australia	1	1	7	1	7
China	2	1	7	1	7
Japan	1	1	7	1	7
	4	3	21	3	21
TOTAL	19	14	100	14	100

Table 4.14 ITA Questionnaire Response on Lining Design

4.4.2.2 Results of the Survey

One of the questions involving an aspect which is highly consequential regarding the lining loads, asked "what are the values chosen for the primary stress-field before the tunnel is excavated" (Duddeck, Op.cit.:167). All respondents but two, provided answers to this question indicating that they take the overburden vertical total stress as a major principal stress, but different assumptions were evident regarding the horizontal total stress. Figure 4.7 shows that most of the respondents estimate a ratio horizontal to vertical total stress from the coefficient of earth pressure at rest, K_o, as determined from measurements (in situ tests inclusive) or from local experience. The second most popular approach is to arbitrarily assume a fixed value for K, usually between 0.4 and 0.6. A third group assumed that the coefficient K is a function of Poisson's ratio.

At another point, the practitioners were asked "what would be the loads or ground pressures assumed" for the design of the lining of a shielded or mined tunnel (Duddeck, Op.cit.:167). As shown in Figure 4.8, the answers were classified into four categories. For the shielded tunnel situation, the majority of the responses (54%) indicated full overburden, which implies the assumption that the lining is already installed before the ground is excavated. A second group of responses indicated the use of the full or reduced overburden, depending on whether the tunnel is very

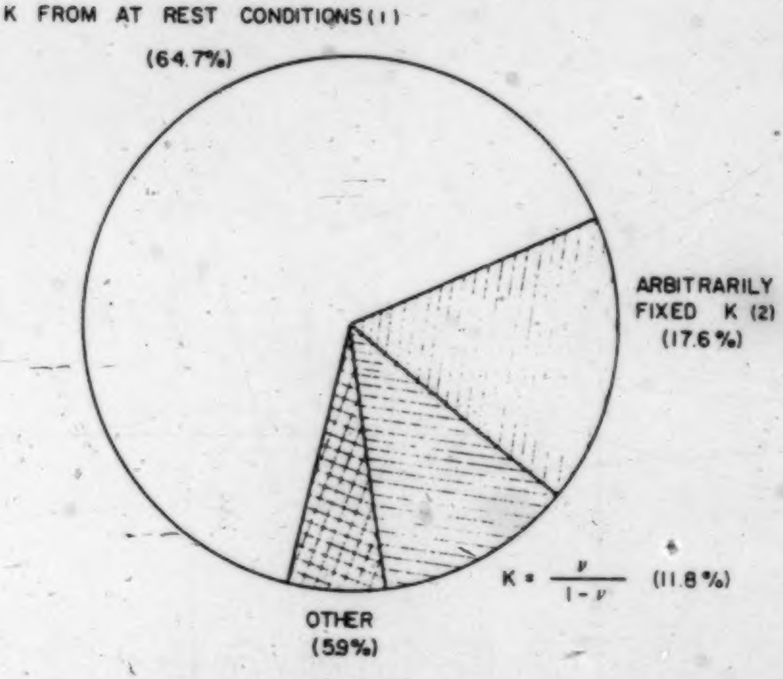

NOTES: (1) Determined from measurements of K_o or from local experience
(2) Typical K value ranging from 0.4 to 0.6
(3) 17 respondents

Figure 4.7 Assumed Ratio Horizontal to Vertical In Situ Stresses used for Design of Shielded or Mined Tunnels in Soil

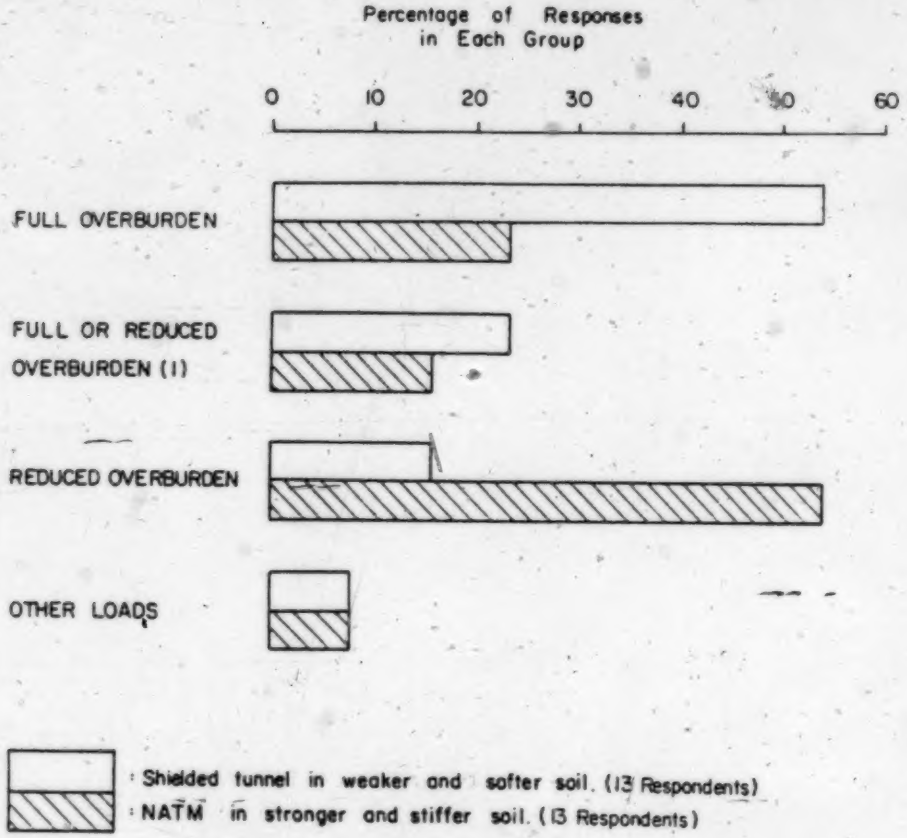

(1) Depending on geometry, type of soil or type of lining.

Figure 4.8 Ground Load Assumption Considered in the Responses for the Design of Shielded and Mined Tunnels

shallow or not, or on the type of soil (sandy or clayey). Just two responses indicated the use of a reduced overburden to account for ground stress relaxation before lining installation. One response revealed that ground load should not be considered in the lining design, but simply loads developed in handling the prefabricated lining, as well as other construction loads.

For the mined tunnel situation, the majority of the responses (54%) indicated a reduced overburden assumption for the lining design. Following this group were those postulating the full overburden hypothesis and those favouring either one of the other, depending on the particular case (relative depth and soil type). According to one respondent, it depends on whether the lining being designed is the primary or the secondary one (reduced load for the former or even for the latter if the tunnel is deep). Unfortunately, it is not very clear if the differences in the assumed ground load conditions for the two tunnelling situations, are due to the different construction technologies, soil properties,r ground conditions, or personal views of the respondents, as noted earlier.

It could be speculated that the predominant assumption of a reduced overburden load for mined tunnels results from the respondents probable understanding that the shotcrete and steel arch lining usually acts as a primary support. On the other hand, as most shielded tunnels use, nowadays, prefabricated linings as combined primary and secondary support, the respondents could have understood that a full overburden load assumption would be more adequate for the long term performance of this lining system. This interpretation was adopted by P. Gesta, who prepared the conclusions for mined tunnels of the ITA survey (Duddeck, Op.cit.:219). He concluded that there is a tendency towards designing primary supports using a reduced ground load, and secondary supports with the full (in situ) ground loads. He cautioned, however, that this is not a unanimous philosophy of the practitioners. Indeed, a careful review of the 13 responses on the subject revealed that only P. Gesta himself indicated that the ground load assumption depends on whether the support is the primary or the secondary. Other responses did not indicate this, possibly because the questionnaire did not invite this point to be answered. Although his interpretation might be correct, his conclusion cannot be supported by the explicit answers of the respondents. Although not requested to explain how the reduction in the ground loads would be estimated, the 14 responses (5 for shielded and 9 for mined tunnels) that indicated this assumption, provided indications about the procedure to be used for such an estimate. Figure 4.9 shows that the majority for both tunnelling situations combined (64%), favour the use of Terzaghi's arching theory for this purpose. This group is followed by those 21% who estimate the stress reduction on an arbitrary basis (founded on previous experience). The remaining group of responses use some sort of empirical approach based on classification systems, to evaluate the ground load reduction.

Further on, the questionnaire asked, "what kind of statical system is used for determining the inner stresses, the deformations ..." for the lining design (Duddeck, Op.cit.:167). For each tunnelling situation, 14 respondents offered answers to this question. Some respondents mentioned more than one method for lining load prediction. Considering only those responses that clearly answered the question, the 13 responses for the shielded tunnel situation mentioned 17 lining design methods. For mined tunnels, 13 responses mentioned 26 methods (some applied to the primary and some others to the secondary lining). If all 26 responses for both tunnelling situations are combined, 43 references to lining design methods are evident. The combined statistical results are shown in Figure 4.10, with the design methods classified into four main groups. The percentage of responses was calculated in relation to the total of 26 responses, and the value calculated for each group method gives an indication of how frequently this method was indicated in the responses.

As shown, the methods most frequently referred (69.2%) are those that represent the lining by a ring and the soil by springs. In these models, the structure is submitted to prescribed loads independent of lining deformation, and the ground reaction results from displacement dependent spring

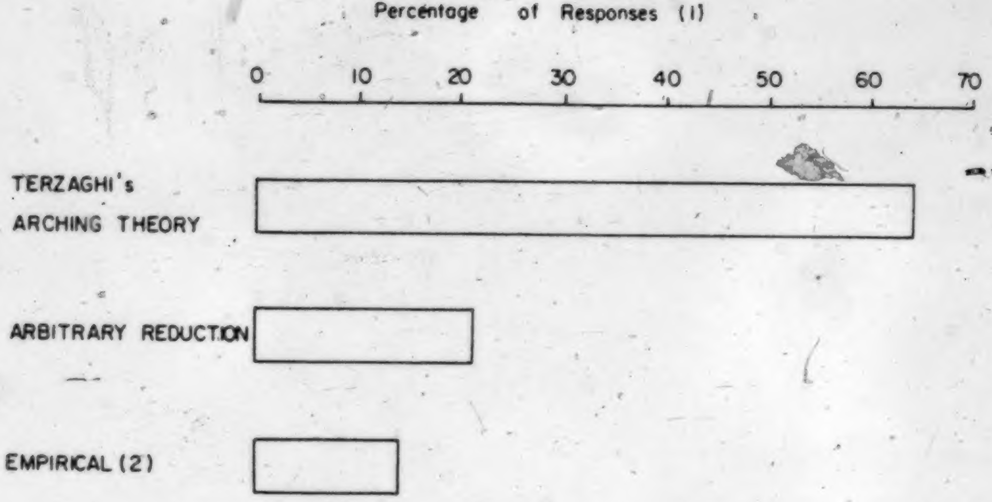

NOTES: (1) Total of 14 responses, combining 5 that reduce ground loads in shielded tunnels and 9 in mined tunnels.

(2) Ground load reduction by Geomechanics classification methods.

Figure 4.9 Criteria Indicated in the Responses for Ground Load Reduction both in Shielded and Mined Tunnels

loads. Some responses indicated methods based on continuous solutions (namely, Schulze and Duddeck, 1964 method), and others seem to use discrete solutions, numerically obtained for an embedment with a finite number of springs. Moreover, 8 responses (4 for the shielded and 4 for the mined tunnel situations), which represents 44% of the responses in this group, or 31% of the total responses, mentioned that they neglect the embedment of the lining in the crown region. In other words, they assume a "gravity load" condition, which is associated with a poor ground control assumption. Most of these came from German speaking respondents, and this is conversant with the local practice or tradition which has been incorporated in the design directives of the German Society for Soil Mechanics and Foundation Engineering (Duddeck, 1980).

The second most indicated procedure (39%) are the empirical methods, followed by ring and plate analytical models (31%) which include closed-form solutions such as Muir-Wood's and the convergence-confinement method. Finally, 27% of the responses indicated the finite element method, in most cases as an alternative approach and sometimes simply to check the solution provided by the simpler models.

Figure 4.11 presents the same data, but this time identifying the distributions of design procedures with respect to the different tunnelling situations. No significant differences are noted, except a tendency towards a more frequent use of empirical procedures and the finite

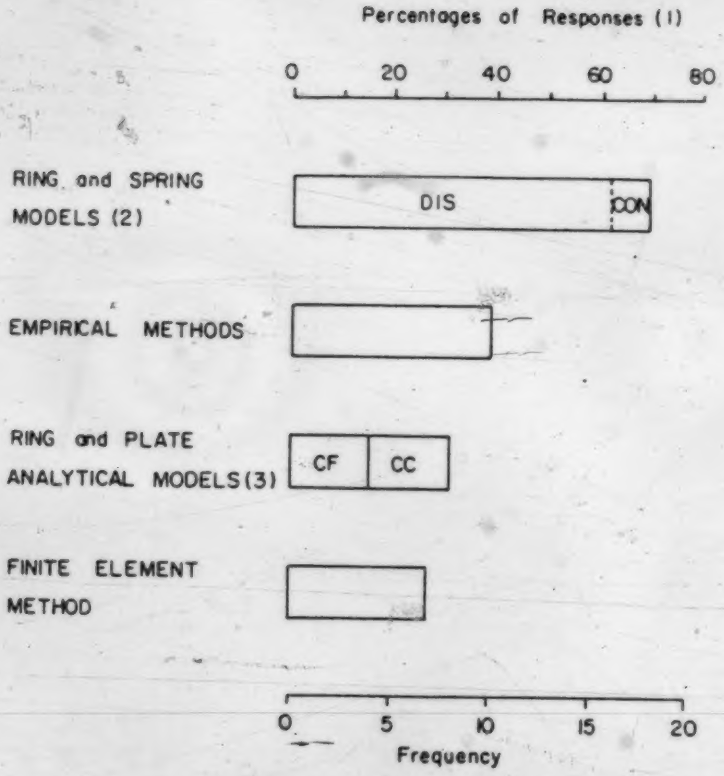

NOTES (1) Some of the 26 responses indicated more than one design method (some for primary support, for secondary support or for both). 43 design methods were mentioned.

(2) The answers did not allow clear separation between numerical (NUM) and analytical (AN) solutions.

(3) Include closed-form (CF) solutions and convergence-confinement (CC) models.

Figure 4.10 Types of Statical Systems used for Assessment of Lining Loads in Shallow Tunnels

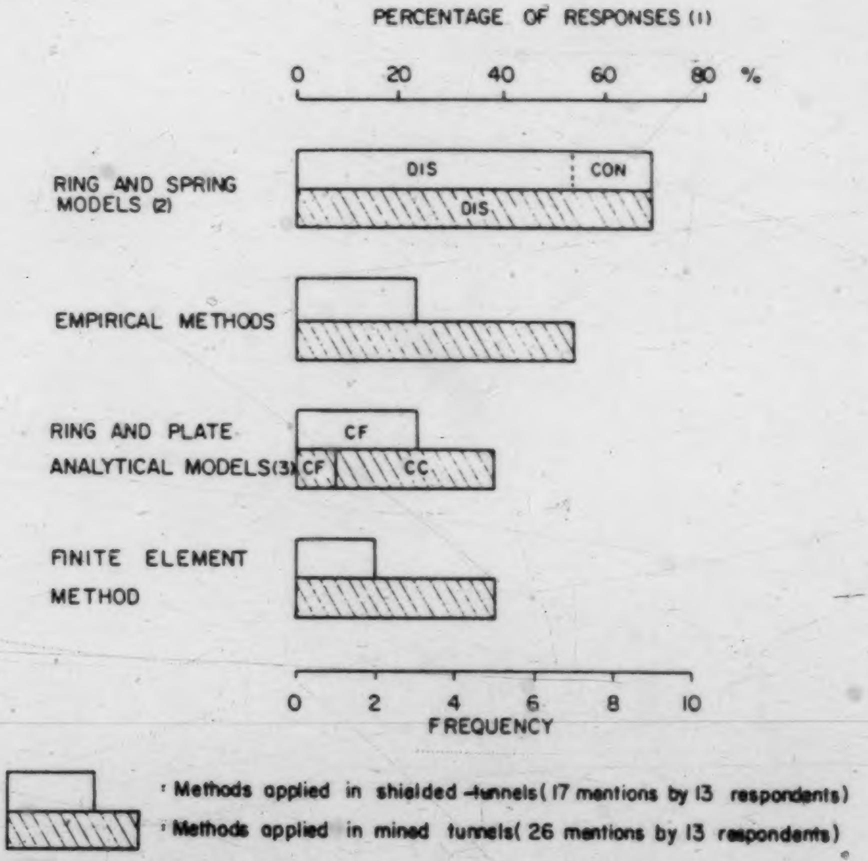

NOTES: see previous figure

Figure 4.11 Statical Systems Applied in Shielded and Mined (NATM) Tunnels

element method for the mined tunnel situation. For both tunnelling situations, the ring and spring models are most popular.

All respondents were asked if there is "any method determining the ground reaction modulus by the measured characteristic of the ground", to be used in ring and spring models. From the 28 responses received for both tunnelling situations, 21 procedures were mentioned that could be classified as shown in Figure 4.12. The remaining 11 responses did not provide an answer or indicated that there is no simple method for this. The most referred to procedure (52%) was the indirect calculation of the radial spring constant (K_r) through elastic parameters (E and ν) obtained from laboratory tests. Included in this group are most of the German speaking respondents, who relate K_r to the constrained modulus of the soil, which is primarily obtained by oedometer tests (see Section 4.3.2.4). A second group of responses mentioned the direct estimate of K_r in situ by plate bearing and pressuremeter tests. The remaining group use spring constants from back analysis of monitored field performance.

Although the respondents were clearly asked to answer if "are the same models employed for 'lining' and for the 'temporary' supports" (Duddeck, 1982:167), 11 of the 14 responses for the shielded tunnelling situation provided no answer to this question. Most of the latter felt that the question was not applicable to this situation, since the

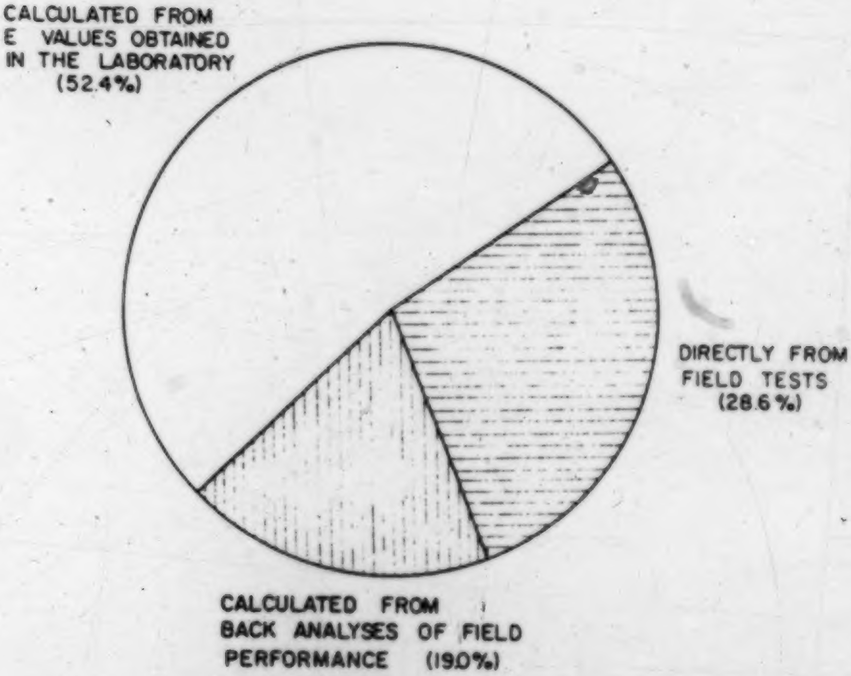

NOTE: 11 responses provided no answer; remaining 17 mentioned altogether 21 procedures. Percentages shown refer to the latter.

Figure 4.12 Procedures for Evaluation of the Spring Constant to be used in Ring and Spring Models for Lining Design of Shielded or Mined Tunnels

support normally used acts as a primary and a secondary lining. Considering only the answers for the mined tunnel situation, in which it is usual to apply a primary and secondary lining, the answers given in the 14 responses (Figure 4.13) indicate a slight tendency towards the use of different design methods for each lining type. Among the 6 respondents who use different lining calculation models, there was a general preference for employing an empirical and simple approach for the design calculations of the primary lining, combined with ring-spring models for the secondary support.

Another question posed was, "is the designing engineer obliged to take into account non-linear behaviour as for example, of the structural elements, of the ground, plasticity, rheology, large deformations?" (Duddeck, Op.cit.:169). From the 28 responses received, two of them (one for each tunnelling situation) were not clear, and could not be classified. Figure 4.14 summarizes the result of the survey for both shielded and mined tunnels. Half of the responses indicated that there is no obligation to take into account non-linearities of the soil or the support. Almost 27% said there is such an obligation, either for the support or for the soil. The remaining indicated that in some instances there would be a need to take that effect into consideration.

It may be questioned whether this statistical result is fully representative of the current practice. The question

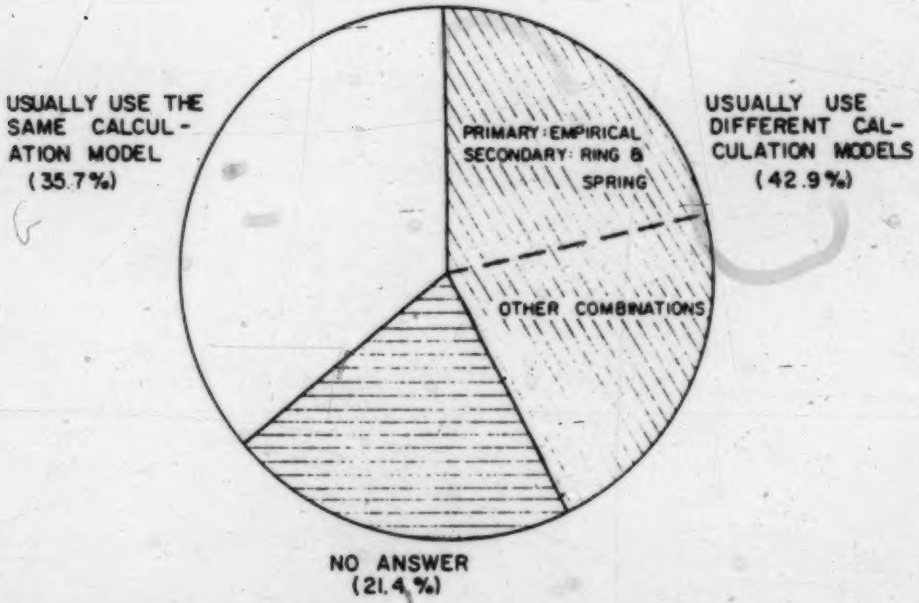

NOTE: 14 responses to the question for mined tunnels.

Figure 4.13 Distribution of Respondents on the Statical System used for the Design of the Primary and Secondary Linings in Mined Tunnels

asked if practitioners are obliged to take the effect into account, and not if they usually do.

Despite this, if the results are separated into shielded and mined tunnels (Figure 4.15), one notes slightly different trends for each. While only 15% of the responses agree that designers are bound to take into account non-linearity effects (for the soil only, however) in the shielded tunnelling situation, 38% of the responses for the mined tunnel and indicate that non-linearity of the soil (23%) is slighly more important than that of the support.

At another point (Duddeck, Op.cit.:169), the questionnaire asked "what kind of statical models are used checking the support actions at the working face? Are three-dimensional effects considered?". All 14 responses for the shielded tunnel situation could have been classified into three categories, as shown in Figure 4.16. However, only 10 responses for the other tunnelling situation could be properly classified.

As shown, the large majority for the shielded tunnel case do not consider any three-dimensional effect. A smaller group stated they may consider it for some occasional and non-specified condition. Only one response indicated that the only three-dimensional effect considered is the stress relaxation of the ground stress reduction by the 3D arching around the face.

For the mined tunnel case, a slightly higher tendency to consider 3D effects is apparent, but still the major part

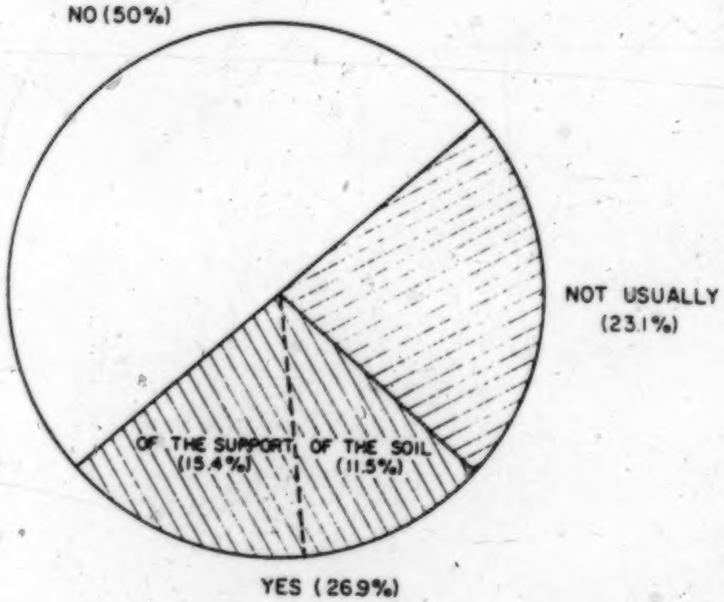

(26 responses ; shielded and mined tunnels combined)

Figure 4.14 Obligation to Account for the Non-Linear Behaviour of the Soil or the Support, in the Design of a Shallow Tunnel in Soil

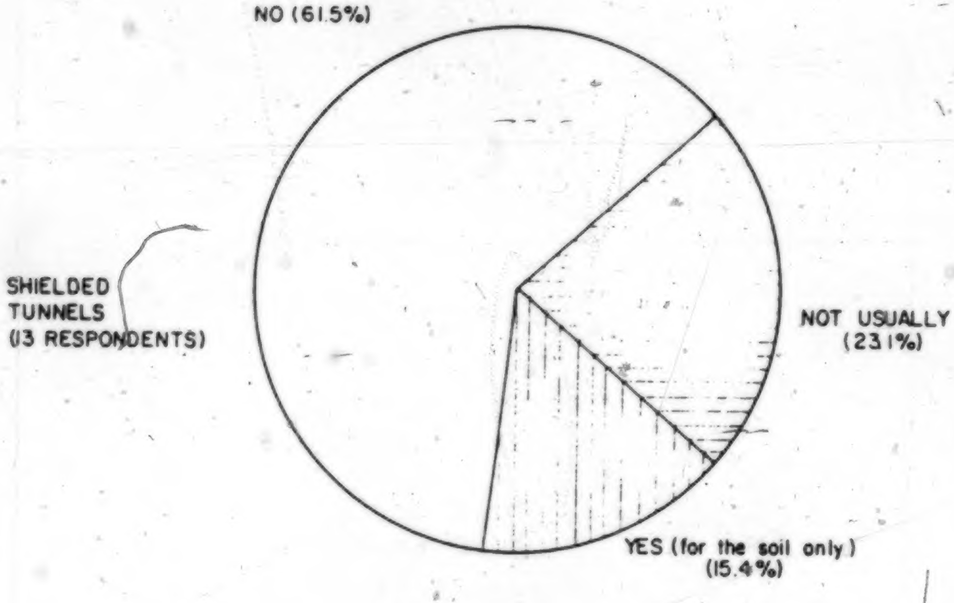

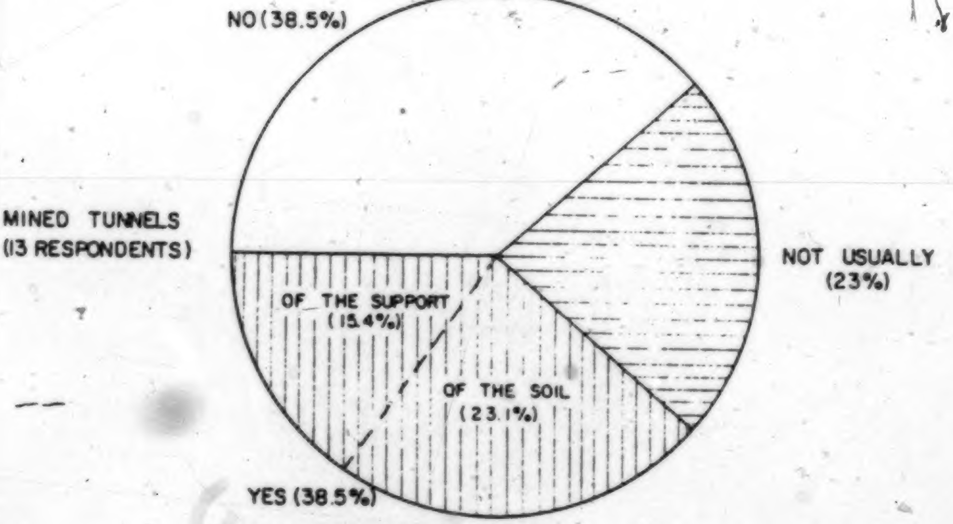

Figure 4.15 Obligation to Account for Non-Linear Behaviour of the Soil or the Support in Shielded and Mined Tunnels

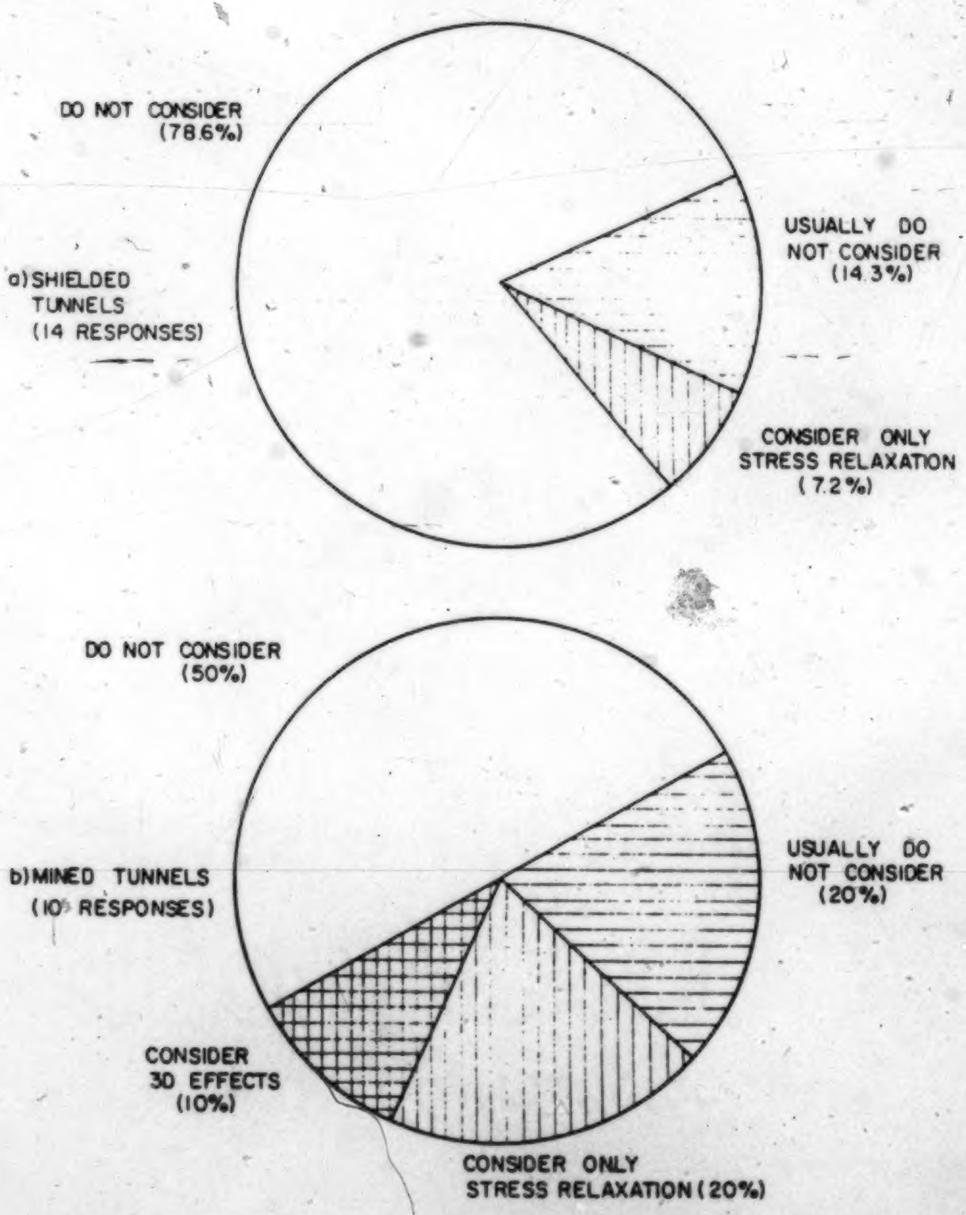

Figure 4.16 Consideration of Three-Dimensional Effects in the Lining Design of Shielded and Mined Tunnels

of the responses indicate no account is taken of these effects. Only one respondent stated that he does consider these effects, but on an empirical basis.

None of the respondents made any mention of possible load concentration in the leading edge of the lining that may result from the 3D soil arching around the unsupported heading. An assessment of the practitioners attitude towards this effect appeared to be the original intention of those who prepared the questionnaire. The responses seem to indicate that this effect is not considered in practice and when some three-dimensional action is considered, it is restricted to the ground stress relaxation induced by the face and heading excavation.

Finally the questionnaire asked (Duddeck, 1982:169) how factors of safety are employed in the lining design practice. Ten responses provided unclear or no answer to this question, and only the remaining 18 can be considered for the statistical analysis (Figure 4.17). No differences in distributions were detected for the mined or shielded cases, so the results are given in a combined form. One notes that the majority of the responses favour the use of partial factors of safety to the support section and to the soil loads. Another group of responses pointed out the use of both partial or global factors depending on the case.

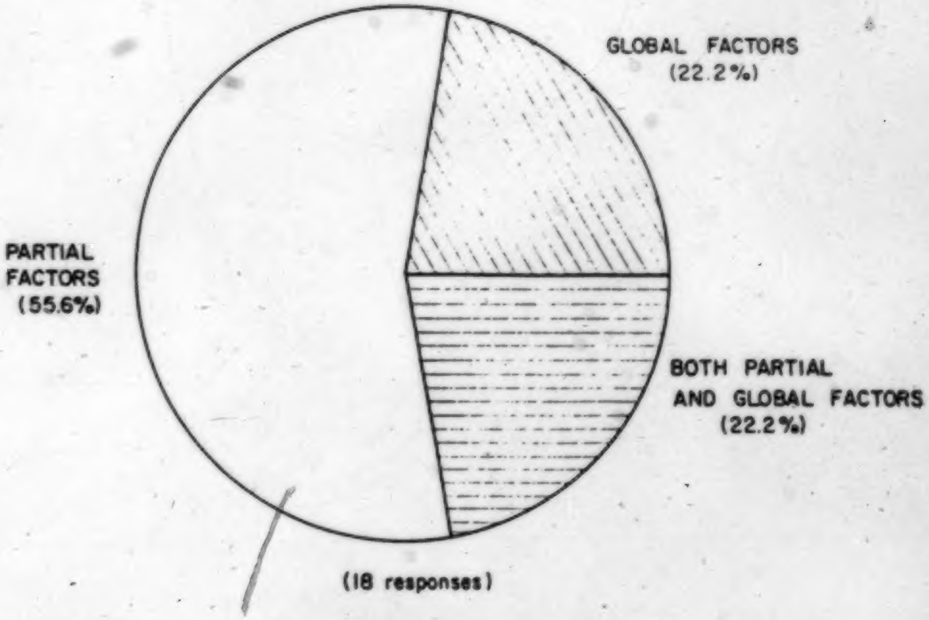

Figure 4.17 Factors of Safety used in the Design of Shallow Tunnels in Soil

4.4.2.3 Final Comments

Despite being recognized that the state of the in situ stresses has a major role in the design of the tunnel lining, a significant number of practitioners seems to believe that, for design purposes, it is sufficient to select a certain stress ratio (K), and use it for design. In so doing, the designer tends to select a conservative value for K, incorporating at the onset, an inbuilt and unknown margin of safety for the design. This reveals considerable departure from a typical design attitude, which is that of anticipating the actual behaviour of a structure under foreseen (even extreme) conditions, and providing it with a known , if possible amount of safety. Moreover, the practice of selecting an arbitrary K value, may in some cases be unsafe. This would be the case of those who fix a low K value, or who estimate it from the Poisson's ratio, if they were to design a tunnel in very overconsolidated soils, like London Clay, at shallow depths where K values in excess of 1.5 (in total stresses) can be observed.

For the shielded tunnel situation, practitioners tend to use a full overburden assumption for the lining design, whereas for the mined situation, they favour a reduced overburden assumption. Other respondents may or may not use the latter assumption in both tunnelling cases, depending on the type of soil, the relative depth of the tunnel or the type of lining. Unfortunately it was not possible from the answers collected, to identify the reasons for the different assumptions made. Parallel to the differences in construction technology in the two situations posed, including different lining systems, the two reference cases involved distinct ground conditions (more competent and water free ground in the mined case). Moreover, not necessarily the same individual replied to the questions for both situations, so that different personnal views might have affected the results. In addition, no details of the construction technology in each case were provided in the questionnaire. The respondents, therefore, were left unbound without a uniform view of how the two tunnels were to be built, and inconsistent interpretations of each situation posed, might have had a role in the results obtained. The conclusions included in the ITA report (Duddeck, 1982:219) suggested that the differences in the ground load assumptions depends on whether the support under consideration is the primary (shotcrete and ribs in the mined case) or the secondary or final lining (possibly prefabricated lining in the shielded case - not explicitly mentioned in the questionnaire, however). Although the writer was also tempted to draw the same conclusion, there is no firm indication from the data gathered that this is the case.

Also not answered by the survey are the reasons why or how those favouring the full overburden assumption support this reasoning. Does it reflect a belief that a shielded driven tunnel does not induce ground movements or stress release before lining application? Does it reflect a belief that the ground strength will be reduced to zero in a long term process? Most practitioners assuming a full overburden assumption take into consideration the interaction between the lining and the soil in the support design. This is in direct conflict if the shear strength of the soil supposedly fully deteriorates with time. Does it reflect an attitude towards providing an additional, built in, and somewhat hidden factor of safety to the structure being designed? Does it reflect an understanding that possible savings in the lining, otherwise designed with inconsistent and conservative assumptions, are marginal with respect to the overall cost of the tunnel (known to be mainly controlled by excavation and ground control costs)? Unfortunately, these questions remained unanswered by this survey and may be suggested as points to be included in similar investigations in the future.

Although empirical methods are still largely used for lining design, the survey indicated that ring and spring models are those most frequently used by the practitioners. This can be attributed to the facility of using available design charts for the continuous solutions, or to the current availability of microcomputers, which allow easy implementation of discrete solutions. These models can furnish good results, provided ground loads and spring constants are properly estimated. The constants usually seem to be calculated from elastic constants obtained through laboratory testing and using some approximate expressions. Not disclosed by the survey was how the elastic parameters are determined from the non-linear responses observed in the testing results. The success in applying these lining calculation models rely heavily on the correct assessment of some 'equivalent' elastic properties, which is not a simple task, especially in a problem in which the non-linear response of the soil is likely to play an important role.

It is interesting to note (particularly in the mined tunnel case), that most practitioners use a reduced overburden assumption for ground loads, combined with a ring and spring model to represent the lining and ground interaction. The usual criterion adopted to estimate the reduced ground loads is Terzaghi's arching theory. This appears to be somewhat inconsistent with Terzaghi's (1943:194) original ideas:

> "Part of the yield of the sand toward the tunnel occurs while the working face passes the section ... and the remainder takes place after timbering has been constructed. Owing to the imperfect fit of the timbers at the joints and the compressibility of supports of the footings of the vertical posts, the yield of the timbering is usually sufficient to reduce the pressure of the sand on the timbering almost to the value corresponding to the state of incipient shear failure in the sand. This state is similar to the state of stress in a mass of sand above a yielding strip."

In other words, Terzaghi suggested that the ground pressures derived from his trapdoor theory would include the effect of ground yielding both before and after lining installation, and the pressures it provides would approximate the final equilibrium pressure against the support.

By applying Terzaghi's reduced ground loads on an elastically embedded frame of a ring and spring model, the active loads will be shared between the latter and the former, according to their relative stiffnesses. The lining will end up sustaining a load at equilibrium which is lower than that given by the arching theory. Moreover, the combination of a limit state type of condition, represented by Terzaghi's theory, with an elastic model for soil-lining interaction analysis can be questioned or at least debated.

The reasons behind the slight trend towards the use of different lining calculation models for the primary and secondary supports were not fully grasped. Since the latter is usually installed far behind the advancing face, probably after the former attains a full equilibrium with ground loads, the secondary support is commonly designed to withstand any long term change in loads, as discussed in Section 4.2.1. Formally there is no apparent reason to require different calculation models. Perhaps that attitude still reflects the old design posture to treat the primary lining simply as a 'temporary' support, relegated in the overall design to a less important role and designed according to any simple empirical rule. At least 20% of the respondents (see Figure 4.13) seem to still share this view which nevertheless, is being changed, as noted in Section 4.2.1.

Most of the respondents did not feel any need to take into account the non-linear behaviour of either the soil or the lining in the shielded tunnel case. For the mined case, it was found that the account was felt to be more necessary, which is slightly surprising as far as the soil non-linearity is concerned. Indeed, in the second case, tunnelling conditions are more favourable and the magnitude of ground deformations are likely to be smaller. The more competent nature of the ground will also help this trend. If a linear elastic analysis was to be adopted in any of the cases, the chances are that the mined case could be better depicted by this approach.

It is apparent from the survey that no account is taken in practice regarding the possible concentration of loads on the lining close to the advancing face. If any three-dimensional effect were considered, it was the stress relaxation of the ground by arching or shear transfer around the face that ultimately reduces the lining loads.

Preference for the use of partial factors of safety was evident among practitioners. This is done by applying a factor to the ground loads and a capacity reduction factor to the lining section (or support strength), as recommended by some codes. Although not disclosed by the responses, it is believed that no fixed load factor is normally established for the ground loads, due to the varying degrees of conservatism frequently included in their evaluation, as noted by Paul et.al. (1983:134). Some factor is usually required to keep stresses and deformations in a structural member within tolerable limits when it is subjected to the operational ground loads. If the loads adopted in the design are the extreme envelope loads, and possibly conservatively estimated, the over-load factor could be less than that required when the lining is designed for the working ground loads which are expected to act on the support. This is so because the component of the load factor that accounts for the uncertainties in the loads, would already be implicitly included in the conservative estimate of the design ground loads. The other load factor which contributes to the overall safety margin, accounts for possible understrength of materials in the lining under operational conditions, and clearly should always be considered. Having this in mind, it seems preferable both in technical and economical terms, to estimate as simply as possible, the ground loads within a given range that are actually expected to act on the lining, rather than to work with a conservative assumption of this load as is frequently done.

4.4.3 Prediction of Ground Settlements

4.4.3.1 Survey of Practice

The principal purpose of this section is to report on the state-of-practice as it exists, regarding the prediction of ground settlements caused by shallow tunnelling. Although the writer was familiar to some extent with this practice in a few countries, both in South and North America as well as in Europe, it was decided to carry out a formal inquiry. This was done in order to avoid reporting the practice as the writer perceives it should be, and to avoid any other possible biased interpretation. Unlike the practice on lining design, which had already been formally surveyed, no inquiry had covered the present topic, to the writer's knowledge.

The inquiry was designed to cover the practice mainly in Western countries, as it stands presently within the designer's community. This was done by means of a questionnaire sent to practitioners known to be actively involved in designing underground urban systems at the time of mailing.

Similar surveys conducted previously by other authors, revealed that a reduced reply rate would be expected if the number of subjects or topics addressed was too large or if the number of questions was too many. For example, an inquiry recently conducted by Focht and O'Neill (1985:188), on the design of deep foundations, required answers to 36 questions, either in multiple choice form or in descriptive form. The questionnaire was sent to 66 active consultants but disappointingly only 11 (17%) of them were returned. Since one of the goals of the present survey was to have a representative reply, it was decided to limit the questionnaire to a single page, including only five questions with multiple choice answers, but allowing free comments. It was suggested to the respondents to indicate only one answer per question, but mulitple answers and any comments included by some were interpreted in the subsequent analyis. To further boost the reply rate, a self addressed envelope was included in the mail. It is believed that these combined measures justified the fairly high return rate of nearly 70%. The price paid for it, however, was that the survey had to cover the subject in a fairly circumscribed and simple manner, since more involved questions, demanding detailed answers were intentionally avoided. Nevertheless, it is believed that the results fulfilled the intended goals.

The questionnaire prepared is reproduced in Table 4.15. As is seen, the questions included a focus on ground displacements caused solely by the construction of shallow tunnels driven in soft ground in urban environments, by means of any type of tunnelling procedure. When answering the questions, the respondents were invited to disregard all components of time dependent movement due to soil consolidation or creep.

The questions were sent to 50 practitioners in 17 countries, where active urban tunnelling practice was evident during the first half of the current decade. Table 4.16 lists the number of questionnaires sent to all those countries, mostly located in Europe and secondly North and South America. Table 4.16 also shows the number of questionnaires returned, the percent returned of number sent, and the percent distribution of total questionnaires returned. The latter provides the weight of each country surveyed on the global results obtained. Therefore answers coming from West Germany affect the statistical results that will be shown, by 18%, followed by Brazil (15%), Canada and the U.S.A. (12% each). Regionally speaking, the survey results will represent firstly the European practice (47%) followed by North and South American practices (26 and 18% respectively).

The returns were approximately in proportion to the number sent, except for a few countries such as Belgium, Argentina, England and Japan, that end up being underrepresented in the survey by their lower return rate.

As noted previously, the questionnaire was sent basically to those involved with routine design practice of shallow tunnels. As indicated in Table 4.17, most of the respondents (74%) are connected with consulting engineering firms or have their private consulting practice. The remaining respondents work in other types of organizations, but also in design related activities. This is notably the case of contractors in West Germany and Japan, which include an in-house consulting or design group to whom the

The questions below focus on ground displacements caused by construction of a shallow tunnel driven in soft ground (including soft rock), in an urban environment, using any type of tunnelling method (TBM, NATM or other). Time dependent settlement components due to consolidation or creep are not part of this research and as such should be disregarded in answering the questions. Please mark only one answer per point.

1) In the design of a tunnel as defined above, do you normally perform a quantitative prediction of settlements induced in the ground?

a) ☐ Yes
b) ☐ No

2) If the answer to question 1 is "Yes", then, what procedure or method do you most often use for your settlement prediction?

a) ☐ Judgement or simple analysis based on past experience in similar conditions

b) ☐ Empirical method using some mathematical function

c) ☐ Peck-Schmidt method

d) ☐ Numerical procedures such as the finite element method

e) ☐ Method developed from parametric numerical analyses (e.g. Reséndiz and Romo, 1981). (Specify which: ....).

f) ☐ Other (Specify: ....).

3) If you could specify just one single most significant factor of the method you indicated above, it would be:

a) ☐ its simplicity
b) ☐ its reliability
c) ☐ its theoretical rigor
d) ☐ its widespread acceptance or use
e) ☐ other (Specify: ....)

4) Under favourable ground control conditions, the loads that finally act on the (primary) support system appear to be related to the magnitude of the displacements induced by tunnelling (concept of the ground-support reaction curves or the convergence-confinement model). In your normal design practice, do you estimate ground settlements according to the estimate of the loads on the primary lining (or vice-versa)? In other words, do you couple settlement and loads predictions?

a) ☐ Yes

b) ☐ No

5) If the answer to question 4 is "Yes", then, how do you do it?

a) ☐ By using the finite element method
b) ☐ By using other numerical methods (Which? ....)
c) ☐ Other (Specify: ....)

Respondent: ....

Address: ....
....
....

Table 4.15 Questionnaire on Ground Movements Caused by Shallow Tunnels

Region/Country	Number sent	Number returned	Percent returned of number sent	Percent of total returned
Europe				
Austria	3	2	67	6
Belgium	1	0	0	0
Czechoslovakia	1	1	100	3
England	3	1	33	3
France	2	1	50	3
W. Germany	6	6	100	18
Hungary	2	2	100	6
Spain	3	2	67	6
Switzerland	1	1	100	3
	22	16	73	47
North America				
Canada	5	4	80	12
U.S.A.	6	4	67	12
Mexico	1	1	100	3
	12	9	75	26
South America				
Argentina	2	0	0	0
Brazil	6	5	83	15
Venezuela	1	1	100	3
	9	6	67	18
Africa				
Egypt	1	1	100	3
Asia				
Japan	6	2	33	6
TOTAL	50	34	68	100

Table 4.16 Questionnaire Response on Ground Movements

questionnaires were sent. The global distribution of the type of practice of respondents is illustrated by the chart in Figure 4.18. The names and affiliations of all contributors are listed in Appendix B.

4.4.3.2 Results of the Survey

The first question asked whether or not a quantitative prediction of ground settlements was normally performed by the practitioner in his tunnel design routine. As shown in Figure 4.19, the vast majority of respondents said yes to this question. A minority group seems to limit their practice in shallow tunnel design to the structural definition of the support system.

The next question asked what procedure or method the designer mostly used in his routine settlement prediction. Although asked to answer only one answer, some respondents (23.5%) marked more than one, without an indication of which is the procedure they most used. These were grouped as "multiple answers", being identified as those who combine different empirical or semi-empirical approaches and those who combine numerical and empirical approaches. The result of the statistical analysis on replies to this question is summarized in Table 4.18. Procedures 1 to 4 in Table 4.18 could be gathered as an "empirical or semi-empirical approach" group. Procedures 5 and 6, could be termed as a "numerical approach" group. Therefore the results could be re-arranged as shown in Figure 4.20. Fifty percent of the respondents favour an empirical or semi-empirical approach.

Region/country	Consulting Engineering	Other (owners, contractors, researchers)
Europe		
Austria	2	-
Czechoslovakia	-	1
England	1	-
France	1	-
W. Germany	2	4
Hungary	2	-
Spain	1	1
Switzerland	1	-
	10	6
North America		
Canada	4	-
U.S.A.	4	-
Mexico	1	-
	9	-
South America		
Brazil	5	-
Venezuela	1	-
	6	-
Africa		
Egypt	-	1
Asia		
Japan	-	2
TOTAL	25	9
	(74%)	(26%)

Table 4.17 Type of Practice of Respondents

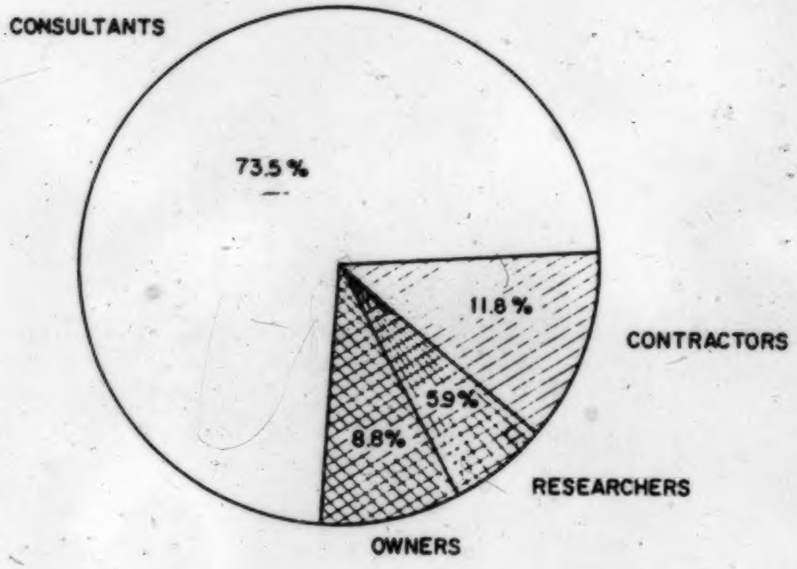

Figure 4.18 Type of Practice of Respondents

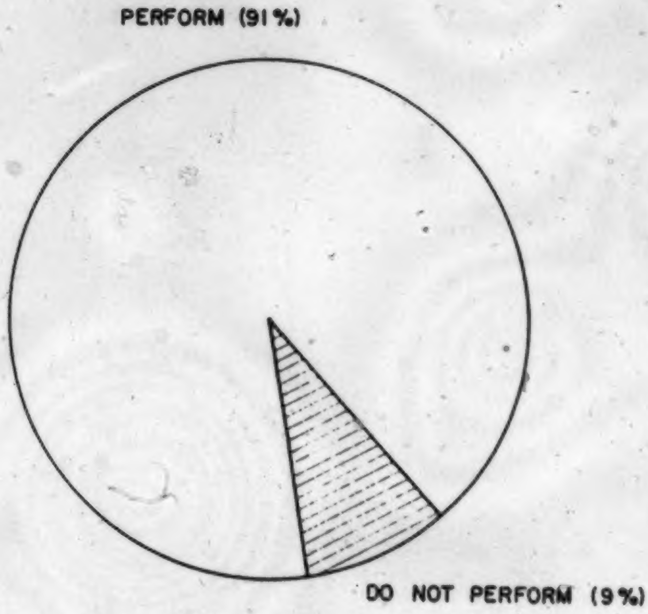

Figure 4.19 Distribution of Respondents that Normally Perform Quantitative Prediction of Settlements Caused by Shallow Tunnelling

That percentage is even higher (62.5%) among European practitioners.

Only 18% of the respondents showed sole preference for a fully numerical prediction. Among this group, the majority (83%) indicated that their preference lies in the finite element method and one respondent indicated the boundary element method as his most frequent choice. Those respondents who indicated that their preference, in routine practice, lies on an equal combination of numerical and empirical approaches amounts to 18% of the total. Among these, only one uses a numerically derived method combined with some empirical procedure. Therefore, 32% of the respondents declared that they normally use a fully numerical approach for ground settlement prediction, either solely or associated with some empirical method. This percentage is lower in Europe (19%) and higher in South America (50%).

Out of the larger group favouring an empirical approach (17 respondents), 35% do so by using judgement or some simple analysis based on past experience in similar conditions. These respondents are followed in number by those who use the Peck-Schmidt method (29%). The use of this method seems to be more frequent in Europe than elsewhere.

The third question asked the practitioner to single out one quality he would ascribe to his most used prediction method, which could be understood as a key attribute explaining the reason for preference. Figure 4.21 shows that

	Procedure/Method	No. of Respondents	Percent of Total
1.	Judgement based on past experience	6	17.6
2.	Empirical with some mathematical function	4	11.6
3.	Peck-Schmidt method	5	14.7
4.	Combined empirical methods	2	5.9
5.	Numerical procedures	6	17.6
6.	Numerically derived method	2	5.9
7.	Combined numerical and empirical methods	6	17.6
8.	No answer or do not predict	3	8.8
	TOTAL	34	100

Table 4.18 Preferred Approaches Indicated by Respondents for Ground Settlement Prediction

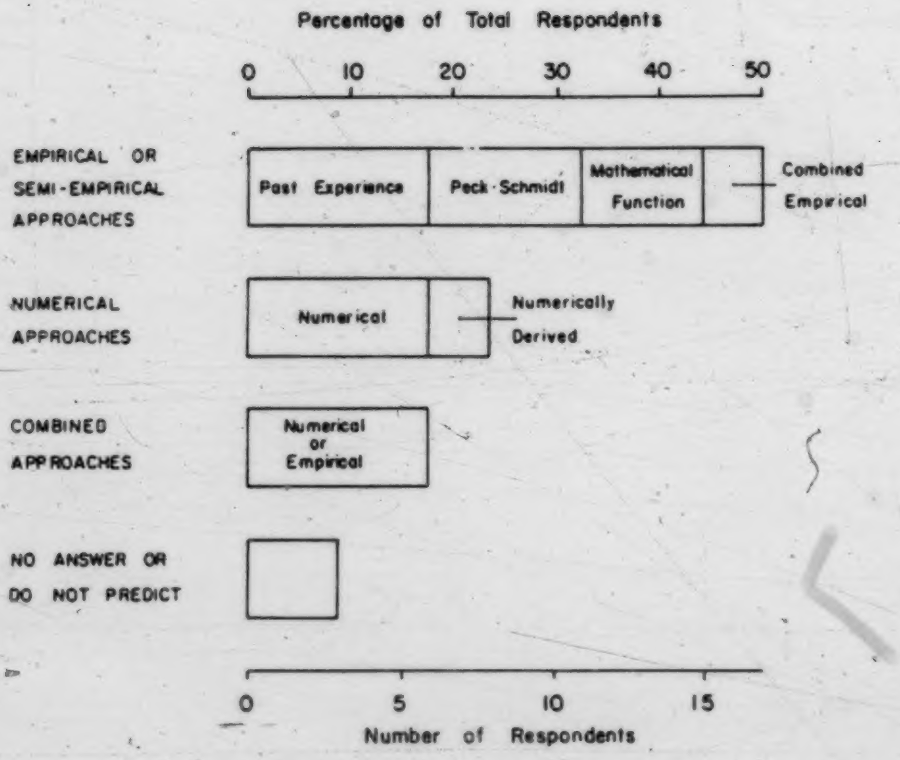

Figure 4.20 Distribution of most often used Methods for Settlement Prediction among Respondents

the leading attributes of a predictive method are its reliability (26.5% of respondents) and its simplicity (23.5%). Hence if a method is proved reliable and simple, it would possibly be accepted by 50% of the practitioners. Moreover, 15% of the respondents did not specify a particular attribute, but follow what is widely accepted or used in practice. In other words, any predictive tool being reliable and simple would be used by almost two-thirds of the design community. On the other hand, a mere 3% of the respondents indicated that their preference lies in the theoretical rigour of the prediction method. Some of the respondents (15%) could not simply select one single quality and pointed out more than one attribute among those listed. Additionally 12% made reference to some non-listed qualities.

If one cross-analyses the answers to the second and third questions, it is possible to identify what method or procedure each attribute is addressed to. The results of this assessment are shown in Table 4.19 and Figure 4.22. The latter summarizes the noted qualities of the "empirical" and of the "numerical" approaches for prediction normally made by the practitioners (17 and 14 individuals respectively). It is interesting to note that the distribution of attributes within each of these two groups of approaches are very different. While reliablity and simplicity is responsible for 76.5% of the qualities preferred by the respondents within the "empirical group", those favouring

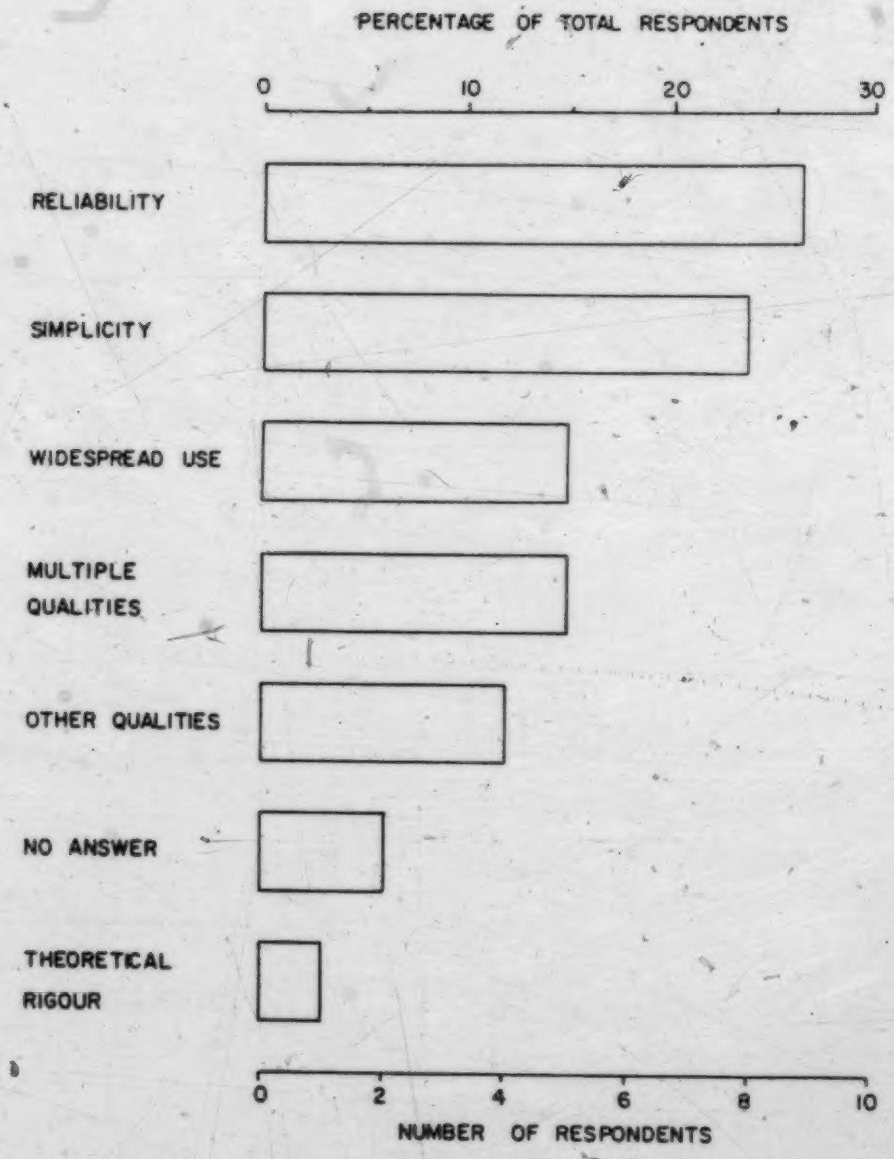

Figure 4.21 Basic Qualities of any Settlement Prediction

the numerical approaches made reference to "multiple qualities", to "widespread use" and to other qualities. Some of the latter qualities referred to were the possiblity of the numerical methods to allow sensitivity studies of certain parameters, to investigate the effect of the staged excavation of the tunnel, or of the effect of non-circular profiles of the tunnel cross section, as well as the possibility of obtaining settlements at points of the ground other than at the surface. Contrary to those who favoured an empirical approach, reliablity is a quality rarely referred to by those preferring a numerical approach. Also interesting is the fact that "theoretical rigour" is a quality seldom noted by those using a numerical approach. Very few respondents admitted that this approach is simple.

The next question asked whether the practitioner does or does not couple ground settlement and lining load prediction in his normal design practice, provided good ground control conditions are anticipated. The question was formulated after being stated that if these conditions prevail, it has been noted that the loads on the (primary) support appear to be related to the magnitude of induced ground displacements. Figure 4.23 shows that the larger part of the respondents (59%) declared that they either do not ever couple lining loads and settlement predictions, or do not usually do it, except under some special circumstances, as for NATM applications or for relatively deep tunnels as quoted by some respondents of the latter group. Among the

Group Method	Simplicity	Reliability	Theoretical Rigour	Widespread Use	Other	Multiple Attributes	No indication of attribute	Total
Empirical or semi-empirical	6	7		2	1	1		17
Numerical	1		1	1	2	1		6
Numerically derived	1				1			2
Combined numerical and empirical		1		2		3		6
No indication of method		1					23	2
Total	8	9	1	5	4	5	2	34

Table 4.19 Noted Qualities for Different Settlement Prediction Procedures

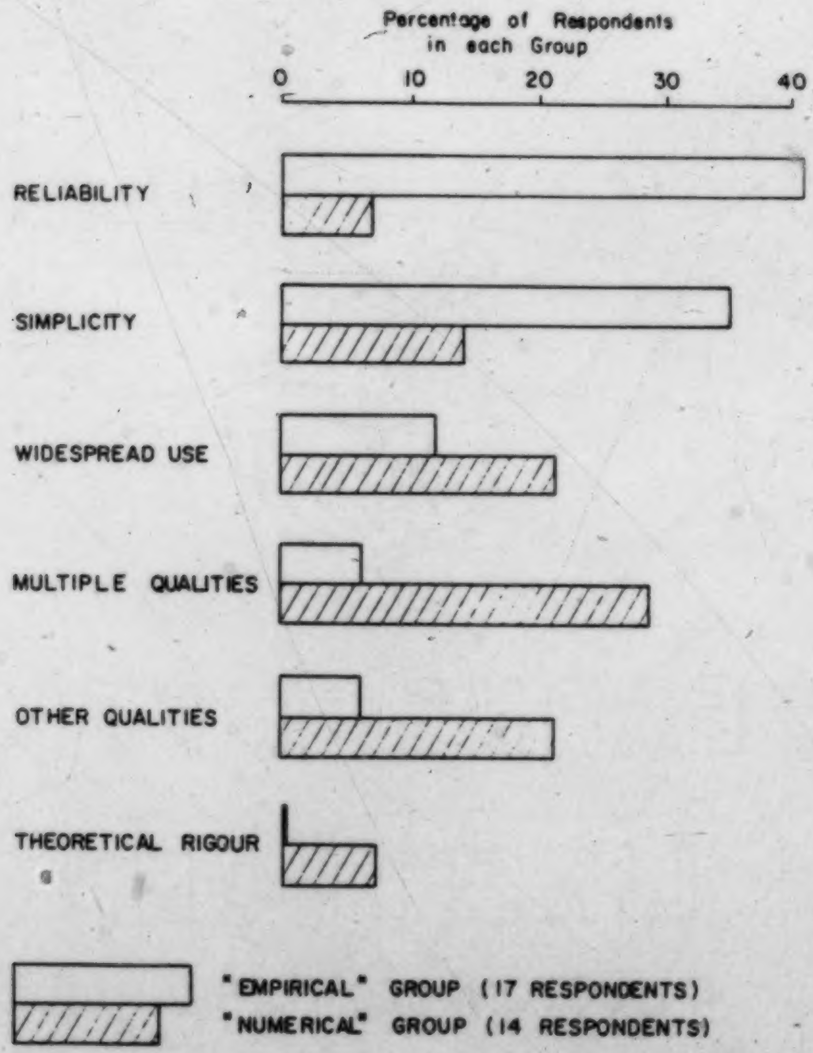

Figure 4.22 Noted Qualities of the "Empirical" and "Numerical" Approaches for Settlement Predictions Routinely Performed by Practitioners

remaining group declaring that they couple load and settlement predictions, one respondent suggested that his normal practice is to design the tunnel for "unfavourable" or "poor ground" control conditions. For these, the stated relationship between loads and displacement may no longer hold, as discussed in Chapters 2 and 3 of this thesis. It will be seen later, that inconsistency has been detected in some replies which makes one think that the number of practitioners actually coupling settlements and lining load prediction to be even smaller than indicated.

The last question asked the practitioner to explain how he does the coupled prediction. The answers by those 14 practitioners who said they usually perform the coupled prediction, are interpreted in Figure 4.24. The majority of those respondents (64%) declared they do it using the finite element method, 21% said they also use the finite element method combined with other procedures, and the remaining individuals declared they use other numerical methods (the boundary element method, for example). Hence, all respondents said that they perform the couple prediction, making use of some numerical tool, the finite element method being most commonly used (86%).

By cross-checking the answers to questions 2, 4 and 5, a few inconsistencies were detected in the replies of six respondents. Typically they admitted in answering question 2 that in their routine practice they favour some simple empirical analysis for ground settlement predition. By

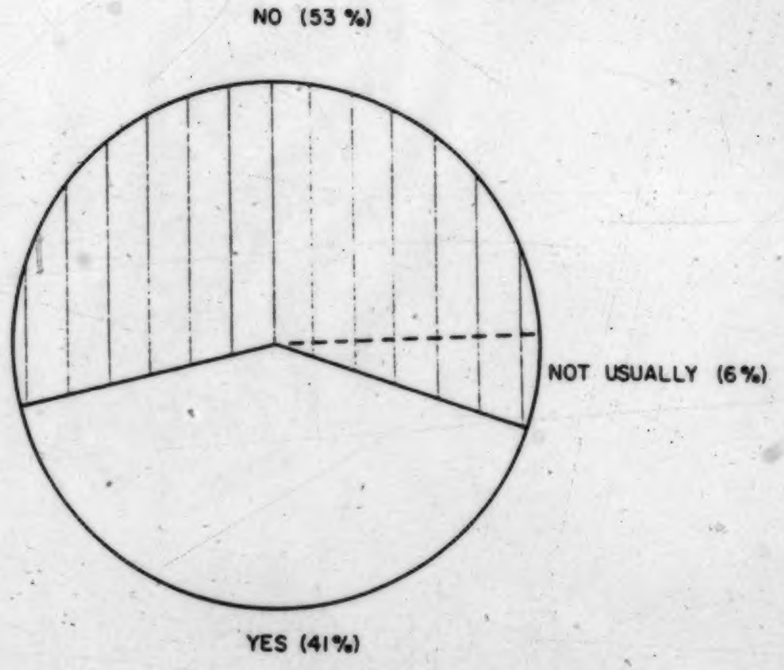

Figure 4.23 Distribution of Respondents Affirming they Couple Settlement and Lining Load Prediction in their normal Design Practice

possibly misunderstanding the statement of question 4, which also invited an answer regarding their routine practice these respondents apparently and contrary to their reply in question 2, admitted in answering question 5 that they use a numerical approach (the finite element method in all cases) to couple settlement and load predictions. Since no further elements were available to ellucidate this point, the answers were accepted as they were and thus included in the statistical analyses. However, if they were to be excluded, then the percentage of practitioners performing coupled prediction of loads and settlement would decrease from 41 to 29%.

4.4.3.3 Final Comments

The survey conducted revealed that quantitative prediction of ground settlements caused by shallow tunnelling in soil is routinely done in practice by almost all designers. It also showed that despite the significant developments in basic and applied soil mechanics, a great deal of empiricism remains in tunnelling design practice. This became apparent through the answers of 50% of the practitioners that still use empirical approaches for the solution of the ground settlement prediction problem. However, it could be expected that this amount may decline with the increasing availability of computer facilities and with further development of other numerically derived design procedures. In fact, the two procedures referred to by respondents, that belong to the latter class of solutions

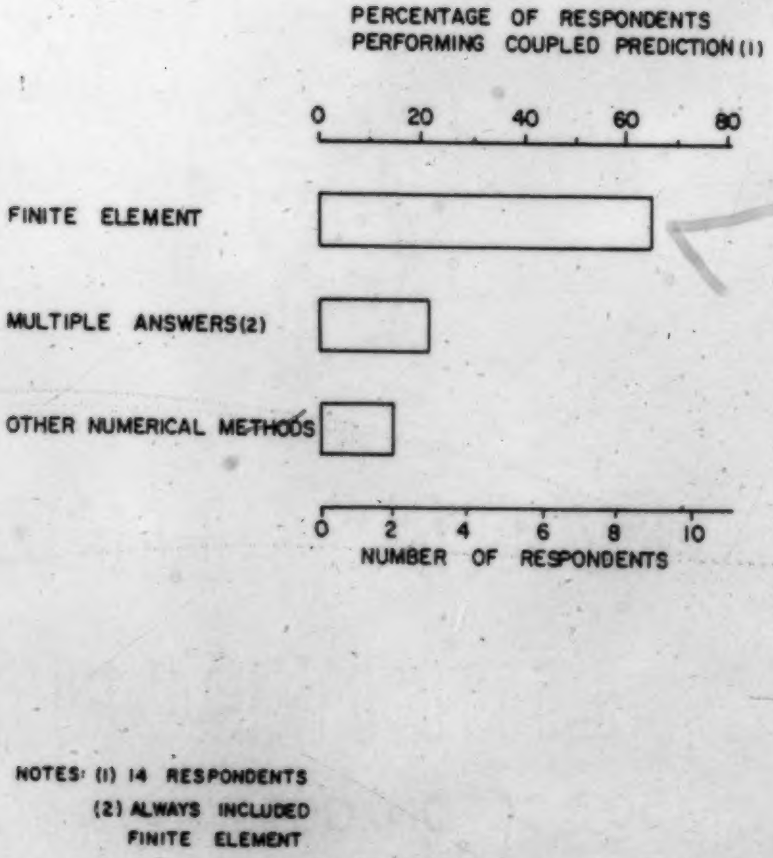

Figure 4.24 Distribution of Approaches Used for Coupling Ground Settlements and Lining Load Predictions

were developed recently and were made available in the early years of this decade (Resendiz and Romo, 1981 and Oteo and Sagaseta, 1982). Regardless of this, it is believed that none of the numerical approaches will ever preclude the use of knowledge based on previous experience.

Reliability and simplicity are the basic qualities required by the majority of practitioners for any method of settlement prediction. These are the two attributes noted by most respondents favouring empirical approaches. It seems commonly accepted that only the methods validated by past experiences are deemed acceptable in practice. Practitioners are not highly demanding with respect to the theoretical rigour of a prediction method.

Innovation in contruction practice tends increasingly towards a better ground control condition, represented by reduced ground movements. Although the dependence between the latter and the magnitude of lining loads is widely recognized particularly under the above conditions, certainly more than half of the practitioners (possibly more than two-thirds of them) do not couple the predictions of settlements and the support loads. Those who couple these predictions do so by means of finite element analyses, generally without claiming that this numerical procedure is either reliable or simple. It seems that the way to proceed is towards the use of simple numerically developed methods, calibrated against and possibly coupled with past experience, to render to the required attribute of reliability.

4.5 Summary and Conclusions

This chapter presented a review of available methods for the geotechnical design of shallow tunnels and a survey of the current design practice.

There are certain features specific to tunnels in soil that make their design slightly dissimilar from the design of other geotechnical structures. Included among these features are the definition of the loads acting on the lining, the need to take into account the lining-ground interaction, the acceptance of fairly low factors of safety, and the rapid development (in time) of deformations induced by the tunnel advance.

Basic Design Requirements

The basic requirements for the geotechnical design of a shallow tunnel were reviewed and discussed as related to the lining design, to the prediction of ground movements and assessment of the damage potential to neighbouring constructions, and to the verification of the excavation stability.

The tunnelling performance, defined by the response of the ground and of the support system, is directly related to the quality of the construction. In the discussion of the design requirements, it was assumed that the tunnel is to be built under what has been termed 'good ground control conditions'. These are represented by controlled and limited ground movements, avoidance of instability processes, limited soil overcutting in TBM excavated tunnels, minimized delay of support activation, good lining-ground contact, and minimized groundwater drainage into the tunnel and the associated consolidation settlements. Although described here in rather qualitative terms, some effort was directed in Chapters 2 and 3, to tentatively define quantitative criteria allowing the identification of such conditions. Under poor ground control conditions, the tunnelling performance may not be entirely predictable.

Regarding the lining design requirements, the discussion was mainly confined to the primary lining, where the geotechnical component of design is more evident. Though the design requirements focussed predominantly on the operational loads for the primary lining, some attention was paid to transient loading conditions that may represent a controlling design factor in certain cases. Under operational loads, for good ground control conditions and good lining-ground contact, the structural failure of a circular tunnel lining can result from the combined action of thrust and bending. Other modes of failure are possible, but are not usually observed.

In the design, it is customary to assume a linear elastic behaviour for the lining. This assumption is usually a conservative one, with respect to the assessment of the lining capacity. In modern design of linings with small eccentricities (and associated small bending moments), the linear elastic assumption does not lead to excessively conservative results.

The requirements for lining design also include the assessment of the lining capacity, of lining response to possible external loading conditions (excavations, parallel tunnel construction, etc.) and of lining deformations.

The design requirements for the secondary lining were also briefly discussed, with comments being made regarding current trends to integrate the design of primary and secondary linings.

The requirements for ground displacement prediction was then discussed, as related to the need for evaluating the potential risk of damage to neighbouring structures and utilities. Similar to the basic lining design requirement, an estimate of relevant quantities is required as well as an assessment of the appropriate capacity (damage potential to existing structures). Unlike lining design, the interaction between the ground and nearby structures is not fully accounted for in usual practice. An exception to this is the procedure presented by Attewell et.al. (1986:237), but it treats the tunnelling induced ground movements in an empirical and oversimplified way.

The existing criteria for assessment of the onset of damage to existing construction at the ground surface were reviewed. Most were derived from observations made in prototypes and are mainly empirical. The different approaches available to evaluate the building performance subjected to ground movements were discussed. Most originated from observations of building damage related to settlement caused by the structure selfweight. Cording et.al. (1976), proposed an empirical criterion derived from field observations made in structures adjacent to tunnels and open cuts, which is more appropriate to the present case. The damage magnitude was related to the average angular distortion of the ground surface (discounting the structure tilt). The need to investigate in future research, the three-dimensional distortional effects on existing constructions upon tunnel advance, was pointed out.

Finally, a brief review was made of the criteria and methods for assessment of the consequences of tunnel induced ground movements on buried pipelines. Considerable advances in the subject have been achieved over the last decade. It is worth mentioning that most methods available take into consideration the interaction between the ground and the buried pipeline. The main limitation of the above procedures is that the tunnel induced displacements are estimated using rather arbitrary assumptions which are predominantly empirically formulated. There is a clear need to supplement these methods with a more adequate treatment of the tunnelling induced ground movements.

The verification of tunnel stability is usually circumscribed to the stability of the unsupported excavation of the heading and face. The problem is three-dimensional and its solution involves considerable approximation.

Plasticity solutions are usually preferred to limit equilibrium approaches, unless the mode of failure is well known. Available plasticity solutions do not allow a treatment in terms of effective stress, so that the influence of pore pressures cannot be explicitly assessed. Two classes of solutions are available, where the soil response is represented either by an ideal undrained condition or by an ideal drained condition (with no pore pressures). Hence, it is important to identify the pore pressure responses in terms of the rate of dissipation, compared with the anticipated rate of tunnel advance. The stability assessment under steady state ground water flow is usually done for idealized two-dimensional conditions, with no solution being available for the actual three-dimensional problem.

The minimum acceptable factor of safety is defined in terms of maximum tolerable ground deformations. An interpretation of tunnel model test data undertaken in Chapter 2 indicated that good ground control conditions are achieved whenever the dimensionless crown displacement (U) is less than 1. This condition corresponds to factors of safety typically greater than 1.5, but this figure is not a rigid reference, since different displacement magnitudes are expected for different soil types, for the same factor of safety. Thus, lower values may be accepted for stiffer or denser soils (possibly 1.3 to 1.4) and higher values may be required for softer or looser grounds (e.g. 1.6 to 1.7).

Another requirement for the stability evaluation is the assessment of the soil strength. This point deserves special consideration when dealing with some stiff fissured clays. An example of this assessment was provided.

If the stability condition is not acceptable, or if ground displacements are excessive, ground control measures should be considered as an integral part of the geotechnical design of the tunnel. These control measures were classified into six groups. The techniques available for each group type were described and the action of each type of measure was identified. Reported examples of application of these control measures in soil tunnelling were furnished.

Having established the main requirements for the geotechnical design of a soil tunnel, a review of available design methods was undertaken.

Available Methods for Prediction of Lining Loads

The methods for prediction of lining loads were classified according to the basis of their development.

The empirical and semi-empirical methods include the earth pressure theories and the methods in which the lining performance is specified beforehand.

In the earth pressure theories, the ground loads are usually independent of the ground displacements and typically, the lining-ground interaction is disregarded. The ground loads to be applied to the lining are normally derived from considerations or theoretical models that imply substantial shear strength mobilization in the ground. This 'external' load (also referred to as 'gravity' load) approach corresponds to conditions of poor ground control, represented by large ground displacements, a large degree of 'loosening' and poor lining-ground contact. Though reflecting conditions commonly found in the past when these methods were developed, they correspond to conditions which are hardly acceptable for present requirements of urban tunnelling. By neglecting the ground-lining interaction, a conservative lining design is attained. However, the displacement independent earth pressure load assumption, may or may not lead to conservative lining design, in cases where the construction quality is good.

The methods that specify tunnel lining performance were developed in the U.S.A. by Peck and co-workers. They represent a development with respect to the older empirical methods just described, as they recognize (in an approximate way) the lining-ground interaction. They are more consistent with modern tunnelling practice, asking for flexible lining design and good construction quality. According to these methods, a circular tunnel lining should be designed for a uniform ring compression, corresponding to the overburden pressure at the springline, plus an arbitrary imposed distortion measured as a percentage change in the lining radius. As noted in Chapter 3, the full overburden assumption is debatable, since in most cases, it is not substantiated by practical or theoretical evidence. The arbitrarily imposed distortion generating bending stresses, is not consistent with the uniform lining compression assumption, since this calls for an ideally flexible and incompressible lining which does not generate bending moments. According to this approach, lining bucking is examined for a uniform load condition, under which, this type of instability is a rare occurrence, for usual tunnel depths and sizes.

The second group of methods reviewed for lining load prediction, included the ring-and-plate analytical solutions.

These solutions are divided into two categories, according to whether the type of in situ stress field they assume is uniform or non-uniform. In both cases, they are analytically developed as closed-form solutions which are very easy to handle.

The uniform stress field solutions include the so called convergence-confinement models. The particular state of stress they assume and the assumption of material isotropy, allow an independent assessment of the ground and of the support reactions. The evaluation of the interaction process, is therefore, greatly simplified, since no distortion of the lining occurs. This simplification allowed the treatment of the ground response using fairly complex constitutive relationships. For that they can be very useful in qualitative design estimates, but the impossibility to account for the lining bending in non-uniform stress conditions, makes the use of these solutions very restrictive for practical use in shallow tunnel design.

The non-uniform stress field solutions assume a state of plane strain and all, but one, assume the circular tunnel to be ideally deep, so that the action of gravity is disregarded. The non-uniformity due to stress ratios different from unity, gives more generality to these analytical solutions, but at the price of having to assume simpler linear elastic material behaviour for the lining-ground interaction analysis. Fourteen different solutions were reviewed, focusing on their assumptions, abilities and limitations. Some assume an external overpressure loading condition which is not applicable to the tunnelling problem. The lining-ground interface is usually treated by a full or non-slip condition. In Chapter 2, it was contended that the latter condition usually represents an assumption closer to reality.

Among the solutions in this group, the most useful, although least used or referred to, it that by Hartmann (1970, 1972). It is the only one that fully accounts for the action of gravity. However, like other approaches, it neglects the presence of the ground surface, but, as indicated in Chapter 2 and further discussed in Chapter 7, this is not a very restrictive assumption, provided the cover to diameter ratio is greater than 1.5. For deep tunnels, the effect of the ground surface on the lining-ground interaction is immaterial, though the influence of the gravitational stress field is not.

The major deficiency of this group of solutions is the lack of ability to account for the effects of delayed lining installation. These are represented by the stress and stiffness changes in the ground prior to lining activation, and are always present in real problems (see Chapter 2). In particular, even if an initial homogeneous ground condition could be accepted, by the time the support is installed, a non-homogeneous ground condition would have been developed, as the non-linear soil at different points around the tunnel, would have undergone different degrees of straining, implying different degrees of stiffness degradation.

The third group of methods for lining load prediction included the ring-and-spring solutions. In these solutions the ground is represented by an infinite or finite number of springs (continuous or discrete ground reactions). Twelve different solutions were reviewed, with emphasis on their assumptions, features and limitations. These closed form solutions were either analytically or numerically approached, through the use of design charts or else requiring a computer program code for application.

Most solutions within this group assume a partial ground embedment, with no ground reaction considered at the crown region. This representation is derived from the assumption that a fully developed failure zone will always be generated above the tunnel, confined by two slip surfaces rising upward from the opening and intercepting the ground surface. This assumption implies accepting an extreme collapse condition, which will not prevail if adequate ground control measures are ensured, as they should be in urban tunnelling. The absence of ground embedment is assumed in the upper 90° or 100°, on the assumption of a tunnel roof collapse. This is also a very arbitrary assumption, as it is known (see Sections 2.2, 3.2 and 4.3.4) that, depending on the soil strength and on the geometry, other modes of collapse may develop. Accordingly, the partial embedment assumption would have to be further extended to the tunnel walls. For normal conditions, the assumption of 'embedment absence' could more sensibly be replaced by a 'weakened' or 'softened embedment' assumption.

In most solutions of this group, only radial springs are considered. Tangential springs are considered in a few cases in an attempt to obtain a better correspondence with the ring-and-plate solutions. The assumption of radial springs only will normally lead to safer estimates of the lining loads.

Some solutions are inaccurate, in that they neglect to consider the shear stresses at the lining-ground interface as an active load. Hence, as in Muir Wood's (1975) original ring-and-plate solution, they do not take into consideration the deformation components due to the full slippage condition.

Two main types of ground load assumptions are normally made: in situ stress and localized gravity loading. In the first, the lining is assumed to be installed in the ground before excavation takes place. This assumption of full ground loads is not consistent with the assumption of partial embedment, which requires considerable ground movement (thus, in situ stress relaxation) to realize it. The acceptance of these two assumptions combined implies assuming zero shear strength and zero shear stiffness along the two slip surfaces in the tunnel cover. This is clearly not realistic and is overconservative. The localized gravity loading at the crown (see Chapter 3) imply an acceptance of localized roof collapse and stable tunnel walls, and once again, these are conditions which are not compatible with good ground control and good lining-ground contact required in urban tunnelling.

Most of the ring-and-spring solutions assume that the tunnel profile is circular but some treat non-circular cross sections. This is one of the features that makes these solutions very attractive for practical use.

Other features reviewed referred to the account of geometric non-linearities and of the gravitational stress field in shallow tunnels.

It was shown that it is possible to find a complete correspondence between ring-and-plate and ring-and-spring solutions, provided in the latter, an infinite number of springs (continuous ground reaction) and that both radial and tangential springs are considered. The equivalence between the two types of solutions was illustrated for an unlined circular tunnel under a gravitational stress field.

The equivalent spring constants were found to depend on the position on the tunnel contour, on the in situ stress ratio, on the relative depth of the tunnel and on the elastic parameters of the corresponding continuum. The equivalence for a lined tunnel could also be found but was not attempted.

It was also shown that a complete correspondence between ring-and-plate and ring-and-spring solutions, with discrete ground reactions is not possible.

The deficiencies of this group of solutions are similar to those discussed for the ring-and-plate since no account of delayed lining activation (ground loads and stiffness reduction) is undertaken. The present solutions seem to show slightly more potential, in that with them, it is possible to account for different ground stiffness changes at the instant of lining activation, by ascribing different spring constants at different points of the tunnel contour. The differential stiffness changes around the tunnel were discussed in Chapter 2.

The fourth group of methods for lining load prediction included the numerical solutions, where the ground is treated as a continuum. The finite element method is the one most frequently used within this group, though other numerical solutions could be included. By treating the soil as a continuum, lining loads and ground displacements can be obtained simultaneously, which is one of the most important features of this group of models. The problem can be treated by two or three dimensional analyses, but the latter tends to be too complex for practical use. The use of finite element techniques in shallow tunnel design was not covered in this chapter but in other sections of this thesis. In Section 5.2.1.1 a brief review is presented on lining representation and on lining material modelling. In Section 5.2.1.2, an attempt is made to assess the ability of two-dimensional finite element analyses to predict lining loads in existing tunnels. Further comments on the subject are included in Section 5.2.2.1 and three-dimensional modelling is discussed in Section 5.3.

Two-dimensional finite element analyses present more potential practical use, though they are still involved and time consuming for routine usage. Putting aside aspects related to the material constitutive laws, the main difficulty involved in two-dimensional simulation is how to account for the actual three-dimensional effects of the tunnel advance. This problem is common in other two-dimensional methods for lining load prediction and the subject is treated separately.

The fifth group of methods for lining load prediction included solutions derived from parametric numerical analyses (numerically derived methods). Five methods within this group were reviewed. All of them used the finite element method as the numerical modelling tool. Most of them treated the ground and the lining as linear elastic materials. Just one assigned an elasto-plastic constitutive law to the soil, but assumed fixed strength parameters which reduced the generality of the results. Three of the methods assumed plane strain conditions. Another assumed a three-dimensional axisymmetric condition with a non-axisymmetric and non-gravitational stress field. The fifth assumed an actual three-dimensional representation of a shallow tunnel with non-circular cross section.

Additional assumptions and features of each method were described and discussed and these included the type of loading assumed in the two-dimensional methods, consideration of the in situ stresses, the presentation of the solution, etc.

The three-dimensional axisymmetric solution with non-symmetric loading by Erdmann (1983) deserves some comment. Though designed as a linear elastic analysis of a deep tunnel, with non-unity in situ stress ratio, the author included a representation of the shotcrete lining hardening with face advance. Support rings closer to the face were assigned lower stiffnesses in some analyses. If the results of these analyses are compared to those where a constant lining modulus was assumed, one concludes that the influence of the increasing shotcrete stiffness with increasing distance to the face, on the lining loads, is nearly equivalent to a net increase in the delay of application of a constant stiffness lining. Though requiring further investigation, it is believed that, for all practical purposes, the influence of the shotcrete lining hardening can be accounted for by using an increased unsupported heading span and a constant stiffness liner. It seems worth investigating in the future some criterion to define this increased span, taking into consideration the rates of shotcrete hardening and of lining placement.

The main deficiency of the available numerically derived methods is related to the usually strict range of validity of their assumptions. The parametric analyses they were based on usually cover conditions (geometric or geotechnical) which are fairly narrow, so that their application in practice is fairly restricted. Moreover, the linear elastic ground response they normally assume is another important limitation. Further limitations of each method were discussed on a case by case basis. However, it is believed that this type of method presents great potential for development in the future.

It is customary to introduce into the two dimensional models for lining load predictions or ground displacement estimates, some sort of approximation in order to get results which are closer to those obtained by three-dimensional methods. The actual three-dimensional longitudinal arching effect is represented in two-dimensional models by the introduction of some balancing internal stresses in the unsupported opening. Four procedures are available to simulate this, of which none are rigorously correct. As faint approximations of the actual three-dimensional condition, these procedures should be interpreted in terms of their degree of simplicity in use and of their ability to offer results that better approximate reality.

Eighteen methods were reviewed, some of them applicable only to numerical (finite element) solutions, but others also applicable to analytical (ring and plate) solutions. According to their development, these procedures are empirical, analytical or numerical. Moreover, according to the type of representation used, they were classified into four groups: core stiffness reduction, progressive core removal, imposed tunnel convergence and ground stress reduction. The advantages and limitations of each approach were discussed.

The core stiffness reduction introduces ficitiously created unknowns: a softened core stiffness and its rate of softening. The progressive core removal is only meaningful in staged tunnel construction and usually underestimates the lining loads. The imposed tunnel closure may be meaningful in TBM excavated schemes, when the soil closes the overcutting gap. Its application for other conditions is not as clear. It always requires an estimate of the closure at the face, which is not known. The ground stress reduction is the more usual procedure, and possibly the simpler one. It introduces one unknown, the amount of ground stress release prior to support activation. This stress release, defined as a fraction of the in situ stress is usually assumed to be uniformly applied to points of the tunnel contour. There is some evidence, however, suggesting that different stress releases may occur at different points of the contour. Even so, the constant release fraction is a simpler and usually safer assumption, as far as the lining design is concerned.

Unfortunately, most of the procedures available are applicable to numerical simulations only. Moreover, the others are to be used mainly in uniform stress field ring-and-plate solutions. The survey indicated that except for some fully empirical procedures, there is not a single solution to account for the three-dimensional effects in non-numerical two-dimensional models, such as the ring-and-plate or ring-and-spring, which could be applicable to shallow tunnels.

Available Methods for Prediction of Ground Displacements

A less extensive survey was made regarding the methods for ground displacement prediction. This is due to the much smaller number of methods available. These methods were classified according to the type of development on which they are based: empirical, semi-empirical, numerical and numerically derived. Numerical methods were not reviewed in this chapter since the use of finite element modelling for ground displacement prediction is covered in detail in Chapter 5 of this thesis.

Twelve methods were reviewed, the output of each were described, their assumptions presented and discussed. The input requirements were also given and the conditions for application of the methods reviewed.

Most of the methods were empirically or semi-empirically developed. The empirical methods have the least general application, as they cannot be used or extrapolated to conditions other than those assumed in their development.

The semi-empirical methods may allow a wider range of application, since they take into account some more or less fundamental parameters that control the phenomenon. However, many fundamental aspects are neglected.

Two types of semi-empirical procedures are distinguished: those that treat the soil as a continuum and those that approximate it by a particulate medium. The last group is the more popular one, in which the ground subsidence is treated as a stochastic problem. The number or volume of particles at a certain location being lost into the tunnel, is related to the probability of these particles moving down into the tunnel. This enables the ground subsidence profile to be approximated by a normal probability curve.

For good ground control conditions, in which local collapse of the ground is prevented, no ground particles are 'lost' and the fundamental soil behaviour is not probabilistic (de Mello, 1981). The essence of the soil response is better portrayed by a continuum mechanics approach, in which stresses and displacements can be related, which is a feature not allowed by the stochastic approach.

For these conditions, the stochastic solutions are reduced to fully empirical methods, with the normal probability function understood as a single curve fitting tool to adjust measured settlement profiles.

All methods within this class require an independent (usually empirical) estimate of the total volume of surface settlement or of the maximum surface settlement.

An extension of these empirical approaches was recently presented, in which the longitudial distribution of settlement was approached by a cumulative probability function. By assuming a zero volume change in the ground and by taking the ground settlement at the face as equal to half the total displacement, Attewell and co-workers further extended the method which can now be used to approximate the distributions of the entire displacement field in the cover of a tunnel being advanced. The ground displacement magnitudes, however, are estimated in an empirical manner.

The numerically derived methods approach the problem by two or three dimensional representations. The latter were developed with very restrictive assumptions, and can be applied only to a narrow range of conditions that make their potential practical use too limited. The limitations of each method were discussed on a case by case basis. A common limitation of available two-dimensional methods is that they always require some empirical assessment of certain parameters and in none of them, are the settlement predictions coupled with the lining load estimate.

Available Methods for Ground Stability Verification

The ground stability verification is usually performed using Plasticity solutions. Twenty-nine methods were reviewed. These were classified according to the stability problem they address. The main assumptions made in each method were identified, as well as the type of solution used (Upper or Lower Bound). The assumptions within the various solutions include the soil being weightless, approximating the problem by two or three dimensional representations, and treating the stability problems in terms of undrained or drained soil strength parameters. The format of each solution was described as well as its development(analytical or numerical).

The limitations of these solutions can be apprehended by their individual features and assumptions. Globally speaking, most of the available methods are strictly valid for homogeneous ground conditions and they do not account for time dependent ground responses. Effective stress stability analysis, with explict account of the pore water pressure effects, cannot be undertaken. The solutions are strictly valid for materials with the associated flow rule, showing a perfectly rigid-plastic type of response. Some of these limitations are further discussed in Chapter 6.

The most general 2D stability solution is that by D'Escatha and Mandel (1974), which is presented in detail in Chapter 6. No solution is available for the 3D tunnel face stability for drained soil strength parameters.

Survey of Lining Design Practice

The current practice of lining design was assessed through a survey carried out by the International Tunnelling Association in the late seventies and early eighties. The answers related to the soil tunnelling section of the survey were reviewed and re-interpreted by the writer.

Details of the survey procedures and its representativeness were given. The answers were provided mainly by designers, consultants and contractors, from 12 different countries. The questions were presented for two tunnelling situations: a TBM driven and a mined (NATM) tunnel, in different but very favourable geotechnical scenarios.

No conclusive answer was found in terms of the use of different design attitudes regarding distinct construction techniques.

A significant number of respondents use rather arbitrary approaches to define the in situ stress ratio, a factor which has an important role in the lining design.

Over half of the practitioners (54%) use a full overburden assumption when designing linings for shielded driven tunnels. On the other hand, a reduced overburden assumption is adopted by the same percentage of the respondents when designing the shotcrete lining of the mined tunnel case. It was not possible to clearly identify the reasons for these different design criteria.

For predictions of the thrust forces and bending moments, ring-and-spring models are those most frequently used (69%). The least frequently used is the finite element method (27%). In 31% of the responses the crown embedment is neglected.

Terzaghi's arching theory is the procedure more frequently used (64%) to define the reduced overburden ground load. The remaining responses indicated a preference for empirical approaches. It was noted that the commonly found use of a ring-and-spring model, with the semi-empirical earth pressure theory by Terzaghi, is somewhat inconsistent. According to his original ideas (Terzaghi, 1943:194), his theory approximates the actual pressures on the tunnel support after yielding of the soil upon the face passage and upon lining deformations under the ground loads. Thus, it approximates the final loads on the support and was not intended for use in a lining-ground interaction analysis.

The survey indicated that the spring constants of the ring-and-spring models, are usually obtained from results of laboratory tests, but did not disclose how this was done.

Some trend was noted towards the use of different design methods for different lining types. Empirical methods were preferentially used for primary lining design, while ring-and-spring models were used for secondary lining.

The majority of respondents do not take into consideration the non-linear behaviour of either the soil or the lining in their practice. They also do not take into account any three dimensional effect in the lining design, except for ground stress relaxation accounted by a few respondents.

Survey of Practice on Ground Settlement Prediction

A questionnaire was prepared and sent to active practitioners in 17 countries. Almost 73% of the respondents were active consultants. Simple questions were prepared to ensure a high return rate, which resulted in 70% of the 50 questionnaires sent. The questions were related to time-independent ground movement only.

The survey showed that 50% of the respondents use solely empirical or semi-empirical approaches for settlement prediction. Those using numerical methods only represented 18% of the respondents.

Reliability and simplicity are the basic qualities required by the majority of the practitioners in the selection of any settlement prediction method. The least demanded quality was the theoretical rigour.

Though the correspondence between ground movements and lining loads is widely recognized, more than half (possibly two-thirds) of the practitioners do not couple settlement and lining load predictions. These two predictions are usually done separately. Those who couple the predictions do so by means of the finite element method, though without claiming that this method is either reliable or simple.

It is apparent that if a new design procedure is to be developed, it would have to be a simple numerically based procedure, and it would have to be validated or calibrated against past experience to render it compatible with the required attribute of reliability.

5. SHALLOW TUNNEL MODELLING

5.1 Introduction

In Chapter 4, the available design procedures and the current design practice for shallow tunnels in soil were reviewed. It was noted that most existing procedures and the most common practices, even in the so called 'good ground control' conditions, do not take into consideration some important features of the ground behaviour or of the ground-support system. These features can be, but not always are, incorporated in designs based on numerical procedures, such as the finite element method. The survey of the practice revealed that only 27 and 32% of the responses to the questionnaire on lining design and on ground movements, repectively, use numerical approaches for design (normally combined with other procedures). Also, possibly two thirds of the practitioners do not couple the predictions of lining loads with ground settlements. This state of affairs seems to result, not so much from lack of knowledge or understanding of the mechanisms involved in a shallow tunnel construction, but rather, on the availability of adequate design tools that allow consideration of these mechanisms.

Practitioners are bound to introduce simplifications in their calculation models that tend to transform the design activity into an exercise of the anticipation of the most adverse conditions (possibly unattainable in the field), rather than an attempt to estimate more closely the likely response of the structure. In other instances the simplifications introduced are inadequate as they are possibly, unsafe.

Therefore, it seems desirable to attempt the development of a design procedure that may improve current practice, allowing for instance, the simultaneous estimate of lining loads and ground movements. Moreover, it seems crucial that this procedure take into consideration those important factors that always affect the tunnel behaviour. It appears that, if such a venture is to have some practical significance in present times, it should not be aimed at the development of a numerical model such as a new FEM code, but rather at a self-contained and simple method that avoids the use of a main frame computer facility. This is particularly important if such a procedure is to be used as an expiditious design tool for a preliminary design assessment, allowing sensitivity studies on the influence of these dominant factors that control the tunnel behaviour.

A method ~~such as the~~ one described above, can result from a systematic modelling of the tunnel behaviour, leading to a process of generalization. The limits of the generalization will clearly depend on the limits of the modelling tool and on its capacity for handling the controlling variables. Further comments on the process of generalization will be be included in the following chapter of this thesis. Otherwise the subject is covered in a paper by Resendiz (1979).

The knowledge accumulated from theory and the experience gathered from laboratory testing and modelling, as well as from field observations in prototypes, allow the identification of the relevant factors or variables that control the behaviour of a shallow tunnel in soil. The influence of some of these factors was discussed in Chapters 2 and 3 of this thesis. Although the inclusion of a very large number of variables in an analysis is theoretically possible, in practice this may not be feasible, particularly if the procedure is to retain simplicity. Therefore, a decision has to be made on which factors should be included and which should not. In order to render the problem tractable and yet to ensure some generality in the proposal, the number of factors or variables to be considered has to be reduced using some sort of criterion. For instance, those factors known to have an important role in most or all cases should ideally be considered. On the other hand, variables, regardless how of influential they might be, that may affect the tunnelling behaviour in one instance, but not in another, may momentarily be put aside and perhaps studied independently.

Following this criterion, it was decided to limit the development to full face excavated circular tunnels under time independent conditions with no ground failure. By excluding the effect of ground pore water pressure changes, the influence of soil consolidation does not have to be addressed and the influence of the tunnelling technology, in terms of the effect of the tunnel advance rate, is somewhat reduced. If ground failure is not involved, hence, on the assumption of good ground control conditions, there seems to be no need to address the effects of shear localization, as suggested in Chapter 2. It was also suggested there that, under those conditions, the effects of shear dilatancy may not be very pronounced, especially if the so called 'loosening' process is inhibited. Evidence shows particularly, that the volumetric strains in overconsolidated clays are very small even for tunnels at a near collapse situation. As additional simplifications, it will be assumed that the ground does not exhibit pronounced anisotropic behaviour or strain softening response. Moreover, non-geostatic loading conditions, represented by existing construction at the surface or subsurface, will be disregarded.

On the other hand, it was decided to include in the development of the design procedure, factors whose actions are known to be present in most common shallow tunnel situations. These are:

a) the effect of the relative position of a horizontal and stress free ground surface (H/D);

b) the action of gravitational body forces generating a stress gradient in the soil across the tunnel profile;

c) the non-uniformity of the in situ stresses generated by a horizontal to vertical stress ratio, K, different from unity;

d) the non-linear response exhibited by soils in terms of their stress-strain relationships, including the dependence on hydrostatic and deviatoric stress levels;

e) the delayed installation of the lining, generating ground movement and stress changes prior to support installation;

f) the interactive nature of the load transfer process developed between the soil and the support system.

Despite the simplifications assumed a priori, and a few others to be discussed later, it is believed that a design procedure that includes the influence of the factors listed above, is still sufficiently general for potential use in practice.

After identifying and reducing the factors or variables to be included in the development, the next step is to model the shallow tunnel problem. The purpose of the present chapter is to select, implement and test a modelling procedure, which allows the influence of these relevant factors to be considered separately. Yet, it must permit a simple representation of the problem, which may ultimately lead to a simple generalized solution for a prescribed range of conditions, without the recourse of additional modelling.

For the purpose envisaged, numerical modelling is the convenient approach to follow. Despite the considerable advance in physical modelling of shallow tunnels (e.g. Schofield, 1980), the ability and ease of studying the controlling factors separately, is far more limited in physical models than in numerical ones. Moreover, finite element simulation presently seems to be the most versatile tool available, widely accepted and used in tunnelling research and practice. It also seems convenient to depict the tunnel performance by some combined two and three-dimensional finite element simulations, in order to simplify the representation and yet still account for the relevant variable involved.

In the next section, overviews of previous studies on finite element modelling of shallow tunnels under time independent conditions will be included. No attempt, however, will be made to review the theoretical aspects of the subject, which are beyond the scope of the present work.

5.2 Two-Dimensional Modelling

5.2.1 Review of Previous Studies

An appreciable volume of contributions on two-dimensional modelling of shallow tunnels using finite element analyses has been observed over the last 20 years. Some of them were directed towards the understanding of the mechanisms associated with tunnelling and to the identification of the controlling factors that govern the tunnel behaviour. This is done by means of sensitivity studies. Some others were aimed at the development of design procedures, by generalization modelling, as shown in Sections 4.3.2.6 and 4.3.3, for lining loads or ground movement predictions, respectively. Finally, others focused on the finite element technique as a modelling tool for a prediction of the behaviour of actual tunnel structures or small scale physical models.

In the present section, an attempt will be made to briefly review previous studies, with emphasis being given to the latter class. The subject was of interest to other workers (for example, Katzenbach, 1981:34, Eisenstein, 1982, Heinz, 1984:78), who reviewed it to a considerable extent. The present assessment will focus on numerical modelling from the user's point of view, and will summarize former works which are mainly related to prediction exercises in time independent situations. Intentionally left out of this review are the theoretical aspects related to the solution techniques of linear and non-linear finite element equations. This subject lies beyond the scope of this thesis.

5.2.1.1 Modelling Aspects

There are no firmly established criteria for modelling a shallow tunnel and, typically, the practical approach is to follow precedents. This task is partly guided by some rules or guidelines established from sensitivity studies, such as those by Kulhawy (1974) for deep tunnels, by Heinz (1984:80) for shallow tunnels and others.

Mesh Design

The finite element mesh is usually designed following guidelines that have resulted from parametric analyses. Most of them assume linear elastic stress-strain relationships for the materials involved. Therefore, they are strictly valid for this condition. Table 5.1 summarizes some of these guidelines, regarding the size of the domain to be discretized, the density of elements and the choice of boundary conditions. Available indications regarding the ideal position of the lateral boundary are not conclusive. During the course of investigations with the numerical model to be presented in Section 5.2.2, it was noted that the position depends not only on the size of the opening, but also on the ratio of cover to diameter, and on the Poisson's ratio of the ground. These facts were also noted by Seneviratne (1979:87). No attempt was made to generalize these findings, although some systematic investigation on the subject would be very useful. The location of the lateral boundary was defined in a case by case basis in the present study. In analyses where the ground is homogeneous with a constant stiffness with depth, the amount of heave at points below the tunnel will depend on the location of the lower boundary. Unrealistic heaves result in this case, unless stiffness-depth variations are considered or the correct location of a 'rigid' boundary can be assumed. The positioning of the lower boundary becomes immaterial when ground stiffness increases with depth.

Some authors (e.g. Kulhawy, 1974:465) advocate the use of elements with linear strain capabilities for the ground representation. Others (e.g. Orr et.al. 1978:123, Medeiros,

Representation Aspect	Case	References	Comments
Mesh discretization	Shallow and deep tunnels	Kulhawy (1974:469) Oteo & Sagaseta (1982:653) Ahrens et al (1984:87) Heinz (1984:87)	Element density affects tunnel convergence more and surface settlements less. Increase density where stress gradients are higher. Discretize tunnel half contour with more than 8 elements (lower order).
Boundary location	Deep tunnels	Kulhawy (1974:470) Almeida & Pereira (1978)	Boundary location affects displacements more than stresses. Locate 'infinite' boundary at more than 3 diameters away from tunnel centre. Location effects depend also on boundary condition.
	Shallow: Lateral Boundary	Oteo & Sagaseta (1982:653) Ahrens et al 1982:264) Heinz, (1984:94)	Effect of boundary negligible when located at more than 8 diameters away from tunnel centre.
	Lower Boundary	Ho (1980:49) Rowe et al (1981:271) Oteo & Sagaseta (1982:654) Rowe et al (1983:14) Heinz (1984:94)	Lower boundary located at 'infinity' result in unrealistically high ground heave below tunnel if ground is elastic and homogeneous. Magnitude and distribution of ground displacements are thus affected. Heave effect mitigates if realistic variation of ground stiffness with depth is assumed or if a higher operating ground modulus is assigned to elements below tunnel floor.
Boundary conditions	Deep tunnels	Almeida & Pereira (1978)	A fixed displacement boundary condition affects the numerical results more than a free boundary, for the same boundary location.
	Shallow tunnels	Heinz (1984;94)	Magnitude and distribution of surface settlements unaffected by type of boundary condition at the lower boundary.

Table 5.1 Some Guidelines for Two-Dimensional Finite Element Mesh Design, Derived from Sensitivity Studies

1979) favour the use of the simpler lower order constant strain elements, despite the need of a higher element density to provide sufficient accuracy. For the lining representation, beam elements are sometimes favoured (e.g. Ahrens et.al., 1982:264, Paul et.al., 1983:85), for their ability to directly furnish the lining internal forces. In this case the integration of element stresses is avoided. Otherwise, layered systems of plane elements may also suffice (e.g. Fleck and Sonntag, 1977,1978).

As noted in Section 2.3.5, while a full slip condition between the ground and the lining is hardly realistic, and a no-slip situation is a better representation, there might be some interest in investigating intermediate slip conditions. For this, interface elements such as those reviewed by Brandt (1985), are adequate. Applications of these element types to tunnelling problems are not abundant but can be found in Rodriguez Roa (1981), in Saha (1982) and in Paul et.al. (1983:86).

Excavation Simulation

The need to take into account the gravitational in situ stress field in shallow tunnel analyses was stressed in Section 2.2. This was also pointed out by Kulhawy (1975:47) who performed numerical analyses considering the action of gravity. He concluded that the latter should be considered for openings at 150 m depth or less. His conclusion, however, cannot be readily generalized since no indication of the size of the opening was given.

The initial stresses are computed directly as a function of depth below ground surface, assuming the vertical and horizontal stresses to be principal stresses. The vertical stress is taken as the overburden stress and the horizontal stress is calculated as K times the vertical. This requires a horizontal ground surface and horizontally layered deposits, with constant lateral earth pressure coefficient K. This approach was favoured by Medeiros (1979:158) and is the most commonly used procedure to introduce the initial stress condition with horizontal ground surfaces (Kulhawy, 1977:531). Otherwise, the initial stress state is implemented by the "switch-on-gravity" approach, in which K is dependent on Poisson's ratio. This restricts the generality of the approach, unless an unbounded Poisson's ratio can be assumed initially in order to render the desired K value, and amended in a second step to comply with the bounds imposed by elasticity. The latter approach was favoured by Chan (1985) and Wong (1986:48) for shallow tunnel simulations.

Three procedures are usually used to simulate the excavation of an underground opening. These are listed in Table 5.2, where some indications of their main features are also included. The limitations of these techniques can be inferred from the comments. The so-called general approach is a more rigorous method, furnishing results which are insensitive to the number of steps or phases into which a staged or incremental excavation is divided. However, for single phase excavation, as for a full face tunnel excavation, the errors involved in the other procedures tend to be small and the results are virtually the same (Kulhway, 1974:467, Ghaboussi and Pecknold, 1984:2061). In this case the discussion on the adequacy of the simulation procedures is merely academic.

In Section 4.3.2.7, a variety of approximate methods to account for three-dimensional effects in two-dimensional models were reviewed. Some of them are strictly applicable to finite element numerical simulations. A summary of the latter is reproduced in Table 5.3. For further examples and specific details of these procedures one is referred to Table 4.10. The procedures in Table 5.3 were classified into four groups, according to particular features and also where each are usually applied; staged (or incremental) and full face tunnel excavation. Moreover, each procedure employs more or less distinct numerical techniques to simulate the excavation. This is also shown in the table.

As suggested in Section 4.3.2.7, all procedures should be taken as rough approximations to bring the 2D solutions closer to the actual conditions. Their qualities should not be analysed in terms of the generality of their assumptions or of their rigour. Rather they should be evaluated by their degree of simplicity and their ability to furnish results closer to reality. For full face, single stepped excavation schemes, procedures 2, 3 and 4 in Table 5.3 are equally applicable. Procedure 1 is inappropriate as it leads to an

Procedure	References	Comments
1. Gravity turn-on	Kulhawy (1974:466)	Require two analyses, with and without the opening. Results furnished by the differences between the analyses. K is not an independent variable but a function of Poisson's Ratio. Do not model a construction sequence. Adequate for one step full face excavation in linear elastic materials.
2. Conventional approaches		
a) Stress reversal	Kulhawy (1974:465) Medeiros (1979:163) Chandrasekaran & King (1974)	Apply equivalent nodal forces with reversed sign along excavation contour and reduce modulus of excavated elements (to at least 10^{-6} times its original value). Forces calculated for instance, by lumping element stresses adjacent to the contour, using different approximate procedures. Results are step number sensitive.
b) Relaxation	Kulhawy (1974:466)	Excavated region not represented in the finite element mesh. In situ stresses applied as nodal forces on tunnel contour to represent action of non-existent core. Contour loads relaxed to simulate excavation. Difficult to follow a stepped construction sequence with simplicity. Procedure reduces approximately to the previous for single step, full face tunnel excavation.
3. General approach (Activation and de-activation)	Ghaboussi & Ranken (1981:254) Ghaboussi & Pecknold (1984:2052) Heinz (1984:83)	Equivalent nodal forces calculated consistently with interelement stress discontinuities across element boundaries that do not form part of the excavation contour, and accounting for weighted element residuals, arising from local equilibrium errors. Excavated elements are deactivated, being omitted in equilibrium equation. More rigorous approach involving less approximations. Insensitive to number of excavation steps. No major differences in relation to previous procedures, for single step, full face tunnel excavation.

Table 5.2 Excavation Simulation Procedures for Tunnel Modelling with Finite Element Techniques

Procedure	Where Usually Applied	Main Features	Excavation Simulation Procedure	Examples of Use[(1)]
1. Progessive Core Removal	Sequential excavation schemes	Gradual removal of elements within tunnel cross section (core), normally following the actual sequence of tunnel excavation. The stresses around the contour of the portion being excavated are usually zeroed and the partial application of the support takes place in the subsequent excavation step.	Stress reversal or general approaches	Baudendistel (1972) Sagaseta (1973) Kulhawy (1975) Wanninger & Breth (1978) Negro et al (1984)
2. Ground Stress Reduction	Full face excavation schemes (non staged)	Complete 'removal' of elements within the entire tunnel cross section with their stiffness reduced to a near zero value or excavated area not represented in the finite element mesh. Boundary stresses at tunnel contour gradually reduced to a prescribed value or until a certain value of section convergence is achieved. At this stage support is installed and remaining boundary stresses are released.	Stress reversal or relaxation approaches (2)	Tan (1977) Rowe et al (1981) Zagottis (1981) Heinz (1984) Baumann et al (1985) Wong (1986) Ng et al (1986)
3. Core stiffness Reduction	Both full face or sequential excavation schemes	Stiffness reduction of elements in certain area within tunnel section. Reduction factor empirically assessed, being usually calibrated by back analyses. Then partial or complete reduction of in situ stresses around the contour of softened area.	Stress reversal and general approaches	Swoboda and Laehmayr (1978) Van Dillen et al (1979) Schikora (1982) Baumann et al (1985)
4. Imposed tunnel Convergence	Full face excavation schemes (non staged)	Imposed displacement boundary conditions at tunnel contour derived from independent numerical simulation accounting for face advance effects or from field observations.	Pre-Determined displacement boundary	Negro and Eisenstein (1981) Ohta et al (1985)

Notes: (1) For further examples see Section 4.3.2.7 and Table 4.10.
(2) General approach can be used but it is reduced to the conventional approach, if boundary stresses and equivalent nodal forces at tunnel contour are inconsistently determined from element boundary tractions or are independently fixed.

Table 5.3 Numerical Procedures to Account Approximately for Three-Dimensional Effects of a Tunnel Advance in Two-Dimensional Finite Element Analyses

unstressed support. Procedure 3 (core stiffness reduction), has the virtue of automatically furnishing the boundary balancing stress around the softened area without a prefixed assumption on the rate of the in situ stress release around the tunnel contour. However, it introduces an additional unknown variable, which is the degree of stiffness reduction (referred to herein as 'softening') of the tunnel core. The assessment of this parameter is inevitably empirical.

Procedures 2 and 4 are basically equivalent. They both require an independent assessment of the degree of stress release at the tunnel contour or of the amount of tunnel convergence. This is to account for the 3D stress transfer and the delayed support application. This can be done with some degree of formalism using few existing methods, but a large amount of empiricism or informal judgement is always required. Available simplified methods (e.g. Ng et.al., 1986:48, Ohta et.al. 1985), are conceptually inadequate as they infer that the losses of ground of a shallow tunnel can be approximated by deep tunnel solutions, with uniform stress field (K=1). In essence, no 2D procedure is presently available to properly relate the degree of stress release or tunnel cross section convergence occurring in the 3D advance of a shallow tunnel. Moreover, in cases where the construction technology used does not make use of a shield machine, the simplified procedure such as that by Ng et.al. (1986) and others, are not readily acceptable.

Lining Material Modelling

As in the ring-and-plate or the ring-and-spring solutions (Sections 4.3.2.3 and 4.3.2.4), most finite element modelling assumes the support as a linear elastic, isotropic and homogeneous material. This is a simpler and usually conservative assumption, for prediction of the working loads on the lining. However, as noted by Paul et.al., (1983:137) and Duddeck and Erdmann (1985:257), if the analysis aims at the assessment of the ultimate capacity of a concrete lining, the assumption of linear elasticity may lead to an overconservative design. Paul et.al., (1983:139) showed that if the actual non-linear behaviour of a reinforced concrete lining is taken into consideration, the capacity thrust value for large eccentricities is typically 1.8 to 2.8 times that estimated from linear elastic analysis. Recognizing however, that a non-linear lining analysis will hardly be carried out routinely, these authors proposed a simplified procedure, applicable to cases where the load eccentricity is large (load path intersecting the moment-thrust interaction diagram below the balance point). Linear elasticity is assumed to obtain the eccentricity and the thrust load, but the ulimate thrust value is obtained from Paul et.al., (1983:142), taking the non-linear effect fully into consideration. For smaller eccentricities, results from linear elastic analyses will not provide overconservative ultimate loads and the lining non-linearity may be neglected.

The case of shotcrete lining represents a special case, as its stiffness changes with time. Hence, with a gradual advance of the tunnel, lining sections at different distances from the face will show different stiffnesses. The net response of the lining will be non-linear, and the degree of non-linearity in its stress-strain behaviour will depend on the rate of the shotcrete stiffness increase in time, on the rate of tunnel advance and shotcrete placement. The subject was studied by Erdmann (1983:185) and by Schikora (1984) who used three-dimensional finite element modelling. As explained in Section 4.3.2.6, Erdmann (Op.cit.) assumed a constant shotcrete modulus in one analysis, and made two assumptions of the variation in the modulus with distance to the face. In both cases, the shotcrete modulus was assumed to increase from a near zero value at the leading lining edge to its final value one diameter behind. In any case, the lining behaviour was assumed to be linear elastic. Two distances of delayed lining installation were considered, measured from the tunnel face to the leading edge; 0.5 and 0.25 times the tunnel diameter. Erdmann's results strongly suggest (Op.cit.:193-195,202-206) that the effect of this variable stiffness on radial displacements, radial stresses, thrust and bending moments, can be quite reasonably taken into account by assuming a constant shotcrete modulus (in a linear elastic analysis) and a nominally increased distance of delayed lining installation. Although Erdmann did not pursue the subject, it seems likely that one could propose some useful rule relating the rate of shotcrete stiffness increase with time and distance, to an equivalent distance of delayed lining application, for a constant shotcrete modulus.

Lining-Soil Interface Modelling

Most of the finite element modelling conducted for soft ground tunnelling assume a non-slip condition between the soil and lining. Few studies assumed a full-slip interface condition, with zero shear transfer from soil to lining (for example, Ranken, 1978:96 and Ahrens, 1982:266, see Section 4.3.2.6). Fewer treated the interface as a non-linear material. Rodriguez Roa (1981) and Saha (1982) modelled it using an interface element, with very high normal stiffness and an elasto-plastic tangential shear-deformation relationship, with failure described by the Mohr-Coulomb criterion.

Soil Modelling

A review of the stress-strain relations applicable to soil modelling is beyond the scope of the present work. The subject was covered comprehensively by Christian (1982), Wroth and Houlsby (1985), Dyer et.al. (1986), among others. Some aspects of these relations which have been used to model tunnels in soil will be briefly discussed.

Figure 5.1 lists examples of different stress-strain relations for soils, which have been used in shallow tunnel modelling for the assessment of stress and displacement, under time independent conditions. Three classes of relationships are identified. The two most commonly used are the elastic and the elasto-plastic models, which are mainly used in connection with finite element applications. A third class of soil model is included, that is used in associated field solutions, which are less popular than finite element for stress-displacement analyses. This class includes rigid-plastic models, which usually satisfy the normality condition of the associated flow rule. But the associated field solutions have been extended to cases where the soil is not at failure everywhere and therefore the flow rule is not associated (Atkinson, 1981:262). Atkinson et.al. (1975:8) presented solutions using the latter approach with a hardening law for shallow tunnels in sand.

For the reasons exposed in Sections 2.3.4.3 and 4.1 linear elastic analyses applied to shallow tunnelling tend to furnish results that are poorer than those from non-linear analyses. Good correspondence may be found between linear elastic prediction and actual performance, if the comparison is defined in terms of a limited number of parameters (e.g., maximum surface settlement). However if a complete comparison is proposed, including vertical and horizontal displacements in the ground mass as well as lining deformations and loads, then a good correspondence between linear elastic prediction and performance seems unlikely for most soils and usual ground control conditions. Consideration of soil anisotropy in these analyses may

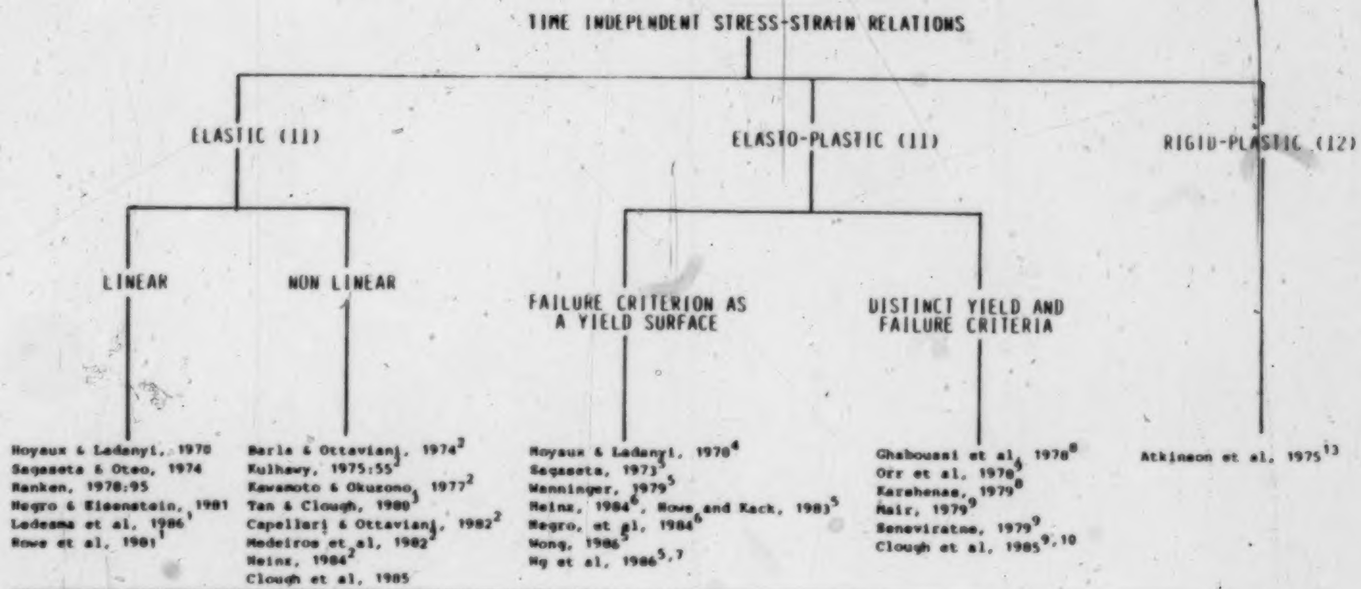
TIME INDEPENDENT STRESS-STRAIN RELATIONS
ELASTIC (11)
ELASTO-PLASTIC (11)
RIGID-PLASTIC (12)
LINEAR
NON LINEAR
FAILURE CRITERION AS A YIELD SURFACE
DISTINCT YIELD AND FAILURE CRITERIA
Hoyaux & Ladanyi, 1970
Sagaseta & Oteo, 1974
Ranken, 1978:95
Negro & Eisenstein, 1981[1]
Ledesma et al, 1986[1]
Rowe et al, 1981[1]
Barla & Ottaviani, 1974[2]
Kulhawy, 1975:55[2]
Kawamoto & Okuzono, 1977[2]
Tan & Clough, 1980[3]
Capellari & Ottaviani, 1982[2]
Medeiros et al, 1982[2]
Heinz, 1984[2]
Clough et al, 1985
Hoyaux & Ladanyi, 1970[4]
Sagaseta, 1973[5]
Wanninger, 1979[5]
Heinz, 1984[6], Howe and Kack, 1983[5]
Negro, et al, 1984[6]
Wong, 1986[5]
Ng et al, 1986[5,7]
Ghaboussi et al, 1978[8]
Orr et al, 1978[9]
Karshenas, 1979[8]
Mair, 1979[9]
Seneviratne, 1979[9]
Clough et al, 1985[9,10]
Atkinson et al, 1975[13]

Notes:

1. Elastic anisotropic model
2. Duncan & Chang (1970) hyperbolic model
3. Hyperbolic model in terms of bulk and shear moduli
4. Tresca's failure criterion
5. Mohr-Coulomb failure criterion
6. Von Mises failure criterion
7. Elastic anisotropic model; parameters defined according to stress path
8. Ghaboussi & Karshenas, 1977 critical state model
9. Modified cam-clay model
10. Prevost, 1980 critical state model
11. Finite element applications
12. Associated field solution
13. Non classic plasticity solution, with limited failure, non-associated flow rule and hardening law.

Figure 5.1 Examples of Stress-Strain Relations for Soil used in Shallow Tunnel Modelling

improve the correspondence, for instance with respect to the maximum slope of the surface settlement trough (e.g., Rowe et.al., 1983:17), but it is improbable that a complete correspondence of all aspects involved would be achieved. Besides, proper assessment of cross anisotropic material properties (e.g., Lo et.al., 1977, Ng and Lo, 1985) involves testing and evaluation procedures which are not routinely used, except in cases where the ground anisotropy is of prime concern and likely controls the tunnel performance.

Potentially the most useful relationships for soil tunnel modelling are non-linear, and are either elastic or elasto-plastic. As it will be seen in the following section, the latter seems to be widely used in numerical predictions for soil tunnelling. This fact would appear to reveal a general belief that for this type of geotechnical structure, the soil non-linearity is an aspect of concern.

Among the linear elasto-plastic models, those in which the failure criterion is adopted as a yield surface are more frequently used. Normality is often assumed, but non-associated flow rules have also been employed. If the construction of the tunnel being simulated is performed under good ground control conditions, so that soil failure is fully prevented or the failed zone is rather limited, these models will mainly portray a linear elastic response. This is a shortcoming of this class of stress-strain soil relationships.

In fact, accurate strain measurements with displacement transducers in the laboratory (Costa-Filho, 1980), have shown that even stiff soils like London Clay, exhibit a clear non-linear stress-strain behaviour at very small deviatoric strains. The study of small strain behaviour of soils (up to 0.1%) under undrained conditions as observed in triaxial testing, has advanced considerably by the use of electrolevel gauges (Jardine et.al., 1984) or of magnetic flux density gauges (Clayton and Khatrush, 1986), that allow the local measurement of strain as opposed to the global one. Jardine et.al. (1985) observed that the undrained stiffness of a stiff clay can show a drop of two-thirds for an increase in strain from 0.01 to 0.1%. A similar response can possibly be anticipated in terms of the drained stiffness.

The results of the laboratory testing by Jardine et.al. (1985) suggest that, at least for London Clay, the account of the non-linear behaviour at small strains is more important than the influence of stress relief due to sampling and of the stress path applied to the sample. Indeed, while the stiffness of this particular clay may change by a factor of two when subjected to undrained compression as opposed to extension, the stiffness at small strains (say at 0.01%) as obtained from external measurements, can be an order of magnitude smaller than the value derived from local strain measurements (Jardine et.al., 1984:331 and Jardine et.al., 1985:511).

Moreover, the large mass of soil in a number of geotechnical structures including excavations, is strained to less than 0.1% deviator strain (Jardine et.al., 1986:394). Therefore, it is not possible to accurately depict soil behaviour before yield by ascribing linear elastic deformation moduli, even if the parameters are backanalysed from field measurements of similar structures (Fourie et.al., 1986:233).

Elasto-plastic stress-strain relations with distinct yield and failure criteria, represent an improvement with respect to other elasto-plastic models. The use of critical state models such as the Modified Cam-Clay model may ameliorate predictions, especially for normally consolidated soils. However, for lightly or overconsolidated clays, Cam-Clay models will still predict an elastic response for the soil at stress levels below yield, both for drained and undrained loading (Bolton, 1979:220, Wroth and Houlsby, 1985:19). The criticism applied to the other elasto-plastic models is also valid here: no account is taken of the pre-yield non-linear response of overconsolidated soils.

Non-linear elastoplastic models (e.g. Evgin and Eisenstein, 1985) would solve this problem. Apparently the use of these models in shallow tunnels has not been reported. Few constitutive models available take into account the complete non-linearity of the stress-strain response of soils. The most popularly used model for analyses of tunnels in soil are those with non-linear elastic incremental formulations of a hyperbolic type (see Figure 5.1). This empirical model will be described and discussed in following sections of this thesis. It is formulated in different ways and it is popular because it is simple and requires a small number of parameters which are easy to obtain.

Jardine et.al. (1986:380) proposed a new non-linear elastic formulation for undrained loading. The stress-strain relation was empirically derived from curve fitting of laboratory results and is represented by a periodic logarithmic function, requiring 5 parameters for its definition. While designed to provide a more accurate fit of the stress-strain relation in the small strain range, it increased the number of required parameters compared with that needed for the more traditional undrained hyperbolic formulation. The new model was tested in a retained excavation scheme and furnished improved predictions of horizontal and vertical displacements of the ground, as compared to an elasto-plastic analysis with the failure criterion as a yield surface. Nevertheless, the merits of this formulation for shallow tunnel modelling remain to be seen.

Figure 5.2 furnishes results of tests on a reconstituted glacio-marine sediment of low plasticity, anisotropically consolidated and subjected to undrained shearing in a Bishop and Wesley triaxial cell (Jardine et.al., 1984:327 and Jardine et.al., 1986:379). The clay had an OCR of 2.05 before shearing, and K_o equal to 1.47. The dots represent results of the triaxial test with locally measured axial strains. The dashed curve corresponds to a simulation using the non-linear elastic-perfectly plastic model of Jardine et.al. (1986). A good agreement with the experiment is obtained using this five parameter model. The full line shown represents a best fit hyperbola described in this case (anisotropic test) by three parameters. A fairly reasonable agreement is also obtained, despite the latter being a simpler model. From this , it can be seen that the hyperbolic formulation can provide an adequate representation of the stress-strain relation of this lightly consolidated clay in the small strain region.

Another example of the suitability of the hyperbolic formulation is shown in Figure 5.3. The dots represent results of an unconsolidated undrained triaxial test in an undisturbed Blue London Clay sample, taken from a depth of 7.3 m below surface the at Canons Park (Jardine et.al., 1985:511). The soil was heavily over-consolidated and had an estimated K_o of 3. The axial strains were also measured locally. A fitted hyperbola accommodates the data reasonably well over a considerable range of deviator strains. An initial tangent modulus from the hyperbola was found to be 91.5 MPa. Had the axial strains been measured externally, with all due corrections included (e.g. cell compliance), the stress-strain curve obtained would be that shown by the chain-dotted line. An initial 'linear elastic' portion would

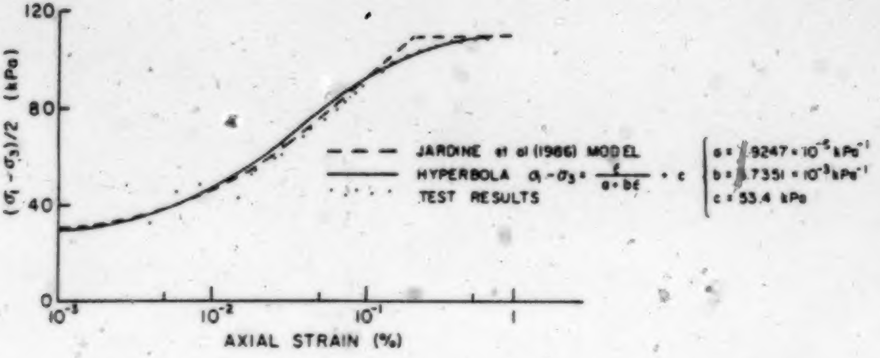

Figure 5.2 Triaxial Test Results on a Lightly OC Clay and Predictions by the Hyperbolic and Jardine et.al. (1986) Models

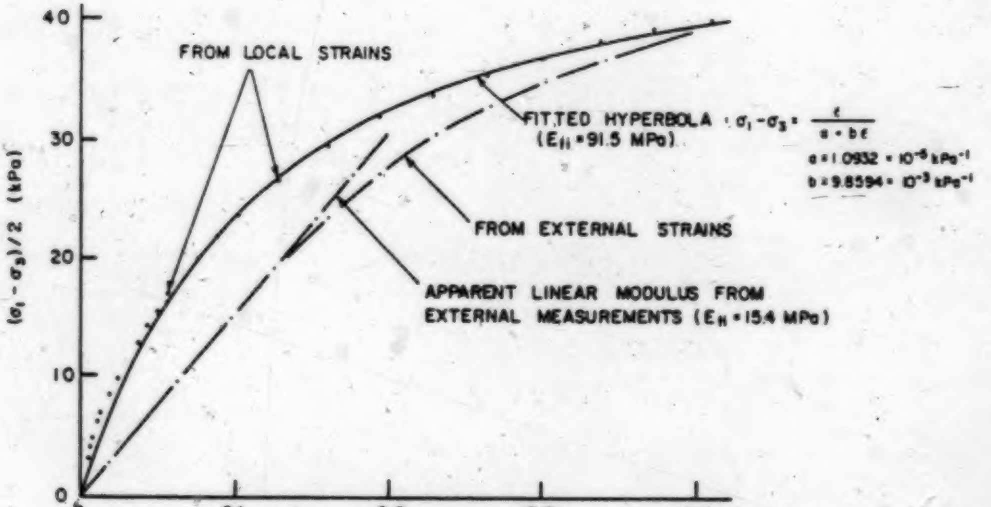

Figure 5.3 Stress-Strain Relations for OC London Clay under Unconsolidated Undrained Triaxial Test (after Jardine et.al., 1985:512, modified)

have been identified giving a Young's modulus of 15.4 MPa. This is about one-sixth of the initial modulus given by the locally measured strain data.

In summary, a good prediction of ground behaviour could be ensured if the complete non-linear stress-strain relation was to be accounted for and if an accurate assessment of the initial tangent modulus was possible. The hyperbolic stress-strain formulation is a simple and adequate way to describe the non-linearity of soil. Assessment of the soil stiffness at the small strain range can be made in the laboratory with good quality undisturbed samples, by means of specially designed strain meters. It can also be evaluated through in situ testing (e.g. Jamiolkowski et.al., 1985:113). Recent studies on seismic or geophysical measurements for the evalution of elastic parameters provided encouraging results (for instance, Abbiss, 1986).

5.2.1.2 Prediction of Performance by Finite Elements

In this section, an attempt will be made to evaluate the capabilities of finite element techniques as a prediction tool for soil tunnelling problems. The role of predictions in soil engineering practice was examined by Lambe (1973) who proposed a classification that is reproduced in Table 5.4.

A comprehensive, but not exhaustive, list of prediction exercises applied to shallow tunnels was prepared and is shown in Table 5.5. The review covers only works published over the last decade, where comparisons between numerical results using two-dimensionsal finite element analyses and field measurements were made available. The list provides brief details of the tunnel location, construction method and type of soil. Laboratory tunnel models are also included. Furthermore, the type of prediction mode is indicated, according to the classification shown in Table 5.4. Each case was classified according to details and descriptions provided by the authors. A relative degree of uncertainty was involved in the classification of a number of cases (38% of the total) and these are marked accordingly.

Table 5.5 also includes some indications of how the numerical simulation was performed, especially how the 3D effects were accounted for in the 2D analyses. The type of stress-strain relation used for the soil is also given. Lining representation was not always included, but when it was, lining material was assumed to be linear elastic, and a no slip condition at the lining-soil interface was assumed.

Finally, Table 5.5 provides a qualitative comparison between the predicted and measured performances. The aspects of performance that were inspected included:

a) surface settlements: magnitudes of the maximum settlement and maximum distortion, plus the overall aspect of the transverse settlement profile;

b) subsurface settlements: magnitudes of the maximum subsurface settlement and the overall distribution of settlements with depth;

Prediction Type	When Prediction Made	Results at Time Prediction Made
A	Before event	-
B	During event	Not known
B1	During event	Known
C	After event	Not known
C1	After event	Known

Table 5.4 Classification of Prediction According to Lambe (1973)

	Author/Year	Tunnel	Soil	Construction Method	Prediction Type$^{(1,2)}$	Numerical Simulation	Stress-Strain Model for Soil	Surface Settlement			Subsurface Settlement		Horiz. Displ.		Lining Loads	
								Mg.	Dist.	Dtr.	Mg.	Dtr.	Mg.	Dtr.	Mg.	Dtr.
1.	Takemoto et al 1977	Odawara-Atsugi	Loam	Side drift	B1? (w)	Progressive core removal	Linear elastic (with creep)	=		G	>	R	<	R	>	P
2.	Kawamoto & Okuzono 1977	Nagoya Subway	Sands	Shield	C1 (w)	Ground stress reduction	Non linear elastic	=	=	G						
3.	Gartung & Bauernfeind 1977	Nuremberg Subway	Keuper Sandstone	NATM	B (z)	Ground stress reduction	Elasto-plastic	>	=	G						
4.	Swoboda & Laabmayr 1978	Munich Subway L8/1	Marls	NATM	B1 (z)	Stress & stiffness reductions	Elasto-plastic								>	G
5.	Ghaboussi et al 1978	Univ of Ill. model	Ottawa sand	Self weight model test	C1 (x)	Imposed tunnel convergence	Elasto-plastic (with cap)	=	>	G						
6.	Orr et al 1978	Cambridge Univ static model	O.C. kaolin	Ext. load drain. test (a)	C1? (x)	Ground stress reduction	Elasto-plastic (mod. Cam-clay)	>	<	R	>		>			
7.	Karshenas 1979	Cambridge Univ static model	Leighton Buzzard sand	Ext. load model test	C1 (x)	Ground stress reduction	Elasto-plastic (with cap)	=	<	R	>					
8.	Mair 1979	Cambridge Univ centrifuge model	O.C. kaolin	Gravit.undr. load (2DP,2DV)	C1? (x)	Ground stress reduction	Elasto-plastic (mod. Cam-Clay)	<	<	R	<					
9.	Seneviratne 1979	Cambridge Univ static model	N.C. kaolin	Ext. load undr. test (UDC)	A? (x)	Ground stress reduction	Elasto-plastic (mod. Cam-clay)	<	<	P	<					
10.	Negro & Eisenstein 1981	ABV water tunnel	Clayey sand	Full face hand mined	C1 (y)	Imposed tunnel convergence	Linear elastic	<	<	R	=	G				
11.	Schikora 1982 and 1983	Munich Subway S6, LW2	Gravel	NATM	C1? (z)	Stiffness & Stress reduct.	Elasto-plastic	=	=	G	=	G			=	R
12.	Garcia C. et al 1984 Saganeta 1973	Madrid Subway L6	Hard Clay	Belgian method	C1 (y)	Progressive core removal	Elasto-plastic	>			=	G			=	P

Table 5.5 Review of Some Numerical Predictions of Shallow Tunnel Behaviour Using Two-Dimensional Finite Element Analyses

Author/Year	Tunnel	Soil	Construction Method	Prediction Type (1,2)	Numerical Simulation	Stress-Strain Model for Soil	Surface Settlement			Subsurface Settlement		Horiz. Displ.		Lining Loads	
							Mg.	Dist.	Dtr.	Mg.	Dtr.	Mg.	Dtr.	Mg.	Dtr.
13. Imaki et al 1984	Narita Airport Shinkansen tunnel	Fine Sand	NATM	A? (w)	Progressive core removal	Visco elasto-plastic	>	=	G	>	G	>	R	<	G
14. Negro et al 1984 Eisenstein et al 1986	Sao Paulo Subway North Extension	Fissured silty clay	NATM	A (x)	Progressive core removal	Elasto-plastic (with harden.)	=	=	G	=	G				
15. Katzenbach 1985	Munich Subway S2, L5/9	Marls	NATM	C1 (w)	Progressive core removal (and dewater)	Elasto-plastic	<			<	G				
16. Clough et al 1985	San Francisco Water Tunnel (N2)	Soft silt and clay	Earth Pressure Balance Shield	C1 (w)	Ground stress reduction	Elasto-plastic with consol. (Mod. Cam Clay)	=	<	R			<	P		
17. Ohta et al 1985	Sewage tunnel	Sands	Slurry Shield	C1? (y)	Imposed tunnel convergence	Elasto-plastic with consol (Mod. Cam Clay)	=	<	G	>	R	>	P		
18. Baumann et al 1985	Munich Subway U5/9-7	Marls	Twin NATM (compr. air)	C1? (w)	Ground stress reduction	Elasto-plastic	=	<	R	<	G			<	R
19. Ng et al 1986	Thunder Bay (Array 1)	Soft silty clay	Shield	C1 (w)	Ground stress reduction	Elasto (anis.) plastic (stress path drain.)	=	>	R	=		>	G		
20. Ledesma et al 1986	Barcelona (Sect C)	Stiff clay	Mined	B (z)	Ground stress reduction	Linear elastic (back anal. param. used)	=			=	G	=	G		
21. Tan (1977:166)	Washington, DC Metro	Ungrouted sand	Shield	C1 (y)	Ground stress reduction	Non linear elastic	=	=	G	>	P	>	P		

Notes: (1) Types of prediction according to Lambe (1973:158) classification. The question mark indicates a certain degree of uncertainty.
(2) x: actual prediction; y: back analyses; z: prediction with previously calibrated model; w: any of the former x, y or z.
(3) Meaning of abbreviations and symbols: HORIZ. DISPL: horizontal displacements; MG: maximum magnitude; DIST: maximum distortion; DTR: overall distribution; =: calculated value approximately equal or equal to measured value; >: calculated value greater than measured value; <: calculated value smaller than measured value; G: good; R: regular; P: poor.

Table 5.5 Review of Some Numerical Predictions of Shallow Tunnel Behaviour Using Two-Dimensional Finite Element Analyses (Continued).

c) horizontal displacements: magnitude of the maximum displacement and the overall distribution of displacements with depth;

d) lining loads: magnitude of the maximum loads defined in terms of either radial ground stresses onto the lining, or thrust, and in a few cases, bending momements.

The calculated value is said to approximately equal the measured value, whenever the latter is within 20% of the former. Otherwise the calculated value is said to be greater or smaller than the measured value. The spatial distributions of displacement or loads were arbitrarily defined as good, regular or poor, after a liberal comparison between prediction and measurements was made.

Most of the literature covering the reviewed cases does not provide a complete set of information regarding both the case history (including construction details) and in depth details of the numerical simulation. The majority of cases fail to include an accurate assessment of the soil properties and their constitutive modelling. This alone could hinder any careful assessment of the models used to simulate the tunnel performances. Moreover, even if this were not the case, there is strong evidence that differences in the application of judgement (always required) between different individuals doing the prediction, are as significant as the different features involved in each modelling tool (Poulos, 1982:2). Ideally, a proper assessment of the modelling capabilities would be done by a single individual carrying out the prediction before the event (type A prediction), using different numerical simulation tools applied to a large number of case histories and covering all aspects of tunnel performance. The only exercise carried out closer to this ideal condition, was that by Clough et.al. (1985). However, they conducted a type C1 prediction, using basically one simulation procedure, three constitutive models for the soil in just one case history and restricted their comparison to ground displacements only. For this particular case (number 16 in Table 5.5) they were able to claim that the critical state model seems to provide the most adequate prediction. However, a brief inspection of their results, described in qualitative terms, shows that they are no better than the results obtained by other individuals, using different simulation procedures or stress-strain models in other locations.

Notwithstanding these facts, an attempt was made to identify the capabilities of the simulations, as related to the soil type, the construction method, and the prediction class, for each group of numerical simulation of tunnel construction and for each group of stress-strain model used. For that, a point rating criterion was tentatively established, and total points recorded for each case. Not suprisingly, the attempt was a fruitless one. Some of the most complete or powerful modelling procedures provided both some of the best and some of the worst predictions. No clear correlation was found between the prediction quality and the soil type, the tunnel construction method or the prediction type. The analysis was partly affected by the fact that, except for the magnitude of the maximum surface settlement, the predictions were compared to different aspects of measured tunnel performance. This is possibly due to the unavailability of field monitoring data on some performance aspects or failure to publish a complete set of comparative data.

Furthermore, it should be noted that most likely, some of the predictions classified as type C1, could actually be labelled as back-analyses of field performance, although not always clearly identified as such by the authors. A tentative identification is appended to the prediction type in Table 5.5, indicating which of the cases are actual predictions, back-analyses, predictions done with previously calibrated models and which are the unidentified cases. It is then observed that even a very simple numerical model, like that by Ledesma et.al. (1986), using a linear elastic relation with parameters derived from back analyses of similar conditions, can rank among those providing the best predictions. In this case, however, the lining installation was not simulated (Ledesma et.al., Op.cit.:337), and therefore the model cannot provide predictions of lining loads.

Because of the noted difficulties in evaluating the modelling abilities in each case, an overall appraisal of the numerical predictions was attempted. A similar assessment was done by Eisenstein (1982) on surface settlement predictions. Here the assesssment is extended to include other aspects of performance.

As a guideline to future interpretation, Table 5.6 has been prepared. It is noted that almost half of the cases studied originated in Europe and that 67% of the soils involved showed a cohesive nature. More than 50% of the cases refer to mining methods of tunnel construction, as opposed to TBM schemes that accounted for 24%. This distribution reflects the trend noted in Section 4.4.2.2 towards a more frequent use of finite element analyses in design practice for mined tunnels. With respect to the numerical simulation, most of the predictions accounted for the 3D effect of tunnel advance by utilizing a ground stress reduction procedure. This is followed in preference by the progressive core removal technique. Regarding the stress-strain model adopted for the ground representation, preference is given to elasto-plastic models (43%), with yield and failure coinciding. These are seconded by elasto-plastic models with distinct yield and failure conditions (33%).

As indicated in Figure 5.4, the majority of cases (67%) refer to type C1 predictions, including cases of actual back-analyses. This is not the ideal type of prediction to evaluate a simulation procedure, but nevertheless, it can provide some insight if this fact is fully appreciated.

Aspects	Percentage of Cases
(1) Case History Aspects:	
a) Tunnel location and study origin	
Europe	48
Asia	19
North America	24
South America	9
b) Type of soil	
Cohesive	67
Cohesionless	33
c) Construction Method	
Mined tunnel	52
Model tests	24
TBM schemes	24
2. Simulation Aspects:	
a) Account of 3D effects in 2D analysis	
Ground stress reduction	52
Progressive core removal	24
Imposed tunnel convergence	14
Core stiffness reduction	10
b) Stress-strain model for soil	
Elasto-plastic (yield=failure)	43
Elasto-plastic (yield≠failure)	33
Linear elastic	14
Non-linear elastic	10

Table 5.6 Overall Aspects of Reviewed Numerical Predictions of Shallow Tunnel Performance

Figure 5.5 shows that in the majority of the cases reviewed (72%), the comparison between calculated and observed performance was limited to ground displacements. A full comparison of the complete ground displacement field and lining loads, which is ideally required for the proper evaluation of a simulation, was achieved in only two cases (10% of total). Whenever one aspect of the performance is not assessed in the comparison, the prediction (or even a back analysis) becomes more flexible and more easily adjustable to the observations, especially those of types B1 and C1.

The results of comparisons between calculated and observed surface settlements are shown in Figure 5.6. The magnitude of the maximum observed surface settlement is very closely matched by the numerical predictions in 60% of the cases. Overprediction or underprediction are observed in equal proportion. This may indicate that finite element simulations are good enough for estimating the magnitude of surface settlement. This is confirmed by the result of the predicted overall distribution of the transverse settlement profile. This is seen to be good to regular, and seldom poor. However, one may also speculate that in those predictions where the result of the performance is known (B1 or C1), the calculation might have been biased towards that result. As noted by Eisenstein (1982), regardless of the type of the analysis or which type of stress-strain model is used, and regardless of the type of soil or construction

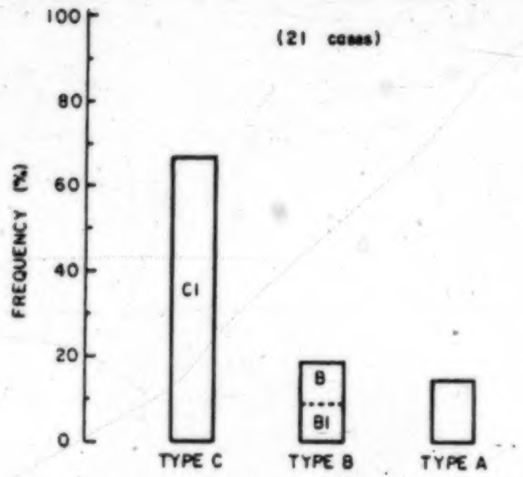

Figure 5.4 Types of Numerical Prediction of Shallow Tunnel Behaviour made by Two-Dimensional Finite Element Analysis

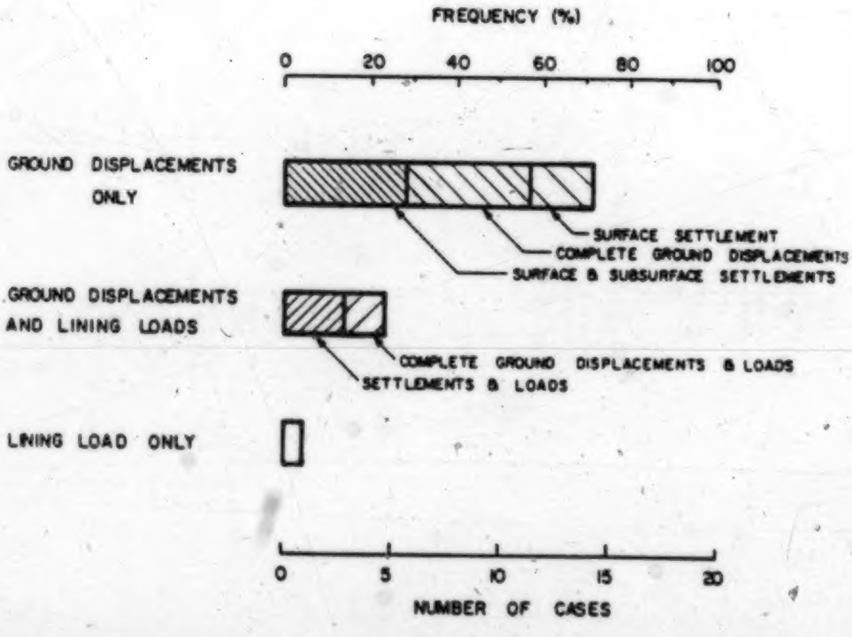

Figure 5.5 Performance Aspects Compared in Numerical Predictions of Shallow Tunnel Behaviour by Two-Dimensional Finite Element Analyses

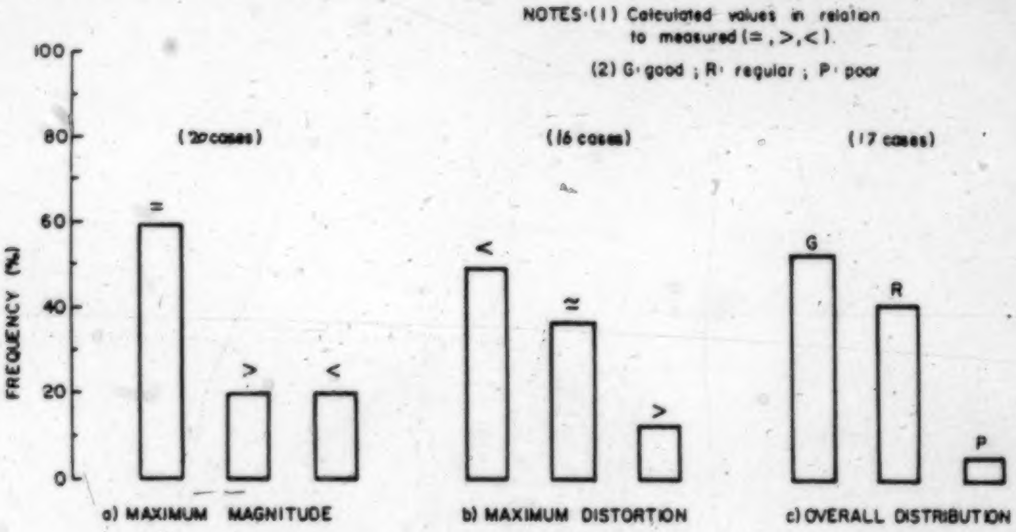

Figure 5.6 Comparison of Surface Settlements Calculated by Two-Dimensional Finite Element Analyses and Measured Values

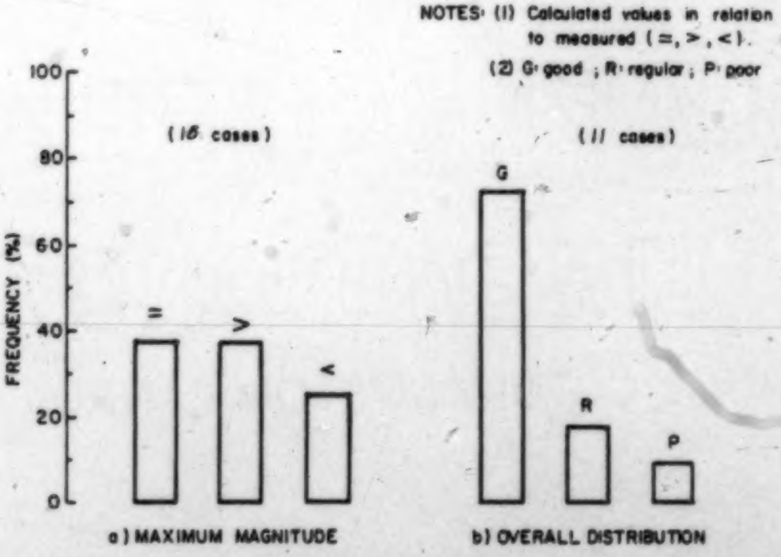

Figure 5.7 Comparison of Subsurface Settlements Calculated by Two-Dimensional Finite Element Analyses and Measured Values

scheme, the numerical simulations appear to furnish smaller surface distortions (maximum slope of the settlement profile) or wider settlement troughs than observed. Some authors (Mair, 1979:132, Eisenstein, Op.cit.) attribute this to the concentration of shear strains into relatively narrow zones. This aspect of soil behaviour is not adequately modelled by most finite element codes and constitutive models presently available.

An immediate consequence appears to be that a finite element approach would underestimate the damage potential to structures located at the ground surface. However, in practice, this may not be as consequential as initially thought. The estimate of surface distortion is only required when there are neighbouring structures. However, the estimate is usually performed ignoring the existence of buildings at the surface. As shown in Section 4.2.2, this simplification leads to an overestimate of the ground distortion, which may compensate the shortfall from the finite element analyses.

Figure 5.7 summarizes comparisons between calculated and observed subsurface settlements with depth. An even trend is noted towards matching or overestimating the maximum magnitude at points closer to the tunnel. As noted in Section 4.1, linear elasticity will hardly provide a good match of displacements at the tunnel contour and at the surface, unless the ground is very stiff or the ground control conditions are extremely good, so that the effect of the always present non-linearity in the stress-strain response of the soil is minimized. It will be shown in the next chapter (Section 6.3.2.3) that depending on the in situ stress ratio, on the relative depth of the tunnel and on the nature of the soil strength (purely cohesive or purely frictional), a match in the crown displacement in a linear analysis may lead to either an overestimate or an underestimate of the maximum surface settlement. Correspondingly, a match in the surface settlement with a linear elastic model, will also be followed by either an over or an underestimate of the crown settlement. Similar trends will be observed in linear elastic-plastic analyses if the amount of soil yielding is limited. Hence, if the cases reviewed in Table 5.5 involved mainly this type of analysis in providing a good match of the maximum settlement at the surface, the results shown in Figure 5.7(a) make sense provided soil yielding has not been extensive.

The calculated overall distribution of subsurface settlements is usually good, as shown in Figure 5.7(b). However, it should be pointed out that this interpretation requires clearer definition, since there are few cases where sufficient field measurements are taken at points very close to the tunnel contour where the strain and displacement gradients tend to be appreciably high. The noted agreement is, broadly speaking, good at points located at more than 30% of the tunnel radius away from its wall.

No immediate explanation is found for the noted trend on the calculated maximum horizontal displacement transverse to the tunnel. In most of the cases where this comparison was available, the results from analyses tended to be greater than the measured values (Figure 5.8). This tendency is noted even in anisotropic elastic-plastic analyses (Ng et.al., 1986:43). This displacement is very dependent on the initial stress ratio and one could speculate that inaccurate estimates of this ratio might explain the observed departures. However, this reasoning would lead to an equal frequency of over and underestimated displacements, which was not observed. Moreover, the noted feature could not be explained in terms of the numerical simulation procedures adopted or of the constitutive models used, as the same procedures or models resulted in both over and underestimates in different cases. Among them, the best agreement noted was in the linear elastic analysis by Ledesma et.al. (1986), using elastic parameters and a stress ratio which had been backanalysed from an instrumented section at the early stages of the tunnel construction.

The comparison between calculated and measured lining loads furnished mixed results (Figure 5.9). Equal frequencies of matched values, overestimates and underestimates were found, regarding the magnitude of the loads. Similarly, the distributions of these calculated loads were found to be equally good, regular and poor, with respect to the measurements. Again, no clear justification

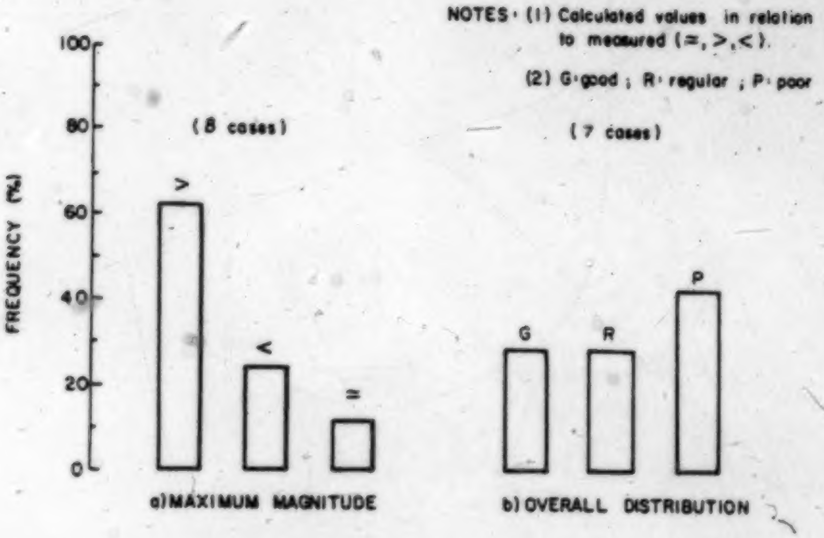

Figure 5.8 Comparison of Horizontal Displacements Calculated by Two-Dimensional Finite Element Analyses and Measured Values

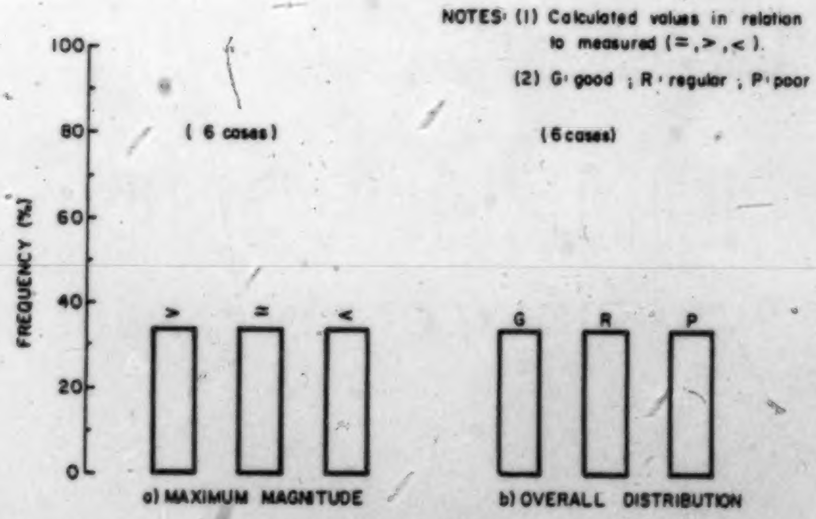

Figure 5.9 Comparison of Lining Loads Calculated by Two-Dimensional Finite Element Analyses and Measured Values

is found for this finding. On purely speculative grounds one could suggest that in most of the cases reviewed, the authors were mainly interested in evaluating the capabilities of their numerical simulation in terms of the ground response, which was usually expressed in terms of ground movements. Since in most of the cases, the results of field measurements were already available at the time the analyses were performed, the calculations could have been manipulated to achieve a better agreement in terms of soil displacement. Lining loads would have resulted as a by-product of the study with not much emphasis being placed on them. This is somewhat confirmed by the results provided by Ng et.al. (1986:45) as well as other authors. On the other hand, the well known difficulties associated with monitoring lining loads should not be overlooked. Consequently, measured loads are frequently treated more suspiciously than measured displacements, and differences between load calculations and measurements are attributed to unrepresentative or erroneous measurements (e.g. Duddeck and Stading, 1985), particularly if pressure cells are used. Moreover, in cases where the ground control and the lining-soil contact are poor, it is very unlikely that any correspondence between calculation and measurements is found. The reasons for this were exposed in the discussion on the idealized action of a support with poor contact with the ground in Section 2.3.5 of this thesis. It was shown there that if the lining contact is poor, and if the so-called loosening condition with "gravity" loads develops, then the support performance is likely to be unpredictable in formal terms.

5.2.2 Numerical Simulation Applied

Having in mind the capabilities of finite element simulations of shallow tunnels as reviewed in Section 5.2.1 and considering the goals of the present study established in Chapter 1, it was decided to make use of a simple finite element program which could incorporate and simulate the factors that most affect the tunnel performance. These were discussed in Chapter 2 and summarized in Section 5.1.

An open finite element code prepared by Medeiros (1979) was found suitable for the proposal. It is based on a simple constant strain triangle formulation, originally developed by Murray (1971) and extended by Medeiros for the solution of incremental supported excavations, allowing non-linear elastic analyses to be performed. This program was modified and implemented to allow the analysis of a shallow tunnel problem.

5.2.2.1 General Description of the Solution

The plane strain tunnel problem is solved by a displacement formulation, allowing the calculation of nodal displacements as primary unknowns and element stresses as secondary quantities. The finite element equilibrium equations are solved directly by the Gauss elimination technique. Constant strain triangles are the element type used.

The initial vertical and horizontal stresses are assumed to be principal stresses (ground surface assumed horizontal). They are specified directly at each element, as the overburden vertical stress and K times this value for the in situ horizontal stress. The former is taken as the bulk specific weight (assumed constant) times the difference in elevation between the ground surface and the centre of the element being considered. A single and constant stress ratio, K, is assumed in the analysis.

The problem is solved in stages, in order to represent different construction phases (typically two). In the first stage, ground excavation is simulated. This is done using the conventional approach (Section 5.2.1.1), in which all elements within the tunnel cross section have their elastic constants reduced to very small values to represent air and have their stresses zeroed to represent a full face excavation. This is followed by the application of boundary loads at the excavated contour, designed to cancel (gradually) the nodal loads equivalent to the initial stresses. These boundary loads correspond to boundary stresses with magnitude equal to a fraction, a, of the in situ stresses, but with a reversed sign. This boundary stress reversal simulates a partial in situ stress release, designed to approximately account for the true three-dimensional stress transfer mechanism in the two-dimensional analysis. To implement this procedure, referred to as 'ground stress reduction' (see Table 5.3), the finite element method requires the boundary stresses to be imposed as equivalent nodal loads. These forces are calculated by integration of the in situ stresses within the elements being excavated. In the first stage of the solution simulation, the fraction, a, of the load magnitudes are applied with reversed sign to partly reduce the initial in situ loads. This is necessary as the excavation should not be left unsupported, as explained in Section 4.3.2.7. The amount of in situ stress reduction, a, is a key issue in the simulation, and has to be independently assessed. The fraction of the stress release is equal to

$$a = 1 - \Sigma \qquad [5.1]$$

where Σ is defined in Section 2.3.2. The same stress reduction factor is uniformly applied to all points around the tunnel profile, and this produces a proportional reduction of the radial and shear stresses along the contour.

The reversed nodal loads applied to reduce the ground stresses are divided into a number of steps of equal magnitude and are applied incrementally. This allows the material non-linearity to be taken into account. The piecewise linear incremental displacements are accumulated to give the total displacement. After each load step the element stresses are updated and new elastic constants are obtained for the next load increment. This procedure is called 'past stress solution', since it uses elastic constants determined from stress levels obtained in the previous load increment. The stiffness matrix is formulated in terms of the tangent moduli. No attempt was made to redistribute the unbalanced loads within each increment.

The stress-strain relationship assumed for the soil is hyperbolic, following the original formulation by Duncan and Chang (1970). The soil is thus treated as a hypoelastic [13] isotropic time-independent material, defined by a variable and stress dependent tangent modulus and a constant Poisson's ratio. As an incremental constitutive model, the state of stress depends on the current state of strain as well as on the stress path followed to reach that state (Chen and Saleeb, 1982:217). As it will be shown in Chapter 6, in order to reduce the number of variables and to make the process of generalization simpler, an incrementally reversible (unique) stress-strain behaviour was assumed. Since no distinction is made between loading, unloading and reloading behaviours, the stress path dependency with respect to loading and unloading is not represented. The hyperbolic model was originally derived as a fitting function for conventional triaxial tests results (Kondner, 1963). Because of this, the shear stress component is simply approximated by the difference between the major and minor principal stresses acting in the plane being considered, and the mean normal stress component is approximated by the minor principal stress in that plane. The out of plane stress is not taken into consideration, as far as the constitutive model is concerned. The present model allows both effective or total stress analyses to be performed, by using the appropriate set of parameters. Details of the hyperbolic stress-strain formulation are given by Duncan and Chang (1970) and are reviewed by Chen and Saleeb (1982:516). A summary of its development is given in Figures 5.10 and 5.11. In its current configuration, the program allows the representation of just one layer of soil with the hyperbolic stress-strain relations, but this can easily be extended to include more than one soil layer.

---

[13] The term 'hypoelastic' model is used to describe the incremental elastic constitutive relations. Such models are used to represent the behaviour of materials where the state of stress is generally a function of the current strain state and of the stress path followed to reach it (Chen and Saleeb, 1982:148).

Once the last load step of the first simulation phase is applied, the remaining boundary stresses acting on the tunnel contour maintain equilibrium, and are equal to a fraction, Σ, of the original in situ stresses. At this stage, the support is applied by assigning properties of the lining material to appropriate elements. The balancing boundary stresses are no longer needed to ensure the 'stability' of the opening and therefore, they are reduced to zero. This is done by applying opposite and equivalent nodal loads incrementally and the reaction provided by the balancing stresses is gradually substituted by the support reaction. The final equilibrium between soil and lining is reached in an interactive form, after the complete removal of the fictitious balancing boundary stresses corresponding to Σ equal to zero or a equal to one (full stress release). No special provision is made to represent the interface between the lining and soil, and therefore, a no-slip contact is assumed.

The support is represented by layered rings of constant strain triangles. The reduced thickness of the lining ring (about 3% of the diameter for a concrete lining) would require a large number of elements for the discretization. However, the stress distribution within the support is not of primary concern in the present study. The overall action of the support in the interaction process with the soil can, therefore, be adequately represented by an equivalent lining ring with slightly increased thickness. This ensures an adequate element aspect ratio (close to 1), but requires selecting artifical material properties, such that the resulting compressibility and flexibility ratios are close to the actual values. This approach is similar to that used by many authors in retaining wall analyses (e.g. Medeiros, 1979:175), by Medeiros et.al., (1982:929) in a complex station-shallow tunnel analysis, and by Kasali and Clough (1983:73) in 3D analyses of shallow tunnels. This expedient simplifies the mesh design since a smaller number of elements can be used to represent the lining, which is assumed weightless. Accordingly, the program sets the initial stresses to zero in the lining. The lining material is treated as homogeneous, isotropic and linear elastic. Lining radial joints are not represented directly in the

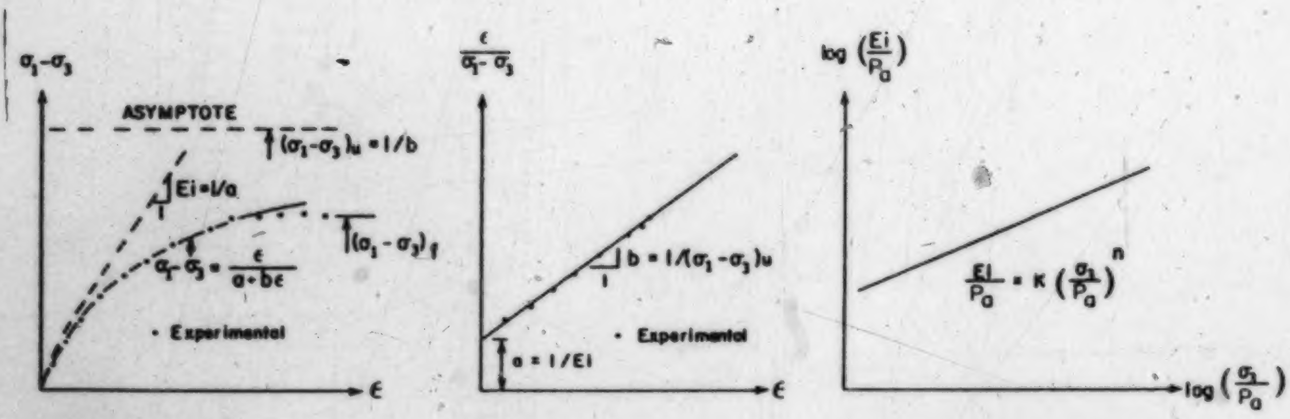
$\sigma_1-\sigma_3$
ASYMPTOTE
$(\sigma_1-\sigma_3)_u = 1/b$
$E_i = 1/a$
1
$(\sigma_1-\sigma_3)_f$
$\sigma_1-\sigma_3 = \frac{\epsilon}{a+b\epsilon}$
• Experimental
ϵ
$\frac{\epsilon}{\sigma_1-\sigma_3}$
$b = 1/(\sigma_1-\sigma_3)_u$
1
$a = 1/E_i$
• Experimental
ϵ
$\log\left(\frac{E_i}{P_a}\right)$
$\frac{E_i}{P_a} = K\left(\frac{\sigma_3}{P_a}\right)^n$
$\log\left(\frac{\sigma_3}{P_a}\right)$

Hyperbolic stress-strain curve by Kondner

Transformed stress-strain curve

Janbu's initial modulus confining stress relation

Figure 5.10 Hyperbolic Model Representation

Kondner (1963) hyperbola:

$$\sigma_1 - \sigma_3 = \frac{\varepsilon_1}{a + b\varepsilon_1}$$

with σ_1, σ_3: major and minor principal stresses and ε_1: axial strain. Material constants:

$$a = \frac{1}{E_i} \quad \text{and} \quad b = \frac{1}{(\sigma_1 - \sigma_3)_u} = \frac{R_f}{(\sigma_1 - \sigma_3)_f}$$

where E_i = initial tangent modulus; $(\sigma_1 - \sigma_3)_u$: ultimate or asymptotic stress difference; $(\sigma_1 - \sigma_3)_f$: stress difference at failure; R_f = stress ratio.

In conventional triaxial compression test σ_3 = constant. Hence the current tangent modulus is:

$$E_t = \frac{\partial}{\partial\varepsilon_1}(\sigma_1 - \sigma_3) \quad \therefore E_t = \frac{a}{(a + b\varepsilon_1)^2}$$

But

$$\varepsilon_1 = \frac{a\,(\sigma_1 - \sigma_3)}{1 - b\,(\sigma_1 - \sigma_3)}$$

Thus

$$E_t = \frac{1}{a}\left[1 - b\,(\sigma_1 - \sigma_3)\right]^2$$

or

$$E_t = E_i\left[1 - R_f\,\frac{(\sigma_1 - \sigma_3)}{(\sigma_1 - \sigma_3)_f}\right]^2$$

Janbu (1963) relation:

$$E_1 - Kp_a\left(\frac{\sigma_3}{p_a}\right)^n$$

where p_a: atmospheric pressure, K and n: dimensionless constants.

Failure in conventional triaxial, with Mohr-Coulomb criterion:

$$(\sigma_1 - \sigma_3)_f = \frac{2c\cos\phi + 2\sigma_3\sin\phi}{1 - \sin\phi}$$

with c: cohesion and ϕ: friction angle.

Therefore

$$E_t = Kp_a\left(\frac{\sigma_3}{p_a}\right)^n\left[1 - R_f\,\frac{(1 - \sin\phi)(\sigma_1 - \sigma_3)}{2c\cos\phi + 2\sigma_3\sin\phi}\right]^2$$

Figure 5.11 Derivation of the Current Tangent Modulus

solution, but their effect in reducing the bending stiffness in the lining can be indirectly taken into account, by Muir Wood's (1975:126) approximation:

$$I_e = I \left(\frac{4}{n}\right)^2 + I_j \qquad [5.2]$$

where I_e is the equivalent moment of inertia (per unit length of tunnel) of a continous ring corresponding to the actual lining, with n joints or segments with moments of inertia equal to I_j and I respectively. Hence for an eight segment lining, with perfectly articulated joints ($I_j \approx 0$), $I_e = I/4$.

The assumed plane symmetry simplifies the shallow tunnel problem, as it allows the analysis of only half of the plane strain section. The mesh design observed the guidelines presented in Section 5.2.1.1. The nodal points in the vertical boundaries were allowed to move freely in the vertical direction and were fixed horizontally (zero horizontal displacement). The nodes lying in the lower boundary, had both vertical and horizontal displacements fixed. The location of the lateral boundary varied from case to case, but typically it was located at 18 tunnel radii away from the tunnel centre. The lower boundary was located at a convenient location representing the position of rigid bedrock. The assumption of an increasing tangent modulus with increasing confining stress (or with depth) in the hyperbolic model formulation (Figure 5.11) lessens the effect of the unrealistic ground heave below the tunnel floor which is evident in analyses with a constant modulus profile. Therefore the position of the lower rigid base becomes irrelevant, as noted in Section 5.2.1.1. As much as possible the elements were designed to show aspect ratios close to unity, both in the ground and in the lining domains. Following the indications given in Table 5.1, a higher element density was adopted around the tunnel contour, where the stress gradients are higher. A typical finite element mesh used is shown in Figure 5.12a, and the details of the discretization around the tunnel are given in Figures 5.12b and c for clarity. This particular mesh contains 332 nodes and 609 elements. For a two phase construction simulation, with five load step increments each, the average CPU time to execute the complete solution using the present computer scheme at the University of Alberta, was 88 seconds with CPU storage of virtual memory integral (VMI) of 367 page-minutes. The band width for this mesh was 150. The program subroutine that reads the problem geometry (READGE) also allows the generation of intermediate nodal points and elements, and this simplifies the input preparation.

The complete listing of the computer program is not included herein, but can be found in the 'Tunnel Excavation' Computer Program Manual edited by Negro (1981), available in the Department of Civil Engineering at the University of Alberta.

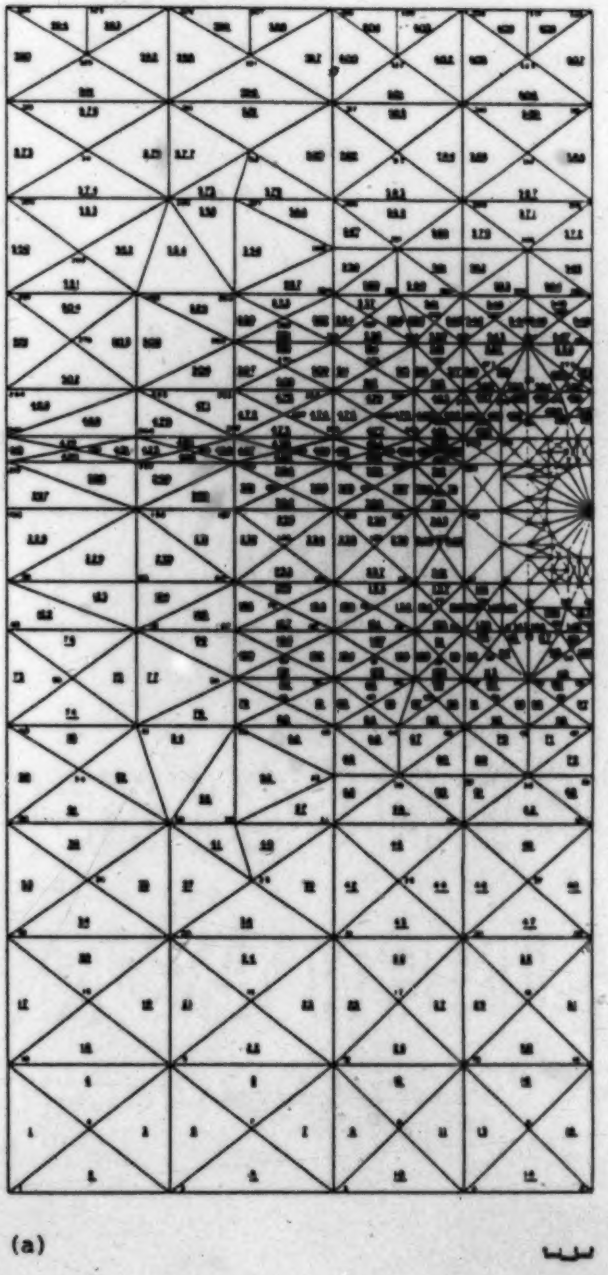

(a)

Figure 5.12 Details of the Finite Element Mesh

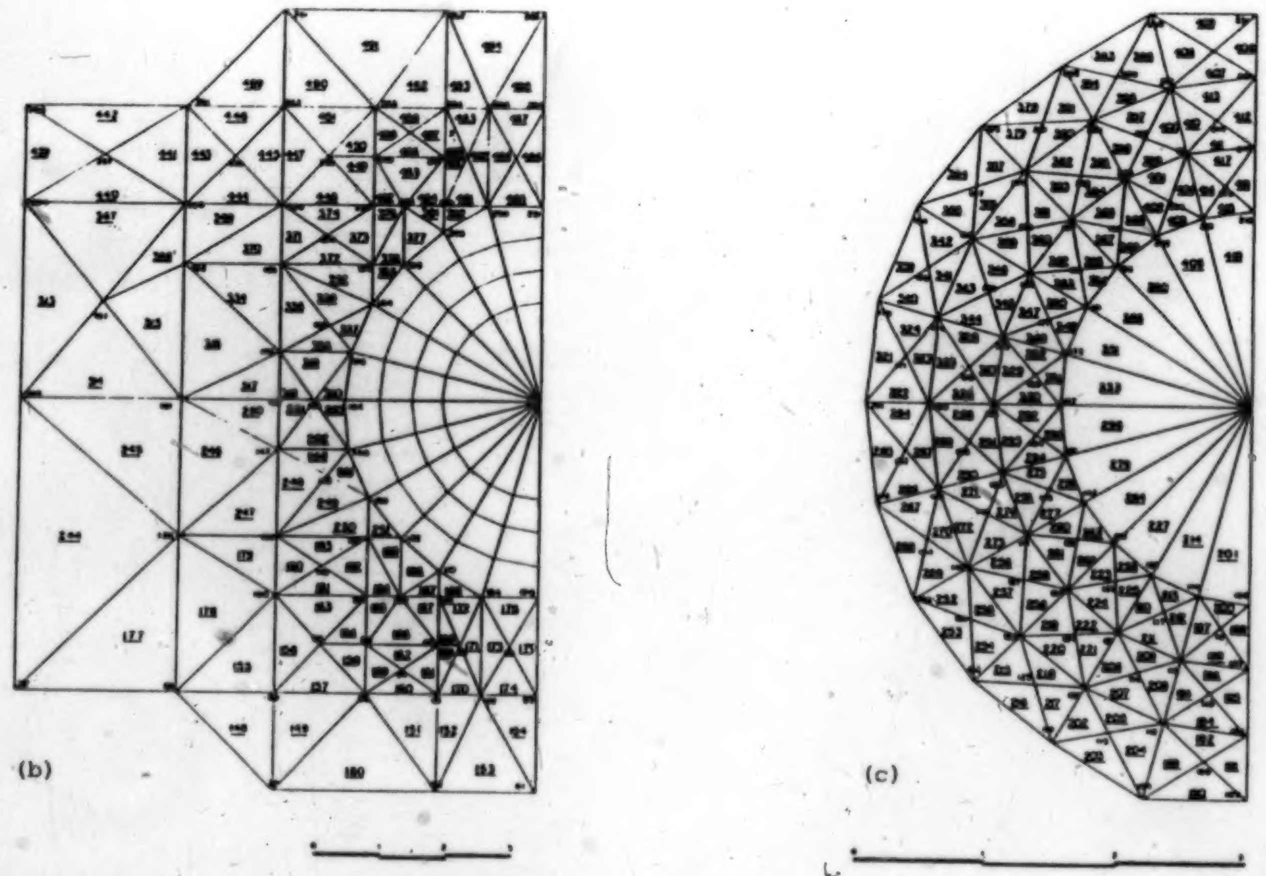

(b) (c)

Figure 5.12 Details of the Finite Element Mesh (Continued).

The manual provides details of the program organization and structure, the flowchart of the solution, a description of the subroutines, a glossary of names of input variables, instructions for data input and an input data sample.

5.2.2.2 Discussion on the Solution Adopted

The justifications of the numerical solution adopted and of the underlying simplifications can be inferred from the discussions included in the former sections of this chapter. Moreover, they are largely supported by the understanding of the behaviour of shallow tunnels presented in Chapters 2 and 3, and by the detected needs of current design practice, as shown in Chapter 4. A few additional points are discussed in this section, in an attempt to better assess the limitations of the solution adopted.

The use of constant strain triangles involves clear limitations which are partly compensated for by employing a larger number of elements. While this enhances accuracy, it increases computing time and cost and adds inconvenience to input and output handling. The problem is less severe in terms of the ground representation than it is for the lining, where higher stress gradients can be anticipated. With respect to the latter, Evison (1987) using the present numerical solution, analysed the problem of a simple fixed cantilever with elastic response, subjected to axial compression and bending. In order to approximate the correct solution for pure bending, it became apparent that an extremely large number of elements would be required, thus rendering the solution impractical. However, for uniform compression it was found that even a coarse mesh could provide a reasonable approximation of the exact solution, both in terms of displacements and stresses. Notwithstanding this, Medeiros (1979) used this solution for a retaining wall analysis, a structure where the behaviour in bending dominates. To compensate for the stiffening effect of the finite element solution, Medeiros (Op.cit.:178) reduced the wall stiffness by 35%, a value derived from the solution equivalence of the fixed cantilever model. Despite these shortcomings, the interactive process between the wall and ground was successfully simulated and the ground response quite satisfactorily represented.

For the tunnel lining, the problem tends to be less severe since, unlike the retaining wall case, compression tends to prevail, particularly in modern designs, where bending is likely to be very small. Moreover load eccentricity will also be minimized in a large group of stiff soils which have an in situ stress ratio between 0.8 and 1.2. The use of an equivalent lining in the analysis, with increased thickness in order to render an adequate element aspect ratio, should not be a matter of concern, provided proper attention is given to the equivalence of the compressibility and flexibility ratios. Kasali and Clough (1983:73) used a similar approach in their three-dimensional analyses of a shallow tunnel. They considered, however, that it would be sufficient to ensure a bending stiffness in the equivalent (thicker) lining comparable to that of the actual support. Accordingly, the modulus of the thicker liner elements was reduced proportionally to the relation between the liner thickness and the bending stiffness (which is proportional to the cube of the liner thickness). Despite being simpler than the criterion selected in the present study, the results of the numerical back-analyses shown in Sections 5.2.4.2, 5.2.4.3 and 5.2.4.4 confirm that the Kasali and Clough (Op.cit.) suggestion is indeed quite reasonable. It will then be shown that the best correspondence between observed and calculated performances is achieved when the flexibility ratios of the real and equivalent lining are comparable. This condition implies, in fact, the equivalence of bending stiffness (EI), provided the average lining radii are equal (which may not be the case).

As noted in Sections 2.3.5.2 and 2.3.5.3, the assumption of a no-slip interface is not a critical one, as only very limited relative tangential displacement is to be expected in the soil-lining contact. Moreover, as shown in that section, the non-slip assumption will tend to furnish both the highest and lowest values of thrust, at different locations in the lining, depending on the geometry of the problem and on the in situ stress ratio.

The premise of a horizontal ground surface, constant specific weight and constant in situ stress ratio is not very restrictive. More so is the assumption of homogeneity of the soil profile. Provided the tunnel cross section is fully embedded in one single layer and the case in study does not involve a mixed face condition, the simplification adopted is quite acceptable.

The solution adopted assumes a full face tunnel excavation. While this may be a reasonable approximation for a TBM excavation scheme, one may argue that it may not be so for a staged excavation. However, in schemes where the tunnel invert is excavated and supported at a small distance behind the leading tunnel face (say, one diameter), it is believed that the effect of the staged excavation may simply be localized and possibly transient. In these cases, the final response of the ground and lining may not be very sensitive to the sequence in which the face is excavated. Although this aspect has not been fully proven so far, the analyses shown in this chapter and in Chapter 7 of this thesis tend to confirm this assertion. Broadly speaking, provided a good soil-lining contact is ensured, as in shotcrete support, and provided the excavation is stable both globally and locally, in either a full-face or in a staged face scheme, the final stress changes in the ground are not dissimilar if the distance between the heading face and the point of closure of the lining invert is the same. The overall final tunnel performance is likely to be similar.

As noted in Section 5.2.1, the use of the conventional approach here for excavation simulation does not induce too much approximation since a full face excavation is represented and it is performed in a single phase. Also, the numerical integration of the in situ stress around the tunnel profile is quite acceptable as the number of elements around it is fairly large.

The ground stress reduction procedure used to simulate the 3D arching process in a 2D analysis, is quite adequate for the problem at hand, as shown in Sections 4.3.2.7 and 5.2.1. As noted, despite some indications that the rate of stress release around the contour may not be uniform as assumed in the present solution, the use of a unique stress reduction factor, a, is simpler and possibly safer, as far as lining bending is concerned. The key issue in this aspect of the simulation lies in how this factor, a, is determined.

The merits and limitations of the incremental procedure, as compared to iterative or mixed procedures, were discussed by Desai and Abel (1972:226). Perhaps the main advantage is that the convergence problems, often associated with iterative approaches, are non-existent, and that it provides complete descriptions of the load-deformation behaviour, since information is rendered at each load increment. The difficulty is associated with the definition of an adequate increment of load. However, experience gained with the present numerical solution, as applied to pre-failure simulations of excavations in fairly stiff soils (Medeiros, 1979:166), indicate that a relatively small number of increments (around four) is sufficient in this past stress incremental solution.

The merits and limitations of the hyperbolic stress-strain model, as implemented in this solution are well known (see, for instance, Morgenstern, 1975:12, Duncan et.al., 1980:20, Duncan, 1980:456, Christian, 1982;193, Chen and Saleeb, 1982:523, Vaid, 1985). A brief summary of these points is presented below.

The model is rather simple both conceptually and mathematically. It requires a small number of parameters, which have readily understood physical significance, although some of them are not fundamental soil properties. As it has been used for more than a decade, a fairly wide data base is available, which facilitates the estimate of parameter values in cases where sufficient data is not available. These values can be determined from the conventional triaxial testing which is routinely performed in geotechnical projects. A considerable amount of experience has been accumulated with this model, in a fairly wide range of practical geotechnical problems, including shallow tunnels, foundations (e.g. Domaschuk and Valliappan, 1975), excavations and retaining structures (e.g. Clough and Tsui, 1977:520), culverts (e.g. Duncan, 1979) and dams (e.g. Kulhawy and Duncan, 1972). This explains to some extent, the degree of confidence yielded in using this simple model. Moreover, the model accounts for non-linearity and stress dependency of soil behaviour and is applicable to both drained and undrained conditions.

As the model is based on incremental elasticity, it is not suitable for conditions where the behaviour of the soil mass is largely controlled by those elements which have already failed. As noted by Duncan (1980:457), the model is useful for predicting movements in basically stable earth masses and not for conditions extending up to the stage of soil mass collapse. Numerical procedures allowing stress redistribution after an element of soil fails ("load shedding") according to some failure criterion, have been developed (Byrne and Janzen, 1984), but were not incorporated into the present solution. The soil behaviour in this model is represented through a variable tangent modulus and a constant Poisson's ratio, which adds difficulty to portraying the soil response at failure. As failure is approached with increasing deviatoric stress, the modulus E_t undergoes a pronounced decrease. If the Poisson's ratio is kept constant, the reduction in E_t entails a proportional reduction of the tangent bulk and shear moduli, which are defined as:

$$B_t = \frac{E_t}{3(1-2\nu)} \qquad [5.3]$$

$$G_t = \frac{E_t}{2(1+\nu)} \qquad [5.4]$$

respectively. While the reduction in G_t is supported by experimental evidence, the pronounced reduction required in B_t is not. The value of the bulk modulus of soils is essentially independent of the magnitude of the deviatoric stresses and depends only on the mean normal stress (Chen and Saleeb, 1982:523). Even after failure, soils are able to sustain additional increases in mean normal stresses. An improved representation of soil behaviour at failure is obtained through hyperbolic models formulated in terms of the tangent bulk and shear moduli as above (e.g. Domaschuk and Wade, 1969) or in terms of the tangent Young's and bulk moduli (e.g. Duncan et.al., 1980). This problem is more pronounced at higher mean normal stress levels. In a plane strain shallow tunnel representation, failure is reached at relatively low stress levels, with decreasing confining stress. Thus, the E_t, ν formulation may suffice, especially if an accurate failure representation is not aimed for.

The present solution is strictly applicable only to soils in which shear dilatancy is not significant. Since the model is incrementally elastic and isotropic, cross effects between hydrostatic and deviatoric response components are disregarded. By uncoupling these components, volumetric changes are solely due to changes in the mean normal stress and those volume changes which are observed in certain soils under pure shear, are not represented. Byrne and Eldridge (1982) extended the original hyperbolic formulation by including an additional dilatancy parameter, which allows shear-volume coupling. This model was tested against some laboratory controlled problems but its potential in actual field conditions remains to be seen.

It has been assumed that the strength parameters, c and ϕ, are constant and stress level independent. Although the variation of the friction angle with the mean normal stress level (Vesic and Clough, 1968) can be easily implemented in the present solution (e.g. Duncan et.al., 1980:30), the conventional approach of assigning a "working" strength parameter, for the expected range of stresses, has been preferred. This range is fairly wide in some geotechnical structures (in a medium sized dam, the mean stresses can vary from zero to more than 1 MPa) and thus, a single representative ϕ value is difficult to define (particularly in cohesionless soils, with pronounced curvature of the failure envelope). In most urban tunnels, especially if a good ground control is ensured, the variations of the mean normal stresses around the opening are usually small (say from 0.1 to 0.3 MPa in a typical subway tunnel). Therefore, a single representative value of the strength parameter can be defined with no major implications.

Results shown by Duncan and Chang (1970:1644, 1646) and by Chang and Duncan (1970:1675), on laboratory testing, foundation and excavation simulations, indicated that satisfactory results may often be obtained using a reasonable estimate for a constant value of Poisson's ratio. Moreover, the experimental difficulties of determining parameters related to Poisson's ratio, indicate that it may be sufficient to assume a constant value in the analyses (Chen and Saleeb, 1982:520).

The stress-strain relationship adopted in the present solution followed a formulation which is compatible with the triaxial compression test. This led to the use of the minor principle stress and of the stress difference (major and minor prinicipal stresses), instead of the formally more appropriate stress invariant components such as the octahedral mean, normal and shear stresses. The latter were used in the hyperbolic model formulation by Domaschuk and Wade (1969), but the triaxial test based formulation gained wider acceptance and popularity, despite its lack of formal rigour. More critical than this is the fact that it is formally applicable only to that particular state of stress, in which the minor and intermediate principal stresses are equal. But, this is not the case in a plane strain or in a more general three-dimensional representation. In the present solution, the effect of the out of plane stress is not included, despite its known influence on both deformational and strength characteristics of soil behaviour. Moreover, by using parameters usually derived from triaxial tests, both characteristics will normally be underestimated in a plane strain analysis, unless some independent correction is included. The effect of the intermediate principal stress in the stress-strain relation of a numerically simulated unconfined compression test, was investigated by Gopalakrishnayya (1973:111), who pointed out that for a lower range of strains, its effect is not significant, but increases with increasing straining. Nevertheless, this effect is possibly less significant than the hyperbolic fitting approximation of the actual stress-strain data.

For the reasons exposed in Section 5.2.2.1, the present solution does not include any unloading and reloading criteria. As noted in Section 2.3.4.1, certain points around the tunnel may experience a rotation of the principal stresses. Consequently, these points will experience a decrease in the stress difference, associated with an increase in the minor principal stresses as the boundary stresses are reduced. This is the case of soil elements above the crown and below the floor of a tunnel, when the in situ stress ratio K is smaller than one. As a result, these elements become less stiff than they would have if an unloading-reloading feature had been implemented. It will be shown, however, that for stiff soils with K not far from unity, this simplification is not critical, as the stress reversal is achieved quite rapidly, and is followed by a monotonic increase in the stress difference. The major asset with this simplification is the allowance of a simpler generalization process as will be seen in Chapter 6.

The inability of the stress-strain model implemented in the present solution to predict the soil response under certain types of stress paths is well known. One of them is the constant stress-ratio paths (σ_1/σ_3) (Duncan and Chang, 1972:497), similar to that experienced in the central part of embankment dams. For these conditions, the strains are overpredicted for primary loading modulus values (Eisenstein, 1974). Another path is that of constant deviator stress under decreasing minor principal stress. For this, the present model would indicate expansion in all directions, while in actual fact compressive stains would be observed in the direction of the major principal stress. This anomaly was noted by many authors, for example, Duncan and Chang (1972) and Verruijt (1976). Chen and Saleeb (1982:524) suggested that this is due to the assumption of co-axiality of stress and strain increments, which result from the assumption of incremental isotropy and linear elasticity of this model. They recalled experimental evidence showing that the principal directions of strain increments coincide more closely with the direction of the principal stresses rather than that of the stress increments, notably at high stress levels and as failure is approached. Fortunately, none of these paths are typical for points around a shallow tunnel (Section 2.3.4.1).

Additional limitations to the present solution are its inability to account for the strain softening behaviour after peak and the fact that the parameters involved are not fundamental soil properties. However, these parameters have clear physical significance which facilitates the comparisons of different soil properties and the appreciation of their effects on the soil response.

Despite all the limitations described, the stress-strain model implemented in this numerical solution has shown its potential in a variety of situations, including the prediction of soil responses under quite unconventional loading conditions as shown by Duncan (1980:245). When used with judgement and making allowance for the uncertainties in the test data serving as input and in the approximations in the model, Duncan (Op.cit.) has shown that reasonable ranges of behaviour are predicted for different soil types.

5.2.3 Parametric Studies

The numerical model described in the previous section was tested for a variety of idealized conditions, before being used for the simulation of actual shallow tunnels. A number of sensitivity studies were undertaken in order to gain experience and to assess the influence of the intervenient parameters and variables.

It was felt that the results of these studies would be better appreciated in connection with the development of a model for generalized shallow tunnel performance. Accordingly, some of the results of these sensitivity studies are presented in Chapter 6. They include assessments of aspects related to the numerical simulation (size of mesh, number of load steps, etc.), to the effect of the in situ stress conditions (tunnel depth, in situ stress ratio), to the influence of the soil strength (cohesion and friction angle), to the influence of the soil deformation properties (Janbu's modulus and exponent, Poisson's ratio), and to the amount of stress release, etc.

5.2.4 Analyses of Some Case Histories

5.2.4.1 Opening Remarks

In order to assess the overall ability of the numerical solution adopted to simulate the performance of actual shallow tunnels, a few case histories were analysed. All analyses are type C1 predictions. Unlike the majority of similar studies reviewed in Section 5.2.1.2, the analyses shown in the following sections attempted a complete comparison between calculated and observed performance, including ground displacements and lining loads.

The selection of case histories for study was guided by a number of factors. Firstly, preference was given to well documented cases with comprehensive and numerous field data, and under well known geotechnical conditions. Secondly, the selected case histories should entail aspects which are understood as typical of the idealized conditions required for the application of the numerical solution. These include geometric aspects, soil properties and soil conditions, construction type, etc. Hence, tunnel cases where the construction quality and the quality of the ground control were recognized as good were intentionally chosen. Finally, preference was given to cases where the writer was directly or indirectly involved in the process of field observation, data acquisition and construction follow-up.

There were three cases chosen for analyses. The first is the 4 m diameter Alto da Boa Vista Tunnel, abbreviated to the ABV tunnel, built in Sao Paulo, through a clayey sand sediment, using the so called New Austrian Tunnelling Method (NATM). The second is the Southbound Edmonton LRT tunnel at Jasper Avenue, driven by a 6 m diameter TBM, through a stiff glacial till. The third is the Edmonton Experimental Sewage tunnel, also driven by a TBM, but with a 2.56 m diameter, through a softer glacial till. Further details of these case histories are summarized in Table 5.7 and will be furnished in the following sections.

In the three cases, soil conditions and properties were fairly well defined or bounded. The major unknown was the amount of stress release to be applied in the 2D analyses representing the 3D mechanism. With respect to this, the study conducted was a back analysis, in which the independent variable was the fraction of ground stress reduction, α, to be considered prior to lining installation, in order to obtain a reasonable match between the observed and computed performances. Besides this variable, some other properties were also varied, but to a lesser degree and covering their possible ranges of values.

The subject of back analysis as applied to geotechnical engineering has received considerable attention in recent years. Also referred to as calibration, characterization or identification processes, the back analysis problem can be solved by "direct" or "inverse" approaches. In the first approach, the solution is obtained by minimizing the differences between observed and computed performances, by correcting the trial values of the unknown parameter. In the

Case	1	2	3
Tunnel	ABV	Edmonton LRT	Edmonton Exper.
Reference	Negro & Eistenstein, 1981	Branco, 1981	El Nahhas, 1980
Soil Condition	Clayey sand (stiff-dense) above W.L.	Stiff glacial till, above W.L.	Softer glacial till, above W.L.
Construction	NATM	TBM	TBM
Primary lining	Shotcrete	Steel ribs and wooden lagging	segmented concrete
External diameter (D)	4.0 m	6.1 m	2.56 m
Cover (H)	6.20	9.0 m	22.5 m
H/D	1.55	1.48	8.79

Table 5.7 Case Histories Selected for Analyses with the Adopted Numerical Solution

second, the governing equations of the problem are "inverted", so that the observed performance quantities are set as input data and the unknown parameters become output of the inverted problem. Since the number of field measurements usually exceeds the number of unknowns, some minimization procedure is required to optimize the solution. The problem can be treated using either a deterministic or a statistical approach. The latter is applied whenever the influence of possible errors or uncertainties in the observed variables are believed to be significant in the results of the analysis. A general review on the subject was presented by Gioda (1985) who discussed different optimization procedures, and the advantages and disadvantages of direct and inverse approaches. Applications to the tunnel problem have been limited to simpler linear elastic constitutive relations (e.g. Gioda and Jurina, 1981:47, Ledesma et.al., 1986). The treatment of non-linear material responses is the subject of ongoing studies by different researchers.

The analyses presented in subsequent sections do not include any of the formalism just described. The best fit conditions were obtained by a direct trial and error approach, where the acceptance of the results relied simply on a balanced judgement of the aspects of the tunnel performance being inspected.

5.2.4.2 Alto da Boa Vista Tunnel

Introduction and Site Geology

This was a medium sized tunnel built in 1978 in the southern area of Sao Paulo, Brazil, to connect two water treatment plants. Details of this project were given by Negro (1979), Negro and Eisenstein (1981), Simondi, Negro and Kuperman (1982), Negro (1983) and were partly summarized by Heinz (1984:273). A very brief description is included herein for completeness.

This 73 m long tunnel was driven as an experimental project, to test the NATM procedure in the construction of an urban tunnel, for the first time in South America. It was driven with an almost circular profile of about 4 m external diameter, and with a soil cover of 6 to 6.5 m. A longitudinal cross section of the tunnel is shown in Figure 5.13, where a simplified geological profile is included which summarizes data from the logs of 7 boreholes.

The soils found at the site represent some of the upper layers of Sao Paulo Sedimentary Basin. This deposit resulted from the combined action of tectonics affecting the Pre-Cambrian metamorphic bedrock (gneiss, migmatite and mica-schist mainly) with simultaneous sedimentation processes. A depressed valley floor was formed and filled with sediments in the early Tertiary. The source of sediments was the residual soil mantle covering adjacent scarps, which was eroded, transported a short distance and finally deposited under an alluvial-lacustrine environment.

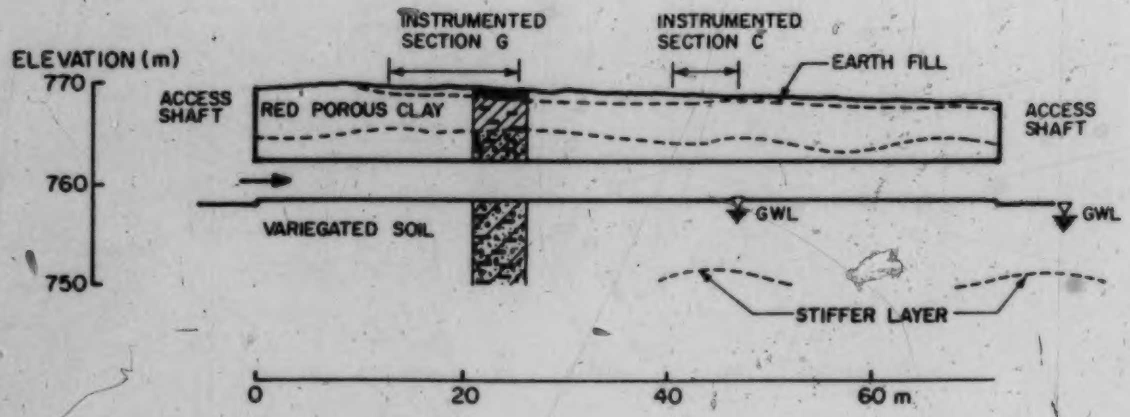
INSTRUMENTED SECTION G
INSTRUMENTED SECTION C
ELEVATION (m)
770
760
750
EARTH FILL
ACCESS SHAFT
RED POROUS CLAY
ACCESS SHAFT
GWL
GWL
VARIEGATED SOIL
STIFFER LAYER
0
20
40
60 m

Figure 5.13 Longitudinal Profile Along ABV Tunnel

The soils thus formed were later subjected to pedological processes under a dry climate, involving chemical weathering of the upper layers.

Below an earth fill layer of some 0.5 m thickness a 3 to 4 m thick layer of a soft lateritic silty clay is found, which is locally called red porous clay. Underlying this is a thick layer of what is locally referred to as the variegated soil, thus named for its diversified colours. The tunnel was entirely driven through this rather heterogeneous material which was predominantly represented at this site by a silty and clayey fine sand of medium density with occasional gravel layers. The ground water level was found 1 or 2 m below the tunnel floor, and a stiffer horizon was detected at some 20 m below the surface.

Geotechnical Properties

The typical index properties of the soils given in Table 5.8 were obtained from samples collected at the site. Of particular interest are the mechanical properties of the variegated soil, which should govern the tunnel response. These are summarized in Table 5.9 and are derived from laboratory tests carried out on undisturbed block samples collected at the site and at other locations. This soil belongs to Groups II and III according to the classification system proposed by Sousa Pinto and Massad (1972), and by Massad (1980). The properties indicated are expressed in terms of effective stresses (drained parameters). While most parameters shown have been obtained from actual laboratory testing (triaxial compression and oedometer tests), the coefficient of earth pressure at rest was estimated from an empirical expression proposed by Mayne and Kulhawy (1982:863):

$$K_o = (1-\sin\phi')OCR^{\sin\phi'} \qquad [5.5]$$

The K_o range shown was calculated for a friction angle of 29°, for the given range of overconsolidation ratios.

The red porous clay overlying the variegated soil, although more homogeneous in appearance than the latter, is in reality very heterogeneous particularly in terms of deformation properties (Massad, 1974 and Massad et.al., 1981). Some mechancial properties of this material as found at the site are shown in Table 5.10. Additional data on this soil can be found, for example in Kupper (1983).

Possibly for a better evaluation of the in situ deformation properties, a few pressuremeter tests were conducted using the same probe and equipment used by Eisenstein and Morrison (1973). Figure 5.14 shows the variations of the Young's modulus, calculated from the pseudo-elastic testing stage on primary loading, using the Gibson and Anderson (1961) interpretation. Tests were conducted at three boreholes, but the results were superimposed for presentation. The considerable scatter of data noted may reflect the erratic nature of the sediments, but there appears to be an overall trend of the E modulus increasing with depth. Results marked with an asterisk were probably affected by the presence of gravels immersed in the

Soil Type	Red Porous Clay	Variegated Soil
Liquid Limit (%)	58 - 72	44 - 64
Plasticity Index (%)	27 - 38	17 - 31
Water Content (%)	30 - 39	13 - 26
Finer than 2 µm (%)	52 - 74	19 - 57
Coarser than 75 µm (%)	10 - 25	14 - 83
Total Unit Weight (kN/m^3)	14.3 - 16.0	17.8 - 19.4
Specific Gravity	2.69 - 2.85	2.68 - 2.84
Void Ratio	~ 1.55	~ 0.86
Degree of Saturation (%)	62	63

Table 5.8 Typical Ranges of Properties of ABV Soils

Cohesion intercept c' (MPa)	0.01 - 0.03 (1)
Friction angle ϕ' (°)	26 - 32 (2)
Failure ratio R_f	0.8 - 1.0
Modulus number K	300 - 400
Modulus exponent n	0.2 - 0.3
OCR	2 - 3
K_0	0.7 - 0.9 (3)
Posson's Ratio ν	0.3 (4)

Notes:
(1) For stresses above the overconsolidation pressure the cohesion intercept is zero.
(2) Range for stresses beyond the overconsolidation pressure. For that C' = 0.
(3) Estimated from Mayne and Kulhawy (1982) expression for $\phi' = 29°$.
(4) Estimated.

Table 5.9 Range of Geotechnical Parameters for the Variegated Soil at the ABV Site

Cohesion intercept c' (MPa)		0 - 0.07 (1)
Friction angle ϕ' (°)		22 - 30 (1)
Oedometer E moduli (MPa)		
Primary loading	(50 to 100 KPa)	5 - 10
Unloading	(100 to 50 KPa)	11 - 16
Reloading	(50 to 100 KPa)	25 - 30
OCR		2.5
K_0		0.8 (2)
Poisson's Ratio		0.2 - 0.4 (3)

Notes:
(1) Drained strength range for stresses below overconsolidation pressure. Data from other locations.
(2) Estimated from Mayne and Kulhawy (1982) expression for ϕ' = 26°.
(3) From Kupper (1983:118) measurements at low confining pressures.

Table 5.10 Range of Geotechnical Parameters for the Red Porous Clay at the ABV Site

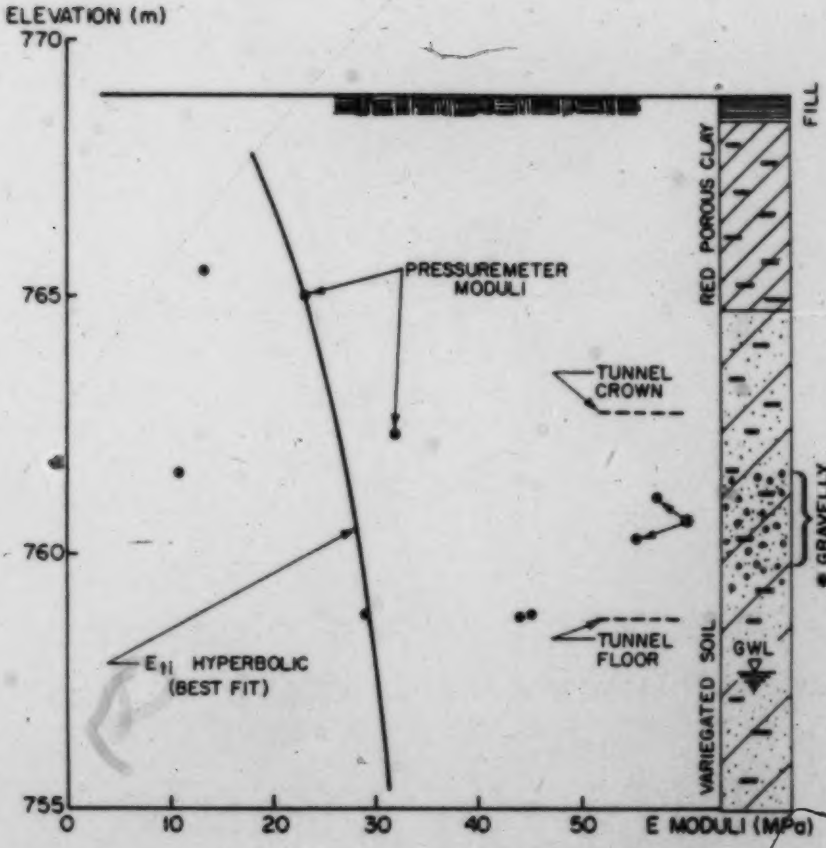

Figure 5.14 Profile of the In Situ Deformation Modulus at the ABV Site

clayey sand layer. Also shown, is the variation of the initial tangent modulus with depth as given by the hyperbolic model formulation (Figure 5.11), for the in situ stress conditions. This modulus distribution was the one used in the best fit back analysis as explained later. It corresponds to K=400, n=0.25, $\phi'=29°$, c'=0, $R_f=1$, $K_o=0.75$ and $\gamma=16$ KN/m³.

Construction Details and Field Monitoring

Tunnel construction was undertaken with a three-stage face excavation (heading, bench and floor) with immediate shotcreting of exposed walls. Details of the transverse and longitudinal sections of the tunnel are shown in Figure 5.15. The cross section of 12.8 m² was fully hand mined, with the heading advance varying from 1 to 1.5 m. Lining invert closure at the instrumented section took place at about 2.6 m behind the heading face. The average construction rate was 1.6 m/day for a single 10 h/day shift and when passing the instrumented section, it peaked at a rate of 2.8 m/day.

The initial support system was a 10 cm thick shotcrete with a light wire mesh placed in the centre of the section. After tunnel completion, an additional 3 cm layer of shotcrete was applied at the lateral walls. This system worked as a primary and secondary support. Perfect material and structural conditions were revealed by a site inspection 40 months after completion. A complete set of information on the construction control and the shotcrete properties and

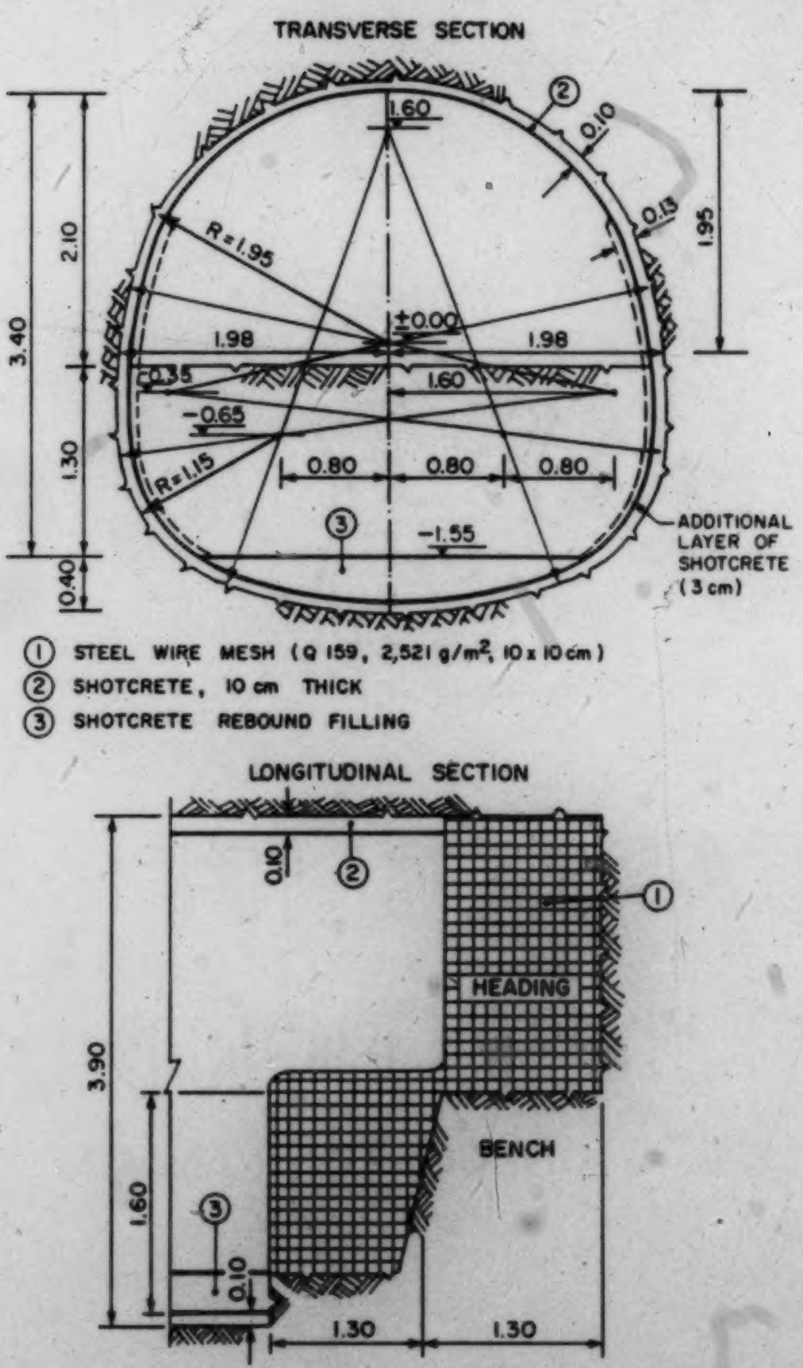
TRANSVERSE SECTION
1.60
②
0.10
0.13
R=1.95
2.10
3.40
1.95
±0.00
1.98
1.98
-0.35
1.60
-0.65
1.30
R=1.15
0.80
0.80
0.80
③
-1.55
0.40
ADDITIONAL LAYER OF SHOTCRETE (3 cm)
① STEEL WIRE MESH (Q 159, 2,521 g/m², 10 x 10 cm)
② SHOTCRETE, 10 cm THICK
③ SHOTCRETE REBOUND FILLING
LONGITUDINAL SECTION
0.10
②
①
HEADING
3.90
BENCH
1.60
③
0.10
1.30
1.30

Figure 5.15 Construction Details at the ABV Tunnel

performance was published by Simondi, Negro and Kuperman (1982). From this data it can be estimated that the Young's modulus of the concrete increased from 2 GPa a few minutes after its application to 20 GPa about 24 hours later. The excavation of the heading and bench proceeded during concrete hardening, before it achieved its final strength. Field monitoring, which included convergence and levelling measurements inside the tunnel and ground movements near the opening, indicated that a substantial part of the lining deformations took place in less than 24 hours following the initial shotcrete application at the heading walls. Lining invert closure took place in less than 24 hours after the heading face reached the instrumented section. Most of the remaining lining deformations took place in the subsequent 24 hours, with the heading face advanced about one diameter ahead of the instrumented section. In other words, most of the interaction processes between the soil and lining took place while the shotcrete was young, at which stage it is difficult to assess its mechanical properties. Moreover, it is appreciated that within the same shotcrete ring, there are portions with different ages, which further complicates the assessment. If a single value of the secant Young's modulus of the shotcrete was to be chosen in order to be represented in a simplified interaction analysis, this value would have to be necessarily low. A reference value of 5 GPa was liberally selected, which is believed to have been the shotcrete secant modulus some 6 to 8 hours after its application. A Poisson's ratio of 0.25 was adopted for the shotcrete. This is slightly higher than is usually assumed for normal concrete. However, it is known that during hardening, the Poisson's ratio decreases from 0.4-0.5 to a final value of around 0.2. To be consistent with the lower reference modulus of deformation, a higher Poisson's ratio had to be assumed.

Field instrumentation comprised surface and subsurface settlement measurements, section convergence monitoring, tunnel crown levelling and contact pressure measurements. The latter was done using hydraulic pressure cells (Interfels type HPG077) located at the lining-soil interface, at the crown, springline and floor of the tunnel. Details of other measuring schemes are given by Negro and Eisenstein (1981), who also provide the results and interpretation of the field measurements.

Numerical Simulation

For the back analysis of this tunnel performance the numerical solution described in Section 5.2.2.1 was used, with a finite element mesh having 273 nodal points and 500 elements. A surficial porous clay layer of 4.2 m thickness and with linear elastic behaviour was initially considered to overlie the non-linear elastic variegated soil layer. A few runs revealed that the results of the analyses were not very sensitive to the elastic properties assigned to the upper layer, for the ranges given in Table 5.10. It will be shown later in Section 6.2.4.2 that the tunnel response is basically controlled by the properties of ground extending a half tunnel diameter above and below the opening. In this case, only variegated soil exists within those limits. It was decided to simulate the problem as a single soil layer, with selected properties representing the variegated soil.

Figure 5.16 furnishes the assumptions that were made and the values of the soil parameters that were used and kept constant in the analyses. Field monitoring indicated that the ground response was basically time-independent and the location of the ground water level below the tunnel floor led to the assumption of a fully drained soil response. The soil parameters were selected accordingly from the range of values shown in Table 5.9. Furthermore, they were chosen so to approximate the in situ modulus distribution provided by the pressuremeter tests results shown in Figure 5.14, both for the variegated soil and for the porous clay. The specific weight shown is a weighted average value for the two soil layers combined. The only soil parameter allowed to vary in the analyses was the coefficient of earth pressure at rest. The range of variation considered for K_o was that shown in Table 5.9 (from 0.7 to 0.9).

A perfect equivalence betwen the actual shotcrete lining and the thicker lining ring used in the numerical simulation would be achieved only if the compressibility and flexibility ratios of both linings were equal. This, however, is not possible since there is one condition too

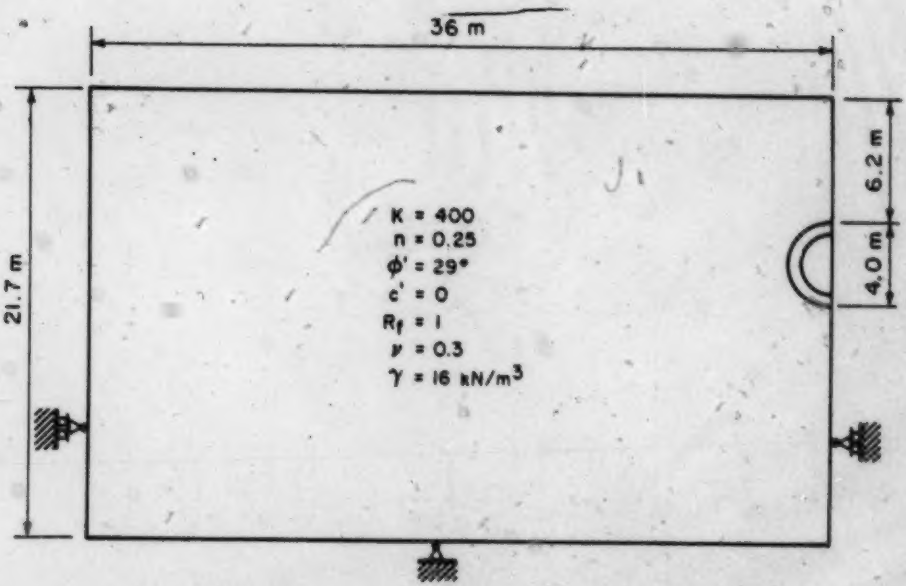

36 m
21.7 m
6.2 m
4.0 m
K = 400
n = 0.25
φ' = 29°
c' = 0
R_f = 1
ν = 0.3
γ = 16 kN/m³

Figure 5.16 Assumptions and Fixed Parameters for ABV Tunnel Back Analyses

many. For the 10 cm thick shotcrete lining, an outside diameter of 4 m, a 5 GPa modulus, and a Poisson's ratio of 0.25, those ratios are equal to 0.11 and 507.8, respectively, using the Einstein and Schwartz (1979) definitions (equations 2.17 and 2.18). To approximate these figures, the 50cm thick equivalent lining of equal external diameter, would require a modulus of either 30 MPa to harmonize with the compressibility ratio or 900 MPA to equal the flexibility ratio. Accordingly, in the back analysis, the lining modulus was assumed to vary within these limits. It was later found that the best agreeement between measured displacements and stress is obtained when the flexibility ratios are similar.

The third and most important parameter to be varied in the analyses, is the amount of stress release taking place prior to the lining installation. An interpretation of the field measurements suggested that it would be sufficient to vary this parameter from 30 to 50%.

Results of the Back Analyses

After a few tentative runs it was concluded that five equal load increments, for each simulation phase (10 unloading steps altogether), allowed an adequate approximation. Table 5.11 summarizes the parameters that were varied in the analyses. Fourteen combinations of these parameters were required to give what was called the best fit case. For the higher lining modulus, the tunnel crown heaved rather than settled as observed in the field. The

Stress release α prior to lining installation (%)	30	40(1)	50	
In situ stress ratio K_0	0.7	0.75(1)	0.8	0.9
Equivalent lining E modulus (MPa)	50(1)	100	200	

Note: (1) Best fitted values

Table 5.11 Parameters Varied in ABV Tunnel Back Analyses

best fit analysis provided a reasonably good match between the calculated and observed performances, both at the final equilibrium situation and before lining installation. This condition was found for 40% stress release prior to the lining installation, for K_0=0.75 and for an equivalent lining modulus of 50 MPa. This modulus value corresponds to a flexibility ratio, F, equal to 293.7 or a shotcrete modulus of about 8.65 GPa. As noted previously, the in situ (initial) tangent modulus distribution with depth is that given in Figure 5.14, which roughly agrees with the pressuremeter test results.

Figures 5.17 and 5.18 compare observed and calculated vertical displacements in the ground, at the surface and below it, when the heading face reached the instrumented section. The calculated values correspond to a stress release of 32%. Figures 5.19 and 5.20 show in turn, the final vertical movements of the ground after full equilibrium between lining and soil. In both situations, a reasonable agreement between observed and calculated movements is found, in terms of the magnitude of the maximum displacements and in terms of their overall distribution, including ground heave below the tunnel floor.

Figure 5.21 compares the final radial stresses onto the lining as measured in the field and as calculated in the best fit finite element run. The latter was obtained by extrapolation of the averaged element stresses in the ground to the lining-soil interface. The contact stresses were

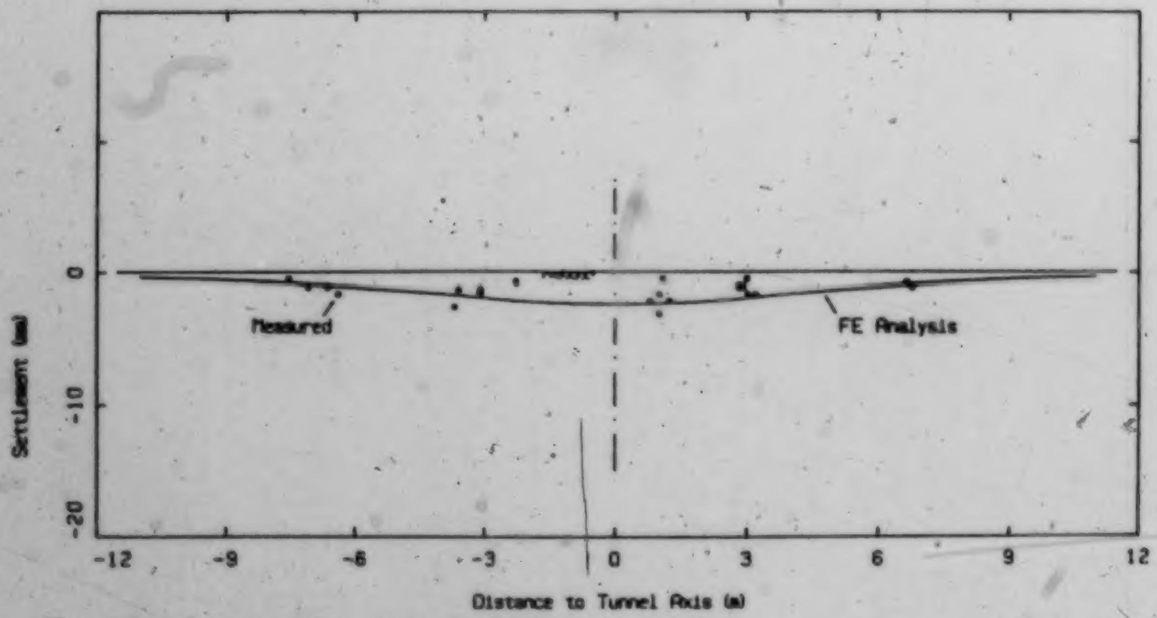

NOTE : MEASUREMENTS AT INSTRUMENTED SECTION C AND G

Figure 5.17 Measured and Calculated Surface Settlements at the Face of the ABV Tunnel

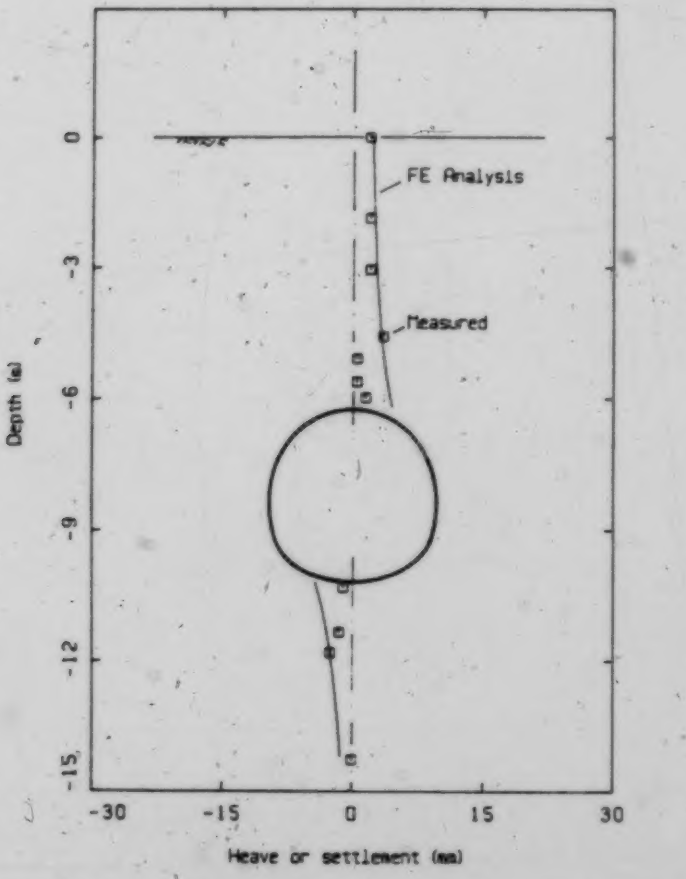

NOTE : MEASUREMENTS AT THE MAGNETIC EXTENSOMETER CCI (SECTION C)

Figure 5.18 Measured and Calculated Subsurface Vertical Displacements at the Face of the ABV Tunnel

measured by three Glotzel type pressure cells located at the crown, springline and floor. Notwithstanding the known difficulties associated with the installation of these type of cells notably at the upper arch of the lining, the agreement between the measured and calculated contact stresses is fairly reasonable. The radial stresses at the crown and springline are overestimated by the FE analysis, and slightly underpredicted at the floor.

Finally, Table 5.12 summarizes the comparisons between measured and predicted performances for this case history. It also includes additional data regarding measurements taken inside the tunnel, for convergence and crown levelling. The major discrepancies found refer to these latter measurements. The maximum horizontal convergence of the lining was appreciably overestimated while the lining roof settlement was underestimated. These disparities are not unexpected, when one considers the three-dimensional arching and ground-lining responses discussed in Section 2.3.6. It was suggested in that section that in heading and bench schemes with immediate application of shotcrete in the tunnel walls, some longitudinal bending of the upper shotcrete shell, which is open at springline elevation, may occur. The field instrumentation seems to support that this was the case in the ABV tunnel. The upper shell seemed to have worked as a cantilever, "fixed" in the closed section further behind. A partial rebound was noted once the invert was closed. The associated spatial squatting

Performance Aspect		Measured(1)	Calculated	C/M
1. Maximum surface settlement at tunnel face	mm	1.6	2.3	1.44
2. Maximum final surface settlement	mm	5.0	4.2	0.84
3. Maximum slope of final settlement trough at surface		1:1300	1:1790	0.73
4. Floor heave at tunnel face	mm	1 - 1.5(2)	3.2(3)	2.13 - 3.2
5. Final floor heave	mm	5 - 9(2)	8.2(3)	0.91 - 1.64
6. Maximum horizontal convergence of the lining	mm	0.85	5.7	6.71
7. Crown settlement at tunnel face	mm	1.5(4)	4.2(4)	2.80
8. Final crown settlement	mm	8.0(4)	7.7	0.96
9. Total settlement of lining roof	mm	4 - 5	2.6	0.52 - 0.65
10. Pressure on lining at the crown	kPa	30	44	1.47
11. Pressure on lining at the springline	kPa	35	49	1.40
12. Pressure on lining at the floor	kPa	55	47	0.85

Notes: (1) Average values.
(2) Measured at 0.2m and 1.2m below tunnel.
(3) Calculated at 0.7 m below tunnel.
(4) At 0.2m above tunnel.

Table 5.12 Measured and Calculated Performance of ABV Tunnel

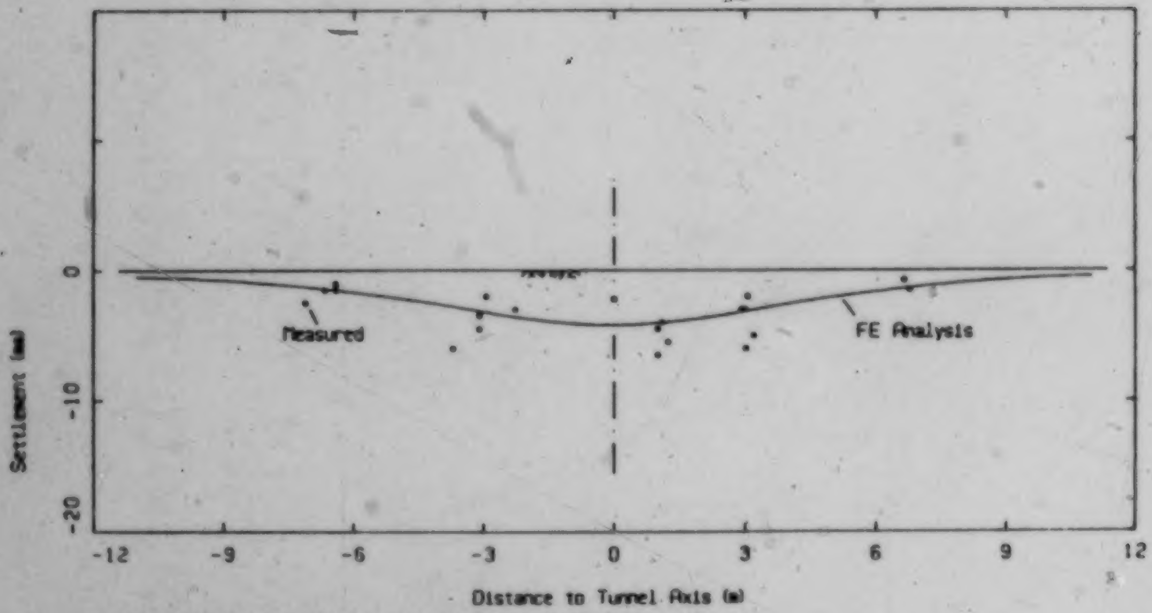

NOTE : MEASUREMENTS AT INSTRUMENTED SECTIONS C AND G

Figure 5.19 Measured and Calculated Final Surface Settlements at the ABV Tunnel

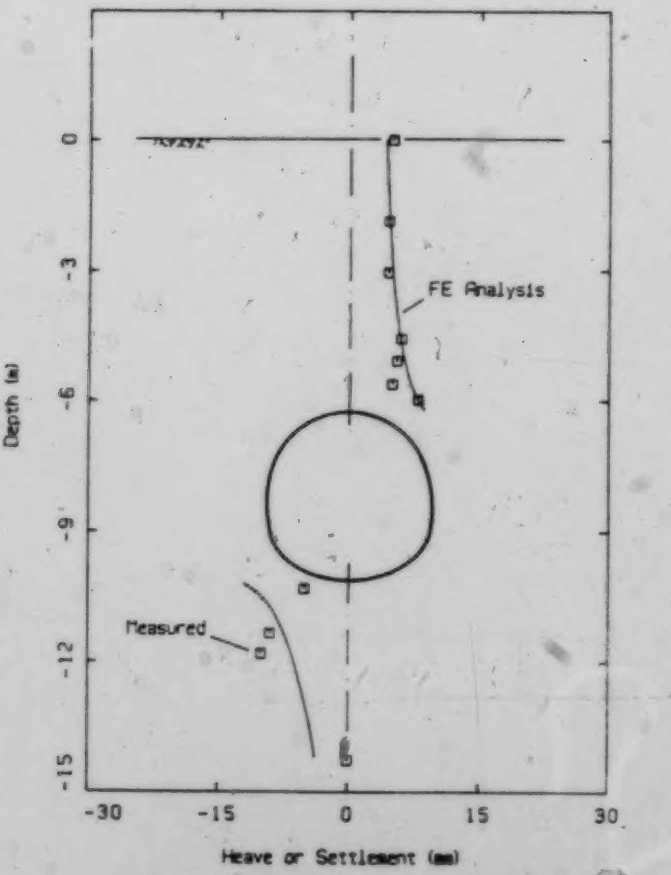

NOTE : MEASUREMENTS AT THE MAGNETIC EXTENSOMETER CCI (SECTION C)

Figure 5.20 Measured and Calculated Final Subsurface Vertical Displacements at the ABV Tunnel

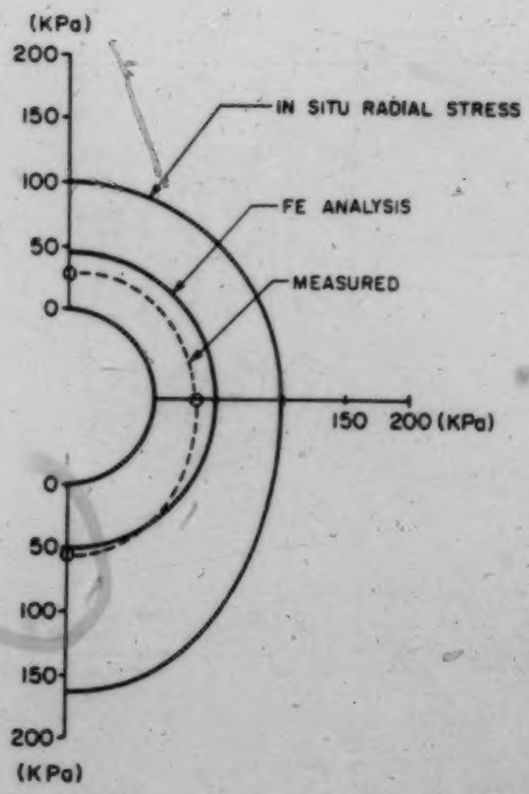

Figure 5.21 Measured and Calculated Final Radial Stresses on ABV Tunnel Lining

of the half cylinder shell which causes the crown to deflect downwards and springline points to move outwards, cannot be simulated with the present simple two-dimensional model, and this could explain the noted discrepancies.

Unfortunately, the readings in the contact pressure cells were not planned to monitor this type of response. It seems worthwhile to confirm this mechanism in similar projects in the future, using adequate monitoring equipment and planning. Moreover, it seems relevant to explore the consequences of this type of response, by using detailed three-dimensional numerical simulations in future research projects. The absence of an adequate treatment of this problem in lining design was indicated in Section 4.2.1. Also, the current lack of appreciation, by practitioners, of this mechanism as a possible source of problems was shown in Section 4.4.2.2.

The same reasons exposed above could explain the poorly predicted magnitude of crown settlement and floor heave at the moment the tunnel face reaches the instrumented section. A simple two-dimensional representation cannot portray with accuracy the ground-displacement field around the tunnel face. While in the present plane strain solution, the vertical displacements along the tunnel axis above crown, will always be shown as attenuating from the opening to the surface, it is known that this may not be the case (see for instance, Casarin, 1977 and Katzenbach, 1981:100). In the planes containing the tunnel face or ahead of it, settlements larger than the crown settlement can be observed above the crown elevation in an actual 3D case. Reciprocally, the same response may occur below the floor elevation. If the aspects of performance that are strongly influenced by the 3D nature of the tunnel problem are put aside (items No. 4, 6, 7 and 9 in Table 5.12), the others are fairly reasonably approximated by the numerical simulation. Although not formally attempted, it was felt in the course of these analyses that 3D dominated aspects could have been fully bracketed by the numerical solution, if allowance for extreme variations of the soil properties had been made.

Unfortunately, no measurements of horizontal ground movements were taken in this case history, and this allowed an additional degree of flexibility in fitting the observed performance. The best fitting process is also made easier by virtue of the fact that three parameters (K_o, E_s, α) were allowed to vary. It should be noted that the K_o value was only allowed to vary within fairly narrow limits. The same cannot be said regarding the lining properties but this does not affect the back analysis of the performance prior to support application, but only after. Hence, it can be accepted that the assessed amount of stress release before lining placement, has been reasonably approximated in this analysis. For similar studies in the future, it would be advisable to undertake careful investigation of the variation in the deformation modulus of the shotcrete with time and with the tunnel advance. This would be affected by means of some in situ monitoring or laboratory testing under variable strain rate control conditions. This would enable a narrower range of properties to be considered, which could improve the accuracy of the stress release estimate.

The back analysis furnished a final all round average radial stress onto the lining which amounts to 40% of the in situ radial stresses. This is compared with the 34% provided by the measurements. The mean thrust in the support was, therefore, overestimated by about 18%. If the bending moments are considered to be proportional to the radial stress difference between the crown (or floor) and the springline, it could be said that the analysis underpredicted the actual bending moments by about 11%. These figures should be taken with a word of caution, because of the known difficulties with pressure cells. It is worth noting that an almost uniform all-round radial stress distribution was obtained from the analysis. This seems to be consistent with the mode of behaviour, which is usually anticipated for unreinforced or lightly reinforced shotcrete linings. In these the final bending moments are expected to be negligible due to the singular process of ground load transfer while the shotcrete is hardening.

Finally, Figures 5.22 and 5.23 illustrate the amount of straining after final equilibrium is reached, that points around the tunnel should be subjected to according to the numerical simulation results. Figure 5.22 indicates that the soil next to the opening underwent compression in the major principal strain direction (up to about 1%) and extension in the minor one (up to about -0.4%), as expected. As a measure of shear straining, principal strain differences were plotted in Figure 5.23. The maximum strain difference is observed around the tunnel springline and amounted to 2%. At distances greater than about one radius from the tunnel the effect has dropped significantly to 0.1% or less. The difficulties in defining a "failure zone" from shear strain contours, was discussed in Section 2.3.4.3. Although no laboratory data is available on samples of the variegated soil tested under the stress path that prevails in this region, available results from conventional triaxial tests (Massad, 1980), suggest that this soil would fail under higher strain differences (around 3 to 6%). In fact, the numerical simulation indicated that no soil element experienced failure, as defined by the Mohr-Coulomb envelope, in any stage of the analysis. Despite this, a substantial decrease in the tangent elastic modulus was observed from its initial in situ value to that calculated for the final situation. This is also illustrated in Figure 5.23, where it is shown that near the tunnel walls, the tangent modulus decreased to about 1% of its original value.

Despite the fact that this tunnel had been built under very good ground control and favourable ground conditions (Negro, 1979, Negro and Eisenstein, 1981), a significant

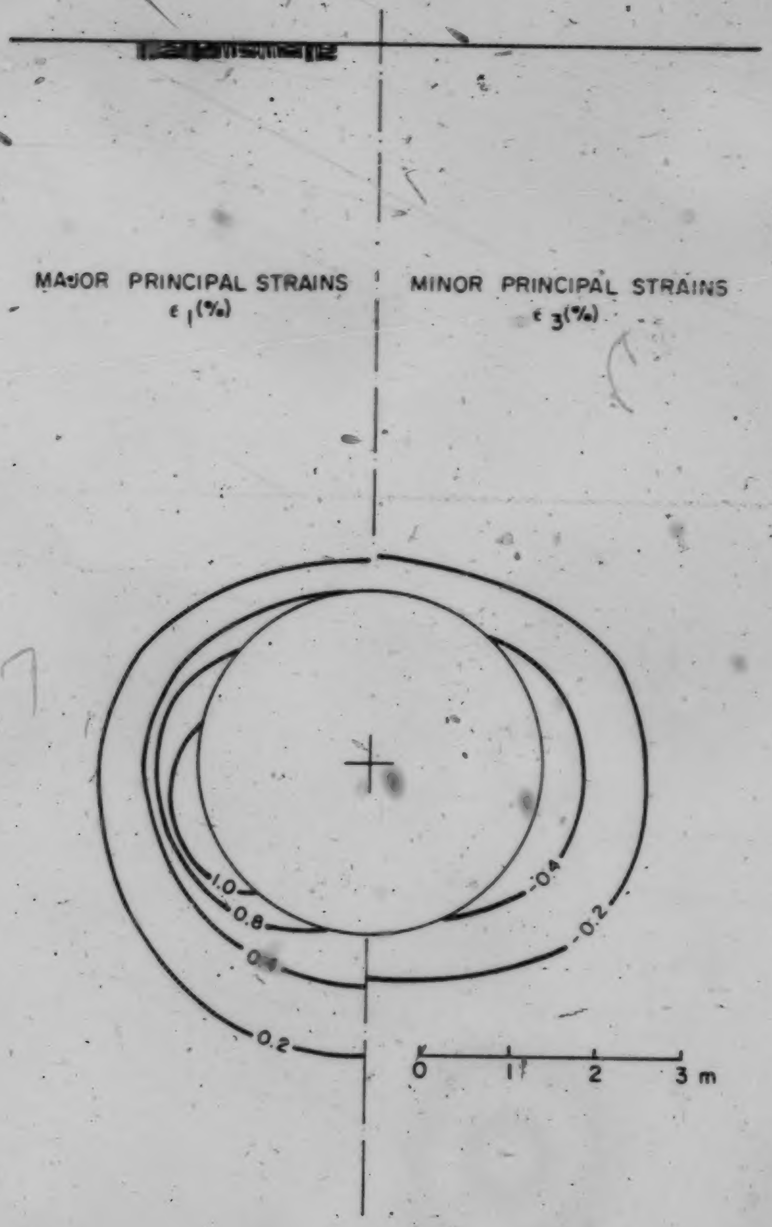
MAJOR PRINCIPAL STRAINS
ϵ_1(%)
MINOR PRINCIPAL STRAINS
ϵ_3(%)
1.0
0.8
0.4
0.2
0.4
0.2
0
1
2
3 m

Figure 5.22 Calculated Contours of Major and Minor Principal Strains Around the ABV Tunnel

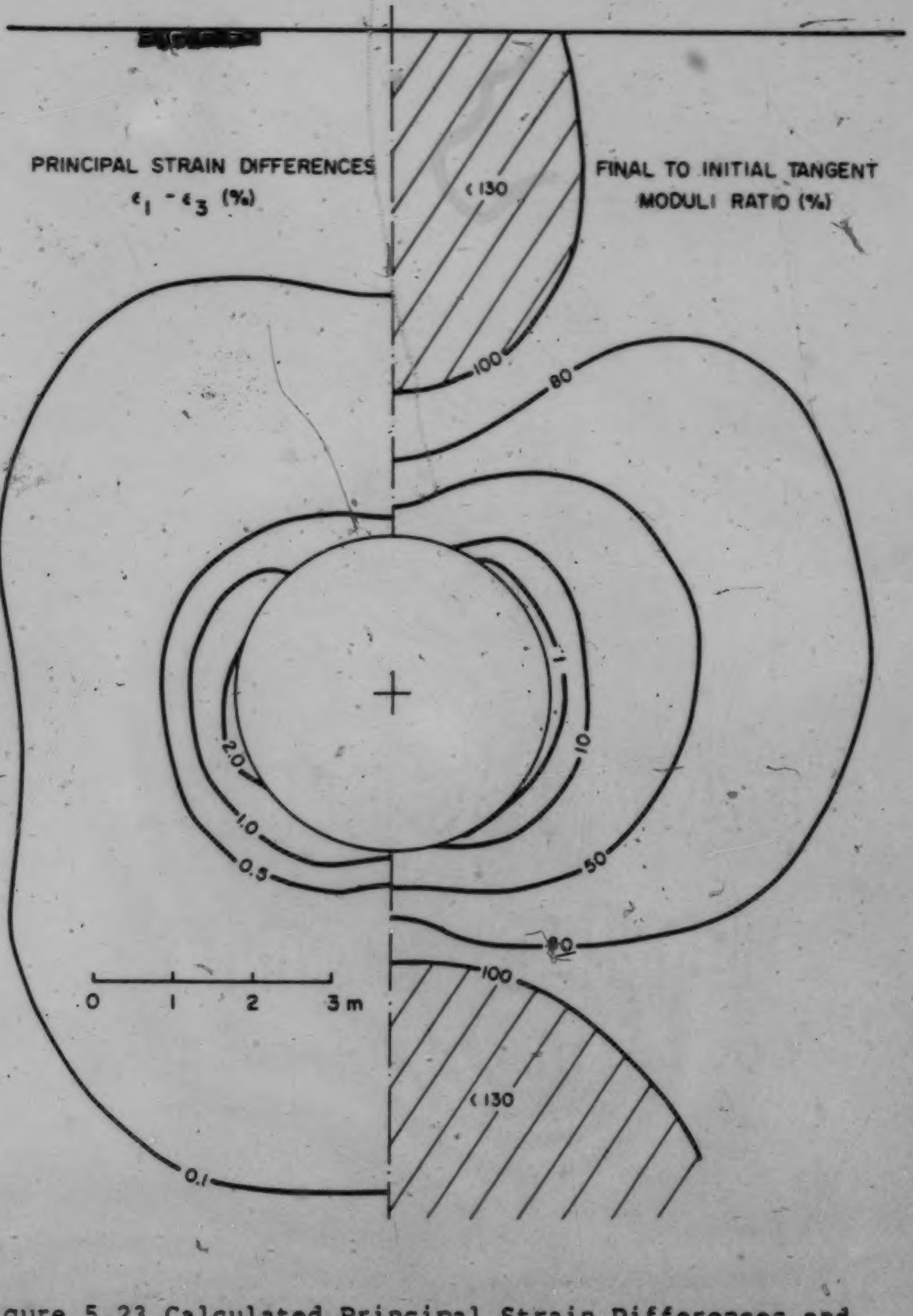
PRINCIPAL STRAIN DIFFERENCES
ε1 - ε3 (%)
FINAL TO INITIAL TANGENT
MODULI RATIO (%)
<130
100
80
1
10
50
80
100
<130
2.0
1.0
0.5
0.1
0
1
2
3 m

Figure 5.23 Calculated Principal Strain Differences and Changes in Tangent Modulus Around the ABV Tunnel

non-linear ground response seems to have occurred. This tends to confirm the aspects discussed in Chapter 2, where it was pointed out that, even if ground failure is avoided by adequate construction procedures, the non-linear response of the soil cannot be neglected when interpreting or simulating the observed the observed tunnel response. Consequently, the associated tunnel performance could not be adequately simulated by a linear elastic model or by some elasto-plastic models (Section 5.2.1.1), unless some aspects of the behaviour are disregarded. This was the case of the linear elastic analysis of the same tunnel carried out by Negro and Eisenstein (1981), where a full stress release was assumed at the excavated tunnel boundary and where the presence of the lining was not explicitly taken into account.

No concentration of shear straining was detected, although one would not expect to obtain this with the present finite element code. But even if the plastic behaviour of soil was represented by an elastic-plastic model, as for instance the Cam-Clay model, the concentration would not have been correctly simulated according to the discussion in Sections 2.3.4.3 (see also Mair, 1979:133 and Seneviratne, 1979:113).

If the action of the lining could be simply reduced to that of a uniform pressure acting against the walls, thus assuming the support to be a very flexible membrane then a factor of safety against global collapse of the tunnel opening could be estimated for the final equilibrium situation. The limiting tunnel pressure causing tunnel collapse could be assessed by the D'Escatha and Mandel (1974) method, (see Sections 4.3.4. and 6.5.2). Using the definition of the factor of safety given by equations 2.11 and 2.14, and working in terms of a uniform average in situ stress field and uniform tunnel pressures, a factor of safety of 1.42 is determined for the average stress produced by the FE analysis and FS=1.26 for the average measured stress. These values are less than the range of safety factors (2 to 3) proposed in Section 2.3.3, below which a non-linear ground response is to be expected. Thus, it tends to confirm the criteria established then.

With the final crown displacement as given by the back analysis or by the field instrumentation (both roughly equal to 8 mm), it is possible to calculate the dimensionless crown displacement, U, given by equation 2.16. This is found to be equal to 0.55, for an initial tangent modulus at the crown elevation, of about 26 MPa. According to the criteria proposed in Section 2.3.4.3, a value of U higher than 1.8 will generally mean a high shear strain concentration and conditions approaching tunnel collapse. In the present case a value of U well below this proposed threshold was found and it is actually lower than the reference unit value proposed for good ground control conditions. As such, it supports the criterion established then. For this condition, no "loosening" effects should be manifested and the numerical model used is adequate for the present simulation.

An additional interesting feature shown in Figure 5.23 is the increase in the tangent modulus at points above and below the tunnel. This aspect of behaviour was anticipated from Section 5.2.2.2, where it was explained that this results from the rotation of principal stresses in those regions. During the initial increments of stress release, it was noted that the shadowed areas touched the opening, and as the unloading proceeded they moved away after complete reversal of the principal stresses. In these regions, the ratios of final to initial tangent moduli varied from 1 to 1.3. Had the unloading-reloading feature of the hyperbolic model been implemented with a modulus solely dependent on the confining pressure, higher moduli ratios would have been found in those areas, since the Janbu's modulus number for unloading is greater than for loading (about 20% more for stiff soils , Duncan et.al., 1980:13).

5.2.4.3 Edmonton Light Rail Transit (LRT) Tunnel

Introduction and Site Geology

This was a large diameter tunnel, built in early 1981 along Jasper Avenue, in Edmonton, Canada, as part of the South Extension of the light Rail Transit System. This extension was about 600 m long and built as a twin tunnel. The case history described herein refers solely to the tunnel driven first, which was the Southbound line on the northern side of Jasper Ave. Details of this project, including field monitoring and its interpretation, were provided by Branco (1981), Eisenstein and Branco (1985), and Branco and Eisenstein (1985). Previous local experience was reported by Eisenstein and Thomson (1978), related to the performance of the first LRT line, thereafter extended through the length currently described.

The 6 m diameter tunnel was driven with a soil cover of 8.5 to 9.5 m. A longitudinal cross of the tunnel is shown in Figure 5.24, where a simplified geological profile is included which summarises data from 18 borehole logs.

The geological and geotechnical conditions of downtown Edmonton were reviewed recently by Thomson et.al. (1982). The bedrock, comprising clay shale, mudstones and sandstones, was uplifted during the Eocene and subaerial erosion led to the formation of a mature drainage system prior to glaciation. During Pleistocene epochs, the preglacial river systems began aggrading, as a result of the only recorded advance of the continental ice sheet into the area. Many of the preglacial valleys became partially infilled with a sequence of dense to very dense sands and gravels termed the Saskatchewan Sands and Gravels. Local advances and retreats of the W[illegible]consin Ice Sheet are said to have laid down two till layers (the Upper or Brown Till and the Lower or Grey Till). While the lower unit has been laid down on the Saskatchewan Sands and Gravels or on the bedrock by an ice lobe moving NW-SW, the upper one resulted from ice advancing from the NE direction. Both till sheets contain lenses of water-deposited sands with thicknesses varying

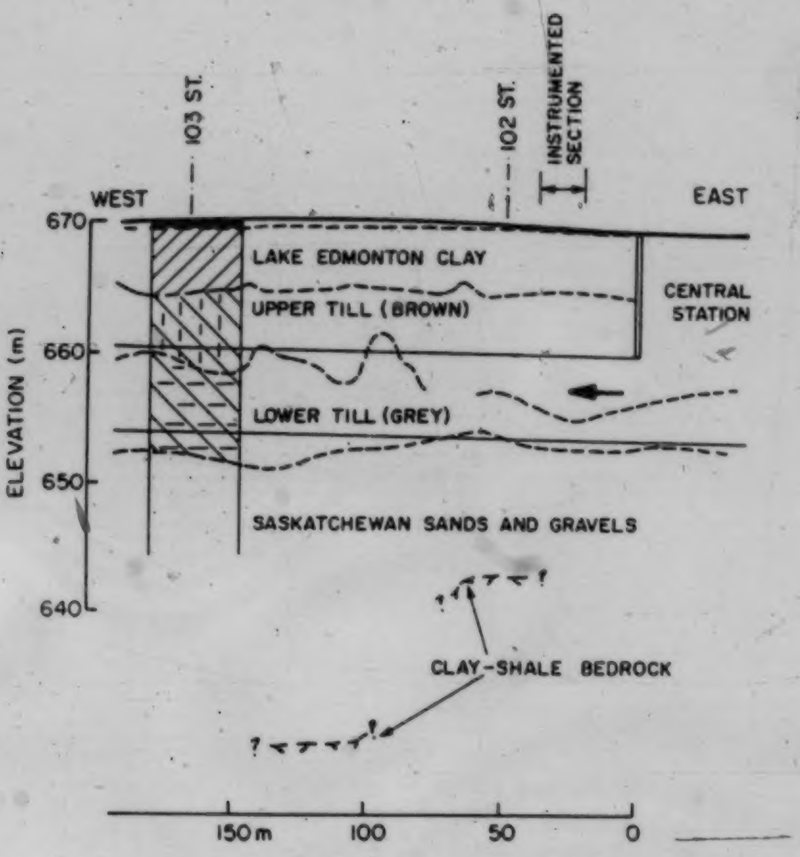
103 ST.
102 ST.
INSTRUMENTED SECTION
WEST
EAST
670
660
650
640
ELEVATION (m)
LAKE EDMONTON CLAY
UPPER TILL (BROWN)
CENTRAL STATION
LOWER TILL (GREY)
SASKATCHEWAN SANDS AND GRAVELS
CLAY-SHALE BEDROCK
150m
100
50
0

Figure 5.24 Subsurface Profile of Southbound LRT Tunnel along Jasper Avenue (after Branco, 1981:modified)

from a few centimeters to several metres, and range in extent from less than one to more than 10 metres. These lenses are frequently water-bearing and randomly located. The surficial deposit is a silty clay, glacial lake sediment, formed in the late Pleistocene and is covered locally by fill material.

As noted in Figure 5.24, the upper fill material is less than a metre thick. The Lake Edmonton Clay is 4 to 5 m thick. The combined till units appear at the site with a total thickness of 12 to 14 m, the upper till being thicker than the lower one at the instrumented section. As elsewhere in the area, the upper till was found to be columnar jointed with joint spacing in the order of some 20 to 40 cm. The lower till is also known to be jointed but in a rectangular fashion. The till body overlies the tertiary Saskatchewan Sands and Gravels, which in turn lie on a Clay-Shale bedrock located at an elevation which is not clearly defined at this site. The bedrock was detected at two locations at depths varying between some 30 to 40 m. Apart from some free water found in a few of the sand lenses detected within the till, a ground water level has not been identified in this site, and may be located well below the tunnel floor.

Geotechnical Properties

Basic geotechnical properties of these soils were given by a number of authors (for example, Thomson, 1969, Morgenstern and Thomson, 1971, Eisenstein and Thomson, 1978, Wittebolle, 1983). The results of tests on samples collected at this particular site were presented by Branco (1981:13, 268-273), and are summarized in Table 5.13. Apart from differences in colour and in the joint systems the two till materials are geotechnically very similar (Thomson et.al., 1982:176). For this reason, single ranges of properties are given for the stiff to hard Edmonton Till. Of particular interest are the mechanical properties of this material since the tunnel was entirely driven through this layer. Some of these properties are summarized in Table 5.14. With the exception of the K_o value and Poisson's ratio, the parameters were obtained from drained axial compression triaxial tests on block and cored samples, which were collected at nearby excavation sites, some 300 m northeast and 400 m west of the present site by Medeiros (1979) and by Wittebolle (1983) respectively. The hyperbolic model parameters were obtained from the drained conventional triaxial test results (confining pressures from 15 kPa to 34 kPa) furnished by Medeiros (1979:78). His data was reinterpreted by the writer who fitted hyperbolae to the stress-strain curves. Some of the curves obtained by Medeiros (Op.cit.) were not closely fitted by a hyperbola. These were the tests with cell pressures between 20 and 26 kPa and were therefore discarded following recommendations by Duncan et.al., (1980:22) on elimination of experimental inconsistencies. The range of modulus constants resulting reflects considerable scatter of data despite the elimination of inconsistent results. The scatter can be

Soil Type	Lake Edmonton Clay	Edmonton Till	Saskatchewan Sands and Gravel
Liquid Limit (%)	34 - 79	27 - 67	-
Plasticity Index (%)	8 - 48	10 - 46	-
Water Content (%)	21 - 39	10 - 29	5(6)
Finer than 2 m (%)	9 - 62	8 - [illegible]5	0(5)
Coarser than 75 m (%)	1 - 13	9 - 48	97.5(5)
Total Unit Weight (kN/m^3)	18 - 20	19 - 23	18.5(6)
Specific Gravity	2.76(2)	2.65(3)	2.67(6)
Void Ratio	~0.9(4)	~0.4(4)	~0.5(4)
Degree of Saturation (%)	95 - 100(4)	90 - 100(4)	28(6)
Undrained Shear Strength (kPa)	44 - 141	94 - 662	-

Notes: (1) All data from Branco (1981:13), except where indicated.
(2) Average value given by Thompson (1969:14).
(3) Average value given by Wittebolle (1983:54).
(4) Calculated typical values.
(5) One sample only.
(6) From Medeiros (1979).

Table 5.13 Range of Basic Soil Properties Found Along LRT Tunnel Alignment at Jasper Avenue

Cohesion intercept c' (MPa)	0	- 0.035	(1)
Friction angle ϕ' (°)	35	- 40	(1)
Failure Ratio R_f	0.75	- 0.95	(2)
Modulus number K	550	- 800	(2)
Modulus exponent n	0.45	- 0.6	(2)
Poisson's Ratio ν		0.4	(3)
K_0	0.5	- 1.2	(4)

Notes: (1) According to Medeiros (1979) and Wittebolle (1983) data.
(2) Based on Medeiros (1979) results from drained axial compression triaxial tests.
(3) Equal to estimated value by Eisenstein and Morrison (1973) and Medeiros (1979).
(4) From selfboring pressuremeter tests by Thurber Consultants (1980).

Table 5.14 Range of Geotechnical Parameters for Edmonton Till at the South LRT Tunnel Line

partly attributed to the fact that each stress-strain curve was obtained from samples taken at different depths in the till thickness (from 7 to 15 m, approximately). Each sample was tested with a confining pressure roughly equal to the overburden pressure at the point it was collected. This testing program exaggerates the effect of the soil variability, thus increasing the scatter of results, but the combined interpretation of these data better reflects the overall behaviour of the till mass. It may be fortuitous that the test results eliminated correspond to samples collected at elevations in the upper metre of the lower till, where the soil is known to be more fractured by the action of the overriding upper till (Eisenstein and Thomson, 1978:336).

Laboratory tests were not conducted on the Lake Edmonton Clay found at this site, but some selfboring pressure meter "quick" tests were available. Their results are given in Table 5.15, following the interpretation furnished by Thurber Consultants (1980).

Medeiros (1979:120) conducted also some conventional drained triaxial tests in block samples of Saskatchewan Sand, collected also at the site northeast of the present project location. The resulting parameters obtained are shown in Table 5.16. No clear relation was found between the initial tangent modulus of the hyperbolae fitted by the writer and the confining cell pressure. This was partly due to the fact that Medeiros (Op.cit.) used a narrow range of cell pressures (38 to 49 kPa), that again corresponded to the overburden stresses at the level of sampling. Hence, to obtain the modulus number K, a modulus exponent n of 0.5 was selected, which is believed to be reasonable for this granular material.

Although both the Till and Saskatchewan Sands have been tested in triaxial cells under stress paths other than axial compression, and in spite of the known influence of stress paths in these soils (Medeiros and Eisenstein, 1983), only results of conventional triaxial tests have been considered. The reasons for this decision bear on the discussion presented in Section 2.3.4.1. and also to be consistent with the aims of the present analysis, stated in Section 5.2.4.1. The numerical solution adopted is based on the original hyperbolic formulation, which in turn is based on parameters derived from conventional triaxial test results.

The deformation properties of these soils were investigated also by pressuremeter testing, conducted along Jasper Avenue by Thurber Consultants (1980). Two types of equipment were used. One is the self-boring pressuremeter and the other is the high pressure pressuremeter which requires a pre-drilled borehole. Details of the equipment, testing procedures and results interpretation are given by Worth and Hughes (1974), Hughes et.al. (1977) and Hughes and Ervin (1980). They are also summarized in Thurber Consultants (1980) report to this particular project. In the self boring equipment a fairly quick probe expansion is done

Friction angle ϕ' (°)	20 - 30
Cu (kPa)	50 - 150
Pressuremeter E moduli (MPa)	6 - 15
Poisson's ratio	0.4 - 0.5(2)
K_0	0.5 - 2.0(3)

Notes: (1) All data from Selfboring pressuremeter (quick expansion) tests by Thurber Consultants (1980) at 104th Street and Jasper Avenue.

(2) Estimated.

(3) Interpreted range. Higher values (in excess of 3) were not considered.

Table 5.15 Range of Geotechnical Parameters for Lake Edmonton Clay at the South LRT Tunnel Line

Cohesion intercept c' (MPa)	$0^{(2)}$
Friction angle ϕ' (°)	39 - 41
Failure Ratio R_f	0.7 - 0.8
Modulus number K	$730 - 940^{(3)}$
Modulus exponent n	$0.5^{(2)}$
Poisson's Ratio ν	$0.25^{(2)}$
K_0	$0.36^{(4)}$

Notes: (1) Data based on Medeiros' (1979) results from drained axial compression triaxial tests.
(2) Assumed
(3) Range calculated for the assumed modulus exponent.
(4) Estimated from Jaky's expression.

Table 5.16 Range of Geotechnical Parameters for Saskatchewan Sands and Gravels at the South LRT Tunnel Line

in discrete increments of air pressure. Pore pressure changes are also monitored during testing. Figure 5.25 shows the variations of the Young's modulus derived from the cell pressure expansion curves obtained in the field, for assumed Poisson's ratios. Tests were done in two boreholes at two locations along the LRT alignment about 200 and 700 m west of the instrumented section, but the test results were superimposed in Figure 5.25 for presentation. Also included in this figure are the results of pressuremeter tests carried out by Eisenstein and Morrison (1973) in the different soil units, at locations not far from the present site. A considerable scatter of data is noticed, reflecting the erratic nature of the locally occurring soils. This feature was referrenced earlier from Thomson et.al. (1982:179).

Also shown in Figure 5.25 is the variation of the initial tangent modulus with depth, as given by the hyperbolic model formulation (Figure 5.11) for the in situ stress conditions. This modulus distribution was the one used in the best fit back analysis, as will be explained later. It corresponds to an upper soil layer with constant E value of 5 MPa, and a lower one described by K=600, n=0.50, $\phi'=40°$, $c'=0$, $R_f=1$, $K_o=0.75$ and $\gamma=19.5$ kN/m^3. The given distribution seems to work nearly as an envelope for the results gathered in the later investigation, and as a lower bound to those tests conducted earlier.

Construction Details and Field Monitoring

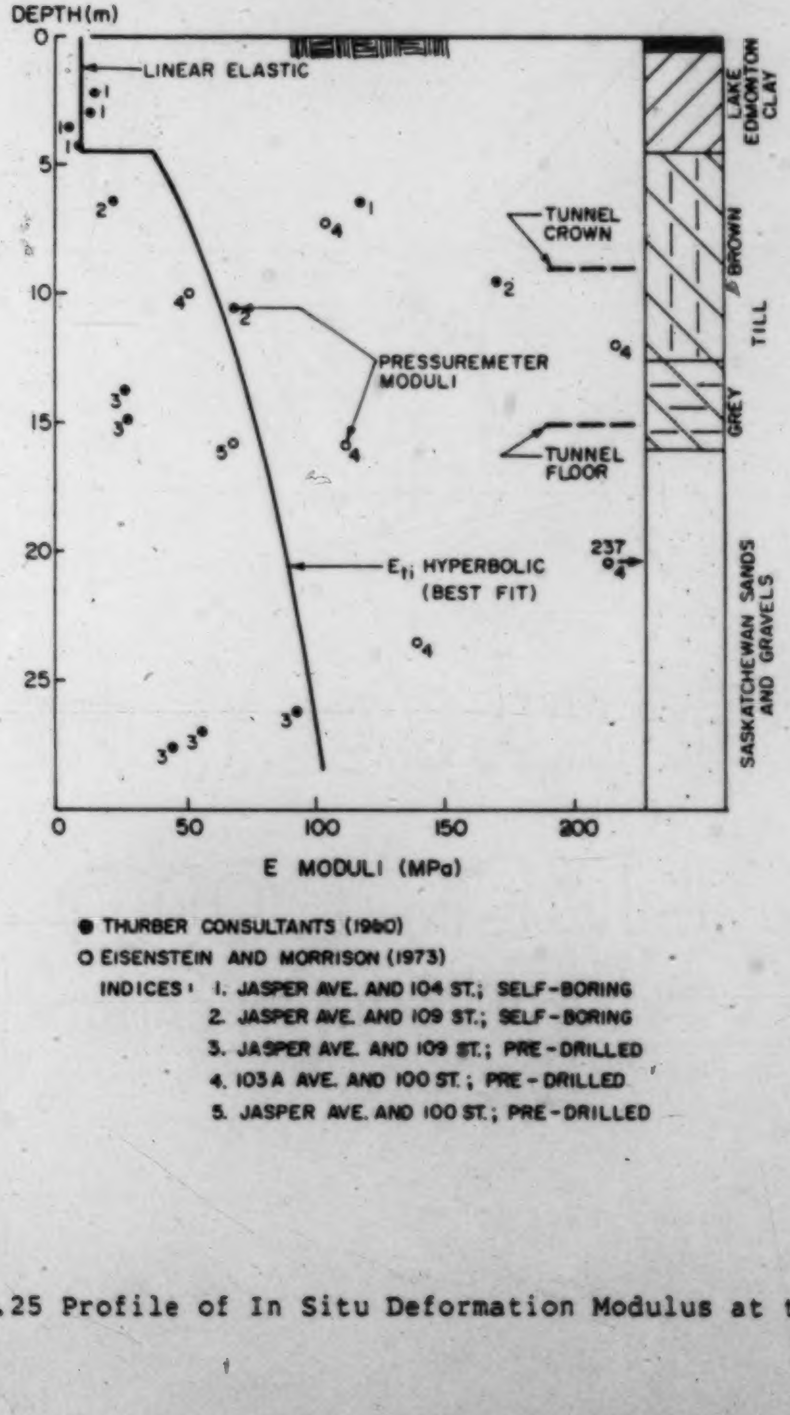

Figure 5.25 Profile of In Situ Deformation Modulus at the LRT site

Tunnel construction was carried out with a full face cutting wheel TBM (a Lovat M-246 Series 2100), whose details are given in Figure 5.26a. The TBM body is 5.5 m long and the cutting profile has a 6.17 m diameter. The cutting head is arranged in such a way that the soil at the face is indented and scraped by staggered teeth protruding outwardly and fixed at six spokes. Consequently, the fairly strong and stiff soil is cut at the heading in a nearly vertical face and left virtually unsupported. A detailed account of the tunnel construction was given by Branco (1981:17). The lining system used is shown in Figures 5.26(b) and (c). The primary lining comprised steel ribs spaced at 1.22 m, each one with four bolted segments, and wooden lagging in between. The support was expanded immediately after the ribs were exposed to the ground. Therefore, the maximum distance between the tunnel face and a fully expanded rib was about 6.7 m. Details of the secondary concrete lining is also given in Figure 5.26. However, they are not particularly relevant to the present study, as the performance of the tunnel being investigated is that observed before the secondary lining installation, which took place after completion of this tunnel. The average construction rate was 2.6 m/day while the TBM passed through the instrumented section. The field instrumentation included surface and subsurface settlement measurements, slope indicator readings, load cell measurements at loosely bolted joints of the steel ribs, load measurements in instrumented steel

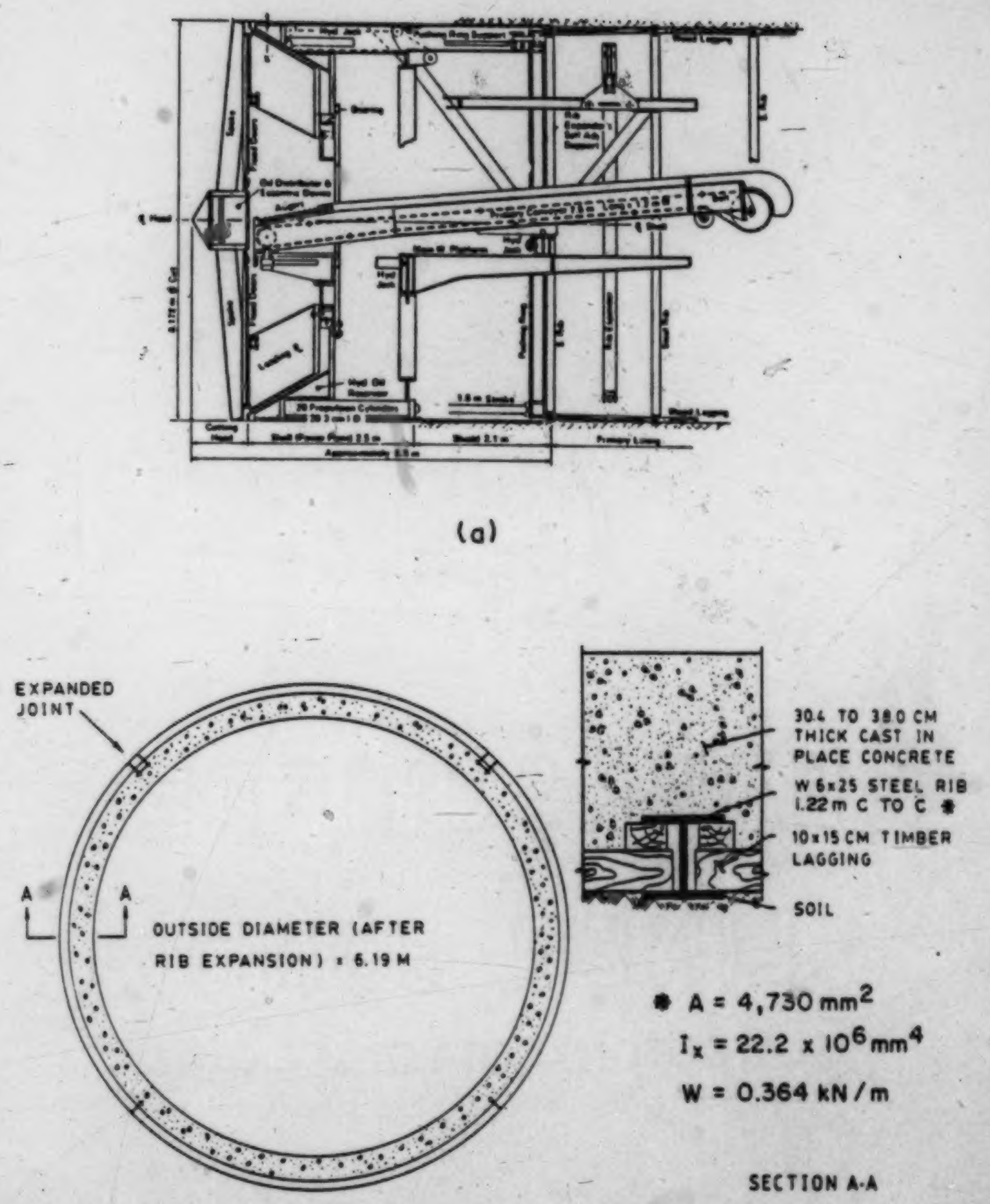
EXPANDED JOINT
A
A
OUTSIDE DIAMETER (AFTER RIB EXPANSION) = 6.19 M
30.4 TO 38.0 CM THICK CAST IN PLACE CONCRETE
W 6x25 STEEL RIB 1.22 m C TO C *
10x15 CM TIMBER LAGGING
SOIL
* A = 4,730 mm²
Iₓ = 22.2 x 10⁶ mm⁴
W = 0.364 kN/m
SECTION A-A

(a)

(b)

(c)

Figure 5.26 TBM and Lining System used at the Edmonton LRT Tunnel (after Branco, 1981:modified)

lagging with the same flexural rigidity (EI) as the timber lagging, convergence measurements of the steel ribs and levelling of two points of the steel set. Branco (1981) presented a detailed account of this rather involved monitoring program.

Numerical Simulation

For the back analysis of this tunnel, a finite element mesh of 298 nodes and 549 elements was used. A surficial layer of Lake Edmonton Clay with 4.5 m thickness and linear elastic behaviour was considered. As in the ABV tunnel case, it was noted again that the results of the analyses were not very sensitive to the elastic properties of this clay in the range given in Table 5.15. Also, it was noted that the deformation properties of the underlying Saskatchewan Sands (Table 5.16) are not dissimilar to those of the till (Table 5.14). As the tunnel was driven entirely through the till layer, it was decided to represent a single soil layer, below the surficial clay, with properties corresponding to that of the till.

Figure 5.27 presents the assumptions that were made and the values of the parameters that were used and kept constant in the back analyses. With the exception of the loads measured in the steel ribs which showed some increase with time, the ground response observed through displacement measurements seemed to be fairly time independent. This appears to be consistent with observations made in other projects in the area (Eisenstein and Thomson, 1978:343, Medeiros, 1979:75). However, the fairly high degree of saturation in the till, despite the fact that the ground water level was located well below the tunnel, may suggest that some pore pressure changes could have happened during tunnel advance.

Recent isotropic consolidation tests, carried out by Wittebolle (1983:56) on intact 10 cm diamter Edmonton Till samples, showed that the coefficient of consolidation (c_v) of this material as measured in the laboratory, for confining stress levels which occur around this tunnel, is about 10^{-3} cm^2/s. This value can be used as a lower bound of the field values for the entire till mass. In fact, the presence of joints or fractures in the mass should considerably increase the rate of pore pressure changes with time. These discontinuities were not present in the laboratory samples (Wittebolle, Op.cit:41), and therefore a lower coefficient should have been obtained. Moreover, the existing sand lenses in the till will act to further accelerate any process of pore pressure equalization. A c_v value of, at least an order of magnitude higher that the laboratory value, can be said to better portray the overall till mass. A value of 10^{-2} cm^2/s was suggested by Medeiros (1979:73) and is used here for discussion.

The tentative criteria developed in Chapter 3 for the identification of the ground response type for a shallow tunnel, in terms of time dependence (Figure 3.23), may be useful in this analysis. As noted by Branco (1981), the

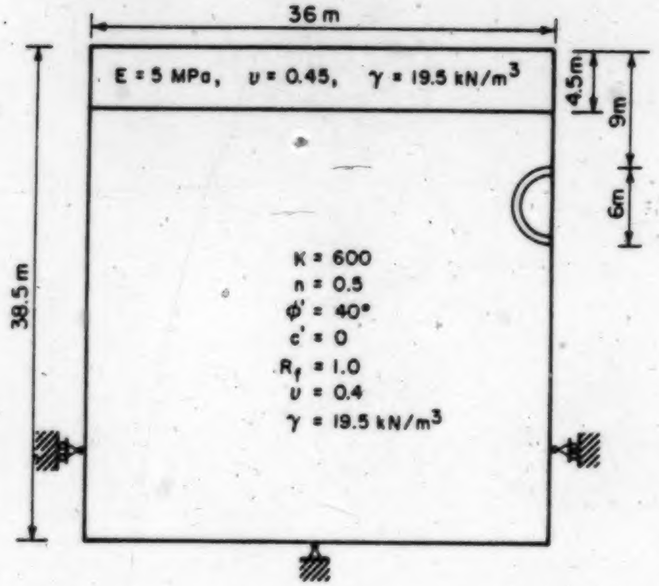
36 m
E = 5 MPa, υ = 0.45, γ = 19.5 kN/m³
4.5m
9m
6m
38.5 m
K = 600
n = 0.5
φ' = 40°
c' = 0
R_f = 1.0
υ = 0.4
γ = 19.5 kN/m³

Figure 5.27 Assumptions and Fixed Parameters for the LRT Tunnel Back Analyses

"immediate" soil movements were observed over a time span of some 20 days, when the tunnel face advanced from a point about 1 to 2 diameters behind the instrumented section to a point 6 to 7 diameters past this section. The primary lining can be assumed to be fully permeable. If a till cover of some 5 m is considered with a c_v of $10^{-2}cm^2/s$, then over a period of time of 20 days, the consolidation of the soil due to drainage towards the tunnel will be partial, but closer to "appreciable" (see Figure 3.23). Had a c_v of $10^{-3}cm^2/s$ been selected, a partial consolidation condition would still result, but a larger percentage of the time dependent process would be occurring after the field measurements were taken.

From this simplified analysis, one would expect some long term ground response for this tunnel. Surface settlement measurements taken 282 days after the "short term" observations were completed (from February 26 to December 5 of 1981), confirmed that some additional ground movements had occurred. However, these movements were small in magnitude (and possibly not reliable). Unlike these, the load cell readings at the steel rib joints indicated a clear increase over the same time interval. The average thrust measured in the upper rib joints increased by 94%. A smaller increase seems to have occurred in the lower joints. Unfortunately not all lower joint cells were measured in the first measuring campaign, but 3 months after the "short term" observations (i.e. May 27) a 20% increase in the average thrust had already been measured for a 31% increase in the upper joints at the same time. Eisenstein et.al., (1983:19) attributed this increase in loads to a progressive loosening of the soil above the crown, associated with a succession of roof failures with time. Branco (1981:187), on the other hand, noted that there was no space left behind the primary lining, a couple of hours after it had left the shield. Furthermore, he noted that a soft and wet clay mixed with sand, had squeezed into and filled the space left behind the wooden lagging. Considering these facts, one could also speculate about the possibility of time-dependent lining load behaviour arising from some pore pressure equalization with time.

Although the reasons for the observed lining load increase with time in the LRT tunnel are not clear, the overall ground response observed should have been close to a drained one. Correspondingly, the soil parameters selected for the back analyses are consistent with those derived from drained tests and were chosen to roughly approximate the in situ modulus distribution provided by the pressuremeter test results, shown in Figure 5.25, both for the till and for the underlying sand. The only soil parameter allowed to vary in the analysis was the coefficient of earth pressure at rest (from 0.7 to 0.9).

An equivalent lining, 50 cm thick, was used in place of the actual primary lining. This gives compressibility and flexibility ratios of 0.3 and 600, according to the Einstein and Schwartz (1979) definitions and for the dimensions given in Figure 5.26. These values are for a soil modulus of 65 MPa and a Poisson's ratio of 0.4, and for a lining modulus of 200 GPa and its Poisson's ratio of 0.2. The contribution from the lagging is disregarded. If the compressibility and flexibility of the rib joints were considered, then the C and F values would be higher. To approximate these ratios, the equivalent lining with a 6 m external diameter would require a modulus of 0.25 or 1.40 GPa to equal either one or the other ratio. Accordingly, in the back analyses, the lining modulus was initially assumed to vary within these limits. However, it was soon found that modulus values lower than 0.25 would have to be investigated, in order to match the observed performance after lining activation. Therefore a new range of moduli from 0.09 to 0.7 GPa was considered. As in the ABV case, the best agreement was obtained when the flexibility ratio of the equivalent lining was set close to the "real" one, rather than matching the compressibility ratios.

The third solution parameter to be varied in the analysis, is the amount of stress release prior to the lining activation. An interpretation of the field measurements, followed by some preliminary computer runs, indicated that it would be sufficient to vary this amount from about 30 to 70%. These tentative runs indicated also that five equal load increments, for each phase of simulation (10 unloading steps altogether) would enable an adequate approximation.

Results of the Back Analyses

Table 5.17 summarizes the parameters that were varied in the analyses. Clearly, not all combinations of these parameters were needed to obtain the best fit case. This was found after fifteen computer runs. The runs using the higher lining modulus furnished unrealistic lining loads and deformations. The best fit analysis provided a reasonably good match between calculated and observed performances, at the final equilibrium situation and also before lining activation. This condition was found for 50% stress release prior to support application, for K_o=0.75 and for an equivalent lining modulus of 0.13 GPa. This modulus corresponds to a flexibility ratio F of 1114, which is almost twice as much the value initially estimated. If the joint flexibility and compressibility were disregarded, the flexural rigidity of the ribs (EI) per unit length of tunnel would be 3.64 MN.m. In the best fit case, EI corresponds to 1.71 MN.m, indicating that the rib joints do have an effect on the overall lining flexibility. It is worth noting again that the wooden lagging was assumed not to contribute to the support stiffness (in compression or bending).

As shown previously, the in situ (initial) tangent modulus distribution with depth is given in Figure 5.25. While this was obtained from drained triaxial test data, the pressuremeter moduli may reflect the soil stiffness under different drainage conditions (and of course, different

Stress release α prior to support activation (%)	33	50(1)	67		
In situ stress ratio K_0	0.70	0.75(1)	0.85	0.90	
Equivalent lining E modulus (GPa)	0.10	0.13(1)	0.16	0.40	0.70

Notes: (1) Best fitted values

Table 5.17 Parameters Varied in the LRT Tunnel Back Analysis

stress paths).

Figure 5.28 compares observed and calculated settlements transverse to the tunnel axis at 3 m below the ground surface, just before lining activation. The measurements were taken when the tunnel face was located 6.3 m (1D) beyond the instrumented section, which is when support expansion was being undertaken. The finite element results correspond, accordingly, to the end of the first phase simulation after a 50% stress release had been applied, but before installation of the lining.

Similarly, Figure 5.29 compares observed and calculated final surface settlements. The measurements were taken when the tunnel face was located 37.6 m (6D) beyond the instumented section. The calculated displacements correspond to the end of the second phase simulation, after equilibrium was reached between the lining and soil.

In both situations depicted in these two figures, a fairly reasonable agreement between observed and calculated measurements is found, both in terms of the magnitude and the overall distribution of the surface settlements.

Figures 5.30 and 5.31 compare the vertical movement in the ground, along vertical lines located at approximately 10 and 4 m off the tunnel centre line, respectively. In each case, calculated and measured displacements are compared at the moment the lining was activated and when final equilbrium was achieved. Both magnitude and distribution of the final movements with depth are fairly reasonably

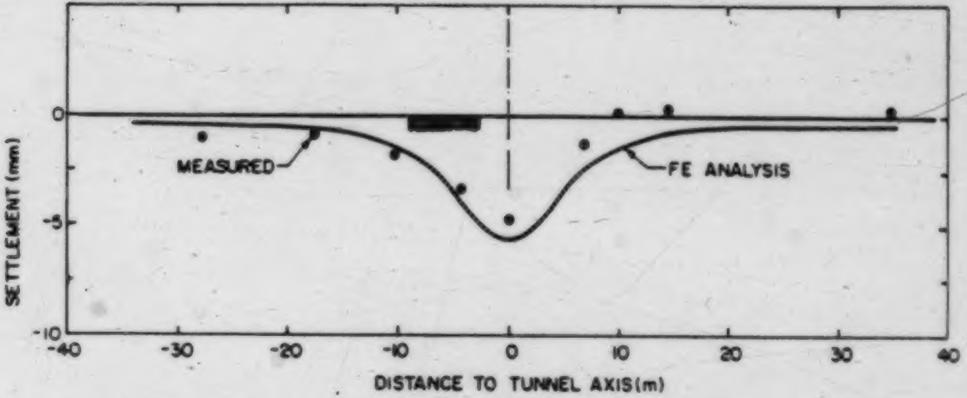

NOTES :
1. MEASURED AND CALCULATED SETTLEMENTS AT POINTS 3m BELOW SURFACE
2. MEASUREMENTS TAKEN WHEN THE TUNNEL FACE WAS 6.3m BEYOND THE INSTRUMENTED SECTION.
3. FIELD DATA FROM BRANCO (1981 : 67)

Figure 5.28 Measured and Calculated Surface Settlements before Lining Activation at the LRT Tunnel

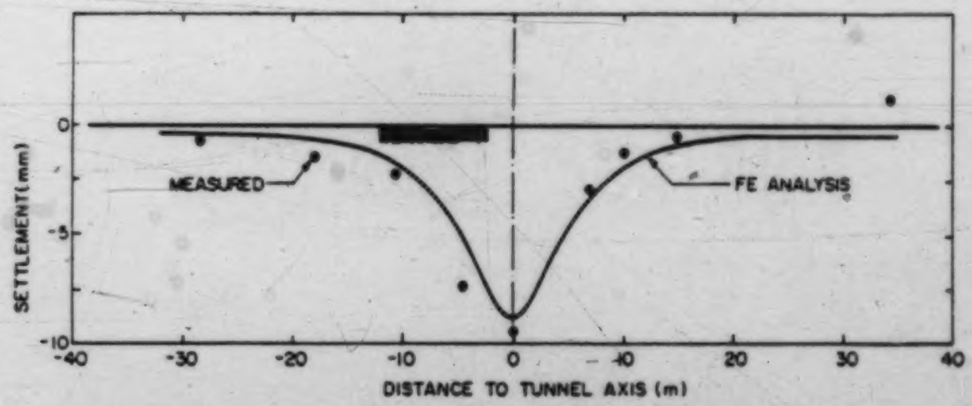

NOTES :
1. MEASURED AND CALCULATED SETTLEMENTS AT POINTS 3m BELOW SURFACE.
2. MEASUREMENTS TAKEN WHEN THE TUNNEL FACE WAS 37.6m BEYOND THE INSTRUMENTED SECTION.
3. FIELD DATA FROM BRANCO (1981 : 67)

Figure 5.29 Measured and Calculated Final Surface Settlements at the LRT Tunnel

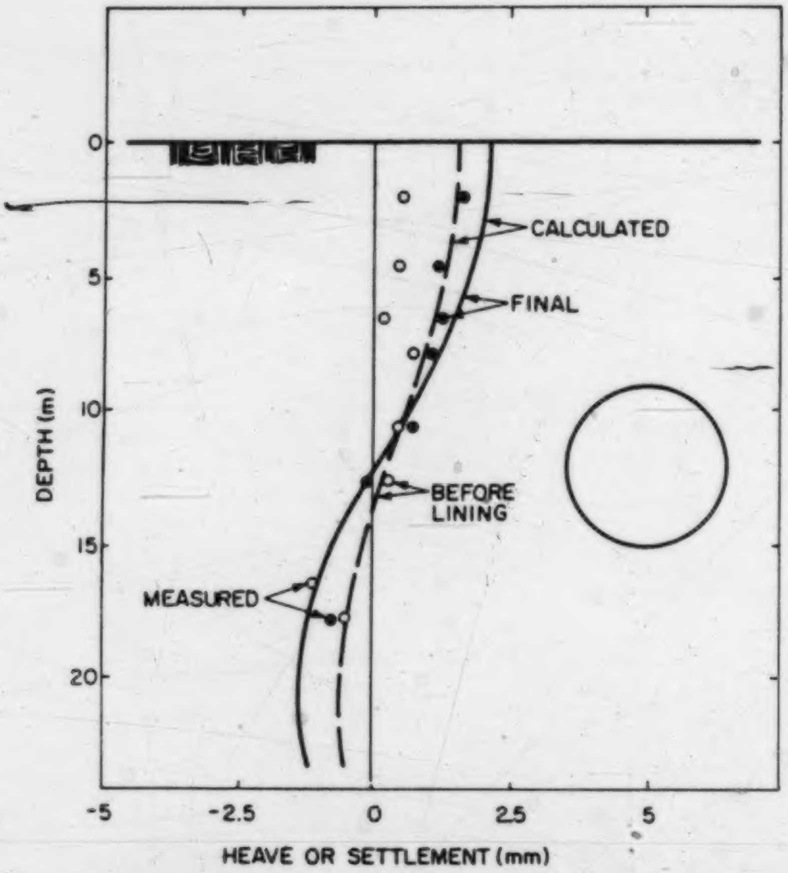

NOTES:

1. MEASUREMENTS AT ME5, 10.4m FROM TUNNEL AXIS.
2. CALCULATED DISPLACEMENTS AT 9.5m FROM TUNNEL AXIS.
3. MEASUREMENTS TAKEN WHEN THE TUNNEL FACE WAS ABOUT 1D AND 6D BEYOND THE INSTRUMENT STATION.
4. FIELD DATA FROM BRANCO (1981: 279 TO 287)

Figure 5.30 Measured and Calculated Vertical Displacements Along a Vertical Line 10 m off the Centreline of the LRT Tunnel

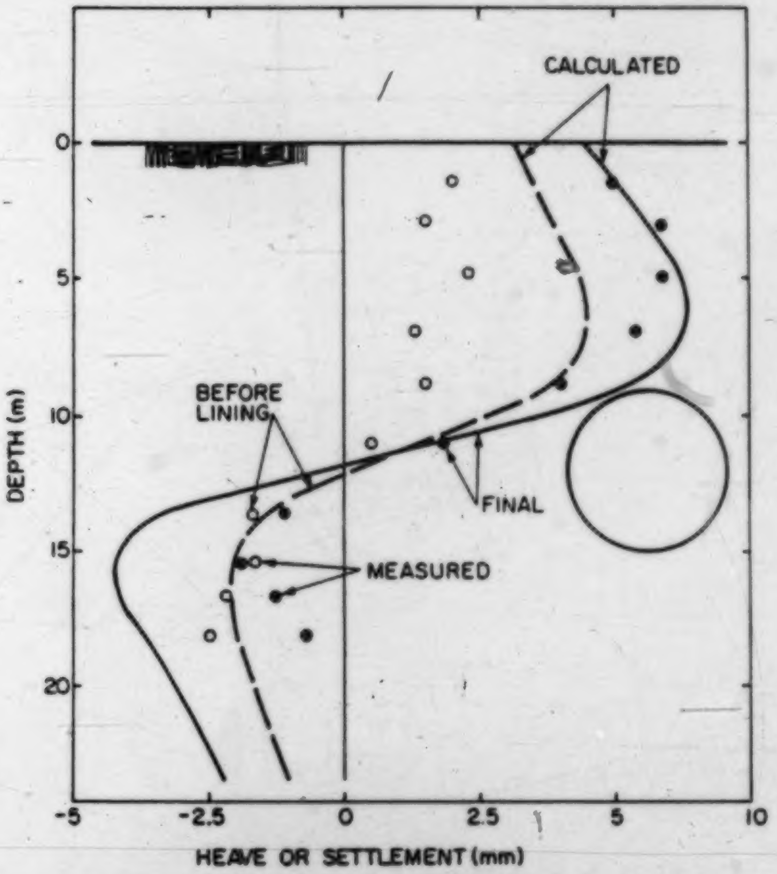

NOTES:

1. MEASUREMENTS AT ME9, 4.3m FROM TUNNEL AXIS.
2. CALCULATED DISPLACEMENTS AT 4m FROM TUNNEL AXIS.
3. MEASUREMENTS TAKEN WHEN THE TUNNEL FACE WAS ABOUT 1D AND 6D BEYOND THE INSTRUMENT STATION.
4. FIELD DATA FROM BRANCO (1981: 288 TO 297)

Figure 5.31 Measured and Calculated Vertical Displacements Along a Vertical Line 4 m off the Centreline of the LRT Tunnel

predicted for points above the tunnel axis elevation, for points below, the analysis tends to overestimate the heave. This is possibly due to the simplifying assumption of introducing a single soil layer below the Lake Edmonton clay. The in situ modulus of the Saskatchewan Sands and Gravels may, in reality, increase faster with increasing confining stress than anticipated. Nevertheless, the results seem acceptable.

On the other hand, the movements predicted at the moment the lining was installed are, in both cases, overestimated for points above the axis elevation. A better agreement is found below it. This result is not suprising, since at a section one diameter behind the tunnel face, the actual displacement field is still affected by the heading advance, and non-zero longitudinal movements are present (see Section 2.3.6 and Eisenstein and Branco, 1985:58). But, when a near plane strain situation is met in the field, the numerical model seems to portray the observed behaviour quite satifactorily.

In Figures 5.32 and 5.33, measured and calculated horizontal displacements are compared along a vertical line beside the tunnel, before lining installation and after final equilibrium is reached. It should be noted that while the measurements refer to data from slope indicators located at 6.4 m and 4.3 m away from the tunnel centreline, the lateral movements were calculated along a vertical line between the slope indicators, some 5.5 m away from the centreline. Some difficulties were experienced with the zero readings of the slope indicators used in the comparison. Movements of as much as 5 mm were detected before the advance of the tunnel face (Branco, 1981:77). The measured displacements indicated in Figures 5.32 and 5.33 were assessed from the Branco (Op.cit.:101) data, but using as a zero reading, the measurements taken three diameters ahead of the face for the slope indicator SI6 and 4 diameters ahead for SI7.

The maximum magnitude of the calculated horizontal movements agrees fairly closely to the maximum observed. However, the distributions of movements are dissimilar. While the numerical models tend to yield maximum lateral displacements at the springline elevation, the observed maxima were noted to be always above the tunnel. This comparison is made with a word of caution since, as noted by Branco (1981:111), the measured movements were small compared to the accuracy of the measuring equipment. Hence, no assurance can be given to the trends of lateral movements observed.

In Figure 5.34, measured and calculated thrust forces at rib joints are compared. The load cell readings included the loads due to the support self-weight, as the zero readings were taken immediately before installation (Branco, 1981:142). The finite element analysis disregards the lining self-weight. For a consistent comparison, the self weight had to be excluded from the load cell readings. Through an

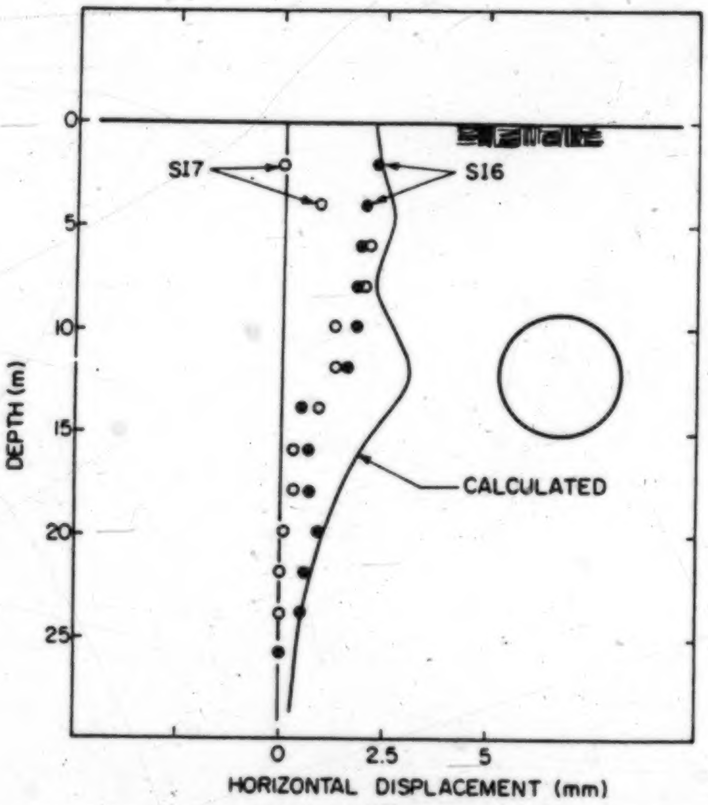

NOTES;

1. CALCULATED DISPLACEMENTS ALONG A VERTICAL LINE 5.5m AWAY FROM TUNNEL CENTRE LINE. SLOPE INDICATORS SI6 AND SI7 LOCATED AT 6.4 m AND 4.3m FROM TUNNEL AXIS.
2. MEASUREMENTS TAKEN WHEN THE TUNNEL FACE WAS ABOUT 1D BEYOND THE SLOPE INDICATORS.
3. FIELD DATA BASED ON BRANCO (1981: 102 AND 103)

Figure 5.32 Measured and Calculated Lateral Movements in the Ground beside the LRT Tunnel before Lining Activation

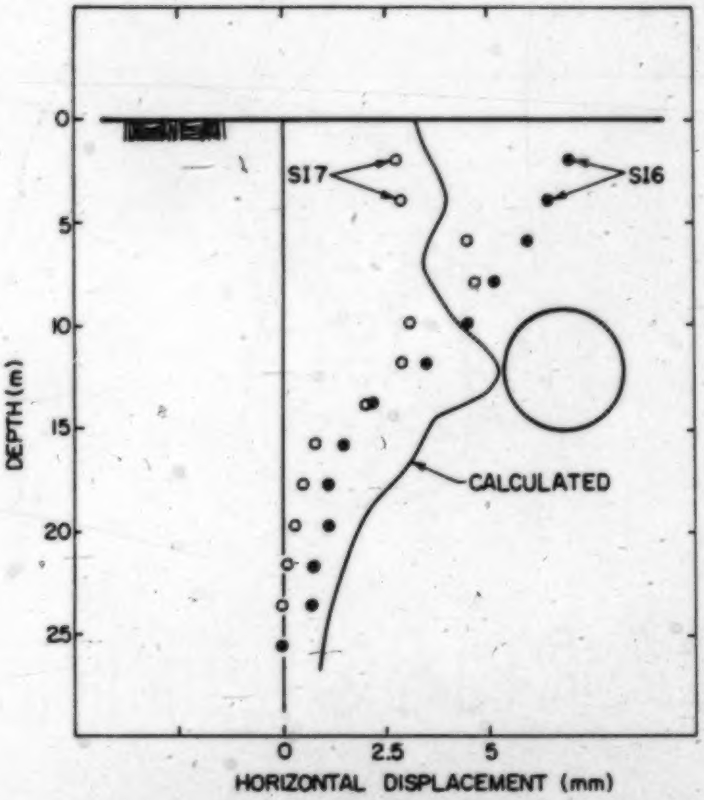

NOTES:

1. CALCULATED DISPLACEMENTS ALONG A VERTICAL LINE 5.5m AWAY FROM TUNNEL CENTRE LINE. SLOPE INDICATORS S16 AND S17 LOCATED AT 6.4m AND 4.3m FROM TUNNEL AXIS.
2. MEASUREMENTS TAKEN WHEN THE TUNNEL FACE WAS MORE THAN 3D BEYOND THE SLOPE INDICATORS.
3. FIELD DATA BASED ON BRANCO (1981:102 AND 103)

Figure 5.33 Measured and Calculated Final Lateral Movements in the Ground beside the LRT Tunnel

approximate calculation, it was estimated that a 2.6 kN reduction in the upper joint thrusts and 7.7 kN in the lower ones were required in order to obtain the thrusts due to the ground loads only. As the calculated forces shown refer to a plane strain section of 1 m thickness, the measured loads in the ribs had to be divided by the rib spacing (1.22 m) to allow proper comparison. The "short-term" measurements are those taken when the shield tail was about 6 diameters away at 16 days after rib installation. The long term readings were taken 293 days after rib erection. The calculated thrusts were obtained at different sections of the lining, by averaging the computed tangential element stresses in those sections, and integrating them along the lining thickness.

As noted in Figure 5.34, the calculated forces tend to be higher than those measured in the "short term". But they seem to agree well with the long term measurements. To illustrate this more clearly, Table 5.18 was prepared. Here the measurements from all cells in the upper joints and in the lower joints were averaged out separately. Note that the values refer to the thrust in each steel rib. The numerical solution underestimates the long term load in the upper joints by only 3.6%. On the other hand, the long term load in the lower joint is underestimated by 7.7%. These results seeem to be quite reasonable, bearing in mind the limitations of the numerical code used, particularly those related to the lining representation, as discussed in

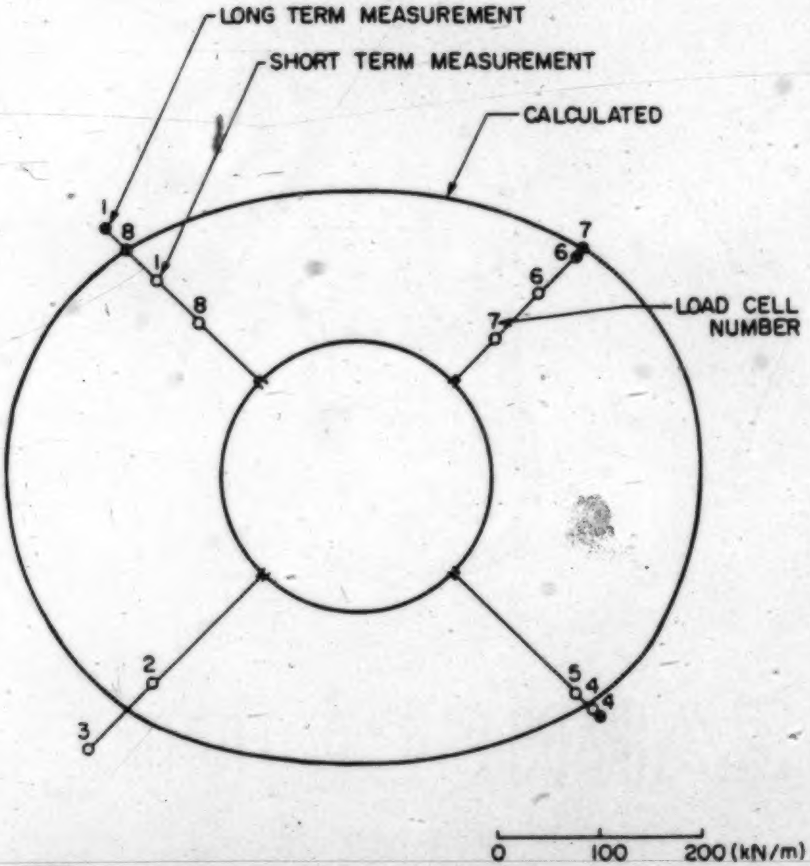
LONG TERM MEASUREMENT
SHORT TERM MEASUREMENT
CALCULATED
LOAD CELL NUMBER
1
8
1
8
7
6
6
7
2
3
5
4
4
0
100
200 (kN/m)

NOTES :

1. SHORT TERM READINGS 16 DAYS AFTER INSTALLATION; 36.4m AWAY FROM SHIELD TAIL
2. LONG TERM READINGS 293 DAYS AFTER INSTALLATION
3. LINING SELFWEIGHT DISCOUNTED FROM READINGS
4. MEASURED AND CALCULATED THRUST VALUES PER UNIT LENGTH OF TUNNEL (1.22m C TO C RIB SPACING CONSIDERED)
5. FIELD DATA FROM BRANCO (1981 : 156) AND FROM EISENSTEIN ET AL (1983)

Figure 5.34 Measured and Calculated Thrust Forces at Rib Joints in the LRT Tunnel

Section 5.2.2.2. The favourable comparison with the load cell measurements was probably due to the small amount of bending carried by the support system in this case history. For this condition, the deficiences of the present finite element formulation in representing the lining are minimized.

Table 5.19 summarizes the comparisons between measured and calculated performances for this case history. It also includes some additional data regarding measurements taken inside the tunnel of convergence and invert levelling. The overall agreement seems quite reasonable. Even the lateral movements in the ground, which were not investigated in the ABV tunnel described before, show a favour~~able~~ comparison, despite the difficulties experienced with the zero readings of the slope indicators. The maximum total heave of the lining invert segment was overpredicted by the calculation. However, as described by Branco (1981:192), the initial measurement was taken only after the TBM tail had been advanced 1.6 m beyond the instrumented rib. In other words, part of the heave occurring between the moment the rib was expanded and the moment the zero reading was taken was not included. The maximum horizontal movement of the lining at the springline was excessively overestimated by the calculation. Part of these movements were also not measured, again due to the delayed zero reading. Branco (Op.cit.:200) threw some doubt on the observed movements because of the reduced number of readings and the possible action of the

	Average Thrust in Rib Joints (kN)		
	Measured(1)		Calculated(4)
Joint	Short Term(2)	Long Term(3)	
Upper	119.3	224.7	216.6
Lower	229.4	242.3(5)	223.7

Notes:
(1) Lining selfweight discounted.
(2) 16 days after installation, 36.4 m away from shield tail.
(3) 293 days after installation.
(4) Considering a rib spacing of 1.22 m c. to c.
(5) Only load cell 4 was read. At 103 days after installation the average thrust was 268.3 kN.
(6) Data based on Branco (1981) and on Eisenstein et al. (1983).

Table 5.18 Measured and Calculated Average Thrust Forces at Rib Joints in the LRT Tunnel

	Performance Aspect		Measured(1)	Calculated	C/M
1.	Maximum surface settlement at lining installation	mm	4.8	5.8	1.21
2.	Maximum final surface settlement	mm	9.3	8.5	0.91
3.	Maximum slope of final settlement trough at surface	-	1:1000	1:1090	0.92
4.	Maximum lateral movement at ground surface	mm	2.5 to 7(2)	3.5	0.5 to 1.4
5.	Maximum total heave at the lower joints of the steel ribs	mm	3.6(3)(7)	5.4	1.5
6.	Maximum horizontal movement of lining at springline elevation	mm	1.2(4)(7)	8.3	6.92
7.	Maximum final deep settlement (4 m from axis)	mm	6.0(5)	6.5	1.08
8.	Final average thrust in upper rib joints	kN	224.7(6)	216.6	0.96
9.	Final average thrust in lower rib joints	kN	242.3(6)	223.7	0.92

Notes:
(1) Data from Branco (1981), Eisenstein et al (1983) and Eisenstein and Branco (1985).
(2) SI7 and 6.
(3) Observed by levelling joint B of ring 8 (Branco, 1981).
(4) At Ring 8
(5) At ME9
(6) Lining selfweight excluded
(7) Zero reading taken 1.6 m behind TBM tail.

Table 5.19 Measured and Calculated Performance of the LRT Tunnel

thrusting forces used to advance the TBM. From experience gained in other projects, using a similarly designed tape extensometer, it can be said that the accuracy of such measurement is frequently very low (up to a few millimeters). It is interesting to note that a poor comparison of horizontal convergence was also obtained at the ABV tunnel, where the same measuring device was used. The reasons for these noted departures require more detailed investigation.

Unfortunately the magnetic extensometer installed in the tunnel axis, was lost when it was hit by the cutting wheel. The distribution of subsurface settlements, above the tunnel crown was therefore not assessed, except ahead of the face where heave was noted throughout the tunnel cover. A second extensometer was intalled later, but a localized collapse of a sand lens at the roof occurred when the tunnel face reached the instrument station and again the measurements were lost (Branco, Op.cit.:110; see also Section 2.3.5.4).

Nevertheless, the larger amount of field data available in this case history, including a fairly complete picture of the displacement field around the opening, created a much more restricted condition for the back analysis than was the case with the ABV Tunnel. The variations allowed in K_o and on the lining properties, still offered some degree of flexibility in fitting the observed performance. But as in the previous case, it is believed that despite these variations, the assessed amount of stress release prior to lining installation was also reasonably approximated in this analysis.

The all-round uniform ground stress, corresponding to the average long term thrust measured in the steel ribs, is estimated to be about 30% of the in situ radial stress. The same figure is found with the numerical solution, noting that a slightly smaller tunnel diameter has been considered here (Figures 5.26 and 5.27). In this regard, a better agreement is found in this case, than in the ABV Tunnel. It is also noted that the present construction scheme led to a slightly higher ground stress reduction, than was observed in the NATM construction scheme. This was due mainly to a delayed support application in the LRT case, compared with the ABV case. In both cases the stress reductions taking place after lining installation are comparable.

The simplified stability assessment for the final plane strain situation, as explained in the former case (Section 5.2.4.2) can be repeated here. Similarly, the support action is reduced to that of applying a uniform internal pressure in the opening walls, so that a factor of safety against global collapse of the ground can be estimated. Both measured or calculated performances convey a factor of safety equal to about 1.3 which is comparable to that noted at the ABV tunnel. Again this figure is less than the range specified in Section 2.3.3, and once more a non-linear ground response would have to be expected. In fact, Figure 5.35 confirms this. Very low tangent moduli were calculated around the opening, but no soil element actually "failed" under the final equilibrium condition. The overall distribution of the elastic modulus around the LRT tunnel was very similar to that in the ABV case, including the increase in modulus above and below the tunnel (not entirely shown). This pattern tended to be not as intense as in the former case. The extent of the "softened" zone in the LRT was a bit larger than in the ABV, for points above and below the tunnel, and smaller in the lateral region. The distribution of the principal strains around the opening was also very similar. Once more, despite the fairly good ground control achieved in this tunnel (Eisenstein and Branco, 1985), a significant non-linear response of the ground appears to have occurred.

Using the final crown displacement of 15.9 mm given by the back analysis, it is possible to calculate the dimensionless crown displacement (U), given by equation 2.16. It is found to be equal to 0.86, for an initial tangent modulus of the soil at the crown equal to about 57 MPa. This value of U is smaller than the reference value of 1.8, set in Section 2.3.4.3, as a threshold figure for a near collapse condition. It was mentioned (Branco, 1981:110) that a localized roof collapse was triggered by a dry sand pocket and by an excessive overcutting. This event cannot be portrayed by this simplified numerical simulation. Had the sand lens been absent, or had a smaller overbreak been

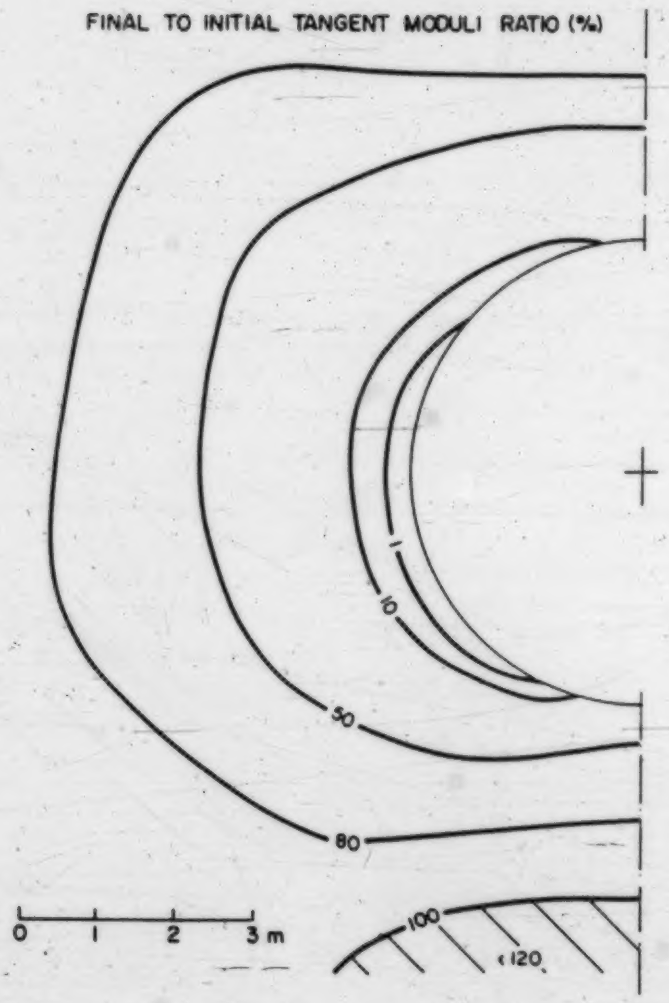
FINAL TO INITIAL TANGENT MODULI RATIO (%)
1
10
50
80
100
<120
0
1
2
3 m

Figure 5.35 Calculated Changes in Tangent Modulus around LRT Tunnel

ensured, such an occurrence would not have been manifested. If this localized phenomenon is put aside then the criteria established seems to operate adequately.

5.2.4.4 Edmonton Experimental Tunnel

Introduction

The small diameter tunnel was built in 1979 as a main storm sewer for the Yellowhead Trail freeway, in northern Edmonton, Alberta. It includes a length of precast segmented concrete lining which was introduced on an experimental basis in the Edmonton area. This case history refers solely to the experimental portion of the tunnel, and does not deal with the remaining length, where a conventional two-phase support system was used. Details of this project are found in El-Nahhas (1980), Eisenstein et.al. (1981a) and in Eisenstein et.al. (1981b).

Site Geology

The 2.56 m diameter tunnel was driven under a soil cover of 22 to 25 m. A longitudinal cross section of the tunnel is presented in Figure 5.36, where a simplified geological profile is included.

A brief overview of the geological conditions in Edmonton was given in the previous section. At the time the present back analysis was initiated, the writer assumed that the geological and geotechnical conditions found in this case were similar to those of the LRT tunnel. A review of the former investigations and analyses then available on this case history did not indicate otherwise. Hence it was

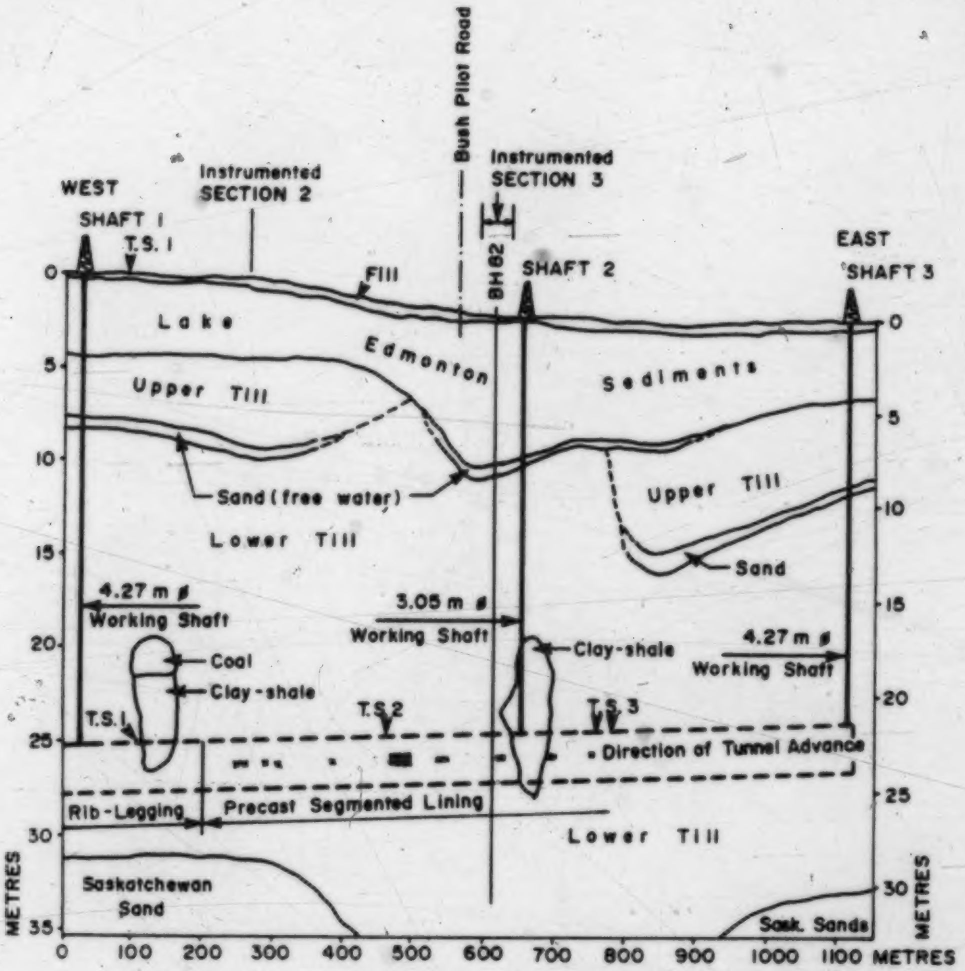
Bush Pilot Road
Instrumented SECTION 2
Instrumented SECTION 3
WEST
SHAFT 1
T.S. 1
BH 82
SHAFT 2
EAST
SHAFT 3
Fill
Lake Edmonton Sediments
Upper Till
Sand (free water)
Lower Till
Upper Till
Sand
4.27 m ø Working Shaft
3.05 m ø Working Shaft
4.27 m ø Working Shaft
Coal
Clay-shale
Clay-shale
T.S. 1
T.S. 2
T.S. 3
Direction of Tunnel Advance
Rib-Legging
Precast Segmented Lining
Lower Till
Saskatchewan Sand
Sask. Sands
METRES
0
5
10
15
20
25
30
35
0
5
10
15
20
25
30
0 100 200 300 400 500 600 700 800 900 1000 1100 METRES

NOTE: ADDITIONAL BOREHOLE BH82 DRILLED IN 29th OCTOBER 1982, 19.7m SOUTH OF TUNNEL AXIS, 44.3 m WEST OF CONSTRUCTION SHAFT 2 (Current Manhole AA14)

Figure 5.36 Subsurface Profile of Edmonton Experimental Tunnel along 125 Avenue (Yellowhead Trail) (after El-Nahhas, 1980:modified)

accepted that the experimental tunnel had also been driven through a stiff, very stiff to hard till. Accordingly, the first preliminary numerical simulations assumed the same 'best-fit' parameters found for the LRT case. These calculations indicated ground movements that were typically five times smaller than that actually measured. This raised the question of whether the tunnel had been driven through one of the soft zones known to exist in the Edmonton till (Thomson et.al., 1982). Available geotechnical data was not sufficient to answer this question. It was thus decided to conduct additional field and laboratory investigations. An exploratory 8" diameter borehole (BH 82 in Figure 5.36) was drilled in late 1982, followed by a testing program. Results of this program will be presented later, but as was anticipated a softer till zone exists in the area.

An examination of the available data on the urban geology of Edmonton (Kathol and McPherson, 1975:20) reveals that the tunnel axis runs almost parallel to the thalweg of the Beverly Preglacial Valley. This is the dominant topographic feature of the Edmonton bedrock and is considered to be the largest and deepest valley present in the area. It shows a gentle downstream gradient to the east (about 0.05%), is locally 7 km wide, and it has a northern side slope of up to 10%. The tunnel runs about 500 m south of its northern flank and about 25 m above its floor. Thomson et.al. (1982) suggested that the commonly used description of two dense basal tills (lodgement tills) in

Edmonton is overly simplistic. They suggested that other types of depositional features could have been present such as rapidly accumulated flow till zones. A review of recently proposed models explaining the formation of glacial sediments was presented by Wittebolle (1983:5).

As noted in Figure 5.36, the fill layer is less than a metre thick (about 3 m at BH 82). At the instrumented section 3, which is of interest to the present study, the base of the lake sediments is 8 m below the surface. The additional borehole BH82 did not detect the free water bearing sand layer underlying the upper sediments as shown in that figure. Instead, small sand lenses or pockets were found in the lower portion of the lacustrine sediments and in the upper region of the subjacent till body. The latter was medium to dark grey in colour and comprised mainly a silty clay (CL), locally including shale pebbles and coal bits, as well as the sand lenses. A careful logging of the twelve 3" diameter shelby samples did not reveal the existence of any joints in the till. The compression tests later conducted did not indicate any fissure controlled mode of failure. The description of the subsurface profile by El-Nahhas (1980:56), who was able to inspect the material in place through a number of construction shafts, large diameter power holes and instrument installation boreholes, does not include any reference to discontinuities in the till mass. Unlike the LRT tunnel, there was no record of localized ground collapses or of failures that were structurally controlled by soil discontinuities. Therefore, it seems probable that the soft till in the area is not jointed. If joint genesis is associated with drying (May and Thomson, 1978:368), then this till may not be dessicated to the same extent as typical Edmonton tills.

Geotechnical Investigations

Some 18 disturbed samples and 12 shelby tube samples were collected and tested. The basic geotechnical profile and properties of the soils found are given in Figures 5.37 and 5.38. The Unified Classification of the grey till is CL. The bedrock and the ground water level were not encountered by the 30.25 m deep borehole, which was drilled using a hollow stem auger. However, the degree of saturation of the till was always found to be greater than 95% and was 100% in most samples. The measured average water content and the in situ void ratio are slightly higher than that found at the LRT tunnel. Very low SPT blow count numbers were detected which were even lower than those found in another soft till zone in downtown Edmonton (Thomson et.al., 1982).

Thin walled shelby tubes turned in to form a cutting edge, were used for 72.9 mm diameter sampling. Sampling locations are given in Figure 5.39. Samplers had an inside clearance (3.9%) and area (20.6%) ratios which were higher than that ideally required for soft to medium clays. Sample length was typically 45 cm. Some of the tube tails had bezel edges protruding inside the sampler close to the fixing holes. This caused two of the samples (I and V) to be

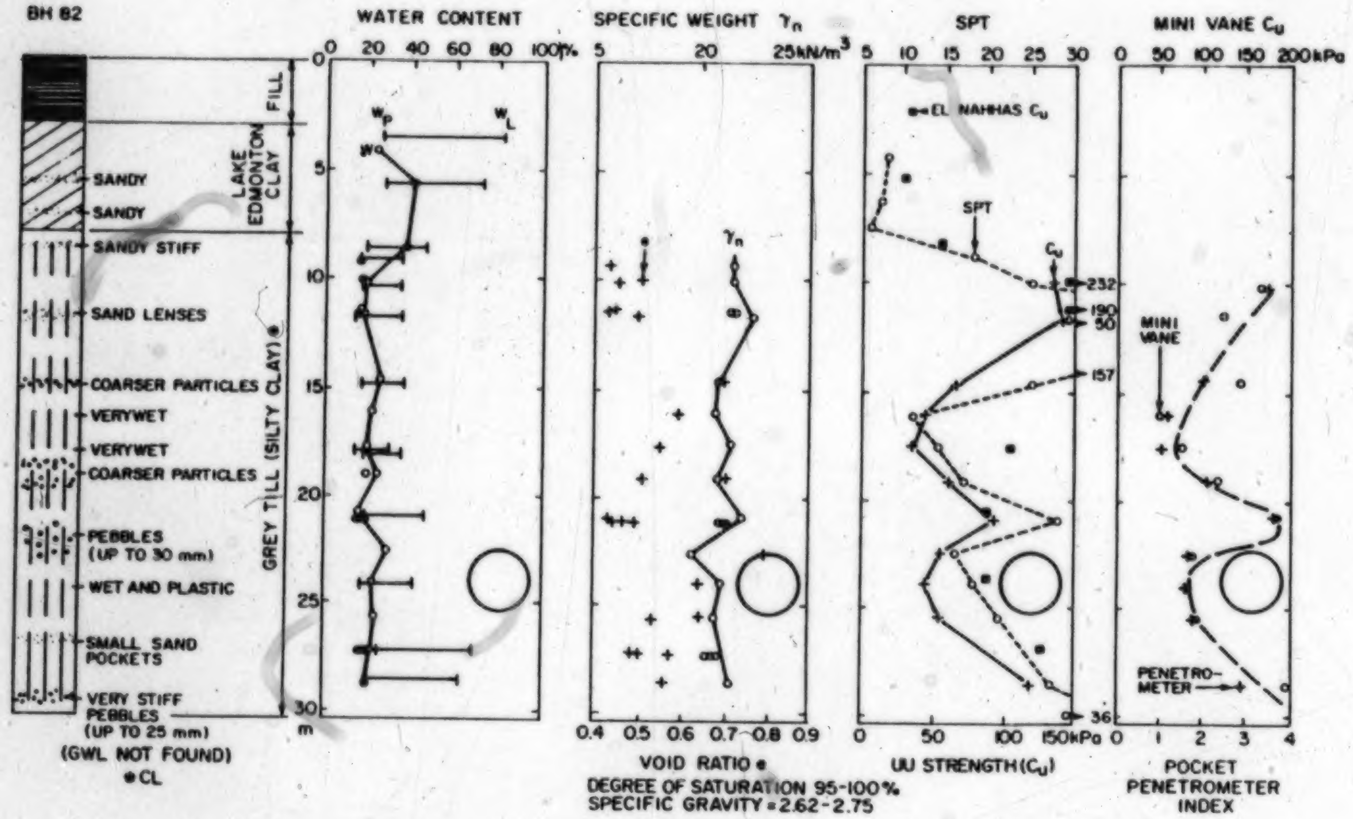

Figure 5.37 Geotechnical Profile at the Instrumented Section 3 of Edmonton Experimental Tunnel

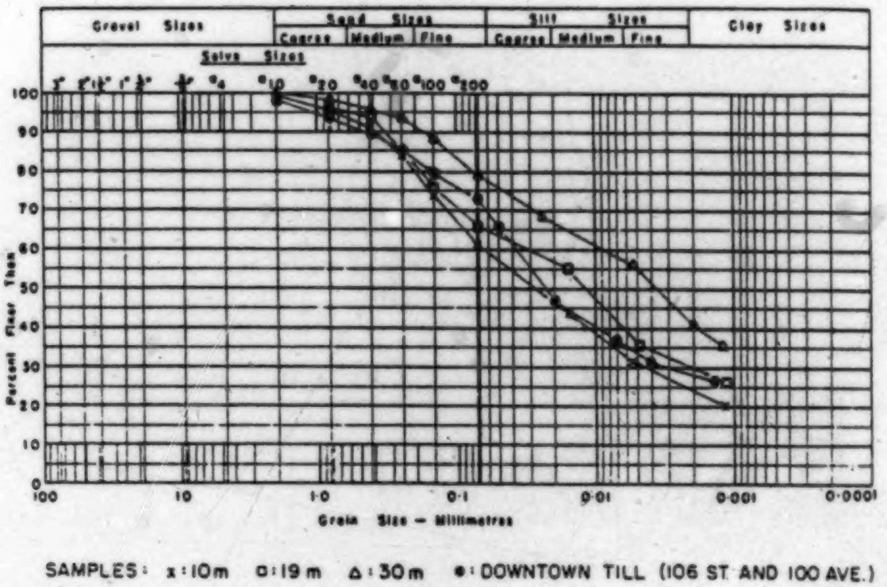

Figure 5.38 Grain Size Distributions

severely disturbed during extrusion. Therefore, it was decided to extrude the remaining samples against the driving direction, (as opposed to the recommended practice). The quality of these samples is regarded as low, and an unknown amount of disturbance would be inherent in the sampling and extruding operations.

Despite this, unconfined undrained tests, mini-vane tests and pocket penetrometer indices indicated trends of undrained strength variation with depth closely resembling that given by the SPT blow counts. Figure 5.37 includes data gathered earlier by El-Nahhas (1981), as well as from the instrumented Section 3. The relatively higher undrained strengths from the El-Nahhas data could be explained by the larger sample size (4") used or by a better quality sampling. Even so, one notes that from 9 to 15 m depth, which roughly corresponds to the very upper portion of the till, the soil strength is considerably higher than at other depths.

Laboratory Testing

Figure 5.39 also furnishes the types of laboratory tests carried out on the shelby samples. Except for the oedometer consolidation tests, conducted on 63 mm diameter samples, all triaxial tests were conducted on 70 mm diameter samples. Figure 5.40 and Table 5.20 furnish the results of some oedometer consolidation tests. The maximum past consolidation stresses at three depths were estimated according to Casagrande's method. As shown in Table 5.20,

Sample	Depth (m)	Compression Index C_c	Initial Void Ratio	Maximum Post Consolidation Stress (kPa)	OCR
II	10.0	0.164	0.50	280	1.33
VII	19.0	0.176	0.60	160	0.26?
XI	25.5	0.194	0.60	300	0.56?

Table 5.20 Results of Oedometer Consolidation Tests on Till for Edmonton Experimental Tunnel

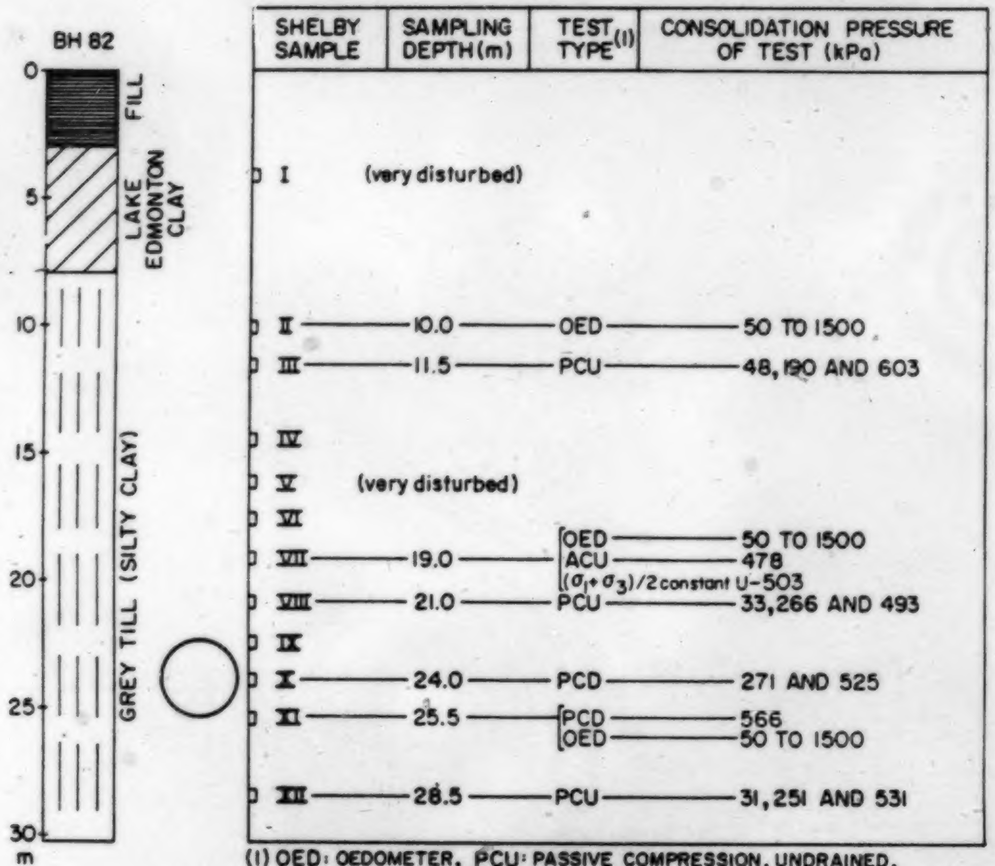

SHELBY SAMPLE	SAMPLING DEPTH (m)	TEST TYPE(1)	CONSOLIDATION PRESSURE OF TEST (kPa)
I	(very disturbed)		
II	10.0	OED	50 TO 1500
III	11.5	PCU	48, 190 AND 603
IV			
V	(very disturbed)		
VI			
VII	19.0	OED ACU $(\sigma_1+\sigma_3)/2$ constant U	50 TO 1500 478 503
VIII	21.0	PCU	33, 266 AND 493
IX			
X	24.0	PCD	271 AND 525
XI	25.5	PCD OED	566 50 TO 1500
XII	28.5	PCU	31, 251 AND 531

(1) OED: OEDOMETER, PCU: PASSIVE COMPRESSION, UNDRAINED,
ACU: ACTIVE COMPRESSION, UNDRAINED,
PCD: PASSIVE COMPRESSION, DRAINED.
TRIAXIAL TEST SAMPLES 10 cm HIGH AND 7 cm DIAMETER, ALL WITH BACKPRESSURE.

Figure 5.39 Location of Shelby Sampling and Types of Test in Edmonton Experimental Tunnel

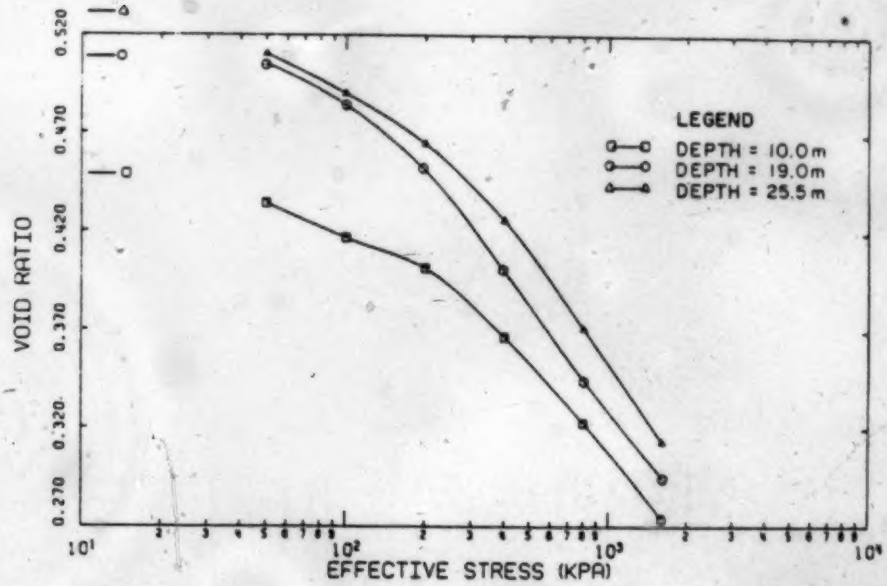

Figure 5.40 Void Ratio - Effective Stress Curves from Oedometer Tests for Edmonton Experimental Tunnel Through Till

sample II which was collected in the upper part of the grey till, is more consolidated than the deeper samples and confirms the higher strength detected in this horizon. The calculated overconsolidation ratios of the deeper samples were less than unity.

The apparent 'underconsolidated' nature of the lower samples could be attributed to localized arching of discrete zones within the till mass. In other words, the stress field would not be simply geostatic, where the vertical stress is equal to the overburden pressure. Wittebolle (1987) suggested that this process could be associated with differential thawing after the till was laid down. The distorted profile of the till surface between stations 450 and 750 m as shown in Figure 5.36, resembles a subsidence trough with a maximum distortion of about 1:20. This could be interpreted as an indication that some arching mechanism might have occurred when ice rich soils which possibly existed in the area, melted out. These zones arch against adjacent soil which act as buttresses. As a result, the ice rich soils would have been later consolidated under vertical stresses lower than the overburden. If this mechanism were correct, one would expect horizontal stresses and K_o values for these soils to be higher than those occurring for normally consolidated state under overburden loads. It is not clear however, if this proposed mechanism could explain the existence of the stiffer upper layer of till which is a feature that seems to be always associated with the softer till lying underneath (see, for instance, Thomson et.al., 1982:179).

On the other hand sampling disturbance effects could also explain, at least in part, the low maximum past consolidation stresses found at depth. Since no definite information is currently available regarding the actual stress field in the area, it will be assumed that the deeper soil samples are normally consolidated under the overburden stress and that the upper layer is lightly overconsolidated.

The coefficient of consolidation of the softer till was found to be 4 to 20 x $10^{-5}cm^2/s$. It will be later shown that even when the higher value of c_v is considered and applying the tentative criteria proposed in Chapter 3, the consolidation in the till induced by the tunnel excavation was probably negligible for several months after the TBM passed the section. Naturally, this is strongly dependent on the assumptions used to develop the simplified criteria, one of which is the soil is fully saturated.

It was decided to conduct both drained and undrained triaxial tests in an attempt to bound the observed field performance. This approach +as used by Chang and Duncan (1970:1674) to calculate the response of a 60 m deep open excavation for a pumping plant in California. Isotropically consolidated undrained tests, however, have been preferred in this study, rather than the unconsolidated tests favoured by Chang and Duncan (Op.cit.). This preference reflects an attempt to minimize the recognized sample disturbance. All

70 mm diameter triaxial test samples had a height to diameter ratio of 1.2 to 1.5 and were loaded with free ends at the top and bottom platens. This follows successful testing experience on glacial tills by Wittebolle (1983:47). All samples in the undrained and drained tests were saturated with back pressures ranging from 400 to 530 kPa. Saturation control, consolidation and strain controlled loading followed the procedures established by Wittebolle (1983:49, 147).

The testing program was set up to provide the required parameters for the hyperbolic model. Accordingly, a suite of passive compression tests (σ_3 constant, σ_1 increasing), both undrained and drained, were carried out. Twelve tests were performed (9 undrained and 3 drained) at the effective consolidation pressures given in Figure 5.39. The results obtained are shown in Figures 5.41 to 5.44. The drained tests showed contraction during loading. The initial sample volumes, after the consolidation stage are indicated in Figure 5.41. Bedding errors were observed in some of the undrained tests which resulted from an initial lack of fit between the sample surface and the lubricated platen. These errors had to be taken into account when the hyperbolic parameters were being obtained. As anticapted, the samples at 11.5 m depth, which is roughly at the midheight of the "stiffer" upper portion of the soft till, showed higher stiffness and strength than the samples below. Unfortunately in one of the tests at this depth, part of the data was lost due to malfunction of the recording system. Most of the samples at all depths considered showed positive pore pressure changes. One exception was the sample at 28.5 m depth, consolidated at 31 kPa (Figure 5.43), where a slight negative trend was noted. This could indicate that, despite sampling disturbance, this sample behaved as an overconsolidated material when reconsolidated in the laboratory at a low effective stress. A similar response was noted in the 11.5 m depth sample under low consolidation stress. All other samples reacted as normally consolidated soils under the test consolidation stress.

Hyperbolic Model Parameters

Using the procedure shown in Figure 5.10 and the recommendations by Duncan et.al. (1980:22), the basic parameters of individually fitted hyperbolae were obtained and are shown in Table 5.21. While the failure ratio result was expected, i.e., being independent of the confining effective stress, the initial tangent modulus was not. Figure 5.45 shows the relation between these two variables, normalized to atmospheric pressure. Two distinct variations of the undrained modulus with confining stress are proposed, one for the stiffer portion of the till (points 1 and 3 - refer to Table 5.21), and one for the softer layer underneath (points 4, 5, 6 and 8). Some of the samples were tested under a confining stress much less than the overburden stress (nominal OCR much greater than unity). Thus, a non-linear modulus-confining stress logarithimic

No.	Depth (m)	Type(1)	σ'_3 Conf. (kPa)	OCR(2)	σ'_3/P_a	R_f	E_i/P_a
1	11.5	Undrained	47.81	5.05	0.472	0.70	78.95
2	11.5	Undrained	189.93	1.27	1.874	-	-(3)
3	11.5	Undrained	602.99	1.00	5.951	0.86	724.06
4	21.0	Undrained	32.50	13.57	0.321	0.98	27.41
5	21.0	Undrained	265.72	1.66	2.622	0.91	217.61
6	21.0	Undrained	493.34	1.0	4.869	0.94	379.6
7	28.5	Undrained	31.21	19.18	0.308	0.96	170.2
8	28.5	Undrained	251.00	2.38	2.477	0.90	180.75
9	28.5	Undrained	530.85	1.13	5.239	0.90	343.87
10	24.0	Drained	270.99	1.86	2.674	0.90	186.20
11	24.0	Drained	524.73	1.00	5.179	0.90	290.27
12	25.5	Drained	566.10	1.00	5.590	0.89	215.28

Notes: (1) Passsive compression tests only.
(2) Nominal value assuming the soil normally consolidated under the overburden stress.
(3) Early portion of stress strain curve was lost.

Table 5.21 Parameters of Fitted Hyperbolae for Softer Till

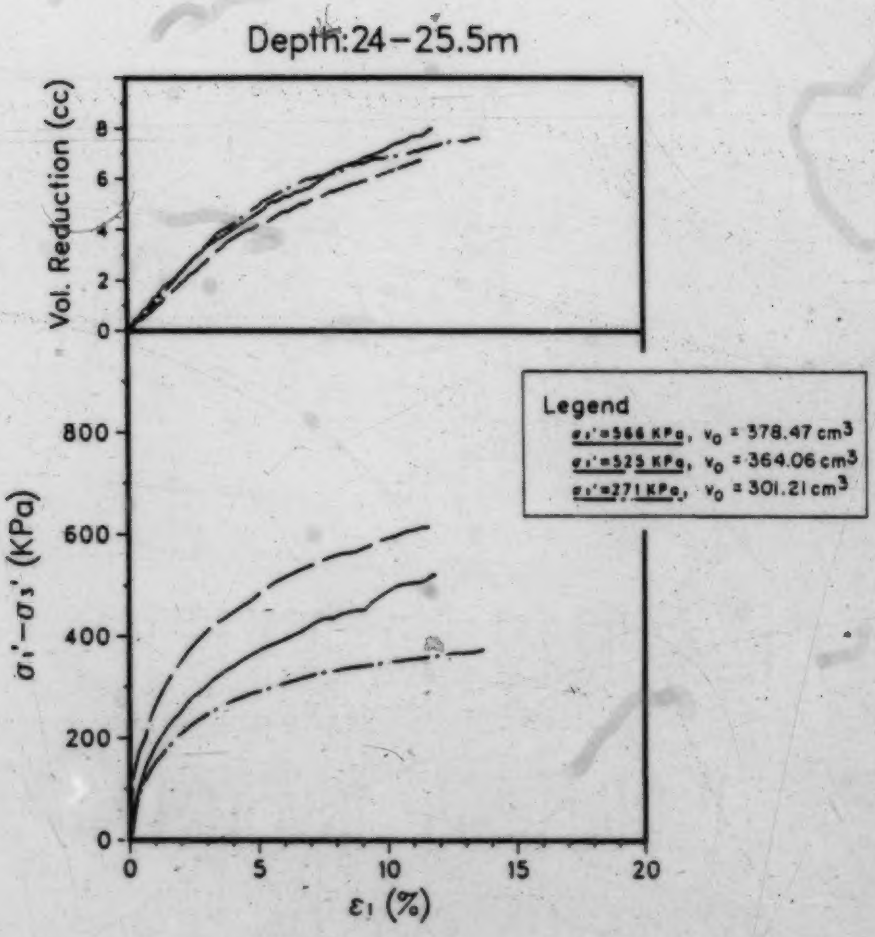

Figure 5.41 Drained Passive Compression Tests in Softer Till (24 - 25 m depth)

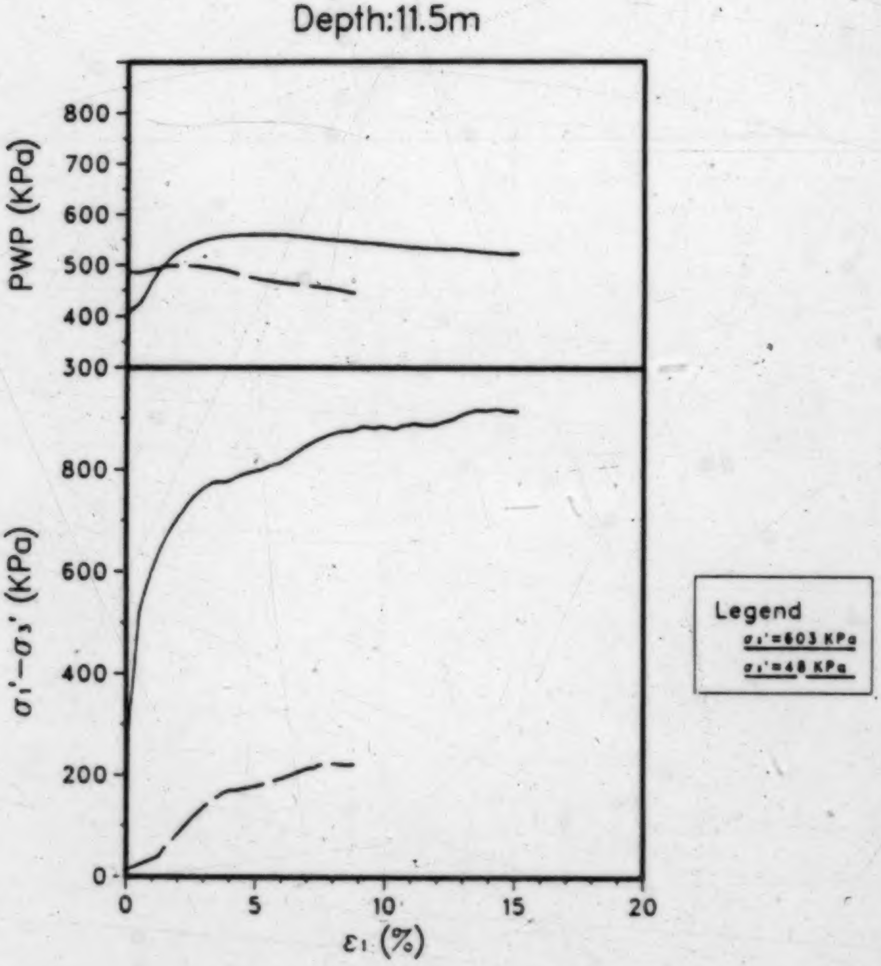

Figure 5.42 Consolidated Undrained Passive Compression Tests in Softer Till (11.5 m depth)

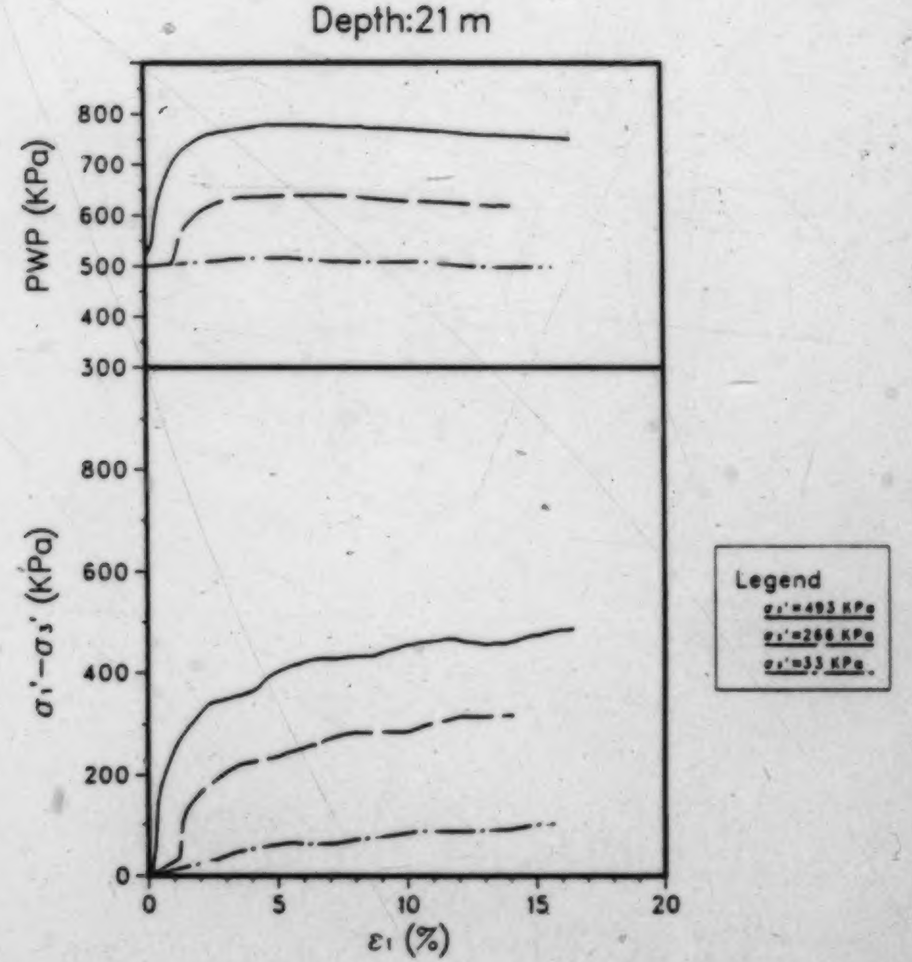

Figure 5.43 Consolidated Undrained Passive Compression Tests in Softer Till (21.0 m depth)

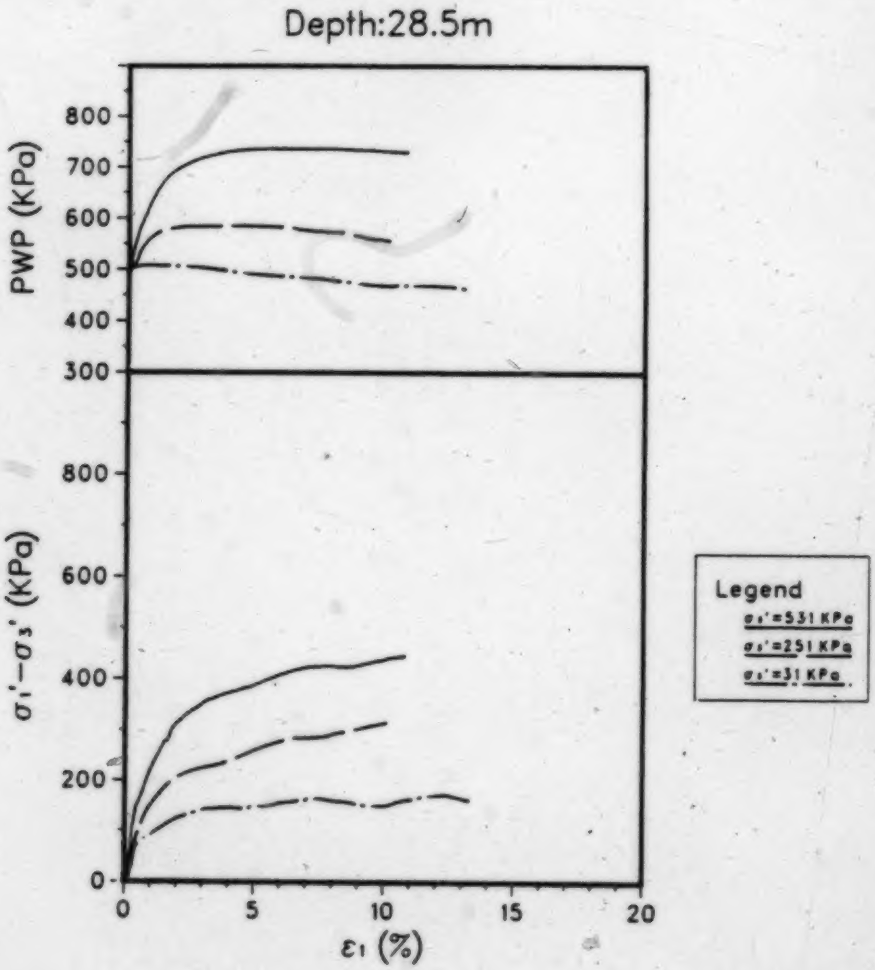

Figure 5.44 Consolidated Undrained Passive Compression Tests in Softer Till (28.5 m depth)

relationship was initially anticipated, as it was recognized that this relation would also depend on the maximum past consolidation stress. This feature, noted by Janbu (1963:21) when investigating the compressibility of natural deposits, was not clearly detected in the present case. A possible exception refers to point 7 in Figure 5.45 which corresponds both to the deepest sample collected and the minimum confining stress used. In this case, a modulus higher than that given by the linear relationship shown in the figure was obtained. This could indicate that the stiffness of this sample is controlled by a maximum past consolidation stress which was higher than the test confining stress. Excluding this point, a modulus number and a modulus exponent were found for the softer till for undrained and drained conditions. For the stiffer layer, a dimensionless initial tangent modulus of 345 (i.e. an elastic modulus of 35 MPa) was found for the average in situ stress at the midheight of the layer (12.35 m depth).

As the deviator stress did not level off or decrease in most tests, failure was defined in terms of the maximum principal stress ratio. This criterion was also favoured by Wittebolle (1983:50) when investigating other tills. As shown in Figure 5.46, two failure lines can be drawn, one for the stiffer and one for the softer till layers which allow the effective stress strength parameters (c', ϕ') to be defined. Similarly, total stress parameters (c, ϕ) can be defined, as shown in Figure 5.47. Despite knowing that the

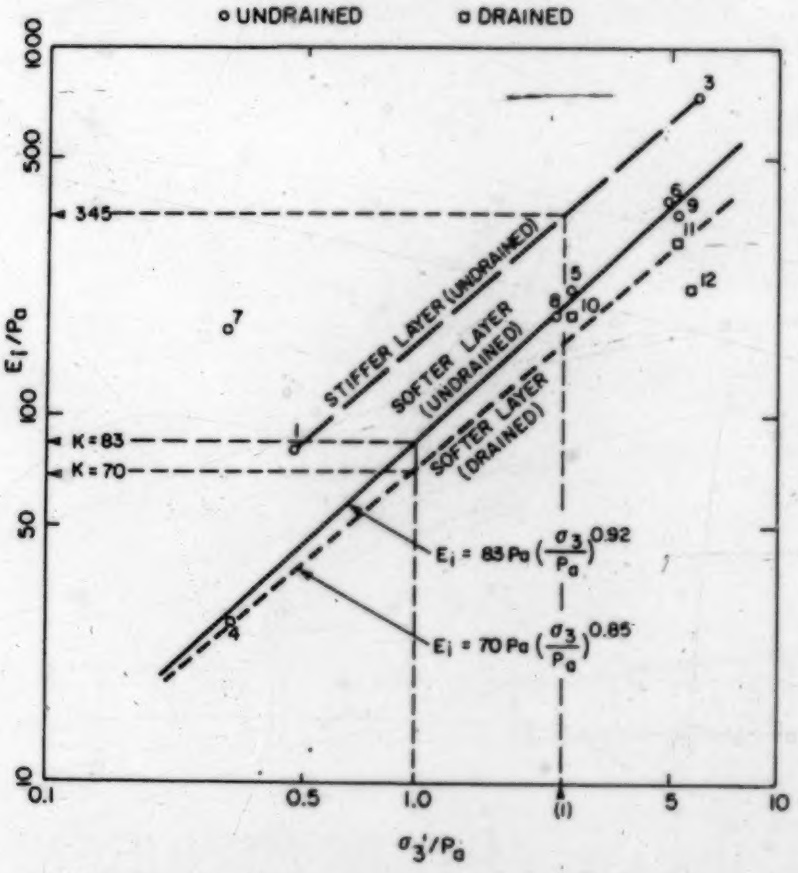

NOTES:

1. AVERAGE IN SITU STRESS AT THE MIDHEIGHT OF THE STIFFER LAYER EQUAL TO 2.56.
2. SEE TABLE 5.21 FOR TEST NUMBER IDENTIFICATION.

Figure 5.45 Variation of Initial Tangent Modulus with Confining Pressure for Till in Edmonton Experimental Tunnel

latter are arbitrary, since they are strongly path dependent, they are needed for an undrained analysis which is discussed later.

The failure ratios shown in Table 5.21 were calculated assuming a deviator stress at failure equal to the maximum observed during the test. As noted, this implied taking the deviator stress at the end of the test, as the stress difference did not level off or decrease. Despite this approximation, the failure ratios were usually greater than 0.90. Perhaps a better estimate of R_f would be a value closer to one. This implies that failure occurs at very high strains, as may have been the case in most samples.

Regarding the in situ stress condition, the coefficient of earth pressure at rest can be estimated from the Mayne and Kulhawy (1982:803) empirical expression. For a friction angle of 22° and an overconsolidation ratio possibly varying between 1 and 2, K_o should range between 0.6 and 0.8. On the other hand, El-Nahhas (1980:195) suggested that K_o should vary between 0.8 and 1.0 in this case, according to his interpretations of the observed ground response to tunnelling. For the present study, K_o was considered to vary from 0.5 to 1.0. It will be shown later that from the best fit analyses, K_o was found to lie between 0.8 and 0.9.

Figure 5.48 furnishes the variations of initial tangent modulus with depth, as given by the hyperbolic model formulation (Figure 5.11), for the most probable in situ stress conditions in both drained and undrained situations.

They were obtained from the data shown in Figures 5.45 to 5.47, and correspond to the analysis that provided the best fit of field performance. Note that the stiffer grey till horizon was represented by a linear elastic material with constant properties (E=35 MPa). The soil below and above this layer was represented by a single non-linear elastic material. Its undrained hyperbolic parameters are K=83, n=0.92, ϕ=16°, c=45 kPa and R_f=1. The drained parameters are K=70, n=0.85, ϕ'=22°, c'=30 kPa and R_f =1.0. The soil was assumed to be fully saturated, with γ = 20 kN/m³, but with zero in situ pore pressure and K_o between 0.8 and 0.9.

Although the parameters above were obtained for the grey till, the resulting in situ modulus for the upper part of the profile shown in Figure 5.48 could well represent that of the Lake Edmonton Clay. This clay was found to have pressuremeter moduli varying between 6 and 15 MPa as reported in the LRT tunnel case (see Table 5.15 and Figure 5.23). These values agree well with the proposed E modulus profiles given in Figure 5.48.

Also shown in Figure 5.48 are the results of pressuremeter moduli obtained by Thomson et.al. (1982:179), in another softer till zone, found elsewhere in Edmonton (107 Str. and Jasper Ave.). It is interesting to note that fair correspondence seems to exist between the proposed in situ tangent modulus profile for the Edmonton Experimental site and the pressuremeter data. These were obtained in pre-drilled boreholes, using the same equipment and

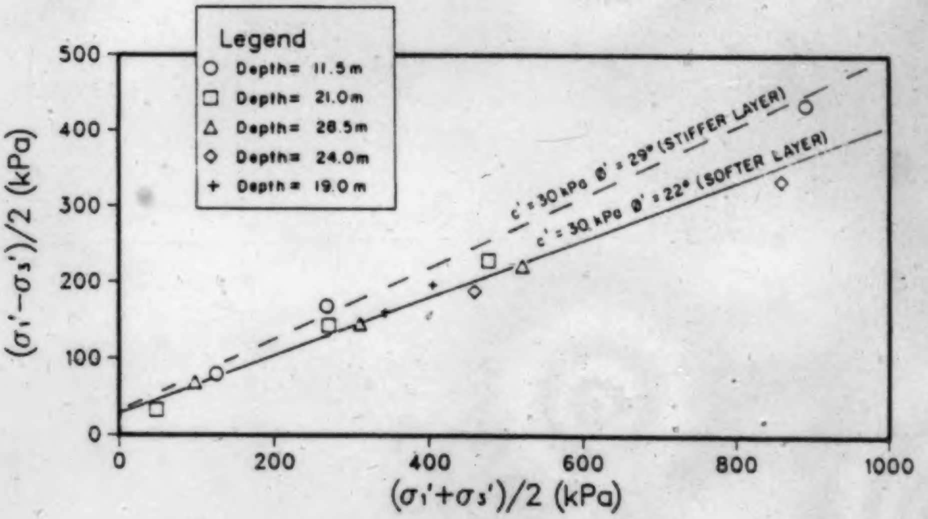

Figure 5.46 Effective Stress Strength Parameters for Till in Edmonton Experimental Tunnel

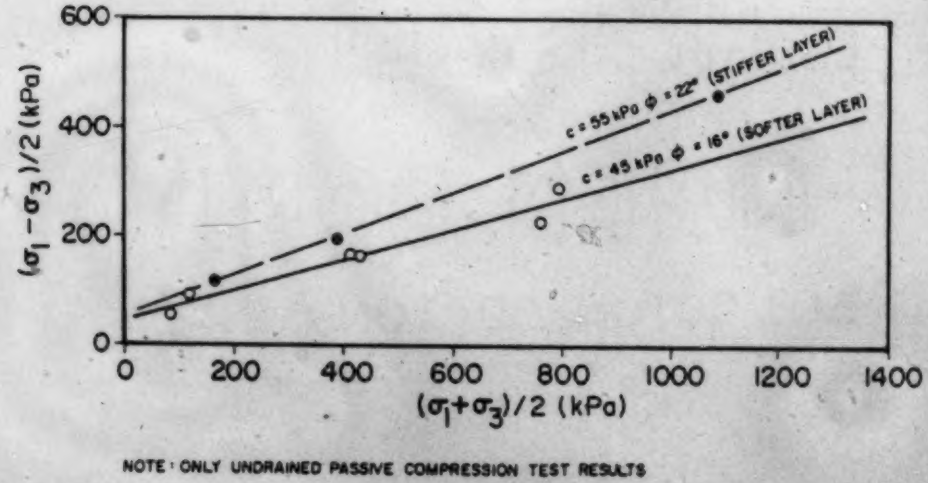

Figure 5.47 Total Stress Strength Parameters for Till in Edmonton Experimental Tunnel

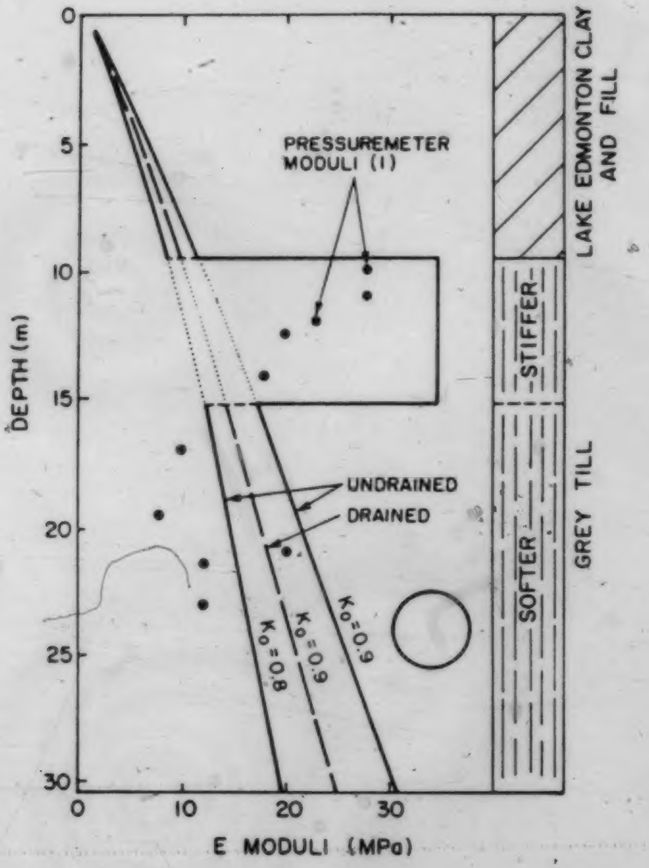

NOTE:
(1) PRESSUREMETER DATA FROM SOFT AREA AT JASPER AVE. AND 107 ST. (BH1A AND BH5A); THOMSON-ET-AL (1982: 179)

Figure 5.48 Profile of In Situ Deformation Modulus at the Edmonton Experimental Tunnel

interpretation procedure described by Eisenstein and Morrison (1973). The correspondence applies even for the stiffer upper horizon of the till. Standard penetration test results exhibit similar trends in both sites. An explanation for the noted similarities has not been presented so far.

Stress Path and Drainage Effects

The input parameters for the numerical back analyses of this case history have been derived from conventional passive compression triaxial tests, despite the known dependency of the stress-strain relationship on stress path. Medeiros and Eisenstein (1983) showed that the stress path effect is well pronounced on the drained behaviour of Edmonton till. This dependency should be less pronounced in undrained loading, as the effective stress path of the saturated soil is less affected by the type of undrained shearing to which it is subjected. To illustrate this point, two additional undrained triaxial tests were performed on a sample collected at 19 m depth. In both tests, the till was consolidated by an isotropic confining stress of about 500 kPa. The testing procedure was the same as in the other tests including the strain rate, but the shear loading paths were different. In the first test, the soil was brought to failure by proportionally increasing the axial stress and decreasing the radial stress, so as to maintain a constant average total stress, $(\sigma_1 + \sigma_3)/2$. In the second test, the till was subjected to an active compression test, by keeping the axial stress constant and reducing the radial stress.

The results of these two tests are shown in Figure 5.49 and 5.50.

The stress-strain curves of these two tests are superimposed in Figure 5.51, together with those from two passive compression tests, one undrained and another drained. Both were consolidated to confining stresses close to 500 kPa, but the tests were conducted on samples collected at slightly different depths (see Figures 5.42 and 5.44). The solid lines shown in Figure 5.51 represent best fit hyperbolae to each test curve. The parameters for each fitted hyperbola are given in Table 5.22. From these, the variations of the tangent modulus with the axial strains can be obtained, as shown in Figure 5.52. Note that due to the particular total stress paths used and due to the fact that the soil is saturated, the Young's modulus in each case is equal to the slope of the deviator stress-axial strain curve. As is seen in Figure 5.52, differences are noted in the undrained modulus variation with strain, but they are appreciably less than that observed for drained moduli (see Medeiros and Eisenstein, 1983:126). The differences can be attributed to the unequal consolidation stresses used, to differences in the inital water content (or void ratio) of each sample, collected at slightly different depths, differences in the past stress histories as well as soil inhomogeneities or anisotropies. Apart from these, differences due to inaccuracies in fitting the curves by hyperbolae should also be considered. An entirely different

Type of Test	Sample Depth (m)	Conf. Stress (kPa)	a $(10^{-5}kPa^{-1})$	b $(10^{-5}kPa^{-1})$	$E_i = 1/a$ (MPa)	$(\sigma_1-\sigma_3)_u=1/b$ (kPa)
A. Passive Compression, Drained	24.0	525	2.72	146.0	36.76	685
B. Passive Compression, Undrained	21.0	493	1.85	213.8	54.05	468
C. Constant $(\sigma_1+\sigma_3)/2$ Test, Undrained	19.0	503	1.70	294.4	58.82	340
D. Active Compression, Undrained	19.0	478	1.35	245.8	74.07	407

Notes: (1) Hyperbola: $\sigma_1 - \sigma_3 = \varepsilon_1/(a + b\varepsilon_1)$; $E_t = a/(a + b\varepsilon_1)^2$

(2) Confining stress always greater than overburden stress.

Table 5.22 Parameters of Hyperbolae Fitted to Stress-Strain Curves of Till, Tested under Distinct Total Stress Paths and Drainage Conditions

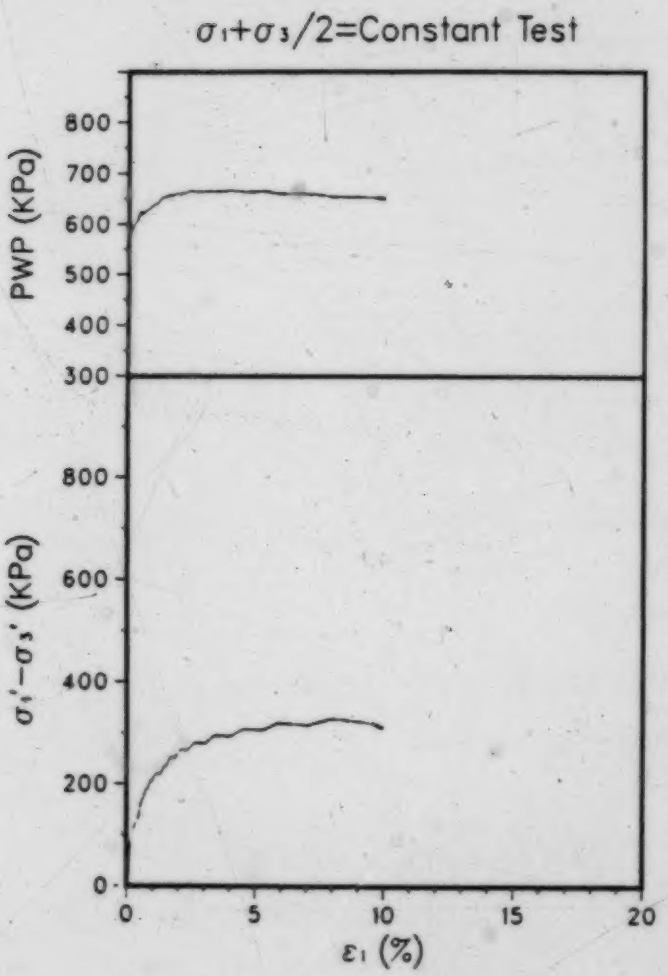

Figure 5.49 Consolidated Undrained Compression Test in Softer Till with Constant Average Stress

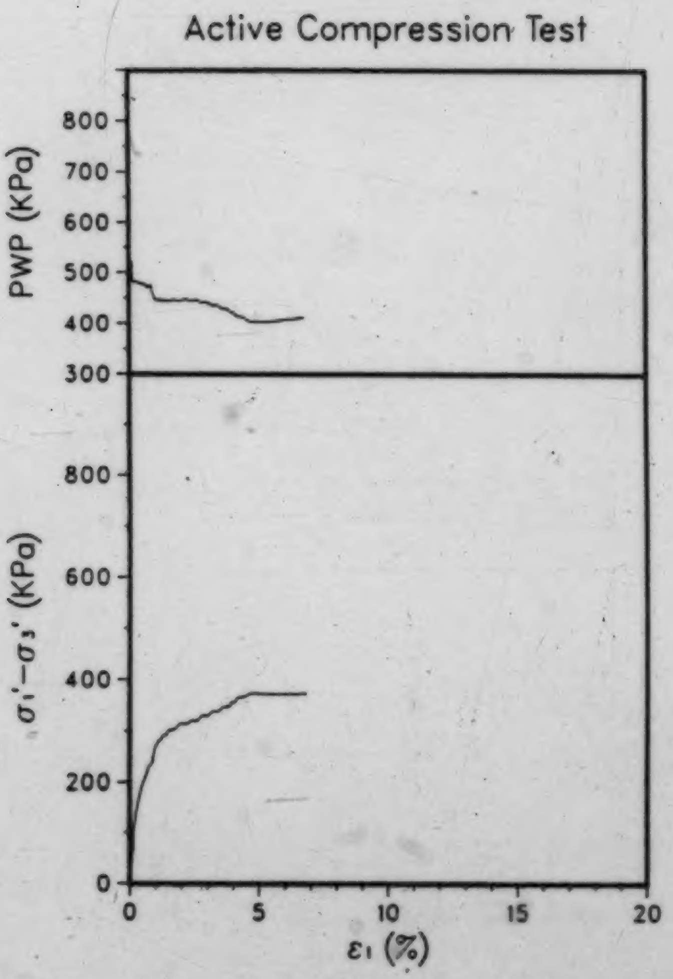

Figure 5.50 Consolidated Undrained Active Compression Test in Softer Till

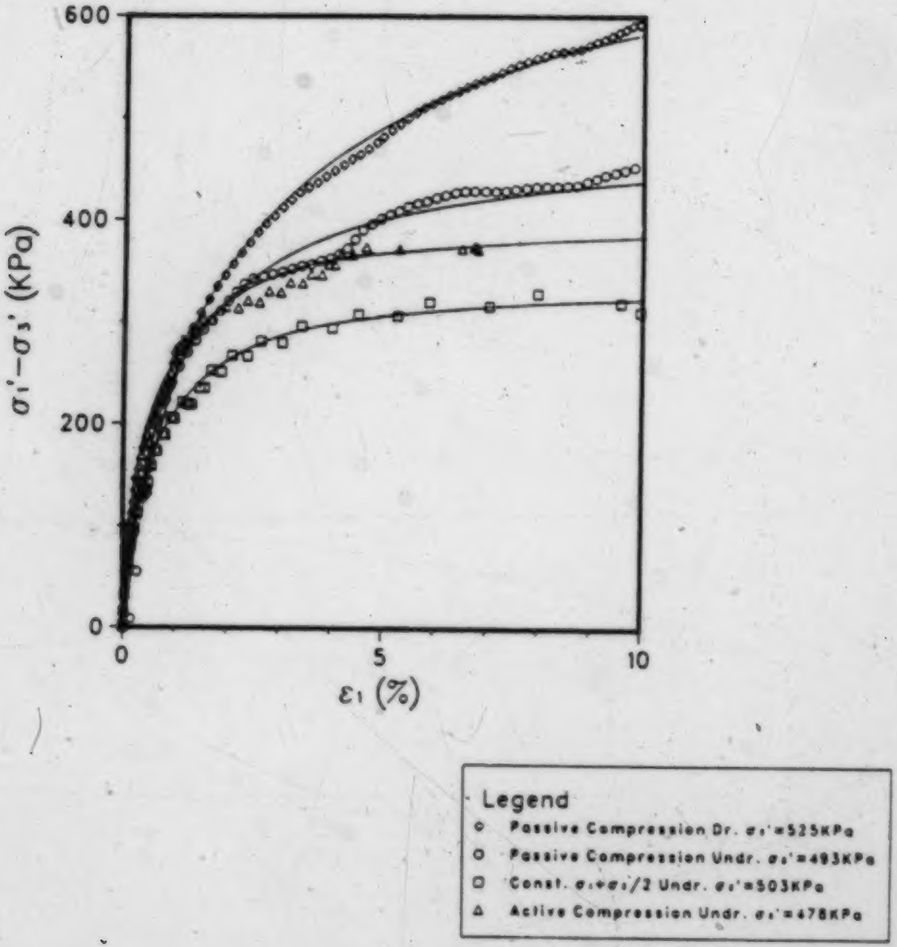

Figure 5.51 Stress-Strain Curves of Softer Till Tested under Distinct Total Stress Paths and Distinct Drainage Conditions

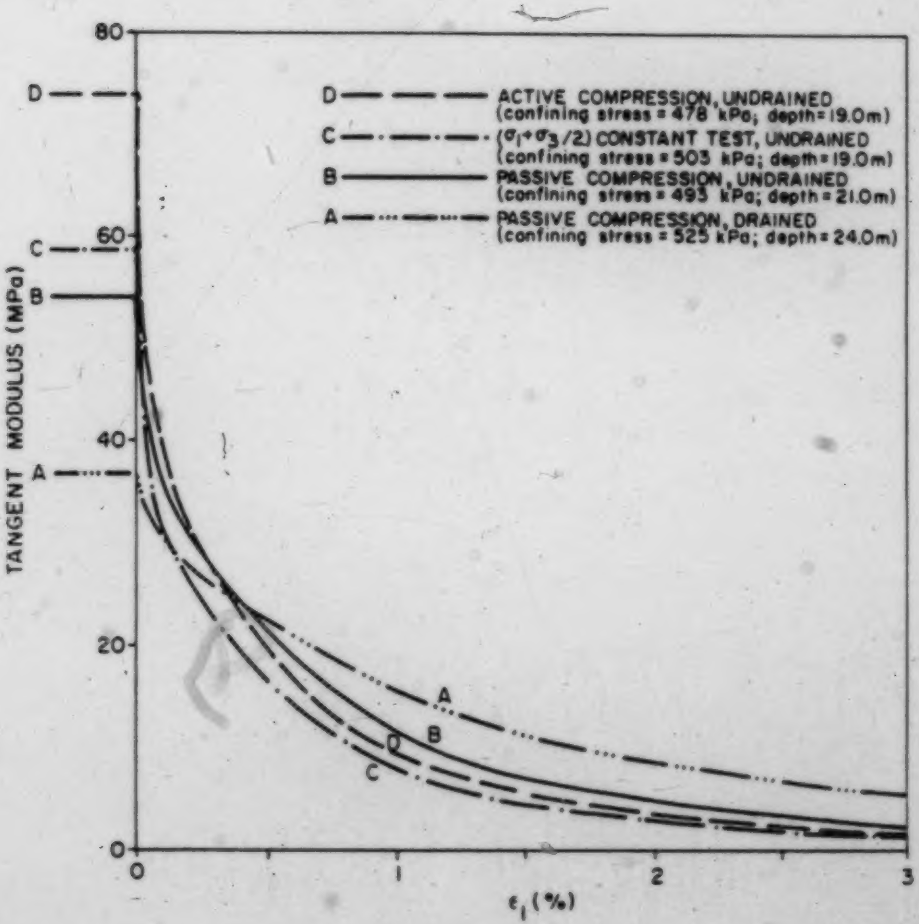

Figure 5.52 Tangent Moduli of Deformation of Till in Edmonton Experimental Tunnel for Distinct Total Stress Paths and Drainage Conditions

modulus variation is noted, however, for the drained test. As indicated earlier, the larger difference here is attributed to the very different effective stress path followed in this case. It is observed in Figure 5.53 that, despite the very distinct total stress paths in the undrained tests, their resulting effective stress paths are not entirely dissimilar, but they are very different from that corresponding to the drained test.

Tunnel Construction and Field Monitoring

Tunnel construction was carried out with a full face cutting wheel TBM (a Lovat M-100 Series 1900), whose details are given in Figure 5.54. The TBM body is 5.96 m long and the cutting profile 2.56 m diameter (including overcutting). Similar to the TBM used at the LRT tunnel, the soil at the face is indented and scraped by staggered teeth, protruding outwardly and fixed at three spokes. The soil is thus cut at the heading in a near vertical face which is left virtually unsupported. A detailed account of the tunnel construction was given by El-Nahhas (1980:60). The lining system used is shown in Figure 5.54. Each support ring, one metre wide, consisted of four trapezoidal precast concrete segments. Each segment was provided with a longitudinal stress raiser which locally reduces the segment thickness from 11 cm to 7 cm. These stress raisers are designed to act as a section of low moment resistance, ideally increasing the lining flexibility. The segments were lightly reinforced with steel mesh at the mid-section. Every ring was expanded radially to

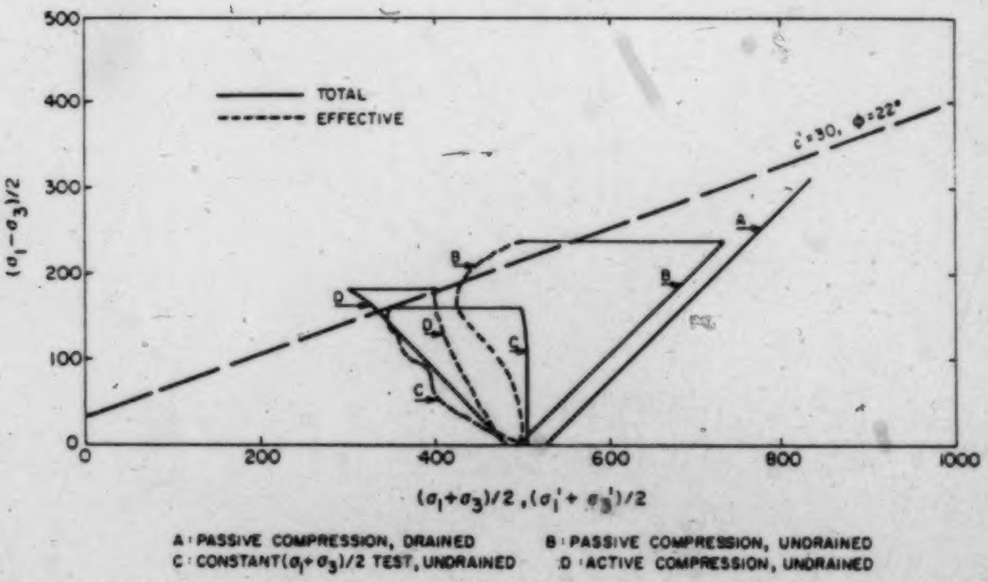

Figure 5.53 Stress Paths of Triaxial Tests on Till in Edmonton Experimental Tunnel

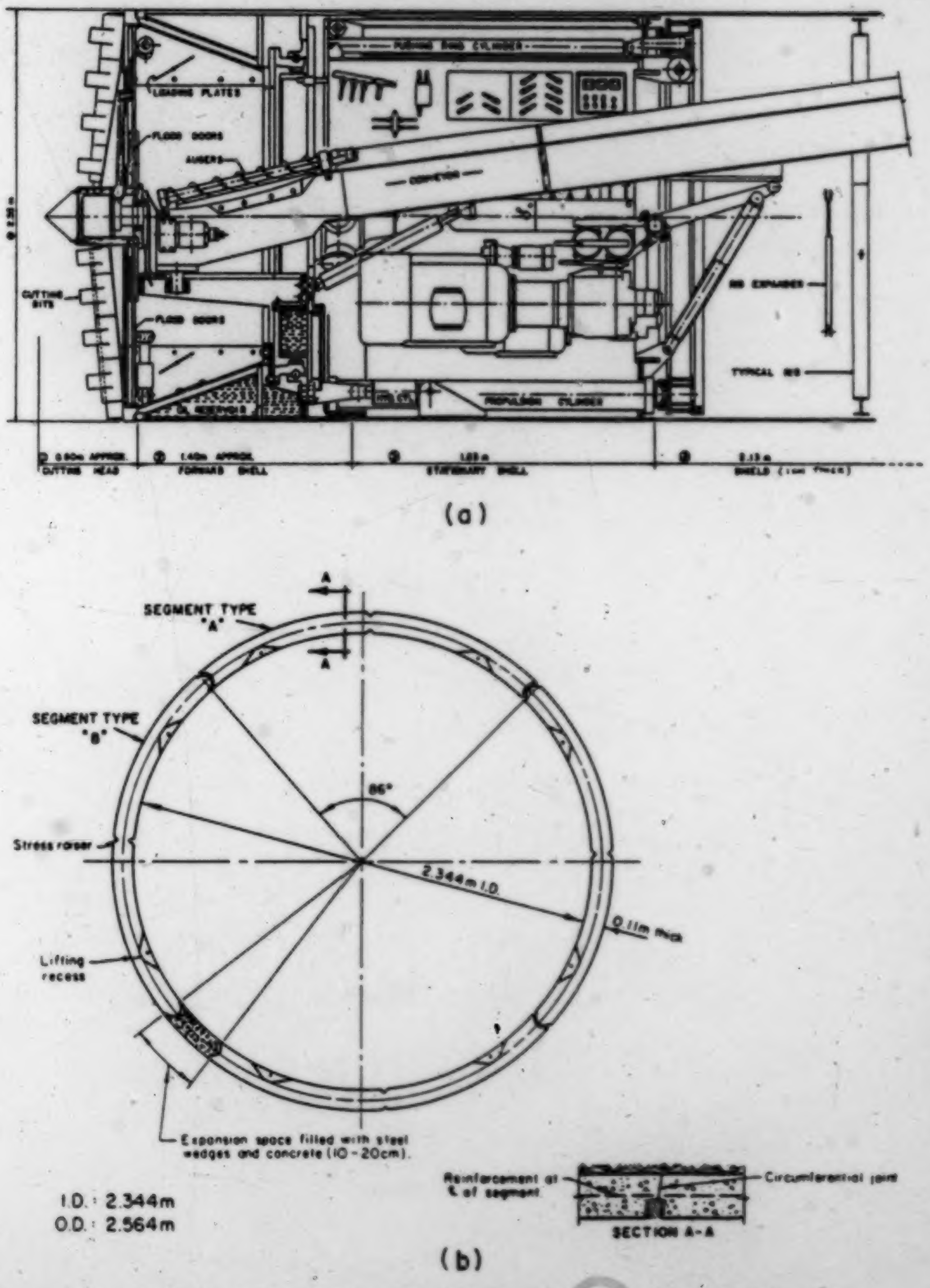
PUSHING RING CYLINDER
LEADING PLATES
FLOOD DOORS
AUGERS
CONVEYOR
CUTTING BITS
FLOOD DOORS
RIB EXPANDER
TYPICAL RIB
PROPULSION CYLINDER
① 0.90m APPROX. CUTTING HEAD
② 1.40m APPROX. FORWARD SHELL
③ 1.83m STATIONARY SHELL
④ 2.13m SHIELD
(a)
A
A
SEGMENT TYPE "A"
SEGMENT TYPE "B"
86°
Stress raiser
2.344m I.D.
0.11m thick
Lifting recess
Expansion space filled with steel wedges and concrete (10 - 20cm).
I.D.: 2.344m
O.D.: 2.564m
Reinforcement at ℄ of segment
Circumferential joint
SECTION A-A
(b)

Figure 5.54 TBM and Lining System used at the Edmonton Experimental Tunnel (after El-Nahhas: 1980: modified)

the excavated surface of the soil, as soon as the shield had advanced beyond that ring. Therefore, the maximum distance between the tunnel face and a fully expanded ring was about 7 m. The average construction rate within the instrumented section was 12.8 m/working day.

The field instrumentation included surface and subsurface settlement monitoring, slope indicator readings, load cell measurements at the lower tangential joints, a few surface and embedded vibrating wire concrete strain gauges (in instrumented section 2 only), tape extensometer measurements for the lining convergence, and levelling of one point on the lining. A detailed account of this field monitoring program is presented by El-Nahhas (1980).

Numerical Simulation

For the numerical back-analyis of this tunnel three finite element meshes were tested beforehand with variable element densities and widths. The maximum surface distortion seemed sensitive to the element density near the ground surface. The use of a slightly narrower mesh was favoured, but with a higher density of elements. This mesh included 388 nodes and 709 elements. The entire ground mass was modelled with properties representing the softer till, except for a 5.7 m thick layer located at 9.5 m below the surface, to which properties representing the stiff till layer was assigned. Figure 5.55 shows the assumptions that were made and the values of the soil parameters that were adopted and kept constant in all numerical analyses. A lower rigid boundary was assumed to exist at 32.42 m below surface.

Both ground instrumentation and lining load monitoring showed some minor but obvious time dependent component. The major part of the ground response in terms of displacements and load magnitudes, developed within 7 days after the TBM face passed the instrumented section. More than two months later the readings had not stabilized, although the increments over that period of time were not very large compared to the recorded "short-term" variations. The time dependent changes were slightly more pronounced in the lining loads. Despite the fact that the ground water level was located well below the tunnel, the grey till was literally saturated throughout its thickness. The observed time dependent responses could thus be attributed to induced pore pressure changes.

One may take as a reference, a liberal value of 10^{-3} cm^3/s for the coefficient of consolidation of the ground mass. This is five times larger than the maximum value found in the laboratory samples, and reflects the effect of macrostructural features in the soil mass that tend to accelerate the process of pore pressure equalization. Again, the approximate criteria shown in Chapter 3 proposed for the identification of the type of ground response, may be used. As noted above, the "immediate" soil movements or lining load build up took place within about one week after the TBM passed the instrumented section. Despite attempts to make it

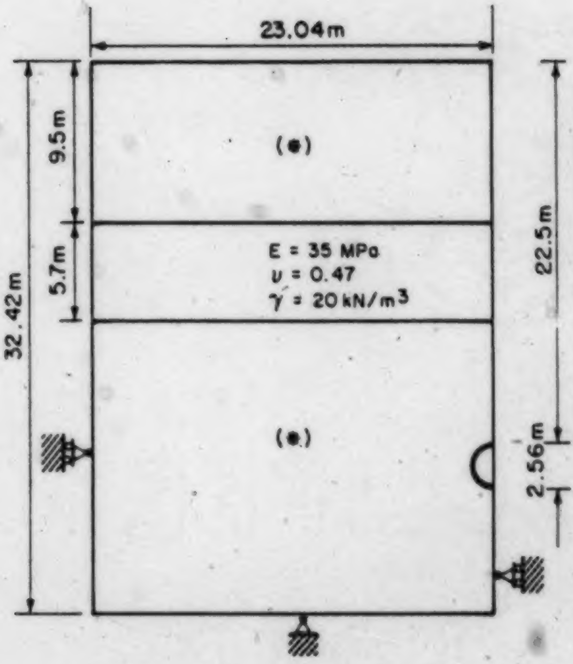
23.04m
9.5m
(*)
5.7m
E = 35 MPa
ν = 0.47
γ′ = 20 kN/m³
32.42m
(*)
22.5m
2.56m

(*)

Parameters	Undrained	Drained
K	83	70
n	0.92	0.85
ϕ(°)	16	22
c (kPa)	45	30
R_f	1	1
ν	0.47	0.3
γ(kN/m³)	20	20

Figure 5.55 Assumptions and Fixed Parameters for the Edmonton Experimental Tunnel Back Analyses

water tight, the segmented lining can be assumed to be fully permeable relative to the the soil. But even if it were not and if the tunnel were supposed to be ideally deep, Figure 3.22 indicates that for a period of time of one week after excavation, "negligible" consolidation may have developed. After two months, the consolidation process is incomplete which is confirmed by the field readings not being stabilized.

If the lining is assumed to be fully permeable (Figure 3.23), then for a till cover of 13 m and taking into account the presence of a continuous sand layer covering the till (actually undetected in BH 82), after one week or one month the consolidation process is virtually negligible.

From this simplified analysis, the ground response, particularly that observed up to a week after the TBM passed the instrumented section, was close to undrained. It was decided to perform both undrained and drained analyses, in order to bound the observed behaviour which may have actually been partly drained over the monitoring period. This would be a reasonable approximation if the soil behaviour was non-linear elastic. In reality, plastic strains may develop during the undrained loading of the soil, especially if failure or plastic yielding is locally induced. Hence, the final strains in the undrained case can be larger than those in a drained situation, in which local failure is less likely to occur. This type of path-dependence of strains is not accounted for in the numerical model being used.

An additional approximation refers to the way in which the undrained analyses were undertaken. Strictly speaking, an undrained analysis would imply $\phi=0$ and a constant strength c_u, for a soil element consolidated at a certain in situ stress level. Total stress changes produced by the undrained tunnelling operation would not cause changes in the undrained strength. Correspondingly, the numerical analysis would have to assign a certain strength c_u for each point of the soil mass, consolidated to a distinct mean effective stress. The present finite element code was developed mainly to portray time independent responses under drained conditions, making allowance for a single non-linear elastic material to be represented. If an adequate representation of an undrained response were to be made, then a very large number of non-linear elastic materials would have to be considered. One would be required for each element stress level with its associated undrained strength. Although the implementation of this feature could have been possible, it departed from the primary aim of the present study. Therefore, an approximation was favoured. This consisted of working in terms of a total stress failure envelope, defined by an undrained cohesion intercept and a friction angle (c, ϕ), obtained from the consolidated undrained passive compression tests shown in Figure 5.47. While this would give a reasonable approximation of the initial undrained strength, it would deviate from the "correct" undrained representation after a certain amount of stress release at the opening, since the current strength will change with changes in the minor principal stress. In other words, the "undrained" strength would have a frictional component depending on the "undrained" friction angle ϕ. The latter is a purely arbitrary parameter and is clearly path dependent. However, it is possible to anticipate the type of error involved in this simplification. Whenever the ground undergoes a decrease in the minor principal stress (for example, at points beside the springline region for $K_o<1$), the soil strength will be underestimated. It will be overestimated at points experiencing an increase in the minor principal stress (crown and floor regions, if $K_o<1$).

The relative stiffness of the segmented lining used can be estimated through the Einstein and Schwartz (1979) definitions. For the dimensions given in Figure 5.54, assuming a Young's modulus of 25.1 GPa (El Nahhas, 1980:166) and a Poisson's ratio of 0.2 for the concrete, and for an average soil modulus of 20 MPa and a Poisson's ratio of 0.47, the stiffness ratios can be calculated. The effect of the four joints and of the four stress raisers can be taken into account using Muir Wood's (1975:126) approximation (see Section 5.2.2.1). Assuming the 8 joints and stress raisers to be perfectly articulated, the equivalent moment of inertia of a continuous ring would be one fourth of the actual lining segment. The compressibility and flexibility ratios are equal to 0.011 and 65.408 respectively. In the numerical analyis, an equivalent liner of 0.32 m is used. To approximate the stiffness ratios, the equivalent lining would have to have a modulus of 0.19 GPa or 7.7 GPa, to equal either one or the other ratio. Accordingly, in the back analysis, the lining modulus was allowed to vary within those limits. As in the other two tunnel cases, the best agreement to observed performance was noted when the flexibility ratio of the equivalent lining was close to the "actual" value.

The only soil parameter allowed to vary in the back analyses was K_o (from 0.7 to 1.0). The remaining solution parameter that was allowed to vary was the amount of stress release prior to the lining activation. An interpretation of field measurements, followed by preliminary computer runs, suggested that it would be sufficient to vary this amount of stress release from about 50 to 70%. These initial runs indicated also that five equal load increments, for each simulation phase (10 unloading steps altogether) would yield an adequate approximation.

Table 5.23 summarizes the parameters that were varied in the analyses. Sixteen computer runs were made for the undrained analyses in order to obtain the best fit case. These corresponded to a 70% in situ stress release prior to lining activation, an equivalent lining modulus of 0.4 GPa and a K_o value of either 0.8 or 0.9. One drained analysis was performed, taking K_o equal to 0.9 after the undrained

Stress release α prior to support activation (%)	55	65	70(1)	
In situ stress ratio K_0	0.7	0.8(1)	0.9(1)	1.0
Equivalent lining E modulus (GPa)	0.1	0.4(1)	1.0	

Note: (1) Best fitted values

Table 5.23 Parameters Varied in the Edmonton Experimental Tunnel Back-Analyses

analyses were completed.

Results of the Back-Analyses

The best fit case provided a reasonably good match between calculated and observed performances before and after lining activation. The equivalent lining modulus found to fit the observed performance best furnished a flexibility ratio F equal to 30.241 which is approximately half the value theoretically estimated. In other words, the back analysed lining behaviour is stiffer than was assessed theoretically at the beginning. This could be partly attributed to assuming the lining joints and stress raisers were perfect articulations with zero moment of inertia and zero bending moments. Uncracked stress raisers in particular would carry moments. If both the joints and stress raisers had moments of inertia equal to that of the reduced concrete section in the stress raiser region (thickness equal to 7 cm), then Muir Wood's (1975:126) approximation would lead to an equivalent moment of inertia 2.03 times that calculated assuming perfect joints. The theoretical value of F for the actual lining would then be 32.21, and this is much closer to the back analysed figure. The flexural rigidity (EI) per unit length of the tunnel would then be equal to 1.41 MN.m, compared with the back analysed rigidity of 1.09 MN.m.

In the following, the comparisons between calculated and observed performances are presented and discussed. It should be noted that the measurements could represent a partial drainage condition in the field which was possibly closer to the ideally undrained situation. A complete comparison of the performance prior to lining installation was not possible. The reason for this was that the case history records (El-Nahhas, 1980) did not include an accurate account of the construction progress with time, or a precise identification of recorded readings relative to the position of the tunnel face. Unlike the previous two cases studied, only a few measurements are clearly identified as occurring just prior to lining activation. Only these were used to make a comparison for this condition. Some field data collected at instrumented Section 2 were included, although a slightly larger cover (25 m) exists, compared with Section 3 (22.5 m cover) where the back-analyses were actually applied.

In Figure 5.56, the final surface settlements transverse to the tunnel axis are compared. The measured range of settlements was that noted after the TBM cutting face had passed the section by more than 18 diameters. As is noticed, the observed maximum surface settlements are fully bounded by the approximate undrained analyses, taking K_o equal to 0.8 and 0.9. The calculated surface distortion, however, tends to be smaller than that measured. Vertical movements at the lateral boundary of the finite element mesh were not zero, indicating that the width of the mesh was too small. A much wider mesh was implemented (52 m width) and still the movements at the lateral boundary were non-zero. Moreover, both meshes produced very similar maximum surface

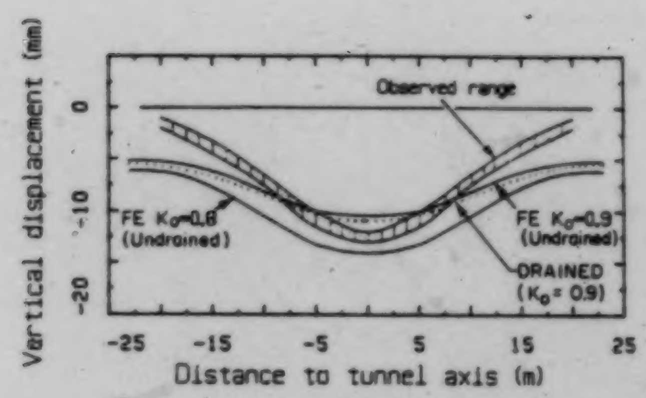

NOTES:

1. MEASUREMENTS AT POINTS 1.5 m BELOW SURFACE, AT SECTIONS 2 AND 3 (SOIL COVERS OF 25 AND 22.5 m RESPECTIVELY)
2. OBSERVED SETTLEMENTS 2 WEEKS AFTER TBM PASSED THE SECTION (TUNNEL FACE AT MORE THAN 18 DIAMETERS AHEAD)
3. CALCULATED (FE) SETTLEMENTS AT POINTS 1.9 m BELOW SURFACE
4. FIELD DATA FROM EL-NAHHAS (1980: 119 AND 125)

Figure 5.56 Measured and Calculated Settlements after Complete Passage of the TBM at the Edmonton Experimental Tunnel

distortions. The inability of the present model to simulate the observed surface distortion is not related to the boundary conditions used in the calculations but, possibly, to its inability to simulate adequately the concentration of shear strains that might have occurred in the soil. This type of problem was addressed in Section 5.2.1.2, where it was shown that it is a common feature in most finite element analyses applied to this type of problem.

The analyses with drained soil parameters furnished the settlement distribution indicated by the dotted curve (Figure 5.56). It gave a maximum "long term" settlement of only 4% larger than the corresponding "short term" value. Unfortunately "long term" readings were not available for most instruments installed. The final readings of the magnetic extensometers at Section 3 were taken almost 3 months after excavation (El-Nahhas, 1980:286). The magnets closer to the ground surface (from 2.24 to 4.19 m below it) indicated an average increase of 28% in the settlements. This is appreciably more than the drained analysis predicted. However, this discrepancy is not suprising, since plastic strains were probably induced in the ground, under the "undrained" loading. This should have led to long term ground movements larger than those given by the non-linear elastic drained analysis, as explained before.

Figures 5.57 and 5.58 compare vertical movements in the ground, along vertical lines at the tunnel centreline and about 2.5 m from it, respectively. The measurements were taken when the tunnel face was more than 20 diameters beyond the instrumented section. One notices that in both cases, the "undrained" ground movements show very good agreement both in magnitude and distribution, for the range of K_o considered. The dotted curves in both figures correspond to the analysis made with drained parameters. It furnished vertical displacements marginally larger than the corresponding undrained analysis, as noted for the surface settlements. The same comments made before regarding the influence of plastic straining in a long term situation, are also entirely applicable.

Perhaps a better view of the subsurface settlements above the tunnel is that ~~seen in~~ Figure 5.59. It includes measurements taken at all magnetic extensometers in Section 3, 8 days after the TBM passed it (tunnel face more than 20 diameters ahead). On the whole, good agreement between the "undrained" settlements is noticed. However, closer to the tunnel, 21.86 m below surface, the agreement is poorer.

A slope indicator located 2.33 m from the tunnel axis (SI33) had readings taken when the tunnel face was located 5 and 11 m past it. Assuming that the lining activation took place with the face 7 m ahead, it was possible to estimate by interpolation, the horizontal displacements that should have occurred at the moment the lining was expanded. A comparison between measured and calculated horizontal movements for this situation is shown in Figure 5.60. Similarly, Figure 5.61 compares measured and calculated

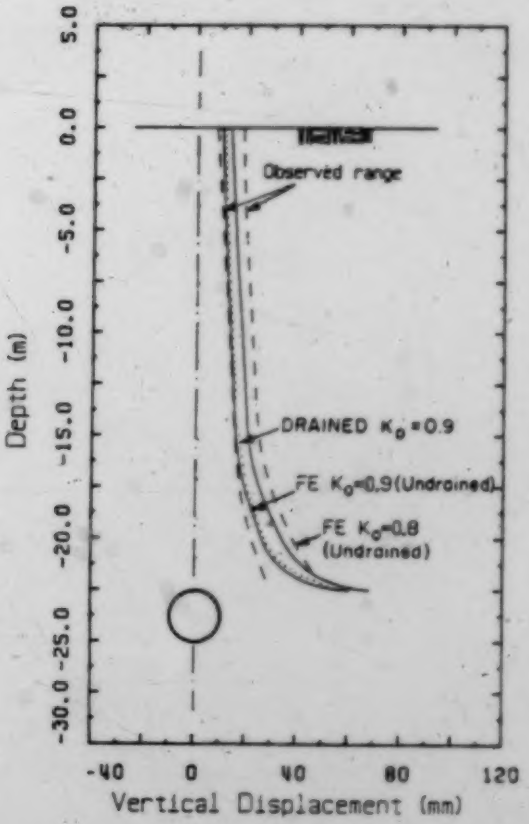

NOTES:

1. MEASUREMENTS AT SECTION 3 (MX 33, MX 38 AND SPX), ALONG TUNNEL VERTICAL AXIS.
2. MEASUREMENTS TAKEN 8 DAYS AFTER TBM PASSED THE SECTION (TUNNEL FACE AT MORE THAN 20 DIAMETERS AHEAD)
3. FIELD DATA FROM EL-NAHHAS (1980:122, 123 AND 124)

Figure 5.57 Measured and Calculated Subsurface Vertical Displacements along the Tunnel Centreline, after Complete Passage of the TBM at the Edmonton Experimental Tunnel

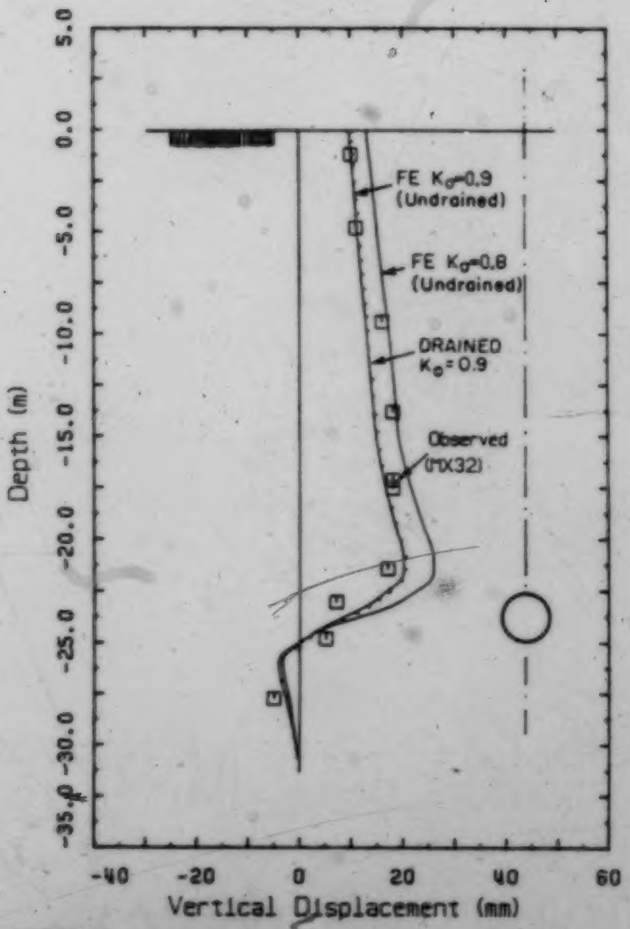

NOTES:

1. MEASUREMENTS AT MX 32 (SECTION 3) LOCATED 2.3 m FROM TUNNEL AXIS.
2. CALCULATED DISPLACEMENTS AT 2.56 m FROM TUNNEL AXIS.
3. MEASUREMENTS TAKEN 8 DAYS AFTER TBM PASSED THE SECTION (TUNNEL FACE AT MORE THAN 20 DIAMETERS AHEAD).
4. FIELD DATA FROM EL-NAHHAS (1980:122)

Figure 5.58 Measured and Calculated Subsurface Vertical Displacements along a Vertical Line 2.5 m off the Centreline, after Complete Passage of the TBM at the Edmonton Experimental Tunnel

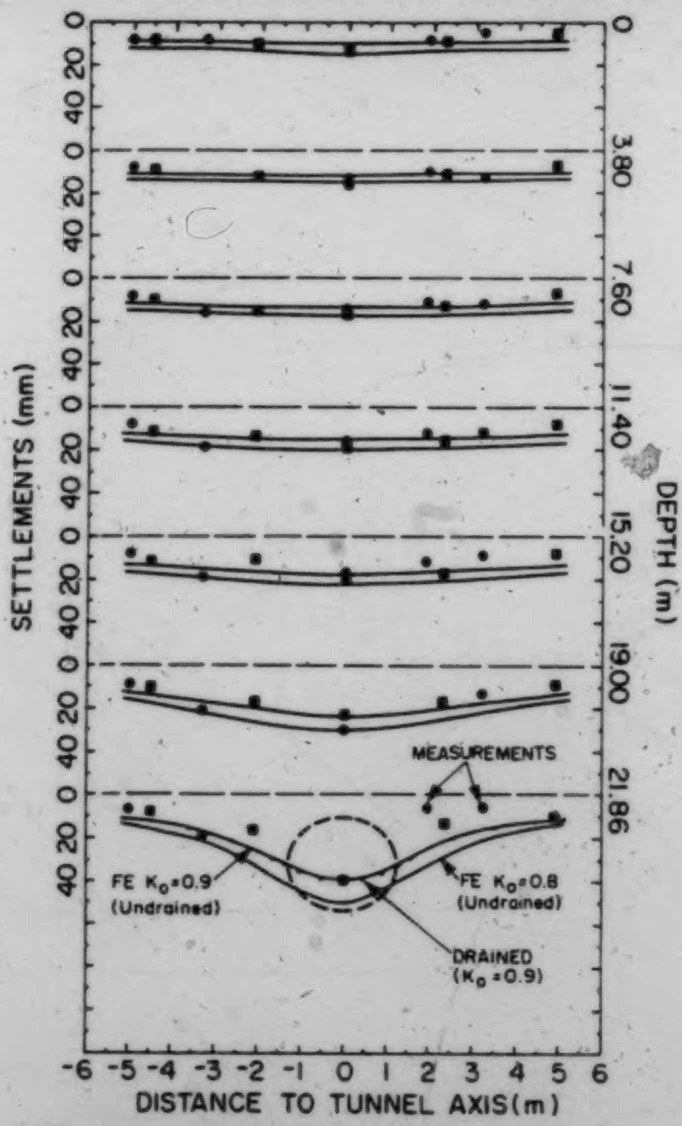

NOTES:

1. MEASUREMENTS TAKEN AT SECTION 3, 8 DAYS AFTER TBM PASSED IT (TUNNEL FACE AT MORE THAN 20 DIAMETERS AHEAD)
2. SQUARE POINTS OBTAINED FROM INTERPOLATION OF READINGS IN MX 31 TO 35 AT DEPTHS INDICATED. RING POINTS FROM MX 36 TO 310.
3. CALCULATED (FE) DISPLACEMENTS AT DEPTHS SHOWN BY DASHED LINES.
4. CALCULATED 'DRAINED' SETTLEMENTS SHOWN ONLY AT DEPTH 21.86m BY DOTTED CURVE. AT OTHER ELEVATIONS THEY VIRTUALLY CONCIDE WITH 'UNDRAINED' SETTLEMENTS FOR K_0 = 0.9
5. TUNNEL CROWN AT ABOUT 22.5m DEPTH
6. ALL FIELD DATA FROM EL-NAHHAS (1980: 122 AND 123)

Figure 5.59 Measured and Calculated Subsurface Settlements after Complete Passage of the TBM, at the Edmonton Experimental Tunnel

lateral movements after the TBM had completely passed the instrumented section (tunnel face at more than 15 diameters ahead, 2 weeks after passing the section). In both cases the agreement is reasonable, especially in terms of the maximum magnitude of the horizontal movement. Above the tunnel crown elevation, the numerical model seems to underpredict the lateral movements, but the overall distributions of displacements seem to agree reasonably well.

It is believed that the load cell readings installed in Sections 2 and 3 provided the most reliable set of information regarding lining loads in this case history. The number of vibrating wire strain gauges embedded in the concrete was, perhaps, too small to allow a reliable picture of lining loads to be drawn. Therefore, only the data gathered from the segmented rings with load cells will be addressed herein. Each of these rings, with 1 m width, were instrumented with two load cells, installed at the lower longitudinal joint. This installation layout was somewhat unfortunate, since it did not allow formation of any conclusion about the distribution of thrusts around the liner. Figure 5.62 shows the measured thrusts in four instrumented rings. The cell readings included the loads due to the lining selfweight, while the finite element analysis disregards it. For a consistent comparison, the selfweight had to be excluded from the readings. Through an approximate calculation, a 5.3 KN/m reduction in the lower joint thrust was estimated, in order to obtain the thrusts due to ground

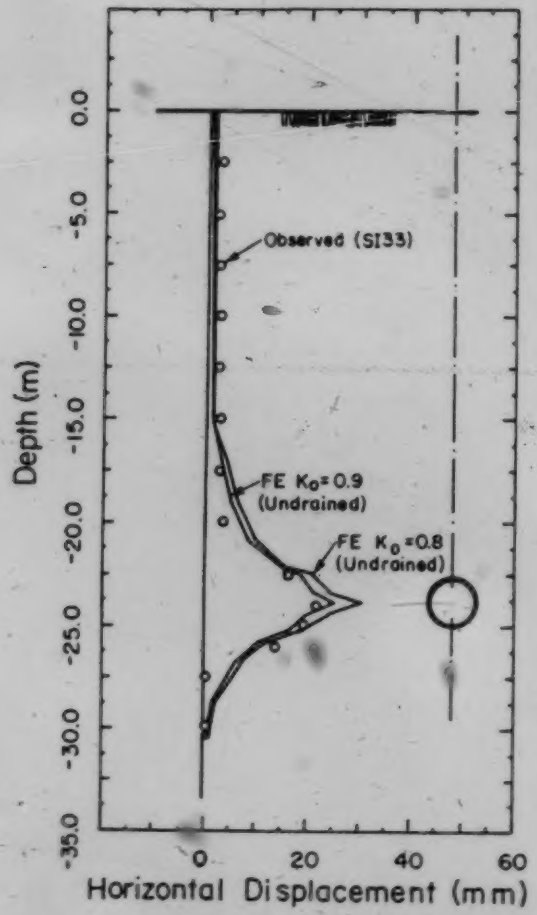

NOTES:

1. MEASUREMENTS AT SI33 (SECTION 3), 2.33m FROM TUNNEL AXIS.
2. CALCULATED DISPLACEMENTS AT 2.56m FROM TUNNEL AXIS.
3. INTERPOLATED MEASUREMENTS FOR THE MOMENT THE LINING WAS EXPANDED (7m BEHIND TUNNEL FACE)
4. FIELD DATA FROM EL-NAHHAS (1980: 302)

Figure 5.60 Measured and Calculated Lateral Movements in the Ground beside the Edmonton Experimental Tunnel before Lining Activation

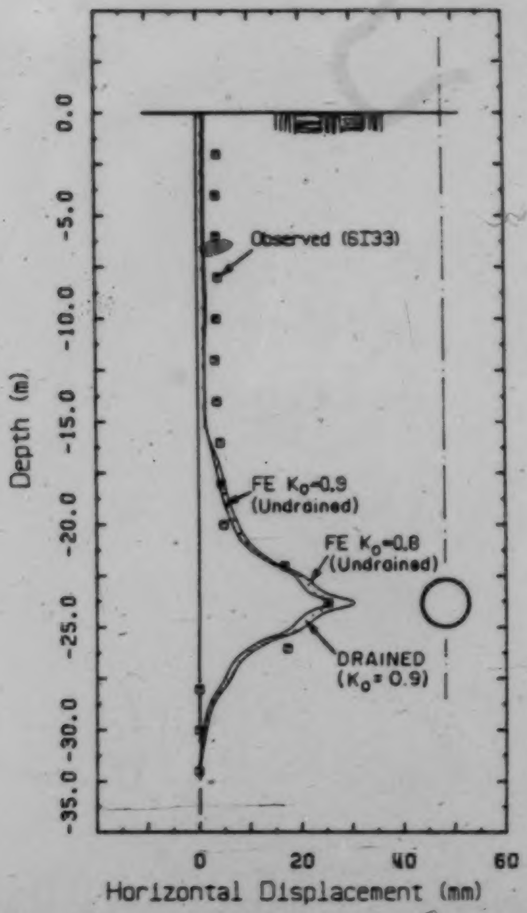

NOTES:

1. MEASUREMENTS AT SI33 (SECTION 3), 2.33 m FROM TUNNEL AXIS.
2. CALCULATED DISPLACEMENTS AT 2.56m FROM TUNNEL AXIS.
3. MEASUREMENTS TAKEN 2 WEEKS AFTER TBM PASSED THE SECTION (TUNNEL FACE AT MORE THAN 15 DIAMETERS AHEAD)
4. FIELD DATA FROM EL-NAHHAS (1980 : 126 AND 302)

Figure 5.61 Measured and Calculated Lateral Movements in the Ground beside the Edmonton Experimental Tunnel after Complete Passage of the TBM

loads only. The "short term" measurements are those taken 7 days after lining installation, when the tunnel face was more than 22 diameters ahead. The "long term" readings were taken 2 months or more later. The calculated thrusts were obtained at different sections of the lining by averaging the computed tangential element stresses in those sections, and integrating them along the equivalent lining thickness. The calculated "undrained" thrusts provide a bound for the "short term" measurements, while the "long term" thrusts are bound by the calculated "drained" values. Table 5.24 furnishes values of the averaged measured thrusts in Section 3 for perhaps a clearer comparison. The reading at instrumented ring number 2 was referred to by El-Nahhas (1980:168, 194) as non-representative as the installation procedure of the load cells in this ring differed from the others. Nevertheless, the results of the comparisons are quite favourable, despite the limitations of the lining representation in the present numerical solution. As in the LRT tunnel, the support systems here seems to carry a small amount of bending and this minimizes the deficiencies of the lining representation.

Table 5.25 summarizes the comparisons between measured and calculated performances for the "short term" condition. It also includes some additional data regarding measurements taken inside the tunnel (convergence and invert levelling). The worst prediction aspect refers to the maximum slope of the surface settlement trough. Also lining convergence and

Condition	Average Thrust(1) (kN/m)			
	Measured		Calculated	
			K_0: 0.8	K_0: 0.9
Short Term(2)	137.0(4)	(149.5)(5)	157.9(6)	166.1(6)
Long Term(3)	158.7(4)	(177.2)(5)	-	172.0(7)

Notes: (1) Per unit length of tunnel. Section 3 only. Loads in the lower joint of the segmented ring. Lining self weight discounted.
(2) 7 days after installation of ring.
(3) 56 to 58 days after installation of ring.
(4) Excluding data from instrumented ring #2.
(5) Including data from instrumented ring #2.
(6) Using undrained parameters.
(7) Using drained parameters.

Table 5.24 Measured and Calculated Average Thrust Forces at the Lower Lining Joint in the Edmonton Experimental Tunnel

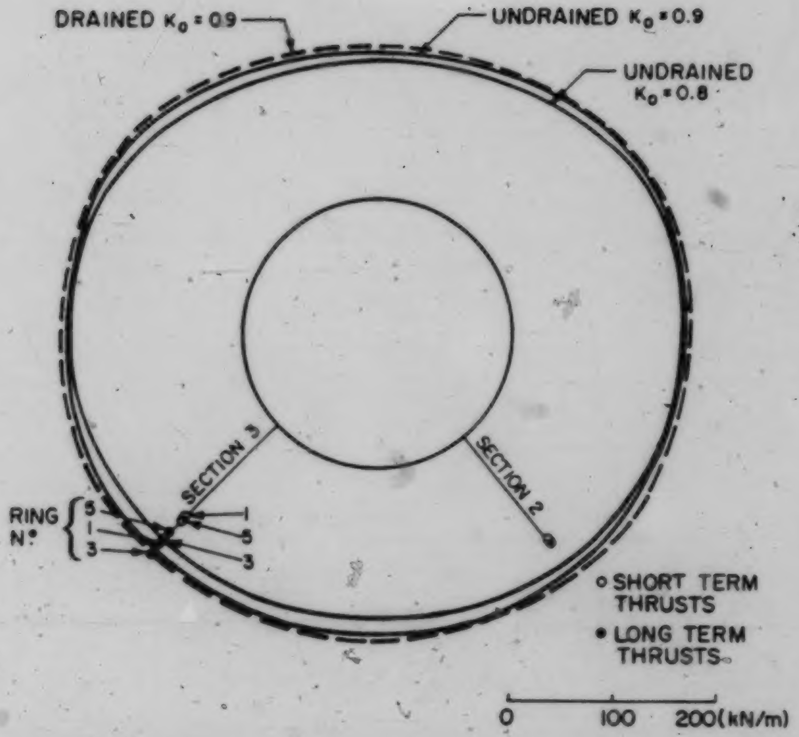
DRAINED $K_0 = 0.9$
UNDRAINED $K_0 = 0.9$
UNDRAINED $K_0 = 0.8$
SECTION 3
SECTION 2
RING N°
5
1
3
1
5
3
○ SHORT TERM THRUSTS
● LONG TERM THRUSTS
0
100
200(kN/m)

NOTES:

1. "SHORT TERM" READINGS 7 DAYS AFTER INSTALLATION; TUNNEL FACE AT MORE THAN 22 DIAMETERS AHEAD THE SECTION.
2. "LONG TERM" READINGS AT SECTION 2 TAKEN 90 DAYS AFTER INSTALLATION. AT SECTION 3 TAKEN 58 DAYS (RINGS 1 AND 3) AND 56 DAYS (RING 5) AFTER INSTALLATION. SOIL COVER IN SECTION 2 - 2.5m AND 22.5m IN SECTION 3.
3. LINING SELFWEIGHT DISCOUNTED FROM MEASUREMENTS.
4. MEASURED AND CALCULATED THRUST VALUES PER UNIT LENGTH OF TUNNEL.
5. FIELD DATA FROM EL-NAHHAS (1980 : 167, 170, 172 AND 173).

Figure 5.62 Measured and Calculated Thrust Forces at Segment Joints in the Edmonton Experimental Tunnel

floor heave were not accurately estimated. The measured figure shown for these two aspects are indicative only, as suggested by El-Nahhas (1980:166).

As in the LRT tunnel, the large amount of field data available in this case history and the reasonable matching achieved in the back analyses, allowed a reasonable assessment of the amount of stress release, prior to the lining activation.

Assuming that the thrust distribution was uniform, the long term measurements in Section 3 (almost 2 months after lining installation) would indicate an all-round uniform ground stress acting on the lining of about 27% of the average in situ radial stress (for K_o=0.9). This construction scheme led to a ground stress reduction slightly higher than seen at the LRT tunnel. This was possibly due to the delayed support activation in the present case, resulting from the use of a relatively longer TBM. On the other hand, the stress reduction occurring after lining activation is smaller in this case, possibly reflecting the stiffer nature of the support used.

The simplified stability assessment for the plane strain (final) situation, as undertaken in the former two case histories, can be repeated here. The support action is one of applying a uniform internal pressure in the opening walls, so that a factor of safety against global collapse of the ground can be estimated. With that all round uniform ground stress, a safety factor of 1.4 is found. Once more,

	Performance Aspect		Measured$^{(1)}$	Calculated$^{(2)}$	C/M
1.	Maximum surface settlement	mm	12.5$^{(3)}$	12.2	0.98
2.	Maximum slope of surface settlement trough	-	1:1300$^{(3)}$	1:2100	0.62
3.	Crown settlement$^{(4)}$	mm	39$^{(3)}$	44	1.13
4.	Maximum deep settlement (2.5 m from axis)	mm	18$^{(5)}$	22	1.22
5.	Maximum lateral movement at lining installation (2.5 m from axis)	mm	22$^{(6)}$	27	1.23
6.	Maximum final lateral movement (2.5 m from axis)	mm	25$^{(6)}$	27.2	1.09
7.	Horizontal diameter change of lining	mm	~2$^{(7)}$	1.5$^{(8)}$	0.75
8.	Floor heave after lining installation	mm	~2$^{(7)}$	3.1$^{(8)}$	1.55
9.	Thrust in lower longitudinal joint	kN/m	137$^{(9)}$	162	1.18

Notes:
(1) Data from El-Nahhas (1980). "Short term" data only, after TBM had passed section 3 entirely.
(2) Averaged calculated response, using "undrained" parameters.
(3) Average value.
(4) About 1.5 m above crown elevation.
(5) At MX32.
(6) At SI33.
(7) At Section 2, according to El-Nahhas (1980:166).
(8) For $K_0 = 0.9$.
(9) Excluding instrumented ring No.2.

Table 5.25 Measured and Calculated Performance of Edmonton Experimental Tunnel

this figure is less than the range given in Section 2.3.4.3, and again, a non-linear ground response would be expected. Despite the good ground control conditions implemented in this tunnel, significant non-linear response of the ground is evident.

With the final crown displacement of 59.4 mm given by the drained back analysis, it is possible to calculate the dimensionless crown displacement (U) given by equation 2.16. This is found to be equal to 1.00, for an initial (drained) tangent modulus of the soil at the crown of about 19.5 MPa. This value is smaller than the threshold figure of 1.8 for a near collapse condition. In fact, although this dimensionless displacement is larger than that found in the other two cases, no sign of ground instability was detected in this case hisory.

Figure 5.63 illustrates the expected degree of straining of the ground around the tunnel after the "short term" equilibrium was reached. The shaded zones correspond to points subjected to maximum shear strains greater than 1%. The calculated shear strains shown on the left hand side correspond to the undrained analysis using K_o=0.9. The righthand side shows the shear strain distribution as deduced by El-Nahhas (1980:245) from his field measurements. The extent of the strained zone around the opening seems comparable but the shape of the zones are dissimilar. Figure 5.64 depicts similar information for maximum shear strains greater than 2%. The measurements indicate that points

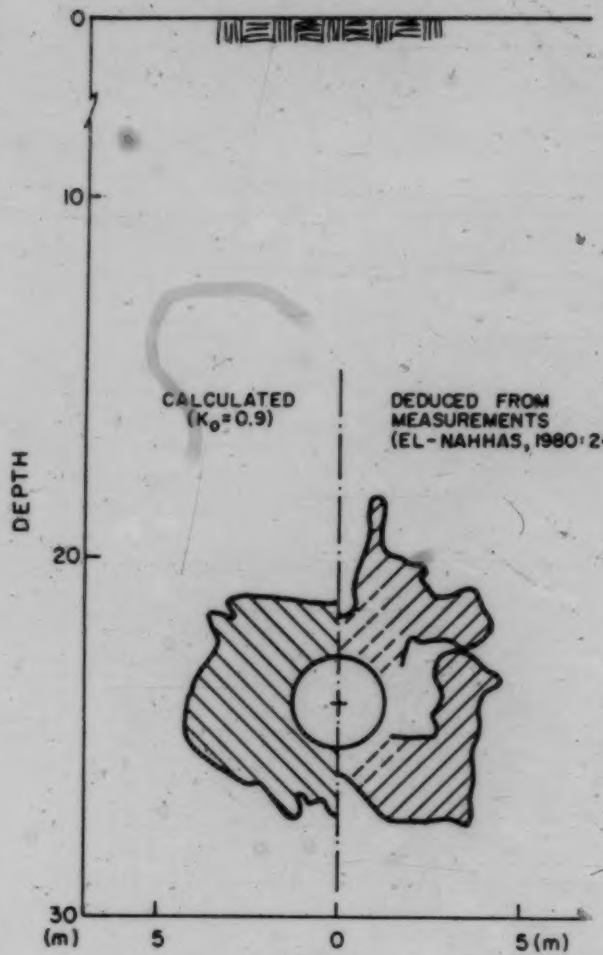
0
10
20
30
(m)
DEPTH
CALCULATED
(K_o=0.9)
DEDUCED FROM
MEASUREMENTS
(EL-NAHHAS, 1980: 245)
5
0
5(m)

Figure 5.63 Calculated and Measured Zones with Maximum Shear Strain Greater than 1% in the Edmonton Experimental Tunnel

slightly farther away from the tunnel had been strained to that level and that, again, the strained zones show different shapes. In both figures one notes that the calculated straining pattern is more uniform and symmetric as compared to the pattern deduced from the field measurements.

The numerical simulation indicated that no soil element around the opening experienced failure as defined by the strength envelope. Nevertheless, a very pronounced decrease in the tangent modulus from its initial value was observed, particularly at springline elevation. In order to identify failure zones from the deduced field strains El-Nahhas (1980:250) suggested that maximum shear strains in excess of 1 to 2% would imply full mobilization of the shear strength. If the higher strain value is considered, and a major principal strain is estimated by using the stress-strain curves of the recent tests conducted, it can be seen that the degree of shear strength mobilization would vary from 40 to 70%, depending on the test stress path. In other words, the possible failure zone might have been much smaller in extent than it was originally thought.

The difference in the shapes of the maximum shear strain contours as given by the measurements and by the numerical model is not an unexpected feature. Variations in the predicted and observed shear strain contours have been noticed by Orr et.al., (1978:136), Mair (1979:131) and Seneviratne (1979:113). The calculated contours and the

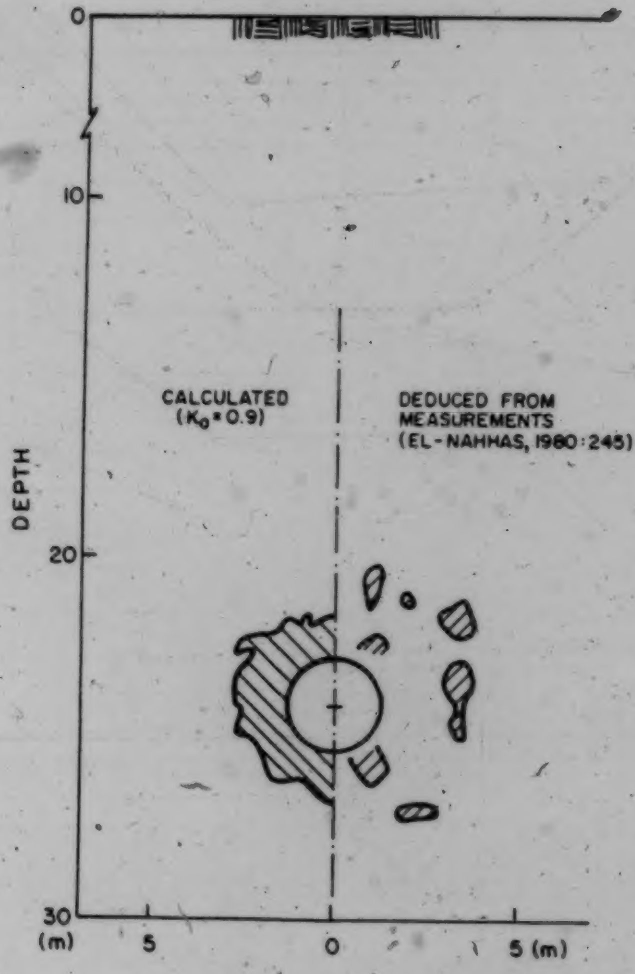
0
10
20
30
(m)
DEPTH
CALCULATED
(K_0 = 0.9)
DEDUCED FROM
MEASUREMENTS
(EL-NAHHAS, 1980:245)
5
0
5 (m)

Figure 5.64 Calculated and Measured Zones with Maximum Shear Strain Greater than 2% in the Edmonton Experimental Tunnel

failure zones, tend to be more axisymmetric than those actually observed. Wong (1986:48,107) using a different numerical solution, also showed that a fairly axisymmetric yield zone would result for the Edmonton Experimental tunnel. As noted in Section 5.2.1.2, the current formulations of most finite element codes, regardless of their constitutive equations, are unable to properly model conditions that involve highly concentrated shear strains. Those preceding the collapse of a tunnel in soil are presented in Section 2.3.4.3. All things considered, the present numerical model was able to yield sensible results compared to the observed field performance of the tunnel.

5.2.5 Summary and Conclusions

This section reviewed the role of two-dimensional numerical modelling in predicting the behaviour of shallow tunnels under time-independent conditions. Relevant modelling aspects were examined, particularly the procedures for excavation simulation and methods to approximately account for the three-dimensional effects involved in the tunnel advance. Examples of stress-strain relations for soils that have been used in shallow tunnel modelling were reviewed and briefly discussed. The need to consider the non-linear behaviour of soils was stressed and some of the advantages of non-linear elastic relationships, such as the hyperbolic model, were assessed. One of these was the suitability of this model to represent the non-linear response of soil even in the "small strain" range of behaviour.

A comprehensive survey of predictive exercises on shallow tunnels using two-dimensional finite element analyses was presented. The survey included only those cases published over the last decade where the capability of the numerical solution to simulate actual behaviour could be evaluated by comparison with measurements. In each case, qualitative indications were provided on the results of these comparisons. Very few cases enabled a complete assessment of the predictive potential of the numerical models. Most cases fail to include a complete picture of the measured and predicted displacement fields and lining loads. It was not possible to relate the quality of the predictions made with the numerical model features or the constitutive relations used. No correlation was found between the quality of the predictions and the soil type, the construction method or the prediction class, as defined by Lambe (1973). Nonetheless, an overall appraisal of the numerical predictions was attempted in a global manner.

The majority of the cases reviewed (67%) referred to predictions after the event, with known results at the time the analyses were made. In most cases (72%) the comparison was limited to ground displacements and most frequently these were surface and subsurface settlements. Only 10% of the cases provided a complete comparison including all displacement fields and lining loads. The magnitude of the maximum surface settlement was closely matched by the numerical simulations in 60% of the cases, but in over half of the cases, the maximum surface distortions were underpredicted. The overall distribution of subsurface settlements was generally well estimated, but the maximum magnitude of these deep settlements was reasonably predicted in less than 40% of the cases. The magnitude of the maximum horizontal displacement in the ground was overestimated in more than 60% of the cases. No dominant trend was noted with respect to the prediction of lining loads. The above findings were discussed in detail and the reasons explaining these facts were either identified or suggested.

The numerical solution used for the present study was described and discussed. Its main features and limitations were analysed in detail in order to provide a basis for judgement and evaluation of its predictive capabilities. The three-dimensional effects of tunnelling advance are approximately accounted for by a partial release of the in situ stress, before the lining is installed. The amount of stress release to be considered in a particular case is unknown, but it should be related to the construction scheme, particularly to the distance between the tunnel face and the point of lining activation and also to the soil conditions.

Three well documented case histories were reviewed and were used to assess the capability of the simple numerical model selected to portray the main features of an actual tunnel performance. Moreover, the analyses of these case histories served as an opportunity to indirectly estimate the amount of stress reduction to be used in order to best fit the observed performances.

The geological and geotechnical aspects of each site were reviewed as well as the contruction details of the tunnels. In all three cases good ground conditions prevailed. A certain degree of uncertainty was present with regard to the in situ stress conditions and to the lining representation. Accordingly, these two additional parameters were included as independent variables in the back analyses. One of the cases, the Edmonton Experimental Tunnel, required additional investigations. These were carried out in order to supply the necessary input for the numerical simulation. The locally occurring till was found to be much softer than originally anticipated.

Despite the inherent approximation involved in the two dimensional simulation for the ground and lining representations, it was possible to find the amounts of stress release that had to be applied to the in situ stresses before support application, in order to yield good estimates of the performances in all three cases. The results of these studies are shown in Table 5.26, prepared in such a way as to allow a direct comparison with Table 5.5, which summarized the results of similar studies carried out with other tunnel cases. The results shown refer only to those aspects of the performance at the final equilibrium situation. As it is seen, the present numerical solution yielded results that compared very favourably with the measurements. Moreover, compared to the results of other simulations applied to other case histories (Table 5.5), it is noticed that the present numerical simulation ranks among those that showed the most favourable results. The fact that the predictions in this study are made after the performance is known (type C1), does not lessen its merit. Most of the analyses shown in Table 5.5 were performed under the same circumstances. Using the same point rating criterion referred to in Section 5.2.1.2, to evaluate the quality of the predictions, the analyses of the LRT and Edmonton Experimental Tunnel were ranked the best in all cases reviewed and were closely followed by the ABV case.

An additional point to be remembered is that in the three cases studied, besides the good agreement found between calculated and measured performances for the final equilibrium situation, fairly good agreement in the ground displacement field before lining installation was found. This agreement would not have been found had the lining been applied very close to the tunnel face. Indeed, the ground stress reduction expedient accounts only partly for the 3D effects involved in a real tunnel, as noted in Sections 4.3.2.7, 5.2.1.1 and 5.2.4.2. Fortunately most shallow tunnels are lined at some distance behind the face (0.5 to 2.0D) where conditions approach that of plane strain, as shown in Section 2.3.6.1.

Tunnel	Main Reference Source	Soil	Construction Method and Support	Cover and Diameter (m)	Distance from Support Appl. to the Face (m)	Back Anal.(2) Amount of Stress Release	Surface(3) Settlement			Subsurface(3) Settlement		Hor.(3) Displ.		Lining(3) Loads	
							Mg.	Dist.	Dtr.	Mg.	Dtr.	Mg.	Dtr.	Mg.	Dtr.
ABV	Negro & Eisenstein (1981)	Clayey sand above W.L.	NATM shotcrete	6.20/4.0-1.55	3.6m (0.65D)	40%	=	>	G	=	G			=	R
LRT	Branco (1981)	Stiff glacial Till above W.L.	TBM, steel ribs and wood lagging	9.0/6.1-1.48	6.7 m (1.09D)	50%	=	=	G	=	G	=	R	=	G
Edm. Exper.	El-Nahhas (1980)	Softer glacial till above W.L. but saturated	TBM segmented concrete	22.5/2.56-8.79	7.0 m (2.73D)	70%	=	>	R	=	G	=	G	=	G?

Notes: (1) See Table 5.5 for the meaning of abbreviations and symbols used.
(2) Applied to the in situ stresses, prior to the support activation.
(3) All refer to the final equilibrium, after lining installation.

Table 5.26 Results of the Numerical Simulations of the Final Tunnel Performance in Three Case Histories

A major limitation is seen in this simulation procedure regarding it potential practical use for class A predictions. This refers to the need of an independent estimate of the amount of ground stress release taking place before lining activation. This stress release was brought into the simulation to represent the three-dimensional ground stress redistributions that take place during the tunnel face advance.

If the ground stress release was uniquely related to the ground displacement by some relationship then an estimate of these ground displacements including the three-dimensional effects of an advancing tunnel, could be a basis of an alternative approach to the solution of this problem. This approach presents several advantages. One is that, while the ground stress release is an artificial expedient without physical meaning, the corresponding ground displacements do have real significance. They would be the actual displacements developing around the opening at the section where the lining is activated.

This reasoning was followed by other authors seeking the solution of similar problems but for axisymmetric conditions. Most of these works have been reviewed in Section 4.3.2.7, and they include treatments by Daemen and Fairhurst (1972), Panet and Guellec (1974), Panet (1976). Baudendistel (1979,1984,1985) also followed this approach, but extended it for a specific non-unifrom stress condition (K_o=0.5) and for a particular cross section of a deep tunnel.

All these works have their value, but they are of little use for the solution of the present problem. They do not deal with the presence of the ground surface, the action of the gravitational stress gradients and the non-hydrostatic in situ stress conditions which are required for the solution of the problem.

In the following section, an attempt will be made to develop an approximate procedure to estimate ground displacements around a shallow circular opening making use of three-dimensional numerical modelling.

THE UNIVERSITY OF ALBERTA

Design of Shallow Tunnels in Soft Ground

by

Arsenio Negro Jr.

©

VOLUME II

A THESIS
SUBMITTED TO THE FACULTY OF GRADUATE STUDIES AND RESEARCH
IN PARTIAL FULFILMENT OF THE REQUIREMENTS FOR THE DEGREE
OF Doctor of Philosophy

Department of Civil Engineering

EDMONTON, ALBERTA
SPRING 1988

Table of Contents VOLUME II

Chapter Page

5.3 Three-Dimensional Modelling 725

5.3.1 Introduction 725

5.3.2 Available Solutions for Estimates of Tunnel Convergence 730

5.3.3 Review of Three-Dimensional Modelling by the Finite Element Method 737

5.3.4 Numerical Solution Adopted 747

5.3.5 Parametric Analyses 753

5.3.5.1 Analyses and Results 753

5.3.5.2 Interpretation of the Results ...774

5.3.6 Application of the Results 804

5.3.6.1 Tunnel Closure 804

5.3.6.2 Ground Movements Ahead of the Tunnel Face 842

5.3.7 Summary and Conclusions 847

5.4 Conclusion 850

6. TWO DIMENSIONAL MODELLING FOR GENERALIZATION 860

6.1 Introduction 860

6.2 Modelling Simplifications and Ranges of Variables 864

6.2.1 Foreword 864

6.2.2 Cohesionless Soil Model 864

6.2.3 Frictionless Soil Model 880

6.2.4 Comments on Some Simplifying Assumptions .894

6.2.4.1 The Effect of Janbu's Modulus K .894

6.2.4.2 The Effect of Janbu's Exponent n 895

6.2.4.3 The Effect of the Cohesive Strength Component 911

6.2.4.4 The Effect of Poisson's Ratio ...923

6.2.5 Ranges of Variables for the Parametric Analyses 931

6.3 Parametric Analyses 939

6.3.1 Details of the Analyses 939

6.3.1.1 Number of Unloading Increments ..939

6.3.1.2 Mesh Design and Influence of the Lower Boundary 946

6.3.2 Results of the Analyses 960

6.3.2.1 Frictionless Soil Model Results .962

6.3.2.2 Cohesionless Soil Model Results .975

6.3.2.3 Relationships Between Surface and Crown Settlements 993

6.4 Generalization of the Results 1013

6.4.1 Opening Remarks 1013

6.4.2 Frictionless Soil Model 1014

6.4.3 Cohesionless Soil Model 1035

6.5 Limits of the Generalized Solution 1078

6.5.1 Extrapolation of the Numerical Results ..1078

6.5.2 Assessment of the Two-Dimensional Stability 1085

6.6 Summary and Conclusions 1102

7. DEVELOPMENT AND VALIDATION OF A DESIGN PROCEDURE ..1115

7.1 Introduction 1115

7.2 Soil-Lining Interaction 1117

7.2.1 Choice of the Model: Hartmann Solution ..1117

7.2.2 Soil-Lining Interaction Analysis for Delayed Lining Installation in a Non-Linear Ground Mass 1131

7.2.3 Influence of the Lining Presence on the Ground Settlements 1153

7.3 Guidelines for Using the Proposed Design Procedure 1158

7.4 An Example of the Use of the Proposed Design Procedure 1168

7.5 Validation of the Proposed Method 1196

7.5.1 Verification Against a Tunnel Model Test 1196

7.5.1.1 Model Test Procedures 1196

7.5.1.2 Soil Conditions in the Test 1198

7.5.1.3 Predicted and Measured Ground Responses 1201

7.5.2 Verification Against a Three-Dimensional Finite Element Analysis of a Shallow Tunnel 1207

7.5.3 Verification Against Actual Case Histories 1212

7.5.3.1 Foreword 1212

7.5.3.2 A Large Shielded Tunnel in Marl: The Frankfurt Baulos 23, Domplatz Tunnel 1214

7.5.3.3 Twin NATM Tunnels in Marl: The Frankfurt Baulos 25, Romerberg Tunnel 1224

7.5.3.4 A Small Shielded Tunnel in Till: The Mississauga (Ontario) Tunnel 1234

7.5.3.5 A Large NATM Tunnel in Granular Soil: The Butterberg Tunnel, in Osterode, near Hannover 1246

7.5.3.6 A Large Shield in Till: The Edmonton LRT Tunnel 1257

7.5.3.7 An NATM Tunnel in Marl: The Munich U - Bahn - Line 8/1, Baulos 18.2 1263

7.5.3.8 An NATM Tunnel Built under Compressed Air: The Munich U-Bahn-Line 5/9, Baulos 7 1269

7.5.3.9 An NATM Tunnel Driven Through Heterogeneous Ground: The Bochum Baulos A2 Double Track Subway Tunnel 1279

7.5.3.10 An NATM Tunnel with Staged Installation of the Lining: The Sao Paulo North Extension Double Track Tunnel 1282

7.5.4 Analysis and Interpretation of the Results Obtained 1293

7.6 Summary and Conclusions 1310

8. CONCLUSIONS 1324

REFERENCES 1341

APPENDIX A - RESULTS OF 3-D FINITE ELEMENT ANALYSES 1406

APPENDIX B - LIST OF RESPONDENTS TO THE QUESTIONNAIRE ..1410

APPENDIX C - NORMALIZED GROUND SETTLEMENTS 1415

APPENDIX D - TWICE NORMALIZED GROUND REACTION CURVES ...1453

List of Tables

Table Page

5.27 Some Solutions for Tunnel Convergence Estimates under Time-Independent Conditions 732

5.28 Review of Some Three-Dimensional Finite Element Simulations of Tunnel Construction 740

5.29 Cases of Three-Dimensional Analyses 755

5.30 Coefficients of the Adopted U and K Relations for Sections at Different Distances Behind the Face 787

5.31 Predicted and Measured Displacements at the Face and at the Point of Support Activation in Shallow Tunnels for the Crown 809

5.32 Predicted and Measured Displacements at the Face and at the Point of Support Activation in Shallow Tunnels for the Springline 813

5.33 Predicted and Measured Displacements at the Face and at the Point of Support Activation in Shallow Tunnels for the Floor 815

5.34 Calculated and Observed Maximum Horizontal Movements of the Tunnel Face 845

5.35 Calculated and Observed Maximum Longitudinal Distortions at the Ground Surface, Ahead of the Tunnel Face 846

6.1 Input Parameters for Finite Element Analyses of Tunnels with the Same H/D and with a Homothetic Hyperbolic Stress-Strain Soil Model with $c=0$ 870

6.2 Invariance of NGRC and Normalized Displacements to Changes in the Unit Weight of the Soil 879

6.3 Input Parameters for Finite Element Analyses of Tunnels with the Same H/D and with Homothetic Hyperbolic Stress-Strain Soil Model with $\phi=0$ 882

Table Page

6.4 Variation of the Maximum Normalized Surface Settlement with the Exponent n and with the Amount of Stress Release Allowed in the Opening 909

6.5 Ratio of Normalized Crown Displacements for n=0 to n>0, for Different Exponents n and Different Amount of Stress Release at the Opening 910

6.6 Variation of the Maximum Normalized Surface Settlement with the Cohesive Strength of the Soil and with the Amount of Stress Release Allowed 916

6.7 Variation of the Dimensionless Crown Displacement for the Different Strength Assumptions made and for the Different Amounts of Stress Release 924

6.8 Selected Variables for the Parametric Finite Element Analyses 940

6.9 Recorded Final Movements below Actual Tunnels and Tunnel Model Tests 957

6.10 Parameters used and Obtained in the Reduction of the Twice Normalized Ground Reaction Curves for the Frictionless Soil Model, for H/D=3 1016

6.11 Parameters used and Obtained in the Reduction of the Twice Normalized Ground Reaction Curves for the Frictionless Soil Model for H/D=1.5 1022

6.12 Parameters Used and Obtained in the Reduction of the Twice Normalized Ground Reaction Curves for the Frictionless Soil Model for H/D=6 1023

6.13 Parameters Obtained in the Reduction of the Twice Normalized Ground Reaction Curves for the Frictionless Soil Model 1024

6.14 Parameters Used and Obtained in the Reduction of the Twice Normalized Ground Reaction Curves of a Tunnel with H/D=3, for the Cohesionless Soil Model with K_o=0.8 1037

Table Page

6.15 Parameters Used and Obtained in the Reduction of the Twice Normalized Ground Reaction Curves for the Frictionless Soil Model and for K_o=0.6 1045

6.16 Parameters Used and Obtained in the Reduction of the Twice Normalized Ground Reaction Curves for the Frictionless Soil Model and for K_o=0.8 1046

6.17 Parameters Used and Obtained in the Reduction of the Twice Normalized Ground Reaction Curves for the Frictionless Soil Model and for K_o=1.0 1047

7.1 Typical Relative Stiffness Ratios for Common Linings and Soils 1122

7.2 Calculation of the Reduced Unit Weight of the Soil for the Lining-Ground Interaction Analyses 1142

7.3 Calculation of the Reduced Average Ground Stiffness at Lining Installation 1146

7.4 Performance at the ABV Tunnel as Measured and as Calculated by the Proposed Procedure 1191

7.5 Measured and Calculated Ground Response in the Centrifuge Model Test 2DP by Mair (1979) 1204

7.6 Typical Properties of Frankfurt Clay used in the Analysis 1216

7.7 Selected Ground Parameters for Drained Analysis of Tunnel in Dense Sand-Clay Till 1237

7.8 Selected Ground Parameters for Analysis of Tunnel in Well-Graded Sandy-Silty Gravel 1249

7.9 Selected Parameters for Munich Marl 1265

7.10 Measured and Calculated Performances at the Munich Line 5/9 Tunnel 1278

7.11 Results of the Application of the Proposed Calculation Procedure to some Case Histories of Shallow Tunnels 1297

Table Page

7.12 Calculated and Measured Widths of the Final Surface Settlement Profiles in Some Case Histories 1306

List of Figures

Figure Page

5.65 Conceptual Relations Between the Amount of Stress Release and Loss of Ground in a Two-Dimensional Representation 728

5.66 Radial Displacements of an Unlined Deep Tunnel in Elastic Ground (after Niwa et.al., 1979) 734

5.67 Three-Dimensional Finite Element Mesh and Input Parameters 749

5.68 Dimensionless Radial Displacements at the Crown of a Lined and Unlined Shallow Tunnel (H/D=1.6 and K=0.75) 756

5.69 Dimensionless Radial Displacements at the Springline of a Lined and Unlined Shallow Tunnel (H/D=1.6 and K=0.75) 757

5.70 Dimensionless Radial Displacements at the Floor of a Lined and Unlined Shallow Tunnel (H/D=1.6 and K=0.75) 758

5.71 Dimensionless Radial Displacements at the Crown of a Lined and Unlined Deeper Tunnel (H/D=2.8 and K=0.75) 760

5.72 Dimensionless Radial Displacements at the Springline of a Lined and Unlined Deeper Tunnel (H/D=2.8 and K=0.75) 761

5.73 Dimensionless Radial Displacements at the Floor of a Lined and Unlined Deeper Tunnel (H/D=2.8 and K=0.75) 762

5.74 Closure of an Unlined Tunnel in Elastic Ground Compared to that of Lined Tunnels in Elasto-Plastic Material 765

5.75 Dimensionless Crown Displacements of the Shallower (H/D=1.6) Unlined Tunnel for Different In Situ Stress Ratios K 767

5.76 Dimensionless Crown Displacements of the Deeper (H/D=2.8) Unlined Tunnel for Different Stress Ratios K 768

5.77 Dimensionless Springline Displacements of the Shallower (H/D=1.6) Unlined Tunnel for Different Stress Ratios K 770

Figure Page

5.78 Dimensionless Springline Displacements of the Deeper (H/D=2.8) Unlined Tunnel for Different Stress Ratios K 771

5.79 Dimensionless Floor Displacements of the Shallower (H/D=1.6) Unlined Tunnel for Different Stress Ratios K 772

5.80 Dimensionless Floor Displacements of the Deeper (H/D=2.8) Unlined Tunnel, for Different Stress Ratios K 773

5.81 Comparison of Dimensionless Crown Displacements of the Shallower and Deeper Unlined Tunnels 775

5.82 Comparison of Dimensionless Springline Displacements of the Shallower and Deeper Unlined Tunnels 776

5.83 Comparison of Dimensionless Floor Displacements of the Shallower and Deeper Unlined Tunnels 777

5.84 Ground Movements in the Vertical Longitudinal Plane of the Shallower (H/D=1.6) Unlined Tunnel 778

5.85 Ground Movements in the Vertical Longitudinal Plane of the Deeper (H/D=2.8) Unlined Tunnel 779

5.86 U and K Relationships for the Section at the Face 781

5.87 U and K Relationship for a Section D/4 Behind the Face 782

5.88 U and K Relationship for a Section D/2 Behind the Face 783

5.89 U and K Relationship for a Section 1.D Behind the Face 784

5.90 U and K Relationship for a Section 2.D Behind the Face 785

5.91 U and K Relationships for the Tunnel Crown 789

5.92 U and K Relationships for the Tunnel Springline 790

Figure Page

5.93 U and K Relationships for the Tunnel Floor 791

5.94 Coefficients of the U and K Relationship for the Crown of an Unlined Shallow Tunnel (1.5<H/D<3.0) as a Function of the Distance to the Face 792

5.95 Coefficients of the U and K Relationship for the Springline of an Unlined Shallow Tunnel (1.5<H/D<3.0) as a Function of the Distance to the Face 793

5.96 Coefficients of the U and K Relationship for the Floor of an Unlined Shallow Tunnel (1.5<H/D<3.0) as a Function of the Distance to the Face 794

5.97 Maximum Horizontal Displacement of the Tunnel Face Expressed in Dimensionless Form, as a Function of the Stress Ratio K 795

5.98 Maximum Angular Distortion Along the Tunnel, at Crown Elevation 799

5.99 Maximum Angular Distortion Along the Tunnel, at an Axis 0.3D Above Crown Elevation, as a Function of the Maximum Crown Distortion 801

5.100 Maximum Angular Distortion of the Ground Surface Along the Tunnel Alignment as a Function of the Maximum Crown Distortion 803

5.101 Comparison Between Niwa et.al. (1979) and the Present (Averaged) Tunnel Closure Solution 807

5.102 Predicted and Measured Crown Displacements at the Face for Different Ground Types 823

5.103 Predicted and Measured Springline Displacements at the Face, for Different Ground Types 826

Figure Page

5.104 Predicted and Measured Crown Displacements at the Face for Different Tunnel Construction Methods 827

5.105 Predicted and Measured Springlne Displacements at the Face, for Different Tunnel Construction Methods 829

5.106 Predicted and Measured Crown Displacements at the Section the Support was Installed for Different Ground Types 831

5.107 Predicted and Measured Crown Displacements at the Section the Support was Installed for Different Tunnel Construction Methods 832

5.108 Dimensionless Crown Displacements Observed when the Support was Installed at Different Distances Behind the Tunnel Face 834

5.109 Predicted and Measured Springline Displacements at the Section the Support was Installed, for Different Ground Types 838

5.110 Predicted and Measured Springline Displacements at the Section the Support was Installed for Different Tunnel Construction Methods 839

5.111 Distributions of Measured Crown Displacements after Support Installation 840

5.112 Distributions of Measured Crown Displacements at the Tunnel Face 843

5.113 Evaluation of the Ground Stress Release at the ABV Tunnel for a Two-Dimensional Numerical Simulation 853

5.114 Evaluation of the Ground Stress Release at the LRT Tunnel for a Two-Dimensional Numerical Simulation 856

Figure Page

5.115 Evaluation of the Ground Stress Release of the Edmonton Experimental Tunnel for a Two-Dimensional Simulation 858

6.1 Example of Homothetic Hyperbolae 866

6.2 Uniqueness of the Normalized Homothetic Hyperbolae for c=n=0 867

6.3 Ground Reaction Curves for the Crown of Geometrically Homothetic Tunnels in a Soil with a Homothetic Hyperbolic Stress-Strain Relationship (cohesionless model) 871

6.4 Ground Reaction Curves for the Springline of Geometrically Homothetic Tunnels in a Soil with a Homothetic Hyperbolic Stress-Strain Relationship (cohesionless model) 872

6.5 Ground Reaction Curves for the Floor of Geometrically Homothetic Tunnels in a Soil with a Homothetic Hyperbolic Stress-Strain Relationship (cohesionless model) 873

6.6 Normalized Ground Reaction Curves of Geometrically Homothetic Tunnels in a Soil with a Homothetic Hyperbolic Stress-Strain Relationship (cohesionless model) 874

6.7 Subsurface Settlements along the Cover of Geometrically Homothetic Tunnels in a Soil with a Homothetic Hyperbolic Stress-Strain Relationship (c=0), for Stress Release of 50% 875

6.8 Surface Settlements over Geometrically Homothetic Tunnels in a Soil with a Homothetic Hyperbolic Stress-Strain Relationship (c=0), for Stress Release of 50% 876

6.9 Ground Reaction Curve for the Crown of Geometric Homothetic Tunnels in a Soil with a Homothetic Hyperbolic Stress-Strain Relationship (frictionless model) 884

Figure Page

6.10 Ground Reaction Curve for the Springline of Geometric Homothetic Tunnels in a Soil with a Homothetic Hyperbolic Stress-Strain Relationship (frictionless model) 885

6.11 Ground Reaction Curve for the Floor of Geometric Homothetic Tunnels in a Soil with a Homothetic Hyperbolic Stress-Strain Relationship (frictionless model) 886

6.12 Normalized Ground Reaction Curves of Geometrically Homothetic Tunnels in a Soil with a Homothetic Hyperbolic Stress-Strain Relationship (frictionless model) 887

6.13 Subsurface Settlements along the Cover of Geometrically Homothetic Tunnels in a Soil with a Homothetic Hyperbolic Stress-Strain Relationship (ϕ=0), for a Stress Release of 50% 888

6.14 Surface Settlements over Geometrically Homothetic Tunnels in a Soil with a Homothetic Hyperbolic Stress-Strain Relationship (ϕ=0), for a Stress Release of 50% 890

6.15 Influence of Janbu's Modulus K on the Ground Reaction Curve of the Tunnel Crown 896

6.16 Influence of Janbu's Modulus K on the Ground Reaction Curve of the Tunnel Springline 897

6.17 Influence of Janbu's Modulus K on the Ground Reaction Curve of the Tunnel Floor 898

6.18 Variations with Depth of the In Situ Tangent Modulus for Three Values of Janbu's Exponent, n 900

6.19 Normalized Ground Reaction Curves for the Tunnel Crown, Calculated for Different In Situ Tangent Modulus Profiles 901

Figure	Page
6.20 Normalized Ground Reaction Curves for the Tunnel Floor, Calculated for Different In Situ Tangent Modulus Profiles	902
6.21 Normalized Ground Reaction Curves for the Tunnel Springline, Calculated for Different In Situ Tangent Modulus Profiles	904
6.22 Ground Reaction Curves for the Crown and Floor, with the Displacements Normalized to the Soil In Situ Stiffnesses at Points Half a Diameter Above and Below the Tunnel Respectively	905
6.23 Normalized Subsurface and Surface Settlements for 50% Ground Stress Release at the Opening, for Different Exponent n Values	907
6.24 Normalized Ground Reaction Curves for the Crown, Calculated for Different Cohesive Strengths of the Soil	913
6.25 Normalized Ground Reaction Curves for the Springline, Calculated for Different Cohesive Strengths of the Soil	914
6.26 Normalized Ground Reaction Curves for the Floor, Calculated for Different Cohesive Strengths of the Soil	917
6.27 Normalized Subsurface and Surface Settlements for 50% Ground Stress Release, Calculated for Different Cohesive Strengths of the Soil	918
6.28 Normalized Ground Reaction Curves for the Crown, Calculated for Different Soil Strengths	921
6.29 Normalized Ground Reaction Curves for the Springline, Calculated for Different Soil Strengths	922

Figure Page

6.30 Normalized Ground Reaction Curves for the Crown, Calculated for Different Poisson's Ratios 926

6.31 Normalized Ground Reaction Curves for the Springline, Calculated for Different Poisson's Ratios 928

6.32 Normalized Ground Reaction Curves for the Floor, Calculated for Different Poisson's Ratios 929

6.33 Normalized Subsurface and Surface Settlements for 50% Ground Stress Release, Calculated for Different Poisson's Ratios 930

6.34 Distributions of Sizes and Depths of Tunnels Reviewed 934

6.35 Distributions of Geotechnical Properties of the Grounds Through Which the Tunnels Reviewed were Driven 935

6.36 Distribution of the In Situ Stress Ratios in the Case Histories Reviewed 937

6.37 Distribution of Construction Methods and Distance of Support Activation in the Tunnels Surveyed 938

6.38 Normalized Ground Reaction Curve for the Springline Calculated for Different Numbers of Unloading Increments 942

6.39 Difference in the Calculated Dimensionless Displacement U for Ten and Twenty Unloading Increments 943

6.40 Differences in the Normalized Ground Settlements for Stress Release of 50%, Calculated for Ten and Twenty Unloading Increments 944

6.41 Normalized Ground Reaction Curves for the Crown, Calculated for Different Positions of the Lower Rigid Boundary 948

Figure Page

6.42 Normalized Ground Reaction Curves for Springline, Calculated for Different Positions of the Lower Rigid Boundary 950

6.43 Normalized Ground Reaction Curves for Floor, Calculated for Different Positions of the Lower Rigid Boundary 951

6.44 Distribution of Subsurface Normalized Settlements for 50% Ground Stress Release, Calculated for Different Positions of the Lower Rigid Boundary 952

6.45 Subsurface Settlement Distribution for 50% Ground Stress Release, Calculated for Different Positions of the Lower Rigid Boundary 954

6.46 Transverse Profiles of Normalized Ground Surface Settlements for 50% Stress Release, Calculated for Different Positions of the Lower Rigid Boundary 955

6.47 Normalized Ground Reaction Curves for H/D=3 and an Undrained Strength Ratio of 1.25 964

6.48 Normalized Subsurface Settlements along Tunnel Axis for H/D=3 and an Undrained Strength Ratio of 1.25, Calculated for Increasing Amount of Stress Release 965

6.49 Normalized Surface Settlements for H/D=3 and Undrained Strength Ratio of 1.25, Calculated for Increasing Amount of Stress Release 966

6.50 Normalized Ground Reaction Curves at the Crown for an Undrained Strength Ratio of 1.25 and Different Tunnel Depths 967

6.51 Normalized Ground Reaction Curves at the Springline for and Undrained Strength Ratio of 1.25 and Different Tunnel Depths 968

6.52 Normalized Ground Reaction Curves at the Floor for an Undrained Strength Ratio of 1.25 and Different Tunnel Depths 969

Figure Page

6.53 Normalized Subsurface and Surface Settlement for an Undrained Strength Ratio of 1.25 and 50% Ground Stress Release, Calculated for Different Tunnel Depths 971

6.54 Normalized Ground Reaction Curves of the Crown for $H/D=3$ and Different Undrained Strength Ratios 972

6.55 Normalized Ground Reaction Curves of the Springline for $H/D=3$ and Different Undrained Strength Ratios 973

6.56 Normalized Ground Reaction Curves of the Floor for $H/D=3$ and Different Undrained Strength Ratios 974

6.57 Normalized Subsurface and Surface Settlements for $H/D=3$ and 50% Ground Stress Release, Calculated for Different Undrained Strength Ratios 976

6.58 Normalized Ground Reaction Curves for $H/D=3$, $K_o=0.8$ and $\phi=30°$ 978

6.59 Normalized Subsurface Settlements for $H/D=3$, $K_o=0.8$ and $\phi=30°$, Calculated for Increasing Amount of Stress Release 979

6.60 Normalized Surface Settlements for $H/D=3$, $K_o=0.8$ and $\phi=30°$, Calculated for Increasing Amount of Stress Release 980

6.61 Normalized Ground Reaction Curves for Different Tunnel Depths, Calculated for $\phi=30°$ and $K_o=0.8$ 982

6.62 Normalized Subsurface and Surface Settlements for Different Tunnel Depths, Calculated for $\phi=30°$, $K_o=0.8$ and 50% Stress Release 983

6.63 Normalized Ground Reaction Curves of the Crown for $H/D=3$ and $K_o=0.8$, Calculated for Different Friction Angles 985

6.64 Normalized Ground Reaction Curves of the Springline for $H/D=3$ and $K_o=0.8$, Calculated for Different Friction Angles 986

Figure Page

6.65 Normalized Ground Reaction Curves of the Floor for H/D=3 and K_o=0.8, Calculated for Different Friction Angles 987

6.66 Normalized Subsurface and Surface Settlements for H/D=3, K_o=0.8 and 40% Ground Stress Release, Calculated for Different Friction Angles 988

6.67 Normalized Ground Reaction Curves of the Crown, for H/D=3 and ϕ=30°, Calculated for Different In Situ Stress Ratios 990

6.68 Normalized Ground Reaction Curves of the Springline, for H/D=3 and ϕ=30°, Calculated for Different In Situ Stress Ratios 991

6.69 Normalized Ground Reaction Curves of the Floor, for H/D=3 and ϕ=30°, Calculated for Different In Situ Stress Ratios 992

6.70 Normalized Subsurface and Surface Settlements for H/D=3, ϕ=30° and 50% Ground Stress Release, Calculated for Different In Situ Stress Ratios 994

6.71 Variation of the Maximum Normalized Surface Settlement with the Amount of Stress Release and other Variables, for the Frictionless Soil Model 997

6.72 Variation of the Maximum Normalized Surface Settlement with the Amount of Stress Release and other Variables, for the Cohesionless Soil Model 999

6.73 Relationships between Normalized Maximum Surface Settlement and Relative Depth of Tunnel, Calculated for the Frictionless Soil Model, for 30% Stress Release 1002

6.74 Relationships between Normalized Maximum Surface Settlement and Relative Tunnel Depth, Calculated for the Frictionless Soil Model, for 50% Stress Release 1003

Figure Page

6.75 Normalized Settlement Ratios for $\phi=40°$ and 30% Stress Release 1004

6.76 Normalized Settlement Ratios for $\phi=40°$ and 50% Stress Release 1005

6.77 Normalized Settlement Ratios for $\phi=30°$ and 30% Stress Release 1006

6.78 Normalized Settlement Ratios for $\phi=30°$ and 50% Stress Release 1007

6.79 Normalized Settlement Ratios for $\phi=20°$ and 30% Stress Release 1008

6.80 Normalized Settlement Ratios for $\phi=20°$ and 50% Stress Release 1009

6.81 Normalized Settlement Ratios Observed in some Case Histories 1011

6.82 Twice Normalized Ground Reaction Curve (NNGRC) for the Crown of a Tunnel with H/D=3, for the Frictionless Soil Model 1017

6.83 Twice Normalized Ground Reaction Curves (NNGRC) for the Springline of a Tunnel with H/D=3, for the Frictionless Soil Model 1019

6.84 Twice Normalized Ground Reaction Curves (NNGRC) for the Floor of a Tunnel with H/D=3, for the Frictionless Soil Model 1020

6.85 Variation of the Coefficient A with Relative Tunnel Depth, for the Frictionless Soil Model 1025

6.86 Variation of the Coefficient B, for the Tunnel Crown, with Strength and Depth Ratios, Calculated for the Frictionless Soil Model 1026

6.87 Variation of the Coefficient B for the Tunnel Springline, with Strength and Depth Ratios, Calculated for the Frictionless Soil Model 1027

6.88 Variation of the Coefficient B for the Tunnel Floor, with Strength and Depth Ratios, Calculated for the Frictionless Soil Model 1028

Figure Page

6.89 Twice Normalized Ground Reaction Curve (NNGRC) for the Crown of a Tunnel with H/D=3, for the Cohesionless Soil Model with K_o=0.8 1038

6.90 Twice Normalized Ground Reaction Curves (NNGRC) for the Springline of a Tunnel with H/D=3, for the Cohesionless Soil Model with K_o=0.8 1040

6.91 Twice Normalized Ground Reaction Curves (NNGRC) for the Floor of a Tunnel with H/D=3, for the Cohesionless Soil Model with K_o=0.8 1041

6.92 Slope of the Arbitrary Axes used to Obtain the NNGRC, Represented as a Function of H/D, for K_o=0.6 1051

6.93 Relationships between α_{ref} and the Friction Angle for K_o=0.6 1052

6.94 Twice Normalized Ground Reaction Curves for Tunnel Crown Calculated for K_o=0.6 1053

6.95 Twice Normalized Ground Reaction Curves for the Tunnel Springline, Calculated for K_o=0.6 1054

6.96 Twice Normalized Ground Reaction Curves for the Tunnel Floor, Calculated for K_o=0.6 1055

6.97 Variations of λ' for the Tunnel Crown, Calculated for K_o=0.6 1056

6.98 Variations of λ' for the Tunnel Springline, Calculated for K_o=0.6 1057

6.99 Variations of λ' for the Tunnel Floor, Calculated for K_o=0.6 1058

6.100 Slopes of the Arbitrary Axes used to Obtain the NNGRC Represented as a Function of H/D, for K_o=0.8 1061

6.101 Relationships between α_{ref} and the Friction Angle of K_o=0.8 1062

6.102 NNGRCs for Tunnel Crown, Calculated for K_o=0.8 1063

Figure Page

6.103 NNGRCs for Tunnel Springline Calculated for K_o=0.8 1064

6.104 NNGRCs for Tunnel Floor, Calculated for K_o=0.8 1065

6.105 Variations of λ' for the Tunnel Crown, Calculated for K_o=0.8 1066

6.106 Variations of λ' for the Tunnel Springline, Calculated for K_o=0.8 1067

6.107 Variations of λ' for the Tunnel Floor, Calculated for K_o=0.8 1068

6.108 Slopes of the Arbitrary Axes used to Obtain the NNGRC Presented as a Function of H/D, for K_o=1.0 1069

6.109 Relationships between a_{rel} and the Friction Angle for K_o=1.0 1070

6.110 NNGRCs for Tunnel Crown, Calculated for K_o=1.0 1071

6.111 NNGRCs for Tunnel Springline, Calculated for K_o=1.0 1072

6.112 NNGRCs for Tunnel Floor, Calculated for K_o=1.0 1073

6.113 Variations of λ' for the Tunnel Crown, Calculated for K_o=1.0 1074

6.114 Variations of λ' for the Tunnel Springline, Calculated for K_o=1.0 1075

6.115 Variations of λ' for the Tunnel Floor, Calculated for K_o=1.0 1076

6.116 Variations of the Initial Slope of the Twice Normalized Ground Reaction Curves with K_o and H/D 1077

6.117 Extension of the NGRCs for H/D=3, K_o=0.8 and ϕ=30° 1081

6.118 Extension of the NGRCs for H/D=3 and $c_o/\gamma D$=1.25 1084

Figure Page

6.119 Reference Values used for Normalizing the NGRC of the Tunnel Crown for the Frictionless Soil Model and Components to Define the Limiting U of the Fitted Function 1086

6.120 Reference Values used for Normalizing the NGRC of the Tunnel Springline for the Frictionless Soil Model and Components to Define the Limiting U of the Fitted Function 1087

6.121 Reference Values used for Normalizing the NGRC of the Tunnel Floor for the Frictionless Soil Model and Components to Define the Limiting U of the Fitted Function 1088

6.122 Lower Bound Solution for Tunnel Collapse Pressure in a Frictionless Soil 1095

6.123 Lower and Upper Bound Solutions for Tunnel Collapse Pressure in a Frictional and Cohesive Soil (ϕ=10°) 1097

6.124 Lower and Upper Bound Solutions for Tunnel Collapse Pressure in a Frictional and Cohesive Soil (ϕ=20°) 1098

6.125 Lower and Upper Bound Solutions for Tunnel Collapse Pressure in a Frictional and Cohesive Soil (ϕ=30°) 1099

6.126 Lower and Upper Bound Solutions for Tunnel Collapse Pressure in a Frictional and Cohesive Soil (ϕ=40°) 1100

7.1 Notations and Conventions used in Hartmann's Solution 1124

7.2 Lining Stresses, Displacements and Internal Forces Given by Hartmann's Solution 1125

7.3 Comparison of Lining Responses Calculated for Different Tunnel Depths, with and without Account of the Influence of the Ground Surface 1129

7.4 Equilibrium Points of the Soil-Lining Interaction at Tunnel Crown 1137

Figure Page

7.5 Equilibrium Points of the Soil-Lining Interaction at Tunnel Springline 1138

7.6 Equilibrium Points of the Soil-Lining Interaction at Tunnel Floor 1139

7.7 Distribution of Final Settlements Calculated for a Tunnel Lined after 40% Stress Release, Compared to the Distributions for an Unlined Tunnel Equal Crown Displacement 1155

7.8 Distribution of Final Settlements Calculated for a Tunnel Lined after 80% Stress Release, Compared to the Distributions for an Unlined Tunnel with Equal Crown Displacements 1156

7.9 Suggested Sequence of Steps for Application of the Proposed Procedure for Shallow Tunnel Design 1161

7.10 Calculation Sheet with Geometric Ground Properties Data and Tunnel Closure at Lining Activation 1169

7.11 Calculation Sheet for Estimates of the Stress Release and Ground Stiffness at the Section the Lining is Activated 1170

7.12 Calculation Sheet for 2D Stability Verification and Lining-Ground Interaction Analysis 1171

7.13 Calculation Sheet for Iterative Analysis of the Lining-Ground Interaction 1172

7.14 Calculation Sheet for Subsurface and Surface Settlements 1173

7.15 ABV Tunnel - Input Data and Tunnel Closure at Lining Activation 1176

7.16 ABV Tunnel - Stress Release and Ground Stiffness at Lining Activation 1179

7.17 ABV Tunnel - Two Dimensional Stability Calculation and Lining-Ground Interaction 1182

7.18 ABV Tunnel - Iterative Calculation for the Lining-Ground Interaction 1185

Figure Page

7.19 ABV Tunnel: Subsurface and Surface Settlement Calculations 1187

7.20 Calculated and Measured Final Subsurface Settlements at the ABV Tunnel 1192

7.21 Calculated and Measured Final Surface Settlements at the ABV Tunnel 1193

7.22 Calculated and Measured Radial Stresses on the ABV Tunnel Lining 1194

7.23 Measured and Calculated Ground Response at Tunnel Crown for the Centrifuge Model Test 1205

7.24 Measured and Calculated Surface Settlement Profiles for the Centrifuge Model Test at Two Internal Pressures 1208

7.25 Subsurface Settlement Distributions Calculated in a Three-Dimensional Analysis and by the Proposed Method 1211

7.26 Profile of Surface Settlements Calculated in a Three-Dimensional Analysis and by the Proposed Method 1213

7.27 Measured and Calculated Final Subsurface Settlements over the South Tunnel in the Frankfurt Baulos 23 (Domplatz) Subway 1220

7.28 Measured and Calculated Final Surface Settlements over the South Tunnel in the Frankfurt Baulos 23 (Domplatz) Subway 1221

7.29 Predicted Lining Loads in the South Tunnel (1st driven) Compared to Measurements in the North Tunnel (2nd driven): Frankfurt Baulos 23 (Domplatz) Subway Tunnels 1222

7.30 Measured and Calculated Subsurface Settlements over the Frankfurt Baulos 25 (Romerberg) Subway 1228

7.31 Measured and Calculated Final Surface Settlements at the Frankfurt Baulos 25 (Romerberg) Subway Tunnel 1229

Figure Page

7.32 Measured and Calculated Final Surface Settlements over Twin Tunnels at the Frankfurt Baulos 25 (Romerberg) Subway 1231

7.33 Predicted Lining Radial Stresses for Single Tunnel and Measured Stresses in Twin Tunnels at the Frankfurt Baulos 25 (Romerberg) Subway 1232

7.34 Measured and Calculated Final Subsurface Settlements over the Mississauga Sewer Tunnel 1242

7.35 Measured and Calculated Final Surface Settlements over the Mississauga Sewer Tunnel 1243

7.36 Measured and Predicted Radial Stress Distributions on the Lining of the Mississauga Sewer Tunnel 1245

7.37 Measured and Calculated Final Subsurface Settlements over the Butterberg Tunnel 1253

7.38 Measured and Calculated Final Surface Settlements over the Butterberg Tunnel 1254

7.39 Measured and Predicted Radial Stress Distributions on the Shotcrete Lining of the Butterberg Tunnel 1256

7.40 Measured and Calculated Final Surface Settlements over the Edmonton LRT Tunnel 1261

7.41 Measured and Calculated Thrust Forces on the Edmonton LRT Primary Lining 1262

7.42 Measured and Calculated Final Subsurface Settlements over the Munich Line 8/1 Tunnel 1268

7.43 Calculated and Measured Radial Stress Distributions on the Shotcrete Lining of the Munich Line 8/1 Tunnel 1270

7.44 Measured and Calculated Surface Settlements over the Munich Line 5/9 Tunnel 1275

Figure Page

7.45 Measured and Calculated Final Subsurface Settlements over the Bochum Baulos A2 Tunnel 1283

7.46 Measured and Calculated Final Surface Settlement Profiles over the Bochum Baulos A2 Tunnel 1284

7.47 Calculated and Measured Radial Stress Distributions on the Shotcrete Lining of the Bochum Baulos A2 Tunnel 1285

7.48 Measured and Calculated Final Subsurface Settlements over the Sao Paulo North Extension Tunnel 1290

7.49 Measured and Calculated Final Surface Settlement Profiles over the Sao Paulo North Extension Tunnel 1291

7.50 Calculated Maximum Surface Distortions Compared to the Observed Maxima 1301

7.51 Calculated Tunnelling Performance Compared to Field Observations 1304

A.1 Radial Stresses and Displacements at the Crown Elevation (L/D=1/2) 1407

A.2 Radial Stresses and Displacements at the Springline Elevation (L/D=1/2) 1408

A.3 Radial Stresses and Displacements at the Floor Elevation (L/D=1/2) 1409

C.1 Normalized Settlements: $K_o=1$, $c_u/\gamma D=2.5$, $H/D=1.5$ 1416

C.2 Normalized Settlements: $K_o=1$, $c_u/\gamma D=1.25$, $H/D=1.5$ 1417

C.3 Normalized Settlements: $K_o=1$, $c_u/\gamma D=0.625$, $H/D=1.5$ 1418

C.4 Normalized Settlements: $K_o=1$, $c_u/\gamma D=0.3125$, $H/D=1.5$ 1419

C.5 Normalized Settlements: $K_o=1$, $\phi=20°$, $H/D=1.5$ 1420

C.6 Normalized Settlements: $K_o=1$, $\phi=30°$, $H/D=1.5$ 1421

Figure Page

C.7 Normalized Settlements: K_o=1, ϕ=40°, H/D=1.5 1422

C.8 Normalized Settlements: K_o=0.8, ϕ=20°, H/D=1.5 1423

C.9 Normalized Settlements: K_o=0.8, ϕ=30°, H/D=1.5 1424

C.10 Normalized Settlements: K_o=0.8, ϕ=40°, H/D=1.5 1425

C.11 Normalized Settlements: K_o=0.6, ϕ=20°, H/D=1.5 1426

C.12 Normalized Settlements: K_o=0.6, ϕ=30°, H/D=1.5 1427

C.13 Normalized Settlements: K_o=0.6, ϕ=40°, H/D=1.5 1428

C.14 Normalized Settlements: K_o=1, $c_u/\gamma D$=2.5, H/D=3 1429

C.15 Normalized Settlements: K_o=1, $c_u/\gamma D$=1.25, H/D=3 1430

C.16 Normalized Settlements: K_o=1, $c_u/\gamma D$=0.625, H/D=3 1431

C.17 Normalized Settlements: K_o=1, ϕ=20°, H/D=3 1432

C.18 Normalized Settlements: K_o=1, ϕ=30°, H/D=3 1433

C.19 Normalized Settlements: K_o=1, ϕ=40°, H/D=3 1434

C.20 Normalized Settlements: K_o=0.8, ϕ=20°, H/D=3 1435

C.21 Normalized Settlements: K_o=0.8, ϕ=30°, H/D=3 1436

C.22 Normalized Settlements: K_o=0.8, ϕ=40°, H/D=3 1437

C.23 Normalized Settlements: K_o=0.6, ϕ=20°, H/D=3 1438

C.24 Normalized Settlements: K_o=0.6, ϕ=30°, H/D=3 1439

Figure Page

C.25 Normalized Settlements: K_o=0.6, ϕ=40°, H/D=3 1440

C.26 Normalized Settlements: K_o=1, $c_u/\gamma D$=2.5, H/D=6 1441

C.27 Normalized Settlements: K_o=1, $c_u/\gamma D$=1.25, H/D=6 1442

C.28 Normalized Settlements: K_o=1, $c_u/\gamma D$=0.625, H/D=6 1443

C.29 Normalized Settlements: K_o=1, ϕ=20°, H/D=6 1444

C.30 Normalized Settlements: K_o=1, ϕ=30°, H/D=6 1445

C.31 Normalized Settlements: K_o=1, ϕ=40°, H/D=6 1446

C.32 Normalized Settlements: K_o=0.8, ϕ=20°, H/D=6 1447

C.33 Normalized Settlements: K_o=0.8, ϕ=30°, H/D=6 1448

C.34 Normalized Settlements: K_o=0.8, ϕ=40°, H/D=6 1449

C.35 Normalized Settlements: K_o=0.6, ϕ=20°, H/D=6 1450

C.36 Normalized Settlements: K_o=0.6, ϕ=30°, H/D=6 1451

C.37 Normalized Settlements: K_o=0.6, ϕ=40°, H/D=6 1452

D.1 NNGRC for Crown, K_o= 0.6, H/D=6 1454

D.2 NNGRC for Crown, K_o= 0.6, H/D=3 1455

D.3 NNGRC for Crown, K_o= 0.6, H/D=1.5 1456

D.4 NNGRC for Springline, K_o= 0.6, H/D=6 1457

D.5 NNGRC for Springline, K_o= 0.6, H/D=3 1458

D.6 NNGRC for Springline, K_o= 0.6, H/D=1.5 1459

D.7 NNGRC for Floor, K_o= 0.6, H/D=6 1460

Figure Page

D.8 NNGRC for Floor, K_o= 0.6, H/D=3 1461

D.9 NNGRC for Floor, K_o= 0.6, H/D=1.5 1462

D.10 NNGRC for Crown, K_o= 0.8, H/D=6 1463

D.11 NNGRC for Crown, K_o= 0.8, H/D=3 1464

D.12 NNGRC for Crown, K_o= 0.8, H/D=1.5 1465

D.13 NNGRC for Springline, K_o= 0.8, H/D=6 1466

D.14 NNGRC for Springline, K_o= 0.8, H/D=3 1467

D.15 NNGRC for Springline, K_o= 0.8, H/D=1.5 1468

D.16 NNGRC for Floor, K_o= 0.8, H/D=6 1469

D.17 NNGRC for Floor, K_o= 0.8, H/D=3 1470

D.18 NNGRC for Floor, K_o= 0.8, H/D=1.5 1471

D.19 NNGRC for Crown, K_o= 1.0, H/D=6 1472

D.20 NNGRC for Crown, K_o= 1.0, H/D=3 1473

D.21 NNGRC for Crown, K_o= 1.0, H/D=1.5 1474

D.22 NNGRC for Springline, K_o= 1.0, H/D=6 1475

D.23 NNGRC for Springline, K_o= 1.0, H/D=3 1476

D.24 NNGRC for Springline, K_o= 1.0, H/D=1.5 1477

D.25 NNGRC for Floor, K_o= 1.0, H/D=6 1478

D.26 NNGRC for Floor, K_o= 1.0, H/D=3 1479

D.27 NNGRC for Floor, K_o= 1.0, H/D=1.5 1480

5.3 Three-Dimensional Modelling

5.3.1 Introduction

It was shown in Sections 5.2.4 and 5.2.5, that the two-dimensional numerical solution adopted in the present study may serve as a reasonable tool to anticipate tunnelling performance. This is so, provided the requirements for validating or applying the numerical solution are fulfilled. Moreover, it was shown that reasonable predictions of the behaviour will only be obtained if the amount of stress release allowed before lining activation is properly estimated. This is, perhaps, the major drawback of this two-dimensional modelling procedure. The model requires an independent estimate of this variable.

Clearly, in a particular case, the stress release should be related to the construction procedures as well as to the ground type. Regarding the construction procedure, the support activation delay seems to be the controlling factor. It is represented by the distance between the tunnel face and the point where the lining and the ground are brought into full contact.

As explained in Section 5.2.5, if the ground stress release was univocally related to the ground displacements, then an estimate of the ground displacements could lead to an evaluation of the stress release. In Sections 2.3.4.2 and 2.3.5.3, the relationship between the radial stresses and displacements in an opening was formulated in a 2D representation, by extending the concept of the ground reaction curve to shallow tunnel conditions. In Section 3.2.3 it was suggested that for this type of representation, an univocal relation between stresses and displacements may indeed exist, provided tunnel collapse and the associated "loosening" process is avoided. But even if these failure processes are present, the tunnel closure is associated with a single ground stress. In Section 2.3.6.2 and 2.3.6.4, it was shown however, that the actual three-dimensional response in terms of stress-displacement relations is far more complex, and that in fact an univocal relation may not exist. This seems to result from the three-dimensional stress redistribution mechanisms. The presence of the lining affects the stress-displacement relation even at unsupported sections between the face and the liner heading edge (see Figures 2.25 to 2.27). This effect is more pronounced for smaller support activation delays. It was suggested however, that a two-dimensional representation may serve to approximate or bound the final equilibrium between liner and soil.

If the final equilibrium condition is the only matter of concern, then the two-dimensional representation may still be useful. This was suitably demonstrated through the back analyses shown in Section 5.2.4. Thus, the lining influence would only be considered in the two-dimensional simulation when the support is activated.

By accepting this simplification, the amount of ground stress release can be directly related to the loss of ground occurring during tunnel advance (Cording and Hansmire, 1975 - see Section 2.3.4.3). If it were possible to identify each component of the ground loss, then one could apportion the stress release to each component within the simplified two-dimensional model. Each construction technology, as applied to a certain ground type or condition, may lead to different compositions of losses of ground, as shown by Negro and Eisenstein (1981). Figure 5.65 illustrates these concepts, making use of an idealized relationship between the amount of stress release and losses of ground for two types of construction scheme. This relation corresponds to an "averaged" ground reaction curve, since by definition in this work, the amount of stress release is related to the applied radial stress and the loss of ground is related to the radial displacements of the tunnel contour. It has been tacitly assumed that ground deformations are not uncontrolled and therefore, stress and strain changes in the ground are gradual and continuous. It has also been assumed that the ground-lining interaction will develop only when the contact between them is fully developed (stage 4 in the TBM scheme) or when the invert is closed (stage 3 in the NATM scheme).

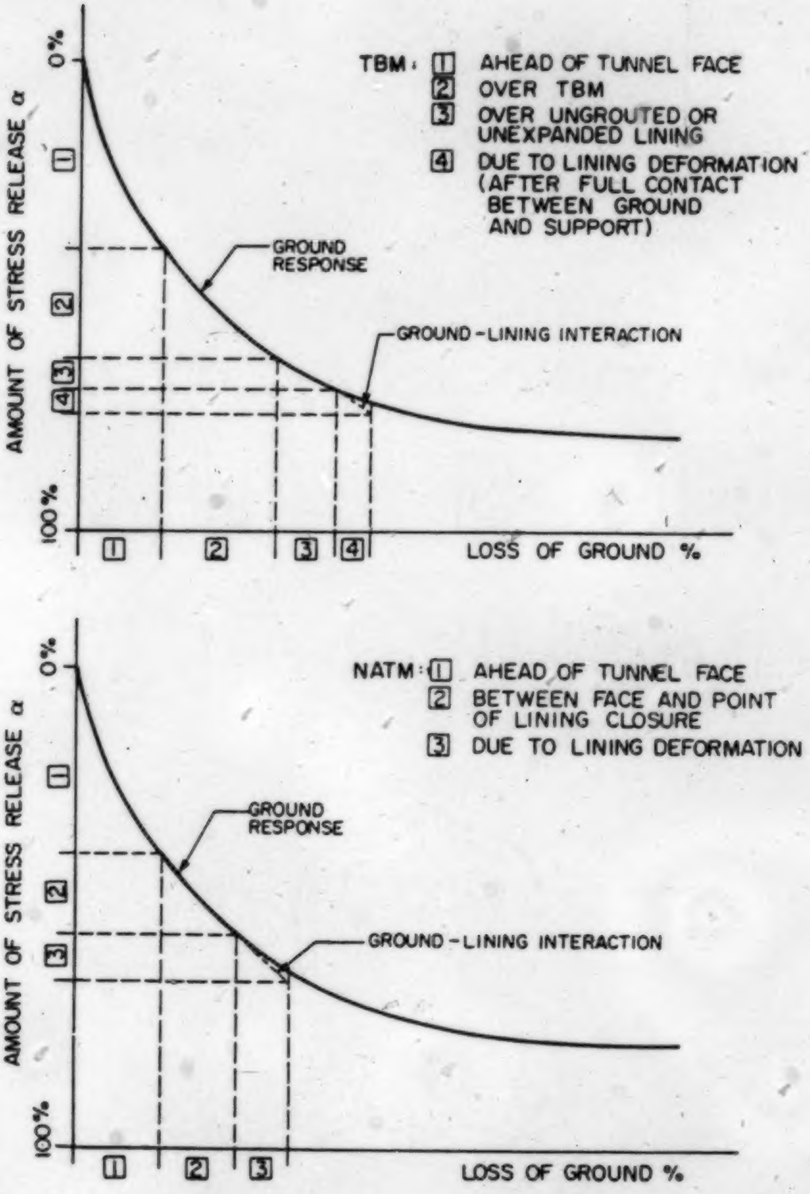
AMOUNT OF STRESS RELEASE α
0%
100%
TBM: 1 AHEAD OF TUNNEL FACE
2 OVER TBM
3 OVER UNGROUTED OR UNEXPANDED LINING
4 DUE TO LINING DEFORMATION (AFTER FULL CONTACT BETWEEN GROUND AND SUPPORT)
GROUND RESPONSE
GROUND-LINING INTERACTION
1
2
3
4
LOSS OF GROUND %
AMOUNT OF STRESS RELEASE α
0%
100%
NATM: 1 AHEAD OF TUNNEL FACE
2 BETWEEN FACE AND POINT OF LINING CLOSURE
3 DUE TO LINING DEFORMATION
GROUND RESPONSE
GROUND-LINING INTERACTION
1
2
3
LOSS OF GROUND %

Figure 5.65 Conceptual Relations Between the Amount of Stress Release and Loss of Ground in a Two-Dimensional Representation

One may consider a few extreme situations. If the support was brought into full contact with the ground at the tunnel face, stages 2 and 3 would be non-existent in the TBM scheme, as well as stage 2 in the NATM case. In another situation, if the soil was highly deformable as in some soft clays, it would close the overcutting void left over the TBM body, and the amount of ground lost at this stage, would be equal to that void volume. Thus, if a full lining contact is ensured as soon as the liner leaves the TBM tail, the ground-support interaction would start after the occurrence of ground movements equal to those developing ahead of the face plus the void size behind the TBM. In these two extreme situations, the amount of stress release to be considered in a two-dimensional representation would be known, provided the ground response the accumulated movement at the tunnel face and the TBM overcutting size are all known.

However, if the soil is only moderately deformable and shows some stand-up time, like some stiff clays, then the overcutting space may not be closed. In this case, the losses of ground at stage 2 in the TBM scheme is, therefore, unknown and the amount of stress release would be undetermined. Nevertheless, portion 1 of the stress release would serve as a lower bound to the unknown release.

If the relationships like those shown in Figure 5.65 were available, then the amount of stress release prior to lining activation, which is to be used in a two-dimensional simulation, would be defined whenever the losses of ground or the total magnitude of ground movement are known at the section where the lining is activated.

Ground reaction curves derived from two-dimensional analyses, as those shown in Sections 2.3.4.2 and 2.3.5.3, could be used to obtain the type of relationships shown in Figure 5.65. The estimate of the ground displacements occurring ahead of the face or at the point where the support is activated, requires consideration of the three-dimensional nature of the problem. It seems therefore necessary to investigate available solutions of opening convergence with the advance of the tunnel face.

5.3.2 Available Solutions for Estimates of Tunnel Convergence

Many authors followed the reasoning exposed in Section 5.3.1 and tried to develop methods that would allow the estimate of the tunnel contour closure at different sections behind the advancing face for time independent conditions. Some of the early works were reviewed and discussed in Section 2.3.6.2. For completeness, Table 5.27 has been prepared. It supplements the former discussions and includes only those methods whose primary goal is the convergence estimate.

These methods were formulated following three main lines of development:

1. methods derived from finite element analyses (either axisymmetric or three-dimensional);

2. methods derived from three-dimensional boundary element analyses;
3. methods semi-empirically derived, using curve fitting techniques.

Unlike the first two classes of methods, the latter, represented by cases 10 and 12 in Table 5.27, are not actual prediction methods. Field data gathered at a certain site and under certain conditions are required for input, and this allows the extrapolation of convergence results for different conditions but at the same location. Therefore, they should be understood as ancillary techniques for the observational method.

Most methods were developed under the assumption that the opening was located far from the ground surface, so that the influence of the gravitational stress gradients could be neglected. The sole exception to this rule is the procedure given in reference 11, Table 5.27. This particular method, described in Section 5.3.5, furnishes the radial displacements of the tunnel contour at a section containing the tunnel face (assumed vertical). In following sections this method will be extended to allow estimates at other points along the tunnel alignment.

The methods developed by Baudendistel (1979, 1984, 1985) and by Erdmann (1983) (see Sections 4.3.2.6 and 4.3.2.7) have not been included in Table 5.27 as they do not explicitly provide the radial displacements of the tunnel contour at different sections along the axis, although these

	Reference	Development	Factors Considered				Notes
			Tunnel Depth	In situ stress Ratio	Stress-Strain Rel. For Ground	Presence of Lining	
1.	Daemen & Fairhurst (1972)	Axisymmetric finite element method	Deep	$K = 1$	linear elastic	unlined	
2.	Descoeudres (1974)	3D finite element method (double symmetry)	Deep	$0.25 < K < 1$	linear elastic	unlined	
3.	Ranken & Ghaboussi (1975)	Axisymmetric finite element method	Deep	$K = 1$	linear elastic and elastoplastic	unlined and lined	Account of non linearily and lining not generalized
4.	Hocking (1976)	3D boundary integral equation method	Deep	$0 < K < 2$	linear elastic	unlined	
5.	Miwa et al (1979)	3D boundary integral equation method	Deep	Any K	linear elastic	unlined	
6.	Schwartz & Einstein (1980)	Axisymmetric finite element method	Deep	$K = 1$	linear elastic and elastoplastic	unlined and lined	Account of non linearily and lining not generalized
7.	Ito & Hisatake (1981)	Curve fitting of axisymmetric FE solution	Deep	$K = 1$	linear elastic	unlined	
8.	Hutchinson (1982)	Axisymmetric finite element method	Deep	$K = 1$	linear elastic	unlined and lined	Accounts of lining effect not generalized.
9.	Hanafy & Emery (1982 and 1980)	Axisymmetric analysis with non symmetric loading	Deep	$K = 1$ and $0.75 < K < 1.25$	linear elastic and elasto plastic	unlined and lined	Accounts of non linearily and lining not generalized
10.	Panet & Guenot (1982) Guenot et al (1985) Sulem et al (1987) Panet (1979) Gaudin et al (1981)	Curve-fitting of field data, semi-empirical	-	-	-	unlined	Observational method. Requires field data as input
11.	Negro et al (1985, 1986)	3D finite element method (single symmetry)	shallow	$0.6 < K < 0.9$	linear elastic	unlined and lined	Convergence at the face only.
12.	Barlow (1986) Barlow and Kaiser (1987)	Curve-fitting of field data. semi-empirical (similar to 10)	-	-	-	lined	Observational method. Requires field data as input.

Table 5.27 Some Solutions for Tunnel Convergence Estimates under Time-Independent Conditions

could be obtained indirectly.

Many methods assume a hydrostatic in situ stress condition, while others assume less restrictive field stresses (K_o not equal to 1). For a deep unlined tunnel, with axisymmetric geometric conditions, a single analysis with K_o equal to zero (uniaxial stress field) is sufficient to obtain a complete solution, provided the material is linear elastic, homogeneous and isotropic. The displacements for any K_o value can be obtained by using the principle of superposition. Therefore, the solutions derived from boundary integral equation analyses, presented by Hocking (1976:336) or by Niwa et.al. (1979:707) for K_o equal to zero, can be extended to any in situ stress ratio. This is summarized in Figure 5.66.

The numerical solutions available which have larger generality, thus applicable to a wider range of situations, are those which assume the ground behaviour to be linear elastic. Those which assume non-linear stress-strain relationships for the ground, cannot be readily generalized to conditions different from the original analyses, although they might be useful in providing insight on the effect of ground yielding.

Similarly, the methods that take into account the presence of the lining in the radial displacements of the opening are not generalized to conditions other than that studied. To achieve a broader generality, a larger number of parametric analyses, combined with components of

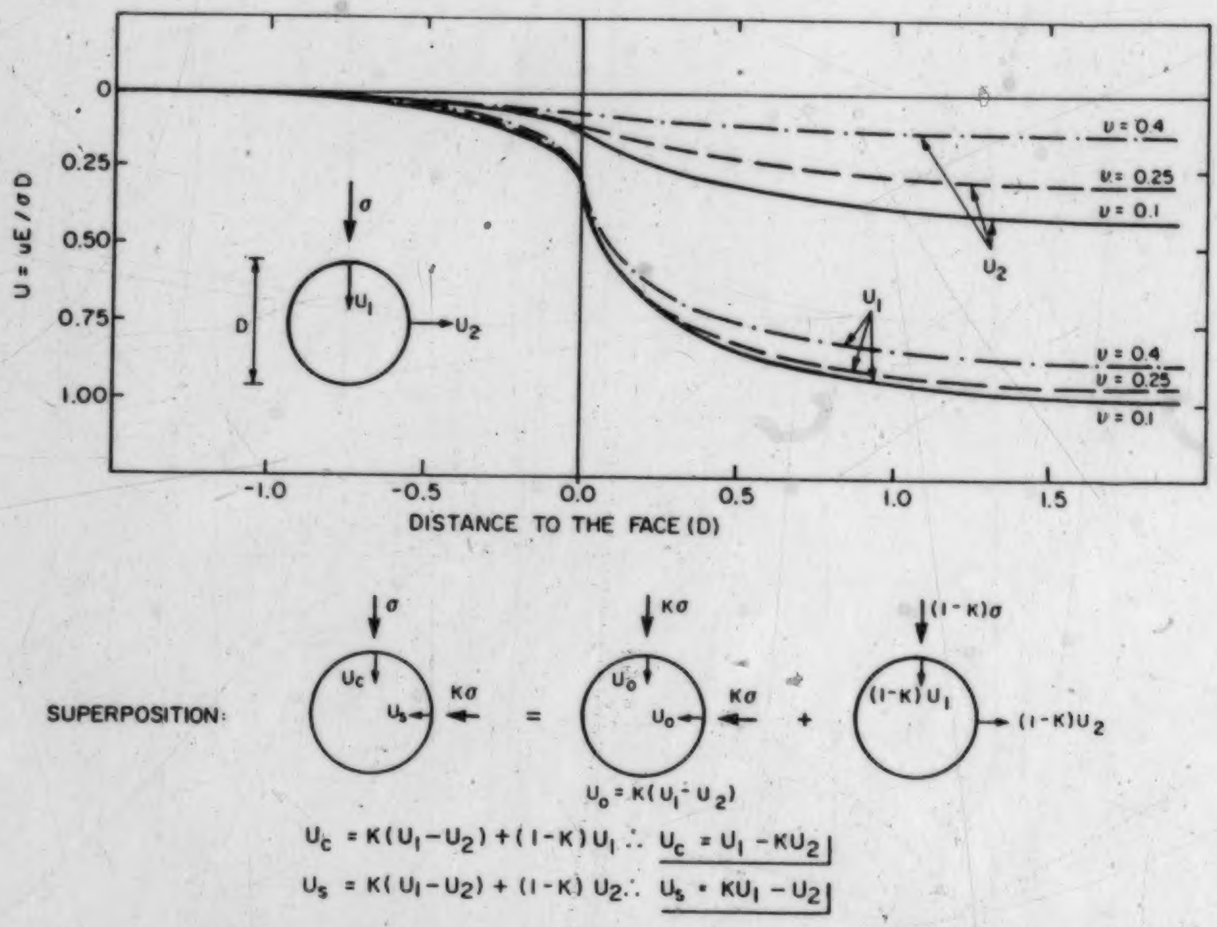

Figure 5.66 Radial Displacements of an Unlined Deep Tunnel in Elastic Ground (after Niwa et.al., 1979)

dimensionless analyses, would be required to obtain such a solution. Barlow (1986:45) achieved this to some extent. This author was able to introduce into the Guenot et.al. (1985) convergence solution, the influence of a lining installed at a certain distance behind the face of the tunnel. His procedure was developed from axisymmetric finite element analyses and, therefore, is strictly valid for hydrostatic in situ stress conditions. For these conditions the liner stiffness can be described in terms of its compressibility ratio only. A more general solution would require the flexibility ratio to be taken into account as well. Such a development is yet to be seen.

Nonetheless, Barlow (1986) has shown that for the conditions he studied (for instance, ground and support assumed elastic), the presence of the lining does have a strong influence on the radial displacements of the tunnel contour over the unsupported tunnel heading, as also shown by Eisenstein et.al. (1984) and as discussed in Section 2.3.6.2. This influence is more pronounced when the liner is placed close to the advancing face. The Convergence - Confinement method usually assumes that the opening deforms as in an unsupported tunnel, until the point of lining activation. The amount of stress release before lining installation can therefore be incorrectly estimated if this effect is neglected. Since the support tends to inhibit the ground movements around the heading, then neglecting the lining presence will likely result in an overestimate of the stress release. This means the support loads are underestimated and leads to an overestimate of the final ground movements. On one hand the assumption is unsafe and on the other it is too conservative. The errors involved in disregarding the lining-ground interaction however tend to be small for increasing distances between the face and the liner leading edge. For linear elastic materials, the results by Barlow (1986:59) showed that for support delays equal to, or greater than, 5/8 of the opening diameter, the tunnel closure at the leading edge of the liner is almost identical to that of an unlined tunnel for the same distance to the face. Since in most shallow tunnels in soil the lining is usually activated at distances from the face greater than this value, the errors involved in that simplifying assumption may not be very high. Moreover, for shotcret lining, its lower modulus at sections closer to the face, will further decrease the differences in the supported and unsupported tunnel closures, in the section the lining is activated. This fact was demonstrated by Erdmann (1983:189) for a non-uniform in situ stress condition. For these reasons, it is believed that possibly, a more critical issue is the linear elastic material assumption made by most of the available solutions.

Through this brief review, it is readily recognized that most of the methods available for the prediction of radial displacements at the tunnel contour which account for the 3D mechanisms involved, are of little help for the solution of the problem at hand. For instance, most methods disregard the presence of the ground surface and the action of the gravitational stress gradients which are always present in a shallow tunnel situation. A large number of solutions were developed to be used in connection with the Convergence - Confinement Method, and the assumption of uniform stress field is far too restrictive for application to the present problem. For the above reasons, it was felt that there was a need to develop another solution, especially designed to the purpose in mind. For convenience, it was decided to attempt this development, making use of three-dimensional finite element modelling. A concise evaluation of former studies using thise type of numerical simulation is included in the following section.

5.3.3 Review of Three-Dimensional Modelling by the Finite Element Method

Following the previous review of two-dimensional modelling studies presented in Section 5.2.1, this section attempts a comprehensive, but not exhaustive assessment of three-dimensional modelling of shallow tunnels driven in soil. Some of the studies referred to herein have already been discussed in Sections 2.3.6 and 4.3.2.6. In particular, Section 2.3.6 covered the main aspects of the three-dimensional stress redistribution and induced displacements associated with the advance of a tunnel. The approximate account for these processes in two-dimensional analyses was discussed in Sections 4.3.2.7 and 5.2.1.1.

In this section, the discussion will focus mainly on the applications of three-dimensional finite element solutions to shallow tunnels in soil. Reference will be made however, to other types of tunnelling conditions, whenever they present sufficient generality to contribute to the subject being focused on. Those studies involving fully axisymmetric assumptions, both in terms of geometry and loading conditions, will not be reviewed. Some of them (for instance, Daemen and Fairhurst, 1972, Panet and Guellec, 1974, Ranken and Ghaboussi, 1975, Schwartz and Einstein, 1980:47, Hutchinson, 1982, and others), have been referred to or partly reviewed (for instance, Sections 2.3.6.1, 2.3.6.2, 4.3.2.7 and 5.3.2). On the other hand, those axisymmetric analyses that consider non-axisymmetric loading assumptions will be referred to herein, as they provide some generality.

Table 5.28 summarizes some representative studies carried out over the last decade, where the use of three-dimensional finite element analyses was made. The studies were classified into three categories, according to their main purposes:

1. Prediction: cases where the aim of the study was mainly an attempt to anticipate the behaviour of a particular tunnel case history, allowing a comparison between calculated and observed performances.
2. Investigation of Behaviour: refers to the cases where

the analyses were conducted mainly to achieve or improve the understanding of some mechanisms or the features of behaviour of tunnelling under idealized conditions.

3. Generalization: cases where an attempt was made to develop some procedure or method that could be generalized and applied to conditions other than that assumed in the actual numerical analyses.

Although most of the cases reviewed could be classified in more than one category, the purpose of the analyses indicated in Table 5.28 reveals which was understood as the main objective of the study conducted.

Most of the cases reviewed used a linear elastic stress-strain model for the ground, assuming a constant elastic modulus or an increasing modulus with depth. The high cost of 3D analyses seems to be the main factor leading to this preference. Even so, a few studies took into account the non-linear behaviour of the ground, by using elasto-plastic or non-linear elastic models. In all cases, the lining was represented by a linear elastic material. In most cases, a constant liner modulus was assumed, but in cases 4, 12 and 14, a variable E modulus was considered, by assigning an increasing value for points at increasing distance from the face. This reflects an attempt to simulate the hardening of shotcrete with tunnel advance.

In the cases where the simulated tunnel was left unsupported and the ground was assumed to be elastic, there was no need to simulate the incremental construction as

	Reference	Purpose of Analyses	Soil Stress-Strain Model	Simulation	Finite Element Features	Comments
1.	Wittke et al. (1974) Wittke (1977:624)	Prediction (type A)	Linear elastic (constant E)	Single step excavation and simultaneous lining application(shallow circular tunnel)	Symmetric mesh, 3.1 x x 4.6 x 6.9D[1]	Analysis of initial length of the Altmuhl Tunnel in W. Germany (clay and sandstone). Poor agreement with measurements attributed to K_0 being higher than what was assumed. Moreover, construction sequence not simulated.
2.	Descoeudres (1974)	Generalization	Linear elastic (constant E)	Unsupported full face excavation in a single step. No gravitational stress gradient (deep circular tunnel).	A quarter sector mesh, 2 x 2 x 4.8D; isoparametric elements; coarse discretization	Parametric analyses, K_0 varying from 0.25 to 1.0. Radial displacements at crown and springline, for sections at different distances to the face. A single elasto-plastic anlaysis was carried out for comparison.
3.	Wittke & Pierau (1976)	Prediction (type C1)	Linear elastic-plastic (approx.) constant E	Single step excavation and simultaneous lining installation. Construction process accounted for by an interative procedure, where changing displacement boundary conditions are used (shallow tunnel).	Symmetric mesh 3.3 x 4.8 x 6.7D (525 nodes)	Analysis of the central length of the Altmuhl Tunnel in W. Germany (sandstone and clay). Simulation procedure allows the use of a smaller mesh. Anchoring and water level lowering considered. Ground displacement generally underestimated. In broad terms a favourable comparison with measurements.
4.	Gartung et al (1979) Bauernfeind et al (1986)	Investigation of behaviour	Linear elastic brittle-plastic (increasing E with confinement)	Incremental construction simulation with heading and bench excavation, delayed shotcrete application (concrete modulus varying with advance) and and delayed anchor installation.	Symmetric mesh; 1.6 x 2.4 x 2.7D (816 elements) PAM-NL program	Evaluation of potential stability problems of a large cross section tunnel of the Nuremberg Subway, under reduced ground cover (Keuper sandstone). The effects of delaying shotcrete or anchor installation were studied. Results indicated the need to consider the 3D loading conditions of the shotcrete shell at the tunnel heading.
5.	Baudendistel (1979, 1984, 1985)	Generalization	Linear elastic (constant E)	Unsupported non circular excavation in three steps: heading, bench and floor (each one in a single step) No gravitational stress gradient (deep tunnel).	Symmetric mesh; 3.5 x 3.5 x 3D (1326 nodes and 1012 isoparametric elements), SAP4 program	Analyses designed to develop ground stress reduction factors for lining design, as a function of the point of lining installation. K_0 = 0.5. Different factors for crown, springline and floor (see Section 4.3.2.7).

Table 5.28 Review of Some Three-Dimensional Finite Element Simulations of Tunnel Construction

Reference	Purpose of Analyses	Soil Stress-Strain Model	Simulation	Finite Element Features	Comments
6. Semprich (1980:161)	Investigation of behaviour	Elasto-plastic (Mohr Coulomb for failure and yield, assoc. flow rule) (constant E)	Simulation procedures similar to 3 above (non circular shallow tunnel)	Symmetric mesh; 3 x 4.2 x 3.6D (isoparametric elements); FEST03 program (Aachen) 704 nodes.	Evaluation of the effect of full face excavation with vertical and inclined tunnel face on the ground response. The effect of delaying the support application was also studied. Analyses applied to a particular tunnel case (a S-Bahn tunnel with 55 m^2 in silt).
7. Meister and Wallner (1977)	Prediction (type C1)	Elastoplastic	NA	Symmetric mesh; 2.4 x 3.2 x 2.6D (650 nodes, 444 elements).	Analysis of a test tunnel in the initial portion of the main Butterberg tunnel in W. Germany (sandy silty gravel). Poor agreement of lining loads and settlements.
8. Katzenbach (1981) Katzenbach & Breth (1981 and 1983)	Prediction (type C1) and investigation of behaviour	Non-linear elastic (Duncan & Chang, 1970)	Incremental construction simulation (stress reversal), with full face stepwise excavation and delayed shotcrete application (constant modulus).	Symmetric mesh; 5.2 x 5.2 x 8.8D, 990 elements with 6 or 8 nodes each; STATAN-15 program (Darmstadt)	Analysis performed to represent a typical NATM construction in Frankfurt clay. Despite simplified, non-staged sequence of construction, very favourable agreement with observations was obtained. No comparison made between calculated and measured lining loads.
9. Pierau (1981, 1982)	Generalization and investigation of behaviour	Linear elastic (constant E)	Simulation similar to 3 above. Shallow tunnel with non-circular cross section $K_0 = v/(1-v)$.	Symmetric mesh; 3 x 3.7 x 4D; isoparametric elements, lining forces and bending from plate elements loaded by calculated displacements, FEST03 program (Aachen), 666 nodes.	Parametric study designed to yield lining thrusts and bending moments at certain points of the lining, as well as maximum surface settlements. Generalization for certain ground covers, lining thicknesses, soil and lining properties, and for a fixed tunnel cross section (see Section 4.3.2.6).
10. Hanafy & Emery (1982, 1980)	Investigation of behaviour	Elastic-plastic (Von Mises, failure and yield criteria) with creep.	Incremental construction simulation, with full face stepwise excavation and delayed liner installation. One excavation step for unlined tunnel case. Axi-symmetric analyses of a deep tunnel with plane symmetric (non-axisymmetric) stress field.	Axisymmetric mesh; 3.5 x 3.5 x 6.4D (equivalent solid dimensions); tri-angular axisymmetric ring elements.	Parametric study conducted for a particular tunnel geometry and ground properties typical for a siltstone. The effect of non hydro-static initial stress field (both in longitudinal and transversal planes) on radial displacements was studied (K_l from 0 to 2 and K_t from 0.75 to 1.25). Also studied the influence of delayed lining installation and of different face advancement rates.

Table 5.28 Review of Some Three-Dimensional Finite Element Simulations of Tunnel Construction (Continued).

Reference	Purpose of Analyses	Soil Stress-Strain Model	Simulation	Finite Element Features	Comments
11. Kasali & Clough (1983)	Investigation of behaviour	Linear elastic (increasing E with depth)	Simulation starts with lining and TBM already in place (tunnel partly built and no gravity). A single step advance is then made (stress reversal) Final displacement field by superposition of results of single step advance.	Symmetric mesh; 4.7 x 3.1 x 7D; isoparametric elements with variable number of nodes (8-21) for soil and lining; modified version of SAP IV program.	Comparative analyses of ground response to tunnelling by conventional TBM, slurry and earth pressure balance shields in soft clay. Numerical solution is approximate as the superposition of displacement is not strictly correct. Losses of ground admitted to develop only at the face and at the tail void.
12. Erdmann (1983) Erdmann & Duddeck (1984)	Generalization	Linear elastic (constant E)	Axisymmetric analyses of a deep tunnel with plane symmetric (non-axisymmetric) stress field as in 10. Incremental construction simulation, with full face stepwise excavation, delayed shotcrete application (varying modulus with advance).	Axisymmetric mesh, with equivalent solid dimensions of 4 x 4 x 5D; program derived from multi-purpose code available in Braunschweig.	Analyses conducted to furnish reduction factors to be applied to the thrusts, bending moments and radial displacements obtained from ring and plate analytical models (see Section 4.3.2.6).
13. Eisenstein et al (1984); Heinz (1984:173) Present study (Section 2.3.6.4)	Investigation of behaviour	Linear elastic (increasing E with depth)	Incremental construction simulation (general approach), with full face stepwise excavation and delayed lining installation (constant modulus).	Symmetric mesh, 3.5 x 4.6 x 4.1D, 8 nodes solid elements for soil and lining; ADINA program (750 nodes).	Evaluation of the ground-lining response under 3D stress transfer conditions, in terms of radial stress-displacement relations, for points of the tunnel contour. Comparisons between 2D and 3D analyses (see Section 2.3.6.4).
14. Schikora (1984)	Investigation of behaviour	Elasto-plastic (constant E Mohr-Coulomb)	Incremental construction simulation, with full face and heading and bench stepwise excavation, delayed shotcrete application (varying modulus).	Not available.	Comparative study of lining response to two different construction schemes, accounting for change in shotcrete modulus with the advance. Assessment of thrust variations in the longitudinal direction, in each support ring. Thrust concentration in leading edge of lining.
15. Heinz (1984:148)	Prediction (Type C1)	Linear elastic (increasing E in depth)	Incremental construction simulation with heading and bench stepwise excavation (general approach) and delayed shotcrete application (with constant modulus).	Symmetric mesh, 3.5 x 4.6 x 5.2D, 8 nodes solid elements for soil and lining; ADINA program (850 nodes).	Analysis applied to the ABV tunnel (clayey sand). Ground displacements at the tunnel face reasonably predicted. Final ground movements underpredicted.

Table 5.28 Review of Some Three-Dimensional Finite Element Simulations of Tunnel Construction (Continued).

Reference	Purpose of Analyses	Soil Stress-Strain Model	Simulation	Finite Element Features	Comments
16. Negro et al. (1985 and 1986) Present study (Section 5.3.5)	Generalization	Linear elastic (Increasing E with depth)	Unsupported circular excavation of shallow tunnel in in a single step. Incremental excavation as in 13 above for lined tunnel cases. Gravitational stress gradient.	Symmetric mesh, 3.5 x 4.6 x 4.1D, 8 nodes solid elements for soil (and lining), 750 nodes; ADINA program.	Parametric analyses yielding a procedure for estimating radial displacements at the tunnel face contour. Consider variable soil cover and variable K_0 values given by (v/1-v). The procedure was applied to about 50 case histories and yielded reasonable estimates.
17. Swoboda (1985)	Investigation of behaviour	Linear elastic (?)	Incremental construction simulation with sequential face excavation and delayed lining application.	376 solid isoparametric elements for the soil and 84 shell elements for the lining. FINAL program (Innsbruck).	Investigation of ground movements immediately ahead of the tunnel face. Excessive soil heave below tunnel floor attributed to unrealistic material properties.
18. Pelli et al (1986)	Investigation of behaviour	Linear elastic (Constant E)	Incremental construction simulation with full face stepwise excavation (general approach) and delayed lining application (constant modulus). Deep tunnel and K_0 = 2 (constant).	A quarter sector mesh, 8 x 8 x 10D, isoparametric solid elements with 8 to 21 nodes; two slices of elements between tunnel face and liner; shell elements representing liner.	Study of mechanisms of stress redistribution process near the tunnel face, for a rock tunnelling situation. Detected radial stress and displacement reversals (to compression) are important for instrumentation analyses. Lining thrust concentrations detected in leading edge of liner, as in 14 above. Thrusts found to depend on round length (depth of advance).
19. Pelli (1987)	Investigation of behaviour	Linear Elastic (isotropic and anisotropic); non-linear elastic; elastic-plastic	Deep circular tunnel. Unlined opening. K_0 = 2. Incremental excavation for for non-linear rock.	Same as above except liner not represented.	Study to provide tools for monitoring data interpretation, including procedure for back-analysis of rock strength and deformational properties. Assessment of the influence of some factors such as the in situ stress state, anisotropy and non-linearity of the stress-strain relationship. Back-analysis of the Donkin-Morien Tunnel (Nova Scotia).

Note: (1) Dimensions of mesh in tunnel diameters (D): width x height x length.

Table 5.28 Review of Some Three-Dimensional Finite Element Simulations of Tunnel Construction (Continued).

explained in Section 2.3.6.4. The excavation was therefore simulated in a single step, on the assumption that the solution of the problem is unique. Ishihara (1971) formally proved the uniqueness of the solution of an excavation problem, assuming the ground to be linear elastic (for a loading which is not path dependent). However, as shown by Ghaboussi and Pecknold (1984:2052), depending on the numerical procedure representing the excavation, the resulting solution may be step-size dependent. As discussed in Section 5.2.1.1, strictly speaking, only the general approach of excavation simulation (see Table 5.2) is step-size independent.

Except for case 1, all other lined cases were simulated through an incremental advance of the tunnel heading followed by an incremental advancement of the lining, which resembles the actual tunnel construction. In order to reduce the cost of the analyses, cases 3, 6 and 9 made use of an expedient through which is avoided the continuously changing geometry of the problem (represented numerically by deactivation and activation of elements). The stiffness matrix of the problem is kept constant, but changing displacement boundary conditions are applied to the tunnel problem according to the displacement output obtained in the previous step, which are then used as an input for the following step. An interactive procedure was developed where the convergence of the solution is monitored through the differences between input and output displacements.

In case 1, a single step excavation and simultaneous lining application was performed. As noted by Wittke and Pierau (1976:1409) and Pierau (1982:1223), the ground displacements taking place before lining installation are not accounted for, and therefore the final calculated movements are too small and the lining stresses too high. To better portray the actual problem, an incremental construction simulation has to be performed for lined tunnels, even if the material behaviour is linear elastic. Having this in mind, the solution adopted in case 11, where the final displacement field was obtained by the superposition of results of a single step advance, is not accurate. Moreover, the numerical superposition is not rigorously valid, since there is a geometric non-linearity resulting from the changing geometry of the problem during the numerical incremental simulation. This inaccuracy however, does not invalidate the conclusions of the comparative study as the same approximation was applied to all cases of TBM performances considered.

With the exception of cases 2, 5, 10, 12, 18 and 19, the studies considered the gravitational in situ stress gradients across the opening, and are therefore actual shallow tunnel analyses. Among these, cases 10 and 12 represent a special type of 3D analysis. They assumed the problem to be geometrically axisymmetric, and made use of solid ring elements with triangular cross sections (Erdmann, 1983:150). However, as explained in Section 4.3.2.6, the solution considers that the stress field is non-symmetric (K_0 not equal to 1), with the stresses and displacements being expanded into Fourier Series.

Very limited data are available to serve as a guide for a 3D mesh design. The 'German Recommendations for Underground Constructions in Rock' (DGEG, 1979:198) provide some indications on where to locate the boundaries in a three-dimensional analysis. According to them, for a symmetric mesh, the width should be greater than or equal to three times the opening diameter (D) and the length of the discretized block along the tunnel axis, should be greater than or equal to 4D. The meshes used in the cases included in Table 5.28, had widths varying between 1.6D (case 4) and 8D (cases 18 and 19), and lengths between 2.7D (case 4) and 10D (cases 18 and 19). In terms of element densities, case 2 is noted as an extreme case of a coarse discretization, and case 8 is one of a refined mesh.

Comments have been appended to each case reviewed in Table 5.28, including indications of some of the main findings. One of them refers to thrust concentrations in the leading edge of a lining ring, noted by Schikora (1984:160) and also by Pelli et.al. (1986). This feature was already discussed in Section 2.3.6.3. Unlike Schikora (1984) who found that the liner was always being compressed, Pelli et.al. (1986) found that the trailing edge of the support ring was submitted to substantial tension. The latter would have resulted from the radial rebounding of the leading edge of the support ring immediately behind. This effect, highly consequential in practical terms, may by attenuated by the limited ability of some actual linings to transfer shear through the circumferential joints, in for instance, segmented concrete linings, or in young shotcrete. It would be interesting to know whether this effect persists for different K_o values, for round lengths (depth of tunnel advance) and support activation delays closer to those found in a soil tunnelling situation. This would be represented by a round length of less than half the tunnel radius, and a delay of about two to four tunnel radii.

5.3.4 Numerical Solution Adopted

For developing a procedure to estimate the convergence of the opening behind the face of a shallow tunnel, a three-dimensional finite element solution was needed. The multipurpose program ADINA (Bathe, 1978) was selected for this purpose. For convenience, the modelling procedures including mesh design, stress-strain relationships, construction simulation, etc., used by Heinz (1984:143, 176) were maintained in the present study.

Briefly, the numerical model treated the soil and the lining as isotropic linear elastic materials. Yet, to better represent actual field conditions, the soil modulus was allowed to increase with depth. The tunnel was driven with a shallow soil cover and a gravitational stress field was considered. A non-hydrostatic stress field was assumed with the in situ stress ratio, K, different from unity.

Finite elements with eight nodal points were used to represent both the ground and the liner. As noted by Heinz (1984:144), lower costs and simulation simplifications were the reasons behind favouring this simpler element type. Since the purpose of this study was mainly limit~~ed to the~~ displacements developing at the opening, the use of more convenient element types for lining stress evaluation was thought to be unnecessary.

The finite element mesh used is that shown in Figure 5.67, which is the same as used by Heinz (1984:180). The boundaries of the mesh were located following the German recommendations provided by DGEG (1979:198), as they are the only guidance available on the subject (see Section 5.3.3). The circular tunnel had an excavated diameter (D) of 3.9 m. The symmetric mesh had a width of 3.513 D and a length of 4.103 D. Two mesh heights were considered, the total element number being kept constant. The first, representing a shallower tunnel, had a cover to diameter ratio of 1.615 and is the one shown in Figure 5.67 (total height of 4.615D). The second mesh (not shown), representing a deeper tunnel, had a soil cover of 2.833D and a total height of 5.833D. This mesh was obtained from the former by shifting up the nodes located at the ground surface and on the horizontal plane immediately below. This was done in order to not increase the size of the problem and to avoid extremely elongated elements (the maximum aspect ratio allowed was

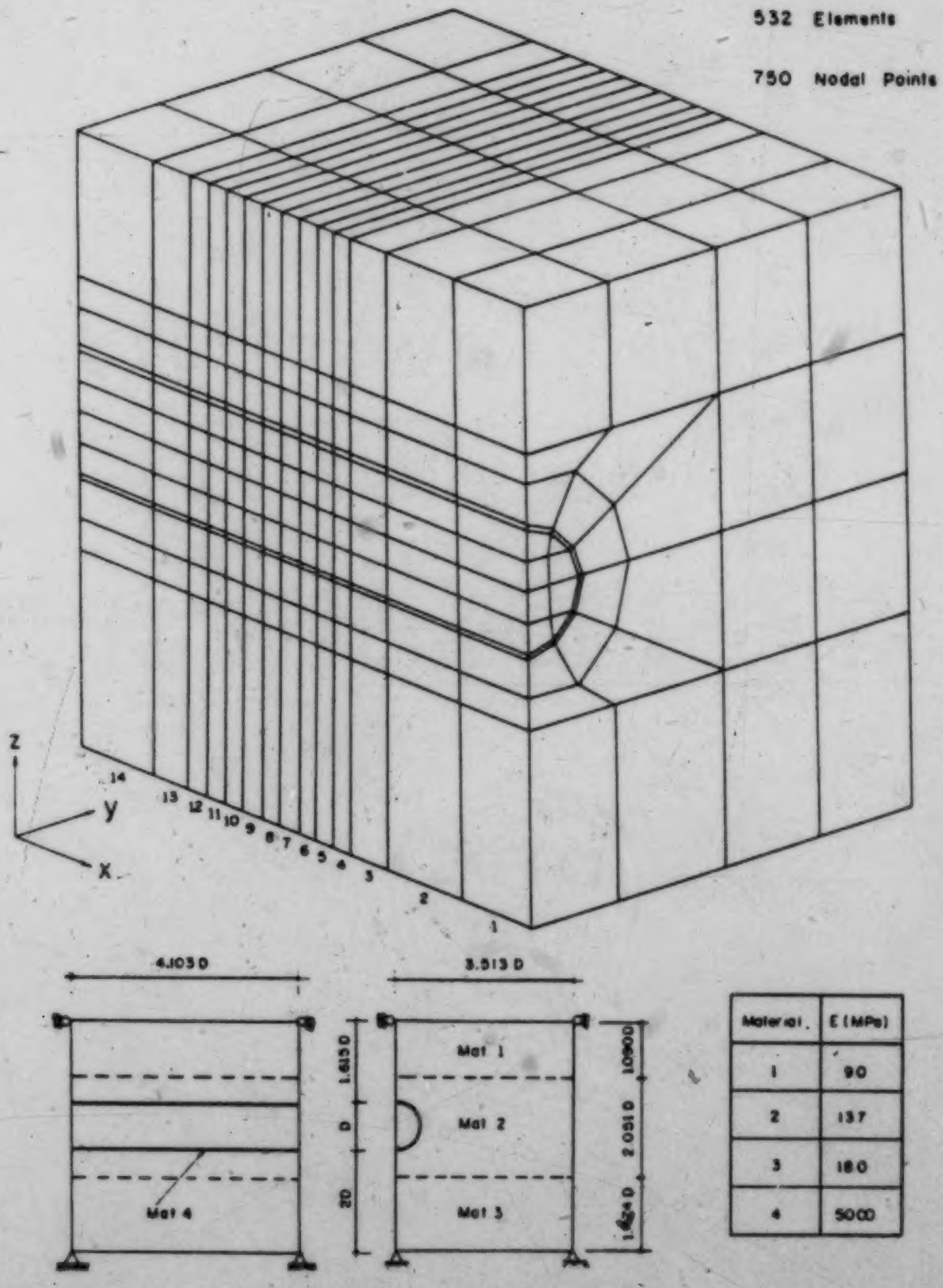
532 Elements
750 Nodal Points
z
y
x
14
13
12
11
10
9
8
7
6
5
4
3
2
1
4.103 D
3.513 D
1.615 D
D
2 D
1.090 D
2.051 D
1.624 D
Mat 1
Mat 2
Mat 3
Mat 4

Material	E (MPa)
1	90
2	137
3	180
4	5000

Figure 5.67 Three-Dimensional Finite Element Mesh and Input Parameters

10).

Each "slice" had 38 solid elements and the full mesh was made out 14 slices (a total of 532 elements). The transverse face of each slice contained 50 nodes, resulting in a 750 nodal point mesh. Compared to the discretizations used by other authors (Table 5.28), and as noted by Heinz (1984:143), this mesh presents an element density which is a compromise between relatively coarser meshes (e.g. Descoeudres, 1974) and finer ones (e.g. Katzenbach, 1981 or Pelli et.al. 1986). The slice thickness decreased towards the centre portion to 1/6 of the tunnel diameter and increased agains towards the opposite end. This resulted in a simulation of the construction sequence in the central area.

All analyses were conducted with a premliminary step corresponding to the establishment of the initial conditions. This was performed by the application of gravity and the in situ stress ratio, K, results as a function of the Poisson's ratio, ν. From then on, two types of construction simulation were implemented depending on the tunnel being lined or unlined. Both simulations assumed a full face excavation. For the unsupported case, there was no need to represent the incremental construction. The excavation was thus simulated in a single step, where the elements within the excavated contour were de-activated from slice 1 to slice 7. For the analysis of the lined tunnel, a stepwise de-activation of excavated elements was implemented, followed by the gradual and delayed (in space) activation of the support. The central part of the mesh was reached after 6 additional steps. In each step, elements of one or two consecutive slices were simultaneously activated and de-activated. This simulation procedure was identical to that used in the work by Eisenstein et.al. (1984), by Heinz (1984:176) and also described in Section 2.3.6.4. In the lined tunnel cases, due to the irregular thickness of slices used, to the varying number of slices being cut through by the excavation, and to the proximity of the boundaries, the radial displacements calculated at the first three slices were found to oscillate irregularly and were thus neglected. The results to be presented refer to the central portion of the mesh more densely discretized with equal thickness slices, through which the face was advanced with constant depth of advance, or round length (always equal to D/3).

The activation or de-activation of elements was performed by the ADINA program using its 'birth-death' option, which allows an excavation simulation that follows the 'general approach' procedure referred to in Section 5.2.1.1 (see Table 5.2). While the excavation round length for the lined cases was kept constant and equal to D/3, the support activation delay was varied in the analyses. Two maximum unsupported distances, L, between the face and the leading edge of the liner were considered: D/2 and 2D/3.

The arbitrary modulus of the materials represented are shown in Figure 5.67, and these were kept constant in all analyses. As it is seen, the ground modulus increased with depth in a discrete manner. The tunnel was totally driven through the material 2 layer. In the supported tunnel analyses, a lining with a thickness of 15 cm was selected. If a Poisson's ratio of 0.25 is assumed for both support and ground, the relative stiffness of the support calculated according to equations 2.17 and 2.18 result in C=0.034 and F=64.2.

In the analyses performed, different in situ stress ratios were considered by varying the Poisson's ratio accordingly. The original version of ADINA used in this work (Heinz, 1984:83), did not allow other approaches besides the "switch - on - gravity" (see Section 5.2.1.1) to represent the in situ stresses in a gravitational stress field. This is a clear shortcoming of the simulation procedure adopted: in actual cases K is independent of ν. The effect of changes in ν alone is however, known to be small at the face or ahead of it, as shown in Figure 5.66 (see also Ranken and Ghaboussi, 1975:3.13).

The assumption of linear elasticity is another drawback of the simulation adopted. The numerical simulation would then be valid only in the case of limited development of yielding zones around the opening. Thus, the results to be presented would be mainly applicable to stiff or dense soils, where a good ground control construction is implemented. It could also be applied to softer or weaker grounds if an internal pressure (compressed air or slurry) is applied to the tunnel walls and face, which would ensure a limited degree of yielding around the tunnel. Results from axisymmetric analyses (Ranken and Ghaboussi, 1975:3.32; Panet and Guenot, 1982:199), have shown that this is the case with tunnels in cohesive soils with stability ratios of up to 1.5. Under these conditions the plastic behaviour of the ground, ignored in the present study, would increase the radial displacements by no more than 20%.

The assumption of linear elaticity is perhaps less restrictive regarding the behaviour of the ground ahead of the face. Under good ground control conditions the amount of straining ahead of the advancing tunnel is limited and the deformation modulus of the soil could be taken as the initial tangent modulus (E) of a representative stress-strain curve of the soil around the tunnel.

5.3.5 Parametric Analyses

5.3.5.1 Analyses and Results

In order to investigate the influence and significance of distinct factors affecting the tunnel convergence, some parametric three-dimensional analyses were conducted.

The tunnel diameter (D) and the ground modulus (E) profile were kept constant in all analyses. With respect to the unlined tunnel cases, the assumption of linear elasticity makes the variation of the ground modulus unnecessary, as the displacements are linearly related to it (for a proportionally changed modulus profile). In the analyses, variations in the unsupported tunnel length (L/D), in the depth of ground cover (H/D) and in the in situ stress ratio ($K=\nu/(1-\nu)$) were allowed. Table 5.29 summarizes the details of the parametric analyses.

It is convenient to express the radial displacements of the tunnel contour in the dimensionless form presented by equation 2.16 in Section 2.3.4.3:

$$U(\theta)= \frac{u.E}{D.\sigma_0(\theta)}$$

where θ defines the point considered at the perimeter of the tunnel, $U(\theta)$ is the radial displacement of this point and $\sigma_0(\theta)$ is the in situ radial stress at that point. The elastic modulus E is the one attributed to the second material layer which fully surrounds the tunnel.

Figures 5.68 to 5.70 present the distribution of the dimensionless radial displacements along the tunnel, at three points of the tunnel contour (crown, springline and floor, respectively) for cases 1, 2 and 3 combined (H/D=1.6). The distributions shown are confined to the central region of the finite element element mesh (about 2D in extent). As explained in Section 5.3.4, the calculated radial displacements at the first three slices in the lined tunnel cases (1 and 2) are not representative and were therefore, disregarded. Nevertheless, the lined cases exhibit some oscillation in the radial displacement distribution, which was a feature explained in Section 2.3.6.3, and was found by other authors in similar studies.

Case	H/D	Type	L/D	ν	K
1	1.615	Lined	1/2	0.430	0.75
2	1.615	Lined	2/3	0.430	0.75
3	1.615	Unlined	-	0.430	0.75
4	1.615	Unlined	-	0.375	0.60
5	1.615	Unlined	-	0.459	0.85
6	1.615	Unlined	-	0.474	0.90
7	2.833	Lined	1/2	0.430	0.75
8	2.833	Lined	2/3	0.430	0.75
9	2.833	Unlined	-	0.375	0.60
10	2.833	Unlined	-	0.474	0.90

Notes: (1) D = 3.90 m
(2) In all cases E = 13,694 KPa around opening (material 2).
(3) In all cases γ = 15.19 kN/m^3 for material 1 and 18.13 kN/m^3 for materials 2 and 3.

Table 5.29 Cases of Three-Dimensional Analyses

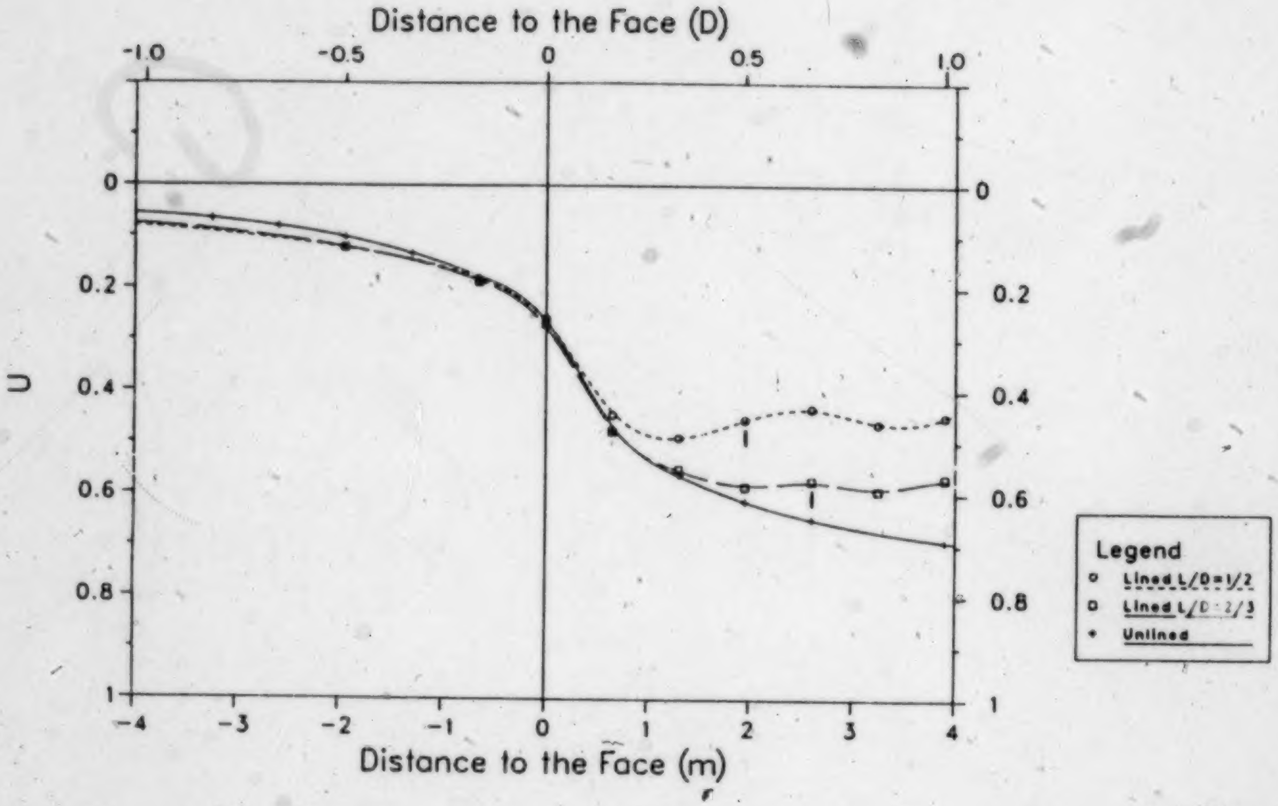

Figure 5.68 Dimensionless Radial Displacements at the Crown of a Lined and Unlined Shallow Tunnel (H/D=1.6 and K=0.75)

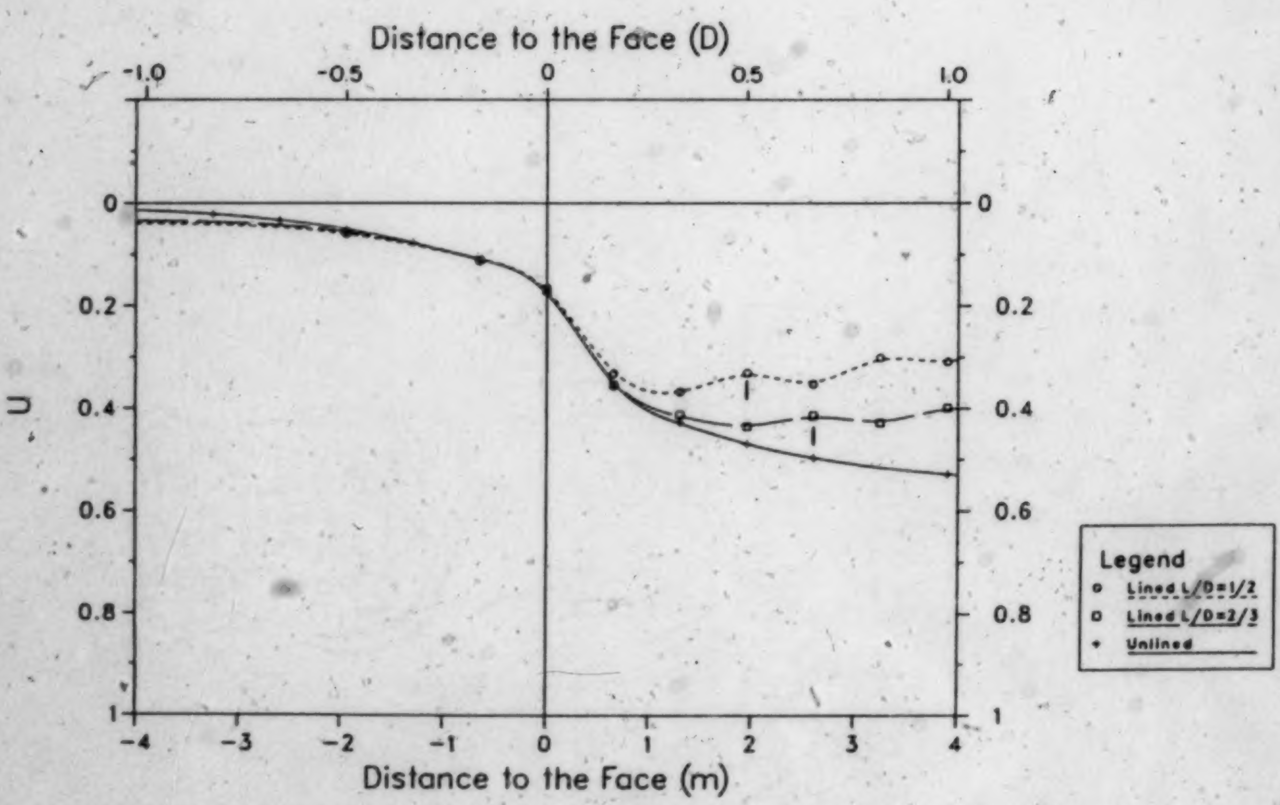

Figure 5.69·Dimensionless Radial Displacements at the Springline of a Lined and Unlined Shallow Tunnel (H/D=1.6 and K=0.75)

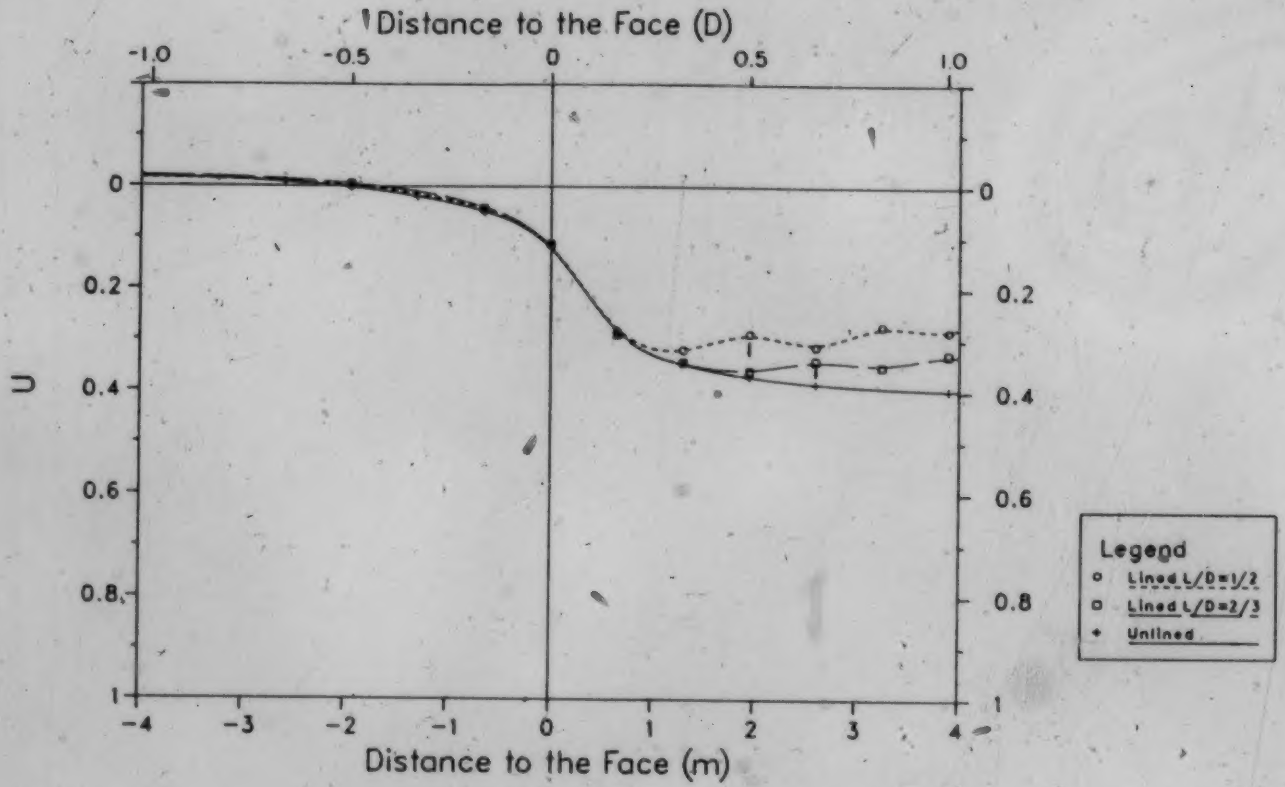

Figure 5.70 Dimensionless Radial Displacements at the Floor of a Lined and Unlined Shallow Tunnel (H/D=1.6 and K=0.75)

It is noted from these figures that the displacements ahead of the tunnel face are not affected much by the presence of the lining. The radial displacements at the face, in particular, are virtually unaffected by the distance to the point of lining placement. This finding confirms conclusions drawn by other authors. Ranken and Ghaboussi (1975:3.57, 3.58) showed that if the lining is installed at distances greater than half a tunnel diameter, the radial displacements at the tunnel face are not affected by the lining installation. Moreover, Erdmann and Duddeck (1984:180) showed that this seems to be correct irrespective of the lining stiffness. The results shown by Pelli et.al. (1986), who used a more refined finite element mesh, support these conclusions.

The same conclusions are drawn by comparing the results of cases 9 and 10, which refer to a deeper tunnel with H/D=2.8. These are shown in Figures 5.71 to 5.73. Note that in these figures, the solid lines represent the unlined case of the shallower tunnel (H/D=1.6). The only difference noted between the two sets of plots for the shallower and the deeper tunnel cases refers to the magnitude of the radial displacements, especially behind the face. Since the radial displacements were normalized to the in situ radial stresses, the effect of the stress level is fully accounted for. However, the effect of the ground surface is not. Therefore, the dimensionless displacements for the shallower tunnel would be expected to be larger than that for the

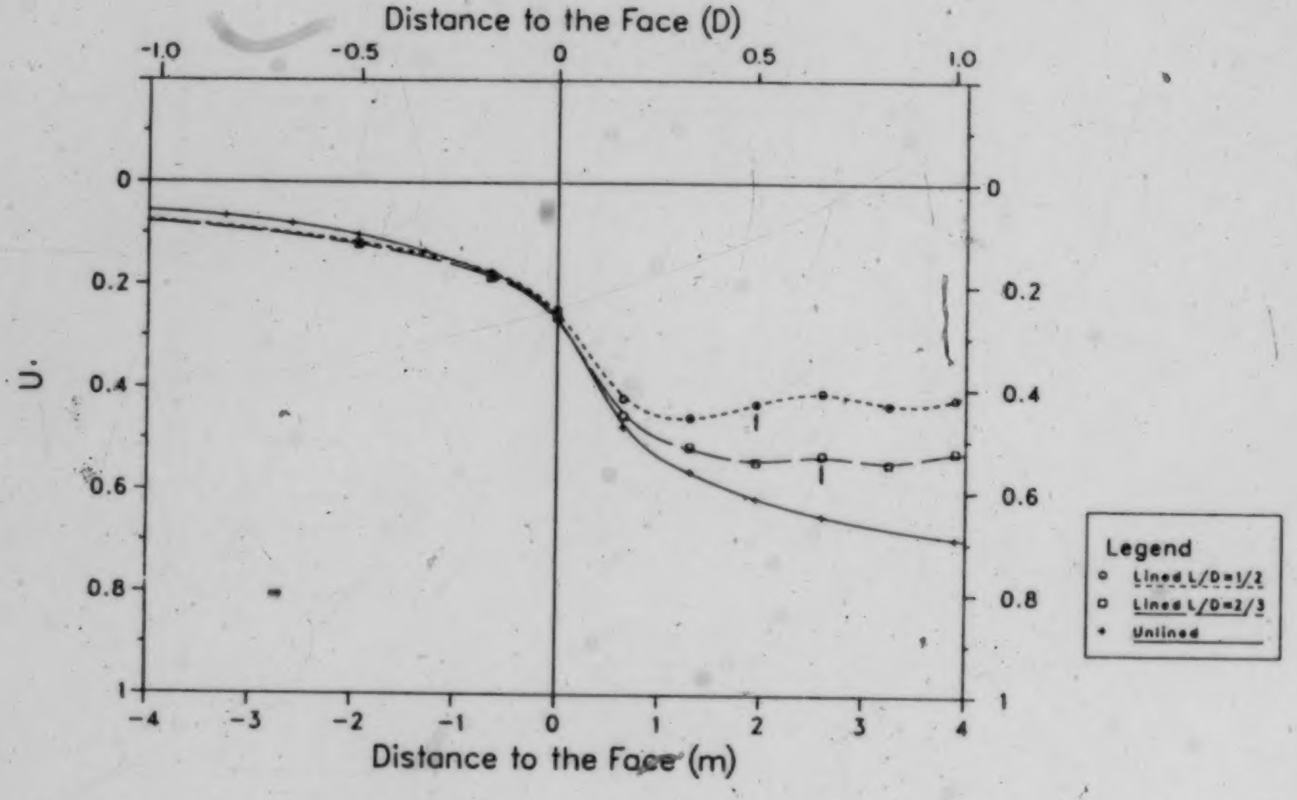

Figure 5.71 Dimensionless Radial Displacements at the Crown of a Lined and Unlined Deeper Tunnel (H/D=2.8 and K=0.75)

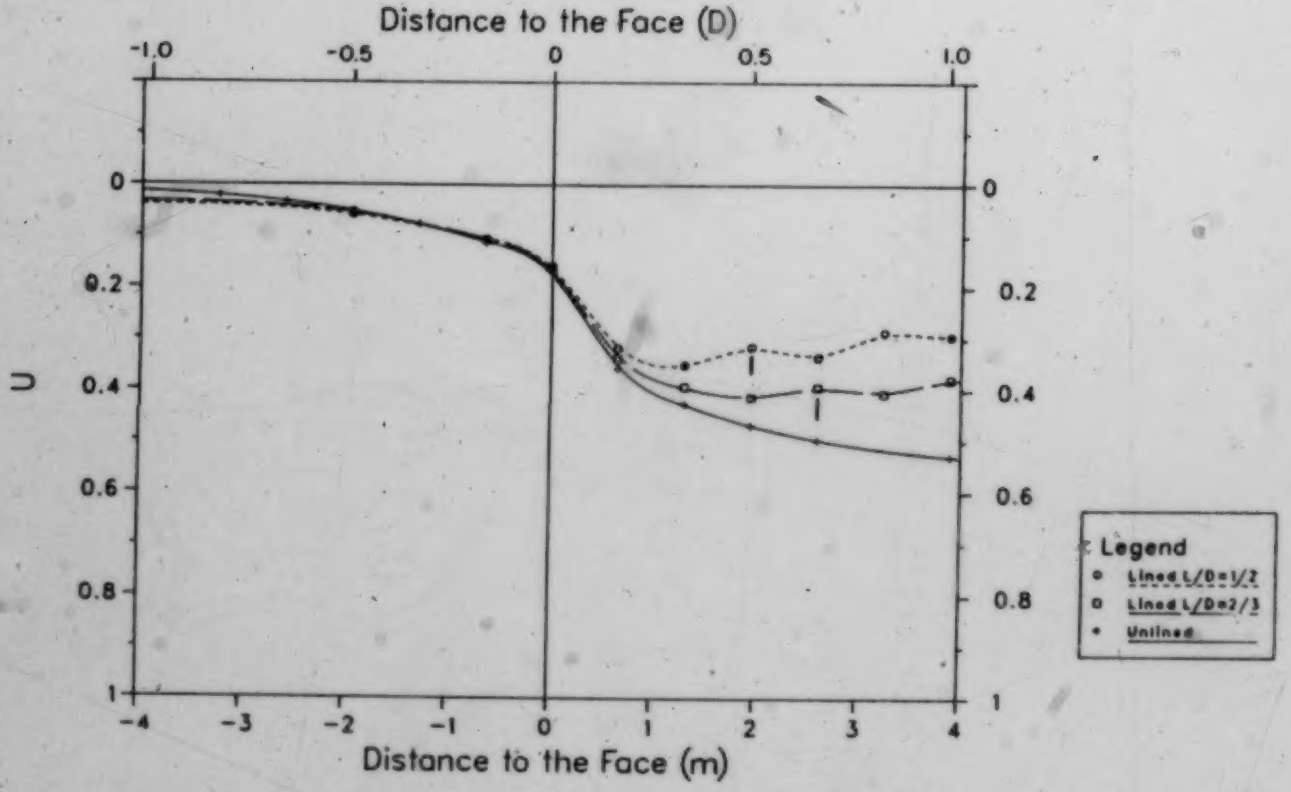

Figure 5.72 Dimensionless Radial Displacements at the Springline of a Lined and Unlined Deeper Tunnel (H/D=2.8 and K=0.75)

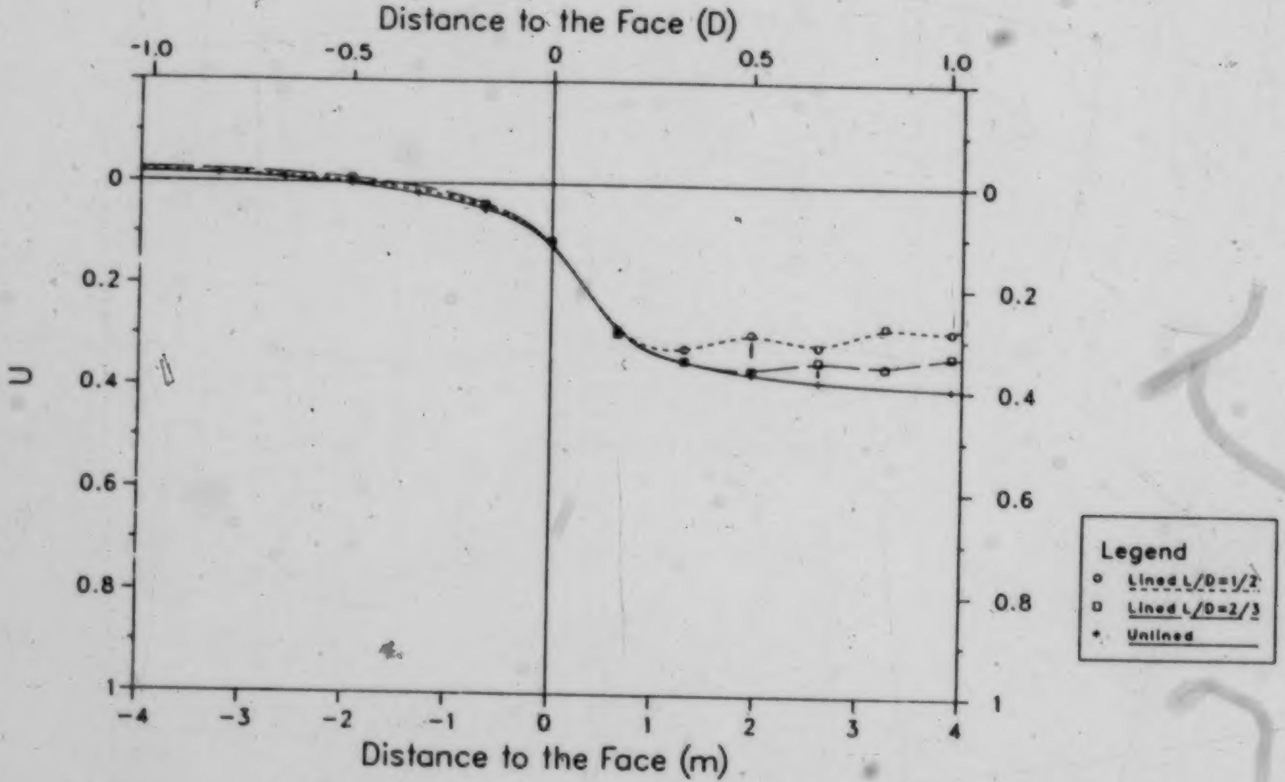

Figure 5.73 Dimensionless Radial Displacements at the Floor of a Lined and Unlined Deeper Tunnel (H/D=2.8 and K=0.75)

deeper configuration, as the thicker cover in the latter case offers a "stiffer" reaction to the stress changes. Notwithstanding this, it appears from the two sets of plots that the differences in the dimensionless displacements amount to less than 10%, for the range of cover to diameter investigated and for the other assumptions made. The difference in the displacements at the face are virtually nonexistent. These results are very much in agreement to what was discussed in Section 2.2. It was shown there that the influence of the ground surface on the behaviour of the lining or on the ground immediately around the opening is negligible for H/D greater than 1.5. The influence of the gravitational stress gradient, however, is evident. The ~~latter~~ is accounted for by using the radial stress at the point being considered, to normalize the corresponding radial displacement.

An additional conclusion from the last two sets of plots is that the tunnel closure at the point of lining installation is affected by the presence of the lining, as already discussed in Section 5.3.2. However, the relative error involved in estimates of the convergence assuming the tunnel is unlined, tends to decrease for increasing support delay lengths, L/D. If the unlined case results were to be used as a basis for evaluating the tunnel closure for a real situation, on one hand they would lead to an overestimate of the tunnel contour displacements. On the other hand, they could lead to underestimates, as the actual non-linear behaviour of the ground is not accounted for. A complete solution to the problem, including the lining action inhibiting the ground movements and the non-linearity of the soil behaviour which increases the movements with respect to the linear elastic solution, is not possible at the moment as it is too complex. As a compromise and as an ad interim solution, it will be assumed that those errors involved in a solution derived from linear elastic unlined tunnel analyses will be compensated for.

To illustrate the last point, Figure 5.74 has been prepared using data from Ranken and Ghaboussi (1975) axisymmetric analyses. The parameters used in these analyses are shown in the figure. The wall closures for an unlined tunnel assuming a linear elastic behaviour, are compared to that of two lined tunnels, with support installed at L/D=0.5 and where an elasto-plastic ground behaviour was assumed. In one case, a purely cohesive behaviour has been postulated and in the other, a c-ϕ material behaviour has been assumed. It is observed that at the point of lining application (0.5D), the dimensionless displacement of the unlined solution is almost equal to those obtained in the lined cases.

It should be pointed out, however, that the compensation for errors cannot always be conceded, as it depends on a number of factors. Thus, considerable caution should be exercised in any attempt to generalize the results of linear elastic unlined tunnel solutions to actual

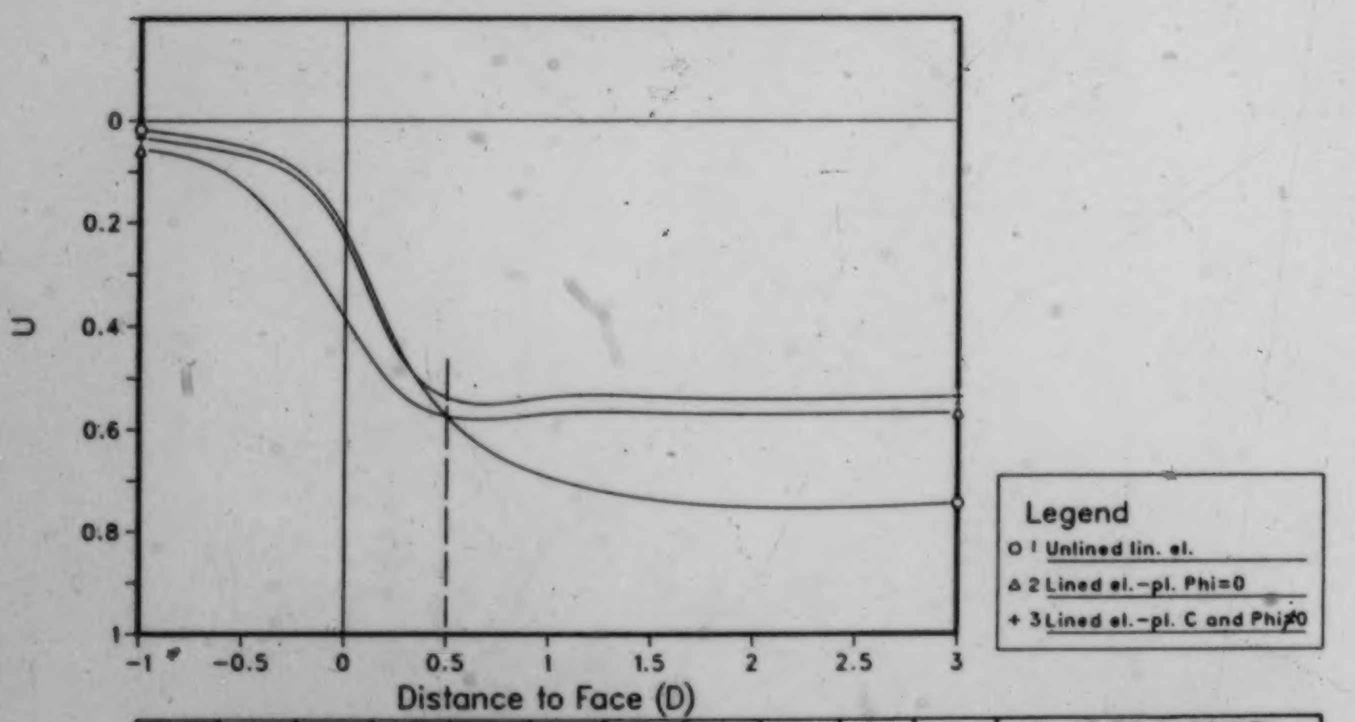

CASE	D (m)	q_0 (kPa)	K_0	E (kPa)	ν	C (kPa)	ϕ (°)	l_s (m)	E_s (GPa)	ν	No. OF FIG. IN RANKEN AND GHABOUSSI (1975)
1	6.096	575	1.0	34.5	0.49	-	-	-	-	-	3.7
2	"	"	"	"	"	96.5	0	0.305	13.8	0.15	3.38
3	"	"	"	"	0.40	"	30	"	"	"	3.47

NOTE; IN CASES 2 AND 3 THE LEADING EDGE OF THE SUPPORT IS LOCATED 0.5 D BEHIND THE FACE.

Figure 5.74 Closure of an Unlined Tunnel in Elastic Ground Compared to that of Lined Tunnels in Elasto-Plastic Material

problems.

The calculated dimensionless displacements at the crown of an unlined tunnel are shown in Figures 5.75 and 5.76, for the shallower tunnel situation (cases 3, 4, 5 and 6 in Table 5.29) and for the deeper cases (9 and 10) respectively. The differences in the distributions of the radial displacements are due to the differences in the in situ stress ratio K, but they also reflect the variation in Poisson's ratio. The influence of the latter is less pronounced since it was varied within fairly narrow limits (from 0.375 to 0.474). The error involved in neglecting the effect of the variation of the Poisson's ratio can be estimated in an approximate way from the solution presented in Figure 5.66, developed the analyses of a deep tunnel (Niwa et.al., 1979). Since in that solution K and ν are independent variables, the influence of each parameter can be assessed individually. For instance, assuming a K value of 0.75, an increase in the Poisson's ratio from 0.25 to 0.4 will cause an increase in the dimensionless radial displacement at the crown or at the floor of about 1.5% for a section at the tunnel face, and of about 4.4% at a section a half diameter behind the face. It will be noted that the influence of the Poisson's ratio is more pronounced on the springline displacements (approximately 4 times larger than at the crown). However, considering the approximate nature of the solution being sought, it will be assumed henceforth that the differences in the displacements shown in the last figures are mainly

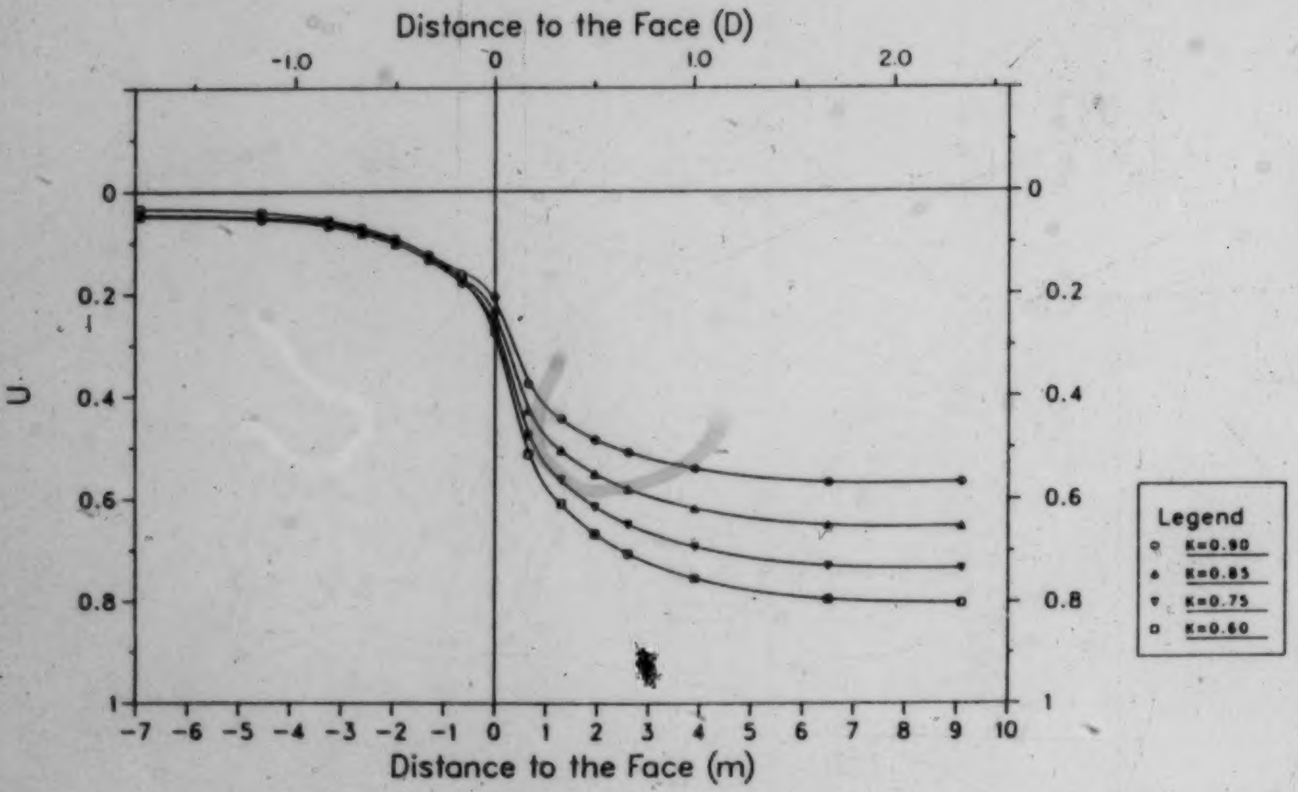

Figure 5.75 Dimensionless Crown Displacements of the Shallower (H/D=1.6) Unlined Tunnel for Different In Situ Stress Ratios K

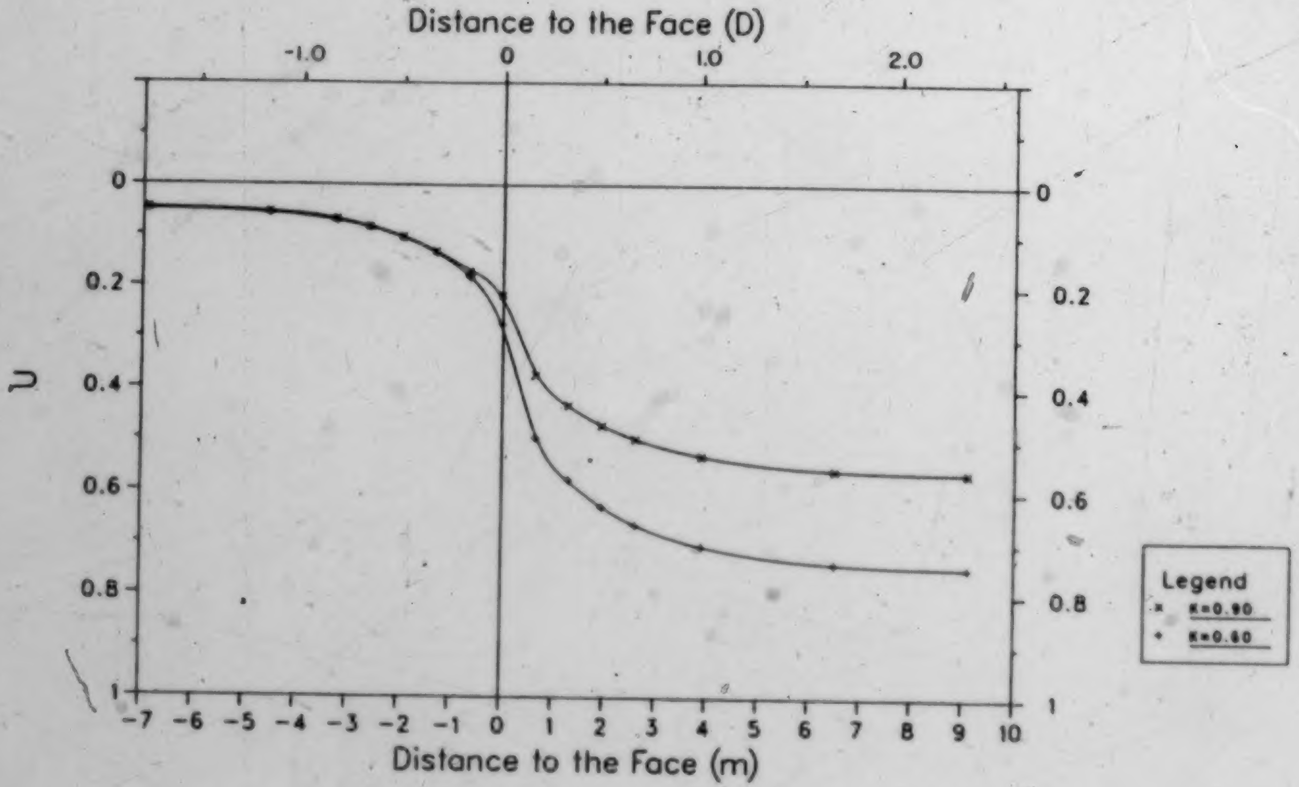

Figure 5.76 Dimensionless Crown Displacements of the Deeper (H/D=2.8) Unlined Tunnel for Different Stress Ratios K

due to the changes in the in situ stress ratio.

Similarly, Figures 5.77 and 5.78 present the dimensionless radial displacements at the springline of an unlined tunnel for the shallower and the deeper tunnel cases, respectively. It should be noted here that, unlike the deep tunnel solution for springline displacement shown in Figure 5.66, the present results of displacements have been normalized to the radial in situ stress at the tunnel springline. Therefore, if the present results are to be compared with those shown in Figure 5.66, they have to be multiplied by the corresponding K value.

Finally, Figures 5.79 and 5.80 furnish the dimensionless radial displacements at the floor of an unlined tunnel for the same cases.

The effect of the ground surface on the dimensionless displacements of the unlined tunnel can be evaluated by comparing the results obtained for the shallower and deeper tunnel cases. These comparisons are provided in Figures 5.81 to 5.83, for the crown, springline and floor of the tunnel respectively. As noted in the lined tunnel cases, the deeper the tunnel is, the smaller the dimensionless radial displacements are. The floor displacements are virtually unaffected by the position of the ground surface. Overall, the differences in the dimensionless radial displacements are relatively small for the two cover to diameter ratios considered, and these fairly well encompass the most frequent situations found in practice. Likewise, the range

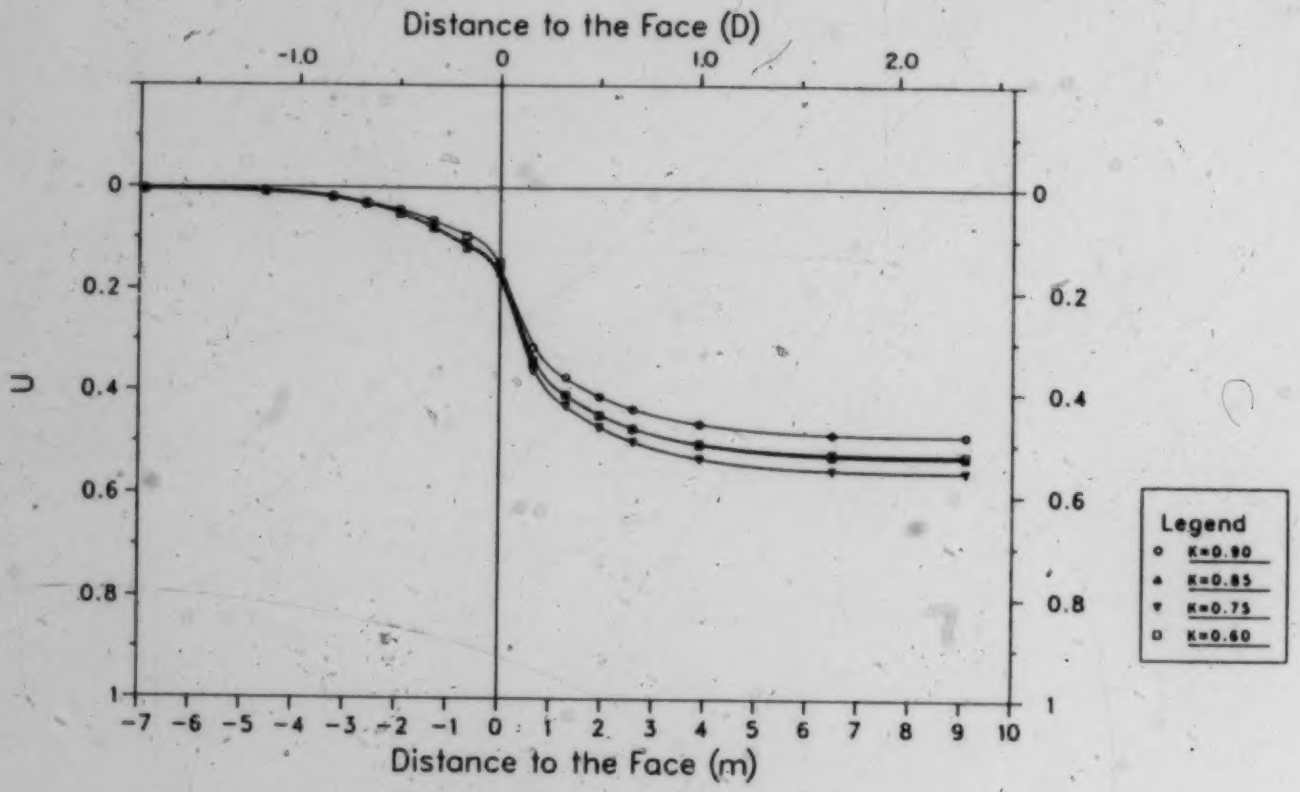

Figure 5.77 Dimensionless Springline Displacements of the Shallower (H/D=1.6) Unlined Tunnel for Different Stress Ratios K

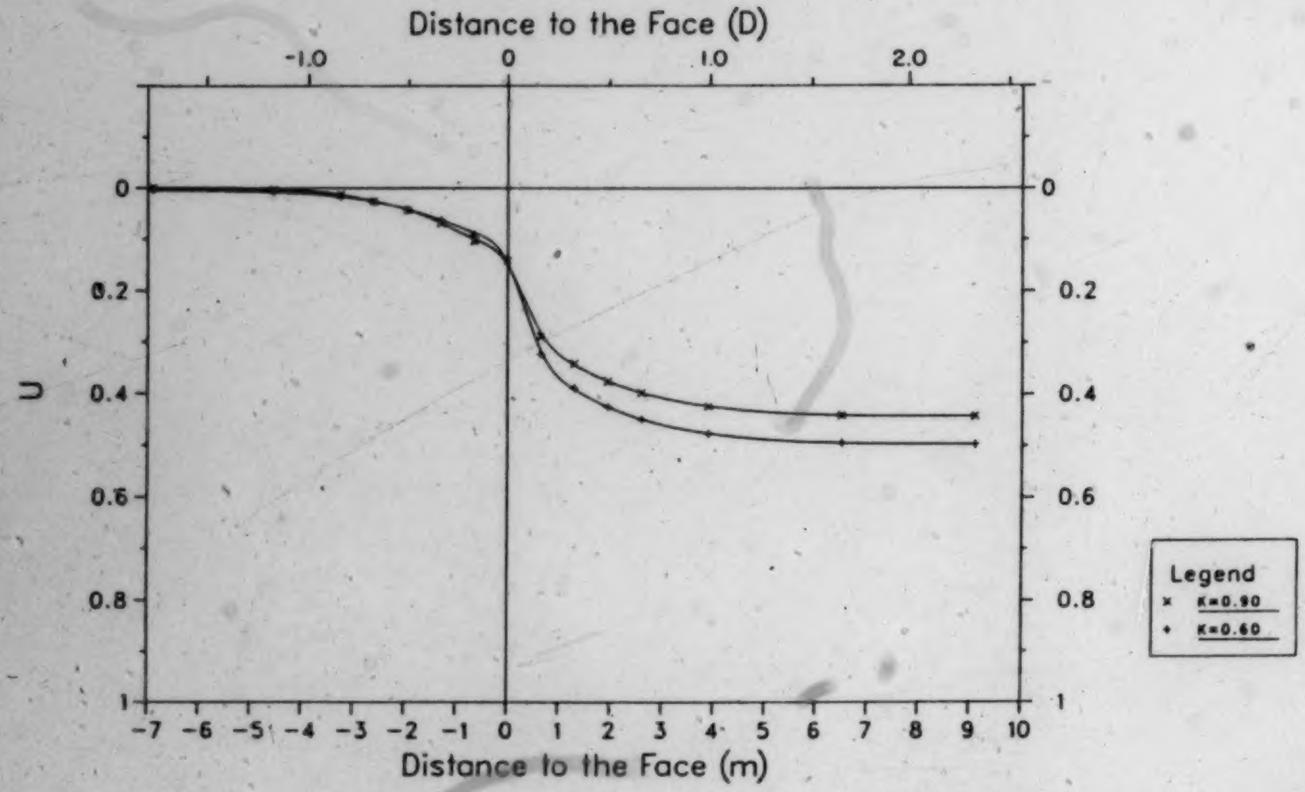

Figure 5.78 Dimensionless Springline Displacements of the Deeper (H/D=2.8) Unlined Tunnel for Different Stress Ratios K

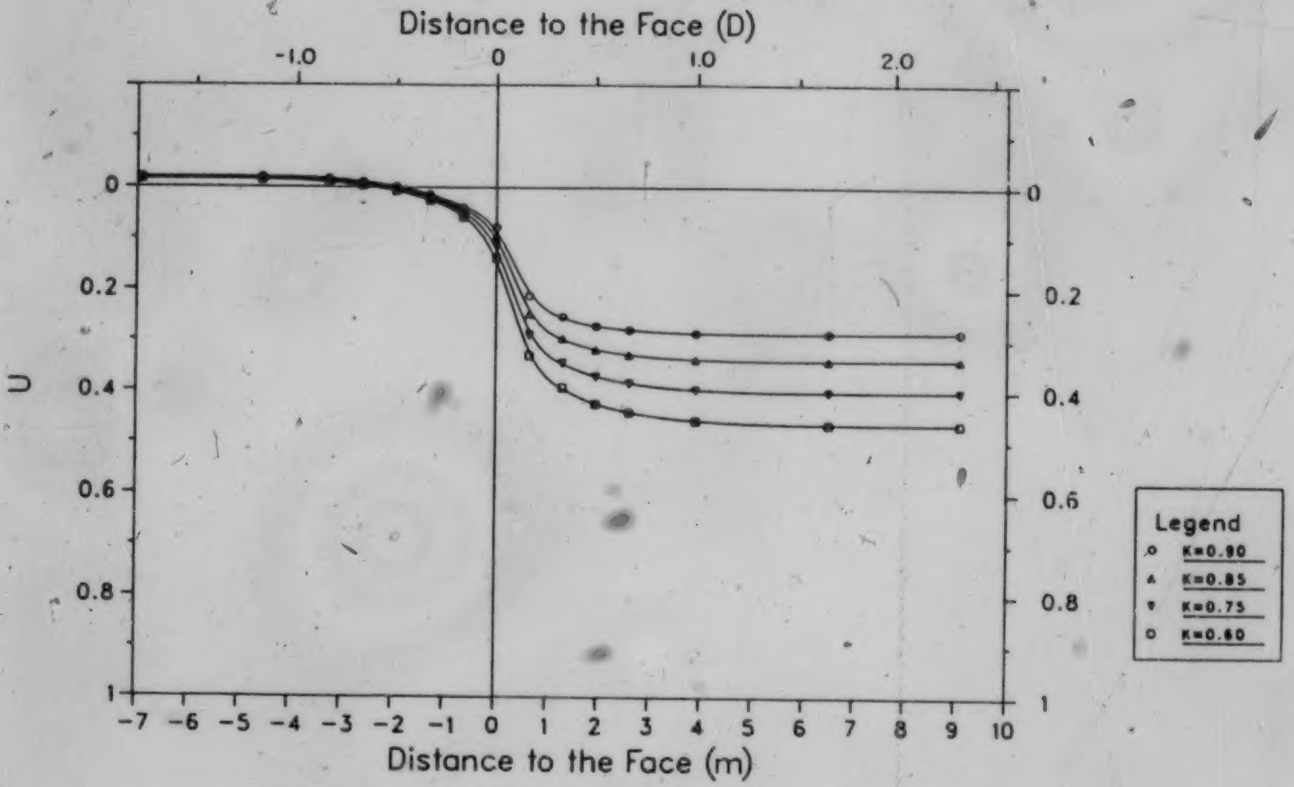

Figure 5.79 Dimensionless Floor Displacements of the Shallower (H/D=1.6) Unlined Tunnel for Different Stress Ratios K

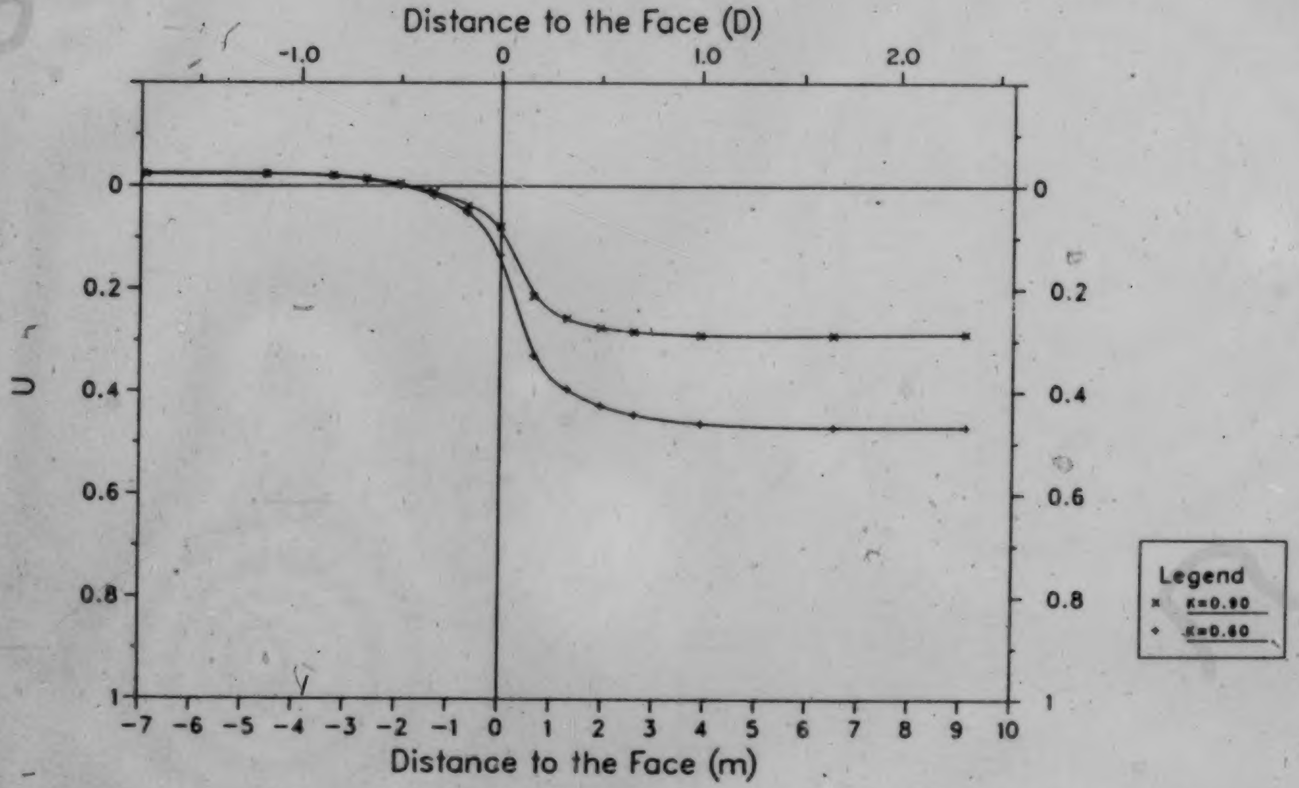

Figure 5.80 Dimensionless Floor Displacements of the Deeper (H/D=2.8) Unlined Tunnel, for Different Stress Ratios K

of the in situ stress ratio considered seems to also include a fairly large number of soil conditions found in practice.

So far the data presented refer to the radial displacement at the tunnel contour. To supplement this information, Figures 5.84 and 5.85 were prepared. They present additional data on the ground displacements around the unlined tunnels. For convenience, the displacements are presented in dimensionless form, and were normalized to the in situ radial stress at the crown of the tunnel. In these figures, the vertical ground movements, either settlement or heave, at four vertical sections are shown, as well as the longitudinal distributions of displacements at the ground surface and at the crown elevation, for the two extreme values of K considered in the parametric analyses. The horizontal displacements of the tunnel face are also presented. The effect of increasing the cover to diameter ratio is apparent by comparing those two figures. The dimensionless displacements tend to decrease everywhere. Ground distortions at the surface or at the crown elevation also decrease. A similar effect is noted by increasing the in situ stress ratio, except with respect to the face horizontal movements, which tend to increase with increasing K.

5.3.5.2 Interpretation of the Results

Closure of an Unlined Tunnel

It was shown in the previous section (Figure 5.65) that for an unlined and ideally deep tunnel, a linear

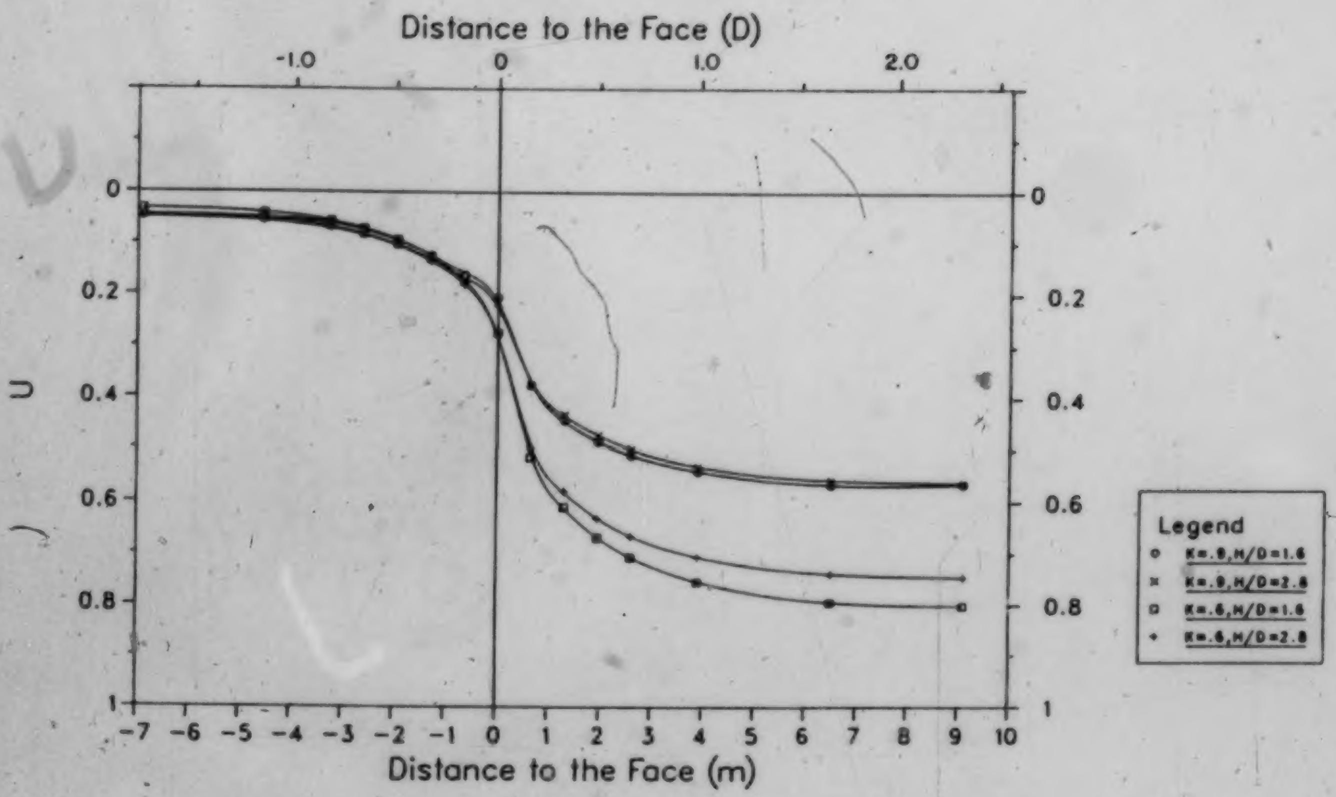

Figure 5.81 Comparison of Dimensionless Crown Displacements of the Shallower and Deeper Unlined Tunnels

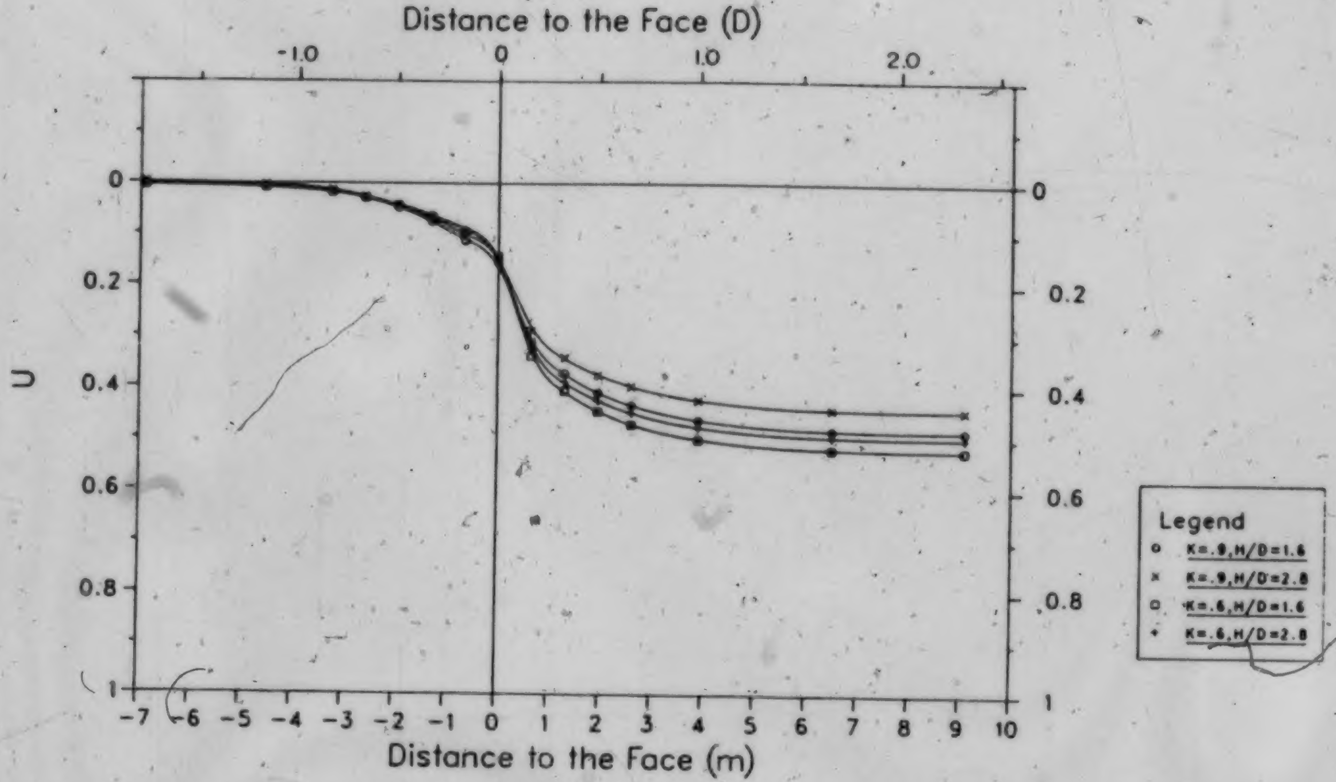

Figure 5.82 Comparison of Dimensionless Springline Displacements of the Shallower and Deeper Unlined Tunnels

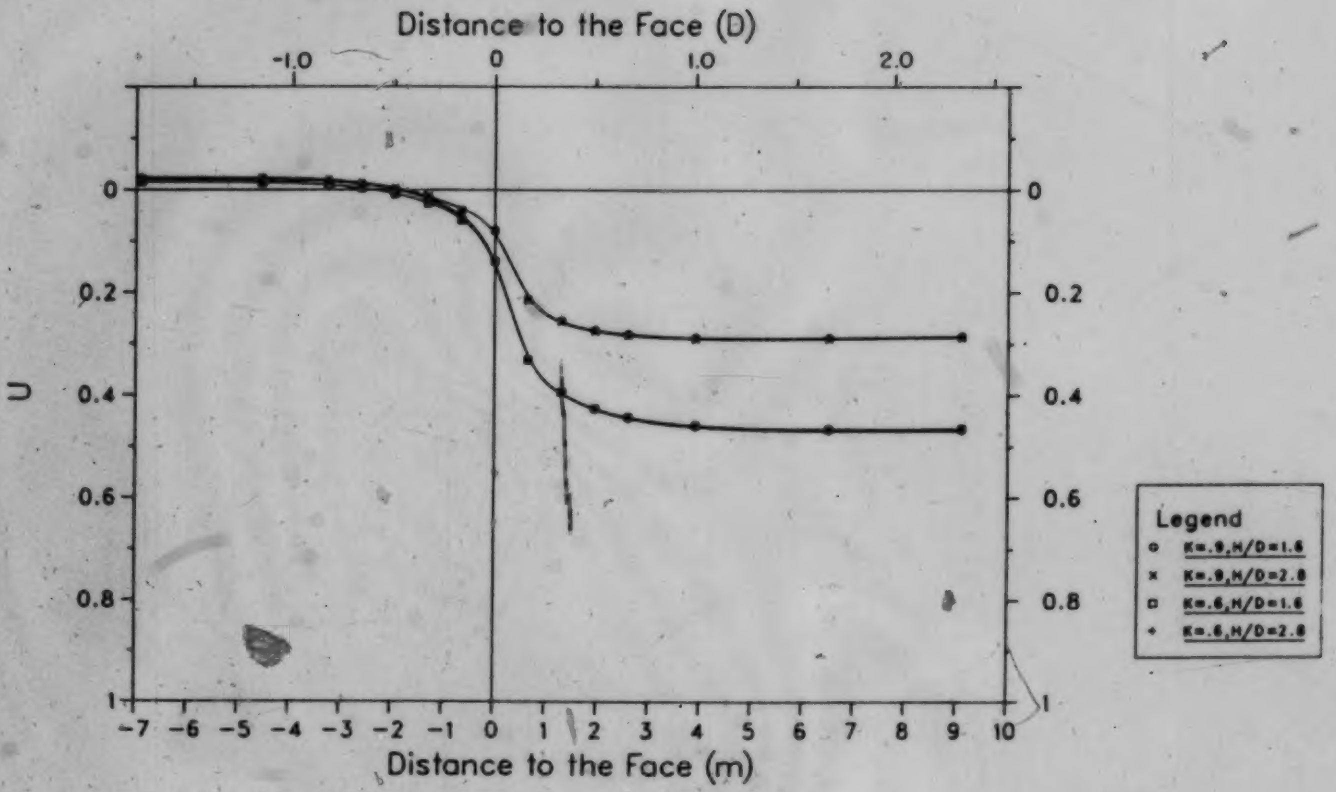

Figure 5.83 Comparison of Dimensionless Floor Displacements of the Shallower and Deeper Unlined Tunnels

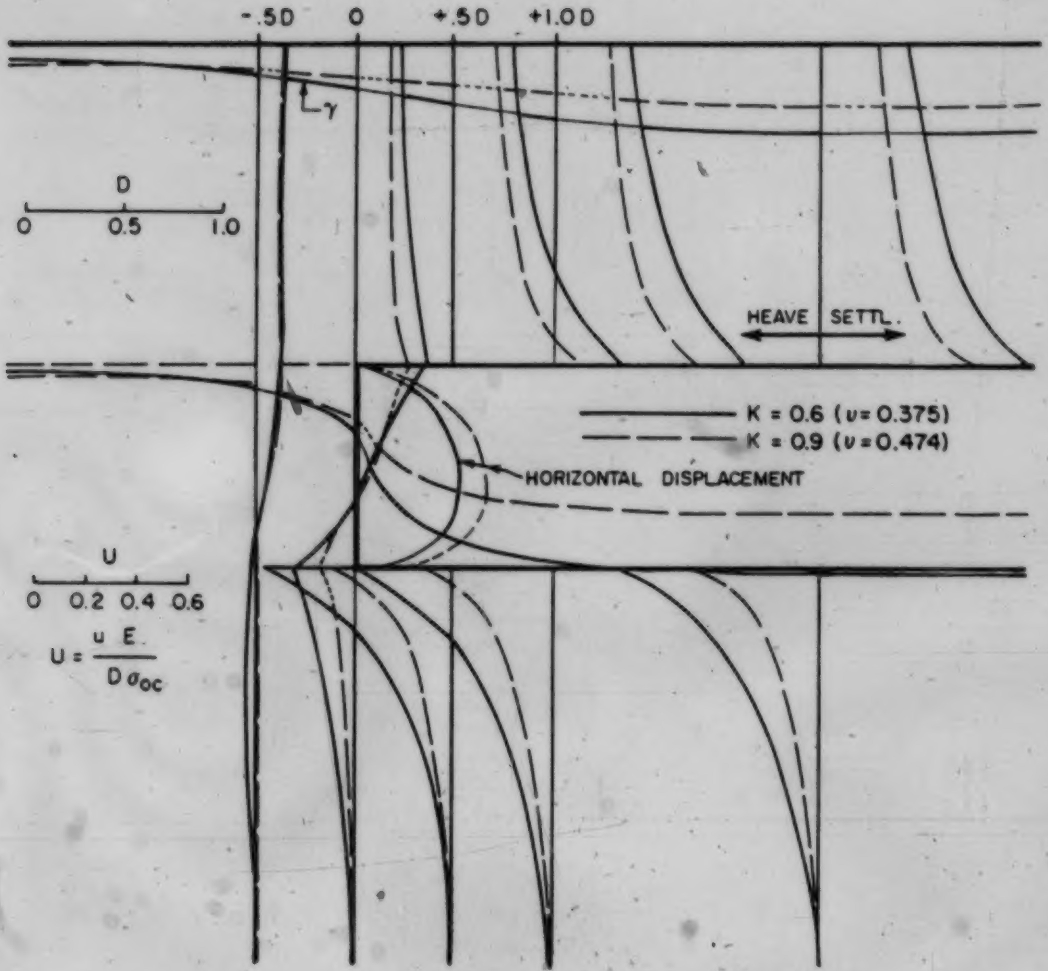

Figure 5.84 Ground Movements in the Vertical Longitudinal Plane of the Shallower (H/D=1.6) Unlined Tunnel

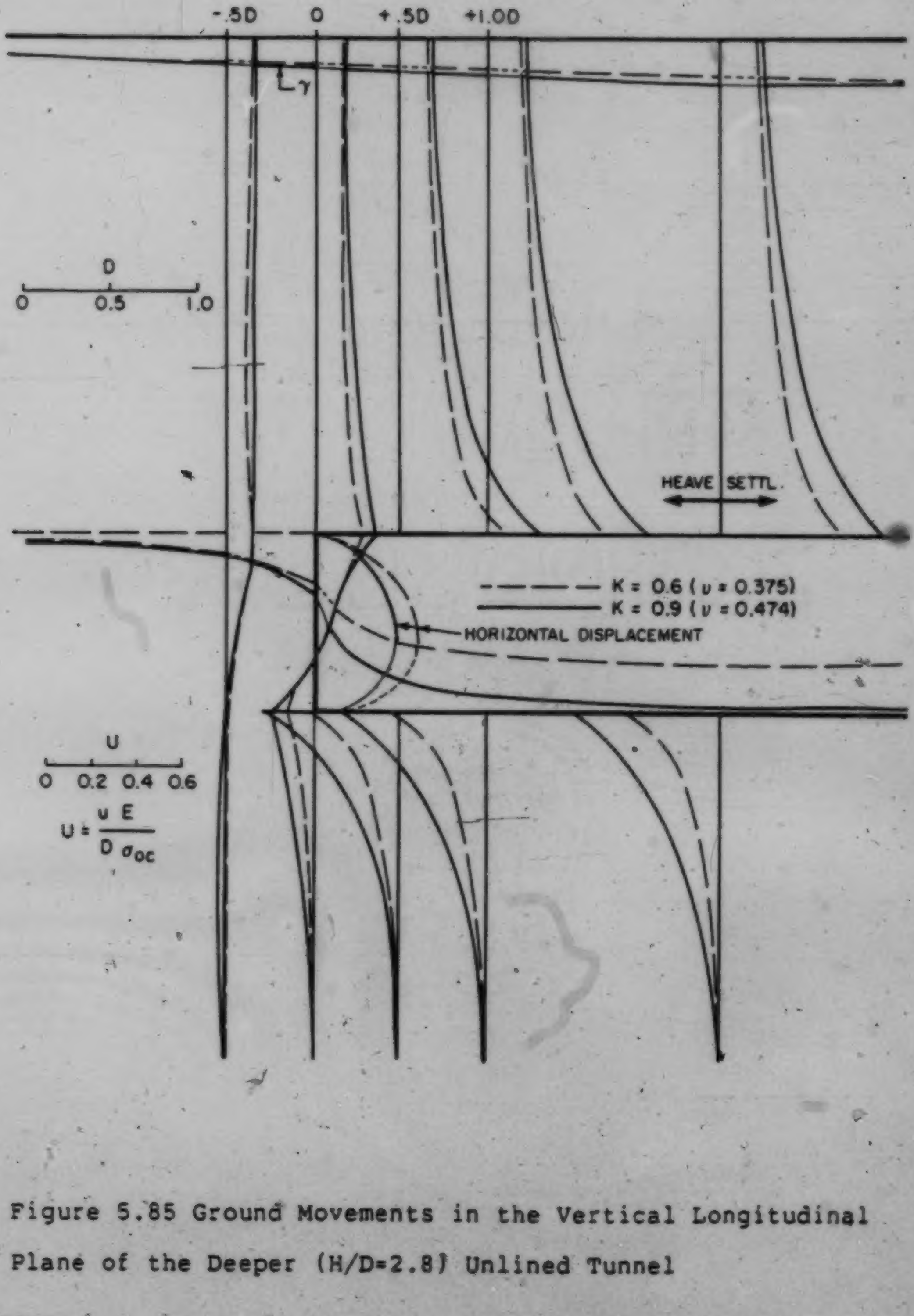

Figure 5.85 Ground Movements in the Vertical Longitudinal Plane of the Deeper (H/D=2.8) Unlined Tunnel

relationship exists between the dimensionless radial displacements of the tunnel wall and the in situ stress ratio, at a given section of the tunnel. If a linear relation is assumed to exist also for a shallow tunnel, one may be tempted to identify such a relationship, from the results obtained through the three-dimensional analyses of the unlined shallow tunnel. For the tunnel crown and floor, this relationship could be expressed as:

$$U = a - bK \qquad [5.6]$$

For the springline, the development shown in Figure 5.66 showed the following relation:

$$U_s = aK - b \qquad [5.7]$$

Considering however the distinct definition of the dimensionless displacement, U, being adopted herein, one obtains at the springline:

$$U = \frac{U_s}{K} \text{ therefore } U = a - b/K \qquad [5.8] \quad [5.9]$$

The coeffiecients a and b for the three particular locations of the tunnel contour (crown, springline and floor), can be obtained at different sections along the tunnel, which are defined in terms of the relative distance, X/D, between the face and the position of this section.

For sections located at X/D = 0 to 2, figures 5.86 to 5.90 present the dimensionless displacement U as a function of K, from the finite element analyses of both the shallower and deeper unlined tunnel cases. At the sections not coinciding with a face of the 3D mesh slices (X/D=0.25 and 2), the displacements were interpolated from adjacent nodal

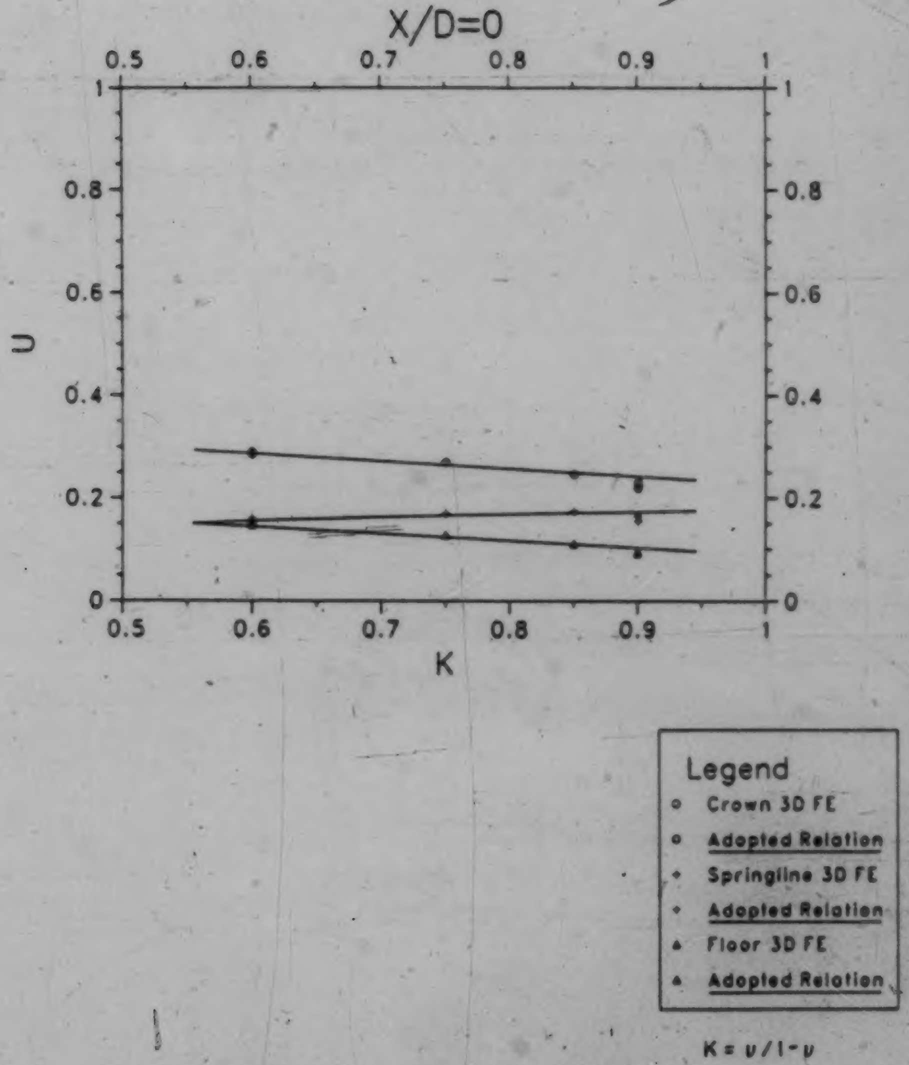

Figure 5.86 U and K Relationships for the Section at the Face

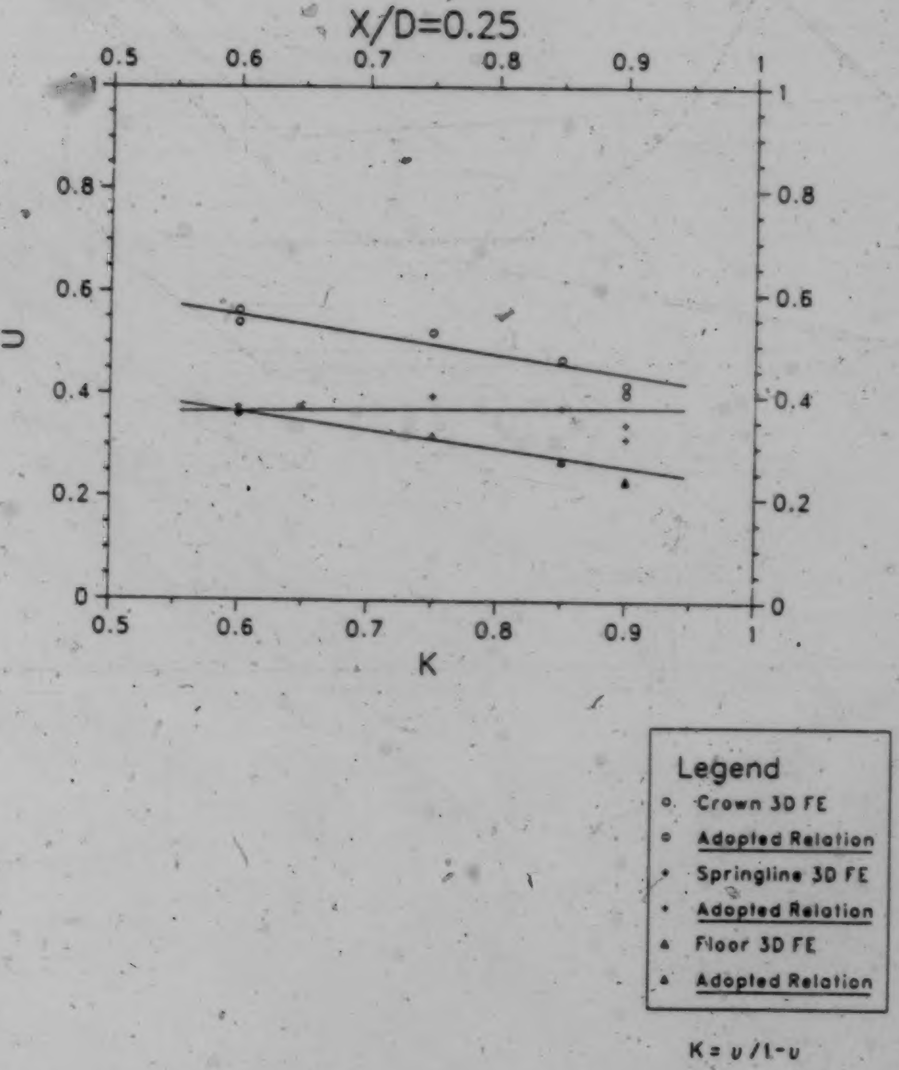

Figure 5.87 U and K Relationship for a Section D/4 Behind the Face

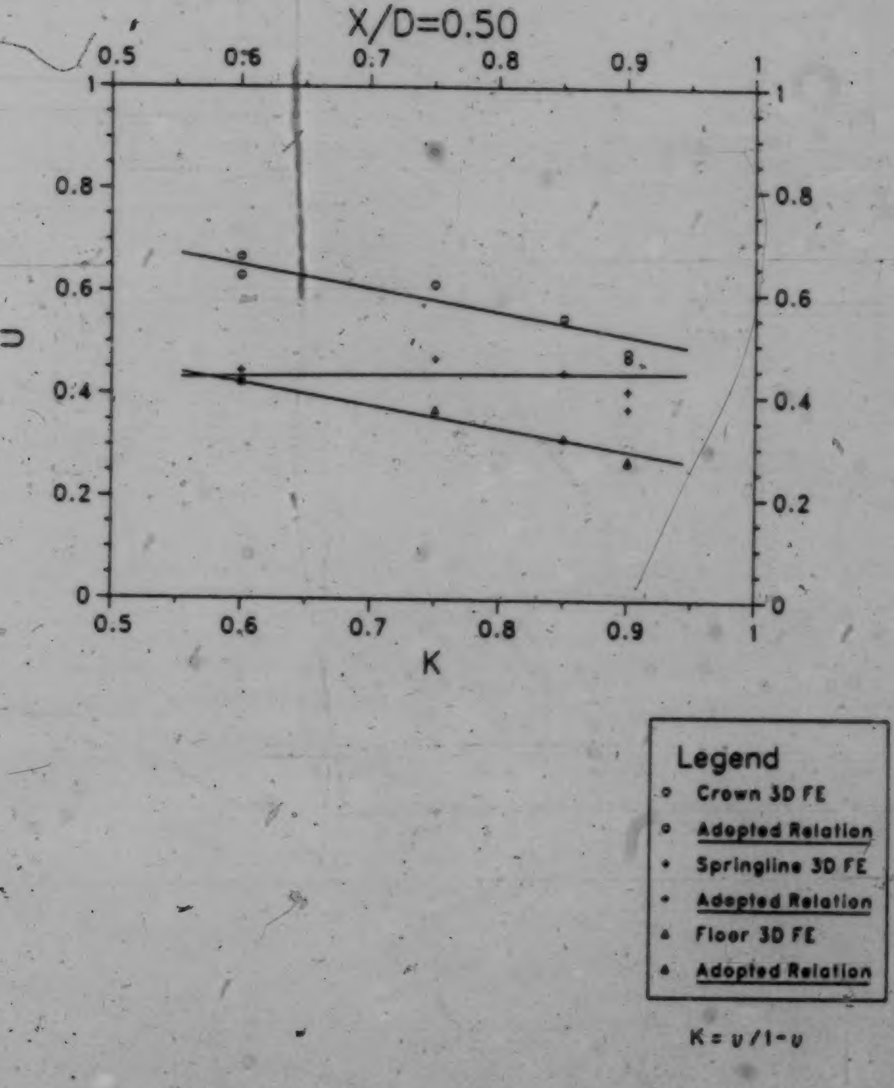

Figure 5.88 U and K Relationship for a Section D/2 Behind the Face

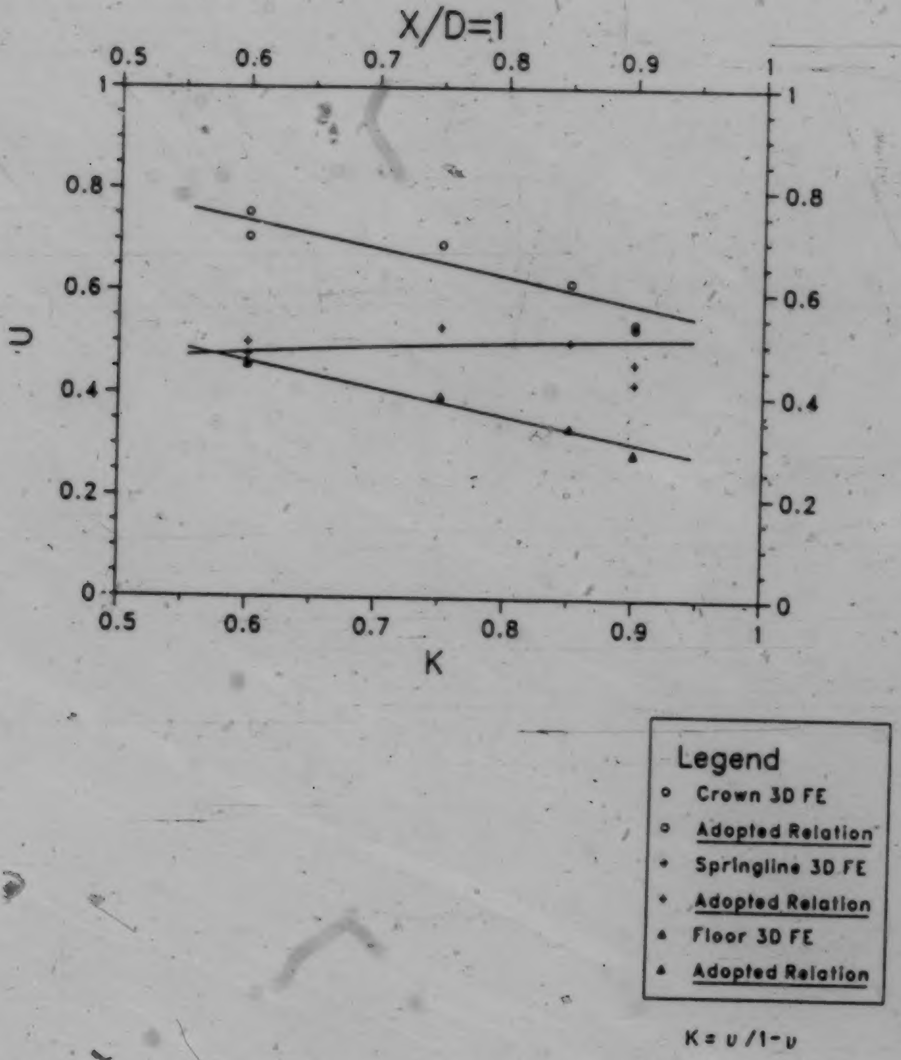

Figure 5.89 U and K Relationship for a Section 1.D Behind the Face

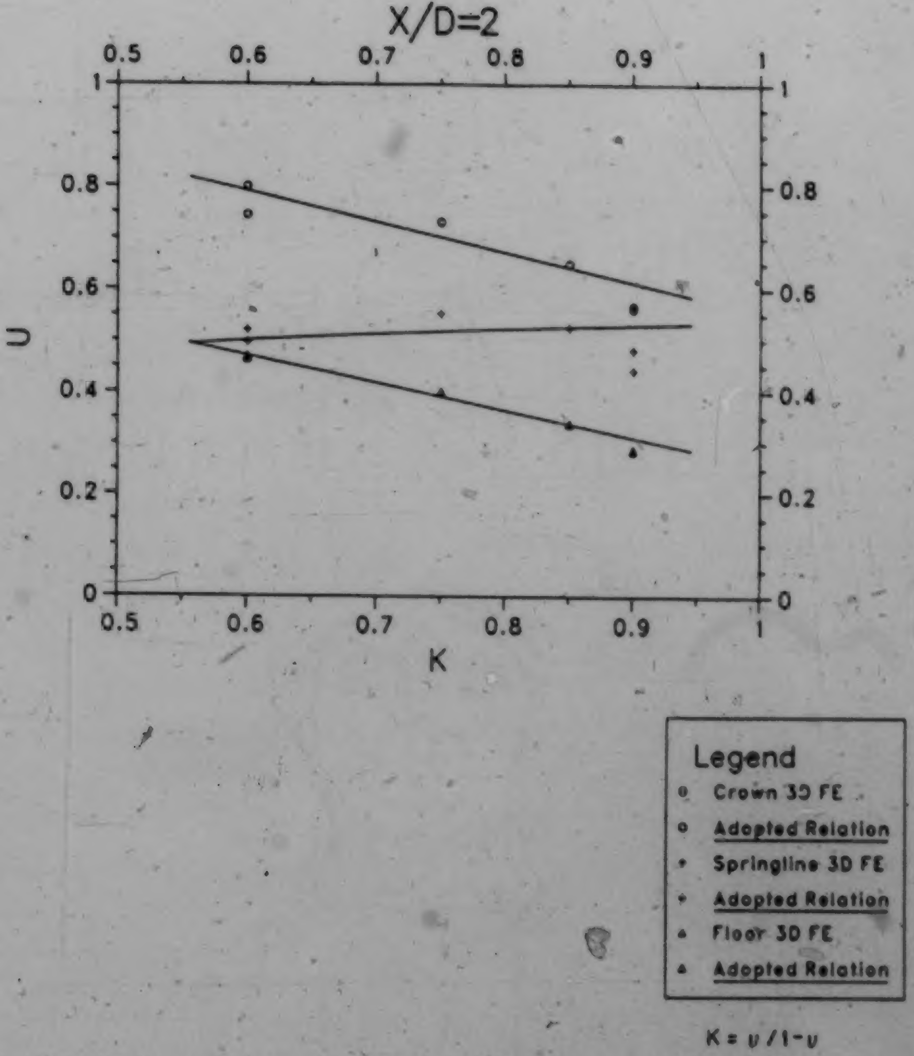

Figure 5.90 U and K Relationship for a Section 2.D Behind the Face

points using the smoothed curves shown in Figures 5.75 to 5.80. At X/D=2, the displacements are almost stabilized.

For each section considered, functions were fitted through the numerically obtained points. These functions are represented as solid lines in Figures 5.86 to 5.90. Since these curves were adjusted through points corresponding to the shallower and the deeper tunnel cases, they represent the typical U-K relationships for tunnels with cover to diameter ratios ranging from approximately 1.5 to 3.0.

Table 5.30 summarizes the values of the coefficients a and b obtained. To further illustrate the aspects of the fitted functions, Figures 5.91 to 5.93 have been prepared. These show for the considered points of the tunnel contour, how the U-K adopted relationships vary with the position of the section behind the tunnel face. One notes that the gradient of radial displacements along the tunnel axis are a maximum at sections just behind the tunnel face, and that is decreases rapidly at sections one to two diameters behind.

This is better seen in Figures 5.94 to 5.96, where the results of these interpretations are assembled in a compact form. From these three plots, one may obtain the coefficients a and b at any position X/D behind the tunnel face and, therefore, one may estimate the radial displacements at three points of the tunnel contour, for any value of K. The format of this solution is very similar to that presented in Figure 5.66, with the coefficients a and b corresponding to the parameters U_1 and U_2 of the deep tunnel

X/D	Crown		Springline		Floor	
	a	b	a	b	a	b
0	0.375	0.147	0.210	0.033	0.226	0.137
0.25	0.783	0.380	0.390	0.014	0.575	0.350
0.50	0.923	0.453	0.460	0.016	0.681	0.433
1.00	1.059	0.537	0.560	0.048	0.774	0.520
2.00	1.144	0.590	0.590	0.054	0.788	0.530

Notes: (1) Crown and Floor: $U - a - bK$

(2) Springline : $U = a - b/K$

Table 5.30 Coefficients of the Adopted U and K Relations for Sections at Different Distances Behind the Face

solution. The new solution is strictly valid for the conditions assumed: linear elastic ground (with modulus increasing with depth), unlined circular tunnel, ground cover to diameter ratio between 1.6 and 2.8 and in situ stress ratio K between 0.6 and 0.9, defined as a function of Poisson's ratio (varied beteen 0.375 and 0.474). Nonetheless it may be of some help in the evaluation of the closure behind or at the face of a shallow tunnel.

Face Displacements

Besides the vertical displacements above and below the unlined tunnels, Figures 5.84 and 5.85 also show the horizontal movements of the vertical tunnel face. The parametric finite element analyses revealed that the maximum dimensionless horizontal displacement of the centre point of the tunnel face depends on the relative depth of the tunnel and on the ratio K.

Figure 5.97 illustrates such a dependency. The maximum face movement towards the tunnel U_F is defined by:

$$U_F = \frac{u_f . E}{D . \sigma_{oc}} \qquad [5.10]$$

where u_f is the horizontal displacement of the face centre, E is the elastic modulus of the soil, D is the tunnel excavated diameter and σ_{oc} is the in situ vertical stress at the tunnel crown elevation. From Figure 5.97 one notes that U_F increases with increasing K and decreases with increasing H/D. Moreover, one notes that increasing the delayed support installation L/D, the dimensionless displacement of the face decreases. This result agrees with that found by Ranken and

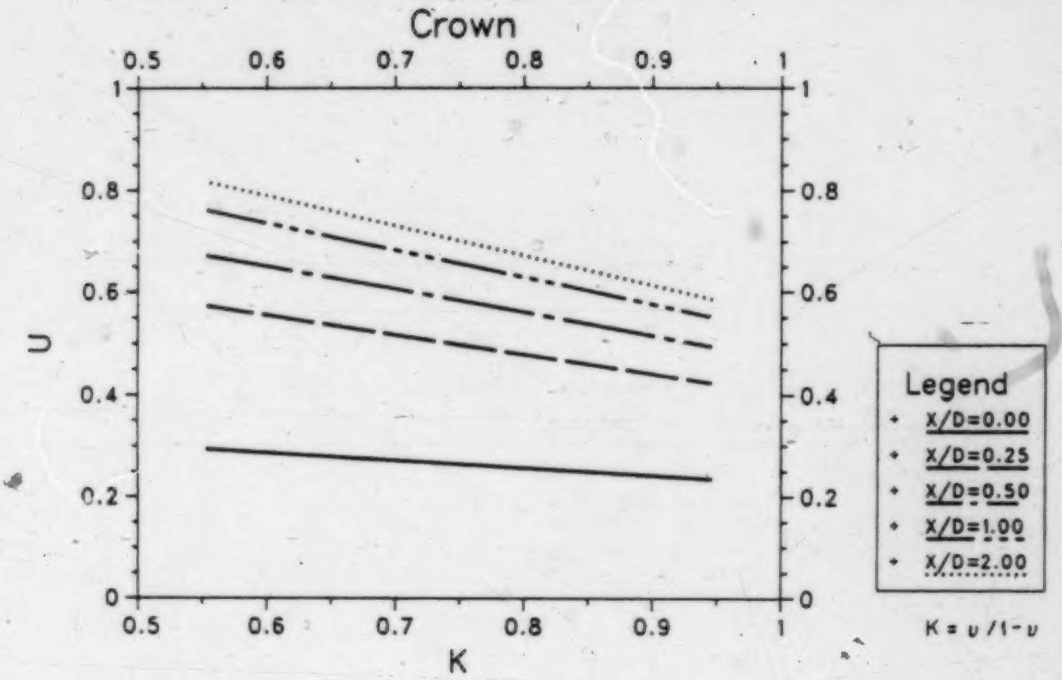

Figure 5.91 U and K Relationships for the Tunnel Crown

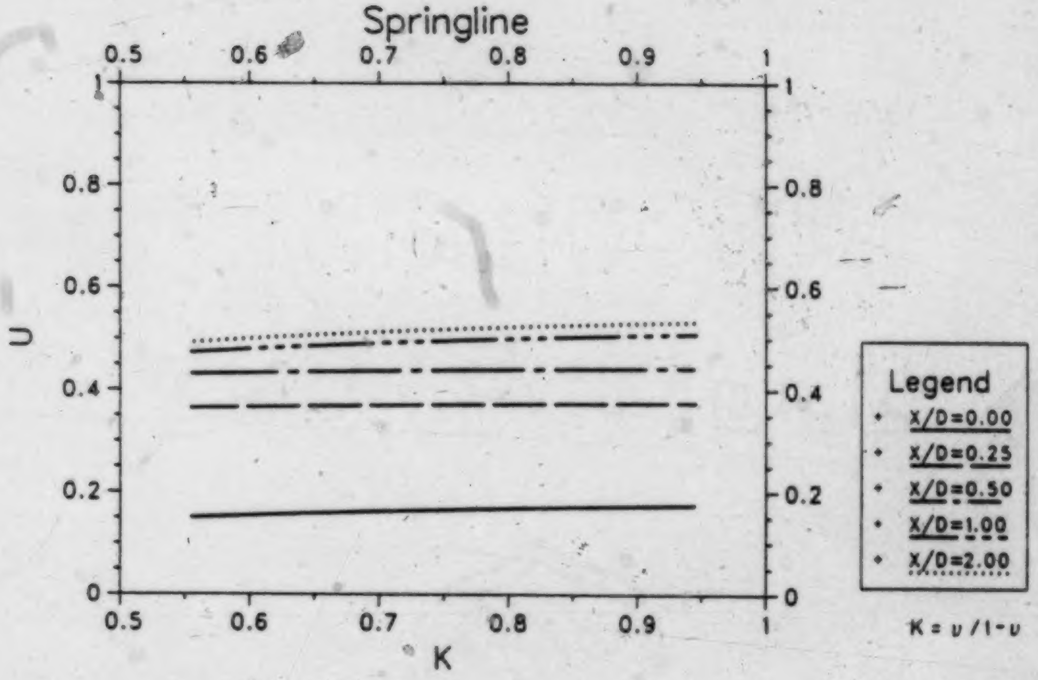

Figure 5.92 U and K Relationships for the Tunnel Springline

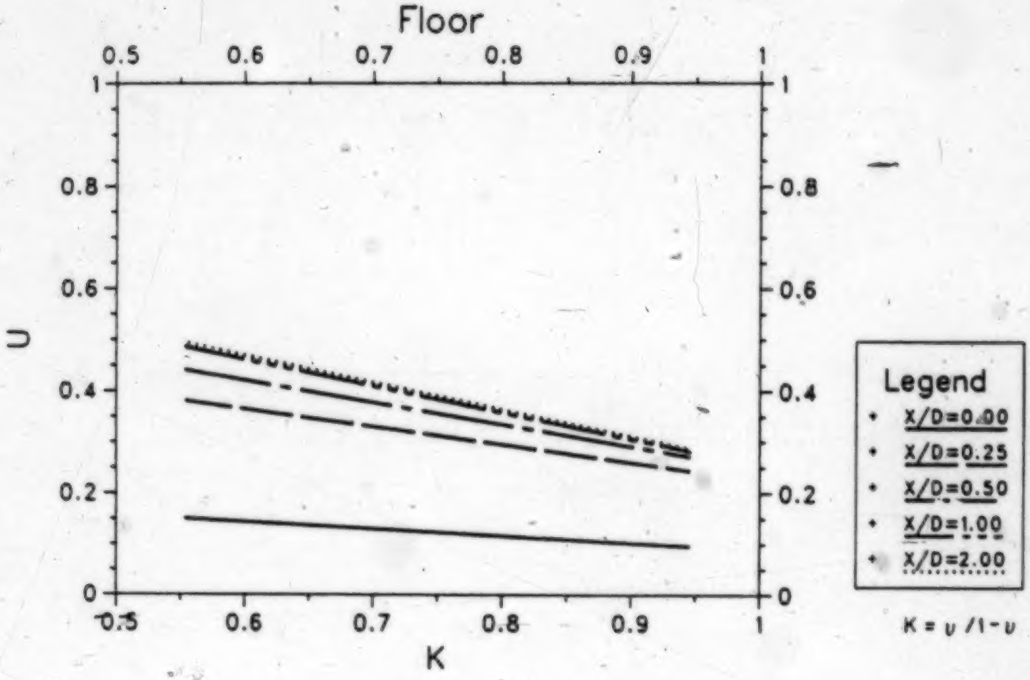

Figure 5.93 U and K Relationships for the Tunnel Floor

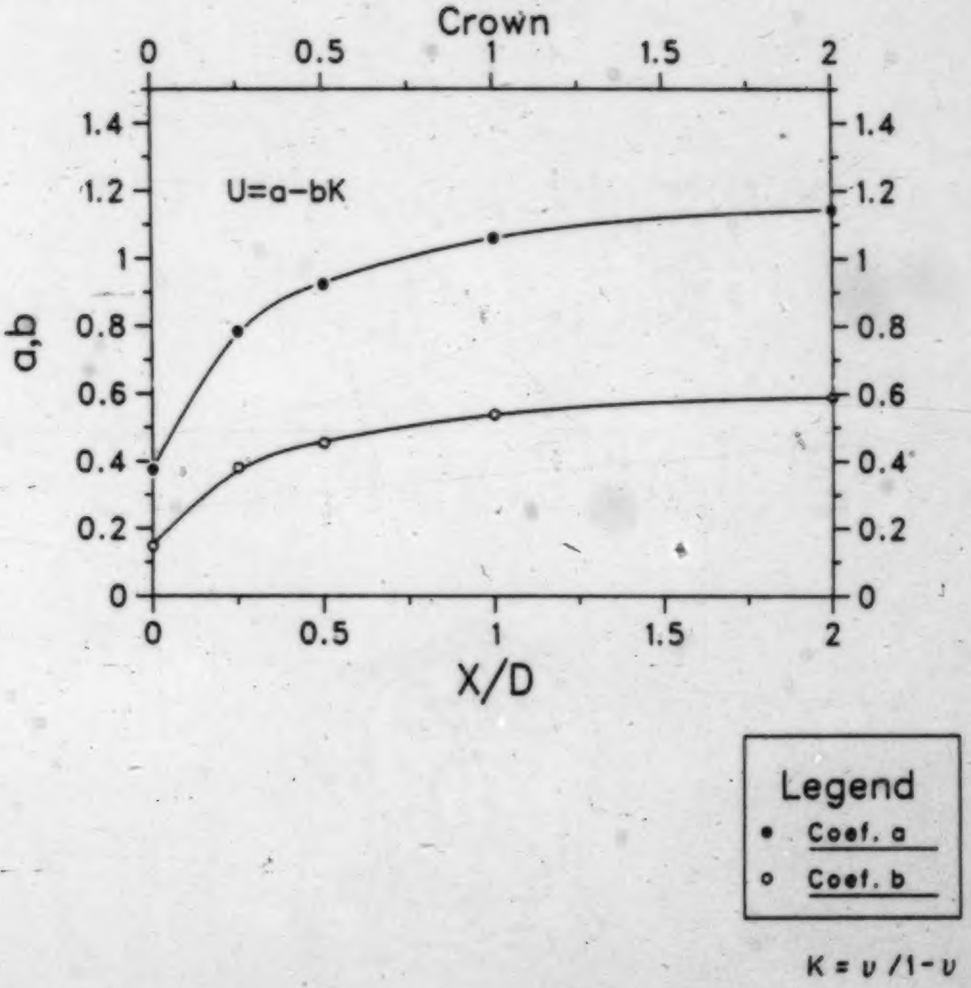

Figure 5.94 Coefficients of the U and K Relationship for the Crown of an Unlined Shallow Tunnel, (1.5<H/D<3.0) as a Function of the Distance to the Face

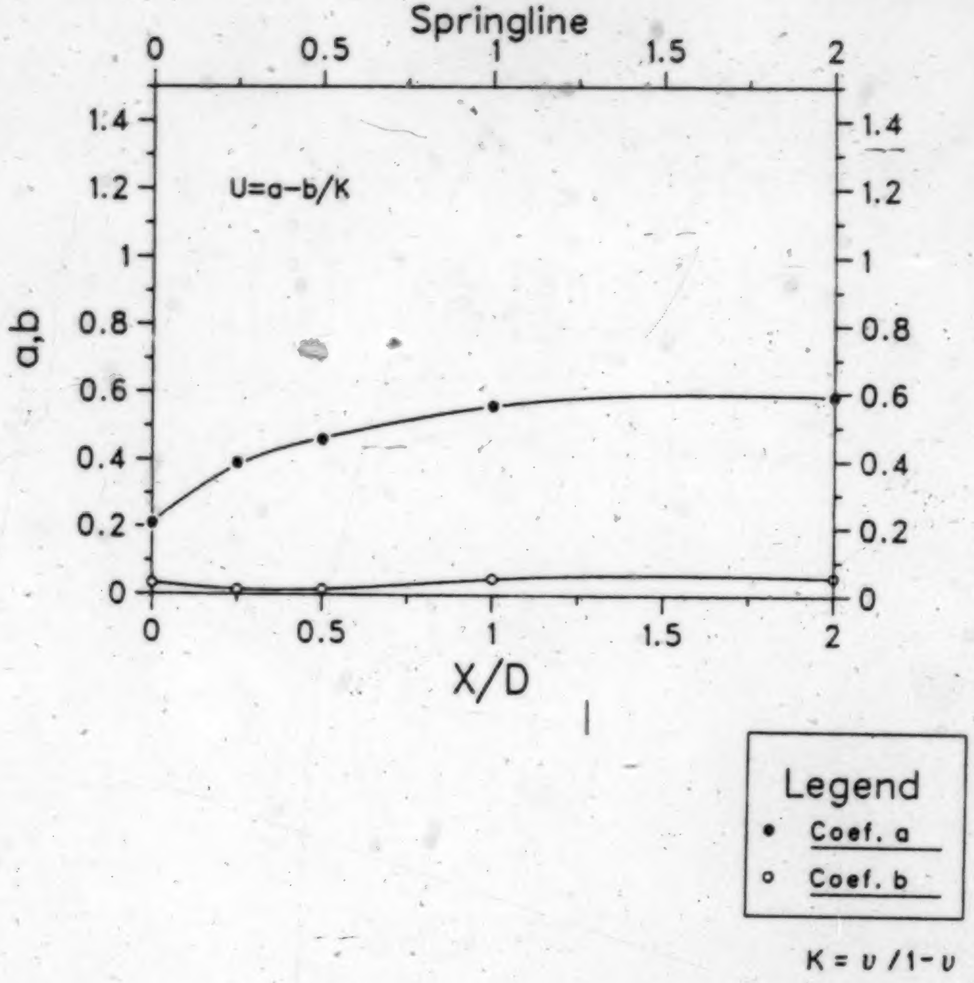

Figure 5.95 Coefficients of the U and K Relationship for the Springline of an Unlined Shallow Tunnel, (1.5<H/D<3.0) as a Function of the Distance to the Face

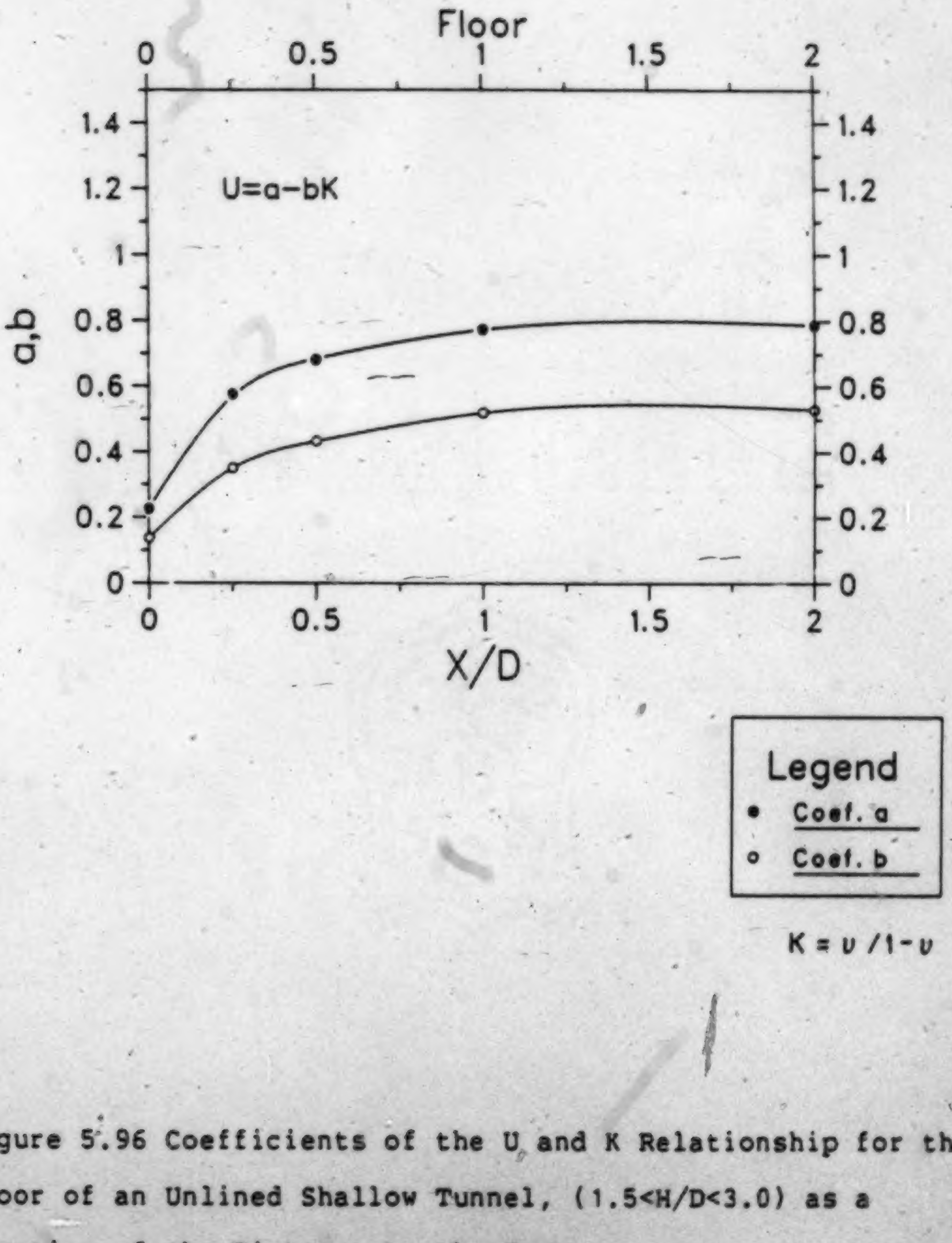

Figure 5.96 Coefficients of the U and K Relationship for the Floor of an Unlined Shallow Tunnel, (1.5<H/D<3.0) as a Function of the Distance to the Face

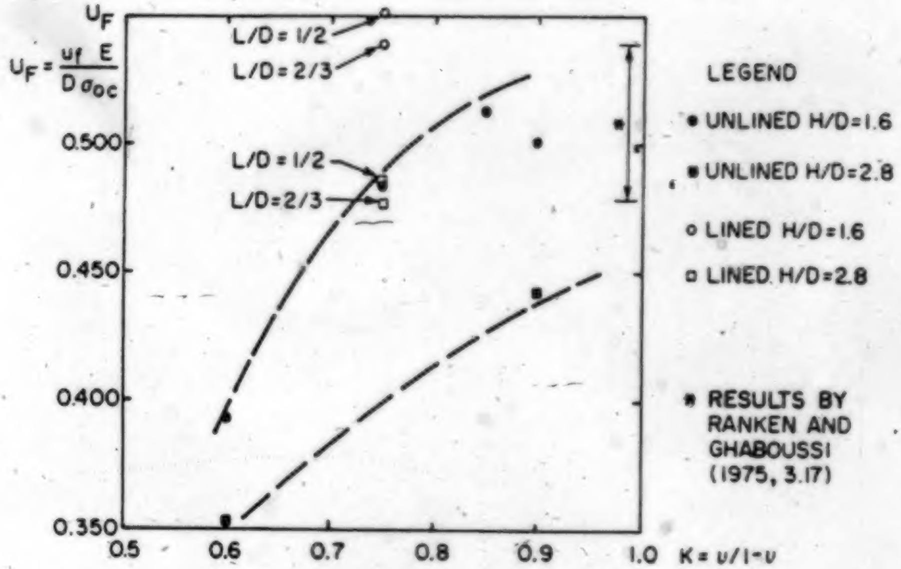

Figure 5.97 Maximum Horizontal Displacement of the Tunnel Face Expressed in Dimensionless Form, as a Function of the Stress Ratio K

Ghaboussi (1975:3.60). Also shown in Figure 5.97 is the range of U_f found by Ranken and Ghaboussi (Op.cit.:3.17), from axisymmetric finite element analyses (K=1) of unlined tunnels, with the Poisson's ratio varying between 0.3 and 0.49.

The dashed curves shown serve as boundaries for U_f estimates (the upper curve applied to shallower tunnels and the lower to deeper ones). Typically, the maximum horizontal displacement of the tunnel face could be estimated on a preliminary basis, by the expression:

$$u_f \approx 0.5\ D\ \frac{\sigma_{oc}}{E} \qquad [5.11]$$

From it, one would conclude that for increasing tunnel depth (thus for increasing σ_{oc}), u_f would increase linearly. However, it should be remembered that for a large number of soils, E is also a function of the stress level (see Figures 5.10 and 5.11) and depending on this, u_f may even decrease with the increasing depth of the tunnel.

Longitudinal Distortions Ahead of The Advancing Tunnel

The results presented in Figures 5.75 and 5.76 show that the maximum gradient of the vertical displacements along the crown elevation develops at a section located about D/12 behind the face of an unlined tunnel. On the other hand, the results shown in Figures 5.68 and 5.71 indicate that if the tunnel is lined, the location of the maximum gradient is not affected and that the magnitude of this distortion is only slightly altered by the action of the support. The effect of the support is likely to decrease the distortion for a decreasing unsupported heading length (L/D).

The maximum longitudinal angular distortion at the crown elevation is given by the maximum gradient of the tunnel closure at the crown:

$$\gamma_{cmax} = \left| \frac{\partial u}{\partial x} \right|_{max} = \left| \frac{\partial U}{\partial (x/D)} \right|_{max} \cdot \frac{\sigma_{oc}}{E}$$

$$= \frac{1}{n_{\gamma c}} \cdot \frac{\sigma_{oc}}{E} \qquad [5.12]$$

The parameter $n_{\gamma c}$ is a measure of the inverse of the maximum longitudinal angular distortion and can be numerically determined from the results of the finite element analyses. Figure 5.98 is thus readily obtained. One observes, in fact, that the lining action is that of positively reducing the distortion. For usual support delays of about one diameter or so, and provided the ground is linear elastic, the longitudinal distortion at the crown can be safely estimated assuming the tunnel to be unlined and using the curves depicted in Figure 5.98. The distortion is found to depend on the ratio K, and decreases as this ratio increases. It is also found to depend on the relative tunnel depth (i.e. the proximity of the ground surface) again decreasing as the tunnel gets deeper. Note, however, that it is directly related to the vertical stress level σ_{oc} at the crown. A quick estimate of the magnitude of the maximum longitudinal distortion of the ground at the crown elevation could be made through the expression:

$$\gamma_{cmax} \simeq 1.5 \, \frac{\sigma_{oc}}{E} \qquad [5.13]$$

From it one sees that the distortion increases as the stress level increases and decreases as the ground becomes stiffer. The relation between the maximum distortion with the tunnel depth is not, however, obvious. It should be recalled, once more, that the modulus of the soil layer the tunnel is being driven through, may be also a function of the stress level. Accordingly, γ_{cmax} may increase, decrease or remain constant, for increasing depths of tunnel cover, depending on the type of soil.

In Section 3.2.2, a practical criterion for the detection of instability problems in the field was discussed. It consists of monitoring variations of the longitudinal distortion index (the angular distortion) with the tunnel advance, through the measurement of vertical movements of the ground just above the tunnel, at measuring points distributed along the tunnel alignment. Changes in the distribution of the longitudinal distortions may serve as an indication of incipient instability problems. It may be useful to know the maximum distortion as a reference for a stable condition. The features shown in Figure 5.98 may assist in this definition, provided the elastic modulus is taken as the initial tangent in situ modulus. However, more frequently than not, the deep settlement points used for this type of monitoring are not installed at the tunnel crown elevation, but rather some distance above it. Once more, the results of the numerical analyses of the unlined tunnel cases, may assist in obtaining the maximum angular distortion above the tunnel crown. Figure 5.99 furnishes the

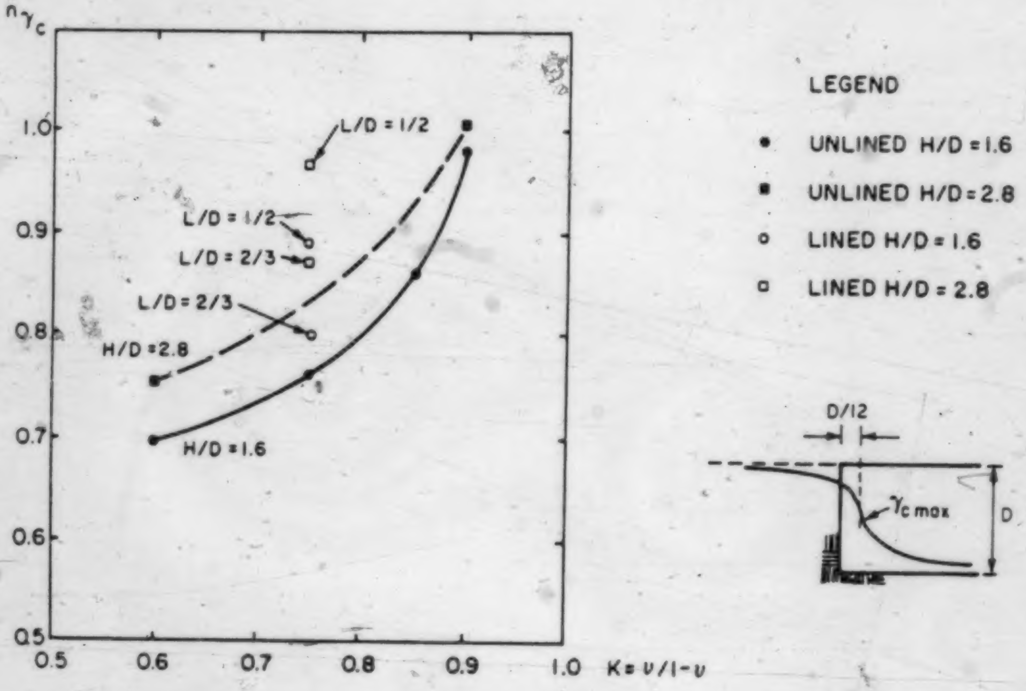

NOTE : MAXIMUM DISTORTION : $\gamma_{c\,max} = \frac{1}{{}^{n}\gamma_c} \cdot \frac{\sigma_{oc}}{E}$, AT $\frac{1}{12}$D BEHIND THE FACE

Figure 5.98 Maximum Angular Distortion Along the Tunnel, at Crown Elevation

ratio of the maximum distortion at crown (γ_{cmax}) to the maximum distortion of the ground at an elevation 0.3D above the crown (γ_{dsmax}). The latter distance is fairly typical for deep settlement points installed above the tunnel. One notes that, for the ranges of K and H/D investigated, the distortion ratio varies within a fairly narrow range. A typical ratio of 2.5 could be selected. Therefore, a rough estimate of the magnitude of the maximum angular distortion in the longitudinal direction, along an axis located 0.3D above the crown, could be made by the expression:

$$\gamma_{dsmax} \simeq 0.6 \frac{\sigma_{oc}}{E} \qquad [5.14]$$

The same comments made for γ_{cmax} are valid here. It was noted that γ_{dsmax} occurs at a section located $D/\sqrt{2}$ behind the tunnel face.

Also of some interest is the maximum longitudinal distortion at ground surface, γ_{smax}, ahead of the tunnel face. Again the action of the support in this case reduces the angular distortion at the surface, by elongating the settlement profile and reducing the magnitude of the maximum movements. As the support is placed closer to the tunnel face, movements are noticed at greater distances from the face and the maximum angular distortion of the ground decreases. This fact was detected from the results of axisymmetric analyses by Ranken and Ghaboussi (1975:3.55), from results of field instrumentation by Negro and Eisenstein (1981) and was broadly confirmed in the present study.

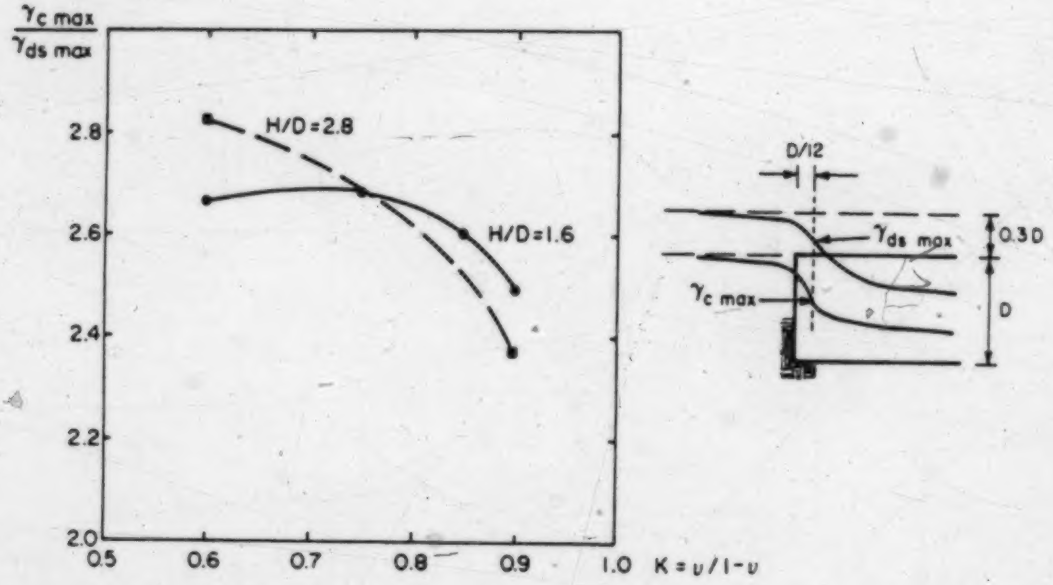

Figure 5.99 Maximum Angular Distortion Along the Tunnel, at an Axis 0.3D Above Crown Elevation, as a Function of the Maximum Crown Distortion

Having this in mind, the numerical results from the 3D analyses of the unlined tunnel, should provide a basis for a safe estimate of the maximum angular distortion ahead of the face. Accordingly, Figure 5.100 was prepared. The maximum surface distortion, γ_{smax}, is related to the maximum crown distortion, as a ratio. This ratio was found to vary with the cover to diameter ratio, increasing as the tunnel gets deeper, as expected. Obviously, when the cover tends towards zero, the ratio should tend towards unity. The in situ stress ratio K was also noted to affect this relationship. While the section where γ_{cmax} occurs was found to be always D/12 behind the face regardless of the depth of the tunnel and the K value, the section where the maximum surface distortion occurs seems to depend on the ratio H/D. For H/D equal to 1.6, γ_{smax} developed at D/4 ahead of the face. For H/D equal to 2.8, γ_{smax} developed further ahead at (21/36)D from the tunnel face. The results of the analyses with linings are also included in Figures 5.100 for comparison. The lined tunnel cases showed less distortion at the surface than the unlined cases, as expected. However, for H/D=2.8 and contrary to expectations, the case with the larger unsupported heading (L/D=2/3) yielded the smaller surface distortion. These results are somewhat suspect, as they may have been affected by the presence of the nearby lateral boundary of the finite element mesh.

Nevertheless, the results shown in Figure 5.100 may be of some help in the estimate of the maximum surface

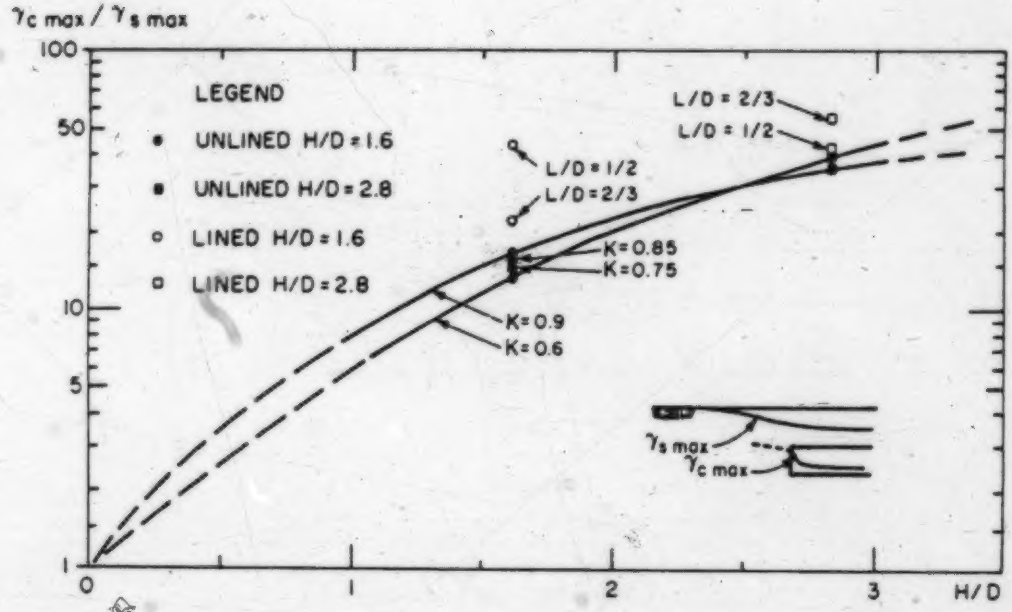

Figure 5.100 Maximum Angular Distortion of the Ground Surface Along the Tunnel Alignment as a Function of the Maximum Crown Distortion

distortion ahead of the tunnel. The use of this solution, or those shown in Figures 5.98 and 5.99, strictly depend on the validity of the simplifying assumptions made. For instance, they cannot be used in cases where substantial yielding develops ahead of the tunnel. An approximate assessment of this condition can be made by evaluating the face stability by using the solutions discussed in Section 4.3.4. Extending the concepts presented in Section 2.3.3 for a plane strain tunnelling situation, if the factor of safety for the face stability is larger than 2 to 3, then the simple methods for evaluation of longitudinal ground distortions ahead of the tunnel may be applicable. Since no other solutions are yet available to treat the present problems, the simplified methods just discussed can perhaps be of some help in practice.

5.3.6 Application of the Results

5.3.6.1 Tunnel Closure

Comparison with other Solutions

The solution developed and presented in Section 5.3.5.2 for estimating the convergence of an unlined tunnel presents a number of peculiarities. Despite this, one is invited to compare it with other solutions available. Among those reviewed in Section 5.3.2, the solutions by Hocking (1976) and Niwa et.al. (1979) display more generality with respect to accounting for the in situ stress ratio. Both solutions were derived from boundary element analyses and yield similar results. The one by Niwa et.al. (1979) however, has been presented in a slightly more convenient form, which allowed the generalization presented in Figure 5.66. Therefore it was selected for comparative purposes.

At least two problems emerge in comparing the presently developed solution with that by Niwa et.al. (Op.cit). The first refers to the nature of the development. The present solution was numerically derived from finite element analyses. The one by Niwa et.al. (Op.cit.) stemmed from boundary element analyses. Being both derived from numerical solutions, they involve numerical approximations, but these are dissimilar and depend on each type of solution. For instance, it has been shown that in the plane strain analysis of an elastic pipe under internal pressure (Brebbia, 1978:162), the displacement calculated by the boundary element method will be slightly larger than that by the finite element method, for equivalent degrees of "discretization". The same conclusion was found by Negro and Kuwajima (1985) in the plane strain elastic analyses of a deep tunnel. On the other hand, it is known that finite element solutions tend to yield displacements smaller than the exact (Zienkiewicz, 1983:36).

The second problem refers to the fact that while the Niwa et.al. (Op.cit) solution was developed for an ideally deep tunnel situation, the present one assumed the tunnel to be shallow, with certain cover to diameter ratios. To make the solutions comparable, the present solution had to be manipulated. In an attempt to "eliminate" the effect of the gravitational stress gradient across the shallow tunnel, the coefficients, a and b, of the proposed U versus K relationship shown in Table 5.30 were averaged in order to obtain the equivalent "deep" tunnel solution. Accordingly, the a and b coefficients for the springline were averaged with the mean values of a and b for the crown and floor, for each section of the tunnel behind the face. In so doing, these average values can be compared to the corresponding values of U_1 and U_2 of Niwa et.al. (Op.cit) solution presented in Figure 5.66. Consequently Figure 5.101 was obtained.

It should be noted that in the present solution, the in situ stress ratio was defined as a function of the Poisson's ratio. Moreover, the elastic modulus of the soil was assumed to increase with depth. These two facts alone would impede any equivalence between the two solutions. Notwithstanding this, the results shown in Figure 5.101 indicate some resemblance beween the solutions. The difference could be attributed to the different features of each case. Moreover, it is observed that the additive component, a, of the dimensionless displacement U given by the present solution is always smaller than that provided by the other solution. Inversely, the subtrahend component, b, is larger. As a result, the final dimensionless radial displacement given by the present solution will usually be smaller than that given by Niwa et.al. (Op.cit.).

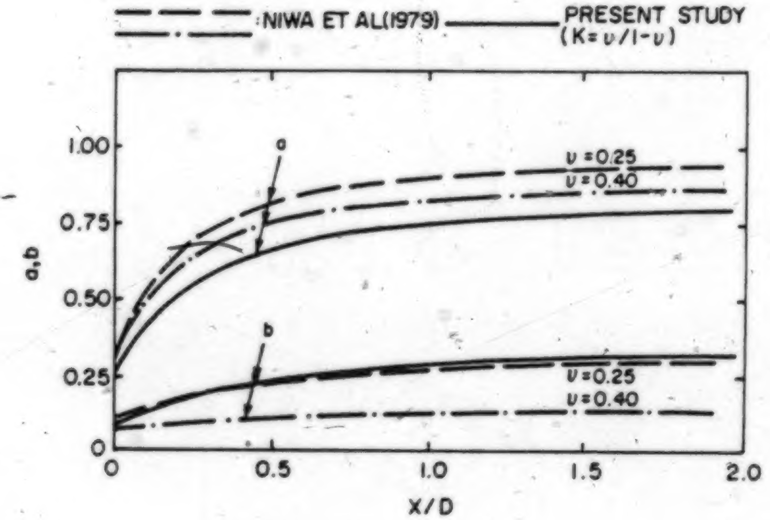

Figure 5.101 Comparison Between Niwa et.al. (1979) and the Present (Averaged) Tunnel Closure Solution

Comparison with Field Measurements

For a proper verification of the proposed method, calculations were performed for cases where field measurements were available. No special criterion was set up for case history selection. The basic requirement was availability of the required data to allow a comparison to be made. Therefore some cases were included which involved conditions lying outside the range those considered in the development of the present solution, either in terms of geometry (H/D) or in situ stresses (K). Not many cases of shallow tunnels in soft clays or sensitive soils were investigated, but at least some were included.

Tables 5.31, 5.32 and 5.33 list the cases investigated, where ground movements at the crown, springline and floor, respectively, have been measured. These tables present also the main source or reference for each tunnel case. They refer to those publications where most of the information shown was drawn from. Additional searches of the literature were undertaken in order to supply data on the ground properties, whenever necessary.

Besides identifying the case history, the tables indicate the instruments or the instrumented sections considered (second column). Indications of the construction method and lining type used are also included, together with a brief description of the ground type and the position of the tunnel with respect to the ground water level. The cases where the ground water level was lowered prior to tunnelling

No.	Tunnel and Section	Method	Lining	Ground	Water Level	Behaviour	D (m)	H (m)	E (MPa)	K	ϕ (°)	c (kPa)
1	Frankfurt 25 Romerberg	NATM$^{(1)}$	Shotcrete	Stiff clay marl CH MH	LO	DR	6.48	11.5	24	0.8	21	37
2	Frankfurt 25 Karmeliterg.	NATM$^{(1)}$	Shotcrete	Stiff clay marl CH MH	LO	DR	6.70	13.0	24	0.8	21	37
3	Frankfurt 25 Blauhandg.	NATM$^{(1)}$	Shotcrete	Stiff clay marl CH MH	LO	DR	6.70	12.5	24	0.8	21	37
4	Frankfurt 17 Bergerstr.	NATM	Shotcrete	Stiff clay marl CH MH	LO	DR	6.70	10.25	52	0.8	21	37
5	Frankfurt 23 Domplatz	Open Shield$^{(2)}$	Precast concrete	Stiff clay marl CH MH	LO	DR	6.70	11.75	24	0.8	21	37
6	Frankfurt 23 Fahrgasse	Open Shield$^{(2)}$	Precast concrete	Stiff clay marl CH MH	LO	DR	6.70	8.6	24	0.8	21	37
7	Butterberg-Osterode	NATM	Shotcrete	Sandy silty gravel GM	A	DR	11.5$^{(3)}$	14.6	150	0.5	33	20
8	Bochum A2 Bahndamm	NATM	Shotcrete	Stiff marl and sand	A	DR	9.03$^{(3)}$	12.2	70	0.8	25	64
9	Munich Los 6 West 2	NATM	Shotcrete	Sandy gravel	A	DR	6.85$^{(3)}$	6.0	100	0.4	37.5	4
10	Munich 8/1 - 10.2	NATM	Shotcrete	Hard marl and sand	LO	DR	6.91$^{(3)}$	22.0	200	1.0	25	40
11	Munich 5/9 - 6$^{(4)}$	NATM	Shotcrete	Hard marl and sand	LO ?	DR?	7.5$^{(3)}$	15.8	200	1.0	25	40
12	Munich 5/9 - 7 (MQ1)	NATM$^{(5)}$	Shotcrete	Hard marl and sand	B	DR?	6.95	20.8	200	1.0	25	40
13	Green Park ext. X1	Open Shield	Cast iron seg.	London clay - CH	B	UN	4.15	29.6	60	1.3	0	250
14	Green Park ext. Y1	Open Shield	Cast iron seg.	London clay - CH	B	UN	4.15	20.8	60	1.3	0	250
15	Green Park ext Z1	Open Shield	Cast iron seg.	London clay - CH	B	UN	4.15	28.2	60	1.3	0	250
16	Regent Park (Sth B) ext. H	Open Shield	Exp. concr. seg.	London clay - CH	B	UN	4.15	32.0	60	1.3	0	250
17	Regent Park (Sth B) ext. K	Open Shield	Exp. concr. seg.	London clay - CH	B	UN	4.15	32.0	60	1.3	0	250
18	Regent Park (Nth B) ext C$^{(7)}$	Open Shield	Exp. concr. seg.	London clay - CH	B	UN	4.15	17.8	30	1.6	0	200
19	Heathrow Cargo (U.K.)	Open Shield	Exp. concr. seg.	London clay - CH	B	UN	10.9	7.3	27	1.9	0	200
20	New Cross (U.K.) ext. B2	Bent. Shield	Cast iron seg.	Dense sand and gravel	A	DR	4.12	8.0	40	0.3	45	0
21	Chinnor (U.K.) ext. P2C	TBM	Steel ribs no lagg.	Lower chalk	A	DR	5.0	5.7	75	0.5	-	q_u=74,200
22	Chinnor (U.K.) ext. P5	TBM	Steel ribs no lagg.	Lower chalk	A	DR	5.0	6.2	75	0.5	-	q_u=74,200
23	Edmonton Exper. ext MX22	Closed Shield	Exp. concr. seg.	'Soft' till - CL	A$^{(10)}$	UN	2.56	25.6	17	0.8	0	100
24	Edmonton LRT (Sth) ext. 1	Closed Shield	Exp. ribs & lagg.	'Stiff' till - CL	A	DR	6.17	8.6	70	0.75	40	0
25	Edmonton Kennedale ext. ME1	Closed Shield	Exp. ribs & lagg.	Till - CL?	A	DR	3.2	12.0	60	1.0	35	10
26	S. Paulo Boa Vista ext. B	Closed Shield$^{(5)}$	Cast iron seg.	Clayey sand - SC	B	UN?	6.19	10.55	50	0.6	0	70

Table 5.31 Predicted and Measured Displacements at the Face and at the Point of Support Activation in Shallow Tunnels for the Crown

No.	σ_{v0} (kPa)	Y (m)	Displ. u at the face (mm) Meas.	Extr.	Predic.	L/D	Displ. u at lining installation or closure (mm) Meas.	Extr.	Predic.	Face Position for Final u (x/D)	Final u (mm) Meas.	Extr.	after Support	Main References
1	213	0.5	21.0	22.6	14.8	0.69	57.0	61.3	33.8	3.09	63.0	67.7	0.111	Edeling and Schulz (1972)
2	240	0.5	14.0	15.0	17.2	0.45	29.0	31.2	36.2	4.03	42.0	45.2	0.209	Stroh and Chambosse (1973)
3	231	0.5	13.0	14.0	16.6	0.22	22.0	23.7	29.0	4.40	34.0	36.6	0.208	Stroh and Chambosse (1973)
4	190	0.05	4.0	4.4	6.3	0.70	13.0	14.4	14.6	NA	19.0	21.1	0.274	Muller, Sauer and Chambosse (1977)
5	210	0.39	5.0	5.3	15.6	1.10	35.0	37.2	37.2	1.49	45.0	47.9	0.177	Chambosse (1972)
6	159	0.58	6.0	6.4	11.4	0.90	50.0	53.2	27.3	2.99	70.0	74.5	0.480	Chambosse (1972)
7	321	2.10	6.0	6.0	7.4	0.61	17.0	19.3	17.7	1.74	24.0	27.3	0.325	Meister & Wallner (1977)
8	244	0.50	8.0	8.5	8.1	0.70	16.0	17.0	18.8	1.74	20.0	21.3	0.137	Jagsch et al (1974), Hofmann (1976)
9	132	0.90	2.0	2.1	(2.8)	0.44	6.0	6.3	(6.5)	NA	7.0	7.4	0.122	Schikora (1983), Krischke & Weber (1981)
10	462	0.60	2.2	2.3	(3.6)	0.87	7.0	7.2	(8.1)	NA	8.5	8.7	0.094	Laabmayr & Weber (1978)
11	332	0	1.9	1.9	2.8	-	-	-	-	-	-	-	-	Amstad and Kovari (1984)
12	376[6]	0	2.1	2.1	(3.0)	0.72	-	-	-	-	--	-	-	Baumann et al (1985)
13	577	2.6	10.5	10.4	(7.3)	0.96	16.0	20.0	(14.4)	7.23	14.0	24.5	-0.088	Attewell and Farmer (1974)
14	562	1.5	8.5	12.0	(7.1)	0.96	12.0	16.9	(14.0)	9.64	15.0	21.2	0.111	Attewell and Farmer (1974)
15	550	1.5	7.5	10.6	(7.8)	0.96	12.0	16.9	(13.7)	12.05	16.0	22.6	0.150	Attewell and Farmer (1974)
16	625	7.15	3.5	9.8	(7.9)	0.96	5.0	14.0	(15.6)	12.85	9.0	25.2	0.259	Barrat and Tyler (1976)
17	625	2.75	6.0	10.2	(7.9)	0.96	7.5	12.8	(15.6)	14.46	11.0	18.7	0.136	Barrat and Tyler (1976)
18	347	1.98	10.0	15.6	(6.7)	0.96	14.0	21.8	(12.0)	10.84	19.0	29.6	0.162	Barrat and Tyler (1976)
19	153	0.91	10.0	11.1	(5.9)	0.33	12.5	13.9	(4.4)	0.55	14.0	15.6	0.028	Muir Wood and Gibb (1971)
20	120[8]	1.30	5.0	6.3	(4.1)	1.33	21.0	26.6	(11.9)	1.82	23.0	29.1	0.152[9]	Boden and McCaul (1979)
21	121	1.0	2.0	2.4	(2.4)	1.10	8.0	9.6	(6.5)	6.0	22.3	26.8	2.132	McCaul et al (1976), O'Reilly et al (1976)
22	132	1.5	3.0	3.6	(2.7)	1.10	8.0	9.6	(7.1)	7.0	18.0	21.6	1.364	McCaul et al (1976), O'Reilly et al (1976)
23	530	3.45	9.5	21.4	(20.9)	2.73	20.0	45.0	(54.4)	9.77	25.0	56.3	0.139	El-Nahhas (1980)
24	163	0.84	3.0	3.5	(3.0)	1.0	11.0	12.8	(9.5)	4.05	34.0	39.4	1.051	Thurber (1982), Branco (1981)
25	220	2.73	2.7	5.2	(2.0)	2.19	6.0	11.5	(6.7)	9.30	10.0	19.2	0.633	Corbett (1984)
26	100[11]	4.36	3.0	5.0	3.8	1.29	18.0	29.9	10.2	4.85	56.0	93.0	3.226[9]	Costa et al (1974)

Table 5.31 Predicted and Measured Displacements at the Face and at the Point of Support Activation in Shallow Tunnels for the Crown (Continued).

No.	Tunnel and Section	Method	Lining	Ground	Water Level	Behaviour	D (m)	H (m)	E (MPa)	K	φ (°)	c (kPa)
27	S. Paulo E.W. Line	Closed Shield(5)	Cast iron seg.	Clayey sand - SC	B	UN?	6.19	21.6	80	0.6	0	120
28	S. Paulo Sanegran I	Open Shield	Precast conc.	Weathered gneiss	LO	DR	5.25	20.0	80	0.6	35	NA
29	S. Paulo Sanegran II	Open Shield(5)	Precast conc.	Dense sand - SP	B	DR	5.25	18.4	80	0.6	40	0
30	S. Paulo Tamanduatei	Closed Shield	Precast conc.	Loose sand - SW	B (18)	DR	1.79	6.2	5	0.5	30	0
31	S. Paulo ABV ext CC1	NATM	Shotcrete	Clayey sand - SC	A	DR	4.04(3)	6.2	28	0.75	29	0
32	S. Paulo ABV ext GG1	NATM	Shotcrete	Clayey sand - SC	A	DR	4.04(3)	6.45	28	0.75	29	0
33	S. Paulo ABV ext BB1	Hand mined	Steel ribs & lagg.	Clayey sand - SC	A	DR	3.99(3)	6.70	28	0.75	29	0
34	S. Paulo N. Ext. S1.9(14)	NATM	Shotcrete	Stiff silty clay CL CH	B	DR?	7.83(3)	10.76	90	0.9	25	3
35	S. Paulo E. Ext. S1.3(14)	NATM	Shotcrete	Stiff silty clay CL CH	B	DR	7.83(3)	11.64	90	0.9	25	3
36	S. Paulo N. Ext. S1.2(14)	NATM	Shotcrete	Stiff silty clay CL CH	B	DR	7.83(3)	11.26	90	0.9	25	3
37	S. Paulo N. Ext. S1.10(14)	NATM	Shotcrete	Stiff silty clay CL CH	B	DR	7.83(3)	10.05	90	0.9	25	3
38	Rio Manqueira ext. 11K(2)	Bernold Shield	Cast in place conc.	Residual soil SM SC	LO	DR	7.0(3)	6.4	15	0.5	40	10
39	Rio Manqueira ext. 23M(2)	Bernold Shield	Cast in place conc.	Residual soil SM SC	LO	DR	7.0(3)	6.4	15	0.5	40	10
40	Washington C-line ext. 10	Open Shield	Exp. rib & lagg.	Sand&silty sand SP SM	B (18)	DR	6.45	11.7	35	0.5	35	0
41	Washington C-line ext. 9	Open Shield	Exp. rib & lagg.	Sand&silty sand SP SM	B (18)	DR	6.45	11.7	35	0.5	35	0
42	Washington L-Route ext. 1	Open Shield	Steel segments	Compact sand SM SP	LO	DR	5.5	17.4	115	0.4	40	0
43	Washington L-Route ext. 3	Open Shield	Steel segments	Compact sand SM SP	LO	DR	5.5	17.4	115	0.4	40	0
44	Washington L-Route ext. 9	Open Shield	Steel segments	Compact sand SM SP	LO	DR	5.5	19.6	115	0.4	40	0
45	Washington L-Route ext. 11	Open Shield	Steel segments	Compact sand SM SP	LO	DR	5.5	19.2	115	0.4	40	0
46	Winnipeg ext. F5	Hand mined	Cast in place conc.	Varved clay CH	B	UN	1.93	11.7	6	0.8	0	70
47	Winnipeg ext. F14	Hand mined	Cast in place conc.	Varved clay CH	B	UN	1.93	11.7	6	0.8	0	70
48	Thunder Bay I	Closed Shield	Precast conc.	Soft silty clay CH	B	UN?	2.47	9.6	7	0.9	0	30
49	Madrid Line 6, ext. 2	Belgian	Cast in place conc.	Hard fiss. clay MH	B	DR?	8.2(3)	17.9	200	0.8	35	10
50	Seville Exp. Sect. 1 and 2	Mined	Brick and conc.	Clay marl CH	B	DR?	4.5(3)	32.5	200	0.9	30	90
51	Mexico Siphon	Open Shield	Steel segments	Lacustrine clay CH	B	UN?	2.95	10.2	5	0.75	0	30
52	Japan B-2	Closed Shield(5)	Precast conc.	Alluvial clay MH CH	B	UN	7.24	24.0	16	0.7	0	50

List of Symbols and Notes used in the table can be found in Table 5.33.

Table 5.31 Predicted and Measured Displacements at the Face and at the Point of Support Activation in Shallow Tunnels for the Crown (Continued).

			Displ. u at the face (mm)				Displ. u at lining installation or closure (mm)			Face Position for Final u (x/D)	Final u (mm)			
No.	σ_{r0} (kPa)	y (m)	Meas.	Extr.	Predic.	L/D	Meas.	Extr.	Predic.		Meas.	Extr.	After Support	Main References
27	254(12)	4.0	6.0	10.0	(5.6)	1.29	15.0	25.1	(15.0)	4.85	25.0	41.8	0.666(9)	Sozio (1978)
28	380	1.5	6.0	7.7	(7.2)	1.56	20.0	25.6	(19.[illegible])	4.76	40.0	51.2	0.642	Azevedo (1983, 1985)
29	258(13)	3.9	3.0	5.7	(4.7)	1.56	5.0	8.2	(12.7)	13.33	8.0	13.1	0.187	Veraki et al (1985)
30	112	0.21	13.0	14.2	(12.1)	3.91	80.0	87.0	(34.0)	8.38	110.0	119.9	0.821	Negro (1984)
31	101	-	3.3	3.3	3.8	0.6	7.4	7.4	8.7	1.50	8.8	8.8	0.096	Negro and Eisenstein (1981)
32	105	-	1.3	1.3	4.0	0.6	2.6	2.6	9.1	4.20	3.9	3.9	0.089	Negro and Eisenstein (1981)
33	109	-	3.3	3.3	4.1	0.25	5.6	5.6	7.7	4.51	17.7	17.7	0.779	Negro and Eisenstein (1981)
34	215	2.0	5.7	5.9	(4.5)	0.84	15.0	15.8	(10.5)	1.79	24.0	26.1	0.551	Negro et al (1985)
35	233	2.0	3.7	3.7	(4.9)	0.83	13.2	13.5	(11.4)	2.39	22.5	23.9	0.513	Negro et al (1985)
36	225	3.02	6.3	6.3	(4.2)	0.64	20.1	22.3	(10.4)	NA	24.9	26.0	0.189	Negro et al (1985)
37	201	2.0	6.3	6.0	(4.2)	0.42	16.1	16.0	(9.0)	NA	25.5	26.0	0.572	Negro et al (1985)
38	115	1.4	13.0(14)	15.0	(16.2)	4.5	350.0	402.5	(45.6)	NA	350	402.5	0	Massa (1981)
39	115	1.4	15.0(14)	17.3	(16.2)	NA	NA	NA	-	NA	120.0	130.0	-	Massa (1981)
40	234	0.46	15.0	15.0	13.0	1.23	280.0	280.0	35.1	2.33	335.0	335.0	1.275	Hanamire (1975)
41	234	0.46	10.0	10.0	13.0	1.23	230.0	230.0	35.1	2.33	320.0	320.0	2.087	Hanamire (1975)
42	347	1.0	2.0	2.7	(5.2)	1.16	18.0	23.9	(14.3)	2.18	30.0	39.9	0.964	Cording et al (1976), Tan (1977)
43	347	1.5	1.5	3.0	(5.2)	1.16	13.0	17.3	(14.3)	2.73	22.0	29.3	0.723	Cording et al (1976), Tan (1977)
44	391	1.7	7.0	9.3	(5.9)	1.16	39.0	51.9	(16.1)	2.36	51.0	67.8	0.850	Cording et al (1976), Tan (1977)
45	383	1.6	2.0	2.8	(5.0)	1.16	11.0	15.4	(15.8)	1.82	15.0	21.0	0.306	Cording et al (1976), Tan (1977)
46	199	1.2	10.0	20.0	(16.5)	2.0	12.5	25.0	(43.0)	5.0	17.0	34.0	0.141	Hardy & Associates (1980)
47	199	0.8	8.5	17.0	(16.5)	2.0	10.5	21.0	(43.0)	NA	16.0	32.0	0.172	Hardy & Associates (1980)
48	183	1.28	7.0	11.3	(15.7)	2.83	60.0	109.7	(39.6)	6.07	75.0	121.0	0.175	Belshaw and Palmer (1978)
49	358	1.40	3.1	3.7	3.8	3.0	10.8	12.9	9.9	NA	12.2	14.5	0.109	Sagaseta (1973), Sagaseta & Escario (1974)
50	649	3.46	2.0	3.6	(3.5)	0.53	-4.0	7.3	(7.7)	-4.0	18.5	33.7	1.808	Uriel and Oteo (1979)
51	115	1.2	40.0	50.8	(18.0)	2.70	-	-	-	NA	170.0	250.0	-	Saenz and Utesa (1971)
52	265(15)	4.0	42.0	75.0	(32.6)	1.25	105.0	189.0	(84.3)	4.5	120.0	216.0	0.166(9)	Hanya (1977)

Table 5.31 Predicted and Measured Displacements at the Face and at the Point of Support Activation in Shallow Tunnels for the Crown (Continued).

No.	Tunnel and Section	Method	Lining	Ground	Water Level	Behaviour	D (m)	H (m)	E (MPa)	K	ϕ (°)	c (kPa)
1	Frankfurt 25 Romerberg Sth I	NATM$^{(1)}$	Shotcrete	Stiff clay marl CH MH	LO	DR	6.48	12.0	24	0.8	20	20
2	Frankfurt 25 Romerberg Sth II	NATM$^{(1)}$	Shotcrete	Stiff clay marl CH MH	LO	DR	6.48	11.5	24	0.8	20	20
3	Green Park Incl. X2	Open Shield	Cast iron seg.	London clay CH	B	UN	4.15	29.6	60	1.3	0	250
4	Green Park Incl. Y2	Open Shield	Cast iron seg.	London clay CH	B	UN	4.15	28.8	60	1.3	0	250
5	Green Park Incl. Z2	Open Shield	Cast iron seg.	London clay CH	B	UN	4.15	28.2	60	1.3	0	250
6	Chinnor Incl. P4	TBM	Steel ribs no lagg.	Lower chalk	A	DR	5.0	6.5	75	0.5	0	q_u=74,200
7	Chinnor Incl. P6	TBM	Steel ribs no lagg.	Lower chalk	A	DR	5.0	6.1	75	0.5	-	q_u=74,200
8	Victoria Line Anchor A	Open Shield	Cast iron seg.	London clay CH	B	UN	4.11	24.0	60	1.4	0	250
9	Edmonton Exper. SI11	Closed Shield	Exp. ribs & lagg.	'Soft' till - CL	A $^{(10)}$	UN	2.56	25.7	17	0.8	16	45
10	Edmonton Exper. SI31	Closed Shield	Exp. conc. seg.	'Soft' till - CL	A $^{(10)}$	UN	2.56	23.2	17	0.8	16	45
11	Edmonton Exper. SI33	Closed Shield	Exp. conc. seg.	'Soft' till - CL	A $^{(10)}$	UN	2.56	23.2	17	0.8	16	45
12	Edmonton LRT Sth SI3	Closed Shield	Exp. ribs & lagg.	'Stiff' till - CL	A	DR	6.17	9.8	70	0.75	40	0
13	Edmonton LRT Sth SI7	Closed Shield	Exp. ribs & lagg.	'Stiff' till - CL	A	DR	6.17	8.9	70	0.75	40	0
14	Edmonton LRT Sth SI6	Closed Shield	Exp. ribs & lagg.	'Stiff' till - CL	A	DR	6.17	8.9	70	0.75	40	0
15	S. Paulo Sanegran I	Open Shield	Precast conc.	Weathered gneiss	LO	DR	5.25	20.0	80	0.6	35	NA
16	Rio Mangueira SI4$^{(14)}$	Bernold Shield	Cast in place conc.	Residual soil SM-SC	LO	DR	7.0$^{(3)}$	6.4	15	0.5	40	10
17	Washington C line SI16	Open Shield	Exp. ribs & lagg.	Sand&silty sand SP SM	B $^{(18)}$	DR	6.45	11.7	35	0.5	35	0
18	Washington C line SI20$^{(2)}$	Open Shield	Exp. ribs & lagg.	Sand&silty sand SP SM	B $^{(18)}$	DR	6.41	11.7	35	0.5	35	0
19	Winnipeg SI	Hand mined	Cast in place conc.	Varved clay CH	B	UN	1.93	11.7	6	0.8	0	70
20	Mississauga SID1	Open Shield	Steel ribs & lagg.	Dense till CL	B $^{(18)}$	DR	4.27	11.5	120	1.0	35	30
21	Thunder Bay I left SI	Closed Shield	Precast conc.	Soft silty clay CH	B	UN	2.47	9.6	7	0.9	0	30
22	Hagenholz L7	Open Shield	Precast conc.	Glacial lacustr. sed.	LO	DR	11.4	28.7	200	0.8	NA	NA

List of symbols and notes used in this table can be found in Table 5.33

Table 5.32 Predicted and Measured Displacements at the Face and at the Point of Support Activation in Shallow Tunnels for the Springline

No.	σ_{z0} (kPa)	Y (m)	Displ. u at the face (mm)			L/D	Displ. u at lining installation or closure (mm)			Face Position for Final u (z/D)	Final u (mm)		ΔU After Support	Main References
			Meas.	Extr.	Predic.		Meas.	Extr.	Predic.		Meas.	Extr.		
1	226	0.5	3.9	4.6	10.3	0.69	7.9	9.2	28.6	1.56	8.8	10.3	0.018	Chambosse (1972)
2	201	0.5	17.0	19.9	9.9	0.69	16.07	16.0	27.6	1.70	13.5	15.8	-0.003	Chambosse (1972)
3	814	1.73	1.0	1.7	(10.4)	0.96	6.0	10.3	(29.3)	9.0	7.0	12.0	0.030	Attewell and Farmer (1974)
4	792	2.15	4.0	6.8	(10.1)	0.96	6.0	10.2	(28.5)	9.0	7.5	12.8	0.047	Attewell and Farmer (1974)
5	779	4.23	1.5	3.9	(9.9)	0.96	2.0	5.2	(20.0)	9.0	3.0	7.8	0.048	Attewell and Farmer (1974)
6	96	0.5	0.6	0.9	(0.9)	1.10	5.7	8.0	(2.9)	6.0	8.9	12.5	0.703	McCaul et al (1976)
7	92	0.5	0.6	0.9	(0.9)	1.10	4.4	6.2	(2.8)	3.0	5.7	8.0	0.293	McCaul et al (1976)
8	710	0.49	2.7	3.3	(9.1)	0.87	9.7	11.8	(24.9)	1.06	12.3	15.0	0.066	Ward (1969)
9	454	0.61	9.0	15.4	(11.5)	2.73	23.0	39.0	(35.7)	NA	27.0	46.0	0.102	El-Nahhas (1980)
10	412	1.12	2.4	5.1	(10.5)	2.73	4.6	9.8	(32.4)	11.0	2.8	2.87	-0.113	El-Nahhas (1980)
11	412	1.05	6.5	13.4	(10.5)	2.73	18.0	37.1	(32.4)	6.0	25.3	52.2	0.243	El-Nahhas (1980)
12	103	1.91	0.5	1.0	2.7	1.0	0.8	1.5	8.0	15.0	3.8	7.4	0.366	Thurber (1982)
13	171	1.21(16)	0.5	1.0	2.5	1.0	2.5	5.0	7.5	4.0	3.1	6.0	0.066	Branco (1981)
14	171	3.31(16)	0.4	1.2	2.5	1.0	1.8	5.2	7.5	4.9	2.5	7.2	0.133	Branco (1981)
15	258	1.58(17)	4.0(17)	7.4	(2.6)	1.56	11.0	20.5	(8.4)	3.8	21.0	39.1	0.687	Azevedo (1983, 1985)
16	89	0.8	3.0	4.5	(6.0)	4.5	20.0	30.0	(20.0)	NA	20.0	30	0	Massa (1981)
17	149	0.03	8.0	8.0	4.0	1.23	25.0	25.0	12.6	6.0	18.0	18.0	-0.255	Hansmire (1975)
18	149	0.72	2.8	3.0	3.8	1.1	22.5	33.8	12.6	1.55	29.6	44.4	0.388	Hansmire (1974)
19	172	0.60	8.0	11.8	(9.3)	2.0	14.0	20.6	(28.9)	4.0	15.0	22.1	0.027	Hardy & Assoc. (1980)
20	327	0.91	2.0	3.0	2.1	1.75	4.0	6.0	6.2	5.27	5.0	7.5	0.129	DeLory et al (1979)
21	178	0.93	12.0	18.5	(10.9)	2.83	3.0	46.0	(33.3)	8.0	33.0	51.0	0.080	Belshaw and Palmer (1978)
22	550	1.92	2.2	3.0	5.3	1.0	NA	-	-	-	-	-	-	Andraskay and Attinger (1979)

Table 5.32 Predicted and Measured Displacements at the Face and at the Point of Support Activation in Shallow Tunnels for the Springline (Continued).

No.	Tunnel and Section	Method	Lining	Ground	Water Level	Behaviour	D (m)	H (m)	E (MPa)	K	φ (°)	c (kPa)
1	Heathrow Cargo (UK)	Open Shield	Exp conc. seg.	London clay CH	B	UN	10.9	7.3	27	1.9	0	200
2	Edmonton LRT (Sth) ME10	Closed Shield	Exp ribs & lagg	'Stiff' till CL	A ?	DR	6.17	8.9	70	0.75	40	0
3	Edmonton Exper. ext. MX37	Closed Shield	Exp conc. seg.	"Soft' till CL	$A^{(10)}$	UN	2.56	23.2	17	0.8	16	45
4	S. Paulo ABV ext. RB1 (B7)	Mined	Steel ribs & lagg.	Clayey sand SC	[illegible]	DR	$3.99^{(13)}$	6.7	20	0.75	29	0
5	S. Paulo ABV ext GG1 (G8)	NATM	Shotcrete	Clayey sand SC	A	DR	4.04	6.5	20	0.75	29	0
6	S. Paulo ABV ext. CC1 (C9)	NATM	Shotcrete	Clayey sand SC	A	DR	4.04	6.2	20	0.75	29	0

No.	σ_{r0} (kPa)	y (m)	Displ. u at the face (mm)				Displ. u at lining installation or closure (mm)			Face Position for Final u (x/D)	Final u (mm)		ΔU After Support	Main References
			Meas.	Extr.	Predic.	L/D	Meas.	Extr.	Predic.		Meas.	Extr.		
1	302	0.30	3.2	4.6	(-5.3)	0.33	NA	NA	-	NA	NA	NA	NA	Muir Wood and Gibb (1971)
2	206	-	2.7	2.7	3.1	1.00	NA	NA	-	NA	NA	NA	NA	Branco (1981)
3	542	$1.3^{(19)}$	2.0	12.0	(9.5)	2.73	2.4	15.0	-	5.4	3.0	19.0	0.049	El-Nahhas (1980)
4	171	0.46	1.0	1.2	3.0	NA	NA	–	–	1.5	3.0	3.6	-	Negro and Eisenstein (1981)
5	171	1.70	3.5	6.2	3.0	0.6	4.5	8.0	9.1	1.0	7.0	12.4	0.170	Negro and Eisenstein (1981)
6	165	1.24	1.5	2.1	2.9	0.6	4.5	6.3	8.7	2.22	9.0	13.5	0.302	Negro and Eisenstein (1981)

Table 5.33 Predicted and Measured Displacements at the Face and at the Point of Support Activation in Shallow Tunnels for the Floor

SYMBOLS	
LO	Water level lowered before construction
A	Tunnel above ground water level
B	Tunnel below ground water level
DR	Drained behaviour (and parameters) assumed
UN	Undrained behaviour (and parameters) assumed
D	Excavation diameter
H	Depth of cover to tunnel crown
E	Average initial tangent modulus of soil around the tunnel (drained or undrained)
K	In situ stress ratio (effective or total stresses)
ϕ	Friction angle (drained or undrained)
c	Cohesion (drained or undrained)
σ_{r0}	Radial stress at the point considered (effective or total stresses)
y	Radial distance between instrument and tunnel contour
Meas. u	Measured radial displacement at a point close to the tunnel contour
Extr. u	Radial displacement extrapolated to the tunnel contour
Predic. u	Predicted radial displacement
L/D	Relative distance between face and point of lining closure or activation

NOTES	
(1)	Twin tunnels driven simultaneously
(2)	Second tunnel built (excluding movements due to the first)
(3)	Equivalent diameter of excavation (non circular profile)
(4)	Data from side drift advance only
(5)	With compressed air
(6)	61 kPa of air pressure discounted
(7)	After southbound tunnel was driven
(8)	40 kPa of bentonite pressure discounted
(9)	Disregarding air or bentonite pressure
(10)	Tunnel above regional water table but possibly below perched water levels. Soil fully saturated
(11)	50 kPa of air pressure discounted
(12)	70 kPa of air pressure discounted
(13)	100 kPa of air pressure discounted
(14)	Tunnel heading only
(15)	95 kPa of air pressure discounted
(16)	Measuring point 0.4 m above springline elevation
(17)	Average of two inclinometers
(18)	Crown below water level. GWL lowered by drainage into the tunnel during advance
(19)	Measuring point 1.9 m off the centreline

Symbols and Notes for Tables 5.31 to 5.33

are also indicated. The geometric data of each case history is summarized in terms of the depth of the cover and in terms of the diameter of the excavation. An equivalent excavation diameter is provided in those cases where the tunnel had a non-circular cut profile. In a few cases, compressed air pressure or slurry pressure was used during construction. In these cases, the radial in situ stress at the point being considered was reduced by an amount equal to that pressure.

Attempts were made in each case to identify the probable response of the ground in terms of the generation and dissipation of pore pressures over the period of time the field measurements were taken up to the instant the lining was installed or closed. For this, the approximate criteria proposed in Chapter 3 were used, and these required an estimate of the coefficient of consolidation of the soil. Whenever this information was not available, that coefficient was evaluated indirectly through the coefficient of permeability and the deformation properties of the ground. To simplify the interpretation of data, only two extreme cases were considered: "drained" or "undrained" behaviour. Those cases where the ground response may have been situated between the two extremes, were labelled according to the extreme response closer to the one that most likely prevailed. A considerable degree of subjective interpretation might, therefore, have been included.

The ground properties were defined in accordance with the above classification. Drained or undrained deformation and strength properties were selected appropriately. Similarly, the in situ stress ratio K was defined in terms of effective or total stresses.

To account for the variations of the in situ deformation modulus with depth, an average E value was taken for points of the ground around the tunnel profile. Whenever the stress-strain data were available for a particular site, the selected E value corresponded to the initial tangent modulus defined at the early portion of a test result. In all cases where neither these nor laboratory tests were available, established correlations have been used to estimate the properties of the ground mass.

When dewatering preceded tunnel construction, the displacements associated with it have been deduced from the observed movements. Hence, the ground movements recorded in the tables refer, as much as possible, to those resulting from the tunnel construction and exclude those due to time dependent responses.

The displacements indicated in the tables are those measured by settlement points or slope indicators installed closer to the opening. Except where indicated, they can be taken as movements radial to the tunnel contour. In each case history, the displacements at three situations were identified: a) when the tunnel face (or the face of the heading in a staged excavation) reached the instrumented section; b) when the lining was activated or when the support ring was closed (in the staged application of a shotcrete lining) at the instrumented section; c) when the movements stabilized (in short term conditions). For situations (b) and (c), the tables provide the relative position of the tunnel face ahead of the measuring section. For shotcrete supports, cast-in-place concrete liners or expanded lining systems, no major difficulty was experienced in identifying the situation (b) at which the support was put in full contact with the ground. For grouted, pre-fabricated linings, however, it was not always simple to identify when this happened. In many cases, this depended on how much behind the face the grouting operation took place, but the information supplied by the references on this particular point are frequently vague or inaccurate. After a careful study of the construction procedures, the section at which the support activation possibly occurred was defined, but no assurance on the accuracy of its location is given, since it also depends on the quality of the grouting operation undertaken. If the grout failed to completely fill the void behind the lining, the support may have not have come in full contact with the soil at that section. Therefore, it cannot be said to have been fully activated there, but only at distances larger than the value shown. The displacements at situation (b) above would be those taking place just before ground-lining interaction starts at the instrumented section. Only when shotcrete is used does there exist some degree of confidence on the estimated distance of delayed support application (L/D), as its contact with the ground is usually "good" (Section 2.3.5). But even in this case, some uncertainty may exist as the records of the construction are not always given in sufficient detail.

Usually, field measurements of displacements are taken not at the tunnel perimeter but at a certain distance away. To allow adequate comparison between the proposed method of estimating the closure of the tunnel profile and the data from case histories, it was necessary to extrapolate the field measurements to the tunnel contour. To achieve this, the results of parametric non-linear elastic finite element analyses were used. These analyses are described and presented in detail in Chapter 6. Their results have partly presented by Eisenstein and Negro (1985:Figure 5). These analyses allowed the definition of the ratio between the perimeter displacement to that measured at a distance y from it (this distance is also shown in the tables). This ratio, as it will be shown in Chapter 6, is mainly a function of y, in relation to the tunnel diameter, of the ratio H/D, of the in situ stress ratio and of the ground properties (mainly ground strength). Clearly, the ratio would not be applicable to cases where localized ground collapse may have occurred. Since this condition could not be identified readily, the extrapolation was undertaken by this method in all cases investigated.

Besides the values of the extrapolated measurements to the tunnel contour, the tables provided the predicted radial displacements for comparison. These were estimated using the data shown in the tables, and the numerically derived solution for tunnel closure as proposed in Section 5.3.5.2 (Figures 5.94 to 5.96). Many of the predicted displacements are placed within brackets in the tables. This indicates that the input parameters used for the prediction lay beyond the formal range of validity of the proposed method of calculation (either in terms of K or H/D). Despite this, the predictions were made as if they were rigorously valid.

Note that the predictions were made only for displacements occurring at the tunnel face and at the point of lining activation. The tables, however, include the final radial displacements. Using the definition of the dimensionless radial displacement given by Equation 2.16, it was possible to calculate the increment, ΔU, of the dimensionless displacement after the support was activated and until the movements stabilized in each case history. This corresponds to the deformations that the support would ideally endure, provided a good lining-ground contact ~~exists~~. A negative sign in the ΔU value reveals an outward movement.

Without exception, all observed radial movements taking place at the face, as well as the increments of displacement between the face and the section at which the support was activated, were positive (inwards). Most of the increments after the support was activated were also positive. A few exceptions to this were noted. One was the Green Park tunnel (extensometer X1), corresponding to case 13 in Table 5.31, where an outward crown movement was observed in this tunnel driven through London Clay. Further exceptions are indicated in Table 5.32 for the tunnel springline: cases 2, 10 and 17 also showed outward springline displacements after the lining was installed. Case 2 corresponds to a shotcrete lining, and cases 10 and 17 to expanded steel ribs and wooden lagging primary support.

Predicted and Measured Radial Displacements at the Face

The radial displacements of the tunnel crown at the face are compared in Figure 5.102 a and b. Figure 5.102 b is simply an enlargement of part of Figure 5.102 a. To help the comparison, the ground was classified into four groups as shown. The "stiff clay" group actually included clayey soils with consistencies ranging from medium to hard. The "soft clay" group includes soils with high clay content and with undrained cohesive strengths smaller than 50 kPa. The "granular soil" group comprises all soils with an appreciable content of sandy or gravelly fractions, with or without fines (silty or clayey). Finally the "soft rock" group includes both weathered and unweathered rocks.

Globally speaking, one notes that, within plus or minus 20%, the extrapolated measurements are approximated by the predicted values in about 50% of the cases. There is a slightly more pronounced trend of the predictive method to

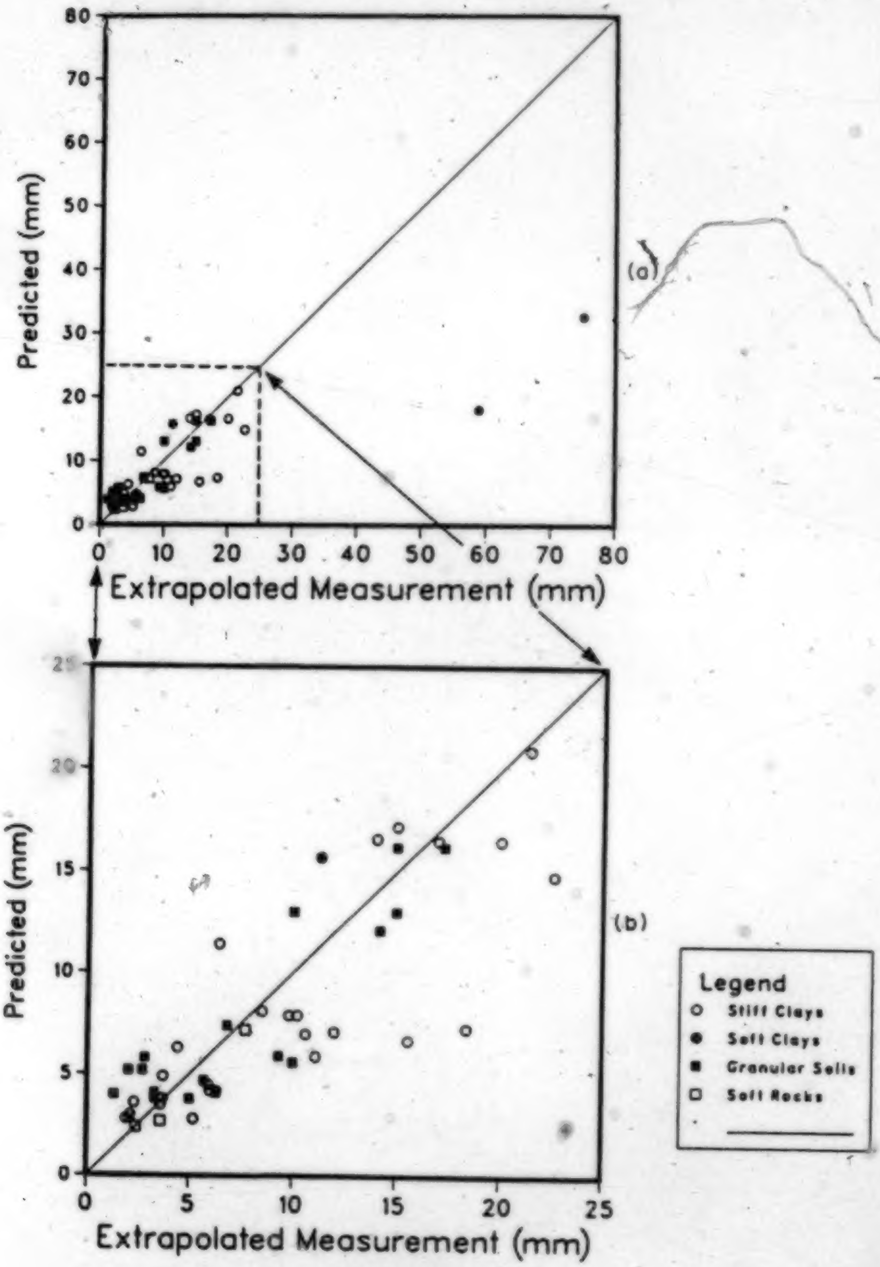

Figure 5.102 Predicted and Measured Crown Displacements at the Face for Different Ground Types

underestimate the displacements than to overestimate them (30% against 20% of the cases approximately). The predictions are based on a linear elastic numerical solution, and make use of the initial tangent modulus of the soil. Whenever departure from linear behaviour is observed in the ground, one would expect the simplified method to underestimate the field measurement. This could explain the noted trend. However, the frequency of cases where the displacements were overestimated is also high. Thus, one may suggest that the correct choice of the parameters of the soil, particularly the E modulus, is far more important than the simplified assumption of linear elasticity, as far as the estimate of displacements at the face are concerned. When applied to soft clays, the method shows a stronger tendency to underpredict the movements, which is explained by the more pronounced non-linear response likely to prevail in these cases.

A similar plot was prepared for the springline radial displacements, and is shown in Figure 5.103. An appreciable scatter is noted, despite the smaller number of cases available for comparison. A slightly more pronounced tendency of the present method to overestimate the displacements is noted. The reasons for this are not clear. One could speculate that the proposed method makes no allowance of ground anisotropy. Certain soils, such as London and Frankfurt clays are known to exhibit anisotropic behaviour, with horizontal deformation moduli larger than the vertical. On the other hand, the larger scatter of points could be explained in terms of the lesser accuracy possible in inclinometer results compared to the accuracy of settlement measurements by extensometers or levelling.

The lack of a sufficient number of case histories where floor heave has been measured does not allow an adequate evaluation of the predictions made for this point. Nevertheless, it is believed that the proposed method can yield sensible results (Table 5.33).

Another possible interpretation of the results presented so far, is to relate the displacement comparison with the construction method used. Accordingly, the data presented in the former two figures was replotted as shown in Figure 5.104 a and b. Three groups of construction methods were identified: (a) NATM construction, (b) Mechanized Construction Methods using TBM's and/or shields; (c) other mining methods. It is soon noticed that better agreement between predictions and measurements was obtained for methods (a) and (c). This is noted in spite of these methods do not always involve a full face excavation, as assumed in the development of the proposed prediction method. At least two reasons can be looked at to explain this. The use of non-mechanized and unshielded heading excavations are normally confined to fairly stable, stiffer and stronger ground. A linear elastic assumption, if applicable to any ground, would be more suitable for this type of soil. Secondly, and perhaps, more importantly, the

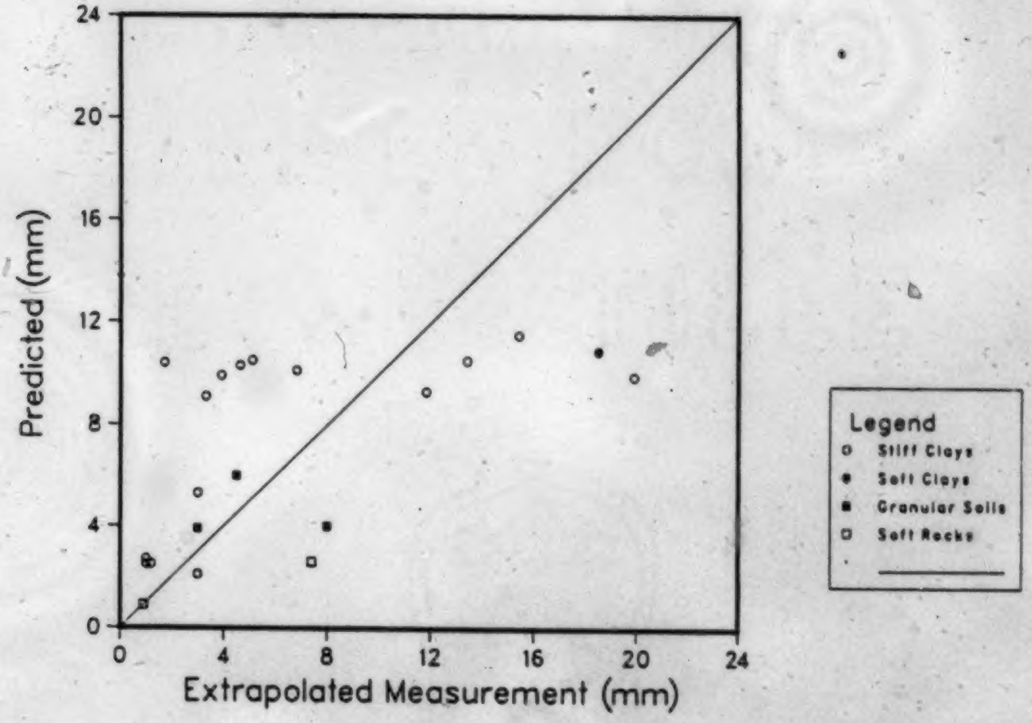

Figure 5.103 Predicted and Measured Springline Displacements at the Face, for Different Ground Types

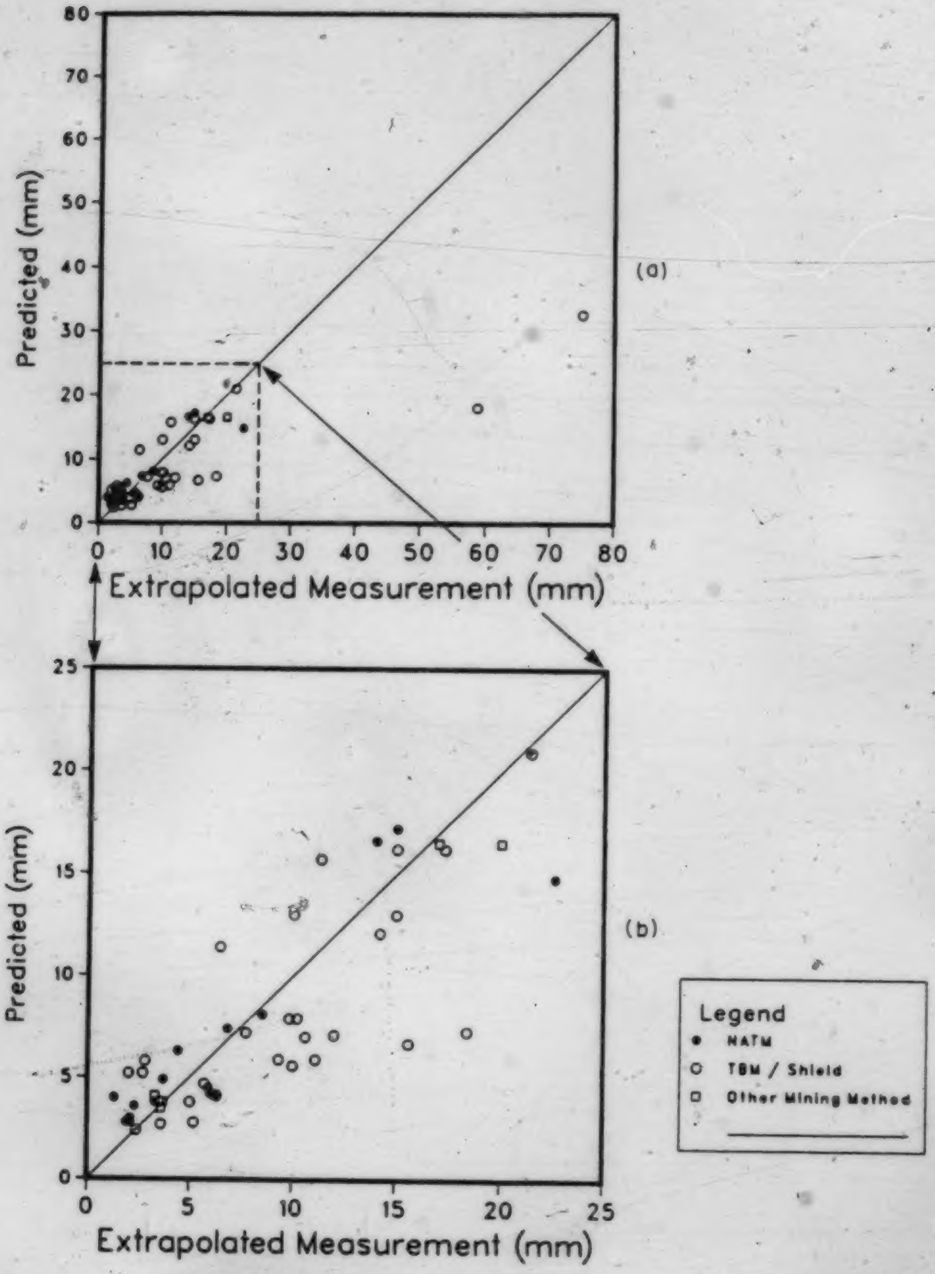

Figure 5.104 Predicted and Measured Crown Displacements at the Face for Different Tunnel Construction Methods

unprotected excavation requires for safety reasons, improved ground control measures. One of these is the earlier activation of the support. Tunnel convergence is restrained sooner by the support being activated closer to the face, and usually is without voids behind it. Most TBM or shielded excavated systems have residual void spaces behind the support. As a consequence, smaller ground stress release would be expected in (a) and (c), and possibly, less pronounced non-linear response in the ground. As for the springline displacements at the face, the results shown in Figure 5.105 do not permit any clear conclusion to be drawn.

The comparison between predicted and extrapolated measurements of radial displacement in the tunnel contour at the face show considerable scatter. It must be borne in mind that the data refers to case histories where a complete and accurate knowledge of ground properties and site conditions were not always available. Also, the predictive method encompasses substantial simplification, while still considering the most important factors. Under these circumstances the results obtained are not completely discouraging. The predicted value of displacement is particularly sensitive to the E modulus, and its correct value is not always known. The variation of this parameter alone for one particular deposit may be responsible to a significant extent, for the scatter observed in the last few figures.

Predicted and Measured Radial Displacements at the Section

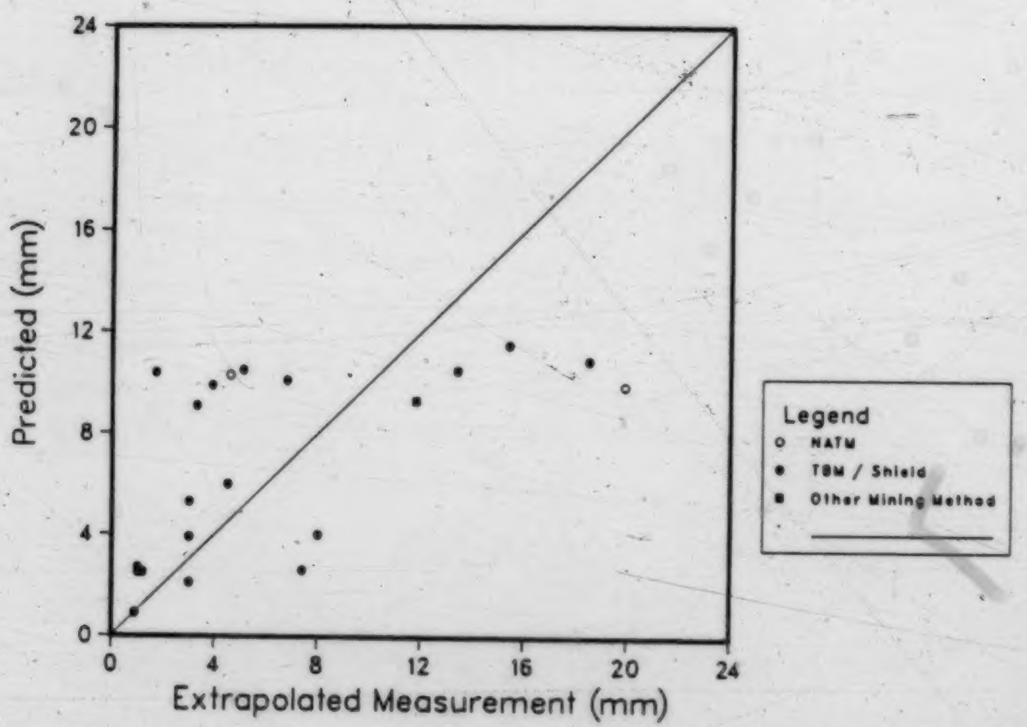

Figure 5.105 Predicted and Measured Springlne Displacements at the Face, for Different Tunnel Construction Methods

of Support Installation

The same interpretations presented for the displacements at the tunnel face were repeated for the ground movements at the tunnel sections where the support was installed. As noted before, these correspond to the sections where the shotcrete ring was closed at the floor in the NATM built tunnels.

Figures 5.106 a and b present the comparison of the crown displacements according to the different types of ground. Here one notes that for both soft clays and granular soils, the displacements tend to be underpredicted. An examination of Figures 5.107 a and b, in which the same results are presented according to the construction methods, reveals that those cases where this tendency was noted, correspond mainly to TBM or shielded excavation schemes. In other words, in TBM or shielded excavations of tunnels in soft clays and in granular soils, the proposed prediction method shows a trend to yield displacements which are smaller than those actually observed. This tendency could possibly be attributed to these soils squeezing in or collapsing to close the gap created by overcutting which is left behind the shield or the lining. In these construction schemes, the support is installed at a greater distance behind the face, and depending on the amount of overcut allowed, and on when and how efficient the grout or lining expansion operations are, the amount of stress release induced in the ground can be larger than in other

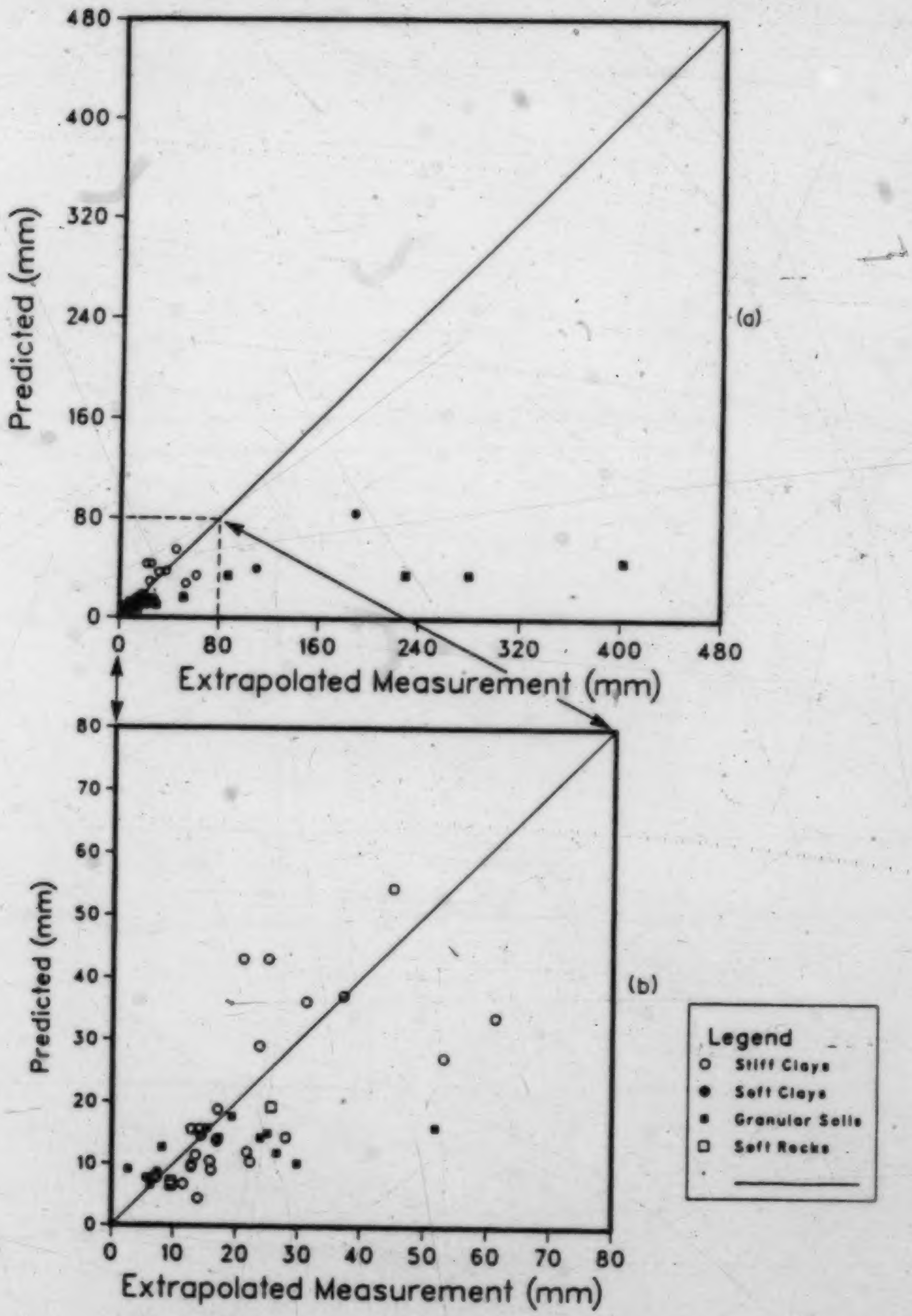

Figure 5.106 Predicted and Measured Crown Displacements at the Section the Support was Installed for Different Ground Types

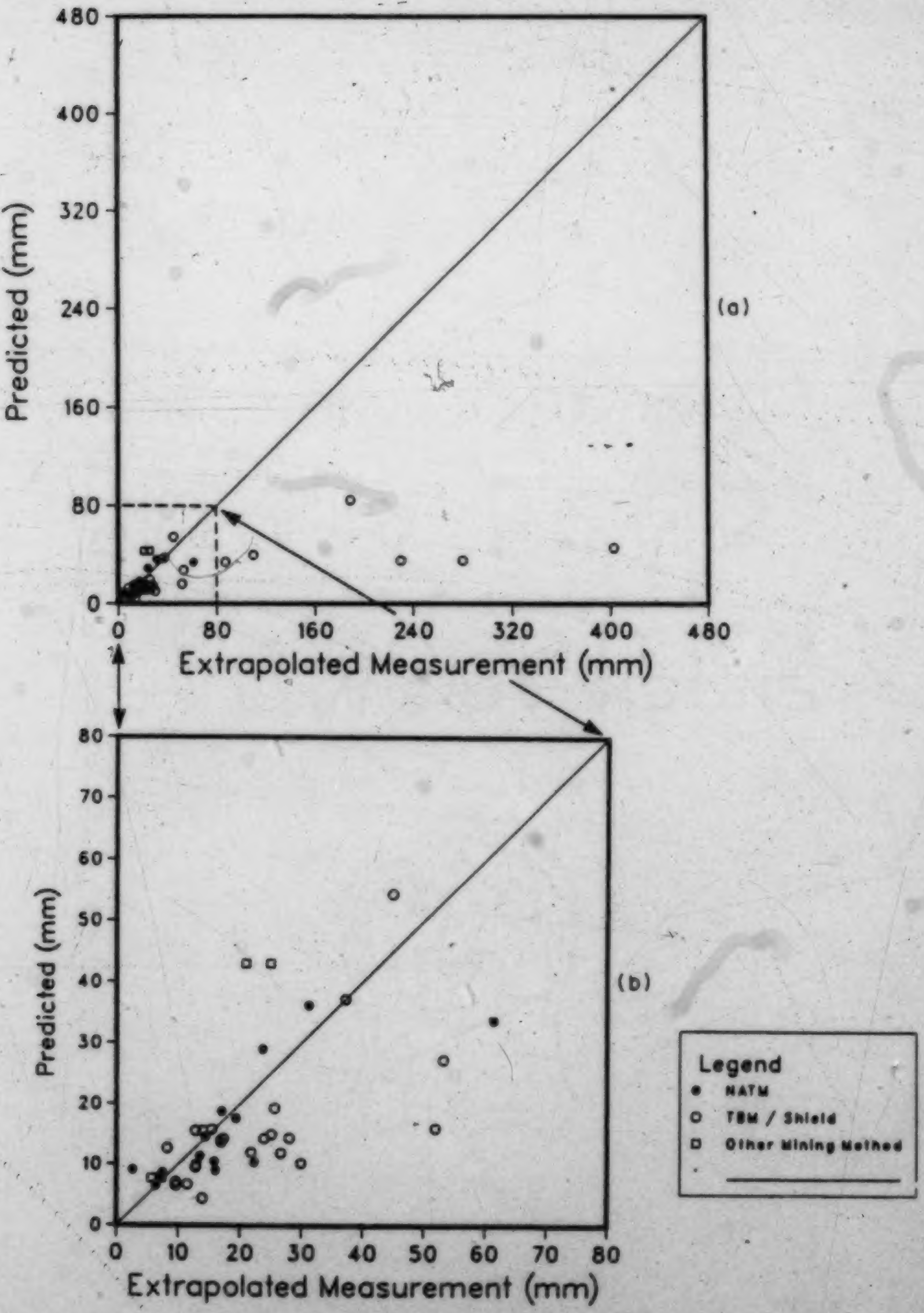

Figure 5.107 Predicted and Measured Crown Displacements at the Section the Support was Installed for Different Tunnel Construction Methods

construction schemes. Hence, a more pronounced departure from the linear response of the ground may be expected, and this leads to movements larger than those anticipated using the proposed method of tunnel closure calculation.

To illustrate this point further, Figures 5.108 a and b were prepared. The dimensionless crown displacements at the sections where the linings were installed, were calculated using the extrapolated measurements and other parameters provided by Table 5.31. These dimensionless displacements were plotted as a function of the distance X/D between the section where the lining was installed and the tunnel face. In (a), the observed data is presented according to the type of ground found in each case. In (b), the data is presented as a function of the construction method used. Included in both (a) and (b) is the distribution of the dimensionless radial displacement along the crown as given by the proposed solution, for K=0.5.

A quick examination of Figures 5.108 a and b confirms that the larger movements are noted for TBM or shielded schemes and are basically associated with soft or granular soils. This is particularly true when the support is installed at distances from the face greater than 1 to 1.2 D. In Section 2.3.4.3, a tentative criterion for ground collapse was proposed in terms of the dimensionless crown displacement. It was noted from tunnel model tests that whenever U exceeded 1.8, a near collapse condition was observed. If this criterion is correct, those points in

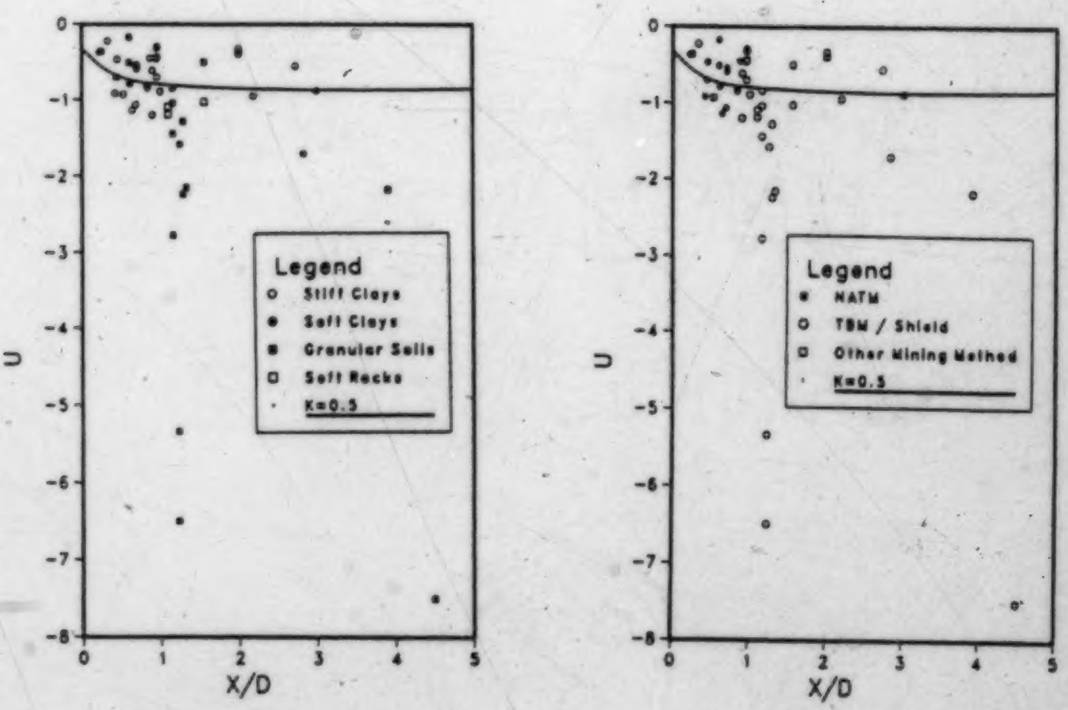

a

b

Figure 5.108 Dimensionless Crown Displacements Observed when the Support was Installed at Different Distances Behind the Tunnel Face

Figure 5.108 showing larger movements represent critical conditions where high shear strain concentration may have developed. These would involve substantial failure zones and ground instabilities such as running sand, fall-outs, etc. A review of the construction records of those case histories involved (e.g. Washington Metro), does reveal that these conditions may indeed have happened.

Recalling the discussion presented in Section 2.3.5.4, it is very likely that in those cases where the larger U values were noted, a poor lining contact may have existed which possibly resulted from excessive overcut. An overbreak larger than that set in Section 2.3.5.4 by the proposed limited overcut bringing about instability may have been the cause of the observed large movements.

While in TBM or shielded schemes the support is installed at distances greater than 1D behind the face, in NATM construction schemes, the shotcrete ring is closed at distances smaller than 1D behind the heading face (see Figure 5.108). Moreover, in the latter schemes, provided the face is stable, instabilities at the roof are seldom noticed, since the depth of unsupported advance of the heading (round length) is usually small (typically between 0.1 and 0.3D). Localized instabilities or collapse are prevented by the immediate shotcreting of the tunnel walls after the short advance. Despite the reduced strength and large deformation properties of the young shotcrete shell, it may be adequate to prevent local ground instabilities, although possibly not enough to completely restrain the ground movements. In other words, it does not impede the tunnel closure but it controls it, allowing the ground to relax without localized instabilities.

Despite the soil type, the NATM construction schemes seem to have yielded U values always smaller than about 1.0 at the section of lining closure. According to the material in Section 2.3.4.3, this value would correspond to factors of safety of about 1.5 or higher and be considered as "good ground control conditions". These conditions seem to have prevailed in all of the NATM constructions investigated, regardless of the ground type. To a great extent, these conditions seem to have existed in the NATM cases as a result of reduced overbreaks and good ground-lining contact.

To complete the picture, Figures 5.109 and 5.110 present comparisons between predicted and measured springline displacements before the support installation. Similar to the displacements at the tunnel face, a considerable scatter is noted, as well as a slightly more pronounced trend for overestimating the displacements at the section the support is installed.

In summary, if the simplified method presented herein for estimating the tunnel wall closure prior to the lining installation was to be successfully applied in practice, it would be only used in cases where good ground control conditions are specified and implemented in the tunnel construction. This seems to imply that this method may render sensible results in NATM construction schemes, regardless of the soil type (but provided the face is stable) and in TBM or shielded schemes when applied to firm grounds or even to less stable grounds, whenever the overcut is small and the lining is activated in full contact with the soil at a short distance from the face.

Measured Crown Displacements after Support Installation

The survey summarized in Table 5.31 allowed an additional set of information to be gathered. This refers to the increment of dimensionless crown displacement (ΔU) taking place after the lining is installed. This was calculated from the increment of the extrapolated crown displacement in the radial direction after the support was installed, until the ground movements stabilized (in the short term).

Figure 5.111 presents the data collected for three groups of support systems: (a) shotcrete; (b) prefabricated lining and grouted behind; (c) prefabricated lining, expanded against the soil. The prefabricated systems include precast segmented concrete linings, cast iron and steel segmented rings, as well as steel ribs and lagging. The data is shown in terms of frequency of cases for different ΔU intervals. The total number of cases for each different support group is shown in the figure.

The distinctions between these support systems are many, but within the present discussion, their main difference refers to what was defined in Chapter 2 as the

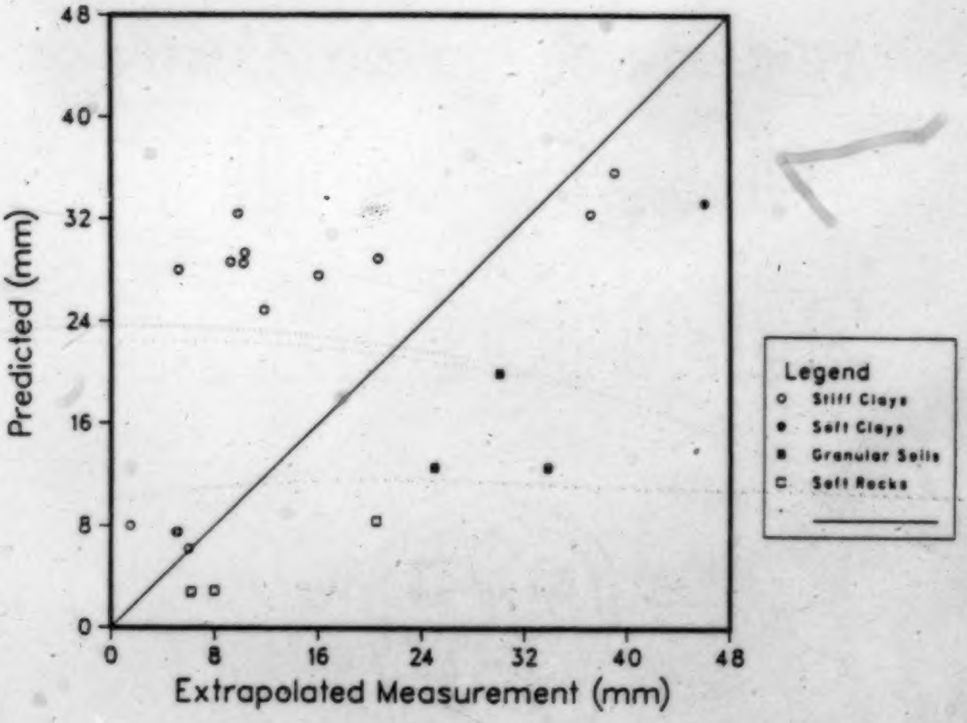

Figure 5.109 Predicted and Measured Springline Displacements at the Section the Support was Installed, for Different Ground Types

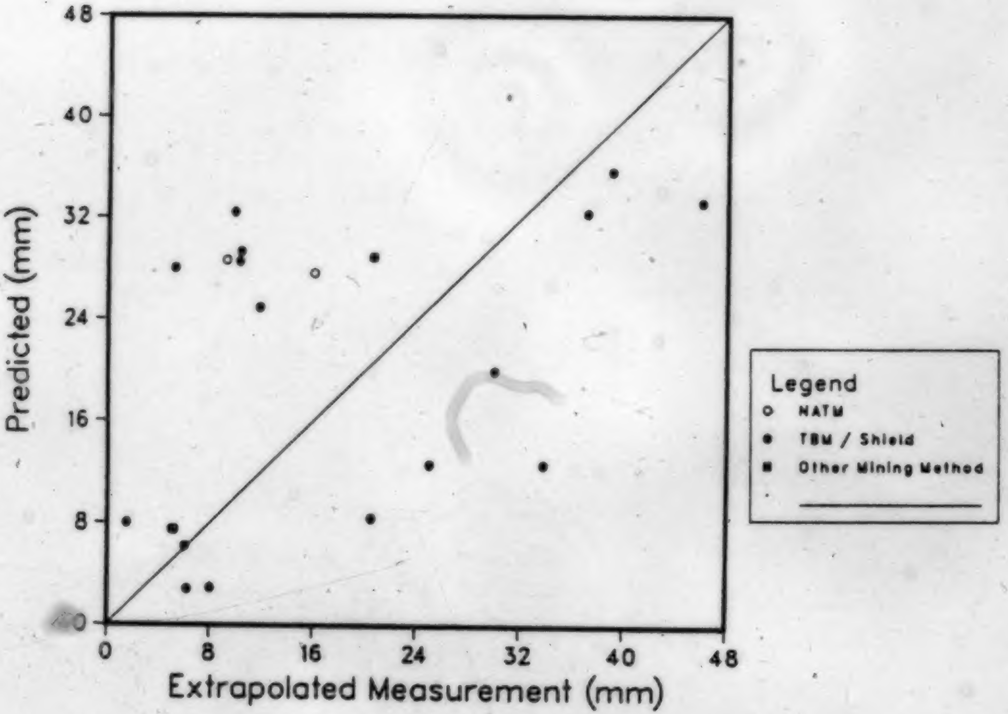

Figure 5.110 Predicted and Measured Springline Displacements at the Section the Support was Installed for Different Tunnel Construction Methods

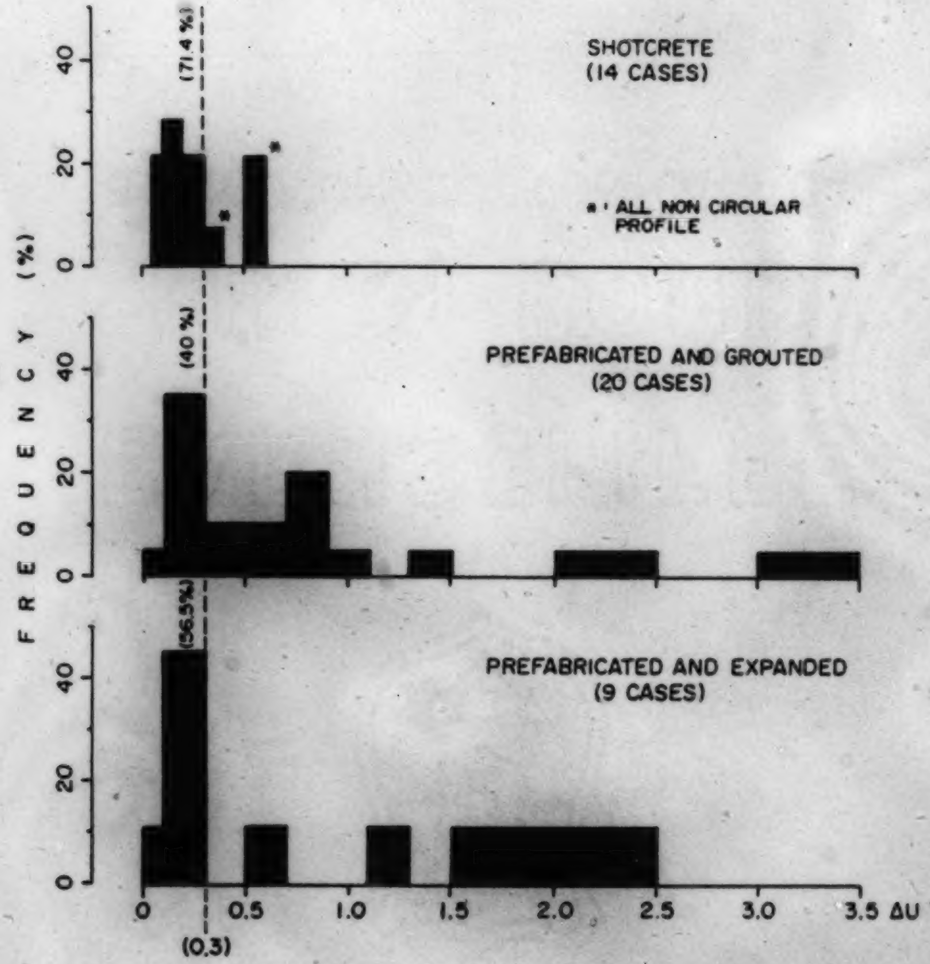

Figure 5.111 Distributions of Measured Crown Displacements after Support Installation

"quality" of the lining-ground contact. While in most shotcrete supports it is reasonable to assume that a full lining-ground contact may exist, in the other groups this may not be the case. The crown movements noted after lining installation in the last two groups may not be solely related to the relative stiffness of the support, but, are to a great degree, also affected by the size of the void left behind the lining.

For shotcrete linings, one notes that in more than 70% of the cases, ΔU is equal to or less than 0.3. If the cases in this group with a non-circular tunnel profiles (with width larger than height) were eliminated, then one could say that for circular shotcrete liners, the increment ΔU is always equal to or less than 0.3. If ΔU equal to 0.3 is taken as a reference value for limiting crown deformation of a lined tunnel with good support-soil contact, one would say that for prefabricated and grouted supports, only 40% of the cases responded as if having such a contact quality. A slightly higher accumulated frequency (56.5%) is noted for prefabricated and expanded supports. The slightly higher frequency would indicate that, in terms of ground control, expanded systems are marginally better than grouted systems.

Figure 5.112 presents the distributions of the frequency of the dimensionless crown displacement at the tunnel face, calculated from the extrapolated radial displacements which are indicated in Table 5.31. Separate distributions are shown for each ground group. One notes that, out of the total number of cases, the value of U at the face is equal to or less than 0.5, in more than 90% of the cases.

By recalling the limiting dimensionless crown displacement of 1.8 proposed in Section 2.3.4.3, a limiting increment of dimensionless crown movement can be established for between the tunnel face and the point of activation of the support in full contact with the soil. This would correspond to the total critical U less the maximum U taking place ahead of the face (0.5) and less the maximum U taking place after the support with good contact with the soil is installed (0.3). This results in the criterion of U=1.0 proposed in Section 2.3.5.4 for a maximum acceptable overbreak over a TBM or shield. The proposed approximate criterion was discussed and justified in that section.

5.3.6.2 Ground Movements Ahead of the Tunnel Face

In Section 5.3.5.2, an approximate equation was proposed to estimate the maximum horizontal movement of the face of a shallow tunnel. Table 5.34 lists a few case histories where that simplified expression was tested. In all cases the horizontal movements ahead of the tunnel face were monitored. It should be noted that while the calculated movements are those right at the face plane, the measurements were taken at some distance behind as indicated in the table. Thus, it would be expected that the predicted values would exceed the observed by some amount. To obtain the calculated maximum displacements, the information given

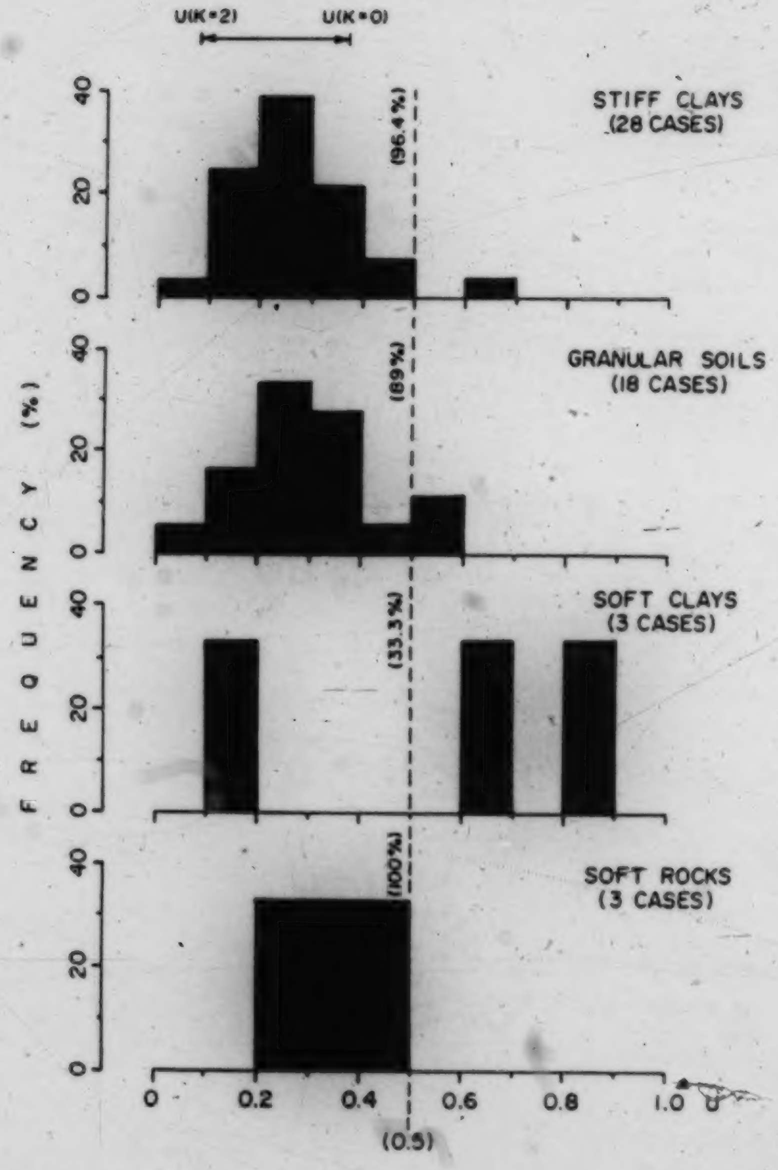

Figure 5.112 Distributions of Measured Crown Displacements at the Tunnel Face

in Table 5.31 was used. As it is observed in Table 5.34, the approximate equation yields fairly sensible results with calculated and measured horizontal movements being of the same order of magnitude.

Section 5.3.5.2 also proposed simplified procedures to evaluate the maximum longitudinal distortions ahead of an advancing tunnel. Unfortunately, not many case histories made this type of information available. In the cases listed in Table 5.35, contour lines of equal surface settlements ahead of the tunnel were presented. Therefore, the maximum surface distortion along the tunnel axis could be adequately estimated and are shown in the table. The calculated surface distortion was obtained by first ascertaining the maximum distortion at the crown elevation, using the approximate equation [5.13]. The maximum surface distortion was then obtained through the relation between the crown and surface distortions shown in Figure 5.100. In each case, the data presented in Table 5.31 served as input for the calculations. The approximate procedure proved to yield fairly sensible results.

The simplified methods for estimating ground movements ahead of the advancing tunnel should not be understood as being actual prediction tools, but rather as simple expedients whose merit is to avoid the need of expensive three-dimensional analyses otherwise required for such estimates. Accordingly, they should be only used to assess the order of magnitude of these movements. On a case by case

Tunnel	Distance to the face when reading was taken (m)	Max. inward movement (mm)		Reference
		Measured	Calculated(1)	
Washington C-Line (1st) SI 17	1.5	6	22	Hansmire (1975:52)
Edmonton LRT (Sth) SI 12	3.6	~4	7	Branco (1981:106)
Butterberg - Osterode	1.3	14	13	Meister and Wallner (1977:926)
Victoria Line anchor A	0	18	24	Ward (1969:323)

Note: (1) $u_f = 0.5D \frac{\sigma_{0c}}{E}$

Table 5.34 Calculated and Observed Maximum Horizontal Movements of the Tunnel Face

	Maximum longitudinal distortion			
	Calculated			
Tunnel	At Crown(1)	At Surface(2)	Measured at Surface	Reference
Washington C-line	1:100	1:1400	1:1200	Hansmire & Cording (1972:383)
Edmonton LRT (Sth)	1:290	1:3200	1:4000	Branco (1981:66)
S. Paulo ABV (NATM)	1:190	1:2500	1:4500	Negro and Eisenstein (1981)
S. Paulo N. Ext. (S1.3 to S1.9) (3)	1:260	1:2340	1:2000	Negro et al (1985)

Notes: (1) $\gamma_{cmax} = 1.5\ \sigma_{0c}/E$

(2) From Figure 5.100

(3) Complete section with D = 9.84 m (non circular profile).

Table 5.35 Calculated and Observed Maximum Longitudinal Distortions at the Ground Surface, Ahead of the Tunnel Face

basis they should be tested and calibrated against field performance in order to make it reliable for predictive purposes within an observational method approach.

5.3.7 Summary and Conclusions

The need to estimate the amount of tunnel closure was explained within the present work, in terms of the need to estimate the amount of ground stress release in a two-dimensional tunnel representation.

Available solutions for estimating the tunnel convergence at and behind the face were reviewed. It was found that they are of little help for solving the shallow tunnel problem. Therefore, it was decided to attempt the development of a new and specific solution for the problem at hand. Moreover, it was decided to make use of three-dimensional finite element modelling for that purpose. Consequently, a brief review on the subject was undertaken, and the main features of previous 3D modelling of shallow tunnels were investigated and discussed. This review guided the selection and implementation of the numerical solution adopted in this study.

The details of the numerical modelling procedure used were presented and discussed. The assumptions, limitations and shortcomings of the solution adopted were examined.

Parametric numerical analyses were conducted and their results presented in terms of longitudinal distribution of dimensionless radial displacements at three points of the tunnel perimeter and at other points within the ground mass.

These results were interpreted and an approximate solution for estimating the tunnel closure of an unlined tunnel in an elastic medium was proposed. The solution allows the radial displacements at crown, springline and floor, to be obtained as a function of the Young's modulus of the soil, of the tunnel diameter and of the radial in situ stresses acting at those points of the tunnel contour, for different sections at or behind the face.

Another simplified solution was developed from the parametric analyses which permits estimates of the maximum horizontal displacement of the tunnel face.

Additional approximate solutions were proposed for the evaluation of the maximum angular distortion along the tunnel at the crown elevation, at some distance above it and at the ground surface. The validity of the approximations made were discussed.

The proposed solution for shallow tunnel closure estimates was compared to another method developed for a deep tunnel situation. Moreover, the presently proposed method was used to predict the convergence of actual shallow tunnels, observed for a number of case histories. Of interest were the radial displacements of the tunnel contour at the face and at the section where the support was installed. Details of each case history were presented.

The comparisons between predicted and measured radial displacements at the face and at the section where the lining was installed were presented and analysed. The ability of the proposed approximate method to predict actual tunnel closure was investigated for each ground type and for each construction method involved in the case histories. The reasons for departures between predictions and measurements were discussed. The ground and construction conditions where the proposed method is likely to yield better estimates were identified as well as the conditions where the method fails to provide good results. The approximate nature of the present solution was emphasized.

The extensive survey of case histories allowed an empirical evaluation of the maximum amount of crown settlement taking place after the installation of the support in full contact with the ground. Furthermore, it allowed the assessment of the maximum magnitude of the crown settlement developing ahead of the tunnel face. By combining the two evaluations with the tentative criterion proposed in Section 2.3.4.3, regarding the limiting crown displacement associated with a near ground collapse condition, the criterion for the maximum acceptable overbreak or overcut, proposed in Section 2.3.5.4 was justified.

Finally, a few comparisons were made available between measurements and approximate predictions of the ground movements ahead of the tunnel face. These include the maximum horizontal displacements of the tunnel face and the maximum surface distortions ahead of the advancing tunnel.

5.4 Conclusion

In Section 5.2, a two-dimensional finite element modelling technique was presented and applied to a few case histories. This modelling technique provided sensible results, if the amount of ground stress release allowed before lining activation was known.

If this stress release could be related to the radial displacements of the tunnel contour, then an estimate of the displacements could lead to an evaluation of the stress release. This approach was proposed and discussed in Sections 5.2.5 and 5.3.1.

In Section 5.3 an approximate method was developed for estimating the radial displacements at the section the lining is activated for three particular points of the tunnel perimeter. This method was developed from parametric three-dimensional finite element analyses. The applicability of this method in actual tunnelling situations was investigated.

To complete the picture, the method for estimating radial displacements should combined with results of the two-dimensional modelling, in order to assess the ability of the proposed procedure to provide estimates of the ground stress release required in the plane strain representation.

This was done for the three case histories analysed in detail in Section 5.2.4.

Alto da Boa Vista Tunnel

Using the parameters of the best fit analysis found for this case history as presented in Section 5.2.4.2, it is possible to obtain the ground reaction curves for points of the tunnel contour subjected to a gradual and complete stress release (in 10 steps). In this additional run, no support was applied to the opening. For convenience, these ground reaction curves can be expressed in terms of the stress release factor

$$\alpha = 1 - \Sigma$$

where Σ is the ratio of the current radial stress to initial radial stress at the tunnel contour. Note that in the modelling technique adopted (Section 5.2.2), the same stress reduction factor is uniformly applied to all points around the tunnel profile and proportionally reduces the radial and shear stresses along that contour. The induced radial displacements can be expressed in the dimensionless form (U). As the in situ initial tangent modulus of the soil in this case history increases with depth (Figure 5.14), an average E value of 30 MPa was adopted to calculate the dimensionless displacement.

The curves presented in Figure 5.113 are thus obtained, for points at the tunnel crown, springline and floor.

The section where the shotcrete support of this NATM tunnel was actually activated is not easily defined. As described in Section 5.2.4.2 the support was installed in stages. The heading walls were immediately shotcreted after excavation (Figure 5.15). Immediate shotcreting also followed the bench excavation. The closure of the lining invert took place at about 2.6 m behind the heading face. From this one may say that the activation of the support system took place at some distance from the face between zero to almost 0.6D. The approximate solution for tunnel closure developed in Section 5.3.5.2 can be used to estimate the dimensionless radial displacements at those extreme situations ($X/D = 0$ and 0.6). The estimates of U at crown, springline and floor are thus shown in Figure 5.113. With these values, stress releases α at those three points can be obtained for each position of X/D considered. One notes that for a given distance behind the tunnel face, different α values are found for the different points of the tunnel contour. As noted above, the two-dimensional modelling technique uses a single reduction factor α for all points of the contour. Accordingly, those different α values obtained have to be averaged out, in order to allow a comparison with the best fit reduction factor found in this case history back analysis. This is easily determined, having in mind the plane symmetry of the problem, which requires the stress reduction computed for the springline point to be counted twice.

From this it is noted that had the lining been installed right at the face ($X/D=0$) the stress reduction factor to be used in a 2D analysis would have been 25.5%. On the other hand, had the lining been activated at 0.6D behind the face (approximately at the point of ring closure), the

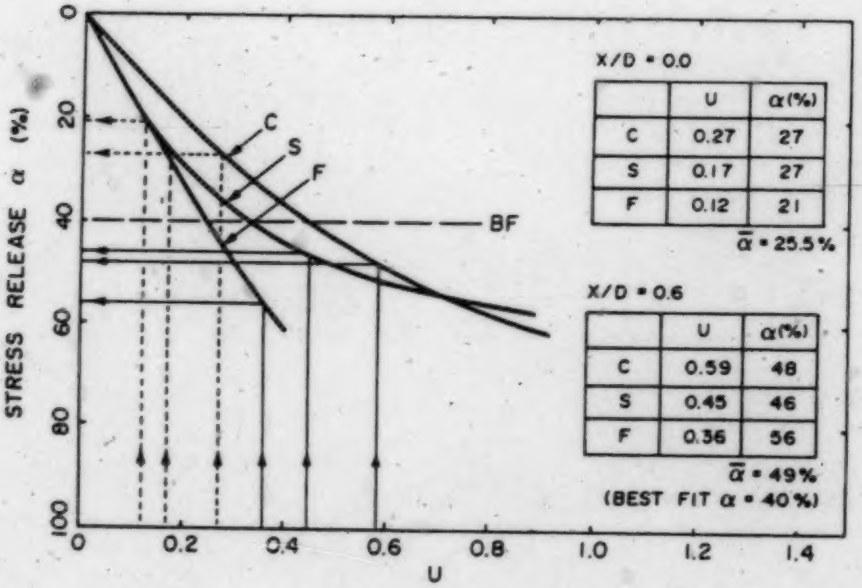

X/D = 0.0

	U	α(%)
C	0.27	27
S	0.17	27
F	0.12	21

$\bar{\alpha}$ = 25.5%

X/D = 0.6

	U	α(%)
C	0.59	48
S	0.45	46
F	0.36	56

$\bar{\alpha}$ = 49%
(BEST FIT α = 40%)

Figure 5.113 Evaluation of the Ground Stress Release at the ABV Tunnel for a Two-Dimensional Numerical Simulation

stress reduction factor to be considered would have been 49%. These two values are to be compared with the 40% stress release prior to the lining application found through the back analyses of this case history, presented in Section 5.2.4.2. The latter value lies within the extreme values given by the approximte procedure suggested, and, actually is closer to the a calculated for the section where the lining ring was closed at the floor. The latter finding seems to confirm that the actual activation of a support installed in stages, takes place at the point when the lining ring is closed.

Edmonton LRT Tunnel

The same reasoning and procedures applied to the ABV tunnel were also applied to the Edmonton Subway Tunnel. The main difference in this case refers to the definition of the section where the lining was activated. The construction procedures described in Section 5.2.4.3 indicate that the support came in full contact with the ground at a distance behind the face of 0.9 to 1.1 times the excavated diameter. Thus the tunnel closure is calculated for a section about 1D behind the face, using the best fit value of the in situ stress ratio found for this case (K=0.75). The ground reaction curves shown in Figure 5.114 were obtained as for the ABV case. Here an average initial tangent modulus of 70 MPa was considered (see Figure 5.25), to calculate the dimensionless displacements.

The radial displacements at the point of lining activation as calculated by the approximate solution are given in Figure 5.114. This enabled the stress reduction factors at the crown, springline and floor to be calculated from the corresponding ground reaction curves, which had been obtained from the 2D finite element analysis of the unsupported opening, using the parameters of the best fit case. Again the stress release factors are averaged out and a mean *a* value of 52% is found. This figure compares well with the best fit amount of ground stress release of 50% found in Section 5.2.4.3 for this case history.

Edmonton Experimental Tunnel

Once more the same procedures were applied to the third case history investigated. Figure 5.115 presents the ground reaction curves derived from a 2D finite element analysis of the unsupported tunnel, using the parameters of the best fit case (Section 5.2.4.4). It also assumes an undrained ground response and an in situ stress ratio, K=0.9. Correspondingly, an average initial tangent modulus of 25 MPa was considered (see Figure 5.48) to calculate the dimensionless radial displacements.

The construction details of the tunnel indicate that the lining was activated in this case, at a section located between 2.3D and 2.7D behind the tunnel face. The approximate tunnel closure solution given in Section 5.3.5.2 indicates however, that at distances greater than 2D behind the face the radial displacements are essentially constant

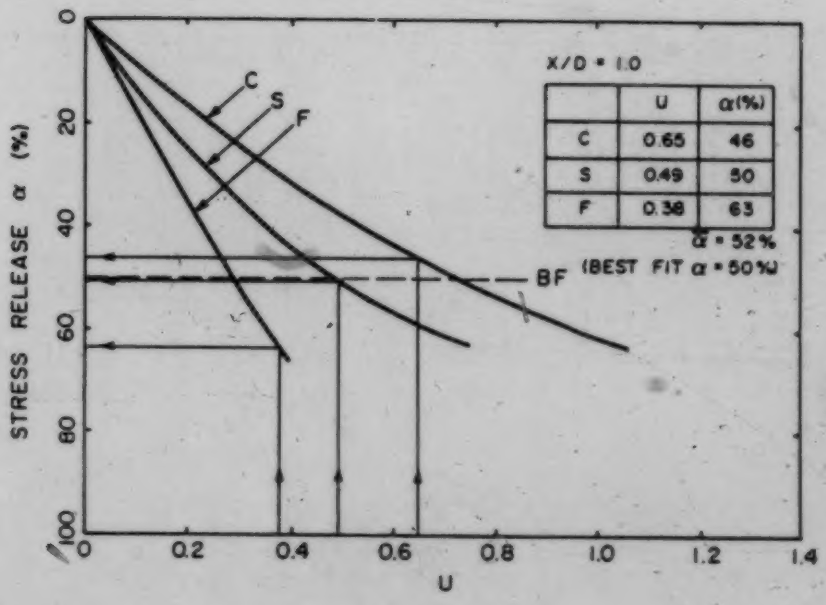

Figure 5.114 Evaluation of the Ground Stress Release at the LRT Tunnel for a Two-Dimensional Numerical Simulation

and fully stabilized. The dimensionless displacements are therefore calculated for X/D=2.0 and the values found are shown in Figure 5.115. The stress release a for the crown, springline and floor are thus determined and an average ground stress reduction factor of 50% is obtained. Unlike the former two case histories, a fairly poor agreement is found with the best fit reduction factor of 70%.

This result emphasizes the limitations of the proposed method for estimating the tunnel closure, as discussed in Section 5.3.6.1. It seems to render good results in tunnels built using the NATM regardless of the soil type but provided the face is stable, and to construction schemes using TBM and shields, where the support is activated at distances from the face smaller than 1 to 1.2 D. On the other hand the method tends to underestimate the tunnel closure when the support is activated at larger distances from the face (especially in softer soils) as in the present case history. As a consequence, the ground stress reduction it yields will be smaller than it should. A two-dimensional analysis using a smaller stress reduction will generally lead to smaller final ground movements and to larger lining loads.

Final Comments

It was shown in this chapter that a shallow tunnel construction can be adequately simulated through the two-dimensional modelling technique presented herein. This simulation requires, however, an independent estimate of the

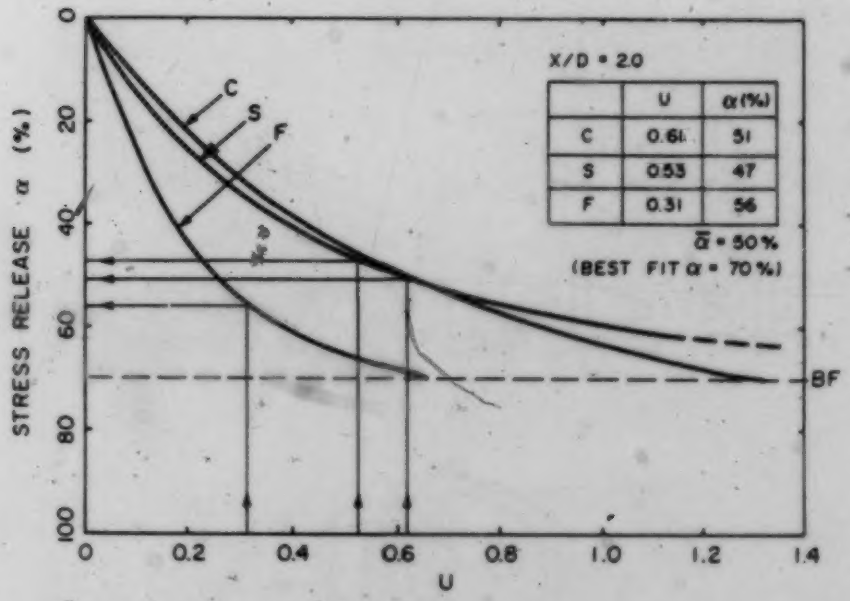

	U	α(%)
C	0.61	51
S	0.53	47
F	0.31	56

Figure 5.115 Evaluation of the Ground Stress Release of the Edmonton Experimental Tunnel for a Two-Dimensional Simulation

amount of ground stress release taking place before the support is activated.

An approximate procedure was developed to assess that amount of stress reduction. It requires an estimate of the radial displacements at the point when the support is activated. It also requires the knowledge of the ground reaction curve of the unsupported opening. This can be obtained from finite element analyses, using the two-dimensional modelling technique mentioned before. The radial displacements prior to supporting the tunnel can be estimated using the approximate method developed from three-dimensional numerical simulations. Combining those two procedures, the stress reduction factor can be assessed or bounded. Caution should be exerted, however, regarding the validity or limitations of the proposed procedure, since these may have an effect on the result of the analysis. Nevertheless, when applied judiciously, the proposed procedure leads to estimates of the ground stress reduction, that ultimately lead to reasonable predictions of the performance of the shallow tunnels, through the two dimensional numerical simulation technique presented in this chapter.

6. TWO DIMENSIONAL MODELLING FOR GENERALIZATION

6.1 Introduction

In Chapter 5, an approximate procedure was proposed to assess the amount of ground stress release to be applied before the lining is activated, in the two dimensional finite element simulation described in Section 5.2.2. This procedure was tested and evaluated in Section 5.4. It requires two basic components: (a) the ground reaction curves at three particular points of the contour of the unsupported opening; (b) the radial displacements of these points at the section the support is activated.

To a large degree, the three-dimensional modelling presented in Section 5.3 was devoted to supplying the fundamentals for requisite (b) above. An approximate solution allowing estimates of radial tunnel closure behind the face of a shallow tunnel was developed in Section 5.3.5.2 and was tested in Section 5.3.6.1. Despite its limitations, this solution presents sufficient generality for practical use.

The other requirement refers to the ground reaction curves of some points of the tunnel contour. In Section 5.4, these were presented in terms of relationships between a non-dimensional radial displacement (U) and a ground stress release factor (α) for the crown, springline and floor of the tunnel. An average stress release factor ($\bar{\alpha}$) is obtained by averaging the factors at these points. The ground reaction curves for three case histories shown in Section 5.4 were obtained through finite element analyses, using the numerical solution presented in Section 5.2.2, and the parameters used or derived from the back analyses presented in Section 5.2.4.

In this chapter, an attempt will be made to develop a procedure which would allow those ground reaction curves or stress release curves to be obtained, without the need of a finite element analysis. Obviously, the development of such a procedure requires a number of finite element analyses. Their results may lead to a generalized solution of the problem which would not demand additional numerical analyses. Through this process of numerical modelling, an additional effort will be made towards simultaneously obtaining the relevant ground displacements induced by the stress reduction at the opening.

To obtain a coupled solution for the ground response in terms of stress release curves and associated ground displacements, a process of generalization may be used. The application of this process to geotechnical problems was described by Resendiz (1979). According to this author, four steps are involved in this process: (a) the identification of the significant variables controlling the problem; (b) the reduction of the variables to a minimum set of mutually independent variables, sufficient to define the problem; (c) the derivation of quantitative relationships between the set of variables through modelling; (d) the validation and calibration of the proposed quantitative relationships against actual field cases.

The process of generalization makes use of similarity techniques through which a physical problem can be described by a set of relationships which are invariant with respect to the scale changes of the physical dimensions. To find these relationships, the theory of dimensional homogeneity or dimensional analysis is used. An application of these concepts to geomechanical problems involving material non-linearities was presented by Winter (1982). Resendiz and Romo (1981) applied these concepts to the solution of settlement over tunnels in frictionless soils exhibiting a hyperbolic stress-strain relationship. Dimensional analysis was also applied to obtain settlement over shallow tunnels in linear elastic soil by Sagaseta and Oteo (1974) and Sagaseta et.al. (1980). Kovari (1977:405) used a similar approach to obtain a solution for lining design on the assumption of linear elasticity for both the support and the ground. A common feature to all these works is the modelling step of the generalization process which made use of finite element analysis.

The steps described for generalization were liberally followed in this study, without the degree of formalism that a dimensional analysis should involve.

The identification of the significant variables controlling the problem at hand were largely discussed in Chapters 2 and 3. The reduction of the number of variables was discussed in Section 5.1 and further simplifications will be discussed in Section 6.2. Some of the variables involved were already reduced to a dimensionless form such as the radial displacements at the tunnel contour (U), or the amount of stress release (α). Other dimensionless variables will be presented later. This chapter will focus mainly on the third step of the generalization process. Having made the assessment in Chapter 5 of the capabilities of the selected modelling tool to simulate the behaviour of a shallow tunnel, the 2D numerical model will be used here to derive quantitative relationships between the reduced variables. The final step regarding the validation and calibration of the solution will be presented in Chapter 7.

A general solution for the ground reaction curves can be expressed in terms of the following equation, which reflects both the selected modelling tool and some simplifications already undertaken:

$$F=f(\sigma_r,u_r,\theta,D,H,\gamma,K_o,\nu,K,n,c,\phi,R_f) \qquad [6.1]$$

The symbols have the meanings established previously.

The next section will discuss some assumptions and simplifications, that will ultimately enable the definition of a minimum number of dimensionless and mutually independent variables which described the function f with sufficient generality.

6.2 Modelling Simplifications and Ranges of Variables

6.2.1 Foreword

Despite the simplifications set earlier in Section 5.1, equation 6.1 still includes a large number of dimensional and dimensionless variables. In order to further reduce this number and to make the modelling step simpler, one may explore some properties of the hyperbolic stress-strain relationship.

The original formulation of the hyperbolic model was presented in Figure 5.11. After inspecting that derivation, one may note that there are groups of hyperbolic relationships with a few peculiar properties as it will be seen in the next sections. Also included are discussions on the consequences of the simplifications introduced and on the ranges of parameters varied in the modelling step.

6.2.2 Cohesionless Soil Model

If the cohesive component of strength is set equal to zero and the Janbu's exponent, n, is also set equal to zero, a special group of hyperbolic stress-strain curves is found. An example of a family of curves of this group is shown in Figure 6.1. These curves present the property of homothety. The centre of homothety or of similitude of these curves is their origin, where the strain and deviatoric stresses are zero. The homothetic transformation maps a curved segment into a parallel segment with a length equal to the ratio of homothety times the length of the original segment. If the coordinates of the homothetic points on these curves (the intersection of the latter with an arbitrary axis through the centre of similitude) are used as reference values, $(\sigma_1-\sigma_3)_{ref}$ and $\epsilon_{1_{ref}}$, and if the deviatoric stresses and the major principal strains of each curve are respectively normalized to these reference values, a single normalized hyperbola is found for the entire ground mass, regardless of the value of the minor principal stress. This is demonstrated in Figure 6.2.

At homothetic points on these curves, the ratio of deviatoric stress to minor principal stress is constant as proved in Figure 6.2. Thus for c=0 and n=0, one gets for the tangent modulus at these points:

$$E_t = K\ p_a\ [1 - R_f\frac{1-\sin\phi}{2\sin\phi}\ \frac{\sigma_1-\sigma_3}{\sigma_3}]^2$$

Hence, for fixed K, R_f and ϕ values, E_t is a constant. This result is not suprising as it is known that a homothety preserves angles between lines of a polygon or gradients of a curve (Dodge, 1972:107). Furthermore, if the in situ stress ratio K_o is constant, the ratio $(\sigma_1-\sigma_3)/\sigma_3$ is constant and the in situ tangent modulus is also constant. This is apparent in Figure 6.1. The in situ or initial tangent modulus is thus given by:

$$E_{ti} = K\ p_a[\ 1-R_f\frac{1-\sin\phi}{2\sin\phi}\ \frac{1-K_o}{K_o}]^2 \qquad [6.2]$$

on the assumption that the ground surface of the soil mass is horizontal and that the major principal stress is vertical. For this ground mass, the initial tangent modulus

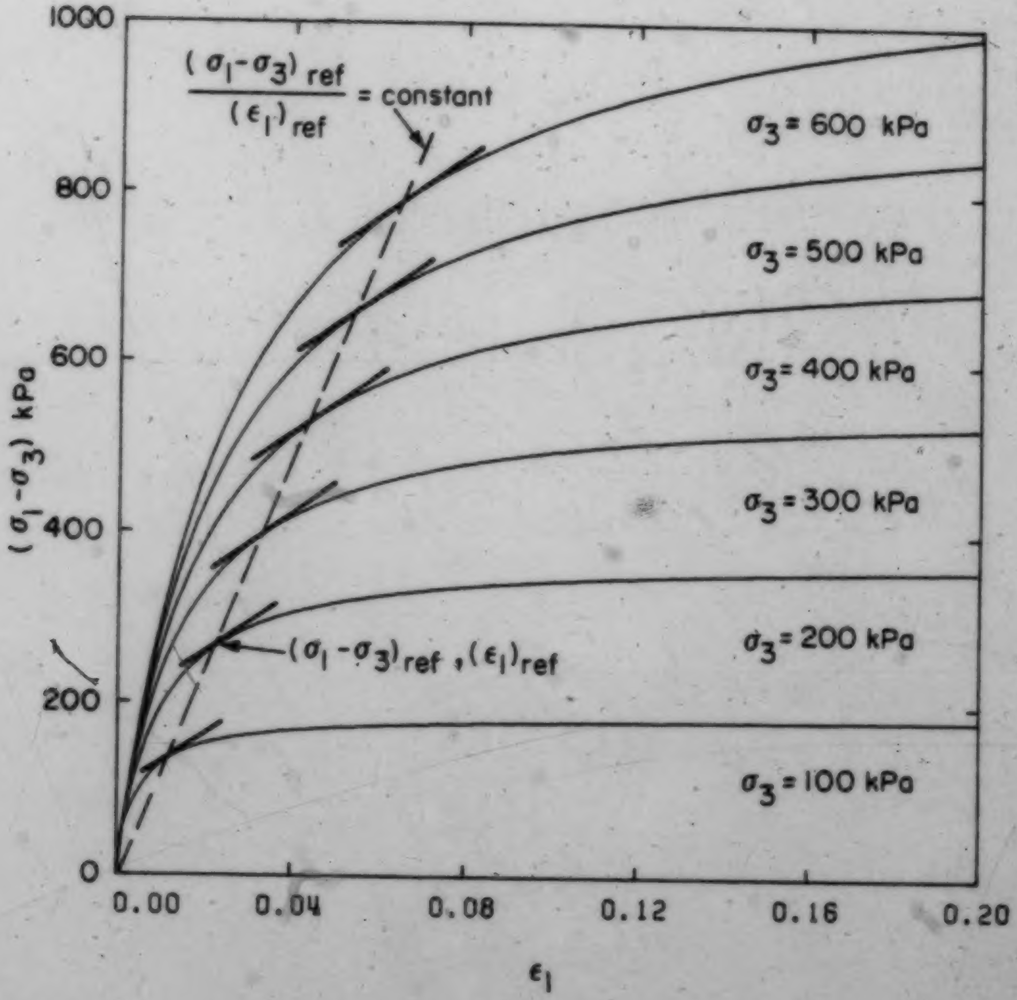

K=400 , n=0.0 , PHI=29 , c=0.0 , Rf=1.0

Figure 6.1 Example of Homothetic Hyperbolae

Hyperbola:

$$(\sigma_1 - \sigma_3) = \frac{\epsilon_1}{a + b\epsilon_1}$$

Dividing by $(\sigma_1 - \sigma_3)_{ref}$ and numerator and denominator of right hand side by $(\epsilon_1)_{ref}$:

$$\frac{(\sigma_1 - \sigma_3)}{(\sigma_1 - \sigma_3)_{ref}} = \frac{\epsilon_1/(\epsilon_1)_{ref}}{a\,\frac{(\sigma_1 - \sigma_3)}{(\epsilon_1)_{ref}} + b\,(\sigma_1 - \sigma_3)_{ref}\,\frac{\epsilon_1}{(\epsilon_1)_{ref}}}$$

If n = 0, then:

$$a = 1/Kp_a$$

Thus, for a given K and a fixed ratio $(\sigma_1 - \sigma_3)_{ref}/(\epsilon_1)_{ref}$:

$$a\,\frac{(\sigma_1 - \sigma_3)_{ref}}{(\epsilon_1)_{ref}} = a_0 \text{ (constant)}$$

If c = 0, then:

$$b\,(\sigma_1 - \sigma_3)_{ref} = R_f\,\frac{1-\sin\phi}{2\sin\phi}\,\frac{(\sigma_1 - \sigma_3)_{ref}}{\sigma_3}$$

However

$$\frac{(\sigma_1 - \sigma_3)_{ref}}{\epsilon_{1\,ref}} = \frac{1}{a + b\epsilon_{1\,ref}}$$

But, for c = 0:

$$b = d/\sigma_3 \quad \text{(d constant for a given } R_f \text{ and } \phi)$$

Then for a fixed $(\sigma_1 - \sigma_3)_{ref}/\epsilon_{1\,ref}$:

$$\epsilon_{1\,ref} = e\,\sigma_3$$

Thus

$$\frac{(\sigma_1 - \sigma_3)_{ref}}{\sigma_3} = f \quad \text{(constant)}$$

Therefore

$$b\,(\sigma_1 - \sigma_3)_{ref} = b_0 \quad \text{(constant)}$$

Hence

$$\frac{(\sigma_1 - \sigma_3)}{(\sigma_1 - \sigma_3)_{ref}} = \frac{\epsilon_1/(\epsilon_1)_{ref}}{a_0 + b_0\epsilon_1/(\epsilon_1)_{ref}}$$

represents a unique hyperbola for a given K, R_f and ϕ.

Figure 6.2 Uniqueness of the Normalized Homothetic Hyperbolae for c=n=0

is therefore constant with the depth.

In a two-dimensional representation, unlined circular tunnels with different diameters will exhibit homothetic geometries if their ratios of cover to diameter (H/D) were the same. If geometrically homothetic tunnels are driven through a ground mass exhibiting homothetic hyperbolic stress-strain curves such as those defined, the ground mass response in terms of stress and strain changes should be also homothetic. If this is so, a unique normalized stress and strain response will be found at corresponding (homothetic) points around those tunnels. Therefore a unique normalized ground reaction curve (NGRC) should be obtained at corresponding points in these tunnels.

To illustrate this point, two finite element analyses were conducted, using the stress-strain parameters of the curves shown in Figure 6.1. Other input variables are given in Table 6.1. The two circular tunnels have different geometries but the same H/D ratio. The ground stresses at the opening were gradually reduced to zero in ten increments and no support was activated. After the 7th load increment, some elements close to the springline "failed" and the results after this event were discarded. In both cases, the in situ tangent modulus was equal to 27.414 MPa.

Figures 6.3 to 6.5 present the ground reaction curves at the crown, springline and floor calculated for both cases. The curves show the radial displacements at those points relative to the ratio of current to in situ radial stresses. Quite distinct curves were obtained for each case. However, if the displacements are normalized to the tunnel diameter and to the ratio of in situ radial stress to the in situ tangent modulus, such that

$$U = \frac{u_r . E_{ti}}{D . \sigma_{ro}}$$

then, single curves result for each point of the tunnel contour as indicated in Figure 6.6. As the in situ stress level at the deeper tunnel is twice that at the shallower one and as the diameter of the former is also twice that of the latter, the displacements in the deeper tunnel are four times larger than those in the shallower position. This is almost exactly the ratio of the displacement found through the numerical analyses.

Figure 6.7(a) presents the distributions of subsurface settlements along the tunnel cover calculated for a ground stress release of 50%. The settlements are plotted against the depth normalized to the tunnel diameter. The settlements for the deeper and larger tunnel are four times larger than those in the other tunnel. Hence, if the settlements are normalized to the settlement of the tunnel crown in each case, then a unique distribution of/normalized settlements with depth is found as shown in Figure 6.7(b). Correspondingly, similar results are found for the surface settlements as indicated in Figures 6.8(a) and (b). When the surface settlements are normalized to the crown settlement, calculated for the same amount of ground stress release, once again, a single normalized distribution of surface

Diameter D (m)	4		8
Cover H (m)	6.2		12.4
H/D		1.55	
K		400	
n		0	
ϕ		29°	
c		0	
R_f		1.0	
ν		0.3	
γ (kN/m^3)		15.97	
K_0		0.75	
V/D$^{(1)}$		2.875	

Note: (1) Definition in Section 6.3.1.2

Table 6.1 Input Parameters for Finite Element Analyses of Tunnels with the Same H/D and with a Homothetic Hyperbolic Stress-Strain Soil Model with c=0

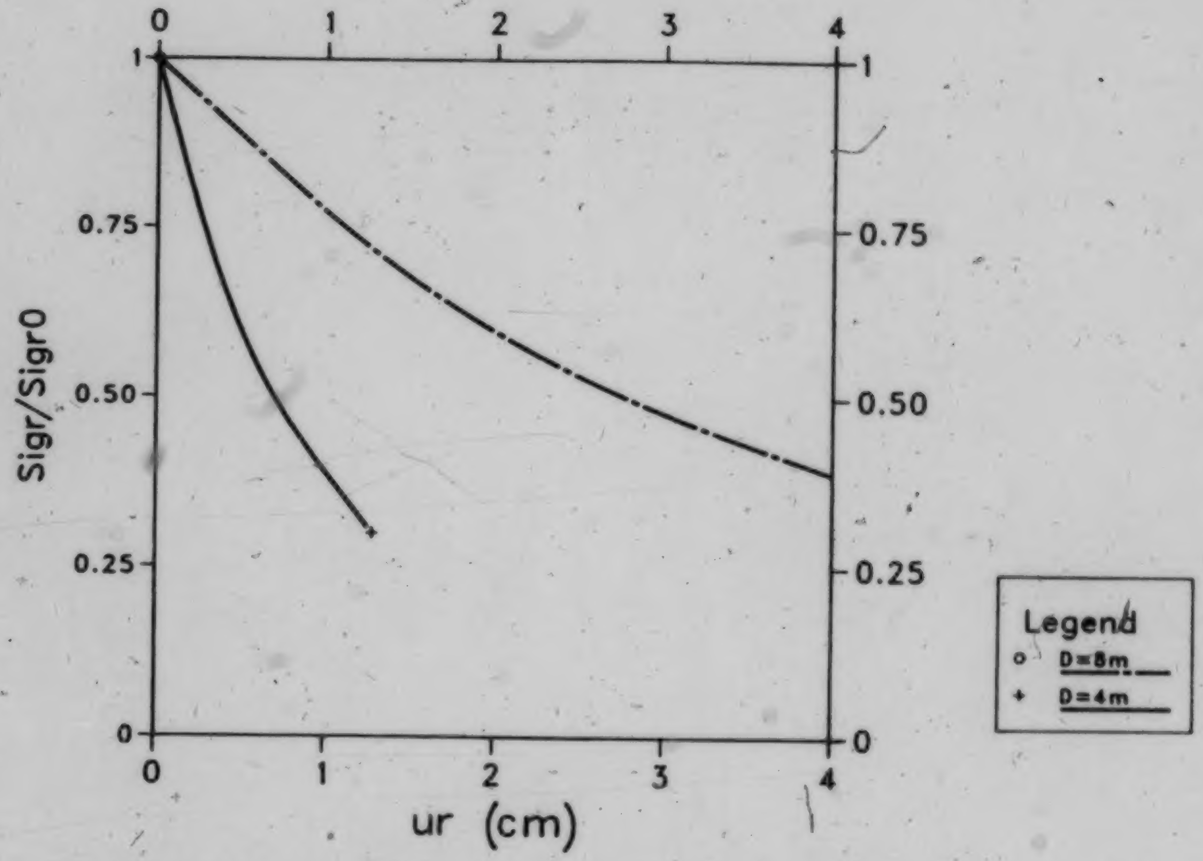

Figure 6.3 Ground Reaction Curves for the Crown of Geometrically Homothetic Tunnels in a Soil with a Homothetic Hyperbolic Stress-Strain Relationship (cohesionless model)

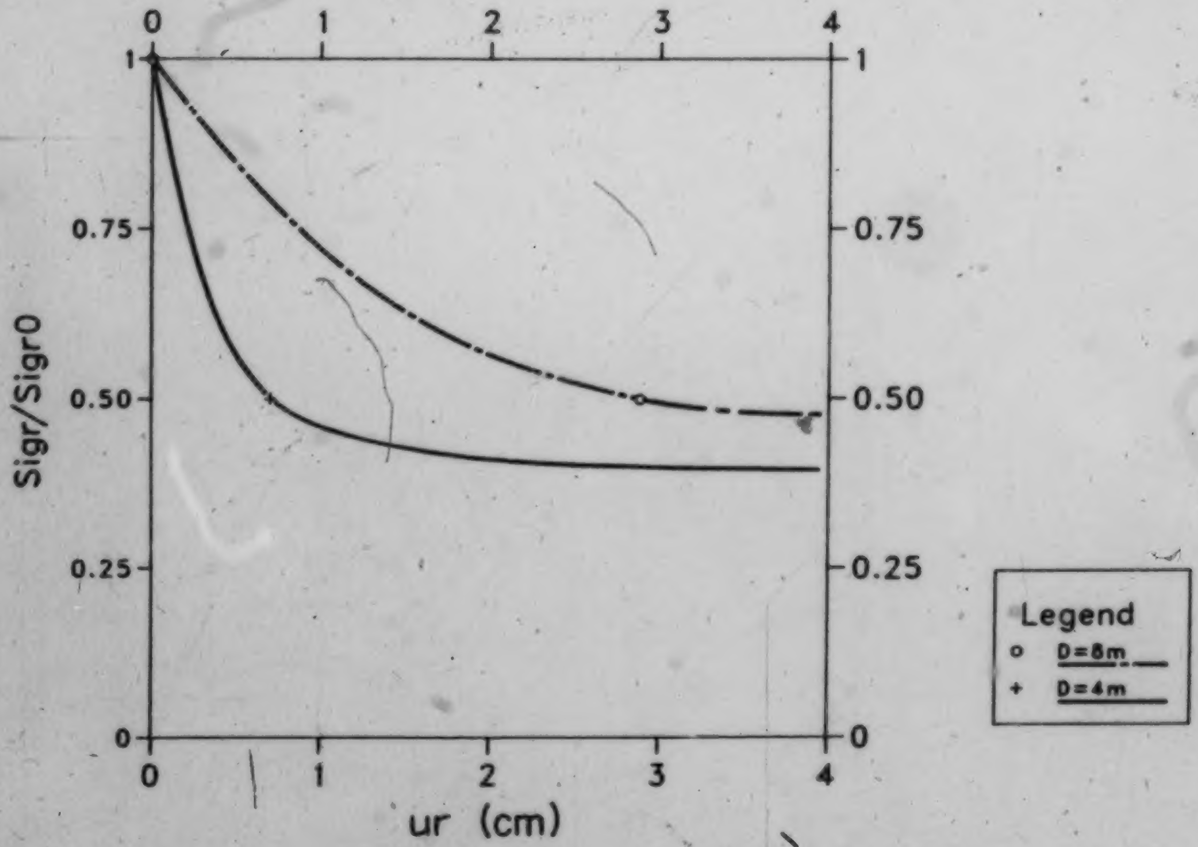

Figure 6.4 Ground Reaction Curves for the Springline of Geometrically Homothetic Tunnels in a Soil with a Homothetic Hyperbolic Stress-Strain Relationship (cohesionless model)

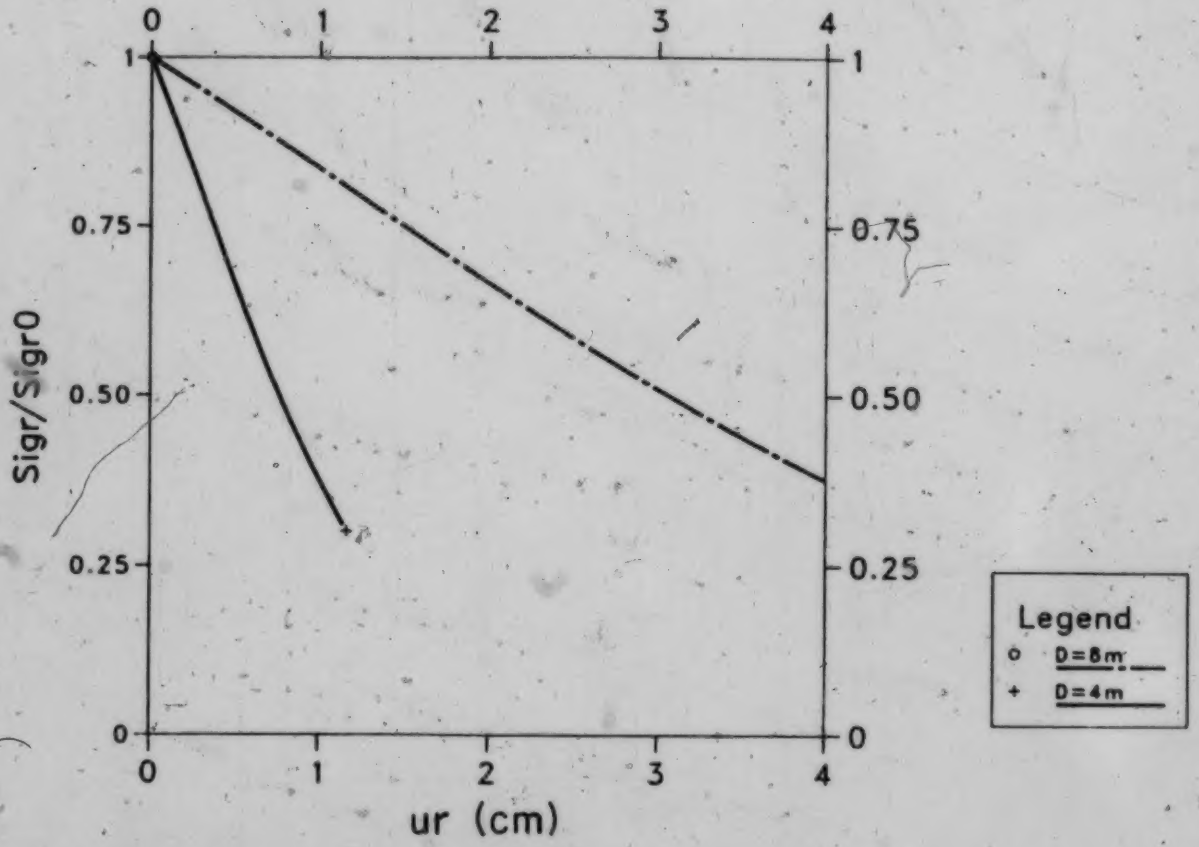

Figure 6.5 Ground Reaction Curves for the Floor of Geometrically Homothetic Tunnels in a Soil with a Homothetic Hyperbolic Stress-Strain Relationship (cohesionless model).

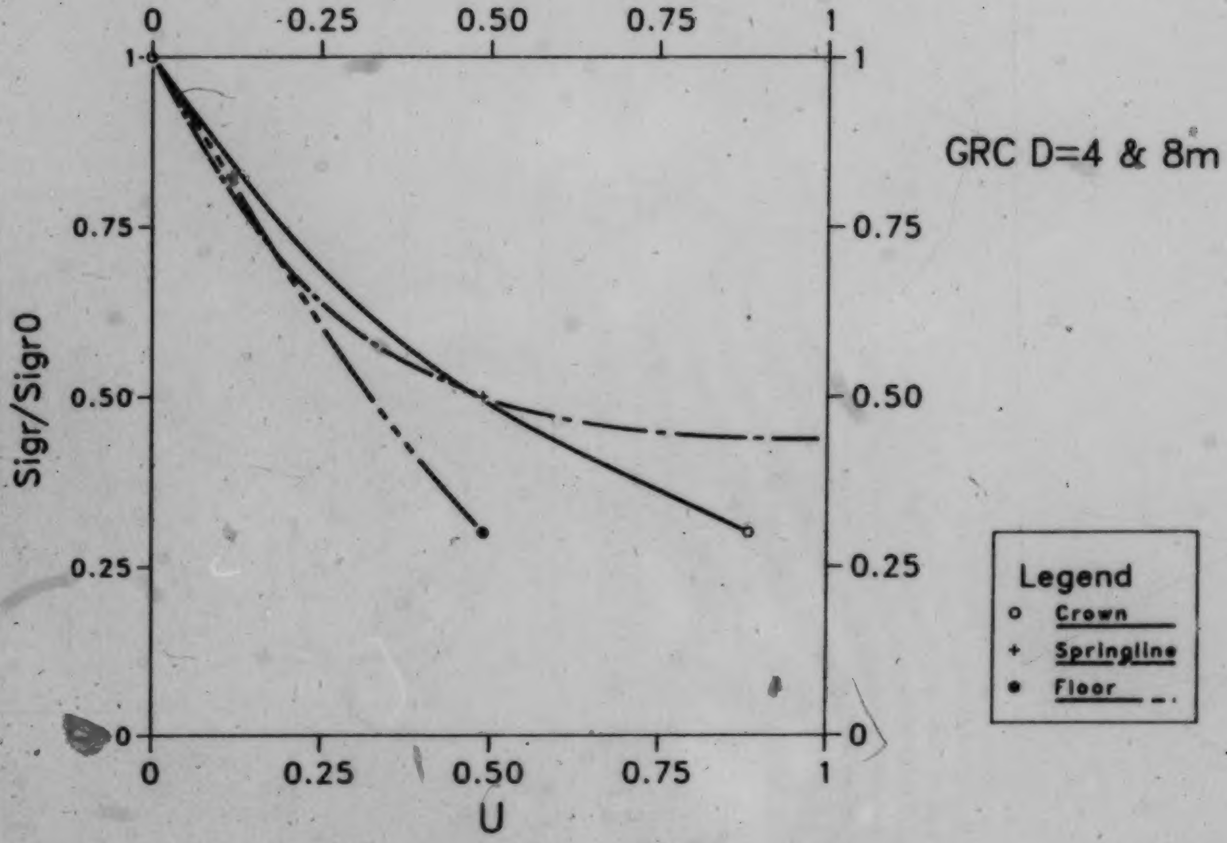

Figure 6.6 Normalized Ground Reaction Curves of Geometrically Homothetic Tunnels in a Soil with a Homothetic Hyperbolic Stress-Strain Relationship (cohesionless model)

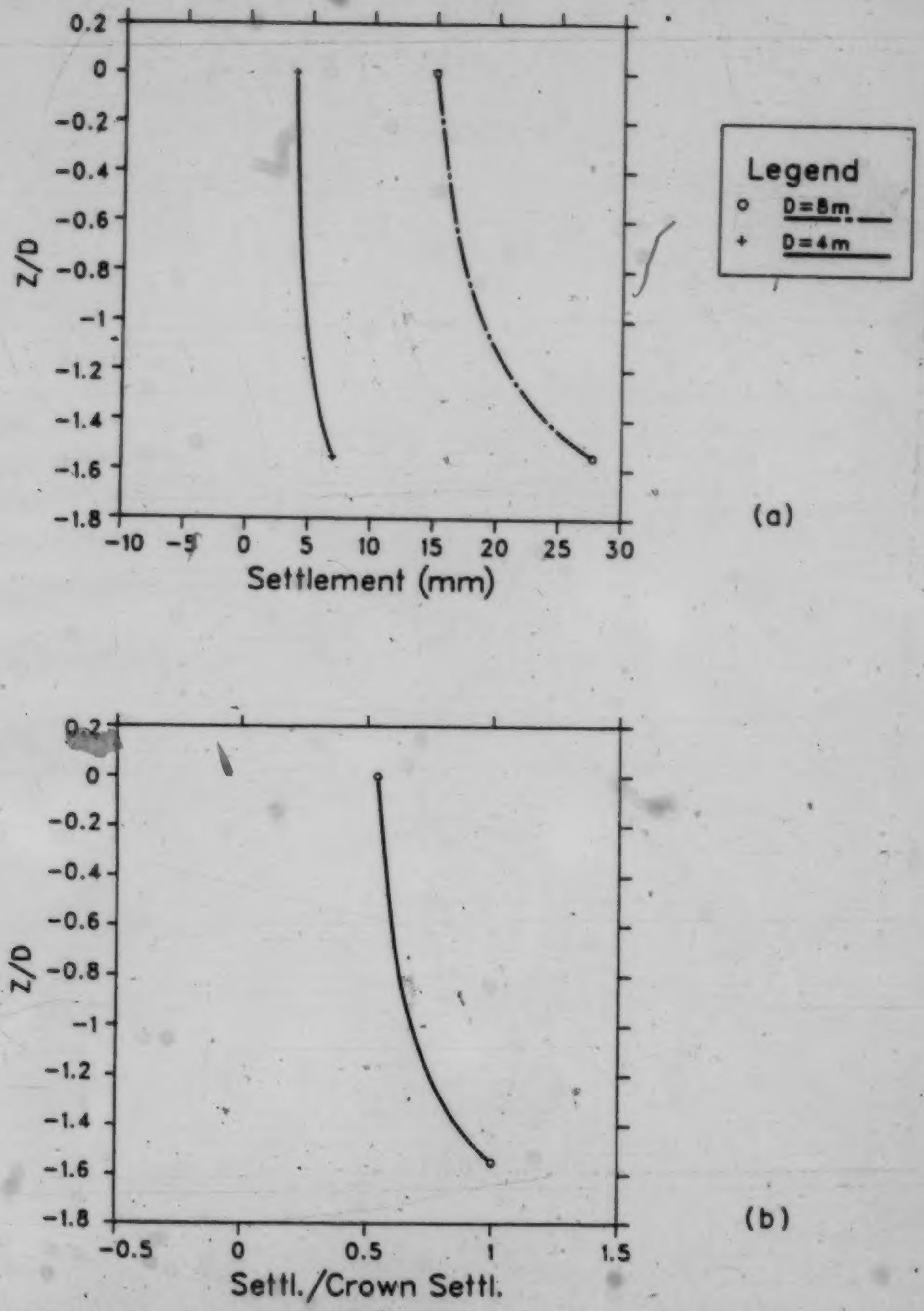

Figure 6.7 Subsurface Settlements along the Cover of Geometrically Homothetic Tunnels in a Soil with a Homothetic Hyperbolic Stress-Strain Relationship (c=0), for Stress Release of 50%

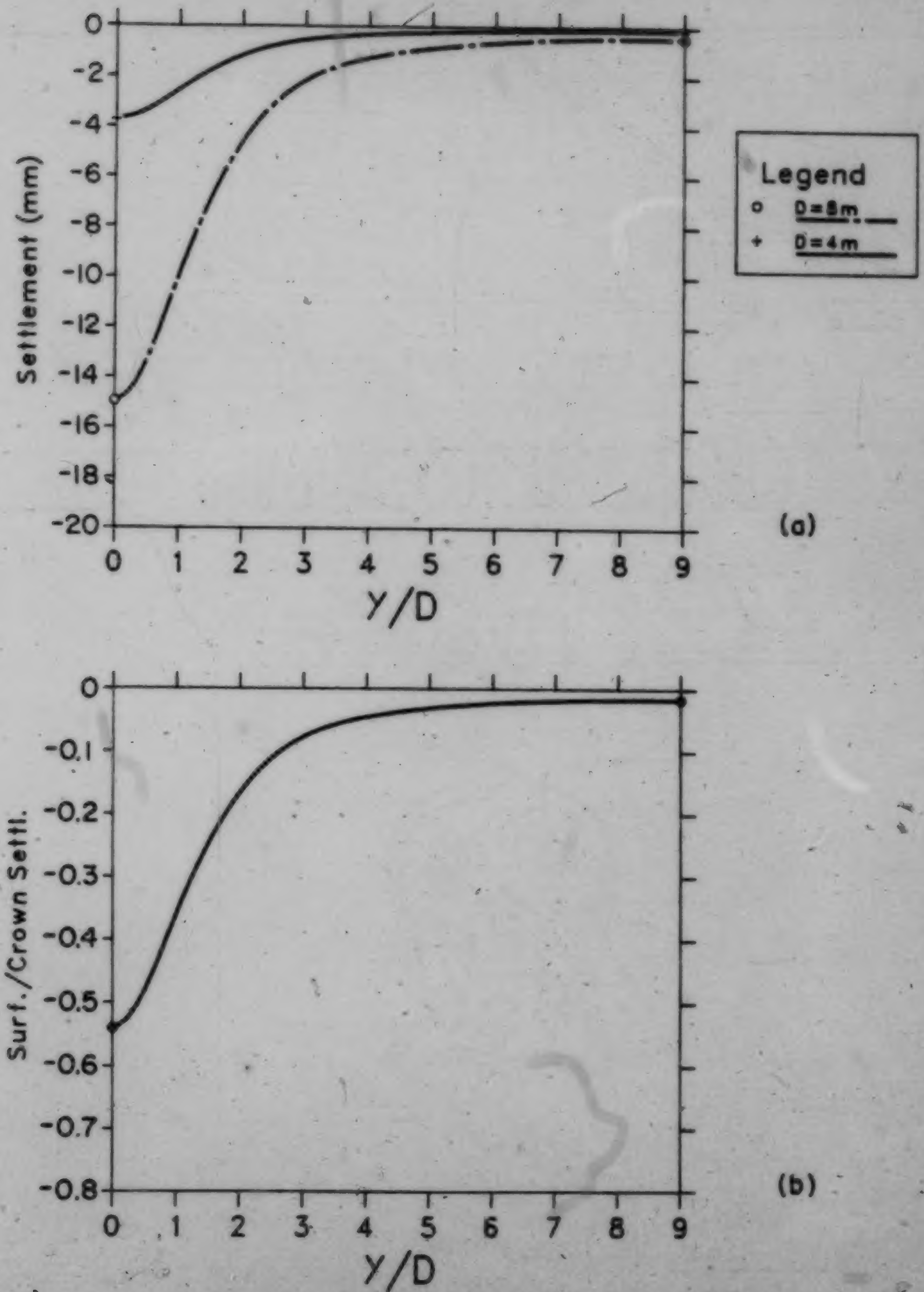

Figure 6.8 Surface Settlements over Geometrically Homothetic Tunnels in a Soil with a Homothetic Hyperbolic Stress-Strain Relationship (c=0), for Stress Release of 50%

settlements is found. Actually, the entire displacement field in one case differs from the other only in magnitude. Moreover, the ratio of displacement magnitudes is constant.

By using the property of homothety, the numerical analyses leading to the generalization of the projected solution will be greatly simplified, as one of the variables in equation 6.1, the tunnel diameter D, will not have to be varied in the parametric analyses, but only the ratio H/D. Furthermore, by making the soil cohesion equal to zero, there will be no need to vary the failure ratio, R_f, in these analyses. By examining Figure 5.11 or equation 6.2, one notes that for a soil with c=0 and with constant ϕ and R_f values, it is always possible to find an equivalent friction angle ϕ_e, associated with a failure ratio (R_{fe}) equal to unity which gives the same tangent modulus. Then:

$$R_f \frac{1-\sin\phi}{2\sin\phi} = R_{fe} \frac{1-\sin\phi_e}{2\sin\phi_e}$$

setting $R_{fe}=1$, then:

$$\sin\phi_e = \frac{1}{1 + R_f(1/\sin\phi) - R_f}$$

and therefore:

$$\phi_e = \text{arc sin}\,(1-R_f+R_f\csc\phi)^{-1} \qquad [6.3]$$

The stress-strain curves and thus the normalized ground reaction curves for a cohesionless soil, with $R_{fe}=1$ and with a friction angle ϕ_e, given by equation 6.3, are identical to that of a cohesionless soil, with R_f not equal to 1 and a friction angle ϕ.

One should also note that the unit weight, γ, of the soil of a homogeneous ground profile which appears in equation 6.1, does not affect the normalized ground reaction curve (NGRC) for n=0. This is because the NGRC is defined in terms of stress and displacements normalized to the in situ stresses. Also not affected are the displacements normalized to the crown settlement. This fact is demonstrated in Table 6.2, which presents the assumptions and results of two finite element analyses which considered identical input parameters except for different unit weights for the soil. The ratios of the normalized radial displacements and of the normalized surface settlements for the two γ values considered are very close to one. The deviations from unity are due to numerical inaccuracies of the calculations. The same results are found for displacements at other points in the ground mass and for other amounts of ground stress release. The invariance of the NGRC and of the ground displacement with respect to γ is in fact general for the simplified conditions considered in the analyses.

The simplifications introduced so far allow equation 6.1 to be expressed in a more compact form:

$$F= f(\theta, \frac{\sigma_r}{\sigma_{ro}}, \frac{u_r E_{ti}}{D\sigma_{ro}}, \frac{H}{D}, K_o, \phi_e, \nu) \quad [6.4]$$

Note that the variables in equation 6.4 are not mutually independent, as E_{ti} is a function of K_o and ϕ_e. They would been independent of each other had the displacements been normalized to Janbu's modulus, K, times the atmospheric pressure, p_a. However, there are some advantages in keeping the equation as shown. It will be shown later in this chapter that the NGRC for given K_o and H/D values, with

Assumptions:

H = 12.0 m D = 4.0 m K_0 = 0.8

K = 400 n = 0

c = 0 ϕ = 30°

ν = 0.4 V/D = 1.5

γ = 15.68 kN/m^3 and 19.60 kN/m^3

E_{ti} = 31.015 MPa (in both cases)

Full ground stress release in 10 equal increments

No lining installed

Results:

Displacements for 50% of stress release

a) Radial displacements at the opening

Point	γ = 15.68 kN/m^3		γ = 19.60 kN/m^3		U (γ = 15.68) / U (γ = 19.60)
	u_r (mm)	U (-)	u_r (mm)	U (-)	
Crown	11.75088	0.48423	14.69135	0.48432	0.99981
Springline	10.18102	0.44951	12.72055	0.44931	1.00045
Floor	8.41449	0.26006	10.56987	0.26134	0.99510

b) Maximum surface settlement

	γ = 15.68 kN/m^3	γ = 19.60 kN/m^3
Settlement (mm)	4.40321	5.50558
Surface Settlement/Crown Settlement	0.37471	0.37474

(Settlement ratio γ = 15.68/Settlement ratio γ = 19.60) = 0.99991

Table 6.2 Invariance of NGRC and Normalized Displacements to Changes in the Unit Weight of the Soil

displacements normalized to E_{ti}, are homothetic curves for any ϕ value. This will provide a greater generality in the projected solution. Had the product Kp_a instead of E_{ti} been selected to define the dimensionless displacement U, the NGRC for different ϕ would not be homothetic.

6.2.3 Frictionless Soil Model

If the frictional component of strength is set equal to zero and the Janbu's exponent n is also set equal to zero, another special group of hyperbolic stress-strain curves is found. With $\phi=0$, the stress-strain relationships become independent of the minor principal stress. For a given modulus K, different curves are obtained for different undrained cohesion (c_u) values. As in the previous case, it is simple to prove that these curves also present the property of homothety. Therefore, if the deviatoric stresses and major principal strains are normalized to the coordinates of arbitrary homothetic points, $(\sigma_1-\sigma_3)_{ref}$ and ϵ_{1ref}, on these curves then a single normalized hyperbola is found for the entire ground mass. A family of curves similar to that shown in Figure 6.1 is found, each one defined for a given c_u value.

The tangent modulus at homothetic points on these curves is given by:

$$E_t = K\, p_a \left[1 - R_f \frac{(\sigma_1-\sigma_3)_{ref}}{2c_u}\right]^2 \qquad [6.5]$$

Likewise to the case of cohesionless soil discussed in the previous section, it is easy to show that the ratio $(\sigma_1-\sigma_3)_{ref}/c_u$ is constant, and thus, for a fixed R_f value, E_t is constant at homothetic points in the stress-strain family of curves. As the stress-strain curve of a soil with a constant c_u profile does not depend on σ_3, the in situ tangent modulus profile for this soil is also constant with depth. For the special case of a hydrostatic stress field ($K_o=1$), the initial tangent modulus is:

$$E_{ti} = K\ p_a \qquad [6.6]$$

It can be shown that in a two-dimensional representation, unlined circular tunnels with different diameters, with the same cover to diameter ratio (H/D) and with the same strength ratio, defined as $c_u/\gamma D$, will exhibit a unique normalized ground response in terms of the ground reaction curves and of the displacement field. This will be so, once more, as a consequence of the homothetic property of the hyperbolic stress-strain curves of this particular soil group, with $\phi=0$, $n=0$ and $K_o=1$.

To illustrate this fact, two finite element analyses were carried out using the parameters shown in Table 6.3. As indicated the two circular tunnels have different geometry but the same H/D ratio. The ground stresses at the opening were gradually reduced to zero in ten equal increments and no support was installed. After the 7th load increment some elements close to the tunnel contour, at about 45° from the crown, underwent tension and the results after this event were discarded. In both cases, the in situ tangent modulus

Diameter D (m)	4		8
Cover H (m)	6		12
H/D		1.5	
K		400	
n		0	
ϕ		0	
c_u (kPa)	98		196
R_f		1.0	
ν		0.49	
γ (kN/m^3)		19.6	
K_0		1	
$C_u/\gamma D$		1.25	
V/D		1.5	

Table 6.3 Input Parameters for Finite Element Analyses of Tunnels with the Same H/D and with Homothetic Hyperbolic Stress-Strain Soil Model with ϕ=0

was equal to 40.494 MPa.

Figures 6.9 to 6.11 present the ground reaction curves at the crown, springline and floor calculated for both cases. The curves are plotted in terms of radial displacements at these points relative to the ratio of current to in situ radial stresses. Distinct curves were obtained for each case. But if the displacements are again normalized to the tunnel diameter and to the ratio of in situ radial stress to in situ tangent modulus, as before, then single curves result for each point of the tunnel contour as indicated in Figure 6.12. As the in situ stress level at the deeper tunnel is twice that at the shallower one, and as the diameter of the former is also twice that of the latter, the displacements in the deeper tunnel are 4 times larger than those in the shallower position. The ratio of the displacements given by the numerical calculations is almost exactly equal to four.

Figure 6.13(a) furnishes the distributions of subsurface settlements along the tunnel cover calculated for a ground stress release of 50%. As in Figure 6.7, the settlements are plotted against the depth normalized to the tunnel diameter. The settlements at the deeper and larger tunnel are four times larger than those at the other tunnel. Therefore, if the settlements are normalized to the crown settlement of each case, then a unique distribution of normalized settlements with depth is found, as shown in Figure 6.13(b). Similar results are found for the surface

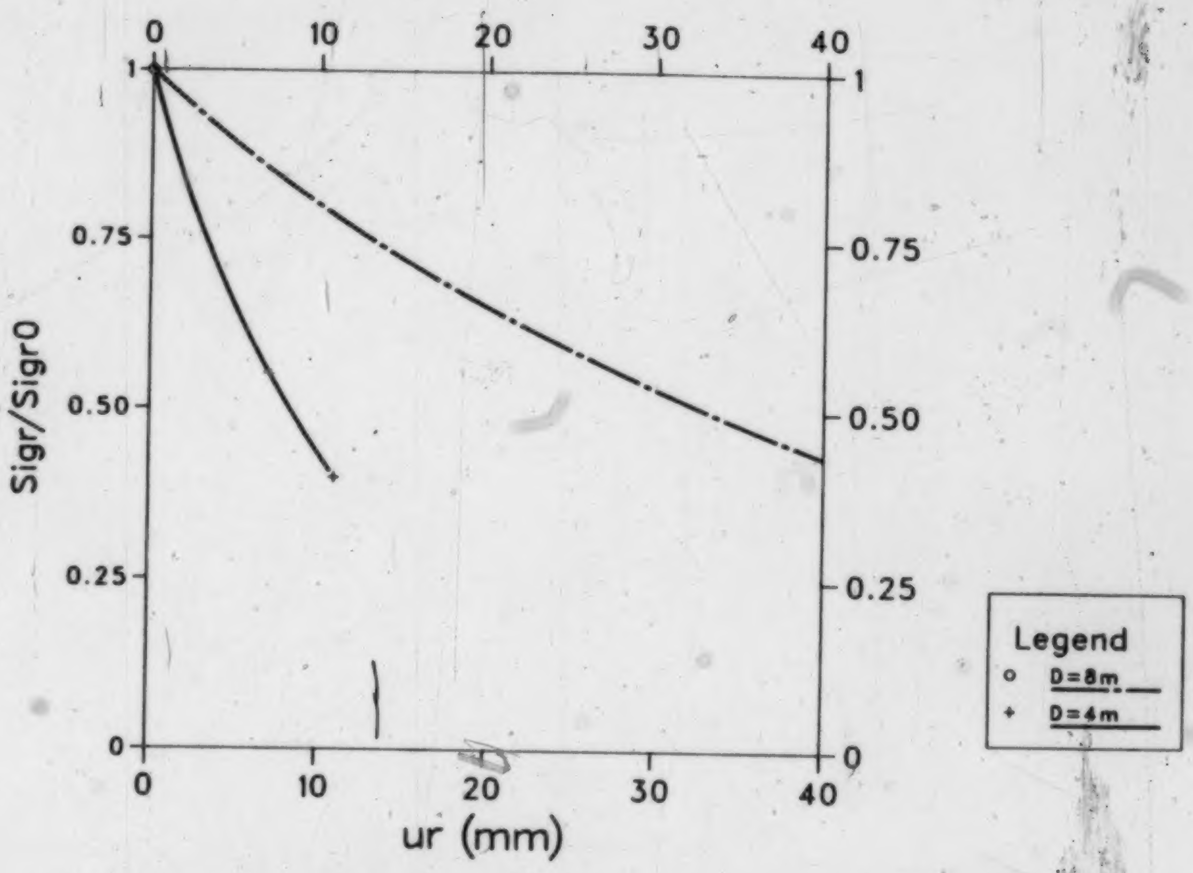

Figure 6.9 Ground Reaction Curve for the Crown of Geometric Homothetic Tunnels in a Soil with a Homothetic Hyperbolic Stress-Strain Relationship (frictionless model)

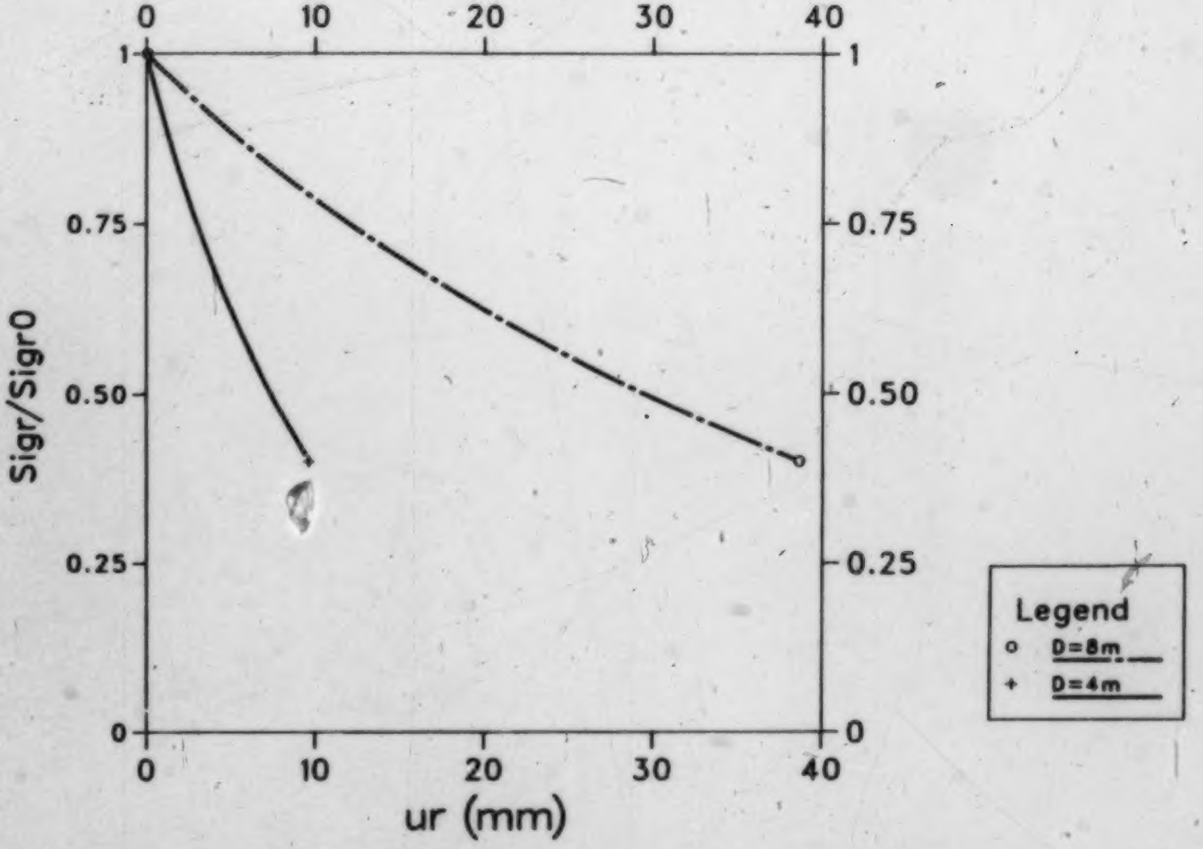

Figure 6.10 Ground Reaction Curve for the Springline of Geometric Homothetic Tunnels in a Soil with a Homothetic Hyperbolic Stress-Strain Relationship (frictionless model)

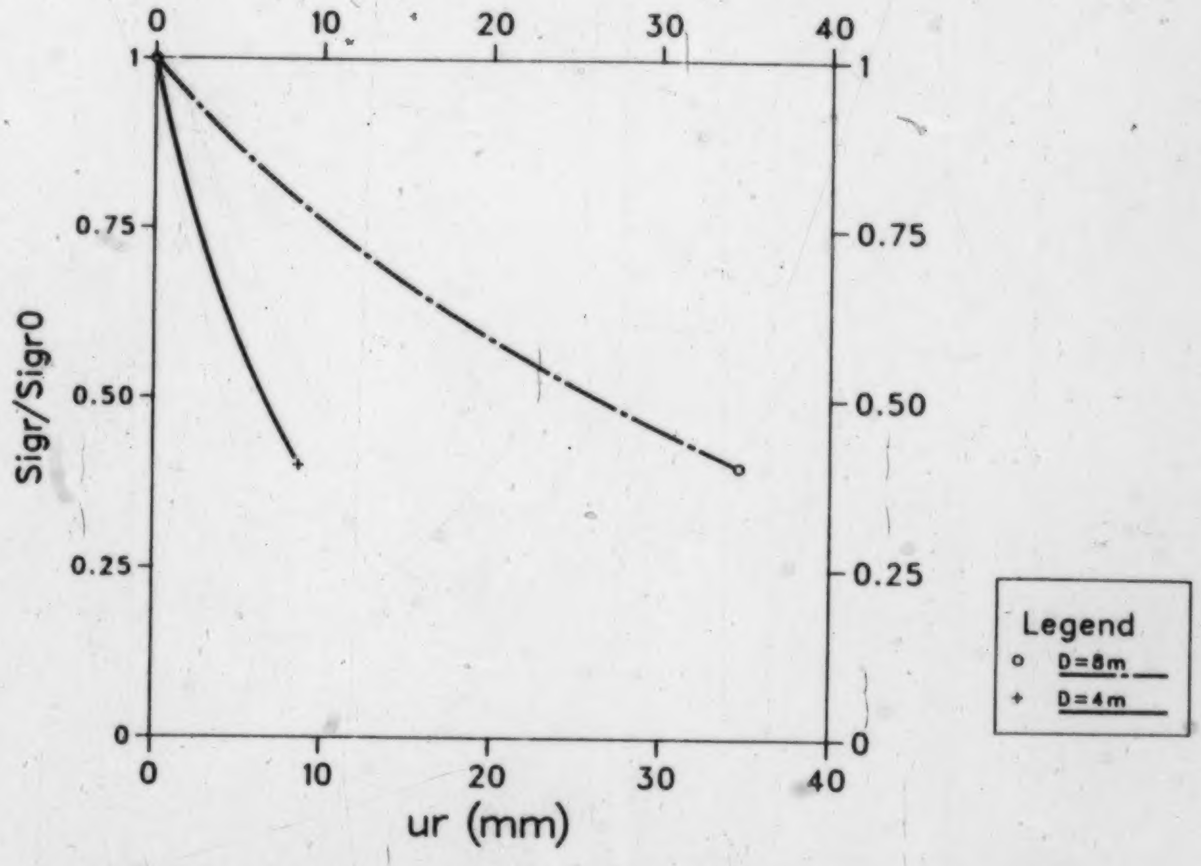

Figure 6.11 Ground Reaction Curve for the Floor of Geometric Homothetic Tunnels in a Soil with a Homothetic Hyperbolic Stress-Strain Relationship (frictionless model)

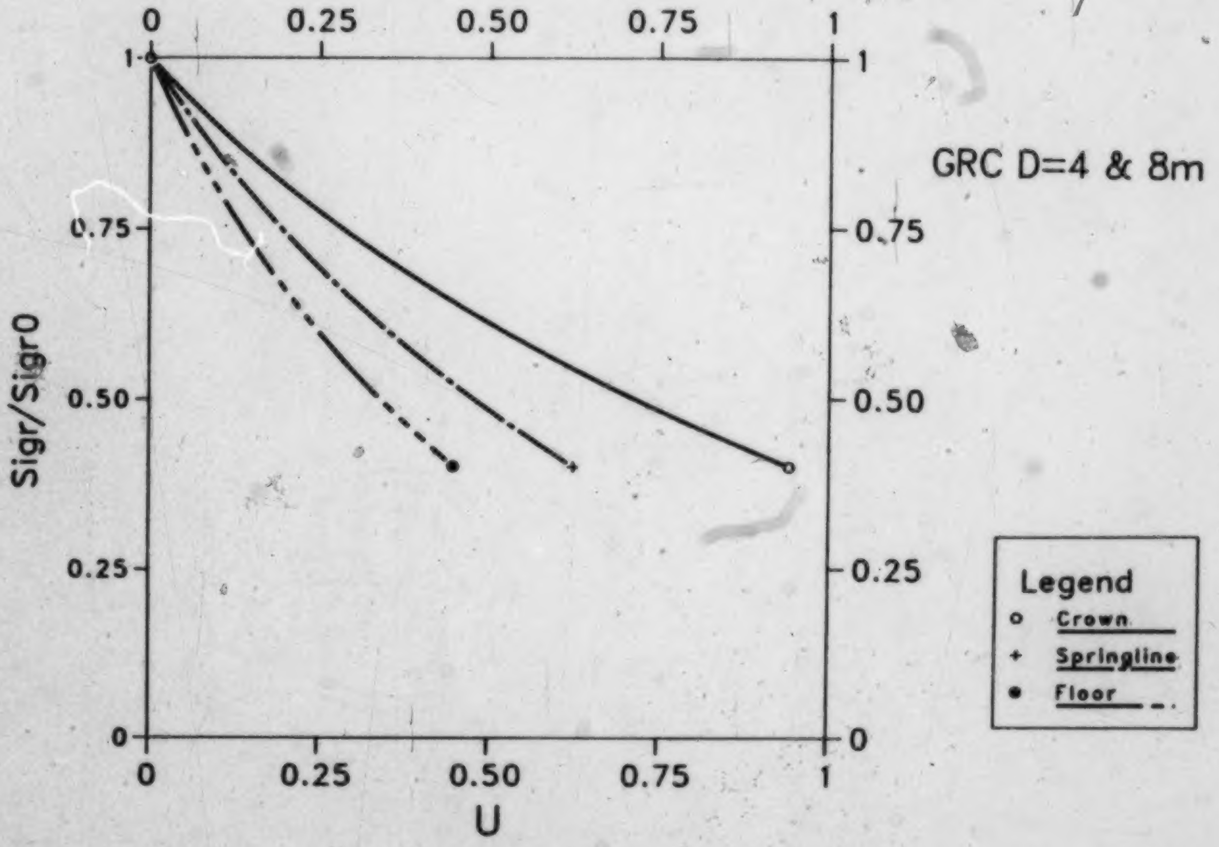

Figure 6.12 Normalized Ground Reaction Curves of Geometrically Homothetic Tunnels in a Soil with a Homothetic Hyperbolic Stress-Strain Relationship (frictionless model)

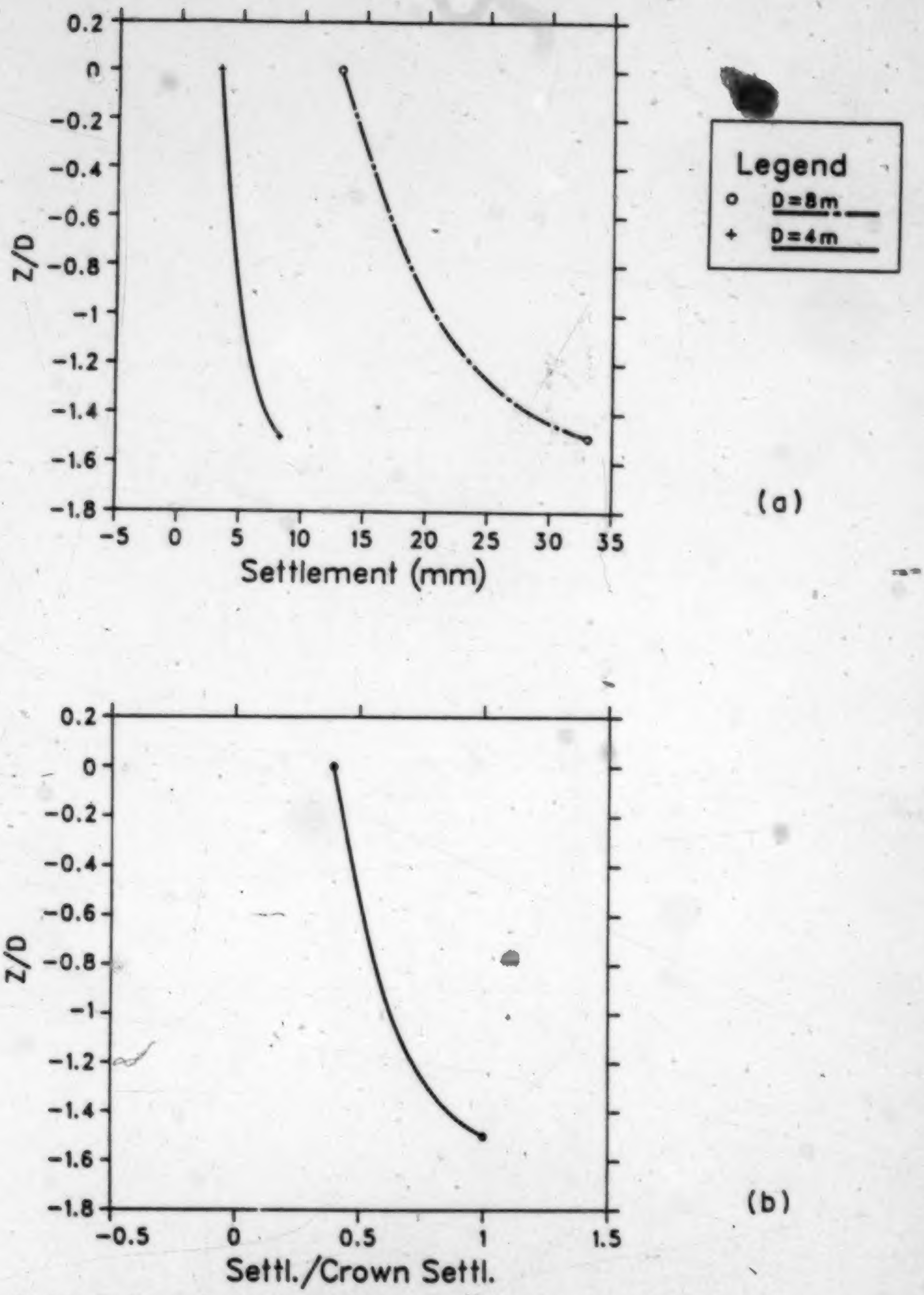

Figure 6.13 Subsurface Settlements along the Cover of Geometrically Homothetic Tunnels in a Soil with a Homothetic Hyperbolic Stress-Strain Relationship ($\phi=0$), for a Stress Release of 50%

settlements as indicated in Figures 6.14(a) and (b). When the surface settlements are normalized to the crown settlement calculated for a certain amount of ground stress release, a unique distribution is found.

As in the case of the cohesionless soil simplification (Section 6.2.2), the property of homothety will simplify the parametric analyses for this case, as the projected solution will not depend on the tunnel size, but simply on the ratio H/D. Obviously, it will depend on the ratio $c_u/\gamma D$, where it is sufficient to vary the values of c_u since, as in the former case, the unit weight of the soil of an homogeneous ground profile does not affect the normalized tunnel response.

Moreover with friction angle set equal to zero, there will be no need to vary the failure ratio, R_f, to obtain a general solution. This is because it is always possible to define an equivalent (undrained) cohesion c_{ue}, associated with a failure ratio (R_{fe}) equal to unity which gives the identical tangent modulus. If the tangent modulus given by equation 6.5 is to be the same, c_{ue} has to be selected in such a way that:

$$R_f \frac{1}{c_u} = R_{fe} \frac{1}{c_{ue}}$$

setting $R_{fe}=1$, then:

$$c_{ue} = \frac{c_u}{R_f} \qquad [6.7]$$

The stress-strain curve and thus the normalized ground response to tunnelling for the frictionless soil, with $R_{fe}=1$ and with an undrained cohesion c_{ue}, given by the equation

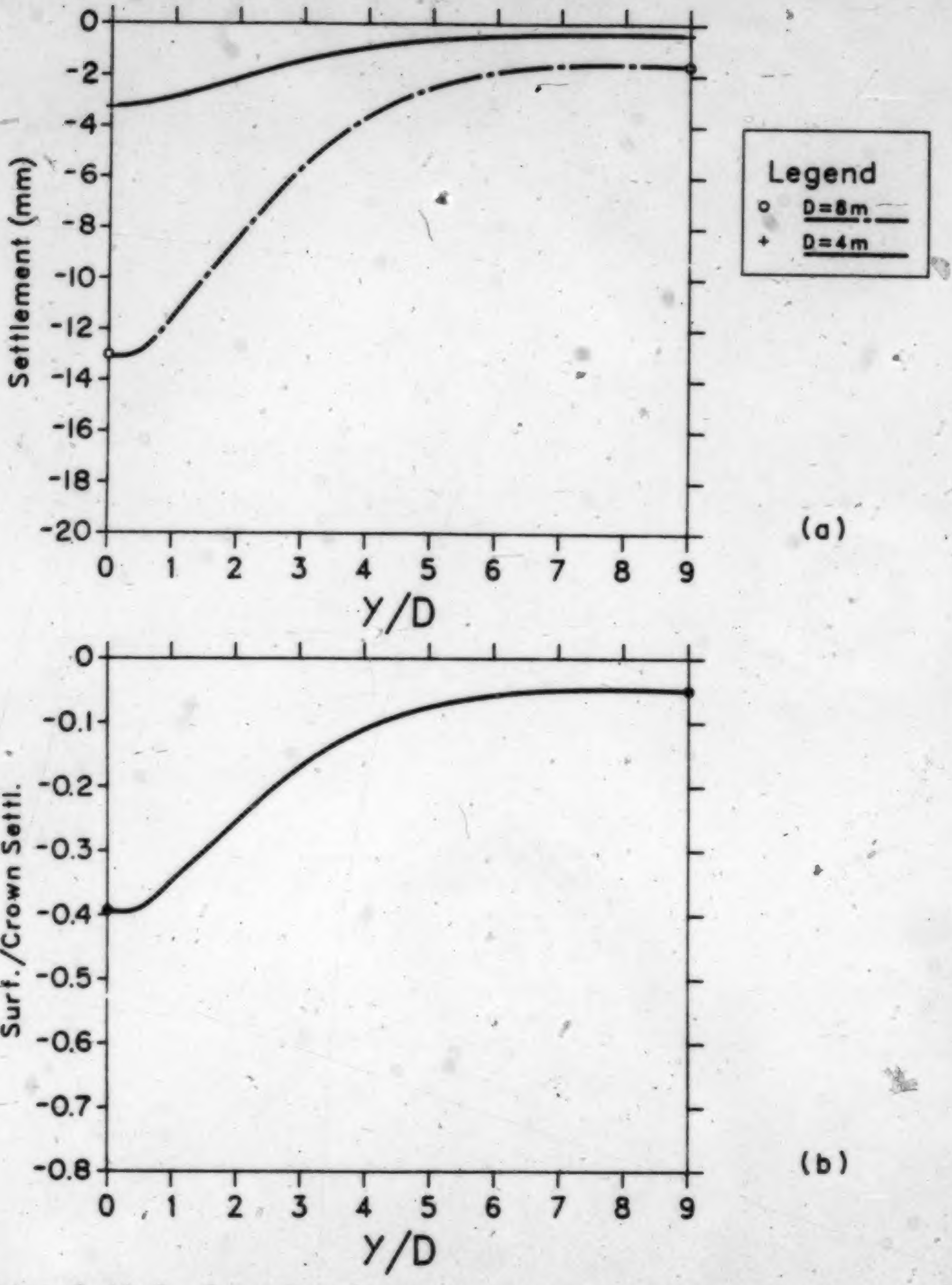

Figure 6.14 Surface Settlements over Geometrically Homothetic Tunnels in a Soil with a Homothetic Hyperbolic Stress-Strain Relationship ($\phi=0$), for a Stress Release of 50%

6.7, are identical to that of the frictionless soil, with R_f not equal to 1 and a cohesion equal to c_u.

The simplifications introduced so far allow equation 6.1 to be expressed in a more compact form, for this group of soil:

$$F = f\left(\theta\ ,\ \frac{\sigma_r}{\sigma_{ro}}\ ,\ \frac{u_r E_{ti}}{D\sigma_{ro}}\ ,\ \frac{H}{D}\ ,\ \frac{c_{ue}}{\gamma D}\ ,\ \nu_u\right) \qquad [6.8]$$

valid for $K_o=1$.

In this particular case, the variables in the above equation are mutually independent, with E_{ti} being solely a function of Janbu's modulus K and of the atmospheric pressure.

When the writer developed the simplifications described above regarding the homothetic soil models for a cohesionless soil (Section 6.2.2) and for a frictionless soil (present section), he was not aware that a similar approach has been used by other authors. In fact, the theoretical solution of settlements above tunnels by Resendiz and Romo, 1981 (see Section 4.3.3) also took advantage of the homothetic property of the hyperbolic model for $\phi=0$ and a c_u constant profile. Even earlier than that, these authors (Resendiz and Romo, 1972:819) used a similar soil model for the study of embankment deformations. In the latter case, a slightly different model was adopted in which the soil was assumed to be consolidated under its own weight and then sheared under undrained conditions, upon addition of subsequent embankment layers (hence a consolidated undrained condition). Resendiz and Romo (1972,1981) expressed their solutions using the original hyperbolic model formulation by Kondner (1963) for cohesive soils. The writer favoured the extended formulation by Duncan and Chang (1970) that makes use of more standard soil parameters. The novel development in the present work is, actually, the first soil model discussed (Section 6.2.2), representing a cohesionless soil. Despite the similarities between the models used by the writer and Resendiz and Romo (1981) for cohesive soils, the subsequent development of the design methods are quite different as will be seen in following sections of this chapter.

A final comment should be added to the present discussion. In section 5.2.2.1, it was pointed out than an incrementally reversible stress-strain relationship was assumed in the two dimensional numerical solution adopted herein. Consequently, no distinction is made between the loading, unloading and reloading behaviours. Had a different unloading - reloading response been specified, like the linear elastic response originally proposed by Duncan and Chang (1970), the uniqueness of the normalized ground response would cease to exist, even for the simplified soil models proposed. It was discussed earlier in this thesis, and especially in Section 5.2.2.2, that some points around the two-dimensionally represented tunnel may have their principal stresses rotating, or commuting directions. This unloading and reloading response may in fact happen around the shallow tunnel, depending on the in situ stress ratio.

It is easy to recognize that if a distinct stress-strain response had been specified for a decreasing principal stress difference, the stress-strain curves representing the soil behaviour would not result homothetic any longer. The similarity of the ground response or its independence on the scale of the problem (tunnel size) would not exist, except approximately.

This difficulty with similarity techniques applied to non-linear incremental laws, with distinct loading and unloading representations, was discussed by Winter (1982:1076). This author suggested that in order to apply these techniques to these types of constitutive laws, one is forced to neglect either the influence of the unloaded zones or of the loaded zones. In the first case, the similarity solution implies more stored energy than it should, and in the second case the converse is true. The last alternative implies in reducing the treatment of the problem to a linear elastic representation and this, as shown earlier in this thesis, is not an acceptable choice.

In order to avoid these difficulties, in the present work makes no distinction between the loading and unloading-reloading soil responses. The numerical model was therefore implemented accordingly. Despite this simplification, the model was tested and proved satifactory in matching the performance of three shallow tunnel case histories (Section 5.2.4). Although this cannot be claimed as proof of the validity of the simplification, it does stand as an indication that it may be acceptable in practical terms.

6.2.4 Comments on Some Simplifying Assumptions

6.2.4.1 The Effect of Janbu's Modulus K

The in situ tangent modulus is directly proportional to the Janbu's modulus K, as shown by equations 6.2 and 6.6. As the normalized displacements are invariant to E_{ti}, they should also be invariant to the modulus K. Figures 6.15 to 6.17 demonstrate this fact. The ground reaction curves shown were calculated numerically, using the cohesionless soil model described in Section 6.2.2 and assuming $\phi=30°$, $n=0$, $\gamma=19.6$ kN/m³, $K_o=1$, $\nu=0.4$, D=4m, H=12 m and three different values for the modulus K. The ground stress release of the unlined circular opening was performed in ten equal increments.

If the displacements are expressed as:

$u_r/D.\sigma_{ro}$

the ground reaction curves are those shown by the solid lines. Clearly, as the K modulus decreases, the tunnel convergence increases proportionally, for the same amount of stress release.

If the displacements are normalized to E_{ti} and therefore to K, the ground reaction curves at each point of the tunnel contour are reduced to a single normalized curve shown by the dashed lines in Figures 6.15 to 6.17. Consequently, there will be no need to vary the value of K in the modelling step, in order to obtain the general solution to the problem.

6.2.4.2 The Effect of Janbu's Exponent n

A fairly restrictive assumption was made in the development of the cohesionless and of the frictionless soil models, presented in Sections 6.2.2 and 6.2.3. It refers to the value of the Janbu's exponent n, which was set equal to zero. This is the parameter controlling the rate of increase of the in situ tangent modulus of a soil deposit with depth. For instance, in a homogeneous and cohesionless deposit, if n is made equal to unity, the in situ tangent modulus increases linearly with depth. In this soil deposit, if n is set equal to zero, a constant modulus with depth is found. Except for some overconsolidated soil deposits, a constant in situ modulus profile does not generally correspond to reality.

The influence of the rate of increase of the in situ modulus with depth on the ground response to tunnelling, was thus investigated. Some typical results of this investigation are presented herein. They refer to three finite element analyses of a tunnel with D=4m and H=12 m, in soil with the following parameters: γ=19.6 kN/m³, K_o=0.8, c=0, ϕ=30°, ν=0.4, and Janbu's modulus K=400. Three exponents n were considered in these analyses: n=0, 0.5 and 1.0. These conditions yielded respectively, the following in situ tangent moduli at the tunnel axis elevation: 31.015 MPa, 45.672 MPa and 67.255 MPa.

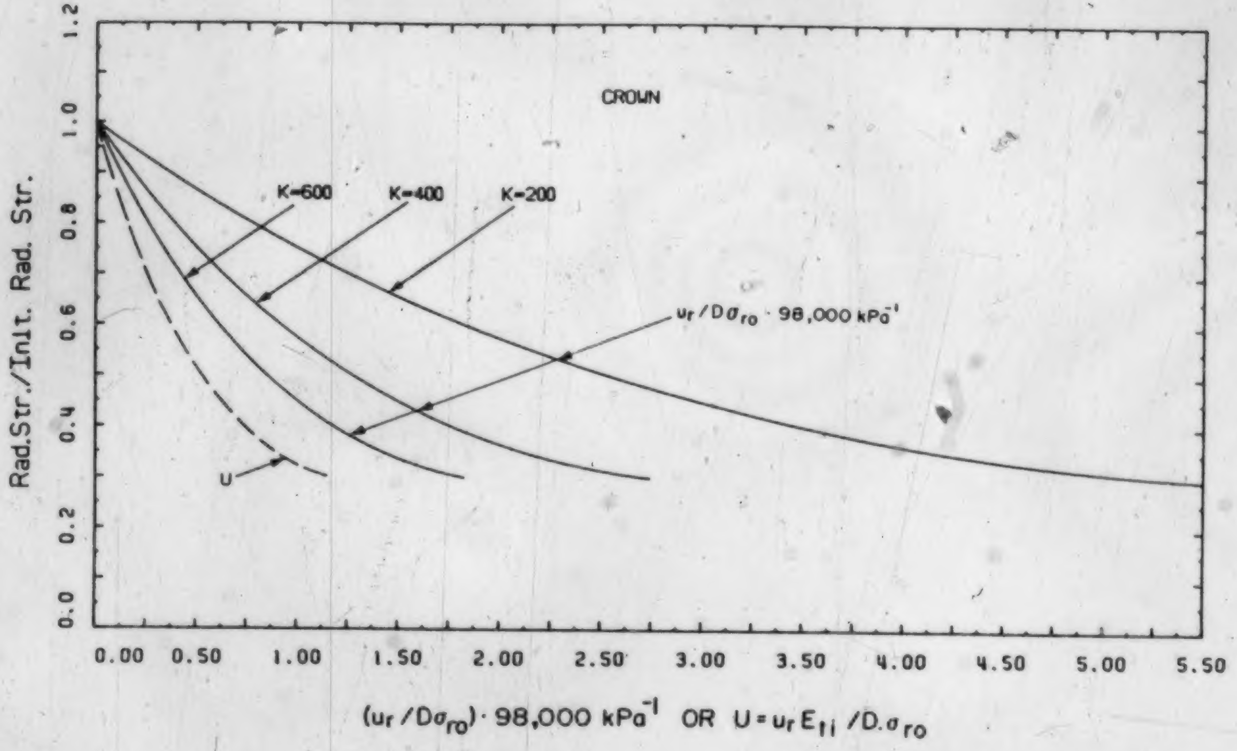

Figure 6.15 Influence of Janbu's Modulus K on the Ground Reaction Curve of the Tunnel Crown

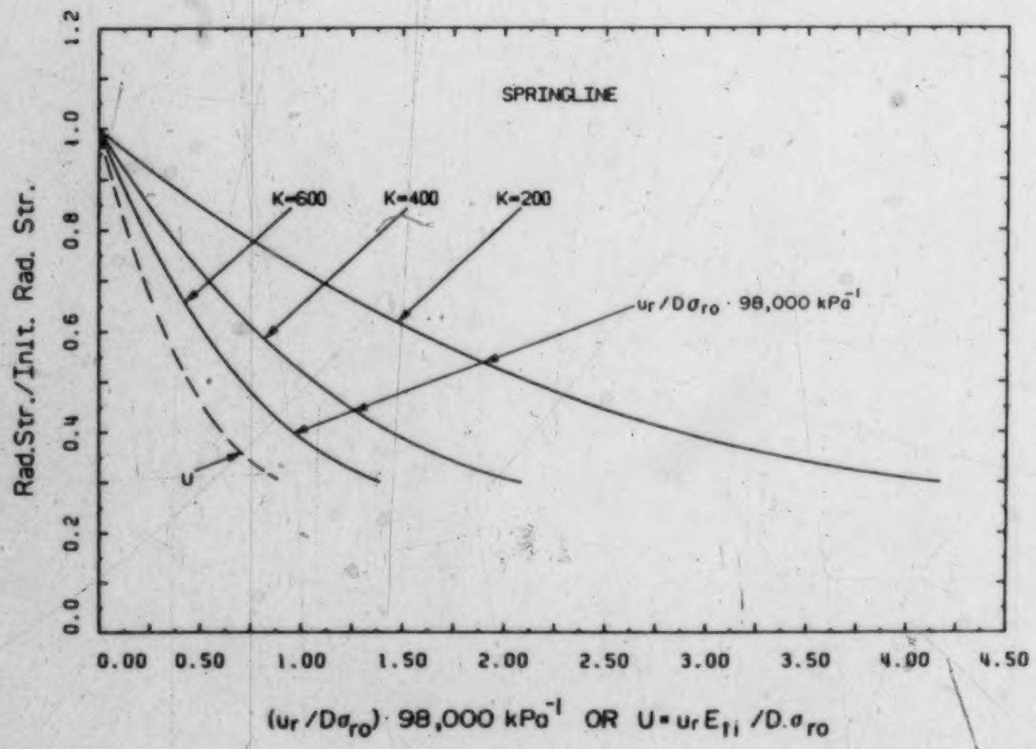

Figure 6.16 Influence of Janbu's Modulus K on the Ground Reaction Curve of the Tunnel Springline

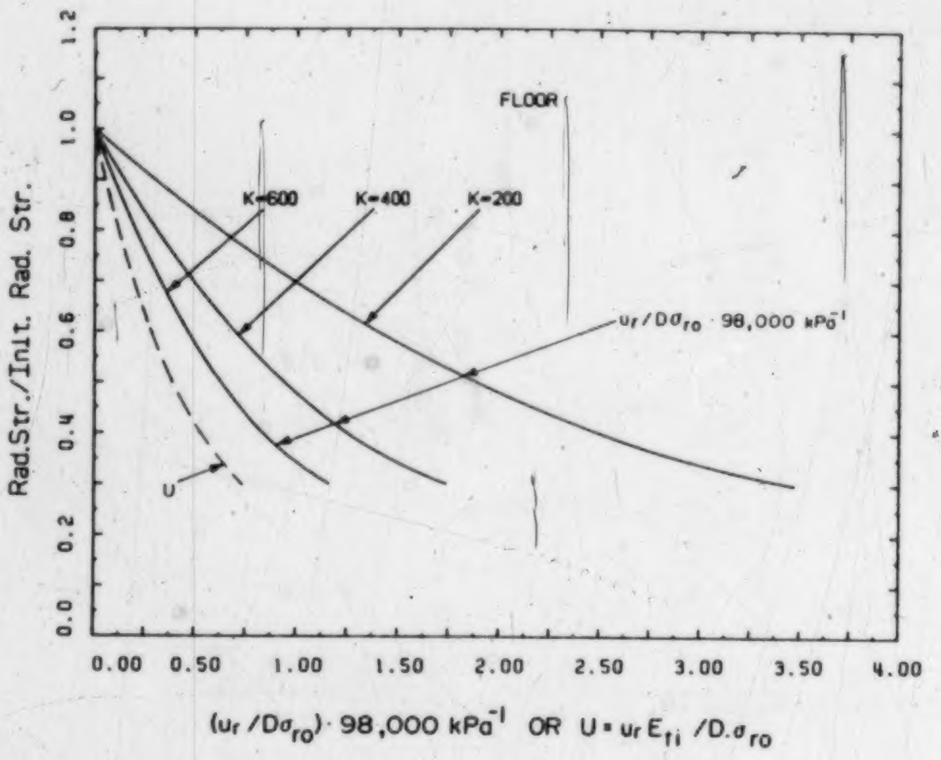

Figure 6.17 Influence of Janbu's Modulus K on the Ground Reaction Curve of the Tunnel Floor

If the in situ tangent modulus at the tunnel axis elevation is normalized to one, the variations of the modulus with depth, for the three cases considered are those shown in Figure 6.18.

The numerical analyses were performed with the gradual release of the ground stresses at the opening in ten increments. After the sixth unloading increment, some elements at the springline failed and the results thereafter were disregarded.

Figure 6.19 presents the calculated normalized ground reaction curves for the tunnel crown. In all cases, the displacements were normalized to the initial tangent modulus taken at the springline elevation. The ground reactions at the crown seem to be basically controlled by the soil cover stiffness. Since the displacements were normalized to the modulus at the tunnel axis, the resulting NGRC for the constant modulus profile (n=0) is stiffer than the other cases. An opposite trend is of course found at the tunnel floor. Figure 6.20 shows that when the modulus increases linearly with depth (n=1), a "stiffer" ground response is noted. The influence of the rate of increase in the ground stiffness with depth on the NGRC is less pronounced at the tunnel springline than elsewhere on the tunnel contour. This is illustrated in Figure 6.21, where the NGRCs appear fairly close together. Nevertheless, like the reponse at the crown, the resulting NGRC for n=0 is stiffer than the others, and this shows that the springline response of this shallow

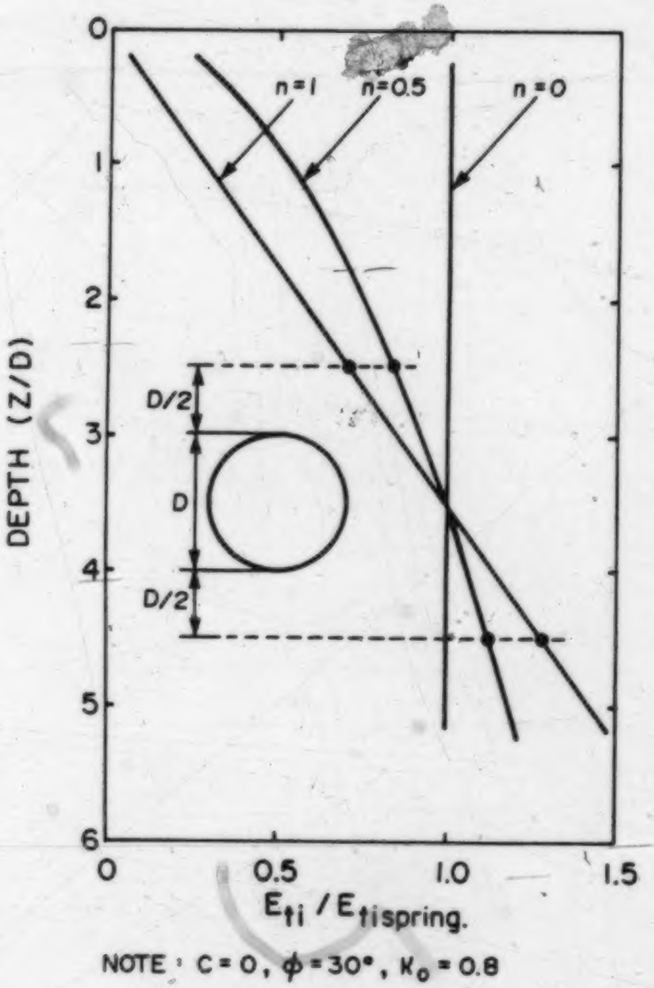

Figure 6.18 Variations with Depth of the In Situ Tangent Modulus for Three Values of Janbu's Exponent, n

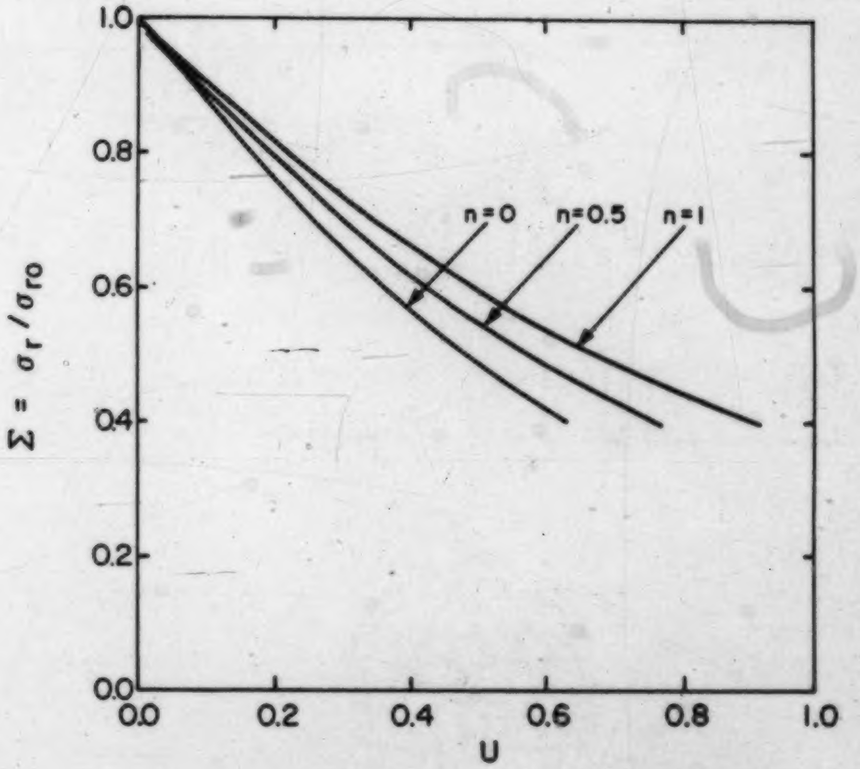

NOTE : C=0, ϕ=30°, K_0=0.8, ν=0.4, H/D=3

Figure 6.19 Normalized Ground Reaction Curves for the Tunnel Crown, Calculated for Different In Situ Tangent Modulus Profiles

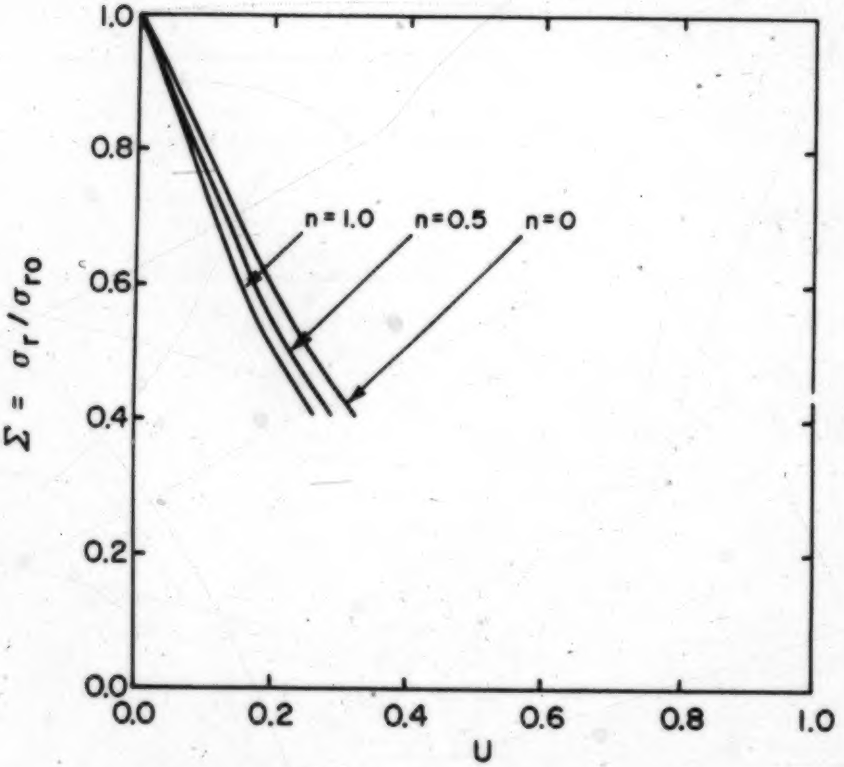

NOTE : C=0, ϕ=30°, K_0=0.8, ν=0.4, H/D=3

Figure 6.20 Normalized Ground Reaction Curves for the Tunnel Floor, Calculated for Different In Situ Tangent Modulus Profiles

tunnel is more affected by the stiffness of the ground above it than below it.

From the trends noted in Figures 6.19 and 6.20, it is observed that the NGRCs at the crown and at the floor reflect some sort of 'average' stiffnesses of the ground above and below the tunnel, respectively. If these average stiffnesses could possibly be determined and used to normalize the corresponding displacements, then a NGRC which would be independent of the rate of increase of the stiffness with depth, could eventually be found. After a few attempts, it was found that if the ground responses at the crown and at the floor were normalized to the in situ stiffness of the ground at points located half diameter above and below the tunnel respectively, the resulting NGRC would be practically independent of the rate of increase of E_{ti} with the depth. For n=0.5, these moduli are equal to 38.514 and 51.744 MPa, at half diameter above and below the tunnel respectively. For n=1.0 they are 47.530 MPa and 85.946 MPa. The new NGRCs for the crown and the floor are shown in Figure 6.22. As one notes, the newly defined response is virtually independent of the exponent n. This artifice thus allows the effect of E_{ti} increasing with depth to be approximately accounted for from the results of analyses where a constant in situ stiffness is assumed. The artifice was tested and found to yield approximately the same results for other geometric situations and soil parameters, within the ranges of variables considered in the

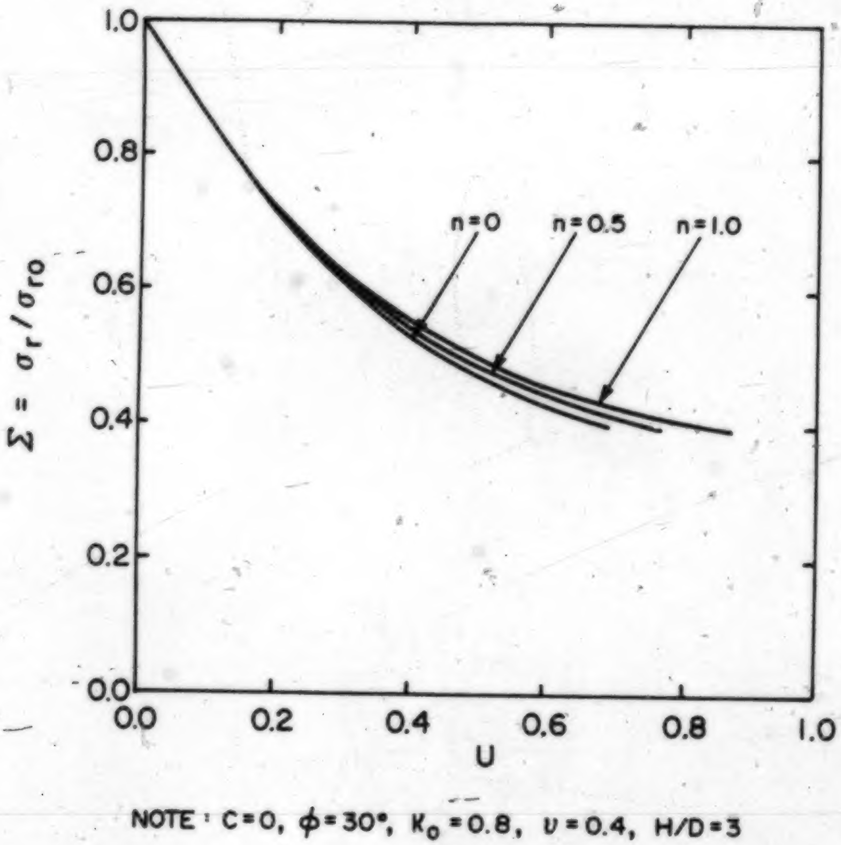

Figure 6.21 Normalized Ground Reaction Curves for the Tunnel Springline, Calculated for Different In Situ Tangent Modulus Profiles

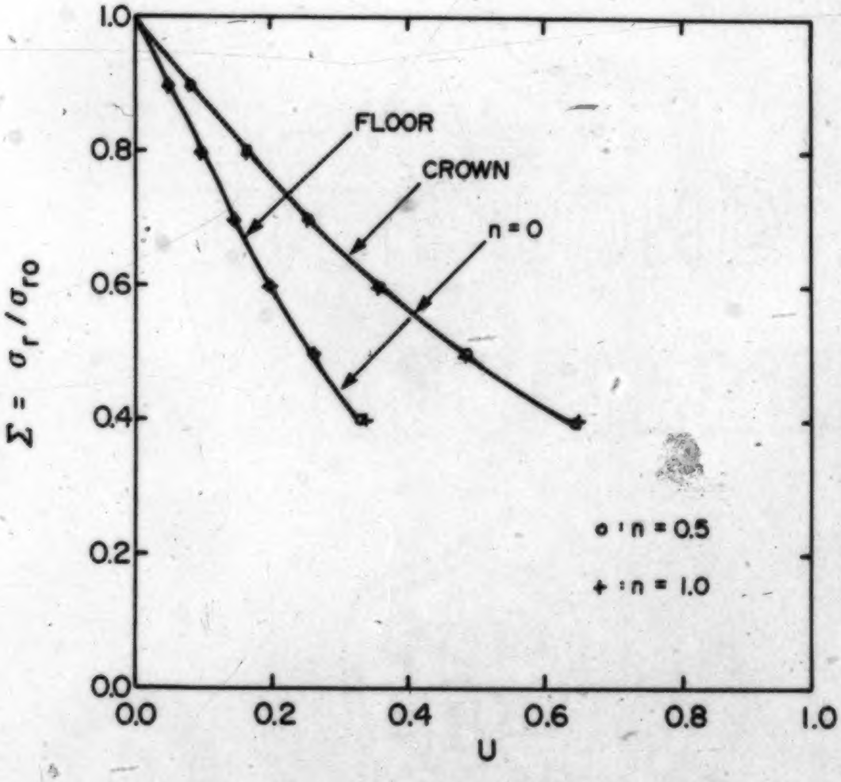

NOTE : C = 0, ϕ = 30°, K_o = 0.8, ν = 0.4, H/D = 3

Figure 6.22 Ground Reaction Curves for the Crown and Floor, with the Displacements Normalized to the Soil In Situ Stiffnesses at Points Half a Diameter Above and Below the Tunnel Respectively

modelling step to be presented later.

If the resulting normalized ground reaction curves are nearly independent of n, one would expect the same with regard to the ground settlements. Figures 6.23 (a) and (b) present the distributions of subsurface and surface settlements normalized to the crown settlement, for n varying from 0 to 1, and for 50% of ground stress release at the opening. Indeed the resulting distributions are very close to each other, although the influence of n is clearly noted. Moreover, one observes that the assumption of n=0 implies a slightly smaller average strain in the tunnel ground cover, as in fact one would expect, and which leads to a marginally higher normalized surface settlement at the tunnel axis. Although the maximum normalized settlement is larger for n=0, the maximum normalized distortion at about 2D off the centerline seems to be insensitive to the exponent n.

The results shown in Figure 6.23 depend slightly on the amount of ground stress release allowed at the opening. Table 6.4 presents the values of normalized maximum surface settlements for different n and different stress releases. The number shown between brackets represent the ratios of normalized settlement for n=0 to n>0. Therefore they represent the amount of approximation involved in the constant modulus profile assumption. By making n=0, one observes that the normalized maximum surface settlement is overestimated by 4 to 11%, depending on the value of n and

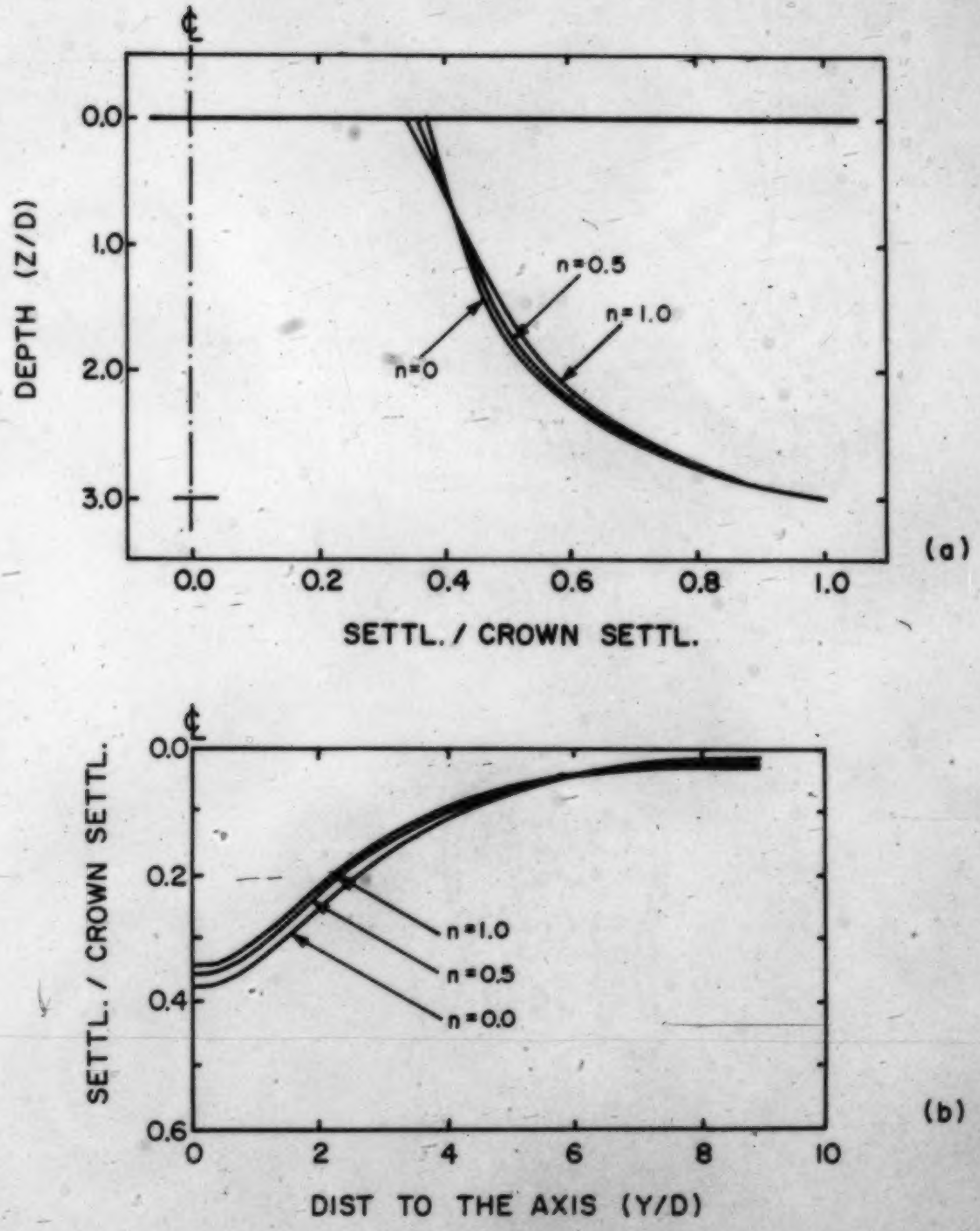

NOTE : C=0, ϕ=30°, K_o=0.8, ν=0.4, H/D=3

Figure 6.23 Normalized Subsurface and Surface Settlements for 50% Ground Stress Release at the Opening, for Different Exponent n Values

on the amount of ground stress release. The error seems to increase as n increases and as the stress release decreases.

To complete the picture, Table 6.5 was prepared. It shows the ratios of normalized crown displacements for n=0 to n>0. The assumption of n=0 may under or overestimate the normalized displacement for n>0, depending on the valaue of n and on the amount of stress release. As the stress release increases, the n=0 assumption tends to underestimate U for n>0. The error in the U estimate with n=0 varies within plus or minus 3%.

If the results of Tables 6.4 and 6.5 are combined one may estimate the final error in the actual maximum ground surface settlement estimate for the assumption of n=0. It will usually be overestimated by 2 to 14%. For n=0.5, the overestimate should not normally exceed 5%.

In summary, one may conclude that the exponent n does have an effect on the ground response to tunnelling. The soil models described in Sections 6.2.2 and 6.2.3 assume n=0. However, the effect of n on the normalized ground reaction curves can be taken approximately into consideration, by using the actual in situ tangent modulus at points located half diameter radially away from the point of the opening being considered. A lower E_{ti} is therefore selected for the crown curve, an intermediate one for the springline and a higher one for the floor.

The subsurface and surface settlements normalized to the crown settlement are not much affected by n, and the

	Maximum Surface Settlement/Crown Settlement		
Stress release	40%	50%	60%
n = 0	0.366 (1.000)	0.375 (1.000)	0.379 (1.000)
n = 0.5	0.350 (1.046)	0.359 (1.045)	0.363 (1.044)
n = 1.0	0.329 (1.112)	0.339 (1.106)	0.343 (1.105)

Note: The ratios of settlement ratios for n = 0 to n > 0 are shown between brackets.

Table 6.4 Variation of the Maximum Normalized Surface Settlement with the Exponent n and with the Amount of Stress Release Allowed in the Opening

	U (n = 0)/U (n > 0) at crown		
Stress release	40%	50%	60%
n = 0.5	1.000	0.990	0.980
n = 1.0	1.023	1.000	0.974

Table 6.5 Ratio of Normalized Crown Displacements for n=0 to n>0, for Different Exponents n and Different Amount of Stress Release at the Opening

assumption of n=0 seems to be a safe one in most cases. Moreover, the degree of overestimation is not excessive. The maximum normalized surface distortions are also not much influenced by n.

6.2.4.3 The Effect of the Cohesive Strength Component

Another fairly restrictive assumption made in the development presented in Section 6.2.2 refers to the zero cohesion assumed in the frictional soil model. Soil cohesion has a clear and important role in the stability of an underground opening as discussed in other sections of this thesis (for instance, Section 4.3.4). To neglect the cohesive component of soil strength may be an unduly conservative assumption.

To investigate the effect of the cohesion on the ground response to tunnelling, some finite element analyses were carried out. An unlined circular tunnel with D=4m and H=12 m was considered in a homogeneous soil profile, with the following properties: $\gamma=19.6$ kN/m^3, $K_o=0.8$, $\phi=30°$, $\nu=0.4$, n=0, and K=400. Three cohesive strengths were considered in these analyses: c=0, c=9.8 kPa and c=19.6 kPa (i.e., $c/\gamma D=0$, 0.125 and 0.250). For those conditions, the following in situ tangent moduli were obtained at the tunnel axis elevation, respecively: 31.015 MPa, 31.653 MPa and 32.211 MPa.

Once more the numerical analyses were performed with the gradual release of the ground stresses at the opening in ten constant increments. For c=0, after the sixth unloading increment, some elements close to the springline failed and the results thereafter were disregarded. In the other cases, the failure of elements close to the springline was noted only after the seventh unloading increment. The increased soil strength in these cases thus allowed a larger stress release to be applied at the opening, without inducing localized soil failure.

Figure 6.24 shows the calculated normalized ground reaction curves for the tunnel crown. The displacements were normalized to the initial tangent modulus at springline elevation. As would be expected, the increase in c, besides making the soil stronger which permitted a larger stress reduction without failure, it also makes the soil stiffer, thus leading to smaller U values for a given stress release. A similar behaviour is noted for the tunnel springline, as indicated in Figure 6.25. A more pronounced non-linear response is noted here which reflects the trend of soil elements at the springline to fail earlier than elsewhere when K_o is less than unity, as in this case. The influence of the cohesion on the ground reaction at the tunnel floor is less pronounced, as indicated in Figure 6.26. Unlike the response at the springline, soil elements close to the floor are likely to fail later, and require a larger stress reduction to cause local soil failure. The ground response shown is thus mainly controlled by the frictional strength of the soil rather than the cohesive component. The higher confining stress level below the tunnel, causes the

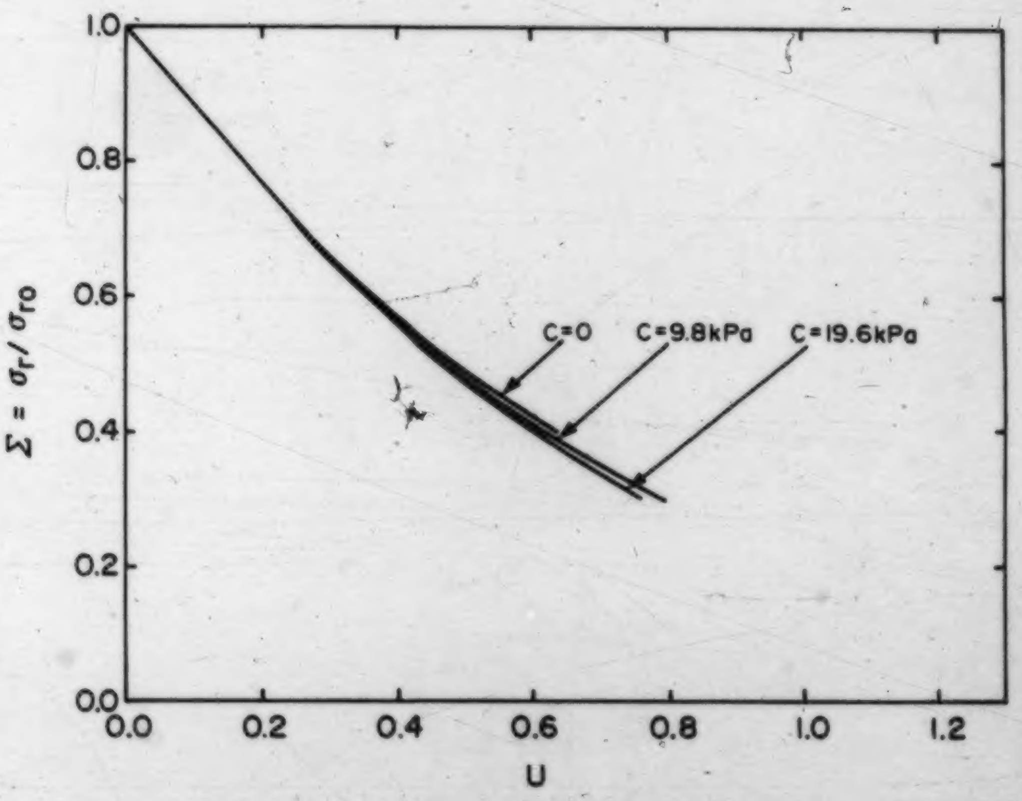

NOTE : $\phi = 30°$, $K_o = 0.8$, $\nu = 0.4$, $n = 0$, $H/D = 3$, $D = 4m$

Figure 6.24 Normalized Ground Reaction Curves for the Crown, Calculated for Different Cohesive Strengths of the Soil

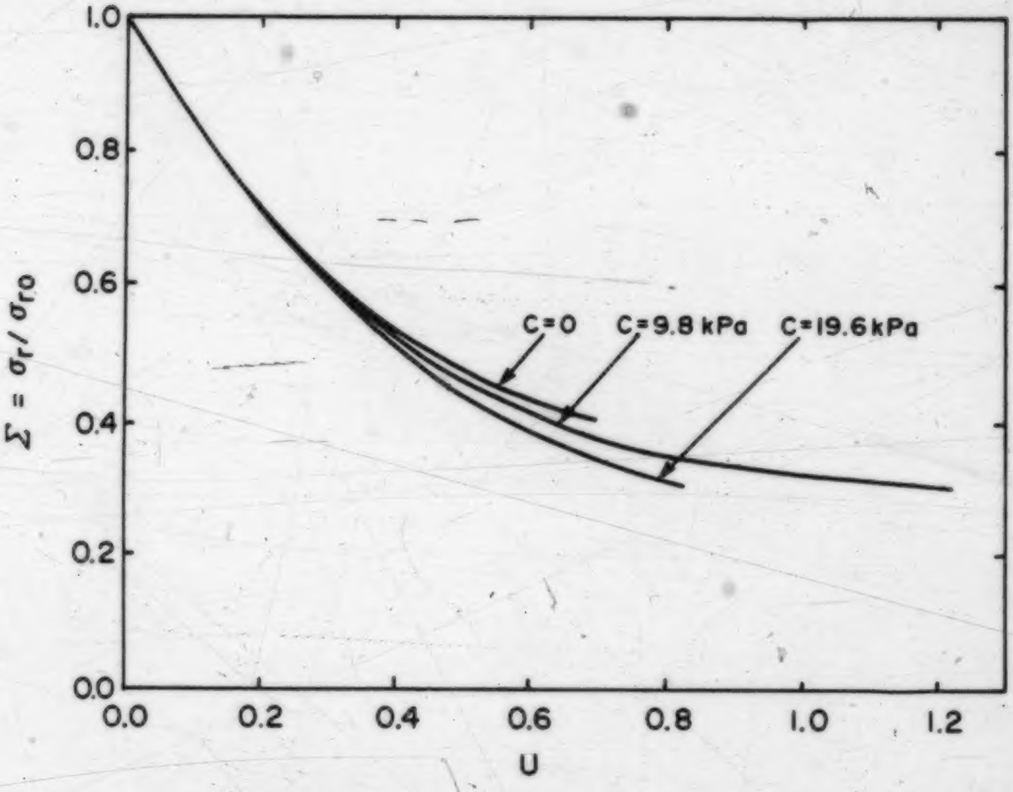

NOTE : $\phi = 30°$, $K_o = 0.8$, $\nu = 0.4$, $n = 0$, $H/D = 3$, $D = 4m$

Figure 6.25 Normalized Ground Reaction Curves for the Springline, Calculated for Different Cohesive Strengths of the Soil

frictional component of strength to dominate the response, and the NGRC for different c values virtually coincide. Similar responses are noted at the crown and springline for smaller amounts of ground stress release (up to about 40% and 30% respectively).

Figures 6.27(a) and (b) present the distributions of subsurface and surface settlements normalized to the crown settlement, for c varying from 0 to 19.6 kPa and for a ground stress release of 50% at the tunnel. For these conditions and parameters, the influence of cohesion is basically immaterial. The maximum normalized ground distortion is virtually insensitive to the soil cohesion. The results shown in this figure depend on the amount of stress release. Table 6.6 presents the values of normalized maximum surface settlements for different c and different stress releases. The numbers shown between brackets represent the ratios of normalized settlements for c=0 to c=0. As for the NGRC, one notes that if the cohesive component of strength is neglected the normalized maximum ground surface settlement is overestimated by 1 to 3%, depending on the value of c and the amount of ground stress reduction. The error involved in neglecting c seems to increase as stress reduction increases and, of course, as the soil cohesion increases. If the cohesion is higher than the values considered herein, then the degree of overconservatism in the c=0 assumption might become excessive. To compensate for this and to get closer to the

	Maximum Surface Settlement/Crown Settlement		
Stress release	40%	50%	60%
c = 0	0.366 (1.000)	0.375 (1.000)	0.379 (1.000)
c = 9.8 kPa	0.362 (1.011)	0.369 (1.016)	0.373 (1.016)
c = 19.6 kPa	0.358 (1.022)	0.365 (1.027)	0.369 (1.027)

Note: The ratios of settlement ratios for c = 0 to c ≠ 0 are shown between brackets.

Table 6.6 Variation of the Maximum Normalized Surface Settlement with the Cohesive Strength of the Soil and with the Amount of Stress Release Allowed

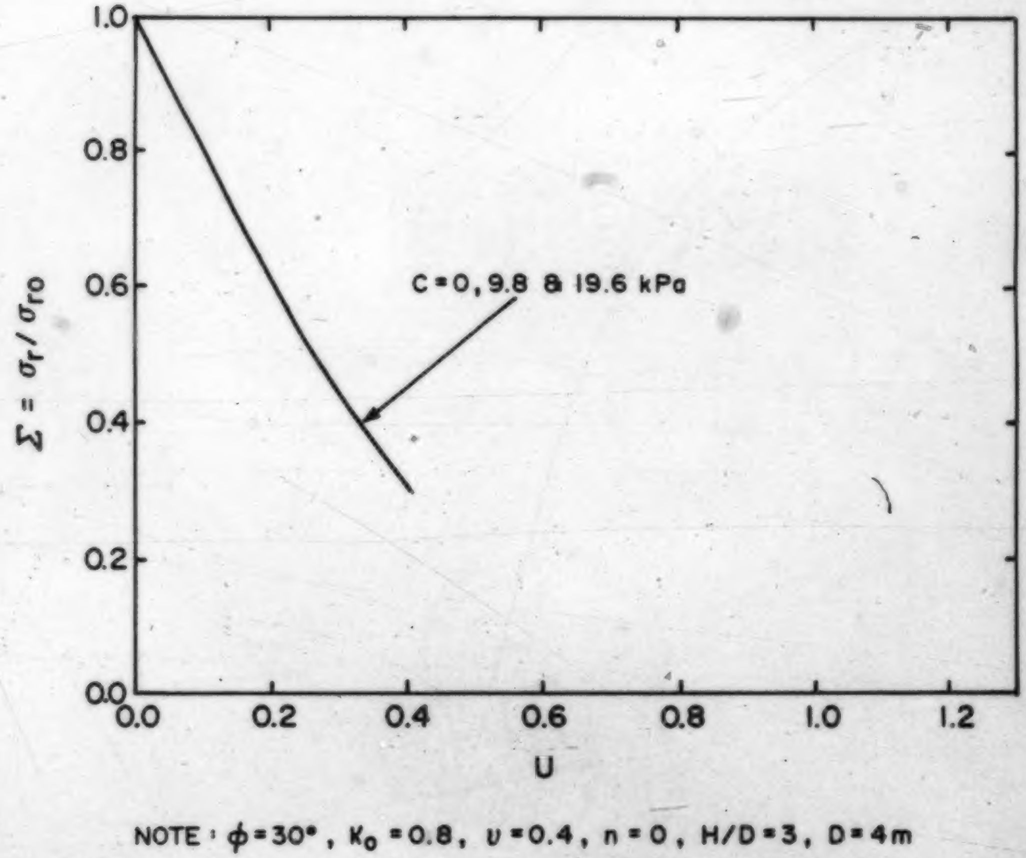

Figure 6.26 Normalized Ground Reaction Curves for the Floor, Calculated for Different Cohesive Strengths of the Soil

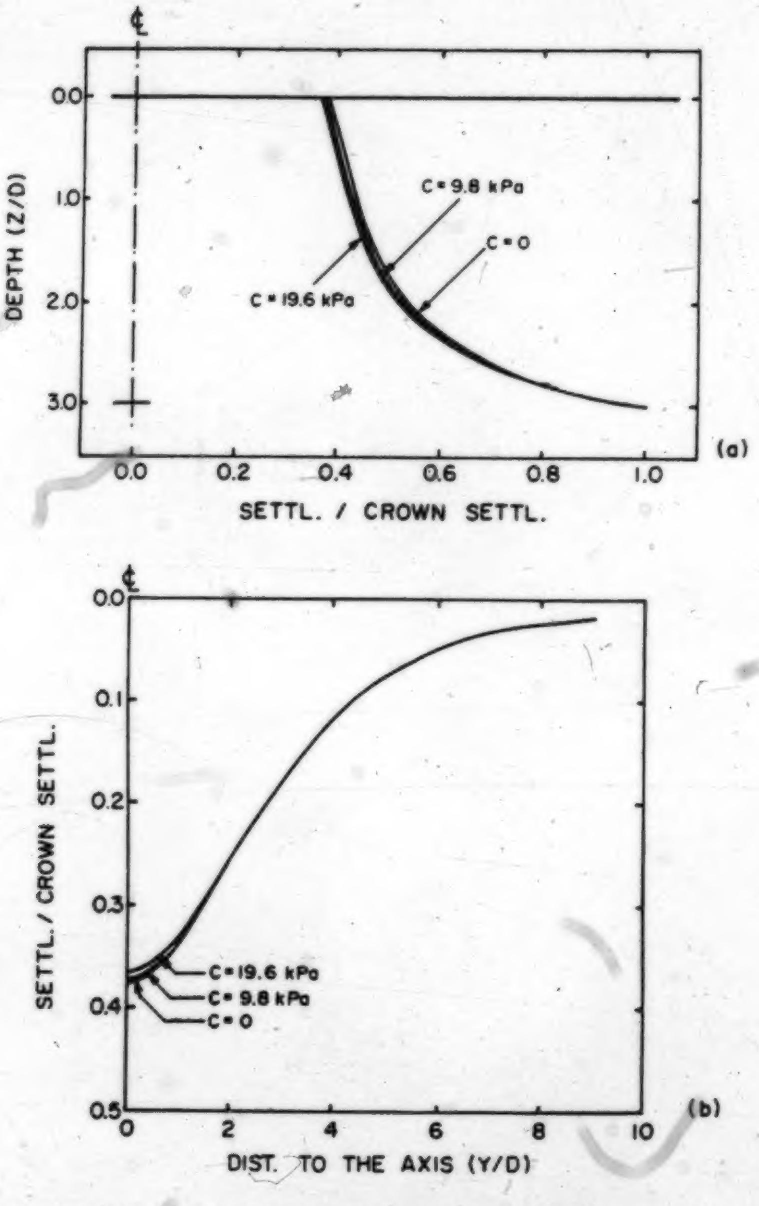

NOTE : $\phi = 30°$, $K_0 = 0.8$, $\nu = 0.4$, $n = 0$, $H/D = 3$, $D = 4m$

Figure 6.27 Normalized Subsurface and Surface Settlements for 50% Ground Stress Release, Calculated for Different Cohesive Strengths of the Soil

response that includes the effects of both frictional and cohesive components of strength, an approximation can be devised. This consists of adjusting the friction angle of the soil with c=0 (so as to not depart from the cohesionless soil model) in such a way that the in situ strength defined in terms of the principal stress difference at the springline elevation, is made equal to the strength of the actual soil with a non-zero cohesion. A problem then emerges, as the stress difference at failure depends on the stress path leading to failure and this is not exactly known.

If it is assumed that at failure the normal stress is equal to the average in situ principal stress $(\sigma_1+\sigma_3)/2$, then the resulting adjusted friction angle is:

$$\phi_a = \arcsin\left[\sin\phi + 2c\cos\phi/\gamma(H+D/2)(1 + K_o)\right] \qquad [6.9]$$

On the other hand, if it assumed that failure is reached by keeping the minor in situ principal stress constant and by increasing the major principal stress, then the adjusted friction angle becomes:

$$\phi_a = \arcsin\left[\frac{1+(\sigma_3/c)\tan\phi}{1+(\sigma_3/c)\sec\phi}\right] \qquad [6.10]$$

If the results of the finite element analysis with the higher cohesion (c=19.6 kPa) is taken as an example, equation 6.9 for ϕ=30° will give an adjusted friction angle of 34.7°, while equation 6.10 leads to $\phi_a=32.4^\circ$. Two additional finite element analyses were then carried out both with $c=0$ and with each of the above adjusted values for friction. Figure 6.28 present the NGRC for the crown derived from these analyses. The use of the adjusted friction angles led to better approximations of the correct NGRC, compared to the result given by the assumption of $c=0$ and $\phi=30^\circ$. Actually, the assumption of $c=0$ and ϕ_a given by equation 6.10 led to a NGRC that virtually coincided with the correct curve. Figure 6.29, on the other hand, presents the NGRC for the springline obtained through these analyses. Once more the analyses with the adjusted friction angles yield better approximations than the $c=0$ and $\phi=30^\circ$ assumption. In this case, however, it was noted that the adjustment given by equation 6.9 (constant normal stress) tends to slightly underestimate the dimensionless displacement U for a given amount of stress release. With regard to the tunnel floor, the NGRC obtained with ϕ_a given by both equations virtually coincided with the correct curve shown in Figure 6.26.

Other assumptions and adjustments of the friction angle were made and tested to conditions different than those considered herein. The best approximations to the correct response were always found using the friction angle given by equations 6.9 and 6.10. However, equation 6.9 sometimes may yield unsafe approximations of the NGRC (a stiffer response), especially for tunnels with small covers in soils with higher cohesion, where the cohesive component of

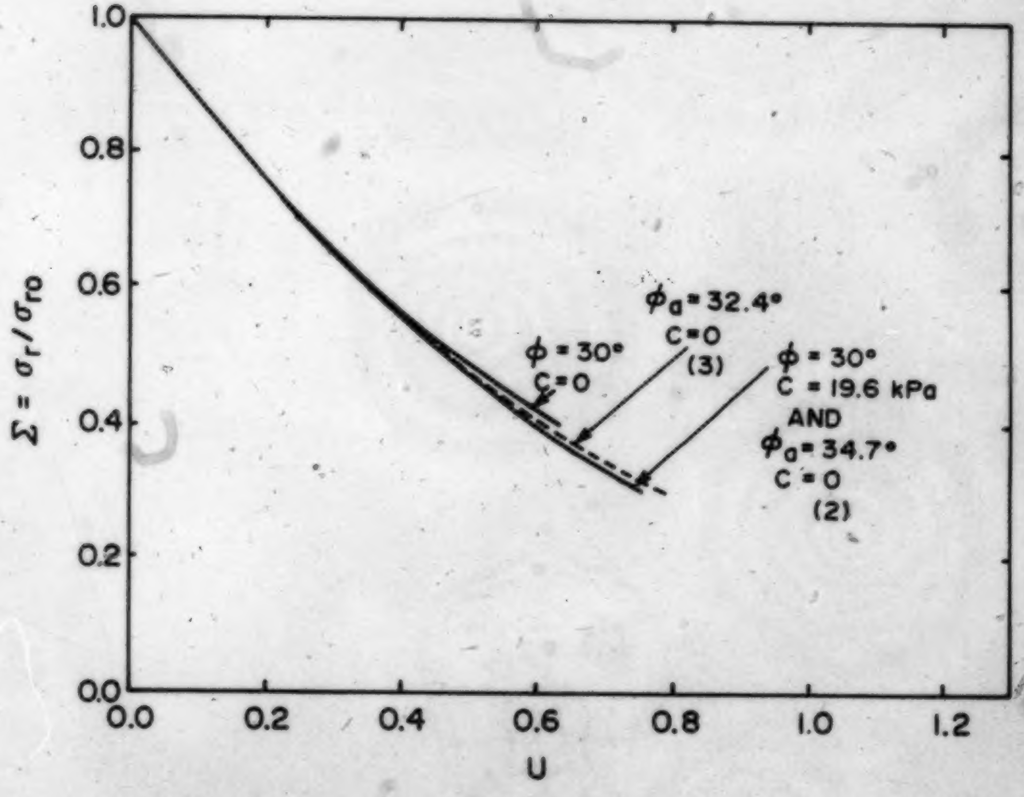

NOTES

1. $K_0 = 0.8$, $\nu = 0.4$, $n = 0$, $H/D = 3$, $D = 4m$
2. ϕ_a BY EQUATION 6.9
3. ϕ_a BY EQUATION 6.10

Figure 6.28 Normalized Ground Reaction Curves for the Crown, Calculated for Different Soil Strengths

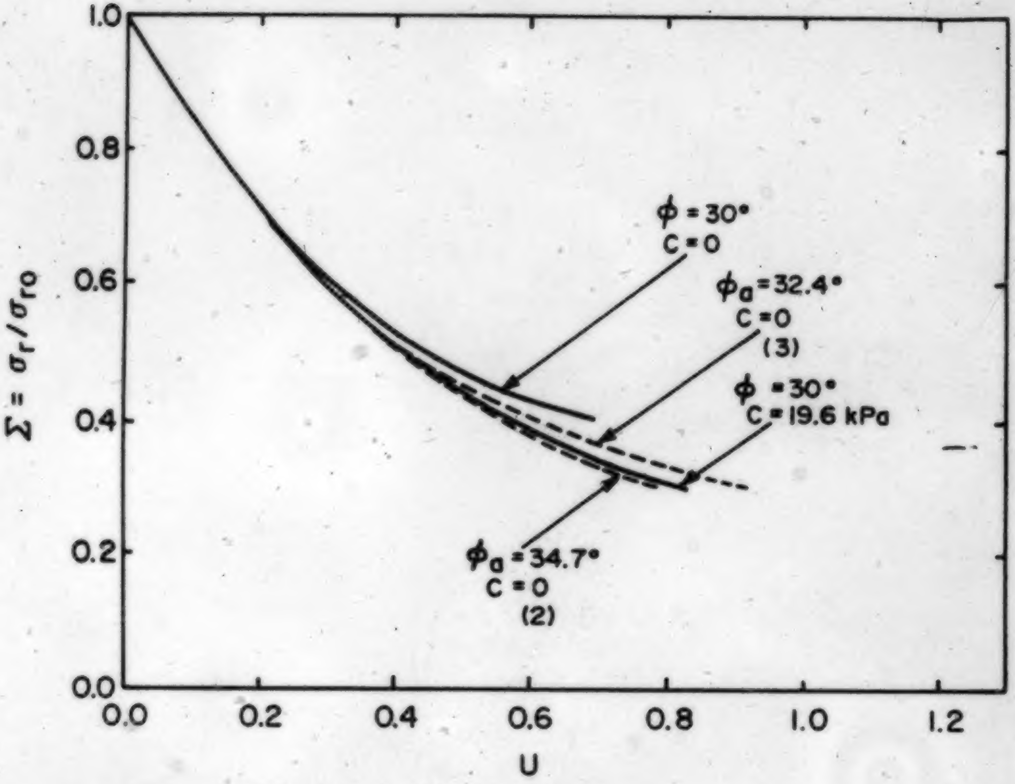

NOTES
1. $K_o = 0.8$, $\upsilon = 0.4$, $n = 0$, $H/D = 3$, $D = 4m$
2. ϕ_a BY EQUATION 6.9
3. ϕ_a BY EQUATION 6.10

Figure 6.29 Normalized Ground Reaction Curves for the Springline, Calculated for Different Soil Strengths

strength therefore dominates the response. For this reason. equation 6.10 will be favoured hereafter. In some special circumstances where the cohesive component of strength predominates, another possible assumption could be made by disregarding the soil's frictional resistance and by using the frictionless soil model. As the adjustments proposed herein are, in fact, simple approximations, each practical situation should be investigated individually and the adjustments should be selected on a case by case basis. In most cases, the approximation given by equation 6.10 with c=0 should prove sufficient.

To summarize the above discussion, Table 6.7 was prepared. It gives the variation of dimensionless displacement at the tunnel crown for the different strength assumptions made and for different amounts of stress release. The numbers between brackets are the ratios correct U for c=0 to the corresponding approximate U for c=0, calculated according to the different assumptions. They give an indication of the approximations involved in each case.

6.2.4.4 The Effect of Poisson's Ratio

As indicated by equations 6.4 and 6.8, the ground responses depend on the values of the Poisson's ratio, ν. The frictionless soil model described in Section 6.2.3 was developed for soils under fully undrained conditions. Therefore, an undrained Poisson's ratio ν_u, of 0.5 should be considered. To avoid numerical problems a ratio close to

Stress release	U at the crown 40%	 50%	 60%
c = 19.6 kPa $\phi = 30°$	0.354	0.465	0.595
(correct)	(1.000)	(1.000)	(1.000)
c = 0 $\phi = 30°$	0.363	0.484	0.635
(1st approx.)	(0.975)	(0.961)	(0.937)
c = 0 $\phi = 34.7°$	0.350	0.460	0.589
(2nd approx., eq. 6.9)	(1.011)	(1.011)	(1.011)
c = 0 $\phi = 32.4°$	0.354	0.475	0.609
(preferred approx.	(1.000)	(0.979)	(0.977)
eq. 6.10)			

Note: The ratios of correct U for c ≠ 0 to the approximate U for c = 0 are shown between brackets.

Table 6.7 Variation of the Dimensionless Crown Displacement for the Different Strength Assumptions made and for the Different Amounts of Stress Release

that value (ν_u=0.49) should be sufficient for the parametric finite element analyses to be carried out in the modelling step. On the other hand, the value of ν for the cohesionless soil model can vary typically from 0.2 to 0.4.

To assess the influence of the Poisson's ratio on the ground response to tunnelling, two finite element analyses were conducted. In both cases, an unlined circular tunnel with D=4 m and H=12 m was considered in a homogeneous soil profile, with the following properties: γ=19.6 kN/m^3, K_o=1.0, ϕ=30°, c=0, n=0,and K=400. One analysis was carried out with ν=0.2 and the other with ν=0.4. In both cases, the in situ tangent modulus of the soil was equal to 40.494 MPa. The analyses were performed with the gradual release of the ground stresses at the opening in ten increments. Local failure of soil elements at the crown, springline and floor was detected after the seventh unloading increment.

The resulting normalized ground reaction curves for the tunnel crown are represented in Figure 6.30. It is noted that for the same amount of stress reduction, ν=0.4 yields dimensionless displacements U usually larger than for ν=0.2, unless the stress release is greater than about 65%.

The normalized ground reaction curves for the springline are shown in Figure 6.31 and for the floor in Figure 6.32. Similar results are found, but the differences in the NGRC for ν=0.2 and 0.4 are less pronounced.

Figures 6.33(a) and (b) present the distributions of subsurface and surface settlements normalized to the

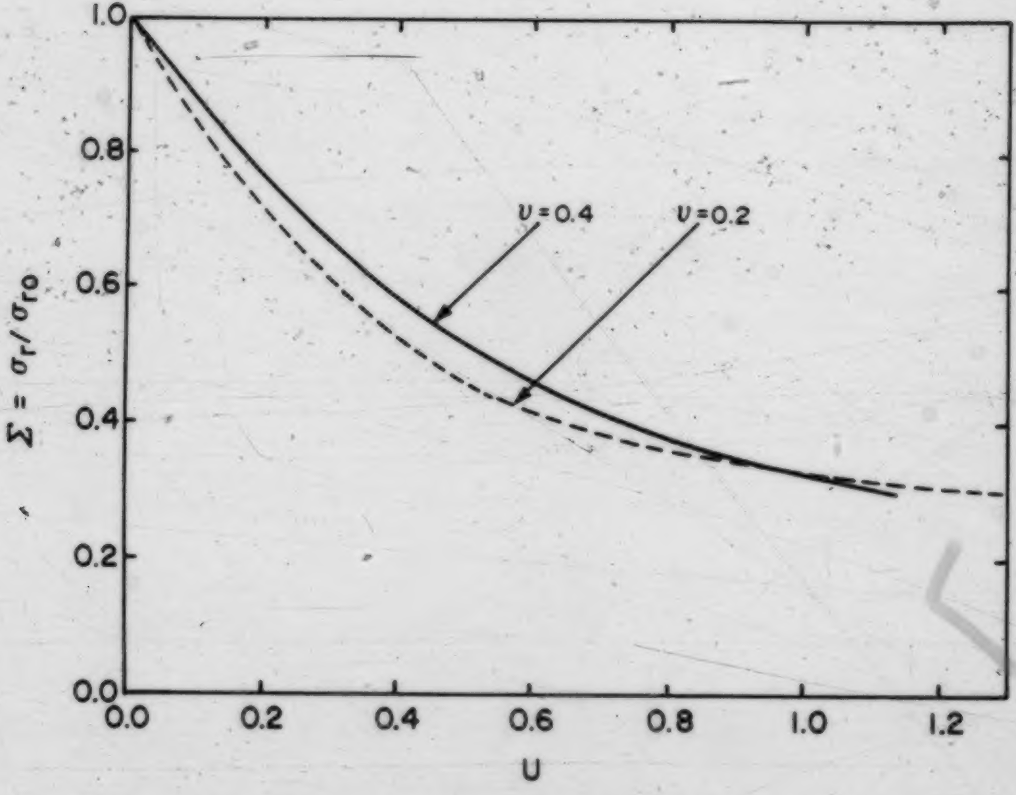

NOTE : C=0, $\phi = 30°$, $K_0 = 1.0$, n=0, H/D=3, D=4m

Figure 6.30 Normalized Ground Reaction Curves for the Crown, Calculated for Different Poisson's Ratios

corresponding crown settlement, for the two Poisson's ratios considered and for a ground stress release of 50%. Similar results are found for other amounts of stress reduction. One notes that the normalized subsurface settlement distribution is not much affected by ν and that the values for ν=0.4 are slightly larger than for ν=0.2.

The analysis with ν=0.4 yielded a maximum normalized ground surface settlement slightly larger than with ν=0.2 (Figure 6.33(b)). The difference between settlement ratios at points other than the centreline tend to increase, with increasing distance to the axis. As a result, the normalized ground distortion at the surface is greater for ν=0.2, than for ν=0.4.

With the exception of the distortion, one notes from Figures 6.30 to 6.33 that for ground stress releases varying between 30% and 65%, the ground displacements seem to increase for an increasing Poisson's ratio. This range of ground stress release can be taken as typical of that occurring before activation of linings in tunnels built under good ground control conditions. In order to reduce the number of independent dimensionless variables in Equation 6.4 and to simplify the modelling step, it was decided to select a single value for Poisson's ratio. In order to be generally on the safe side in terms of ground settlements, the higher value of Poisson's ratio (ν=0.4) will be used in the modelling step analyses. It should be remembered, however, that this simplification may result in unsafe

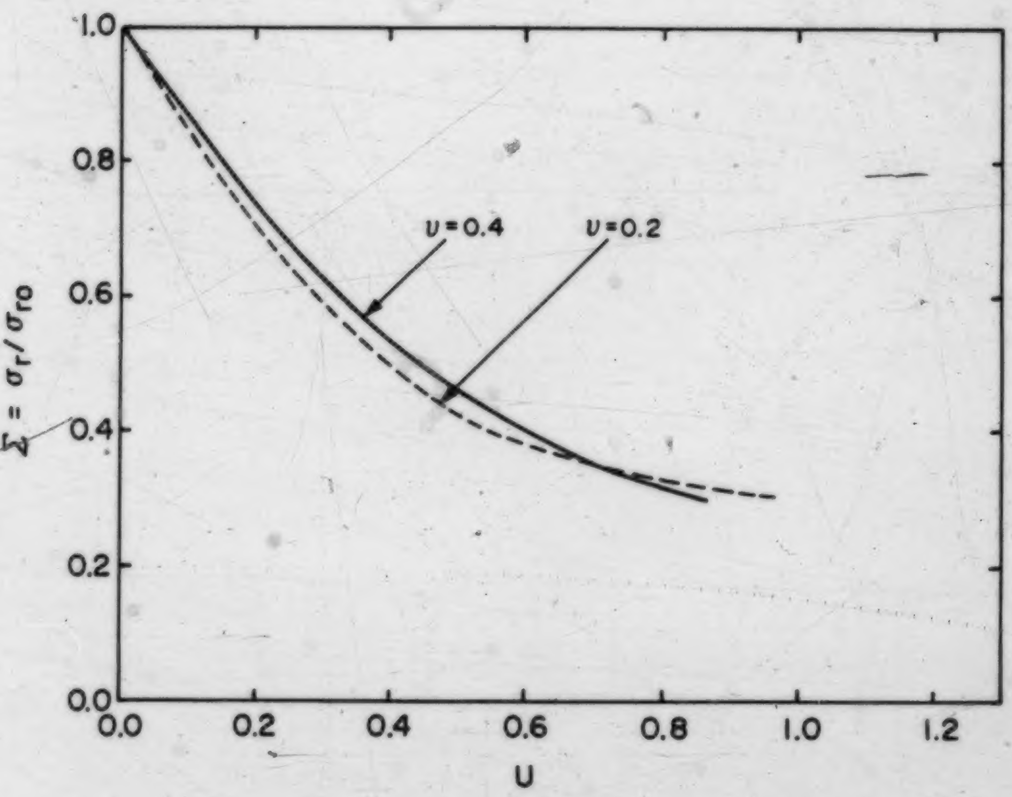

NOTE : $C = 0$, $\phi = 30°$, $K_o = 1.0$, $n = 0$, $H/D = 3$, $D = 4m$

Figure 6.31 Normalized Ground Reaction Curves for the Springline, Calculated for Different Poisson's Ratios

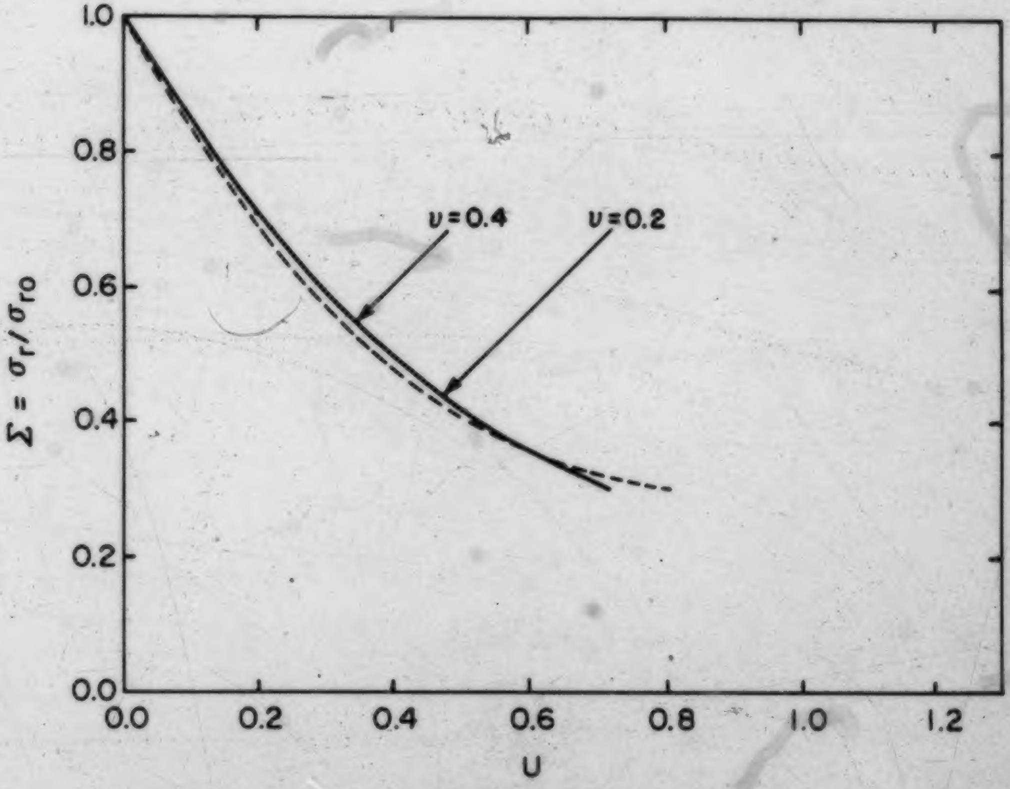

NOTE: $C=0$, $\phi=30°$, $K_0=1.0$, $n=0$, $H/D=3$, $D=4m$

Figure 6.32 Normalized Ground Reaction Curves for the Floor, Calculated for Different Poisson's Ratios

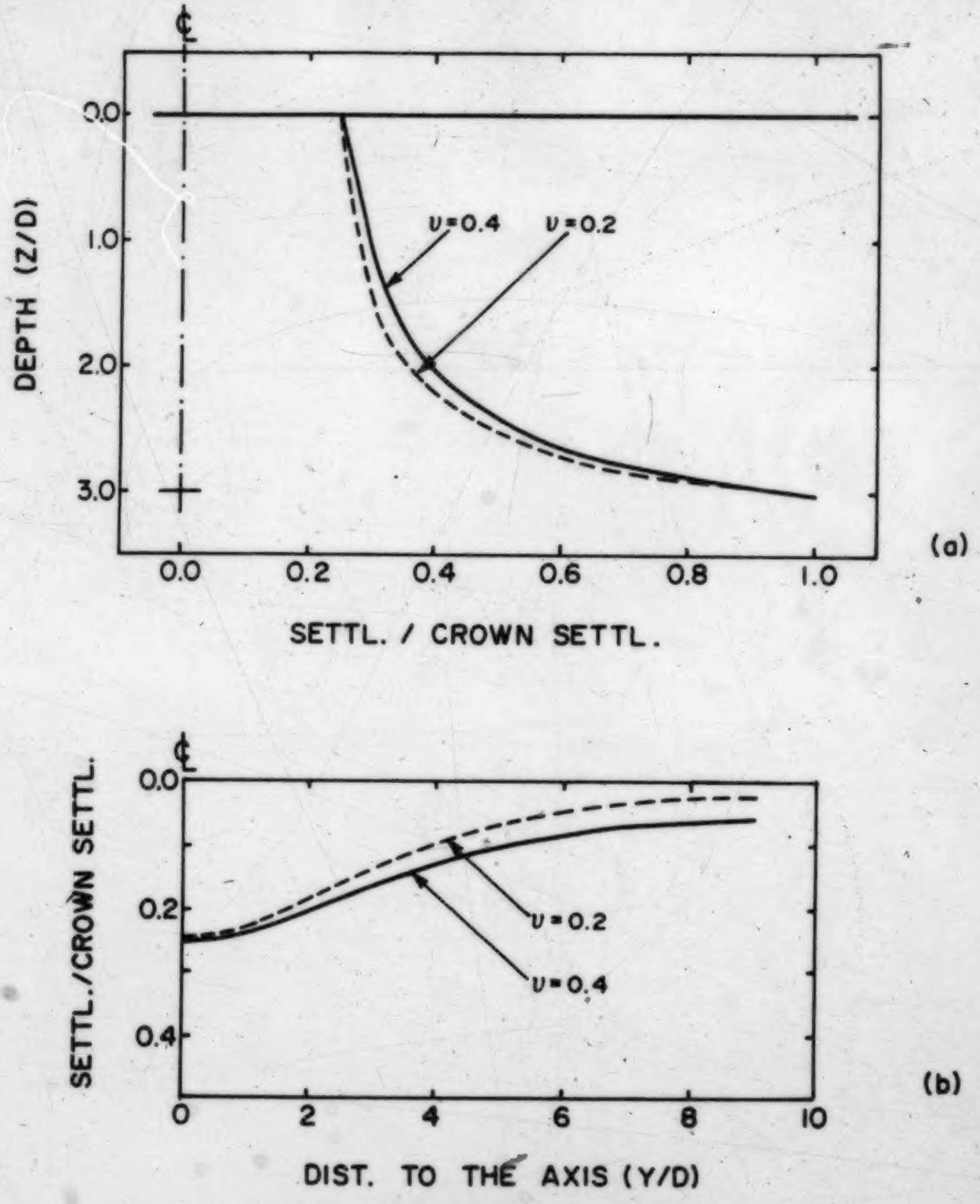

NOTE : C=0 , ϕ=30°, K_0=1.0 , n=0 , H/D=3 , D=4m

Figure 6.33 Normalized Subsurface and Surface Settlements for 50% Ground Stress Release, Calculated for Different Poisson's Ratios

estimates of the maximum normalized surface distortion. As it can be seen from Figure 6.30, this simplification may imply overestimates of the dimensionless crown displacement of 16 to 23% for stress releases between 40% and 60%.

6.2.5 Ranges of Variables for the Parametric Analyses

The simplifications introduced in the previous sections allows the normalized ground reaction curves for a shallow tunnel in a soil whose behaviour is described by the cohesionless soil model presented in Section 6.2.2, to be written as:

$$F = f\left(\theta, \frac{\sigma_r}{\sigma_{ro}}, \frac{u_r E_{ti}}{D\ \sigma_{ro}}, \frac{H}{D}, K_o, \phi_e\right) \qquad [6.11]$$

Similarly for the frictionless soil model:

$$F = f\left(\theta, \frac{\sigma_r}{\sigma_{ro}} \frac{u_r E_{ti}}{D\sigma_{ro}}, \frac{H}{D}, \frac{c_{ue}}{\gamma D}\right) \qquad [6.12]$$

The above equations, in these general forms, will be useful for the definition of the ranges of variables to be considered in the parametric numerical analyses. These ranges should be selected in order to cover the most common situations found in practice. To identify the latter, the data gathered in Tables 5.31 to 5.33 may be of some help. Data from some 53 case histories were included there. However, they may not be entirely representative of all practical situations to be encountered in practice for at least three reasons. The first refers to the fact that they include a fairly large number of tunnels built in certain locations, such as Frankfurt, London, Sao Paulo and Washington. This will have an effect on the conclusions drawn, since they will tend to be more representative of the conditions found at those locations. Secondly, the survey was conducted for a different purpose than the present one. It covered only case histories where substantial subsurface instrumentation data were available. Although this kind of instrumentation is fairly common in practice, it tends to be used only in relatively important projects. Therefore, the cases reviewed are typically large diameter tunnels, mainly for subway systems and only a few cases of smaller size tunnels, like those for sewerage or drainage, were analysed. Thirdly, the survey refers to tunnels that were predominantly built under good ground control conditions, which are normally found in good quality construction practices and in favourable grounds. Usually the cases did not entail ground collapses or pronounced time dependent responses. This is reflected in the review by the inclusion of a large number of tunnels driven through stiffer clays and only a few in softer clays or in other less stable grounds.

With these aspects in mind, the data contained in Tables 5.31 and 5.32 may be interpreted accordingly. Figure 6.34 presents the frequency distributions of the geometric variables. The majority of the cases reviewed had excavation diameters ranging between 5 and 7 m and soil cover between 10 and 14 m. Most frequently the ratio H/D varied between 1 and 2. It was shown, for both soil models proposed, that the NGRC does not depend on the size of the opening. Therefore, an arbitrary value of D, equal to 4 m, was selected and kept constant in the parametric analyses. The geometric variable to be considered is simply the H/D ratio. Three ratios of H/D were selected: 1.5, 3 and 6. These values cover most of the cases reviewed as noted in Figure 6.34.

Figure 6.35 shows the distributions of soil properties encountered in the case histories reviewed. As explained in Section 5.3.6.1, these properties represent average values for the ground around the tunnel profile. The E_{ti} values indicated represent drained as well as undrained moduli, depending on the type of ground response that was anticipated at each particular case history. This is explained in Section 5.3.6.1 and shown in Tables 5.31 and 5.32. The zero friction angle cases correspond to those tunnels driven through saturated clayey soils, where an undrained ground response may have developed. The non-zero friction angles correspond to cases classified as showing drained behaviour. The undrained cohesion values, of course, refer to those cases where the ground response was defined as undrained. About 28% of all tunnel cases reviewed were grouped in the undrained category.

As explained in previous sections in this chapter, particularly Section 6.2.4.1, the normalized ground response is independent of E_{ti} or of the Janbu's modulus K. Thus in the parametric analyses for the modelling step, it will be sufficient to arbitrarily choose any value of K. A constant K value equal to 400 has been therefore selected.

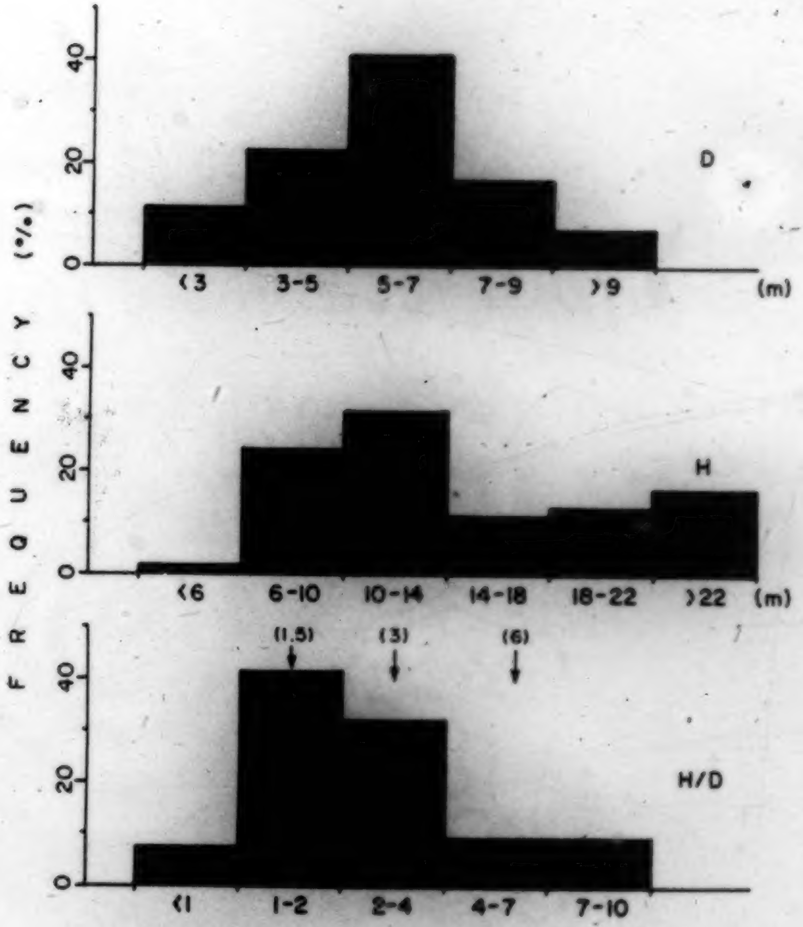

NOTES:
1. FREQUENCY FOR 53 CASES.
2. H/D SELECTED FOR THE PARAMETRIC ANALYSES, SHOWN IN BRACKETS.

Figure 6.34 Distributions of Sizes and Depths of Tunnels Reviewed

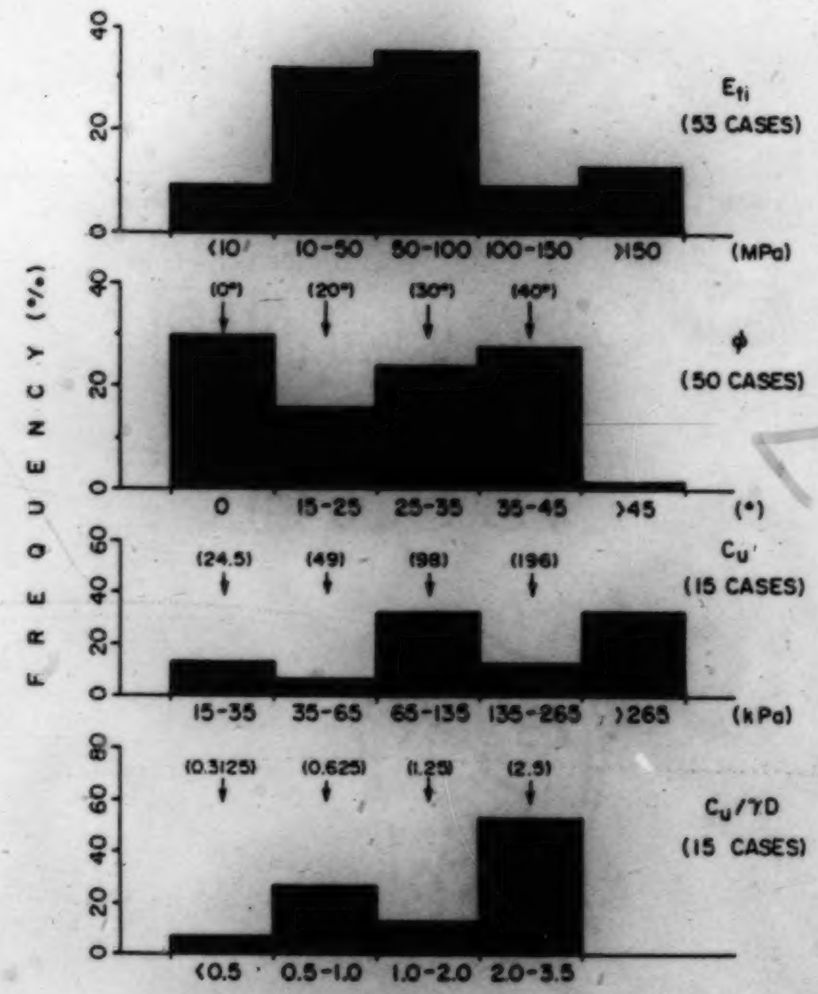

NOTE : STRENGTH PROPERTIES SELECTED AS INPUT FOR THE PARAMETRIC ANALYSES, SHOWN IN BRACKETS.

Figure 6.35 Distributions of Geotechnical Properties of the Grounds Through Which the Tunnels Reviewed were Driven

The friction angles found in the surveyed case histories varied considerably. Appropriately four values for ϕ were selected: zero (for the frictionless, undrained soil model), 20°, 30° and 40^0. These values almost entirely cover the ranges of friction angles likely to be encountered in practice, as indicated in Figure 6.34.

Four values of the undrained cohesion, c_u, were selected, covering almost the full range of c_u found in the survey (c_u=24.5 kPa, 49 kPa, 98 kPa and 196 kPa). More importantly, the undrained strength ratio, $c_u/\gamma D$, entirely covers the corresponding range found in the reviewed cases. Note that, as explained in Section 6.2.2, the normalized ground response does not depend on the unit weight of the soil. Thus a single and constant γ value equal to 19.6 kN/m³ was selected and used in the parametric analyses.

Figure 6.36 shows the distribution of the in situ stress ratio, defined in terms of either total or effective stresses. Three values for in situ stress ratio have been selected for the parametric analyses: 0.6, 0.8 and 1.0. These values, as shown in the figure, typically cover more than 75% of the cases reviewed. Moreover, it was noted that the average in situ stress ratio for the undrained cases is close to unity, in support of the assumption made for the frictionless soil model set up in Section 6.2.3.

For completeness, Figure 6.37 was prepared in order to show the distribution of the construction methods used in the tunnels reviewed. It also includes the distance from the

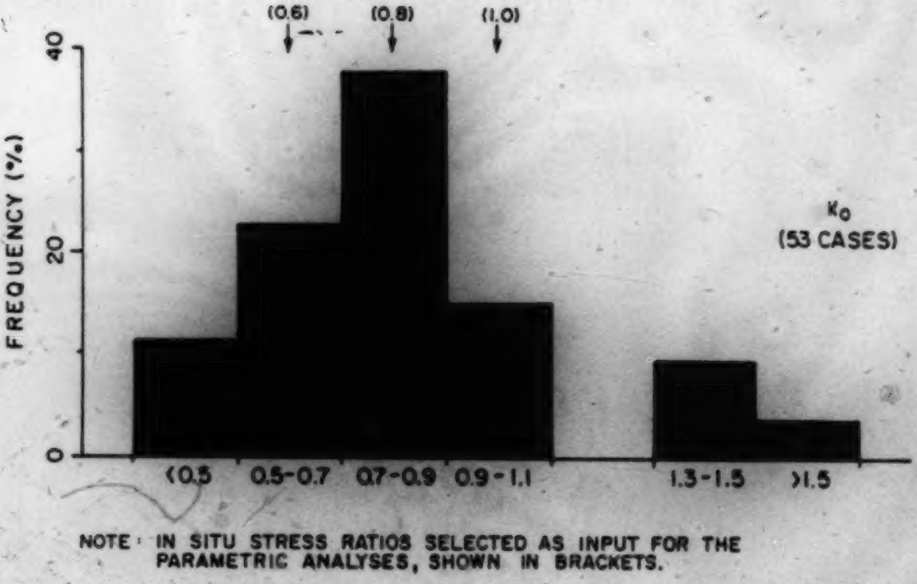

Figure 6.36 Distribution of the In Situ Stress Ratios in the Case Histories Reviewed

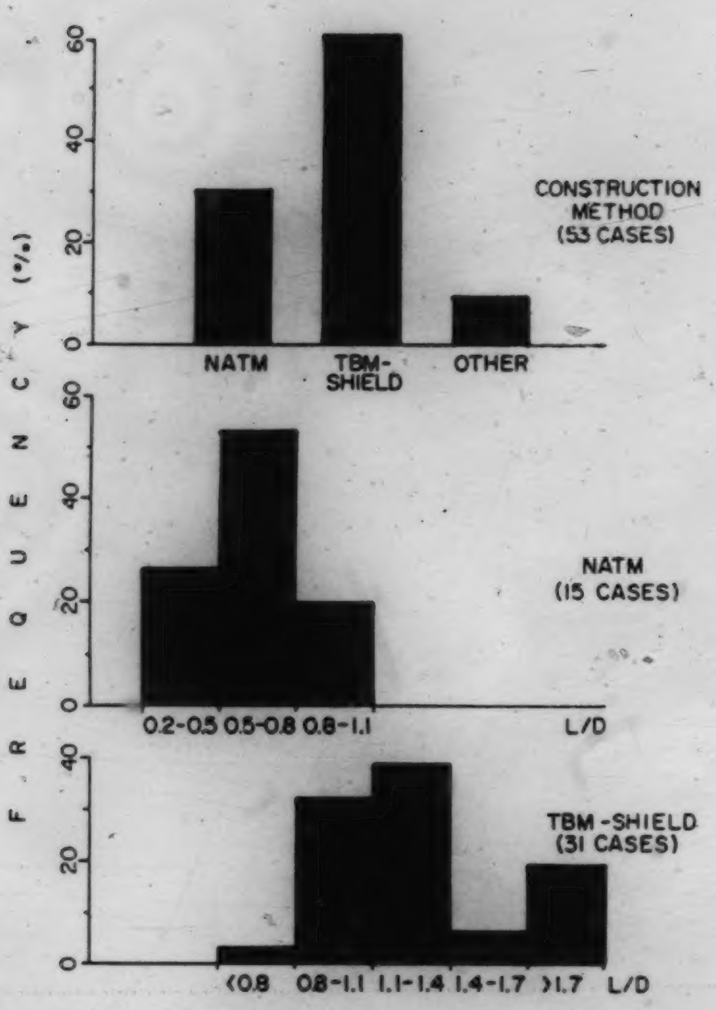

Figure 6.37 Distribution of Construction Methods and Distance of Support Activation in the Tunnels Surveyed

face at which the support was activated. One notes that while in the NATM cases, the lining is frequently closed at 0.5 to 0.8D behind the face, in TBM-shielded constructions the support is applied usually at 1.1 to 1.4D.

In summary, Table 6.8 lists the variables selected for the parametric analyses for both soil models. For the cohesionless soil model, 27 analyses were performed combining the parameters shown in the table. For the frictionless soil model, 10 analyses were conducted. The smallest undrained ratio $c_u/\gamma D$, was used only in connection with the smallest H/D case. These 37 parametric analyses were supplemented by some additional calculations which are described later on.

6.3 Parametric Analyses

6.3.1 Details of the Analyses

6.3.1.1 Number of Unloading Increments

All two dimensional finite element analyses were performed as described in Chapter 5 with full ground stress release in a single phase and with no lining installed. The number of steps adopted for the incremental unloading was defined after a number of trial runs, where different numbers of increments were tested, for different geometries and soil properties. To illustrate the influence of this factor, Figure 6.38 was prepared. It shows the NGRC for the

Cohesionless soil model

H/D	1.5	3.0	6.0
ϕ(°)	20	30	40
K_0	0.6	0.8	1.0
c (kPa)	0		
n	0		
K	400		
γ (kN/m^3)	19.6		
ν	0.4		
D (m)	4.0		
R_f	1.0		

Frictionless soil model

H/D	1.5	3.0	6.0	
C_u (kPa)	(24.5)	49	98	196
$C_u/\gamma D$	(0.3125)	0.625	1.25	2.5
K_0	1.0			
ϕ(°)	0			
n	0			
K	400			
γ (kN/m^3)	19.6			
ν	0.49			
D (m)	4.0			
R_f	1.0			

Table 6.8 Selected Variables for the Parametric Finite Element Analyses

tunnel springline for the case with H/D=3, ϕ=30° and K_o=1.0. The results of the two analyses are shown, one using ten constant increments to release the in situ stresses and another using twenty. In both cases, after 70% of the stress release, some elements at the crown, springline and floor failed and the numerical results thereafter were discarded.

It is noted that by increasing the number of steps, the ground response gets 'softer', with larger displacements being calculated for the same amount of stress release, as would be expected in an incremental solution of this kind. Unfortunately, the exact solution is not available for an assessment of the errors involved. A decision had to be made, therefore, balancing both technical and cost aspects.

Figure 6.39 furnishes the percentage by which the dimensionless displacement U at the tunnel contour calculated for 20 increments exceeds U calculated for 10 increments. For up to 60% of the stress release, the differences in U are typically less than 6%. However, as local failure is approached, that difference increases substantially. However, the differences in the calculated grounds settlement normalized to the crown settlement are appreciably smaller. Figures 6.40 (a) and (b) provide the differences in the normalized settlements along the depth of the cover and at the ground surface for a stress release of 50%. Although the absolute settlements for 10 increments are typically 4% smaller than that calculated for 20 increments, the normalized settlements for 10 increments are always

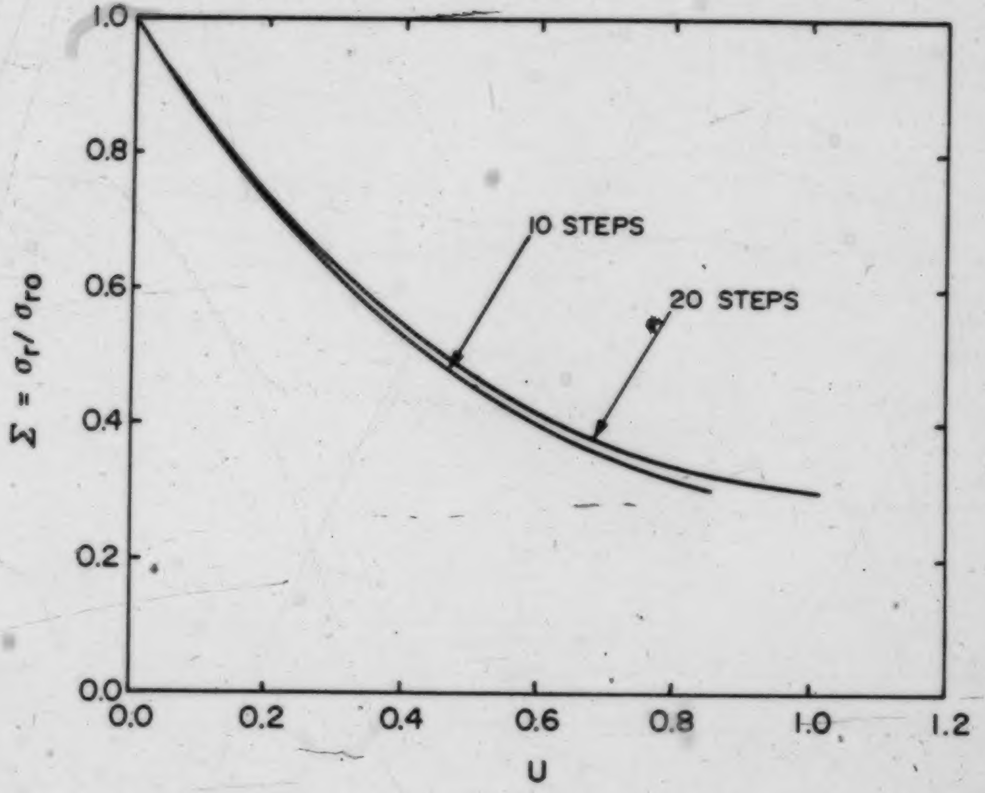

Figure 6.38 Normalized Ground Reaction Curve for the Springline Calculated for Different Numbers of Unloading Increments

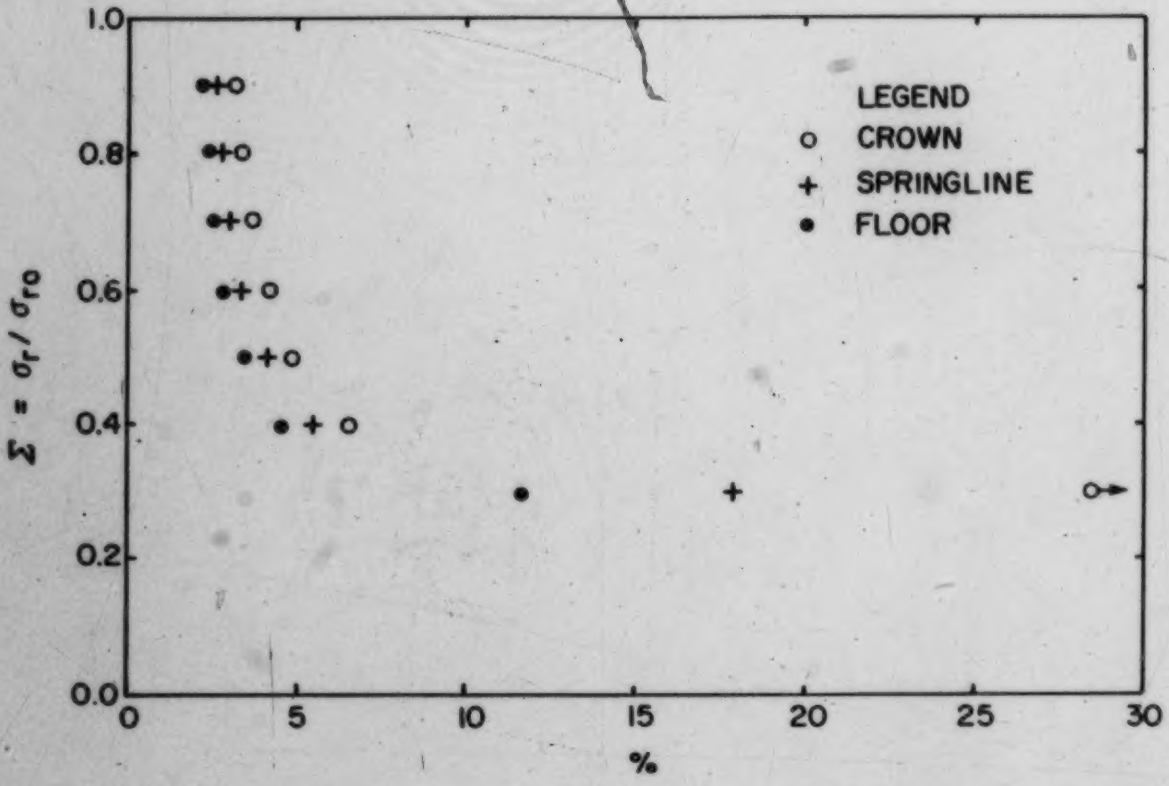

Figure 6.39 Difference in the Calculated Dimensionless Displacement U for Ten and Twenty Unloading Increments

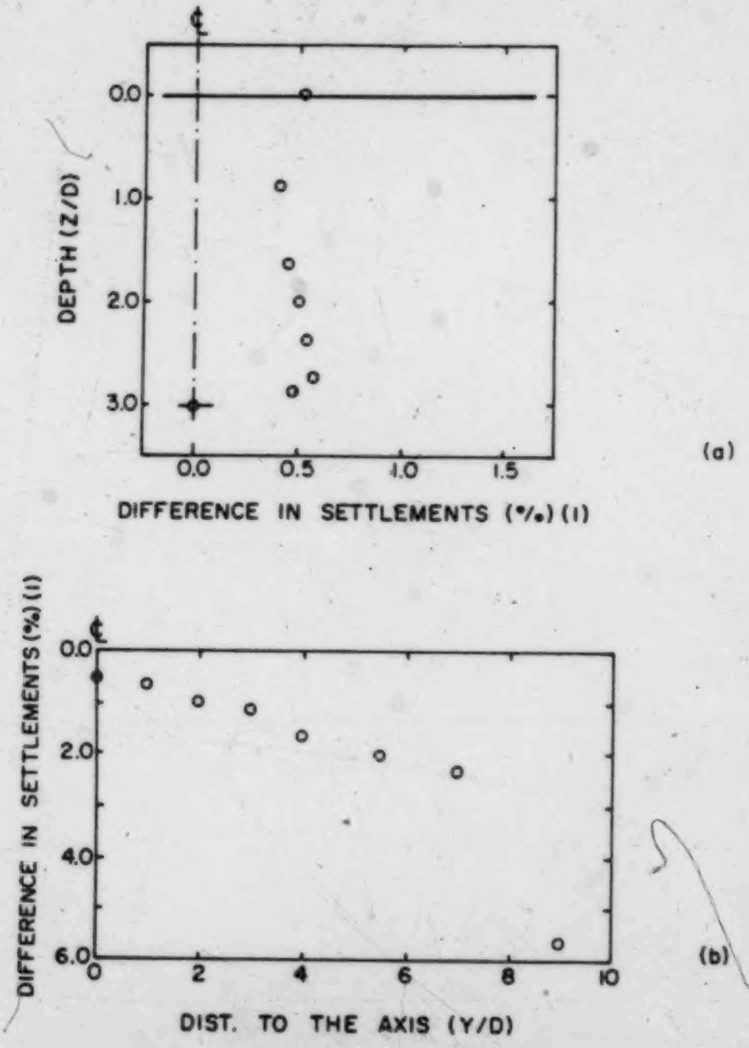

NOTE : DIFFERENCE IN SETTLEMENTS DEFINED AS : $\{[\delta/\delta_c\ (N=10)] - [\delta/\delta_c\ (N=20)]\} \ / \ [\delta/\delta_c\ (N=20)]$ WITH N = NUMBER OF INCREMENTS, δ = SETTLEMENT, δ_c = CROWN SETTLEMENT.

Figure 6.40 Differences in the Normalized Ground Settlements for Stress Release of 50%, Calculated for Ten and Twenty Unloading Increments

larger than for 20 increments. The subsurface normalized settlements for 10 steps exceed those for 20 steps by about 0.5%, as indicated in Figure 6.40(a). For the ground surface settlements, the difference is a minimum at the centreline and it increases with the distance to the axis, never exceeding 6% in this case.

Bearing in mind the other approximations introduced earlier and considering that the cost[14] of the analysis is directly related to the number of steps used, the 10 increment option was favoured and adopted. It should be remembered that the back analyses of case histories presented in Section 5.2.4 were all performed with five unloading increments for each construction phase, thus amounting to 10 increments altogether. Fairly reasonable results were obtained. The parametric analyses in 10 steps would thus roughly approximate the conditions met in the back analyses[15].

Regardless of the number of steps used, the incremental analysis will always yield an NGRC which will lie on the unsafe side where less displacement occurs for a given stress release. This error might be compensated for by other assumptions which led to conservative estimates of the NGRC (for instance, the c=0 and ν=0.4 assumptions), but this compensation cannot be assured. Some correction may possibly be introduced by considering a reduced soil strength.

---

[14] The unit cost of a 20 step computer run was about $45.00, at the low system rate. This was for a run involving 90 seconds of CPU time and 400 page-minute of CPU storage of virtual memory integral, at the U.of A. computer scheme, at 1984 costs. The ten increments run cost was about half that figure (Post-processing costs not included).

[15] Tan (1977:181) conducted similar non-linear analyses, also using a hyperbolic stress-strain model, and found it adequate to simulate the tunnel construction of a particular case history and to run parametric analyses using eight load increments.

6.3.1.2 Mesh Design and Influence of the Lower Boundary

The finite element mesh used in the parametric analyses was designed in accordance to the guidelines presented in Section 5.2.1.1 and as described in Section 5.2.2.1. A standard mesh, quite similar to that shown in Figures 5.12(a) to (c), was used. Layers of elements above the tunnel were removed or added according to the particular geometry of the problem being studied.

A major inconvenience resulted in adopting the constitutive soil models developed in Sections 6.2.2 and 6.2.3. This refers to the constant initial tangent modulus profile. While it provided potential generality to the projected solution, by ensuring similarity conditions not found otherwise, it made the calculated soil response to the tunnelling simulation sensitive to the position of the lower boundary of the finite element mesh. The influence of the position of this boundary on the surface settlements, calculated through a linear elastic soil model, was pointed out by Oteo and Sagesta (1982:654). When a non-linear elastic model is used, this influence is less pronounced but still discernible (see for instance, Tan, 1977:81). This is particularly true when the initial tangent modulus is constant with depth. All back-analyses of the case histories presented in Section 5.2.4 took into account the increase of the soil stiffness with depth. As explained in Section 5.2.1.1, for this condition, the position of the lower boundary does not have much effect on the results of the analysis.

To illustrate this aspect, some typical numerical results will be presented herein. They refer to finite element analyses carried out in ten unloading increments for the following conditions: $H/D=1.5$, $K_o=0.6$, $\phi=40°$, $c=0$, $n=0$, $K=400$ and $D=4$ m. In these analyses, the position of the lower boundary, where the nodal displacements were set equal to zero (rigid boundary), was varied. The vertical distance, V, between the tunnel floor and the rigid boundary was made equal to four distinct values: 0.5 D, 1.5D, 3D and 6.125D. In all cases, some elements at the springline failed after the ground stresses were released by 70%. The results after this event were disregarded. Figure 6.41 shows the NGRC of the tunnel crown, obtained through the gradual unloading of the unlined opening. As it is observed, as the rigid base is moved towards the tunnel floor (V/D decreasing), the crown response becomes "softer" and larger U values are obtained for the same amount of stress release. This behaviour does not reflect any "softening" mechanism of the tunnel cover. Rather, by reducing the thickness of the soil underlying the tunnel, the overall ground heave associated with the reduction of the ground stresses at the opening is reduced. The mechanism involved in the developement of such a heave

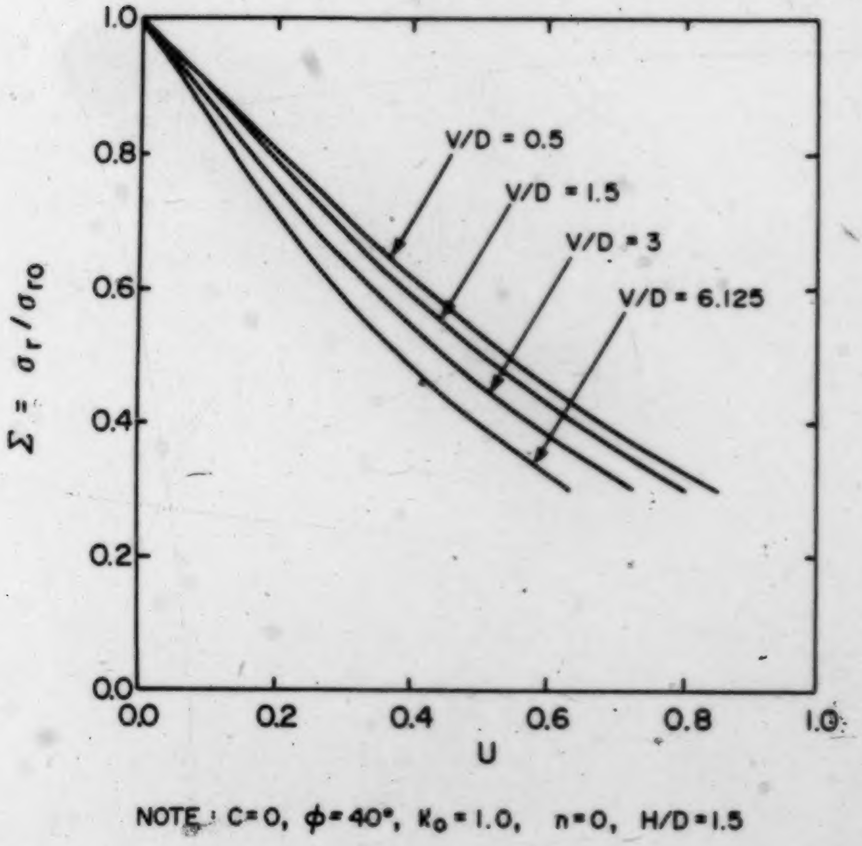

Figure 6.41 Normalized Ground Reaction Curves for the Crown, Calculated for Different Positions of the Lower Rigid Boundary

was discussed in Chapter 2, where it was explained to be a consequence of the gravitational stress gradient which is always active in a shallow tunnel. This heave is one of the components of the ground displacement. Thus, points above the tunnel which otherwise would move downwards as a result of the tunnel excavation, may show reduced net settlements. An infinitely thick layer of soil below the invert would theoretically lead to infinite upwards movement in the ground. Accordingly, by increasing V/D, the net settlement at the crown decreases.

By applying the same reasoning to the tunnel springline, one would conclude that its NGRC should not be much sensitive to V/D. Figure 6.42 does in fact demonstrate this: for all practical purposes the NGRC's do not change much for changes in V/D. A minor trend towards a "stiffer" response at this point is noted as the rigid base gets closer to the tunnel.

The strongest effect of the position of the lower boundary is noted, of course, at the tunnel floor. Figure 6.43 shows that as V/D decreases, the floor reaction gets "stiffer" and smaller invert heaves are noted for a given stress reduction.

The effect of the overall ground heave in partly compensating for the trend of the ground cover to settle is better illustrated in Figure 6.44. It shows the distinction between the normalized settlements of the ground cover along the tunnel axis, for a ground stress release of 50%. Note

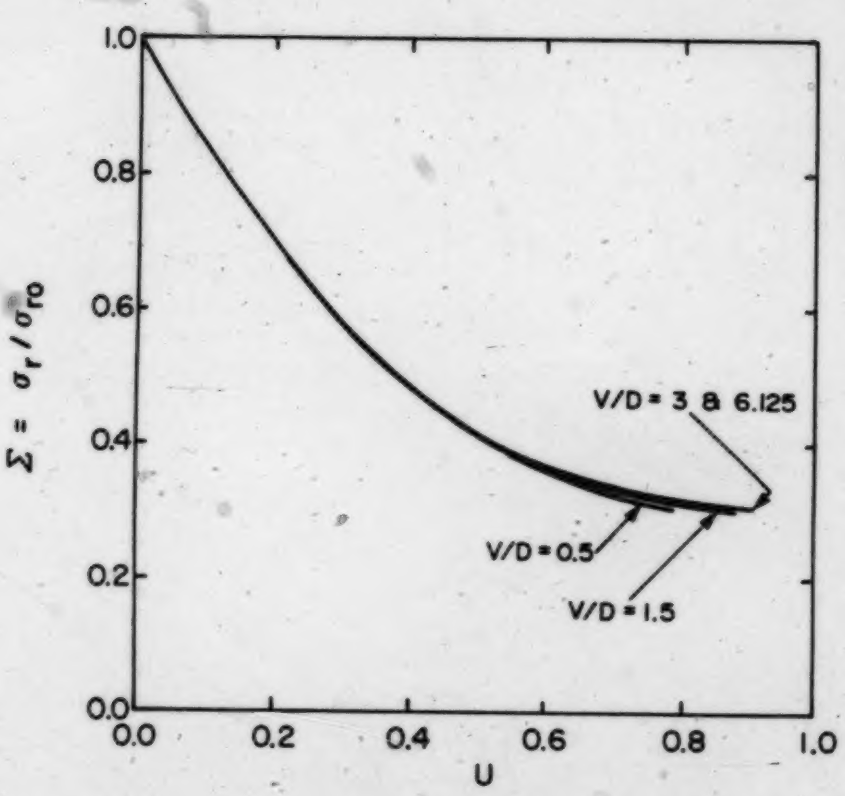

NOTE : C = 0, ϕ = 40°, K_o = 1.0, n = 0, H/D = 1.5

Figure 6.42 Normalized Ground Reaction Curves for Springline, Calculated for Different Positions of the Lower Rigid Boundary

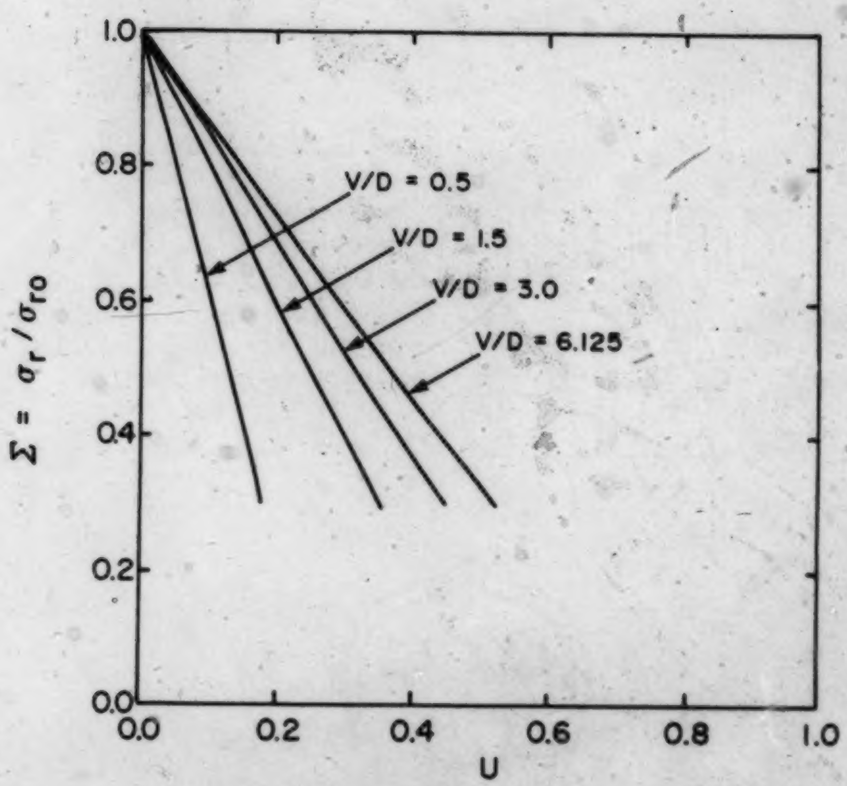

NOTE : C=0, ϕ=40°, K_0=1.0, n=0, H/D=1.5

Figure 6.43 Normalized Ground Reaction Curves for Floor, Calculated for Different Positions of the Lower Rigid Boundary

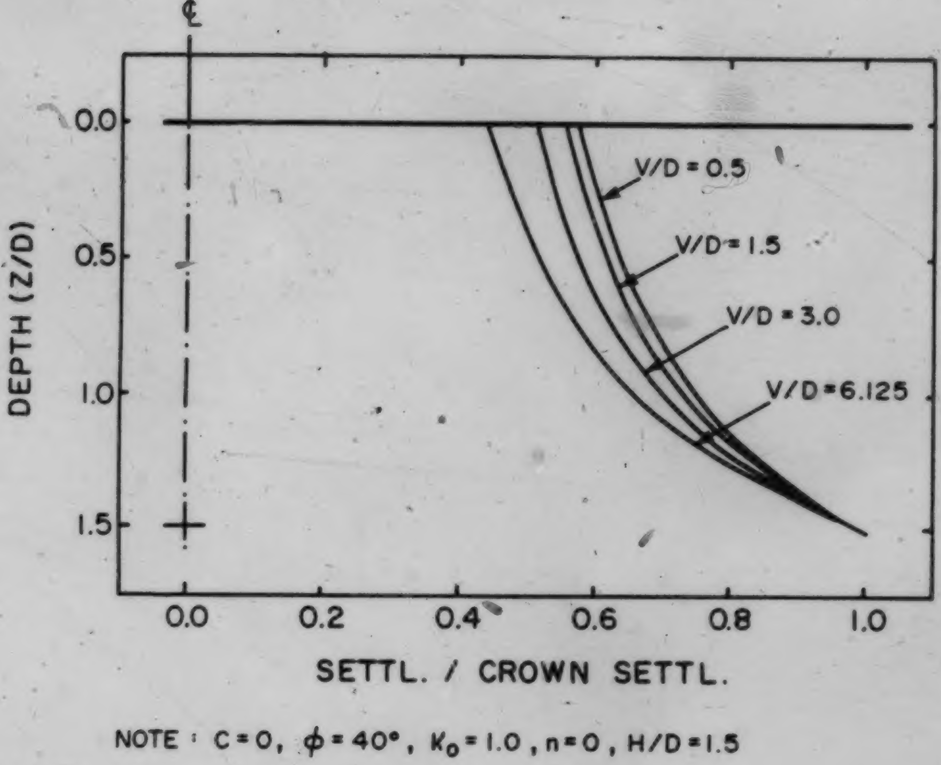

Figure 6.44 Distribution of Subsurface Normalized Settlements for 50% Ground Stress Release, Calculated for Different Positions of the Lower Rigid Boundary

that as before, the settlements were normalized to the corresponding crown settlement which leads to a settlement ratio of one at the crown. If the settlements are not normalized, as shown in Figure 6.45, the ground heave effect is perhaps clearer. The upward displacement components seem to act uniformly with depth in the cover along the tunnel axis, as the settlement difference at the crown and surface remains almost constant with V/D increasing.

Figure 6.46 presents the transverse profiles of the normalized ground surface settlements for a stress release of 50%, calculated for different V/D. The maximum normalized surface distortion does not appear to be affected much by V/D. However, the variation in V/D exerts considerable influence on the maximum normalized settlement and on the overall distribution of these settlements. The ground heave component does not seem to act uniformly over the ground surface and the resulting net distribution of settlements may depart considerably from the usual trough shaped profile. For certain conditions, the net surface movement beomes a heave, and again this is a very unrealistic result.

Other unrealistic results become evident as V/D increases. If it is remembered that in the present case where H/D=1.5, the ratio of radial in situ stresses at the tunnel floor and crown is equal to 5/3, an equal crown and floor displacement will be obtained when the ratio of dimensionless crown and floor displacements is also 5/3. It follows that by comparing Figures 6.41 and 6.43, one

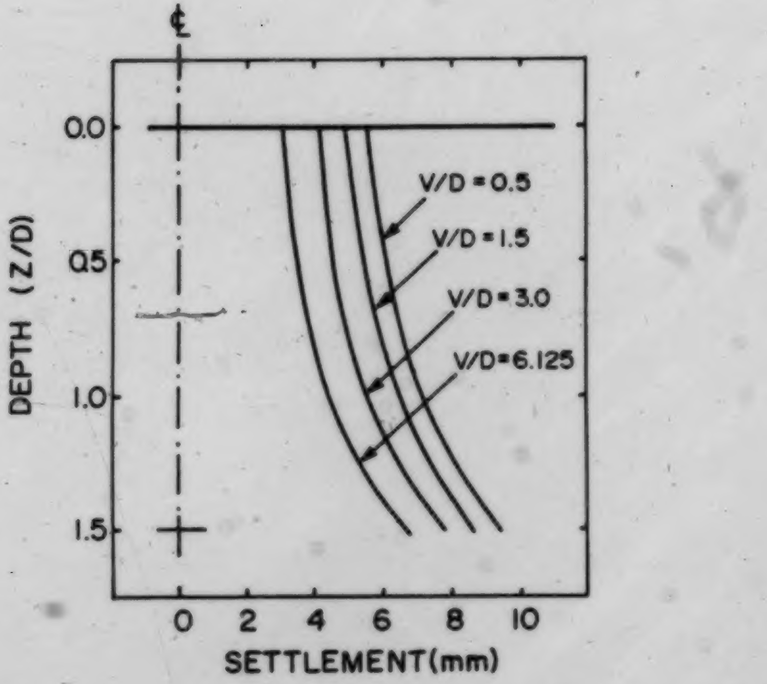

NOTE: C=0, ϕ=40°, K_0=1.0, n=0, k=400, H/D=1.5, D=4m

Figure 6.45 Subsurface Settlement Distribution for 50% Ground Stress Release, Calculated for Different Positions of the Lower Rigid Boundary

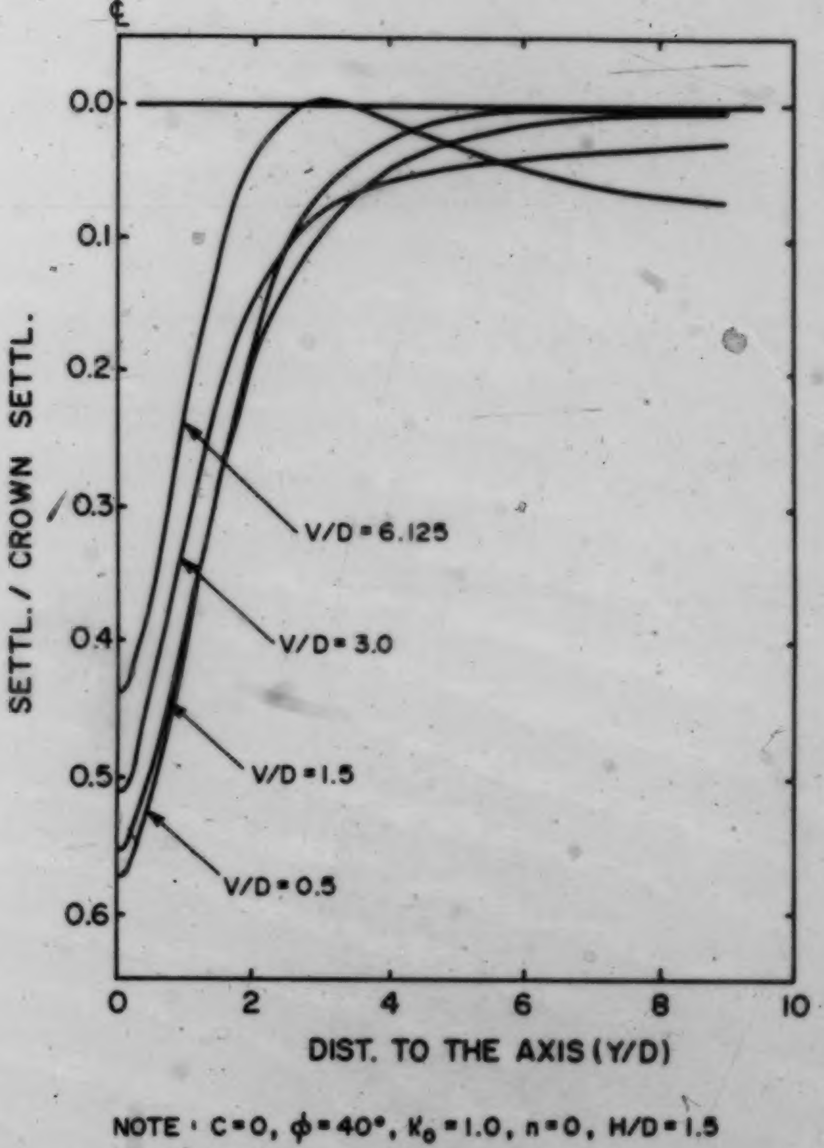

Figure 6.46 Transverse Profiles of Normalized Ground Surface Settlements for 50% Stress Release, Calculated for Different Positions of the Lower Rigid Boundary

concludes that for V/D equal to or greater than 3, the radial displacements at the floor are larger than that at the crown. This is also a result that is not substantiated in reality. To support this, Table 6.9 was prepared. It gives indications of final movements measured below the floor elevation in actual tunnels and in tunnel model tests. Unfortunately, it is not common practice to observe ground displacements in that region. Nevertheless, it is noted that the ratio of floor to crown displacements (u_f/u_c) is seldom greater than 0.5, and in particular, ratios exceeding 1.0 have never been recorded.

Table 6.9 also includes the location of points below the tunnel where no vertical movements were observed. The position of these points is given by y_o, the horizontal distance between the measuring point and the tunnel axis, and by z_o, the depth of this point below floor elevation. From this, one notes that ground movements were never observed at distances greater than 1.4D below the tunnel floor. Normally, the zero heave condition is noted at depths smaller than 1.0D below the floor.

From what has been discussed so far, one may conclude that by fixing the lower rigid base at distances greater than about 3D below the tunnel, unrealistic ground responses may result. These appear as excessive heave below the floor, and unlikely displacement fields above the crown. One would be thus tempted to reduce this distance to a minumum, and expect safer estimates of the ground movements above the

No.	Tunnel	Reference	D (m)	H/D	u_c (mm)	u_f/u_c	$y_0^{(1)}$ (m)	$z_0^{(2)}$ (m)	z_0/D	Notes
1	Frankfurt L82	Bren (1981)	10	1.10	8.4	-	6.1	>1.8	>0.18	
2	Butterberg-Osterode	Meister and Wallner (1977)	11.5	1.27	$27.3^{(3)}$	-	7.5	1.9	0.17	
3	Regent Park (Sth B)	Barrat and Tyler (1976)	4.15	7.71	$25.2^{(3)}$	-	3.8	$5.8^{(4)}$	1.4	1st tunnel
4	Regent Park (Nth B)	Barrat and Tyler (1976)	4.15	4.29	$29.6^{(3)}$	-	4.0	$5.8^{(4)}$	1.4	2nd tunnel
5	Heathrow Cargo	Muir Wood and Gibb (1971)	10.9	0.67	$15.6^{(3)}$	$0.3^{(4)}$	0	$1.0^{(4)}$	0.1	
6	New Cross	Boden and McCaul (1974)	4.12	1.94	$29.1^{(3)}$	-	0	$4.0^{(4)}$	1	
7	Chinnor	McCaul et al (1976)	5.0	1.14	$26.0^{(3)}$	-	0	$5.0^{(4)}$	1	
8	Edmonton Experimental	Eisenstein et al (1981)	2.56	10.0	$56.3^{(3)}$	$0.4^{(4)}$	0	$2.5^{(4)}$	1	
9	Edmonton SLRT (5th)	Branco (1981)	6.17	1.44	$39.4^{(3)}$	-	4.3	3.2	0.3	
10	S. Paulo ABV-MATH CC1	Negro and Eisenstein (1981)	4.04	1.54	8.0	0.0	0	4.2	1.04	
11	S. Paulo Horseshoe	Negro and Eisenstein (1981)	3.99	1.60	$17.7^{(3)}$	0.2	0	4.4	1.1	
12	S. Paulo - ARMCO	Negro and Eisenstein (1981)	3.66	1.50	20	≥0.15	0	2.8	0.77	
13	Thunder Bay II	Palmer and Belshaw (1980)	2.47	4.0	105	-	0	2.5	1	
14	Mulheim/Ruhr	Elmer (1980)	~9	1.2	26	-	6	≥4	≥0.44	Bentonite Shield in sand
15	Acton Grange (Sect. A)	Ryley et al (1980)	2.87	1.59	-	-	2	1.4	0.48	
16	Newcastle Sewer (BHJ)	McCaul et al (1983)	3.49	3.20	-	-	2.5	3.3	0.96	
17	Static Model Test (TH1)	Casarin (1977)	0.038	1.20	6.5	0.30	0	0.015	0.4	Lining at X/D = 0.11
18	Static Model Test (TH3)	Casarin (1977)	0.038	1.28	1.5	0.4	0	0.015	0.4	Lining at X/D = 0.41
19	Static Model Test (No.3)	Cording et al (1976)	0.151	2.36	5.6	0.1	0	0.15	1	
20	Centrifuge Model Test (2BP)	Mair (1979)	0.060	1.60	7.0	0.14	0	0.06	1	LF=1
21	Centrifuge Model Test (2DV)	Mair (1979)	0.060	3.10	8.0	0.13	0	0.03	0.5	LF=1
22	Static Model Test (DC)	Seneviratne (1979)	0.060	0.95	1.5	0.27	0	0.03	0.5	LF=0.6
23	Munich U 519 87 MQ1	Baumann et al (1985)	6.95	3.2	-	-	0	6.0	0.86	Sliding micrometer
24	Munich U 519 86 MQ21	Amstad and Kovari (1984)	10.09	1.6	-	-	0	10.80	1.07	Sliding micrometer

Notes:
(1) Distance to the axis of point below tunnel floor where no ground movement was observed.
(2) Difference between floor elevation and elevation of point where no movement was observed.
(3) Extrapolated displacement to tunnel contour as indicated in Table 5.31.
(4) Estimated from displacement field around tunnel.

Table 6.9 Recorded Final Movements below Actual Tunnels and Tunnel Model Tests

opening. But this creates another difficulty which is explained in the following.

The general solution projected for the NGRC expressed by equations 6.11 or 6.12, would allow an estimate of the amount of stress release taking place before the lining activation, as explained in Sections 5.3.1, 5.4 and 6.1. Besides this, the NGRC could also provide an indication of the degree of ground "softening" taking place, while the ground stresses are reduced. This would be particularly helpful if the intended solution was to be used in connection with a ring-and-spring or a ring-and-plate model, in order to analyse the ground-lining interaction phase of the tunnel construction. The non-linear response of the ground could be partly taken into account in either of these models, by assigning elastic moduli to the soil that were compatible with the degree of straining taking place before the support is activated. In fact, this approach will be presented and discussed in following sections and in Chapter 7.

The slope of a ground reaction curve can be understood as corresponding to the radial spring constant or modulus of a ring-and-spring model. This type of model was reviewed in Section 4.3.2.4. If a single radial spring constant is to be used in this model to represent the ground, it was demonstrated in that section that, for tunnels in gravitational stress fields, with H/D between 1.5 and 6.0 and K_o between 0.6 and 1.0, a mean spring constant would be given approximately by:

$$\bar{k}_r = \frac{1}{1+\nu}\,\frac{E}{R} \qquad [6.13]$$

where E and ν are average elastic properties of the ground around the opening and R is its radius.

The development that led to the above equation assumed a gravitational stress field acting on a plate of infinite extent. In a shallow tunnel situation as the one being considered, the slope of the NGRC will of course reflect the limited depth of the cover or the presence of a rigid base. Hence, for a given set of elastic properties, k_r at the crown would decrease as H/D decreases and k_r at the floor would increase as V/D decreases. Not only would the local spring constant be altered by the position of the boundaries, but the average spring constant $\bar{k}_r$ would also be affected by them.

It was shown in Sections 5.2.4.2, 5.2.4.3 and 5.2.4.4 how the original in situ modulus of the tunnel is reduced as a result of stress release applied to the opening. It will be shown later in this chapter and in the following, how it is possible to obtain an estimate of the reduced soil modulus at the instant the lining is activated. Despite some degree of stiffening that may occur locally at the crown or floor due to the rotation of principal stresses, the ground modulus decreases on average as the in situ stresses are reduced at the opening. A reduced soil modulus should result even if the lining is installed right at the tunnel face (L/D=0).

If the rigid lower boundary is located too close to the tunnel floor, its effect on the floor NGRC can be so pronounced that the average ground modulus for a lining installed at the face may be greater than the in situ initial tangent modulus. This condition is not realistic and thus unacceptable. It was found to occur when V/D was set equal to 0.5 or less. After a very large number of trials covering different geometries, strength parameters and in situ stress ratios, it was found that the problem is avoided completely whenever V/D is set equal to 1.5 or more.

As a consequence of the above findings, it was decided to locate the lower boundary at a fixed distance below the tunnel floor equal to 1.5 D, in all parametric analyses. The results to be presented in the following sections are, therefore, strictly valid for a soil profile interrupted by a rigid horizontal base at 1.5 D below the tunnel. The results presented earlier in this chapter were derived from analyses where different V/D values were adopted: 1.5 (in Tables 6.2 and 6.3 and in Sections 6.2.4.2 and 6.2.4.3), 2.875 (in Table 6.1) and 3.0 (in Sections 6.2.4.1, 6.2.4.4 and 6.3.1.1).

6.3.2 Results of the Analyses

The large amount of data that was generated in the parametric analyses required a decision to be made regarding which aspects of the ground behaviour should be collated and interpreted. The need to relate tunnel closure to the amount of ground stress release at the opening called for the interpretation of the ground reaction curves at, at least three points of the tunnel profile (crown, springline and floor - represented shortly by C, S and F, respectively). Regarding the induced ground displacements, the minimum information required in the distribution of the ground settlements at the surface, and the distribution of subsurface settlements along the tunnel axis. The monitoring of these movements at these locations is the most frequently implemented activity in the observational control of shallow tunnel constructions.

Even after reducing it to a minimum, the numerical output data to be collated and interpreted amounted to something in excess of 5 000 pairs of data. This had to be classified and post-processed. To organize this information and to present it in a condensed form, a few routines were developed and included in the finite element program. The results to be presented and discussed herein refer to this post-processed output.

Recall that in all analyses after a certain amount of stress release had been imposed, soil failure developed locally at points adjacent to the opening. Whenever this happened, the finite element program assigned a very low tangent modulus to the failed elements. It was soon found that after this event, the ground stress-strain response ceased to be homothetic, and a unique normalized ground response could not be obtained. When the failure criteria was locally violated, the subsequent ground response, both in terms of NGRC or normalized settlement distributions, could not be reliably defined. This problem, in fact, was not unexpected, as the selected numerical model is actually unable to simulate this type of condition (see Sections 5.2.2.1 and 5.2.2.2). Accordingly, all numerical output after local failure occurred was disregarded.

In all analyses with the cohesionless soil model, failure was a consequence of excessive shearing. In some analyses with the frictionless soil model, tensile stresses developed. No attempt was made to numerically simulate the soil failure under tension and the resulting stress redistribution. As in the case of ground failure by shear, all numerical output after the local development of tensile stresses was disregarded.

The results of the parametric analyses in terms of normalized subsurface and surface settlements are included in Appendix C, in a compact graphic form. Some of these results are presented and discussed in the following sections.

6.3.2.1 Frictionless Soil Model Results

Effect of the Amount of Stress Release

Figures 6.47 to 6.49 present the results of an analysis for H/D=3 and $c_u/\gamma D=1.25$. One notes through the NGRC shown in Figure 6.47 a 'softer' response at the tunnel crown and a 'stiffer' one at the floor, due to the presence of the free stress ground surface closer to C, and to the rigid boundary closer to F respectively. As the stresses at the opening decrease, the non-linearity of the ground response becomes more pronounced.

Figures 6.48 and 6.49 show that the normalized ground displacements in this case, are not affected much by the amount of stress release. It is noted, however, that the ratio of maximum surface settlement to crown settlement increases slightly (up to 10%) as the stress release is increased (up to 70%). Figure 6.49 also shows that the point of maximum surficial distortion (at about 1.6D off the axis) does not change location with increasing stress release but that the normalized distortion increases slightly.

The last two figures illustrate the format in which all results of the analyses are presented in Appendix C.

Influence of the Tunnel Depth

Figures 6.50 to 6.53 show results of three analyses where the undrained strength ratio $c_u/\gamma D$, was kept constant and equal to 1.25 and the tunnel cover to diameter ratio varied from 1.5 to 6. The NGRC for the crown of a deeper tunnel presents a slightly 'stiffer' response at the early stage of stress release with associated smaller displacements, when compared with a shallower tunnel. This reflects the influence of the proximity of the ground surface, which is also apparent in the springline NGRC, but not at the floor. As the amount of stress release increases the NGRCs become more non-linear. This effect is more pronounced as the tunnel gets deeper. Indeed, ground

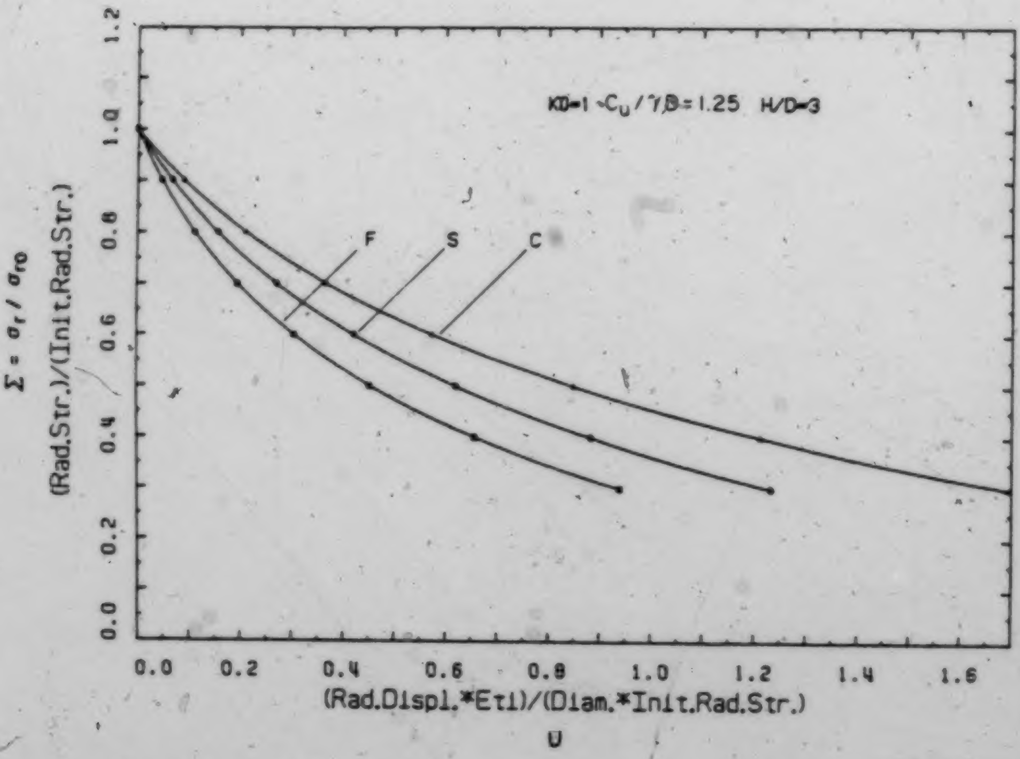

Figure 6.4.7 Normalized Ground Reaction Curves for H/D=3 and an Undrained Strength Ratio of 1.25

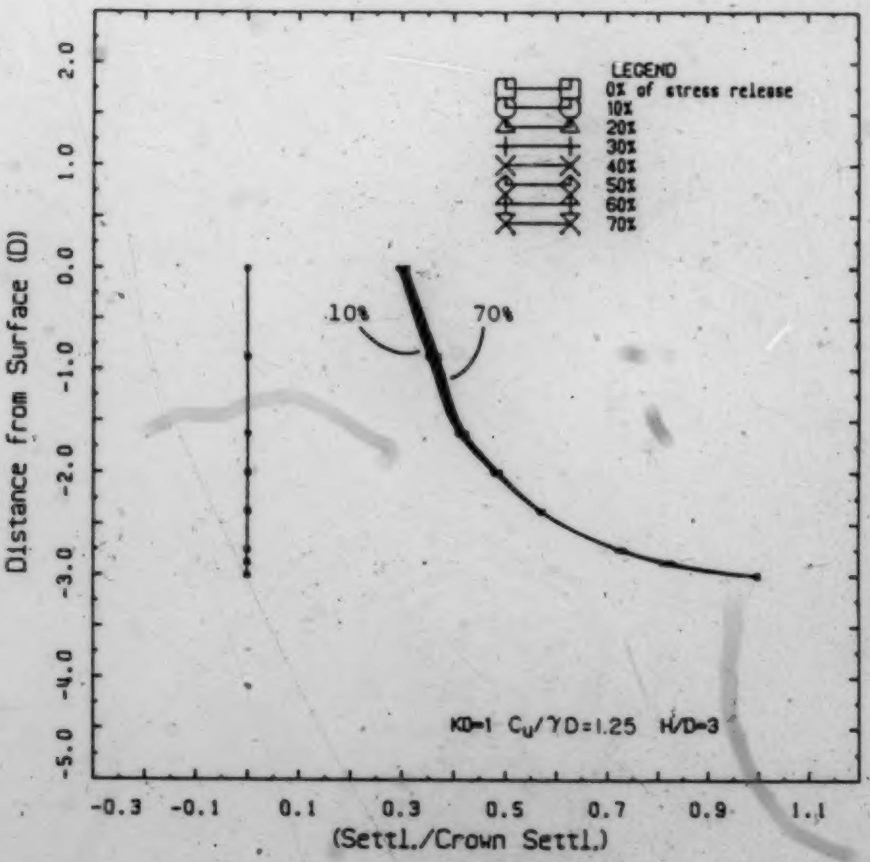

Figure 6.48 Normalized Subsurface Settlements along Tunnel Axis for H/D=3 and an Undrained Strength Ratio of 1.25, Calculated for Increasing Amount of Stress Release

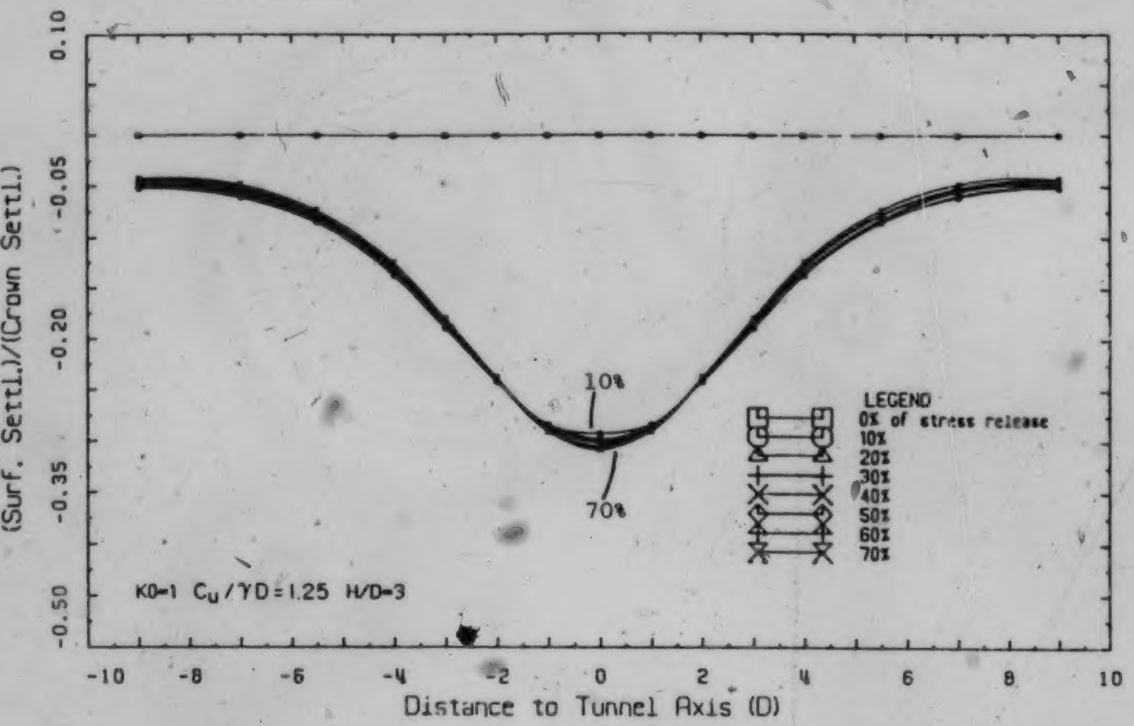

Figure 6.49 Normalized Surface Settlements for H/D=3 and Undrained Strength Ratio of 1.25, Calculated for Increasing Amount of Stress Release

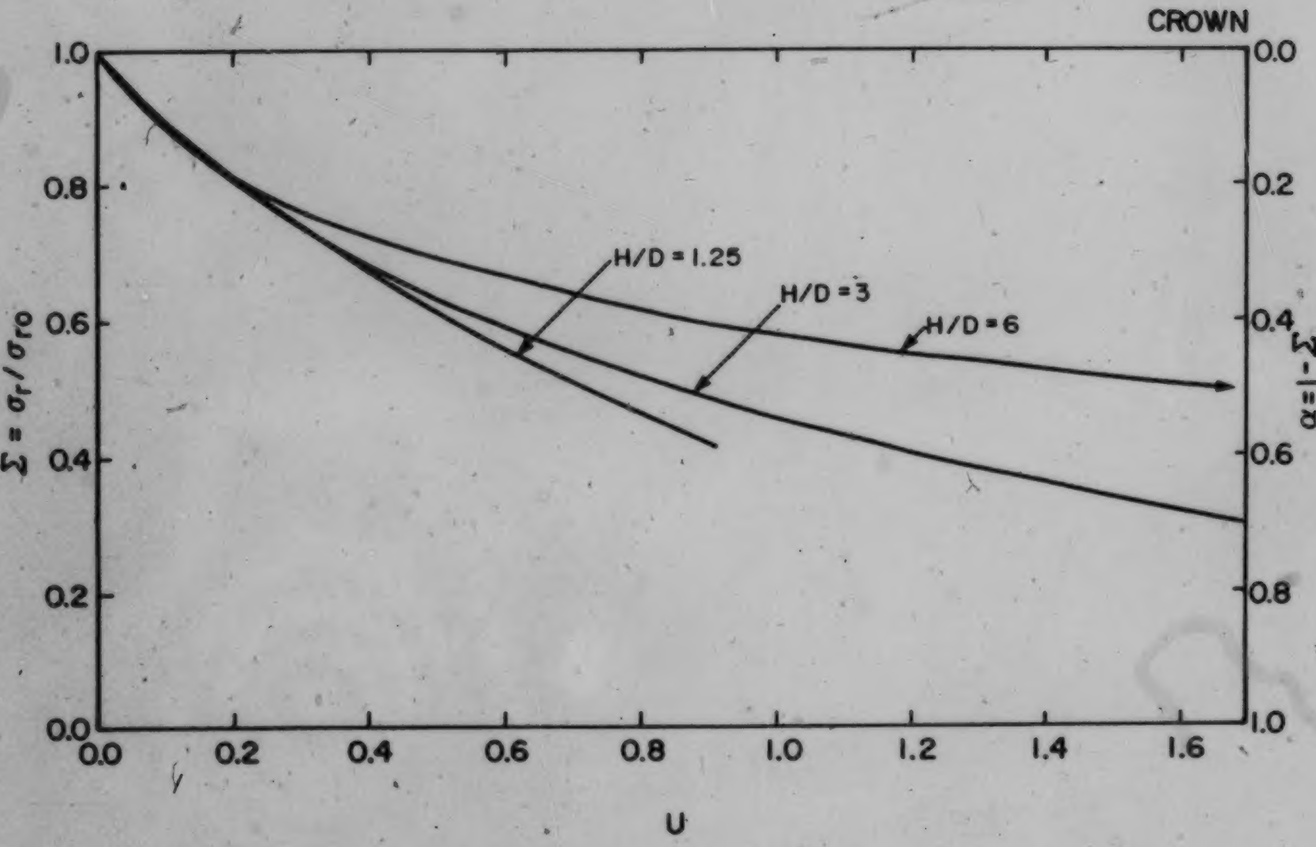

NOTE: $C_u/\gamma D = 1.25$, $K_o = 1.0$

Figure 6.50 Normalized Ground Reaction Curves at the Crown for an Undrained Strength Ratio of 1.25 and Different Tunnel Depths

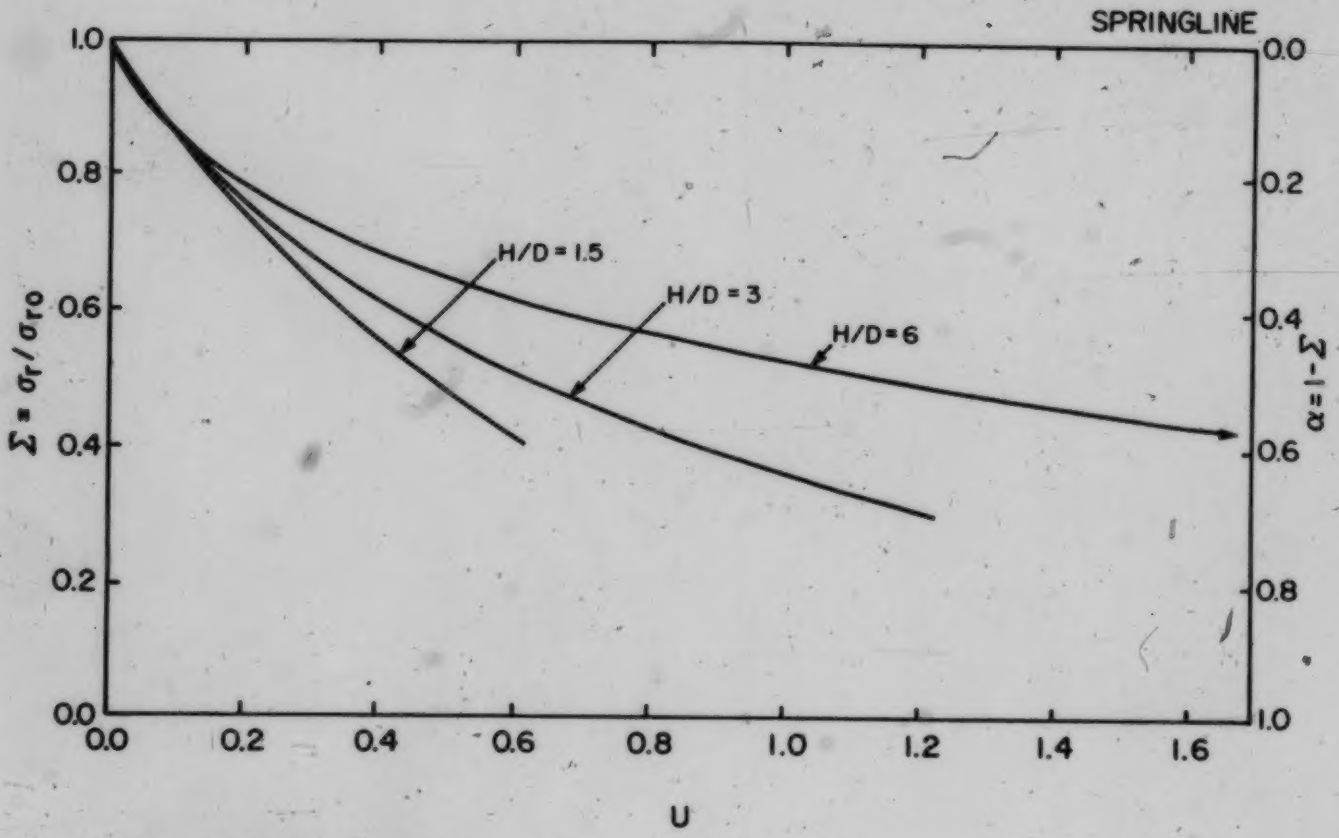

NOTE: $C_u/\gamma D = 1.25$, $K_0 = 1.0$

Figure 6.51 Normalized Ground Reaction Curves at the Springline for and Undrained Strength Ratio of 1.25 and Different Tunnel Depths

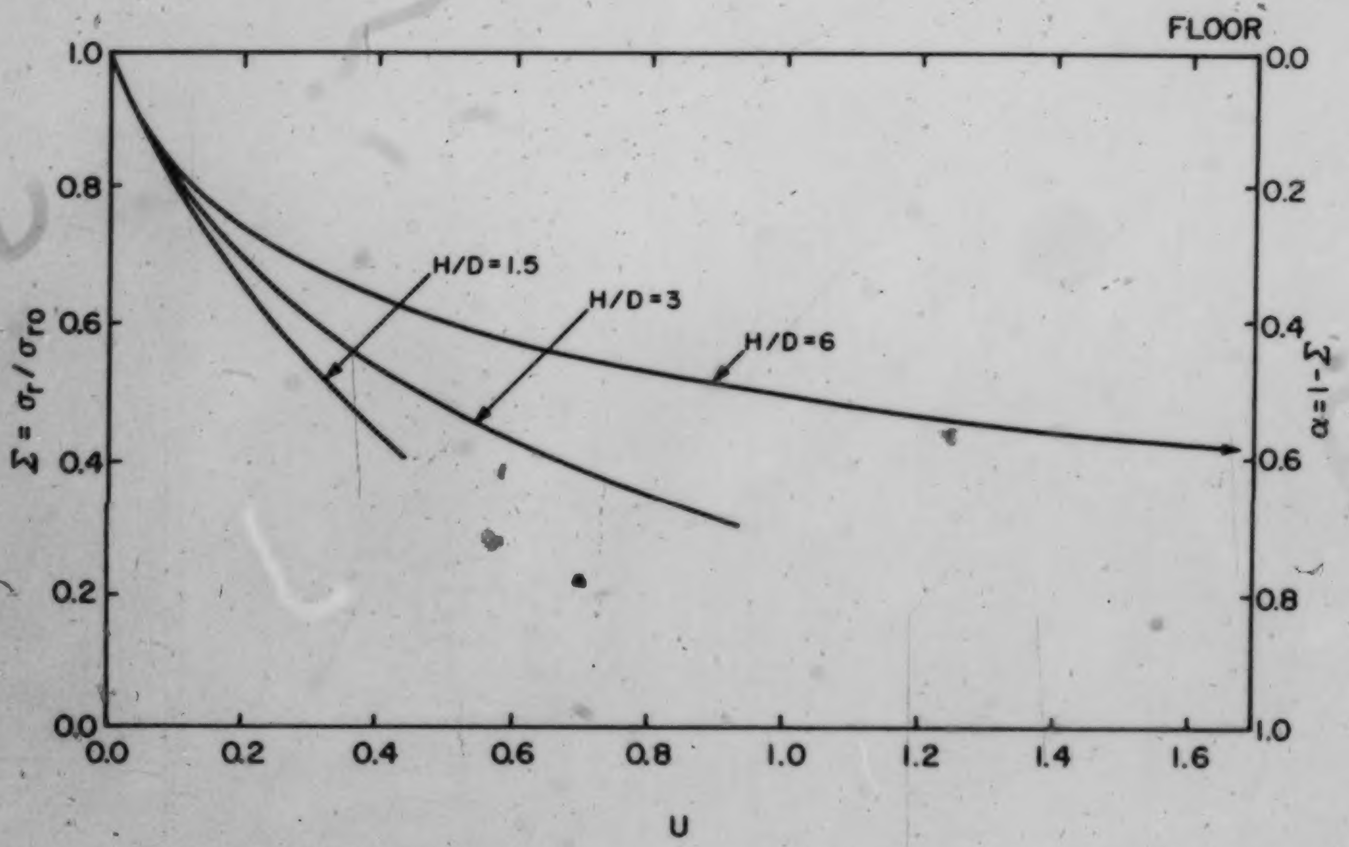

NOTE: $C_u/\gamma D = 1.25$, $K_o = 1.0$

Figure 6.52 Normalized Ground Reaction Curves at the Floor for an Undrained Strength Ratio of 1.25 and Different Tunnel Depths

collapse is approached more rapidly as H/D increases, with the soil undrained strength kept constant.

With respect to the normalized settlements, one notes in Figure 6.53 that the thicker soil cover permits a more rapid attenuation of the ground movements. This leads to the smaller maximum normalized settlement at the surface and the smaller normalized maximum distortion for a given amount of stress release.

Influence of the Undrained Strength Ratio

Figures 6.54 to 6.57 show the results of three analyses, where the relative depth of the tunnel was kept constant (H/D=3) and the undrained strength ratio $c_u/\gamma D$ was varied from 0.625 to 2.5. Clearly as the strength decreases, the larger the displacements are for a given radial stress ratio. A special feature is also apparent in Figures 6.54 to 6.56: the NGRCs for different strengths are nearly homothetic. The centre of similitude of these curves is their origin ($\sigma_r/\sigma_{r0}=1$ and U=0). The coordinates of homothetic points on these curves are defined by the intersections of the latter with arbitrary axes through the centre of similitude (shown by dashed lines). It will be shown in Section 6.4 that if these points were used as reference values and if each curve is transformed into another with coordinates normalized to their respective reference values, then these normalized curves almost coincide. Single curves for each point of the tunnel contour can thus be formulated, regardless of the value of the

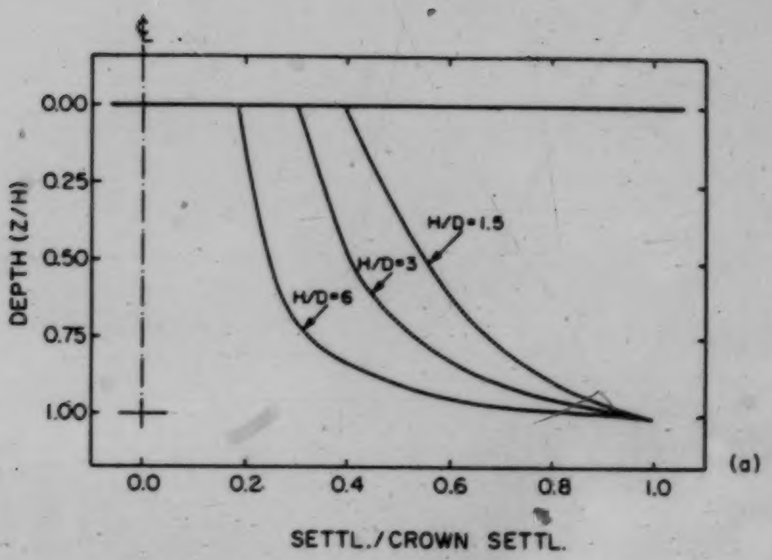

NOTE : $C_u/ D=1.25$, $K_0=1.0$, 50% RELEASE

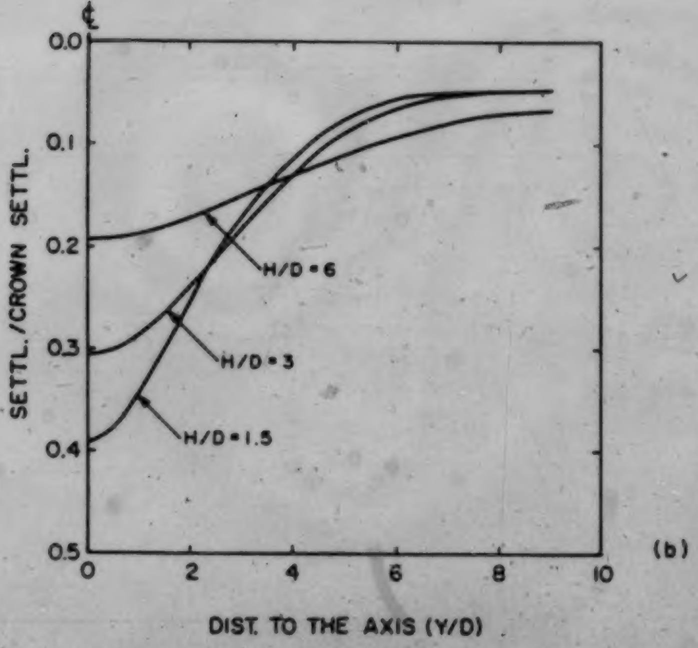

NOTE : $C_u/\gamma D=1.25$, $K_0=1.0$, 50% RELEASE

Figure 6.53 Normalized Subsurface and Surface Settlement for an Undrained Strength Ratio of 1.25 and 50% Ground Stress Release, Calculated for Different Tunnel Depths

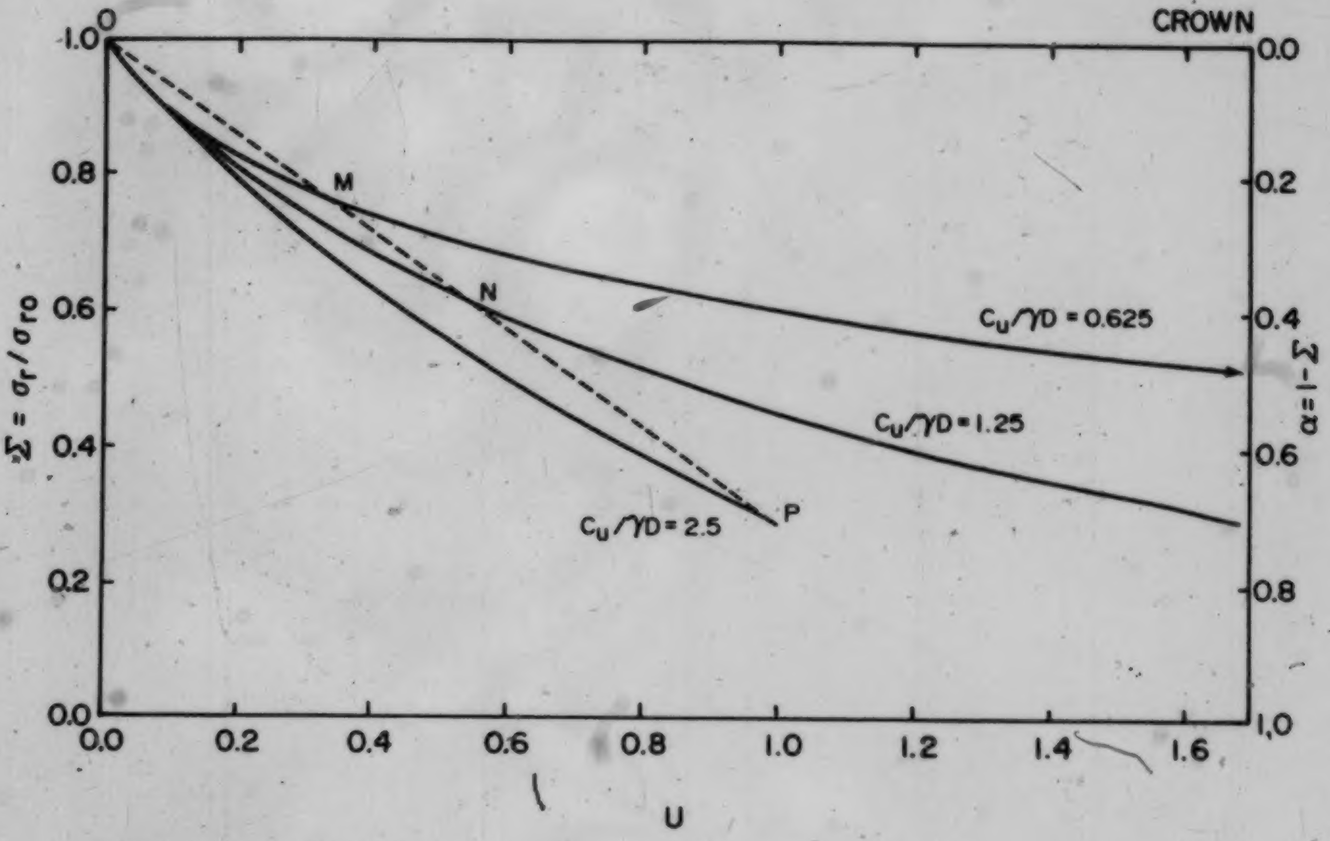

NOTE: $H/D = 3$, $K_o = 1.0$

Figure 6.54 Normalized Ground Reaction Curves of the Crown for H/D=3 and Different Undrained Strength Ratios

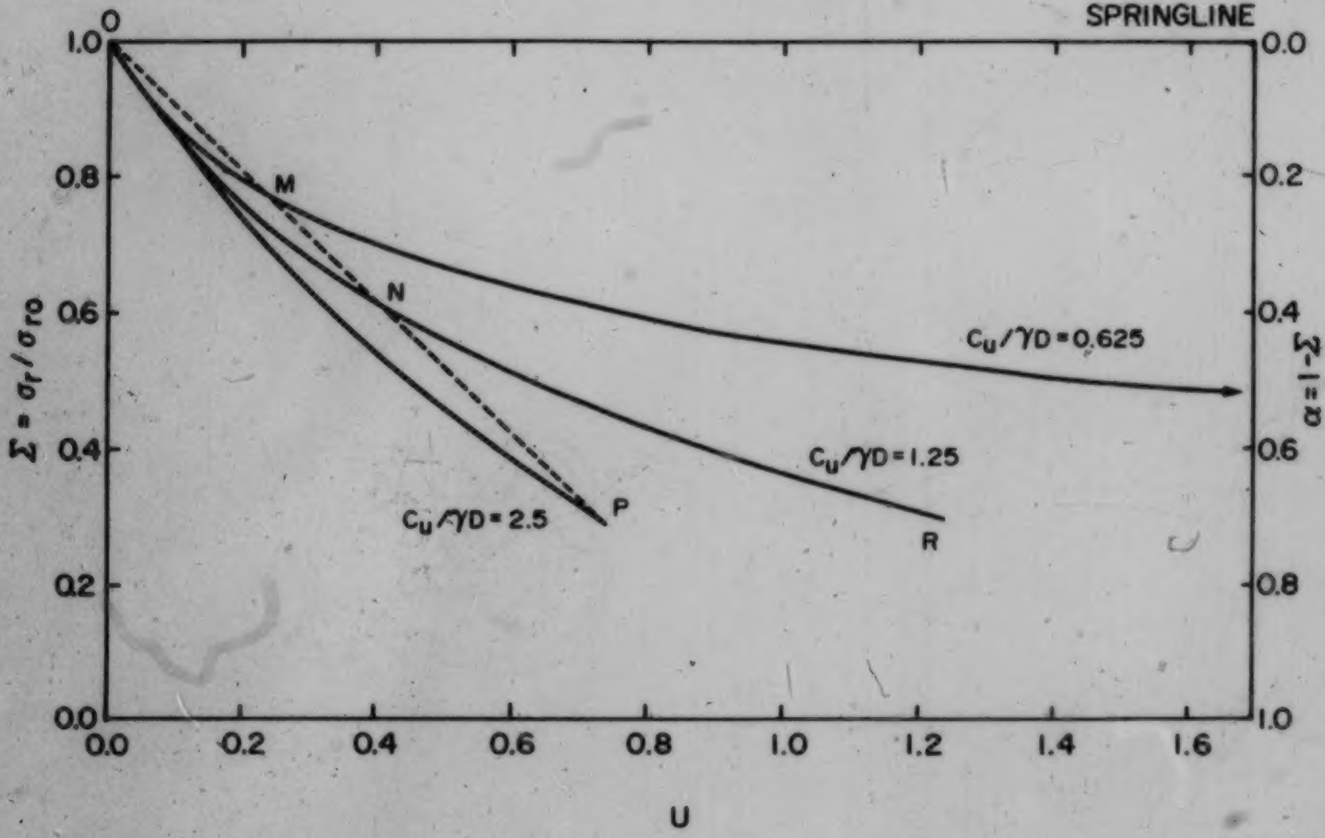

NOTE: H/D=3, K_o=1.0

Figure 6.55 Normalized Ground Reaction Curves of the Springline for H/D=3, and Different Undrained Strength Ratios

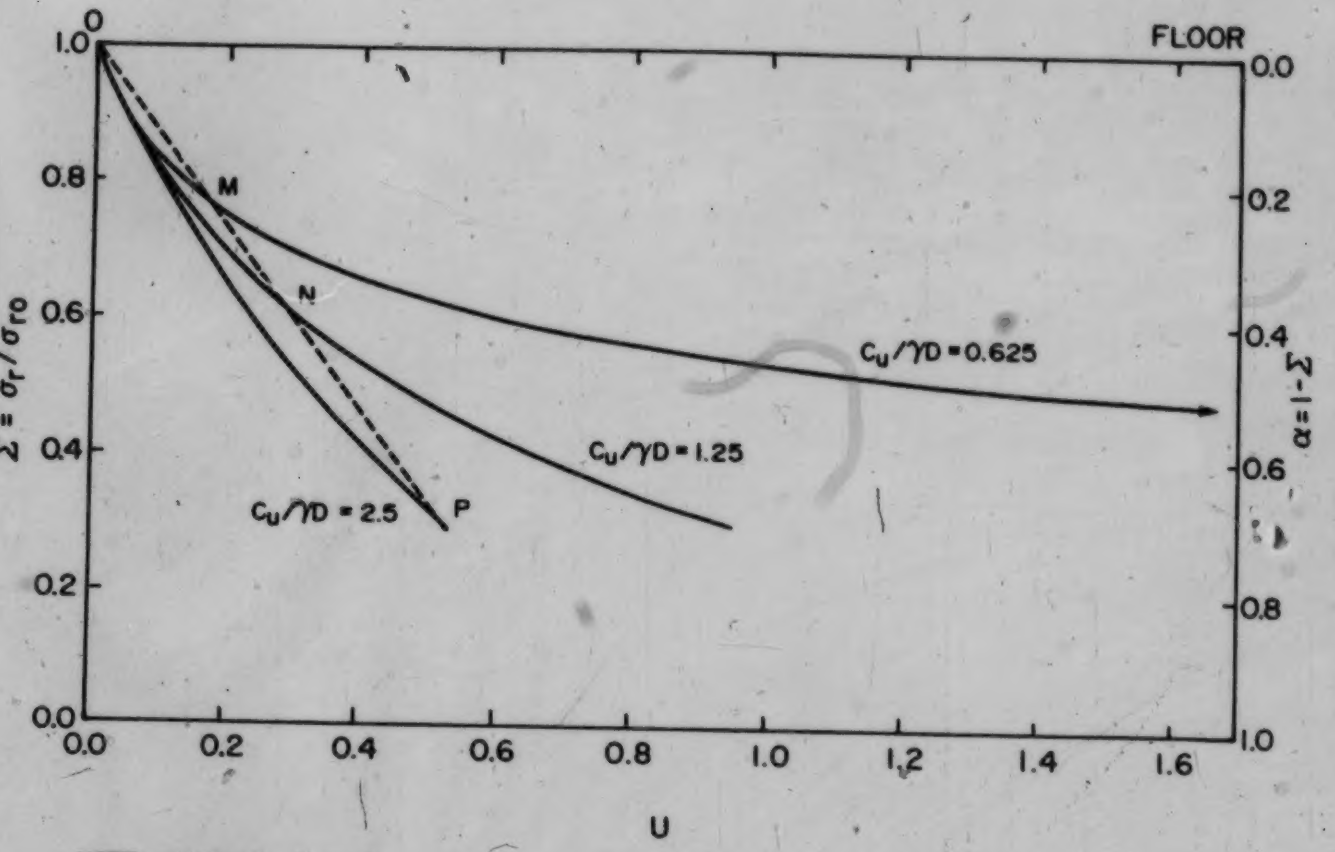

NOTE: $H/D = 3$, $K_o = 1.0$

Figure 6.56 Normalized Ground Reaction Curves of the Floor for H/D=3 and Different Undrained Strength Ratios

undrained strength ratio. This finding will give more generality to the projected solution as will be discussed later.

Figures 6.57(a) and (b) present the distributions of normalized ground settlements at the surface and subsurface for an equal amount of stress release of 50%. As the ground strengths are different in each case, for a fixed radial stress ratio (σ_r/σ_{ro}) the factor of safety against collapse increases as the strength increases. In other words, for the 50% release, the case with lower value of $c_u/\gamma D$ will be closer to collapse (but with an FS greater than unity). Despite this, the distributions of normalized subsurface settlements almost coincide, as shown in Figure 6.57(a). The distributions of surface settlements are also very close to each other. It is apparent, however, that the weaker the soil is (thus, the lower the factor of safety is), the larger the normalized surface distortion is, as expected.

6.3.2.2 Cohesionless Soil Model Results

Effect of the Amount of Stress Release

Figures 6.58 to 6.60 present typical results for a cohesionless soil with ϕ=30°, K_o=0.8 and H/D=3. The "stiffness" of the ground can be measured by the derivative of the NGRC. At the springline (Figure 6.58), one notes that the ground softens progressively, as the stress release increases. At the crown and floor, however, during the initial stages of stress reduction, the ground seems to stiffen slightly but below a certain radial stress ratio,

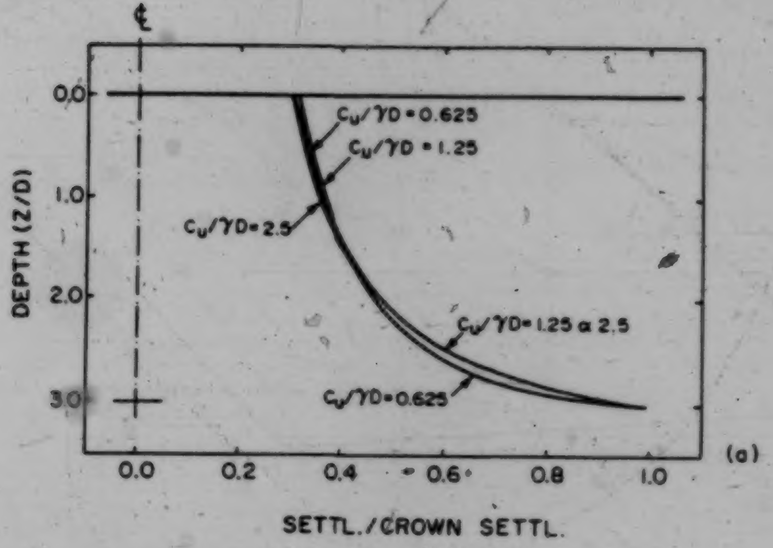

NOTE: $H/D = 3$, $K_0 = 1.0$, 50 % RELEASE

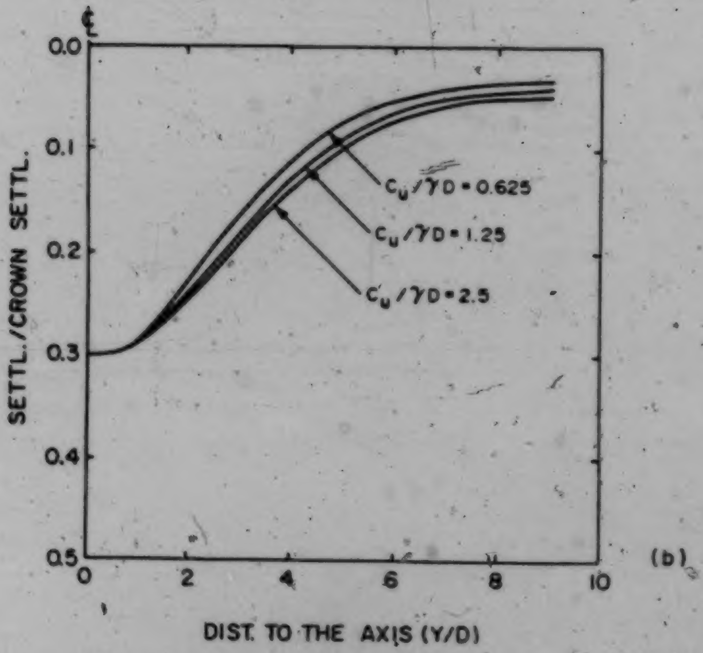

NOTE: $H/D = 3$, $K_0 = 1.0$, 50% RELEASE

Figure 6.57 Normalized Subsurface and Surface Settlements for H/D=3 and 50% Ground Stress Release, Calculated for Different Undrained Strength Ratios

the response is also that of softening for increasing stress release. That initial stiffening response, was not observed for the frictionless soil, where K_o was set equal to unity. When K_o is less than unity, the ground at the crown or floor initially experiences an increase in the minor principal stress (in the horizontal direction), which leads to an increase in the tangent modulus and thus a stiffer response. After the principal stress directions reverse so that the radial stress becomes the minor principal stress, a progressive softening is also noted at crown and floor.

The distribution of normalized subsurface settlements for the cohesionless soil model seems to be more affected by the amount of stress release, than for the frictionless model. As indicated in Figure 6.59, as the amount of stress release increases, larger normalized settlements are observed. The same effect is noted for the normalized surface settlements, in Figure 6.60, when it is also seen that larger normalized surface distortions are observed for increasing stress reductions.

Influence of the Tunnel Depth

Figures 6.61 and 6.62 present results of analyses for K_o=0.8 and ϕ=30°, carried out for three tunnel depths. As it is noted, the NGRC for the tunnel crown is more sensitive to the relative depth than are the other points of the tunnel contour. In fact, the curves at springline and floor almost coincide. Moreover, as the tunnel gets deeper, the effect of the proximity of the ground surface on the NGRCs of the

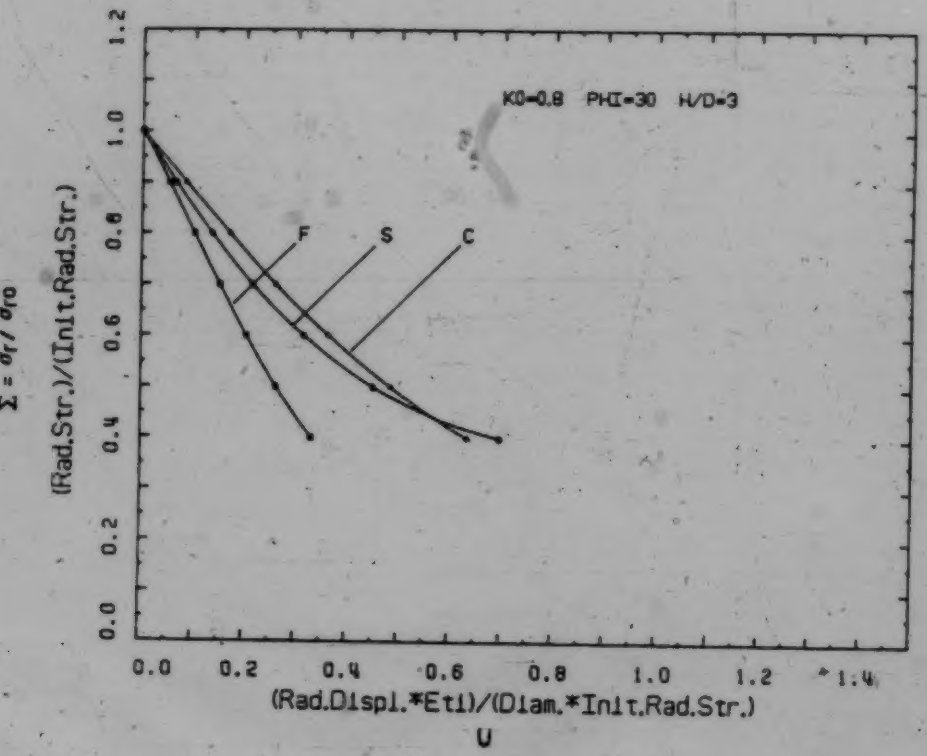

Figure 6.58 Normalized Ground Reaction Curves for H/D=3, K_o=0.8 and ϕ=30°

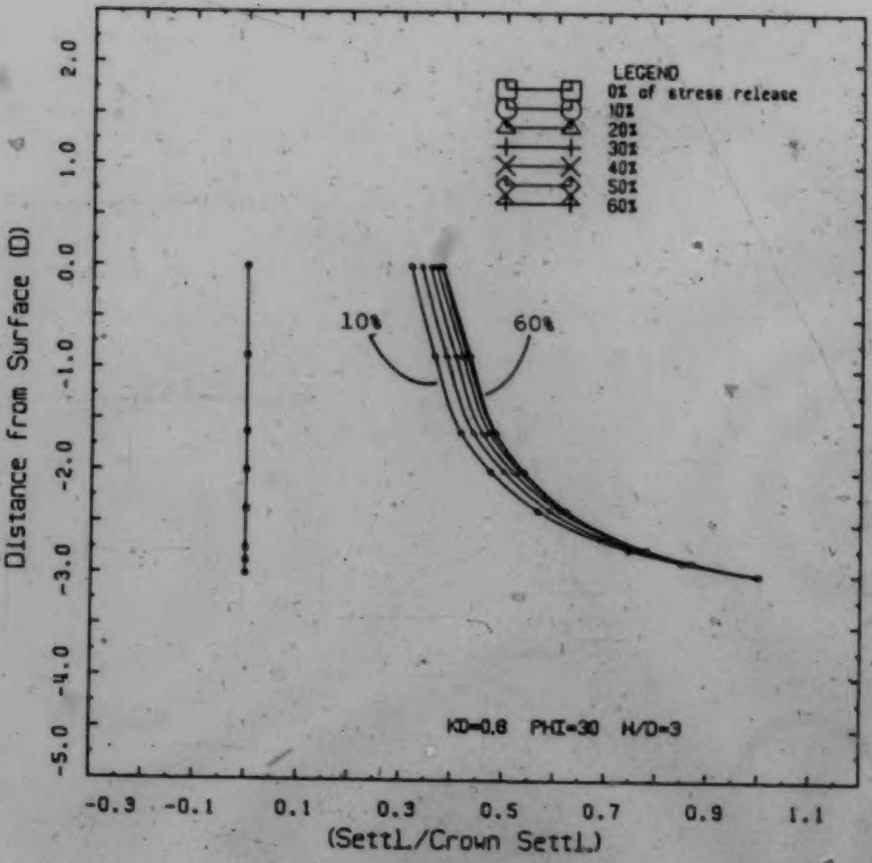

Figure 6.59 Normalized Subsurface Settlements for H/D=3, K_o=0.8 and ϕ=30°, Calculated for Increasing Amount of Stress Release

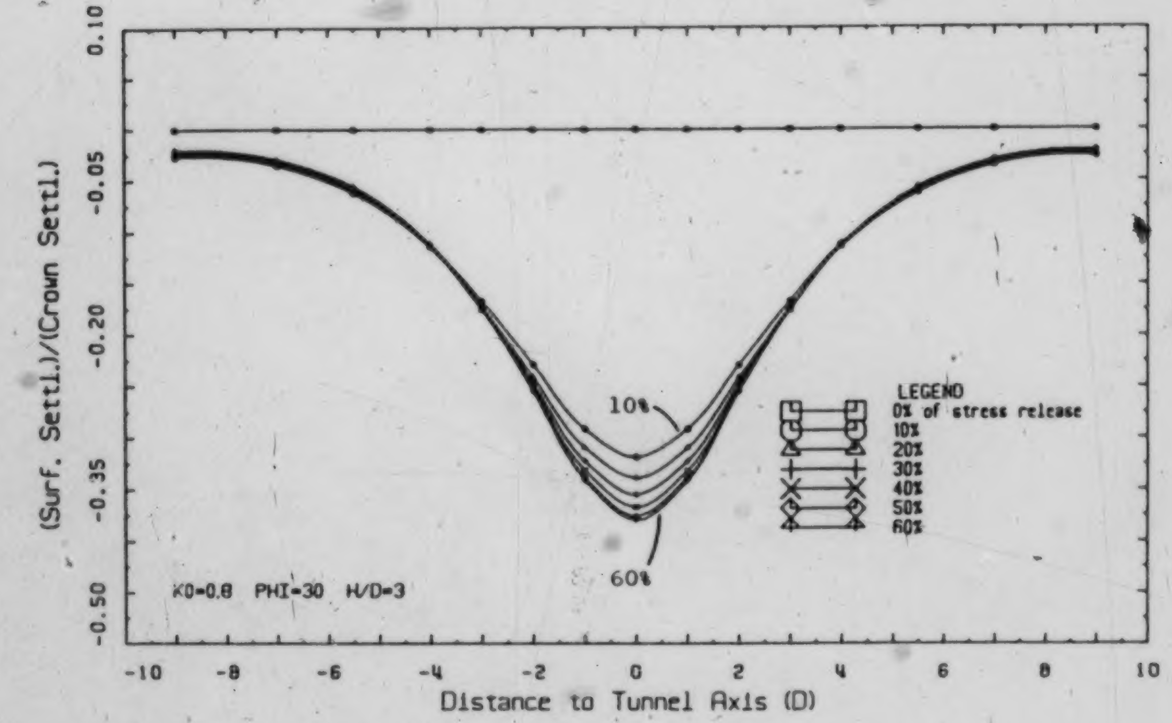

Figure 6.60 Normalized Surface Settlements for H/D=3, K_o=0.8 and ϕ=30°, Calculated for Increasing Amount of Stress Release

crown is reduced and these curves move down and get closer together. This is exactly opposite to the trend noted in the frictionless soil model in which the soil strength was kept constant. In this cohesionless counterpart, the the shear strength increases as the tunnel gets deeper and this explains the noted behaviour. As would be expected when the tunnel gets deeper, the normalized subsurface settlements become smaller as indicated in Figure 6.62(a). These settlements are plotted against the depth ratio z/H (solid lines) and against the depth ratio z/D (dashed curves). The effect ~~of settlement at~~tentuation in the soil cover is perhaps better appreciated through the latter plots. Figure 6.62(b) shows that as the tunnel gets deeper, the normalized surface distortions decrease and the settlement trough gets wider. Recall that the settlements shown in Figure 6.62 correspond to a stress reduction of 50%. Since the friction angle is the same in all cases, the ground strength is higher for deeper tunnels. Thus, for equal stress reduction, the factors of safety are not the same in each case, and are smaller for the shallower tunnel case.

Influence of the Friction Angle

Figures 6.63 to 6.66 present the results of analyses where H/D=3, K_0=0.8 and three values for friction angles were considered (ϕ=20°, 30° and 40°). A stronger non-linear response is noted in the NGRC of the tunnel springline, reflecting that the soil at this point approaches failure earlier than elsewhere around the tunnel. This is consistent

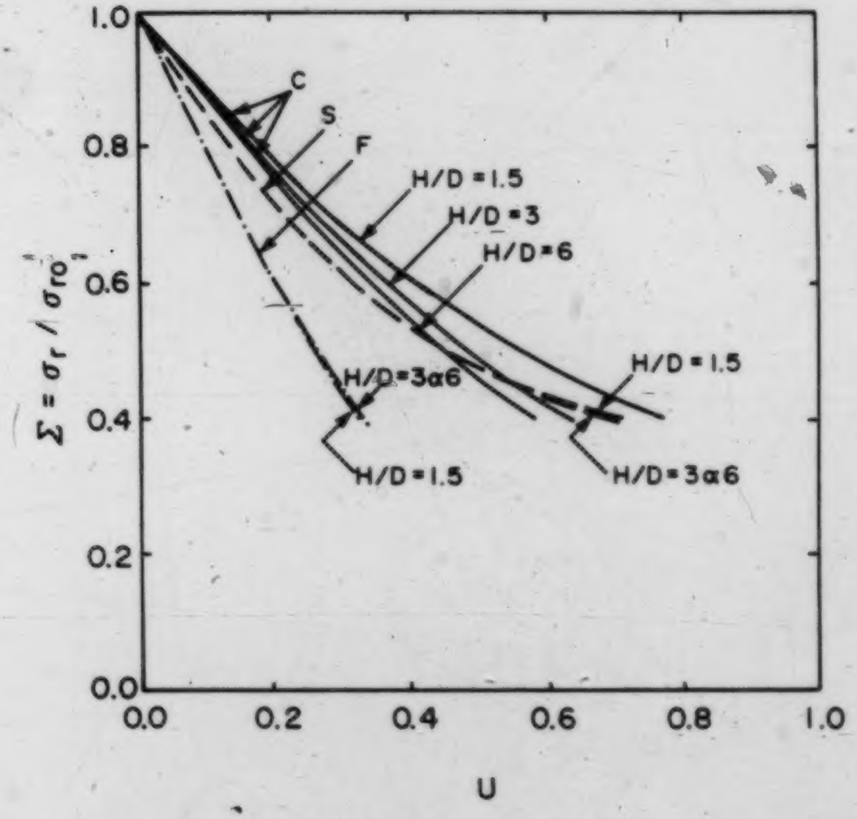

NOTES ;

1. ϕ = 30°, K_0 = 0.8
2. C = CROWN , S = SPRINGLINE , F = FLOOR

Figure 6.61 Normalized Ground Reaction Curves for Different Tunnel Depths, Calculated for ϕ=30° and K_o=0.8

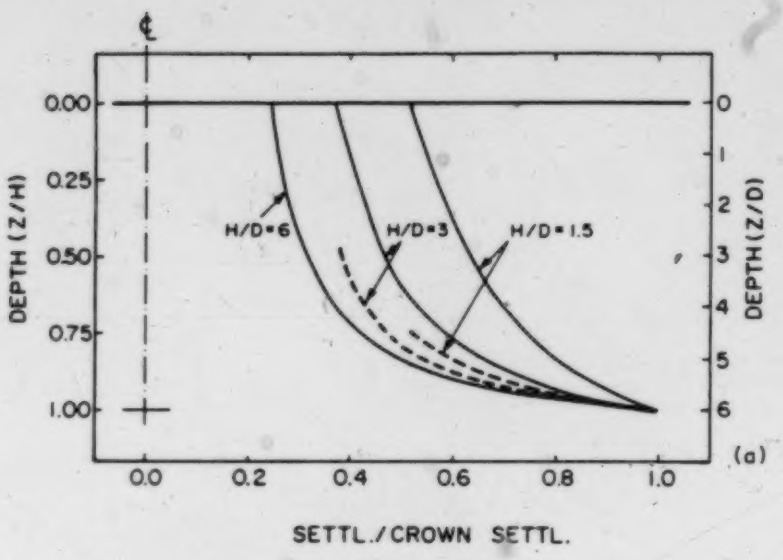

NOTE : $\phi = 30°$, $K_0 = 0.8$, 50% RELEASE

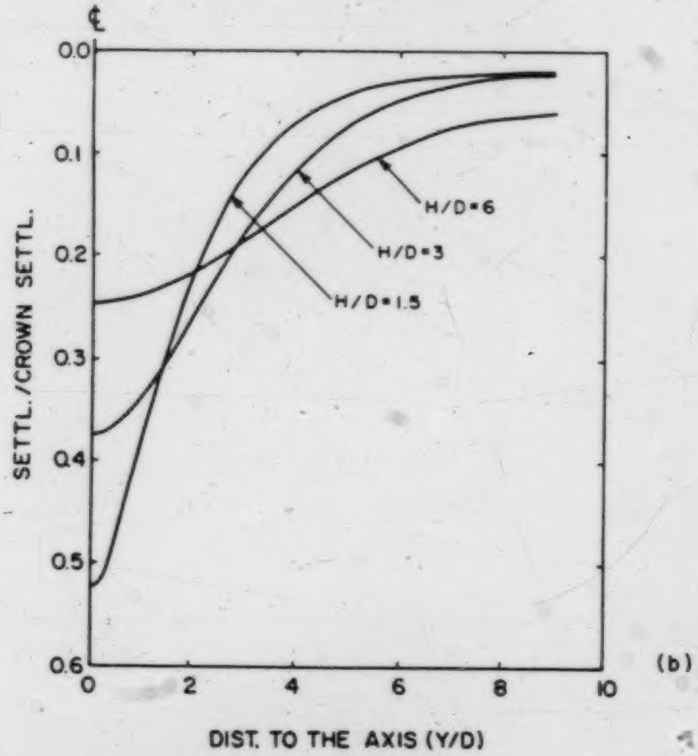

NOTE $\phi = 30°$, $K_0 = 0.8$, 50% RELEASE

Figure 6.62 Normalized Subsurface and Surface Settlements for Different Tunnel Depths, Calculated for $\phi=30°$, $K_o=0.8$ and 50% Stress Release

with the selected K_o value which is smaller than unity.

The NGRCs for different friction angles shown in Figures 6.63 to 6.65 were also found to be nearly homothetic, with the centre of similitude at their origin (Σ=1 and U=0). The coordinates of homothetic points on these curves are defined by the intersection of the latter with arbitrary axes through the centre of similitude. It is shown in Section 6.4 that if these points were used as reference values and if each curve is transformed into another with coordinates normalized to their respective reference values, then these normalized curves almost coincide. Single curves for each point of the tunnel contour can thus be formulated independently of the friction angle. This finding will give more generality to the projected solution.

Figure 6.66 presents the distribution of normalized ground settlements at the surface and subsurface, for a stress release of 40%. The noted differences in the settlement distributions can be partly attributed to the differences in shear straining in each case. As the amount of stress release is the same, but the strengths are different, the factor of safety against collapse in each case is different. Correspondingly, the displacement fields should differ. Higher normalized surface distortions are found for decreasing ϕ but the width of the surface settlement trough does not change much.

Influence of the In Situ Stress Ratio

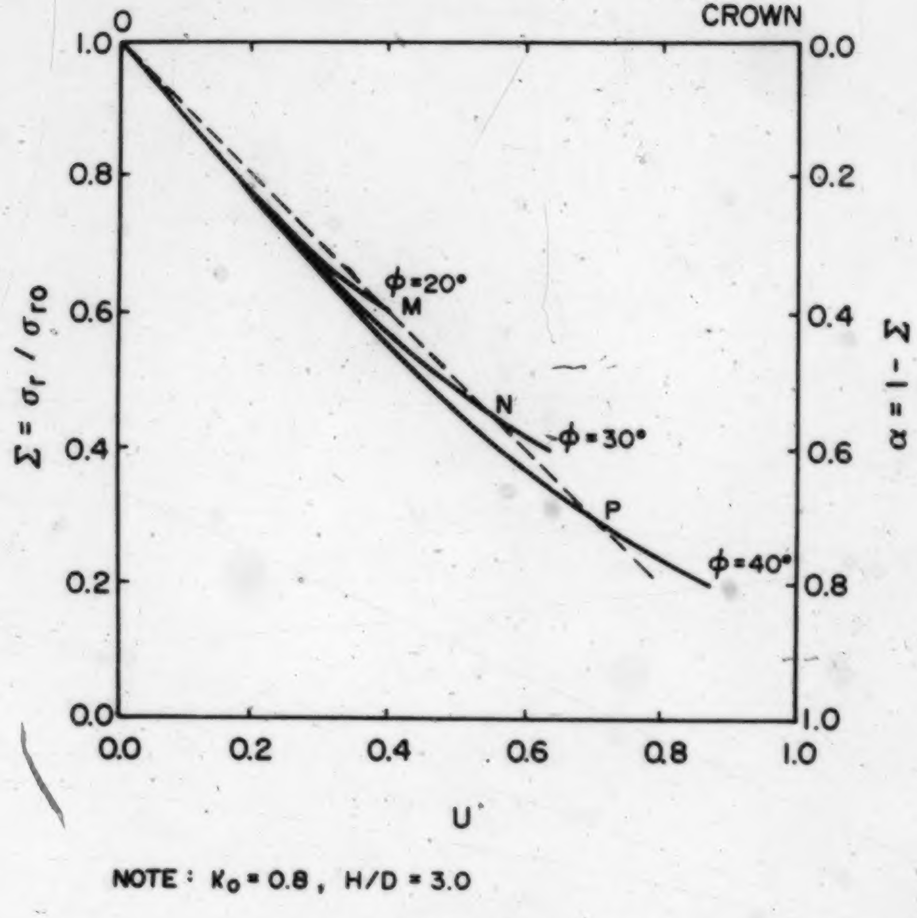

NOTE: K_0 = 0.8, H/D = 3.0

Figure 6.63 Normalized Ground Reaction Curves of the Crown for H/D=3 and K_o=0.8, Calculated for Different Friction Angles

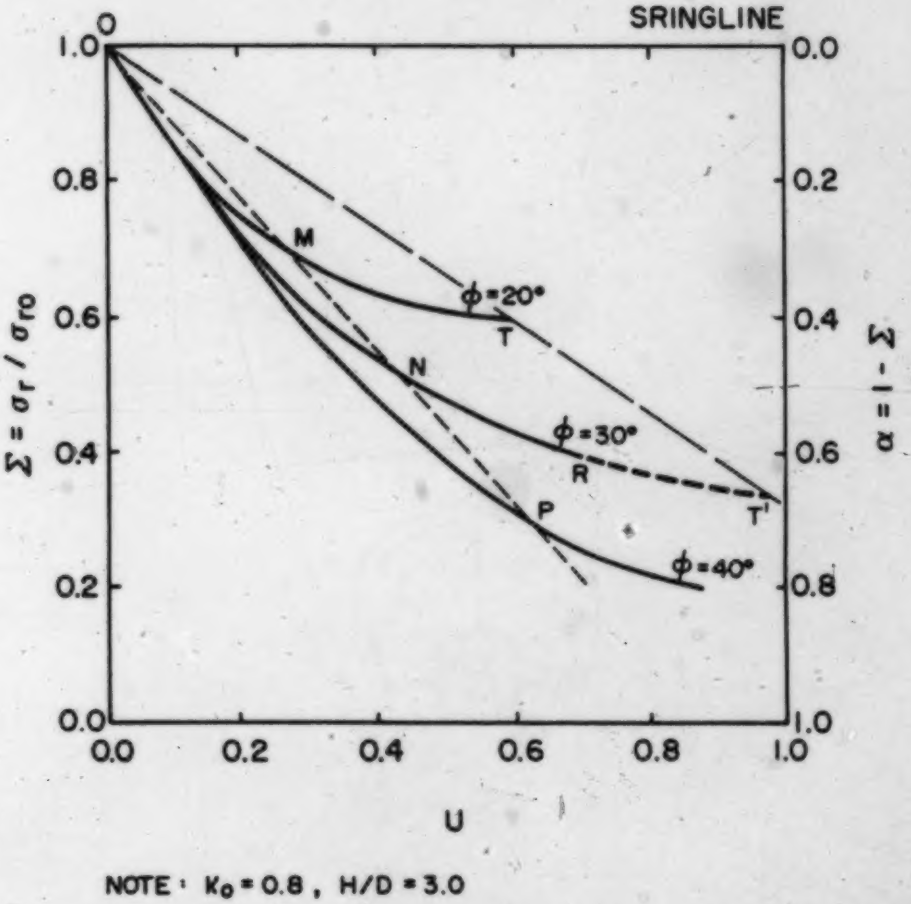

Figure 6.64 Normalized Ground Reaction Curves of the Springline for H/D=3 and K_o=0.8, Calculated for Different Friction Angles

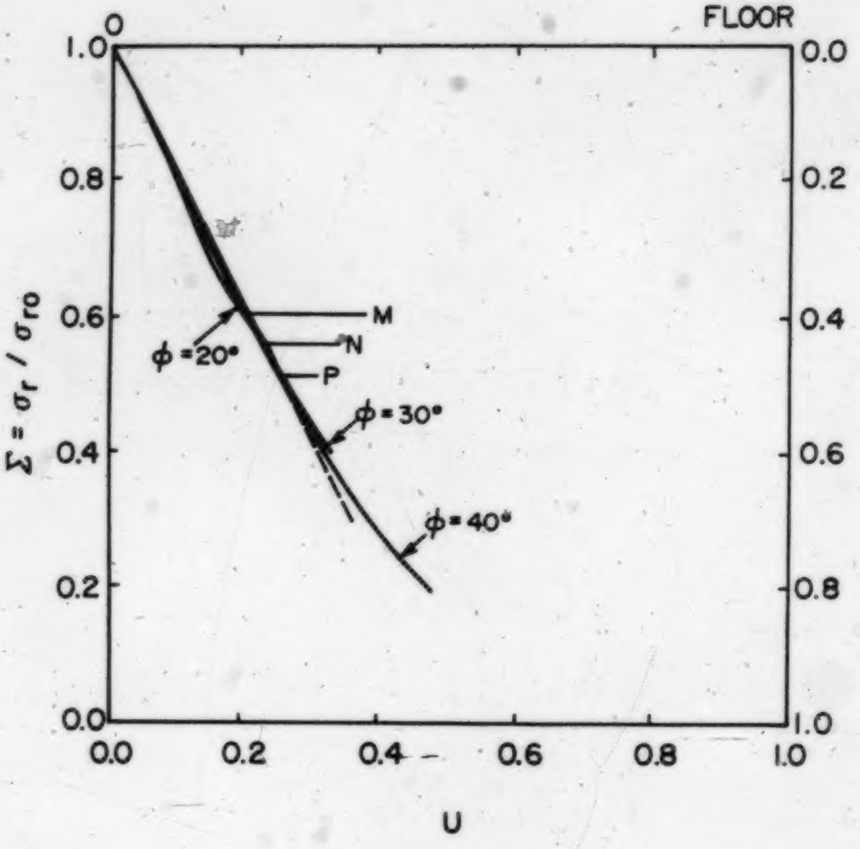

NOTE : $K_0 = 0.8$, $H/D = 3.0$

Figure 6.65 Normalized Ground Reaction Curves of the Floor for H/D=3 and K_o=0.8, Calculated for Different Friction Angles

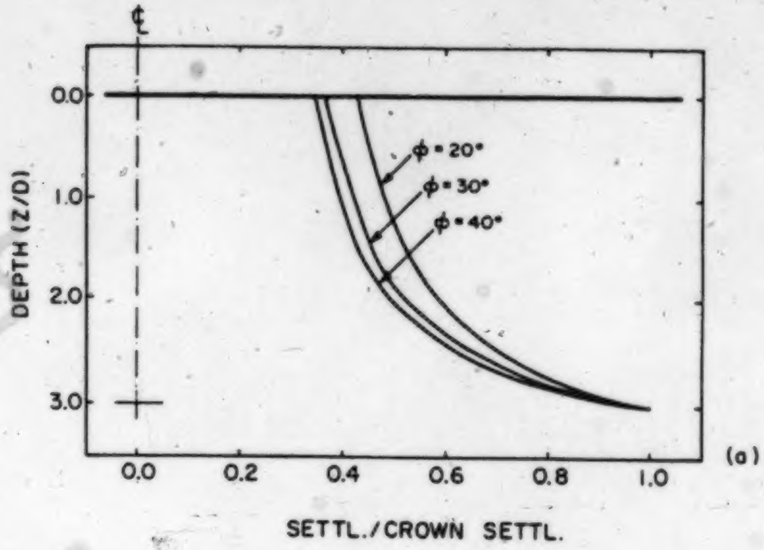

NOTE : $K_0 = 0.8$, $H/D = 3$, 40% STRESS RELEASE

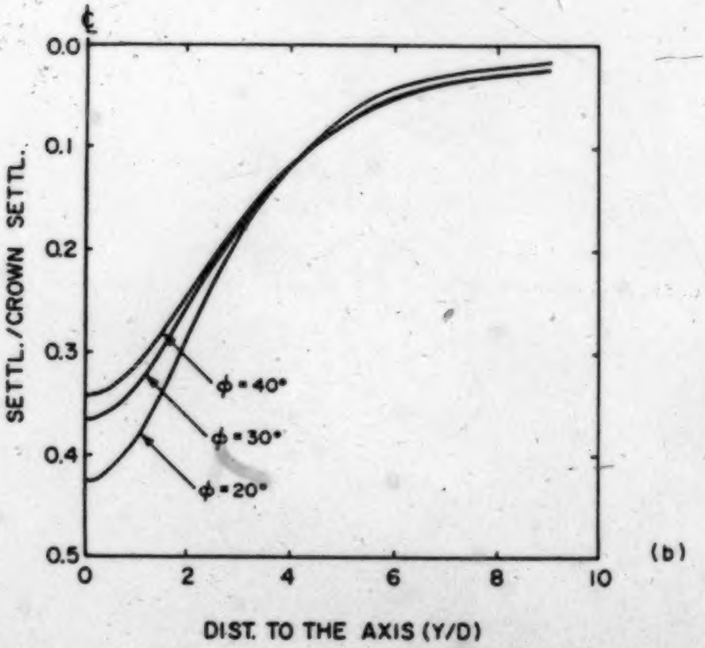

NOTE : $K_0 = 0.8$, $H/D = 3.0$, 40% STRESS RELEASE

Figure 6.66 Normalized Subsurface and Surface Settlements for $H/D=3$, $K_o=0.8$ and 40% Ground Stress Release, Calculated for Different Friction Angles

While for the frictionless soil model, a single value of K_o was considered, in the parametric analyses for the cohesionless model, different K_o values were assumed.

Figures 6.67 to 6.70 present the results of analyses for H/D=3, ϕ=30° and for three in situ stress ratios, (K_o=0.6, 0.8 1.0).

For K_o smaller than unity, soil elements close to the springline undergo local failure before other points at the tunnel contour. This fact is apparent from the NGRCs, which show a more pronounced non-linear aspect at the springline than at elsewhere (Figures 6.67 to 6.69). For K_o equal to unity, soil elements at the springline, crown and floor reach local failure at approximately the same amount of ground stress release.

As noted earlier in this section, when K_o is smaller than unity, the NGRC at the crown and floor, exhibit a 'stiffening' response due to the increase in the minor principal stress in the early stages of the unloading process. This effect is not noted when K_o=1.

Figures 6.70(a) and (b) show the distribution of normalized displacements at the surface and subsurface. It is evident that K_o has a marked influence on the distributions. A lower K_o value promotes a larger maximum normalized settlement, higher normalized surface distortions and a narrower settlement trough. Although the dimensionless displacement U at the crown for K_o=1 is larger than U for K_o smaller than unity, the absolute surface settlement at the

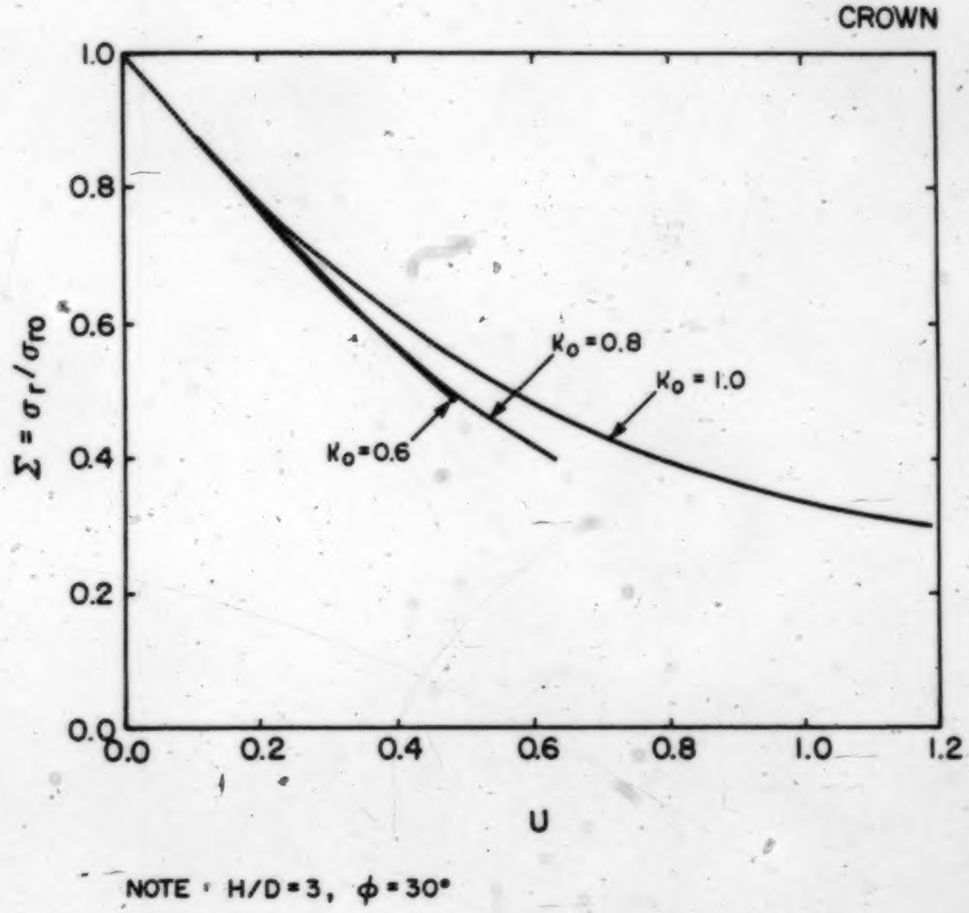

Figure 6.67 Normalized Ground Reaction Curves of the Crown, for H/D=3 and ϕ=30°, Calculated for Different In Situ Stress Ratios

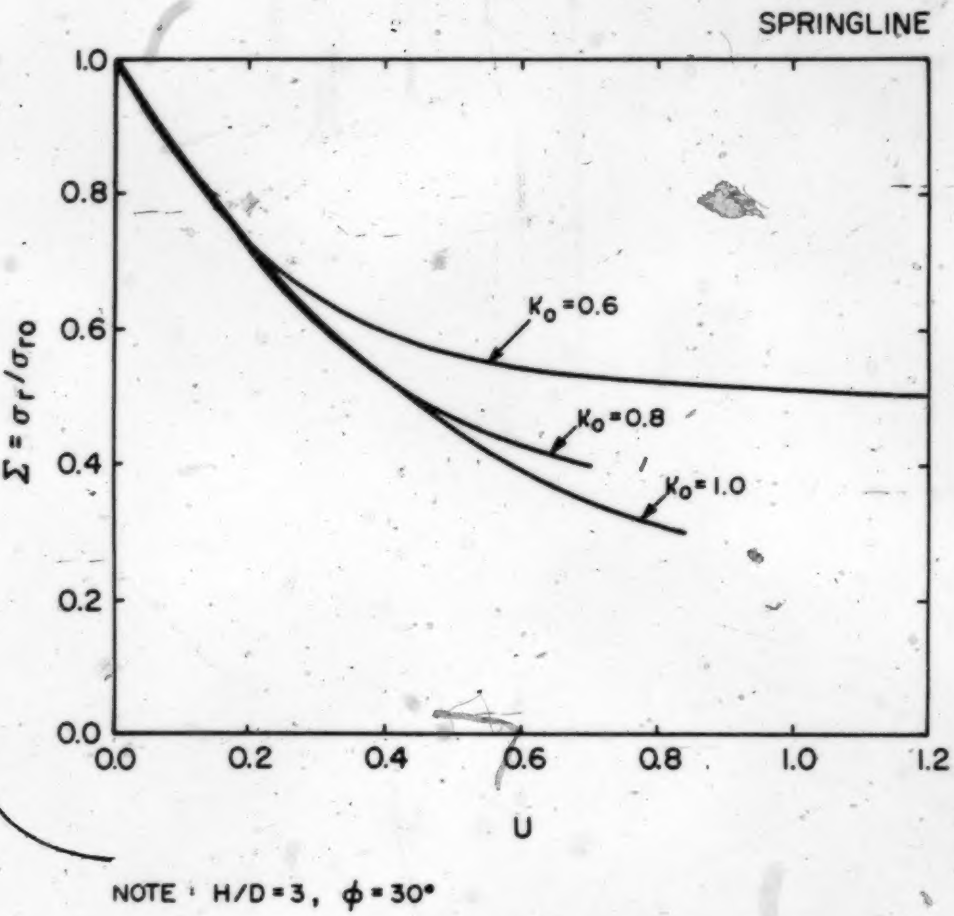

Figure 6.68 Normalized Ground Reaction Curves of the Springline, for H/D=3 and ϕ=30°, Calculated for Different In Situ Stress Ratios

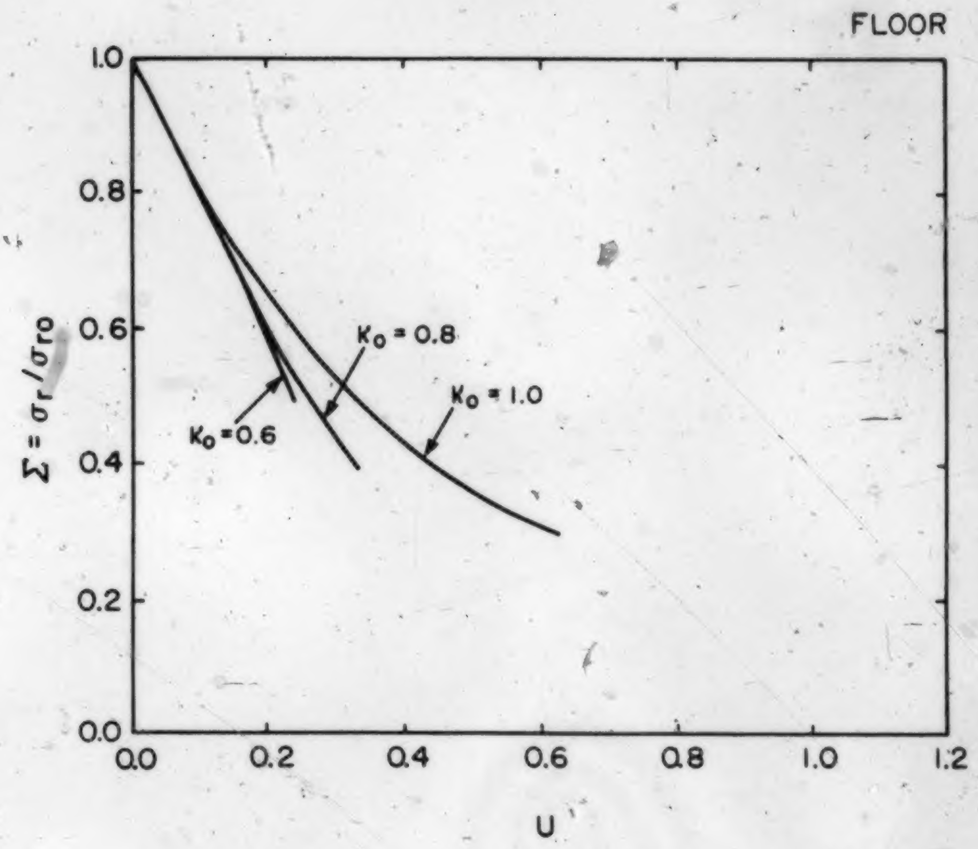

NOTE : H/D=3, ϕ=30°

Figure 6.69 Normalized Ground Reaction Curves of the Floor, for H/D=3 and ϕ=30°, Calculated for Different In Situ Stress Ratios

centreline for $K_o<1$ is always larger than that for $K_o=1$, for the same initial tangent modulus and the same amount of stress release. In other words, for K_o decreasing, the average vertical strain in the ground cover above the tunnel axis decreases.

6.3.2.3 Relationships Between Surface and Crown Settlements

The practical interest that exists in relating the crown settlement (u_c) to the surface settlement at the tunnel centreline (S) is derived from the fact that once the former is assessed in some way, the latter could be readily estimated through some relationship. Many authors investigated the subject and proposed different procedures to accomplish this.

Atkinson and Potts (1977:318) proposed simple expressions relating the normalized surface settlement (S/u_c) to the relative depth of cover (H/D) and the soil type. Their expressions were semi-empirically developed from observation of displacements in tunnel model tests, before ground collapse (FS>1). A similar approach was followed by Seneviratne (1979:56) once more using model test results. Ward and Pender (1981:265) explored the subject further and pointed out some of the limitations of the above approaches. Moreover, they discussed the limitations of the S/u_c relationships derived from linear elastic analyses (for instance, Oteo and Sagaseta, 1982:657). Resendiz and Romo (1981:72) developed a relationship through non-linear

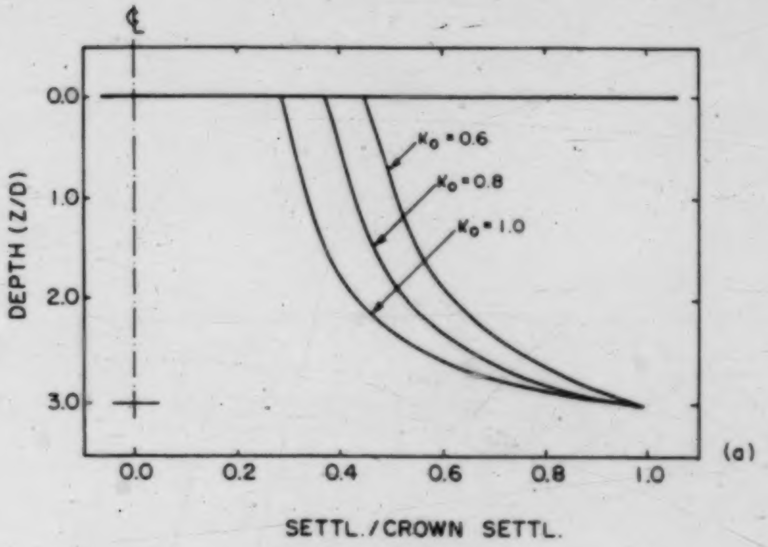

NOTE : H/D = 3, φ = 30°, 50% RELEASE

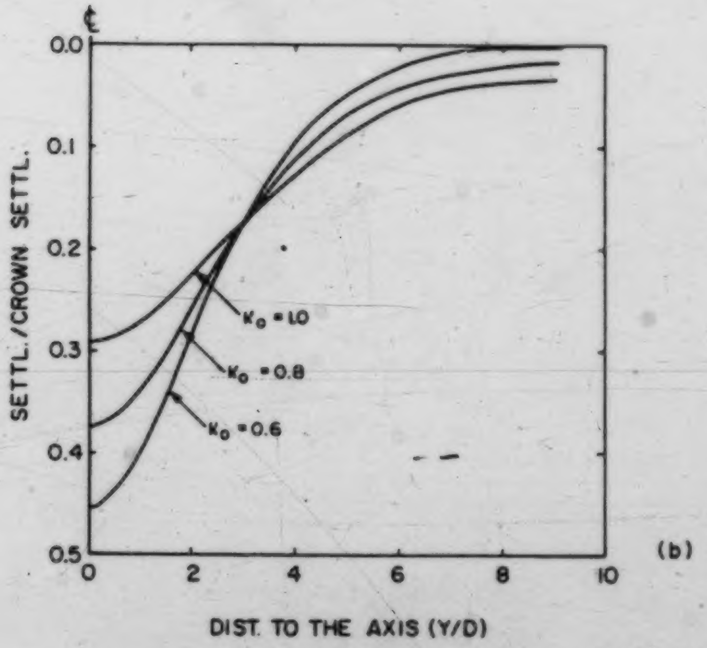

NOTE : H/D = 3, φ = 30°, 50% RELEASE

Figure 6.70 Normalized Subsurface and Surface Settlements for H/D=3, φ=30° and 50% Ground Stress Release, Calculated for Different In Situ Stress Ratios

elastic numerical modelling and suggested that the normalized surface settlement should be a function of H/D and of the soil strain at failure, as determined in an undrained triaxial test. Wong and Kaiser (1987:331) proposed a conceptual model relating the normalized surface settlement to the amount of stress release allowed. They contended that upon the reduction of ground stresses at the opening, the settlement ratio (S/u_c) remains fairly constant initially, increasing rapidly with yielding and subsequent collapse at which stage it approaches unity.

If general relationships to estimate the S/u_c ratio were to be derived for pre-collapse situations (i.e., for good ground control conditions), and if they were to be based on the two soil models introduced earlier (Sections 6.2.2 and 6.2.3), then they would have to be expressed as:

$$F=f\left(\frac{S}{u_c},\frac{\sigma_r}{\sigma_{ro}},\frac{H}{D},\ K_o,\ \phi_e\right) \qquad [6.14]$$

for the cohesionless soil model, and as

$$F=f\left(\frac{S}{u_c},\frac{\sigma_r}{\sigma_{ro}},\ \frac{H}{D},\ \frac{c_{ue}}{\gamma D}\right) \qquad [6.15]$$

for the frictionless soil model.

The results of the parametric analyses included in Appendix C could be helpful in establishing these relationships. To assess the role of the dimensionless variables shown in the equations 6.14 and 6.15 on the settlement ratio, it seems worthwhile to examine some of those results. Figure 6.71, for instance, presents how the settlement ratio for the frictionless soil model, varies with the stress ratio Σ, with the undrained strength ratio and with the tunnel depth. One notes that at the early part of the unloading process and especially for the higher strength soils, the normalized surface settlement is virtually independent of the amount of stress release applied to the opening. Consequently, it does not depend on the factor of safety at pre-collapse stages, despite the pronounced non-linear response one notes even for the stronger soils (see, for instance, Figure 6.54).

The above result is not new as it was noted earlier by Atkinson and Potts (1977:318), through static tunnel model test results in overconsolidated Kaolin, performed in Cambridge by Cairncross (1973) and Orr (1976). In these tests, the undrained shear strength ratio ranged from 0.4 to 0.8 and the H/D ratio from 0.35 to 1.2. For deeper tunnels or weaker soils, however, one notes in Figure 6.71 that the normalized surface settlement becomes more affected by the stress ratio, Σ. Therefore, the Atkinson and Potts (1977) conclusion and proposed correlation for the S/u_c ratio is valid only for the conditions they studied (for instance, very shallow tunnels) and cannot be generalized to other situations. Moreover, the linearity between S/u_c and H/D suggested by the Atkinson and Potts (Op.cit.) relationship have not been confirmed by centrifuge model test results obtained later by Mair (1979:127), also in Kaolin with $c_u/\gamma D$ of about 0.38 and larger cover to diameter ratios (up to 3.11).

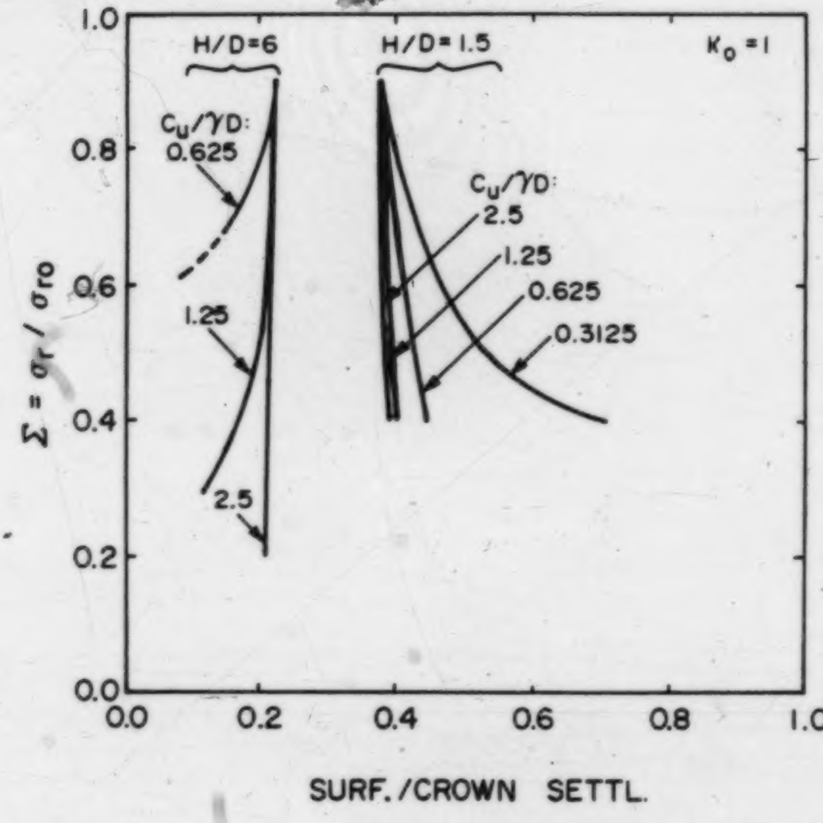

Figure 6.71 Variation of the Maximum Normalized Surface Settlement with the Amount of Stress Release and other Variables, for the Frictionless Soil Model

Another feature that is apparent from Figure 6.71 is that depending on the depth ratio, as ground failure is approached the settlement ratio may either increase or decrease. This seems to reflect the mode of collapse that prevails in shallower or deeper tunnels, with the surface settlement developing at a faster or slower rate compared to the crown settlements. Similar results are found for the cohesionless soil model. These are shown in Figure 6.72 for H/D=3. Once more the normalized surface settlements seem to be unaffected by Σ for small amounts of ground stress release or for larger amounts provided the soil strength is high. Moreover, the influence of the stress ratio K_o now becomes apparent. While for low K_o values, the settlement ratio seems to increase as failure is approached, for higher K_o, that settlement ratio may in fact decrease. The previous criticisms to Atkinson and Pott's (1977) relationship for clays are also applicable for their proposed relations for sand.

The above results indicate ~~that~~ the surface settlement ratio depends on H/D, on the soil strength ($c_u/\gamma D$ or ϕ), on the in situ stress ratio, K_o, and on the amount of stress release allowed (σ_r/σ_{ro}), as is stated by the expressions 6.14 and 6.15. Furthermore they indicate that the S/u_c ratio, regardless of the soil model considered (fully undrained or fully drained), may either increase or decrease with Σ decreasing and ground collapse approaching. Therefore, the conceptual model proposed by Wong and Kaiser

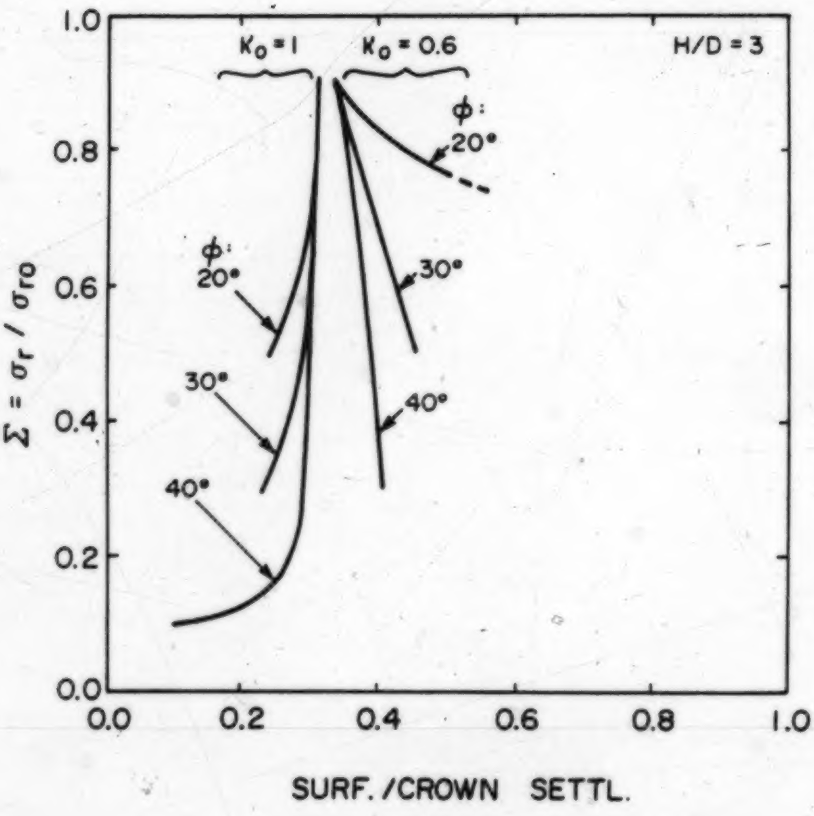

Figure 6.72 Variation of the Maximum Normalized Surface Settlement with the Amount of Stress Release and other Variables, for the Cohesionless Soil Model

(1987:332) is incomplete, as it assumes that in the pre-failure regime, the settlement ratio is always increasing as yielding occurs. In fact, some results by Wong (1986) (not included in Wong and Kaiser, 1987) actually demonstrate the opposite. Wong (1986) studied the subject through finite element modelling using an elasto-plastic stress-strain relationship. For $H/D=2$, $K_o=1.3$ and $\phi=30°$ (analysis ST3 by Wong, 1986:97), the numerical results indicate that the settlement ratio may decrease as the stress ratio Σ decreases. The Wong and Kaiser (1987:333) suggestion that, regardless of the mode of behaviour of the ground defined by its properties, the tunnel depth and the in situ stresses, the settlement ratio S/u_c at collapse becomes unity is yet to be proven. The ratio of settlement increments $\Delta S/\Delta u_c$ may possibly tend toward unity at a complete ground collapse condition but the settlement ratio may not.

To complete the discussion, Figures 6.73 and 6.74 were prepared. They represent graphically the relationship given by the equation 6.15, for the frictionless soil model, and for ground stress releases of 30 and 50% respectively. These amounts of stress reductions in the 2D model could correspond in an actual tunnelling situation, to transverse sections located near the tunnel face and at some distance behind it. Comparing these two figures, one notes that the normalized surface settlement is not very sensitive to the undrained strength ratio, or to the amount of stress reduction. The settlement ratio is more dependent on the relative tunnel depth. Note also that it has been inferred that as H/D tends toward zero, the settlement ratio should tend towards unity. Observe that in Figure 6.74, the results of Mair's (1979) centrifuge model test in kaolin have been included (tests 2DP and 2DV). The undrained strength ratio of this soil was about 0.34.

Similarly, Figures 6.75 to 6.80 were prepared for the cohesionless soil model. It should be noted that the data referring to the 50% stress release, for $\phi=20°$, $K_o=0.6$ and 0.8 were calculated after a few elements of soil at the springline had failed. As explained, the numerical model was not designed for this condition. However, since the failed zone was limited to a fairly small region next to the springline, it is believed that it had negligible effect on the settlement above the crown. The failed zone extended to no more than D/4 beyond the tunnel contour and up to no more than 45° measured from the horizontal axis towards the crown or floor. The area of failed elements corresponds typically to less than 7% of the tunnel area. The suite of plots shown in the last six figures represents the function given by equation 6.14. They may serve as practical design charts for estimating the settlement ratio, for conditions differing from those considered in the parametric analyses whose results were included in Appendix C.

To illustrate the subject further, Figure 6.81 reproduces data from 28 case histories gathered by Ward and

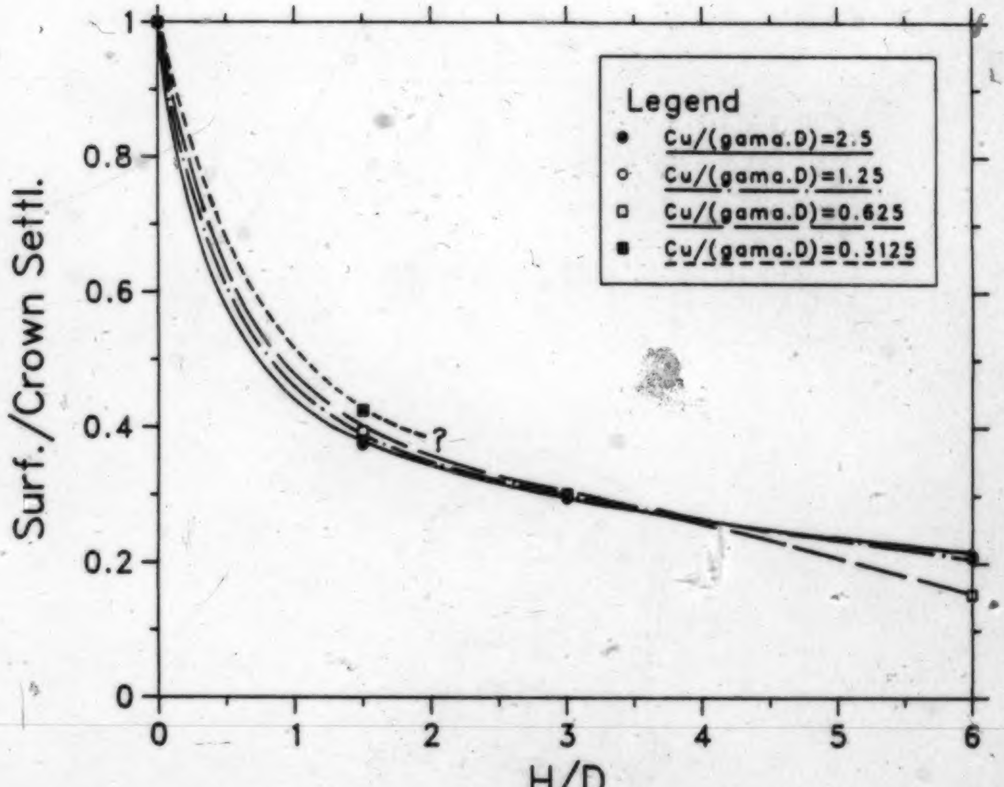

Figure 6.73 Relationships between Normalized Maximum Surface Settlement and Relative Depth of Tunnel, Calculated for the Frictionless Soil Model, for 30% Stress Release

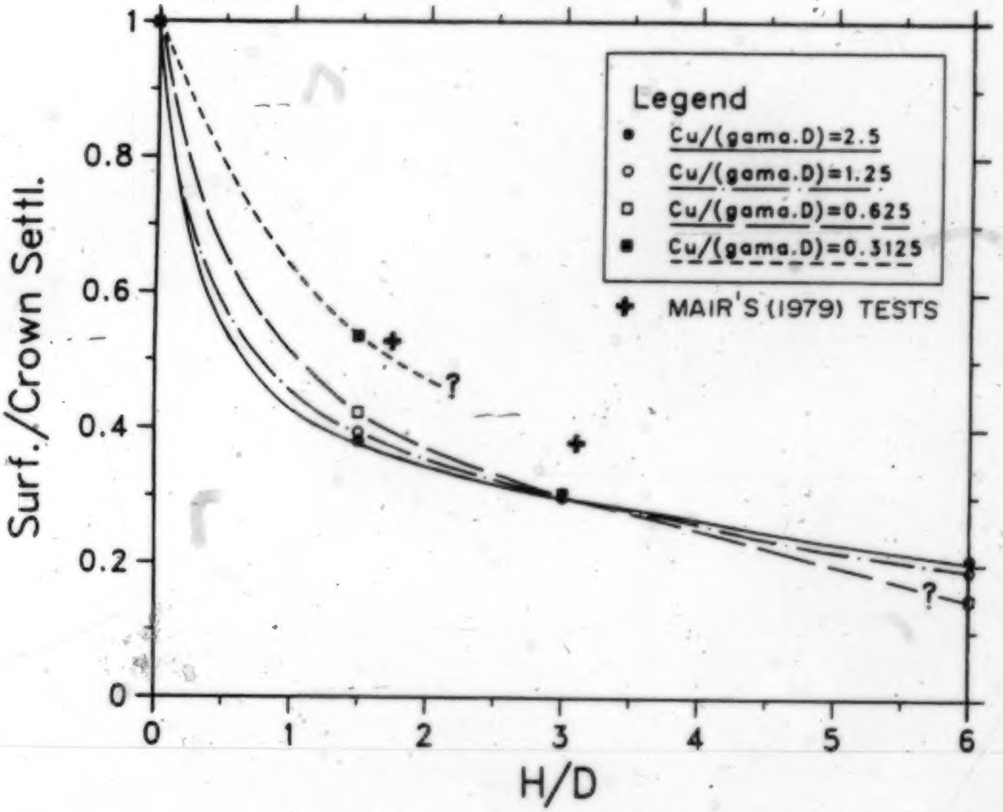

Figure 6.74 Relationships between Normalized Maximum Surface Settlement and Relative Tunnel Depth, Calculated for the Frictionless Soil Model, for 50% Stress Release

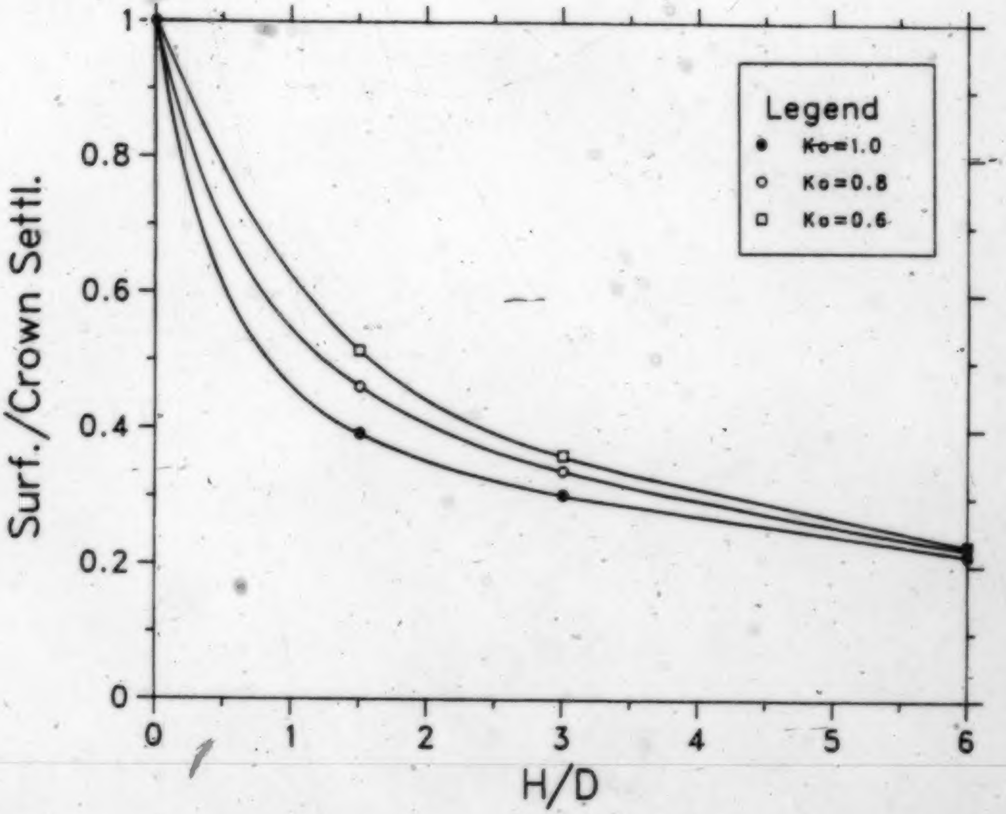

Figure 6.75 Normalized Settlement Ratios for $\phi=40°$ and 30% Stress Release

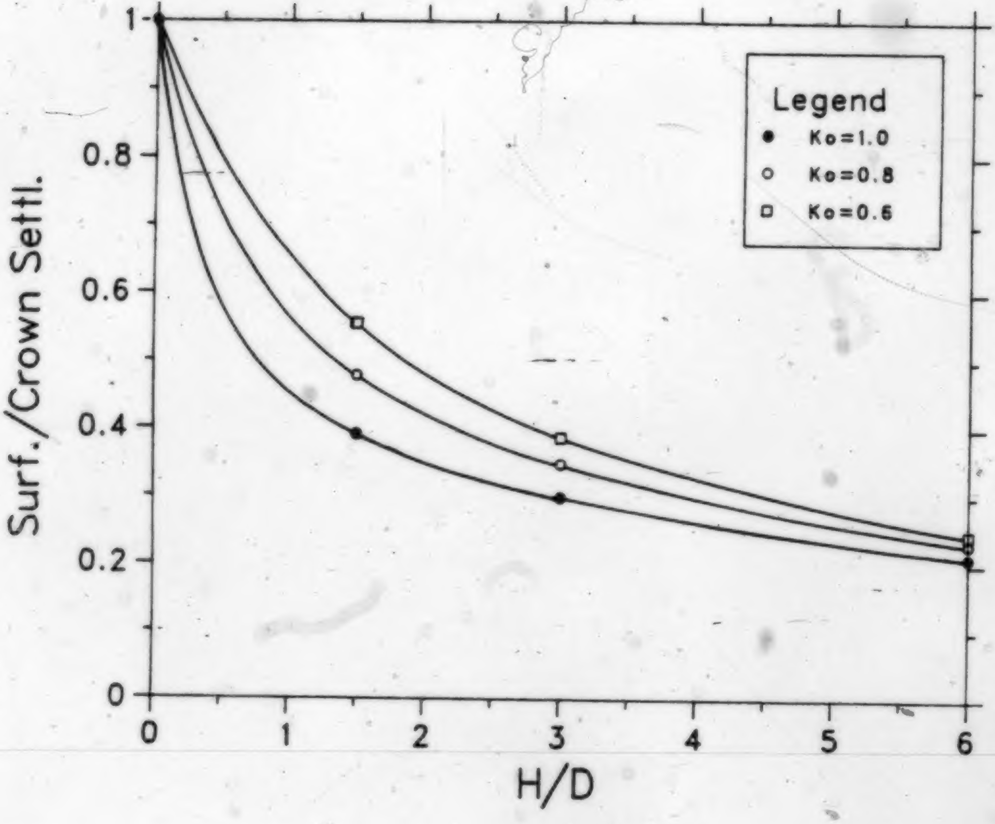

Figure 6.76 Normalized Settlement Ratios for $\phi=40°$ and 50% Stress Release

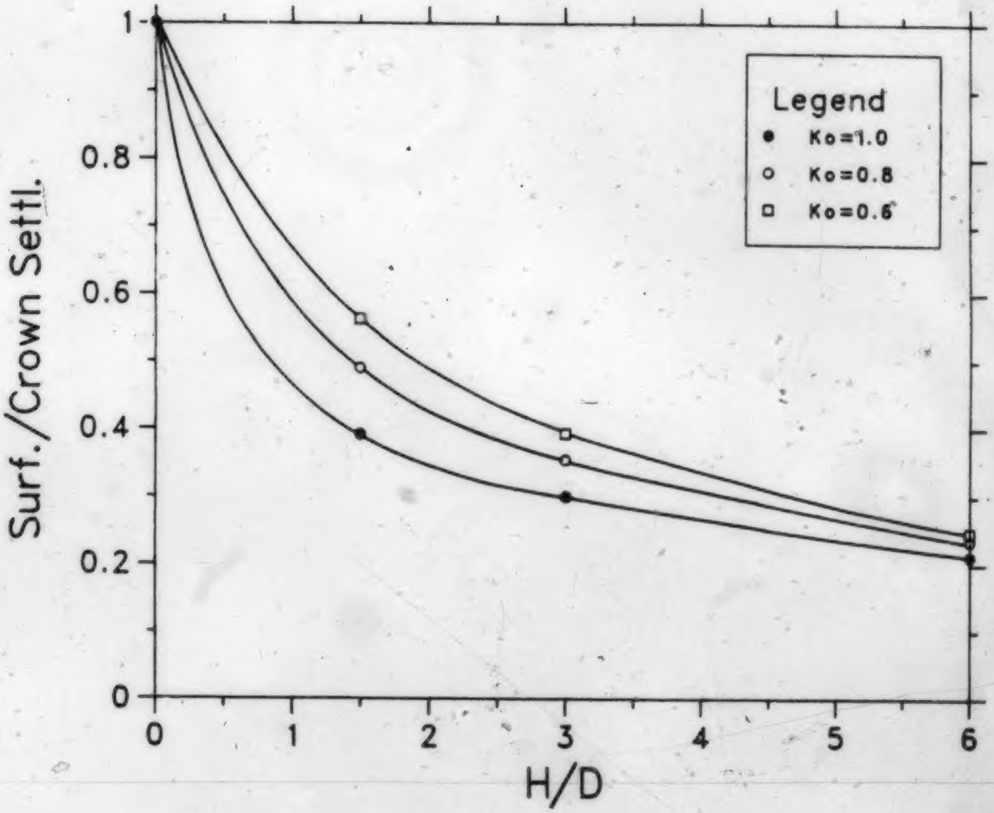

Figure 6.77 Normalized Settlement Ratios for $\phi=30°$ and 30% Stress Release

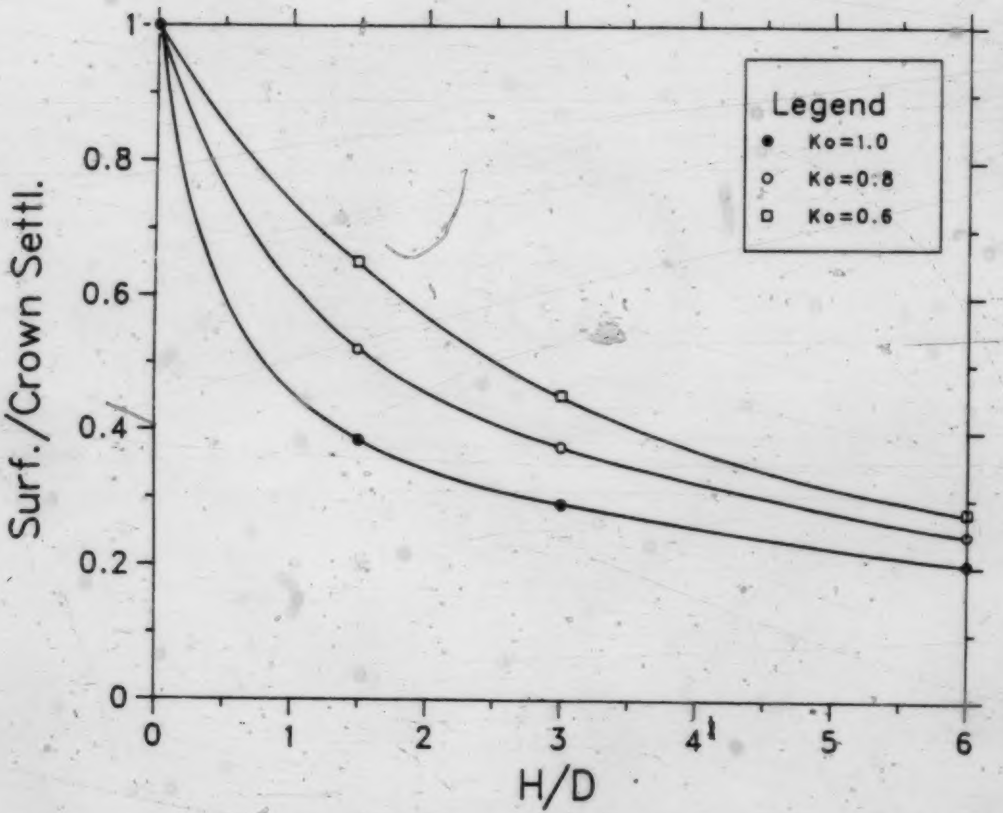

Figure 6.78 Normalized Settlement Ratios for $\phi=30°$ and 50% Stress Release

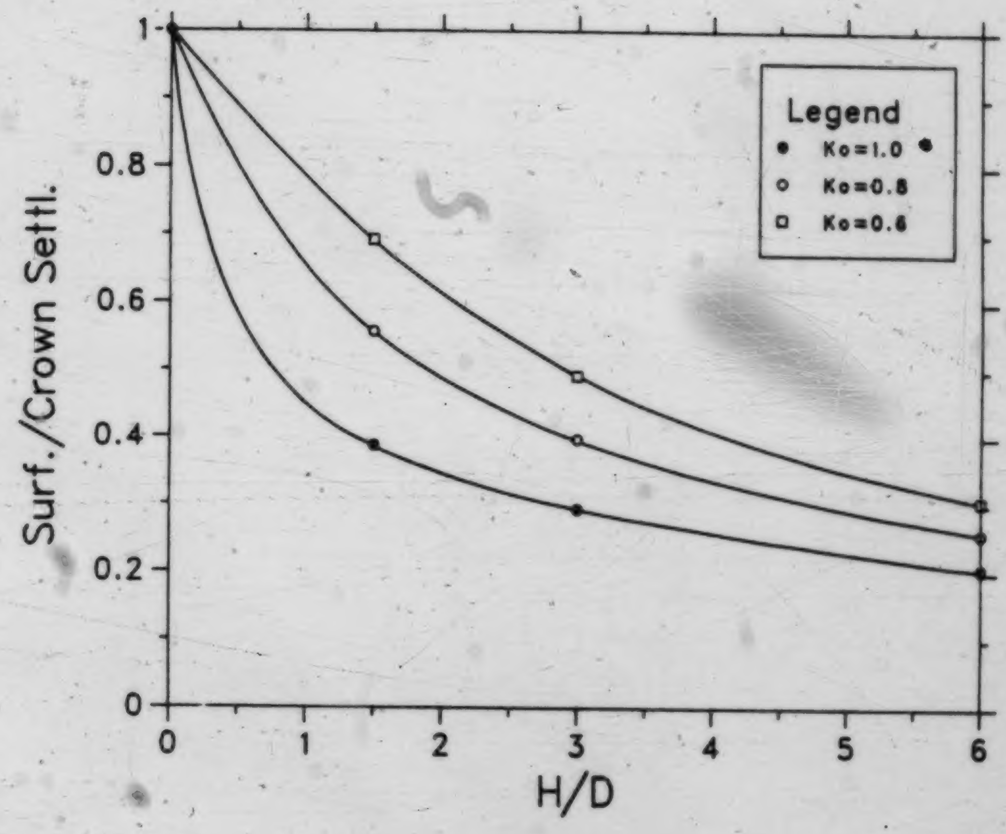

Figure 6.79 Normalized Settlement Ratios for ϕ=20° and 30% Stress Release

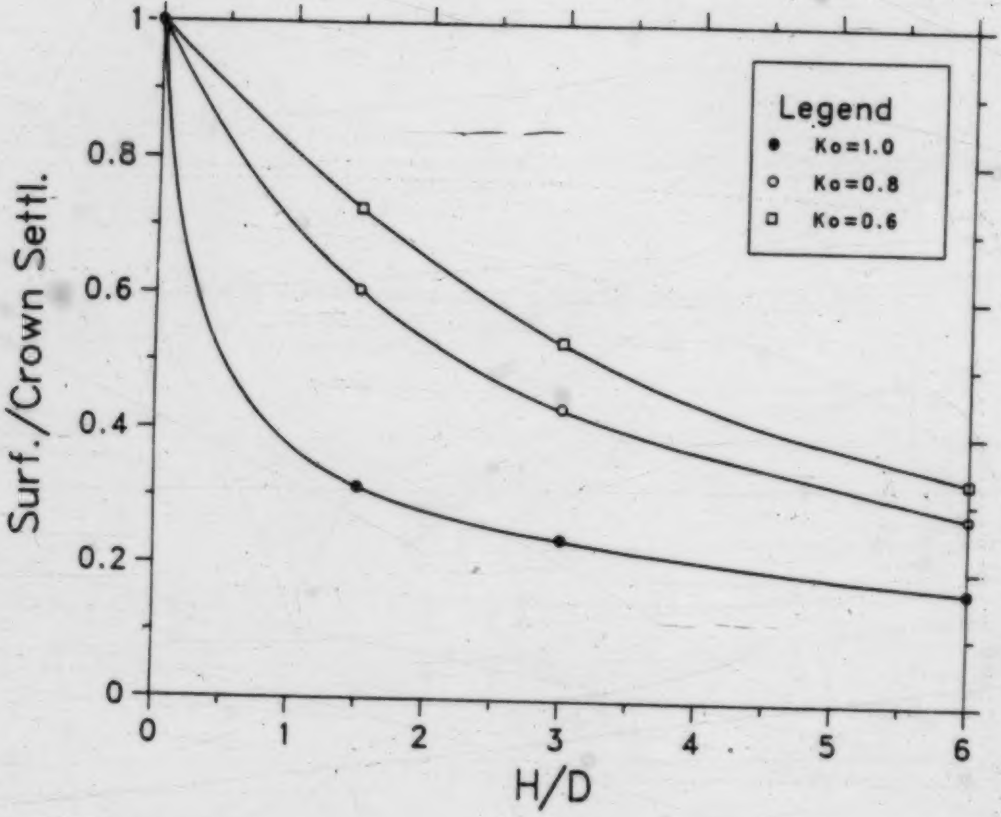

Figure 6.80 Normalized Settlement Ratios for $\phi=20°$ and 50% Stress Release

Pender (1981:267). It shows the ratios of surface to crown settlements measured by field instrumentation, plotted against the cover to diameter ratio. In most cases, the deep settlement measurements were taken somewhat above the tunnel crown. So, in general, the S/u_c ratio is larger than the actual one. Ward and Pender (Op.cit.) tried to include only short-term displacements, excluding those due to drainage, but it is doubtful whether this has been really achieved. For instance, Cases 17, 18, 24 and 25[14], are respectively, the Mexico Siphon tunnel (see Table 5.31), a tunnel in Buenos Aires, a sewer tunnel in Belfast (see Section 3.3.4.2), and the Thunder Bay tunnel (see Table 5.31 and Section 3.3.4.2) and may have, very possibly, included ground displacement caused by partial drainage and consolidation. In cases like these, one would expect to find settlement ratios larger than those experienced under time independent conditions, as assumed in the present study (see Section 3.3.4.2).

Two extreme curves are superimposed on the Ward and Pender data in Figure 6.81. These were obtained in the present study and correspond to 50% stress release, for a soil with $\phi=20°$ and $K_o=0.6$ and 1.0. It is noted that a large number of cases is bound by those two curves, which also bound a similar set of data collected by Heinz (1984:49) of NATM case histories (not shown). This may not be claimed as

---

[14] For identification of the cases numbered in Figure 6.81, the reader is referred to Table 1 in Ward and Pender, (1981:266, 267).

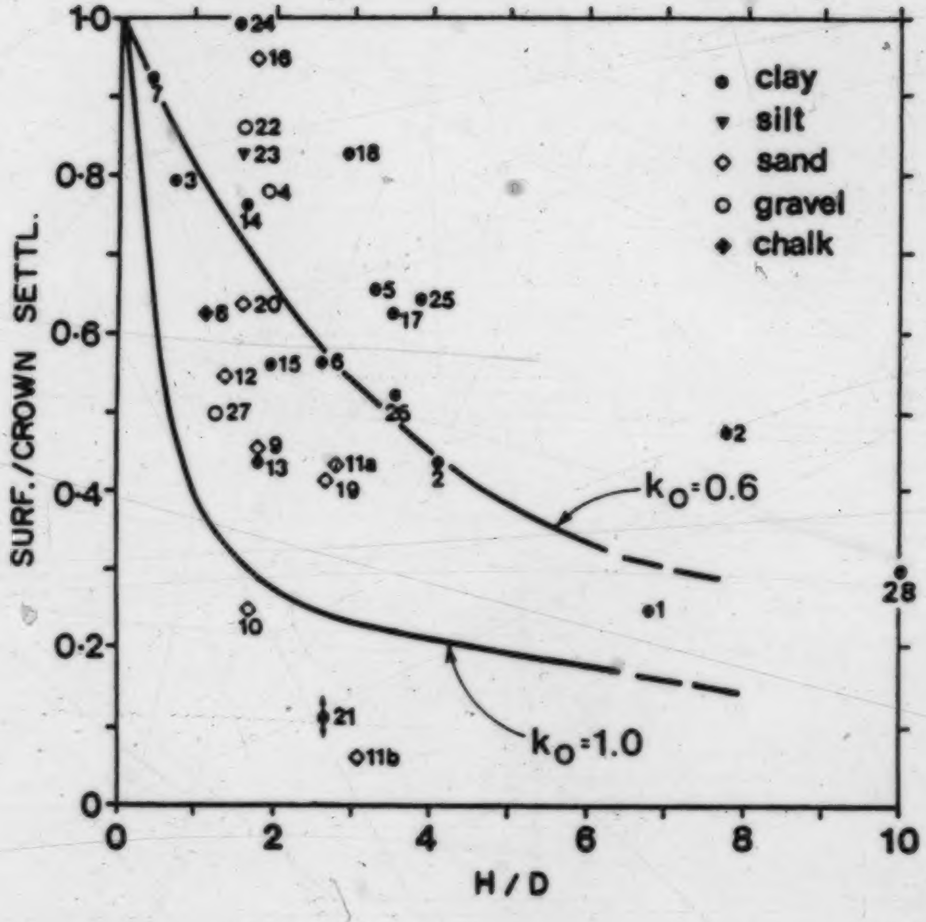

Note: See Ward and Pender (1981:266) for identification of the case histories.

Figure 6.81 Normalized Settlement Ratios Observed in some Case Histories

a proof of the validity of the presently proposed settlement ratios relationships. However, the relationships derived herein may be used to explain the apparently chaotic set of field data shown in Figure 6.81. The scatter of data can possibly be elucidated in terms of differences in K_o, in soil strength and in the amounts of stress release associated with the different case histories.

In Section 5.2.1.2, it was mentioned that a linear elastic finite element back analysis of a shallow tunnel case history could lead to either an overestimate or an underestimate of the maximum surface settlement, whenever a match in the crown displacement is achieved. Conversely, if a match between measured and backcalculated surface settlement is attained, then either an over or an underestimate of the crown settlement may be obtained. The reasons behind these statements are now, perhaps, clearer. In a linear elastic analysis, the surface to crown settlement ratio is always constant, regardless of the amount of stress release. When a non-linear response is taken into account this may not happen, as indicated by the results shown in Figure 6.71 or 6.72, or in the results shown in Appendix C. For a non-linear ground response, the surface to crown settlement ratios can either increase or decrease, with respect to the decreasing stress ratio, Σ. It depends on the type of soil model being considered (the 'undrained' - frictionless soil model, or the 'drained' - cohesionless soil model), on the cover to diameter ratio, on the in situ stress ratio and on the soil strength. These facts explain the above statements and the comments included in Section 5.2.1.2 regarding Figures 5.6 and 5.7. Note that in Figures 6.71 and 6.72, the starting points at Σ=0.9, for all curves shown (after the first 10% of ground stress release), give the settlement ratios for linear elastic analyses under the conditions considered. The ground response after the first unloading increment, as calculated by the present piecewise elastic numerical solution, is identical to the result a linear elastic analysis would yield.

6.4 Generalization of the Results

6.4.1 Opening Remarks

In this section, an attempt will be made to achieve the objective established in Section 6.1: the development of a general procedure that would allow the ground reaction curves or stress release curves of shallow tunnels to be obtained, without the need of additional finite element analyses.

The parametric analyses that were carrried out allowed those curves to be obtained for certain specific conditions, defined in terms of soil properties (for example, a particular soil strength) or geometry (H/D). In practice, conditions differing from those will normally be found and interpolation between the NGRCs obtained will usually be required. If some general expression, such as that given by equations 6.11 or 6.12, could be obtained, then the problem would be simplified. Moreover, if some practical situation is found to lie beyond the range of the variables considered, one may attempt an extrapolation of the results of the parametric analyses through these expressions. This could involve some degree of uncertainty and may yield unreliable results, if certain conditions are not fulfilled. Some of these conditions will be discussed later.

The generalization of the NGRC will be developed separately for the frictionless soil model representing an undrained soil response, and for the cohesionless soil model representing a drained soil response.

6.4.2 Frictionless Soil Model

It was anticipated in Section 6.3.2.1 that, for a given cover to diameter ratio, the NGRCs of points of the tunnel contour for different undrained strength ratios, are nearly homothetic. This can be demonstrated taking, for example, the results shown in Figures 6.54 to 6.56. Assume that the origin of the NGRCs, point O, defined by the stress release, $a=1-\Sigma=0$ and the dimensionless displacement $U=0$, is the centre of similitude. Through O, draw an arbitrary axis OP. The point P can be taken, for instance, as the extreme point of the NGRC for $c_u/\gamma D=2.5$. The line OP will intersect the NGRC for $c_u/\gamma D=0.625$ and 1.25 at points M and N. Read the coordinates of points M, N and P. For instance, for the NGRC of the tunnel crown (Figure 6.54), these coordinates are those shown in Table 6.10. Then use these coordinates as reference values and normalize each of the NGRCs to each corresponding reference value. In other words, replot the results of the numerical analysis with the normalized coordinates a/a_{ref} and U/U_{ref}. If this procedure is applied to the curves for the tunnel crown, Figure 6.54 will be reduced to that shown in Figure 6.82. One notes that the twice normalized ground reaction curves (NNGRC) virtually coincide (Points M, N and P of Figure 6.54 do coincide in Figure 6.82), and it is said that the original NGRCs (Figures 6.54) were nearly homothetic. If they were perfectly homothetic, then they would coincide exactly. Rigorously, this is not the case but, for all practical purposes it can be said that they do coincide.

Moreover, if it is attempted to find out what function fits best the points shown in Figure 6.82, it is soon found that a hyperbola can be quite well adjusted through them. The NNGRC could then be expressed as:

$$a/a_{ref} = (1-\Sigma)/(1-\Sigma_{ref}) = \frac{U/U_{ref}}{a + b\ U/U_{ref}} \qquad [6.16]$$

This function presents two advantages. It has a finite limiting value when U/U_{ref} tends to infinity, as a ground reaction curve should have when a tunnel collapse condition is approached. Secondly, the hyperbola can be transformed into a linear function (see Figure 5.10) and a linear regression analysis can be applied to the transformed normalized points. If this transformation of coordinates is

Position	$C_u/\gamma D$	$\alpha_{ref} = 1-\Sigma_{ref}$	U_{ref}	$\frac{\alpha_{ref}}{U_{ref}}$	a	b	r
Crown	2.5	0.700	0.9930	0.7049	0.6444	0.3253	0.9977
	1.25	0.382	0.5419	0.7049			
	0.625	0.220	0.3121	0.7049			
Springline	2.5	0.700	0.7290	0.9602	0.6575	0.3255	0.9990
	1.25	0.382	0.3978	0.9602			
	0.625	0.220	0.2291	0.9603			
Floor	2.5	0.700	0.5260	1.3308	0.6351	0.3536	0.9999
	1.25	0.382	0.2870	1.3308			
	0.625	0.220	0.1653	1.3309			

Table 6.10 Parameters used and Obtained in the Reduction of the Twice Normalized Ground Reaction Curves for the Frictionless Soil Model, for H/D=3

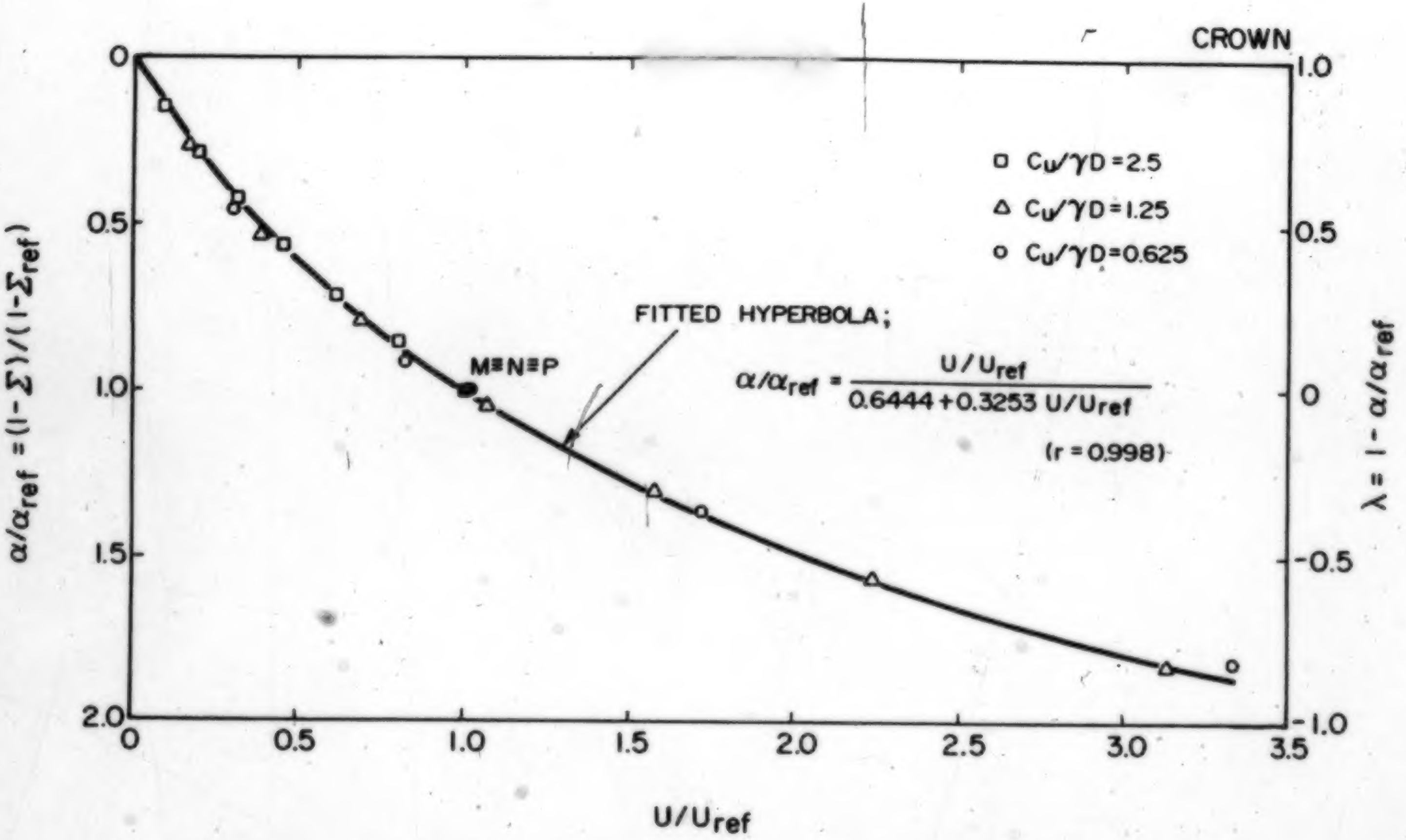

Figure 6.82 Twice Normalized Ground Reaction Curve (NNGRC) for the Crown of a Tunnel with H/D=3, for the Frictionless Soil Model

made and a linear regression is undertaken for the data shown in Figure 6.82, then it is found that the coefficients in equation 6.16 are:

$a = 0.6444$

$b = 0.3253$

and that the correlation coefficient is:

$r = 0.9977$

which is an indication of the goodness of the fit. The fitted hyperbola representing the NNGRC was superimposed on Figure 6.82 and it is seen that the function found for the tunnel crown does fit the transformed numerical results quite well.

If the above process is repeated for the springline and floor curves, then the twice normalized curves shown in Figures 6.83 and 6.84 are obtained. The reference values used for normalizing these curves are also shown in Table 6.10. Note that for each point of the tunnel contour, the ratio α_{ref}/U_{ref} should be constant, as it represents the slope of the selected axis OP used in the transformation process. If the fitted hyperbolae shown in Figures 6.82 to 6.84 are compared, one notes that they come very close together but do not coincide.

If the above procedures are repeated for the other relative tunnel depths considered, then Tables 6.11 and 6.12 are similarly obtained for H/D=1.5 and 6 respectively. In all cases, the correlation coefficient, r, was found to be larger than 0.99, indicating that a good fit was obtained in

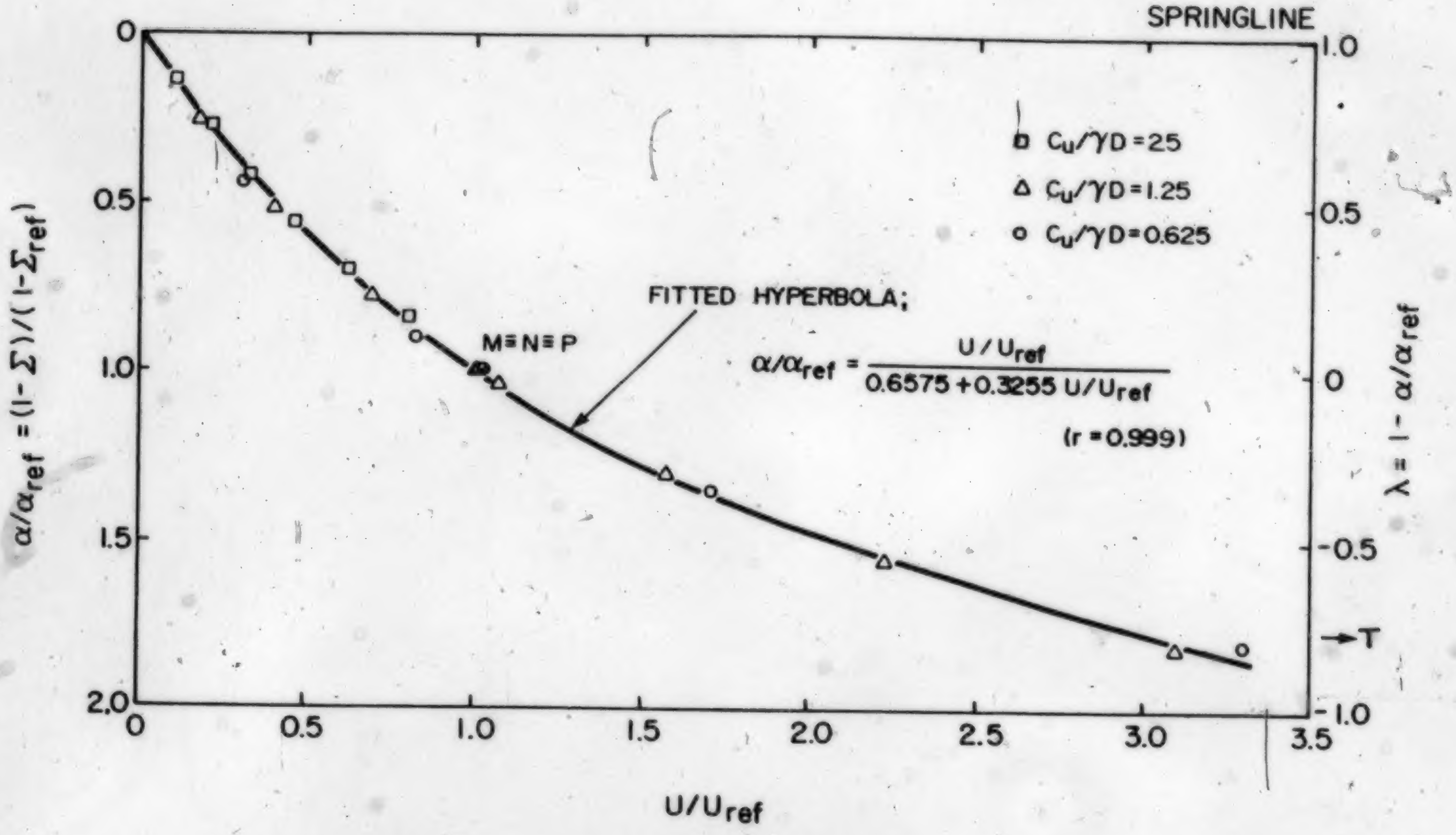

Figure 6.83 Twice Normalized Ground Reaction Curves (NNGRC) for the Springline of a Tunnel with H/D=3, for the Frictionless Soil Model

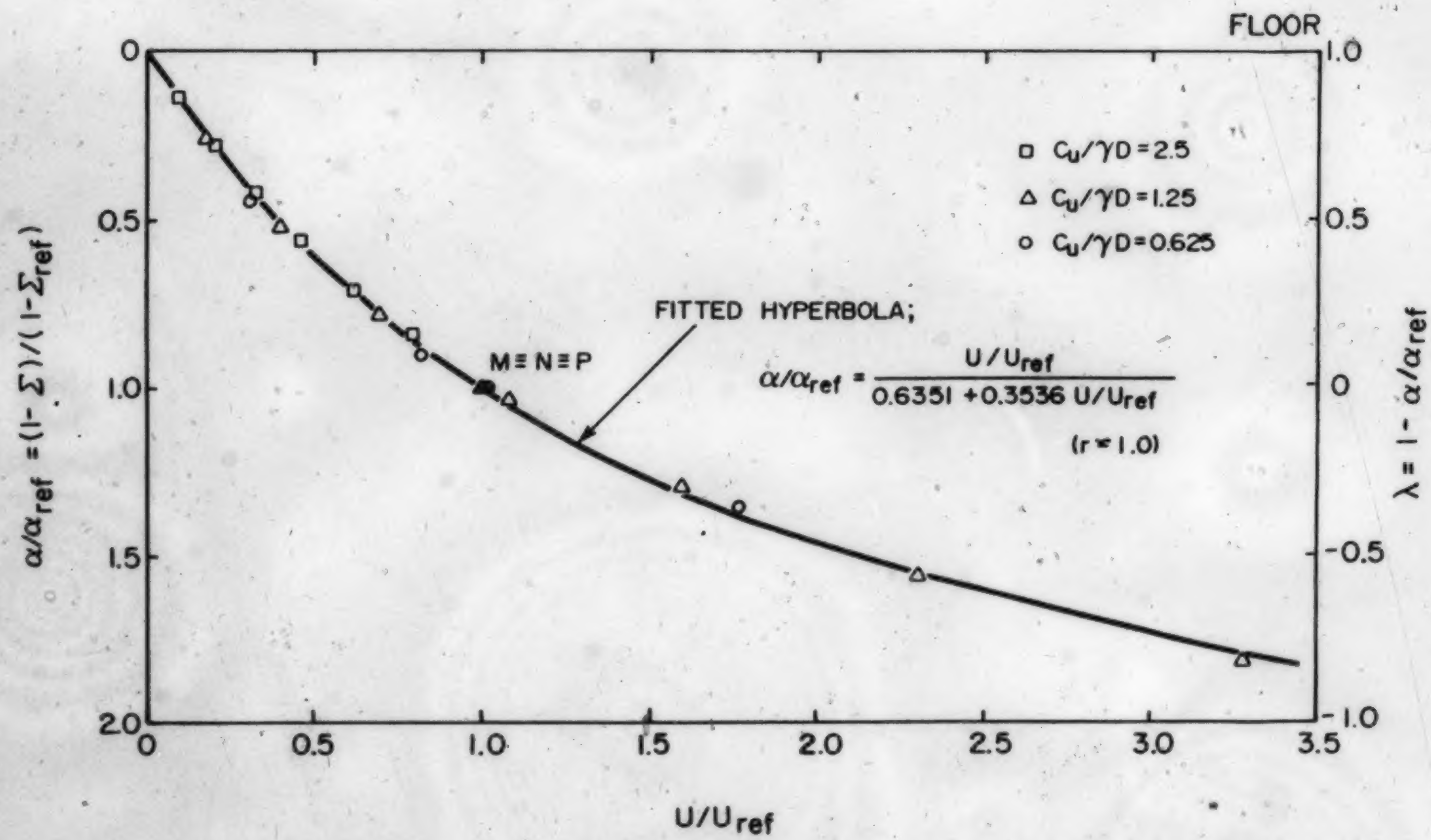

Figure 6.84 Twice Normalized Ground Reaction Curves (NNGRC) for the Floor of a Tunnel with H/D=3, for the Frictionless Soil Model

all situations.

In order to eliminate the arbitrary reference values appearing in equation 6.16, it can be further transformed as below:

$$\alpha = \frac{\alpha_{ref}}{U_{ref}} \cdot \frac{U}{a + b\,U/U_{ref}}$$

Thus:

$$\alpha = 1 - \Sigma = \frac{U}{[a/(\alpha_{ref}/U_{ref})] + [b/\alpha_{ref}].U}$$

or:

$$\Sigma = 1 - \frac{U}{A + B.U} \qquad [6.17]$$

where

$A = a/(\alpha_{ref}/U_{ref})$

$B = b/\alpha_{ref}$

The newly defined parameters can be calculated from Tables 6.10 to 6.12 and thus Table 6.13 is obtained.

The coefficient A is independent of the strength ratio and Figure 6.85 shows how A varies with the relative depth of the tunnel, for three points of the tunnel contour. The coefficient B for each point of the tunnel contour is found to vary with both the soil strength and the tunnel depth. Figures 6.86 to 6.88 summarize these dependencies. In each of these figures, in order to facilitate the interpolation of B for intermediate values of strength or depth ratios, the coefficient B has been plotted against the strength ratio, for constant H/D values (solid lines) and against the depth ratio, for constant $c_u/\gamma D$ values (broken lines).

Equation 6.17 and charts given in Figures 6.85 to 6.88, represent the proposed generalized solution for obtaining

Position	$C_u/\gamma D$	$\alpha_{ref} = 1-\Sigma_{ref}$	U_{ref}	$\frac{\alpha_{ref}}{U_{ref}}$	a	b	r
Crown	2.5	0.600	0.7390	0.8119	0.7218	0.2803	0.9936
	1.25	0.345	0.4250	0.8118			
	0.625	0.219	0.2698	0.8117			
	0.3125	0.152	0.1872	0.8119			
Springline	2.5	0.600	0.5000	1.2000	0.7349	0.2693	0.9928
	1.25	0.360	0.3000	1.2000			
	0.625	0.216	0.1800	1.2000			
	0.3125	0.150	0.1250	1.2000			
Floor	2.5	0.600	0.3520	1.7045	0.7250	0.2693	0.9970
	1.25	0.3389	0.1988	1.7047			
	0.625	0.2087	0.1224	1.7045			
	0.3125	0.1337	0.0784	1.7045			

Table 6.11 Parameters used and Obtained in the Reduction of the Twice Normalized Ground Reaction Curves for the Frictionless Soil Model for H/D=1.5

Position	$C_u/\gamma D$	$\alpha_{ref} = 1-\Sigma_{ref}$	U_{ref}	$\frac{\alpha_{ref}}{U_{ref}}$	a	b	r
Crown	2.5	0.700	1.4470	0.4838			
	1.25	0.382	0.7896	0.4838	0.4540	0.5090	0.9980
	0.625	0.220	0.4548	0.4837			
Springline	2.5	0.700	1.1010	0.6358			
	1.25	0.382	0.6008	0.6358	0.4628	0.4969	0.9969
	0.625	0.220	0.3460	0.6358			
Floor	2.5	0.700	0.8220	0.8516			
	1.25	0.382	0.4486	0.6515	0.4598	0.5322	0.9993
	0.625	0.220	0.2583	0.8517			

Table 6.12 Parameters Used and Obtained in the Reduction of the Twice Normalized Ground Reaction Curves for the Frictionless Soil Model for H/D=6

Position	H/D	$C_u/\gamma D$	$\frac{\alpha_{ref}}{U_{ref}}$	a	$A = \frac{a}{\alpha_{ref}/U_{ref}}$	α_{ref}	b	$B = b/\alpha_{ref}$
Crown	1.5	2.5				0.600		0.4672
		1.25				0.345		0.8125
		0.625	0.8118	0.7218	0.8891	0.219	0.2803	1.2799
		0.3125				0.152		1.8441
	3.0	2.5				0.700		0.4647
		1.25	0.7049	0.6444	0.9142	0.382	0.3253	0.8516
		0.625				0.220		1.4786
	6.0	2.5				0.700		0.7271
		1.25	0.4838	0.4540	0.9384	0.382	0.5090	1.3325
		0.625				0.220		2.3136
Springline	1.5	2.5				0.600		0.4488
		1.25				0.360		0.7481
		0.625	1.2000	0.7349	0.6124	0.216	0.2693	1.2468
		0.3125				0.150		1.7953
	3.0	2.5				0.700		0.4650
		1.25	0.9602	0.6575	0.6848	0.382	0.3255	0.8521
		0.625				0.220		1.4795
	6.0	2.5				0.700		0.7099
		1.25	0.6358	0.4628	0.7279	0.382	0.4969	1.3008
		0.625				0.220		2.2586
Floor	1.5	2.5				0.600		0.4488
		1.25				0.339		0.7946
		0.625	1.70457	0.7250	0.4253	0.209	0.2693	1.2904
		0.3125				0.134		2.0142
	3.0	2.5				0.700		0.5051
		1.25	1.3308	0.6351	0.4772	0.382	0.3536	0.9257
		0.625				0.220		1.6073
	6.0	2.5				0.700		0.7603
		1.25	0.8516	0.4598	0.5399	0.382	0.5322	1.3932
		0.625				0.220		2.4191

Table 6.13 Parameters Obtained in the Reduction of the Twice Normalized Ground Reaction Curves for the Frictionless Soil Model

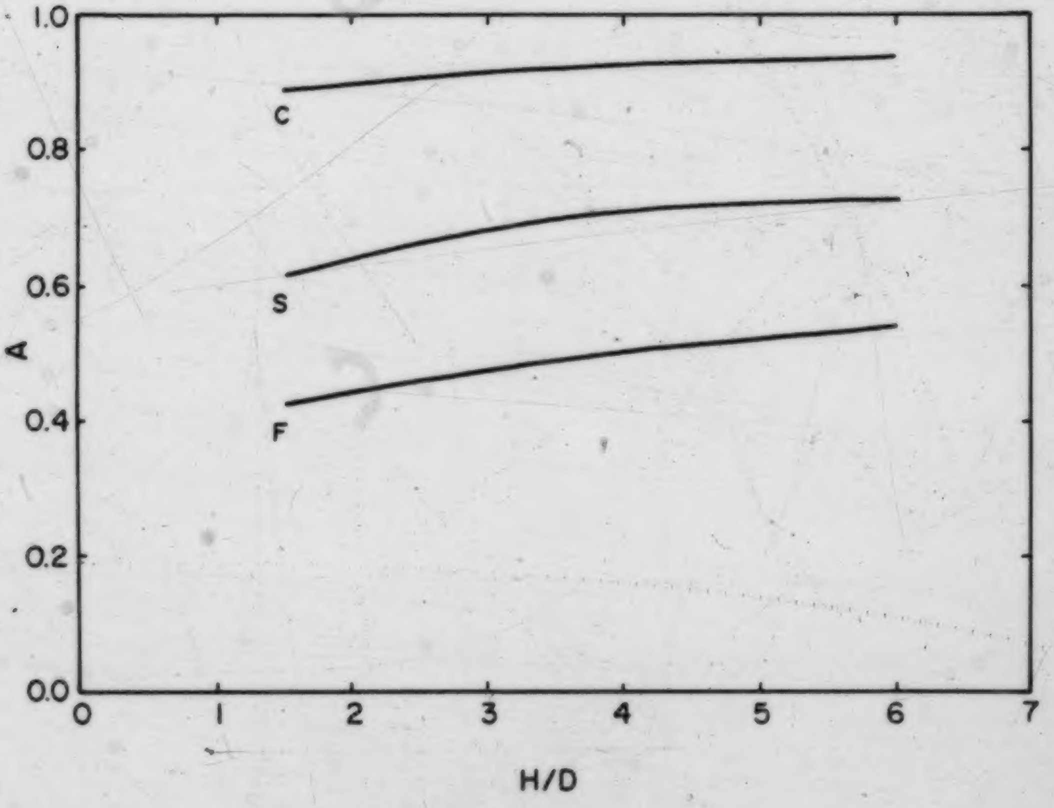

NOTE : C = CROWN , S = SPRINGLINE , F = FLOOR

Figure 6.85 Variation of the Coefficient A with Relative Tunnel Depth, for the Frictionless Soil Model

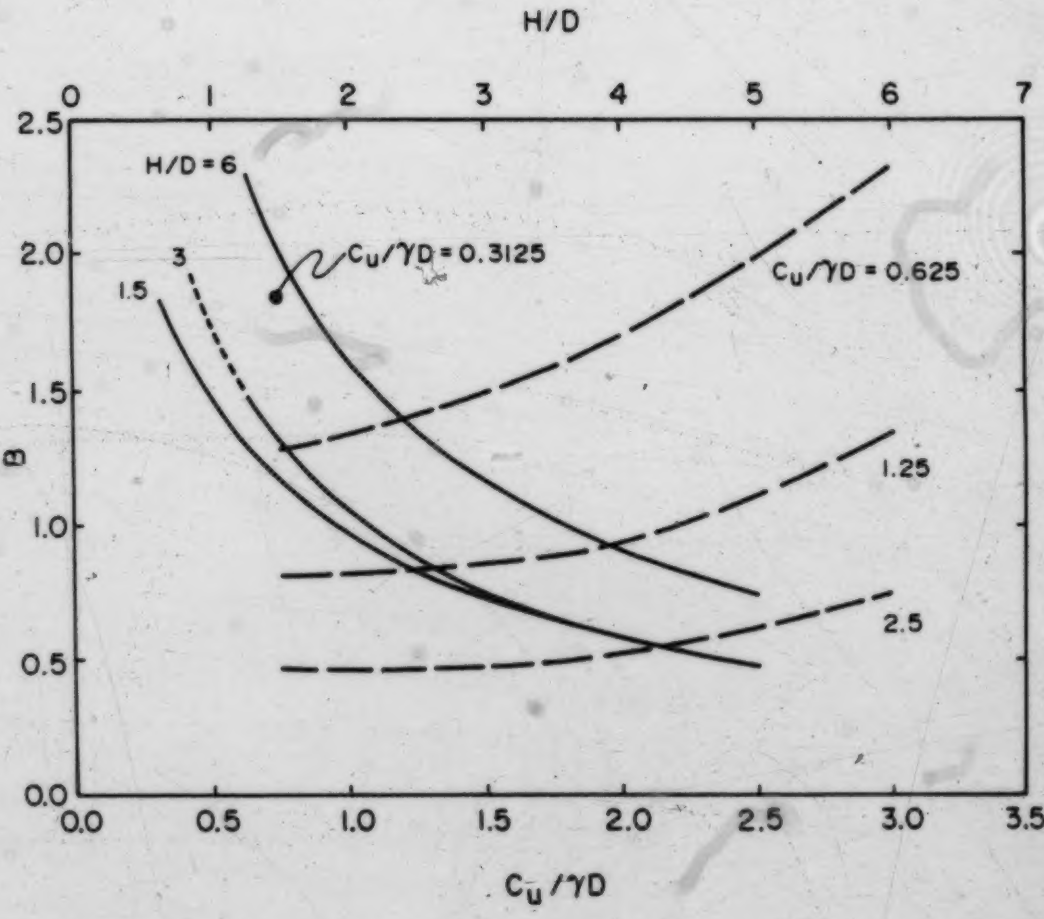

Figure 6.86 Variation of the Coefficient B, for the Tunnel Crown, with Strength and Depth Ratios, Calculated for the Frictionless Soil Model

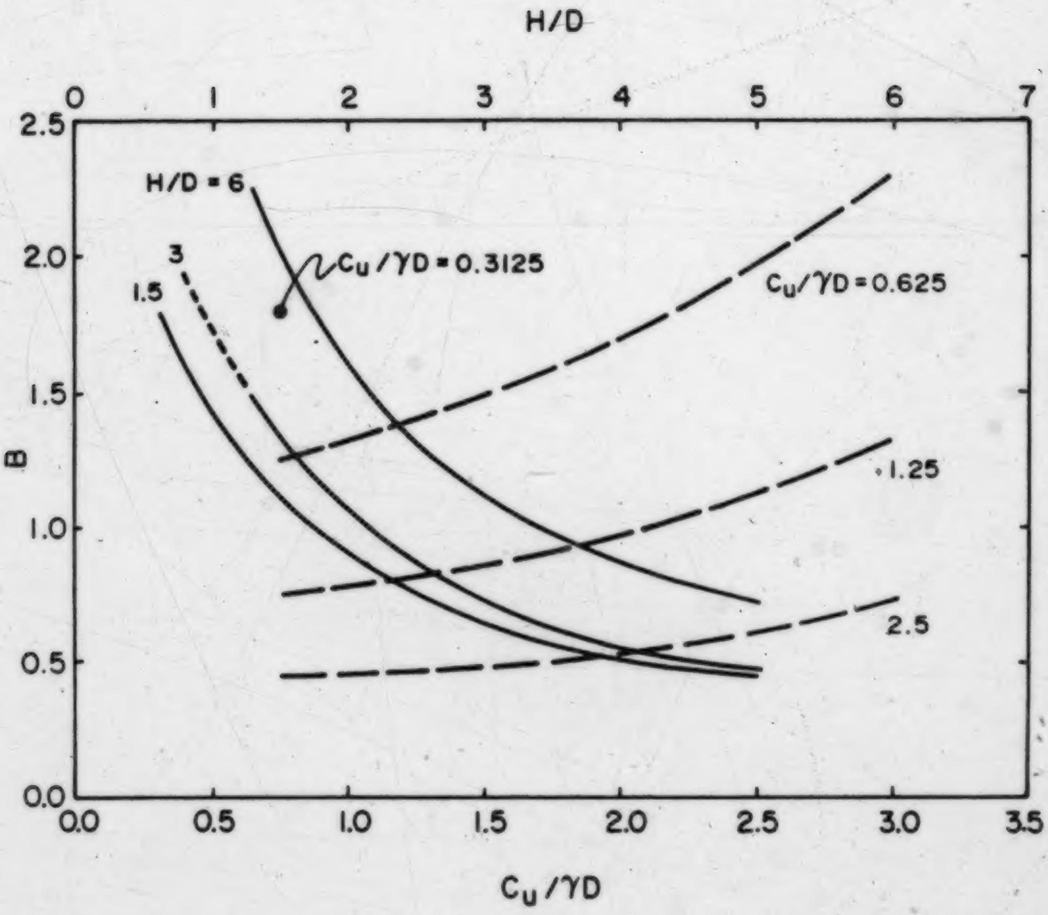

Figure 6.87 Variation of the Coefficient B for the Tunnel Springline, with Strength and Depth Ratios, Calculated for the Frictionless Soil Model

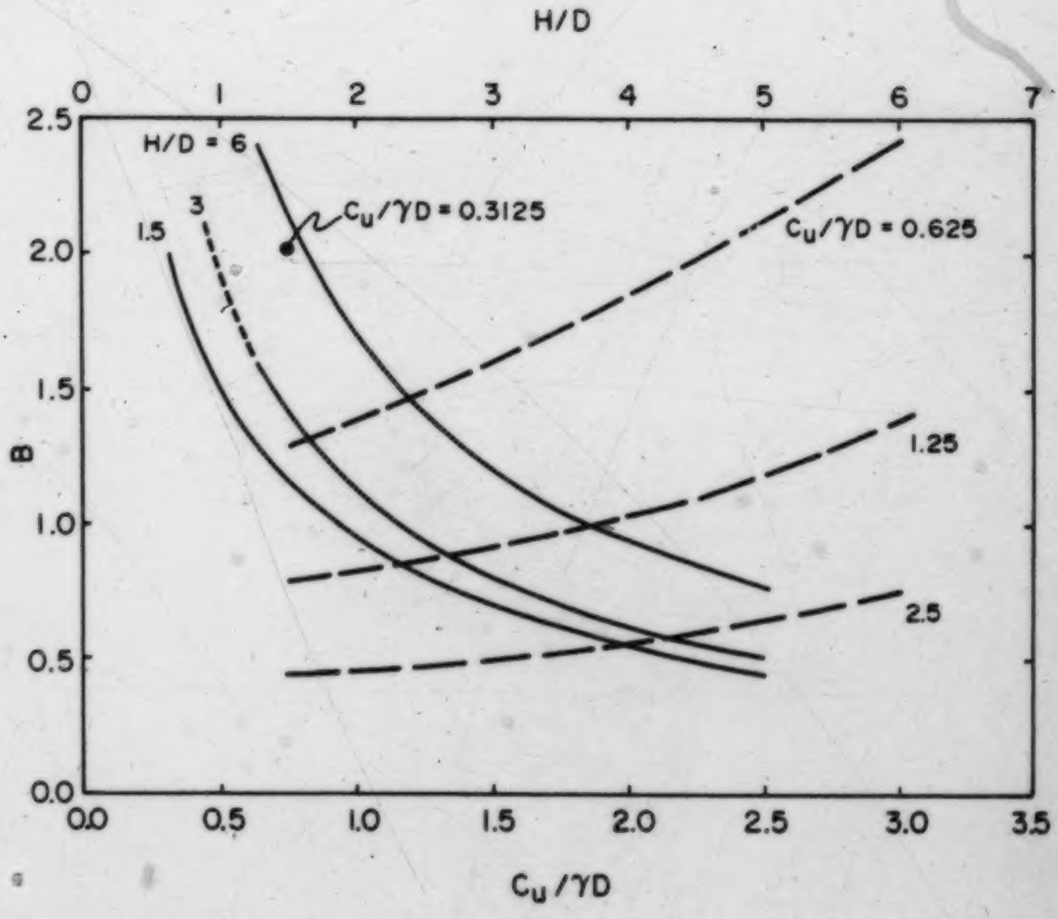

Figure 6.88 Variation of the Coefficient B for the Tunnel Floor, with Strength and Depth Ratios, Calculated for the Frictionless Soil Model

the ground reaction curves for three points on the contour of a shallow tunnel in a soil represented by the frictionless model (equation 6.12). Both coefficients, A and B have some physical meaning. The above solution was designed for applications within the common ranges of variables defined in Section 6.2.5 and its validity is not suggested to hold beyond those ranges. However, it seems interesting to investigate the limits of the solution, in order to assess the physical meaning of the coefficients A and B, in simple qualitative terms.

In the limit for U approaching infinity, equation 6.17 becomes:

$$\Sigma_u = 1 - \frac{1}{B} \qquad [6.18]$$

This would be the limiting stress ratio acting on the opening at a condition of very large radial displacements. One notes that Σ_u does not depend on A, but only on B, which in turn is a function of the soil strength and of the depth of the tunnel. Thus, B is a parameter reflecting the ultimate state of the tunnel at collapse. Since B is related to a limiting stress at tunnel collapse, it should depend on the ground strength and on the tunnel depth, as indicated by any limit analyses solution applied to shallow tunnels.

Moreover, for constant H/D and $c_u/\gamma D$ approaching infinity, Figures 6.86 to 6.88 suggest that B tends towards zero. Under these conditions, for U tending towards infinity, equation 6.18 indicates that Σ_u would tend towards an infinitely large and negative value, which indeed would be required in such infinitely strong ground to cause its collapse. On the other hand, for H/D constant and $c_u/\gamma D$ tending to zero, Figures 6.86 to 6.88 suggest that B would tend towards infinity. Thus, for U approaching infinity, Σ_u would tend towards unity. This is again a consistent result for an extremely weak ground, which would collapse under any amount of stress release at the opening. A similar result is obtained by making $c_u/\gamma D$ constant and H/D increasing towards infinity. In this case, B would also tend to infinity and Σ_u to unity. The extremely high in situ stress in such a deep tunnel, driven through a soil of finite strength, would lead to collapse for any amount of stress release at the opening.

The coefficient A reflects the in situ stiffness of the ground. The partial derivative function of equation 6.17 is easily found as:

$$\Sigma' = \frac{\delta\Sigma}{\delta U} = \frac{A}{(A+BU)^2} \qquad [6.19]$$

in which the negative sign of the partial derivative has been dropped. For zero displacement, the slope of the NGRC is found to be equal to 1/A. In other words, the coefficient A is inversely proportional to the in situ stiffness of the ground, as reflected by the initial slope of the ground reaction curves at each point of the tunnel contour. As noted in Section 6.3.2.1, and illustrated in Figure 6.47, for a constant in situ tangent modulus profile, the initial slope of the NGRC decreases from the tunnel floor towards the crown. This result reflects the 'stiffening' action of the lower boundary, affecting the floor reaction and the 'softening' action of the free ground surface allowing the ground at the crown to move more freely towards the opening upon the stress release. The initial slope of the springline curve should thus show an intermediate initial slope. Accordingly, the coefficient A should not depend on soil strength, as it indeed does not, but should depend on the position of the ground surface, which is manifested by its dependence on H/D, as shown in Figure 6.85. Furthermore, from the above discussion one would expect to get a larger A for the crown and a smaller one for the floor, as is the case.

Besides supplying components for the prediction of the ground reaction curves, the general solution may also provide a means to estimate the degree of 'softening' of the ground around the tunnel upon the reduction of the in situ stresses. This is particularly relevant in assessing the 'current' ground stiffness to be considered in a ground-lining interaction analyses. As the support is activated after some tunnel closure has developed, the interaction process will be controlled not by the initial ground stiffness, but by that existing at the instant the lining is installed. The effect of the ground 'softening', as a result of unloading, on the ground-lining interaction process was presented and discussed in Section 2.3.5.3.

If the ground-lining interaction analysis is to be performed using a ring-and-spring model, such as reviewed in Section 4.3.2.4, one would need to know, for instance, what radial spring constant (k_r) should be adopted to account for the non-linear response of the ground and its associated degree of ground 'softening', taking place before the support is activated. Since the stress ratio is $\Sigma=\sigma_r/\sigma_{ro}$ and $U=u_r E_{ti}/\sigma_{ro}.D$, it follows that the partial derivative of Σ is given by:

$$\Sigma' = \frac{\delta\Sigma}{\delta U} = \frac{D}{E_{ti}}\,\frac{\delta\sigma_r}{\delta u_r}$$

But $\delta\sigma_r/\delta u_r$ is the radial spring constant (k_r) as defined in Section 4.3.2.4. Therefore:

$$k_r = \Sigma'\,\frac{E_{ti}}{D}$$

Using equation 6.19, one gets:

$$k_r = \frac{A}{(A+BU)^2}\,\frac{E_{ti}}{D} \qquad [6.20]$$

The above equation would thus solve the posed problem, yielding different spring constants at each point (C, S, F) of the tunnel contour.

Note that if no stress release is allowed and the radial displacements are zero, equation 6.20 would reduce to a linear elastic spring. Therefore:

$$k_{ri} = \frac{1}{A}\,\frac{E_{ti}}{D} = \frac{1}{2A}\cdot\frac{E_{ti}}{R} \qquad [6.21]$$

It was shown in Section 4.3.2.4 that if a single average radial spring constant ($\bar{k}_r$) is to be considered, as used in most ring-and-spring models, then, for a uniform E_{ti} ground profile:

$$\bar{k}_{ri} = \left(\frac{1}{2A}\right)_{av}\frac{E_{ti}}{R} \simeq \frac{1}{1+\nu}\,\frac{E_{ti}}{R}$$

thus,

$$A_{av} \simeq \frac{1+\nu}{2}$$

In fact, this approximate equation is confirmed by the results shown in Figure 6.85 or Table 6.13. Depending on H/D, A_{av} is found to vary from 0.635 to 0.734, which is not entirely dissimilar to 0.745 obtained from $(1+\nu)/2$, for $\nu=0.49$, the Poisson's ratio used in the parametric numerical analyses. For H/D increasing, A_{av} gets closer to $(1+\nu)/2$, as it should for a deep tunnel.

If the ground-lining interaction analyses is to be performed using a ring-and-plate model, such as reviewed in Section 4.3.2.3, one would need to know the current tangent Young's modulus of the ground (E_t), at the instant the support is installed. If it is assumed that this modulus is directly proportional to the spring constant (or the slope of the GRC), then:

$$\frac{E_t}{E_{ti}} = \frac{k_r}{k_{ri}}$$

Substituting equations 6.20 and 6.21 into the above, one gets:

$$E_t = \left(\frac{A}{A+BU}\right)^2 . E_{ti} \qquad [6.22]$$

Different current moduli would be found at distinct points around the tunnel contour. The available ring-and-plate solutions normally operate with constant ground modulus[17]. Thus:

$$\bar{E}_t = \left(\frac{A}{A+BU}\right)^2_{av} . \bar{E}_{ti}$$

---

[17] If a numerical ring-and-spring model with discrete beams and springs (see Section 4.3.2.4), is to be used, then different spring constants could be assigned at distinct points of the tunnel contour. This would account for the different degrees of ground 'softening' observed around the opening.

or

$$\bar{E}_t = A_{av}.\bar{\Sigma}'.\bar{E}_{ti} \simeq \frac{1+\nu}{2}\,\bar{\Sigma}'\bar{E}_{ti}$$

Any of the above expressions can be used to estimate the average current tangent modulus at the instant the support is activated.

It should be pointed out that the current tangent modulus given by equation 6.22 reflects a "weighted" average of all the ground mass affecting the ground response at a certain point of the tunnel contour. Therefore, it is neither equal to the modulus of the soil elements immediately adjacent to the opening nor to that of elements far away. A closer inspection of the results of the parametric analyses, revealed that the moduli given by equation 6.22, for a certain point of the tunnel contour, correspond approximately to the current tangent moduli of elements located radially away from the contour, at distances varying from 0.25D to 0.65D. The magnitude of this distance was found to vary according to the tunnel depth H/D and, to a lesser degree, to the amount of stress release.

As a reasonable approximation, it may be said that the moduli derived from equation 6.22 for the tunnel crown and floor, are nearly equal to the moduli of elements located, respectively, at half diameter above and below the tunnel. The springline modulus also corresponds to the modulus of an element situated at about D/2 radially measured from that point.

As stated earlier the solution presented is strictly valid only within the ranges of the variables considered in the numerical analyses that supplied the data for the generalization. Although apparently unbounded, equation 6.17 may not be valid for large amounts of stress release (or low Σ). Large dimensionless displacements U may involve ground failure. The numerical model used to develop the present solution does not represent this behaviour properly and all data obtained after this event were disregarded in the generalization process. In fact, for large displacements, the solution presented can furnish values of the stress ratio Σ that may violate the failure criteria. This subject will be discussed in Section 6.5.

6.4.3 Cohesionless Soil Model

It was mentioned in Section 6.3.2.2 that for a given cover to diameter ratio, the NGRCs of each point of the tunnel contour, for different friction angles, are nearly homothetic. This can be demonstrated considering, for example, the results shown in Figure 6.63 (crown, $K_o=0.8$, $H/D=3.0$). Assume that the origin of the NGRCs, point O, defined by the stress release $\alpha=1-\Sigma=0$ and the dimensionless displacement $U=0$, is the centre of similitude. As for the frictionless soil model (Section 6.4.2), draw through O an arbitrary axis, OP. Point P can be taken, for instance, as the point on the curve for $\phi=40°$ corresponding to $\alpha=0.7$ ($\Sigma=0.3$). The line OP will intersect the NGRC for $\phi=20°$ and

30° at points M and N. The coordinates of these points (a_{ref}, U_{ref}) are indicated in Table 6.14. Use these coordinates as reference values and normalize each NGRC in Figure 6.63 to each respective reference value. Replot the numerical results in terms of the normalized coordinates, $1 - a/a_{ref}$ and U/U_{ref}. The curves in Figure 6.63 would thus be transformed into Figure 6.89. The preferred new ordinate variable, λ, is defined as:

$$\lambda = 1 - \frac{a}{a_{ref}} = 1 - \frac{1-\Sigma}{1-\Sigma_{ref}} = \frac{\Sigma-\Sigma_{ref}}{1-\Sigma_{ref}} \qquad [6.23]$$

Note that once the results of the numerical analyses for ϕ=20°, 30° and 40°, are twice normalized as explained, a series of points are obtained and it seems possible to fit a single curve through them. The twice normalized ground reaction curves (NNGRC) are almost coincident (Points M, N and P, of course, coincide), and this confirms that the original NGRCs (Figure 6.63) are nearly homothetic.

Repeating the above process to the NGRCs of the tunnel springline and floor shown in Figures 6.64 and 6.65, then the twice normalized points of the ground reaction curves shown in Figures 6.90 and 6.91, respectively, are obtained. The reference values (points M, N, P in Figures 6.64 and 6.65) used for normalizing the numerical resullts are also shown in Table 6.14. Note that the ratios a_{ref}/U_{ref} shown represent the slope of the arbitrary axes OP used in the reduction process. As was seen for the tunnel crown, the twice normalized points of the springline and floor seem arranged in such a way that a single curve can be well

Position	ϕ (°)	α_{ref}	U_{ref}	$\frac{\alpha_{ref}}{U_{ref}}$	P_1	P_2	P_3	P_4	P_5
Crown	20	0.390	0.3911	0.9972	0.5055	0.4191	2.8752	3.6904	6.8780
	30	0.540	0.5415						
	40	0.700	0.702						
Springline	20	0.290	0.2552	1.1364	0.4197	0.5380	3.4339	2.6640	14.5739
	30	0.490	0.4312						
	40	0.700	0.6160						
Floor	20	0.400	0.1990	2.0101	0.7328	0.2234	3.8938	-3.9446	15.8681
	30	0.440	0.2189						
	40	0.490	0.2438						

Table 6.14 Parameters Used and Obtained in the Reduction of the Twice Normalized Ground Reaction Curves of a Tunnel with H/D=3, for the Cohesionless Soil Model with K_o=0.8

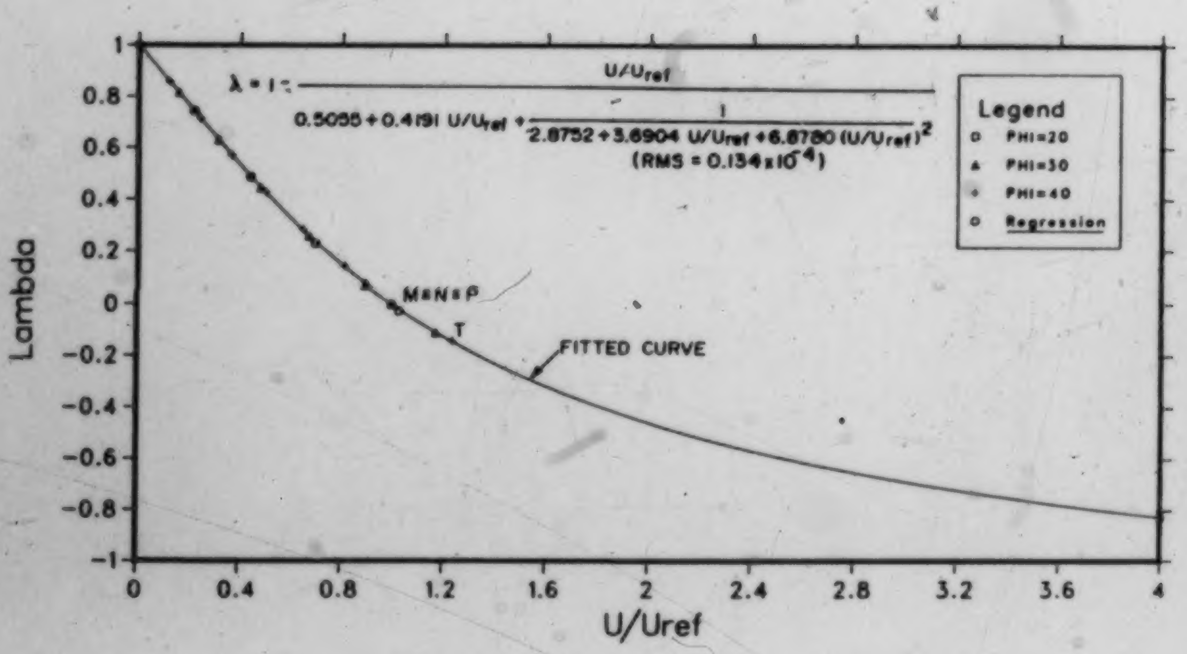

Figure 6.89 Twice Normalized Ground Reaction Curve (NNGRC) for the Crown of a Tunnel with H/D=3, for the Cohesionless Soil Model with K_o=0.8

fitted through them. Some points appear to deviate slightly from the fitted curve, but, for all practical purposes it can be said that all NGRC at different points of the tunnel contour for different friction angles, seem to be very close to homothetic, as single (but distinct) normalized NGRCs can be found for each of these points.

The next step undertaken was to define what function fits best the points shown in the last three figures. Hyperbolae such as were used to fit the data from the frictionless soil model (equation 6.16) did not yield good results. The main reason for this was that this function could not accommodate the apparent inflexion noted in the early part of the curve for the floor (See Figure 6.91) and to a lesser extent, for the crown. It has been mentioned in other sections in this chapter that, when K_o is smaller than unity, elements of the ground at the crown and floor exhibit a stiffening response, resulting from the stress changes that occur at those points (an increase in the minor principal stress). Once the direction of the principal stresses are fully changed, the ground response is again that of softening, as for the springline. A hyperbola could not, therefore, fit this response, as its derivative function is monotonic and does not show a change in sign in its second derivative.

On the other hand, it seemed reasonable to assume that the suitable function should have a definable limit, which is approached monotonically, as in the case of a hyperbola.

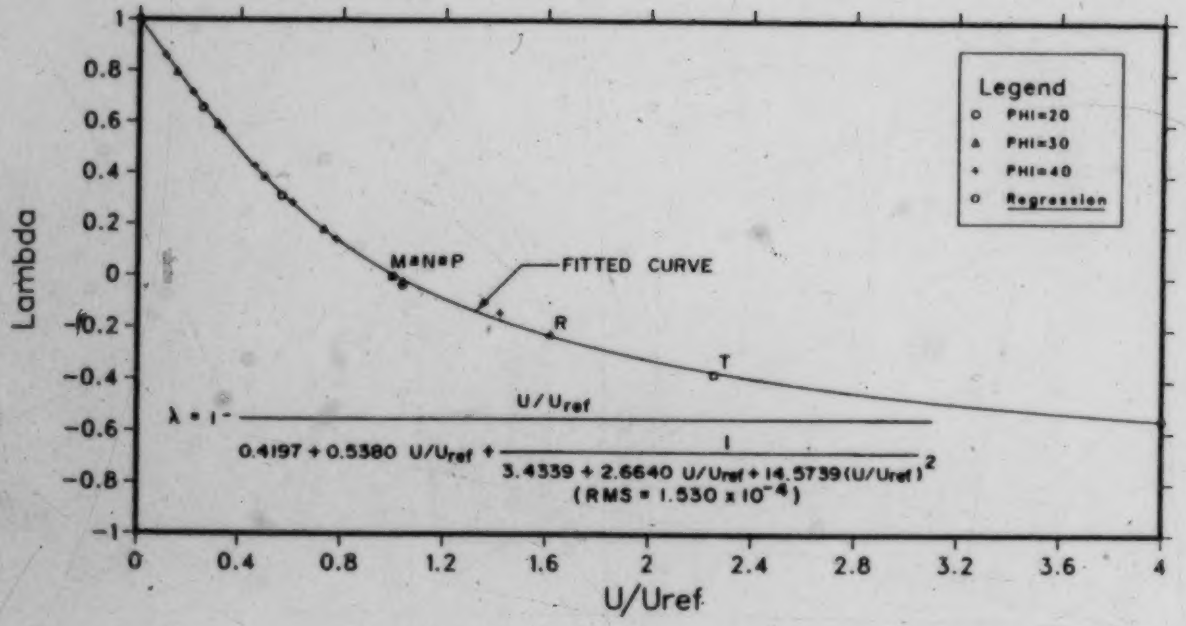

Figure 6.90 Twice Normalized Ground Reaction Curves (NNGRC) for the Springline of a Tunnel with H/D=3, for the Cohesionless Soil Model with K_o=0.8

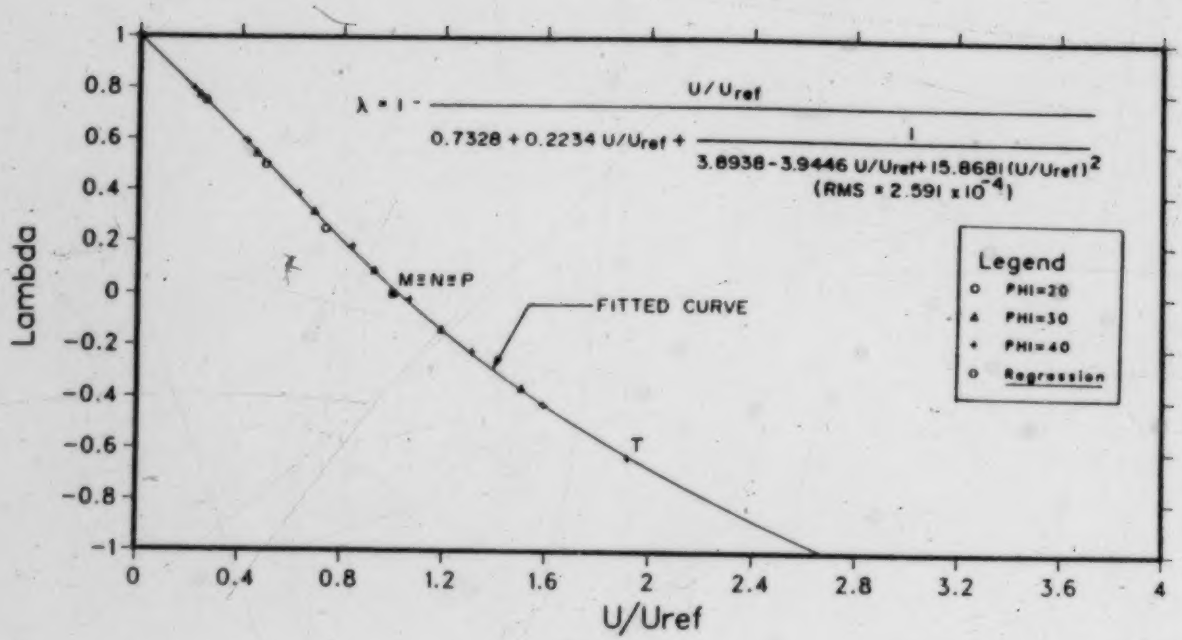

Figure 6.91 Twice Normalized Ground Reaction Curves (NNGRC) for the Floor of a Tunnel with H/D=3, for the Cohesionless Soil Model with K_o=0.8

In other words, it seems reasonable to assume that a collapse radial stress exists at each point of the tunnel contour, which is approached asymptotically upon large displacements.

Moreover, it was decided to select a single function type, that would fit the normalized numerical results found at the three points of the tunnel contour in all of the cases covered in the parametric analyses.

Six types of functions were thoroughly investigated and tested to best fit the requirements. Making a/a_{ref}=y and U/U_{ref}=x, these functions were the following:

a) $y = x/(P_1 + P_2x + P_3e^{P_4x}$

b) $y = x/(P_1 + P_2x + P_3e^{P_4+P_5x+P_6x^2}$

c) $y = x/(P_1 + P_2x + P_3(P_4+x)^{P_5} . e^{P_6(P_4+x)})$

d) $y = x/(P_1 + P_2x + (1/(P_3+P_4x)))$

e) $y = x/(P_1 + P_2x + (1/(P_3+P_4x+P_5x^2+P_6x^3)))$

f) $y = x/(P_1 + P_2x + (1/(P_3+P_4x+P_5x^2)))$

To test these functions, a non-linear least-squares regression technique was used, where the unknown parameters, P_i, were allowed to vary, to establish a 'best-fit' through the known pair of data (x,y). This was accomplished using the computer program BMDP3R, Non-linear Regression (Revised Version, October, 1983), which is part of a statistical package developed at the University of California. Besides the data set with the (x,y) pairs, the program requires the function to be described by FORTRAN statements as well as the function partial derivatives of the function with respect to the parameters, P_i.

Some numerical difficulties were found for certain sets of data (especially for the floor), when applying the program to those functions including exponential terms, a, b and c (floating point overflows and exponential errors). The investigations therefore were concentrated on functions d, e and f above. Visual inspection of the fitted curves on the numerical data revealed that function f was the best fit for all sets of data tested (basically all cases analysed for H/D=1.5).

Besides the visual inspection, a comparative analysis of the quality of the fitting for the different functions can be made through the residual mean square calculated by the program (Torgerson, 1986). This index is defined as:

$$\text{RMS} = \frac{\text{Residual Sum of Squares}}{\text{Degrees of Freedom}} = \frac{\Sigma(y - g)^2}{(N-p)}$$

where y is the observed value of the dependent variable, g is the evaluation of the function, N is the total number of samples (x,y) and p is the total number of independent parameters (P_i) in the function. The function fitting the data best would furnish the lowest RMS value. Through this criterion it was confirmed that function f provided the best fitting of the numerical results. Accordingly function f was selected and used to fit all normalized numerical data. This function expresses the twice normalized ground reaction curve as:

$$\lambda = 1 - \frac{a}{a_{ref}} = 1 - \frac{1-\Sigma}{1-\Sigma_{ref}}$$

$$=1-\frac{U/U_{ref}}{P_1+P_2U/U_{ref}+1/(P_3+P_4U/U_{ref}+P_5(U/U_{ref})^2} \qquad [6.24]$$

The parameters P_i (i=1,5) for the crown, springline and floor of a tunnel with H/D=3, and K_o=0.8 are shown in Table 6.14, and the equation of the best fitted curves for these points are reproduced in Figures 6.89 to 6.91.

The above procedure was repeated to all cases analysed and the results of these reduction process are summarized in Tables 6.15, 6.16 and 6.17, for K_o=0.6, 0.8 and 1.0 respectively. In all cases ,the RMS varied between 10^{-3} to 10^{-5}. All normalized numerical results and corresponding best fitted curves are included in Appendix D. There is not a reference value for RMS that would allow an assessment of the goodness of fit in absolute terms. The RMS is usually interpreted in relative terms, for comparitive purposes. However, one can appreciate that quite satisfactory fitting was obtained in all cases.

At this stage, one notes that the equations for the NNGRC's have been derived for each point of the tunnel contour, for each H/D and K_o, and are independent of the friction angle. The dependence on ϕ is represented by the different a_{ref} or U_{ref} values associated with each friction angle. But this dependence can be expressed separately. The relationships between the slope of the arbitrary axes a_{ref}/U_{ref} used in the transformation process, and the depth ratio H/D (note that this slope is constant for any ϕ value) can be expressed separately.

Position	H/D	ϕ (°)	a_{ref}	U_{ref}	$\frac{a_{ref}}{U_{ref}}$	P_1	P_2	P_3	P_4	P_5	RMS/10^{-4}
Crown	6	20	0.183	0.1552							
		30	0.365	0.3095	1.1792	0.7863	0.1643	5.8485	-0.9192	15.2721	0.162
		40	0.500	0.4240							
	3	20	0.183	0.1605							
		30	0.365	0.3285	1.1111	0.7592	0.1959	5.5995	-1.8853	18.2108	0.052
		40	0.500	0.4500							
	1.5	20	0.183	0.1856							
		30	0.365	0.3701	0.9862	0.5830	0.3175	2.9017	1.5671	5.6173	0.094
		40	0.500	0.5070							
Springline	6	20	0.130	0.1072							
		30	0.296	0.2267	1.3055	0.3270	0.5378	2.2039	1.3714	4.4509	6.923
		40	0.500	0.3830							
	3	20	0.130	0.1070							
		30	0.296	0.2261	1.3089	0.3262	0.5428	2.3007	1.1162	4.9612	8.026
		40	0.500	0.3820							
	1.5	20	0.130	0.1064							
		30	0.296	0.2250	1.3158	0.3173	0.5517	2.2334	1.0538	5.0694	7.602
		40	0.500	0.3800							
Floor	6	20	0.150	0.0765							
		30	0.210	0.1071	1.9608	0.7550	0.0791	4.2389	-2.7928	4.6785	4.452
		40	0.300	0.1530							
	3	20	0.150	0.0765							
		30	0.210	0.1071	1.9608	0.8201	0.0550	6.3141	-6.6624	8.7052	4.021
		40	0.300	0.1530							
	1.5	20	0.150	0.0770							
		30	0.210	0.1078	1.9481	0.8312	0.0476	6.4333	-5.5703	7.8069	3.749
		40	0.300	0.1540							

Table 6.15 Parameters Used and Obtained in the Reduction of the Twice Normalized Ground Reaction Curves for the Frictionless Soil Model and for K_o=0.6

Position	H/D	ϕ (°)	α_{ref}	U_{ref}	$\frac{\alpha_{ref}}{U_{ref}}$	P_1	P_2	P_3	P_4	P_5	RMS/10^{-4}
Crown	6	20	0.39	0.3655							
		30	0.54	0.5061	1.0671	0.5480	0.3849	3.0527	2.9276	9.9043	0.415
		40	0.70	0.6560							
	3	20	0.39	0.3911							
		30	0.54	0.5415	0.9972	0.5055	0.4191	2.8752	3.6904	6.8780	0.134
		40	0.70	0.7020							
	1.5	20	0.39	0.4350							
		30	0.54	0.6200	0.8589	0.5052	0.4630	3.6081	5.5775	17.3331	0.356
		40	0.70	0.8150							
Springline	6	20	0.29	0.2548							
		30	0.49	0.4305	1.1382	0.4223	0.5317	3.4086	3.2167	12.6102	1.413
		40	0.70	0.6150							
	3	20	0.29	0.2552							
		30	0.49	0.4312	1.1364	0.4197	0.5380	3.4339	2.6640	14.5739	1.530
		40	0.70	0.6160							
	1.5	20	0.29	0.2569							
		30	0.49	0.4340	1.1290	0.4096	0.5500	3.4225	2.1201	15.7848	1.732
		40	0.70	0.6200							
Floor	6	20	0.40	0.1990							
		30	0.44	0.2189	2.0101	0.7230	0.2316	3.5999	-2.8499	14.5303	2.476
		40	0.49	0.2438							
	3	20	0.40	0.1990							
		30	0.44	0.2189	2.0101	0.7328	0.2234	3.8938	-3.9446	15.8681	2.591
		40	0.49	0.2438							
	1.5	20	0.40	0.1980							
		30	0.44	0.2178	2.0202	0.7171	0.2256	3.6040	-2.8964	11.6415	3.048
		40	0.49	0.2426							

Table 6.16 Parameters Used and Obtained in the Reduction of the Twice Normalized Ground Reaction Curves for the Frictionless Soil Model and for $K_o=0.8$

Position	H/D	ϕ (°)	α_{ref}	U_{ref}	$\frac{\alpha_{ref}}{U_{ref}}$	P_1	P_2	P_3	P_4	P_5	$RMS/10^{-4}$
Crown	6	20	0.38	0.4418	0.8602	0.4274	0.5208	4.2706	4.9524	9.1674	0.925
		30	0.58	0.6743							
		40	0.80	0.9300							
	3	20	0.38	0.4774	0.7960	0.4097	0.5446	4.4999	5.3435	10.7461	1.247
		30	0.58	0.7286							
		40	0.80	1.0050							
	1.5	20	0.38	0.5700	0.6667	0.3575	0.6118	5.1904	5.6765	17.2042	2.966
		30	0.58	0.8700							
		40	0.80	1.2000							
Springline	6	20	0.38	0.3596	1.0568	0.4416	0.4977	4.0454	5.6946	6.1024	0.637
		30	0.58	0.5488							
		40	0.80	0.7570							
	3	20	0.38	0.3610	1.0526	0.4484	0.5015	4.6854	3.7948	10.6789	0.803
		30	0.58	0.5510							
		40	0.80	0.7600							
	1.5	20	0.38	0.3672	1.0349	0.4207	0.5227	4.0515	4.5578	8.2557	0.799
		30	0.58	0.5604							
		40	0.80	0.7730							
Floor	6	20	0.38	0.2755	1.3793	0.4323	0.5090	4.0270	5.0692	7.6430	0.741
		30	0.58	0.4205							
		40	0.80	0.5800							
	3	20	0.38	0.2707	1.4035	0.4574	0.4914	4.3206	4.2243	10.4066	0.717
		30	0.58	0.4132							
		40	0.80	0.5700							
	1.5	20	0.38	0.2655	1.4311	0.4258	0.4880	3.2546	4.6773	3.4674	0.454
		30	0.58	0.4053							
		40	0.80	0.5590							

Table 6.17 Parameters Used and Obtained in the Reduction of the Twice Normalized Ground Reaction Curves for the Frictionless Soil Model and for $K_o=1.0$

The same development applied to the frictionless soil model (Section 6.4.2) for assessing the changes in the ground stiffness with the reduction of the in situ stresses can be applied here. The partial derivative of λ with respect to $U/U_{ref}(\lambda')$ can be related to a 'current' ground spring constant (k_r), that could be used in ring-and-spring models to analyse the ground-lining interaction developing once the support is installed, after a certain amount of stress release. Recalling equation 6.23 and the definitions of the stress ratio, $\Sigma=\sigma_r/\sigma_{ro}$, and of the dimensionless displacement, $U=u_rE_{ti}/\sigma_{ro}.D$, it can be demonstrated that:

$$\lambda' = \frac{\delta\lambda}{\delta U/U_{ref}} = \frac{U_{ref}}{\alpha_{ref}}\,\frac{D}{E_{ti}}\,\frac{\delta\sigma_r}{\delta u_r}$$

Since $\delta\sigma_r/\delta u_r$ is equal to k_r, then

$$k_r = \frac{\alpha_{ref}}{U_{ref}}\,\frac{E_{ti}}{D}\,\lambda' \qquad [6.25]$$

On the other hand, λ' can be obtained by differentiating equation 6.24

$$\lambda' = \frac{\delta\lambda}{\delta U/U_{ref}} = \left[P_1 + P_2\frac{U}{U_{ref}} + 1/\left(P_3 + P_4\frac{U}{U_{ref}} + P_5\frac{U^2}{U^2_{ref}}\right)\right]^{-1} -$$

$$\frac{U}{U_{ref}}.\left[P_1 + P_2\frac{U}{U_{ref}} + 1/\left(P_3 + P_4\frac{U}{U_{ref}} + P_5\frac{U^2}{U^2_{ref}}\right)\right]^{-2} \times$$

$$\left[P_2 - \left(P_4 + 2P_5\frac{U}{U_{ref}}\right).\left(P_3 + P_4\frac{U}{U_{ref}} + P_5\frac{U}{U_{ref}}\right)^{-2}\right] \qquad [6.26]$$

in which the negative sign of the derivative has been dropped.

Knowing the parameters, P_i (i=1,5) and the reference values α_{ref} and U_{ref} (Tables 6.15 to 6.17), it is possible to define, using equation 6.24 the amount of stress release α associated with a certain dimensionless displacement U.

Moreover, with equations 6.25 and 6.26, the radial spring constant corresponding to U, can also be determined.

If instead, a ring-and-plate model is to be used for the ground-lining interaction analysis, one would need to know the current tangent modulus of the ground (E_t), rather than the spring constant. If it is assumed that this modulus is directly proportional to the spring constant (or the slope of the GRC), then:

$$\frac{E_t}{E_{ti}}=\frac{k_r}{k_{ri}}$$

and, from equation 6.25:

$$E_t = \frac{\lambda'}{\lambda'_i}.E_{ti} \qquad [6.27]$$

remembering that a_{ref}/U_{ref}, E_{ti} and D are constant for a particular tunnel situation. Note that λ'_i is the derivative of λ for zero stress release at the opening.

Distinct current moduli (or current spring constants) would be found for the crown, springline and floor. The available ring-and-plate models operate with a constant ground modulus. Hence an operational modulus could be considered by averaging the moduli at those points of the tunnel contour (the springline modulus being counted twice). This modulus would then be (for a uniform E_{ti} ground profile):

$$\bar{E}_t = \left[\frac{\lambda'}{\lambda'_i}\right]_{av} E_{ti} \qquad [6.28]$$

The value of the partial derivative of λ for zero stress release, λ'_i, is obtained by setting U=0 in equation 6.26. It represents the initial slope of the NNGRC and therefore is related to the in situ tangent modulus of the ground. Thus:

$$\lambda'_i = \frac{1}{P_1 + 1/P_3} \qquad [6.29]$$

The equations furnished above, together with the data summarized in Tables 6.15 to 6.17, represent the proposed solution for obtaining the ground reaction curves or stress release functions for three points of the tunnel contour of a shallow tunnel, in a soil represented by the cohesionless model as indicated by equation 6.11. Although these results could be easily programmed for calculations, it seems convenient to have them presented in form of charts. Accordingly, Figures 6.92 to 6.99 were prepared and represent the complete solution for K_o=0.6. This sequence of charts is described below.

Figure 6.92 furnishes the ratio of a_{ref}/U_{ref} or $(1-\Sigma_{ref})/U_{ref}$ as a function of the relative depth of the tunnel. It was mentioned earlier that this ratio does not depend on ϕ. As it is noted in Table 6.15, the reference values for the amount of stress release, a_{ref} or $(1-\Sigma_{ref})$, were selected for the reduction process in such a way as to make them independent of H/D. They resulted in depending on the friction angle ϕ only. Figure 6.93 shows how that reference value varies with ϕ, expressed here through the function:

$$m-1 = \frac{1+\sin\phi}{1-\sin\phi} - 1 = \frac{2\sin\phi}{1-\sin\phi} \qquad [6.30]$$

Note that (m-1) is the ratio of stress difference to minor principal stress at failure that appears in equation 6.2. With Figure 6.92 and 6.93, one can get U_{ref} for K_o=0.6 and

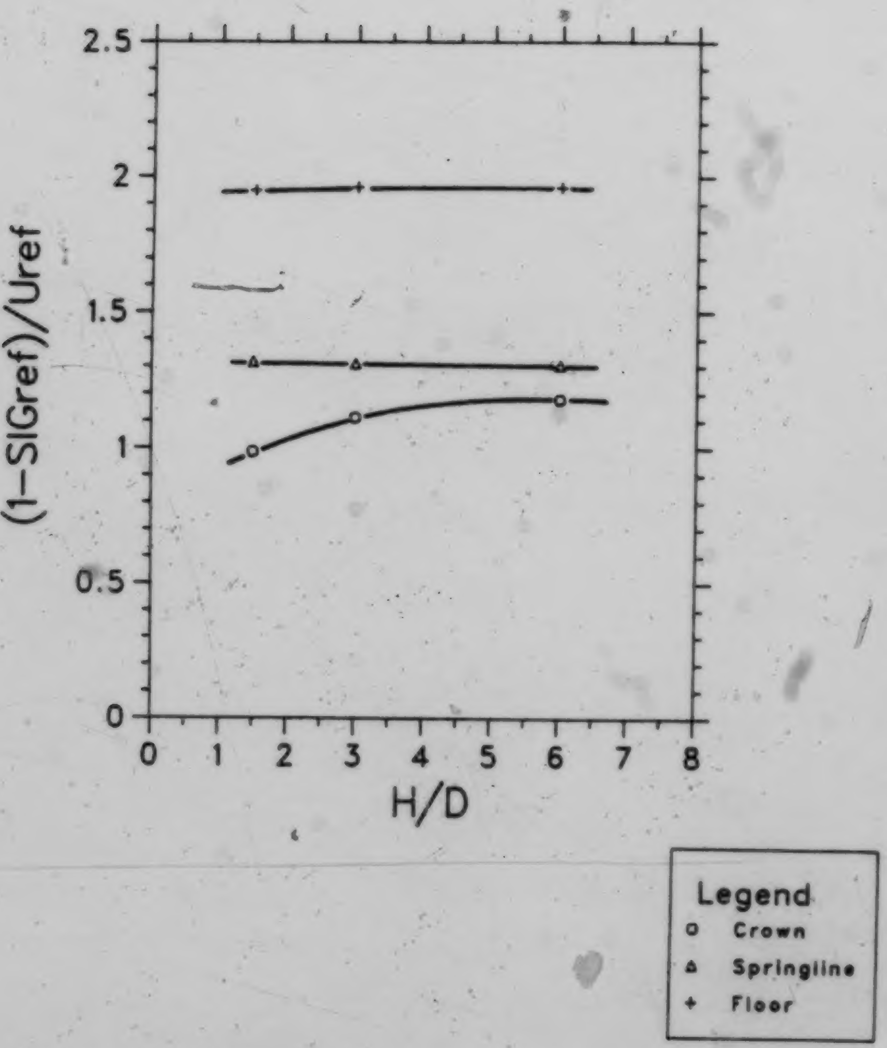

Figure 6.92 Slope of the Arbitrary Axes used to Obtain the NNGRC, Represented as a Function of H/D, for K_o=0.6

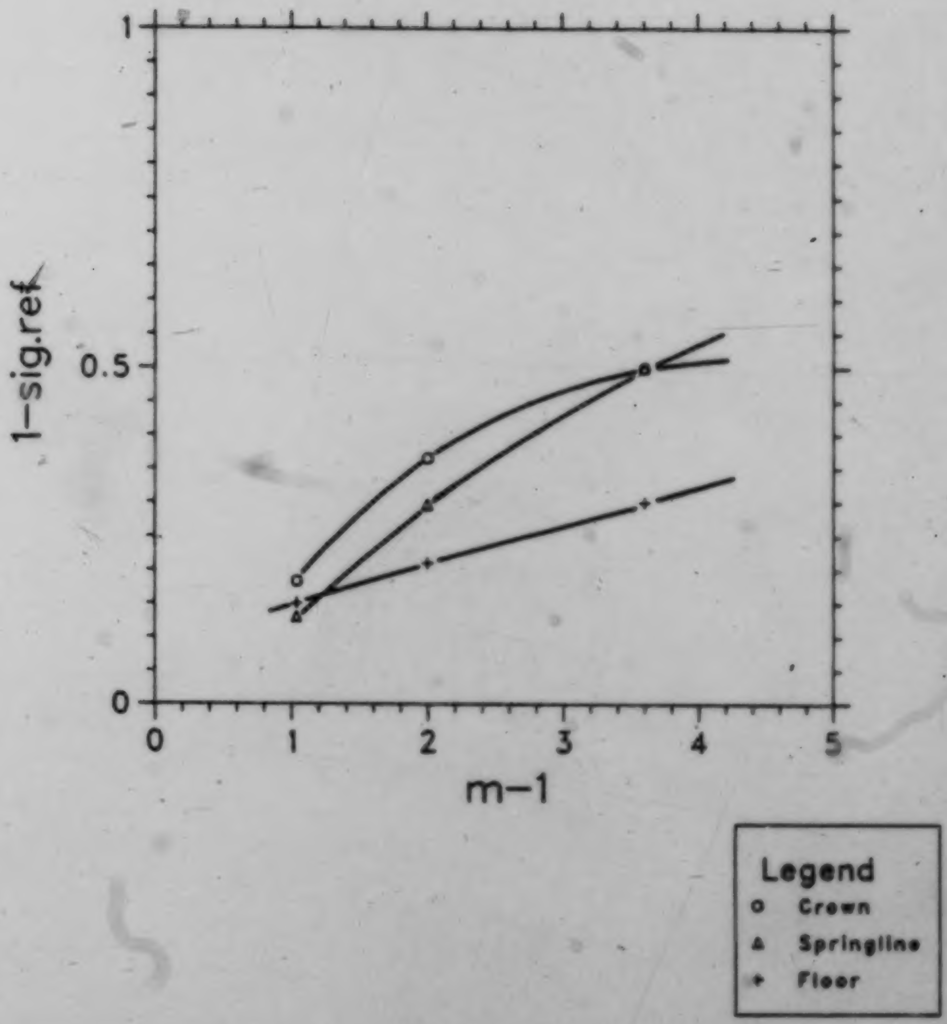

Figure 6.93 Relationships between α_{ref} and the Friction Angle for K_o=0.6

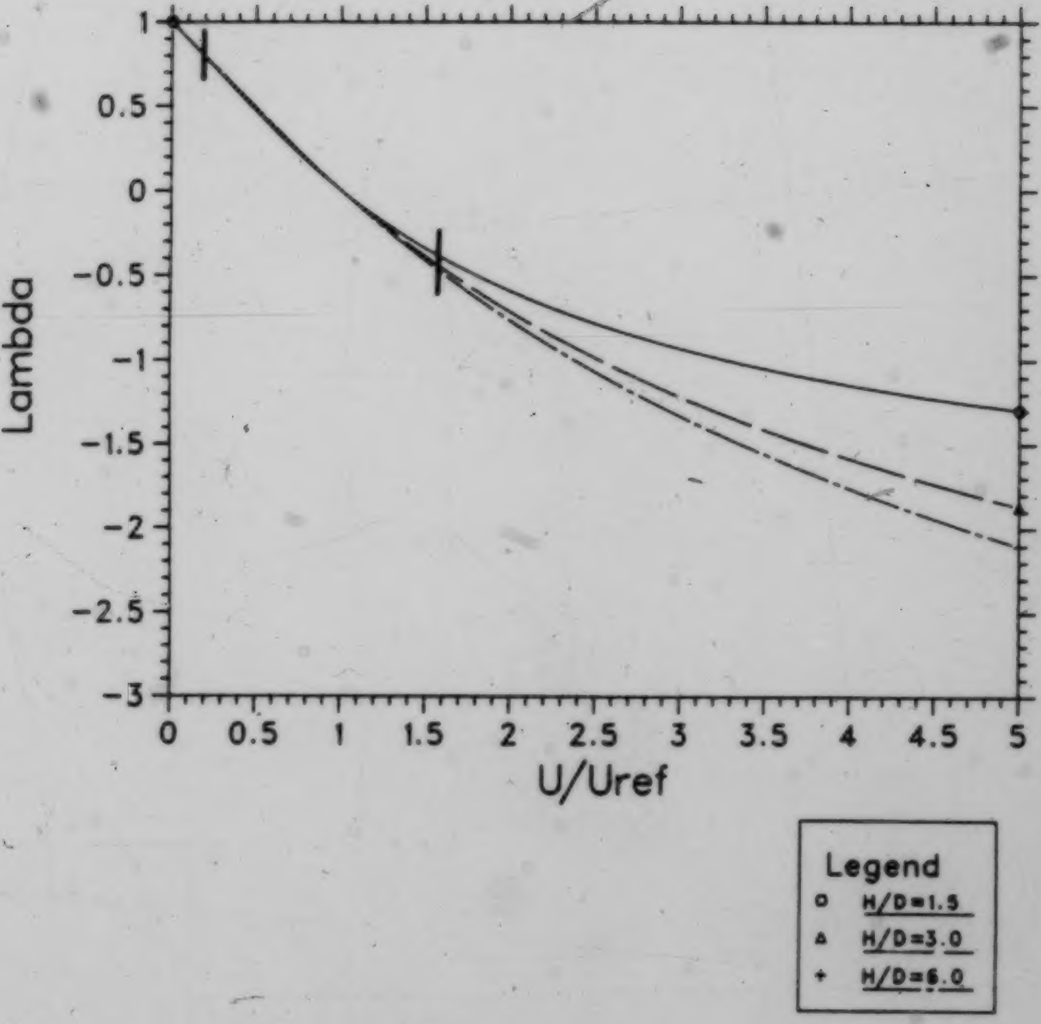

Figure 6.94 Twice Normalized Ground Reaction Curves for Tunnel Crown Calculated for K_o=0.6

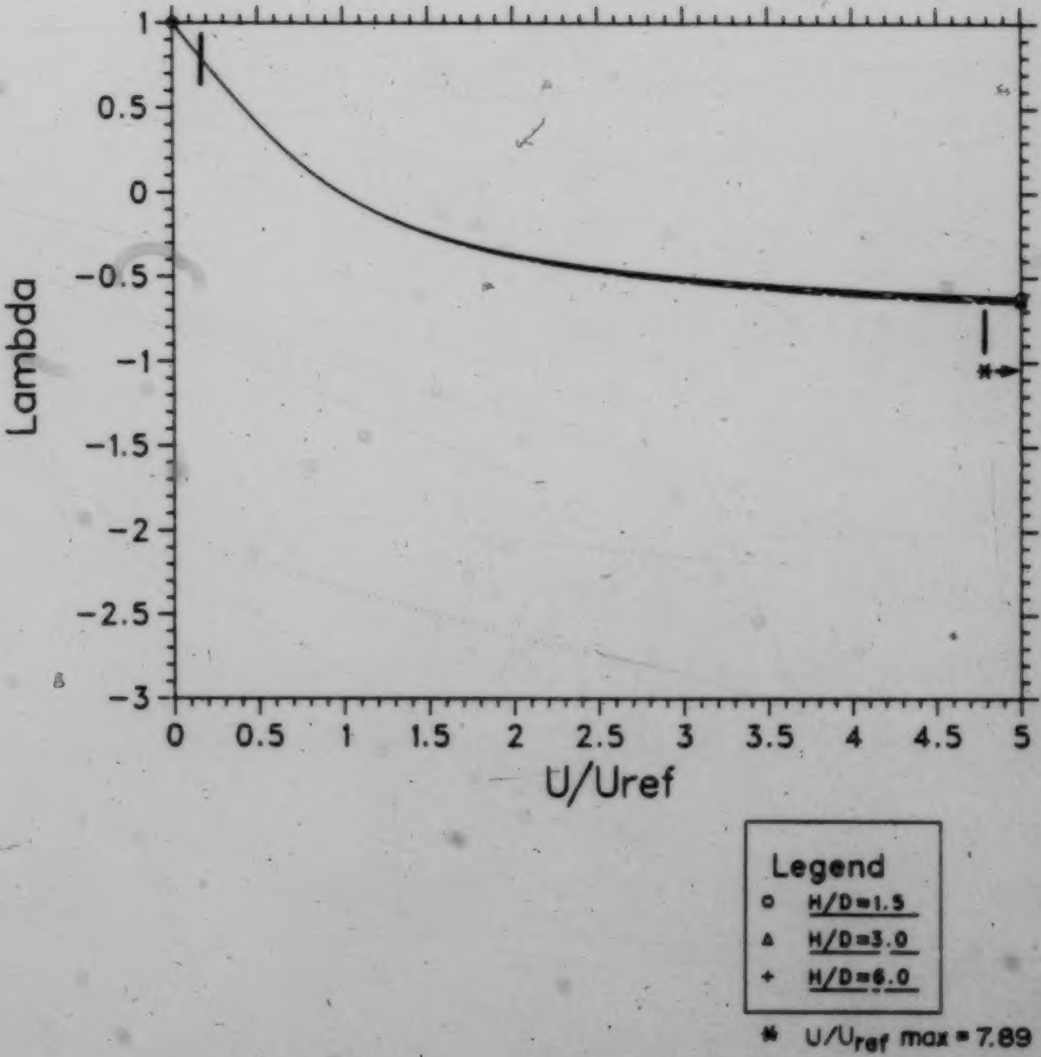

Figure 6.95 Twice Normalized Ground Reaction Curves for the Tunnel Springline, Calculated for K_o=0.6

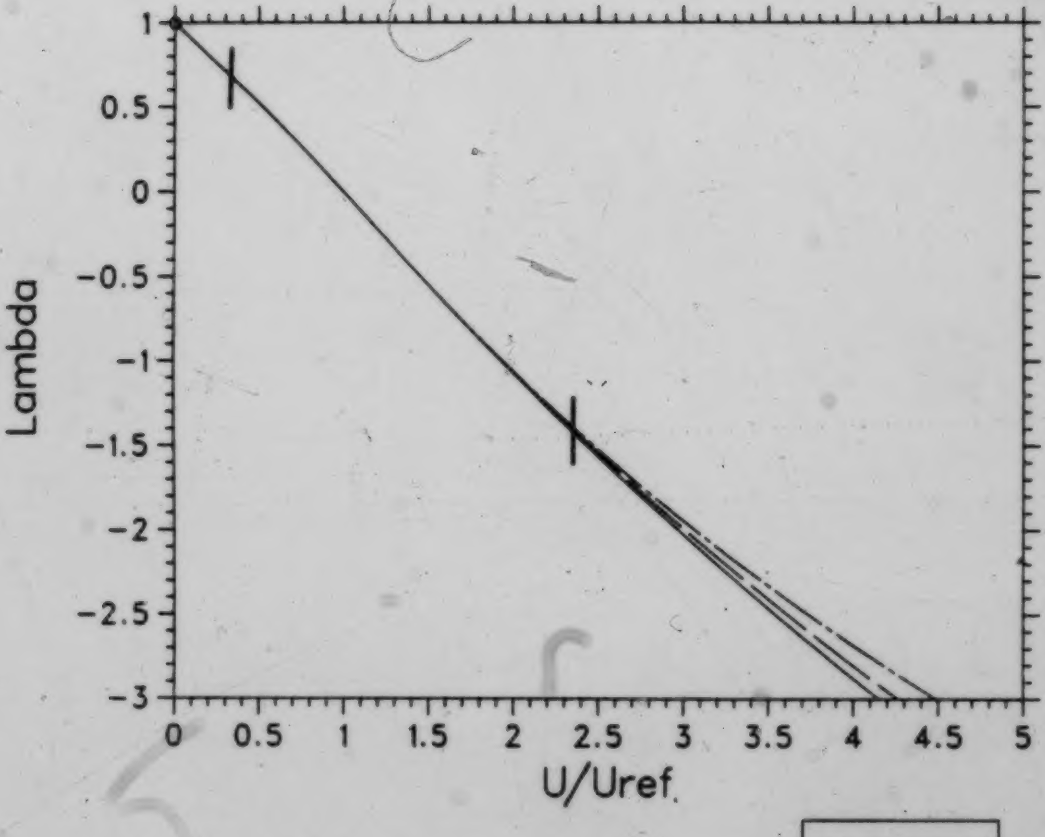

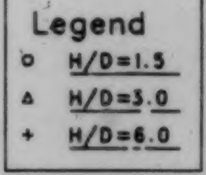

Figure 6.96 Twice Normalized Ground Reaction Curves for the Tunnel Floor, Calculated for K_o=0.6

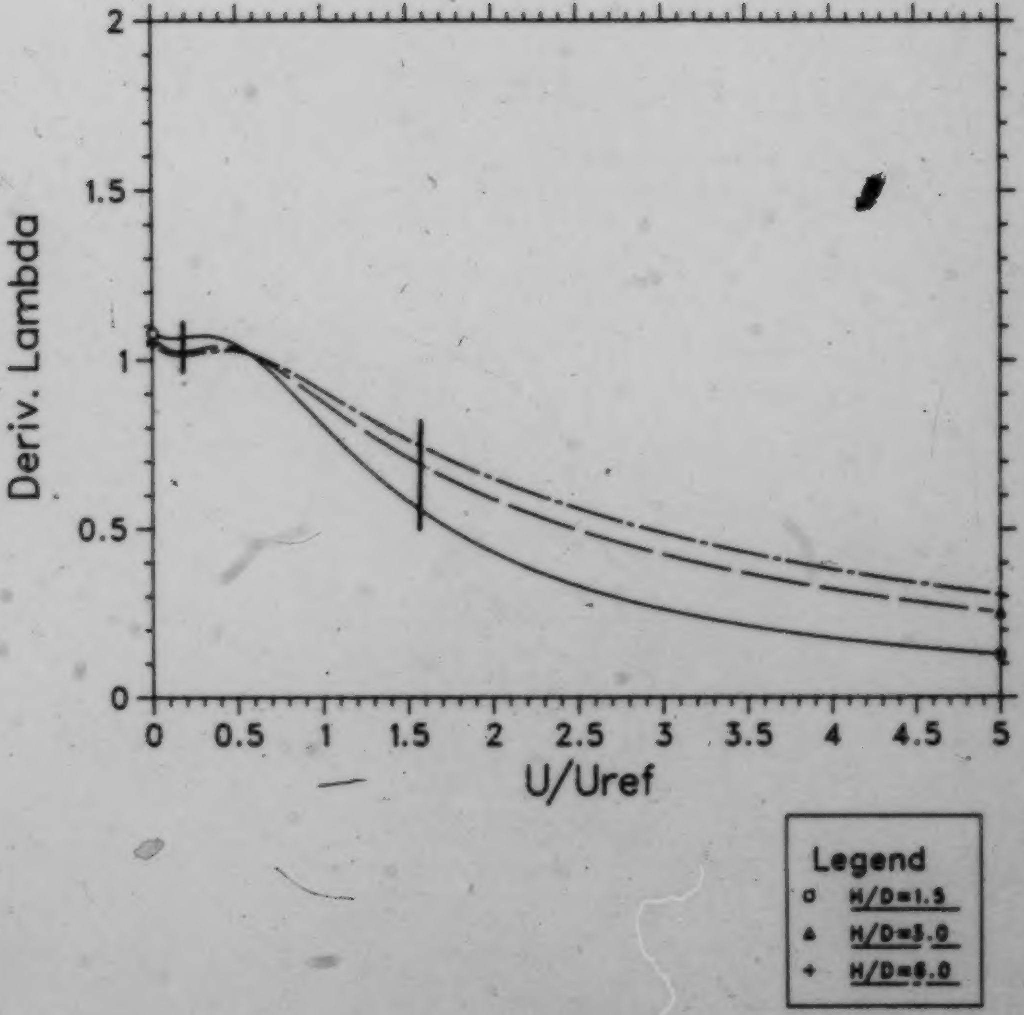

Figure 6.97 Variations of λ' for the Tunnel Crown, Calculated for K_o=0.6

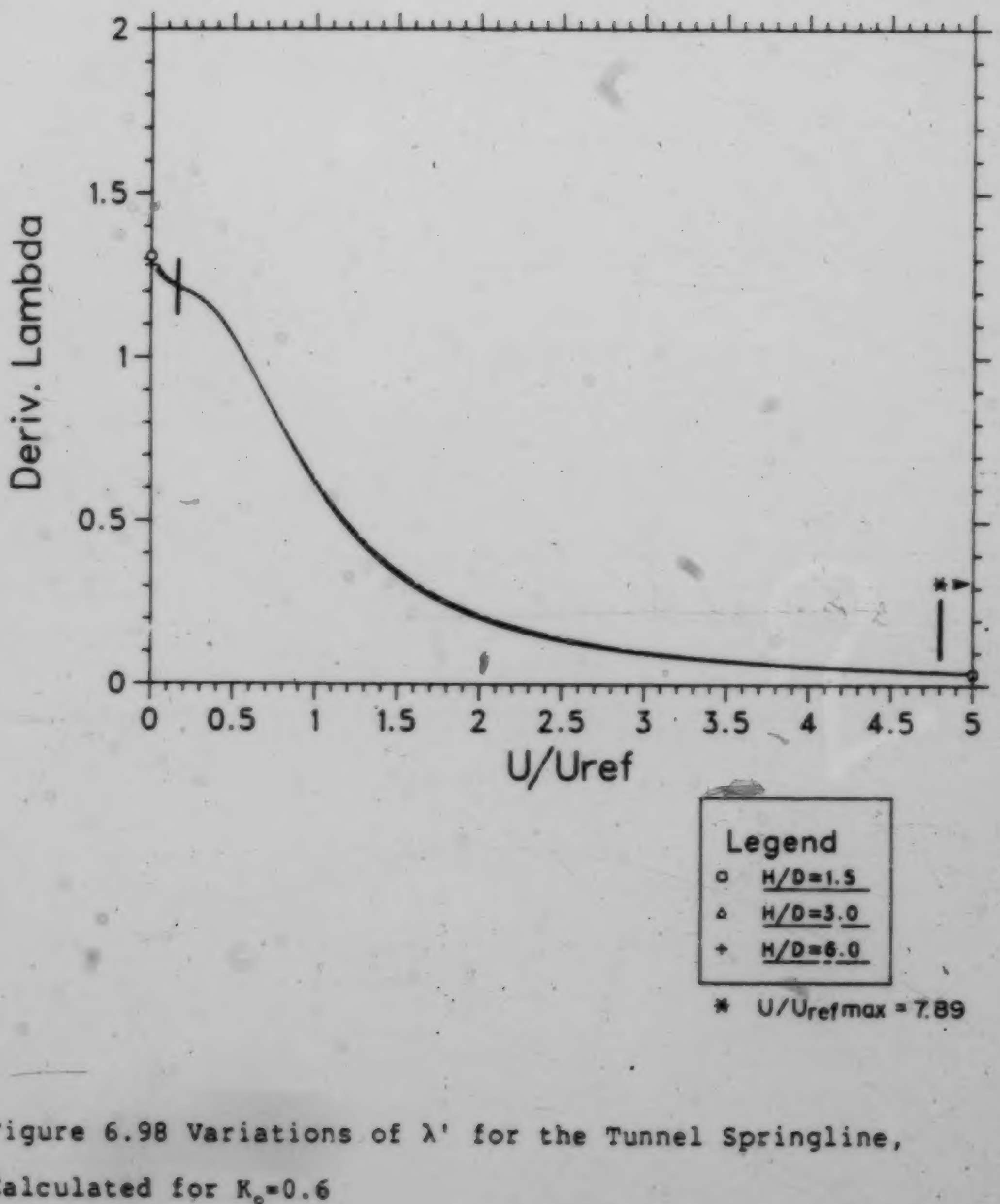

Figure 6.98 Variations of λ' for the Tunnel Springline, Calculated for K_o=0.6

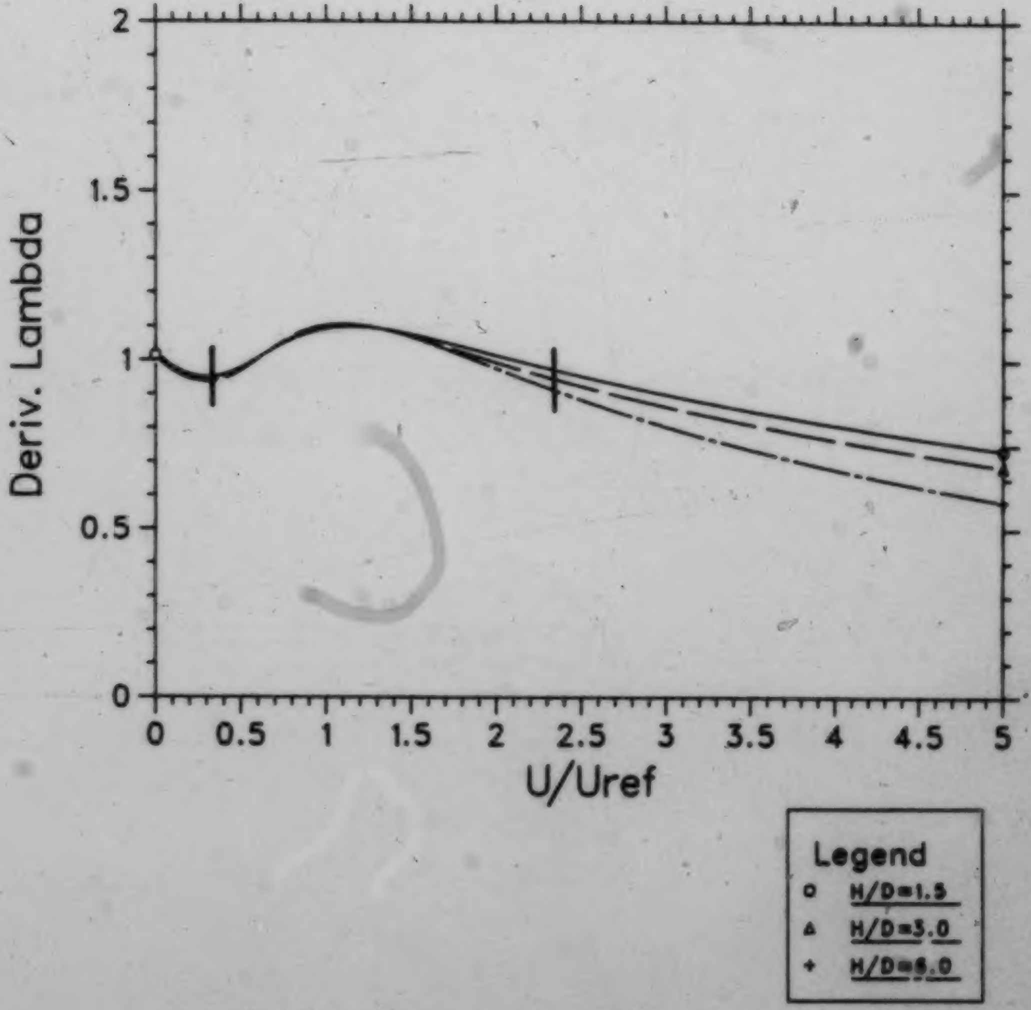

Figure 6.99 Variations of λ' for the Tunnel Floor, Calculated for K_o=0.6

for any H/D and ϕ covered by the parametric analyses.

Figures 6.94 to 6.96 present the twice normalized ground reaction curves (NNGRC) for K_o=0.6, calculated for the tunnel crown, springline and floor, respectively. Note that in each of these figures, the NNGRCs for distinct ratios of H/D have been plotted together. With the exception of the crown, the NNGRC's virtually coincide. This tends to indicate that the effect of H/D is more pronounced at the crown than elsewhere. By understanding this, it seems quite feasible to interpolate data between the curves and to estimate NNGRCs for tunnel depth ratios other that those considered in the parametric analyses. Figure 6.95 indicates that for K_o=0.6, failure at the springline is approached more rapidly for U/U_{ref} increasing than at the other two points of the tunnel contour. The short vertical lines intersecting the NNGRCs in the last three figures delimit the regions where numerical data were available and through which the curves were fitted. The portions of the curves to the right of these regions represent extrapolations of the numerical results. The validity of the functions beyond the region delimited can not be assured. Although the assumption that the fitting functions have always an asymptote and that a good fitting of the numerical results was achieved, there is not the assurance that the extrapolated results can correctly portray the ground behaviour upon large displacements. This subject will be discussed further in the following section.

Figures 6.97 to 6.99 represent equation 6.26 and they provide relationships between the first partial derivative of λ and U/U_{ref}, (λ'), that are needed to assess either the current spring constants through equation 6.25 or the current tangent moduli of the ground through equation 6.27. Note that the values of λ'_i (equation 6.29) can be obtained from these curves by setting U/U_{ref} equal to zero. The last three figures were plotted like the NNGRCs and the same comments made regarding the latter curves are also applicable here. The initial rises in the λ' curves for the crown and floor reflect the 'stiffening' response of the ground noted during the early part of the unloading process.

A similar sequence of charts were prepared for K_o=0.8 (Figures 6.100 to 6.107) and for K_o=1.0 (Figures 6.108 to 6.115). The suite of plots just described represent the proposed generalized solution (equation 6.11) that can be used to estimate both the amount of stress release and the stiffness of the ground after a certain closure of the opening. The solution was formulated in a discrete form for H/D and K_o and this may require interpolation of data for intermediate depth ratios and in situ stress ratio. For instance, this could be done graphically, through the charts given. Figure 6.116, for example, presents a chart for obtaining the initial slope of the NNGRC, λ'_i, for intermediate in situ stress ratios or depth ratios.

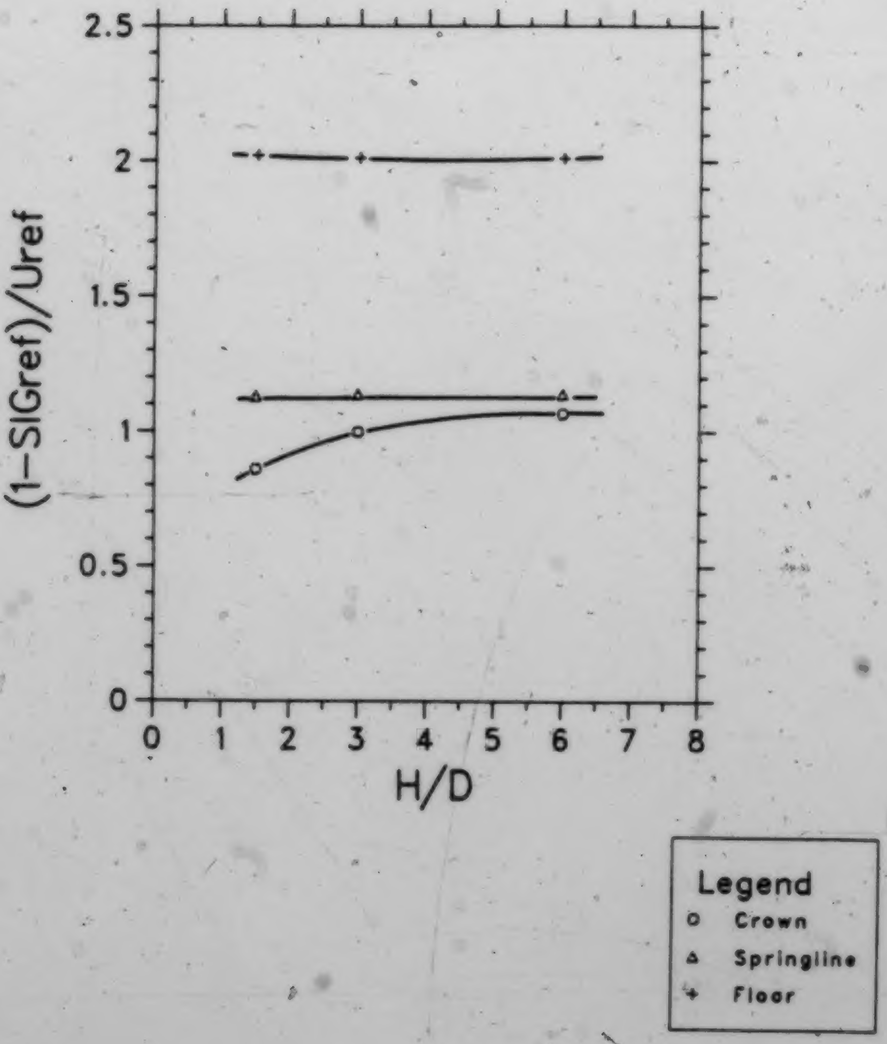

Figure 6.100 Slopes of the Arbitrary Axes used to Obtain the NNGRC Represented as a Function of H/D, for K_o=0.8

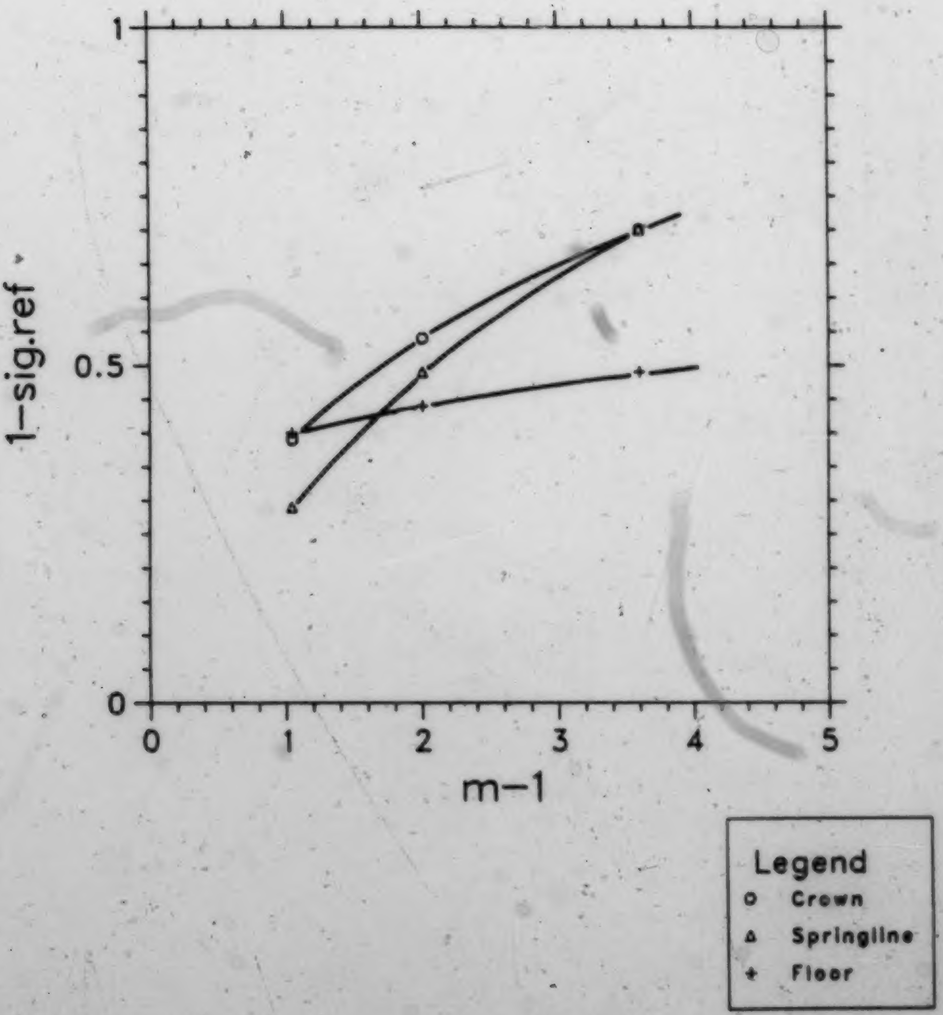

Figure 6.101 Relationships between α_{ref} and the Friction Angle of K_o=0.8

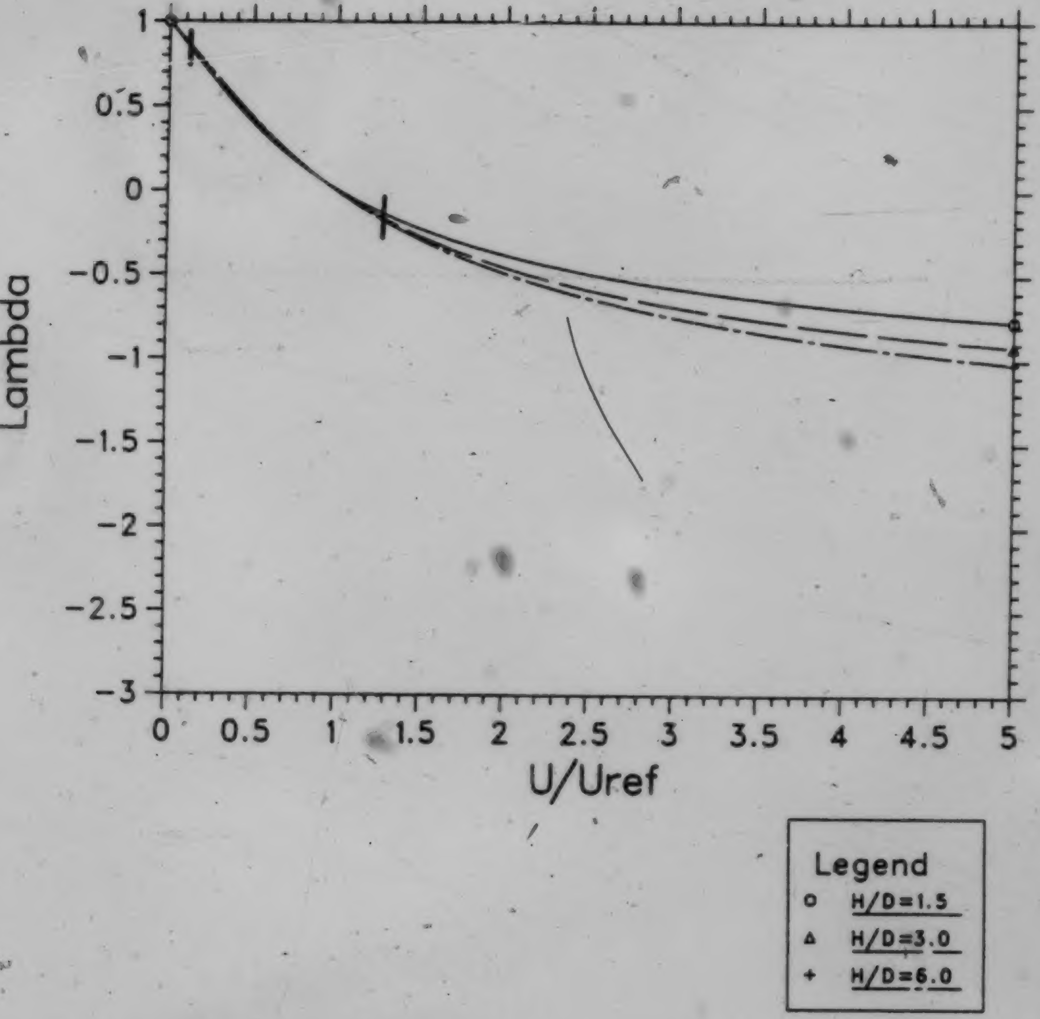

Figure 6.102 NNGRCs for Tunnel Crown, Calculated for K_o=0.8

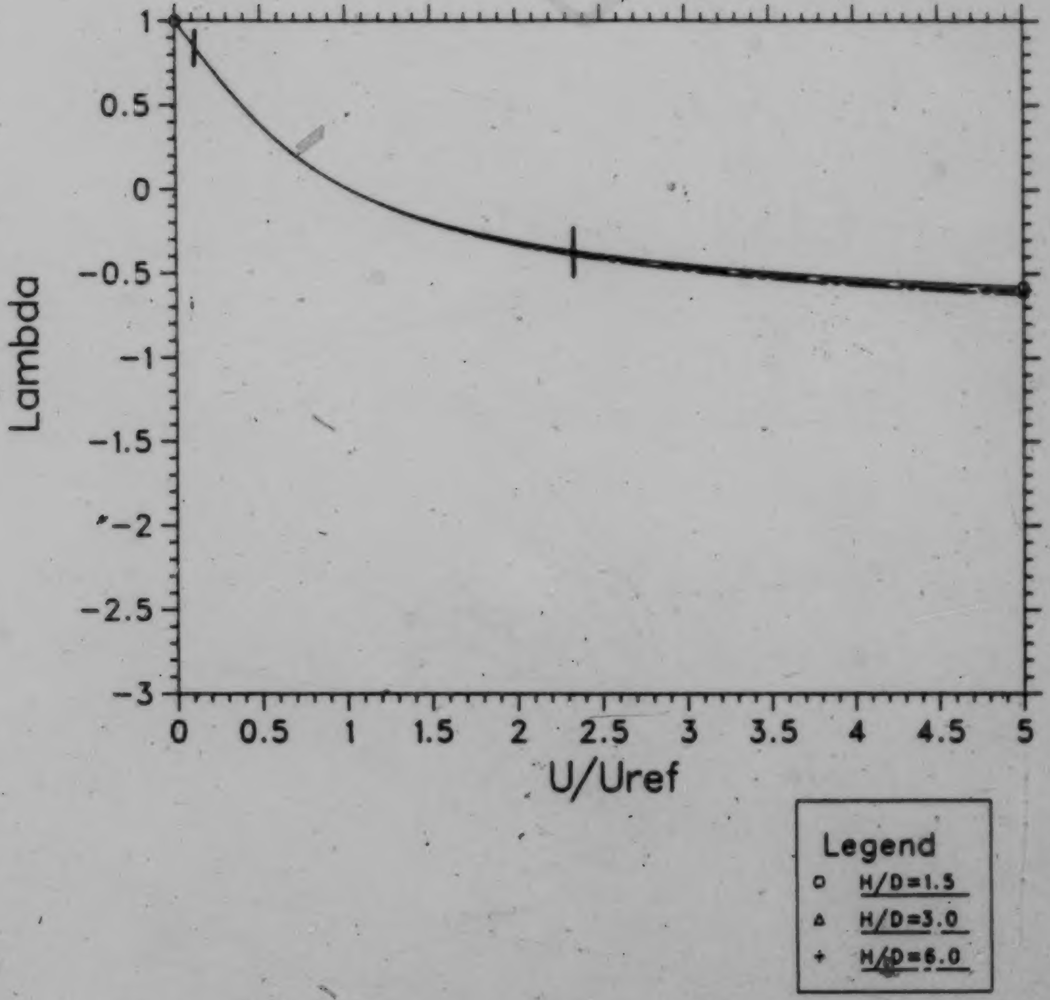

Figure 6.103 NNGRCs for Tunnel Springline, Calculated for K_o=0.8

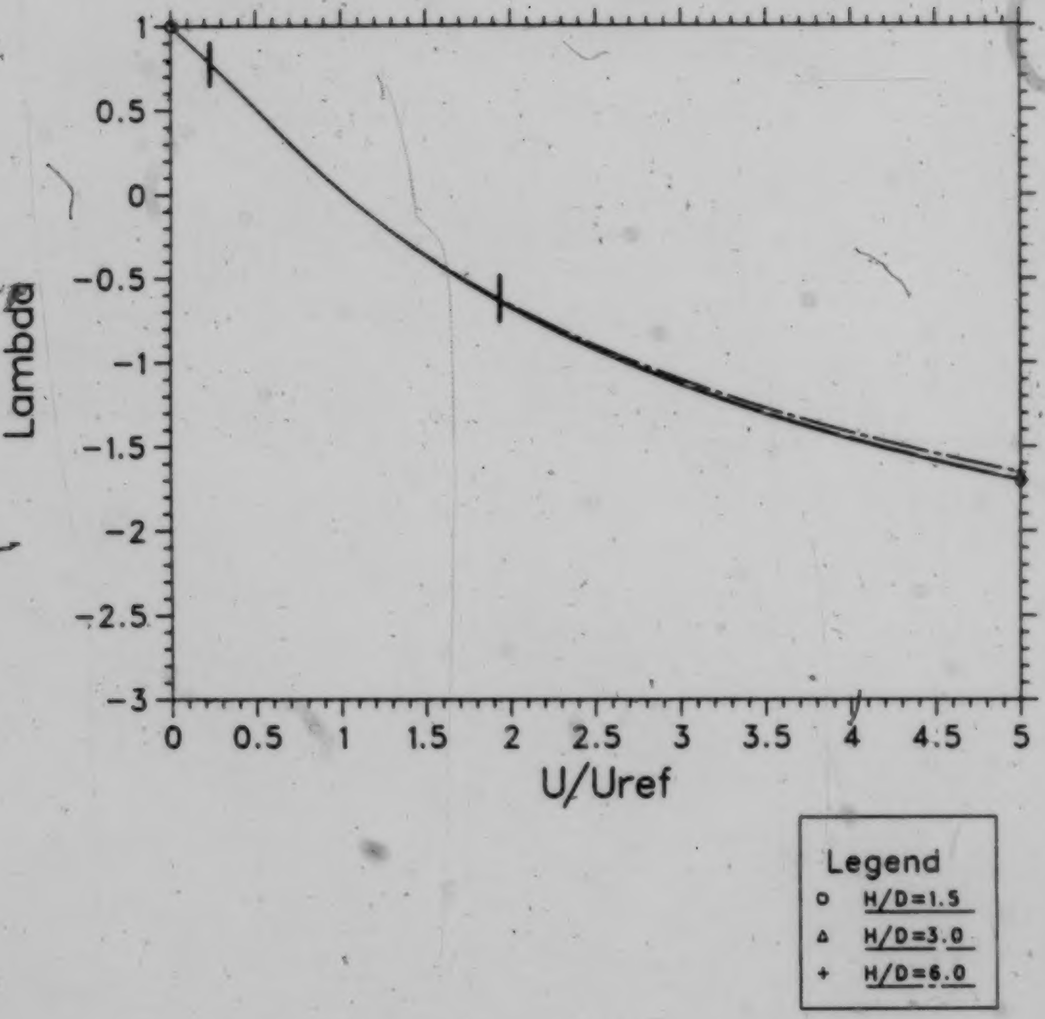

Figure 6.104 NNGRCs for Tunnel Floor, Calculated for K_o=0.8

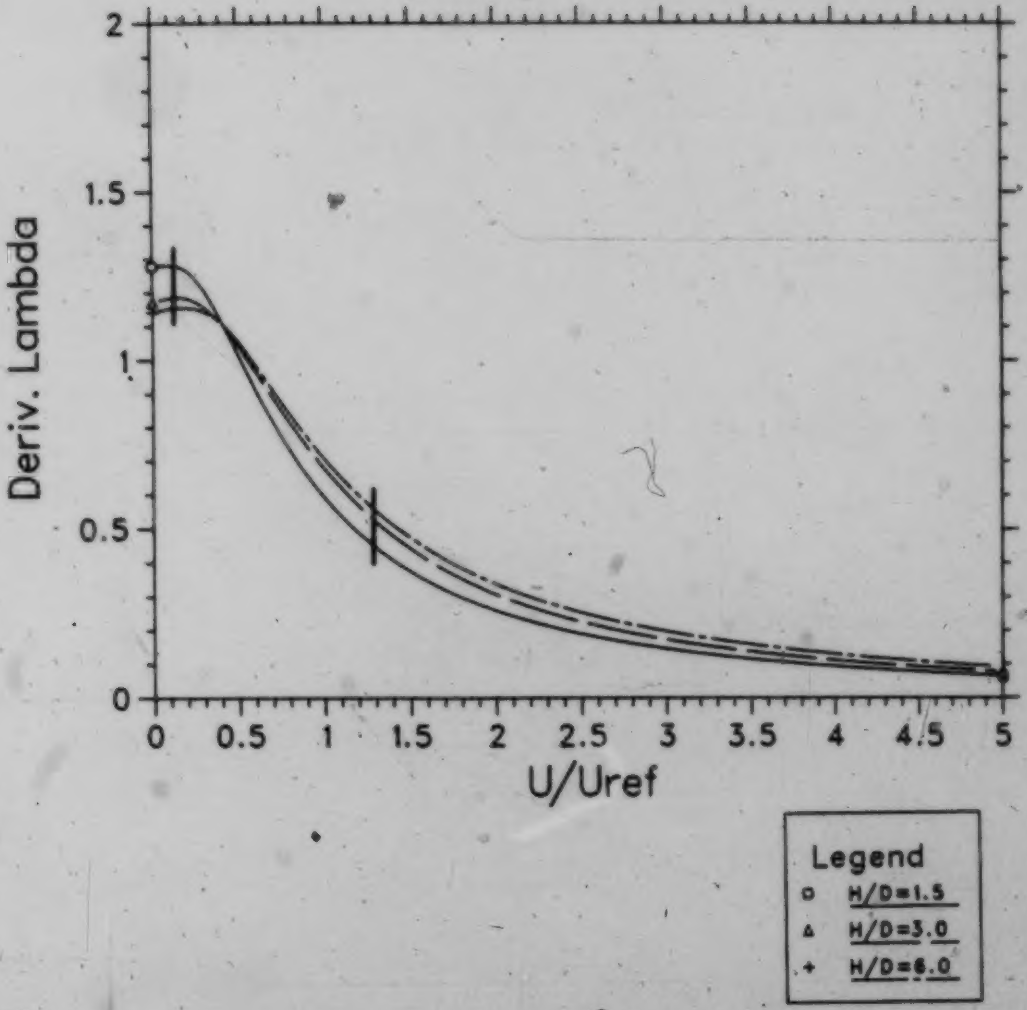

Figure 6.105 Variations of λ' for the Tunnel Crown, Calculated for K_o=0.8

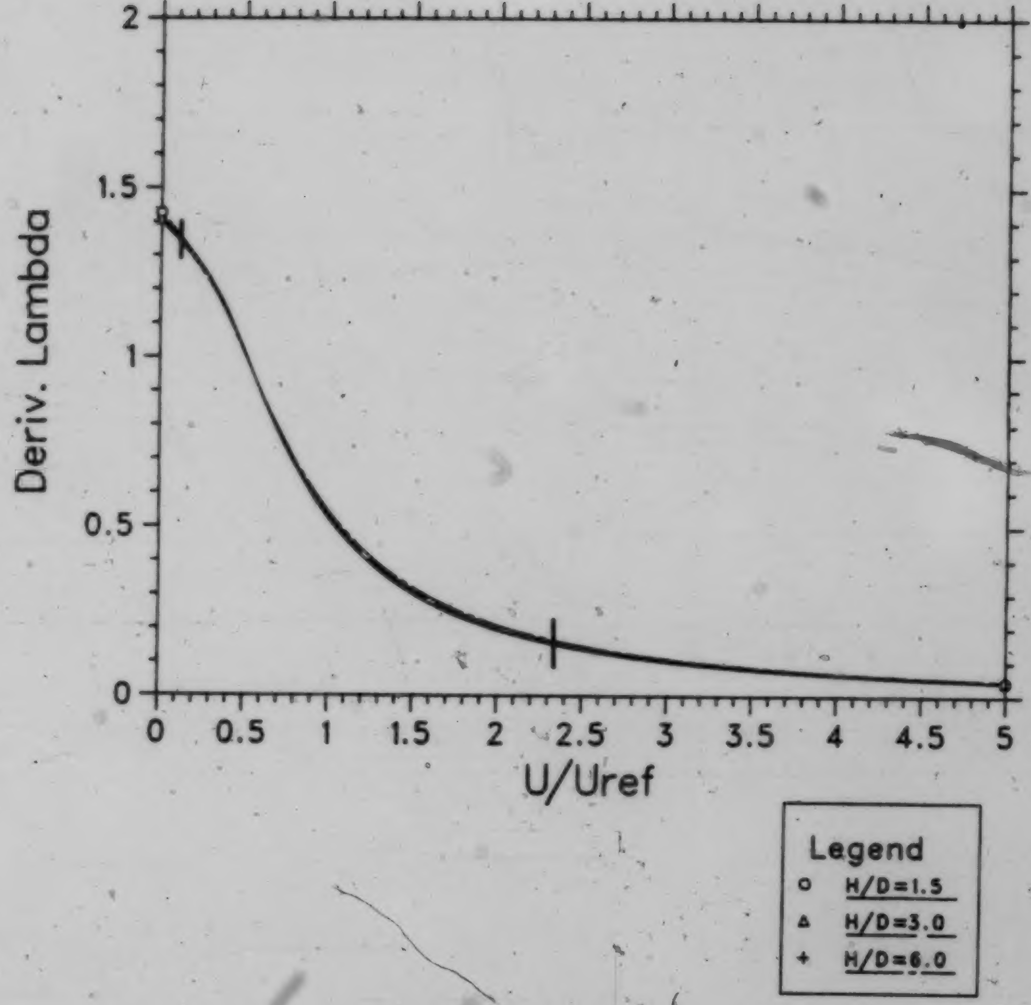

Figure 6.106 Variations of λ' for the Tunnel Springline, Calculated for K_o=0.8

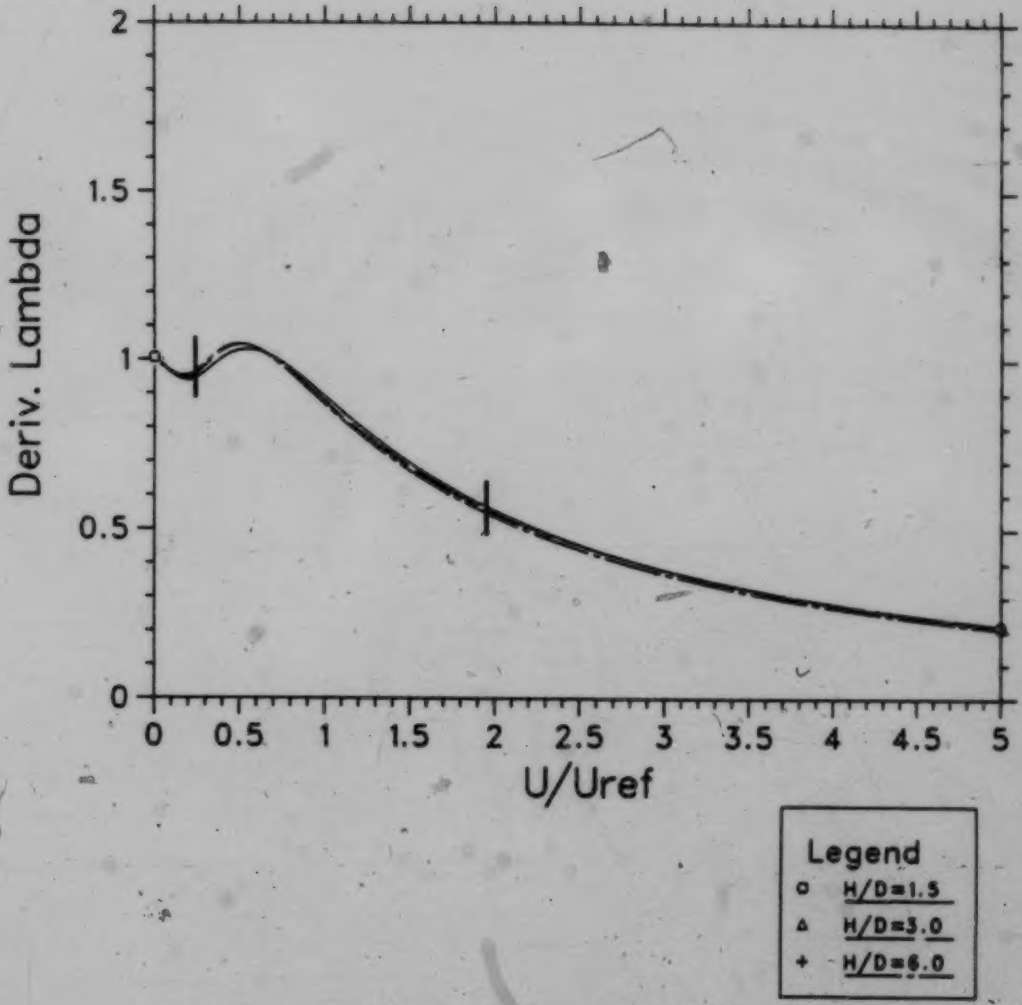

Figure 6.107 Variations of λ' for the Tunnel Floor, Calculated for K_o=0.8

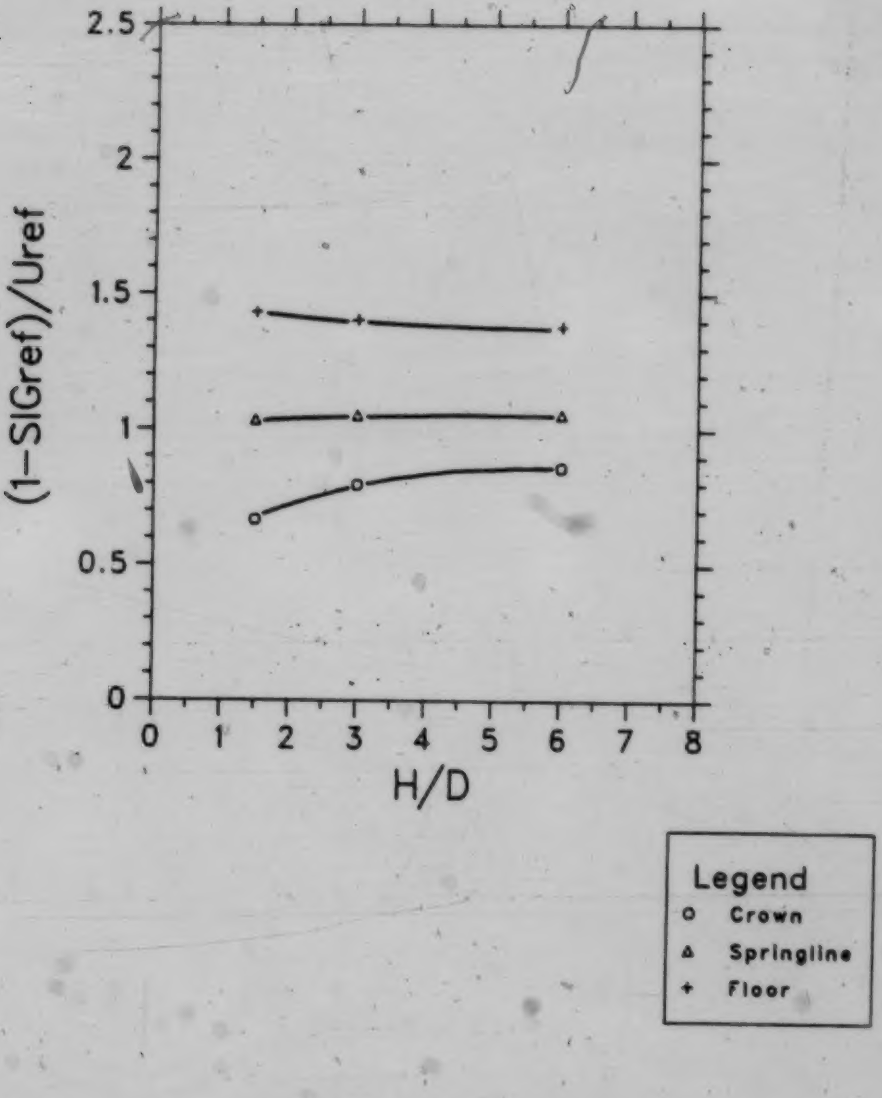

Figure 6.108 Slopes of the Arbitrary Axes used to Obtain the NNGRC Presented as a Function of H/D, for K_o=1.0

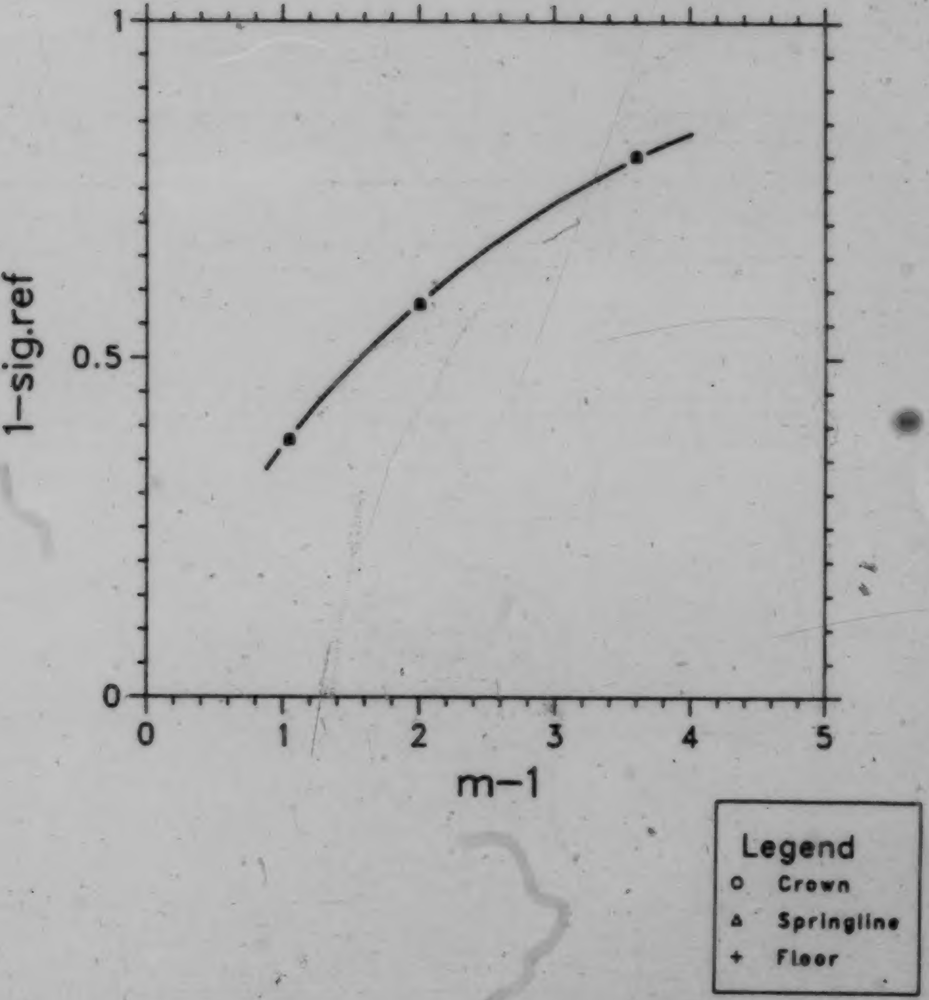

Figure 6.109 Relationships between a_{ref} and the Friction Angle for K_o=1.0

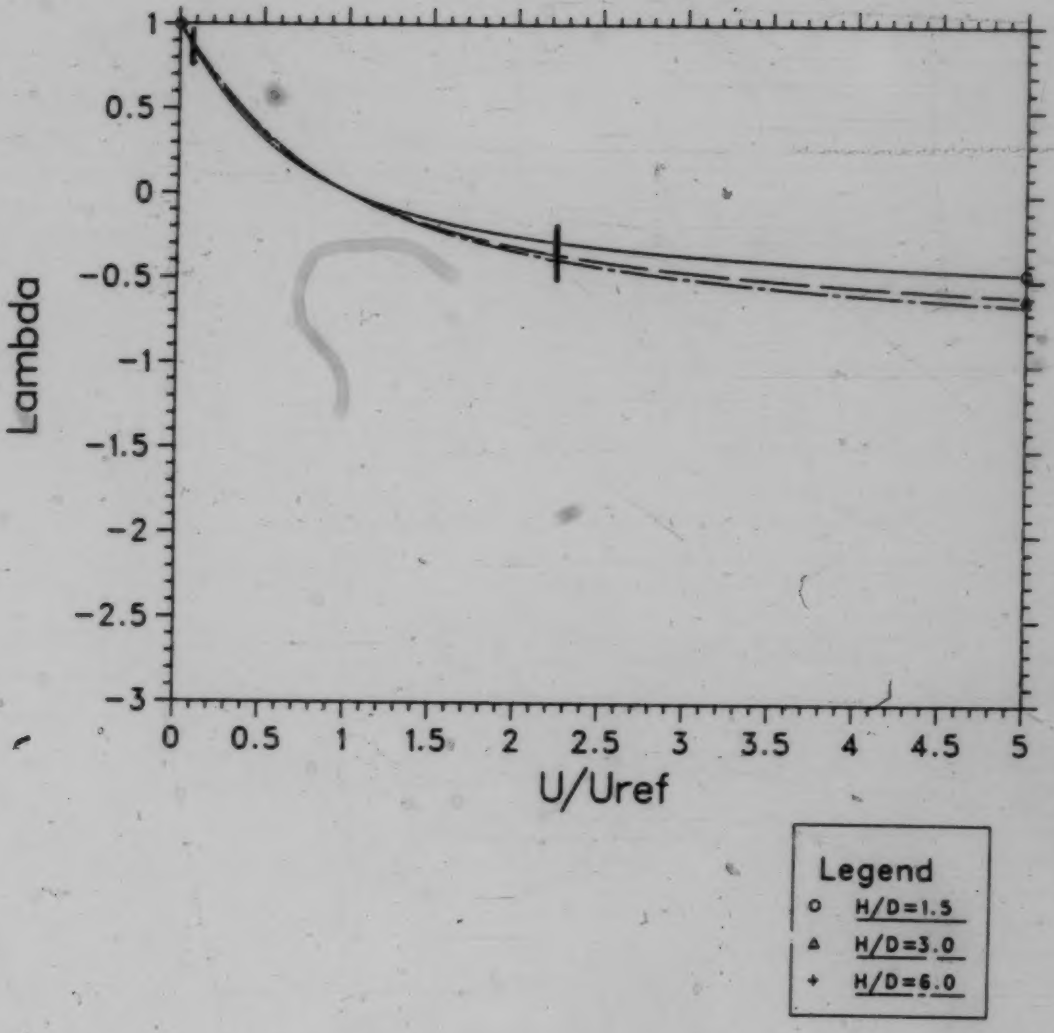

Figure 6.110 NNGRCs for Tunnel Crown, Calculated for K_o=1.0

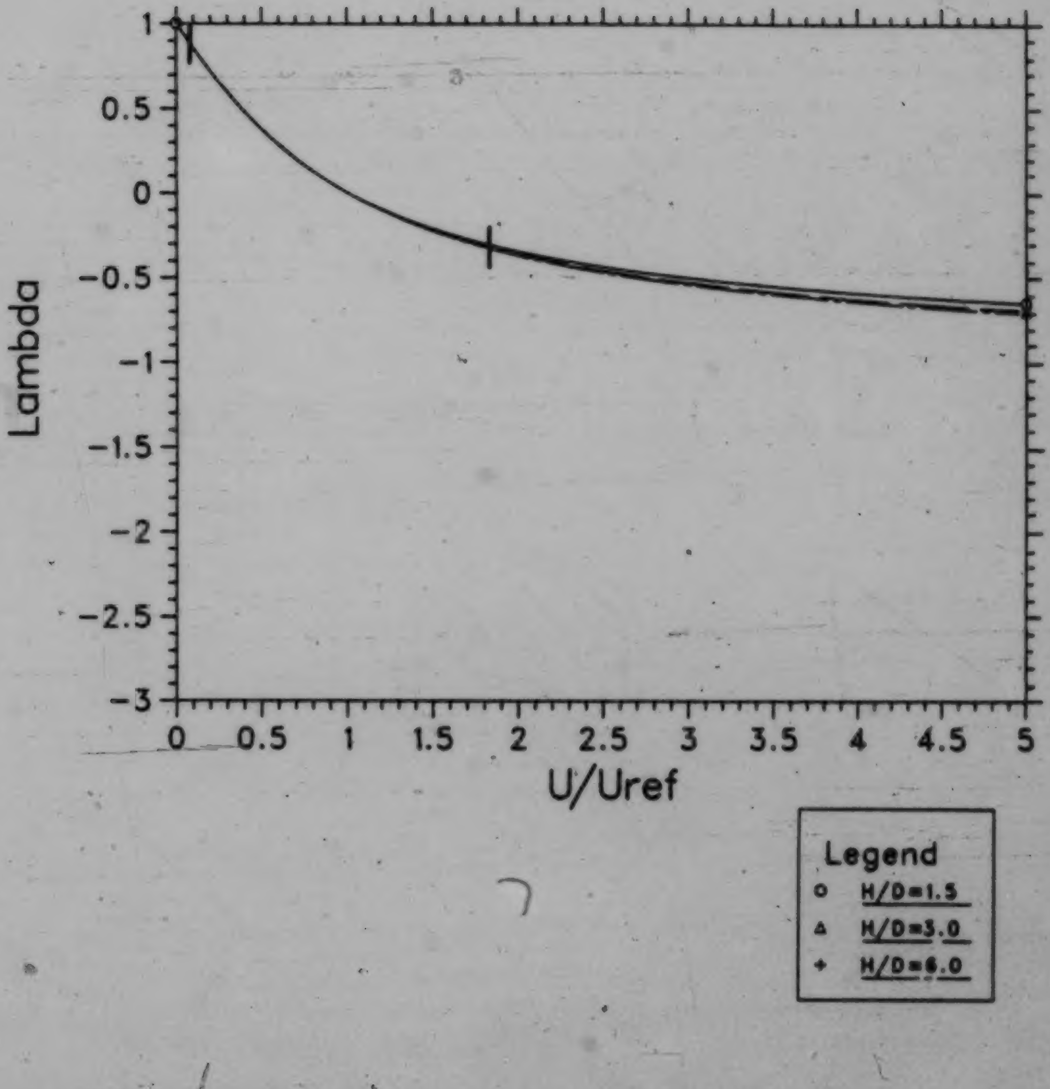

Figure 6.111 NNGRCs for Tunnel Springline, Calculated for K_o=1.0

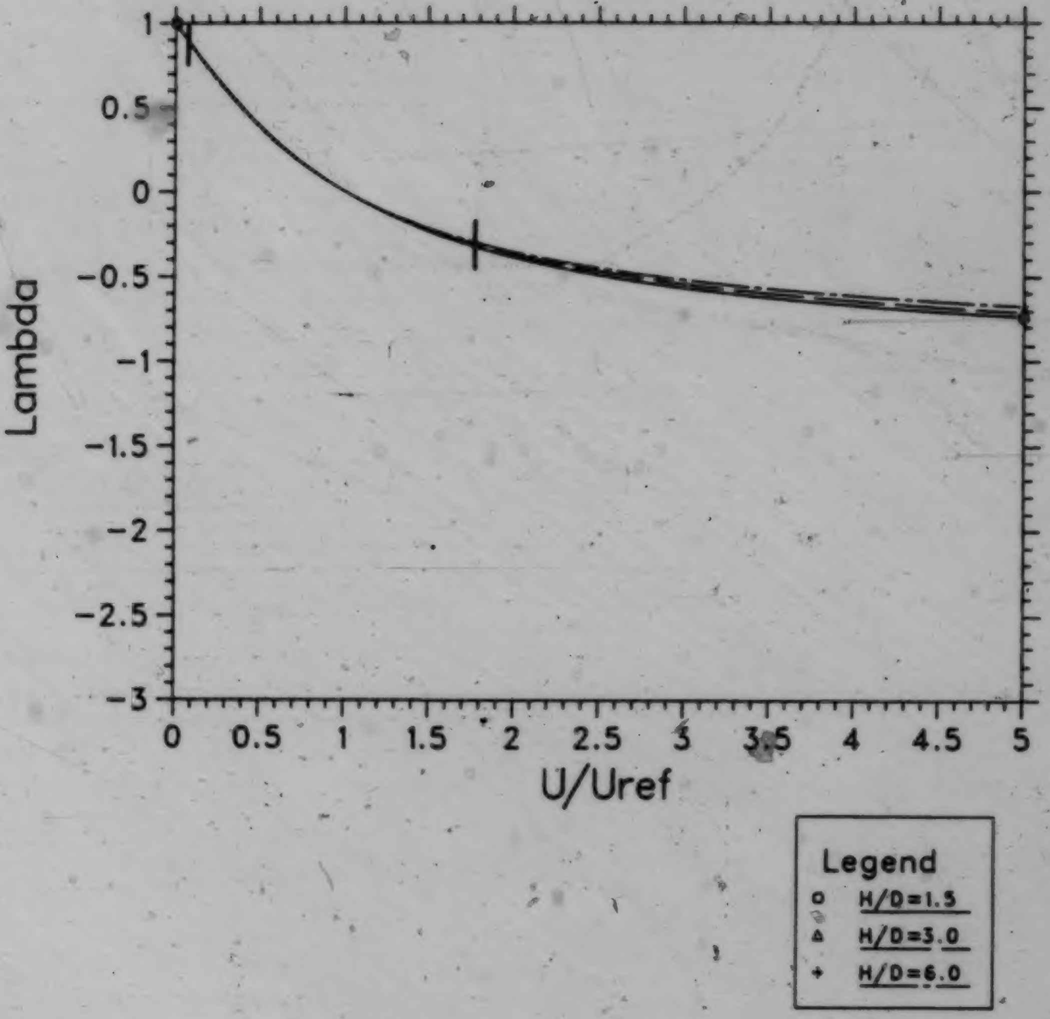

Figure 6.112 NNGRCs for Tunnel Floor, Calculated for K_o=1.0

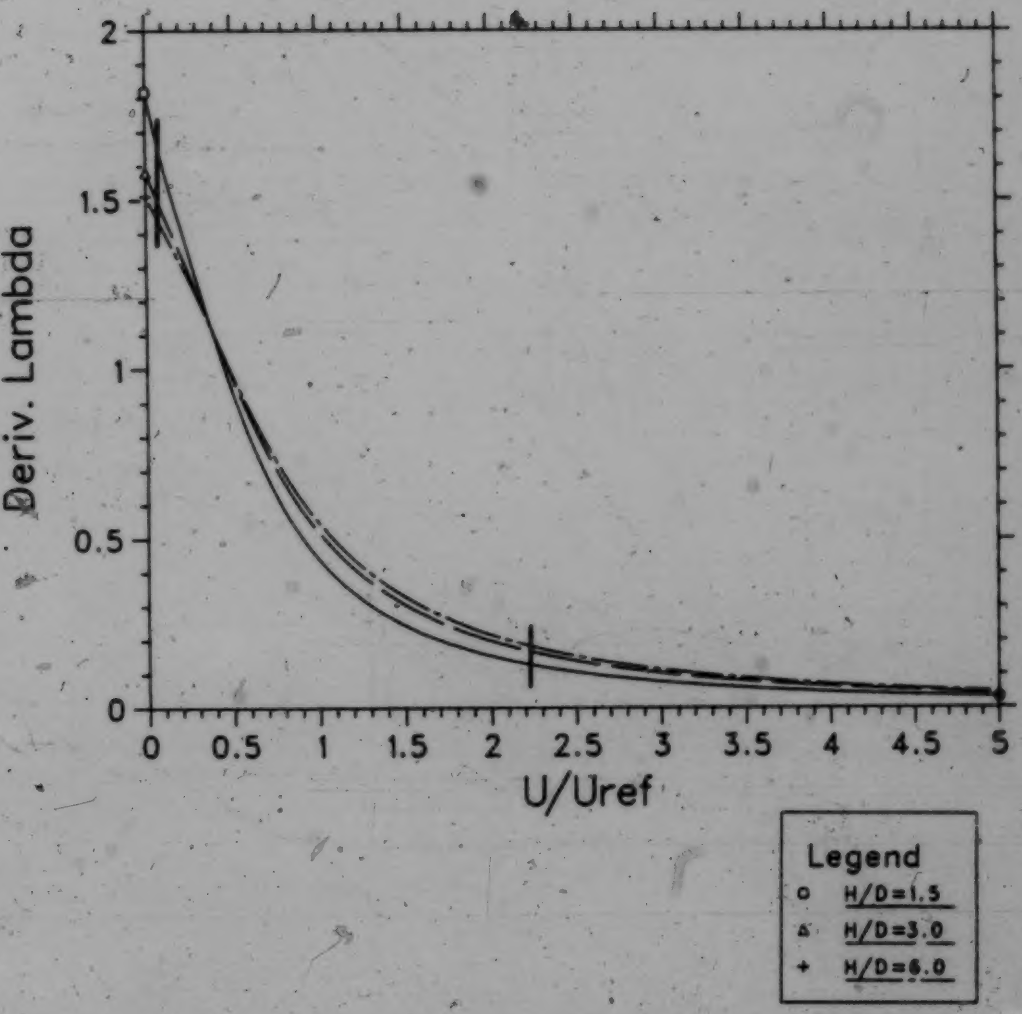

Figure 6.113 Variations of λ' for the Tunnel Crown, Calculated for K_o=1.0

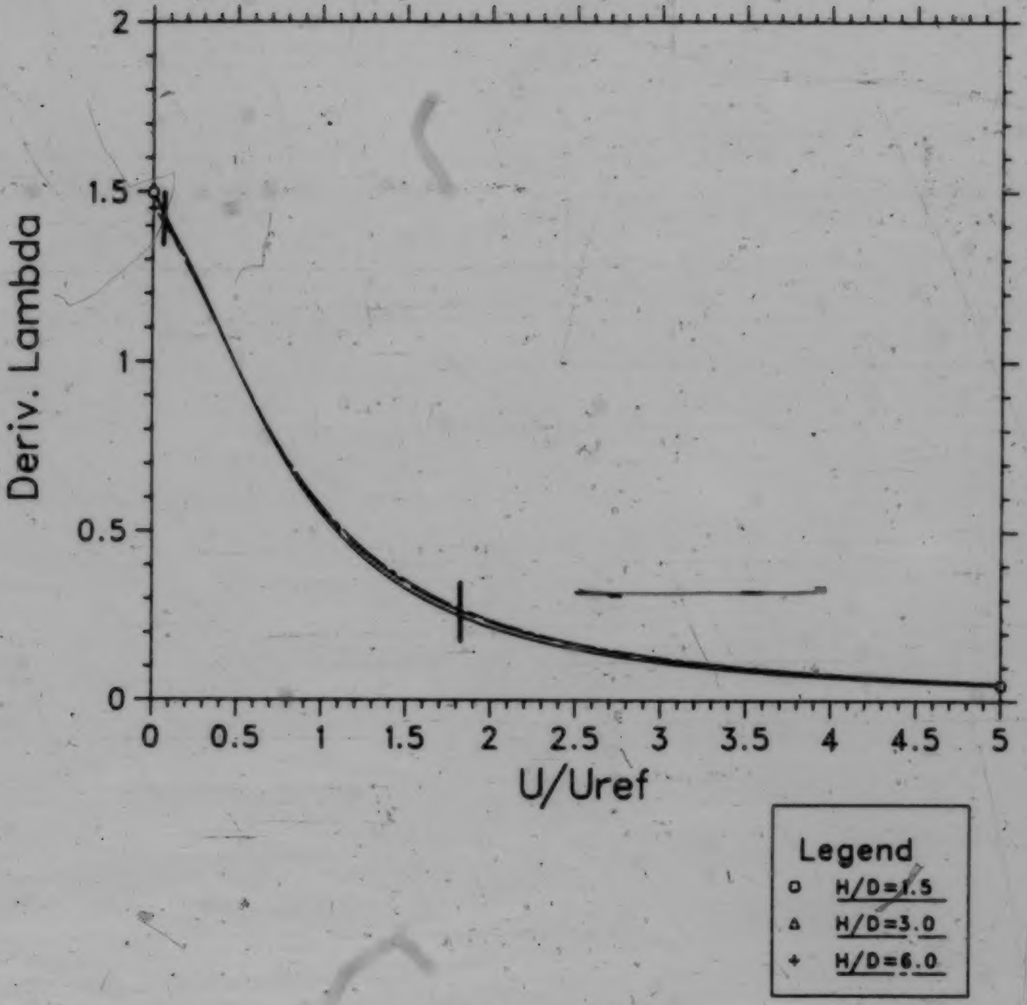

Figure 6.114 Variations of λ' for the Tunnel Springline, Calculated for K_o=1.0

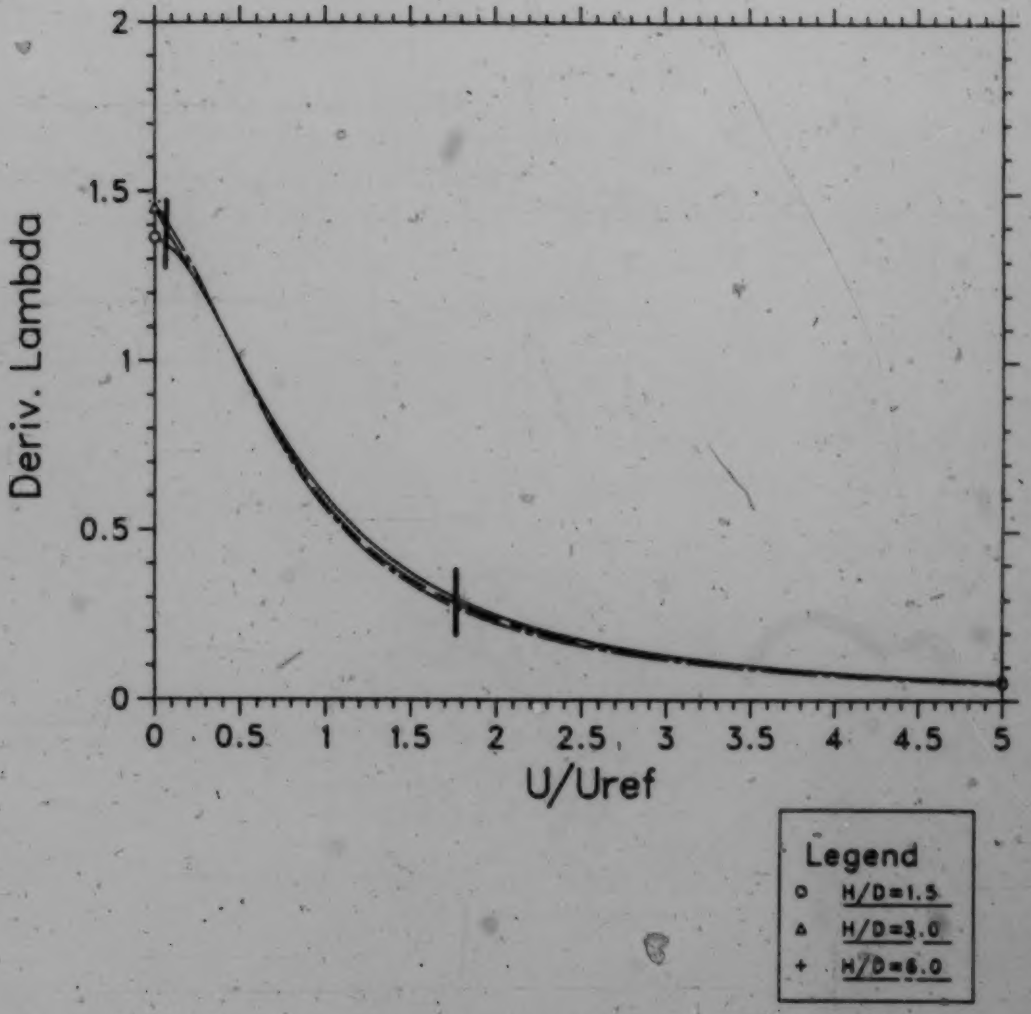

Figure 6.115 Variations of λ' for the Tunnel Floor, Calculated for K_o=1.0

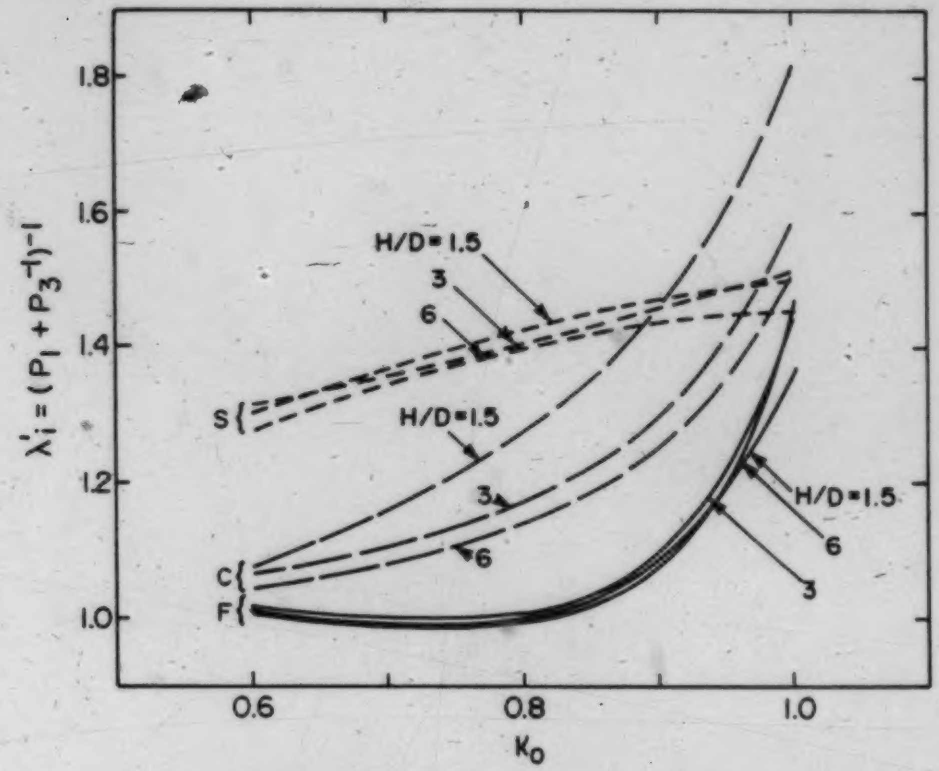

	H/D	λ'_i		
		$K_0 = 0.6$	$K_0 = 0.8$	$K_0 = 1.0$
C	6	1.0446	1.1421	1.5116
	3	1.0663	1.1719	1.5825
	1.5	1.0780	1.2782	1.8176
S	6	1.2808	1.3973	1.4518
	3	1.3143	1.4066	1.5110
	1.5	1.3071	1.4249	1.4981
F	6	1.0092	0.9992	1.4692
	3	1.0210	1.0105	1.4517
	1.5	1.0135	1.0055	1.3641

Figure 6.116 Variations of the Initial Slope of the Twice Normalized Ground Reaction Curves with K_o and H/D

6.5 Limits of the Generalized Solution

6.5.1 Extrapolation of the Numerical Results

It was pointed out earlier that, for the generalization of the parametric analyses results in terms of ground reaction curves, all numerical output after local failure had developed was disregarded (Section 6.3.2). The reasons behind this decision were: a) the numerical model used was not designed to represent this type of behaviour (for instance, the failure criteria can be violated); b) the GRC resulting after local failure of an element or group of elements to which a low tangent modulus is assigned ceases to be homothetic; c) the generalized solution was not intended to cover responses approaching soil failure or ground collapse.

In order to achieve the projected generalization and to find out the functions reprsenting the GRC for the particular soil models investigated (e.g., equations 6.11 and 6.12), some curve fitting techniques were used. The NGRCs were found to be described by equations such as 6.17 and 6.24, obtained by applying non-linear regression techniques to the numerical results of the parametric analyses.

The numerically derived functions that resulted were unbounded and they therefore, may be used to interpolate data between the discrete numerical results of the parametric analyses, and also they may be used for the extrapolation of these results beyond the range of the data investigated. Although the latter use of these functions was not initially envisaged, it was found that~~,~~ for practical use and under certain circumstances, some limited extrapolation of data could be required. This may happen when the resulting calculated GRC was "too short" as can be the case in soils with low ϕ and under low K_o, where local failure is attained at small amounts of ground stress release. An approach to this problem could be to accept the onset of global collapse simultaneously with the event of local failure. Accordingly, this would imply a horizontal extension of GRCs at the points of local failure so that very large displacements develop for a certain amount of stress release.

Clearly, this alternative presents an inconvenience: it may be too conservative in terms of ground stress displacement (and thus loads onto the support) and in terms of opening closure. With this problem in mind, it was contemplated that the use of the fitted functions to extrapolate the ground reaction curves could be a more sensible alternative, provided the implications of this operation are fully recognized and caution is exerted in interpreting the extrapolated results.

To illustrate this point, consider the NGRCs shown in Figure 6.58 for $H/D=3$, $\phi=30°$ and $K_o=0.8$. These curves are reproduced in Figure 6.117 by the solid lines OR. R represents the end points of the curves shown in Figure

6.58 and correspond to the numerical results obtained in the last unload increment, prior to the load step at which local failure developed (at an element next to the springline in this particular case). If the NGRCs are extended beyond R, using equation 6.24 and the corresponding parameters found in Table 6.16, the dashed curves shown in Figure 6.117 are obtained. One notes that the extrapolated portions of the NGRCs do not present any significant discontinuity at point R.

By now examining Figure 6.64, we identify point R of the springline NGRC for ϕ=30°, as the end point of this curve for Σ=0.4. This point reappears in the NNGRC shown in Figure 6.90 also as R. Note that, in the latter figure, to the right of R there exists another point (T), which is the end point of the NGRC for ϕ=20° (Figure 6.64). By virtue of the homothety, to this last point there exists a corresponding homothetic point (T') in the NGRC for ϕ=30° which coincides with T in the twice normalized ground reaction curve (Figure 6.90). This point could not be numerically obtained as the unloading increment used was too large. In this particular case, had this increment been about 7% instead of the standard 10%, point T' on the NGRC for ϕ=30° in Figure 6.64 would have been obtained numerically. Regardless of this, it was possible to identify point T' from point T in Figure 6.64, by assuming that the NGRCs are homothetic and by taking the similitude axis OT and defining T' as the intersection of this axis with the

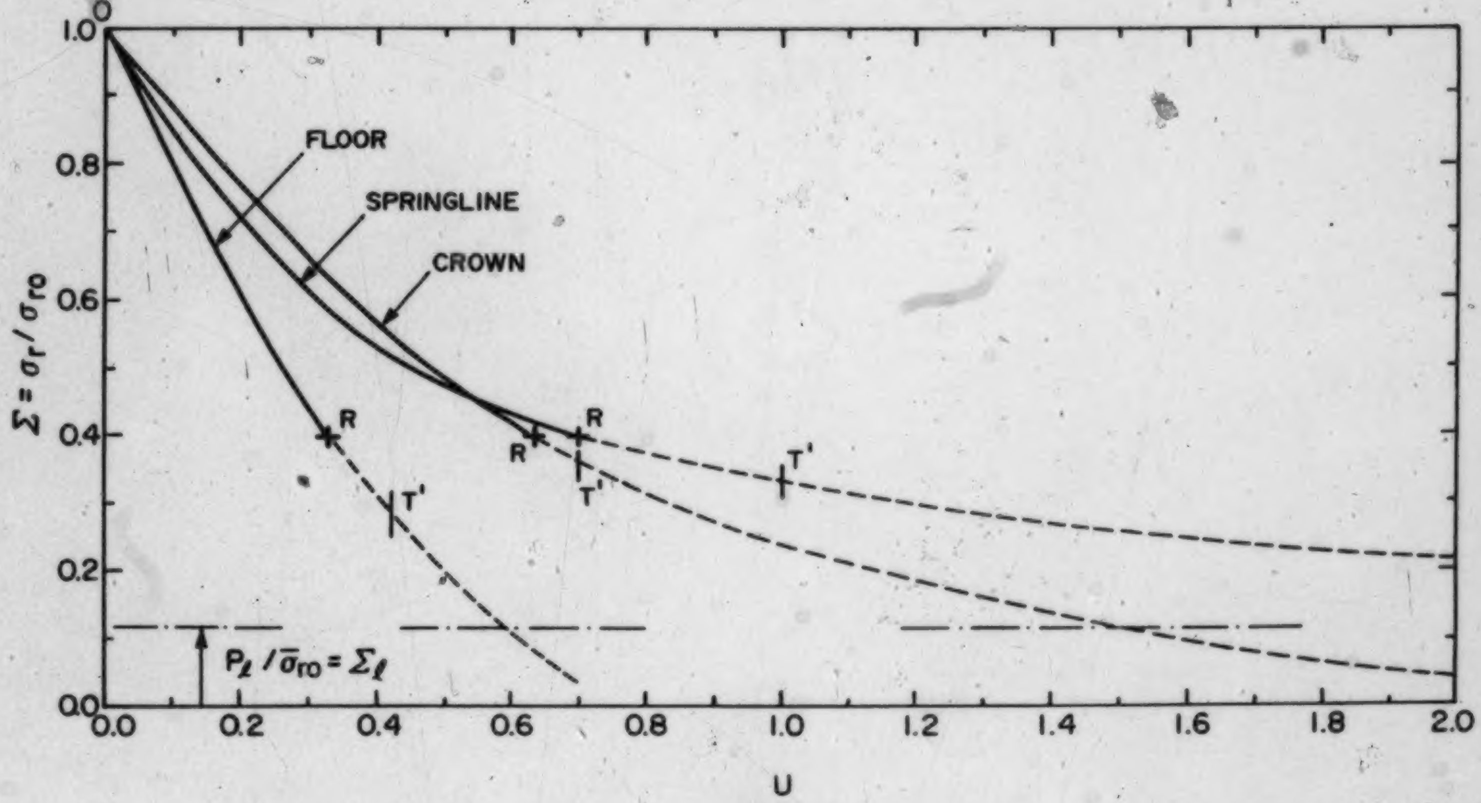

Figure 6.117 Extension of the NGRCs for H/D=3, K_o=0.8 and ϕ=30°

extended NGRC for $\phi=30°$.

If the property of homothety can be accepted for the NGRCs of different ϕ values, then the extended portion RT' of the curves in Figure 6.117 are fully admissible. The terminal points T' of the extended NGRCs are easily found through the ratio U/U_{ref} of the extreme rightward point T shown in Figure 6.90, and indicated by the right vertical bar in all λ versus U/U_{ref} curves (Figures 6.94 to 6.96, 6.102 to 6.104 and 6.110 to 6.112). In brief, the results given by these curves up to these points can be used with no restrictions. However, beyond them (to the right of points T' in Figure 6.117), there is not assurance that the relationships between stresses and displacement are correct. In particular, stresses giving stress ratios below $\Sigma_{T'}$ may either violate the failure criteria or may be smaller than the minimum required to maintain stability of the opening. In other words, the stresses given by the extrapolated NGRC beyond T' may not ensure the equilibrium of the system.

Unfortunately, there is no simple way to check if the failure criteria is being locally violated. In fact, one may assess the global stability of the tunnel, to evaluate how close to tunnel collapse one is, when using acting stresses lower than that at T'. A stability calculation may give some indication as to whether or not the acting stresses are high enough to ensure global equilibrium but it will not ensure that local equilibrium is attained. Neither will it guarantee that the failure criteria is not being violated locally. Consequently, the displacements associated with these stresses are likely to be in error, and are possibly smaller than the correct ones. In spite of these limitations, if one still needs to go beyond T' in Figure 6.117, the least that can be done is to ensure that the factor of safety for the acting stresses is greater than unity.

The discussion just presented referred to the cohesionless soil model but it applies to the frictionless soil model as well. The extension of the NGRCs shown in Figure 6.47 for H/D=3 and $c_u/\gamma D$=1.25 is presented in Figure 6.118. The same notation used before is adopted herein. The extension beyond point R is obtained using equation 6.17 and the corresponding parameters found in Table 6.13 or in Figures 6.85 to 6.88. Similarly the reader is referred to Figures 6.55 and 6.83. Note that in the latter, point T lies outside the figure. The positions of points T' in Figure 6.118 are shown in the inset. The same comments made regarding Figure 6.117 are valid here. The main difference lies in how the points T' are found for the frictionless soil model. As the general solution for this case was presented in a slightly different format, some additional information is needed for establishing T'. This is supplied by Figures 6.119 to 6.121 which provide the values of U_{ref} for different $c_u/\gamma D$ and H/D values. Note that U_{ref} was deliberately chosen as to result in a linear function of the strength ratio. In the inset shown in each of these three

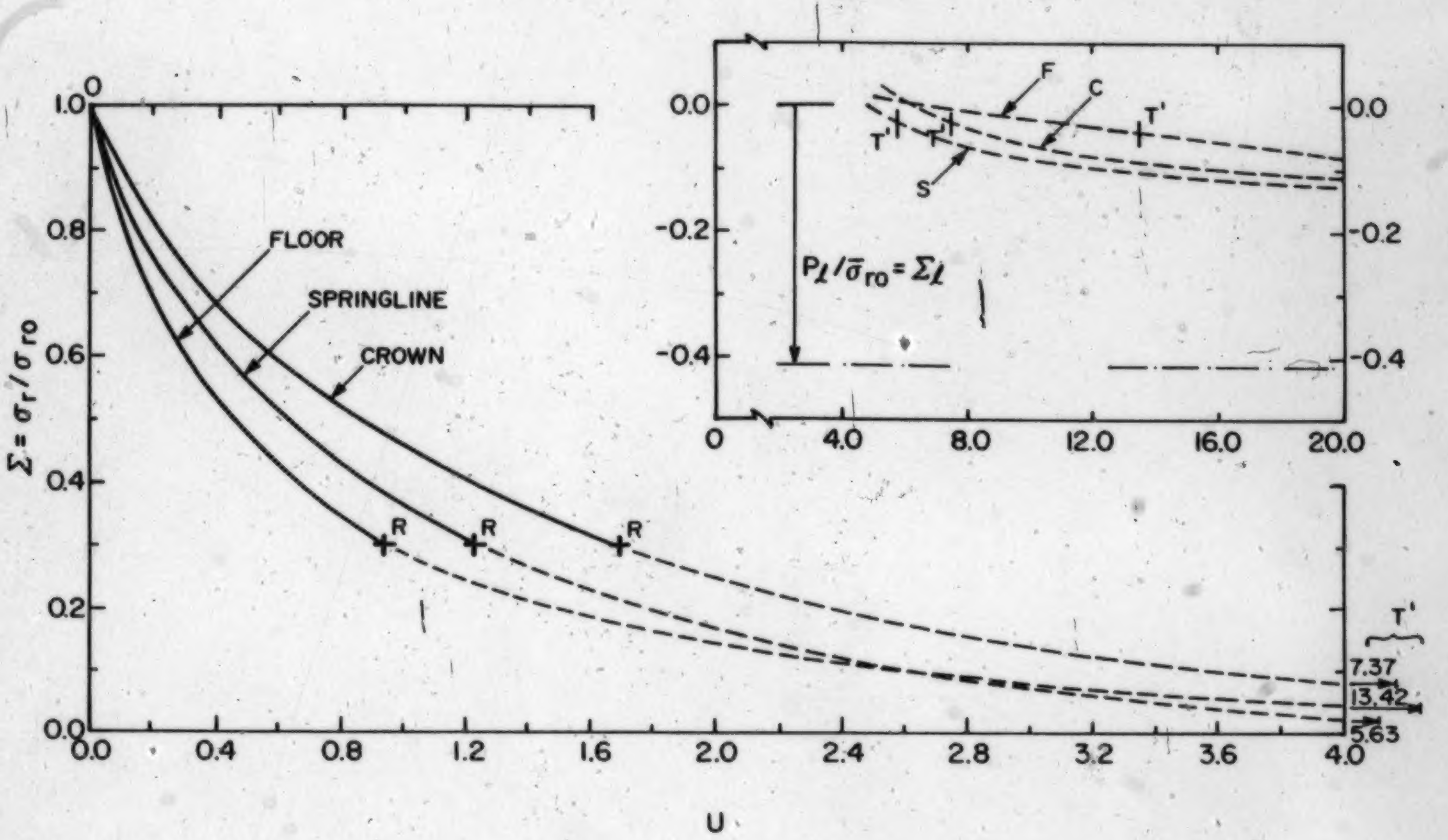

Figure 6.118 Extension of the NGRCs for H/D=3 and $c_u/\gamma D$=1.25

figures, the maximum value of U/U_{ref} calculated for each H/D is also given. This maximum normalized dimensionless displacement corresponds to the terminal point T identified by the vertical bars shown in the NNGRCs for the cohesionless soil.

Another peculiarity found in the results of some analyses with the frictionless soil model was that tensile stresses developed in some elements around the opening, before the development of shear failure. This was noted mainly in the shallower tunnel cases with higher strength ratios. As explained in the introductory remarks to Section 6.3.2, all numerical data output obtained following the development of any tension in the ground was disregarded.

6.5.2 Assessment of the Two-Dimensional Stability

Although not recommended by the reasons exposed in the previous section, if one is forced to use the generalized solutions beyond their terminal points, an assessment of the two-dimensional tunnel stability is required. It should be stressed that this does not secure that the extrapolation is correct, but this evaluation can provide indications of whether or not the calculated stresses for a certain closure of the opening are sufficiently high to keep it stable. Though the excavation stability verification is usually circumscribed to the tunnel face and heading (See Section 4.2.3), in this particular case the two-dimensional stability evaluation also becomes important. The subject was

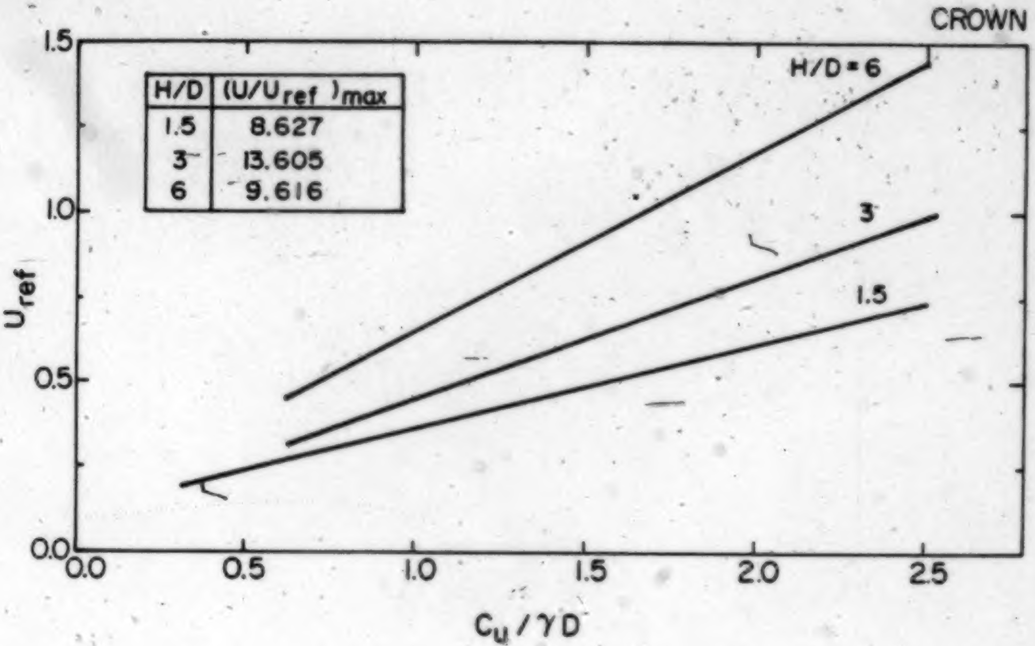

Figure 6.119 Reference Values used for Normalizing the NGRC of the Tunnel Crown for the Frictionless Soil Model and Components to Define the Limiting U of the Fitted Function

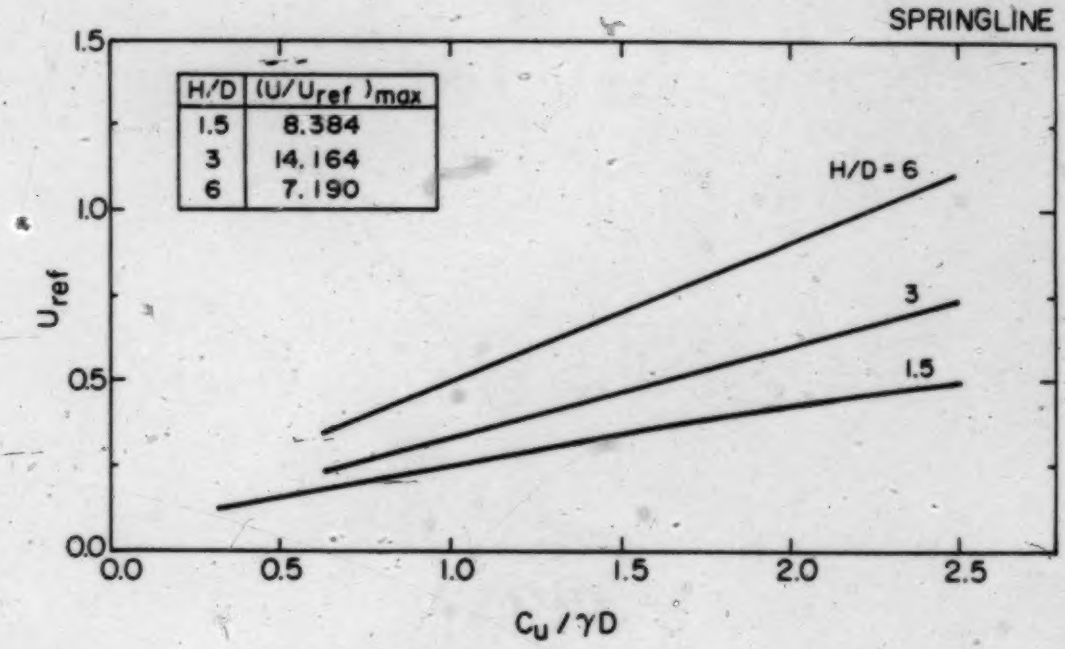

Figure 6.120 Reference Values used for Normalizing the NGRC of the Tunnel Springline for the Frictionless Soil Model and Components to Define the Limiting U of the Fitted Function

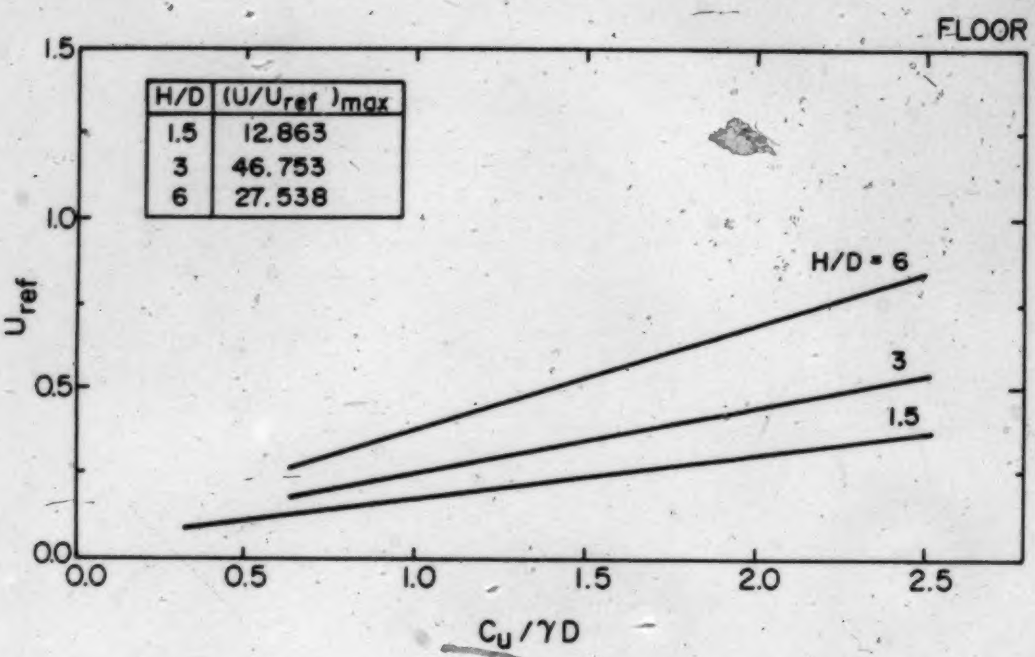

Figure 6.121 Reference ~~Values~~ used for Normalizing the NGRC of the Tunnel Floor for the Frictionless Soil Model and Components to Define the Limiting U of the Fitted Function

discussed and reviewed in different sections of this thesis, especially in Section 4.3.4.

The possibility of violating the boundary or failure conditions in limit equilibrium analyses of the ground mass suggests the use of plasticity solutions. The available plasticity solutions for estimating the two-dimensional stability of a shallow tunnel are based on the Limit Theorems (Lower and Upper Bound). These theorems can be proved for materials with an associated flow rule, where the angle of dilation, ψ, is equal to the friction angle, ϕ. While this assumption provides a good approximation in the case of a saturated soil under undrained loading, in which $\psi=\phi=0$, in general it does not properly represent the actual soil behaviour at ultimate failure under drained loading, when usually ψ is not equal to ϕ. Davis (1968:352) showed that the Upper Bound Theorem can be proved to be correct even for this condition (see also Atkinson, 1981:117). No complete proof of validity of the Lower Bound Theorem was found so far for this condition. There are some indications, however, that it may be valid for ϕ not equal to ψ and $\psi=0$ (for instance, Cox, 1963 - quoted by Davis, 1968:345 and Palmer, 1966).

Davis (1968:346) suggests that while the plastic deformations may strongly depend on the flow rule, the collapse loads may not. Atkinson (1981:118) seems to share this opinion and suggests that the approximate lower bounds calculated for a soil with ψ not equal to ϕ by assuming $\psi=\phi$

are unlikely to exceed the true collapse loads.

An additional aspect of the plasticity solutions is that a unique collapse load is steadily approached, and remains constant at its maximum once collapse is fully developed. This can be proved to hold (Davis, Op.cit.:346) on the condition that the geometry of the problem is not changed significantly. Regarding the tunnel problem, this implies that a unique collapse load can be found provided 'loosening' effects and associated changes in the geometry of the problem does not occur (see Section 3.2.3). In other words, plasticity solutions could be used to approach the stresses associated with point E in Figure 3.8. Beyond it, the changes in geometry would have to be considered in order to investigate the loads associated with point G in Figure 3.8, which lies on the speculated sweeping upward ground reaction curve as discussed in Section 3.2.3. If the displacements are limited as in good ground control tunnelling conditions, which are usually required in urban environments, it will be sufficient to investigate the ground stability on the assumption of uniqueness of the plasticity solution.

The available plasticity solutions to the two-dimensional shallow tunnel problem usually represent the internal stress acting on the circular opening as a uniform pressure which, at ground collapse, is denoted by p_1. An exception to this rule are solutions that assume the cavity being filled by a heavy and non-permeating fluid with a density equal to the soil density (for instance Caquot, 1934:81, or D'Escatha and Mandel, 1974). In both cases, it is noted that the conditions assumed do not correspond exactly to the loading conditions assumed in the two-dimensional numerical modelling adopted in the present study. As described in Section 5.2.2, in any stage of the unloading process, the tunnel contour is subjected to stresses that correspond to a fraction $\Sigma=1-\alpha$ of the in situ stresses, which can be calculated through the expressions given in Figure 2.14. One notes that while in the plasticity solutions the opening walls are subjected only to normal (radial) stresses, the numerical modelling adopted herein assumes that both normal and shear stresses act on the opening contour, which are equal to $\Sigma\sigma_{ro}$ and $\Sigma\tau_o$ respectively, with σ_{ro} and τ_o given in Figure 2.14. Even for $K=1$ (i.e., $\tau=0$), the conditions in the numerical model do not fully correspond to that in the plasticity solution, where the tunnel is assumed to be filled with a fluid with density equal to γ. The latter implies the existance of a pressure gradient across the tunnel, from crown to floor, equal to γ, whereas this gradient is equal to $\Sigma\gamma$ in the numerical model adopted (with Σ smaller than unity).

Even when working in terms of stresses averaged around the tunnel contour, there will always be a non-zero residual shear stress acting on the shallow tunnel walls, whose effect on the limiting tunnel pressure has not been fully assessed. Besides affecting local failure, these shear stresses may affect the global collapse condition and therefore the limiting tunnel load. For K not equal to 1, they may lead to an increase in p_l. For K=1, p_l may also increase since $\Sigma\gamma$ is less than γ. Increased limiting tunnel pressure implies a smaller factor of safety. defined as (see Chapter 2):

$$FS=\frac{\sigma_o - p_l}{\sigma_o - \sigma_i} \qquad [6.31]$$

where σ_o is the in situ vertical stress at the tunnel axis and σ_i is the current internal stress in the tunnel. As the latter, in the numerical model, varies from point to point of the contour, it seems convenient to define σ_i as the current average radial stress acting on the tunnel profile. Thus:

$$\sigma_i = \Sigma\bar{\sigma}_{ro} \qquad [6.32]$$

where $\bar{\sigma}_{ro}$ is the average in situ radial stress, which is given by:

$$\bar{\sigma}_{ro} = \frac{1+K_o}{2}\gamma(H + \frac{D}{2}) \qquad [6.33]$$

Therefore:

$$FS = \frac{1 - \Sigma_l((1+K_o)/2)}{1 - \Sigma((1+K_o)/2)} = \frac{(1-K_o)/(1+K_o) + \alpha_l}{(1-K_o)/(1+K_o) + \alpha} \qquad [6.34]$$

with Σ_l equal to the ratio $p_l/\bar{\sigma}_{ro}$ and $\alpha_l=1-\Sigma_l$.

It should be remembered that the collapse pressure given by plasticity solutions is independent of the initial stresses acting in the ground before the tunnel is built and also independent of the sequence in which the stress release is applied to the opening, provided it is steadily increased during unloading (Davis, 1968:346,347, D'Escatha and Mandel, 1974:46). Hence p_1 does not depend on K_o, although the local failure in the ground during the unloading process does depend on K_o. Note that FS expressed by equation 6.31 or 6.34 is dependent on K_o, not through p_1 but through the current average radial stress acting on the opening contour. Note, moreover, that this definition of FS is approximate since the effect of the shear stresses acting on the contour was disregarded.

Safe estimates of p_1 can possibly be made through solutions developed from applications of the method of characteristics. As it is based on a statically admissible stress field not violating the failure criteria, the solution it provides is a lower bound (theoretically safe) estimate of the exact solution. In other words, the p_1 value estimated is higher than (or equal to) that actually causing the tunnel collapse. On the other hand, an upper bound (unsafe) solution will provide an estimate of p_1 which is lower than (or equal to) the correct value.

If the flow rule is associated, with $\psi=\phi$, then the stress characteristics line coincide with the velocity characteristics (or slip lines). Therefore one can assume that, at collapse, the soil strength is fully mobilized along the slip lines and the safe collapse load can be estimated through the method of characteristics (see, for example, Wu, 1966:215).

For a purely cohesive soil, D'Escatha and Mandel (1974) and Seneviratne (1979:79) (reproduced in Davis et.al., 1980) presented lower bound solutions for the two-dimensional shallow tunnel problem which are shown together in Figure 6.122. The solutions by these authors are intrinsically the same and assume that the opening is supported by a uniform pressure ($\gamma_t=0$). They differ slightly (see curves for $c_u/\gamma D=0.25$ and 1.00) because Seneviratne's characteristic net was less refined than D'Escatha and Mandel's. The tunnel contour was divided into 16 equal segments in the former and into 60 in the latter. The D'Escatha and Mandel solution is therefore numerically more accurate. However, it does not provide solutions for the intermediate range of strength ratios which is of considerable practical interest and for this reason, both solutions are reproduced in Figure 6.122.

Also plotted in Figure 6.122 are the results of some two-dimensional centrifuge model tests (Series I) by Mair (1979:121). It can be appreciated that the interpolated plasticity solution provides a very close estimate of the collapse tunnel (internal) pressures observed in the tunnel model tests.

For a cohesive and frictional soil, D'Escatha and Mandel (1974) also presented 'safe' estimates of the collapse tunnel pressure, once more assuming $\psi=\phi$. These are given by the curves shown in Figures 6.123 to 6.126, for ϕ equal to 10° to 40° and different cohesion, c, expressed in terms of the ratio $c/\gamma D$. Again, this solution assumes that

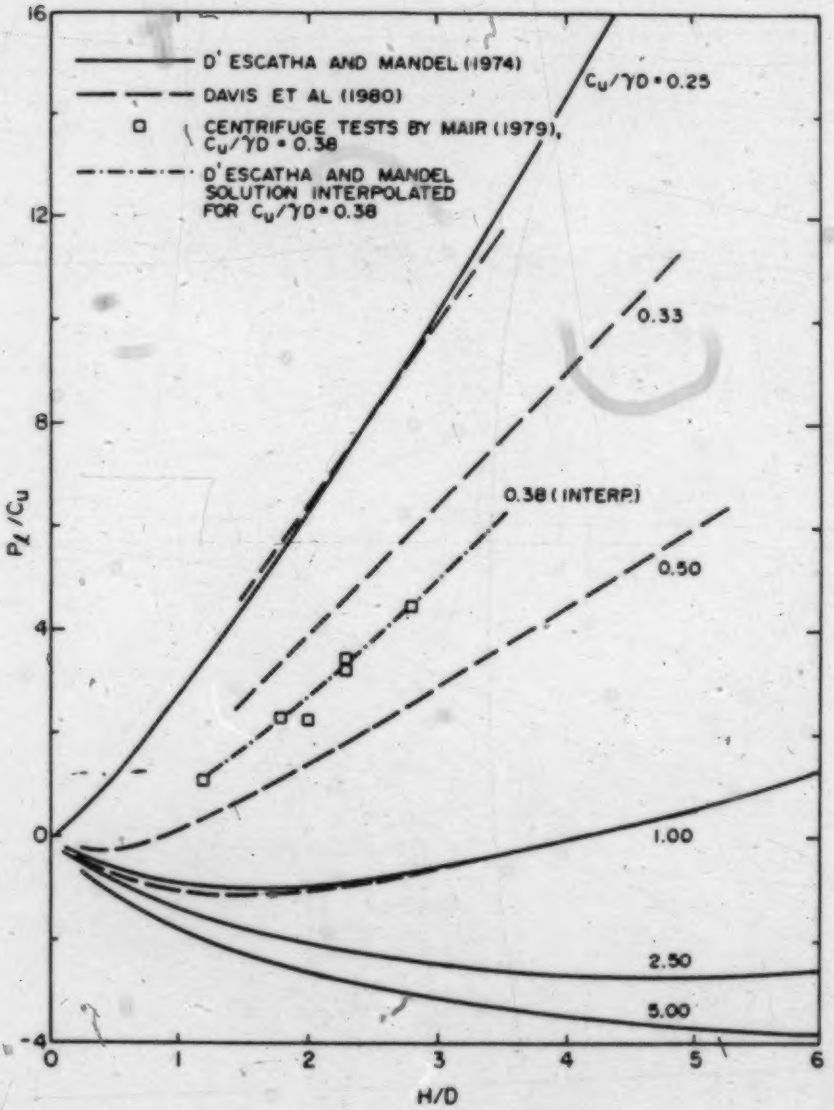

Figure 6.122 Lower Bound Solution for Tunnel Collapse Pressure in a Frictionless Soil

the tunnel walls are submitted to a uniform pressure, p_1.

An upper bound solution for local collapse of a wedge of cohesionless soil at the tunnel crown (See Figure 3.7) can easily be obtained by a work calculation assuming $\psi=\phi$. This solution, which gives a tunnel pressure which is lower than (or equal to) the actual internal pressure at collapse was first proposed by Atkinson et.al., (1975:84) and is given by:

$$\frac{p_1}{\gamma D}=\frac{1}{4\cos\phi}\left[\frac{1}{\tan\phi}+\phi-\frac{\pi}{2}\right] \qquad [6.35]$$

provided that the sides of the wedge do not intersect the ground surface. In other words, provided

$$\frac{H}{D}>\frac{1}{\sin\phi}-1 \qquad [6.36]$$

Values of the $p_1/\gamma D$ given by equation 6.35 and the restriction given by 6.36 are shown in Figures 6.123 to 6.126 by chaindotted lines. It can be observed that for any ϕ this Upper Bound solution always provides a p_1 value lower than that given by the lower bound solution (for $c/\gamma D=0$).

If the above solutions are compared to results of tunnel model tests carried out under drained conditions, mixed results are obtained. The lower and upper bound solutions are found to bracket the loads associated with local collapse as observed in static tests in sand by Atkinson et.al., (1975:84). However, under some circumstances they do not approximate the collapse pressures found by Seneviratne (1979:64) in drained static tests in normally consolidated kaolin. The lower bound solution given was found to underpredict the observed collapse pressure of

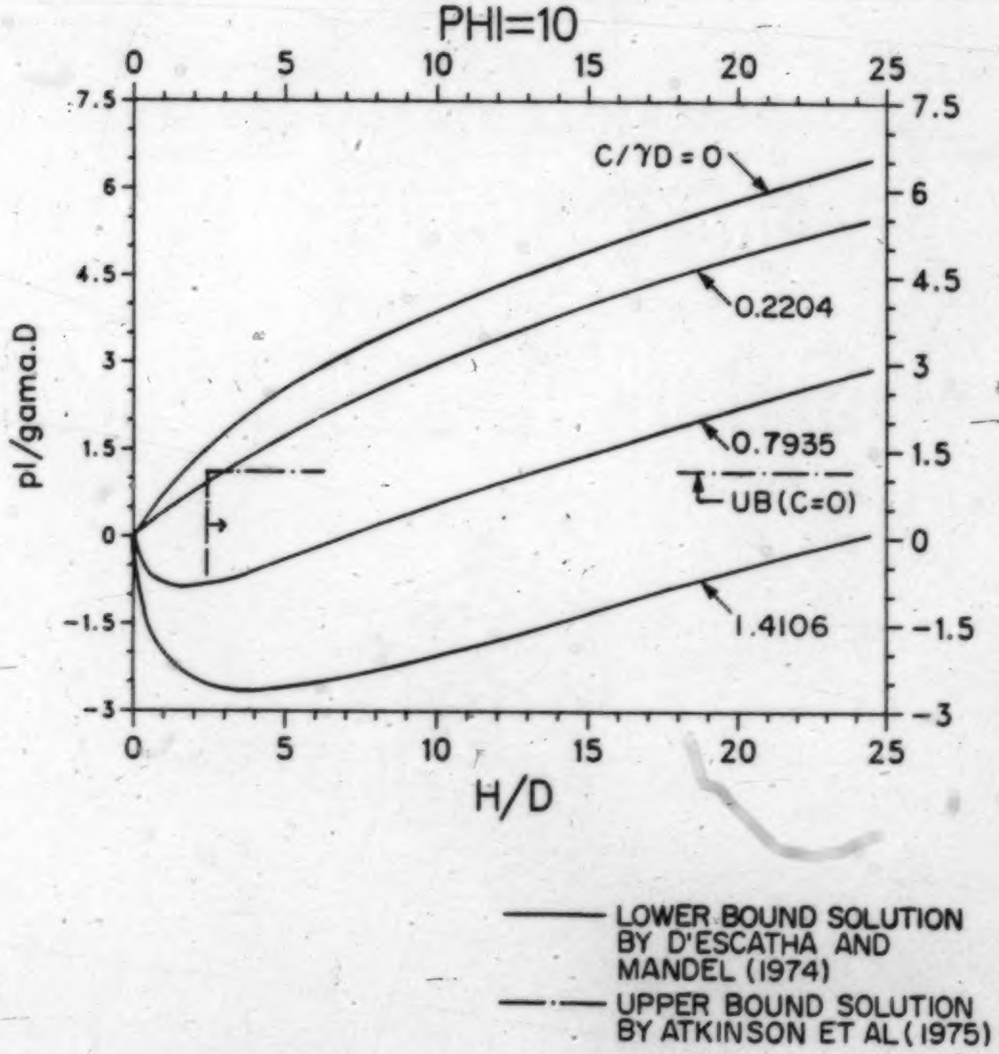

Figure 6.123 Lower and Upper Bound Solutions for Tunnel Collapse Pressure in a Frictional and Cohesive Soil (ϕ=10°)

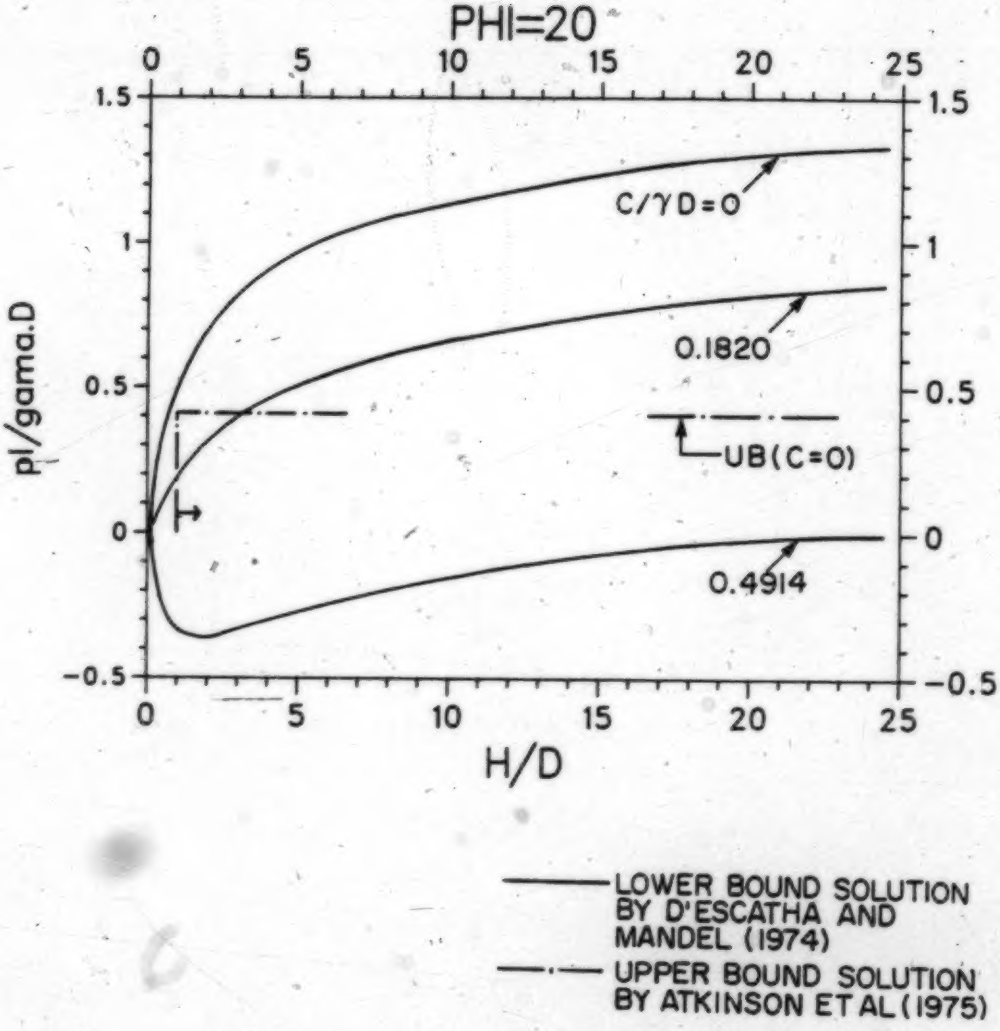

Figure 6.124 Lower and Upper Bound Solutions for Tunnel Collapse Pressure in a Frictional and Cohesive Soil (ϕ=20°)

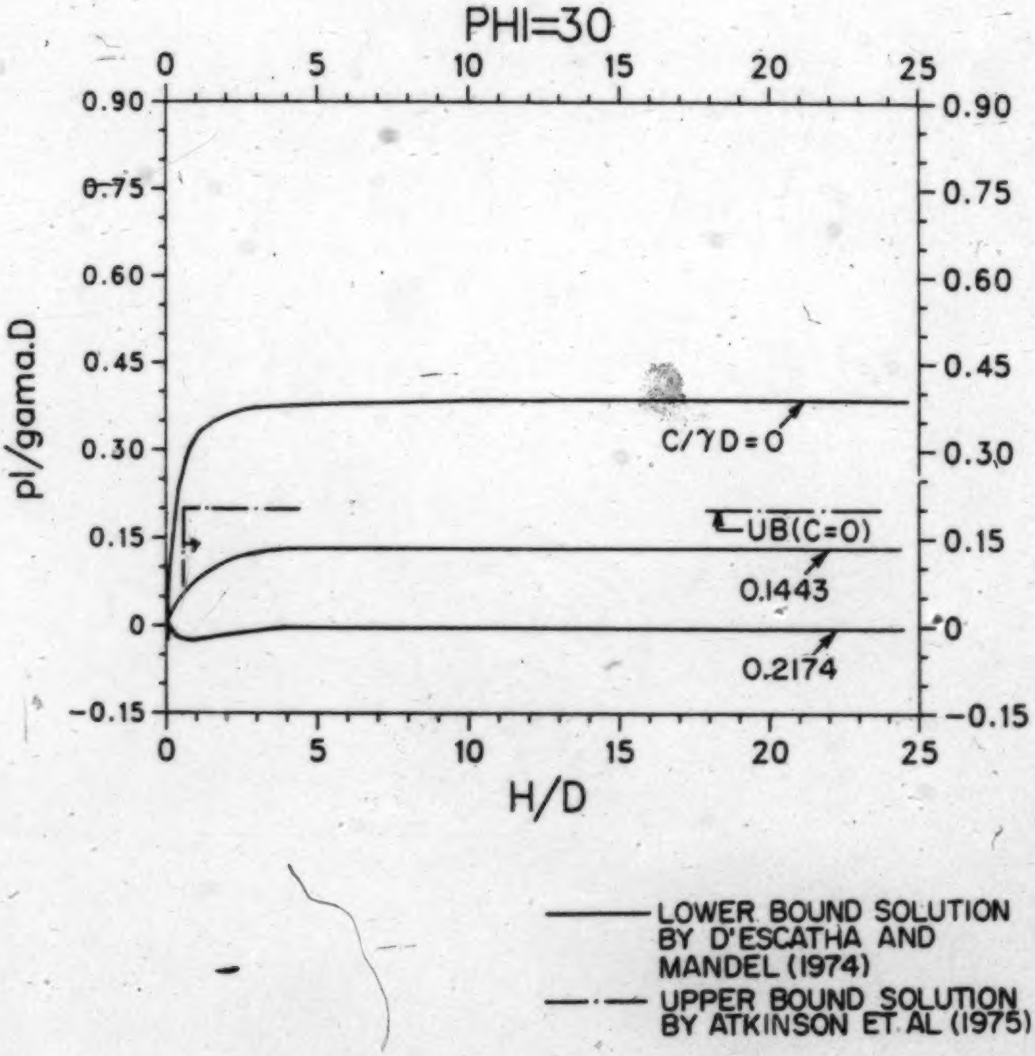

Figure 6.125 Lower and Upper Bound Solutions for Tunnel Collapse Pressure in a Frictional and Cohesive Soil (ϕ=30°)

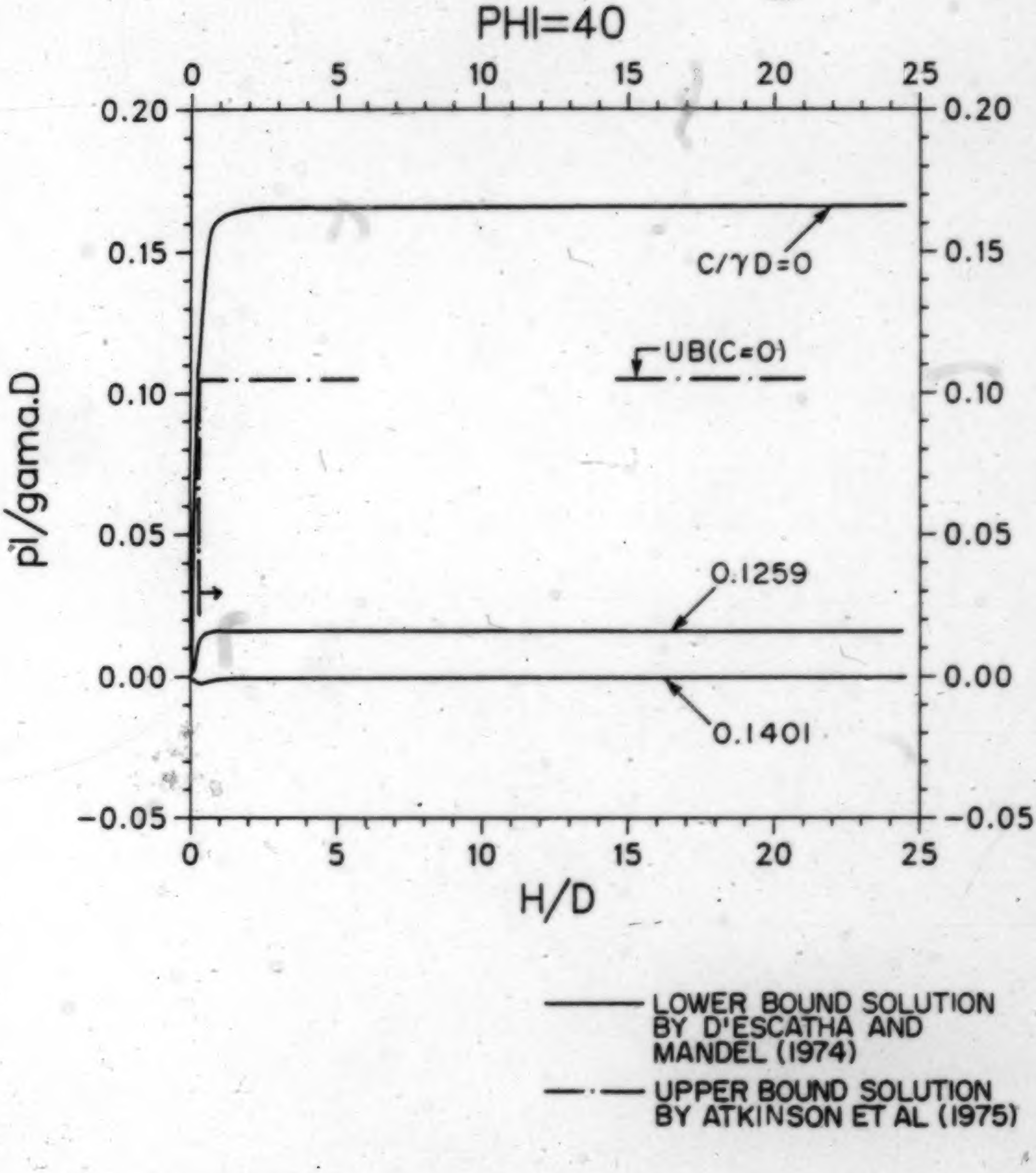

Figure 6.126 Lower and Upper Bound Solutions for Tunnel Collapse Pressure in a Frictional and Cohesive Soil (ϕ=40°)

these tests conducted with small cover to diameter ratios. This may be an indication that, in fact, the solution does not provide 'safe' estimates of the collapse load for materials with a non-associated flow rule behaviour. Another interpretation would be that the deformations in the soil prior to collapse do have an effect on the collapse pressure (see Section 4.3.4). Nevertheless, whatever the reasons are, these findings suggest that caution should be always excercised when using the above solutions, and it is considered good practice to allow as much safety as possible or preferably to avoid any extrapolation of the NGRCs.

If the above lower bound solutions are applied to the conditions assumed in the analyses that led to the results shown in Figure 6.117 and 6.118, the corresponding p_1 and $\Sigma_1=p_1/\bar{\sigma}_{ro}$ are found. These are shown by the chaindotted lines also plotted in these two figures. Those points in the NGRCs below the $\Sigma=\Sigma_1$ line would thus imply stresses acting on the opening smaller than those needed to keep it in a state of limit equilibrium. Note in Figure 6.117 that the dimensionless displacement, U, at the tunnel crown corresponding to $\Sigma=\Sigma_1$ is about U=1.5, which is not dissimilar to the limiting value of U=1.8 suggested in Section 2.3.4.3 for a near collapse situation. Note also that in Figure 6.118 the NGRCs are not intersected by the $\Sigma=\Sigma_1$ line and thus they always give stresses which are higher than those at collapse. This feature is observed for some situations in the generalized solution for the frictionless soil model, but only when $R_f=1$. When the failure ratio is smaller than unity, the NGRC becomes steeper and the $\Sigma=\Sigma_1$ line may intersect them.

6.6 Summary and Conclusions

The main objective of this chapter was to develop a procedure that would allow the ground reaction or stress release curves of points at the contour of a shallow tunnel to be obtained without the need of finite element analyses. In parallel with this development, it was also attempted to obtain the relevant ground displacements associated with the reduction of the in situ stresses, with the tunnel construction being represented by a two-dimensional simulation.

To achieve these aims, some additional simplifications were introduced into the 2D finite element model presented in Chapter 5. These simplifications led to the establishment of two stress-strain models: the frictionless soil model and the cohesionless soil model. The first would represent the behaviour of a saturated soil under undrained conditions, whereas the second would simulate the drained behaviour of frictional soil without cohesion. Both models originated from the hyperbolic model presented in Section 5.2.2.1. The first was obtained by setting $\phi=0$, $K_o=1$ and by making the Janbu's exponent n equal to zero. The second was obtained by setting both the cohesion, c, and the exponent, n, equal to zero. With these simplifications, it was found that the resulting stress-strain curves for these two groups of soil present the property of homothety. This property allows the responses of homothetic circular tunnels (tunnels with the same cover to diameter ratio) to be normalized and become represented by a unique response. Unique normalized ground reaction curves (NGRC) are thus found at corresponding points on the contour of homothetic tunnels. Furthermore, unique normalized distributions of ground settlements at the surface and in the subsurface are also found. These findings facilitate the generalization of the numerical results since they become independent of the scale of the problem.

It was shown that the normalized responses calculated for these models are invariant with regard to the unit weight of the soil. It was also demonstrated that the normalized responses calculated for a certain failure ratio R_f are easily extended to different R_f values. This enables the projected solutions to be developed for a fixed R_f value equal to unity. For R_f different from unity, either the undrained strength, c_u, or the friction angle, ϕ, would be transformed into an equivalent strength parameter (c_{ue} or ϕ_e) using equations 6.3 and 6.7. By implementing the equivalent strength parameters an identical solution is obtained.

It was demonstrated that the normalized responses are invariant to the Janbu's modulus K. Both models set Janbu's modulus n equal to zero, therefore assuming that the in situ tangent modulus is constant with depth. This is restrictive since the normalized ground response was shown to be sensitive to the increase of the in situ modulus with depth, notably at the crown and at the floor. A simple expedient was devised to make the NGRC at those points less sensitive to the modulus increase with depth. It consists of normalizing the displacements at the contour to the in situ stiffness of the ground at points located a half diameter radially away from the tunnel. This artifice provided favourable results and one can approximate the increase of the in situ modulus with depth in both soil models.

The use of the cohesionless soil model for soils in which the cohesive component of strength is not zero was investigated. The normalized ground response was found, of course, to depend on the soil cohesion. By neglecting its influence an unduly conservative ground response may be obtained. To bring the results of the cohesionless soil model closer to the correct one, another approximation was proposed and provided reasonable, yet safe, results. It consists of increasing the friction angle in the cohesionless soil model, so that the in situ strength at the springline elevation is equal to the actual strength, defined in terms of the principal stress difference at failure. The adjusted friction angle to be used in the $c=0$ model is given by equation 6.10 and is found to depend on the actual c and ϕ values and on the in situ minor principal stress at the tunnel axis elevation.

In order to further reduce the number of variables, the effect of Poisson's ratio on the normalized ground response was investigated. For the frictionless model, the assumption of a ratio close to 0.5 was justified as representing the behaviour of a saturated soil under undrained conditions. For the cohesionless model, the ground response for two typical values of Poisson's ratio was studied, which lead to the adoption of a Poisson's ratio of 0.4.

After the introduction of the above simplifications, general equations describing the NGRC for the two soil models were presented in terms of dimensionless and independent variables (equations 6.11 and 6.12). Parametric finite element analyses were the modelling tool used to establish the relationships among these variables. It was decided to investigate these relationships within ranges of variables which would include the most common situations found in practice. These ranges were established by investigating 53 case histories of shallow tunnels. Most of these were identified as having been built under good ground control conditions where collapse and pronounced time dependent responses were not entailed. The most typical ranges in situ stress ratios, of cover to diameter ratios and strength parameters (ϕ and $c_u/\gamma D$) were identified. As a consequence of this investigation, the variables for the parametric finite element analyses were finally defined as ($H/D=1.5$ to 6, $\phi=0$ to 40°, $c_u/\gamma D=0.3125$ to 2.5, $K_o= 0.6$ to 1.0.

Details of the 2D parametric finite element analyses were presented, including the number of unloading increments used, the assessment of its effect on the numerical results, the finite element mesh design and particularly the effect of the fixed lower boundary. The latter was found to have a significant effect on the numerical output, mainly because of the constant modulus profile assumption. Unrealistic numerical results in terms of the ground settlements and ground reaction curves were obtained depending on its position. In order to select the most convenient location for this boundary a very large number of cases were processed. A distance of 1.5D below floor elevation was selected as being a position close enough to the tunnel invert to minimize excessive ground heave and far enough away to minimize its effect on the stiffness expressed by the ground reaction curves.

The generalization of the parametric analyses data was limited to pre-failure conditions because the numerical model is unable to simulate the soil failure. These results are included in Appendix C and D in compact graphic form, in terms of the distributions of normalized ground surface and subsurface settlements and of the NNGRCs for three points of the tunnel contour.

Some of these results for both soil models were presented and discussed in detail. The influence of each dimensionless variable on the ground response was individually assessed. This included the effects of the amount of stress release, the relative tunnel depth, the undrained strength ratio, the friction angle and the in situ stress ratio. Conclusions regarding these assessments can be found in specific sections of this chapter. Of particular interest was the normalized ground reaction curves for different strengths (either expressed in terms of $c_u/\gamma D$ or ϕ) that are homothetic with the centre of similitude at their origins ($\Sigma=1$ and $U=0$). Therefore, if the NGRCs are normalized once more, unique twice normalized ground reaction curves (NNGRC) are found irrespective of the soil strength. This finding had a major impact on the generalization of the numerical modelling results, as the projected solution could be extended to soil strengths other than those used in the parametric analyses.

Relationships between surface and crown settlements (S and u_c) were derived from the results of the numerical analyses. These relations were found to depend on the relative tunnel depth (H/D), on the strength parameters ($c_u/\gamma D$ or ϕ) and on the in situ stress ratio. Moreover, it was found to be a function of the amount of stress release allowed. The ratio, S/u_c, was found to either increase or decrease depending on the stress relief, on K_o and on the geometry of the problem. Results obtained by other authors regarding this aspect were critically assessed and previously proposed relationships for the settlement ratio S/u_c were analysed. The relations proposed herein were found to bound field observations, and it is suggested that they could be used to define the maximum surface settlement above a shallow tunnel whenever the crown settlement is assessed.

The results obtained were used to explain the limitations of linear elastic analyses which, when used to back-analyse actual tunnel performances, lead to either over or underestimates of surface settlement, whenever a match in the crown displacements is achieved.

The results of the numerical modelling were further generalized in an attempt to define expressions relating the variables controlling the ground response. Such expressions would allow one to obtain the ground reactions for conditions or variables other than those considered in the modelling stage. It would serve as a tool to furnish the ground reaction curves for any tunnel size, at any intermediate depth, in soils described by any in situ stiffness or strength. This generalization process was undertaken in parallel for both the frictionless and the cohesionless soil models.

A single expression (6.17) relating the radial stress ratio Σ and the radial dimensionless displacement U, with two parameters (A and B), was found to be a good representation of the normalized ground reaction curve for the frictionless soil model. Parameter A was found to depend on the point of the tunnel contour being considered and on the relative tunnel depth. Parameter B was also found to vary around the contour but to a lesser degree, and depends largely on the undrained strength ratio $(c_u/\gamma D)$ and the relative depth of the tunnel (H/D). The first parameter was shown to reflect the in situ stiffness of the ground and the second, the ultimate collapse state of the ground. Charts were prepared, which allow A and B to be estimated for three points of the tunnel contour (crown, springline and floor), for any cover to diameter ratio or any undrained strength ratio.

The partial derivative of the function expressing the NGRC for the frictionless soil model is easily related to the ground stiffness at any stage of the tunnel unloading process. Therefore, it can provide estimates of the 'current' radial spring constant (k_r) for any amount of tunnel closure (equation 6.20). These constants vary from point to point of the tunnel contour, and could be used as input parameters for a ground-lining interaction analysis using conventional ring-and-spring models such as reviewed in Chapter 4.

If instead, ring-and-plate models were to be used for the interaction analysis, the 'current' tangent Young's modulus (E_t) could also be derived from the derivative of the general NGRC function (equation 6.22).

These derivations would enable an approximation of the degree of 'softening' experienced by the ground around a shallow tunnel and the amount of stress release associated with a certain degree of opening closure taking place before the lining is installed or activated. This would serve to improve the approximations for the actual mechanisms involved in the ground-lining interaction process and perhaps lead to better estimates of tunnelling performance.

Even though more difficult, similar reasoning and development were applied to the cohesionless soil model. The homothetic responses of the ground in terms of the NGRC for different friction angles, allowed an additional normalization of the NGRC. The twice normalized ground reaction curves (NNGRC or λ - curves) could then be fitted by a single five parameter function (equation 6.24). Best fit parameters were then found through a non-linear regression technique using a statistical program package, for each point of the tunnel contour, for each cover to diameter ratio and for each in situ stress ratio. The λ curves obtained for each of the three points of the tunnel contour were found to be relatively insensitive to the cover to diameter ratio (except for the tunnel crown) but more sensitive to the in situ stress ratio. The first finding assures that the definition of the ground reaction curves for intermediate H/D values could be easily achieved by data interpolation. Interpolation of data for intermediate in situ stress ratios could also be made, but with a larger degree of uncertainty. Estimates of the ground reaction curves for any tunnel size, depth, soil stiffness, strength, or in situ stress ratio can thus be obtained, either using the basic general expression and appropriate parameters or through the prepared design charts.

Once more, estimates of 'current' radial spring constant (k_r) or 'current' tangent Young's modulus (E_t) could be obtained by partial differentiation of the basic function giving the NNGRC. Through equations 6.25 to 6.27 the ground stiffness could be assessed for any amount of stress release prior to ground failure, or for any amount of tunnel closure. To facilitate this assessment, a suite of convenient design charts was also prepared and presented. As before, through these derivations, one would be in position to approximately account for the degree of 'softening' and the degree of stress release associated with a given amount of tunnel closure. These factors could be used as input for traditional ground-lining interaction solutions, using either ring-and-spring or ring-and-plate models. Since most of these models operate with a constant spring constant or a constant ground modulus, average stiffness values would have to be estimated from the values found for the crown, springline and floor.

Although the solutions obtained were developed for use within the ranges of variables considered, one may be tempted to use them beyond the ranges of stress release covered by the parametric analyses. In some instances, the NGRC may be "too short" and some limited extrapolation may be needed for certain practical applications. The limits of validity of the solutions were then explored and defined. The terminal points, T, of the functions were identified both for the cohesionless and for the frictionless model solutions. The validity of extrapolations beyond those points cannot be assured, as the corresponding stresses eventually obtained may violate the failure criteria or they may not be sufficient to keep the opening stable. The associated displacements will likely be in error (possibly smaller than the correct values). The generalized solutions are not recommended beyond their terminal points, but if required, an assessment of the 2D tunnel stability is needed. The limitations of plasticity solutions for this purpose were assessed and discussed. Lower bound solutions such as those by D'Escatha and Mandel (1974) or Davis et.al., (1980) were presented and the shortcomings of their application to the posed problem were discussed. The factor of safety assessed using the collapse tunnel pressures that these solutions provide are interpreted, at best, as a crude estimate of the actual factor of safety. While these solutions seem to operate quite satisfactorily for the frictionless soil model (ϕ_u=0), they may not provide good approximations of the collapse loads in soils under drained conditions (c and ϕ not equal to 0). Unsafe estimates of the collapse tunnel pressure may be obtained. It was then advised to allow as much safety as possible or, preferably, to avoid any extrapolation of the NGRC beyond its terminal point. An additional criteria that could be evoked is the limiting dimensionless crown displacement, U=1.8, derived in Section 2.3.4.3 from observations in tunnel model tests. Recall that above this value a ground collapse condition was noted in the physical models.

A compact generalization of the numerical results in terms of ground settlement, similar to that undertaken for the ground reaction curves, was not attempted, although it could possibly be implemented. In fact, Resendiz and Romo (1981) succeeded in doing so, using a model similar to the frictionless model used herein. Nevertheless, the charts included in Appendix C, with normalized surface and subsurface settlements, do present sufficient generality for practical use, simply requiring interpolation of results for conditions other than those considered in the parametric analyses. An example of the interpolation procedure required was presented in terms of the relations between the maximum surface and crown settlements discussed earlier.

Finally, the approximate nature of the generalized solution must be emphasized. It reflects the simplifications introduced, the very approximate nature of the numerical model used, of the simplified constitutive models employed, the approximations related to the finite number of increments used to describe the degradation of the soil stiffness in the pre-failure regime, etc. Although these approximations have been introduced with some degree of discernment and judgement, which in turn requires equal consideration when using these solutions, it is important to test them against actual field cases. This is the last step in the development of the projected design procedure. It would include the validation of the proposed method, comparing its results with measured tunnel performance. The proposed method needs to be calibrated by assessing the deviation of predictions and by identifying the reasons for these deviations. This is the next natural step in the generalization process, following the modelling step just completed in the present Chapter. Accordingly, this will be one of the goals of the next chapter.

However, before this undertaking, an additional and important aspect of the tunnel design should be addressed. This refers to the ground-lining interaction phase of the tunnel construction representation, only briefly discussed in this chapter. The development presented so far attempted to portray the ground response through a 2D representation, up to the instant the support is activated. The first part of the next chapter will present and discuss procedures to represent the interaction process, taking into consideration the main features of the ground response prior to the support installation. With this, a design procedure for shallow tunnels would have been completed.

7. DEVELOPMENT AND VALIDATION OF A DESIGN PROCEDURE

7.1 Introduction

In Chapter 6, an approximate procedure was developed through which relationships between radial stresses and radial displacements at a point of the contour of a shallow tunnel could be obtained without the need of finite element modelling. These relationships, expressed for two idealized soil models in both algebraic and graphic forms, allow the amount of ground stress release in a two-dimensional representation to be determined from the knowledge of the tunnel closure. Other relationships were derived from which the change in the ground stiffness could be assessed by also relating it to the amount of tunnel closure. The first type of relationship expresses the stress transfer, or two-dimensional 'arching' process around a stable opening upon its closure, by a reduction of the stresses acting on its contour. The second portrays the response of the ground, in terms of changes in its stiffness associated with this stress transfer and of the tunnel closure.

Concurrently with these developments, relationships were established between the amount of stress release allowed at the opening and the settlements induced at the ground surface and subsurface. All relations were presented in a non-dimensional and scale independent form to allow generality.

The above derivations assumed that the opening was supported by internal radial and shear stresses which had been gradually and continuously reduced to a fraction Σ of the in situ stresses. This was in order to simulate the ground stress transfer process in an advancing tunnel. A simplification in this simulation process was to disregard the action of an actual lining support (see Sections 2.3.5 and 2.3.6). Both in a simplified 2D representation or in a 3D simulation, it is known that the lining does affect the ground response, as it interacts with the soil by inducing changes in stresses that may alter its stiffness.

In the present chapter the soil-lining interaction will be discussed and a simple model representing the process will be presented and evaluated. The effects of the lining action in the 2D ground response will be addressed. An approximate procedure to account for these effects in the tunnel design will be proposed and evaluated. Within this procedure, the ground stress reduction by arching and the changes in ground stiffness taking place prior to lining activation (in a 2D representation) will be taken into consideration. Subsequently, a complete sequence for design will be proposed, in which the ground settlements and lining loads will be obtained simultaneously. This newly proposed method is verified against results of simulations of shallow tunnels through numerical and physical modelling. Some of the limitations of the proposed procedure will be discussed. Finally, the method will be validated by comparing its predictive capabilities against observed field performances in some case histories.

7.2 Soil-Lining Interaction

7.2.1 Choice of the Model: Hartmann Solution

The basic aspects of the soil-lining interaction process were discussed in Sections 2.3.5 and 2.3.6. The available models representing this process were reviewed in Section 4.3.2. The most simple lining design methods that take into account the interaction between the ground and the support in the lining loads calculation, are those reviewed in Sections 4.3.2.3 and 4.3.2.4, i.e., the ring-and-plate and the ring-and-spring models, respectively. It was shown in Section 4.4.2.2 that the latter is perhaps the most popular type of statical system used for assessment of lining loads in shallow tunnels. Any of the above models could be used in connection with the design procedure being developed in this thesis. If fact, the ring-and-spring models, with ground reaction represented by discrete springs or bars, could be the most convenient one to be used. These models could allow different ground stiffnesses to be considered at distinct points of the tunnel contour. This would permit, as suggested in Section 2.2, taking into account a 'weakened' or 'softened embedment' condition whenever applicable. Certain criteria would have to be established and tested in order to assign different spring constants (radial and tangential) for points at intermediate locations between crown, springline and floor.

The effect of such differential degradation of the ground stiffness around the tunnel could not be considered if other soil-lining interaction models were chosen. An averaged ground stiffness would have to be defined, as these models assume a constant modulus of deformation, to represent the linear elastic behaviour of the ground. The accuracy lost with this assumption is in turn compensated by a gain in the compactness of the solution, particularly if a closed form analytical solution is selected. The latter, furthermore, would offer considerable ease in the design procedure since it permits simpler handling of parametric or sensitivity analyses which are sometimes required at initial design stages. Additionally, it is believed that if such an analytical solution could be coupled with the design procedure, the further simplifications it requires would not be discordant with the overall approximate nature of other components in the design procedure.

These aspects lead to favouring a closed form ring-and-plate solution to analyse the soil-lining interaction phase of the design procedure and to serve as a tool for the lining load prediction. The consequences and limitations of this choice will be further discussed in this and in the following sections. A number of options are offered with this choice but by inspecting the solutions reviewed in Section 4.3.2.3, not many are found that would not introduce further approximations. In fact, Hartmann's (1970, 1972) approach is the only one that makes full allowance for the non-uniform stress field existing in a shallow tunnel, which is generated by in situ stress ratios different from unity and by the action of gravity. Therefore, this solution seems to be the most convenient for the problem at hand, in that it partly accounts for one of the features of a shallow tunnel situation: the gravitational stress gradient across the opening. It neglects, however, the effect of the ground surface, since the ground is approximated by an infinite plate subjected to a gravitational stress field. It was shown in Section 2.2 that the effect of the ground surface on the lining response can be considered as neglible for H/D greater than 1.5 but that the influence of the gravity cannot be disregarded in the interaction analysis for most shallow tunnels.

Hartmann's original solution treats both soil and lining as linear elastic, isotropic and homogeneous materials. The opening is assumed to be circular, the ground mass is represented by an infinite plate and the lining by a weightless thin cylindrical shell of constant thickness. The lining is assumed to be installed in the opening before any displacement occurs in the ground. Moreover, lining and ground are assumed to be in full contact, so a non-slip condition at the interface is admitted. More recently (Hartmann, 1986: unpublished report) a full slip solution was derived but will not be discussed herein for reasons presented in Section 2.3.5.

A zero stress horizontal surface represents the ground surface, so that the principal in situ stresses are vertical (γz) and horizontal ($K\gamma z$), where z is the depth to a point measured from the ground surface, γ is the unit weight of the soil and K is the in situ stress ratio.

The lining is activated by an excavation loading condition (see Section 4.3.2.3). The solution is formulated for both plane strain and plane stress, the former being more relevant to the tunnel problem and is presented herein. The equilibrium and compatibility conditions are formulated in terms of polar coordinates. The internal forces in the lining are computed using Flügge's (1962:134) differential equations relating lining thrust, shear and bending moments to the lining displacements.

The relative stiffness of the lining-ground system is expressed in terms of two coefficients, referred to as the compressibility (α) and the flexibility (β) ratios. These are defined as:

$$\alpha=\frac{E_s A_s(1+\mu)}{E.r_o(1-\mu_s^2)} \qquad [7.1]$$

$$\beta=\frac{E_s I_s(1+\mu)}{E.r_o^3(1-\mu_s^2)} \qquad [7.2]$$

where r_o is the tunnel radius, E, μ and E_s, μ_s are elastic constants for the ground and the support, A_s is the cross sectional area of the lining per unit length of the tunnel (A_s=d=lining thickness) and I_s is the moment of inertia of the support per unit length of the tunnel (I_s=d^3/12).

Note that these ratios are related to the corresponding ratios used in the Einstein and Schwartz (1979) derivation (C and F, see Section 2.3.5.2) by:

$$\alpha = \frac{1}{C(1-\mu)}$$

$$\beta = \frac{1}{F(1-\mu)}$$

Typical flexibility and compressibility ratios can be found in Table 7.1. These were calculated using both the Hartmann and Einstein and Schwartz definitions. The ratios were calculated for six soil types and three common lining systems. The assumptions made are given in the table. Note that the deformation moduli given correspond to initial tangent values at a confining stress of 0.1 MPa. As indicated in Section 2.3.5.3, different stiffness ratios would have to be considered if the effect of the global 'softening' of the ground on the decrease of the in situ stresses with tunnel advance, was to be considered.

The notation and conventions used in Hartmann's solution are shown in Figure 7.1. Note that stresses are positive in compression. A summary of the solution is presented in Figure 7.2, where the equations for lining stresses, displacements and internal forces are given. It should be noted that v'_{ro} and $v'_{\phi o}$ given by equations 7.7 and 7.9 are the components of the total radial and tangential displacements, to which the overall heave component v''_{zo} given by equation 7.10, should be added in order to obtain the total lining displacements v_{ro} and $v_{\phi o}$, as shown in equations 7.6 and 7.8. Note moreover, that the heave v''_{zo} is

Soil		Steel ribs and lagging(2)		Precast concrete segments(3)		Shotcrete(4)	
Type	E_t(1) (MPa)	β	F	β	F	β	F
Soft clay	8	0.030	40	0.140	10	0.040	35
Medium clay	25	0.010	125	0.040	30	0.012	110
Stiff clay	100	0.003	500	0.010	120	0.003	450
Loose sand	40	0.007	200	0.030	50	0.008	170
Medium sand	60	0.004	300	0.020	70	0.005	250
Dense sand	120	0.002	600	0.009	150	0.002	550
		$\frac{\dot{\alpha}}{\beta} = \frac{F}{C} \cong 1{,}300$		$\frac{\dot{\alpha}}{\beta} = \frac{F}{C} = 1{,}200$		$\frac{\dot{\alpha}}{\beta} = \frac{F}{C} = 2{,}800$	

Notes: (1) Typical initial tangent values at a confinement pressure of 0.1 MPa (tunnel at 10 m depth in a soil with γ = 17 kN/m^3 and K_0 = 0.7).

(2) Lagging stiffness disregarded. Influence of joints in β disregarded. Joint compressibility partly accounted. E_s = 100 GPa, $d/r_0 = 1.3 \times 10^{-3}$, $I_s/r_0 = 10^{-6}$.

(3) Influence of joints in β disregarded. Joint compressibility partly accounted. E_s = 10 GPa, $d/r_0 = 0.1$, $I_s = d^3/12$.

(4) Hardening effect partly accounted. E_s = 10 GPa. Presence of ribs or lattice girders disregarded. $d/r_0 = 0.065$, $I_s = d^3/12$.

(5) In all cases $\mu = \mu_s$.

Table 7.1 Typical Relative Stiffness Ratios for Common Linings and Soils

dependent on r_1, which is the radius of an arbitrary circle at which the vertical heave displacement is set equal to zero. If this boundary is located at infinity, an infinite heave would be calculated. Therefore, for practical applications, r_1 is to be chosen according to the position of a stiffer horizon below the tunnel floor or to the location of points below the floor, where no displacements are noted. From what was shown in Table 6.9 (Section 6.3.1.2), the ratio r_0/r_1 is likely to be larger than 1/4 or 1/3. It should be pointed out that the shear force Q_ϕ given by equation 7.13 was not included in Hartmann's original solution, but it could be obtained by differentiating the bending moments ($Q_\phi=(1/r_0)\partial M/\partial\phi$).

Hartmann's solution includes second-order terms that are frequently neglected in similar derivations (for example, see Schwartz and Einstein, 1980:367). The first term in the expression for the bending moments (equation 7.12 in Figure 7.2) represents the influence of the lining perimeter reduction, caused by the action of the thrust forces. A decrease in the lining diameter produces an increase in the lining curvature that leads to bending stresses. These stresses will be present even under an ideal isotropic loading condition ($K=1$ and $z_0 >> r_0$). In most cases this term is of small magnitude. The second term in the expression for M_ϕ gives the influence of the overburden stress γz_0 on the bending moment and the third describes the influence of the gravitational stress gradient across the

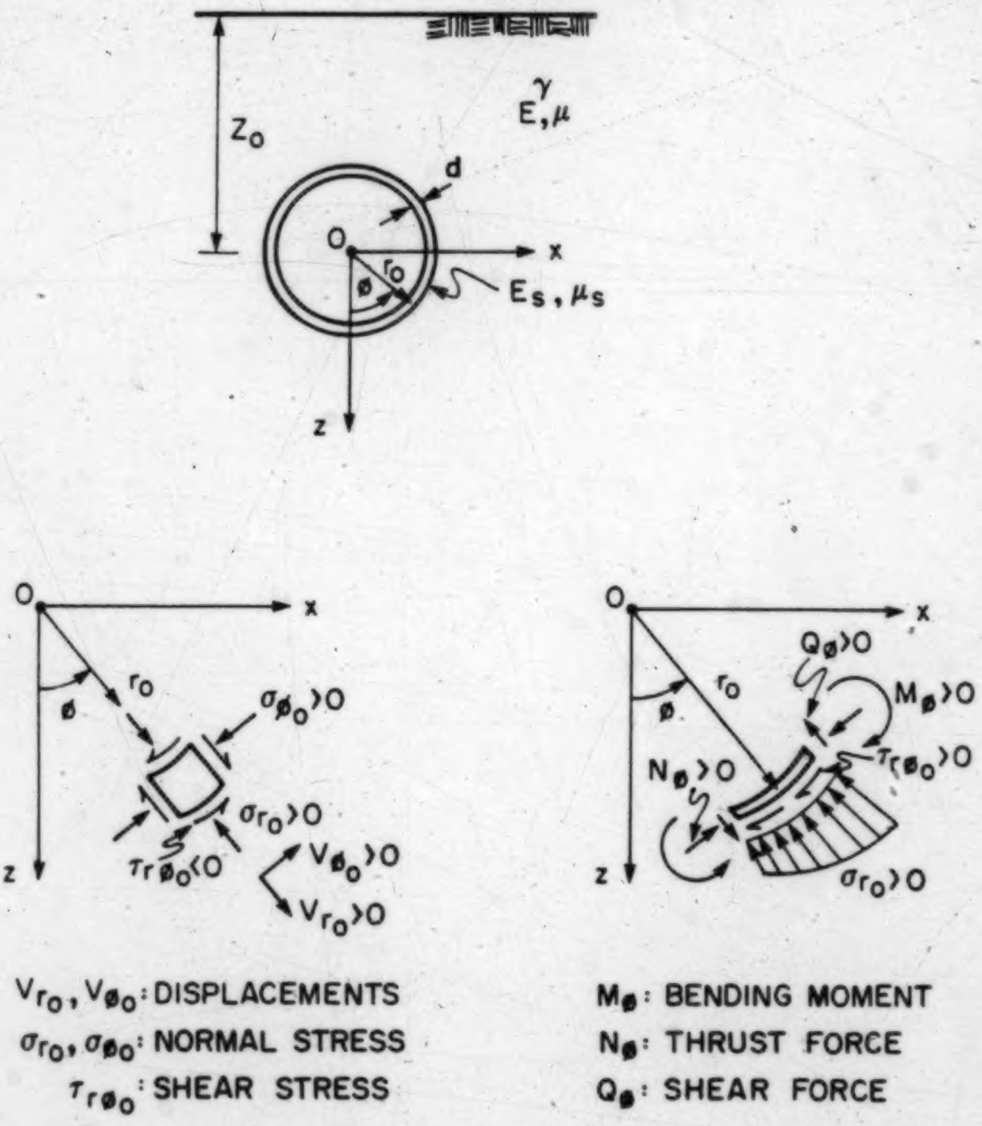
γ
E, μ
Z_o
d
O
x
r_o
ϕ
E_s, μ_s
z
O
x
r_o
ϕ
$\sigma_{\phi_o} > 0$
$\sigma_{r_o} > 0$
$\tau_{r\phi_o} < 0$
$V_{\phi_o} > 0$
$V_{r_o} > 0$
z
O
x
$Q_\phi > 0$
r_o
$M_\phi > 0$
ϕ
$\tau_{r\phi_o} > 0$
$N_\phi > 0$
$\sigma_{r_o} > 0$
z
V_{r_o}, V_{ϕ_o}: DISPLACEMENTS
$\sigma_{r_o}, \sigma_{\phi_o}$: NORMAL STRESS
$\tau_{r\phi_o}$: SHEAR STRESS
M_ϕ: BENDING MOMENT
N_ϕ: THRUST FORCE
Q_ϕ: SHEAR FORCE

Figure 7.1 Notations and Conventions used in Hartmann's Solution

$$\dot{\alpha}=\frac{E_sA_s(1+\mu)}{E\,r_0(1-\mu_S^2)}\qquad(7.1)\qquad\qquad \beta=\frac{E_sI_s(1+\mu)}{E\,r_0^3(1-\mu_S^2)}\qquad(7.2)$$

$$\sigma_{r0}=\frac{(1+K)(\dot{\alpha}+\beta)}{2(1+\dot{\alpha}+\beta)}\gamma z_0+\frac{(1+K)\dot{\alpha}}{4(1+\dot{\alpha})}\gamma r_0\cos\phi-\frac{(1-K)(3-4\mu)(\dot{\alpha}-9\beta-12\dot{\alpha}\beta)}{2\{1+(3-2\mu)\dot{\alpha}+3[5-6\mu+4(3-4\mu)\dot{\alpha}]\beta\}}\gamma z_0\cos(2\phi)-\frac{(1-K)(3-4\mu)(\alpha-32\beta-72\dot{\alpha}\beta)}{4\{1+(5-4\mu)\dot{\alpha}+8[7-8\mu+9(3-4\mu)4]\beta\}}\gamma r_0\cos(3\phi)\qquad(7.3)$$

$$\sigma_{\phi 0}=\frac{(1+K)(2+\dot{\alpha}+\beta)}{2(1+\dot{\alpha}+\beta)}\gamma z_0+\frac{2+\dot{\alpha}+(K-\mu-\mu K)(4+3\dot{\alpha})}{4(1-\mu)(1+\dot{\alpha})}\gamma r_0\cos\phi-\frac{(1-K)\{4+(3+4\mu)\dot{\alpha}+3[11-12\mu+4(3-4\mu)\dot{\alpha}]\beta\}}{2\{1+(3-2\mu)\dot{\alpha}+3[5-6\mu+4(3-4\mu)\dot{\alpha}]\beta\}}\gamma z_0\cos(2\phi)-\frac{(1-K)\{4+(5+6\mu)\alpha+8[16-16\mu+9(3-4\mu)\dot{\alpha}]\beta\}}{4\{1+(5-4\mu)\dot{\alpha}+8[7-8\mu+9(3-4\mu)\dot{\alpha}]\beta\}}\gamma r_0\cos(3\phi)\qquad(7.4)$$

$$\tau_{r\phi 0}=\frac{(1+K)\dot{\alpha}}{4(1+\dot{\alpha})}\gamma r_0\sin\phi-\frac{(1-K)(3-4\mu)(1+6\beta)\dot{\alpha}}{1+(3-2\mu)\dot{\alpha}+3[5-6\mu+4(3-4\mu)\dot{\alpha}]\beta}\gamma z_0\sin(2\phi)-\frac{3(1-K)(3-4\mu)(1+24\beta)\dot{\alpha}}{4\{1+(5-4\mu)\dot{\alpha}+8[7-8\mu+9(3-4\mu)\dot{\alpha}]\beta\}}\gamma r_0\sin(3\phi)\qquad(7.5)$$

$$v_{r0}=v'_{r0}+v''_{z0}\cos\phi\qquad(7.6)$$

$$v'_{r0}=-\frac{1+\mu}{E}\left(\frac{1+K}{2(1+\dot{\alpha}+\beta)}\gamma z_0r_0+\frac{(1+K)}{8(1+\dot{\alpha})}\gamma r_0^2\cos\phi+\frac{(1-K)(3-4\mu)(1+2\dot{\alpha})}{2\{1+(3-2\mu)\dot{\alpha}+3[5-6\mu+4(3-4\mu)\dot{\alpha}]\beta\}}\gamma z_0r_0\cos(2\phi)+\frac{(1-K)(3-4\mu)(1+3\dot{\alpha})}{8\{1+(5-4\mu)\dot{\alpha}+8[7-8\mu-9(3-4\mu)\dot{\alpha}]\beta\}}\gamma r_0^2\cos(3\phi)\right)\qquad(7.7)$$

$$v_{\phi 0}=v'_{\phi 0}+v''_{z0}\sin\phi\qquad(7.8)$$

$$v'_{\phi 0}=\frac{1+\mu}{E}\left(-\frac{1+K}{8(1+\dot{\alpha})}\gamma r_0^2\sin\phi+\frac{(1-K)(3-4\mu)(1+\dot{\alpha}+3\beta)}{2\{1+(3-2\mu)\dot{\alpha}+3[5-6\mu+4(3-4\mu)\dot{\alpha}]\beta\}}\gamma z_0r_0\sin(2\phi)+\frac{(1-K)(3-4\mu)(1+\dot{\alpha}+16\beta)}{8\{1+(5-4\mu)\dot{\alpha}+8[7-8\mu+9(3-4\mu)\dot{\alpha}]\beta\}}\gamma r_0^2\sin(3\phi)\right)\qquad(7.9)$$

$$v''_{z0}=\frac{(1+\mu)(3-4\mu)}{4(1-\mu)E}\gamma r_0^2\ln\frac{r_0}{r_1}\qquad(7.10)$$

$$N_\phi=\frac{(1+K)(\dot{\alpha}+\beta)}{2(1+\dot{\alpha}+\beta)}\gamma z_0r_0+\frac{(1+K)\dot{\alpha}}{4(1+\dot{\alpha})}\gamma r_0^2\cos\phi-\frac{(1-K)(3-4\mu)(\dot{\alpha}+3\beta+12\dot{\alpha}\beta)}{2[1+(3-2\mu)\dot{\alpha}+3[5-6\mu+4(3-4\mu)\dot{\alpha}]\beta]}\gamma z_0r_0\cos(2\phi)-\frac{(1-K)(3-4\mu)(\dot{\alpha}+4\beta+36\dot{\alpha}\beta)}{4\{1+(5-4\mu)\dot{\alpha}+8[7-8\mu+9(3-4\mu)\dot{\alpha}]\beta\}}\gamma r_0^2\cos(3\phi)\qquad(7.11)$$

$$M_\phi=-\frac{(1+K)\beta}{2(1+\dot{\alpha}+\beta)}\gamma z_0r_0^2+\frac{3(1-K)(3-4\mu)(1+2\dot{\alpha})\beta}{2\{1+(3-2\mu)\dot{\alpha}+3[5-6\mu-4(3-4\mu)\dot{\alpha}]\beta\}}\gamma z_0r_0^2\cos(2\phi)+\frac{(1-K)(3-4\mu)(1+3\alpha)\beta}{1+(5-4\mu)\alpha+8[7-8\mu+9(3-4\mu)\alpha]\beta}\gamma r_0^3\cos(3\phi)\qquad(7.12)$$

$$Q_\phi=-\frac{3(1-K)(3-4\mu)(1+2\dot{\alpha})\beta}{\{1+(3-2\mu)\dot{\alpha}+3[5-6\mu+4(3-4\mu)\dot{\alpha}]\beta\}}\gamma z_0r_0\sin(2\phi)-\frac{3(1-K)(3-4\mu)(1+3\dot{\alpha})\beta}{1+(5-4\mu)\dot{\alpha}+8\,[7-8\mu+9(3-4\mu)\dot{\alpha}]\beta\}}\gamma r_0^2\sin(3\phi)\qquad(7.13)$$

Figure 7.2 Lining Stresses, Displacements and Internal Forces Given by Hartmann's Solution

opening. Correspondingly, the first and third terms in the expression for N_ϕ (equation 7.11) represents the influence of the overburden stress, while the second and fourth terms describe the influence of the gravity. Moreover, in the latter equation, the first and second terms reflect the effect of the mean normal in situ stress, while the third and fourth terms reflect the effect of the mean in situ stress difference.

Provided the thickness of the lining is small in comparison with the tunnel radius, the second order moments are small. Moreover, if the tunnel is deep (a large z_o/r_o ratio), then Hartmann's solution becomes equivalent to other deep tunnel solutions. In fact, it yields results which are basically identical to Windels (1967), Curtis-Muir Wood (1976), Einstein and Schwartz (1979) and Ahrens et.al., (1982) closed form solutions, as discussed in Section 4.3.2.3. It is simple to show that if the lining is disregarded, (i.e., $\alpha=\beta=0$), Hartmann's expression for the tangential stresses at the opening contour reduces to Mindlin's solution for an opening in an infinite plate under gravity with lateral restraint (Mindlin, 1940:1136 - equation 58).

In order to assess the consequences of the infinite plate assumption in Hartmann's solution, a comparison between this solution and the results of a finite element analysis of a shallow tunnel would be required. Unfortunately, the lining representation adopted in the 2D finite element model presented in Chapter 5 does not permit a direct comparison to be made, particularly regarding bending moments. Ranken (1978), however, performed a few finite element analyses of circular shallow tunnels, whose results can be used for this comparison. Five linear elastic analyses were carried out, for different cover to diameter ratios that varied between 0.5 and 4.5. Details of this study were presented by Ranken (Op.cit.:96) and will not be repeated herein, except for essential information. In all analyses, the in situ stress ratio in the ground was kept constant and equal to 0.5. The ratio of the soil to lining Young's modulus was set equal to 0.0205. The Poisson's ratio of the soil was 0.25 and the lining was 0.1562. The lining thickness was 10% of the tunnel radius. The resulting relative stiffness ratios were α=6.25 and β=0.0052. As indicated in Table 7.1, these values would be typical for a rib and lagging lined tunnel, in a medium to loose sand. The lining was installed before any release of ground stresses took place. A fixed lower boundary was set up at three diameters below the tunnel floor. A gravitational field stress condition was considered, so the results incorporate both the action of the ground surface and of the in situ stress gradient across the opening. Although both full and no slip conditions were considered for the lining-ground interface, only the results of the latter case will be examined herein.

The solution by Hartmann, as summarized in Figure 7.2, was applied to these cases and some representative results are shown in Figure 7.3. The results of the closed form solution are presented by continuous lines, whereas the numerical results by Ranken are shown by discrete points. In the upper part of Figure 7.3, the calculated thrust forces and bending moments at the crown of the tunnel lining are plotted together. The lower part shows the calculated crown vertical displacement and some diameter changes. All results were conveniently normalized to allow the comparison. Fairly similar results were found at other points of the contour.

Apart from inaccuracies that could be attributed to numerical approximations, the differences in the results by the two approaches can be ascribed to the influence of the ground surface, included in the finite element analyses. As expected, these differences seem to increase as the tunnel becomes shallower. Hartmann's solution seems to furnish results which are either approximately equal to or greater in magnitude than the finite element solution. Moreover, it is noted that both solutions tend to yield very similar results for cover to diameter ratios greater than 1.5. This tends to confirm that the effect of the ground surface on the lining response seems indeed negligible for H/D greater than 1.5 (see Section 2.2). Moreover, even for smaller ratios, the analytical solution seems to furnish results which are greater in magnitude than the numerical solution. Therefore, the Hartmann solution may provide conservative

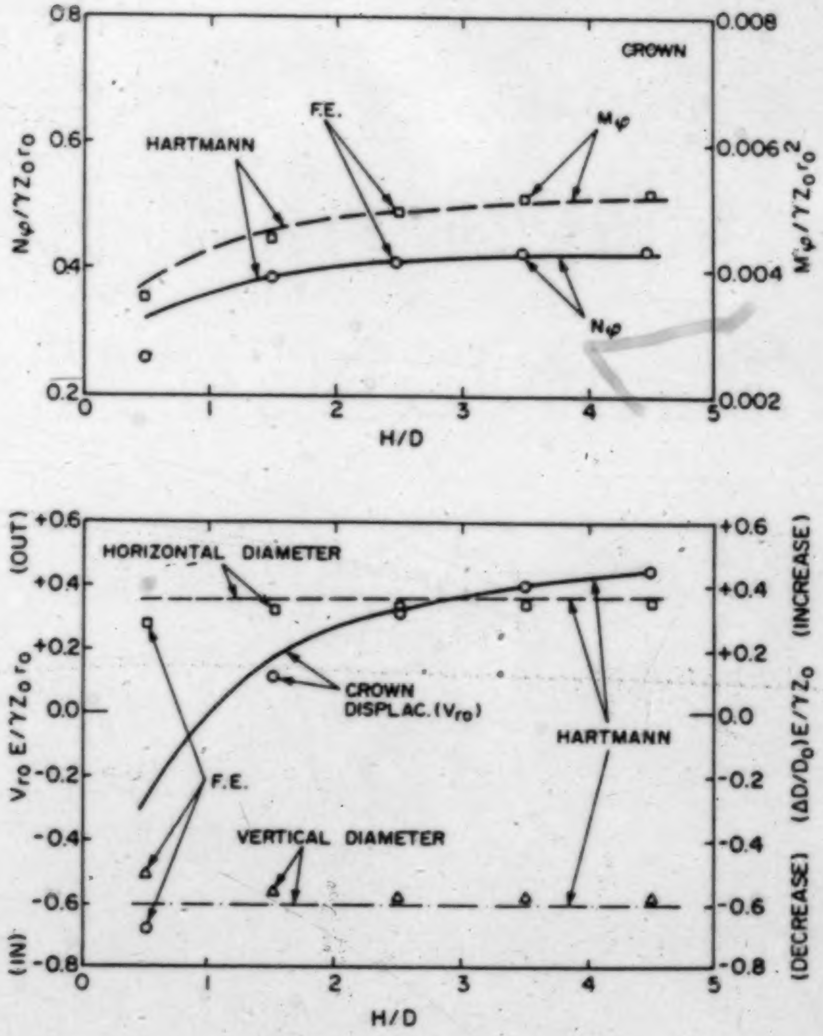

Figure 7.3 Comparison of Lining Responses Calculated for Different Tunnel Depths, with and without Account of the Influence of the Ground Surface

estimates of the lining response for H/D smaller than 1.5. These findings are valid not only for the tunnel crown but for other points of the contour.

The largest discrepancy noted refers to the magnitude of the crown displacement. This result is not surprising since it is the one that involved a larger degree of approximation. As can be noted in Figure 7.2, the radial displacement v_{ro} (equation 7.6) depends on the ground heave v''_{zo} given by equation 7.10. Two approximations are involved in estimating this component of the crown displacement. The first refers to r_1, defined earlier as the radius of an arbitrary circle at which the heave is equal to zero. To simulate the conditions involved in the finite element analyses, r_1 was set equal to 3.5D (thus $r_o/r_1=1/7$), so that such a circle is tangent to the lower boundary of the finite element mesh. This correspondence is, however, not exact and differences in the displacement calculation may result. Secondly, as noticed in equation 7.10, the heave v''_{zo} depends only on the ground modulus E, and is independent of the lining stiffness. Except for the soil to lining modulus ratio, Ranken (1978) did not provide the value of soil modulus used in his analyses. A modulus of 20.09 MPa has been chosen in the present calculation, which may differ from that selected by Ranken.

In summary, it may be concluded that, subject to the assumptions made (notably that of a linear elastic behaviour for soil and lining), Hartmann's solution seems to provide a good approximation for the two-dimensional ground-lining interaction process, despite not taking the influence of the ground surface into account.

7.2.2 Soil-Lining Interaction Analysis for Delayed Lining Installation in a Non-Linear Ground Mass

Hartmann's solution, like other two-dimensional closed form solutions, assumes the lining to be in place before the excavation loading develops. It was shown in Sections 4.3.2.7 and 5.2.1.1 that there is no rigorous procedure to account for the effects resulting from delaying (in space) the installation of the lining, which involves three-dimensional stress changes in a simpler two-dimensional representation. It was also explained earlier in this thesis why the approximate procedure of the gradual reduction of the in situ stresses around the tunnel was favoured in the present work, to simulate the delayed placement of the lining in a 2D model.

In essence, this approximation mimics the actual stress changes or arching process that leads to smaller ground loads being transferred to the lining as a result of the interaction process within the soil. In Chapter 5 it was shown that, although approximate, this procedure may indeed furnish sensible results in terms of estimates of the tunnel performance.

If Hartmann's solution is to be used to analyse the soil-lining interaction phase of the tunnelling process, instead of the finite element simulation used in Chapter 5, then that ground load reduction should be introduced into the solution. Provided that in this analysis the lining response, in terms of its loads and displacements, is the only matter of interest, then the reduction of ground loads can be easily implemented. It can be represented by a reduction in the ground stress field, which can be introduced by a reduction in the unit weight of the ground. This in turn, can be related to the amount of stress release (α) taking place up until the instant the support is installed. The reduced unit weight of the soil would then be:

$$\gamma_{red} = \gamma(1-\alpha) = \gamma\Sigma \qquad [7.14]$$

where γ is the actual in situ weight of the ground.

It should be remembered that in the two dimensional representation adopted in this study (see Section 5.2.2.1) which led to the generalized results presented in Chapter 6, the same stress reduction factor is applied uniformly to all points of the tunnel profile and reduces both radial and shear stresses in the same proportion. Due to this assumption, the current stresses acting on the perimeter of the 2D opening after a certain ground stress release α, and immediately before the support installation against the ground of unit weight γ and in situ stress ratio K_o, are exactly equal to the in situ stresses acting on the contour of a tunnel with same geometry, yet to be excavated in an undisturbed ground mass, which has the same in situ stress ratio K_o but with a reduced unit weight given by equation 7.14. Provided that a linear elastic behaviour can be ensured, the ground-lining response will not depend on the stress and strain changes developing in the ground prior to the support installation. The magnitude of the lining loads and lining displacements furnished by Hartmann's solution, with a field stress reduced through a reduced soil unit weight, will be correct, despite the stress changes and displacements induced within the ground mass being incorrect. The reduced unit weight approximation does not account for the stress changes and displacements induced prior to lining activation. Apparently there is no formal impediment to adapt Hartmann's solution for this new condition, which would explictly include a stress release factor $(1-\Sigma)$ in the derivation, and take into account the stress and strain changes in the ground prior to installing the support. In fact, the Schwartz and Einstein (1980:393) derivation, incorporating a 'soft core' region (see Section 4.3.2.7) that leads to 'pre-support' ground movements is an example of how such a solution could be worked out. Nevertheless, such an undertaking was felt to be out of scope of the present work and therefore was not attempted.

If the non-linear behaviour of the ground is taken into consideration, then the above approach is merely an approximation. The stress changes in the ground prior to the lining installation do have an impact on the ground-lining interaction, as the ground stiffness is inevitably changed.

This point was raised and discussed earlier in Section 2.3.5.3. Moreover, the separate analyses of the pre-support ground response and of the soil-support interaction phase require a superposition of effects for the final equilibrium condition to be found. The validity of such superposition in a non-linear problem is debatable. Furthermore, there is nothing to support a linear elastic interaction analysis in a soil that exhibits a non-linear response. Perhaps the only argument that could be raised in its favour, is that, provided the increments of ground displacements taking place after lining installation are small in comparison with those developing in the finite unloading increment imposed to the ground before that, then the linear elastic approximation may not be entirely discordant with the non-linear, yet piecewise elastic model used herein. But this argument may not be valid under certain practical situations. Therefore, if the linear elastic interaction analysis using Hartmann's solution is used in connection with the design procedure being developed herein, it must be regarded as an approximation whose consequences should be assessed accordingly.

For this end, the numerical analyses described in Section 2.3.5.3 can be helpful. Three analyses were carried out there, with different amounts of ground stress release at the circular opening prior to lining installation: 0%, 40% and 80%. An additional calculation was performed allowing a full stress release. The ground properties were as given earlier in that section. The soil strength including both frictional and cohesive components and the in situ tangent modulus increasing with depth, were maintained in all analyses. The tunnel with a 4 m diameter and 6.2 m cover was intentionally lined with a very soft and flexible support, so that substantial displacements could develop after its installation. This condition is therefore a critical one in terms of enhancing the effect of the non-linear response of the soil on the ground-lining interaction process. For the reasons exposed in Chapter 5, a fairly thick lining with 0.5 m thickness was used with constant elastic properties, which led to a compressibility ratio α of 0.8 ($C=1.8$) and a flexibility ratio β of 0.017 ($F=86$). These were calculated with respect to the in situ elastic modulus of the soil at tunnel axis elevation. Such values could correspond to a flexible and compressible shotcrete lining in a medium clay.

The equilibrium points in terms of radial stresses and radial displacements at crown, springline and floor, as obtained by the finite element analyses, are shown in Figures 7.4, 7.5 and 7.6, respectively. The continuous solid curves shown are the ground reaction curves for these three points, as calculated for a full stress release without installing the lining. The dashed lines link the points representing the equilibrium to the starting point of lining activation. The abscissae of the latter points give the radial closures of the opening when the support was activated. Unlike the radial displacements that were calculated at nodal points, the radial stresses at equilibrium were obtained by extrapolating the calculated element stresses to the tunnel contour.

Following this, an attempt was made to obtain the equilibrium points (L and E as explained later), using Hartmann's solution coupled with the generalized solution presented in Section 6.4 for obtaining the ground reaction curves. In order to achieve this, a few additional assumptions had to be made and these are discussed in the following.

As stated earlier, the closed form interaction analyses require an assessment of a reduced unit weight, γ_{red}, for the soil. It is necessary to evaluate the ratio of current stress to initial stress (Σ) at tunnel contour when the support is installed, so that γ_{red} can be determined through equation 7.14. If the GRC given by the generalized solution presented in Section 6.4 coincided with the GRC calculated in the finite element analysis, then there would be no need to calculate Σ at lining installation, as it would be equal to that imposed in the analysis. However, since the GRCs do not coincide, as the generalized solution is an approximation of the correct GRC, that need is justified.

To assess Σ, one could assume that the radial displacements at the instant of lining installation are known and equal to those given by the finite element calculation. In a more general case, these displacements

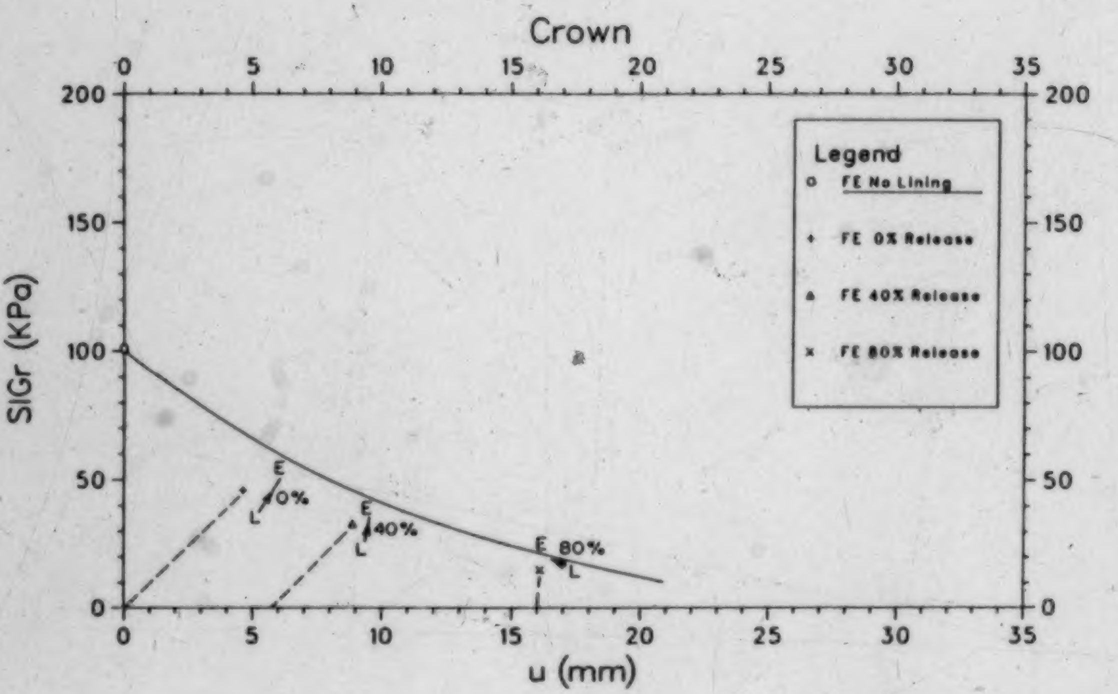

Figure 7.4 Equilibrium Points of the Soil-Lining Interaction at Tunnel Crown

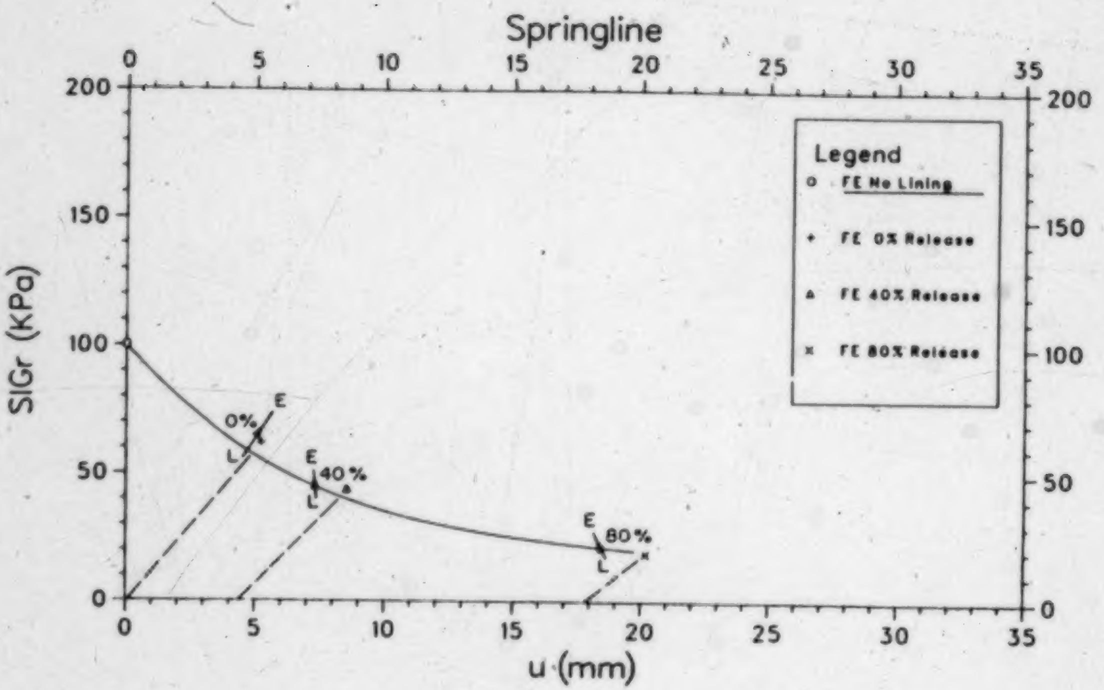

Figure 7.5 Equilibrium Points of the Soil-Lining Interaction at Tunnel Springline

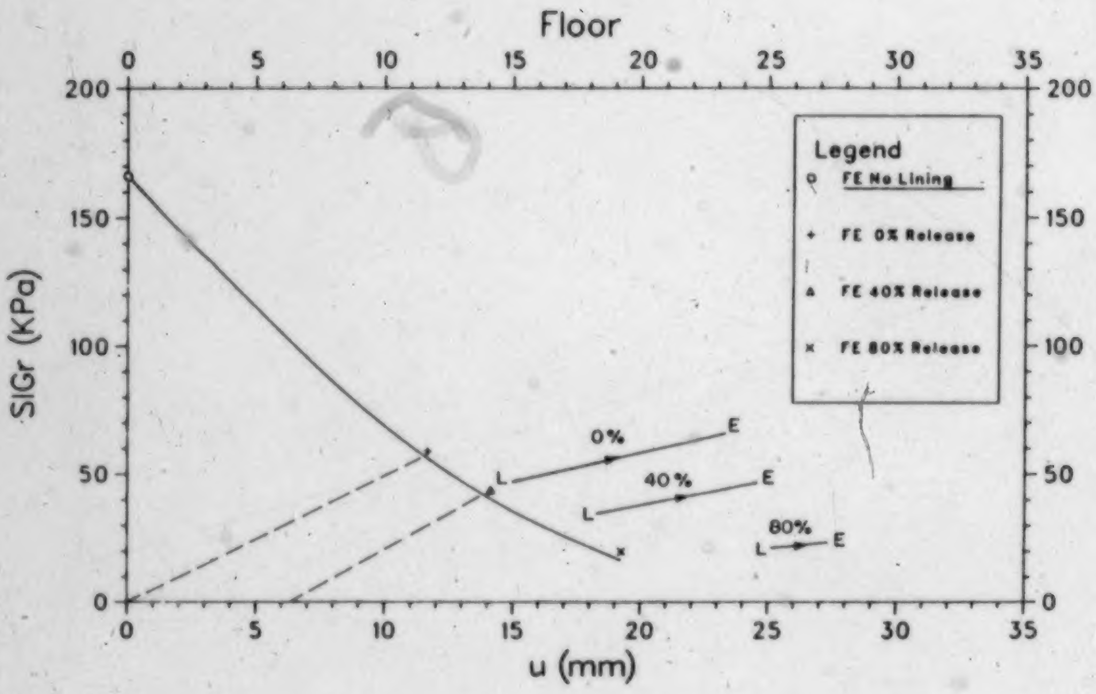

Figure 7.6 Equilibrium Points of the Soil-Lining Interaction at Tunnel Floor

could be estimated by the approximate procedure presented in Section 5.3.5.2 for the assessment of tunnel closure at sections behind the face. With the radial displacements developing before lining installation, it is possible to determine the value of α or Σ at crown (C), springline (S) and floor (F). This is done through the NNGRC or λ curves given by equation 6.24. Before that, however, one has to define $\alpha_{ref}=1-\Sigma_{ref}$, for C, S and F, which is a function of (m-1), which, as indicated by equation 6.30, is a function of the friction angle, ϕ. The friction angle to be used for this purpose is the one obtained after adjusting the actual ϕ to account for the non-zero cohesion, as indicated by equation 6.10. In this case, there is no need to amend the friction angle since the failure ratio, R_{ref}, is equal to one. Otherwise ϕ would have to be adjusted according to equation 6.3. After defining the α_{ref} values, the U_{ref} values should be obtained through the function relating α_{ref}/U_{ref} to H/D. This requires interpolating the reference values between the solutions given by two consecutive K_o curves which bracket the K_o used in the finite element analyses (0.75). Alternatively, one could simply assume the solution set with K_o closer to the required value. This alternative was favoured herein and the reference values for α and U were taken from the solution set for K_o equal to 0.8.

Note also that since a variable in situ modulus profile has been assumed in the numerical analysis, the dimensionless radial displacements U should be normalized to the in situ tangent moduli of the soil at points located half diameter radially away from the opening profile, as explained in Section 6.2.4.2.

The resulting parameters obtained following the above sequence of calculations are given in Table 7.2. One notes that different Σ ratios are obtained at different points of the tunnel contour, thus a mean Σ should be considered to get γ_{red}, by averaging the calculated ratios (springline being counted twice). For the 40% stress release considered in the finite element analysis, the approximate solution yielded 38.2% for the same radial closure of the opening. For the 80% stress release, the approximate solution furnished 75.4%. In both cases, the calculated amount of stress release for the same radial displacement at lining installation, is slightly smaller than the correct one, indicating that the approximate solution furnishes 'safer' estimates of the current ground stresses at the instant the support is activated.

It should be noted that only for the springline in the 80% stress release case, the generalized solution for the GRC was used beyond its limits, as defined in Section 6.5.1.

In summary, the reduced unit weight of the soil which simulates the reduction of the ground loads for the lining-ground interaction analyses, was obtained through the solution presented in Section 6.4.3. It was assumed that the radial closure is known at the instant the support is activated. The reduced unit weight is calculated directly

GEOMETRY: $H = 6.2$ m, $D = 4.0$ m

PROPERTIES: $\gamma = 16$ kN/m^3, $K_0 = 0.75$, $C = 39$ KPa, $\phi = 21°$,
$R_f = 1.0$, $K = 330$, $n = 0.23$, $\mu = 0.3$
Thus:
$(E_{ti})_C = 23.53$ MPa, $(E_{ti})_S = 24.68$ MPa,
$(E_{ti})_F = 25.22$ MPa
And:
$\phi_a = 32.2°$, $(m - 1) = 2.278$

REFERENCES VALUES: $H/D = 1.55$, $K_0 = 0.8$ and $(m - 1) = 2.278$
Thus:

	α_{ref}	α_{ref}/U_{ref}	U_{ref}
C	0.572	0.860	0.665
S	0.528	1.125	0.469
F	0.448	2.020	0.222

REDUCED UNIT WEIGHT:

a. For FE with 0% stress release: $\gamma_{red} = \gamma = 16$ kN/m^3

b. For FE with 40% stress release:

	u (mm) before lining	U	U/U_{ref}	λ	Σ
C	5.77	0.336	0.505	0.400	0.657
S	4.35	0.267	0.570	0.330	0.646
F	6.35	0.248	1.116	-0.070	0.521

Thus $\overline{\Sigma} = 0.618$ and $\gamma_{red} = \gamma\,\overline{\Sigma} = 9.88$ kN/m^3

c. For FE with 80% stress release:

	u (mm) before lining	U	U/U_{ref}	λ	Σ
C	15.98	0.930	1.399	-0.200	0.314
S	17.91	1.102	2.350	-0.380	0.271
F	15.04	0.570	2.568	-0.950	0.126

Thus $\overline{\Sigma} = 0.246$ and $\gamma_{red} = \gamma\,\overline{\Sigma} = 3.93$ kN/m^3

Table 7.2 Calculation of the Reduced Unit Weight of the Soil for the Lining-Ground Interaction Analyses

from the NNGRC or λ curves.

The other key aspect to be assessed is the ground modulus to be used in the interaction analyses. Had a fairly stiff lining been used, one could use an average modulus calculated at the instant the lining is installed, ~~following~~ the procedures set up in Section 6.4.3 (equation 6.26 and 6.29). The lining presently considered, however, is very deformable and large displacements are thus expected to occur. Therefore, the ground stiffness when the equilibrium with the liner is eventually achieved, is likely to be very different from that at the instant the lining is installed.

Regardless of what ground stiffness is to be considered or how it should be considered, an important assumption has to be made. It will be assumed that the tangent stiffness of the ground is uniquely related to the tunnel radial closure (U), through the derivative function of λ (λ') presented in Section 6.4. In other words, it will be assumed that the ground stiffness does not depend on the action of the lining. This is obviously a simplification which actually may not be correct. It was shown in Section 2.3.5 that the presence of the lining does affect the ground response, as it induced stress changes in the ground which in turn may cause changes in its stiffness. This effect will be disregarded by assuming that the λ' curves are not affected by the interaction between lining and ground.

This assumption also implies that the λ' curves can provide the ground stiffness either upon unloading or loading. That is to say that the stiffness of the ground can be assessed through these curves both for increasing or decreasing tunnel radial closure. The latter could occur, for instance, at the springline of a lined tunnel squatting and forcing the soil to move outwardly. Note that the fully reversible stress-strain behaviour assumed in the 2D numerical model used in this work (Section 5.2.2.1) does not necessarily ensure the reversibility of behaviour in terms of the λ' curves.

An unstated assumption related to the use of both λ and λ' curves for each point of the tunnel contour, is that they have an independent existence. In other words, the sequence of loading or closure at different points of the opening profile, does not affect the response noted at a particular point of the contour which is always given by a unique λ or λ' curve. It was shown that the twice normalized ground reaction curves were derived from the parametric analyses, where a gradual stress reduction was simulated by applying a uniform amount of stress release (a) at the opening. Thus, the λ and λ' curves were obtained for this particular unloading condition and other unloading sequences could have led to different responses in terms of the λ and λ' curves. Therefore, in using the generalized solution developed, one may disregard the loading condition originally imposed and may operate with the curves for each point of the tunnel contour, as if they were unaffected by responses at other points of the contour. This is equivalent to assuming that the ground response could be as that given by a series of radial springs, one for each point of the contour but not connected to each other. Obviously this is not true, as the responses expressed in terms of the λ and λ' curves do reflect the interactive responses of all points of the soil mass. The error involved in this assumption will be reduced considerably when the stress ratio, Σ, or tangent stiffness, E_t, obtained independently for each point of the tunnel profile are averaged and single Σ or $\bar{E}_t$ values are defined.

The idea of using a reduced ground stiffness compatible with the tunnel closure in a non-linear ground mass, for a lining-ground interaction analysis was proposed earlier by Kaiser (1981:265) for uniform stress field conditions. In this case, a simpler approach was favoured by approximating the ground response by a bilinear elastic model.

The average tangent stiffness of the ground at the instant the lining is installed can be readily estimated. With the U/U_{ref} given in Table 7.2, E_t is obtained through the λ' curves (or equation 6.26) and equation 6.27. The tangent moduli caculated for the tunnel crown, springline and floor are then averaged as indicated by equation 6.28. The calculations and results obtained are summarized in Table 7.3. As it is noticed, the delayed installation of the lining in the second finite element calculation (40% stress release) caused a drop in ground stiffness of about 27% and of about 75% in the third analysis (80% stress release).

a. F.E. with 0% stress release

$\lambda' = \lambda'_i \quad \therefore E_t = E_{t_i}$

Thus $\bar{E}_t = (E_{t_i})_C + 2\,(E_{t_i})_S + (E_{t_i})_F\ /4 = 24.53$ MPa

b. F.E. with 40% stress release

$E_t = (\lambda'/\lambda'_i)\ E_{t_i}$

With U/U_{ref} at lining installation (see previous table)

	U/U_{ref}	λ'	λ'_i	E_t (MPa)
C	0.505	1.000	1.278	18.41
S	0.570	0.940	1.425	16.28
F	1.116	0.840	1.006	21.07

Thus $\bar{E}_t = 18.01$ MPa

c. F.E. with 80% stress release

With U/U_{ref} at lining installation (previous table)

	U/U_{ref}	λ'	λ'_i	E_t (MPa)
C	0.930	0.420	1.278	7.73
S	1.102	0.160	1.425	2.77
F	0.570	0.440	1.006	11.04

Thus $\bar{E}_t$: 6.08 MPa

Table 7.3 Calculation of the Reduced Average Ground Stiffness at Lining Installation

At this point, the lining-ground interaction analysis can be performed. For each case (0, 40 and 80% release), the analytical solution summarized in Figure 7.2 was applied, using the data presented in Tables 7.2 and 7.3 as input. The radial stresses at the crown, springline and floor were found from equation 7.3, after calculating the relative stiffness ratios from equations 7.1 and 7.2. These are the equilibrium stresses acting on the lining at those points. The incremental radial displacements at these points resulting from the lining-ground interaction can be calculated from equations 7.6, 7.7 and 7.10. Note that the value of the in situ stress ratio (K_o or K) to be considered, is the value used in the finite element calculations (0.75). The value of r_1 to be used in equation 7.10, for assessment of the ground heave, v''_{20}, as explained in Section 7.2.1, is the distance between the tunnel centre and the lower (fixed) boundary of the finite element mesh. In this case r_1 is equal to 13.5 m. The final (total) radial displacements are obtained by adding the incremental displacements to the displacements that took place before lining installation.

The values of final radial stresses and displacements thus obtained furnish the equilibrium points indicated by letter "L" in Figures 7.4, 7.5 and 7.6. One notes that in almost all cases and at all points of the tunnel contour, the stresses at L are smaller than the radial stresses at equilibrium calculated in the corresponding finite element analysis. This result is not suprising, as it is a consequence of the criteria used to define the ground stiffness $\bar{E}_t$ adopted in this analysis. It has been assumed that the soil modulus during the lining-ground interaction remained equal to the soil modulus immediately prior to support activation. Since the increments of ground displacements after support installation in this particular case, are quite substantial due to the very compressible lining used, there is also a substantial change in the ground stiffness during the interaction process. Tunnel closure increases during this process and ground stiffness decreases accordingly. Hence at equilibrium the average soil modulus is likely to be appreciably less than that when the support was activated. Therefore, if no allowance is made to account for the additional 'softening' of the ground after the support is installed, then the calculated lining loads will likely be less than the correct ones as the support will be more compressible and more flexible relative to the soil than it should be.

A possibly better and safer assumption regarding the lining loads is to perform the interaction analysis, by assigning the ground its final stiffnesses, defined at the point of equilibrium. This would take into account the additional ground stiffness degradation due to the increment of tunnel closure after the lining is installed. However, this incremental closure is not known beforehand. An iterative procedure would have to be devised to solve the problem. The lining-ground interaction analysis would be started by assigning the ground a stiffness compatible with the tunnel radial closure at the instant the support is activated, as it was done before. An incremental tunnel closure would then be calculated and a new ground stiffness would thus be estimated. The process would then be repeated until convergence is obtained, when the estimated ground stiffness at equilibrium is equal to the assigned ground stiffness used in the interaction analysis.

This algorithm was applied to the three cases being studied. For the 0% stress release case, five iterations were needed for solution convergence. An average modulus, $\bar{E}_t$ of 13.37 MPa was finally found, which represents 45% additional degradation of the ground stiffness resulting from the lined tunnel incremental closure. For the 40% stress release case, four iterations were needed and the resulting average ground modulus was equal to 9.79 MPa, representing a decrease of about 46% relative to the modulus at lining installation. For the 80% stress release case, only three iterations were needed and the resulting average ground modulus was 4.58 MPa, thus 25% lower than that at support activation.

The resulting equilibrium points found through these calculations are those indicated by letter "E" in Figures 7.4 to 7.6. The reduction in the adopted ground stiffness resulted, as expected, in higher radial stresses than at corresponding points L. More importantly, however, the equilibrium stresses at E are systematically higher than the equilibrium stresses given by the finite element calculations. This indicates that, the adoption of the ground tangent stiffness calculated for the total tunnel closure at the final equilibrium situation is a safer assumption, though not excessively so, with respect to the ground loads acting on the tunnel. Conservative estimates of bending moments and thrust forces, as well as larger eccentricities are obtained with the latter assumption.

With respect to the radial displacements at equilibrium, mixed results are obtained. At the crown and floor (Figures 7.4 and 7.6), the displacements at both points L and E are larger than those found in the finite element analyses. While at the crown, the movements given by the approximated procedure are not excessively greater than the correct one, at the floor the displacements are substantially overestimated. It seems that this results from an overestimation of the ground heave component calculated by equation 7.10. The heave has been estimated using the same ground modulus used in the interaction analysis. This modulus seems to represent well the soil around the opening which is participating in the lining-ground interaction process. However, it may not approximate the stiffness of the ground below the tunnel, which would be underestimated by the procedure used.

At the springline, the displacements at both points L and E tend to be smaller than that calculated by the finite element analysis. The degree of underestimation, however is not excessive.

With respect to displacements, those calculated at tunnel crown are of primary importance in the design procedure being developed. This is because all settlements developing above the tunnel are related to the crown displacement, through the normalized settlement distributions. As indicated in Figure 7.4, the approximate method for ground-lining interaction tends to furnish slightly conservative estimates of the crown displacements, which is likely to lead to conservative estimates of surface and subsurface settlements.

The arrows indicated in the last three figures give the directions followed by the equilibrium points, in the proposed analysis, during the iterative calculations. Although depicted as straight vectors, the path from L to E in the iterative analyses is, in fact, a non-linear one.

The above results indicate that, despite the approximate assumptions introduced, a very reasonable estimate of the equilibrium points is possible using the generalized solution developed in Chapter 6, coupled with the closed form solution presented in Section 7.2.1. Moreover, the procedure, derived to account for the delayed installation of a lining in a non-linear elastic ground, seems to furnish safe estimates of lining loads and displacements at the opening which in turn lead to safe estimates of the ground settlements. It should be noted that the generalized solution for the ground response was used without restrictions and, indeed, at certain points and situations, it was used beyond its limits of strict validity (Section 6.5.1).

For design purposes, it seems preferable to use a ground modulus compatible with the final tunnel closure for the tunnel closure. As this is not known beforehand, a simple algorithm was developed to generate the solution, which is found after 3 to 5 iterations.

In solving the problem at hand, a calculation sequence emerged. This sequence will be summarized and discussed in Section 7.3 as a guideline for practical use. Other sequences or assumptions could have been introduced, and were in fact, attempted with end results that did not differ entirely from those shown. The one presented herein, however, seemed to be the most convenient and easiest for practical use.

There were two basic assumptions in the development of the above solution. Firstly, the effect of the delayed lining installation is accounted for by reducing the ground stress field, through a reduction of the unit weight of the soil. The latter is obtained from an average amount of stress release, calculated using the λ curves (normalized ground reaction curves), for an estimated tunnel closure at the point the support is installed. Secondly, the reduced tangent stiffness of the ground to be considered in the interaction analysis, is that given by the λ' curves or the derivative of the normalized ground reaction curves. It is assumed that the ground stiffness is uniquely related to the tunnel closure through these curves, which are assumed to be unaffected by the lining action.

7.2.3 Influence of the Lining Presence on the Ground Settlements

The parametric analyses presented in Chapter 6 considered the tunnel to be unlined and, therefore, the resulting normalized settlement distributions shown, for instance, in Figures 6.48, 6.49, 6.59 and 6.60 (see also Appendix C) disregard the influence of a lining on the ground movements. If a fairly rigid lining is installed after a substantial amount of stress release, the increment of ground movements during the soil-lining interaction may not be very significant compared to the magnitude of movements developed in the pre-support phase. Hence, the settlements developing in the pre-support stage will tend to dominate. However, if the lining is flexible or compressible, then the settlement after lining installation can also be significant. This component of the total ground movement is the one affected by the presence of the lining in a two-dimensional tunnel representation.

The results of the finite element analyses discussed in Section 7.2.2 are helpful for the assessment of the lining influence on the ground settlements. The solid curves in Figures 7.7 and 7.8 represent the final distributions of subsurface and surface settlements, calculated for the cases with ground stress release of 40 and 80% prior to lining installation. The broken curves represent the distributions calculated for an unlined opening, with crown settlements approximately equal to the final crown displacement calculated for the two lined tunnel cases. Since the geometries and soil properties are the same in all cases, the differences between solid and broken curves reflect the influence of the lining on the ground settlements. In the first case, the settlements for the unlined tunnel correspond to a stress release of 55%, to which a crown settlement of 8.97 mm was calculated (against 8.88 mm obtained in the lined case). In the second case, the settlements for the unlined case correspond to a stress release of 80%, and a 16.60 mm crown displacement (compared with 16.10 mm obtained in the corresponding lined case). To obtain a match of crown settlements for the lined and unlined cases, interpolation of displacements between consecutive unloading steps in the unlined case would have been required, but this was not attempted.

For equivalent crown displacements, one notes that the related settlements in both lined cases are smaller than those obtained for the unlined situation. Although the ground surface distortions are not much different for the lined and unlined cases, the latter tend to be marginally higher.

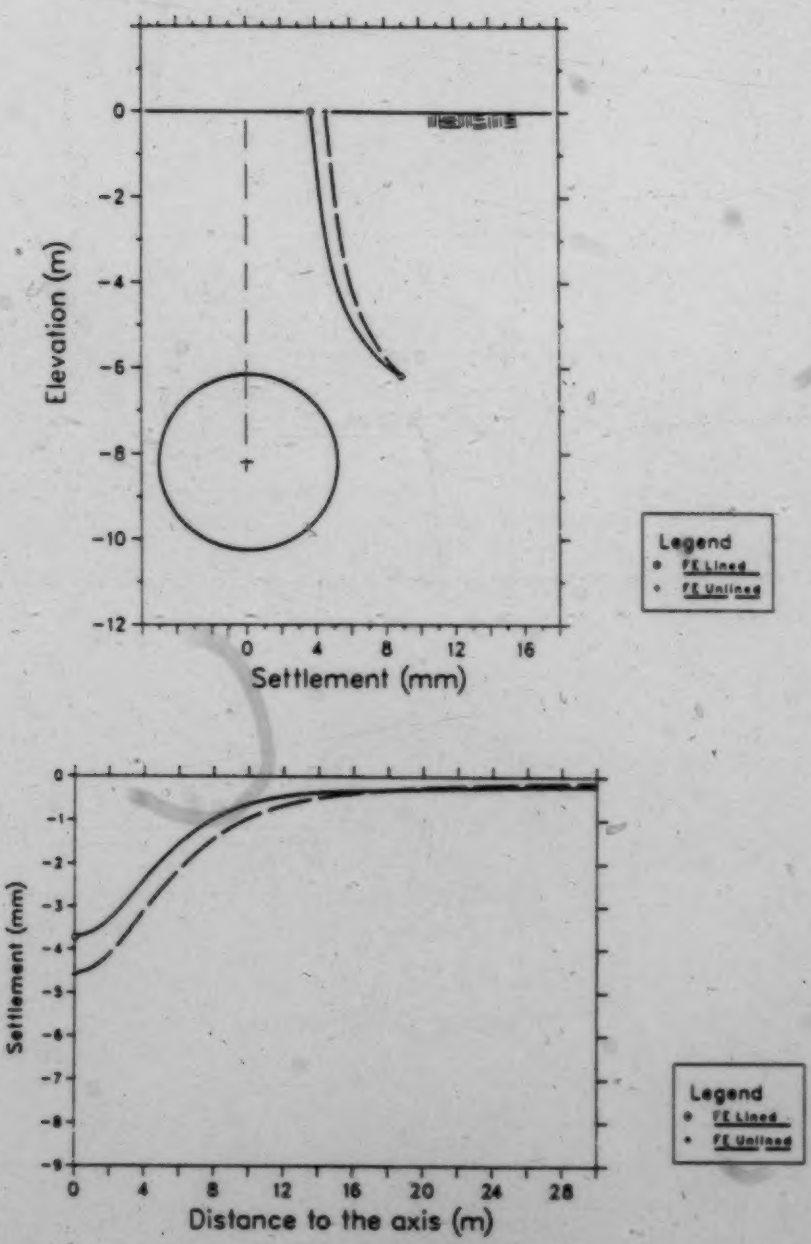

Figure 7.7 Distribution of Final Settlements Calculated for a Tunnel Lined after 40% Stress Release, Compared to the Distributions for an Unlined Tunnel Equal Crown Displacement

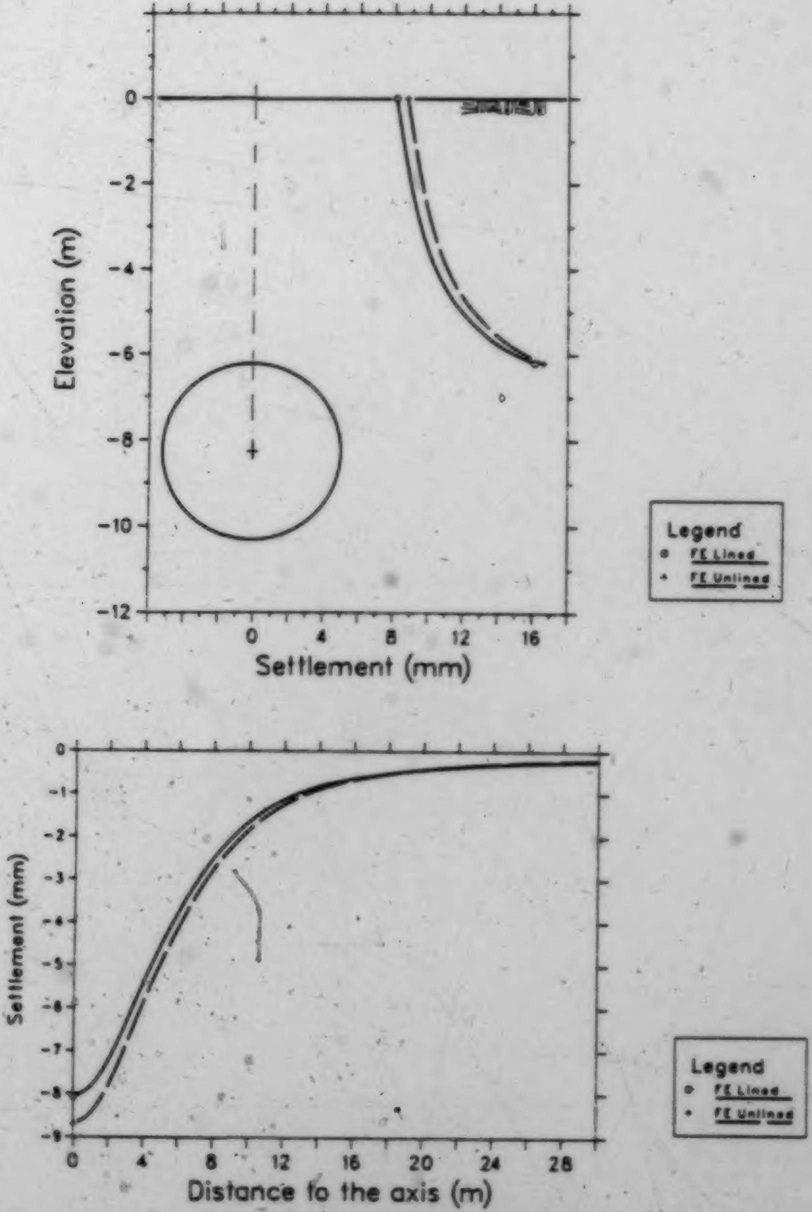

Figure 7.8 Distribution of Final Settlements Calculated for a Tunnel Lined after 80% Stress Release, Compared to the Distributions for an Unlined Tunnel with Equal Crown Displacements

One notes, furthermore, that as the amount of ground stress release before supporting the tunnel increases, the differences in settlements for the lined and unlined cases decrease. The pre-support displacements tend to dominate over the after-support movements as the lining installation is increasingly delayed. The incremental movements after the liner is installed tend to reduce as the ground stress reduction increases, but also as the support becomes stiffer relative to the ground with increasingly delayed installation of the lining. At the instant the lining is installed for the 40% stress release case, the relative stiffness ratios are: β=0.005 and α=0.96. For the 80% stress release case, they are β=0.015 and α=2.85. The additional ground softening resulting from the extra 40% ground stress release, caused the same lining to behave three times stiffer.

The presence of a lining inhibits the 'flow' of soil into the tunnel which is unrestrained in the unlined case. Thus, the volume of soil being lost into the opening is reduced. Moreover, if the lining squats, soil elements adjacent to the opening will be pushed outwardly and this may generate an opposing displacement field in the ground.

This mechanism was found to develop for other ground and lining conditions, and it may be said that by neglecting the presence of the lining, a conservative estimate of the ground settlement distributions above the tunnel will normally be found.

Accordingly, the normalized settlement distributions obtained in the parametric analyses and presented in Appendix C, can be used in practice, since it is sufficient to calculate the amount of stress release in the unlined tunnel solution, which causes the same crown settlement obtained in the lining-ground interaction analyses. This amount of stress release is easily obtained from the normalized ground reaction or λ curves defined for the tunnel crown by inputting the calculated dimensionless crown displacement found at equilibrium. As the sets of normalized settlement distributions were obtained for particular values of H/D, K_o, ϕ or $c_u/\gamma D$, and amounts of stress release, some data interpolation may be needed. Alternatively, the sets of data corresponding to the ground properties nearest the actual one are selected and the data interpolation is restricted to finding the normalized settlements for intermediate values of H/D or stress releases.

7.3 Guidelines for Using the Proposed Design Procedure

The purpose of the present section is to suggest and discuss a sequence of steps to be followed when applying the proposed design procedure.

Following the general scope of the present work, emphasis is given to some of the geotechnical aspects of a shallow tunnel design. No attempt is made to address, for instance, the structural design of the lining, although, the output of the present procedure may serve as input for this.

Geological and geotechnical investigations, though playing a paramount role in underground project designs (see, for example, U.S. National Committee on Tunnelling Technology, 1985) are discussed just briefly with reference to what directly concerns the proposed procedure.

Considering the relative simplicity of the procedure, and in spite of its identified limitations which are derived from the assumptions adopted in its development, the proposed method seems to be useful for sensitivity studies. These are frequently performed in feasibility projects and in basic designs, regarding alignment optimization, selection of construction procedures, the assessment of influence of parameter variability, etc. Moreover, its simplicity offers considerable attraction for design reevaluation during tunnel construction, as part of an observational design approach. The method can be applied and calibrated simultaneously with field monitoring, thus serving as an auxiliary tool for design feed-back and for decisions being made during construction. All calculations involved are simple and easy to perform. The entire procedure can be implemented in a small micro-computer.

The guidelines presented herein were developed for the cohesionless soil model described in Chapter 6. However,it can be easily adapted to the frictionless soil model which provides a better representation of the behaviour of saturated soils under undrained loading conditions.

Figure 7.9 shows a flow chart that summarizes the main sequential steps of the proposed procedure for shallow tunnel design. The geometry of the problem is initially assessed. A range of tunnel covers along the alignment is defined or critical sections are selected. If the tunnel contour is non-circular, and provided it does not deviate too much from a circle, the diameter of a circular profile with equal excavation area is defined.

The geological conditions are then assessed. The design procedure was developed for time independent conditions, so it is important to identify the groundwater conditions, soil permeabilities and coefficients of consolidation. The method asks for uniform ground conditions, at least in the subsurface profile from half diameter above to half diameter below the tunnel. One has to verify whether or not ground uniformity can be assumed for this horizon. Mixed face conditions, for instance, cannot be handled by the proposed procedure. Typical ground properties, or their ranges are then defined. If triaxial test results from good quality undisturbed samples are available, the input parameters for the hyperbolic model can be obtained. Undrained or drained parameters are defined according to the type of analyses to be carried out. A profile of an in situ tangent modulus is carefully defined, and possibly adjusted according to available results of in situ tests (for instance, pressuremeter tests). A reliable estimate of the in situ stress conditions is also needed. This is an important issue

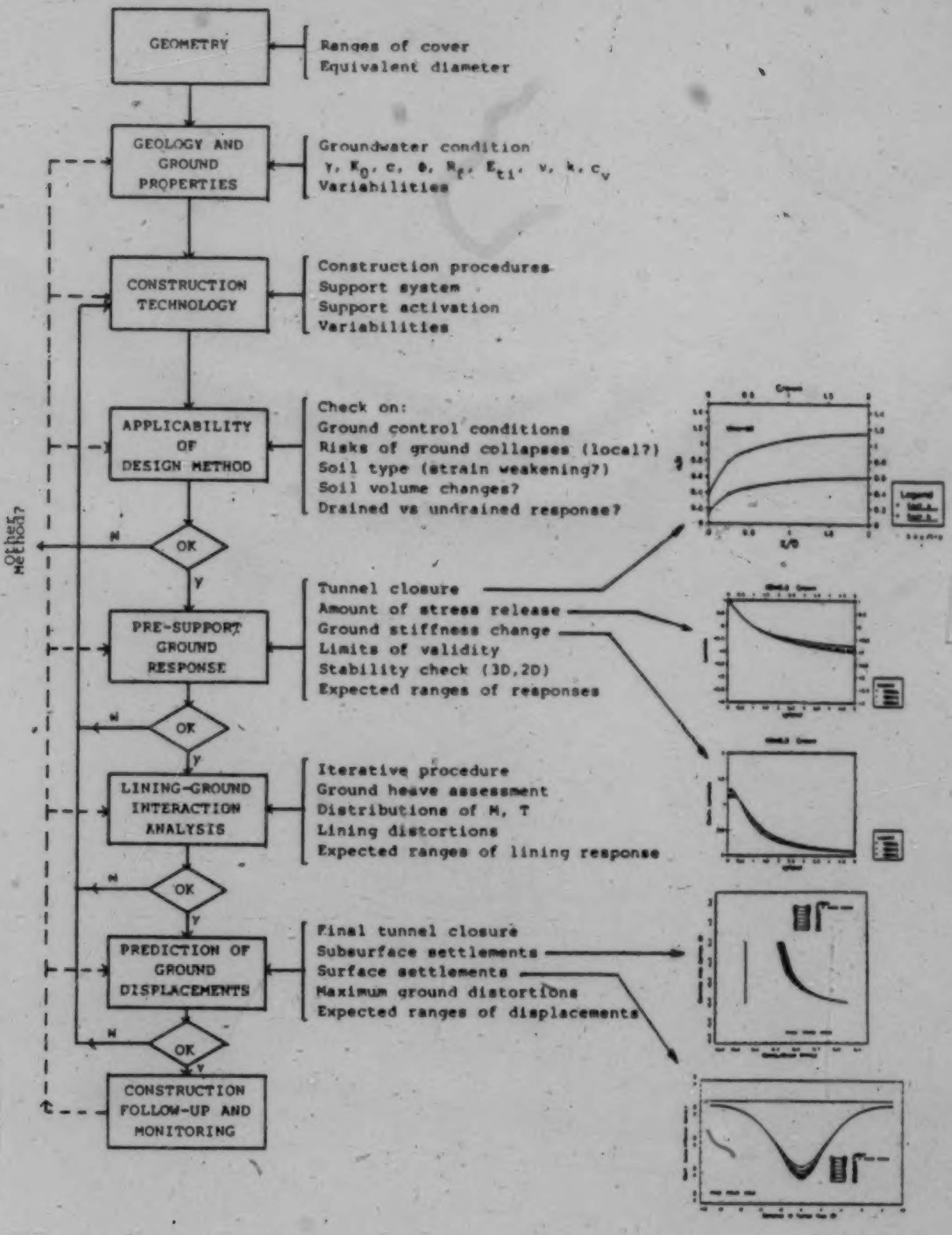
GEOMETRY
Ranges of cover
Equivalent diameter
GEOLOGY AND GROUND PROPERTIES
Groundwater condition
γ, K0, c, φ, Rf, Eti, ν, k, cv
Variabilities
CONSTRUCTION TECHNOLOGY
Construction procedures
Support system
Support activation
Variabilities
APPLICABILITY OF DESIGN METHOD
Check on:
Ground control conditions
Risks of ground collapses (local?)
Soil type (strain weakening?)
Soil volume changes?
Drained vs undrained response?
OK
N
Y
Other Method?
PRE-SUPPORT GROUND RESPONSE
Tunnel closure
Amount of stress release
Ground stiffness change
Limits of validity
Stability check (3D,2D)
Expected ranges of responses
OK
N
Y
LINING-GROUND INTERACTION ANALYSIS
Iterative procedure
Ground heave assessment
Distributions of M, T
Lining distortions
Expected ranges of lining response
OK
N
Y
PREDICTION OF GROUND DISPLACEMENTS
Final tunnel closure
Subsurface settlements
Surface settlements
Maximum ground distortions
Expected ranges of displacements
OK
N
Y
CONSTRUCTION FOLLOW-UP AND MONITORING
Legend

Figure 7.9 Suggested Sequence of Steps for Application of the Proposed Procedure for Shallow Tunnel Design

in the analysis, since both soil and lining performances are very dependent on these conditions. Unfortunately, measurement of K_o in soils is not a simple task. Recent development in push-in stress cells in soft to medium clays have shown promising results (Chan and Morgenstern, 1986). If specific site data is not available, information and field evidence from excavations in nearby areas can provide some help. Additionally, the variability of strength properties, deformation parameters, etc, should be carefully assessed in order to define parameter envelopes. Special attention should be paid to geological features that may likely control local stability conditions. This includes fissures, bedding, sand lenses, etc. Local collapses or cave-ins typify poor ground control conditions under which the present design procedure ceases to be valid. Such occurrences however, can be entirely avoided by appropriate construction techniques or properly chosen construction methods.

Regarding the latter, the design procedure requires a complete knowledge of the method of tunnelling to be undertaken. As originally developed, the present design method is strictly applicable to full face tunnelling, or to tunnelling with minor face excavation staging. In section 7.5, however, the procedure is tested against a few cases that deviate from these conditions. A key issue is the identification of the location where the support is activated and this does not necessarily coincide with the point of lining assembly, especially in grouted or expanded lining systems. In shotcrete linings, the activation point seems to correspond to the section where the support ring is closed. The proposed method is also strictly valid to good lining-ground contact conditions. While this is normally ensured in shotcrete linings, it may not prevail in some prefabricated linings installed in sections with large overbreaks caused by excessive overcutting or local collapses, or in poorly grouted or backfilled supports. The support characteristics and properties should be defined, and their variability assessed (particularly for a shotcrete support). The expected ranges of lining installation delay also have to be estimated.

The proposed design procedure should be used preferably within its range of applicability, avoiding for instance, extrapolation of results beyond the established limits (see Section 6.5) of the stress release and stiffness reduction normalized curves or corresponding equations (Section 6.4). Accordingly, interpolation of data should be performed within the ranges of variables used in the parametric analyses (Section 6.2.5). Similarly, the estimates of tunnel closure using the approximate solution developed in Chapter 5 should be made having in mind the limitations and restrictions discussed in Sections 5.3.5.2 and 5.3.6.1. Broadly speaking, the method should be used only when good ground conditions are ensured, so that near collapse situations are precluded. A tentative criterion to identify such situations was set up in Section 2.3.4.3. Results of tunnel model tests indicated that a limiting value for the dimensionless crown displacement associated with near collapse conditions can be defined. Values of U in excess of 1.8 were generally indicative of near collapse conditions in those tests. A good ground control condition would necessarily mean U values at the crown smaller than that figure and possibly less than 1.0. The interpretation of field data in a number of case histories (see Section 5.3.6.1) seemed to confirm the proposed criteria.

The lining-ground interaction analysis used in the proposed design procedure is strictly applicable to good lining-ground contact, as defined in Section 2.3.5. The quality of this contact depends on different factors as discussed in that section. In prefabricated lining systems it depends to a large degree on the size of the space left unfilled behind the support. As suggested in Section 2.3.5.4, the maximum allowable overbreak at the tunnel crown can be calculated from a limiting increment of dimensionless crown displacement, which was estimated to be 0.5 to 0.65.

Moreover, the proposed design procedure is not to be used for soils with stress-strain behaviour departing appreciably from that described by a hyperbolic relationship. Conditions involving appreciable ground volume changes (dilation, consolidation) also cannot be handled by the proposed procedure. The type of analysis to be performed, which can be either undrained or drained, should be assessed independently, according to the ground profile, soil type, its properties and the construction scheme to be used (lining type, rate of advance, etc). The simplified criteria set up in Section 3.3.4.5 can be helpful for this assessment.

The next step in the design sequence is the evaluation of the pre-support ground response. This requires an estimate of the tunnel closure, which can be made through the procedure developed in Section 5.3.5.2. The dimensionless radial displacements at three points of the tunnel contour can be estimated once the distance (x) behind the face where the support will be activated and the in situ stress ratio K_o are both known. If a drained analysis is made using the cohesionless soil model, then the amount of stress release and the ground stiffness changes at the point the support is activated can be assessed, using the solutions derived in Section 6.4.3 and as explained in Section 7.2.2. Adjustments of the friction angle will be needed for soils with a non-zero cohesive strength component and with failure ratios different from unity. For a variable in situ deformation modulus profile, the radial displacements at the tunnel contour are normalized to the in situ moduli at points located half diameter radially away from the opening, as explained in Section 6.2.4.2. Reference values for the amount of stress release (α_{ref}) and for the dimensionless displacements at tunnel contour (U_{ref}) are found for the particular geometry (H/D), the in situ stress ratio (K_o) and for the adjusted friction angle (m-1). The reduced unit weight of the soil and reduced ground stiffnesses are found by averaging the stress ratios (Σ) and the current stiffnesses (E_t) at the point where the support is activated. These are obtained through the twice normalized ground reaction curves and their derivative functions λ and λ' curves, see Section 6.4.3).

The three dimensional stability condition of the tunnel is verified, both at the face and at the unsupported heading, through some of the methods discussed in Section 4.3.4. A check of the two-dimensional tunnel stability is also made, using for example, the solutions presented in Section 6.5.2, taking into account the reduction of the ground stress calculated at the point the support is to be activated. Provided the calculated factors of safety are acceptable (greater than or equal to 1.3 to 1.6; see data and discussions on Sections 2.3.4.3 and 4.2.3), the construction procedure is applicable and the proposed design method can be used. Otherwise, changes in the construction method have to be considered or additional ground control procedures, such as those discussed in Section 4.2.3, should be implemented.

Expected ranges of pre-support ground response are thus defined and used as input for the lining-ground interaction analysis. The latter is carried out using the solution presented in Section 7.2.1, following the iterative procedure described in Section 7.2.2. Attention should be paid to the evaluation of ground heave, which tends to be overestimated by the solution given in Section 7.2.1. Distributions of lining loads are obtained, including bending moments and thrust forces, calculated for the ranges of expected ground responses. They are used in the independent structural design of the lining. Lining loads and distortions are checked for acceptability. Total tunnel closure is calculated and checked if admissible. If the estimated lining-ground response is not acceptable the construction technology has to be reviewed accordingly, and may require changes to the lining system or in the construction procedures.

The total crown displacement is then obtained. The associated amount of stress release is calculated through the λ curve for the tunnel crown, as explained in Section 7.2.3. Finally the subsurface and surface ground settlements are calculated using the distributions of normalized settlements included in Appendix C, and may require some data interpolation. If the calculated ranges of surface and subsurface settlements are not acceptable or if the risk of damage to existing structures is high (see Section 4.2.2), then again, the construction procedures have to be reassessed or additional ground control measures considered.

Finally, during the construction follow up and field monitoring, the anticipated ground and lining performances can be verified. Reasons for possible departures from the predicted behaviour can be assessed and back analysis of performance can be made, calibrating the proposed procedure to a particular site condition. This feedback process may provide further insight on the tunnelling activities and may help in reevaluating the design and construction, as well as support new decisions to be made.

To facilitate some of the calculations involved in the application of the design sequence described, Figures 7.10 to 7.14 were prepared. As explained earlier, they were developed for applications using the cohesionless soil model, but they can be easily adapted for the frictionless model. The present calculation sheets include the geometry of the problem, the ground properties and the tunnel closure at lining activation (Figure 7.10), reference values used to assess the amount of stress release and the ground stiffness at the section the support is activated (Figure 7.11), the two dimensional ground stability verification and input data for the lining-ground interaction analysis (Figure 7.12), a sheet for the iteration calculations (Figure 7.13) and finally a sheet for the subsurface and settlement calculations (Figure 7.14). For easier reference, some of the equations that are used were reproduced in the calculation sheets.

7.4 An Example of the Use of the Proposed Design Procedure

The Alto da Boa Vista Tunnel built in Sao Paulo, Brazil, is used as an example of the application of the proposed design procedure. This case history was described

1. GEOMETRY

H = ☐ D = ☐ H/D = ☐

2. GROUND PROPERTIES

γ = ☐ K_o = ☐

$(\sigma_3)_{axis}$ = ☐ c = ☐ ϕ = ☐ R_f = ☐

$$\phi_a = \text{arc sin}\left[\frac{1+(\sigma_3/c)\tan\phi}{1+(\sigma_3/c)\sec\phi}\right] = \square$$

$$\phi_e = \text{arc sin}\,(1-R_f+R_f\csc\phi_a)^{-1} = \square$$

$$(m-1) = \frac{2\sin\phi_e}{1-\sin\phi_e} = \square$$

K = ☐ n = ☐ p_a = ☐ μ = ☐

$$E_{ti} = K\,p_a\left(\frac{\sigma_3}{p_a}\right)^n\left[1-\frac{R_f\,(1-\sin\phi)(\sigma_1-\sigma_3)}{2c\cos\phi+2\sigma_3\sin\phi}\right]^2$$

Location	σ_3	σ_1	E_{ti}
1/2 D above C			
at S			
1/2 D below F			

3. TUNNEL CLOSURE AT LINING ACTIVATION

X = ☐ X/D = ☐ K_o = ☐ $u_r = (D\sigma_{ro}/E_{ti})U$

Location	U	σ_{ro}	$D\,\sigma_{ro}/E_{ti}$	u_r
C				
S				
F				

Figure 7.10 Calculation Sheet with Geometric Ground Properties Data and Tunnel Closure at Lining Activation

4. REFERENCE VALUES

$H/D=$ $K_0=$ $(m-1)=$

	$1-\Sigma_{ref}=\alpha_{ref}$	α_{ref}/U_{ref}	U_{ref}
C			
S			
F			

5. STRESS RELEASE AND STIFFNESS CHANGE AT LINING ACTIVATION

	U	U/U_{ref}	Beyond Limit?	λ	λ'
C					
S					
F					

STRESSES : $\Sigma = 1-(1-\lambda)\alpha_{ref}$

	$(1-\lambda)$	Σ
C		
S		
F		

$\overline{\Sigma}=(\Sigma_C+2\Sigma_S+\Sigma_F)/4 =$

$\overline{\alpha} = 1-\overline{\Sigma} =$

$\gamma_{red} = \gamma \cdot \overline{\Sigma} =$

STIFFNESS : $E_t = (\lambda'/\lambda'_i)E_{ti}$

	λ'_i	E_{ti}/λ'_i	E_t
C			
S			
F			

$\overline{E}_t = (E_{tC}+2E_{tS}+E_{tF})/4 =$

Figure 7.11 Calculation Sheet for Estimates of the Stress Release and Ground Stiffness at the Section the Lining is Activated

6. 2D STABILITY VERIFICATION

$\bar{\alpha} = \boxed{\quad}$ $\quad \bar{\sigma}_{ro} = \frac{1+K_0}{2}\gamma(H+\frac{D}{2}) = \boxed{\quad}$ $\quad \phi = \boxed{\quad}$ $\quad c/\gamma D = \boxed{\quad}$ $\quad H/D = \boxed{\quad}$

$\therefore P_\ell/\gamma D = \boxed{\quad}$ $\quad P_\ell = \boxed{\quad}$ $\quad \alpha_\ell = 1 - P_\ell/\bar{\sigma}_{ro} = \boxed{\quad}$

$$FS = \frac{[(1-K_0)/(1+K_0)+\alpha_\ell]}{[(1-K_0)/(1+K_0)+\bar{\alpha}]} = \boxed{\quad}$$

7. LINING-GROUND INTERACTION

GEOMETRY : $Z_0 = \boxed{\quad}$ $\quad r_0 = \boxed{\quad}$ $\quad r_1 = \boxed{\quad}$

SOIL : $\bar{E}_t = \boxed{\quad}$ $\quad \mu = \boxed{\quad}$ $\quad \gamma_{red} = \boxed{\quad}$ $\quad K_0 = \boxed{\quad}$

LINING : $E_s = \boxed{\quad}$ $\quad \mu_s = \boxed{\quad}$ $\quad d = \boxed{\quad}$ $\quad I_s = \boxed{\quad}$

ITERATION No.: ________ $\quad \bar{E}_t = \boxed{\quad}$ $\quad \dot{\alpha} = \boxed{\quad}$ $\quad \beta = \boxed{\quad}$

	u_r	Δu_r	$u_{rf} = u_r + \Delta u_r + V''_{ZO}$	U	U/U_{ref}	λ''	E_t	σ_r
C								
S								
F								

$V''_{ZO} = \frac{(1+\mu)(3-4\mu)}{4(1-\mu)\bar{E}_t}\gamma_{red}\cdot r_0^2 \ln\frac{r_0}{r_1} = \boxed{\quad}$ $\quad (\bar{E}_t)_{new} = (E_{tC} + 2E_{tS} + E_{tF})/4 = \boxed{\quad}$

Figure 7.12 Calculation Sheet for 2D Stability Verification and Lining-Ground Interaction Analysis

ITERATION No.: ______ $\overline{E}_t$ = ☐ $\dot{\alpha}$ = ☐ β = ☐

	u_r	Δu_r	$u_{rf} = u_r + \Delta u_r + v''_{ZO}$	U	U/U_{ref}	λ'	E_t	σ_r
C								
S								
F								

v''_{ZO} = ☐ $(\overline{E}_t)_{new}$ = ☐

ITERATION No.: ______ $\overline{E}_t$ = ☐ $\dot{\alpha}$ = ☐ β = ☐

	u_r	Δu_r	$u_{rf} = u_r + \Delta u_r + v''_{ZO}$	U	U/U_{ref}	λ'	E_t	σ_r
C								
S								
F								

v''_{ZO} = ☐ $(\overline{E}_t)_{new}$ = ☐

Figure 7.13 Calculation Sheet for Iterative Analysis of the Lining-Ground Interaction

8. SUBSURFACE SETTLEMENTS

CROWN SETTL. = ☐ U/U_{ref} = ☐ λ_c = ☐ $\alpha_c = (1-\lambda_c)\alpha_{ref}$ = ☐

K_o = ☐

ϕ = ☐

DEPTH Z (m)	Z/H	SETTLEMENT/CROWN SETTL.			SETTLEMENT
		H/D=	H/D=	H/D=	
H=	1.000	1.000	1.000	1.000	

9. SURFACE SETTLEMENTS

α_c = ☐

K_o = ☐

ϕ = ☐

DIST. Y (m)		0.0
Y/D		0.0
SETTL./CROWN SETTL.	$\frac{H}{D}$=	
	$\frac{H}{D}$=	
	$\frac{H}{D}$=	
SETTL.		

MAX. DISTOR.: 1: ☐

AT: ☐

Figure 7.14 Calculation Sheet for Subsurface and Surface Settlements

in detail in Section 5.2.4.2, where it was back-analysed through the two-dimensioal finite element model presented in Chapter 5. In the present section, as well as in the following, no attempt will be made to best fit the observed performance. The case history data are used as a design case, where the most likely tunnel response in geotechnical terms, is the matter of interest. For consistency, however, and to allow a comparison with the results of the numerical back-analysis performed earlier, the same parameters then used will be applied here.

The tunnel had a soil cover of 6.2 m and a near circular excavation profile with 3.9 m height and 4 m width. The equivalent diameter of a circular excavation with an equal area is 4 m.

The tunnel was driven above the water table through the variegated silty sand and a drained analysis using effective stress parameters and zero pore pressures is justified. The ground properties and geometric data are reproduced in Figure 7.15. The justifications for using these soil parameters were given in Section 5.2.4.2. An in situ stress ratio of 0.8 was selected in the present analysis (as opposed to the 0.75 ratio back analysed earlier), in order to simplify the application of the generalized solution. Interpolation of data regarding the K_0 value was thus eliminated. Note that since the soil cohesion is zero and its failure ratio is equal to one, there is no need to adjust the friction angle using equations 6.3 and 6.10 which are reproduced in Figure 7.15. The variation of the in situ tangent modulus with depth is given by the last equation in Figure 5.11, using the calculated in situ principal stresses. The in situ modulus at half a tunnel diameter above the crown, at the springline elevation and half a tunnel diameter below the floor are thus calculated and will be used to normalize the radial displacements at the corresponding points of the tunnel contour. The moduli obtained are marginally higher than those used in the numerical back-analysis, as a slightly higher K_o was assumed here. However, they are not discordant with the in situ deformation modulus profile, as obtained through pressuremeter tests (see Figure 5.14).

In a routine design application, ranges of geotechnical parameters, such as those given in Table 5.9 for the variegated soil, would be used instead of the single 'most likely' set of parameters being considered herein.

As described in Section 5.2.4.2, the tunnel construction was performed under good ground control conditions, that were provided both by the favourable ground and by the good construction quality achieved. The shotcrete support and the face excavation were installed in stages. As suggested earlier in different sections of this thesis, it seems reasonable to allow in such a support type, that its activation takes place when the shotcrete ring is closed at the floor. Therefore, the radial closure of the opening, at the point the lining is activated, is calculated at a

I. GEOMETRY

H = 6.2 m D = 4.0 m H/D = 1.55

2. GROUND PROPERTIES

γ = 16 kN/m³ K_0 = 0.8

$(\sigma_3)_{axis}$ = 104.12 kPa c = 0 ϕ = 29° R_f = 1.0

$$\phi_a = \arc\sin\left[\frac{1+(\sigma_3/c)\tan\phi}{1+(\sigma_3/c)\sec\phi}\right] = \boxed{29°}$$

$$\phi_e = \arc\sin\,(1-R_f+R_f\csc\phi_a)^{-1} = \boxed{29°}$$

$$(m-1) = \frac{2\sin\phi_e}{1-\sin\phi_e} = \boxed{1.882}$$

K = 400 n = 0.25 p_a = 101.33 kPa μ = 0.3

$$E_{ti} = K\,p_a\left(\frac{\sigma_3}{p_a}\right)^n\left[1-\frac{R_f(1-\sin\phi)(\sigma_1-\sigma_3)}{2c\cos\phi+2\sigma_3\sin\phi}\right]^2 = 30477.682\,(\sigma_3/101.33)^{0.25}$$

Location	σ_3 kPa	σ_1 kPa	E_{ti} MPa
1/2 D above C	53.76	67.20	26.01
at S	104.32	130.40	30.70
1/2 D below F	154.88	193.60	33.89

av. 30.325

3. TUNNEL CLOSURE AT LINING ACTIVATION

X = 2.6 m X/D = 0.65 K_0 = 0.8 $u_r = (D\sigma_{ro}/E_{ti})U$

Location	U	σ_{ro} kPa	$D\,\sigma_{ro}/E_{ti}$	u_r mm
C	0.587	49.20	0.015255	8.95
S	0.469	104.32	0.018592	6.37
F	0.352	161.60	0.019026	6.70

Figure 7.15 ABV Tunnel - Input Data and Tunnel Closure at Lining Activation

section located 2.6 m behind the heading face (x/D=0.65). Possible variations in the depth of heading advance or distance of lining closure behind the face, would have to be considered in a real design calculation and thus a range of tunnel closures at the lining installation point would have to be considered. For the present, it is sufficient to contemplate the most probable delay of support application in this case history. Being a shotcrete support, the lining-ground condition can be defined as good.

Tunnel closure at crown, springline and floor are estimated using the approximate solution given in Section 5.3.5.2 (Figures 5.94 to 5.96). If the design procedure was being used during construction, the actually observed tunnel closure would possibly be known. The measured radial displacements would, thus, be used instead of the estimated values. As shown in Figure 7.15, the dimensionless crown displacement is smaller than 1.0 and this is consistent with the good ground control conditions met in this case history.

The stress-strain curves of the variegated soil are very closely represented by a hyperbolic relationship. In an actual design activity, the risk of local ground collapse would have to be assessed through a close inspection of the locally occurring geological features and through available stability solutions which can provide the means for assessing the face and unsupported heading stability. In the present analysis this is not needed since the tunnel was already built, and no local or global instability process was detected during construction. Except for some contraction likely to occur in this soil upon shearing, the overall volume changes expected in this ground were small, and this is partly due to the good ground control conditions implemented. No appreciable volumetric changes associated with changes in the mean normal stresses were expected, partly because the overconsolidated nature of the deposit. For all these reasons, the proposed design method seemed to be fully applicable to the case history considered.

The next step consists of the evaluation of the ground stress release and of the ground stiffness at the point of support activation. The corresponding calculations are shown in Figure 7.16. The solution set for K_o=0.8, summarized in Figures 6.100 to 6.107, is used. With the calculated strength factor (m-1) (Equation 6.30), α_{ref} is obtained from Figure 6.101 and the ratio α_{ref}/U_{ref} is determined through Figure 6.100, for the cover to diameter ratio being considered. The reference dimensionless displacements at the crown, springline and floor are thus obtained. The corresponding ratios U/U_{ref} are then calculated and checked if they are greater than the limiting ratios defined in the solution generalization. In this case, the U/U_{ref} values lie to the left of the terminal points of the fitted function, represented by the right vertical bars in Figures 6.102 to 6.104, and so no data extrapolation is involved. Using the last three figures, the values of λ are obtained and the corresponding stress ratios (Σ) at the crown, springline and

4. REFERENCE VALUES

H/D= $\boxed{1.55}$ K_0= $\boxed{0.8}$ (m-1)= $\boxed{1.882}$

	$1-\Sigma_{ref}=\alpha_{ref}$	α_{ref}/U_{ref}	U_{ref}
C	0.525	0.87	0.603
S	0.465	1.12	0.415
F	0.435	2.02	0.215

5. STRESS RELEASE AND STIFFNESS CHANGE AT LINING ACTIVATION

	U	U/Uref	Beyond Limit?	λ	λ'
C	0.587	0.973	No	0.03	0.62
S	0.469	1.130	No	-0.05	0.45
F	0.362	1.637	No	-0.45	0.65

STRESSES : $\Sigma = 1-(1-\lambda)\alpha_{ref}$

	$(1-\lambda)$	Σ
C	0.97	0.491
S	1.05	0.512
F	1.45	0.369

$\overline{\Sigma} = (\Sigma_C + 2\Sigma_S + \Sigma_F)/4 = \boxed{0.471}$

$\overline{\alpha} = 1 - \overline{\Sigma} = \boxed{0.529}$

$\gamma_{red} = \gamma \cdot \overline{\Sigma} = \boxed{7.536}\ kN/m^3$

STIFFNESS : $E_t = (\lambda'/\lambda'_i) E_{ti}$

	λ'_i	E_{ti}/λ'_i	E_t MPa
C	1.278	20.362	12.618
S	1.425	21.544	9.695
F	1.005	33.721	21.919

$\overline{E}_t = (E_{tC} + 2E_{tS} + E_{tF})/4 = \boxed{13.482}$ MPa

Figure 7.16 ABV Tunnel - Stress Release and Ground Stiffness at Lining Activation

floor are calculated using the definition given by equation 6.23. The stress ratios are averaged and the reduced unit weight of the soil (γ_{red}) is calculated according to the definition given by equation 7.14.

Similarly, the derivative of the twice normalized ground stress release curve (λ') are found, for the calculated U/U_{ret} values at lining installation, using the curves given in Figures 6.105 to 6.107. The current ground moduli are then calculated using equations 6.27 and 6.29 (or Figure 6.116). They are then averaged and E_t is obtained.

It should be noted that since the ratio H/D lies between two values considered in the parametric analyses (1.5 and 3.0), some interpolation of data may be needed to obtain λ and λ'. Since the solutions for those two values lie very close together, a linear interpolation is sufficient. As an alternative, the nearest available solution (H/D=1.5) could be used, as the error involved is insignificant. If the analysis is done through a programmed solution, λ and λ' would be calculated from equations 6.24 and 6.26, using the parameters, P_i, shown in Table 6.16.

One can note from Figure 7.16 that at the section the lining was installed, the ground stress had been reduced by 52.9% and the average ground modulus had been also reduced but by 55.6%. The former ground stress reduction is higher than that found in the back analysis of this case history presented in Section 5.2.4.2 (40%) and also higher than the amount given in Section 5.3.7 (59%). This is because a slightly higher K_o value has been adopted herein, as well as considering an increased distance between face and point of lining activation (x/D=0.65), and other approximations involved in the proposed calculation method.

A two-dimensional stability check would then be made. This is done here using the lower bound solution presented in Section 6.5.2. For instance, one could say that $\phi \approx 30°$ and the tunnel collapse pressure, p_1, is obtained from Figure 6.125, with c=0 and H/D=1.55. The factor of safety of the ground is calculated using equation 6.34 and it is found to be about 1.4 (see Figure 7.17). This value is totally acceptable, thus the construction procedure and the proposed design method are applicable.

The next design step is the ground-lining interaction analysis. The values of γ_{ref} and $\bar{E}_t$ are used as input in this analysis. The depth to the tunnel axis is taken as the soil cover plus the half tunnel diameter. The analytical solution assumes the lining thickness to be small. Thus, an average lining radius of 1.95 m (for a shotcrete lining 10 cm thick) is considered. Following the discussions presented in Section 5.2.4.2, a reduced shotcrete modulus of 10 GPa is adopted (instead of the 8.65 GPa modulus back analysed in Section 5.2.4.2). The radius, r_1, of the arbitrary circle at which the vertical ground heave displacement is set equal to zero (see Section 7.2.1), would be chosen as that tangent to a stiffer horizon below the tunnel. According to the description of the local geology (Section 5.2.4.2), it would

6. 2D STABILITY VERIFICATION

$\bar{\alpha} = \boxed{0.529}$ $\bar{\sigma}_{ro} = \frac{1+k_0}{2}\gamma(H+\frac{D}{2}) = \boxed{117.36\ kPa}$ $\phi \overset{\sim}{=} \boxed{30°}$ $c/\gamma D = \boxed{0}$ $H/D = \boxed{1.55}$

$\therefore P_\ell/\gamma D \overset{\sim}{=} \boxed{0.35}$ $P_\ell = \boxed{22.4\ kPa}$ $\alpha_\ell = 1 - P_\ell/\bar{\sigma}_{ro} = \boxed{0.809}$

$$FS = \frac{[(1-k_0)/(1+k_0)+\alpha_\ell]}{[(1-k_0)/(1+k_0)+\bar{\alpha}]} = \boxed{1.437}$$

7. LINING-GROUND INTERACTION

GEOMETRY : $Z_0 = \boxed{8.15m}$ $r_0 = \boxed{1.95\ m}$ $r_1 = \boxed{8.15m}$ tongent to surface

SOIL : $\bar{E}_t = \boxed{13.482\ MPa}$ $\mu = \boxed{0.3}$ $\gamma_{red} = \boxed{7.536\ kN/m^3}$ $K_0 = \boxed{0.8}$

LINING : $E_s = \boxed{10\ GPa}$ $\mu_s = \boxed{0.25}$ $d = \boxed{0.1\ m}$ $I_s = \boxed{8.33.10^{-5}}\ m^4/m$

ITERATION No.: 01 $\bar{E}_t = \boxed{13.482\ MPa}$ $\dot{\alpha} = \boxed{52.745}$ $\beta = \boxed{1.156.10^{-2}}$

* No heave between brackets ( )

	u_r mm	Δu_r mm	$u_{rf} = u_r + \Delta u_r + V''_{zo}$	U	U/Uref	λ'	E_t MPa	σ_r kPa
C	8.95	1.683	8.093 * (10.633)	0.531 (0.697)	0.881 (1.156)	0.69 (0.52)	14.043 (10.583)	44.24
S	6.37	-1.378	4.992 (4.992)	0.367	0.884	0.62	13.357	57.81
F	6.70	1.847	11.087 (8.547)	0.583 (0.449)	2.712 (2.088)	0.42 (0.53)	14.163 (17.872)	57.14

$v''_{zo} = \frac{(1+\mu)(3-4\mu)}{4(1-\mu)\bar{E}_t}\gamma_{red}\cdot r_0^2 \ln\frac{r_0}{r_1} = \boxed{2.540\ mm}$ (zero)

$(\bar{E}_t)_{new} = (E_{tC} + 2E_{tS} + E_{tF})/4 = \boxed{13.730\ MPa}$ * (13.792)

Figure 7.17 ABV Tunnel - Two Dimensional Stability Calculation and Lining-Ground Interaction

be at 11.85 m. This is however, more than the depth of the tunnel axis, and would likely lead to excessive ground heave. Instead, r_1 is selected so that the arbitrary circle becomes tangent to the ground surface (r_1=8.15 m). The coefficients of relative stiffness can then be calculated (equations 7.1 and 7.2) and are found to be α=52.7 and β=0.0116 (Figure 7.17), which are typical for a shotcrete lining in a medium clay (Table 7.1).

The overall ground heave is calculated using equation 7.10 (Figure 7.2) and it is found to be 2.54 mm (see Figure 7.17). The analysis is conducted using the solution shown in Figure 7.2 (equations 7.3 and 7.7). Increments of radial displacement Δu_r are found. Using equation 7.6, these are added to the heave displacement. The final radial displacements are found after adding those calculated at lining installation (Figure 7.15). New U and U/U_{ref} values are found for the three points of the contour. New λ' and E_t are thus obtained and a new $\bar{E}_t$ is found to be equal to 13.73 MPa, which is to be compared to that formally calculated (13.482 MPa). The new modulus is found to be 1.8% greater than the previous one. A second iteration analysis is thus performed, using the new modulus as input. (Figure 7.18). A new ground heave is calculated and the calculation is repeated. Another $\bar{E}_t$ is found (13.623 MPa), which differs from the old value by less than 0.6%. Therefore, no more iterations are needed. The final radial stresses and displacements are thus found, as shown in Figure 7.18. As explained in Section 7.3, bending moments and thrust forces in the lining are also obtained in this calculation but are not discussed. Note, moreover, that the normalized final dimensionless displacement (U/U_{ref}) at the tunnel floor exceeded the limit of the fitted λ and λ' functions for this point (see Figures 6.104 and 6.107), unlike at the other points of the tunnel contour. Notwithstanding this, the extrapolation of data at the floor did not impair the quality of the results obtained, as will be seen later.

A total crown settlement of 8.1 mm is obtained, which leads to a U/U_{ref} value of 0.882. Using the λ curves shown in Figure 6.102, it is found that this crown displacement corresponds to λ equal to 0.1 and, therefore, to a stress release at the crown of 47.25%. As recommended in Section 7.2.3, the induced ground settlements are obtained through the results of the parametric analyses (Appendix C) for the unlined tunnel case, considering the amount of stress release (≈47%) which causes, in the unlined tunnel, the same crown settlement obtained in the lining ground interaction analysis (Figure 7.19).

To obtain the distribution of subsurface settlements, the normalized subsurface settlement plots, such as the one shown in Figure 6.59, are used. The corresponding sets of normalized plots which bracket the case in hand are selected in Appendix C. These are taken as the plots for $K_o=0.8$ and $\phi=30°$, and for $H/D=1.5$ and 3.0. Curves for these two cover to diameter ratios, for 47% stress release are obtained by

ITERATION No.: 02 $\bar{E}_t$ = 13.730 MPa $\dot{\alpha}$ = 51.793 β = 1.351.10⁻²

	u_r mm	Δu_r mm	$u_{rf} = u_r + \Delta u_r + v''_{zo}$	U	U/U$_{ref}$	λ'	E_t MPa	σ_r KPa
C	8.95	1.658	8.113 (10.608)	0.532 (0.695)	0.882 (1.153)	0.69 (0.52)	14.043 (10.583)	44.21
S	6.37	-1.352	5.018	0.369	0.889	0.61	13.142	57.80
F	6.70	1.820	11.015 (8.520)	0.579 (0.448)	2.693 (2.084)	0.42 (0.53)	14.163 (17.872)	57.10

v''_{zo} = ☐ $(\bar{E}_t)_{new}$ = 13.623 (13.685)

ITERATION No.: ______ $\bar{E}_t$ = ☐ $\dot{\alpha}$ = ☐ β = ☐ $(\bar{E}_t)_{new} \geq \bar{E}_t$ ∴ ok

	u_r	Δu_r	$u_{rf} = u_r + \Delta u_r + v''_{zo}$	U	U/U$_{ref}$	λ'	E_t	σ_r
C								
S								
F								

v''_{zo} = ☐ $(\bar{E}_t)_{new}$ = ☐

Figure 7.18 ABV Tunnel - Iterative Calculation for the Lining-Ground Interaction

linear interpolation (see Figure 7.19), from the curves which bracket that amount of stress release (i.e., the 40% and 50% curves). Curves similar to those shown in Figure 6.62(a) are thus obtained. This is followed by another data interpolation, at equal normalized depth to cover ratios (z/H), so that the normalized settlement curve for H/D=1.55 is obtained (see Figures 6.62a and 7.19). The distribution of subsurface settlements is immediately calculated as the crown settlement is known. Note that to find the distribution for the actual friction angle (ϕ=29°), the process would have to be repeated once more for ϕ=20°, and the normalized displacements would have to be interpolated from those found for the 20° and 30° friction angles. It is simpler, as well as sufficient, to select the set of normalized plots for the friction angle which is closer to the actual one, or to assume the angle that leads to a more conservative settlement estimate. The same comments apply to intermediate values of the in situ stress ratio (K_o). The above calculations can be relatively tedious to perform if done manually. However, they can easily be programmed and performed in a small micro-computer.

The distribution of surface settlements are obtained through an identical procedure, except for using the normalized surface settlement plots, such as the one shown in Figure 6.60. Similar interpolation procedures are undertaken, after selecting the sets of normalized plots from Appendix C which bracket the case being investigated.

8. SUBSURFACE SETTLEMENTS

CROWN SETTL. = 8.11 (10.61) U/U_{ref} = 0.882 (1.153) λ_c = 0.1 (-0.075) $\alpha_c = (1-\lambda_c)\alpha_{ref}$ = 0.473 (0.564)

47% (56%)

K_o = 0.8

ϕ = 30°

* No heave between brackets ( )

DEPTH Z (m)	Z / H	SETTLEMENT/CROWN SETTL.			mm SETTLEMENT
		H/D= 1.5	H/D= 3.0	H/D= 1.55	
0	0	0.515 (0.521)	0.375 (0.378)	0.510 (0.516)	4.14 (5.48)
1.862	0.300	0.575 (0.586)	0.422 (0.430)	0.570 (0.580)	4.62 (6.15)
3.044	0.491	0.624 (0.632)	0.460 (0.467)	0.619 (0.627)	5.02 (6.65)
4.568	0.737	0.732 (0.740)	0.580 (0.580)	0.727 (0.735)	5.90 (7.79)
5.080	0.819	0.782 (0.787)	0.642 (0.642)	0.777 (0.782)	6.30 (8.30)
5.613	0.905	0.855 (0.860)	0.765 (0.765)	0.852 (0.857)	6.91 (9.09)
5.982	0.965	0.940 (0.940)	0.873 (0.873)	0.938 (0.938)	7.61 (9.95)
H = 6.20	1.000	1.000	1.000	1.000	8.11 (10.61)

9. SURFACE SETTLEMENTS

α_c = 47% (56%)

K_o = 0.80

ϕ = 30°

DIST. Y (m)		0.0	2.0	4.0	8.0	12.0
Y/D		0.0	0.5	1.0	2.0	3.0
SETTL./ CROWN SETTL.	$\frac{H}{D}$=1.5	0.515 (0.521)	0.470 (0.475)	0.375 (0.375)	0.220 (0.215)	0.122 (0.117)
	$\frac{H}{D}$=3.0	0.375 (0.378)	0.360 (0.365)	0.335 (0.340)	0.254 (0.255)	0.175 (0.175)
	$\frac{H}{D}$=1.55	0.510 (0.516)	0.466 (0.471)	0.374 (0.374)	0.221 (0.216)	0.124 (0.119)
SETTL. mm		4.14 (5.48)	3.78 (5.00)	3.03 (3.97)	1.79 (2.30)	1.00 (1.26)

MAX. DISTOR.: 1: 2,000 (1,800)

AT:

Figure 7.19 ABV Tunnel: Subsurface and Surface Settlement Calculations

The interpolations are performed at equal normalized distances to the tunnel axis (Y/D). The resulting calculations are summarized at Figure 7.19, where the calculated maximum surface distortion is also indicated.

If it was only necessary to know the maximum surface settlement, then the above calculations would not be needed. It would be adequate to use the relationships between surface and crown settlements presented in Section 6.3.2.3. For the present case, the solution would be found using the relationships given in Figure 6.77 to 6.80.

The calculations above complete the basic geotechnical design. Obviously, the lining design is an activity in itself, which will not be covered herein. The structural design of the support can, however, make use of the lining internal forces (N_ϕ, M_ϕ, Q_ϕ) calculated through equations 7.11 to 7.13, (Figure 7.2) with the input parameters used in the second and final iteration (Figure 7.18).

It was suggested in Section 7.2.2 that the ground heave as calculated through equation 7.10 tends to be excessive. In fact, Hartmann's solution for this aspect of the shallow tunnel entails an indeterminate degree of approximation, represented by the value of the arbitrary radius r_1. Before a comparison between calculated and measured behaviour is made, it seems convenient to explore the influence of the calculated heave on the overall tunnel response. For this, the calculations presented in Figure 7.17 were repeated, assuming, that v''_{z0} was equal to zero. The resulting calculations are depicted between parentheses in Figures 7.17 and 7.18. As expected, the total radial displacement at the crown increases, as the floor displacement decreases, while the springline radial displacement remains unchanged. The average ground modulus $\bar{E}_t$, calculated at the end of each iterati~~on, however~~, does not change by any significant degree. This seems to reflect the compensating effect of the increased crown displacement against the decreased floor heave. As a result, the radial stresses onto the support at equilibrium, do not change significantly. In essence, the effect of the overall ground heave given by equation 7.10 is mostly restricted to the vertical displacements at the floor and crown. Therefore, it should affect the subsurface and surface settlements which are normalized to the crown settlement. Settlement distributions were calculated with the zero heave assumption (not shown in Figure 7.19), and it was found that the amount of stress release in the unlined tunnel solution, which produces the same final crown settlement obtained in the interaction analysis (10.61 mm), was about 56%.

Figure 7.20 presents a comparison between the observed and calculated final subsurface settlements at the ABV tunnel. The calculated ground movements neglecting the heave component given by equation 7.10 are larger than the measured values, showing that this assumption leads to conservative settlement predictions. The calculated settlements including the heave component are, on the other hand, very much in agreement with the field measurements.

A similar comparison regarding surface settlements is presented in Figure 7.21. Again the zero heave assumption leads to conservative estimates of the surface movements. The larger number of measurements includes a greater scatter of data so that both the heave and the no heave assumptions lead to results are contained well within the measurements.

The calculated and measured radial stresses acting on the lining are shown in Figure 7.22. Note that the calculated stresses are not sensitive to the heave assumption. The proposed design procedure seems to overestimate the ground loads onto the lining, except at the floor, where a good match is obtained. Bearing in mind the known difficulties associated with the installation of contact pressure cells notably at the upper arch of the lining, the agreement between measured and calculated stress seems fairly reasonable.

Finally, Table 7.4 summarizes the comparisons between the measured and calculated performance for the ABV tunnel. Note that the tunnel radial closure at the face was calculated using the approximate solution presented in Section 5.3.5.2 (aspects 3 and 6). The maximum horizontal convergence of the lining (aspect 5) was calculated by discounting the springline movements that took place ahead of the tunnel face (not measured). The total settlement of the lining roof (aspect 8), measured by internal levelling in the field, was calculated by discounting the crown

Performance aspect		Measured(1)	Calculated	
			Heave(2) Included	Heave(3) Excluded
1. Maximum final surface settlement	mm	5.0	4.1	5.4
2. Maximum slope of final settlement trough at surface	-	1:1,300	1:2,000	1:1,800
3. Floor heave at tunnel face	mm	1-1.5(4)	2.2	2.2
4. Final floor heave	mm	5-9(4)	11.0	8.5
5. Maximum horizontal convergence of the lining	mm	0.85	2.7	2.7
6. Crown settlement at tunnel face	mm	1.5(5)	3.9	3.9
7. Final crown settlement	mm	8.0(5)	8.1	10.6
8. Total settlement of lining roof	mm	4-5	4.2	6.7
9. Pressure on lining at the crown	kPa	30	44	44
10. Pressure on lining at springline	kPa	35	58	58
11. Pressure on lining at the floor	kPa	55	57	57

Notes:
(1) Average values.
(2) Taking into account the ground heave in the lining-ground interaction analysis.
(3) Disregarding the ground heave in the lining-ground retraction analysis.
(4) Measured at 0.2 m and 1.2 m below tunnel.
(5) At 0.2 m above tunnel.

Table 7.4 Performance at the ABV Tunnel as Measured and as Calculated by the Proposed Procedure

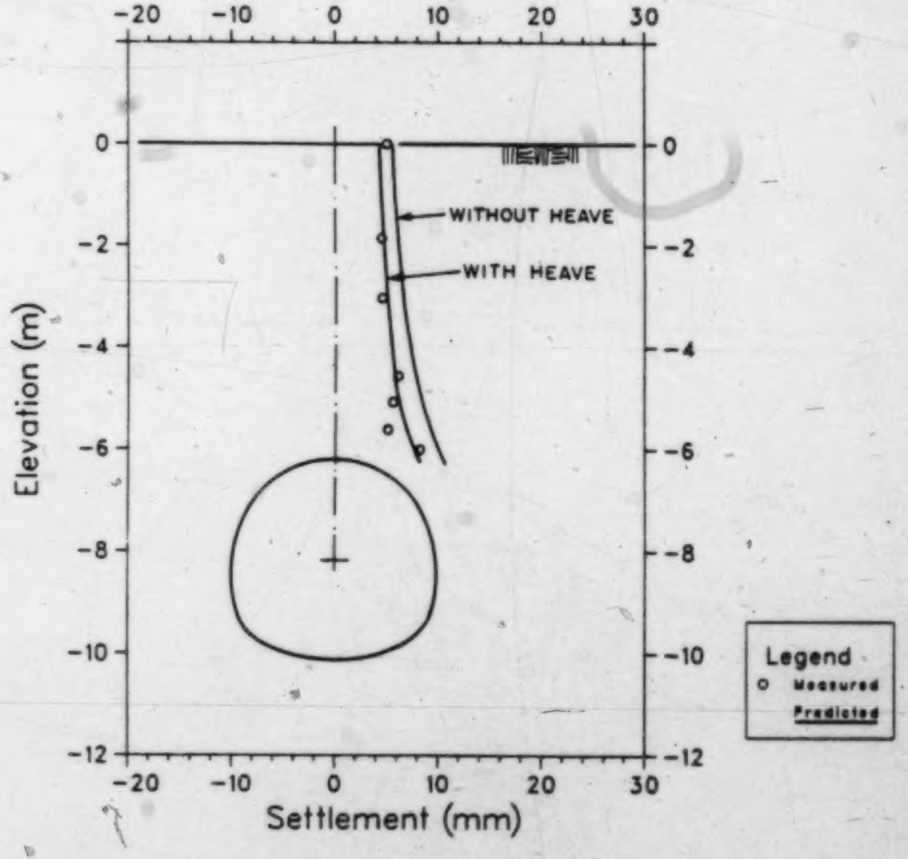

Figure 7.20 Calculated and Measured Final Subsurface Settlements at the ABV Tunnel

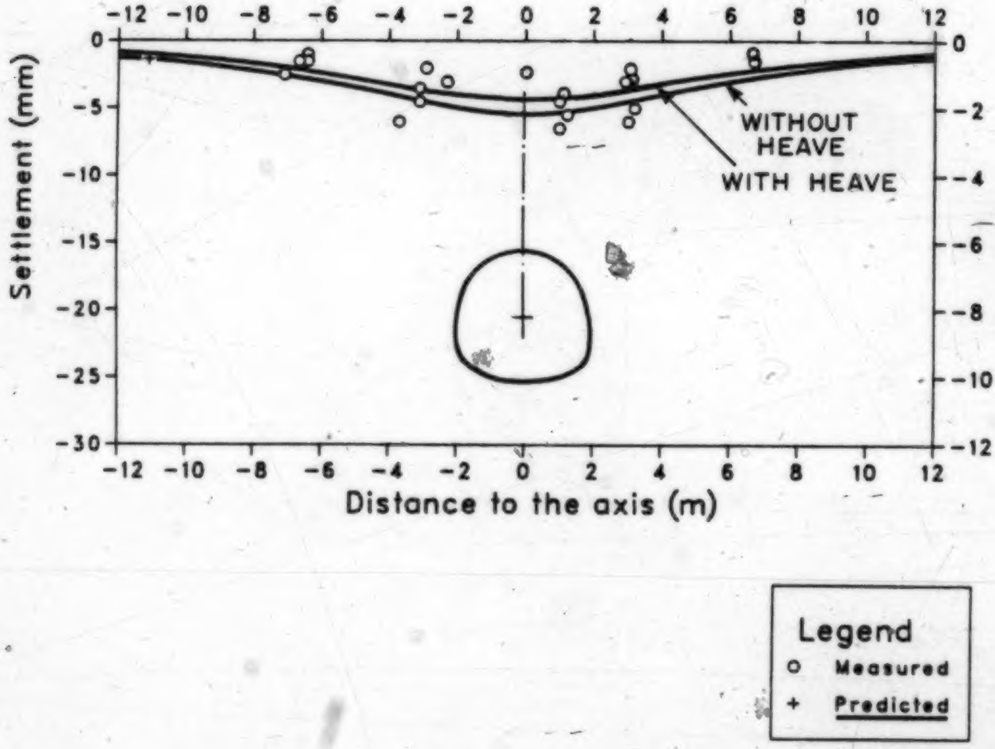

Figure 7.21 Calculated and Measured Final Surface Settlements at the ABV Tunnel

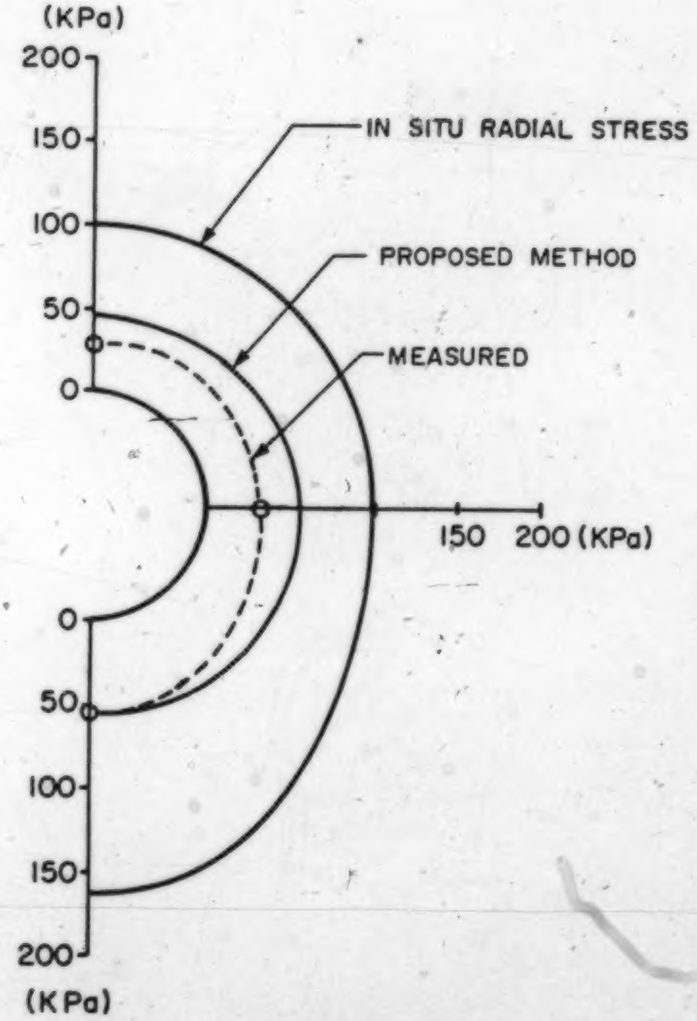

Figure 7.22 Calculated and Measured Radial Stresses on the ABV Tunnel Lining

settlement that also developed ahead of the face.

Regardless of the assumption made with respect to the ground heave, the comparisons shown speak for themselves. If the results of the present calculations are compared with those of the best fit finite element analysis shown in Section 5.2.4.2 (Figure 5.19 to 5.21 and Table 5.12), one may appreciate that they are similar, if not better. In fact, the introduction of a procedure, although approximate, to estimate the tunnel closure prior to lining installation which takes into account the three dimensional nature of the problem, did improve some of the predicted aspects of the performance, particularly aspect numbers 3, 5, 6 and 8, which are those more affected by the 3D nature. On the other hand, the approximations and simplifications introduced in developing the proposed method did not seem to deteriorate the predictions of the remaining aspects.

The time required for someone to use this design procedure for the first time, with the help of a programmable calculator, should not exceed an hour, or less with a microcomputer, provided the input data is fully digested and well defined.

The agreement between calculations and measurements might have been unintentionally biased by the familiarity with this case study that the writer gained earlier through its numerical back analysis. The purpose of the present section was to illustrate the use of the proposed design procedure, more than to validate it. For the latter purpose, additional comparisons between measured and predicted tunnel performances are needed, and are provided in the next section for a representative range of practical situations.

7.5 Validation of the Proposed Method

7.5.1 Verification Against a Tunnel Model Test

Some tunnel model tests conducted in Cambridge in the seventies, present almost ideal conditions to test the validity of the proposed procedure to estimate the ground response around a tunnel. A number of verification calculations were undertaken using these experimental test results. One of them is presented in this section. It refers to an undrained centrifuge test in kaolin, carried out by Mair (1979), in which the ground reaction curve of the tunnel crown was obtained by simultaneous measurement of the applied internal tunnel pressure and the associated displacements at a point immediately above the crown. The measured ground reaction is compared with that calculated through the procedure proposed herein.

7.5.1.1 Model Test Procedures

The experimental result being focussed on, refers to test 2DP (series II), described by Mair (Op.cit.:62). Very briefly, a plane strain model test was conducted at 75g acceleration in the Cambridge Geotechnical Centrifuge (see Schofield, 1980), using Spestone kaolin as the modelling material. The two dimensional apparatus, housing the model test, was completely sealed, so that it allowed the modelling of a saturated soil under undrained conditions. A special grease and grease application technique ensured a plane strain condition to be met. A kaolin slurry with a water content twice the liquid limit was placed in the apparatus, and was fully consolidated under a final vertical stress of 171 kPa. After unloading and removing the entire front of the apparatus conveniently tilted back, silvered perspex balls at 10 mm spacing were pressed into the clay surface, as markers for displacement measurements. Pore pressure transducers were also inserted. The model apparatus was then assembled in the centrifuge and an equilibrium stage achieved at 130 r.p.m, which corresponds to 75 g at a 4 m radius. Water was sprayed to the top surface of the model to ensure saturation and a water level coinciding with this surface. After a few hours, pore pressure equilibrium was noted. The gravity scaling factor and model dimensions were such that, at equilibrium, the vertical effective stresses everywhere in the soil were less then the consolidation pressure applied earlier (171 kPa). The kaolin was therefore overconsolidated, with the degree of overconsolidation increasing towards the top surface.

The centrifuge was then stopped, and a circular opening representing the tunnel with a 60 mm diameter, was cut using a specially designed tool. Test 2DP was prepared in such a way that the cover to diameter ratio was equal to 1.67. A greased rubber bag was then inserted into the tunnel. The centrifuge was restarted and equilibrium conditions restored at 75 g. Concomitant with centrifuge speed build-up, the tunnel internal pressure was steadily increased to maintain it equal to the vertical overburden stress at the tunnel axis. This was ensured by a pressure line connected to the tunnel bag.

Once the design acceleration was reached the centrifuge was kept at constant speed and the tunnel internal pressure immediately reduced in rapid increments, until ground collapse was observed. Simultaneously, photographs of the model were being taken, for each applied internal pressure reduction. The changes in the position of the silvered perspex balls could be monitored through the photographs. Ground strains and displacements could thus be obtained using specially developed techniques and data reduction procedures.

7.5.1.2 Soil Conditions in the Test

If the model is scaled back to gravitational conditions, then the prototype tunnel dimensions are found:

$D = 75 \times 0.06 = 4.5$ m

$H = 1.67\ D = 7.515$ m

The depth of the tunnel axis is equal to 9.675 m.

Through laboratory testing and the measurements taken, Mair (1979) was able to define the profiles of the 'in situ' effective stress, of K_o, OCR and the undrained strength, c_u, with depth. These were shown in Figure 5.17 in Mair (Op.cit.) and are not reproduced here. The overconsolidation ratio was found to decrease from 5 at half diameter above the tunnel, to 2 at half diameter below it, so that an average OCR would be 2.8 at the tunnel axis elevation. The value of K_o was found to vary from about 1.3 to 0.85 between those two points, and, at axis elevation, K_o was found to be approximately equal to 1.0. Since the 'ground water level' was maintained at the top surface, the resulting in situ total stress ratio also equal to one. The undrained strength varied from 22 to 26 kPa between those two points with an average c_u of 24 kPa at the axis. These values corresponded to the undrained strength of the kaolin in plane-strain extension (Mair, 1979:99,103), consolidated to the effective stress acting at those points.

At tunnel axis elevation and assuming full saturation, the soil water content was found to be about 61%, corresponding to a void ratio of 1.59 and a specific gravity of 2.61. The unit weight of this saturated soil was equal to 16 kN/m³.

The initial tangent modulus for the kaolin can be estimated from parameters determined by many research workers who investigated this type of soil at Cambridge. According to critical state concepts, the response of a lightly or overconsolidated saturated kaolin under undrained loading, is close to linear elastic, until the stress path reaches the state boundary surface. With the usual Cambridge notation (see Atkinson and Bransby, 1978, for example), the undrained elastic modulus for this soil at stress levels below yield, is calculated by:

$$E_u = \frac{1+\mu_u}{1+\mu'} E' \qquad [7.15]$$

as the shear modulus of a soil is the same in effective or total stress terms. In this expression, E' and μ' are the Young's modulus and Poisson's ratio in terms of effective stress and μ_u is the undrained Poisson's ratio (0.5). According to Seneviratne (1979:Table 2.1), μ' for this soil is equal to 0.33. The modulus E' can be calculated from the bulk modulus K', through:

$$E' = 3(1-2\mu')K' \qquad [7.16]$$

and K' of an overconsolidated soil can be obtained from the slope k of the swelling curve of a isotropic compression test:

$$K' = \frac{v\ p'}{k} \qquad [7.17]$$

where v is the specific volume (1+e) and p' is the octahedral normal effective stress invariant $((\sigma'_v + 2K_0\sigma'_h)/3)$. The swelling curve of clay in the v x ln(p') representation of the isotropic compression, is approximated by a straight line in the Cam-Clay model. The slope, k, of this line for kaolin was found to vary from 0.04 to 0.06 (Mair, 1979:124). As one is interested in obtaining the initial tangent modulus, the lower k seems to be the most respresentative value.

Combining the equations above one gets:

$$E_u = \frac{1+\mu_u}{1+\mu'}.3.(1-2\mu')\frac{v\ p'}{k} \qquad [7.18]$$

With p' and v calculated at a point half diameter above the tunnel crown, one obtains E_u. Mair (Op.cit.:Figure

5.16a) indicated that the soil water content at this point was equal to 62% and from it, the specific volume can be calculated, and is equal to 2.62. Mair (Op.cit.:Figure 5.17) indicated that p' at this point was about 40 kPa. The undrained Young's modulus is, thus, found to be equal to about 3.0 MPa. This value is the initial tangent modulus that will be used to normalize the displacements at tunnel crown.

A failure ratio, R_f, of about 0.9 is calculated from undrained triaxial test results on this soil, presented by Roscoe and Burland (1968).

7.5.1.3 Predicted and Measured Ground Responses

The generalized solution derived for the frictionless soil model (Section 6.4.2) will be used to estimate the ground reaction curve for the tunnel crown. It should be pointed out that the solution derived for the frictionless soil model does not completely represent the model test condition. In the latter, a uniform pressure was applied inside the tunnel, which was a fraction of the overburden vertical stress at the axis elevation. The derived solution on the other hand, assumes a non-uniform stress applied over the opening contour, which results from the initial gravitational stress field. However, if in both cases, the acting stresses onto the tunnel are normalized to their respective initial values, a comparison between the observed and calculated responses can perhaps be made.

For $K_o=1$ and $\phi=0$, the normalized ground reaction curve is given by equation 6.17:

$$\Sigma = 1 - \frac{U}{A+BU} \qquad [6.17]$$

The coefficient A for the tunnel crown can be obtained from Figure 6.85. For a cover to diameter ratio of 1.67, A is found to be equal to 0.89. The coefficient B, also for the tunnel crown, can be obtained from Figure 6.86. The undrained strength of this soil has to be adjusted, according to equation 6.7, since its failure ratio is less than unity. The equivalent cohesion is thus calculated as $c_{ue} = c_u/R_f \simeq 26.67$ kPa. Therefore, the equivalent undrained strength ratio becomes $c_{ue}/\gamma D=0.37$. In Figure 6.86, B is found to be equal to 1.74. Thus:

$$\Sigma = 1 - \frac{U}{0.89+1.74U} \qquad [7.19]$$

This equation relates the ratio of radial stress at the crown to the normalized crown displacement. In the model test, however, the displacements were not measured exactly at tunnel crown but at some distance above it. From Mair (1979:Figure 5.26), one may suggest that this distance could have been about 20 mm or D/3. The distribution of the normalized subsurface settlements for H/D=1.5 and $c_u/\gamma D=0.3125$, included in Appendix C, shows that at that normalized distance above the crown, the normalized settlement is almost independent of the amount of stress release and is equal to 0.72. For H/D=3, the settlement ratio is about 0.66. Hence for H/D=1.67, it should be 0.713. Thus, the resulting crown settlement (u_c) is equal to 1.402

times the settlement at the displacement marker (u). The normalized crown displacement is:

$$U=\frac{u_c.E_{ti}}{D.\sigma_{ro}}$$

where u_c=1.402u, E_{ti}=3 MPa, D=4.5 m and σ_{ro}=120.24 kPa. Therefore:

$$U\simeq 34.98\,\frac{u}{D} \qquad [7.20]$$

Table 7.5 shows the displacement ratios u/D measured at the point above the crown by Mair (1979:Figure 7.8), for different tunnel internal pressure ratios Σ_T. The radial stress ratio, Σ, at the crown was calculated by equation 7.19, for the normalized crown settlement calculated from equation 7.20. The predicted and observed response are shown in Figure 7.23. A certain degree of uncertainty exists in the calculated response, since the exact position of the point where the displacements were measured is not exactly known. Accordingly, the calculations were repeated, assuming now that this point was located at 10 mm above the tunnel crown. The dimensionless crown displacement is then: $U\simeq 30.81$ u/D.

The ground reaction curve calculated with this assumption is also included in Figure 7.23. One notes that, regardless of the assumption made regarding the position of the marker used for measuring the displacements above the crown, the agreement between predicted and observations is good.

The limiting U beyond which the solution represented by equation 7.19 ceases to be formally valid, can be calculated

$\Sigma_T^{(1)}$	$u/D^{(2)}$	$U^{(3)}$	$\Sigma^{(4)}$
1.000	0	0	1.000
0.800	0.009	0.315	0.781
0.713	0.015	0.525	0.709
0.617	0.036	1.259	0.591
0.513	0.083	2.903	0.511

Notes: (1) Ratio of applied internal pressure in the model test tunnel.

(2) Displacement ratio measured in model test at a point above the crown.

(3) Normalized settlement at the crown.

(4) Predicted radial stress ratio at crown for (3).

Table 7.5 Measured and Calculated Ground Response in the Centrifuge Model Test 2DP by Mair (1979)

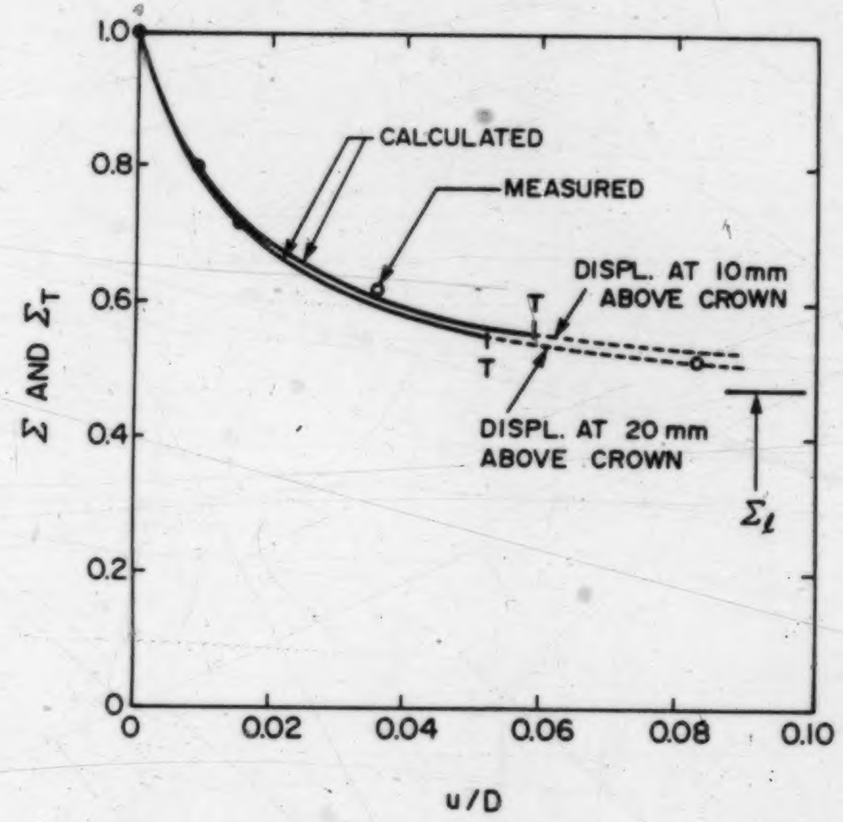

NOTE: TEST 2DP BY MAIR (1979)

Figure 7.23 Measured and Calculated Ground Response at Tunnel Crown for the Centrifuge Model Test

through Figure 6.119. This is found to be equal to 1.812, which corresponds to u/D equal to 0.052 or 0.059, depending on the assumed position of the measuring point (20 mm or 10 mm above the crown respectively). To the right of point T, the dashed curves represent numerical data extrapolation, and nothing ensures that the ground response predicted by the theoretical solution beyond T is correct. Notwithstanding this, the curves bound the experimental observation even beyond their limits.

Figure 7.23 also indicates the ratio of the collapse to initial tunnel pressure, Σ_1. This was calculated through the lower bound solution shown in Figure 6.122. For a strength ratio $c_u/\gamma D=0.33$ (not adjusted) and H/D=1.67, the collapse pressure is estimated as 73.2 kPa, while the initial internal pressure applied was equal to the overburden stress at axis elevation, i.e., 154.8 kPa. Hence, Σ_1 resulted in being 0.473, a value that seems to agree with test and calculated results.

Finally, Figure 7.24 compares the measured and calculated surface settlement profiles at two internal pressures (107 and 92 kPa), corresponding to Σ=0.71 and 0.61. The experimental results were presented by Mair (1979:Figure 5.18) and Mair et.al., (1981:326). The crown displacements were calculated through equation 7.19, and were found to be equal to 0.83×10^{-2} and 4.27×10^{-2} times the opening diameter. The profiles were obtained through the distributions of normalized surface settlements included in

Appendix C, using the procedure given in Section 7.3 and exemplified in Section 7.4. While it provided settlement magnitudes close to those observed, the shape of the settlement troughs furnished by the proposed calculation method did not fully agree with the measurements. This is particularly true for the larger amount of stress release, when Σ gets closer to the collapse stress ratio (0.473). Figure 7.24 shows that the surface distortions are underestimated by the proposed method. This result, however, is not surprising and the reasons behind it were discussed in different occasions in Chapter 5. It was shown there, that this type of result is a common feature in finite element modelling of shallow tunnel behaviour.

7.5.2 Verification Against a Three-Dimensional Finite Element Analysis of a Shallow Tunnel

Katzenbach (1981) performed a fairly refined three dimensional finite element analysis of a shallow tunnel, where the ground was represented by a non-linear elastic stress-strain relationship using the orginal hyperbolic model formulation (Duncan and Chang, 1970). Some results of this study were published by Katzenbach and Breth (1981) and some features of this analysis were reviewed in Section 5.3.3 of this thesis. While in Section 7.5.1, the new design method was verified against an ideal plane strain situation, this finite element analysis may serve to check it against an idealized three-dimensional condition.

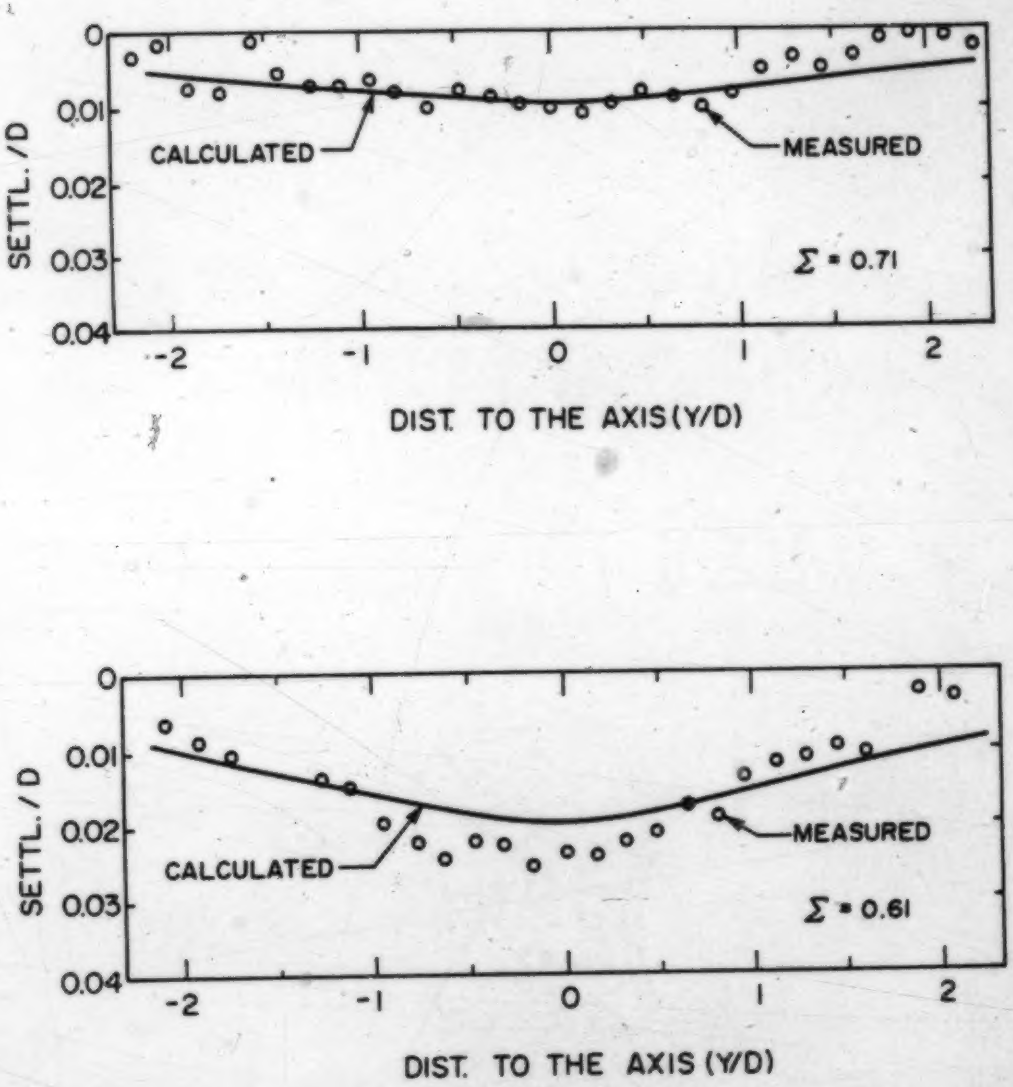

NOTE: TEST 2DP BY MAIR (1979)

Figure 7.24 Measured and Calculated Surface Settlement Profiles for the Centrifuge Model Test at Two Internal Pressures

In the analysis, the ground mass was assumed to be uniform, with the following parameters: $\gamma=18.5$ kN/m³, $K_o=0.8$, $c=20$ kPa, $\phi=20°$, $R_f=0.9$, Janbu's modulus $K=225$, Janbu's exponent $n=0.6$, and $\mu=0.45$. The tunnel was assumed to be circular, with an excavated diameter of 6.7 m and with a soil cover of 11.35 m. The support was represented by cylinder, 0.2 m thick, with elastic parameters given by $E=12.6$ GPa and $\mu=0.2$ (Katzenbach, 1981:39). An incremental construction simulation was performed with a full-face stepwise excavation and delayed support application. Some uncertainty existed in the definition of the distance from the face at which the lining was installed. The reason for it was that, in the numerical simulation, this distance was not kept constant throughout the analysis. When the support ring immediately behind the control section was activated (see LS13 in Katzenbach; Op.cit.:Figure 37b), the distance between its middle point and the vertical tunnel face was 6.25 m. The support ring immediately beyond the control section, on the other hand, was installed at 7.25 m behind the face. For calculation purposes, it will be assumed that lining installation occurred at 1D behind the face.

The proposed calculation method was applied to this problem, using the same parameters and considering the same conditions found in the 3D analyses. At lining activation, the reduced unit weight of the soil was found to be 9.46 kN/m³, corresponding to about 49% stress release. The averaged soil modulus at this point was calculated to be

9.24 MPa, representing a 68% decrease in the ground stiffness, resulting from the delayed application of the support. The lining-ground interaction was carried out neglecting the overall ground heave developing after lining installation, otherwise calculated by equation 7.10. A final crown settlement of 55.3 mm was obtained, which corresponded to 54.4% stress release at the crown in the 2D unlined tunnel solution.

The distributions of final subsurface settlements along the tunnel axis are compared in Figure 7.25. A fairly good agreement between the results of the 3D finite element analysis and of the proposed calculation method is observed. A good agreement was also found for settlements at sections between the face and the point of lining activation. Poorer agreement was noted for sections at or ahead of the face, where the three-dimensional effects, not fully accounted for in the proposed method, are more pronounced.

In Figure 7.26, the profiles of final surface settlements are compared and, once more a reasonable agreement is noted. The zero settlement noted in the 3D finite element analysis at the furthermost point from the tunnel axis, resulted from the imposed zero displacement condition adopted by Katzenbach (Op.cit.) at the lateral boundary of his finite element mesh. The latter was located closer to the tunnel axis, than was the case in the parametric analyses that generated the present solution.

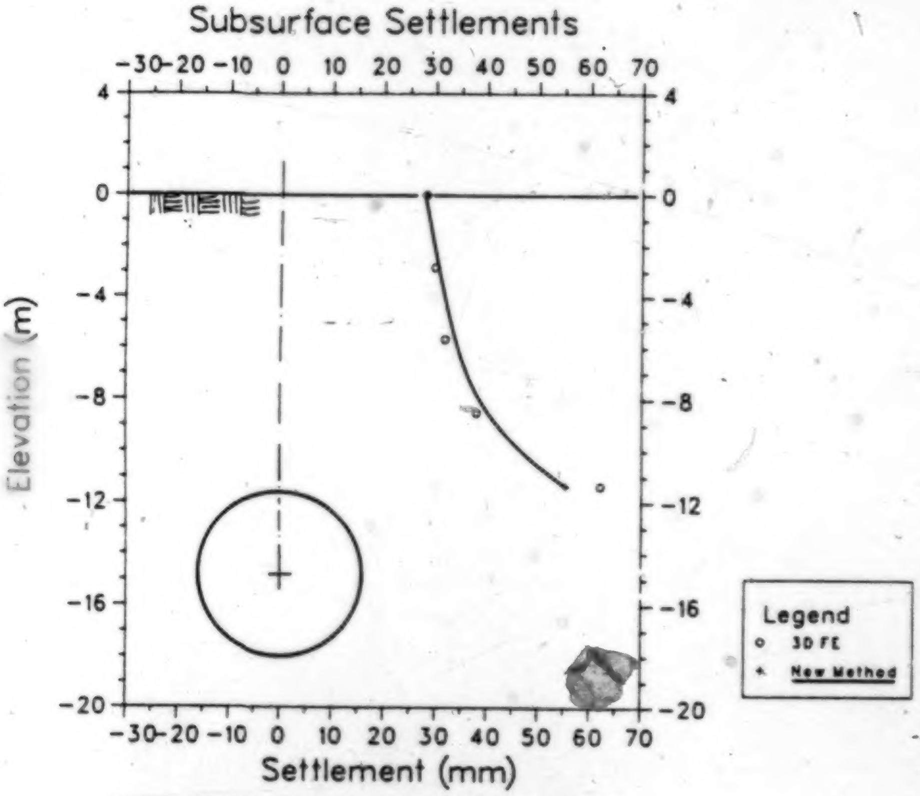

NOTE: 3D FE RESULTS BY KATZENBACH(1981:100)

Figure 7.25 Subsurface Settlement Distributions Calculated in a Three-Dimensional Analysis and by the Proposed Method

Unfortunately, Katzenbach (1981) did not present either the resulting ground loads onto the lining or the opening radial displacements. However, the displacements and ground stresses he provided at nodal points and elements located at some distance away from the tunnel contour, seem to be consistent with those presently calculated at the lining-ground interface.

7.5.3 Verification Against Actual Case Histories

7.5.3.1 Foreword

In order to complete the validation of the proposed design procedure, it was tested against a number of case histories. They included both shielded and non-shielded driven tunnels, mainly through fairly firm ground. The case histories were selected according to the availability of adequate or sufficient published field instrumentation data. The comparison between predicted and observed performances was restricted to cases where good ground control conditions were met. Some of these cases, however, included conditions that deviate from those originally covered by the proposed calculation method. These were included to test the applicability of the new method, for practical situations outside its formal range of validity. The calculations were performed without attempting to best fit, or bracket the observed performance. The input parameters were selected by the writer, on the basis of available information and to best represent the most probable conditions found in each

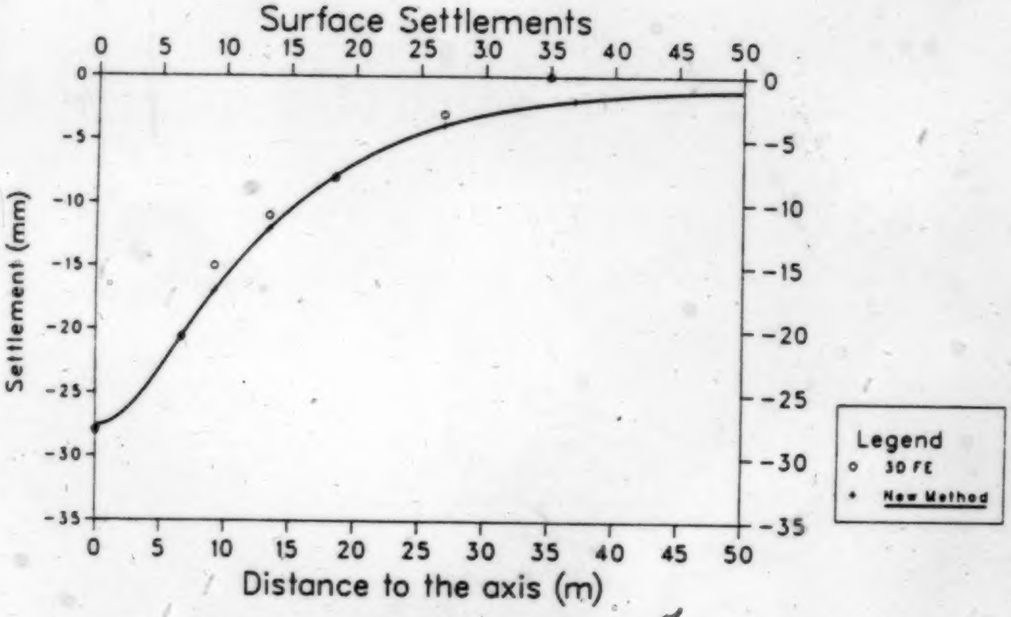

NOTE: 3D FE RESULTS BY KATZENBACH (1981: 103)

Figure 7.26 Profile of Surface Settlements Calculated in a Three-Dimensional Analysis and by the Proposed Method

case. A general appraisal of the results obtained are included in Section 7.5.4.

7.5.3.2 A Large Shielded Tunnel in Marl: The Frankfurt Baulos 23, Domplatz Tunnel

This case history refers to a subway tunnel built in 1970-1971, north of the Frankfurt Cathedral and described by Chambosse (1972). A twin tunnel system (13.2 m centre to centre) was built, with 6.7 m excavated diameter and cover of 11.8 m. The analysis here is concentrated to the south tunnel which was driven first.

The subsurface soil profile included a 9 m thick surficial layer of quaternary sand and gravel, covering a tertiary clayey marl, locally known as Frankfurt clay. The tunnel was entirely driven through this layer, which is intercepted by occasional limestone bands (up to 2 m thick), which are usually water bearing. The ground water level was originally located at about 5 m below the surface, but it was lowered by an extensive dewatering program, initiated one year before excavation started, so that tunnel construction was undertaken through a fully dewatered ground.

The Frankfurt clay is an overconsolidated fissured soil (CH) which was fairly intensively investigated by laboratory testing at the Univeristy of Darmstadt. Katzenbach (1981) summarized the results of these investigations and prepared a table with typical properties for this clay (also reproduced by Heinz, 1984:239). As input data for the analysis of this case history, ground parameters equal to the mean between the maximum and minimum properties provided by Katzenbach (Op.cit:Table 4) were selected and are shown in Table 7.6.

An open face shield 6 m long, with working platforms at the face, was used for the construction, which proceeded at a 5 m/day rate of advance. The lining system included a five segment precast concrete ring, 90 cm wide and 35 cm thick with tongue and groove longitudinal joints, which were assembled under the shield tail protection. The fifth segment was a smaller key segment located at 30° from the tunnel floor. The external diameter of the concrete lining was 6.55 m, so that a nominal void space of 7.5 cm had to be filled, all around the ring, once the shield was advanced. Chambosse (1972) did not provide details of the grout filling operation, but it is believed that it took place typically at every second ring installed.

Tunnel construction was carried out under fairly good ground control conditions, with no localized ground collapses or instabilities having been reported. The presence of fissures in the marl could have been a point of concern regarding the applicability of the proposed design procedure. However, recent theoretical and experimental evidence on other fissured overconsolidated soils (Costa-Filho, 1984) seem to suggest that the effect of discontinuities on the pre-failure initial portion of the stress-strain curve is reduced, provided they are (and

Unit weight	γ	kN/m^3	18.5
In situ stress ratio	K_o	-	0.8$^{(1)}$
Effective cohesion intercept	c'	kPa	37.5
Effective friction angle	ϕ'	(°)	21.5
Failure ratio	R_f	-	0.8
Janbu's modulus	K	-	175
Janbu's exponent	n	-	0.6
Poisson's ratio	μ	-	0.3$^{(2)}$

Notes: (1) Suggested by Katzenbach (1981).
(2) Adopted value.
(3) All other parameters are mean values calculated from extremes provided by Katzenbach (1981: Table 4).

Table 7.6 Typical Properties of Frankfurt Clay used in the Analysis

remain) closed. A fully drained behaviour was assumed, consistent with the assumption that the ground water level was lowered below the tunnel invert. The ground settlements associated with the changes in pore pressure induced by the dewatering had, in fact, almost stabilized before tunnel construction commenced. Accordingly, both the predictions and measurements, to be presented later, refer only to those additional ground movements caused by the tunnel excavation. Although the Frankfurt clay cover at the instrumented section was a little less than half tunnel diameter, the analysis assumed that the soil profile could be approximated by a uniform layer of marl, and the presence of the limestone bands was disregarded.

An adjusted friction angle of about 30° was found and an average in situ modulus of 21.79 MPa was estimated for this soil. It is uncertain when the lining was brought in full contact with the soil, as the amount of overcutting over the shield as well as the details of the grouting operation were sparse. It was, thus, assumed that lining activation took place at the middle point of the second ring leaving the shield tail and that the soil did not close over the shield body. This results in a distance of 7.35 m behind the face or at about 1.1D. The calculated amount of stress release at this section resulted in being equal to 56% and the current average tangent modulus at this point was estimated as 9.61 MPa. The two-dimensional ground stability verification for this condition furnished a factor of safety of 1.66, indicating that the opening was stable and the ground far from collapse. The lining-ground interaction analysis was then conducted. No allowance was made for the possible increase in lining flexibility, resulting from the presence of joints. In fact, Muir Wood's (1975) correction for the moment of inertia of a jointed lining is only applicable when more than four equal segments are included. In this case, the fifth segment is the key element, which was much smaller than the others. A Young's modulus of 29.4 GPa was assumed for the lining, as this was the value adopted by Chambosse (1972:77) on the lining measurements data reduction. This modulus is likely to be slightly high, knowing that the longitudinal joints normally increase the compressibility ratio of the support. This is particularly true, for instance, when bitumen strips or neoprene sheets are used as seals, which however, was not the case herein. Had these materials been used, the lining compressibility would have been entirely controlled by their stiffnesses. The flexibility and compressibility ratios defined in Section 7.2.1 were calculated as 0.5 and 468, respectively. The ground heave after the support was activated was assumed to be zero. Only one iteration was needed to define the equilibrium conditions, which reflects the very stiff nature of the lining.

The final crown settlement was estimated as about 59 mm (U=0.657) and the associated amount of stress release at the crown was calculated as 56.7%. The distributions of final subsurface and surface settlements were immediately obtained and are shown in Figures 7.27 and 7.28. A maximum surface settlement of about 30 mm was calculated. In these figures, field measurements are included for comparison. The settlements due to dewatering prior to the drivage were subtracted from the measurements (Chambosse, Op.cit.:Figure 74). One notes that the predicted settlements agree quite well with the measurements.

The predicted distributions of thrust forces (N_ϕ) and bending moments (M_ϕ) in the three upper segments are shown in Figure 7.29. The notation and sign convention used is that given in Section 7.2.1. The position of the longitudinal joints are indicated by the letter 'J', and the crown and springline by 'C' and 'S', respectively. Unfortunately no load measurements were undertaken in the South tunnel lining. Lining instrumentation was introduced 9 months later in the second driven North tunnel. Thrust forces and bending moments were calculated through strain measurements in seven niches cast in the inner sides of the three upper lining segments. Each niche housed six pairs of steel reference pins, fixed against the niche's transverse wall, so that the strain distributions across the half thickness of the lining could be obtained using a DEMEC type mechanical strain gauge. A linearized stress distribution across the lining thickness was calculated, assuming a Young's modulus of 29.4 MPa, and from it, the thrust forces and bending moments were obtained.

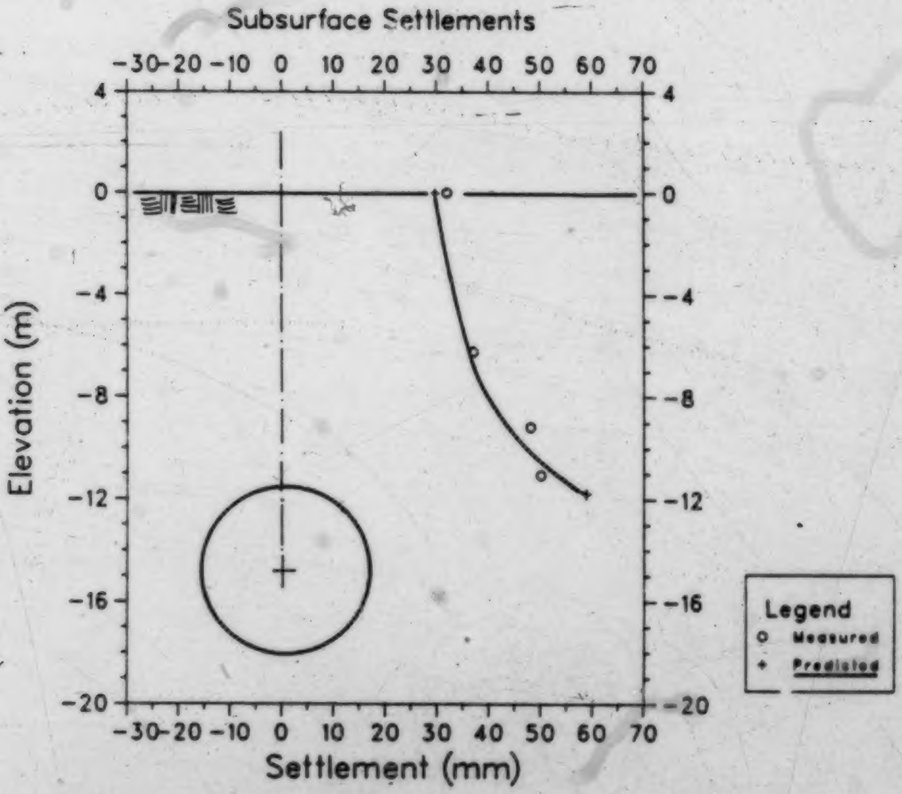

NOTES :

1. SETTLEMENTS CAUSED BY THE FIRST TUNNEL MEASURED AT EXTENSOMETER T4, FROM CHAMBOSSE (1972, FIGURE 19)
2. THE SETTLEMENTS DUE TO GWL LOWERING WERE SUBTRACTED FROM MEASUREMENTS.

Figure 7.27 Measured and Calculated Final Subsurface Settlements over the South Tunnel in the Frankfurt Baulos 23 (Domplatz) Subway

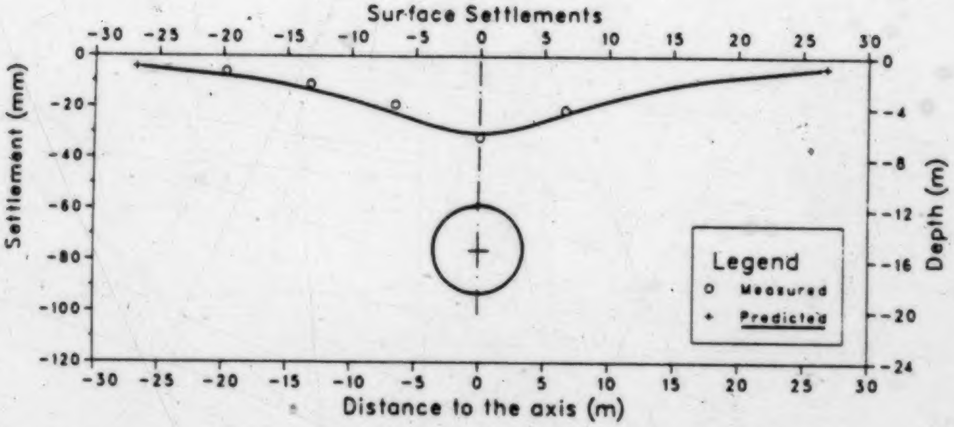

NOTES:

1. MEASUREMENTS AT DOMSTRASSE INSTRUMENTED SECTION AFTER FIRST TUNNEL CONSTRUCTION, FROM CHAMBOSSE (1972, FIGURE 19)
2. THE SETTLEMENTS DUE TO GWL LOWERING WERE SUBTRACTED FROM MEASUREMENTS.

Figure 7.28 Measured and Calculated Final Surface Settlements over the South Tunnel in the Frankfurt Baulos 23 (Domplatz) Subway

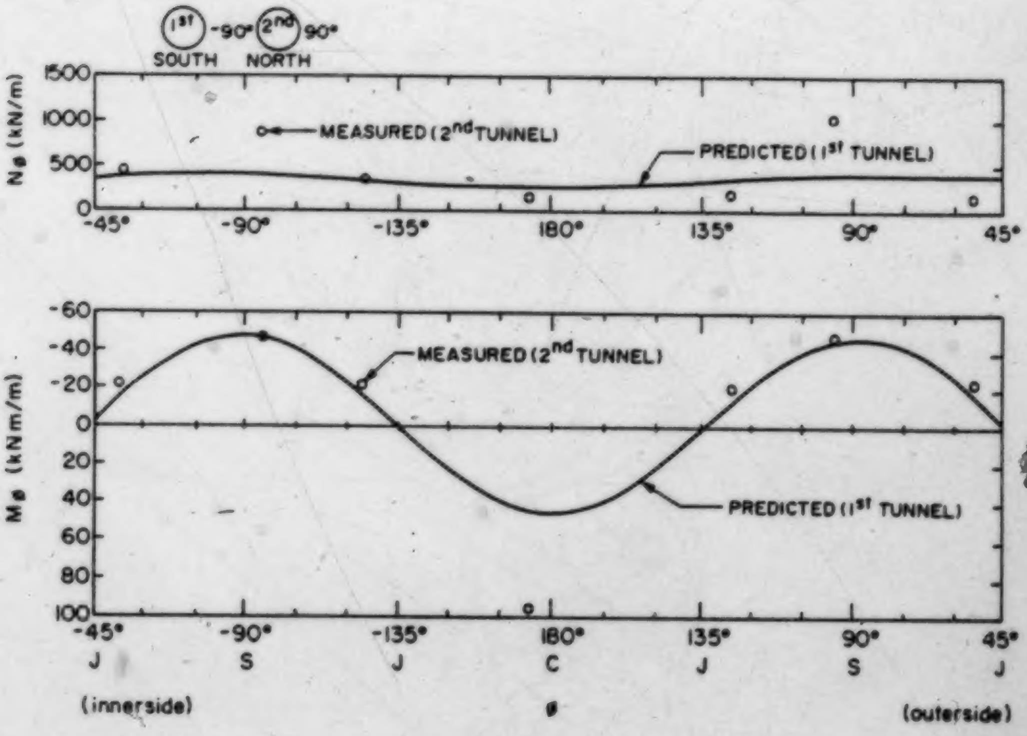

Figure 7.29 Predicted Lining Loads in the South Tunnel (1st driven) Compared to Measurements in the North Tunnel (2nd driven): Frankfurt Baulos 23 (Domplatz) Subway Tunnels

The width of the central soil pillar separating the two tunnels was about one tunnel diameter. The lining measurements taken in the second tunnel were very probably affected by the first tunnel already built. Notwithstanding this, the measurements recorded in the second, are presented together with the lining loads predicted for the first in Figure 7.29. Although an immediate comparison is not formally valid, one notes that the results are not entirely discordant. The differences between predicted and measured loads could be partly attributed to the changes in ground stiffness and in ground stresses induced by the first tunnel construction. The transverse arching process triggered by the first drivage may partly explain the higher thrust forces measured at the springline in the second tunnel, as well as the higher bending moment at the crown. This interpretation is supported, in qualitative terms, by the numerical results obtained by Ranken (1978:219, case C) who studied the lining responses in two parallel tunnels consecutively driven, assuming a linear elastic response for both soil and lining.

The overall agreement between predicted and observed performances in this case history was quite satisfactory, despite no attempt having been made to best fit the observations. In a real design situation, it is believed that the observed performance could have been totally bracketed, had the variabilities of the ground properties and construction operations been taken into consideration.

7.5.3.3 Twin NATM Tunnels in Marl: The Frankfurt Baulos 25, Romerberg Tunnel

This case history refers to a twin subway tunnel built in 1970, at the Romerberg, Frankfurt, that was described by Chambosse (1972), Edeling and Schulz (1972) and Schulz and Edeling (1973). More recently, this case history was reviewed by Heinz (1984:236). It was in this project that the so called New Austrian Tunnelling Method was first used for the construction of an urban tunnel in soil. The two parallel tunnels were advanced simultaneously at a distance of 12.7 m from centre to centre. Each tunnel had a circular profile with a 6.48 m excavated diameter. The soil cover at the instrumented sections was 11.5 m. Although the proposed design procedure was developed for a single and isolated tunnel, it seems interesting to assess the influence of a parallel and simultaneous tunnel construction.

The ground conditions were similar to that found at the Frankfurt Domplatz Tunnel (Section 7.5.3.2), built nearby. The tunnels were entirely driven in the Frankfurt clay marl, which is overlain here by a 4 m thick layer of sand and gravel, which in turn is covered by a 2.5 m thick fill. The marl is also interbedded with limestone bands although thinner than at Domplatz (less than 1 m thick). The clay marl cover at the instrumented section was about 5 m thick. The ground water level, originally located at 4 m depth, was also lowered through deep wells to elevations below the tunnel invert. Dewatering was initiated six months before tunnel construction started (Chambosse, 1972:48). The ground settlements associated with dewatering had stabilized before construction commenced, so that it was possible to separate these movements from those resulting from the tunnel construction proper. The ground mass, as it appeared during tunnel advance was free of water (Chambosse, Op.cit.:6), so that a drained behaviour could be assumed in the analysis. The relevant ground properties for the Frankfurt clay were already presented in Section 7.5.3.2. The same parameters used for the Domplatz Tunnel will be considered herein.

The simultaneous tunnel construction was carried out with sequential excavation of the face in three stages: heading, bench and invert. The shotcrete lining was also applied in stages, immediately after the ground was exposed. An average rate of advance of 1.2 m/day was achieved. The excavation round length was about 1.2 m, which corresponded to the spacing of light segmented steel ribs, with a channel profile (TH 48, 16.5 kg/m). A steel mesh (Q188) was also incorporated into the support system. The total shotcrete thickness varied between 15 and 18 cm. When the tunnels passed the instrumented section II, the support ring closure at the floor took place typically at 5.7 m behind the face (Edeling and Schulz, 1972:Figure 11). The steel ribs were fixed to the ground by 3 to 4 m long anchors which were found later to have contributed nothing to the opening support (Schulz and Edeling, 1973:251). Tunnel construction was undertaken under good ground control conditions and no ground instabilities were reported.

The analysis was conducted neglecting the presence of the second tunnel, and assuming a uniform layer of clay marl. An adjusted friction angle of about 30° was found and adopted for the cohesionless soil model. The average in situ tangent modulus was estimated as 21.49 MPa, with the parameters shown in Table 7.6. The lining activation was assumed to have taken place when the shotcrete lining ring was closed at the floor, 5.7 m behind the face. The calculated amount of stress release at this point was 55.5% and the current average tangent ground modulus at this section was estimated as 9.63 MPa. The ground stability verification yielded a factor of safety of 1.67, which confirmed that the opening was stable.

The lining-ground interaction analysis was carried out neglecting the action of the light steel ribs, but considering a nominally increased shotcrete thickness of 20 cm. A lining modulus of 10 GPa was considered as well as a Poisson's ratio of 0.2. The flexibility and compressibility ratios were estimated as 0.03 and 90, respectively, which are typical for a shotcrete lining in a soft to medium clay (see Table 7.1). A single iteration was required to define the equilibrium condition. The ground heave after the support was activated was neglected.

The final crown settlement was estimated as 59.1 mm (U=0.694) and the associated amount of stress release at the crown was calculated as 57.8%. The calculated distributions of final subsurface and surface settlements are presented in Figures 7.30 and 7.31. Included in these figures are the measured displacements that were caused by the simultaneous construction of the two parallel tunnels. One notes in Figures 7.30 that, while the displacements of points closer to the tunnel are well approximated by the proposed procedure, those at the surface are substantially underestimated. This result was indeed expected, as the prediction did not take into acount the second tunnel construction. Ranken (1978:197) studied the development of surface settlements over twin tunnels built simultaneously, through linear elastic finite element analyses. He showed that the interaction between two shallow tunnels (H/D=1) is small provided the centre to centre distance is greater than 2 diameters. In other words, for this condition, the settlement profile obtained by superimposing two single tunnel settlement distributions is approximately equal to the actual profile from the two parallel tunnels simultaneously built. In the present case history, the tunnels were built at slightly more than two diameters apart. However, unlike the conditions focused on by Ranken (Op.cit.), the tunnels were deeper and the soil response was definitely non-linear. Nevertheless, if the superposition of surface settlements is accepted, then the profile found is that shown in Figure 7.32. One observes now, that a better agreement between measured and predicted responses is attained, at least with regard to the maximum surface

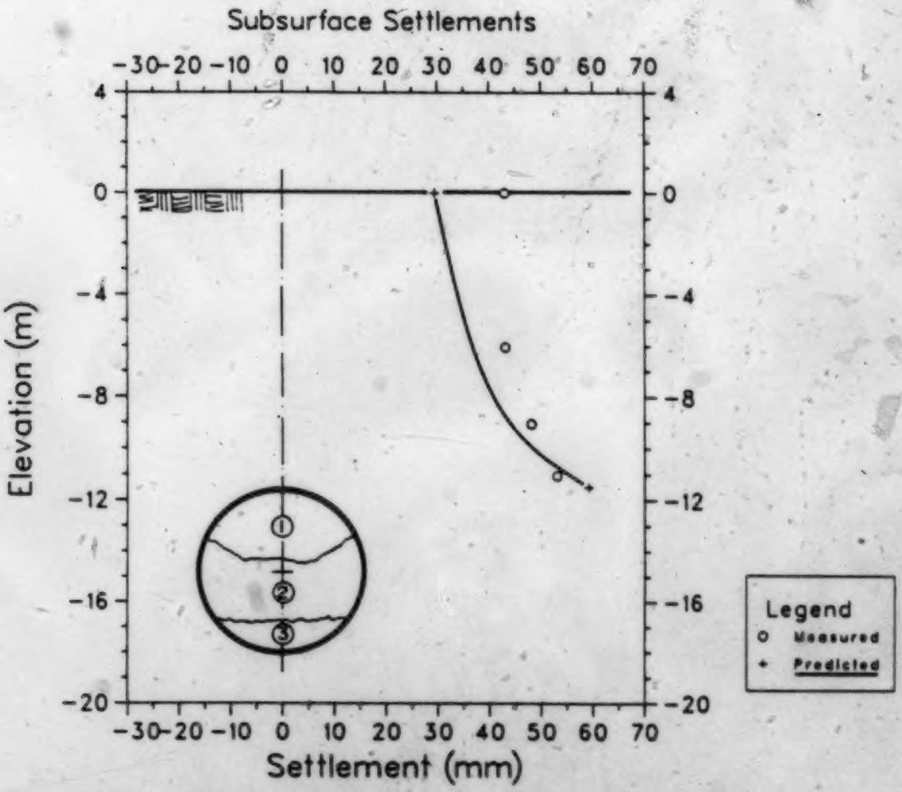

NOTES:

1. MEASUREMENTS AT EXTENSOMETER D2 OVER THE NORTH TUNNEL, AT THE INSTRUMENTED SECTION II, FROM CHAMBOSSE (1972:52)
2. THE SETTLEMENTS DUE TO GWL LOWERING WERE SUBTRACTED FROM MEASUREMENTS.
3. MEASURED SETTLEMENTS CAUSED BY SIMULTANEOUS CONSTRUCTION OF THE TWO PARALLEL TUNNELS.

Figure 7.30 Measured and Calculated Subsurface Settlements over the Frankfurt Baulos 25 (Romerberg) Subway

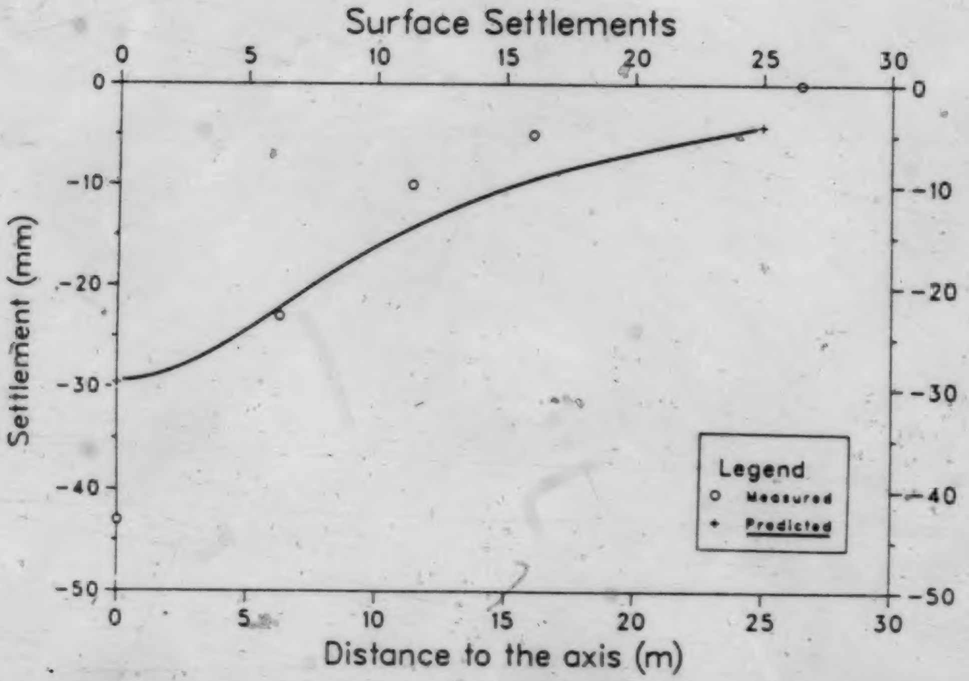

NOTES
1. CALCULATED SETTLEMENTS FOR A SINGLE TUNNEL CONSTRUCTION.
2. MEASUREMENTS AT THE INSTRUMENTED SECTION II, OVER THE SOUTH TUNNEL, FROM CHAMBOSSE (1972 ·52)
3. THE SETTLEMENTS DUE TO GWL LOWERING WERE SUBTRACTED FROM MEASUREMENTS.
4. MEASURED SETTLEMENTS CAUSED BY SIMULTANEOUS CONSTRUCTION OF THE TWO PARALLEL TUNNELS.

Figure 7.31 Measured and Calculated Final Surface Settlements at the Frankfurt Baulos 25 (Romerberg) Subway Tunnel

settlements. The maximum surface distortion is however, underestimated by this approximate calculation procedure.

Figure 7.33 presents the calculated and measured radial stresses acting on the upper arch of the shotcrete lining, after equilibrium was achieved. The stresses were measured by Glotzl contact pressure cells (15 x 25 cm). Note that, while the prediction was made for a single tunnel, the measured stresses include the effect of the twin tunnels simultaneous construction. Note, moreover, that the measurements were taken at both tunnels, and for easier comparison, they were plotted together by making the relative position of the measuring points with respect to the central soil pillar to coincide. Accordingly, the measurements at the springlines (S) facing the central pillar (innerside) are plotted together at the +90° position (measured from the floor), whereas those at the outer abutment springlines (outer side) are plotted at the -90° position. The predicted radial stresses seem to be closer to the average stress measured, except at the springlines, where the measured stresses are underestimated, notably at the inner springline, on the pillar side. If it is admitted that the readings are correct, one could speculate that the interaction between the two tunnels forced them to squat more and to mobilize higher radial stress at the springline elevation. This interpretation, however, is not clearly supported by Ranken's (1978:194) numerical results, which suggested that shallow twin tunnels built simultaneously, at

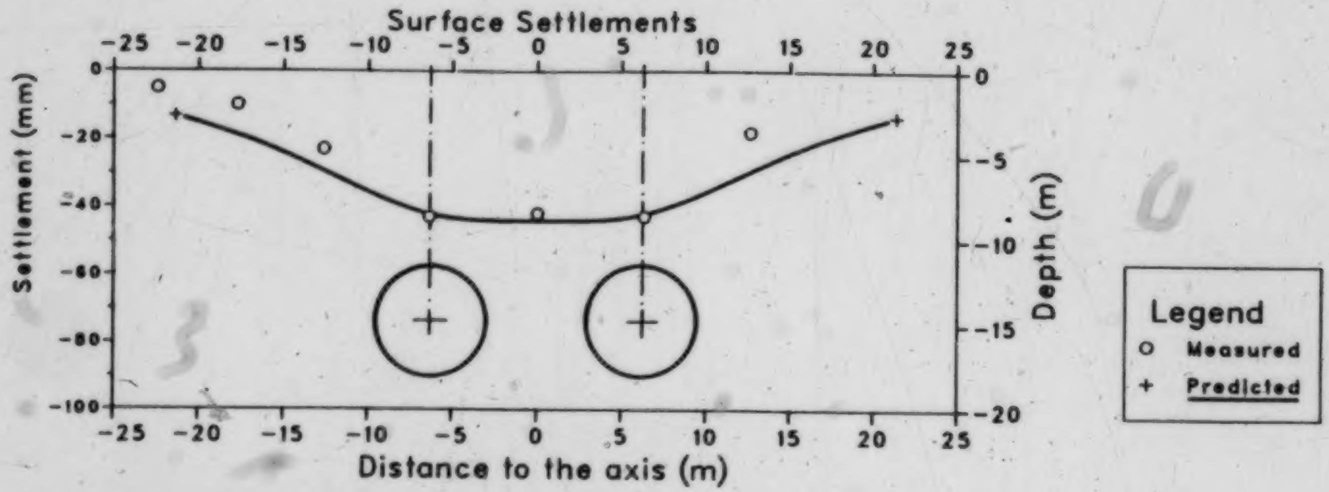

NOTES:

1. CALCULATED SETTLEMENTS OBTAINED BY SUPERPOSITION OF SINGLE TUNNEL PROFILE.
2. MEASUREMENTS AT THE INSTRUMENTED SECTION II, FROM CHAMBOSSE (1972:52)
3. MEASURED SETTLEMENTS CAUSED BY SIMULTANEOUS CONSTRUCTION OF THE TWO PARALLEL TUNNELS, WITH MOVEMENTS DUE TO GWL LOWERING PRIOR TO EXCAVATION DISCOUNTED.

Figure 7.32 Measured and Calculated Final Surface Settlements over Twin Tunnels at the Frankfurt Baulos 25 (Romerberg) Subway

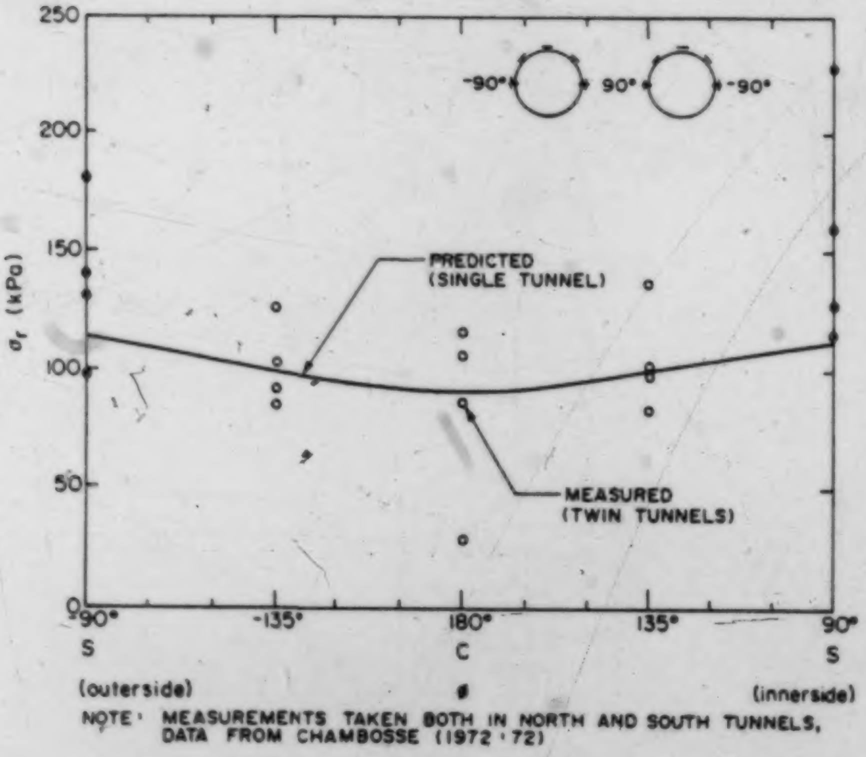

Figure 7.33 Predicted Lining Radial Stresses for Single Tunnel and Measured Stresses in Twin Tunnels at the Frankfurt Baulos 25 (Romerberg) Subway

one diameter apart (centre to centre), exhibit lining loads that do not differ greatly from those for a single tunnel. However, the generality of Ranken's suggestion is debatable, since he assumed linear elastic responses for both soil and liner, and more importantly, he assumed that the linings in both tunnels were installed before soil excavation (no stress relaxation before support application).

A special device, designed by Interfels, installed from the surface, allowed the measurement of horizontal displacements in the ground at the springline elevation, 0.5 m away from the tunnel contour. A maximum horizontal movement towards the opening of about 19.5 mm was measured at Section II, in the outer abutment of the tunnel, just prior to the closure of the shotcrete ring at the invert (Chambosse, 1972:Figure 75). This value is compared with the 31.9 mm of inward radial displacement calculated at the springline of the single tunnel contour at lining installation.

Horizontal diameter changes were also measured in three shotcrete rings in the North Tunnel (Edeling and Schulz, 1972:357). An increase of the horizontal diameter of 12 to 13 mm after completion of the invert was recorded (10.5 to 13 mm according to Chambosse, 1972:66). The lining-ground interaction analysis indicated that this increase amounted to 11.1 mm, which compares favourably with the measurements.

The comparison between calculated and observed performances in this case history should be carefully interpreted, since the proposed procedure does not account for the interaction of two parallel tunnels. However, one can observe that the resulting calculations are consistent with the observations and that the noted differences could be attributed to the interaction between the tunnels.

7.5.3.4 A Small Shielded Tunnel in Till: The Mississauga (Ontario) Tunnel

This case history refers to a small sewer tunnel, built in 1972 in Mississauga, about 29 km from central Toronto (Ontario), and described by Seychuk (1977) and by DeLory et.al. (1979). The tunnel was bored with a 4.27 m diameter, under a soil cover of 11.5 m at the installed instrumented section.

The soil profile included a 3.5 m superficial layer of recent alluvial sands and gravel, covering a very dense 12.5 m thick, sand-clay till layer. Underneath it, there was another till layer, of 4 m thickness, comprising a dense silty sand. The shale bedrock was found at about 20 m below the surface. The ground water level was about 6 m below the surface before construction started.

According to DeLory et.al. (1979), the tunnel was driven entirely through the very dense upper sand-clay till (SPT in excess of 100), which was found to be a relatively uniform soil, with 20% clay, 36% silt and 44% sand and gravel. The till liquid limit was about 22%, the plastic limit 15% and the natural water content 8%. Its unit weight was 24 kN/m^3 and the in situ effective stress ratio was estimated as 0.9 to 1.0. The effective friction angle was measured in the laboratory and was found to be 35°. The effective cohesion intercept was not given by those authors, but data from Nipawin and Edmonton Till (Wittebolle, 1983), suggest that it could be greater than 30 kPa. These data also indicated that the failure ratio from drained triaxial tests for this soil may vary from 0.7 to 1.0.

Menard pressuremeter tests carried out in boreholes adjacent to the tunnel gave values of the in situ modulus from 55 to 160 MPa. Assuming that the tests were conducted rapidly and that some disturbance might have been caused by boring, a value of 140 MPa can be taken as typical for the undrained tangent in situ modulus of this till at the tunnel axis elevation. If a drained Poisson's ratio of 0.3 is assumed for the soil, then a drained modulus of about 120 MPa is calculated, provided that (at small strains) the soil behaviour is approximately linear elastic. No details of those tests or of the variation of the pressuremeter moduli with depth are given. It was then assumed that the drained soil modulus varied linearly with the square root of the vertical in situ effective stress (See Lambe and Whitman, 1969:159). In situ drained moduli of 105 and 134 MPa, were therefore estimated at a half diameter above and below the tunnel respectively.

Piezometers installed from the surface above and near the tunnel, showed that there was a lowering of the water pressure near the tunnel after construction. The piezometric head at the axis elevation, at a point 2.1 m away from the springline decreased from 7 m to 1.4 m or less (DeLory et.al. 1979:193), after the tunnel was built. The original water pressures around the tunnel were not re-established after tunnel completion, which seems to have acted as a drain. If an option had to be made between an undrained and a drained analysis, one could suggest that the observed performance might have been closer to the latter condition rather than to the former. Accordingly, the selected ground parameters, defined in terms of effective stresses, that were considered for the analysis of this case history are those given in Table 7.7.

An open face shield, 5.18 m long, was used for construction. Excavation was by an Alpine miner road header, with the face being undercut some 0.6 to 1.5 m ahead of the shield hood (Seychuck, 1977). The cut profile was about 75 to 100 mm less than the shield outside diameter. The shield shaved off the remaining soil annulus as it was advanced. The rate of advance was about 5 m/day when passing the instrumented section. The primary lining system consisted of steel set rings (H section, 100 x 100 mm) in four segments and concrete planks (75 x 200 x 1200 mm), assembled inside the shield in 1.22 m lengths. As the primary lining emerged from the tail, it rested on the tunnel floor and a space of about 50mm between planks and ground was left at the sides and of about 100 mm at the crown. According to DeLory et.al. (1979:192), this void was filled with pea gravel, and was

Unit weight		γ	kN/m^3	24
In situ stress ratio		K_o	-	1.0 (1)
Effective cohesion intercept		c'	kPa	30 (1)
Effective friction angle		ϕ'	(°)	35°
Failure ratio		R_f	-	0.8 (1)
E_{t_i} (drained)	1/2 D above crown		MPa	105 (2)
	at springline		MPa	120 (2)
	1/2 D below floor		MPa	134 (2)
Poisson's ratio (drained)		μ	-	0.3 (1)

Notes: (1) Assumed value.

(2) Derived from pressuremeter tests.

Table 7.7 Selected Ground Parameters for Drained Analysis of Tunnel in Dense Sand-Clay Till

later grouted with cement. While the filling and grouting operations took place, for most of the tunnel length, at distances greater than 12 m behind the face, at the instrumented section it is estimated that these operations happened after the face had advanced about 7.5 m past the section. It is unlikely that the grout completely filled the gravel voids, particularly at the crown. An excessively robust unreinforced concrete liner, 460 mm thick, was installed about 3 months after passing the instrumented section.

Thanks to the good ground conditions rather than to the quality of the construction, no instability process was observed. The ground response was good, despite some poor construction procedures, such as face undercutting, the use of a long shield or the delay in filling and grouting the void behind the liner, to name a few. The ground drainage caused by the tunnel construction, induced changes in pore pressures which, in itself, may have induced ground displacements. The magnitudes of these were likely to be small, as the till is very dense, has a low void ratio (about 0.22) and a high bulk modulus. The soil volume changes due to consolidation induced by the dewatering were, thus, probably small. Probably the volumetric strains caused by the shear and mean normal stress changes induced by the tunnel excavation were also small. A factor of safety in excess of 1.7 was calculated in the two dimensional ground stability verification, for the instant the support was activated. From what was shown in Section 2.3.4.4, for this safety level (load factor smaller than 0.6), the volumetric expansion in this soil was probably small.

Since the proposed design procedure does not take into account the consequences of pore water pressure changes, it was conveniently assumed that the ground was entirely dewatered, so that those pressures were equal to zero. However, the in situ ground moduli considered, (Table 7.7) are drained moduli corresponding to effective stress levels existing in situ, prior to dewatering. In other words, the possible gain in stiffness, which results from the increase in the effective stress level that would follow the ground water drawdown (either the hypothetical or the actual one) was neglected.

Having in mind the above discussion and considering the fairly uniform nature of the ground, it was felt that the proposed design procedure could be applied to this case history, and a comparison between the predicted and observed performances could be made. However, as noted above, it should be remembered that the latter may reflect not only the response resulting from the tunnel excavation, but also that resulting from changes in the pore water pressures.

An adjusted friction angle of about 40° was calculated, on account of the cohesive strength component and of the non-unity failure ratio. A certain degree of uncertainty existed regarding when the lining was brought in full contact with the soil. The exact grouting procedures were not clear, as well as the amount of overcutting over the shield. It was, thus, assumed that lining activation took place 7.5 m behind the face, as mentioned earlier. A smaller distance would have to be considered if the shield had been advanced without an overcutter head. But this is unlikely, since high thrust forces are required to propel the shield in such a strong material, without some overcutting rim. The amount of stress release at lining activation was about 57% and a reduced average tangent modulus of 70.13 MPa was obtained (41% less than the original value).

Although an attempt was made to jack the concrete planks together circumferentially (DeLory et.al., 1979:195) it is very unlikely that they all came in full contact. If a minor gap of 0.5 mm had been left on average between each of the 64 or so planks used, a uniform convergence of more than 10 mm in the lining diameter would be required to put all the planks in full contact with each other. This convergence is an order of magnitude higher than the expected lining convergence. Therefore, it is reasonable to accept that, besides not being able to carry any bending in the plane transverse to the tunnel, the concrete plank lagging was very compressible under uniform transverse loading, and thus unable to carry tangential thrust. If a fully compressible contact between the planks is conceded, then they operate simply by transferring the ground loads in the longitudinal direction, to their supporting ribs. Accordingly, the relative stiffness of the lining would be that given by the steel ribs at 1.22 m spacing only. Thus, a lining with a moment of inertia of 3.615 x 10^{-6} m^4/m and a cross sectional area of 2.016 x 10^{-3} m^2/m was considered for the lining-ground interaction, with elastic properties of steel (E_s=200 GPa and μ=0.2). The interaction analysis was conducted with the reduced unit weight of the soil and the reduced ground modulus mentioned earlier. Two iterations, in which the ground heave after support activation was neglected, were needed to define the equilibrium condition. An average ground modulus of 60.49 MPa was found for this condition, and the flexibility ratio (β) and compressibility (α) ratios resulted in values of to 1.92x 10^{-3} and 4.44 respectively. As can be observed in Table 7.1, these values are typical for this type of support in dense sand or stiff clay. The ground modulus at equilibrium is roughly half of the in situ modulus value.

The final crown settlement was estimated as about 7.3 mm (U=0.648) and the associated amount of stress release at crown was calculated as 60%. The distributions of the final subsurface and surface settlements were then obtained and are presented in Figures 7.34 and 7.35, together with the results of the field measurement program given by DeLory et.al. (1979:194). Seychuk (1977) made reference to problems regarding survey accuracy and thermal effects affecting the readings. Notwithstanding this, the predicted values broadly conform to the measurements, but it is clear that the maximum surface distortion is underpredicted by the

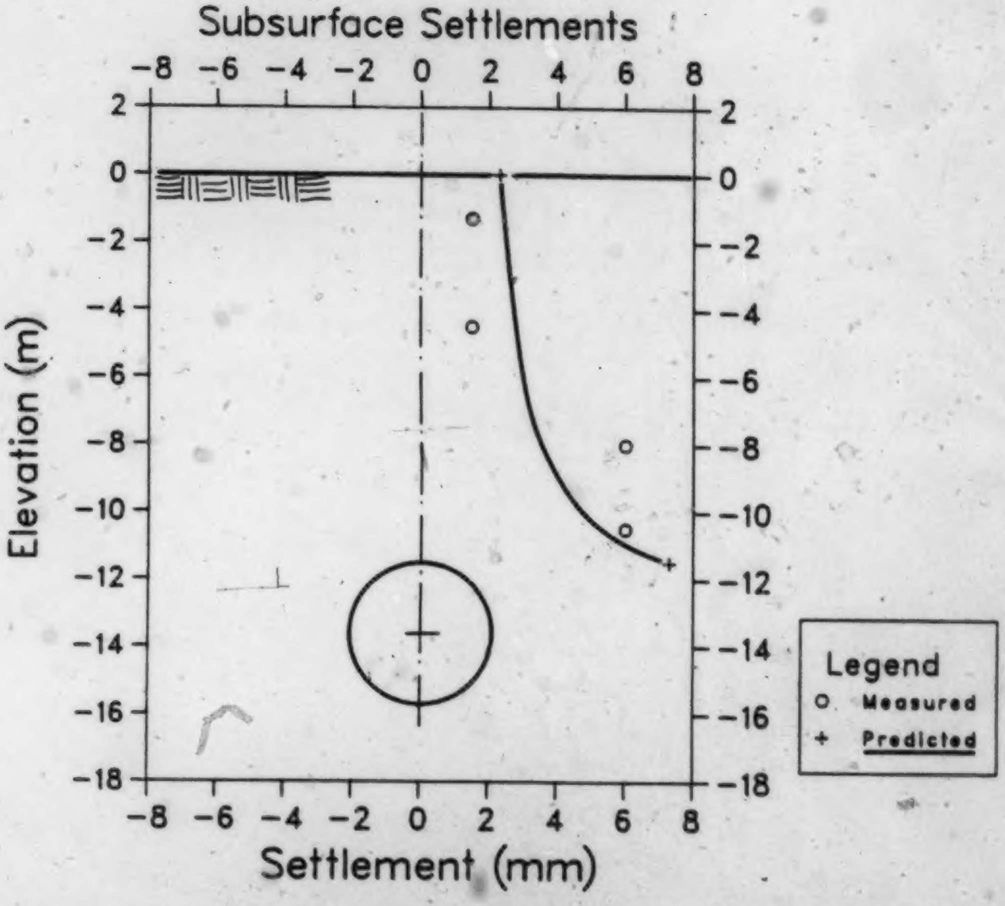

NOTE: MEASUREMENTS RECORDED AT POSITION C (TUNNEL AXIS) BY DELORY ET AL (1979: 194)

Figure 7.34 Measured and Calculated Final Subsurface Settlements over the Mississauga Sewer Tunnel

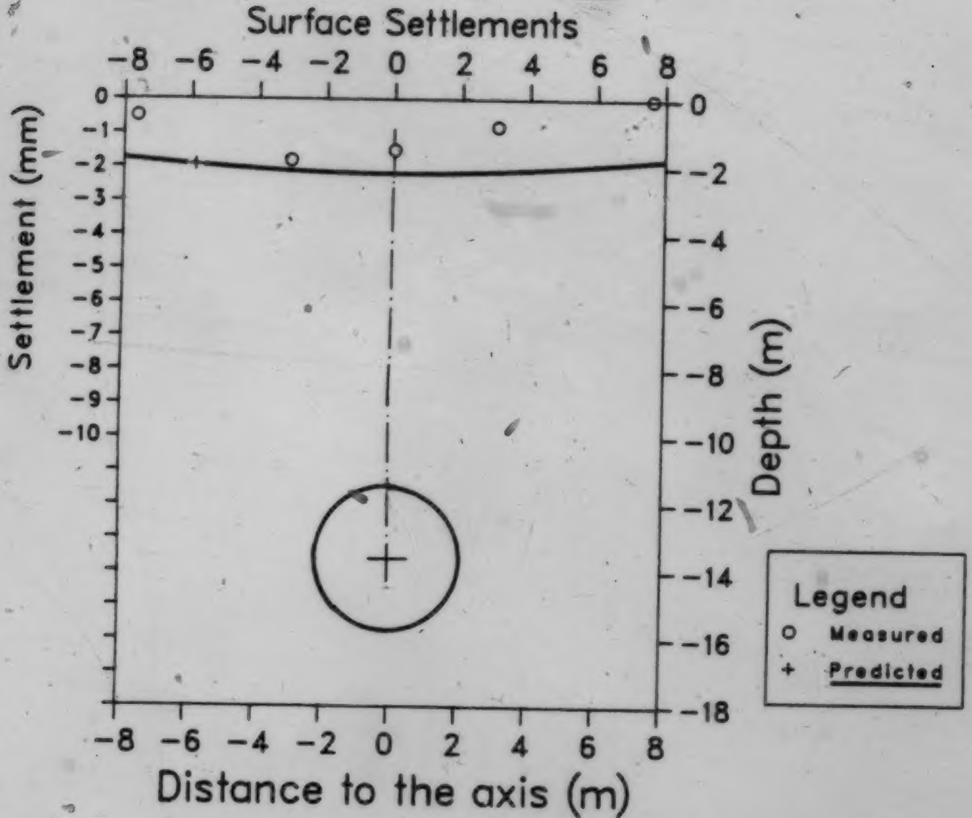

NOTE: MEASUREMENTS PRESENTED BY DELORY ET AL (1979 : 194)

Figure 7.35 Measured and Calculated Final Surface Settlements over the Mississauga Sewer Tunnel

calculations.

The predicted distribution of radial stress acting upon the lining is shown in Figure 7.36. The measured radial stresses, also shown in this figure, were recorded by 250 mm diameter flat contact cell pressures, installed between the primary lining and the ground. The cells were placed in the void behind the lining and were packed on each face with a soil-bentonite-cement mixture, to fill the space between the soil and support. The mixture was designed to have mechanical properties similar to the surrounding till. Twelve cells were used but one at springline (270°) ceased to operate some time after installation. Four of them installed in the upper arch (three at the crown and one at 45° off) seem to have had faulty installation. As explained by DeLory et.al. (1979:195), "the cells near the crown acted as hard spots taking more than their share of the load". In fact, stresses more than 100% in excess of the overburden stress were recorded in these four cells. Their results are, thus, unreliable and therefore not included in Figure 7.36. The measurements indicated correspond to final long term readings, one year after installation, although they do not differ to any substantial degree, from the short term readings taken a few weeks after the cells were installed (DeLory et.al., Op.cit.:195).

A substantial scatter in the cell pressure measurements is noted, possibly reflecting the effects of the installation procedure adopted. However, if an average

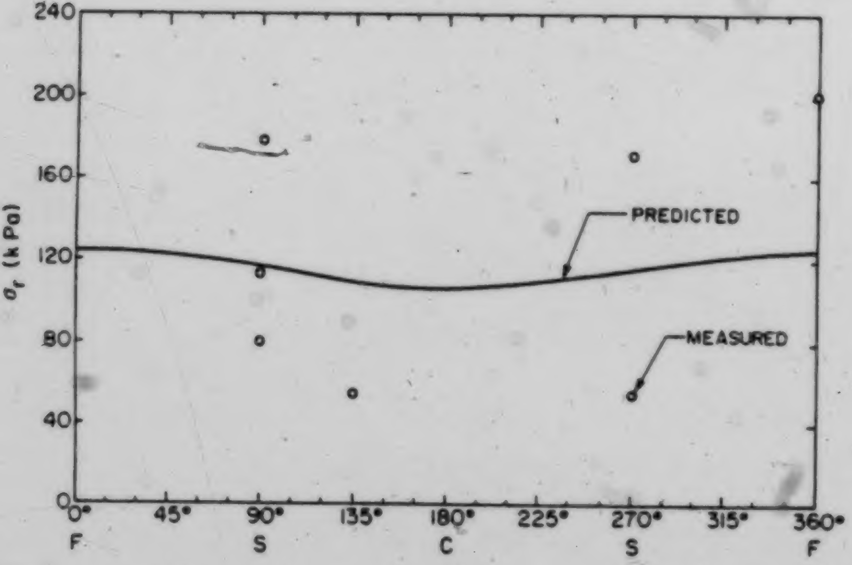

NOTE: LONG TERM MEASUREMENTS BY DE LORY ET AL (1979:196). DATA FROM FIVE FAULTY CELLS WERE EXCLUDED.

Figure 7.36 Measured and Predicted Radial Stress Distributions on the Lining of the Mississauga Sewer Tunnel

distribution of radial stresses were to be defined, it would not lie far from the predicted distribution.

A slope indicator was installed at 0.91 m away from the tunnel springline. DeLory et.al., (Op.cit.:Figure 3), presented a plot of radial movements in the ground, at the springline elevation, with tunnel advance. If an average curve is fitted through the points shown in that plot and if the displacements are extrapolated to the tunnel contour following the procedure used in Section 5.3.6.1, one would find that, at the point of lining activation, the radial closure at the springline would have been equal to 6 mm and equal to 7.5 mm at final equilibrium. These values are to be compared with the calculated closures of 6.3 and 7.4 mm respectively. The total increase of about 2.3 mm in the horizontal lining diameter, after its activation (i.e., after grouting), is in agreement with the convergence measurements taken in the field (DeLory et.al. Op.cit.:193).

7.5.3.5 A Large NATM Tunnel in Granular Soil: The Bütterberg Tunnel, in Osterode, near Hannover

This case history refers to a large road tunnel built in 1977-1979 in Osterode, about 50 km southeast from Hannover (Germany), that was described by Duddeck et.al., (1979 and 1981). The initial portion of the job, completed earlier in 1975-1976, served as a test tunnel designed to supply information on tunnelling performance for the main tunnel. The investigations carried out in this experimental length were reported by Meister and Wallner (1977). The tunnel had a non-circular profile of 10.11 m high and 11.70 m wide. The area of excavatiion was about 100 m^3/m, corresponding to an equivalent diameter of 11.5 m. At the main instrumented section the ground cover was 13.6 m.

The ground profile at the instrumented section included a thick Quaternary terrace deposit (Pleistocene Epoch) consisting of a well graded sandy-silty gravel (GM) with a of silt component of 10% and with boulders of diameters up to 1 m. The tunnel, at this section, was entirely driven through this granular soil. Underneath it, some 12 m below the tunnel floor, there was a limestone bedrock. The groundwater level was not identified by the exploratory boreholes drilled down below the tunnel floor. Some local seepage was detected at the portal region, associated with rainfall infiltration. Otherwise the quaternary deposit was water free.

Laboratory and in situ direct shear tests were conducted on the granular soil and showed that the effective shear strength parameters were $c'=20$ kPa and $\phi'=33°$. This soil showed some strength loss after peak, with residual values given by $c'_r=5$ kPa and $\phi'_r=30°$. The soil deformation behaviour was investigated by plate bearing tests in test pits and inside the tunnel. From these tests, an average constrained modulus for the 'intact' material of 330 MPa was estimated (Duddeck et.al., 1979:208). For a Poisson's ratio of 0.3, a Young's modulus of 245 MPa is found for this soil at a depth of about 24 m. If that value is taken as the in situ tangent modulus, and if it is assumed to be proportional to the square root of the vertical effective stress, in situ moduli of 141 MPa, 217 MPa and 279 MPa are estimated at points located half a diameter above the tunnel crown, at the springline elevation and half a diameter below the tunnel floor, respectively.

The failure ratio (R_f) for this material is not known, but results from triaxial tests on similar materials when compacted (Duncan et.al., 1980), suggest that R_f should be close to 0.7. The unit weight of this soil is 22 kN/m^3 and an in situ stress ratio of 0.5 was suggested by Duddeck et.al. (1979:208). A drained analysis is justified for this case, and the corresponding parameters adopted are summarized in Table 7.8. Peak strength parameters are assumed on the grounds that the soil around the opening was not strained to failure.

The tunnel construction was carried out with the segmented excavation of the face in stages: heading, bench and invert. The bench and invert excavations were undertaken in steps, in such a way that a central core was always left supporting the tunnel face (see Figure 7.37). The heading was advanced in two successive rounds of one metre each. This was followed by a 2 m advance of the bench, floor excavation following this in 4 m sections. An average rate of advance of 2 m/day was maintained during construction. The excavation at the crown was carried out under the protection of short forepoling (1.3 m long).

			(1)	
Unit weight	γ	kN/m^3	22	
In situ stress ratio	K_o	-	0.5	
Effective cohesion intercept	c'	kPa	20	(2)
Effective friction angle	ϕ'	(°)	33	(2)
Failure ratio	R_f	-	0.7	(3)
E_{t_i} (drained)	1/2 D above crown	MPa	141	(4)
	at springline	MPa	217	(4)
	1/2 D below floor	MPa	279	(4)
Poisson's ratio	μ	-	0.3	

Notes: (1) Average values provided by Duddeck et al (1979:208).

(2) Peak strength parameter.

(3) Estimated.

(4) Derived from the average constrained modulus from plate bearing tests by Duddeck et al (Op.cit).

Table 7.8 Selected Ground Parameters for Analysis of Tunnel in Well-Graded Sandy-Silty Gravel

The primary lining consisted of a shotcrete layer 30 cm thick, steel wire mesh and light steel ribs at 1 m spacing (GI profile, 130 mm high, 37 kg/m in the instrumented tunnel length). Steel ribs were not installed at tunnel invert. At the instrumented section, the shotcrete ring closure at the floor took place when the face was 9.5 m past the section. This was the distance between the middle point of the shotcrete section at the invert and the heading face (Duddeck et.al., 1979:Figure 16).

A very careful construction procedure was undertaken. The two dimensional ground stability verification at lining closure, furnished a factor of about 1.21, which is, in fact, slightly low. However, no ground instability was observed during construction. Such a low factor of safety may indicate that some shear stress concentration in the ground might have happened. If this is so, the development of some shear dilatancy in this fairly dense granular soil could be expected. The proposed design procedure does not take into account this type of ground response, as well as the effects of some strain weakening that might have also developed around the opening, possibly at the tunnel shoulders. Notwithstanding this, the analysis was carried out neglecting such likely occurrences.

An adjusted friction angle of 41.5° was calculated on account of the cohesive strength component and of the failure ratio different from unity. At lining closure (0.826 D behind the face), the amount of stress release was about

64% and a reduced tangent ground modulus of 115.82 MPa was calculated (46% less than the original average value). In these calculations, the generalized λ and λ' curves for K_o=0.6 were used for simplicity and to avoid the need of extrapolating the numerical results for the selected in situ stress ratio. At lining closure, the U/U_{ref} values for the crown and the springline did not exceed the limits of the fitted solutions. For the floor, however, it was necessary to use the solutions beyond their formal limits.

The lining-ground interaction analysis was carried out neglecting the contribution of the light steel ribs and the shotcrete reinforcement. A lining modulus of 10 GPa was considered, as well as a Poisson's ratio of 0.2. These are the same parameters used for the Romerberg Tunnel (Section 7.5.3.3). Meister and Wallner (1977:930) also used this Young's modulus for the lining in their numerical analysis of this case history. Four iterations, in which the ground heave after support activation was neglected, were needed to obtain the equilibrium condition. An average ground modulus of 144.78 MPa was found for this condition which was higher than that found at lining closure. This modulus increase resulted from the mode of deformation where the lining squatted and pushed the soil outwards at the springline region. The radial confinement increase in this area caused the soil to become locally stiffer and this led to an increase in the average ground modulus, which at equilibrium, was now only 32% lower than the in situ average value. For this condition, the flexibility (β) and compressibility (α) ratios were found to be about 5 and 0.0012, which are typical for shotcrete linings in dense sand (See Table 7.1).

The final crown settlement was estimated as 22.1 mm ($U=0.906$) and the associated amount of stress release at the crown was about 70%. The resulting distributions of subsurface and surface settlements were calculated for $K_o=0.6$ and $\phi=40°$, which are not far from the values which that should actually have been considered. An inevitable numerical extrapolation was required regarding the normalized settlements, with respect to the cover to diameter ratio. In this case study, this ratio was equal to 1.183, whereas the parametric numerical results (Appendix C) furnishes distributions for $H/D=1.5$ and 3.0. A linear extrapolation was made, and the distributions obtained are those shown in Figures 7.37 and 7.38. Included in these figures are the settlements measured in the instrumented section MS3 (Duddeck et.al., 1979:214).

From Figure 7.37, one notes that, although a reasonable agreement was obtained between predictions and measurements, the proposed method underestimated the ground movements close to the tunnel. One could speculate that this is due to the unaccounted for influence of the volumetric expansion of the soil above the tunnel (see Figure 2.9, d and e). Plastic dilation in the ground is known to increase the tunnel convergence, for a given amount of stress release (e.g.,

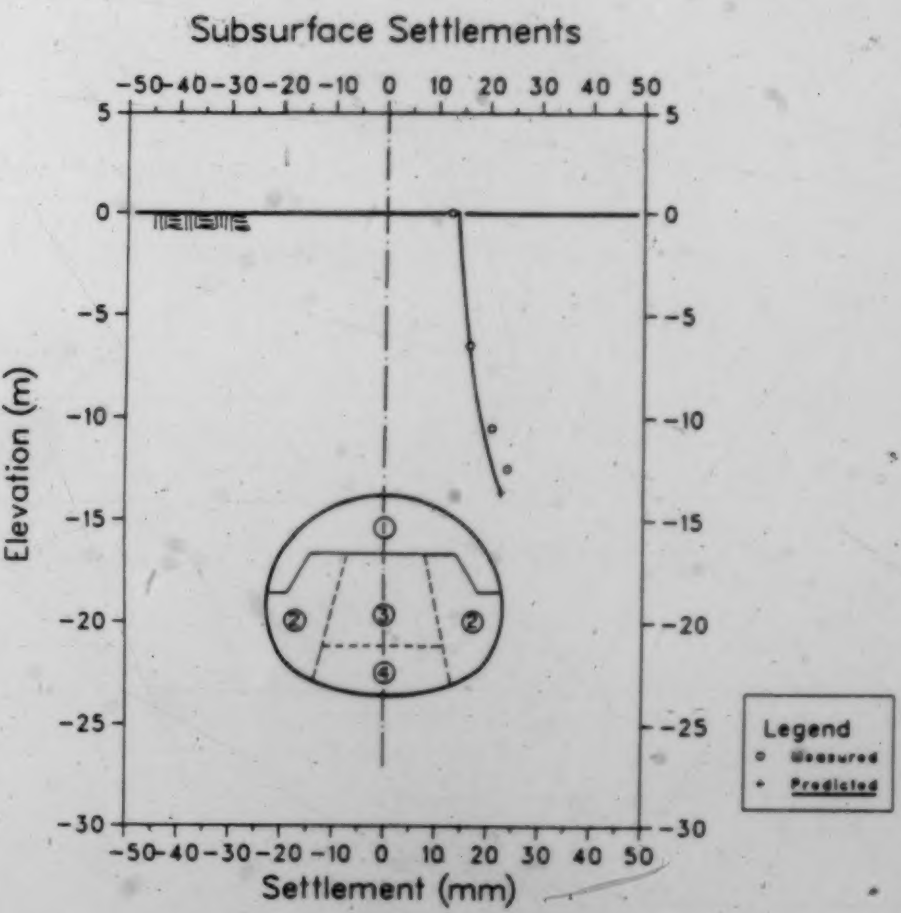

NOTE · MEASUREMENTS AT SECTION MS3, BY DUDDECK ET AL (1979·214)

Figure 7.37 Measured and Calculated Final Subsurface Settlements over the Butterberg Tunnel

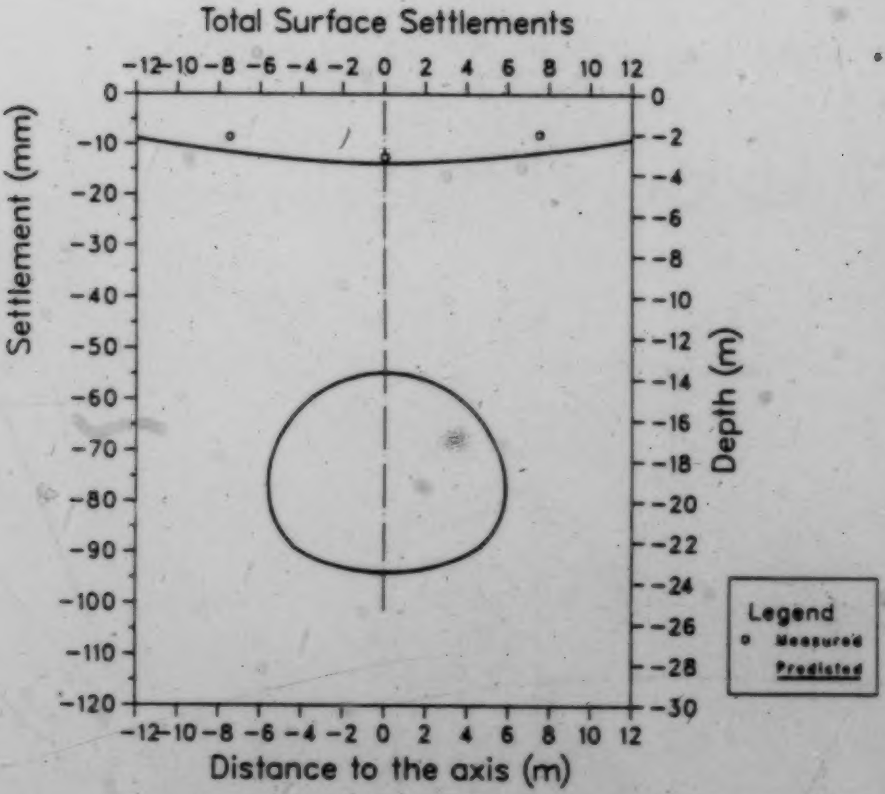

NOTE: MEASUREMENTS AT SECTION MS3', BY DUDDECK ET AL (1979: 214)

Figure 7.38 Measured and Calculated Final Surface Settlements over the Butterberg Tunnel

Lombardi, 1973, Ladanyi, 1974). The non-circular shape of the tunnel cross section could also be evoked to explain the underestimation of the crown displacements. From Figure 7.38, one notes that the magnitude of the maximum surface settlement observed at surface, was reasonably estimated by the proposed method, but once more the distortions were underestimated.

Predicted and measured radial stress onto the lining are shown in Figure 7.39. The measurements were taken with Maihak pressure cells (Duddeck et.al., 1981:181), but details of their installation were not given. One set of measurements was taken in the experimental tunnel length, while the other was taken during the main tunnel construction under similar conditions. One notes that the shapes of the predicted and measured stress distributions show some sort of broad agreement. However, the predicted stresses are typically twice the stresses measured. Although, it was shown that the proposed method may tend to slightly overestimate the final lining loads (see Section 7.2.2), this fact does not explain the result obtained in this case. Had a smaller shotcrete modulus been assumed a slightly better agreement could have been obtained. A smaller modulus would imply, however, a poorer agreement regarding the lining convergence results. A horizontal diameter increase of 3.96 mm was measured in the field (Duddeck et.al., 1981:180) after the shotcrete ring closure. The predicted increase in the horizontal diameter was 3.74

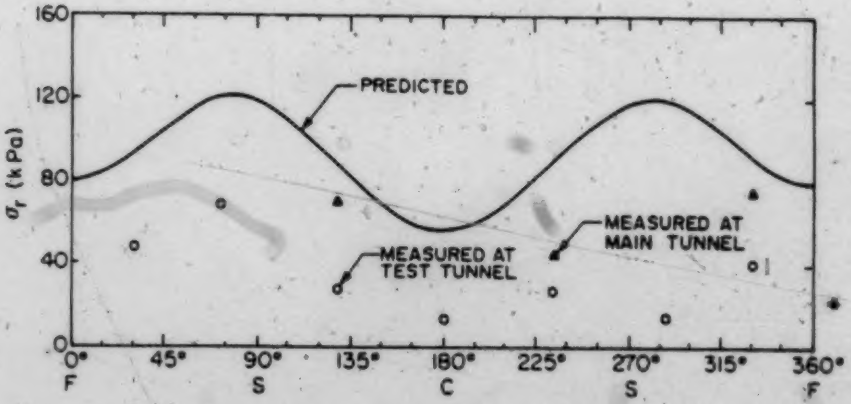

NOTE: MEASUREMENTS BY DUDDECK ET AL (1979: 213 AND 215)

Figure 7.39 Measured and Predicted Radial Stress Distributions on the Shotcrete Lining of the Butterberg Tunnel

mm, which agrees very well with the observed value. Had a 'softer' lining been considered, this agreement would not have been so good.

7.5.3.6 A Large Shield in Till: The Edmonton LRT Tunnel

This case history was described in detail in Section 5.2.4.3, where it was back analysed through the two dimensional finite element model presented in Chapter 5. Basically, the same parameters used in the best fit case were considered in the present analysis.

The tunnel was driven with a 6.172 m diameter under an 8.9 m cover of soil. A uniform till layer was considered with a friction angle of 40° and zero cohesion (R_f=1). For an in situ stress ratio of 0.75, in situ tangent moduli of 45.35 MPa, 65.18 MPa and 80.22 MPa were calculated, at points half a diameter above the crown, at the springline elevation and half a diameter below the tunnel floor, respectively.

Assuming that the lining was activated at one diameter behind the tunnel face, the amount of stress release immediately before liner installation could be calculated. To avoid data interpolation, the λ curve for K_o=0.8 was used for this purpose. The average stress release was about 60% and a reduction of about 43% in the ground modulus was found. The former value is higher than that found in the back analysis presented in Section 5.2.4.3 (50%), which results from the approximation above and from others which are built into the proposed calculation procedure. The two dimensional ground stability verification at the section the lining was activated furnished a factor of safety of 1.35.

In shielded driven tunnels, it is convenient to check if the soil stood up over the TBM body, in order to assess if the assumed distance between the tunnel face and the section of lining activation is correct. This verification could not be performed in the Domplatz and in the Mississauga tunnel cases, since no information was available regarding the amount of overcutting used. In the LRT tunnel, the ground was bored with a diameter 19 mm larger than the outer diameter of the TBM body (Branco, 1981:23).

By using the approximate solution for tunnel closure presented in Section 5.3.5.2 and the in situ ground moduli estimated earlier, one can calculate the increments of radial displacement at the crown and floor, from the tunnel face to the shield tail. The latter extended to 5.5 m behind the face (0.89D). From this, one finds that the vertical diameter of the bored opening reduced by 14.5 mm from the face to shield tail. This value is less than the clearance provided by the overcutting (19 mm). The reduction in the horizontal diameter was also less than the above clearance. Therefore, one could say that the soil did not close over the shield body. This, in fact, happened whenever the tunnel was bored through uniform till. In some locations, however, (see Section 2.3.5.4), sand pockets were cut at the crown and localized instabilities were observed. Some soil ran into the unsupported heading, over the cutting wheel, and some soil blocks may have rested over the TBM. But the remainig till mass, otherwise stable, did not come in contact with the TBM body. In other words, in the present case, it is valid to assume that the opening was virtually unsupported until the lining left the shield and was expanded against the opening profile, about one diameter behind the tunnel face.

For the lining-ground interaction analysis, it was assumed that the wooden lagging did not contribute to the lining stiffness. Its action was, thus, limited to longitudinally transferring the ground loads to the steel ribs (E_s=200 GPa, μ_s=0.2, I_s=1.82 x 10^{-5} m^4/m) at 1.22 m spacing. Two iterations were needed to find the equilibrium condition, which yielded an average ground modulus of 34.85 MPa, and relative flexibility (β) and compressibility (α) lining ratios of 0.0055 and 10.74, respectively (typical for this type of support in stiff clays or medium sands).

The final crown settlement was calculated as 17.5 mm (U=0.754) and the associated amount of ground stress release at the crown was about 65%. The final subsurface settlements could not be measured in this case history, since the magnetic extensometer installed at the tunnel axis was lost when the TBM reached the instrumented section (Branco, 1981:77, 110). Accordingly, only the final surface settlements were calculated and are compared to the measurements in Figure 7.40. Note, however, that while the settlements were measured at points located 3 m below the surface, the calculated movements refer to points on the actual ground surface. If the calculation method allowed the estimate of settlement distributions in horizontal planes below the surface, a better agreement with the observations would have been found, with a larger maximum displacement and a narrower settlement trough. In fact, the settlement at the tunnel axis, 3 m below surface, was calculated as 9.7 mm, while the actually measured settlement was 9.65 mm. Nevertheless, the agreement between calculations and measurements is reasonable, although it is again noted that the proposed procedure tends to underestimate the ground distortions.

The calculated thrust forces in the steel ribs are shown in Figure 7.41. Thrust forces were measured at rib joints by loads cells, as decribed in Section 5.2.4.3. Note that the calculated and measured thrusts have been reduced for the tunnel unit length, on a 1.22 m rib spacing basis. Note also that the lining self weight was discounted from the readings. The predicted thrusts seem to very closely bound the long term load cell measurements (taken 293 days after installation), while the short term reading (16 days, tunnel face 36.4 m ahead of the instruments) tend to lie below the calculated levels.

In general terms, the tunnel performance predicted herein, agrees well with the back calculated tunnel performance presented in Section 5.2.4.3 using the two dimensional finite element method, as well as with the field

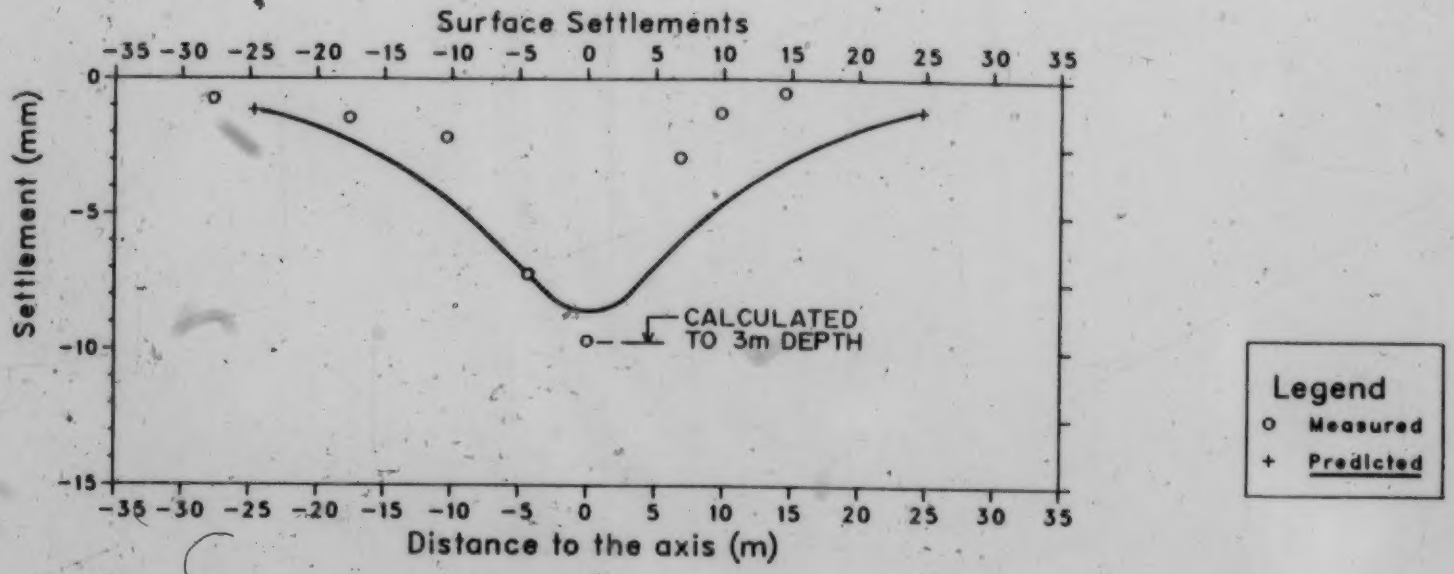

NOTES:
1. MEASUREMENTS TAKEN AT POINTS 3m BELOW SURFACE. CALCULATED SETTLEMENTS AT GROUND SURFACE.
2. FIELD DATA FROM BRANCO (1981 : 67). READINGS TAKEN WHEN THE TUNNEL FACE WAS 37.6m BEYOND THE INSTRUMENTED SECTION.

Figure 7.40 Measured and Calculated Final Surface Settlements over the Edmonton LRT Tunnel

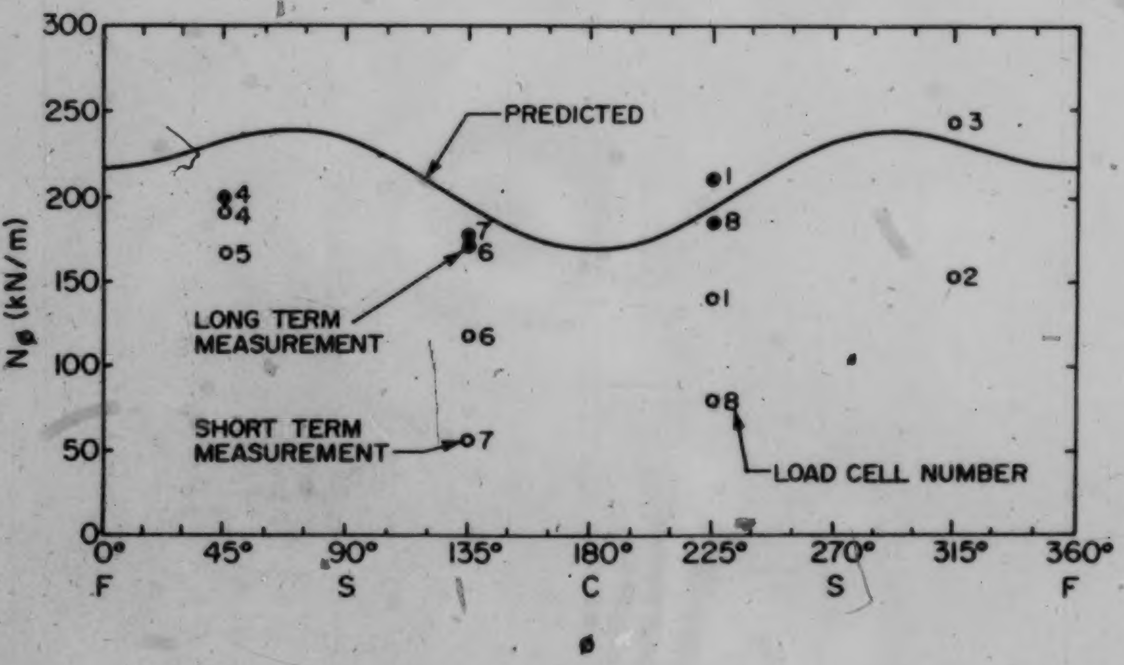

NOTES:
1. FIELD DATA FROM BRANCO (1981:156) AND FROM EISENSTEIN ET AL (1983)
2. SEE OTHER NOTES IN FIG. 5.34

Figure 7.4.1 Measured and Calculated Thrust Forces on the Edmonton LRT Primary Lining

measurements.

7.5.3.7 An NATM Tunnel in Marl: The Munich U - Bahn - Line 8/1, Baulos 18.2

This case study refers to a subway tunnel built in 1975-1976 in Munich (W. Germany), that was described by Laabmayr and Pacher (1978) and Laabmayr and Weber (1978). Two parallel tunnels were driven consecutively, each one with a near circular cross section, 6.98 m high and 6.32 m wide. The area of excavation of each tunnel was 37.50 m^3/m, corresponding to an equilvalent diameter of 6.91 m. At the instrumented section (MQ4), under the Mathilde Covent (by Mathildenstrasse), the ground cover was 22 m and the tunnels were driven almost 19 m apart (centre to centre), i.e., with a central pillar width of almost 2 diameters. The analysis and instrumentation results to be discussed refer to the first tunnel driven only.

The geological and geotechnical conditions found in Munich, and especially at the site were described by Laabmayr and Pacher (1978), Gebhardt (1980) and Krischke and Weber (1981) and were summarized by Steiner et.al., (1980) and Heinz (1984:267). At the instrumented section, the subsurface profile included a 10 m thick superficial layer of quaternary sands and gravels, underlain by a 7 m thick layer of tertiary dense sand rich in mica (Flinzsande). Below this layer, there was a thick layer of stiff to hard calcareous clay marl (Flinzmergel), also from the Tertiary, which is locally intercepted by other tertiary sand layers.

A perched water table was found at about 15 m below surface, within the upper tertiary sand layer. The other sands layers, within the marl, were found to be saturated and under pressure. A deep dewatering system was installed and operated for more than three months before tunnel construction commenced. The ground settlements due to dewatering had been completely stabilized before the tunnel was driven through the stiff marl, and, during excavation, the ground was found to be almost water-free. A drained analysis could, thus, be considered.

It will be assumed that the ground response was controlled mainly by the marl, although the tunnel cross section was intercepted by a tertiary sand layer between the haunches and the floor. The geotechnical properties of the marl summarized by Steiner et.al. (1980:170) and by Krischke and Weber (1981:11) were used as a basis for the definition of the input parameters for the present analysis (see Table 7.9). A coefficient of earth pressure at rest slightly higher than that suggested by these authors (0.8) has been assumed, perhaps more consistent with the higher overconsolidation of this soil, compared with the Frankfurt marl. No indications were found regarding the variation of the deformation modulus of the Flinzmergel with depth. Accordingly, a constant initial tangent modulus was assumed, corresponding to the upper bound value given by those authors. Since no information was provided regarding the failure ratio, the same R_f used for the Frankfurt marl was

Unit weight	γ	kN/m^3	21
In situ stress ratio	K_o	-	1.0
Effective cohesion intercept	c'	kPa	40
Effective friction angle	ϕ'	(°)	25°
Failure ratio	R_f	-	$0.8^{(2)}$
Initial tangent modulus	E_{t_i}	MPa	200
Poisson's ratio	μ	-	0.25

Notes: (1) Parameters based on data published by Steiner et al (1980:170) and Krischke and Weber (1981:111).
(2) Assumed equal to that for the Frankfurt marl.

Table 7.9 Selected Parameters for Munich Marl

adopted herein.

The tunnel construction was carried out with the sequential excavation of the face in three stages, heading, bench and invert, with immediate application of shotcrete over the exposed ground. The rate of advance when the tunnel face passed the instrumented section was about 4 m/day. The excavation round length was 1 m at the heading and bench, and 2 m at the invert. The primary lining also included horseshoe shaped segmented steel ribs with a channel profile (TH 21/58), at one metre spacing, which were not closed at the floor. The shotcrete total thickness was 16 cm from crown to haunches, and was increased to 20 cm in the invert. The support ring was closed, at the instrumented section, 7 m behind the face (Laabmayr and Weber, 1978:89). Similarly to the Romerberg Tunnel in Frankfurt, ground anchors were also installed here, but again, their effectiveness in controlling the ground behaviour was questioned (Laabmayr and Weber, Op.cit.:82).

The tunnel construction was undertaken under good ground control conditions, wtih no ground instabilities being reported.

An adjusted friction angle of 31° was calculated. At lining activation the amount of stress release resulted was about 51% and the average ground modulus was 97.69 MPa, which corresponds to a 51% decrease from the in situ value. The 2D ground stability verification at lining closure furnished a factor of safety of 1.91.

The lining-ground interaction analysis was carried out neglecting the action of the steel ribs, and considering a shotcrete lining 0.16 m thick, with a modulus of 10 GPa and a Poisson's ratio 0.2. Two iterations were needed to define the equilibrium condition, neglecting the ground heave after the support was activated. A ground tangent modulus of 79.82 MPa was found at equilibrium, from which flexibility and compressibility ratios of 0.0015 and 7.73 were calculated, respectively.

A final crown settlement of about 9.9 mm was calculated (U=0.616), for which a stress release of about 55% resulted at tunnel crown. At the instrumented section, the surface settlement profile could not be determined due to interference from existing constructions. The ground movements were measured only at two points, as shown in Figure 7.42. Here, only those movements observed during tunnel construction are considered: the displacements due to dewatering were discounted. Figure 7.42 shows also the calculated final subsurface settlement distribution. It seems to agree with the sparse field data available.

Figure 7.43 presents the calculated and measured radial stresses acting around the lining contour. The stresses were measured by Glotzl contact pressure cells and they correspond to the final readings, taken 7 months after the instruments were installed. The measurements indicated some load increase with time. It is not known when the second tunnel was built and therefore, it is not known if these

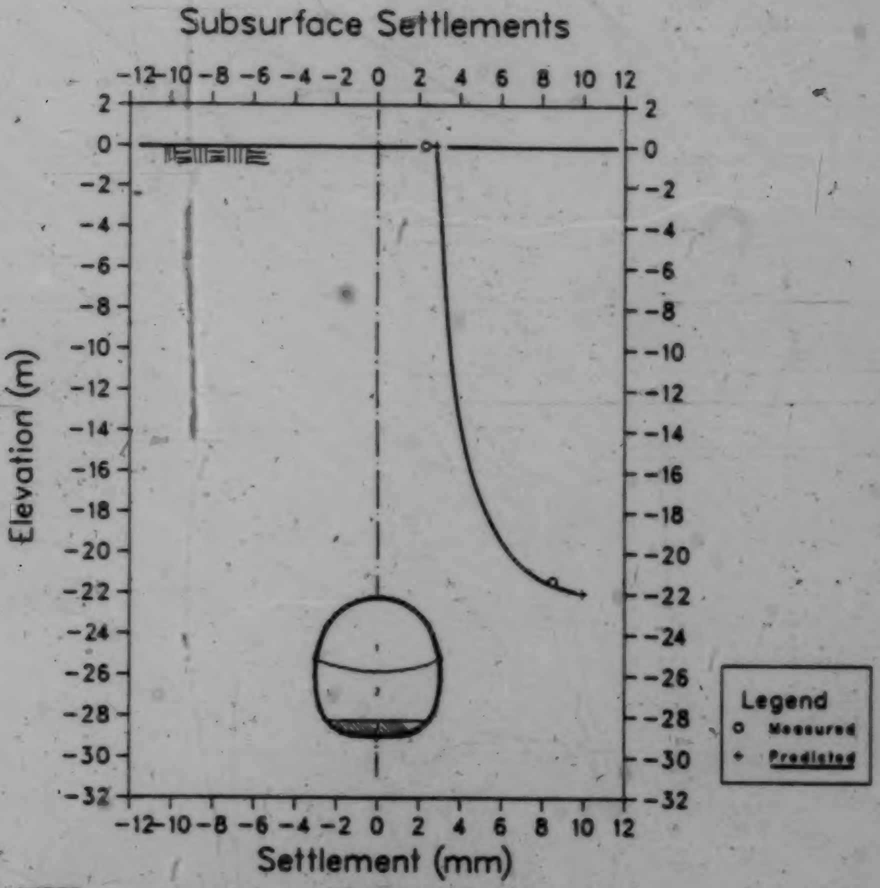

NOTES
1. MEASUREMENTS AT EXTENSOMETER E3, FROM LAABMAYR AND WEBER (1978·85)
2. SETTLEMENTS DUE TO DEWATERING DISCOUNTED.

Figure 7.42 Measured and Calculated Final Subsurface Settlements over the Munich Line 8/1 Tunnel

readings were affected by the parallel tunnel construction. If they were, the effect may have not been very pronounced as the second tunnel was built almost three diameters apart from the first one. A substantial scatter was observed in the field data. The predicted stresses tend to bound the measurements.

No convergence measurements were reported at the instrumented section MQ4. However, they were taken at another section (MQ1), some 400 m from MQ4, where not much dissimilar conditions were encountered (Laabmayr and Weber, Op.cit.:81). A fairly uniform lining closure was observed, confirming the in situ stress ratio adopted in the analysis. Horizontal diameter decreases of up to 2.3 to 3.9 mm after the shotcrete ring closure at the floor, were measured at two different convergence bases (H1 and H2). These values compare well with the 3.2 mm horizontal diameter reduction predicted in the lining-ground interaction analysis.

7.5.3.8 An NATM Tunnel Built under Compressed Air: The Munich U-Bahn-Line 5/9, Baulos 7

The present case history refers to a subway tunnel built in the early eighties in Munich (W. Germany), that was described by Baumann et.al. (1985). It represented one of the first experiences in using shotcrete combined with compressed air (Weber, 1984).

Two parallel tunnels were driven consecutively, each one with a near circular cross section, 7.0 m high and 6.5 m wide. The excavation area of each tunnel was 38 m^3/m, which

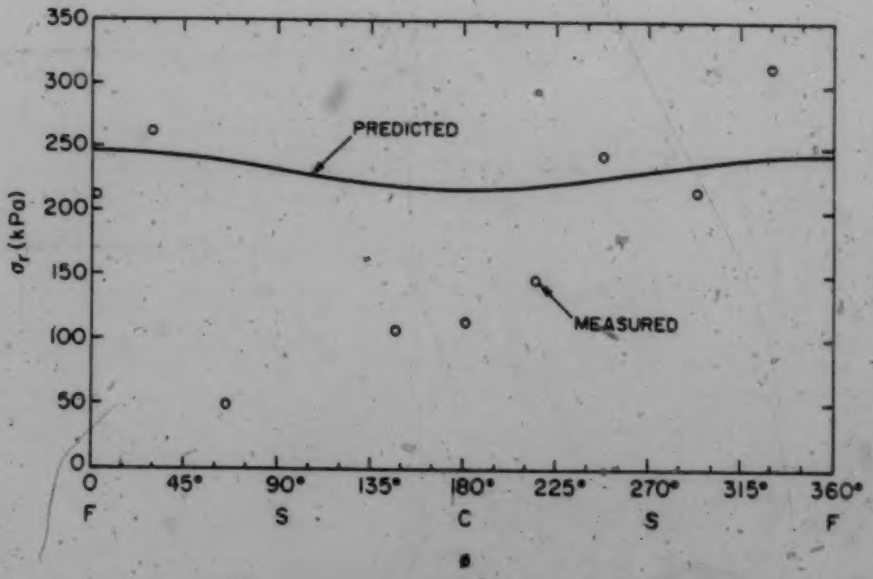

NOTE: MEASURED AT MQ4, TAKEN 7 MONTHS AFTER INSTALLATION (LAABMAYR AND WEBER, 1978 · 87)

Figure 7.43 Calculated and Measured Radial Stress Distributions on the Shotcrete Lining of the Munich Line 8/1 Tunnel

corresponds to an equivalent diameter of 6.95 m. At the instrumented section MQ7, located West of the Maximilianeum, not far from the Isar River bank, the ground cover was 20 m and the tunnels were driven about 13 m apart (centre to centre), leaving a central pillar of slightly less than one diameter between the two tunnels. The analysis and instrumentation results to be presented refer to the first tunnel driven only. The second tunnel passed the instrumented section MQ7 4 months after the first tunnel had passed it.

The geological and geotechnical conditions found at this site are similar to that described in Section 7.5.3.7. At the instrumented section, the subsurface profile included a 4.5 m thick superficial layer of quaternary sands and gravels, underlain by a thin marl layer (2.5 m thick). Below it, a 10 m layer of fine to medium dense tertiary sand was found. Underlying this, a thick layer of stiff to hard tertiary marl was encountered, through which the tunnel was driven. The marl cover above the crown was slightly less than half tunnel diameter. At floor elevation the marl was cut by a metre thick sand layer.

A perched water table was found at the quaternary granular soil. Another one was found 15 m below the surface within the thick sand layer. The thinner sand layer below the tunnel was also saturated and under pressure. A compressed air pressure of 60 kPa was used in this section.

For the analysis, it was assumed that the ground response at the crown was controlled by the stiffness of the sand layer located above the tunnel, with an in situ drained modulus estimated as 144 MPa from data presented by Krischke and Weber (1981:111). For the springline and floor, a tangent modulus of 200 MPa was assumed for the stiff marl as for the U-Bahn-Line 8/1.

Based on data from Krischke and Weber (1981:111) and Steiner et.al., (1980:170), the coefficient of consolidation of the marl was estimated as 2×10^{-2} cm^2/s. The likely ground response in terms of pore pressure development, can be estimated through the tentative criterion proposed in Section 3.3.4.5. If the pore pressure changes in the 3 m marl cover were solely caused by the change in the hydraulic boundary condition at the tunnel contour, one could use the criterion given in Figure 3.23. It would then be found that over one week, the marl cover would experience partial consolidation, but over a time span of a month, appreciable consolidation (more than 90%) would have developed. If an average rate of advance of 3 m/day is admitted (Weber, 1984:26), then the 'short term' ground response, corresponding typically to an advance of the face from a section, say, 2D behind the instrumented section, to a point 4D past this section, would take place in a two week time interval. The 'short term' response would thus involve some amount of ground consolidation, and could not be defined as 'undrained'. Accordingly, a drained analysis was favoured, and the same 'drained' parameters used for the Munich 'Flinzmergel' in Section 7.5.3.7, were adopted presently.

The tunnel construction was similar to that used in the U-Bahn-Line 8/1, except that here the shotcrete ring was closed at a shorter distance from the heading face (5.5 m typically). The minimum shotcrete thickness used was 15 cm, and at some locations it was increased to 18 cm. A single steel mesh (Q188) was laid on the inner side of the shotcrete lining. Lattice girders at one metre spacing were installed instead of steel ribs.

The tunnel construction was carried out under good ground control conditions, and no ground instabilities were reported.

An adjusted friction angle of 31.2° was calculated on account of the cohesive strength component and of the failure ratio equal to 0.8. In calculating the tunnel closure at the instant of lining activation (0.8D behind the face), allowance had to be made regarding the compressed air pressure being applied. To take it approximately into account, the in situ radial stresses at crown, springline and floor were reduced by 60 kPa, the magnitude of the air pressure. This approach was used earlier by Deere et.al. (1969:87). This is equivalent to reducing the soil cover depth by 2.9 m (for a soil unit weight of 21 kN/m³). In so doing, the amount of stress release at lining activation was about 49% and the mean ground modulus was 95.03 MPa. The latter corresponded to about a 49% decrease of the original in situ ground modulus. The 2D ground stability verification of lining closure furnished a factor of safety of 2.01.

The lining-ground interaction analysis was carried out neglecting the action of the steel mesh or of the lattice girders. A nominal 16 cm thickness for the lining was considered. As on other occasions, a shotcrete modulus of 10 GPa and a Poisson's ratio of 0.2 were assumed. Two iterations were required to define the equilibrium condition, neglecting the ground heave after support activation. A tangent modulus of 80.18 MPa was found for the ground at equilibrium (about 43% if the in situ value). Flexibility and compressibility ratios of 0.0014 and 7.67 were calculated, respectively.

A final crown settlement of 10.05 mm was calculated (U=0.578), which corresponds to about 52% of the stress release at the tunnel crown. The field instrumentation at section MQ7 did not include the measurement of the subsurface settlements along the tunnel vertical axis. Only surface settlements were measured, as indicated in Figure 7.44. Two measured profiles are indicated, one corresponding to a 'short term' condition (10 days after the face passed the section) and another corresponding to a 'long term' condition (140 days after passage, immediately prior to the second tunnel drivage). Both at the short or long term conditions, the tunnel was being submitted to the same compressed air pressure. The calculated settlement profile is included in Figure 7.44 and one notes that it agrees

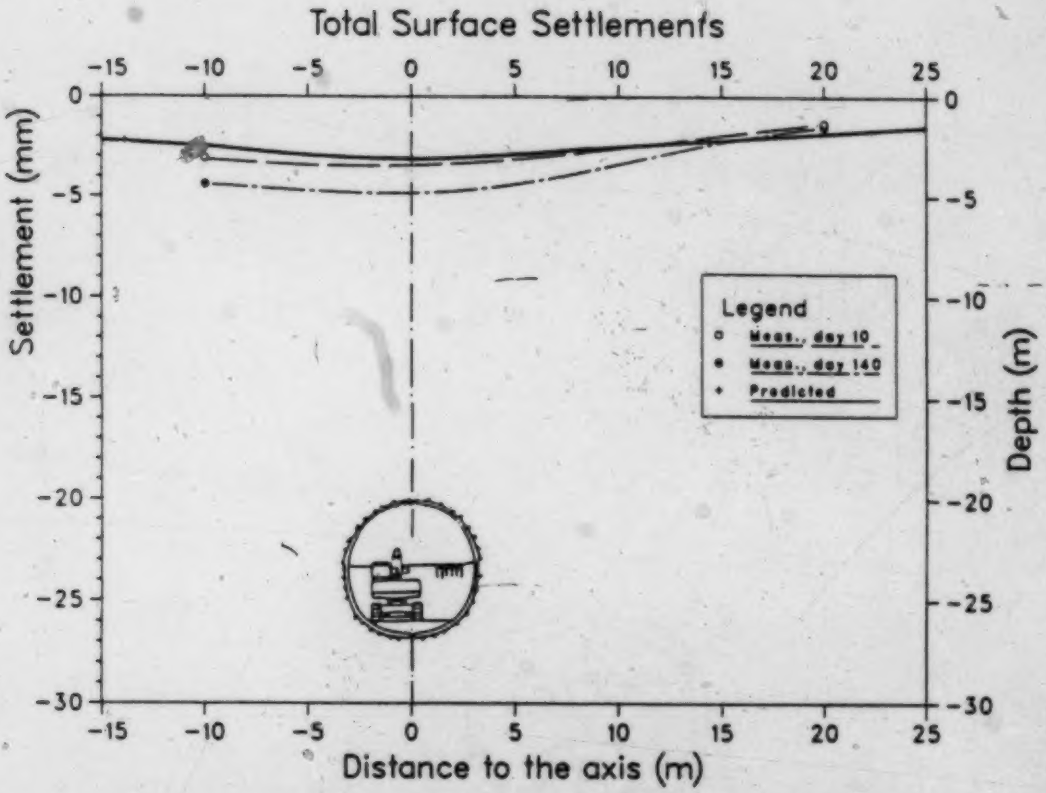

NOTE: MEASUREMENTS AT SECTION MQ7, DATA FROM BAUMANN ET AL (1985: 336)

Figure 7.44 Measured and Calculated Surface Settlements over the Munich Line 5/9 Tunnel

roughly well with the 'short term' profile. This agreement, however, may be claimed as fortuitous, since there is not a complete correspondence between the 'partial consolidation' condition, that may have actually developed in the short term, and the completely drained behaviour (with "zero" pore pressures) assumed in the calculations. On the other hand, it is not unexpected that the measured 'long term' settlements are larger than those calculated. The proposed calculation method does not take into account the ground volume changes and associated consolidation settlements resulting from porewater pressure changes and ground water drainage into the tunnel (see Section 3.3.4.2).

The tunnel convergence was also measured at the instrumented section. Reference points at the springline were installed right at the face, so that the changes in the horizontal tunnel diameter before and after shotcreting the invert could be observed. The radial displacements at the face were calculated using the approximate solution presented in Section 5.3.5.2. The reduction in the horizontal diameter, from a section at the face to the section where the shotcrete lining ring was closed, was thus calculated to be 9.36 mm. This compares favourably with the 10 mm reported by Baumann et.al. (1985:336). After closure of the shotcrete ring, the lining-ground interaction analysis furnished an additional reduction in the horizontal diameter of 2.66 mm, which also agrees well with the 2.5 mm measured.

Specially designed load cells were installed to measure thrust forces and bending moments in the shotcrete lining (Baumann et.al., 1985:450). The measuring system was developed by Philipp Holzmann AG Munchen. Details of this patented measuring gauge were not disclosed. Apparently it consisted of a 2 m long, 0.2 m high and 0.12 m wide steel box, installed at the lining haunches and shoulders, and interrupted the whole shotcrete lining thickness. It is not clear how the system measured the bending moment (or normal force eccentricities). The calculated thrust forces exceeded the forces actually measured both in the short and the long term. As noted in Section 2.3.6.3, a non-uniform thrust force distribution was observed, along the 2 m long embedded gauge. For a given position of the face, the highest thrust force was recorded at the cell end closer to the face. The measured values indicated in Table 7.10 correspond to the mean values provided by Baumann et.al. (1985:336). The eccentricities measured ranged between 1 and 3 cm, while those calculated were one order of magnitude smaller (about 0.06 cm). That could be an indication that the in situ stress ratio is not equal to one, as assumed. But this would be conflicting with the mode of lining deformation, which was well estimated by the calculations. Nothing further can be advanced, as the reliability of these measurements cannot be assessed due to the paucity of the information made available.

Performance aspect	Unit	Calculated	Measured Short Term(2)	Measured Long Term(2)
1. Maximum surface settlement	mm	3.00	3.45	4.9
2. Horizontal diameter change from face to the section the support ring is closed	mm	9.36	10.0	-
3. Final horizontal diameter change of shotcrete lining after invert closure	mm	2.66	-	2.50
4. Thrust force at haunches (45°)	kN/m	693	476	550
5. Thrust force at shoulders (135°)	kN/m	617	305	400

Notes: (1) Measurements at Section MQ7. Data from Baumann et al (1985:336).

(2) Short term: 10 days after the tunnel face passed the section. Long term: 140 days after passage.

Table 7.10 Measured and Calculated Performances at the Munich Line 5/9 Tunnel

7.5.3.9 An NATM Tunnel Driven Through Heterogeneous Ground: The Bochum Baulos A2 Double Track Subway Tunnel

This case history refers to a double track subway tunnel that was described by Jagsch et.al. (1974), by Hofmann (1976) and reviewed by Heinz (1984:69). It was built in 1973 in Bochum (W. Germany) and was one of the first NATM cases with large cross-sectional area built in an urban environment.

The tunnel cross section was non-circular being 8.3 m high and 10.1 m high. It had an excavation area of 64 m^3/m, which corresponds to an equivalent diameter of 9.03 m. At the instrumented section MQI, the ground cover was 12.2 m.

A fairly heterogeneous subsurface profile was found at this site. It included a 7 m thick superficial fill layer, which was the embankment of an existing railway line. Below it there was a sloping layer of a fairly hard chalk-marl about 7 m thick at the tunnel axis. Underlying this, there was a softer sandy-marl, 4 m thick, that rested over a succession of sandstone, shale and coal. The ground water level lay below the tunnel floor. A mixed face condition was thus encountered, with a stiffer marl at crown, a softer marl down below the springline and sedimentary rocks at the floor.

Wittke and Gell (1980:113) presented the geotechnical properties of some of these materials, found however, at a different location (Bochum Baulos B3). While the stiffer marl had an "elastic" modulus of 100 MPa, the softer one had a modulus of 40 MPa. The proposed calculation method was clearly not designed to be used in such heterogeneous ground conditions. However, it would be interesting to test it under such conditions. A constant in situ tangent modulus of 70 MPa was thus assumed for the entire ground mass. The drained friction angle of these deposits did not vary much and it was assumed to be equal to 25°. The cohesive strength of these materials varied appreciably, within almost one order of magnitude. For the analysis, it was decided to consider the lowest cohesion value, corresponding to that of the softer sandy-marl, which was equal to 64 kPa. An average unit weight of 20 kN/m^3 was estimated for the ground mass. No data was available regarding the failure ratio of these materials. An arbitrary value of 0.9 was thus selected. No indications were provided regarding the in situ stress ratio (K_o) in the ground. It is believed that it should not differ much from other marls found in the Frankfurt or in the Munich areas. A stress ratio of 0.8 was thus liberally assumed. Wittke and Gell (Op.cit.:113) suggested that the Poisson's ratio for this soil should be about 0.3.

A very careful construction was carried out, with the face excavated in a variation of the heading-bench-invert scheme, classified as type T3 by Eisenstein et.al., (1985:711). The depth of each excavation round was 0.8 m at the heading and bench and 1.6 m at the invert. A 25 cm thick shotcrete lining was installed as well as steel sets at 0.8 m spacing. The average rate of advance was 2 m/day. The closure of the shotcrete lining at the floor took place 6.4 m behind the face. Some 3 m long ground anchors were installed to hold in place the steel ribs during their assemblage.

The adjusted friction angle was calculated and was about 35°. At lining closure, a stress release of about 57% was estimated and an average ground modulus of 37.58 MPa was obtained (almost 54% of the assumed in situ value).

The lining-ground interaction analysis was carried out neglecting the steel ribs, and considering a shotcrete modulus of 10 GPa and a Poisson's ratio of 0.2. Two iterations were required to find the equilibrium conditions, neglecting the ground heave after support activation. A 36.31 MPa ground modulus was found at this condition, which enabled the flexibility and compressibility ratios of 0.0057 and 21.24 to be calculated, respectively. These values are typical for shotcrete in stiff clays or medium sands.

A final crown settlement of 22.4 mm resulted (U=0.712), for which a stress release of 60% at the crown was estimated. The calculated final subsurface settlements are compared to those measured (Jagsch et.al., 1974:13) in Figure 7.45. The predicted magnitudes of the ground movements are comparable to the measured but the estimated shape of the settlement distribution does not agree with the observations, which involved less vertical straining. The departure could be attributed to the crude simplifications introduced (e.g. the uniform modulus profile) as well as to the non-circular shape of the excavation.

Similar results were obtained regarding the surface settlement profile (Figure 7.46). As in other case histories, the surface distortions were underestimated by the proposed calculation method, although the magnitudes of the displacements are closely estimated.

Finally, Figure 7.47 shows the predicted and measured final radial stresses acting on the shotcrete lining. The measurements do not reveal any clear trend. If a mean measured stress distribution could be defined, the calculated radial stress distribution seems to approximate it. The non-circular tunnel contour, as well as the heterogeneity of the ground around the tunnel could partly explain the disagreement between the calculated and observed stress distributions.

7.5.3.10 An NATM Tunnel with Staged Installation of the Lining: The Sao Paulo North Extension Double Track Tunnel

This case study refers to a large subway tunnel built in 1984 in Sao Paulo (Brazil), that was described by Cruz et.al. (1985), Negro et.al. (1985a & b) and by Eisenstein et.al. (1986). The double track tunnel was built with a non-circular cross section, with an area of 76.1 m², 8.5 m high and 11.4 m wide (9.84 m equivalent diameter). At the instrumented sections S1-3 and S1-9, the ground cover was about 11.2 m.

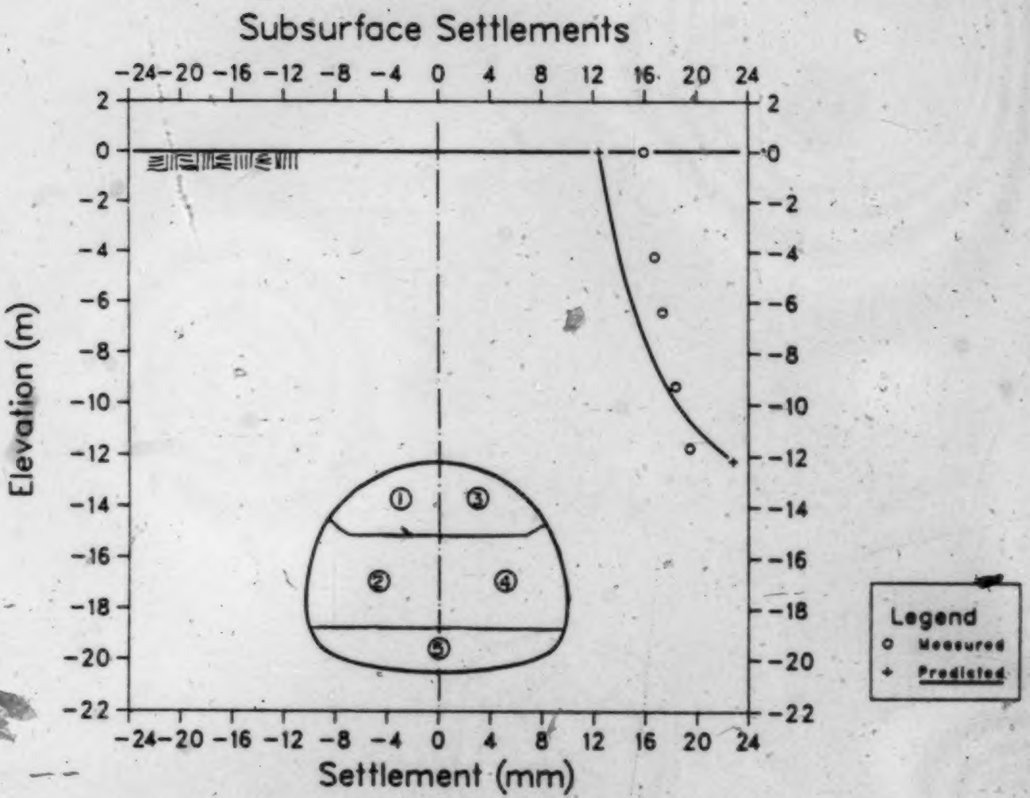

NOTE: MEASUREMENTS AT EXTENSOMETER E3, FROM JAGSCH ET AL (1974:13)

Figure 7.45 Measured and Calculated Final Subsurface Settlements over the Bochum Baulos A2 Tunnel

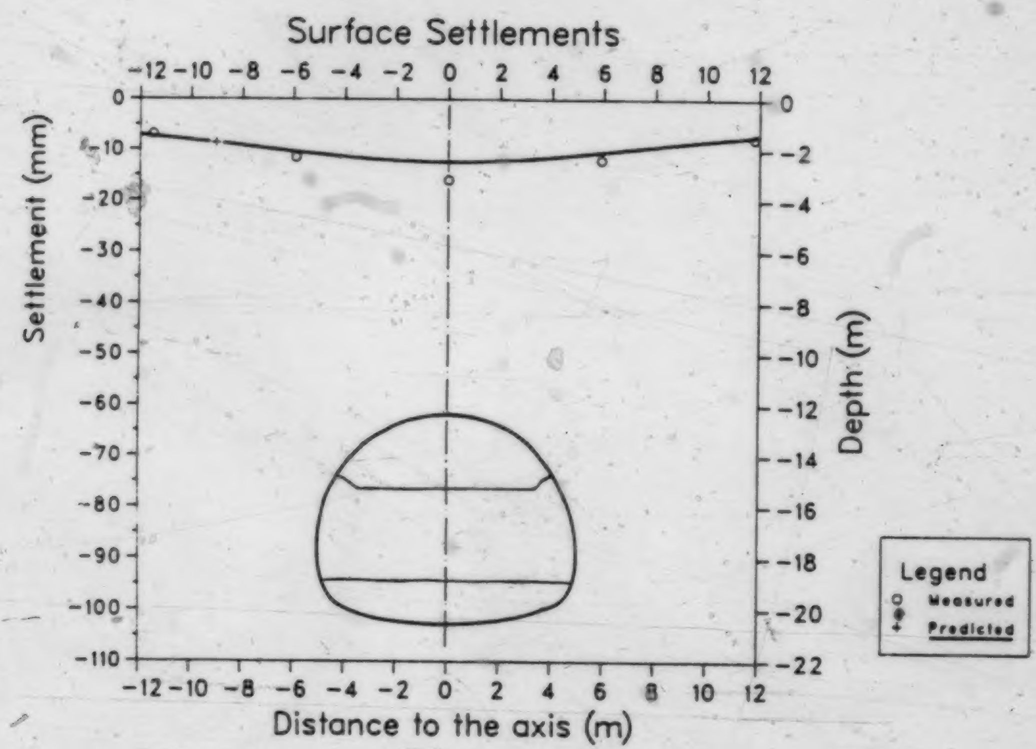

NOTE: MEASUREMENTS AT THE INSTRUMENTED SECTION MQ1; DATA FROM JAGSCH ET AL (1978:13)

Figure 7.46 Measured and Calculated Final Surface Settlement Profiles over the Bochum Baulos A2 Tunnel

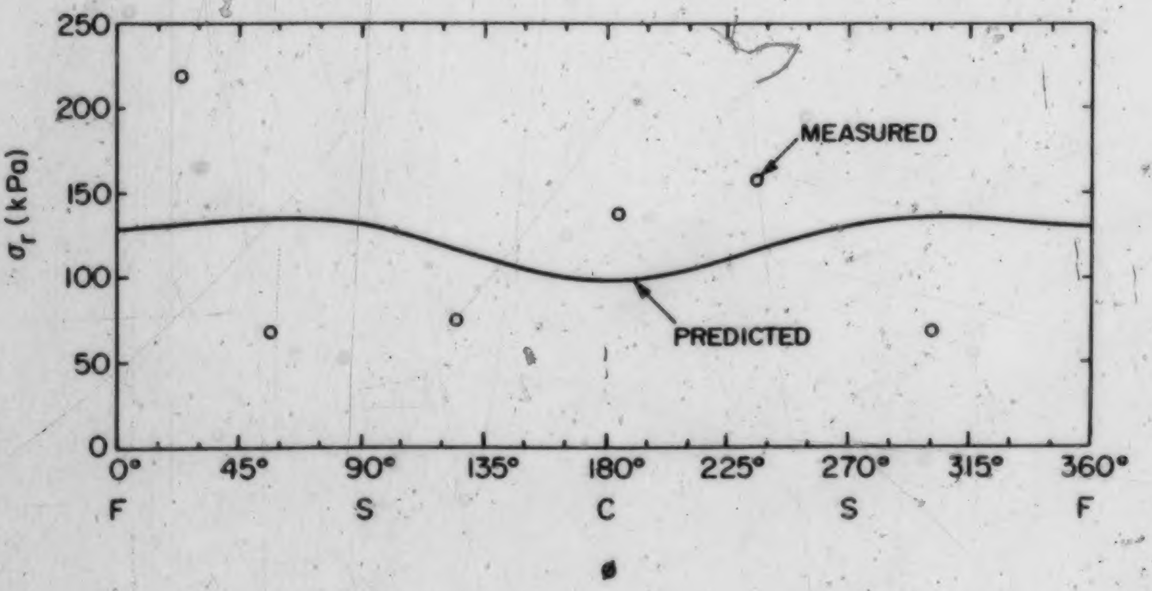

NOTE: MEASUREMENTS AT MQI; DATA FROM JAGSCH ET AL (1974:13)

Figure 7.47 Calculated and Measured Radial Stress Distributions on the Shotcrete Lining of the Bochum Baulos A2 Tunnel

The tunnel was driven through an overconsolidated stiff and fissured clay layer, about 12 m thick, which is a sediment of the Sao Paulo Tertiary formation. This soil underlay a superficial fine clayey sand layer, about 9 m thick, and overlay a 4 m thick fine clayey sand layer, below the tunnel floor. A perched water table was found 3 m below the surface, in the upper sand layer. The piezometric level in the lower sand layer showed that a nearly uniform pore water pressure distribution with depth existed in the stiff clay layer (in situ pore pressures of about 60 kPa). Some dewatering was undertaken at the portal area, about 80 m away from the measuring section, and caused a 30 kPa reduction in the porewater pressures in the lower aquifer, prior to the tunnel excavation. The settlements associated with this operation were separated from those that developed during tunnel advance.

Negro et.al. (1985:57) showed that the tunnel acted as a drain, and that the 2 to 3 m cover of stiff clay above the crown resulted in being appreciably consolidated from this drainage during the drivage process. Accordingly, in the analysis of this case history, it will be assumed that the ground response was controlled by the drained parameters of these soils. Triaxial tests on the stiff clay furnished a friction angle of 25°, a 3 kPa cohesion and a failure ratio of 0.75. The in situ effective stress ratio of this soil was estimated as 0.9 and an average unit weight of 20 kN/m^3 was determined for this sedimentary deposit. The in situ (drained) tangent modulus for the stiff clay at the tunnel springline elevation was estimated also from triaxial tests and resulted as 124 MPa. The modulus of the soil located half a diameter above the crown (the fine sand) was estimated as 47 MPa and that half a diameter below the floor (also the fine sand) was 64 MPa.

The tunnel construction was carried out in two main phases: heading excavation with a temporary shotcrete invert and bench excavation. At the instrumented sections, the temporary inverted arch was demolished and bench excavation took place when the heading face was about 19 m past the section. The heading face was always advanced leaving a central supporting ground core. The face was excavated in one metre round depths, and the temporary invert was shotcreted in 2.5 to 3 m lengths. The average distance between the mid-section of the temporary invert being shotcreted and the heading face was 7.7 m at the instrumented section. The depth of bench advance varied between 2.5 and 3 m. The final shotcrete invert was installed immediately after bench excavation.

Besides a 0.25 m thick shotcrete, the support system included two steel wire meshs (4.48 kg/m^2) and polygonal steel sets (I 8") at one metre spacing. The shotcrete lining thickness was increased to 0.40 m, after tunnel completion, and an additional steel mesh included. This tunnel is quoted as being the first subway tunnel in soil where shotcrete was used as the final support. The average excavation progress was 3 m/day for the heading and 6 m/day for the bench. The overall rate of completed tunnel construction was about 1 m/day.

The conditions involved in this case history, depart considerably from those envisaged for the application of the proposed calculation procedure. The tunnel was driven below the ground water level, with minor dewatering. The tunnel cross-section was non-circular, and, more importantly, the staged application of the lining, with a temporary invert at the heading, respresented a condition not considered in the development of the calculation method.

The analysis was conducted for a circular opening with the same excavated area as in the Bochum case history. The ground parameters were defined for the effective stress levels prior to tunnel construction. However, the stress release at the opening was calculated assuming that the pore pressures were zero in the ground mass, as for the Mississauga tunnel case. To account, at least partly, for the particular sequence of construction, it was assumed that the delay distance of lining activation was equal to the distance between the heading face and the mid point of the temporary invert section (7.7 m), plus the distance between the bench face and the mid point of the final invert section being shotcreted (about 1.4 m). In other words, it was assumed tht the lining deformations developed only after the shotcrete ring was closed at the floor of the completed tunnel section. Although this approximation may lead to unrealistic estimates of the displacements at sections between the heading face and the bench face, it was felt that it could be reasonable in estimating the final equilibrium condition.

An adjusted friction angle of 30° was calculated. At lining activation, 0.925D behind the face, a ground stress release of about 53% was estimated and an average ground modulus of 36.71 MPa was calculated (almost 60% reduction from the in situ value). The 2D ground stability verification at this instant furnished a factor of safety of 1.35.

The lining-ground interaction was analysed for the completed tunnel section, neglecting the existence of the steel sets and meshes, and considering the 0.25 m shotcrete with a 10 GPa modulus and a Poisson's ratio of 0.2. Two iterations were required to find the equilibrium condition, neglecting the ground heave after support activation.

A final crown settlement of 29.6 mm was calculated (U=0.631), for which at stress release of about 50% resulted at tunnel crown. The comparison between calculated and measured performances was restricted to surface and subsurface settlements, as lining loads were not measured in this case history. While the measured settlements shown in Figures 7.48 and 7.49 do not include the ground movements due to dewatering at the portal areas prior to tunnel excavation, they do include those settlement components resulting from ground drainage and consolidation, which were

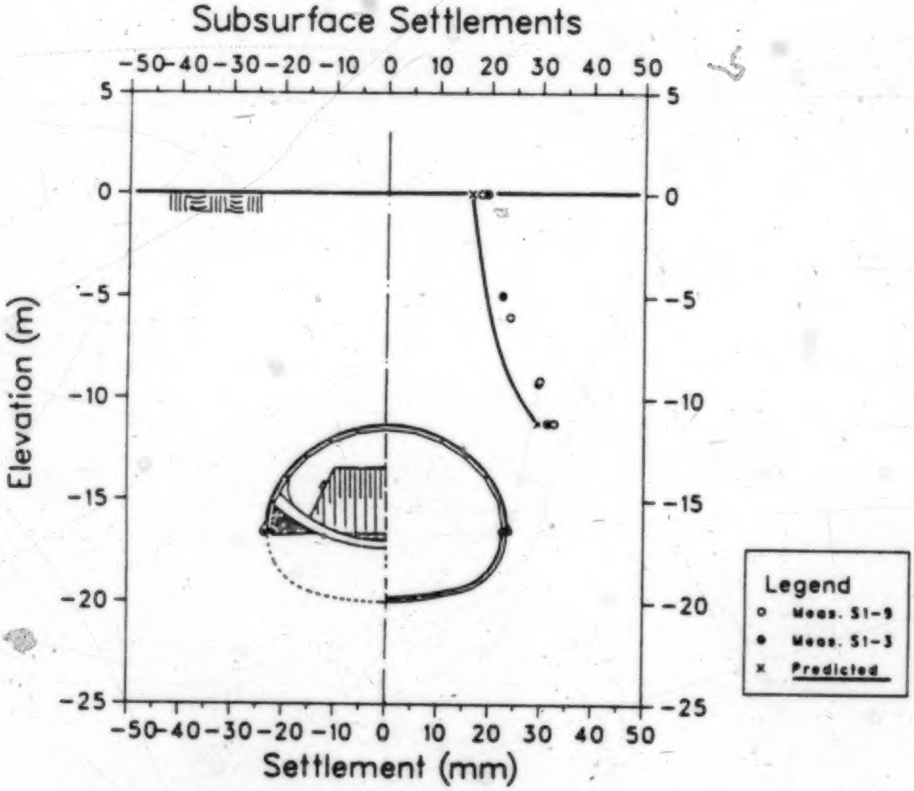

NOTE MEASUREMENTS AT SECTIONS S1-3 & S1-9. DATA FROM NEGRO ET AL (1985)

Figure 7.48 Measured and Calculated Final Subsurface Settlements over the Sao Paulo North Extension Tunnel

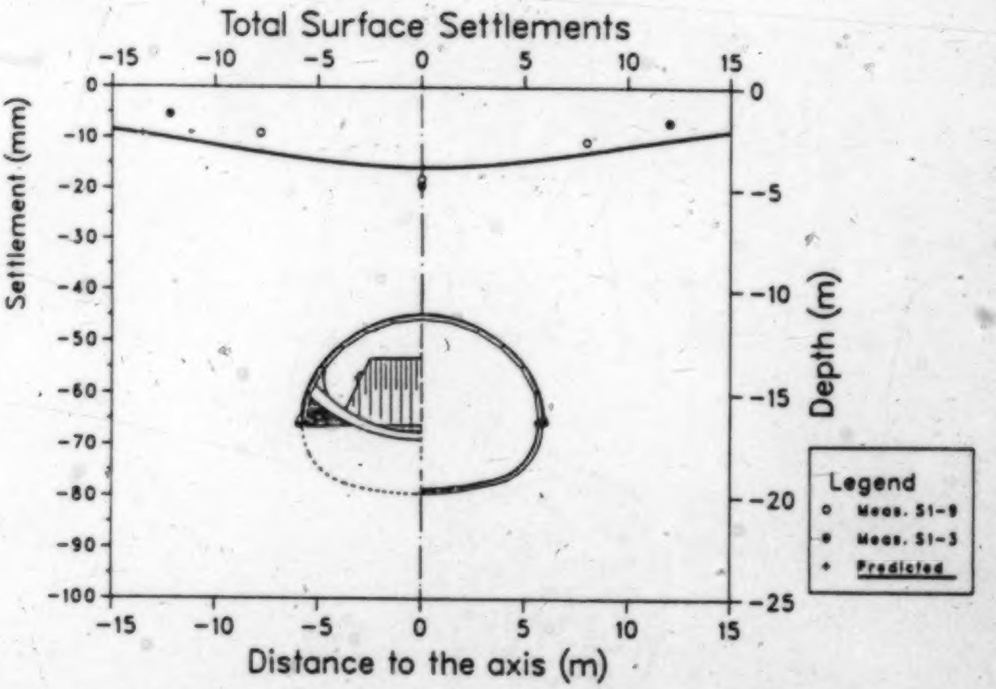

NOTE MEASUREMENTS AT SECTION S1-3 & S1-9. DATA FROM NEGRO ET AL (1985)

Figure 7.49 Measured and Calculated Final Surface Settlement Profiles over the Sao Paulo North Extension Tunnel

not accounted for in the calculations. As it is noted in those figures, the settlements were underpredicted by this approximate analysis. Also underestimated were the ground surface distortions.

The shape of the cross section of this tunnel deviates considerably from a circular profile. In fact, from all cases investigated, this is the one that presents the lowest opening height to width ratio (h/w=0.746). This can partly explain the underestimation of the magnitude of the crown and of the maximum surface settlement. The former was underpredicted by about 8% and the latter by about 14%, using the calculation, where a circular cross section of equal area was assumed.

In order to assess the influence of the cross section shape on the crown settlement, the solution numerically derived by Negro and Kuwajima (1985) may be of some help. This solution was obtained from 2D linear elastic parametric bounday element analyses of deep unlined tunnels, with cross section shapes similar to the present one. The dimensionless crown displacement is given by:

$$U = 1.058 - 0.179\frac{h}{w} - 0.385K_o \qquad [7.21]$$

where the symbols have the usual meaning. When the height to width ratio is reduced from 1 to 0.746, as in this case, for K_o equal to 0.9, one finds that the crown displacement increases 8.5%. This value is of the same order of magnitude of the underprediction quoted earlier.

7.5.4 Analysis and Interpretation of the Results Obtained

The application of the proposed calculation procedure, to simulate shallow tunnel performance obtained through three-dimensional numerical modelling, through centrifuge model testing and through field observation of full scale prototypes, revealed that it does yield sensible results. With the above exercise, the proposed method was tested and its use exemplified for a variety of conditions that may be found in actual practice.

In only one case, the centrifuge model test, the calculation procedure made use of the frictionless soil solution. In another few cases, although the ground was saturated in situ, the analyses were carried out assuming a fully drained soil behaviour. While in the former, an undrained condition could be assumed, in the latter, evidence showed that partly drained conditions had prevailed, so that the use of the frictional soil solution was preferred.

In the applications of the method to actual tunnel cases, no attempt was made to best fit the observed performances. These tests were not back analyses, since it was assumed that all of the parameters governing the tunnel response were known. Accordingly, these parameters were selected, and in a few cases, assumed, so that they would represent the most probable conditions found in each case. The departures noted in each case study were discussed and tentatively explained. In the present section,.a general appraisal of the results is attempted, with minor references to particular cases.

In some cases, the proposed method was tested to conditions that deviate considerably from those originally set up in the development of the method. As mentioned earlier, some cases investigated (Mississauga, Munich 5/9 and Sao Paulo North Extension) involved constructions below the groundwater level, under partly drained conditions. In these cases, drained ground parameters were estimated for the in situ effective stress conditions. However, the ground stress release and lining-ground interaction analyses were carried out assuming the ground mass was fully drained, with zero pore pressures. Obviously, this does not correspond to reality but it was necessary to use this approximation since the proposed calculation method does not allow an effective stress analysis to be performed with proper consideration of the pore pressure effects. Notwithstanding this, the results obtained with that simplifying assumption compared well with the observed performances. The agreement partly resulted from the fact that, in those cases, the ground was overconsolidated, stiff or dense, and less susceptible to volume changes induced by porewater pressure changes.

In some cases, the method was applied to construction conditions that also departed from those originally admitted. In the Munich 5/9 tunnel, compressed air was used during excavation. In the Sao Paulo North Extension Subway, the tunnel was advanced in stages, using a temporary invert in the heading excavation, which was later removed. These singular operations were accounted for in the calculations, through simplified, yet conscious approximations. In the former, the ground cover was reduced proportionally to the compressed air pressure. In the latter, the support activation delay was calculated assuming that the first stage lining (with the temporary invert) did not deform: lining activation was assumed to occur only after the invert of the completed tunnel section was installed. In the Romerberg tunnel (Frankfurt), the simultaneous construction of the twin tunnels was partly accounted for by superimposing the settlement solution of single isolated tunnel, and neglecting the interaction between the tunnels, on the assumption they were sufficiently far apart. The approximations introduced in these cases were found to be sufficient to make the calculated performance closer to that observed.

In three cases (Butterberg, Bochum and Sao Paulo North Extension), the tunnel profile deviated considerably from the circular section which was assumed in the development of the calculation method. Some of the noted disagreement in these cases (e.g., the underestimation of final crown settlement) could be attributed to this fact.

Having in mind these peculiarities, the overall results obtained can be better assessed through a table summarizing the analyses conducted (Table 7.11). In all calculation results, the overall ground heave component resulting from the trend the opening exhibits to 'float' after the lining is activated (equation 7.10), was neglected. Of course, the heave component prior to lining installation is included in the displacement field provided by the proposed method. The reasons and consequences of this assumption were presented and analysed in Section 7.4.

One notes that most of the cases analysed involved fairly favourable ground conditions (stiff or dense soils), and in all of them fair to good construction quality was ensured. In most cases, the tunnel was driven above the in situ water table (A) or above the lowered phreatic surface (LO). In a few cases, discussed earlier, the tunnel was advanced below the groundwater table (B), without dewatering.

In a large number of cases, the tunnel was built following the so called NATM, using shotcrete as the main support element. In all cases, it was assumed that the lining was solely represented by the shotcrete ring activated at the section where it was closed at the floor, and always considering a Young's modulus of 10 GPa and a Poisson's ratio of 0.2. In the shield driven tunnels, steel ribs and lagging or segmented concrete linings were used. The support systems used in the case studies investigated ranged very widely, from very stiff to very flexible. The flexibility ratio, β, was found to vary, in these cases, from about 0.5 to 0.0014. The compressibility ratio α, on the other hand, varied from about 468 to 4.44. These ranges

Tunnel Case No.	1	2	3	4	5	6	7	8	9	10	11	12
Soil	Clayey-sand	O.C. Kaolin	O.C. Kaolin	Clay Marl	Clay Marl	Till	Sandy Gravel	Till	Hard Marl	Heter. Marl	O.C. Clay	Hard Marl
Water Level	A	B	B	LO	LO	B	A	A	B	A	B	LO
Construction	NATM	Model Test	Model Test	Shield	NATM(a)	Shield	NATM	Shield	NATM-c.air	NATM	NATM	NATM
Lining	Shotcrete	Rubber	Rubber	Segm.concr.	Shotcrete	Ribs&lagg.	Shotcrete	Ribs&lagg.	Shotcrete	Shotcrete	Shotcrete	Shotcrete
β	0.0135	0	0	0.497	0.0303	0.0019	0.0119	0.0055	0.0014	0.0057	0.0042	0.0015
α	51.79	0	0	467.79	89.60	4.44	4.98	10.74	7.67	21.24	18.35	7.73
H/D	1.550	1.670	1.670	1.761	1.775	2.693	1.183	1.442	2.880	1.351	1.138	3.184
Shape	non-circ.	circ.	circ.	circ.	circ.	circ.	non-circ.	circ.	non-circ.	non-circ.	non-circ.	non-circ.
h/w	0.975	1.0	1.0	1.0	1.0	1.0	0.864	1.0	1.077	0.822	0.746	1.104
ϕ_e/Cue:γD	29°/0	0°/0.37	0°/0.37	30°/0	30°/0	40°/0	41.5°/0	40°/0	31.2°/0	35.6°/0	30°/0	31°/0
K_0	0.8	1.0	1.0	0.8	0.8	1.0	0.5	0.75	1.0	0.8	0.9	1.0
Lining activation X/D	0.65			1.10	0.88	1.75	0.826	1.00	0.8	0.7	0.925	1.013
$\bar{I}$ at L.A.	0.471	(0.710)	(0.610)	0.440	0.445	0.434	0.363	0.383	0.508	0.434	0.471	0.490
E_t/E_{ti} at L.A	0.445			0.441	0.448	0.586	0.542	0.573	0.511	0.537	0.409	0.488
E_t/E_{ti} at Equil.	0.449			0.438	0.451	0.505	0.678	0.545	0.431	0.519	0.412	0.399
FS at L.A. (b)	1.437	(1.817)	(1.351)	1.655	1.667	1.767	1.210	1.353	2.010	1.694	1.346	1.910
Extrapolation needed?	Yes	No	No	No	Yes	No	Yes	No	No	No	No	No
Where?	F				F		C,F					
Final U at crown	0.695	0.517	1.065	0.657	0.694	0.648	0.906	0.754	0.578	0.712	0.631	0.616
Surface Settlements												
Max. Magnitude	=	=	=	=	=	=	=	=	=(c)	<	=	=
Max. Distortion	<	<	<	=	=	<	=	<(d)	<	<	<	
Distribution	G	G	R	G	R	P	R	R	G(c)	G	R	
Subsurface Settlements												
Max. Magnitude	=	=	=	=	=	=	=		=	=	=	
Distribution	G			G	P	R	G		P	G	G	
Horiz. Converg. of Liner												
Magnitude	>				=	=	=	>	=			=
Lining Loads												
Aver. Magnitude	>	=	=	=(e)	=	=	>	>	>	=		>
Distribution	R			G(e)	G	R	G	G	G	R		P

Notes:
(1) ABV - Sao Paulo
(2) Centrifuge model test (ε = 29%)
(3) Centrifuge model test (ε = 39%)
(4) Domplatz-Frankfurt
(5) Rom erberg-Frankfurt
(6) Mississauga
(7) Butterberg
(8) Edmonton LRT
(9) Munich 5/9
(10) Bochum
(11) Sao Paulo-North Extension
(12) Munich 8/1
a. Twin tunnels simultaneously driven
b. For actual strength parameters
c. Short term measurement
d. Measurements 3 m below surface
e. Measurements in the 2nd tunnel

Table 7.11 Results of the Application of the Proposed Calculation Procedure to some Case Histories of Shallow Tunnels

entirely cover the spectrum of relative lining stiffness likely to be found in practice (see Table 7.1).

The calculation procedure was tested in tunnels with ratios of cover to diameter ranging from 1.14 to 3.18, and with opening height to width ratio (h/w) ranging from 0.75 to 1.08. The lining activation was assumed to have taken place at 0.65D to 1.75D behind the tunnel face.

The adjusted friction angles of the ground involved varied from 29° to 41.5°. Only in the centrifuge model test a ϕ=0 condition was assumed, and an undrained strength ratio of 0.37 was considered. The in situ stress ratios varied from 0.5 to 1.0.

The calculated amount of ground stress release at lining activation (L.A.) varied from 0.29 to 0.64. Excluding the model tests, the average amount of stress release found in the case histories was 56%. Incidentally, this value compares very favorably with the arbitrary 50% stress reduction proposed by Muir Wood (1975:124) for lining design. At lining activation, it was found that the ratio of average current to in situ tangent ground moduli varied from 0.41 to 0.59. This ratio, at the equilibrium condition, was estimated to vary from 0.40 to 0.68. These findings indicate that for a quick lining-ground interaction analysis, it may be sufficient to assume a 50% reduction in both the ground stresses and in the ground in situ stiffness, provided that the ground control conditions are comparable to those of the present case histories.

The two dimensional stability verifications, at the sections where the linings were activated, yielded factors of safety varying from 1.21 to 2.01, with the median value being about 1.6. It could be said that the proposed calculation method can be successfully applied to predict the performance of a tunnel, whenever this factor of safety is within or above that range. As discussed in Section 2.3.4.3, for this safety range, the ground displacements are small, and high shear strain concentrations in the ground are minimized or avoided. On the other hand, it was shown in Section 2.3.3, that for this range of factors of safety, a non-linear ground response is to be expected. In fact, ground stiffness reductions in the order of 50% were, indeed, calculated in these case histories, despite the good ground control conditions met.

Only in three case histories was there a need to use the extrapolated part of the twice normalized stress release or ground reaction curves. The extrapolation beyond the formal limit of the generalized solution was needed mainly for the tunnel floor. Despite this, the results obtained in these cases were comparable to those where no extrapolation of results was needed.

The final dimensionless crown displacement (U) was found to vary between 0.5 to 1.0, approximately. The latter figure was suggested, in Section 2.3.4.3, as a reasonable bound for crown settlements in tunnels built under good ground control conditions. Thus, quick estimates of the final crown displacement, under these tunnelling conditions, could be performed assuming U=1.0.

The results of the comparisons between measured and calculated performances are presented in Table 7.11 in simple qualitative terms. The same criteria used to evaluate the prediction of performance by the finite element method (Section 5.2.1.2, Table 5.5) was adopted herein. The calculated value is said to approximately equal the measured value (≃), whenever the latter is not more than 20% different than the former. Otherwise the calculated value is said greater (>) or smaller (<) than the measured value. The spatial distributions of displacements or loads were arbitrarily defined as good (G), regular (R) or poor(P), after a liberal comparison between prediction and measurements was made. This qualification is likely to be more subjective and may vary among individuals.

A quick inspection of these results reveals that the proposed calculation procedure consistently yielded unsafe estimates of the maximum surface distortion (the maximum slope of the surface settlement trough). For the other performance aspects, the calculation method provided either a good or a safe estimate. If the calculated maximum distortions (γ_c) are plotted against the observed maxima (γ_o), then the results shown in Figure 7.50 would emerge. If the calculated and observed distortions were equal, the points would be accommodated along the full continous line shown. However, the points that were actually obtained were

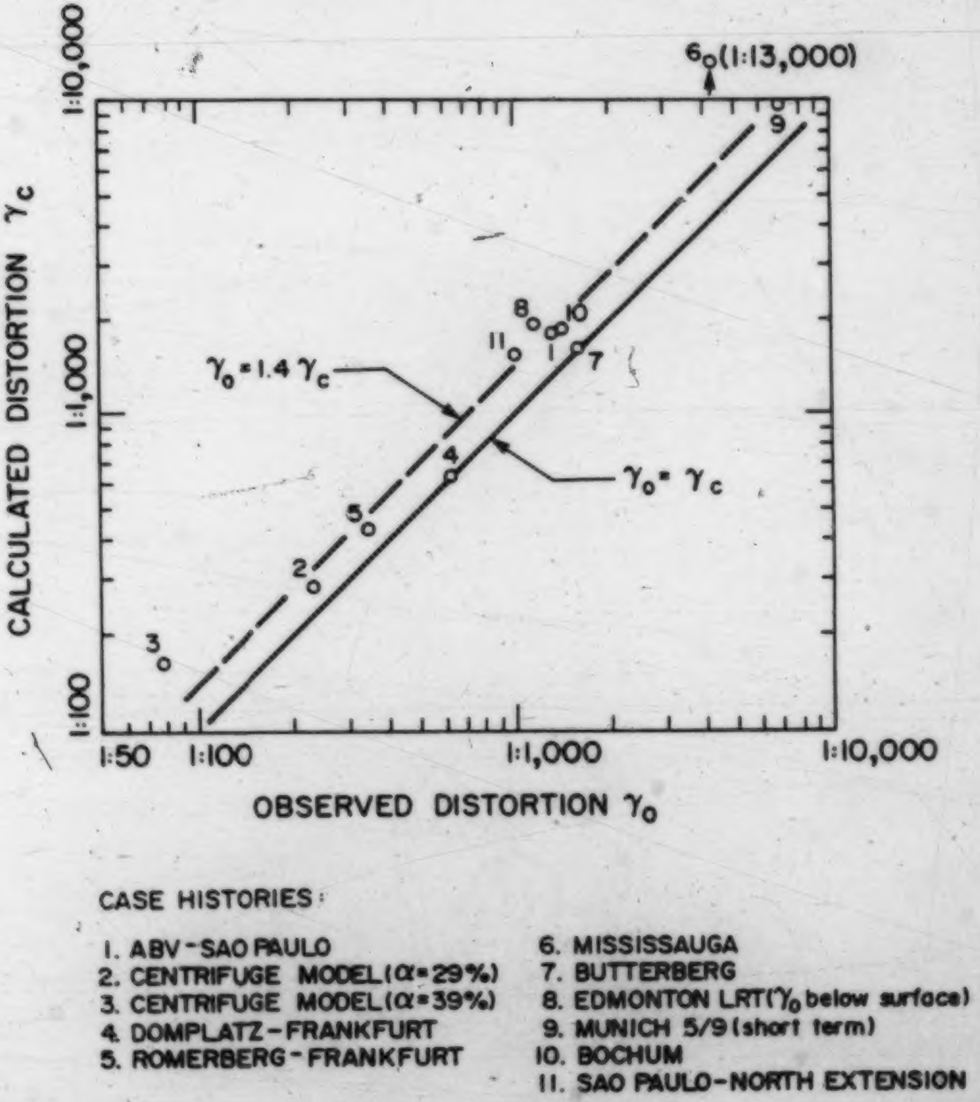

Figure 7.50 Calculated Maximum Surface Distortions Compared to the Observed Maxima

found to lie close to the broken line. This line yields observed distortions which are on average, 40% greater than those calculated. This result was not unexpected, as it reflects a common trend shown by most finite element calculations (see Section 5.2.1.2).

In order to compensate for this effect, it seems advisable to introduce an empirical correction into the calculated distortion (γ_c). The corrected distortion (γ_{cc}) would, thus, be obtained through:

$$\gamma_{cc} \simeq 1.4\ \gamma_c \qquad [7.22]$$

If the above correction was applied to the cases investigated, a better agreement between calculations and observations would be obtained. A possible exception would be case 6 in Figure 7.50. It corresponded to the Mississauga Tunnel, where, as noted in Section 7.5.3.4, some difficulties were experienced in levelling the settlement points in the field.

A pictorial representation of results is given in Figure 7.51. One notes that the calculation method, in the majority of the cases, provided a close estimate of the maximum surface settlement (within a ±20% margin). In only one case (No. 10, Table 7.11), the maximum surface settlement was underestimated. This case (the Bochum Tunnel) involved, however, very peculiar ground conditions (mixed face, heterogeneous profile), that deviates appreciably from the conditions idealized for the application of the calculation method.

The surface distortions were underestimated in 73% of the cases and were never overestimated. In more than half of the cases, the predicted overall distribution of surface settlement was regular or poor. The calculation method tends to furnish settlement troughs which are wider than the observed. This does not seem to be a matter of serious concern, as the theoretical result is safe. Though the criticisms on the use of the error function or normal probability curve are known, it appears that this curve tends to fit actually observed surface settlement profiles better than the distributions proposed by the present calculation method. With this fact in mind, one could suggest a correction on the width of the calculated surface settlement profile, as follows.

The distance (i) between the point of inflexion of the settlement trough and the tunnel axes could be estimated assuming that the maximum surface settlement (S_{max}) is that given by the proposed calculation method, and that the maximum slope of the settlement trough is given by equation 7.22. If the shape of the settlement trough follows a normal probability curve, then:

$$i = 0.606 \frac{S_{max}}{\gamma_{cc}} \qquad [7.23]$$

The width of the settlement trough (w_s) is defined as the distance between the tunnel axis and the point beyond which the settlements are insignificant (i.e., smaller than 4.3% of S_{max}). For a normal probability curve, this point is given by:

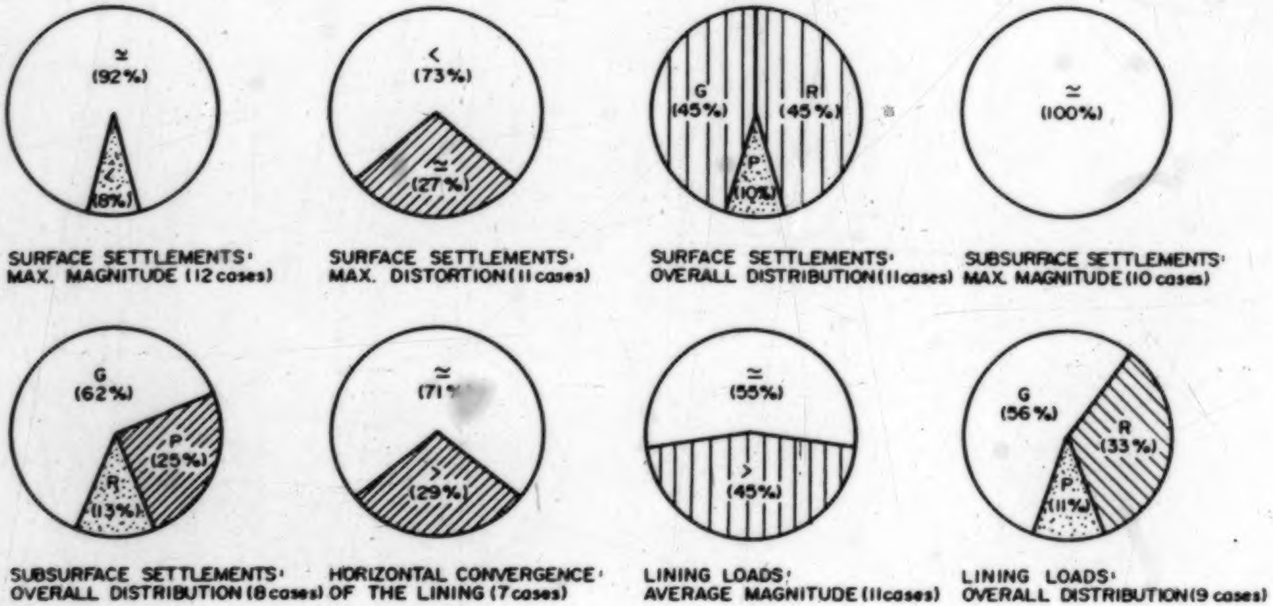

SURFACE SETTLEMENTS: MAX. MAGNITUDE (12 cases)

SURFACE SETTLEMENTS: MAX. DISTORTION (11 cases)

SURFACE SETTLEMENTS: OVERALL DISTRIBUTION (11 cases)

SUBSURFACE SETTLEMENTS: MAX. MAGNITUDE (10 cases)

SUBSURFACE SETTLEMENTS: OVERALL DISTRIBUTION (8 cases)

HORIZONTAL CONVERGENCE OF THE LINING (7 cases)

LINING LOADS: AVERAGE MAGNITUDE (11 cases)

LINING LOADS: OVERALL DISTRIBUTION (9 cases)

Figure 7.51 Calculated Tunnelling Performance Compared to Field Observations

$$w_s = \sqrt{2\pi}\ i$$

therefore

$$w_s \simeq 1.52\ \frac{S_{max}}{\gamma_{cc}} \qquad [7.24]$$

The above semi-empirical correction was tested in the case histories investigated (see Table 7.12) and was shown to give reasonable results. Note that the "measured" trough width is actually an estimated value, based on the measurements available, which in most cases were not extended to a sufficient distance from the tunnel axis to adequately define w_s.

As is also shown in Figure 7.51, the magnitude of the maximum observed subsurface settlement was always closely estimated with the proposed calculation method. The distribution of settlement with depth was good to regular in 75% of the cases. 'Poor' distributions were noted in Case 5 (Table 7.11), which corresponded to twin tunnels simultaneously built and in Case 10, where a heterogeneous ground condition was encountered. For these two particular conditions, it would be expected that the calculated distribution could not compare favourably with the measurements.

Figure 7.51 indicates further, that the horizontal convergence of the lining after its activation was very well estimated in 71% of the cases available. Moreover, the support convergence was never underestimated by the calculation procedure. These results seem to indicate that the assumption that the activation of a shotcrete lining

Case	Tunnel	S_{max}	γ_c	γ_{cc}	w_s	
					Calc.	Meas.
1.	ABV - Sao Paulo	5.4 mm	1:1800	1:1286	10.57 m	10 - 12 m
2.	Centrifuge Test (α = 29%)	8.812 10^{-3}D	1:290	1:207	2.78 D	2.5 - 3 D
3.	Centrifuge Test (α = 39%)	19.68 10^{-3}D	1:167	1:119	3.57 D	2.5 - 2.8 D
4.	Domplatz-Frankfurt	29.4 mm	1:638	1:456	20.37 m	20 - 24 m
5.	Romerberg- Frankfurt	42.5 mm$^{(1)}$	1:425	1:304	19.61 m$^{(2)}$	12 - 18 m$^{(2)}$
6.	Mississauga	2.3 mm	1:13000	1:9286	32.46 m	8 - 11 m
7.	Butterberg	13.9 mm	1:1600	1:1143	24.11 m	20 - 23 m
8.	Edmonton LRT	8.5 mm	1:1933	1:1381	17.92 m$^{(3)}$	15 - 30 m$^{(4)}$
9.	Munich 5/9	3.0 mm	1:9756	1:6969	31.78 m	~ 30 m$^{(5)}$
10.	Bochum	12.2 mm	1:1846	1:1319	24.45 m	20 - 23 m
11.	Sao Paulo - North Extension	16.4 mm	1:1579	1:1097	27.38 m	15 - 19 m

Notes:
(1) Over 1st tunnel driven
(2) Measured on the outer sides of the twin tunnels
(3) At ground surface
(4) 3 m below surface
(5) In short term
(6) γ_{cc} calculated through equation 7.22
(7) w_s calculated through equation 7.24
(8) w_s is the half width of the full surface settlement trough

Table 7.12 Calculated and Measured Widths of the Final Surface Settlement Profiles in Some Case Histories

takes place at the section where it is closed at the tunnel floor, is a reasonable one. Additionally, they tend to confirm that, under this assumption, the arbitrary shotcrete modulus of 10 GPa adopted, combined with the assumption of no contribution of the steel ribs to the relative stiffness of the lining, are also reasonable approximations.

It is difficult to perform an accurate assessment of the ability of the proposed method to estimate lining loads. This is mainly due to the fact that in most cases, contact pressure cells were used to measure the ground loads acting on the support. Depending on the installation procedure, this type of instrument is known to either overestimate or underestimate the actual contact stresses (see, for example, Hanna, 1985:205). A special class of problem arises when pressure cells are used in concrete - soil interfaces, and is related to the heat generated during the setting of fresh concrete (Hanna, Op.cit.:444). Due to these facts, it was decided to compare "average" lining loads, in the hope that the over-reading and the under-reading errors would balance each other. In terms of these qualitatively estimated average lining loads obtained from field measurements, it was noticed (Figure 7.51) that the calculation procedure either matched these loads or overestimated them. Large average load estimates (up to 50%) were noted in the Butterberg and in the Munich 8/1 Tunnels, where Maihak and Glotzl cells were used in the soil-shotcrete contact. This result may be associated with the formation of gaps between the cell and the concrete after the concrete temperature dropped (the full contact might have been lost at the interface). On the other hand, this effect may have not been present at the Munich 5/9 tunnel, where specially designed load cells were embedded in the shotcrete. Even so, the lining thrusts in this case, were also overestimated by 20 to 50%.

Actually, the proposed calculation procedure was developed in such a way that it may indeed, lead to overestimation of the lining loads. Firstly, as explained in Section 7.2.2, the use of the final equilibrium ground stiffness, defined at the point of equilibrium, will normally lead to higher loads, unless the in situ stress ratio is low and the outward lining displacement at springline is appreciable. This was the case in the Butterberg tunnel, where the overall ground stiffness increased from the instant of lining activation to equilibrium (see Table 7.11). Secondly, if the tunnel closure at the instant of lining activation is large, the combination of the 3D elastic solution for closure estimate, with the 2D non-linear elastic solution for the stress release estimate, may also lead to estimating higher lining loads. With regard to this aspect, an improvement on the closure estimate solution would be beneficial, particularly for cases where the delay in the lining activation is large. For activation at sections more than 1.5D behind the face, the 3D closure solution furnishes radial displacements which are basically independent of that distance. Hence, for distances greater than 1.5D, the tunnel closure is virtually constant and the resulting amount of stress release is also constant.

In reality, for most soils, the tunnel closure will increase if lining activation is delayed more than 1.5D. The failure of soil elements around the opening will increase the radial displacements and further reduction of the ground stress is attained, before a collapse condition emerges. This additional reduction in the ground stresses cannot be represented by the present calculation procedure, unless another solution for the tunnel closure is developed (including the ground non-linear response) and is coupled to the 2D ground stress release solution. In its present form, the proposed procedure will tend, for these conditions, to estimate smaller tunnel closures and higher lining loads. This limitation of the proposed method was discussed earlier in Section 5.3.7, where the problem was exemplified through the Edmonton Experimental Tunnel case, where the lining was activated at a section more than 2D behind the face. Fortunately, in most cases (See Figure 6.37) and under good ground control conditions, this distance is less than 1.5D.

Also not assessed in the lining load estimate evaluation are the effects of the tunnel shape, and the differential soil stiffness degradation around its contour. It seems interesting to explore these two aspects in future research. The second factor could, perhaps, be investigated using a ring and spring calculation model, where the spring moduli would vary from point to point along the tunnel profile, according to the stiffness provided by the generalized solution developed in Chapter 6 (the λ' curves, for instance).

Finally, it should be pointed out that the overall results obtained in this chapter with the proposed calculation method, are equivalent to those obtained by the finite element modelling exercises reviewed in Section 5.2.1.2. In fact, if the diagrams shown in Figure 7.51 are compared to those presented in that section, it would be noted that the proposed procedure presented improved results. Using the same point rating criterion referred to in Section 5.2.1.2, to evaluate the quality of the prediction, some of the analyses summarized in Table 7.11 top ranked and none showed results below the average.

7.6 Summary and Conclusions

In this chapter, the soil-lining interaction phase of the shallow tunnel problem was addressed. A simple linear elastic analytical model was selected to study this interaction in a two dimensional representation. The preference towards a ring-and-plate solution was justified, and of these, Hartmann's (1970, 1972) closed form solution was favoured as it is the only one that makes full allowance for the non-uniform stress field existing in a shallow tunnel.

The assumptions involved in the soil-lining interaction solution were described and the main aspects of its derivation were discussed. The relative stiffness of the lining to the ground mass was expressed through two coefficients, the compressibility ratio (α) and the flexibility ratio, (β). Typical values for common linings and soils were given. The closed form solution was presented in an abbreviated form (Figure 7.2) and its significance was assessed.

The selected analytical solution assumes the ground to be represented by an infinite plate under a gravitational stress field. The consequences of this assumption were investigated, by comparing the results of the analytical solution with that obtained from finite element analyses of a shallow tunnel. Since in both cases the action of gravity is included, the differences in the results could be attributed to the influence of the ground surface, if the numerical inaccuracies are ignored. Numerical and analytical solutions were found to yield similar results for cover to diameter ratios greater than 1.5, which confirms the discussions presented in Section 2.2. Moreover, the analytical solution furnished conservative estimates of the lining response for smaller H/D ratios. Some of the discrepancies noted were attributed to the procedure adopted in the analytical solution used to account for the overall ground heave (the trend exhibited by a shallow tunnel to "float").

In order to account for the effects of the delayed lining installation in the soil-lining interaction analysis, the use of the analytical solution had to be adapted. The first effect resulting from a delayed lining activation is the reduction of ground loads and this was introduced through the use of a reduced unit weight for the soil (equation 7.14). Though this artifice may be valid for linear elastic materials, for a non-linear elastic ground it is understood to be an approximation. The second effect, resulting from a delayed support installation, refers to the degradation of the soil stiffness, associated with the tunnel closure developing before the lining is activated.

The reduction in the unit weight of the soil, can be assessed through the twice normalized ground reaction curves (λ curves) derived in Chapter 6, once the radial displacements of the tunnel contour at the instant of lining activation are known.

The degradation of the soil stiffness can be assessed through the derivative functions of the twice normalized ground reaction curves (λ' curves). An important assumption then had to be made: the tangent stiffness of the ground was assumed to be uniquely related to the tunnel radial closure (U), through the derivative functions presented in Section 6.4. The implications of this assumption were assessed and discussed.

To evaluate the ground stress and stiffness reductions associated with the delayed support activation, the twice normalized support activation, and their derivatives, at different points of the tunnel contour, are assumed to have an independent existence. In other words, the sequence of loading or closure at different points of the opening profile, is assumed to not affect the response noted at any other point of the contour. The approximation involved in this assumption is minimized when the stress ratios (Σ) or the tangent stiffnesses (E_t) obtained indepently for each point of the tunnel profile, are averaged.

To assess the consequences of the preceding simplifying assumptions, the proposed procedures for ground stress and stiffness reductions were tested against the results of 2D non-linear elastic finite element analyses, where different amount of stress release, representing varying degrees of delaying the support activation, were imposed prior to the lining installation. Accordingly, the closed form solution was used, coupled with the generalized solutions for ground reactions derived in Chapter 6. Through these solutions, an average tangent stiffness of the ground, at the instant the lining is installed, could be estimated. This value and the reduced soil unit weight, were used in the lining-ground interaction analysis. The ground loads onto the support at equilibrium, were found to be underestimated by this calculation procedure. This resulted from the assumption that the ground stiffness remains unchanged during the interaction process. The additional soil stiffness degradation, upon further closure of the now lined opening, would necessarily imply that increased lining loads would exist on the support.

A better and safer assumption would be to assign the ground its stiffness as defined at final equilibrium. This, however, is not known, as the incremental closure of the opening after lining installation is unknown. To solve the problem, an iterative procedure was devised, in which the average ground stiffness is updated after each iteration. The process is repeated until convergence is obtained, which required not more than five iterations. With this algorithm, the calculation procedure was repeated and new ground loads acting on the lining were found. As expected, loads higher than those previously obtained were calculated. More importantly, these resulting ground loads were slightly higher than those given by the finite element analyses. Moreover, the radial displacements of the lining were closely estimated by the approximate analyses, except at the tunnel floor where the displacements were overestimated. This was attributed to an overestimation of the ground heave at points below the tunnel in the analytical approach.

Briefly, the approximate solution developed by coupling the generalized solution for the ground response developed in Chapter 6, with the closed form solution for the lining-soil interaction analysis, furnished reasonable (and safe) estimates of the lining-ground equilibrium condition, both in terms of final stresses acting on the lining as well as final tunnel closure.

The parametric analyses presented in Chapter 6 considered the tunnel to be unlined and, therefore, the resulting normalized settlement distributions disregard the influence of a lining on the ground movements. The influence on ground displacements that a lining has, when installed after allowing some stress release in the ground, was evaluated through the results of the non-linear elastic finite element analyses just discussed. The final settlement distributions obtained for the lined and unlined tunnel cases, were compared by estimating the amount of stress release required in each case to produce the same crown settlement. It was found that the unlined tunnel analysis causing an equal crown displacement, furnished settlement distributions similar to those obtained for the lined cases, and slightly higher settlement magnitudes. In other words, by neglecting the presence of the lining, conservative estimates of the ground settlements above the tunnel are found. Accordingly, the normalized distributions presented in Appendix C, can be used in practice, since it is sufficient to calculate the amount of stress release in the unlined tunnel solution, which causes the same crown settlement obtained in the lining-ground interaction analysis. That amount of stress release is easily obtained through the normalized ground reaction curve for the tunnel crown.

As a result of the above analyses and verifications, a calculation sequence emerged. It was possible to produce a flow chart, to guide the application of the presently proposed design procedure (Figure 7.9). Its main sequential steps involve:

a) The assessment of the geometric conditions of the problem;

b) The evaluation of the geological and geotechnical aspects involved, including the definition of ground parameters;

c) The assessment of the construction technology to be applied, including details of the support system;

d) The assessment of the applicability of the proposed design procedure, including the anticipation of likely ground conditions to be encountered (risk of collapse, drained or undrained ground responses, soil volume changes, etc);

e) The evaluation of the pre-support ground response (tunnel closure, amount of stress release, ground stiffness change, ground stability verification, etc);

f) The analysis of the lining-ground interaction including the calculation of thrust forces and bending moments, lining distortions, etc;

g) The prediction of the ground movements, including final tunnel closure, subsurface and surface settlements, and maximum ground distortions.

The results obtained in each step, from (e) to (g), should be interpreted accordingly and their acceptability verified. If the results obtained after any step are not acceptable (e.g., unstable pre-support response, excessive lining loads, excessive ground movements), then the construction technology should be reviewed and modified. If the anticipated tunnel performance is acceptable, then construction follow-up and monitoring are carried out, and the data collected are used for feed-back in each design step, as an on-going process, as part of an observational design approach.

Details of each design step were discussed and analysed. Special attention was given to the formal range of applicability of the proposed calculation method: absence of ground heterogeneities (mixed face conditions, for instance), absence of ground collapse, good lining contact, time independent ground response, limited ground volume changes, etc. Whenever possible, quantitative criteria were proposed to define the conditions for application of the method.

When the proposed method is applied to actual design problems, sensitivity analyses should be undertaken, so that the variability of the ground conditions are assessed, ranges of variation of soil properties are covered and the variabilities of the construction procedure are accounted for. The method can therefore be used in connection with a probabilistic design approach, and expected ranges of ground and lining responses can be defined.

All the calculations involved are simple and easy to program. The entire procedure can be implemented in a small micro-computer, allowing quick on-site re-evaluation of any design step during the tunnel construction. The method can be applied and calibrated concurrently with field monitoring, thereby serving as an auxiliary tool for decisions being made during construction.

In order to facilitate some of the calculations involved in the application of the design sequence described, a set of calculation sheets was prepared. A complete example of the use of the proposed design procedure was presented. Each design step was covered in detail, for a particular case history (The Alto da Boa Vista Tunnel). The use of the normalized design charts presented in Chapter 6 was exemplified. The lining-ground interaction analysis was conducted using two separate assumptions regarding the overall ground heave taking place after lining installation. Firstly, the ground heave was calculated and incorporated into the method, according to the original formulation of the analytical solution. It was shown that the heave estimate entails an indeterminate degree of approximation, normally leading to an excessive estimation of this ground movement. Secondly, the design procedure was applied assuming that this ground movement component was negligible. It was then shown that the ground heave does not influence the lining loads, but it does affect the radial displacements at floor and crown, and consequently the settlement distribution above the tunnel. A comparison between the calculated settlements using the two assumptions and the ground displacements measured in the field, revealed that the zero heave assumption leads to slightly conservative estimates of field settlement.

The proposed calculation method was verified against the results of a plane strain centrifuge model test of a shallow tunnel under undrained conditions, carried out by Mair (1979). For that, the frictionless soil model solution, developed in Chapter 6, was used. The calculated responses in terms of the ground reaction curve and surface settlements compared very favourably with the test results. The proposed calculation method proved, however, to furnish progressively poorer predictions of the maximum distortion of the surface settlement trough, as collapse was approached in the test. Nevertheless, as noted in Chapter 5, this result was expected.

The proposed procedure was then compared with the results of a 3D finite element analysis. The latter was carried out by Katzenbach (1981), who used a hyperbolic stress-strain relationship to represent the soil behaviour. Details of the 3D analysis were summarized and the results of the comparison were discussed. Again, the proposed method yielded sensible results which compared very favourably with the 3D analysis results.

Finally, the proposed method was verified against a large number of actual case histories. The latter were selected according to the availability of adequate or sufficient field instrumentation data. Intentionally, the case studies selected always exhibited good ground control conditions, reflecting either good construction practice and/or good quality ground. Ground instabilities or local collapses were not reported in any of the cases investigated. To test how the method would perform in actual practice required the inclusion of some cases with complex conditions which deviated considerably from those originally set up in the method development. These conditions were represented by tunnelling below the water table with partial consolidation of the soil mass, construction involving the use of compressed air, staged excavation of the tunnel face with a temporary invert in the heading excavation, non-circular tunnel profiles, etc. Additional assumptions and approximations had to be incorporated in order to deal with these distinct features. Despite this, the calculation method yielded sensible results, in terms of both the ground and the lining responses.

It should be remembered that in all applications of the method, no attempt was made to best fit or bound the observed performances. These tests were not back-analyses of case histories, as it was assumed that all parameters and variables governing the tunnel response were known and would represent the most probable conditions found in each case.

The results of the verification tests were put together (Table 7.11) and the overall ability of the proposed calculation procedure to predict actual tunnel performance was generally appraised.

A global inspection of the range of conditions covered in these tests was undertaken. The tests covered both shielded and unshielded tunnel construction, different support systems and lining stiffnesses, a wide range of geometric conditions and a fairly wide range of soil types.

The output revealed that the amount of stress release at lining activation ranged from 29 to 64%, with an average of 56%. This value compares favourably with Muir Wood's (1975:124) arbitrary reduction by 50% of the in situ stress, suggested for lining design. The reduction in the ground stiffness resulting from the ground stress relaxation was found to vary from 32 to 60%. These findings indicate that, for a quick lining-ground interaction analysis, it may be adequate to assume a 50% reduction for both the ground in situ stresses and the in situ (tangent) ground stiffness, provided the ground control conditions are comparable to those found in the cases studied.

The two-dimensional stability verification, at the section where the linings were activated, yielded factors of safety varying from 1.2 to 2.0, with the median value being about 1.6. It was suggested that the proposed calculation procedure seems to provide reasonable predictions of the tunnelling performance, whenever this factor of safety is within or above that range. Tunnel model test results reviewed in Section 2.3.4.3 indicated that, for this range of safety factors, the ground displacements are usually small and that high shear strain concentrations in the ground are minimized or avoided.

The final dimensionless crown displacement (U) was found to vary between 0.5 and 1.0. The latter figure was suggested, in Section 2.3.4.3, as a reasonable bound for the crown displacement in tunnels built under good ground control conditions. Hence, quick, and possibly, conservative estimates of the final crown displacement under these tunnelling conditions, could be performed by making U=1.0.

The results from the comparisons between calculated and measured performances were presented in simple qualitative terms, following a similar criterion introduced earlier in Section 5.2.1.2. The worst result obtained was related to the maximum ground surface distortions, which were, in more than two-thirds of the cases, unsafely estimated by the proposed calculation procedure. Using the results found, a correction factor was empirically introduced, which indicates that the calculated maximum distortions should be increased by 40%, in order to make them closer to the measured values (see Figure 7.50).

A similar trend was noted regarding the width of the surface settlement profile since the calculation method usually led to troughs wider than the observed. Once more, in order to make the estimated widths closer to the observed, a semi-empirical correction was suggested (equation 7.24). This was tested in the case histories investigated and furnished reasonable results.

The results of this comparative study were then summarized in graphic form (Figure 7.51), where it was shown that the calculation method did furnish good estimates of the maximum surface and subsurface settlements and of the lining convergence. Some difficulties were found in interpreting the results of lining loads. To a large degree, this was due to the fact that most of the lining load measurements were taken with contact pressure cells, and the difficulties associated with this type of instrument are fairly well known. However, it was shown that the proposed calculation procedure, furnished lining loads which either matched the average lining loads measured or overestimated them by up to 50%. Although this figure cannot be taken as definitive, as the accuracy of the measurements can be questioned, especially in shotcrete-soil contact, the noted trend of the calculation method to overestimate lining loads was discussed and explained. Possible improvements on this aspect were discussed and suggestions for future research work on the subject were addressed.

8. CONCLUSIONS

The present research work dealt with the design of shallow tunnels in soil. In an attempt to avoid redundancy, this chapter reviews only the main points and conclusions of the work and the reader is referred to the summaries presented at the end of each chapter for a condensed, yet comprehensive review of all studies undertaken.

The aims of the research were presented in Chapter 1. They included attempts to:

a) identify unsolved or partly solved problems that affect existing practice;

b) more adequately appreciate the mechanisms involved in the soil and in the behaviour of the supporting structures, identifying the controlling parameters, whenever possible;

c) develop procedures to solve these problems and consequently to propose a new design method;

d) summarize the results of the research work in a comprehensive manner and in a way that may be used by the practitioner;

e) validate the results of the research by application o practical problems and defining ranges of validity.

Point (a) above was briefly addressed in Chapter 1 and more thoroughly in Chapter 4. The surveys presented in Chapter 4 revealed that there was no adequate and simple method to couple lining loads and ground settlement predictions. They also revealed that no satisfactory procedure was available to sensibly account for the effects associated with delaying the activation of the support. These effects are mainly represented by the ground stress relaxation and by the ground stiffness degradation. The importance of such effects seems to be recognized by many. However, since no sensible criteria were available to account for them, the practitioner was compelled to adopt extreme assumptions. Examples of these include the 'full overburden' and partial ground embedment assumptions in lining design, or the assumption of full ground stress release for settlement predictions. With these conflicting assumptions, the design ceases to be an exercise of anticipating the 'most probable' performance, with allowance for adequate safety margins. Instead, it becomes an activity of bounding possible tunnelling performances, which makes the assessment of the safety margins more difficult.

Point (b) was comprehensively addressed in Chapters 2 and 3, where the soil tunnel behaviour was studied through idealizations exemplified by available theoretical and experimental modelling tools and supplemented by observational evidence from prototypes. Through this activity, some of the parameters controlling the behaviour were identified. Soil tunnels in urban environments are designed under requirements that lead to conditions where collapse mechanisms are usually avoided. Accordingly, most of the discussion was confined to the behaviour in pre-collapse stages.

Although urban tunnels are usually designed for and built under 'good ground control' conditions, it was shown that the factor of safety against ground collapse is fairly low, typically 1.2 to 1.7. Moreover, it was shown that for these low safety factors, a non-linear response in terms of ground stress and strain relationships should always be expected. Considerable departures from linear responses were noted in model and prototype behaviour whenever the factor of safety was less than 2 to 3.

A reasonably clear relationship appears to exist between the factor of safety and the dimensionless displacement (U) of the tunnel crown. An interim criterion, based on results of plane section model tunnel tests, was proposed to define a 'good ground control condition', for which the ground movements are generally acceptable and ground collapse is precluded. The test results indicated that near collapse conditions are generally met when U is greater than 1.8 and that values smaller than 1.0 would represent a 'good ground control condition'. Although tentative, this criterion proved to be sensible and to have potential use in practice.

Another tentative criterion was derived from the above. It refers to the limiting dimensionless crown displacement increment for ground movement into a void space behind the lining, which might produce a near collapse ground condition. This dimensionless movement was suggested as equal to 1.0. From this, one may define a maximum crown overcut in a TBM excavated tunnel. Once more, this is a tentative criterion which may be improved in the future, by further data collation and interpretation and by experimental and theoretical modelling.

It was illustrated that if the overcutting is excessive and the ground displacements are large, 'gravity loads' may act on the lining and that its response may not be predictable. To avoid this condition, a 'good' lining-ground contact should be ensured and ground movements should be limited to levels below those associated with a near collapse stage. A speculative discussion was attempted to analyse the consequences of the development of uncontrolled ground deformations and the associated ground 'loosening' process. A conceptual model was proposed and the need for experimental or theoretical investigations to confirm it, were suggested.

Although of some value at the design stage, the above criteria of limiting displacements may be of little help during construction. For this, a criterion for ground stability assessment in the field was suggested, which is based on the interpretation of longitudinal ground distortions from displacements measurements at points above the tunnel crown.

While the present work focuses on the ground response under time independent conditions, it was felt necessary to analyse the role of groundwater on the ground behaviour. Among others, the effect of pore pressure generation and dissipation on tunnel stability was addressed for idealized conditions. The difference in the soil response to that observed in other geotechnical structures was explained by the existence of a different intervening parameter: the degree of stress relaxation. Moreover, this analysis illustrated the practical need to identify the ground response in either undrained or drained terms. Examples of how to anticipate these responses were given through approximate criteria derived from simplified theoretical analyses. The need to extend these approaches was suggested.

Another feature studied, still within point (b), was the three-dimensional arching and ground-lining responses associated with the tunnel advance. The stress-displacement responses for points around the tunnel contour were reviewed, as well as some evidence of the three-dimensional stress transfer effects. The role of some of these effects in controlling the tunnel lining design has not been clearly established, for instance, load concentrations or longitudinal bending of the support. Further investigation of these aspects would be of considerable interest, bearing in mind their potential consequences.

After assessing points (a) and (b) described earlier, point (c) was addressed mainly in Chapter 5. To solve this problem, detected in current practice, it was decided to develop an integrated procedure that would allow lining load predictions and settlement estimates taking into account some of the most important factors controlling the tunnel behaviour. These are:

1. the effect of the relative position of a horizontal and stress free ground surface;
2. the action of gravitational body forces generating a stress gradient in the soil across the tunnel profile;
3. the non-uniformity of the in situ stresses generated by a horizontal to vertical stress ratio different from unity;
4. the non-linear response exhibited by soils in terms of their stress-strain relationships, including the dependence on hydrostatic and deviatoric stress levels;
5. the delayed activation of the lining generating ground movements and associated stress and stiffness changes in the ground, prior to support application;
6. the interactive nature of the load transfer process developed between the soil and the support.

The decision to include these factors in the development of the projected design procedure lies in the fact that they have an important role in most, if not all, shallow tunnel cases. Those factors, that are sometimes influential in one instance but not in others, had to be set aside, and, perhaps studied separately.

Accordingly, in order to render the problem tractable and yet to ensure some generality, it was decided to limit the development to full face excavated circular tunnels, under time independent conditions, in situations not involving ground failure, shear dilatancy and post peak softening, among others.

The finite element method was selected as an appropriate modelling tool to derive the projected method. A fairly extensive review of previous studies on shallow tunnel modelling using that method was undertaken. Through it, the ability and limitations of this method to portray shallow tunnel performance was critically assessed. This review led to the adoption of a simple two dimensional finite element code developed and tested earlier in this University for analyses of retained excavations. The program was adapted and implemented for the present project, where the soil behaviour is described by a non-linear elastic stress-strain relationship (the hyperbolic model).

Through this program, tunnel construction is represented in stages and the delayed lining installation and associated stress transfers are represented by a partial release of the ground in situ stresses. This two dimensional simulation mimics the three-dimensional stress changes by the introduction of an additional variable, the amount of stress release, α. Three well documented case histories in which good ground control conditions were present, were used to test this numerical solution. It was proved that good estimates of the final displacement field and lining loads are obtained whenever the factor, α, is appropriately selected. Like similar codes, this program seems useful only for the prediction of pre-failure responses. It is evident that there is a need to develop numerical modelling techniques that portray the ground response for conditions approaching collapse with the formation of shear strain concentrations.

The main limitation of the selected simulation technique is the need for an independent estimate of the amount of stress release taking place before support activation. However, if this stress release was univocally related to the ground displacement, then an estimate of the latter, including the three-dimensional effects of an advancing tunnel, could be sought as an alternative approach to the solution of this problem.

The need to develop a procedure to estimate the amount of tunnel closure at the section at which the support is activated was thus justified and undertaken through parametric three-dimensional finite element analyses. An approximate solution for estimating the closure of an unlined shallow tunnel in an elastic medium was proposed. It allows estimates of radial displacements at three points of the tunnel contour, for different sections at or behind the face. These analyses also allowed simplified solutions to be obtained for estimates of the maximum horizontal displacement of the tunnel face and of the maximum longitudinal distortions for the ground surface and the subsurface ahead of the face.

This approximate method for estimating convergence was used to predict radial displacements for comparison with observed values in a large number of case histories. It was shown that it can yield sensible results whenever good ground control conditions are specifed and implemented in tunnel construction. Furthermore, it was shown that the method can be successfully applied to NATM construction schemes regardless of the soil type (but provided the face is stable), and to TBM or shielded schemes in firm grounds or even in less stable soils, whenever the overcut is small and the lining is activated in full contact with the ground at a short distace from the face. For conditions different from the above, the simplified method yielded poorer results. Improvements to its predictive capabilities could be attempted in the future by incorporating the non-linear ground behaviour and by accounting for the support installation, both of which are presently neglected.

To validate the proposed approach, the above approximate method was tested against results from the two dimensional modelling of the three case histories studied. By combining the estimates of the radial displacements at the tunnel contour from this method, with ground reaction curves obtained by the two dimensional modelling, reasonable estimates of the amount of stress release at the instant of lining activation were obtained.

The above approach requires the use of a 2D finite element program to generate stress-displacement curves from which it is possible to assess the amount of stress release. The survey of practice presented in Chapter 4 showed that this may represent an inconvenience since this type of analysis is not always used in routine practice. Accordingly, an attempt was made to develop a procedure which would allow these stress-displacement relationships to be obtained without the need for further finite element analyses. Parallel to this development, an attempt was made to obtain the relevant ground displacement associated with the reduction of the ground stresses, representing the tunnel construction in a two-dimensional simulation.

To achieve these aims, some additional simplifications were introduced into the 2D finite element model presented in Chapter 5. These simplifications led to the establishment in Chapter 6 of two non-linear elastic stress-strain models: the frictionless model representing an undrained soil response, and the cohesionless soil model representing a drained response. These models exhibit stress-strain relationships presenting the property of homothety, which allows these relationships to be normalized into unique stress-strain curves. Moreover, this property causes the response of geometrically homothetic tunnels to become unique when this response is conveniently normalized. These findings facilitated the generalization of results through the similitude they show, as they become independent of the scale of the problem.

Through parametric numerical modelling, the role of each variable affecting the response of unlined tunnels was investigated. Finally, generalized normalized ground reaction curves (NGRC or λ curves) were obtained for points at the crown, springline and floor of a shallow tunnel, and were presented as equations and charts. The limits of this generalization were identified. The partial derivatives of the NGRC (λ' curves) were related to the ground stiffness at any stage of the tunnel unloading process. The two sets of curves (λ and λ') thus allow estimates of the amount of ground stress relaxation and ground stiffness degradation for any amount of tunnel closure defined by the dimensionless radial displacement, U, taking place at the section where the support is activated. These solutions allowed such estimates to be made for ranges of geometric and geotechnical conditions that were shown to cover most of the cases likely to be encountered in practice. The solutions also permitted some extrapolation of data beyond the ranges of conditions which had been focused on, though considerable care should be taken in this regard.

Parallel with the development of these generalized solutions, normalized subsurface and surface ground displacement distributions were obtained for different amounts of stress relaxation associated with a given amount of tunnel closure.

The soil-lining interaction phase of the shallow tunnel problem was addressed in Chapter 7. Once more, to avoid the need of finite element modelling in the development of the projected design procedure, preference was given to the use of a linear elastic, closed form solution that treats this problem, with full account of the non-uniform stress field existing in a shallow tunnel, including the effect of gravity. This analytical solution was adapted to take into consideration the effects of the delayed lining installation, represented by the stress relaxation and ground stiffness degradation. These were accounted for through the use of a reduced unit weight of the soil and a reduced ground stiffness, calculated from the normalized ground reaction curves and their derivative functions. The tangent stiffness of the ground was assumed to be uniquely related to the tunnel radial closure. This and other simplifying assumptions were carefully assessed and their consequences evaluated through 2D finite element simulations.

It was demonstrated that adequate and safe estimates of final lining loads and displacements can be obtained by combining the generalized solution for non-linear ground response, with the analytical solution for soil-lining interaction. For this, it is sufficient to estimate the ground stress relaxation prior to lining activation and the ground stiffness at the final lining-ground equilibrium condition. Since the equilibrium condition is not known beforehand, a simple iterative procedure was devised to solve this problem.

The present development could also be of some help, if, alternatively the soil-lining interaction analysis were done through the use of ring - and - spring solutions reviewed in Chapter 4. With them, the non-uniform degradation of the ground stiffness around the tunnel contour could be taken into consideration.

Regarding the effect of the lining on the ground movements, parametric finite element studies revealed that the unlined tunnel analyses, with a crown displacement equal to the final crown settlement calculated in the lined tunnel case, furnished settlement distribution similar, yet slightly conservative, to those found in the latter case. Thus, the normalized settlement distribution obtained in the parametric analyses can be used for settlement prediction. It is sufficient to calculate the amount of stress release in the unlined tunnel solution, causing the same crown displacement obtained in the lining-ground interaction analysis. This is easily assessed through the generalized ground reaction curves for the tunnel crown.

With these developments, the aims described in point (c), given earlier in this chapter, were fulfilled. The following point, (d), required that the findings accumulated so far be organized in a comprehensive manner to enhance their use in practice. Appropriately, a flow chart was prepared to serve as a guide for using the presently proposed design procedure (Figure 7.9). Each step of the procedure was presented and discussed, with emphasis being given to the assessment of its applicability.

Moreover, to facilitate the calculations involved in the design sequence suggested, a set of calculation sheets was prepared, and an example was worked. It was shown that all calculations are simple and easy to program, therefore allowing quick on-site re-evaluation of any design step during tunnel construction. Thus, the method can be applied and calibrated simultaneously with field monitoring serving as an auxilary tool for decisions being made during construction. Furthermore, at the design stage, the method allows sensitivity analyses to be undertaken, where the variability of ground conditions, construction procedures, geometric conditions, etc. can be taken into account. Accordingly, the expected ranges of ground and lining responses could be defined. The last point to be addressed, (e), referred to the validation of the proposed design procedure. This was also undertaken in Chapter 7, where the method was verifed against results of plane strain centrifuge model tests of a shallow tunnel. It was also tested against available results of a 3D finite element analysis in which the ground was represented by a hyperbolic stress-strain relationship. In both cases, very favourable results were obtained.

Finally, the proposed method was verifed against a large number of actual case histories. These always involved good ground control conditions, reflected either by good construction quality or simply good ground quality. In order to test the performance of the method in actual practice, some of the case histories included conditions that deviated considerably from those originally set up in the development of the method. These conditions were represented by tunnelling below the water table with partial consolidation of the soil mass, construction involving the use of compressed air, staged excavation of the tunnel face with a temporary invert in the heading excavation, non-circular tunnel profiles, mixed face conditions. Additional approximations were introduced to account for these distinct features. Despite this, the calculation method yielded sensible results, both in terms of ground and lining responses. Noted discrepancies were duly explained in terms of the limitations of the method.

It should be pointed out that in all applications, no attempt was made to best fit or to bound the observed performances. These tests were not back analyses of prototypes, as it was assumed that all parameters and variables governing the tunnel response were known and supposedly represented the most probable conditions found in each case.

A global assessment of the results obtained was undertaken and the ability of the proposed procedure to predict tunnel performance was carefully investigated (Table 7.11 and Figure 7.51).

This comparative exercise covered both shielded and unshielded tunnels, different support support systems and lining stiffnesses, a wide range of geometric conditions and a fairly wide range of soil types. This study revealed that for a quick lining-ground interaction analysis, it may be sufficient to assume a 50% reduction in the ground in situ stresses and in the in situ tangent ground stiffness, provided the ground control conditions are comparable to those found in the cases studied.

It was suggested that the proposed calculation method seems to provide reasonable predictions of the tunnel performances, whenever the factor of safety of the ground at the section the support is activated, is within or above the calculated range factors found in these cases (from 1.2 to 2.0). The final dimensionless crown displacement, U, was found to vary between 0.5 and 1.0, and according to the criterion set up earlier in Chapter 2, this confirms that ground control conditions were good and high shear strain concentrations in the ground were minimized or avoided. It was suggested that quick, and possibly, conservative estimates of the final crown displacement under these tunnelling conditions, could therefore be performed by making U=1.0.

Except for the width of the settlement trough or the maximum ground surface distortion, the proposed design procedure yielded performance predictions that either matched or overestimated the observed behaviour. The surface distortions were underestimated in the majority of cases. To compensate for this not unexpected and unsafe trend, a correction factor was empirically introduced. Accordingly, a semi-empirical correction was also suggested for the assessment of the width of the surface settlement profile. In both cases, the proposed corrections improved the predictions, making them closer to the observed performances.

With this, the aims of the present research project have been fulfilled. Suggestions for future research work have been presented in this chapter and in the summary sections of other chapters. Moreover, it is believed that the present approach could be extended to other conditions not covered by this work, such as twin tunnels and non-circular tunnel profiles.

REFERENCES

Abbiss, C.P., 1986. The effects of damping on the interpretation of geophysical measurements. Geotechnique 36, No. 4, pp. 565-580.

Ahrens, H. 1976. Geometrisch und physikalisch nichtlineare Stabelemente zur Berechnung von Tunnelauskeidungen. Bericht aus dem Institut fur Statik der Technischen Universitat Braunschweig Nr. 76-14, 110p.

Ahrens, H., Lindner, E. and Lux, K.H. 1982. Zur Dimesionierung von Tunnelausbauten nach den Empfehlungen zur Berechnung von Tunneln im Lockergestein (1980). Die Bautechnik, 59, pp. 260-273; 303-311 (see also 'Taschenbuch fur den Tunnelbau' 1983, Verlag Gluckauf, Essen).

Almeida, M.S.S. and Pereira, P.R., 1978. Consideraçoes Relativas a aplicacao de elementos finitos a problemas de Escavacoes Subterraneas profundas. Proceedings 6th Brazilian Congress of Soil Mechanics and Foundation Engineering (Rio de Janeiro), pp 1-19.

Amberg, W.A. and Lombardi, G., 1974. Une method de calcul elasto-plastique de l'etat de tension et de deformation autour d'une cavite souterraine. Proceedings 3rd Congress of the International Society for Rock Mechanics (Denver), pp.1055-1060

Amstad, C. and Kovari, K. 1984. Strain monitoring in the subsoil of the Munich subway. Proceedings of the 2nd Conference on Mass Transportation in Asia (Singapore).

Andraskay, E, and Attinger, R., 1979. Behaviour of the prefabricated lining in shield driven tunnels (in German). Proceedings of the 4th International Congress on Rock Mechanics (Montreux), Vol. 2, pp 9-15.

Andraskay, E., Hofmann and Jemelka, p., 1972. Berechnung der Stahlbetontubbinge fur den Heitersbergtunnel, Los West. Schweizerische Bauzeitung, 90 Jahrgang, Heft 36 (September), pp. 864-868.

Atkinson, J.H., 1981. Foundations and slopes, An introduction to applications of critical state soil mechanics. Halsted Press - John Wiley and Sons, New York, 382 p.

Atkinson, J.H. and Bransby, P.L., 1978. The mechanics of soils, An introduction to critical state soil mechanics. McGraw-Hill Book Co. (U.K.), London, 375 p.

Atkinson, J.H., Brown, E.T. and Potts, D.M., 1975. Collapse of shallow unlined circular tunnels in dense sand. Tunnels and Tunnelling, May, pp. 81-87.

Atkinson, J.H., Brown, E.T. and Potts, D.M., 1977. Ground movement near shallow model tunnels in sand. In Proceedings Conference of Large Ground Movement and Structures. Cardiff, United Kingdom, pp. 372-387.

Atkinson, J.H. and Cairncross, A.M., 1973. Collapse of a shallow tunnel in a Mohr-Coulomb material. Proceedings of the Symposium on the Role of Plasticity in Soil Mechanics, Cambridge, pp. 202-206.

Atkinson, J.H., Cairncross, A.M. and James, R.G., 1974. Model tests on shallow tunnel in sand and clay. Tunnels and Tunnelling, July, pp. 28-32.

Atkinson, J.H. and Mair, R.J., 1981. Soil mechanics aspects of soft ground tunnelling, Ground Engineering (July), pp. 20-26 and 38.

Atkinson, J.H. and Mair, R.J., 1983. Loads on leaking and watertight tunnel linings, sewers and buried pipes due to groundwater. Geotechnique 33, No. 3, pp. 341-344.

Atkinson, J.H., Orr, T.L.L. and Potts, D.M., 1975. Research studies into the behaviour of tunnels and tunnel linings in soft ground . TRRL Supplementary Report 176 UC.

Atkinson, J.H. and Potts, D.M. 1977(a). Subsidence above shallow tunnels in soft ground. Journal of the Geotechnical Engineering Division - American Society of Civil Engineers, Vol. 103, pp.307-325.

Atkinson, J.H. and Potts, D.M., 1977(b). Stability of a shallow circular tunnel in cohesionless soil.

Geotechnique, Vol. 27, No. 2, pp. 203-215.

Atkinson, J.H., Potts, D.M. and Schofield, A.N., 1977. Centrifugal model tests on shallow tunnels in sand. Tunnels and Tunnelling, January, Vol. 9, No.1, pp. 59-64.

Attewell, P., 1977. Ground movements caused by tunnelling in soil. In: Large Ground Movements and Structures (edited by J.D. Geddes), Pentech, London, pp. 812-948.

Attewell, P.B. and Farmer, I.W., 1974(a). Ground deformation resulting from shield tunnelling in London clay. Canadian Geotechnical Journal, Vol. 11, pp. 380-395.

Attewell, P.B. and Farmer, I.W., 1974(b). Ground disturbance caused by shield tunnelling in a stiff overconsolidated clay. Engineering Geology, 8:4, pp. 361-381.

Attewell, P.B. and Farmer, I.W., 1975. Ground settlement above shield driven tunnels in clay. Tunnels and Tunnelling, Vol. 7, No.1, pp. 58-62.

Attewell, P.B. and Woodman, J.P., 1982. Predicting the dynamics of ground settlement and its derivatives caused by tunnelling in soil. Ground Engineering, Vol. 15, No.8, pp. 13-22 and 36.

Attewell, P.B. and Yeates, J., 1984. Tunnelling in soil. In: Ground Movements and their Effects on Structures. Edited by P.B. Attewell and R.K. Taylor (Surrey University Press), pp. 132-215.

Attewell, P.B. and Yeates, J. and Selby, A.R., 1986. Soil movements induced by tunnelling and their effects on pipelines and structures. Blackie and Son (Glasgow), 325 p.

Azevedo, N., 1983. Personal Communication.

Azevedo, N., 1985. Medidas das deformacoes do solo ao redor de tunnel em Shield em Sao Paulo. Anais do 2.° Simposio Sobre Excavacoes Subterraneas - ABGE (Rio de Janerio).

Babendererde, S., 1976. Tunnelvortrieb mit Messerschild und Sprizbetonausbau. Forschung+Praxis (STUVA), Band 19, pp.50-55.

Babendererde, S., 1986. Extruded concrete lining. Proceedings of the International Congress on Large Underground Openings, ITA (Firenze), Vol.I, pp. 607-611.

Baker, W.H., Cording, E.J. and MacPherson, H.H., 1983. Compaction grouting to control ground movements during tunnelling. Underground Space, Vol. 7, pp. 205-212.

Balla, A., 1963. Rock pressure determined from shearing resistance. Proceedings European Conference on Soil Mechanics and Foundation Engineering (Budapest), pp.461-471.

Barla, G. and Ottaviani, M., 1974. Stresses and displacements around two adjacent circular openings near to the ground surface. Proceedings 3rd Congress of the International Society for Rock Mechanics (Denver), Vol. II, part B, pp. 975-980.

Barlow, J.P., 1986. Interpretation of tunnel convergence measurements. M.Sc. Thesis, University of Alberta. 235 p.

Barlow, J.P. and Kaiser, P.K., 1987. Interpretation of tunnel convergence measurements. Proceedings 6th Congress of the International Society for Rock Mechanics (Montreal).

Barratt, D.A. and Tyler, R.G., 1976. Measurements of ground movement and lining behaviour on the London underground at Regents Park. TRRL Laboratory Report 684 (UK).

Bathe, K.J., 1977. Static and dynamic geometric and material nonlinear analysis using ADINA. Report 82448-2, Massachusetts Institute of Technology, 240 p.

Bathe, K.J., 1978. ADINA: A finite element program for automatic dynamic incremental nonlinear analysis. Report 82448-1, Massachusetts Institute of Technology, 385 p.

Baudendistel, M., 1972. Wechselwirkung von Tunnelauskleidung und Gebirge. Veroffentlichungen des Institutes fur Bodenmechanik und Felsmechanik der Universitat Fridericiana, Karlsruhe, Heft 51, 1972. (English translation by BRE, U.K.).

Baudendistel, M., 1973. Zur Bemessung von Tunnelauskleidungen in wenig festem Gebirge. Rock Mechanis, Supplementum 2 (1973), pp.279-312.

Baudendistel, M., 1974. Abschatzung der Seitendruckziffer λ und deren Einfluss auf den Tunnel. Rock Mechanics, Supplementum 3 (1974), pp. 89-96.

Baudendistel, M., 1979. Zum Entwurf von Tunneln mit grossem Ausbruchquerschnitt. Rock Mechanics (Springer, Vienna), Suppl. 8., pp.75-100.

Baudendistel, M., 1984. Die Bedeutung der freien Stutzweite im Tunnelbau. Felsbau 2, Nr.2, pp. 78-83.

Baudendistel, M., 1985. Significance of the unsupported span in tunnelling . Proceedings Tunnelling '85 (Brighton). The Institution of Mining and Metallurgy, pp. 103-109.

Bauernfeind, P., Gartung, E. and Adams, F.J., 1986. Large subway tunnel cross sections at Nuremberg. Proceedings of the International Congress on Large Underground Openings, ITA, (Firenze), Vol. I, pp. 634-643.

Bauernfeind, P., Muller, F. and Muller, L. 1978. Tunnelbau unter historischen Gebauden in Nurnberg. Rock Mechanics (Springer, Vienna), Suppl. 6, pp. 161-192.

Baumann, T., 1985. Messung der Beanspruchung von Tunnelschalen. Bauingenieur 60, pp. 449-454.

Baumann, T., Sulke, B-M. and Trysna, T., 1985. Einsatz von Messung und Rechnung bei Spritzbetonbauweisen im Lockergestein. Bautechnik, 10, pp.330-337 und 11, pp. 368-374.

Belshaw, D.J. and Palmer, J.H.L., 1978. Results of a program of instrumentation involving a precast segmented concrete-lined tunnel in clay. Canadian Geotechnical Journal, Vol. 15, No.4, November, pp.573-583.

Berest, P. and Nguyen, M.D., 1979. Etude en grandes deformations de la contraction et de l'expansion de cylindres creux de revolution elastoplastiques avec radoucissement. Journal de Mecanique Applique, Vol. 3, No. 4, pp. 463-487.

Berest, P., Nguyen Minh, D. and Panet, M., 1978. Contribution a l'etude de la stabilite d'une cavite souterraine dans un milieu avec radoucissement. Revue Francaise de Geotechnique No. 4 (Juin), pp. 65-72.

Bevington, P.R., 1969. Data reduction and error analysis for physical sciences, McGraw-Hill, 336 p.

Bierbaumer, A., 1913. Die Dimensionerung des Tunnelmauerwerks, Engelmann (Leipzig) (quoted by Steiner and Einstein, 1980).

Bishop, A.W., 1966. The strength of soils as engineering materials. 6th Rankine Lecture, Geotechnique Vol. 16, No. 2, pp.91-128.

Bishop, A.W. and Bjerrum, L., 1960. The relevance of the triaxial test to the solution of stability problems. Proceedings of American Society of Civil Engineers Reseach Conference on Shear Strength of Cohesive Soils (Boulder), pp. 437-501.

Bishop, A.W., Webb, D.L. and Lewin, P.I., 1965. Undisturbed samples of London clay from the Ashford Common shaft; strength-effective stress relationships. Geotechnique, Vol.15, No.1, pp.1-31.

Bishop, A.W. and Wesley, L.D., 1975. A hydraulic triaxial apparatus for controlled stress path testing. Geotechnique, Vol.25, No.4, pp.657-670.

Bjerrum L., and Eide, O., 1956. Stability of strutted excavations in clay. Geotechnique, Vol.6, No.1, pp.32-47.

Blight, G.E., 1986. Pressures exerted by materials stored in silos: part I, coarse materials. Geotechnique 36, No.1, pp.33-46.

Blight, G.E., 1986. Pressures exerted by materials stored in silos: part II, fine powders. Geotechnique, 36, No.1, pp.47-56.

Blindow, F.K., Edeling, H. and Hofmann, H., 1979. Engstenhende tunnel und deren Verschneidungen. Bauingenieur, 54, pp.213-221.

Blindow, F.K. and Wagner, H., 1978. Grenzfalle bei der Anwendung der Neuen Osterreichischen Tunnelbauweise am Beispiel des Pfaffensteiner Tunnels. Forschung+Praxis (Alba, Dusseldorf), 21, pp.30-36.

Boden, J.B. and McCaul, C., 1974. Measurement of ground movements during a bentonite tunnelling experiment. TRRL Laboratory Report 653 (U.K.)

Bolton, M., 1979. A Guide to Soil Mechanics. MacMillan Press. 439p.

Brady, B.H.G. and Brown, E.T., 1985. Rock Mechanics for Underground Mining. George Allen and Unwin (London) 527p.

Branco, P., 1981. Behaviour of a shallow tunnel in till. M.Sc. Thesis, Department of Civil Engineering, University of Alberta, 351p.

Branco, P., 1987. Ph.D. Thesis in prepartion. University of Alberta.

Branco, P. and Eisenstein, Z., 1985. Convergence-confinement method in shallow tunnels. Proceedings of the 11th International Conference on Soil Mechanics and Foundation Engineering, Section 8 (San Francisco).

Brandt, J.R.T., 1985. Behaviour of soil-concrete interfaces. Ph.D. Thesis, University of Alberta, 376 p.

Brebbia, C.A., 1978. The Boundary Element Method for Engineers. Pentech Press, 189p.

Brem, G., 1981. U-Bahnhof Schweizer Platz in Frankfurt am Main: Berechnungs-und Messergebnisse fur die dreischiffige unteridisch aufgefahrene Bahnhofshalle. Forschung+Praxis (Berlin), 27, pp.137-146.

Breth, H. and Chambosse, G., 1975. Settlement behaviour of buildings above tunnels in Frankfurt clay. Proceedings of the Conference on Settlement of Structures, Pentech Press, London, pp.329-336.

Britto, A.M. and Kusakabe, O., 1985. Upperbound mechanisms for undrained axisymmetric problems. Proceedings of the 5th International Conference on Numerical Methods in Geomechanics (Nagoya), pp.1691-1698.

Broms, B., 1978. Subsidence due to seepage to tunnels in rock. Proceedings of the International Conference on Evaluation and Prediction of Subsidence (Pensacola Beach).

Broms, B.B. and Bennermark, H., 1967. Stability of clay at vertical openings. Journal of the Soil Mechanics and Foundations Division, American Society of Civil Engineers, Vol.93, pp.71-94.

Brown, E.T., Bray, J.W., Ladanyi, B. and Hoek, E., 1983. Ground response curves for rock tunnels. Journal of Geotechnical Engineering, American Society of Civil Engineers, Vol. 109, pp.15-39. (Discussion with corrections on the original paper in the same journal, January, 1984, pp.140-141.

Bull, A., 1946. Stresses in the linings of shield-driven tunnels. American Society of Civil Engineers, Proceedings, Nov. 1944.

Burland, J.B. and Fourie, A., 1985. The testing of soils under conditions of passive stress relief. Geotechnique, Vol. 35, No.2, pp.193-198.

Burland, J.B. and Wroth, C.P., 1974. Allowable and differential settlements of structures including drainage and soil-structure interaction. Proceedings of the Conference on Settlement of Structures, Pentech Press, London, pp.611-764.

Burns, J.Q. and Richard, R.M., 1964. Attenuation of stresses for buried cylinders. Proceedings of the Symposium on Soil-Structure Interaction. Tucson, pp. 378-392.

Byrne, P.M. and Eldridge, T.L., 1982. A three parameter dilatant elastic stress-strain model for sand. Proceedings of the International Symposium on Numerical Methods in Geomechanics. (Zurich), pp.73-80.

Byrne, P.M. and Janzen, W., 1984. INCOIL: A computer program for nonlinear analysis of stresses and deformations in oil sand masses. Report to the Alberta Oil Sands Technology and Research Authority, 104p.

Cairncross, A.M., 1973. Deformations around model tunnels in stiff clay. Ph.D. Thesis, Cambridge University.

Calladine, 1969. Engineering Plasticity (U.K.).

Capellari, G. and Ottaviani, M., 1982. Predicted surface settlements due to shield tunnelling with compressed air. Proceedings of the 4th International Conference on Numerical Methods in Geomechanics. (Edmonton), Vol.2, pp.531-536.

Caquot, A., 1934. Equilibre des Massifs a Frottement Interne, Gauthier-Villars (Paris).

Caquot, A. and Kerisel, J., 1956. Traite de Mecanique des Sols. Gauthier-Villars (3^e Edition).

Carder, D.R., Ryley, M.D. and Symons, I.F., 1985. Ground movements caused by deep trench construction in Boulder clay and their effect on an adjacent service pipeline. Proceedings of the 3rd International Conference on Ground Movements and Structures (Cardiff), pp.3-23.

Carter, J.P. and Booker, J.R., 1982(a). The analysis of consolidation and creep around a deep circular tunnel in clay. Proceedings of the 4th International Conference on

Numerical Methods in Geomechanics, (Edmonton), Vol.2, pp.537-544.

Carter, J.P. and Booker, J.R., 1982(b). Elastic consolidation around a deep circular tunnel. International Journal for Solids and Structures, Vol.18, No.12, pp.1059-1074.

Carter, J.P. and Booker, J.R., 1983. Creep and consolidation around circular openings in infinite media. International Journal for Solids and Structures, Vol.19, No.8, pp.663-675.

Carter, J.P. and Booker, J.R., 1984. Elastic consolidation around a lined circular tunnel. International Journal for Solids and Structures, Vol.20, No.6, pp.589-698.

Casarin, C., 1977. Soil deformations around tunnel headings in clay. M.Sc. Thesis, Cambridge University.

Casarin, C. and Mair, R., 1981. The assessment of tunnel stability in clay by model tests. Soft-Ground Tunnelling, Failures and Displacements (Ed. D. Resendiz and M.P. Romo), A.A. Balkema (Rotterdam), pp.33-44.

Chambosse, G., 1972. Das Verformungsverhalten des Frankfurter Tons beim Tunnelvortrieb - Berichte uber Messungen in der Frankfurter Innenstadt. Mitteilungen der Versuchsanstalt fur Bodenmechanik und Grundbau der Technischen Hochschule Darmstadt, Heft 10.

Chan, D., 1985. Finite element analysis of strain-softening materials. Ph.D. Thesis. Department of Civil Engineering, University of Alberta, Edmonton, Alberta. 355p.

Chan, A.C.Y. and Morgenstern, N.R., 1986. Measurement of lateral stresses in a lacustrine clay deposit. Proceedings of the 39th Canadian Geotechnical Conference (Ottawa), pp.285-290.

Chandrasekaran, V.S. and King, G.J.W., 1974. Simulation of excavation using finite elements. Journal of the Geotechnical Engineering Division. ASCE GT9, pp.1086-1088.

Chang, C.Y. and Duncan, J.M., 1970. Analysis of soil movement around a deep excavation. Journal of the Soil Mechanics and Foundation Division, ASCE, Vol.96, SM5, pp.1655-1679.

Chen, W.F. and Saleeb, A.F., 1982. Constitutive Equations for Engineering Materials. Volume 1: Elasticity and Modelling. John Wiley & Sons, 580 p.

Christian, J.T., 1982. The application of generalized stress-strain relations. In: Application of Plasticity and Generalized Stress-Strain in Geotechnical Engineering (edited by R.N. Yong and E.T. Selig), American Society of Civil Engineers, pp.182-204.

Christian, J.T. and Wong, I.H., 1973. Errors in simulating excavation in elastic media by finite element. Soils and Foundation, Vol.13, No.1, pp.1-10.

Clayton, C.R.I. and Khatrush, S.A., 1986. A new device for measuring local axial strains on triaxial specimens. Geotechnique, Vol. 36, No. 4, pp.593-597.

Clough, G.W. 1980. Advanced soil and soft rock tunneling technology in Japan. Stanford University Technical Report No. CE-252.

Clough, G.W., 1981. Innovations in tunnel construction and support techniques. Bulletin of the Association of Engineering Geologists, Vol. XVIII, No.2, pp.151-167.

Clough, G.W. and Schmidt, B., 1981. Design and performance of excavations and tunnels in soft clay. In: Soft Clay Engineering (edited by E.W. Brand and R.P. Brenner), Elsevier, pp.569-634.

Clough, C.W., Shirasuna, T. and Finno, R.J., 1985. Finite element analysis of advanced shield tunnelling. Proceedings of the 5th International Conference on Numerical Methods in Geomechanics (Nagoya), pp.1167-1174.

Clough, G.W., Sweeney, B.P. and Finno, R.J., 1983. Measured soil response to EPB shield tunneling. Journal of Geotechnical Engineering Division of the ASCE, Vol. 109, No. 2, pp.131-149.

Clough, G.W. and Tsui, Y., 1977. Static analysis of earth retaining structures. In: Numerical Methods in Geotechnical Engineering (edited by C.S. Desai and J.T. Christian), McGraw Hill, pp.506-527.

Corbett, I., 1984. Load and displacement variation along a tunnel. M.Sc. Thesis. Department of Civil Engineering, University of Alberta, Edmonton, Alberta, 246p.

Cording, E.J. and Hansmire, W.H., 1975. Displacements around soft ground tunnels. Proceedings of the 5th Pan-American Conference on Soil Mechanics and Foundation Engineering, Buenos Aires, Vol.4, pp.571-633.

Cording, E.J., Hansmire, W.H., MacPherson, H.H., Lenzini, P.H. and Vonderohe, A.P., 1976. Displacement around tunnels in soil. Report DOT-TST 76T-22, National Technical Information Service (Springfield, Virginia).

Cording, E.J., O'Rourke, T.D. and Boscardin, M., 1978. Ground movements and damage to structures. Proceedings of the International Conference on Evaluation and Prediction of Subsidence (Pensacola Beach) pp.516-537.

Costa, F.M., de Mariano, M., Monteiro, J.T. and Kira, Y., 1974. Passagem dos shields sob o Viaduto Boa Vista, observacoes de movimento da Estrutura. Anais do 5. Congresso Brasileiro de Mecanica dos Solos (Sao Paulo), Vol. I, pp.323-338.

Costa-Filho, L.M., 1980. A laboratory investigation of the small strain behaviour of London Clay. Ph.D. Thesis, University of London.

Costa-Filho, L.M., 1984. A note on the influence of fissures on the deformation characteristics of London clay. Geotechnique, Vol.34, No.2, pp.268-272.

Cox, A.D., 1963. The use of non-associated flow rules in soil plasticity. R.A.R.D.E. Rep (B) 263. (Quoted by Davis, 1968:345).

Craig, R.N. and Muir Wood, A.M., 1978. A review of tunnel lining practice in the United Kingdom. Department of the Environment, Department of Transport, TRRL Supplementary Report 335: Crowthorne, (Transport and Road Research Laboratory).

Crofts, J.E., Menzies, B.K. and Tarzi, A.I., 1977. Lateral displacements of shallow buried pipelines due to adjacent deep trench excavations. Geotechnique, Vol. 27, No.2, pp.161-179.

Crofts, J.E., Menzies, B.K. and Tarzi, A.I., 1978. Discussion: Lateral displacements of shallow buried pipelines due to adjacent deep trench excavations. Geotechnique, Vol.28, No.2, pp.217-220.

Cruz, H.J.V., Couto, J.V.S., Hori, K., Salvoni, J.L. and Ferrari, O.A., 1982. Os tuneis do prolongamento norte - uma primeira avaliacao do NATM em area urbana. Proceedings 'Simposio sobre Escavacoes Subterraneas', Rio de Janeiro, published by ABGE - Brazilian Association of Engineering Geology), pp.297-316.

Cruz, H.J.V., Hori, K., Ferrari, O.A. and Ferreira, A.A., 1985. A construcao em NATM e em area urbana, de um tunel de grande secao - O tunel de Via dupla do Prolongamento Norte. Proceedings of the 2nd Symposium on Underground Excavation (ABGE), Vol. 1, pp.391-411 (Rio de Janeiro).

Curtis, D.J., 1974. Visco-elastic tunnel analysis. Tunnels and Tunnelling. November, pp.38-39.

Curtis, D.J., 1976. The circular tunnel in elastic ground. Discussion. Geotechnique, Vol.26, pp.231-237.

Daemen, J.J., 1975. Tunnel support loading by rock failure. Ph.D. Thesis. Department of Civil Engineering, University of Minnesota, Minnesota.

Daemen, J.J. and Fairhurst, C., 1970. Influence of failed rock properties in tunnel stability. 12th Symposium on Rock Mechanics. Rolla, Missouri, pp.855-875.

Daemen, J.J. and Fairhurst, C., 1972. Rock failure and tunnel support loading. Proceedings of the International

Symposium on Underground Openings, Lucerne, pp.356-369.

Dar, S.M. and Bates, R.C., 1974. Stress analysis of hollow cylindrical inclusions. Journal of the Geotechnical Engineering Division, ASCE, Vol.100, No. GT2, February, pp.123-138.

Davis, E.H., 1968. Theories of soil plasticity and the failure of soil masses, Soil Mechanics: Selected Topics. Ed. Lee, I.K., pp.341-380, Butterworth.

Davis, E.H., Gunn, M.J., Mair, R.J. and Seneviratne, H.N., 1980. The stability of shallow tunnels and underground openings in cohesive material. Geotechnique 30, No.4, pp.397-416.

Deere, D., Peck, R.B., Monsees, J.E. and Schmidt, B., 1969. Design of tunnel liners and support systems, Report No. PB-183799 (NTIS - National Technical Information Service, U.S. Department of Commerce, Springfield, VA 22161).

DeLory, F.A., Crawford, A.M. and Gibson, M.E.M., 1979. Measurements on a tunnel lining in very dense till. Canadian Geotechnical Journal, Vol.16, pp.190-199.

Desai, C.S. and Abel, J.F., 1972. Introduction to the Finite Element Method. A numerical method for engineering analysis. van Nostrand Reinhold Comp., New York.

Descoeudres, F., 1974. Analyse tridimensionelle de la stabilite d'un tunnel au voisinage du front de taille dans une roche elasto-plastic. Proceedings 3rd. Congress of the International Society for Rock Mechanics, Denver, Vol.II-B, pp. 1130-1135.

Detournay, E. and Fairhurst, C., 1982. Generalization of the ground reaction curve concept. Proceedings of the U.S.A. Rock Mechanics Symposium, pp. 924-934.

DGEG - Deutsche Gesellschaft fur Erd- und Grundbau e.V. 1979. Empfehlungen fur den Felsbau Untertage. In; Taschenbuch fur den Tunnelbau 1980. Verlag Gluckauf Essen, pp. 157-239.

Dickin, E.A. and King, G.J.W., 1982. The behaviour of hyperbolic stress-strain models in triaxial and plane strain compression. Proceedings of the International Symposium on Numerical Models in Geomechanics (Zurich), pp.303-311.

Diniz, R.A.D.C., 1978. Schnittgrossen in kreisformigen und elliptischen Tunnelwandungen aus Beton. Dissertation, TU Munchen, Nov.

Dodge, C.W., 1972. Euclidean geometry and transformations. Addison-Wesley Publishing Company, 295 p.

Domaschuk, L. and Valliappan, P., 1975. Nonlinear settlement analysis by finite element. Journal of the Geotechnical Engineering Division, ASCE, Vol.101, No. GT7, pp.601-614.

Domaschuk, L. and Wade, N.H., 1969. A study of bulk and shear moduli of sand. Journal of the Soil Mechanics and Foundations Division, ASCE, Vol. 95, No. SM2, pp. 561-581.

Duddeck, H., 1972. Zu den Berechnungsmethoden und zur Sicherheit von Tunnelbauten. Bauingenier 47. H.2, pp.43-52.

Duddeck, H., 1973. Schildvorgetriebene Tunnel, Entwicklungstendenzen in Forschung and Ausfuhrung. Rock Mechanics, Supplementum 2, pp.257-278.

Duddeck, H., 1980(a). Empfehlungen zur Berechnung von Tunneln im Lockergestein (1980). Die Bautechnik, 10, pp.349-356.

Duddeck, H., 1980(b). On the basic requirements for applying the Convergence Confinement Method. Underground Space, Vol.4, No.4, pp.241-247.

Duddeck, H., 1981, Views on structural design models for tunnelling. Synopsis of answers to a questionnaire (ITA). Advances in Tunnelling Technology and Subsurface Use. Vol.2, No.3, pp.155-228.

Duddeck, H. and Erdmann, J., 1982. Structural design models for tunnels. Proceedings, Tunnelling '82 (edited by M.J. Jones), The Institution of Mining and Metallurgy, London, pp. 83-91.

Duddeck, H. and Erdmann, J., 1985. On structural design models for tunnels in soft soil. Underground Space, Vol.9, pp.246-259.

Duddeck, H., Meister, D., Werner, E., Schlegel, R. and Theurer, M., 1979. Road tunnel in very soft soil in terrace deposits in the Harz Mountains, Germany. Tunnelling '79, pp.205-215.

Duddeck, H., Meister, D., Werner, E., Schlegel, R. and Theurer, M., 1981. Strassen-Tunnel Butterberg in Osterode/Harz. Bauingenieur, 56, pp.175-185.

Duddeck, H. and Stading, A., 1985. Entwurfskonzept und Realitat beim Standsicherheitsnachweis von Tunneln im deutschen Mittelgebirge. Proceedings of STUVA Meeting, (Hannover).

Duncan, J.M., 1979. Behaviour and design of long-span metal culverts. Journal of the Geotechnical Engineering Division, ASCE, Vol. 105, No. GT3, pp.399-418.

Duncan, J.M., 1980(a). Strains predicted using hyperbolic stress-strain relationships. Proceedings of the Workshop on Limit Equilibrium, Plasticity and Generalized Stress-Strain in Geotechnical Engineering (McGill University), pp.245-253.

Duncan, J.M., 1980(b). Hyperbolic stress-strain relationships. Proceedings of the Workshop on Limit Equilibrium, Plasticity and Generalized Stress-Strain in Geotechnical Engineering (McGill University) pp.443-460. (comments on pp.333-335).

Duncan, J.M., Byrne, P., Wong, K.S. and Mabry, P., 1980. Strength, stress-strain and bulk modulus parameters for finite element analysis of stresses and movements in soil masses. Report UCB/GT/80-01, University of California, Berkeley, 77p.

Duncan, J.M. and Chang, C.V., 1970. Nonlinear analysis of stress and strain in soils. Journal of the Soil Mechanics and Foundations Division. American Society of Civil Engineers, Vol.96, pp.1629-1653.

Duncan, J.M. and Chang, C.V., 1972. Discussion closure of "Nonlinear analysis of stress and strain in soils". Journal of the Soil Mechanics and Foundation Division. American Society of Civil Engineers, Vol.98, No.SM5, pp.495-498.

Dyer, M., Jamiolkowski, M. and Lancellota, R., 1986. Experimental soil engineering and models for geomechanics. Proceedings of the 2nd International Symposium on Numerical Models in Geomechancis (Ghent), pp.873-906.

Dysli, M. and Fontana, A., 1982. Deformations around the excavations in clayey soil. Proceedings International Symposium on Numerical Methods in Geomechanics, Zurich, September, pp.634-642.

Ebaid, G.S. and Hammad, M.E., 1978. Aspects of circular tunnel design. Tunnels and Tunnelling (July), pp.59-63.

Edeling, H. and Schulz, W., 1972. Die Neue Osterreichische Tunnelbauweise im Frankfurter U-Bahnbau. Der Bauingenieur, 47, pp.351-362. (English translation by BRE, UK).

Eden, W.J. and Bozosuk, M., 1969. Earth pressures on Ottawa outfall sewer tunnel. Canadian Geotechnical Journal, 6, pp.17-32.

Egger, P., 1974. Gebirgsdruck im Tunnelbau und stuzwirkung der Ortsbrust bei Uberschreiten der Gebirgsfestigkeit. Proceedings of the 3rd Congress of the International Society for Rock Mechanics. (Denver), pp.1007-1011.

Egger, P., 1980. Deformations at the face of the heading and determination of the cohesion of the rock mass. Underground Space, Vol.4, No.4, pp.313-318.

Eigenbrod, K.D., 1975. Analysis of the pore pressure changes following the excavation of a slope. Canadian

Geotechnical Journal, 12, pp.429-440.

Einstein, H.H., Azzouz, A.S., Schwartz, C.W. and Steiner, W., 1979. Improved design of tunnel supports: Executive summary. Report UMTA-MA-06-0100-79-15. NTIS (Springfield, Virginia) 49p.

Einstein, H.H., and Schwartz, C.W., 1979. Simplified analysis for tunnel supports. Journal of the Geotechnical Engineering Division, American Society of Civil Engineers, V. 106, pp.499-518 (Discussion with corrections on the original paper in the same journal, July, 1980, pp.835-838).

Eisenstein, Z., 1974. Application of finite element method to analysis of earth dams. State-of-the art-report, Proceedings of the 1st Brazilian Seminar on Applications of Finite Element Method in Soil Mechanics (Rio de Janerio), pp. 457-528.

Eisenstein, Z., 1982. The contribution of numerical analysis to design of shallow tunnels. Proceedings, International Symposium on Numerical Models in Geomechanics, Zurich, pp. 135-165.

Eisenstein, Z. and Branco, P., 1985. Observational method applied to ground control at the Edmonton LRT Tunnel. Canadian Tunnelling (TAC), pp.51-65.

Eisenstein, Z., El-Nahhas and Thomson, S., 1981(a). Pressure-displacement relations in two systems of tunnel lining. Soft Ground Tunnelling, Failures and Displacements (Ed. D. Resendiz and M.P. Romo) A.A. Balkema (Rotterdam), pp.85-94.

Eisenstein, Z., El-Nahhas, F. and Thomson, S., 1981(b). Strain field around a tunnel in stiff soil. Proceedings, 10th International Conference on Soil Mechanics and Foundation Engineering (Stockholm), Vol.1, pp.283-288.

Eisenstein, Z., Heinz, H. and Negro, A., 1984. On three-dimensional ground response to tunnelling. Proceedings, Geotech' 84, American Society of Civil Engineers (edited by K.Y. Lo), pp.107-127.

Eisenstein, Z., Heinz, Jr., H. and Negro, A., 1986. Multiple excavation schemes for large openings in soft ground. Proceedings, International Congress on Large Underground Openings (Firenze), Vol. 1, pp.710-719.

Eisenstein, Z., Kulak, G.L., MacGregor, J.G. and Thomson, S., 1977. Report on geotechnical and construction performance of the twin tunnels. Unpublished report prepared for the City of Edmonton Engineering Department. Edmonton, Alberta, 77p.

Eisenstein, Z. and Medeiros, L.V., 1983. A deep retaining structure in till and sand. Part II: Performance and analysis. Canadian Geotechnical Journal, Vol.20, pp.131-140.

Eisenstein, Z. and Morrison, N.A., 1973. Prediction of foundation deformation in Edmonton using an in situ pressure probe. Canadian Geotechnical Journal, Vol.10, pp.193-210.

Eisenstein, Z. and Negro, A., 1985(a). Excavations and tunnels in tropical lateritic and saprolitic soils. General Report for Session 5, 1st International Conference on Geomechanics in Tropical Lateritic and Saporlitic Soils (Brasilia), Vol.3, pp.299-333.

Eisenstein, Z. and Negro, A., 1985(b). Comprehensive design method for shallow tunnels. ITA/AITES, International Conference, Underground Structures in Urban Area, Prague, Czechoslavakia, pp.7-20.

Eisenstein, Z. and Thomson, S., 1978. Geotechnical performance of a tunnel in till. Canadian Geotechnical Journal, Vol.15, pp.332-345.

Eisenstein, Z., Thomson, S. and Branco, P., 1983. South LRT extension, Jasper Avenue twin tunnel, instrumentation test section at 102nd Street, Part II: Northbound Tunnel. Report submitted to LRT Project Office, Edmonton Transit, The City of Edmonton.

Elmer, H., 1980. Zusammenhang zwischen Bauverfahren und geringstmoglichen setzungen beim Bau eines doppelgleisigen Stadtbahntunnels in Mulheim a.d. Ruhr. Forschung+Praxis (Koln), 23, pp.160-165.

El-Nahhas, F., 1980. The behaviour of tunnels in stiff soils. Ph.D. Thesis, Department of Civil Engineering, University of Alberta, 305p.

Engelbreth, K., 1961. Correspondence to Tunnel stress analysis. Geotechnique 11, pp.246-248.

Erdmann, J., 1983. Vergleich ebener und Entwicklung raumlicher Berechnungsverfahren fur Tunnel. Bericht Nr. 83-40, Institut fur Statik der Technischen Universitat Braunschweig, 220p.

Erdmann, J. and Duddeck, H., 1983. Statik der Tunnel im Lockergestein-Vergleich der Berechnungsmodelle. Bauingenieur, 58 Jahrgang, pp.407-414.

Erdmann, J. and Duddeck, H., 1984. Stress-displacement fields at the face of rock tunnels. Proceedings, 1st Latin-American Congress of Underground Construction -ITA (Caracas), Vol.I, pp.177-183.

D'Escatha, Y. and Mandel, J., 1974. Stabilite d'une galerie peu profonde en terrain meuble. Revue de L'Industrie Minerale (Special Issue), Avril, pp.45-53.

Evgin, E. and Eisenstein, Z., 1985. Performance of an elastoplastic model. Canadian Geotechnical Journal, Vol. 22, No. 2, pp.177-185.

Evison, S., 1987. M.Sc. Thesis in preparation. University of Alberta.

Ewoldsen, H.M., 1968. The near surface tunnel in a gravitating medium. Proceedings of the 10th Symposium of Rock Mechanics, University of Texas, p.677-698.

Fenner, R., 1938. Untersuchungen zur Erkenntnis des Gebirgsdrucks. Gluckauf Berg- und Huttenmannische Zeitschrift 74, Nr. 32, 681-695, Nr.33, 705-715.

Fitzpatrick, L., Kulhawy, F.H and O'Rourke, T.D., 1981. Flow patterns around tunnels and their use in evaluating construction problems. Soft-Ground Tunnelling, Failures and Displacements (Ed. D. Resendiz and M.P. Romo), A.A.

Balkema (Rotterdam), pp. 95-103.

Fleck, H., and Sklivanos, S., 1978. Statische Berechnung gebetteter Hohlraumaussteifungen (Auskleidungen) bei Berucksichtigung einer tangentialen Bettungmodulwirkund und Vergleich mit Ergebnissen nach der Kontinuumstheorie. Forschung Ing.-Wessen 44 (1978), Heft 4, 101-136, VDI Dusseldorf pp. 149-156.

Fleck, H. and Sonntag, G., 1977. Statische Berechnung gebetteter Hohlraumskleidungen mit einem ortsveranderlichen, last-und verformungsabhangigen Bettungsmodul aus der Method der Finite Elemente. Die Bautechnik 5, pp.149-156.

Fleck, H. and Sonntag, G., 1978. Ermittlung der Biegung von Hohlraumassteifungen (Auskleidungen) aus den Krummungsanderungen der Ausbruchkontur. Bauingenieur 53, Heft 12, pp.471-478.

Flugge, W., 1962. Statik und Dynamik der Schalen, 3. Auflage. Springer-Verlag (Berlin), 292 p.

Focht, J.A. and O'Neill, M.W., 1985. Piles and other deep foundations. Proceedings of the 11th International Conference on Soil Mechanics and Foundation Engineering (San Francisco), 4, pp.187-209.

da Fontoura, S.A.B. and Barbosa, M.C., 1985. Superficial settlements caused by a small diameter tunnel excavated in a residual sandy soil (in Portuguese). Geotecnia (Lisbon), pp. 67-87.

Fourie, A.B., Potts, D.M. and Jardine, R.J., 1986. The determination of appropriate soil stiffness parameters for use in finite element analyses of geotechnical problems. Proceedings of the 2nd International Symposium on Numerical Models in Geomechanics (Ghent), pp. 227-235.

Fredriksson, B. and Mackerle, J., 1983. Stuctural Mechanics Finite Element Computer Programs. Advanced Engineering Corp. (Sweden), Box 3044, S-580 03 Linkoping.

Fujita, K., 1982. Prediction of surface settlements caused by shield tunnelling. Proc. Conf[illegible]ncia Internacional de Mecanica de Suelos (Sociedade Mexicana de Mecanica de Suelos), Vol.1, pp. 239-246.

Gais, W.H., Harpf, R. and Herg, M., 1985. Hohlraumsicherung beim Nurnberger U-Bahnbau - Messergebmisse zum Tragverhalten, Forschung + Praxis, 29 (STUVA), pp. 196-201.

Gais, W.H., Harpf, R. and Herg, M., 1986. Langzeitige Lastentwiklung in der Auskleidung von Tunneln in Spritzbetonbauweise: Beispeil U-Bahn Munchen. In: Forschung + Praxis (Alba, Dusseldorf), 30, pp. 59-68.

Garcia Gonzalez, J.M., Escario, V., Moya, F.J., Oteo, C.S. and Sagaseta, C., 1984. The Madrid subway extension and its associated geotechnical problems. Proceedings of the 1st Latinamerican Congress of Underground Construction (ITA Caracas), Vol.I, pp. 209-224.

Gartung, E. and Bauernfeind, P., 1977. Subway tunnel at Nurnberg - Predicted and measured deformations. Proceedings of the International Symposium on Field Measurements in Rock Mechanics (Zurich), pp. 473-483.

Gartung, E. and Bauernfeind, P., 1983. Construction of adjacent tubes by NATM. Proceedings, 5th Congress of the International Society for Rock Mechanics, Melbourne, D 163-166 (reprint).

Gartung, E., Bauernfeind, P. and Bianchini, J.C., 1979. Three-dimensional finite element method study of a subway tunnel in Nurnberg. Proceedings, Rapid Excavation and Tunnelling Conference. Atlanta, Vol. 1, pp. 773-789.

Gaudin, B., Folacci, J.P., Panet, M. and Salva, L., 1981. Soutenement d'une Galerie dans le Marnes du Cenomanien. Proceedings 10th International Conference on Soil Mechanics and Foundation Engineering (Stockholm), Vol. 1, pp.293-296.

Gebhardt, P., 1980. Hydrogeologische und geotechnische Probleme bei Planung und Bau der U-Bahn-Linie 8/1. In; U-Bahn fur Munchen, U-Bahn Linie 8/1 (published by U-Bahn-Referat Munchen), pp.65-87.

Gesta, P., Kerisel, J., Londe, P., Louis, C. and Panet, M., 1980. Tunnel stability by Convergence-Confinement Method. Underground Space, Vol. 4, pp. 225-232.

Ghaboussi, J. and Gioda, G., 1977. On the time dependent effects in advancing tunnels. International Journal for Numerical and Analytical Methods in Geomechanics, Vol.1, pp.249-271.

Ghaboussi, J., Hansmire, W.H., Parker, H.W. and Kim, K.J., 1983. Finite element simulation of tunnelling over subways. Journal of Geotechnical Engineering (ASCE), Vol.109, No.3, pp.318-334.

Ghaboussi, J. and Karshenas, M., 1977. On the finite element analysis of certain material nonlinearities in geomechanics. Proceedings of the International Conference on Finite Elements in Nonlinear Solids and Structural Mechanics (Norway) (quoted by Ghaboussi et.al., 1978:191).

Ghaboussi, J. and Pecknold, D.A., 1984. Incremental finite element analysis of geometrically altered structures. International Journal for Numerical Methods in Engineering, Vol.20, pp.2051-2064.

Ghaboussi, J. and Ranken, R., 1974. Tunnel design considerations: Analysis of medium-support interaction. Report FRA - ORD and D75-24, NTIS (Springfield, Virginia).

Ghaboussi, J. and Ranken, R.E., 1981. Finite element simulation of underground construction. Proceedings, Symposium on Implementation of Computer Procedures and Stress-Strain Laws in Geotechnical Engineering (Chicago), pp.253-265.

Ghaboussi, J., Ranken, R.E. and Karshenas, M., 1978. Analysis of subsidence over soft ground tunnels. Proceedings of the International Conference on Evaluation and Prediction of Subsidence (Pensacola Beach), pp. 182-196.

Gibson, R.E. and Anderson, W.F., 1961. In situ measurement of soil properties with the pressuremeter. Civil Engineering Public Works Rev. (London), Vol.56, No.5, pp.615-620.

Gioda, G., 1985. Some remarks on back analysis and characterization problems in geomechanics. Proceedings of the 5th International Conference on Numerical Methods in Geomechanics (Nagoya), pp.47-61.

Gioda, G. and Jurina, L., 1981. Identification of earth pressure on tunnel liners. Proceedings of the 10th International Conference on Soil Mechanics and Foundation Engineering (Stockholm), Vol.1, pp.301-304.

Glossop, N.H., 1978. Ground movements caused by tunnelling in soft soils. Ph.D. Thesis, University of Durham.

Glossop, N.H. and Farmer, I.W., 1979. Settlement associated with removal of compressed air pressure during tunnelling in alluvial clay. Geotechnique 29, No.1, pp.67-72.

Gopalakrishnayya, A.V., 1973. Analysis of cracking of earth dams. Ph.D. Thesis, The University of Alberta.

Guatteri, G., Teixeira, A.H. and Martins, A., 1986. Solution of stability problems in tunnelling by the CCP method. Proceedings of the International Congress on Large Underground Openings - ITA (Firenze), Vol.II, pp.190-197.

Gunn, M.J., 1977. The use of the finite element method for the design of tunnels in soft ground. Cambridge University Engineering Department Supplementary Research Report to the Director of the Transport and Road Research Laboratory.

Gunn, M.J., 1984. The deformation of ground near tunnels and trenches. Cambridge Univeristy Engineering Department Research Report to the Director of the Transport and Road Research Laboratory.

Gunn, M.J. and Taylor, R.N., 1985. Discussion of Atkinsonn and Mair. Geotechnique 35, No.1, pp.73-75.

Hain, H. and Horst, H., 1970. Spannungstheorie 1. and 2.

Ordnung fur beliebige Tunnelquerschnitte unter Berucksichtigung der einseitigen Bettungswirkung des Bodens. Strasse Brucke Tunnel 22, Heft 4, pp.85-94.

Hain, H. and Horst, H., 1971. Gultigekeitsgrenzen der Theorie 2. Ordnung bei der Berechnung kreisformiger Tunnelquerschnitte. Strasse Brucke Tunnel 23, Heft 3, pp 64-68.

Hain, H. and Horst, H., 1974. Zur Frage der radialen und tangentialen Bettung schildvorgetriebener Tunnel. Strasse Brucke Tunnel 26, Heft 1, pp. 12-20.

Hanafy, E.A. and Emery, J.J., 1980. Advancing face simulation of tunnel excavations and lining placement. Proceedings of the Underground Rock Engineering, 13th Canadian Rock Mechanics Symposium, CIM Special Volume 22, pp. 119-125.

Hanafy, E.A. and Emery, J.J., 1982. Three-dimensional simulation of tunnel excavation in squeezing ground. Proceedings of the 4th International Conference on Numerical Methods in Geomechnics (Edmonton), Vol.3, pp. 1203-1209.

Handy, R.L., 1985. The arch in soil arching. Journal of Geotechnical Engineering Division, ASCE, Vol. 111, No.3, pp.302-319.

Hanna, T.H., 1985. Field Instrumentation in Geotechnical Engineering. Transtech Publications (Germany), 843 p.

Hansmire, W., 1975. Field measurements of ground displacements about a tunnel in soil. Ph.D. Thesis, University of Illinois at Urbana-Champaign. 334p.

Hansmire, W.H., 1984. Example analysis for circular tunnel lining. Proceedings, Geotech '84, ASCE. (Ed. by K.Y. Lo), pp.30-45.

Hansmire, W.H. and Cording, E.J., 1985. Soil tunnel test section: Case history summary. Journal of the Geotechnical Engineering Division. American Society of Civil Engineers, Vol. 111, No. 11, pp. 1301-1320.

Hansmire, W.H., Parker, H.W., Ghaboussi, J., Casey, E.F. and Lentell, R.L., 1981. Effects of shield tunnelling over subways. Proceedings, 3rd Rapid Excavation and Tunnelling Conference (San Francisco), Vol. 1, pp.254-276.

Hanya, T., 1977. Ground movements due to construction of shields-driven tunnel. Proceedings, 9th International Conference on Soil Mechanics and Foundation Engineering (Tokyo), Case History Volume, pp.759-790.

Hardy Associates. 1980. City of Winnipeg, Tunnel Instrumentation Project. Geotechnical Consideration. Year 1 Report for the City of Winnipeg, Waterworks Waste and Disposal Division (December).

Hartmann, F., 1970. Elastizitatstheorie des ausgekleideten Tunnelhohlraumes und des eingebohrten kreisformigen Rohres. Strasse Brucke Tunnel 22 (1970), Heft 8, 209-215, Heft 9, 241-246, und Jg. 24 (1972), Heft 1, 13-20, Heft 2, 39-45.

Hartmann, F., 1985. Einfache Berechnung uberschutteter, kreisformiger Rohre von beliebiger Steifigkeit Elastizitatstheorie des uberschutteten Rohres. Bautechnik, 62, Heft 7, pp.224-235.

Hartmann, F., 1986. Personal Communication.

Heilbrunner, J., Gais, W.H., Herg, M., 1981. Neue Messergebnisse zum Tragverhalten von Verbaubogen und Spritzbeton bein der Hohlraumsicherung im U-Bahnbau. Forschung + Praxis (STUVA - Berlin), pp.129-136.

Henkel, D.J., 1960. The relationship between the effective stresses and water content in saturated clays. Geotechnique, Vol.10, p.41.

Heinz, H., 1984. Applications of the New Austrian Tunnelling Method in urban areas. M.Sc. Thesis. Department of Civil Engineering, University of Alberta, Edmonton, 320 p.

Heinz, H., 1987. Ph.D. Thesis in preparation. University of Alberta.

Henry, K., 1974. Grangemouth tunnel sewer. Tunnels and Tunnelling (January)., pp.25 and 29.

Hereth, A., 1979. Der Pfaffensteiner Tunnel in Regensburg. Rock Mechanics (Springer, Vienna), 12, pp.47-60.

Herzog, M., 1985. Die Setzungsmulde uber Seicht liegenden Tunneln. Bautechnik, 11, pp.375-377.

Hewett, B. and Johannesson, S., 1922. Shield and Compressed Air Tunnelling. McGraw Hill, New York.

Ho, S.K., 1980. An investigation into the behaviour of shallow tunnels in elastic soils. B.Eng.Sc. Report, Faculty of Engineering Science, University of Western Ontario.

Hocking, G., 1976. Three-dimensional elastic stress distribution around the flat end of a cylindrical cavity. International Journal of Rock Mechanics, Mining Sciences and Geomechanical Abstracts. Vol. 13, No. 12, pp. 331-337.

Hoeg, K., 1968. Stresses against underground structural cylinders. Journal of the Soil Mechanics and Foundation Engineering Division. ASCE, Vol. 94, No. SM4, July, pp. 833-858.

Hoek, E. and Brown, E.T., 1980. Underground excavations in rock. 1st ed., The Institution of Mining and Metallurgy, London, 527 p.

Hofmann, H., 1976. Progonose und Kontrolle der Verformungen und Spannungen im Tunnelbau. Forschung+Praxis (Alba, Dusseldorf), 19, pp.94-100.

Holmsen, G., 1953. Regional settlements caused by a subway tunnel in Oslo. Proceedings of the 3rd International Conference on Soil Mechanics and Foundation Engineering (Zurich), Vol. I, pp. 381-383.

Horiuchi, Y., Kudo, T., Tashiro, M. and Kimura, K., 1986. A shallow tunnel enlarged in diluvial sand. Proceedings of the International Congress on Large Underground Openings

- ITA (Firenze), Vol. I, pp.752-760.

Howe, M., 1982. Damage control for distribution systems. Gas Engineering and Management. Journal of Institution of Gas Engineers (London), Vol. 22, Oct., pp. 377-399.

Howland, A.F., 1981. The prediction of the settlement above soft ground tunnels by considering the groundwater response with the aid of flow net constructions. Proceedings of the 2nd International Conference on Ground Movements and Structures (Cardiff), pp. 345-358.

Hoyaux, B. and Ladanyi, B., 1970. Gravitational stress field around a tunnel in soft ground. Canadian Geotechnical Journal, Vol. 7, No. 1, pp. 54-61.

Hubbard, H.W., Potts, D.M., Miller, D. and Burland, J.B., 1984. Design of the retaining walls for the M25 cut and cover tunnel at Bell Common tunnel. Geotechnique 34, No.4, pp. 495-512.

Hughes, J.M.O. and Ervin, M.C., 1980. Development of a high pressure pressuremeter for determining the engineering properties of soft to medium strength rocks. Proceedings of the 3rd Australia and New Zealand Geomechanics Conference, (Wellington).

Hughes, J.M.O., Wroth, C.P. and Windle, D., 1977. Pressuremeter tests in sands. Geotechnique, Vol. 27, No. 4, pp.455-477.

Hungr, O., 1985. Discussion of Atkinson and Mair, Geotechnique 35, No. 1, p73.

Hutchinson, D.E., 1982. Effect of construction procedure on shaft and tunnel performance. M.Sc. Thesis, Department of Civil Engineering, University of Alberta.

Imaki, J., Masumoto, H., Ueda, S., Amano, M. and Kurihara, H., 1984. Execution of large cross section tunnel by New Austrian Tunnelling Method in sandy soil with small cover. Proceedings of the 1st Latinamerican Congress of Underground Constructions (ITA, Caracas), Vol. I, pp. 503-508.

Ishihara, K., 1970. Relations between process of cutting and uniqueness of solution. Soils and Foundation, Vol. X, No. 3, pp. 50-65.

Ito, T. and Hisatake, M., 1981. Analytical study of NATM. Proceedings of the 10th International Conference on Soil Mechanics and Foundation Engineering (Stockholm), Vol. 1, pp. 311-314.

Ito, T. and Hisatake, M., 1982. Three-dimensional surface subsidence caused by tunnel driving. Proceedings of the 4th International Conference on Numerical Methods in Geomechanics (Edmonton), Vol. 2, pp.551-559.

Jagsch, D., Muller, L. and Hereth, A., 1974. Bericht uber die Messungen und Messergebnisse beim Bau der Stadtbahn Bachum Los A2. Interfels Messtechnik Information, pp. 11-13.

Jamiolkowski, M., Ladd, C.C., Germaine, J.T. and Lancellotta, R., 1985. New developments in field and laboratory testing of soils. Proceedings of the 11th International Conference on Soil Mechanics and Foundation Engineering (San Francisco), Vol. 1, pp. 57-153.

Janbu, N., 1963. Soil compressibility as determined by oedometer and triaxial tests. European Conference on Soil Mechanics and Foundation Engineering, Wiesbaden, Germany, Vol. 1, pp.19-25.

Jardine, R.J., Fourie, A., Maswoswe, J. and Burland, J.B., 1985. Field and laboratory measurements of soil stiffness. Proceedings of the 11th International Conference on Soil Mechanics and Foundation Engineering (San Francisco), Vol. 2, pp. 511-514.

Jardine, R.J., Potts, D.M., Fourie, A.B. and Burland, J.B., 1986. Studies of the influence of non-linear stress-strain characteristics in soil-structure interaction. Geotechnique, Vol. 36, No. 3, pp. 377-396.

Jardine, R.J., Symes, N.J. and Burland, J.B., 1984. The measurement of soil stiffness in the triaxial apparatus. Geotechnique. Vol. 34, No. 3, pp. 323-340.

Jeffrey, G.B., 1920. Plane stress and plane strain in bipolar coordinates. Transaction of the Royal Society, London, Series A, Vol.221, pp. 265-293.

Johnston, P.R., 1981. Finite element consolidation analyses of tunnel behaviour in clay. Ph.D. Dissertation, Stanford University, 224p.

Johnston, P.R. and Clough, G.W., 1983. Development of a design technology for ground support for tunnels in soil. Volume I: Time-dependent response due to consolidation in clays. Report UMTA-MA-06-0100-82-1, NTIS (Springfield, Virginia), 218p.

De Jong, J. and Harris, M.C., 1971. Settlements of two multistory buildings in Edmonton. Canadian Geotechnical Journal, 8, pp. 217-235.

Kaiser, P.K., 1981. A new concept to evaluate tunnel performance - influence of excavation procedure. Proceedings of the 22nd U.S. Rock Mechanics Symposium, (Boston), pp. 264-271.

Kaiser, P.K., 1982. Proposal for new design approach. In: Course Notes for Design and Construction of Tunnels and Shafts (Chapter 3), Department of Civil Engineering, University of Alberta.

Kaiser, P.K., 1985. Rational assessment of tunnel liner capacity. Proceedings of the 5th Annual Canadian Tunnelling Conference (Montreal).

Kaiser, P.K. and Barlow, J.P., 1986. Rational assessment of tunnel liner capacity. Canadian Tunnelling Canadien, pp. 31-44.

Kaiser, P.K. and Hutchinson, D.E., 1982. Effects of construction procedures on tunnel performance. Proceedings of the 4th International Conference on Numerical Methods in Geomechanics, 2, pp.516-569.

Karlsrud, K. and Sander, L., 1978. Subsidence problems caused by rock-tunnelling in Oslo. Proceedings of the International Conference on Evaluation and Prediction of Subsidence (Pensacola Beach), pp. 197-213.

Karshenas, M., 1979. Modeling and finite element analysis of soil behaviour. Ph.D. Thesis. University of Illinois at Urbana-Champaign. 279 p.

Kasali, G. and Clough,G.W., 1983. Development of a design technology for ground support for tunnels in soil. Volume II: Three-dimensional finite element analysis of advanced and conventional shield tunneling. Report UMTA-MA-06-0100-82-2 NTIS (Springfield, Virginia), 218 p.

Kastner, H., 1949. Uber den echten Gebirgsdruck beim Bau tiefliegender Tunnel. Osterr. Bauzeitschr., 10-11 (Quoted by Szechy, 1973:176).

Kastner, H., 1971. Statik des Tunnel und Stollenbaues. Springer Berlin.

Kathol, C.P. and McPherson, R.A., 1975. Urban geology of Edmonton. Alberta Research Council, Bulletin 32, 61p.

Katzenbach, R., 1981. Entwicklungstendenzen beim Bau und der Berechnung oberflachennaher Tunnel in bebautem Stadtgebiet. Mitteilungen der Versuchsanstalt fur Bodenmechnik und Grundbau der Technischen Hochschule Darmstadt, Heft 24.

Katzenbach, R., 1985. The influence of soil strength and water load to the safety of tunnel driving. Proceedings of the 5th International Conference on Numerical Methods in Geomechanics (Nagoya), pp. 1207-1213.

Katzenbach, R., and Breth, H., 1981. Nonlinear 3-D analysis for NATM in Frankfurt clay. Proceedings of the 10th International Conference on Soil Mechanics and Foundation Engineering, Stockholm, Vol. 1, pp. 315-318.

Katzenbach, R., and Breth, H., 1983. Zur Standsicherheit oberflachennaher Tunnel. Bauingenieur, 58, pp. 201-207.

Kawamoto, T. and Okuzono, K., 1977. Analysis of ground surface settlement due to shallow shield tunnels. International Journal for Numerical and Analytical Methods in Geomechanics, Vol. 1, No. 3, pp.271-281.

Kenney, T.C. and Uddin, S., 1974. Critical period for stability of an excvated slope in clay soil. Canadian Geotechnical Journal, 11, pp. 620-623.

Kerisel, J., 1975. Old structures in relation to soil conditions. 15th Rankine Lecture. Geotechnique 25, No. 3, pp. 433-483.

Kerisel, J., 1980. Commentary on the General Report. In: Analysis of tunnel stability by the Convergence-Confinement Method. Translation of the Proceedings of the Paris Conference, Underground Space, Vol. 4, No. 4, pp. 233-239.

Kimura, T., and Mair, R.J., 1981. Centrifugal testing of model tunnels in soft clay. Proceedings of the 10th International Conference on Soil Mechanics and Foundation Engineering (Stockholm), Vol. 1, pp. 319-322.

Kirsch, G., 1898. Die Theorie der Elasticitat und die Bedurfnisse der Festigkeitslehre. Zeitschrift des Vereines Deutscher Ingenieure, 42:29, 1.

Kochen, R. and Negro, A., 1985. Analise da Ruptura do tunel Oeste. Prolongamento da Linha Norte-Sul do Metro de Sao Paulo. Report MD-1.20.00.00/6G9-204 to Cia. Metro de Sao Paulo.

Kochen, R., Negro, A., Heinz, Jr., H. and Rottmann, E., 1985. Finite element simulations of underground excavations. Proceedings of the 2nd Symposium on Underground Excavations (ABGE) (in Portuguese), Vol. 1, pp. 195-217 (Rio de Janeiro).

Kocken, R., Negro, A., Hori, K., Ferrari, O. and Maffei, C., 1987. Longitudinal displacements induced by the excavation of a shallow tunnel. Proceedings of the International Conference on Soil Structure Interactions (Paris, May'87), pp.405-411.

Koenz, P. and Garbe, L., 1986. Railway tunnel construction under the old city of Zurich. Proceedings of the International Congress on Large Underground Openings - ITA (Firenze), Vol. I, pp. 761-770.

Kommerell, O., 1912 and 1940. Statische Berechnung von Tunnelmauerwerk. Grundlagen und Anwendung auf die wichtigsten Belastungsfalle. Ernst u. Sohn, Berlin 1940.

Kondner, R.L., 1963. Hyperbolic stress-strain response: cohesive soils. Journal of the Soil Mechanics and Foundation Division, ASCE, Vol. 89, SM 1, 115-143.

Kondner, R.L. and Zelasko, J.S., 1963. A hyperbolic stress-strain formulation for sands. Proceedings of the 2nd Panamerican Conference on Soil Mechanics and Foundation Engineering, Vol. 1, Brasil, pp. 289-324.

Kovari, K., 1977. The elasto-plastic analysis in the design practice of underground openings. Finite Elements in Geomechanics, Wiley, 377-412.

Kovari, K., Hagendorn, H. and Fritz, P. 1976. Parametric studies as a design aid in tunnelling. Proceedings of the 2nd International Conference on Numerical Methods in Geomechanics (Virginia), Vol. II, pp. 773-790.

Krischke, A. and Weber, J., 1981. Erfahrungen bei der Erstellung grosser Tunnelquerschnitte in Teilvortrieben beim Munchener U-Bahn-Bau. Rock Mechanics (Springer, Vienna), Suppl. 11, pp. 107-126.

Kuesel, T.R., 1986. Principles of tunnel lining design. Tunnelling Technology Newsletter, U.S. National Committee on Tunnelling Technology, No. 53, pp. 1-8.

Kulhawy, F.H., 1974. Finite element modeling criteria for underground openings in rock. International Journal of Rock Mechanics and Mining Sciences and Geomechanics Abstracts, Vol. 11, pp. 465-472.

Kulhawy, F.H., 1975. Stresses and displacements around openings in homogeneous rock. International Journal of Rock Mechanics and Mining Sciences and Geomechanics Abstracts, Vol. 12, pp. 43-57.

Kulhawy, F.H., 1977. Embankments and excavations. In: Numerical Methods in Geotechnical Engineering (edited by C.S. Desai and J.T. Christian), McGraw Hill, pp. 528-555.

Kulhawy, F.H. and Duncan, J.M., 1972. Stresses and movements in Oroville Dam. Journal of the Soil Mechanics and Foundations Divisions, ASCE, Vol. 98, No. SM7, pp. 653-665.

Kupper, A.M.A.G., 1983. Caracteristicas Tensao x Deformacao x Resistencia de Uma Amostra da Argila Vermelha do Terciario de Sao Paulo. M.Sc. Thesis. Catholic University, Rio de Janeiro.

Kusakabe, O., Kimura, T., Ohta, A., Takagi, N. and Nishio, N., 1985. Centrifige model tests on the influence of axisymmetric excavation on buried pipes. Proceedings of the 3rd International Conference on Ground Movements and Structures (Cardiff), pp. 113-128.

Kyrou, K., 1980. The effect of trench excavations induced ground movements on adjacent buried pipelines. Ph.D. Thesis, Department of Civil Engineering, University of Surrey, (U.K.) (quoted by Rumsey and Dorling, 1985).

Kyrou, K. and Kalteziotis, N.A., 1985. The effect of trenching on adjacent pipelines. Proceedings of the 11th International Conference on Soil Mechanics and Foundation Engineering (San Francisco), Vol. 3, pp. 1657-1660.

Laabmayr, F. and Pacher, F., 1978. Projekt Sondervorschlag U-Bahn Linie 8/1 Los 9/18.2. In: Moderner Tunnelbau bei der Munchner U-Bahn, Springer (edited by H. Lessmann), pp. 29-53.

Laabmayr, F., Swoboda, G., 1979. Zusammenhang zwischen elektronischer Berechnung und Messung, Stand der Entwicklung fur seichtliegende Tunnel. Rock Mechanics, Suppl. 8, 29-42.

Laabmayr, F., and Weber, J., 1978. Messungen, Auswertung und ihre Bedeutung. In: Moderner Tunnelbau bei der Munchner U-Bahn, Springer, (edited by H. Lessmann), pp. 73-96.

Ladanyi, B., 1966. Short term behaviour of clay around a circular tunnel. Universite Laval, Departement de Genie Civil, Rapport S-8.

Ladanyi, B., 1974. Use of long-term strength concept in the determination of ground pressure on tunnel linings. Proceedings of the 3rd International Congress on Rock Mechanics, (Denver), Vol. 2B, pp. 1150-1156.

Ladanyi, B., 1980. Direct determination of ground pressures on tunnel lining in non-linear viscoelastic rock. 13th Canadian Rock Mechanics Symposium, CIM Special Volume 22, Canadian Institute of Mining and Metallurgy. pp. 126-132.

Ladanyi, B., 1982. Issues in rock mechanics: A personal view. Conference Keynote Address. Proceedings of the 23rd Symposium on Rock Mechanics (Berkeley), pp.3-14.

Ladanyi, B. and Hoyaux, B., 1969. A study of the trap-door problem in a granular mass. Canadian Geotechnical Journal, 6, pp. 1-14.

Lambe, T.W., 1973. Predictions in soil engineering. 13th Rankine Lecture, Geotechnique 23, pp. 149-202.

Lambe, T.W. and Whitman, R.W., 1969. Soil Mechanics, John Wiley & Sons, New York, 553 p.

Larnach, W.J. and Wood, L.A., 1972. The effect of soil-structure interaction on settlements. Proceedings of the International Symposium on Computer-Aided Structural Design (Coventry), pp. Gl. 1- Gl. 13.

Ledesma, A., Gens, A., and Alonso, E.E., 1986. Identification of parameters in a tunnel excavation problem. Proceedings of the 2nd International Symposium on Numerical Models in Geomechanics (Ghent), pp. 333-344.

Limanov, I.A., 1957. Surface settlements in Cambrian clay due to tunnel construction (in Russian). Inst. Inzh. Zhelezn. Transport (Leningrad) - quoted by Szechy (1973:1045)

Lo, K.Y, Leonards, G.A. and Yuen, C., 1977. Interpretation and significance of anisotropic deformation behaviour of soft clay. Norwegian Geotechnical Institute Report No. 117 (Oslo, Norway) (quoted by Ng and Lo, 1985:380).

Lo, K.Y., Ng, M.C. and Rowe, R.K., 1984. Predicting settlement due to tunnelling in clay. Tunnelling in Soil and Rock. Geotech '84 (ASCE)/ pp. 46-75.

Lo, K.Y. and Rowe, R.K., 1982. Prediction of ground subsidence due to tunnelling in clays. Research Report GEOT-10-82 for NRC of Canada, Faculty of Engineering Science, Univeristy of Western Ontario, 353 p.

Lombardi, G., 1970. The influence of rock characteristics on the stability of rock cavitities. Tunnels and Tunnelling, Vol. 2, pp. 104-109.

Lombardi, G., 1972. Diskussionsbeitrag zum Thema 2. Proceedings Internationales Symposium fur Untertagbau (Luzern), pp. 370-378.

Lombardi, G., 1973. Dimensioning of tunnel linings with regards to constructional procedure. Tunnels and Tunnelling, Vol. 5, pp. 340 -351.

Lombardi, G., 1974. The problems of tunnel supports. Proceedings of the 3rd Congress of the International Society for Rock Mechancis (Denver), Vol. III, pp. 109-113.

Lombardi, G., 1980. Some comments on the Convergence-Confinement Method. Underground Space, Vol. 4, No. 4, pp. 249-258.

Lombardi, G. and Amberg, W., 1979. L'Influence de la Methode de Construction sur l'Equilibre final d'un Tunnel. Proceedings, 4th Congress of the International Society for Rock Mechanics, Montreux, Vol. 1, pp. 475-484.

Loudon, P.A., 1967. Some deformation characteristics of kaolin. Ph.D. Thesis, Cambridge University.

Lunardi, P. and Louis, C., 1985. Methodes de presoutenement et pre-etanchement pour le travaux en souterrain. Proceedings of the International Symposium in Tunnelling in Soft and Water-Bearing Grounds. AFTES, Lyon, A.A. Balkema (Rotterdam), pp. 119-124.

Lunardi, P., Mongilardi, E., Tornaghi, R., 1986. Il preconsolidamento mediante jet-grouting nella realizzazione di opere in Sotteraneo. Proceedings of the International Congress on Large Underground Openings -ITA (Firenze), Vol. II, pp. 601-612.

Maffei, C.E.M., 1982. Analise dos modelos calculo de Suportes e Revestimentos. Anais do Simposio Sobre Escavacoes Subterraneas (ABGE - Rio de Janeiro), pp. 157-184.

Maidl, B., 1984. Handbuch des Tunnel - und Stollenbaus. Band I: Konstruktionen und Verfahren. Verlag Gluckauf GmbH, 423 p.

Mair, R.J., 1977. Behaviour of tunnels in soft ground. CUED - Soils Report to TRRL (September), University of Cambridge.

Mair, R.J., 1979. Centrifugal modelling of tunnel construction in soft clay. Ph.D. Dissertation, Cambridge University.

Mair, R.J., Gunn, M.J. and O'Reilly, M.P., 1981. Ground movements around shallow tunnels in soft clay. Proceedings of the 10th International Conference on Soil Mechanics and Foundation Engineering (Stockholm), Vol. 1, pp. 323-328.

Mandel, J. and Halphen, B., 1974. Stabilite d'une cavite spherique souterraine. Proceedings of the 3rd Congress of the International Society for Rock Mechanics (Denver), Vol. II, Part B, pp. 1028-1032.

Marsland, A., 1972. The shear strength of stiff fissured clays. In: Stress-Strain Behaviour of Soils. Roscoe Memorial Symposium, Cambridge (edited by R.H.G. Parry), pp. 59-68.

Marsland, A. and Randolph, M.F., 1977. Comparisons of the results from pressuremeter tests and large in situ plate tests in London clay. Geotechnique, Vol. 27, No. 2, pp. 217-243,

Massa, E.M., 1981. Projeto e construcao do Tunel de

Mangueira. Metro do Rio de Janeiro. Special Publication of the Brazilian Association of Soil Mechanics (ABMS - Rio de Janeiro), 43 p.

Massad, F., 1974. Caracteristicas geotecnicas das argilas porosas vermelhas de Sao Paulo. Proceedings of the 5th Brazilian Congress on Soil Mechanics and Foundation Engineering (Sao Paulo), Vol. 2, pp.131-144.

Massad, F., 1980. Caracteristicas e propriedades geotecnicas de alguns solos da Bacis de Sao Paulo. Anais de Mesa Redonda Aspectos Geologico e Geotecnicos da Bacia Sedimentar de Sao Paulo (ABGE - SBG), Sao Paulo - IPT, pp. 53-93.

Massad, F., 1981(a). O problema do coeficiente de empuxo em repouso dos solos terciarios da cidade de Sao Paulo. Proceedings, Simposio Brasileiro de Solos Tropicais em Engenharia (published by ABMS - Brazilian Society for Soil Mechanics), pp. 91-101.

Massad, F., 1981(b). Resultados de Investigacao Laboratorial sobre a deformabilidade de alguns solos terciarios da cidade de Sao Paulo. (Laboratory investigation on the deformability of some Sao Paulo city Tertiary Soils). Proceedings, Brazilian Symposium on Tropical Soils in Engineering (Rio de Janeiro), pp. 66-90.

Massad, F., Niyama, S. and Aleoni, N.A.O., 1981. Analise de provas de cargas horizontais em tubuloes executados num solo lateritico. Proceedings 'Symposio Brasileiro de Solos Tropicais em Engenharia' (ABMS), pp.668-682.

Matheson, D.S., 1970. A tunnel roof failure in till. Canadian Geotechnical Journal, 7, pp. 313-317.

Matsuzaki, S., Yamada, K. and Tanaka, H., 1986. An example of observational construction for risk reduction against existing underground structures in shield tunnelling. Proceedings of the International Congress on Large Underground Openings - ITA (Firenze), Vol. II, pp. 630-639.

May, R.W. and Thomson, S., 1978. The geology and geotechnical properties of till and related deposits in the Edmonton, Alberta, area. Canadian Geotechnical

Journal, Vol. 15, pp. 362-370.

Mayne, P.W. and Kulhawy, F.H., 1982. K_o-OCR relationships in soil. Journal of the Geotechnical Engineering Division, American Society of Civil Engineers, Vol. 108, June, pp. 851-872.

Medeiros, L.V., 1979. Deep excavations in stiff soils. Ph.D. Thesis. Department of Civil Engineering, University of Alberta.

Medeiros, L.V and Eisenstein, Z., 1983. A deep retaining structure in till and sand. Part I: Stress path effects. Canadian Geotechnical Journal. Vol. 20, No. 1, pp. 120-130.

Medeiros, L.V., El-Nahhas, F., Smith, L.B. and Eisenstein, Z., 1982. Modelling of the construction of an underground station. Proceedings of the 4th International Conference on Numerical Methods in Geomechanics (Edmonton), Vol. 2, pp. 929-934.

Meister, D. and Wallner, M., 1977. Instrumentation of a tunnel in extremely bad ground and interpretation of the measurements. Proceedings, International Symposium on Field Measurements in Rock Mechanics, Zurich (edited by K. Kovari), pp. 919-933.

de Mello, V.F.B., 1969. Foundations of buildings in clay. Proceedings of the 7th International Conference on Soil Mechanics and Foundation Engineering, State-of-the-Art Volume (Mexico), pp. 49-136.

de Mello, V.F.B., 1977, Reflections on design decisions of practical significance to embankment dams. Geotechnique 27, No. 3, pp. 279-355.

de Mello, V.F.B., 1981. Proposed bases for collating experiences for urban tunneling design. Proceedings of the Syposium on Tunnelling and Deep Excavations in Soils, Sao Paulo, (published by ABMS - Brazilian Society for Soil Mechanics), pp. 197-23

de Mello, V.F.B. and Sozio, L.E. 1983. Proposed bases for collating experiences for urban tunneling design (in

Portuguese). Course Lecture Note, Department of Civil Engineering, PUC, (Rio de Janeiro).

Menzies, B.K., Sutton, H. and Davies, R.E., 1977. A new system for automatically simulating K_o consolidation and K_o swelling in the conventional triaxial cell. Geotechnique, Vol. 27, pp. 593-596.

Mettier, K., 1979. Messungen und Ergebnisse bei der Anwendung des Gefrierverfahrens im Tunnelbau. Mitteilungen der Schweizenschen Gelleschaft fur Boden und Felsmechanik , No. 100. pp. 53-59.

Migliacci, A., Campagna, D., Levati, S., Riva, P. and Curzio, A.Q., 1986. Le gallerie scavate in terreno cementato. Analisi Strutturali e sperimentzioni. Proceedings of the International Congress on Large Underground Openings - ITA (Firenze), Vol. I, pp. 804-813.

Mindlin, R.D., 1938. Gravitational stresses in bipolar coordinates. Proceedings of the 5th International Congress of Applied Mechanics (Cambridge, MA), pp. 112-116.

Mindlin, R.D., 1939. Stress distribution around a tunnel. Proceedings of the American Society of Civil Engineers, Vol. 65, pp. 619-642. Also in 1940, Trans. ASCE, Vol. 105, pp. 1117-1153.

Mohraz, B., Hendron, A.J., Ranken. R.E. and Salem, M.H., 1975. Liner medium interaction in tunnels. Journal of the Construction Division, American Society of Civil Engineers, Vol. 101, No. CO1, March, pp. 127-141.

Morgan, H.D., 1961. A contribution to the analysis of stress in a circular tunnel. Geotechnique, Vol. 11, pp. 37-46.

Morgenstern, N.R., 1975. Stress-strain relationships for soils in practice. Proceedings of the 5th Panamerican Conference on Soil Mechanics and Foundation Engineering (Buenos Aires), Vol. 1, pp. 1-41.

Morgenstern, N.R. and Eisenstein, Z., 1970. Methods of estimating lateral loads and deformations. Proceedings of the ASCE Specialty Conference on Lateral Stresses and Retaining Structures, Cornell University, pp. 51-102.

Morgenstern, N.R. and Tchalenko, J.S., 1967. Microscopic structures in kaolin subjected to direct shear. Geotechnique, Vol. 17, pp. 309-328.

Morgenstern, N.R. and Thomson, S., 1971. Comparative observations of the use of the Pitcher sampler in stiff clay. ASTM Special Technical Publication 483, pp. 180-191.

Muhlhaus, H.B., 1983. Critical geometry and material parameters of shallow tunnels. Proceedings of the 5th Congress of the International Society for Rock Mechanics (Melbourne), Vol. I, pp. C263-C268.

Muhlhaus, H.B., 1985. Lower Bound Solutions for Circular Tunnels in Two and Three Dimensions. Rock Mechanics and Rock Engineering, 18, pp. 37-52.

Muir Wood, A.M., 1969. Contribution to discussion. Proceedings of the 7th International Conference on Soil Mechanics and Foundation Engineering (Mexico), Vol. 3, pp. 363-365.

Muir Wood, A.M., 1975, The circular tunnel in elastic ground. Geotechnique, Vol. 25, pp. 115-127.

Muir Wood, A.M. and Gibb, F.R., 1971. Design and construction of the cargo tunnel at Heathrow, London. Proceedings ICE, Vol. 48 (Jan), pp. 11-34. Discussion: Proceedings ICE, Vol. 50 (Oct.), pp. 187-201.

Muller, L. 1977. The use of deformation measurements in dimensioning the lining of subway tunnels. Proceedings of the International Symposium on Field Measurements in Rock Mechanics (Zurich), pp. 451-471.

Muller, L. 1978. Removing misconception on the NATM. Tunnels and Tunnelling, October, pp. 29-32.

Muller, L., 1979. Die Bedeutung der Ringschlusslange und der Ringschlusszeit im Tunnelbau. Proceedings of the 4th

Congress of the International Society for Rock Mechanics (Montreux), Vol. 1, pp. 511-519.

Muller, L., Sauer, G. and Chambosse, G., 197[illegible] Berechnungen, Modellversuche und in situ Messungen bei einem bergmannischen Vortrieb im tonigen Untergrund. Bauingenieur 52, Heft 1, pp. 1-8.

Mullins, W.W., 1977. Stochastic modeling of gravity induced particulate flow. In: Probability Theory and Reliability Analysis in Geotechnical Engineering. Ed. D.A. Grivas (Rensselaer Polytechnic Institute, New York), pp. 36-51.

Murayama, S. and Matsuoka, H., 1969. On the settlement of granular media casued by local yielding in the media. Proceedings of the Japan Society of Civil Engineers (in Japanese), 172, pp. 31-41.

Murray, D.W., 1971. Simple two dimensional finite element program - constant strain triangle. Internal Note. Department of Civil Engineering, The University of Alberta.

Myer, L.R., Brekke, T.L., Dare, C.T., Dill, R.B. and Korbin, G.E., 1981. An investigation of stand-up time of tunnels in squeezing ground. Proceedings of the Rapid Tunneling Excavation Conference (San Francisco), Vol. 2, pp. 1415-1433.

McBean, R.J. and Harries, D.A., 1970. The development of high-speed soft ground tunnelling pre-cast concrete segments and tunnelling machines. Proceedings of the South African Conference on Tunnelling (Johannesburg), pp. 129-134.

McCaul, C.,1978. Settlements caused by tunnelling in weak ground at Stockton-on-Tees. Department of the Environment, Department of Transport, TRRL Supplementary Report 383: Crowthorne, 1978 (Transport and Road Research Laboratory). Also Tunnels and Tunnelling (November, 1978), pp. 63-67.

McCaul, C., Dobson, C., Cooper, I., and Spencer, I.M., 1983. Ground movements caused by tunnelling in loose fill. TRRL Supplementary Report 781 (Crowthorne, U.K.).

McCaul, C., Morgan, J.M. and Boden, J.B., 1976. Measurement of ground movement due to excavation of a shallow tunnel in Lower Chalk. TRRL Supplementary Report 199UC (U.K.).

Nadarajah, V., 1973. Stress-strain properties of lightly overconsolidated clays. Ph.D. Thesis. Cambridge University.

Nath, P., 1983. Trench excavation effects on adjacent buried pipes: finite element study. Journal of Geotechnical Engineering (ASCE), Vol. 109, No. 11, pp. 1399-1415.

Negro, A., 1979. Quality of construction and tunnelling behaviour. Unpublished contribution to the Specialty Session on Tunnels in Soft Ground - 6th Panamerican Conference on Soil Mechanics and Foundation Engineering, Lima.

Negro, A., 1981. Computer program manual: Tunnel excavation. Internal Note. Department of Civil Engineering. The University of Alberta (November)

Negro, A., 1983. Soil tunnels: Construction procedures and induced ground displacements. Journal of Engineering. FAAP, Sao Paulo, Vol. 2, n.3, pp. 14-23 (in Portuguese).

Negro, A., 1984. Avaliacao do sistema Mecanizado de construcao de Tuneis da ETESCO. Report to ETESCO S.A. Comercio e Construcoes (Novembro).

Negro, A. and Eisenstein, Z., 1981. Ground control techniques compared in three Brazilian water tunnels. Tunnels and Tunnelling, Oct., pp. 11-14, Nov., pp.52-54, Dec. pp. 48-50.

Negro, A., Eisenstein, Z. and Heinz, Jr., H., 1985. Three-dimensional displacements at the face of shallow tunnels (in Portuguese). Proceedings of the 2nd Symposium on Underground Excavation (ABGE), Vol. 1, pp. 270-286 (Rio de Janeiro).

Negro, A., Eisenstein, Z. and Heinz, Jr., H. 1986. Prediction of radial displacements at the face of shallow tunnels. Proceedings of the 2nd International Conference on Numerical Models in Geomechanics (Ghent), pp. 837-843.

Negro, A., Heinz, Jr., H. and Eisenstein, Z., 1984. Urban tunnels with large cross section (in Portuguese). Solos e Rochas, Vol. 7, pp. 7-29.

Negro, A. and Kochen, R., 1985. Discussion on Session III, Underground Construction and Building Foundations (in Portuguese). Proceedings of the Symposium on Special Foundations (ABMS/FAAP), Vol. II, pp. 115-120. (Sao Paulo, Sept.).

Negro, A., Kochen, R. and Rottmann, E., 1985. Analise da Instrumentacao de Campo e Avaliacao do comportamento: Tunnel Duplo. Prolongamento da Linha Norte Sul do Metro de Sao Paulo. Report MD-1.20.00.002/6G9 - 205 to Cia Metro de Sao Paulo.

Negro, A. and Kuwajima, F., 1985. Prediction of displacements around underground caverns (in Portuguese). Proceedings of the 2nd Symposium on Underground Excavations (ABGE), Vol. 1, pp. 234-249 (Rio de Janeiro).

Newmark, N.M., 1964. The basis of current criteria for the design of underground protective construction. Proceedings of the Symposium on Soil-Structure Interaction (Tuscon), pp. 1-24.

Ng, R.M.C., 1984. Ground reaction and behaviour of tunnels in soft clays. Ph.D. Thesis. University of Western Ontario.

Ng, R.M.C. and Lo, K.Y., 1985. The measurements of soil parameters relevant to tunnelling in clays. Canadian Geotechnical Journal, 22, pp. 375-391.

Ng, R.M.C, Lo, K.Y., and Rowe, R.K., 1986. Analysis of field performance - the Thunder Bay tunnel. Canadian Geotechnical Journal, 23, pp. 30-50.

Nguyen Minh, D., 1986. Modeles Rheologigues pour l'anlyse du comportement differe des galeries profonds. Proceedings of the International Congress on Large Underground Openings - ITA (Firenze), Vol. II, pp. 659-666.

Nguyen Minh, D. and Berest, P., 1977. Contraction d'une sphere creuse elastoplastique avec radouscissement. Journal de Mecanique Appliquee, Vol. 1, No. 1, pp. 85-109.

Nguyen Minh, D. and Berest, P., 1979. Etude de la stabilite des cavites souterraines avec un modele de comportement elastoplastique radoucissant. Proceedings of the 4th Congress of the International Society for Rock Mechanics (Montreux), Vol. I, pp. 249-256.

Nishiwaki, S., 1984. Measures for reinforcing ground in tunnel in sandy strata with small overburden. Proceedings of the 1st Latinamerican Congress of Underground Constructions - ITA (Caracas), Vol. I, pp. 457-466.

Niwa, Y., Kobayashi, S. and Fukui, T., 1979. Stress and displacements around an advancing face of a tunnel. Proceedings of the 4th Congress of the International Society for Rock Mechanics (Montreux), Vol. I, pp. 703-710.

Novak, J., 1984. Use of extruded concrete in subway tunnels. Proceedings of the 1st Latinamerican Congress of Underground Constructions - ITA (Caracas), Vol. I, pp. 425-429.

Ohnishi, Y., Nishagaki, Y., Kishimoto, H. and Tanaka, Y., 1982. Analysis of advancing tunnel by 2-dimensional F.E.M. Proceedings of the 4th International Conference on Numerical Methods in Geomechanics (Edmonton), Vol. 2, pp. 571-578.

Ohta, H., Kitamura, H., Itoh, M. and Katsumata, M., 1985. Ground movement due to advance of two shield tunnels. Proceedings of the 5th International Conference on Numerical Methods in Geomechanics (Nagoya), pp. 1161-1166.

Oliveira, M. and Ferreira, A.A., 1982. Consolidacao de Solo aluvionar mole: relato de um tratamento por injecao de cimento para escavacao de de tunel urbano na cidade de Sao Paulo. Anais do Simposio sobre Escavacao Subterraneas (Rio de Janeiro), Vol. 1, pp. 335-353.

OMTC 1976. Tunnelling Technology: an appraisal of the State-of-the-Art for applications to transit systems. Published by Ontario Ministry of Transportation and Communications, Toronto, 166p.

O'Reilly, M.P., Roxborough, F.F. and Hignett, H.J., 1976. Programme of laboratory, pilot and full-scale experiments in tunnel boring. Proceedings Tunnelling '76 (U.K.), pp. 287-299.

O'Reilly, M.P., Ryley, M.D., Barratt, D.A. and Johnson, P.E., 1981. Comparison of settlements resulting from three methods of tunnelling in loose cohesionless soil. Proceedings of the 2nd International Conference on Ground Movements and Structures (Cardiff), pp. 359-376.

O'Rourke, T.D., 1978. Discussion:Lateral displacement of shallow buried pipelines due to adjacent deep trench excavations. Geotechnique, Vol. 28, No. 2, pp. 214-216.

O'Rourke, T.D., Cording, E.J. and Boscardin, M., 1978. Damage to brick-bearing wall structures caused by adjacent braced cuts and tunnels. Proceedings of the Conference on Large Ground Movements and Structures (Cardiff), pp. 647-671.

O'Rourke, T.D. et.al., 1984. Guidelines for Tunnel Lining Design. Prepared by the UTRC Technical Committee on Tunnel Lining Design. ASCE Geotechnical Engineering Division. 82 p.

Orr, T.L.L., 1976. The behaviour of lined and unlined model tunnels in stiff clay. Ph.D. Thesis. Cambridge University.

Orr, T.L.L., Atkinson, J.H. and Wroth, C.P., 1978. Finite element calculations for the deformation around model tunnels. Computer Methods in Tunnel Design. Institution of Civil Engineers (London), pp. 121-144.

Oteo, C.S. and Moya, J.F., 1979. Estimation of the soil parameters of Madrid in relation to tunnel construction. Proceedings of the 7th European Conference on Soil Mechanics and Foundation Engineering (Brighton), Vol. 3, pp. 239-247.

Oteo, C.S. and Sagaseta, C., 1982. Prediction of settlements due to underground openings. Proceedings of the International Symposium on Numerical Models in Geomechanics (Zurich), September, pp. 653-659.

Palmer, A.C., 1966. A limit theorem for materials with non-associated flow rules, Journal de Mecanique, 5(2), 217-22.

Palmer, J.H.L. and Belshaw, D.J., 1979. Long-term performance of a machine-bored tunnel with use of an unreinforced, precast, segmented concrete lining in soft clay. Proceedings of the 2nd International Symposium Tunnelling '79 (IMM, London), pp. 165-178.

Palmer, J.H.L. and Belshaw, D.J., 1980. Deformations and pore pressures in the vicinity of a precast, segmented, concrete-lined tunnel in clay. Canadian Geotechnical Journal, Vol. 17, pp. 174-184.

Panet, M., 1976. Stabilite et Soutenement des tunnels. La mechanique des roches appliquee aux ouvrages du Genie Civil, Chapitre IX, pp.143-168. L'Ecole Nationale des Ponts et Chausses.

Panet, M. and Guellec, P. 1974. Contribution to the problem of the design of tunnel support behind the face. Proceedings, Third Congress, International Society for Rock Mechanics, Denver, Vol. 2, Part B, pp. 1163-1168. (in French).

Panet, M. and Guenot, A. 1982. Analysis of convergence behind the face of a tunnel. Tunnelling 1982, the Institution of Mining and Mettallurgy, pp. 197-204.

Paul, S.L., Hendron, A.J., Cording, E.J., Sgouros, G.E. and Saha, P.K., 1983. Design recommendations for concrete tunnel linings. Volume II: Summary of research and proposed recommendations. Report UMTA-MA-06-0100 83-3. National Technical Information Service, Springfield, Virginia, 22161.

Peck, R.B., 1969. Deep excavations and tunnelling in soft ground. Proceedings, 7th International Conference on Soil Mechanics and Foundation Engineering, Mexico, State-of-the-Art Vol., pp. 225-290.

Peck, R.B., 1981. Weathered rock portion of the Wilson Tunnel, Honolulu. Soft-Ground Tunnelling, Failures and Displacements (Ed. D. Resendiz and M.P. Romo), A.A. Balkema (Rotterdam), pp. 13-22.

Peck, R.B., Deere, D.U. and Capacete, J.L., 1956. Discussion on Skempton and MacDonald. Proceedings, Institution of Civil Engineers. Part II, Vol. 5, p. 778.

Peck, R.B., Hendron, A.J. and Mohraz, B., 1972. State-of-the-Art of soft grond tunnelling. Proceedings, 1st North American Rapid Excavation and Tunnelling Conference, Vol. 1, pp. 259-286.

Pelli, F., 1987. Near Face Behaviour of Deep Tunnels in Rock. Ph.D. Thesis, University of Alberta, 406p.

Pelli, F., Kaiser, P.K. and Morgenstern, N.R., 1986. Three-dimensional simulation of rock-liner interaction near tunnel face. Proceedings NUMOG II, Numerical Models in Geomechanics (Ghent).

Pender, M.J., 1980(a). Elastic solutions for a deep circular tunnel. Geotechnique, Vol. 30, pp. 216-222.

Pender, M.J., 1980(b). Simplified analysis for tunnel. Discussions. ASCE, GT7, p. 833-835.

Pender, M.J., 1980(c). Discussion of "Stress path method: second edition". Journal of the Geotechnical Engineering Division, ASCE, Vol. 106, No. GT9, pp. 1068-1071, September.

Penman, A.D.M., 1986. On the embankment dam. 26th Rankine Lecture. Geotechnique, Vol. 36, No. 3, pp. 301-348.

Penman, A.D.M. and Charles, J.A., 1974. Measuring movements of embankment dams. Proceedings, Symposium on Field Instrumentation in Geotechnical Engineering, Butterworths, pp. 341-358.

Pierau, B., 1981. Tunnelbemessung unter Berucksichtigung der raumlichen Spannungs-Verformungszustande an der Ortsbrust. Publication of the 'Institut fur Grundbau, Bodenmechanik, Felsmechanik und Verkehrswasserbau der. R.W. Technische Hochschule Aachen, Heft 9, 182 p.

Pierau, B., 1982. Tunnel design with respect to the three-dimensional state of stresses and displacements around the temporary face. Proceedings, 4th International Conference on Numerical Methods in Geomechanics, Edmonton, (edited by Z. Eisenstein), Vol. 3, pp. 1221-1231.

Polshin, D.E. and Tokar, R.A., 1957. Maximum allowable non-uniform settlement of structures. Proceedings, 4th International Conference on Soil Mechanics and Foundation Engineering, (London), Vol. 1, pp. 402-405.

Potts, D.M., 1976. Behaviour of lined and unlined tunnels in sand. Ph.D. Thesis. Cambridge University.

Potts, D.M. and Burland, J.B., 1983. A numerical investigation of the retaining walls of the Bell Common tunnel. TRRL Supplementary Report 783 (U.K.).

Poulos, H.G., 1982. Simplicity a desirable end-point of geotechnical research. Ground Engineering, pp. 2 and 6.

Poulos, H.G. and Davis, E.H., 1980. Pile foundation analysis and design. John Wiley and Sons (New York), 397 p.

Prevost, J.H., 1980. Constitutive theory for soil. Proceedings of the Workshop on Limit Equilibrium, Plasticity and Generalized Stress-Strain in Geotechnical Engineering (McGill University), pp.745-814.

Ranken, R.E., 1978. Analysis of ground liner interaction for tunnels. Ph.D. Thesis. Univeristy of Illinois (Urbana-Champaign), 427 p.

Ranken, R.E. and Ghaboussi, J., 1975. Tunnel design considerations: analyses of stresses and deformations around advancing tunnels. Report UILU-ENG75-2016 (NTIS - National Technical Information Service, U.S. Department of Commerce, Springfield, VA 22161).

Read, H.E. and Hegemier, G.A., 1984. Strain softening of rock, soil and concrete. A review article. Mechanics of Materials 3, pp. 271-294.

Rebull, P.M., 1972. Earth responses in soft ground tunnelling. Proceedings, Specialty Conference on Performance of Earth and Earth Supported Structures. (Lafayette), Vol. 1, Part 2., pp.1517-1535.

Resendiz, D., 1979. Full-scale observation, numerical modeling, and generalization in soil mechanics. Opening Lecture at the International Symposium on Soil Mechancis (Oaxaca), Publication E-37, Universidad Nacional Autonoma de Mexico.

Resendiz, D. and Romo, M.P., 1972. Analysis of embankement deformations. ASCE Specialty Conference on Performance of Earth and Earth-Supported Structures, Vol. 1, Part 1, pp. 817-836.

Resendiz, D. and Romo, M.P., 1981. Settlements upon soft-ground tunneling: theoretical solution. Soft-Ground Tunneling - Failures and Displacements. Edited by D. Resendiz and M.P. Romo (A.A. Balkema), pp. 65-74.

Reyes, S.F. and Deere, D.U., 1966. Elastic-plastic analysis of underground openings by the finite element method. Proceedings, 1st Congress International Society of Rock Mechanics, Lisbon 1966, Vol. II, pp. 477-483.

Ritter, W., 1879. Die statik der tunnelgewolbe. Springer, Berlin (quoted by Steiner and Einstein, 1980:37).

Rocha, M., 1975. Rock Mechanics in Underground Projects (in Portuguese). Lecture Notes, EPUSP (Sao Paulo).

Rodriguez, L.B., Ruelas, S.A. and Frausto, L.G., 1983. Movimientos presentados durante la excavacion de un tunel con escudo. Proceedings of the 7th Panamerican Conference on Soil Mechanics and Foundation Engineering (Vancouver), Vol. I, pp.425-437.

Rodiguez Roa, F., 1981. Some considerations for tunnel design. Proceedings, 10th International Conference on Soil Mechanics and Foundation Engineering (Stockholm), Vol. 1, pp. 353-356.

Romo, M.P. and Diaz, C.M., 1981. Face stability and ground settlement in shield tunnelling. Proceedings, 10th International Conference on Soil Mechanics and Foundation Engineering. Vol. 1, pp. 357-360.

Romo, M.P. and Resendiz, D., 1982. Observed and computed settlements in a case of soft-ground tunnelling. Proceedings, 4th International Conference on Numerical Methods in Geomechanics. (Edmonton), Vol. 2, pp. 597-604.

Roscoe, K.H., 1970. The influence of strains in soil mechanics. Geotechnique 20, No. 2, pp. 129-170.

Roscoe, K.H. and Burland, J.B., 1968. On the generalized stress-strain behaviour of 'wet' clay. Engineering Plasticity, Eds. J. Heyman and F.A. Leckie, Cambridge University Press, pp. 535-609.

Rowe, R.K., 1986. The prediction of deformations caused by soft ground tunnelling - Recent trends. Canadian Tunnelling.

Rowe, R.K. and Kack, G.J., 1983. A theoretical examination of the settlements induced by tunnelling: four case histories. Canadian Geotechnical Journal, 20, pp. 299-314.

Rowe, R.K., Lo, K.Y. and Kack, G.J., 1981. The prediction of subsidence above shallow tunnels in soft soil. Proceedings, Symposium on Implementation of Computer Procedures and Stress-Strain Laws in Geotechnical Engineering (Chicago), pp.266-280.

Rowe, R.K., Lo, K.Y. and Kack, G.J., 1983. A method of estimating surface settlement above tunnels constructed in soft ground. Canadian Geotechnical Journal, 20, pp. 11-22.

Rozsa, L., 1963. Die Bemessung kreisformiger Tunnelwundungen aus prafabrizierten Stahlbetonelementen nach dem Verfahren der Grenzbelastungen. Bauingenieur 38, Heft 11, pp. 434-441.

Rumsey, P.B. and Dorling, C., 1985. The prediction of ground movement and induced pipe strain caused by trench excavation. Proceedings, 3rd International Conference on Ground Movements and Structures (Cardiff), pp. 24-49.

Ryley, M.D., Johnson, P.E., O'Reilly, M.P. and Barrat, D.A., 1980. Measurements of ground movements around three tunnels in loose cohesionless soil. TRRL Laboratory Report 938 (Crowthorne, U.K.).

Saenz, J.T. and Utesa, L.V., 1971. Settlement around shield driven tunnels (in Spanish). Proceedings, 4th Panamerican Conference on Soil Mechanics and Foundation Engineering (Puerto Rico), Vol. II, pp. 225-241.

Sagaseta, C., 1973. Estado tenso-deformacional alredor de un tunel excavado en un medio elasto-plastico, con special consideracion de la influencia del proceso construtivo. Ph.D. Thesis. Escuela Tecnica Superior de Ingenieros de Caminos, Canales y Puertos de Madrid.

Sagaseta, C., Moya, J.F. and Oteo, C.S., 1981. Estimation of ground subsidence over urban tunnels. Proceedings of the 2nd International Conference on Ground Movements and Structures (Cardiff), pp. 331-344.

Sagaseta, C. and Oteo, C., 1974. Analisis Teorico de la Subsidencia Originada por la Excavacion de Tuneles. Proceedings, 1er Simposic Nacional Sobre Tuneles (Madrid), II-10, pp. 1-10, discussion pp. 76-79.

Sakurai, S., 1970. Stability of tunnel in viscoelastic-plastic medium. Proceedings, 2nd Congress of the International Society for Rock Mechanics (Beograd), pp. 521-529.

Sakurai, S., 1981. Direct strain evaluation technique in construction of underground openiong. Proceedings, 22nd US Symposium on Rock Mechanics: Rock Mechanics from Research to Application (MIT), pp. 278-282.

Sakurai, S., Yamamoto, Y., 1976. A numerical analysis of the maximum earth pressure acting on tunnel lining. Proceedings, 2nd International Conference on Numerical Methods in Geomechanics (Blacksburg), Vol. II, pp. 821-833.

Samarasekera, L., 1987. Ph.D. Thesis in preparation. University of Alberta.

Sasanabe, M., Matsubara, H. and Nakao, T., 1986. Planning and results of large diameter tunnel driven by soil plasticizing shield. Chichibu section of Nagoya Municipal Subway. Proceedings, International Congress on Large Underground Openings - ITA (Firenze), Vol. I, pp. 925-932.

Sauer, G. and Jonuscheit, P. 1976. Krafteumlagerung in der Zwischenwand eines Doppelrohrentunnels in Zuge eines Synchronvortriebes. Rock Mechanics (Springer, Vienna), 8, pp. 1-22.

Sauer, G. and Sharma, B., 1977. A system for stress-measurement in constructions in rock. Proceedings, International Symposium on Field Measurements in Rock Mechanics (edited by K. Kovari), Zurich, Vol. 1, pp. 317-329.

Schikora, K., 1982. Calculation model and measuring results for a double tunnel with low overburden in quarternary soil. Tunnel ('STUVA - Studiengesellschaft fur unterirdische Verkehrsanlagen' - Cologne 3/82, pp. 153-161.

Schikora, K., 1983. Double tunnel in the Munich underground. Tunnel (STUVA - Cologne), 2/83, pp. 71-79.

Schikora, K., 1984. Plane and spatial finite element calculations in tunnelling. Tunnel (STUVA - Cologne), 3/84, pp. 158-161.

Schikora, K. and Fink, T., 1982. Berechnungsmethoden moderner bergmannischer Bauweisen beim U-Bahn-Bau. Bauingenieur 57, pp.193-198.

Schmid, H., 1926. Statische Probleme des Tunnel - und Druckstollenbaues und ihre gegenseitigen Beziehungen, Springer, Berlin Wien 1926.

Schmidt, B., 1969. Settlements and ground movements associated with tunneling in soil. Ph.D. Thesis. University of Illinois at Urbana-Champaign.

Schmidt, B. 1970. Gravitational stress field around a tunnel in soft ground: Discussion. Canadian Geotechnical Journal, Vol. 7, pp. 346-348.

Schmidt, B., 1984. Tunnel lining design - do the theory work?, Proceedings, 4th Australia - New Zealand Conference on Geomechanics, (Perth), May.

Schmidt, B. and Sousa Pinto, 1983. Geotechnical engineering for transportation structures - general report. Proceedings, 7th Panamerican Conference on Soil Mechanics and Foundation Engineering, (Vancouver), Vol. III, pp. 1001-1034.

Schmitter, J.M. and Moreno, A.F., 1983. Tunel con Deformaciones Excesivas. Proceedings, 7th Panamerican Conference on Soil Mechanics and Foundation Engineering (Vancouver), pp. 401-411.

Schneebeli, G., 1957. Une analogie mecanique pour l'etude de la stabilite des ouvrages en terre a deux dimensions. Proceedings 4th International Conference on Soil Mechanics and Foundation Engineering (London), Vol. II, pp. 228-232.

Schofield, A.N., 1980. Cambridge geotechnical centrifuge operations. Geotechnique, Vol. 30, No. 3, pp. 227-268.

Schulz, W. and Edeling, H., 1973. Die Neue Osterreichische Tunnelbauweise beim U-Bahnbau in Frankfurt am Main. Rock Mechanics (Springer, Vienna), Supplement 2, pp. 243-256.

Schulze, H., and Duddeck, H., 1964(a). Statische Berechnung schildvorgetriebener Tunnel. Festschrift "Beton- und Monierbau AG 1889-1964", Dusseldorf, pp. 87-114.

Schulze, H., and Duddeck, H., 1964(b). Spannungen in Schildvorgetriebenen Tunneln. Beton-und Stahlbetonbau (Berlin), Heft 8, 59 Jahrgang, pp. 169-175.

Schwartz, C.W., Azzouz, A.S. and Einstein, H.H., 1980. Improved design of tunnel supports: Vol. 2 - Aspects of Yielding in ground-structure interaction. Report UMTA-MA-06-0100-80-5, NTIS, U.S. Department of Commerce, Springfield, VA 22161.

Schwartz, C.W. and Einstein, H.H., 1980. Improved design of tunnel supports: Vol. 1 - Simplified analysis for ground structure interaction in tunnelling. Report UMTA-MA-06-0100-80-4 (NTIS - National Technical Information Service, U.S. Department of Commerce, Springfield, VA 22161).

Selby, S.M., 1970. Handbook of tables for mathematics (4th edition), Publisher: The Chemical Rubber Co. (Ohio).

Semprich, S., 1980. Berechnung der Spannungen und Verformungen im Bereich der Ortsbrust von Tunnelbauwerken im Fels. Veroff. D. Inst. f. Grundbau, Bodenmechanik, Felsmechanik und Verkehrswasserbau der RWTH Aachen, Heft 8.

Seneviratne, H.N., 1979. Deformations and pore-pressures around model tunnels in soft clay. Ph.D. Thesis. University of Cambridge.

Seychuk, J.L., 1977. Discussion presented to 30th Canadian Geotechnical Conference.

Sgouros, G.E., 1982. Structural behaviour and design implications of concrete tunnel linings based on model tests and parameter studies. Ph.D. Thesis, University of Illinois at Urbana-Champaign., 385 p.

Simondi, S., Negro, A. and Kuperman, S., 1982. The use of shotcrete as secondary lining of a urban tunnel through soil (in Portuguese). Proceedings, Symposium on Concrete for Foundation and Underground Structures (Brazilian Concrete Institute), pp. 42-68, Sao Paulo.

Sizer, K.E., 1976. The determinations and interpretation of ground movements caused by shield tunnelling in silt alluvium at Willington Quay, North-East England. M.Sc. Thesis. University of Durham.

Skempton, A.W., 1951. The bearing capacity of clays. Building Research Congress, England.

Skempton, A.W., 1954. The pore-pressure coefficients A and B. Geotechique, Vol. 4, pp. 143-147.

Skempton, A.W., 1961. Horizontal stresses in overconsolidated Eocene clay. Proceedings, 5th International Conference on Soil Mechanics and Foundation Engineering (Paris), Vol. 1, pp. 351-357.

Skempton, A.W., 1964. Long-term stability of clay slopes. 4th Rankine Lecture, Geotechnique, 14, pp. 77-101.

Skempton, A.W., 1977. Slope stability of cuttings in Brown London Clay. Proceedings, 9th International Conference on Soil Mechanics and Foundation Engineering (Tokyo), pp. 261-269.

Skempton, A.W. and MacDonald, D.H., 1956. Allowable settlement of buildings. Proceedings of the Institute of Civil Engineers, Part III, Vol. 5, pp. 727-768.

Sketchley, C.J., 1973. The behaviour of kaolin in plane strain. Ph.D. Thesis, Cambridge University.

Sonntag, G. and Fleck, H., 1973. Ahnlichkeitsgerechte kohasionslose Modellboden fur Modellversuche an Hohlraumauskleidungen. Strasse Brucke Tunnel, 25 Jahrung, Heft 4, pp. 85-90.

Sonntag, G. and Fleck, H., 1976. Zum Bettungsmodul bei Tunnelauskleidungen. Ingenieur - Archiv 45, pp. 269-273.

Sousa Pinto, C. and Massad, F., 1972. Caracteristicas dos solos variegados da cidade de Sao Paulo. Publicacao No. 984, Instituto de Pesquisas Tecnologicas, Sao Paulo, 31 p.

Sozio, L.E., 1978. Settlements in a Sao Paulo shield tunnel. Tunnels and Tunnelling (September), pp. 53-55.

Steiner, W. and Einstein, H.H., 1980. Improved design of tunnel supports: Volume 5 - Empirical methods in rock tunneling - review and recommendations. Report UMTA-MA-06-0100-80-8, NTIS (National Technical Information Service), U.S. Department of Commerce, Springfield, VA 22161.

Steiner, W., Einstein, H.H. and Azzouz, A., 1980. Improved design of tunnel supports: Vol. 4 - Tunnel practices in Austria and Germany. Report UMTA-MA-06-0100-80-7, NTIS (National Technical Information Service), U.S. Department of Commerce, Springfield, VA 22161.

Stini, J., 1950. Tunnelbaugeologie. Springer (Vienna). (quoted by Steiner and Einstein, 1980).

Strobl, B., 1986. NATM under compressed air - geomechanical aspects and numerical modelling. Proceedings, International Congress on Large Underground Openings, ITA (Firenze), Vol. II, pp. 686-692.

Stroh, D. and Chambosse, G., 1973. Messungen und Setzungsursachen beim Tunnelvortrieb im Frankfurter Ton. Strasse Brucke Tunnel, Heft 2, pp. 38-42.

Sulem, J., Panet, M. and Guenot, A., 1987(a). Closure analysis in deep tunnels, International Journal of Rock Mechanics, Mining Sciences and Geomechanics Abstract, Vol. 24, No. 3, pp. 145-154.

Sulem, J., Panet, M. and Guenot, A., 1987(b). An analytical solution for time-dependent displacements in a circular tunnel. International Journal of Rock Mechanics, Mining Sciences and Geomechanics Abstract, Vol. 24, No. 3, pp. 155-164.

Sungur, T., 1984. A modern design for tunnel lining. Tunnels and Tunnelling, November, pp. 21-22.

Sweet, A.L. and Bogdanoff, A.L., 1965. Stochastic model for predicting subsidence. Journal of the Engineering Mechanics Division, A.S.C.E., EM 2, pp. 21-45.

Swoboda, G., 1979. Finite element analysis of the New Austrian Tunnelling Method (NATM). Proceedings, 3rd International Conference on Numerical Methods in Geomechanics, Aachen (edited by W. Wittke), Vol. 2, pp. 581-586.

Swoboda, G., 1982. Special problems during the geomechanical analysis of tunnels. Proceedings, 4th International Conference on Numerical Methods in Geomechanics (Edmonton), Vol. 2, pp. 605-609.

Swoboda, G., 1985. Interpretation of field measurements under consideration of the three-dimensional state of stress, the viscoelasticity of shotcrete, and viscoplastic behaviour of rock. Proceedings, 5th International Conference on Numerical Methods in Geomechanics (Nagoya), pp. 1651-1658.

Swoboda, G. and Laabmayr, F., 1978. Beitrag zur Wieterentwicklung der Berechnung flachliegender Tunnelbauten im Lockergestein. In: Moderner Tunnelbau bei der Munchner U-Bahn, Springer, (edited by H. Lessmann), pp. 55-71.

Symons, I.F., 1978. Discussion: Lateral displacement of shallow buried pipelines due to adjacent deep trench excavations. Geotechnique, Vol. 28, No. 2, pp. 212-214.

Szechy, K., 1973. The art of tunnelling. 2nd English Edition. Akademiai Kiado, Budapest, 1097p.

Takagi, N., Shimamura, K. and Nishio, N., 1985. Buried pipe responses to adjacent ground movements associated with tunnelling and excavations. Proceedings of the 3rd International Conference on Ground Movements and Structures (Cardiff), pp. 97-112.

Takemoto, T., Ryoke, K. and Teramoto, T., 1977. Creep behaviour of soft ground tunnel. Proceedings, International Symposium on Field Measurements in Rock Mechanics (Zurich), pp. 669-682.

Tan, D.Y., 1977. Finite element analysis and design of chemically stabilized tunnels. Ph.D. Thesis. Stanford University.

Tan, D.Y. and Clough, G.W., 1980. Ground control for shallow tunnels by soil grouting. Journal of the Geotechnical Engineering Division, American Society of Civil Engineers, Vol. 106, No. GT9, pp.1037-1057.

Tarzi, A.I., Menzies, B.K. and Crofts, J.E., 1979. Bending of jointed pipelines in laterally deforming soil. Geotechnique, Vol. 29, No. 2, pp. 203-206.

Taylor, R.N., 1980. Modelling of tunnel failure in silt.

CUED/D - Soils Report TR81 (University of Cambridge).

Taylor, R.N., 1984. Ground movements associated with tunnels and trenches. Ph.D. Thesis. Cambridge University. (quoted by Gunn, 1984).

Terzaghi, K., 1936. Stress distribution in dry and in saturated sand above a yielding trap-door. 1st International Conference on Soil Mechanics and Foundation Engineering, Vol. 1, pp. 307-311.

Terzaghi, K., 1942. Shield tunnels of the Chicago subway. Journal of the Boston Society of Civil Engineers, Vol. 29, pp. 163-210.

Terzaghi, K., 1943(a). Theoretical Soil Mechanics. John Wiley and Sons, Inc., New York.

Terzaghi, K., 1943(b). Liner-plate tunnels on the Chicago (Ill.) subway. Transactions of the American Society of Civil Engineers, 108, pp. 970-1007.

Terzaghi, K., 1946. Rock defects and loads on tunnel supports. In: Rock Tunneling with Steel Supports (Ed. by R.V. Proctor and T.L. White), pp. 17-102.

Terzaghi, K., 1956. Discussion on Skempton and MacDonald. Proceedings, Institution of Civil Engineers. Part II, Vol. 5, p.775.

Thomson, S., 1969. A summary of laboratory results on Lake Edmonton clay. Internal Note SM2, (April 24), Department of Civil Engineering, University of Alberta.

Thomson, S., Martin, R.L., and Eisenstein, Z., 1982. Soft zones in the glacial till in downtown Edmonton. Canadian Geotechnical Journal, Vol. 19, pp. 175-180.

Thurber Consultants Ltd., 1980. South LRT Extension, Geotechnical Report No. 5, In situ pressuremeter tests, 104th and 107th street stations, Unpublished report to Edmonton Transit.

Thurber Consultants Ltd., 1982. South LRT Extension. Geotechnical Report No. 14, Tunnel section, instrumentation test section at 105th street. Report submitted to LRT Project. Edmonton Transit (February 4).

Togerson, R., 1986. Personal Communication.

Uriel, S. and Oteo, C.S., 1979. Measurements in an experimental tunnel bored in the Sevilla Blue Marls and recommendations for the subway design. Proceedings, 4th Congress of the International Society for Rock Mechanics (Montreux), pp. 697-703.

Vaid, Y.P., 1985. Effect of consolidation history and stress path on hyperbolic stress-strain relations. Canadian Geotechnical Journal, Vol. 22, pp.172-176.

Van Dillen, D. and Fellner, R.W., 1979. A two-dimensional finite element technique for modeling rock/structure interaction of a lined underground opening. Proceedings, 20th U.S. Symposium on Rock Mechanics (Austin), pp. 251-258.

Van Sin Jan, M.L. and Cording, E.J., 1984. Ground and lining behaviour of shallow underground rock chambers for the Washington D.C. subway. Proceedings of a Symposium on Design and Performance of Underground Excavations (Cambridge, U.K.) pp. 415-422.

Vardoulakis, I.G., 1986. Stability and bifurcation in geomechanics. Notes of a short course. University of Alberta. (June 2 to 6).

Vardoulakis, I.G., Graf, B. and Gudehus, G., 1981. Trap-door problem with dry sand: a statical approach based upon model test kinematics. International Journal for Numerical and Analytical Methods in Geomechanics, Vol. 5, pp.57-78.

Vasishth, V., 1986. Mount Baker Ridge Tunnel. Proceedings, International Congress on Large Underground Openings - ITA (Firenze), Vol. I, pp. 579-587.

Vaughan, P.R., 1974. Embankment dams. Course notes. Imperial College, Department of Civil Engineering, University of

London.

Vaughan, P.R. and Walbancke, H.J., 1973. Pore pressure changes and the delayed failure of cutting slopes in overconsolidated clay. Geotechnique 23, No. 4, pp. 531-539.

Verruijt, A., 1976. Non-linear elastic approximations of the behaviour of soils. Proceedings, 2nd International Conference on Numerical Methods in Geomechanics (Virginia), Vol. III, pp. 1321-1328.

Verski, A., Cesar, S.E.D.M. and Ibri, I.A., 1985. Observacao da interacao solo-estrutura atraves da instrumentacao de uma secao tipica do interceptor Tiete do Sistema SANEGRAN. Proceedings of the 2nd Symposium on Underground Excavation (ABGE), Vol. 1, pp. 475-492.

Vesic, A.S. and Clough, G.W., 1968. Behaviour of granular materials under high stresses. Journal of the Soil Mechanics and Foundations Division, ASCE, Vol. 94, No. SM3, pp.661-688.

Voellmy, A., 1937. Eingebettete Rohre. Leemann u. Co., Zurich Leipzig.

Wanniger, R., 1979. New Austrian Tunnelling Method and finite elements. Proceedings, 3rd International Conference on Numerical Methods in Geomechanics, Aachen (edited by W. Wittke), Vol. 2, pp. 587-597.

Wanniger, R. and Breth, H., 1978. Moglichkeiten und Grenzen numerischer Rechenverfahren im Grundbau. Bauingenieur, 53, Heft 12, pp. 465-470.

Ward, W.H., 1956. Discussion on Skempton and MacDonald. Proceedings of the Institution of Civil Engineers, Part III, Vol. 5, pp. 782.

Ward, W.H., 1969. Discussion in Main Session 4. Proceedings, 7th International Conference on Soil Mechanics and Foundation Engineering (Mexico), Vol. 3, pp. 320-325.

Ward, W.H., 1978. Ground supports for tunnels in weak rock.

18th Rankine Lecture. Geotechnique, Vol. 28, pp. 133-171.

Ward, W.H., Coats, D.J., and Tedd, P. 1976. Performance of tunnel support systems in the Four Fathom Mudstone. Tunnelling '76, London, March, pp. 329-340, Discussion, pp. 348-367.

Ward, W.H. and Pender, M.J., 1981. Tunnelling in soft ground. General report, Session 2, 10th International Conference on Soil Mechanics and Foundation Engineering, Stockholm, Vol. 4, pp. 261-275.

Watanabe, T., 1984. Several cases of large size slurry shield tunnelling in heterogeneous soils. Proceedings, 1st Latinamerican Congress of Underground Constructions - ITA (Caracas), Vol. I, pp. 329-337.

Weber, J., 1984. Experience using compressed air drivage and shotcreting. Tunnel 1/84, pp. 16-27.

Wilson, A.H., 1981. Stress and stability in coal ribsides and pillars. Proceedings, 1st Annual Conference on Ground Control in Mining (West Virginia University), pp. 1-12. Quoted by Brady and Brown (1985:374).

Windels, R., 1966. Spannungstheorie zweiter Ordnung fur den teilweise gebetteten Kreisring. Bautechnik 43, Heft 8, pp. 265-274.

Windels, R., 1967. Kreisring im elastischen Kontinuum. Bauingenieur 42. Jahrgang, Heft 12, pp. 429-439.

Winter, H., 1982. Similarity technique for numerical methods in geomechanics. Proceedings, 4th International Conference on Numerical Methods in Geomechanics (Edmonton), Vol. 3, pp. 1073-1080.

Wittebolle, R.J., 1983. The influence of microfabric on the engineering properties of glacial tills. M.Sc. Thesis. University of Alberta.

Wittebolle, R.J., 1987. Personal Communication.

Wittke, W., 1977(a). Static analysis for underground openings in jointed rock. Numerical Methods in Geotechnical Engineering (Ed. by C.S. Desai and J.T. Christian), McGraw Hill, pp. 589-638.

Wittke, W., 1977(b). New design concept for underground openings in rock. Finite Elements in Geomechanics (Ed. by G. Gudehus), John Wiley and Sons, pp. 413-478.

Wittke, W., Carl, L. and Semprich, S., 1974. Felsmessungen als Grundlage fur den Entwurf einer Tunnelauskleidung. Interfels Messtechnik Information, pp. 3-11.

Wittke, W., Feiser, J. and Krieger, J., 1986. Stability analysis of an advanced vault excavation with unlined invert according to the finite element method. International Journal for Numerical and Analytical Methods in Geomechanics, Vol. 10, pp. 259-281.

Wittke, W. and Gell, K., 1980. Raumliche Standsicherheitsuntersuchungen fur einem oberflachennachen Tunnelabschnitt des Bauloses B3 der Stadtbahn Bochum. Geotechnik, Heft 3, pp. 111-119.

Wittke, W., and Pierau, B., 1976. Stability analysis of tunnels in jointed rock. Proceedings, 2nd International Conference on Numerical Methods in Geomechancis, Blacksburg, Vol. III, pp. 1401-1418.

Wittke, W. and Semprich, S., 1974. Messungen als felsmechanische Grundlage beim Entwurf eines Stollens. Discussion in the Proceedings of the 3rd Congress of the International Society for Rock Mechanics (Denver), Vol. III, pp. 121-123.

Wong, R.C.K., 1986. Design and performance evaluation of tunnels and shafts. Ph.D. Thesis. University of Alberta. 308 p.

Wong, R.C.K. and Kaiser, P.K., 1986. Ground behaviour near soft ground tunnels. Proceedings, International Congress on Large Underground Openings (Firenze), Vol. I, pp. 942-951.

Wong, R.C.K. and Kaiser, P.K., 1987. Prediction of ground movements above shallow tunnels. Proceedings of the International Symposium on Prediction and Performance in Geotechnical Engineering (Calgary), pp. 329-343.

Wroth, C.P. and Houlsby, G.T., 1985. Soil Mechanics - Property characterization and analysis procedures. Proceedings, 11th International Conference on Soil Mechanics and Foundation Engineering (San Francisco), Vol. 1, pp. 1-55.

Wroth, C.P. and Hughes, J.M.O. (1974). Development of a special instrument for the in situ measurement of the strength and stiffness of soils. Proceedings, Engineering Foundation Conference on Subsurface Exploration for Underground Excavations and Heavy Construction, N.E. College, Henniker, (New Hampshire), pp. 295-311.

Yamaguti, S., 1929. On the stresses around a horizontal circular hole in a gravitating elastic solic. Journal of the Civil Engineering Society of Japan, Vol. 15, pp. 291-303. Quoted by Mindlin, 1940:1118).

Yeates, J., 1985. The response of buried pipelines to ground movements caused by tunnelling in soil. Proceedings, 3rd International Conference on Ground Movements and Structures (Cardiff), pp. 129-144.

Yoshida, K., Kondoh, H., Kibe, T., and Takasaki, H., 1986. Tunnelling work in sandy-gravel stratum in urban area. Countermeasures and its results against environmental problems. Proceedings, International Congress on Large Underground Openings -ITA (Firenze), Vol. I, pp. 952-958.

Yoshikoshi, W., Watanab, O. and Takagi, N., 1978. Prediction of ground settlements associated with shield tunnelling. Soils and Foundations, Vol. 18, No. 4, pp. 47-59.

Zagottis, D.L. 1981. An application of finite element non-linear plane analysis to tunnel decision. Proceedings, Symposium on Implementation of Computer Programs and Stress-Strain Laws in Geotechnical Engineering (Chicago), pp. 281-290.

Zienkiewicz, O.C., 1983. The Finite Element Method, Third

Edition. McGraw Hill, London.

APPENDIX A - RESULTS OF 3-D FINITE ELEMENT ANALYSES

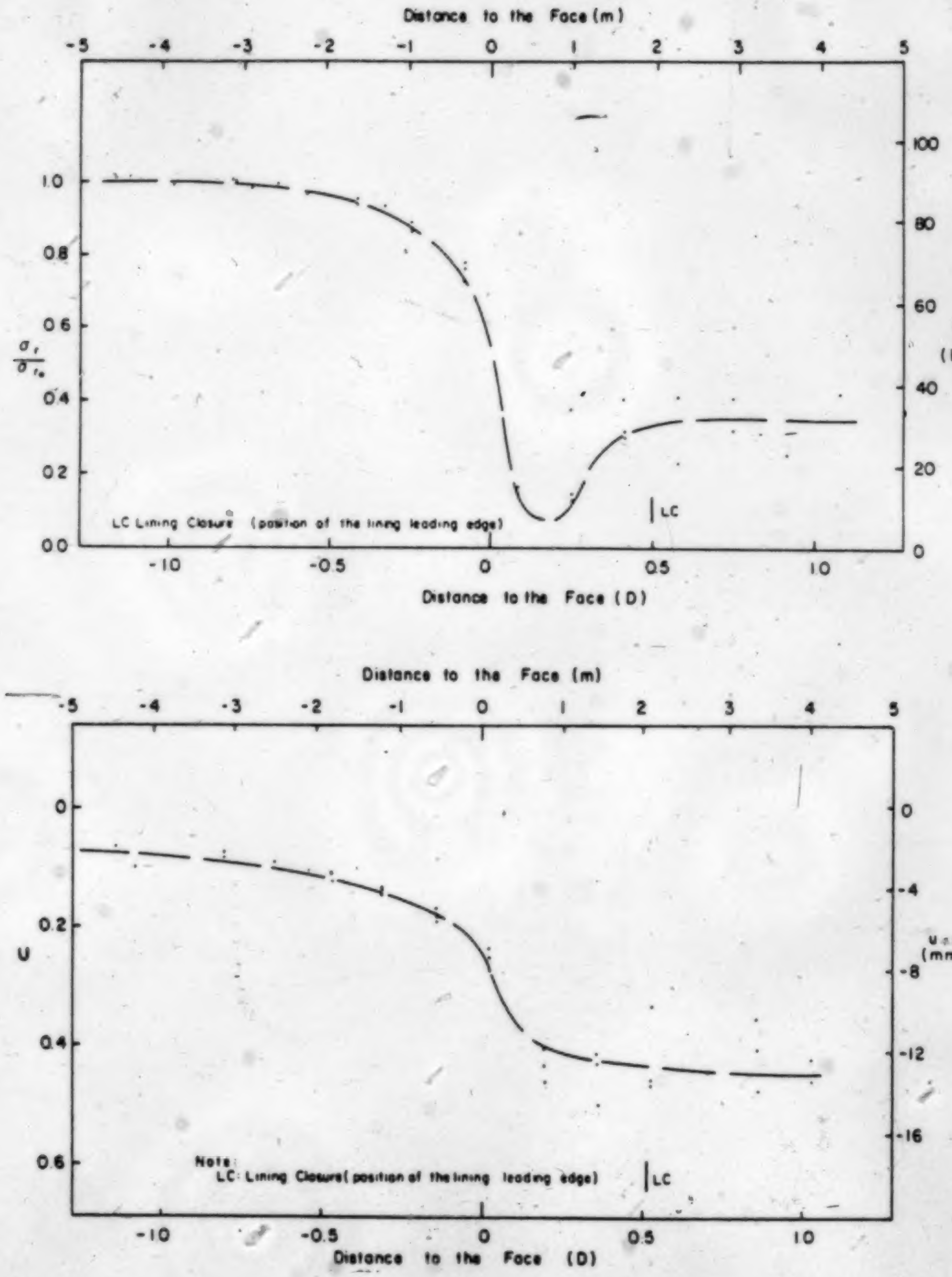

Figure A.1 Radial Stresses and Displacements at the Crown Elevation (L/D=1/2)

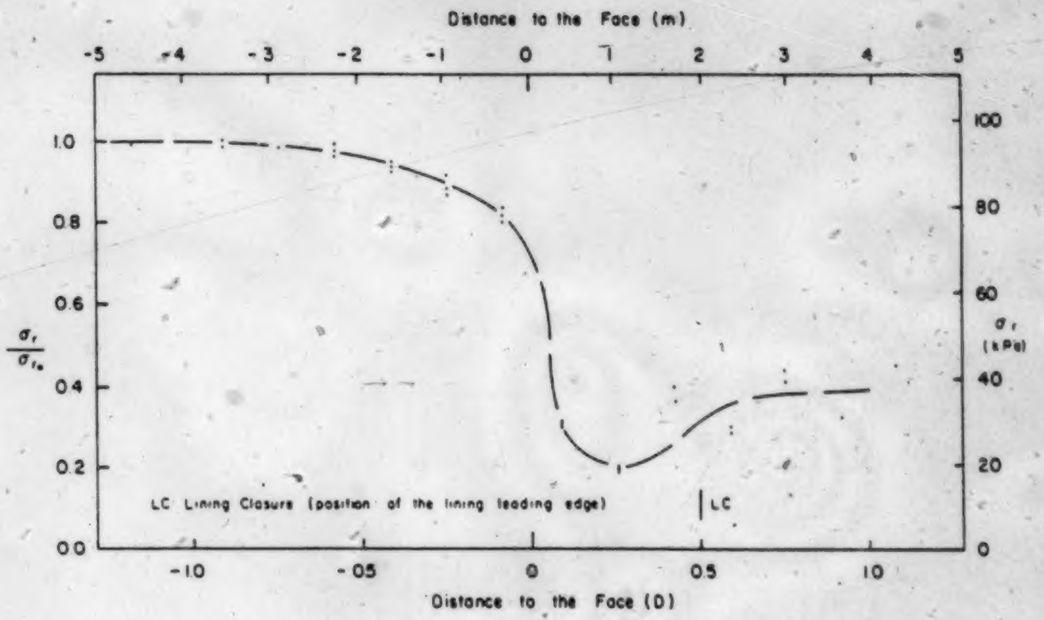

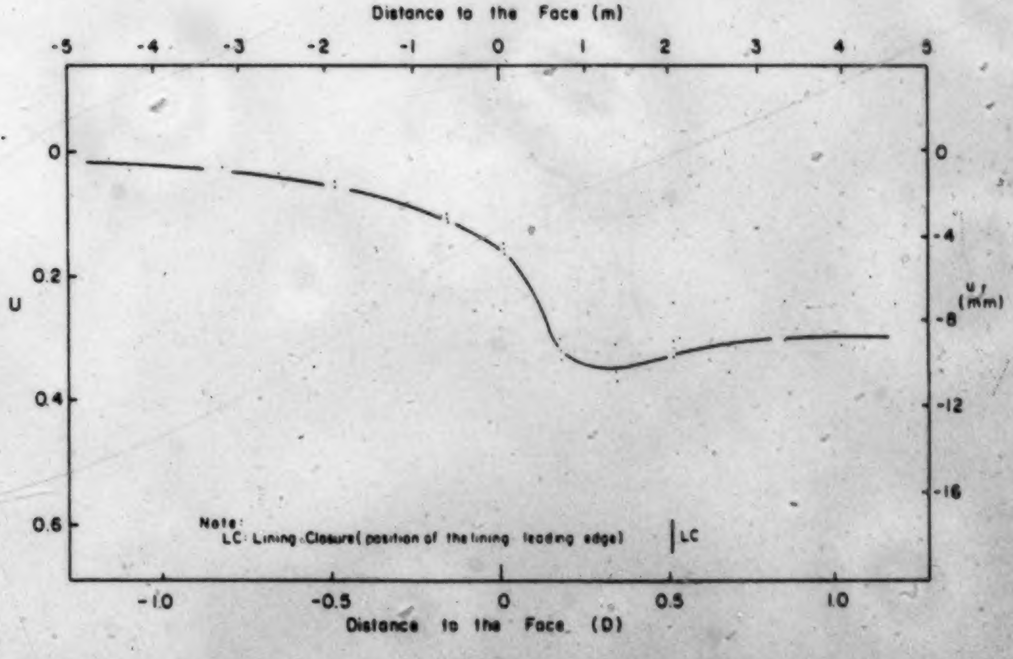

Figure A.2 Radial Stresses and Displacements at the Springline Elevation (L/D=1/2)

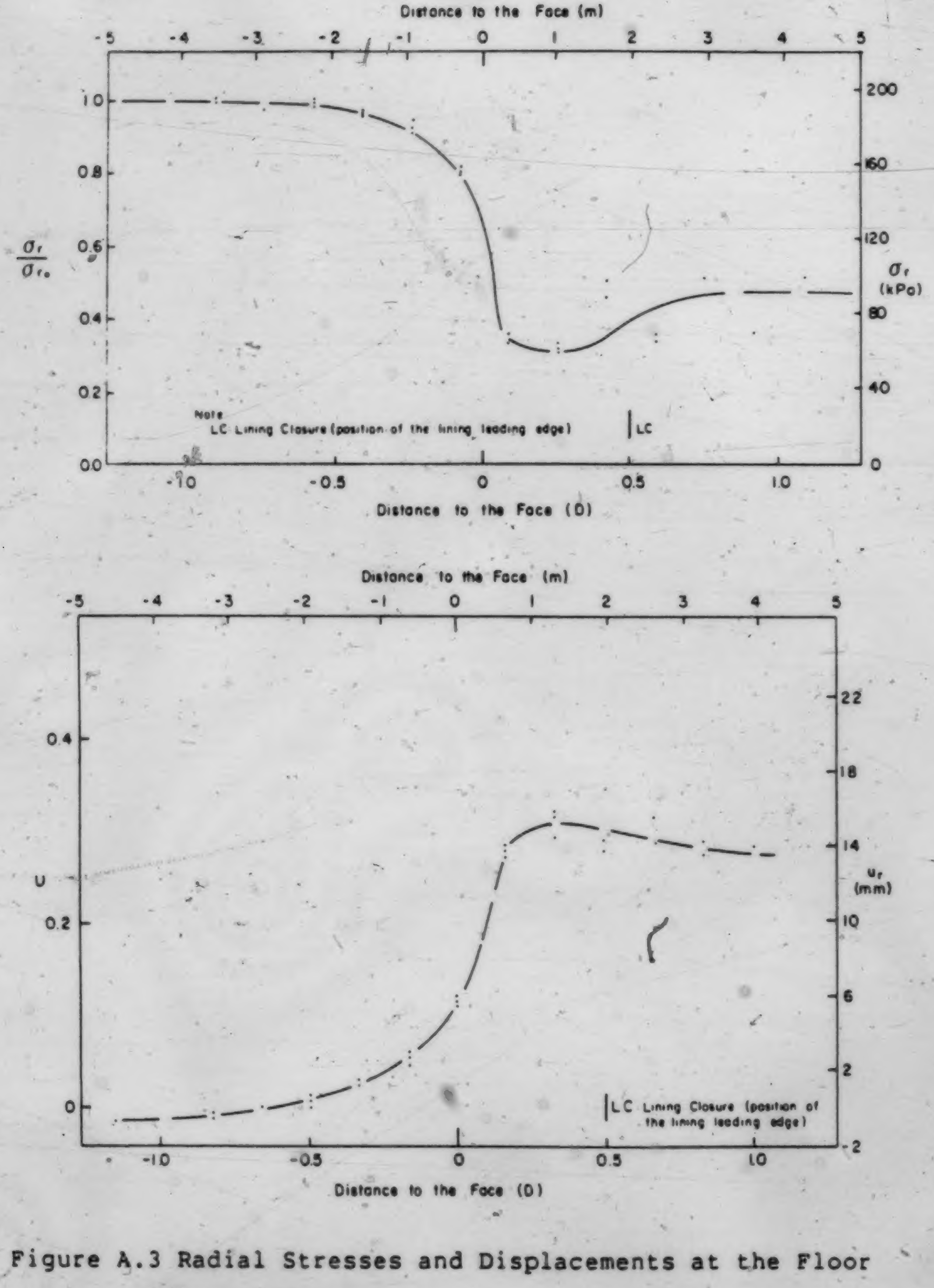

Figure A.3 Radial Stresses and Displacements at the Floor Elevation (L/D=1/2)

APPENDIX B - LIST OF RESPONDENTS TO THE QUESTIONNAIRE

AUSTRIA

1. Prof. Franz Pacher and Mr. N. Ayaydin
Franz Josef-Strasse 3
A-5020 Salzburg

2. Mr. Klaus Mussger and Mr. G. Schicktanz
c/o Geoconsult Consulting Engineers
Sterneckstrasse 55
A-5020 Salzburg

CZECHOSLOVAKIA

3. Mr. Josef Novak
Vodni stavby, o.p.
Delnicka 12
Praha 7

ENGLAND

4. Mr. D. Buckley
c/o Sir William Halcrow and Partners Ltd.
Vineyard House
44 Brook Green
London W6 7BY

FRANCE

5. Mr. Marc Panet
c/o Simecsol
115 Rue Saint Dominique
75007 Paris

WEST GERMANY

6. Dr. T. Baumann
c/o Philip Holzmann AG
Herzog-Heinrich-Strasse 20-22
8000 Munchen 2

7. Prof. Heinz Duddeck

Consulting Engineer
Greifwaldstrasse 38
3300 Braunschweig

8. Dr. Fritz Hartmann
Consulting Engineer
Bahnhofstrasse 39
2248 Hemmingstedt

9. Dr. S. Babendererde
c/o Hochtief AG
Rellinghauser Strasse 53-57
4300 Essen

10. Dr. F. Blennemann
c/o Studiengesellschaft STUVA
Mathias-Bruggen-Strasse 41
5000 Koln 30

11. Mr. J. Weber
c/o U-Bahn-Referat
Viktualienmarkt 13
8000 Munchen 2

HUNGARY

12. Dr. Laszlo Rozsa
c/o UVATERV
Jozsef Attila u. 8
1051 Budapest

13. Mr. G. Greschik
c/o FTV Consulting Engineers
Reviczky utca 4
1088 Budapest

SPAIN

14. Mr. J.M. Gutierrez Manjon
Cardinal Belluga 21
28028 Madrid

15. Dr. C. Sagaseta
c/o E.T.S. Ingenieros de Caminos

Avda. de Los Castros, s/n
39005 Santander

SWITZERLAND

16. Dr. E. Andraskay
c/o Basler and Hofmann AG
Forchstrasse 395
8029 Zurich

CANADA

17. Mr. D.J. Phelps and Dr. J.R.T. Brandt
c/o UMA Engineering
17007-107 Avenue
Edmonton, Alberta
T5S 1G3

18. Mr. E.W. Brooker
c/o EBA Engineering
14535-118 Avenue
Edmonton, Alberta
T5R 0B9

19. Mr. John Yan Egmond
c/o Trow Ltd.
1595 Clarke Blvd.
Brampton, Ontario
L6T 4V1

20. Mr. M. Walia
10180 - Shellbridgeway
Richmond, British Columbia
V6X 2W7

USA

21. Dr. Birger Schmidt
c/o Parsons Brinckerhoff
1625 Van Ness Avenue
San Francisco,
California, 94109

22. Dr. Gerard Sauer

Consultant Engineer
11403 Orchard Green CT.
Reston (Washington, D.C.)
Virginia, 22090

23. Mohamad Irshad
c/o DeLeuw, Cather and Co.
600 Fifth Street, NW
Washington, D.C., 20001

24. Dr. D.R. McCreath
c/o Golder Associates Inc.
4104 148th Avenue, NE
Redmond
Washington, 98052

MEXICO

25. Mr. J. Schmitter
c/o Solum S.A. de C.V.
Rio Becerra 27 5.° Piso
Col. Napoles
03810 Mexico, DF.

BRAZIL

26. Mr. Claudio Casarin
c/o THEMAG Engenharia Ltda.
Rua Beija Flor 34, Vilage 1
Lagoa da Conceicao
88000 Florianopolis, S.C.

27. Dr. Carlos Eduardo Moreira Maffei
Consulting Engineer
Al. Austria, 772, Alphaville Residencial I
06400 Barueri, SP

28. Mr. Mosze Gitelman and Mr. Roberto Kochen
c/o Figueiredo Ferraz Ltda.
Rua Conde de Iraja, 118
04118 Sao Paulo, SP

29. Messrs. Hamilton G. de Oliveira, Alexandre Verski and
Sergio E.D.M. Cesar
c/o Hidroservice (MS)

Rua Afonso Celso, 235
04119 Sao Paulo, SP

30. Mr. Luis E. Sozio
c/o Promon Engenharia
A.V. Juscelino Kubitschek 1830, 5°
04543 Sao Paulo

VENEZUELA

31. Mr. Roberto Centeno Werner
Consulting Engineer, Metro de Caracas
Avenida Sojo, Quinta Chichi
El Rosal
Caracas 106

EGYPT

32. Mr. M.E. Abdel Salam
National Authority for Tunnels
56 Riad Street
Elmohandiseen
Cairo

JAPAN

33. Mr. Yoshio Mitarashi
c/o Kumagai Gumi Co. Ltd.
Institute of Construction Technology
17-1, Tsukudo-CHO, Shinjuku-Ku
Tokyo, 162

34. Dr. Keiichi Fujita
c/o Hazama-Gumi, Ltd.
2-5-8, Kita-Aoyama
Minato-Ku
Tokyo 107

APPENDIX C - NORMALIZED GROUND SETTLEMENTS

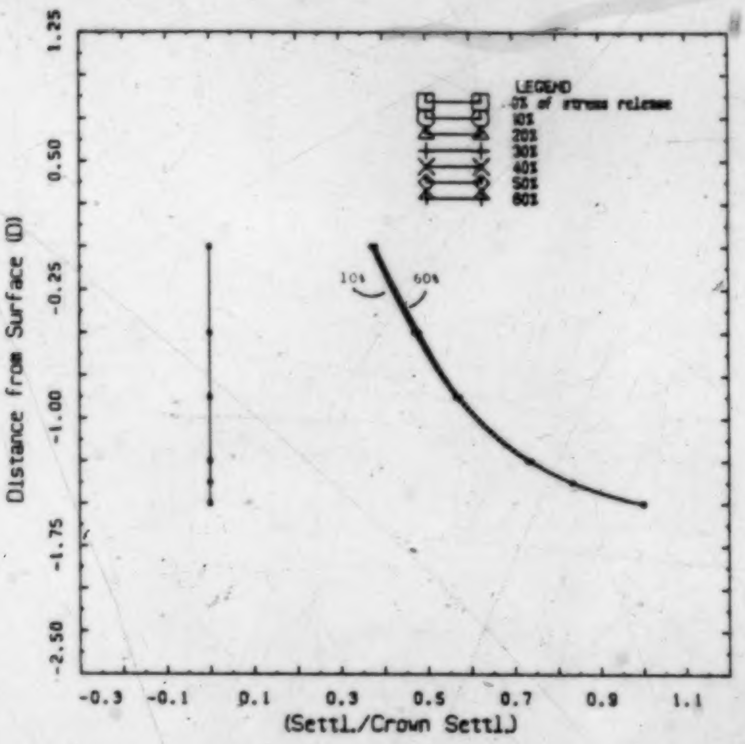

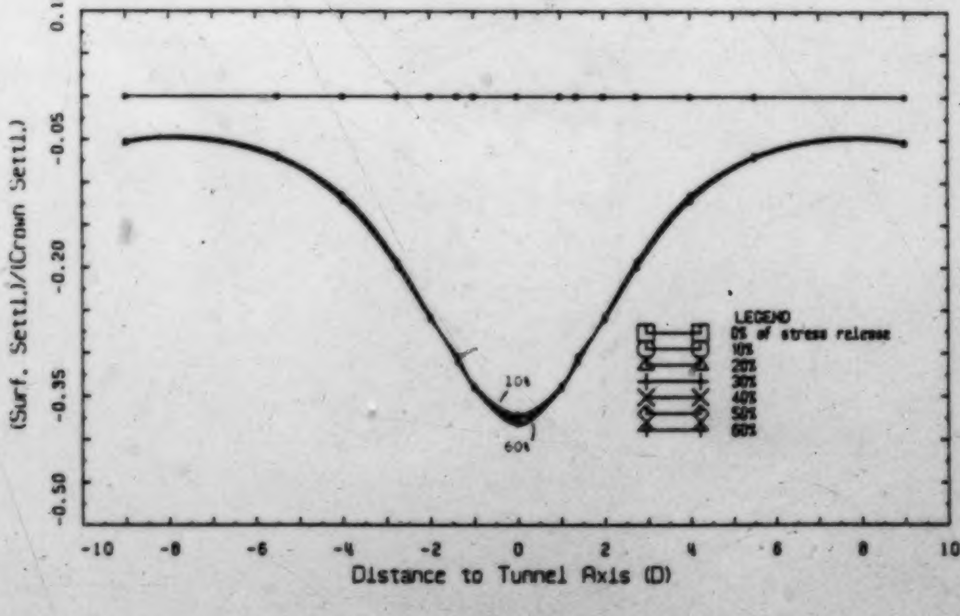

Figure C.1 Normalized Settlements: $K_o=1$, $c_u/\gamma D=2.5$, $H/D=1.5$

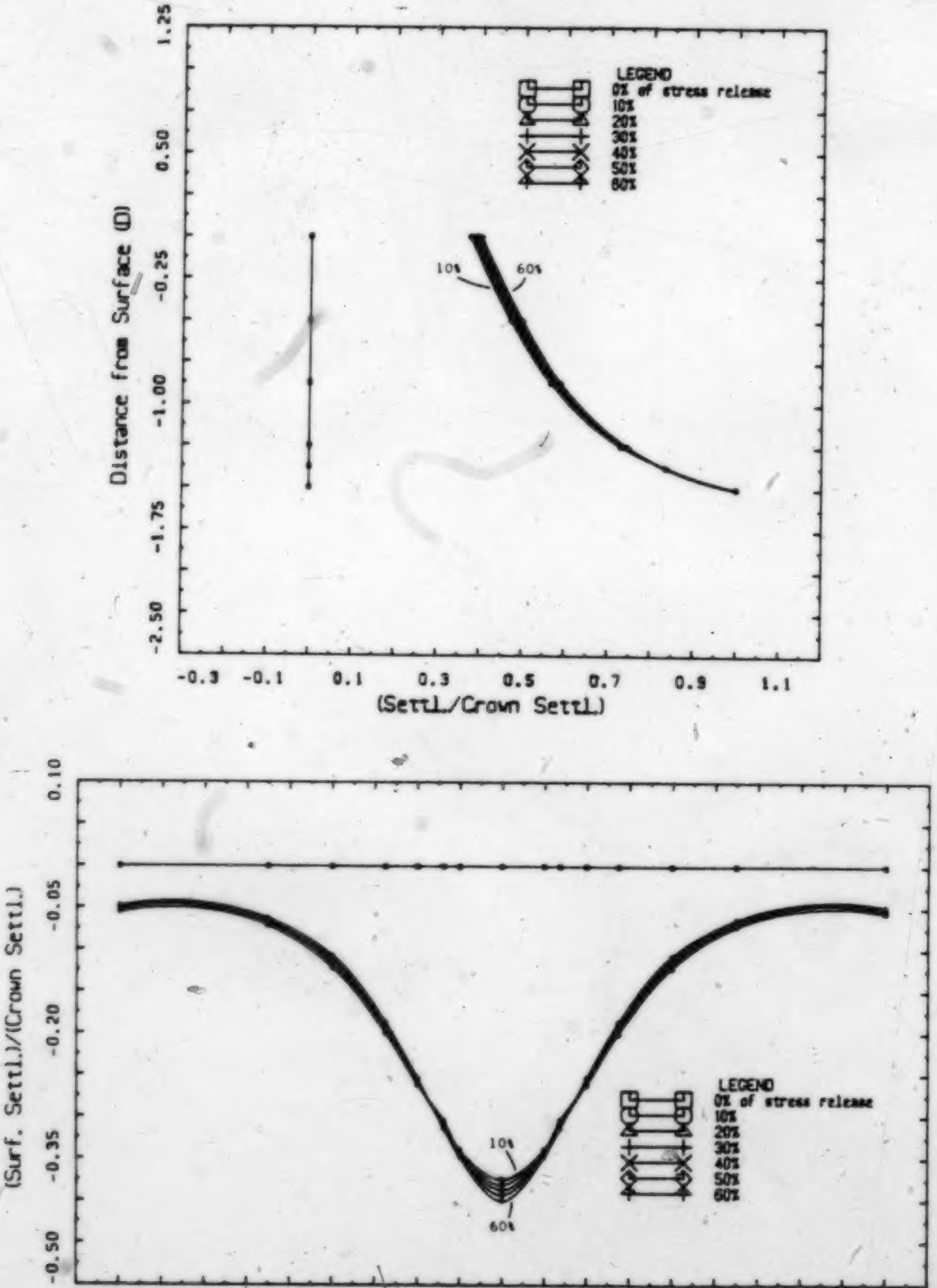

Figure C.2 Normalized Settlements: $K_o=1$, $c_u/\gamma D=1.25$, $H/D=1.5$

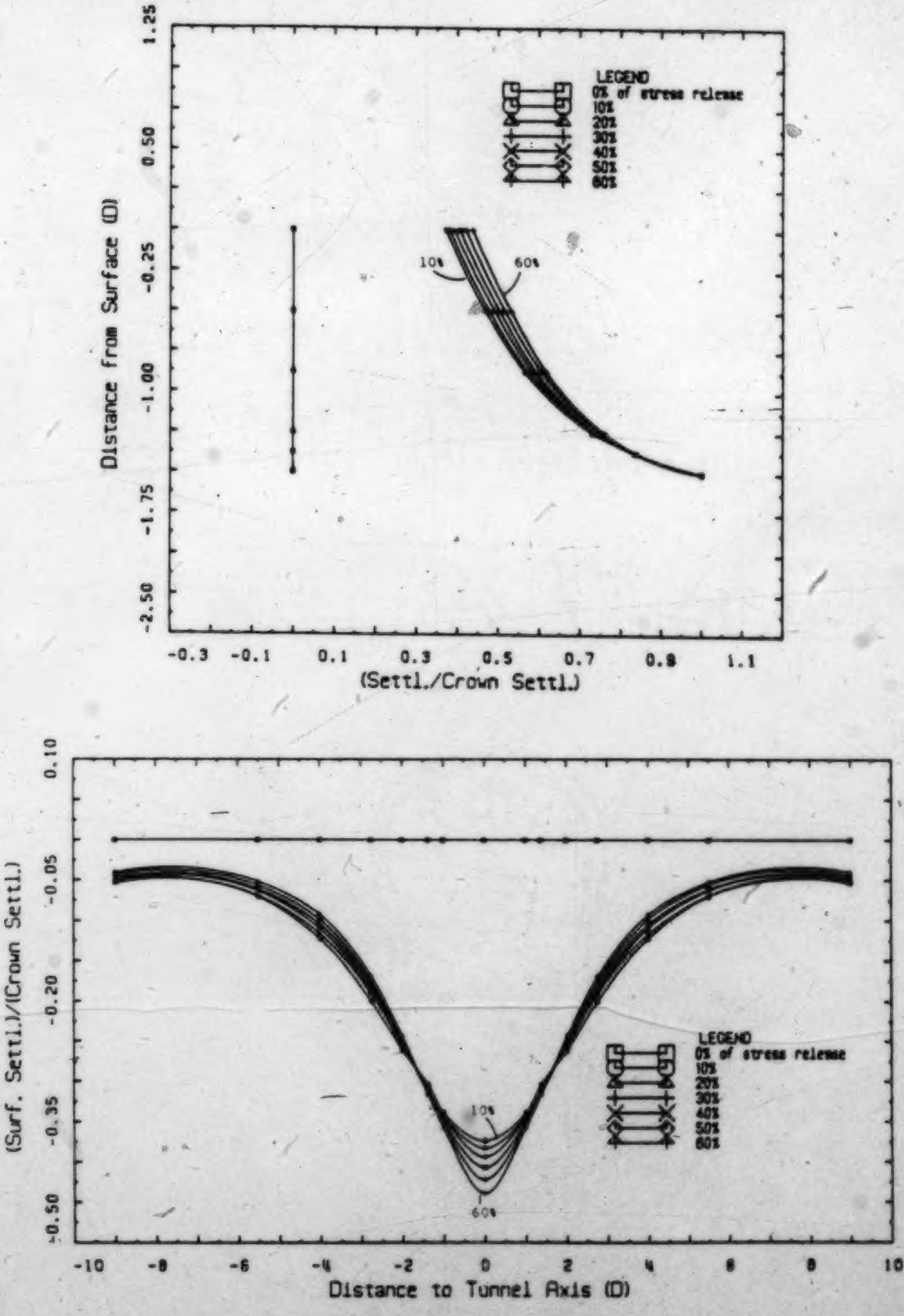

Figure C.3 Normalized Settlements: $K_o=1$, $c_u/\gamma D=0.625$, $H/D=1.5$

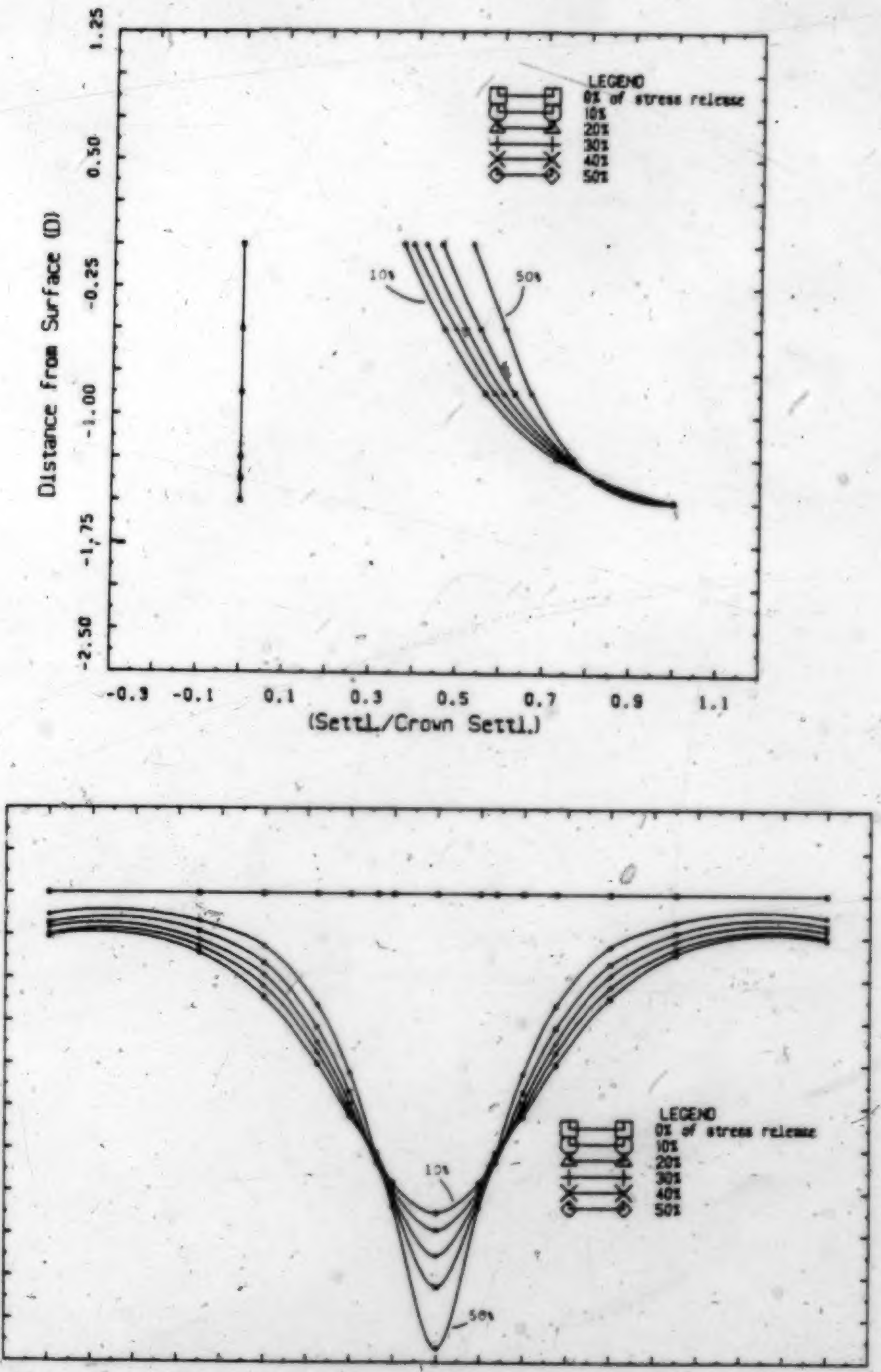

Figure C.4 Normalized Settlements: $K_o=1$, $c_u/\gamma D=0.3125$, $H/D=1.5$

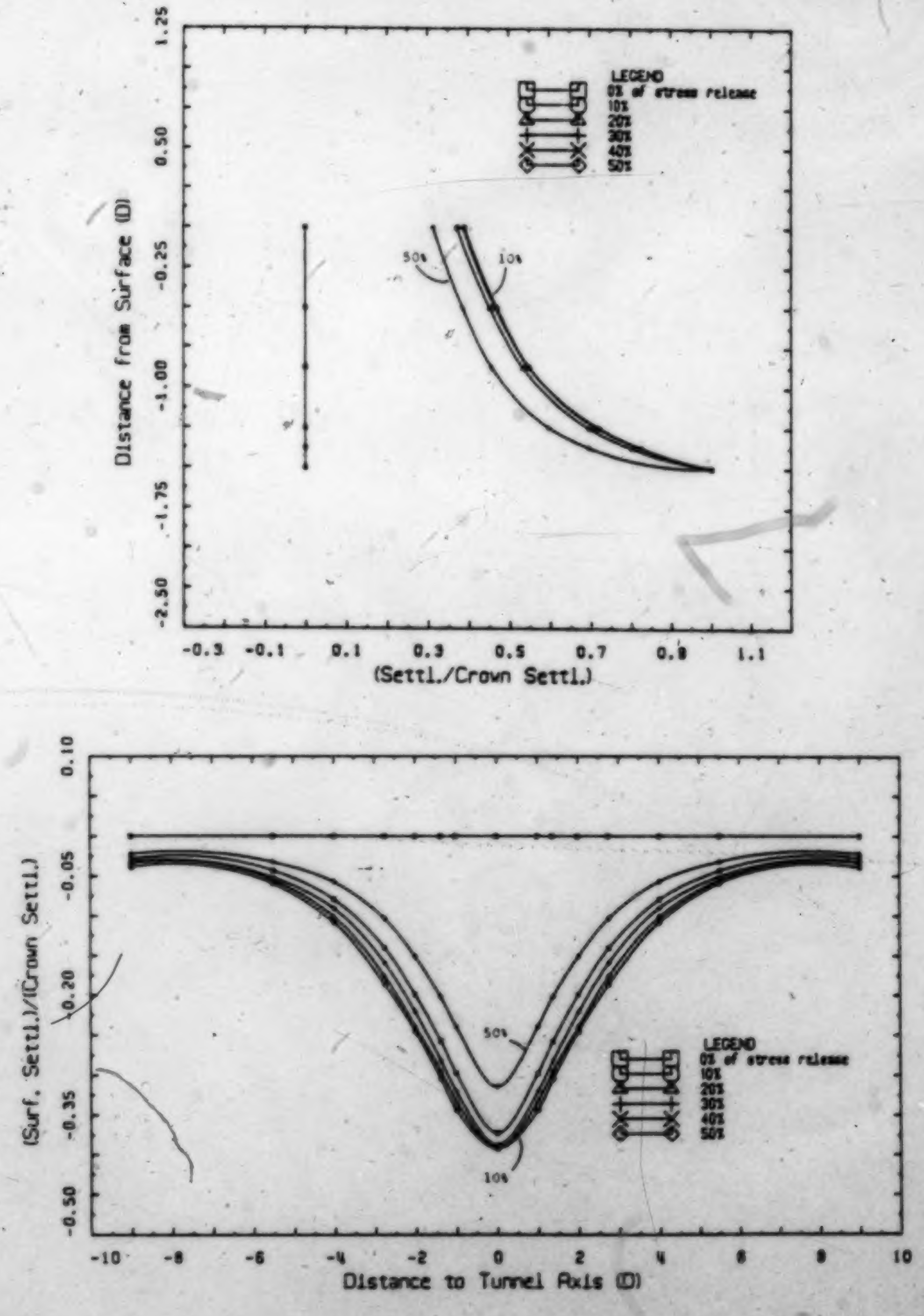

Figure C.5 Normalized Settlements: $K_o=1$, $\phi=20°$, $H/D=1.5$

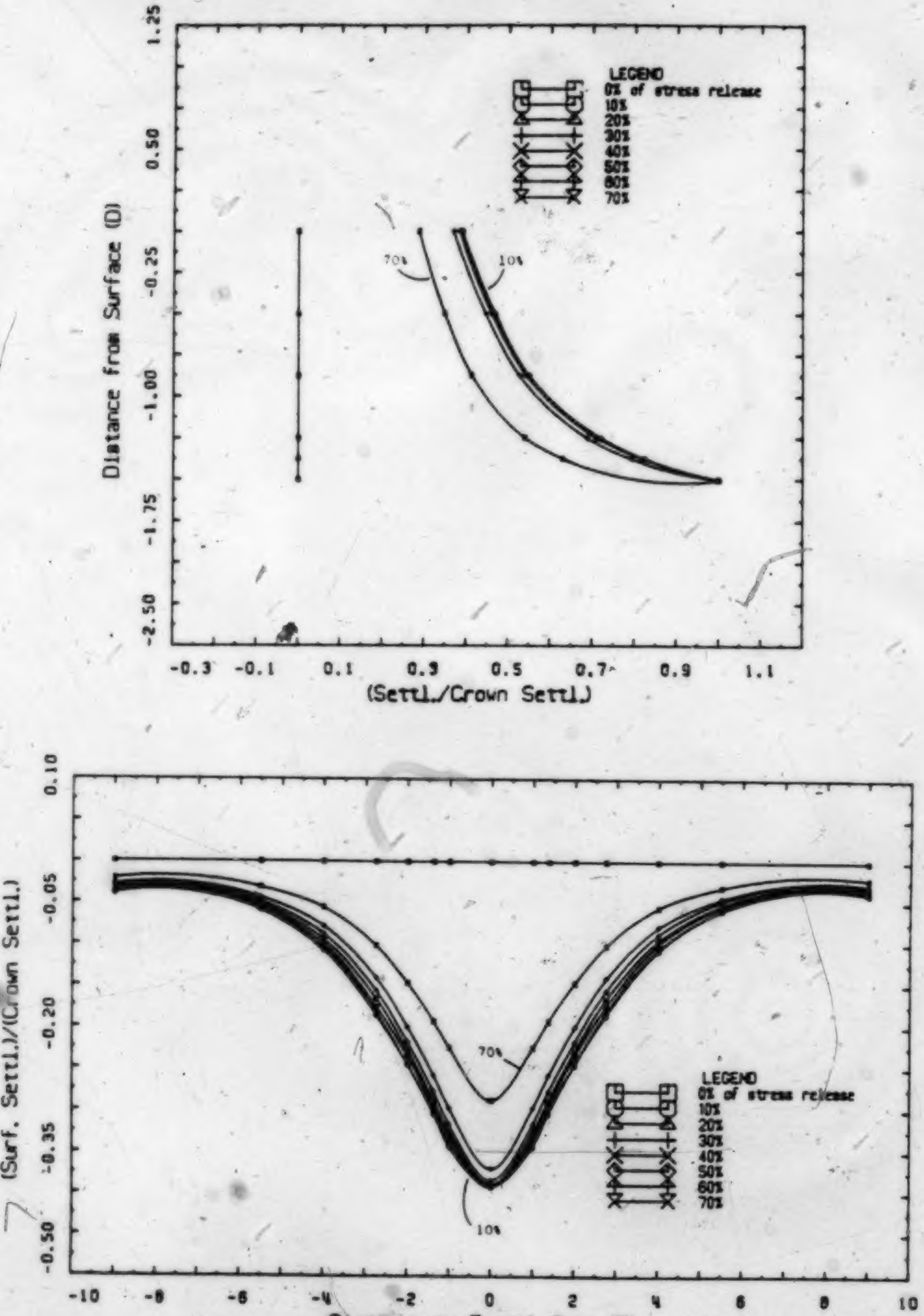

Figure C.6 Normalized Settlements: $K_o=1$, $\phi=30°$, $H/D=1.5$

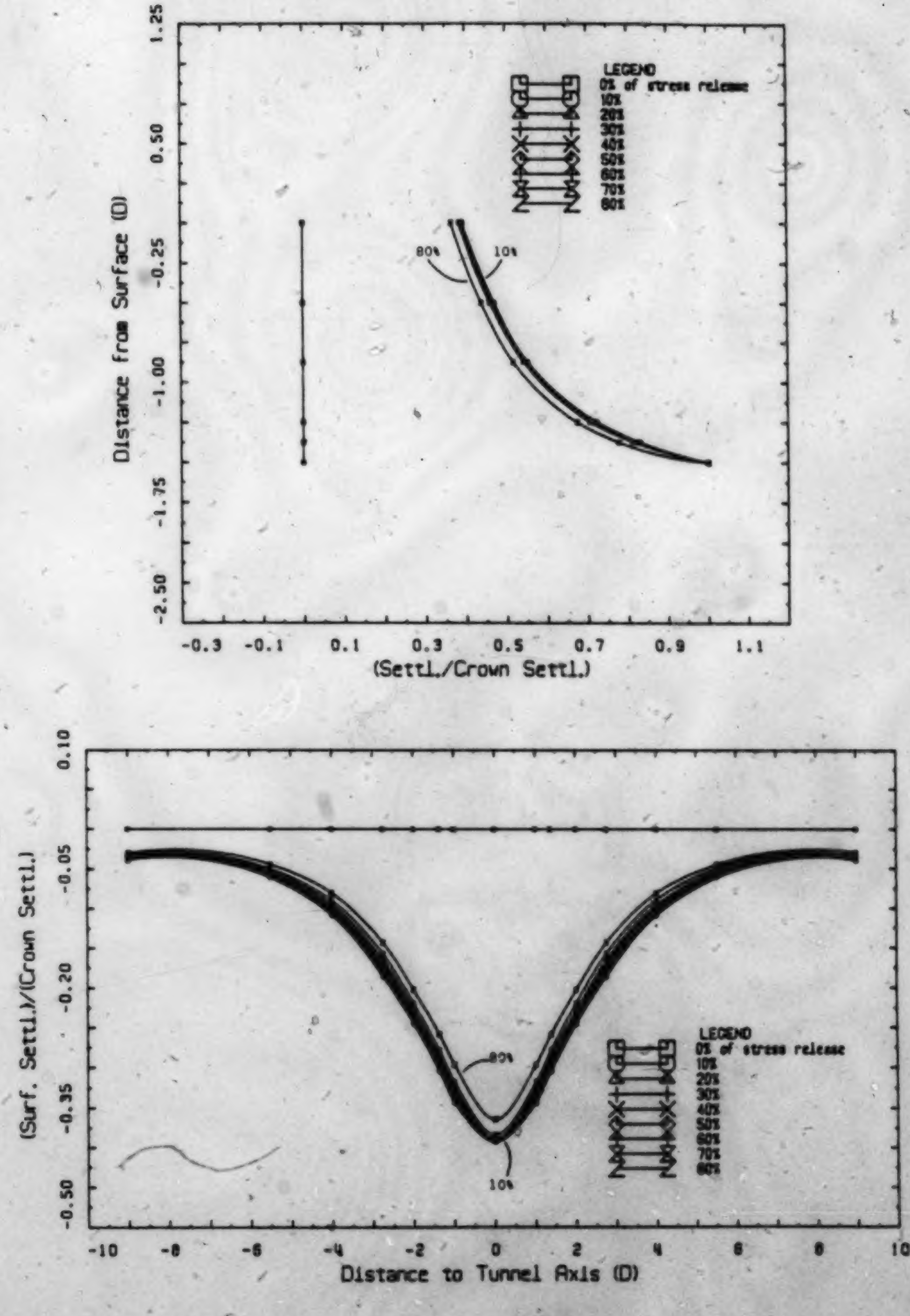

Figure C.7 Normalized Settlements: $K_o=1$, $\phi=40°$, $H/D=1.5$

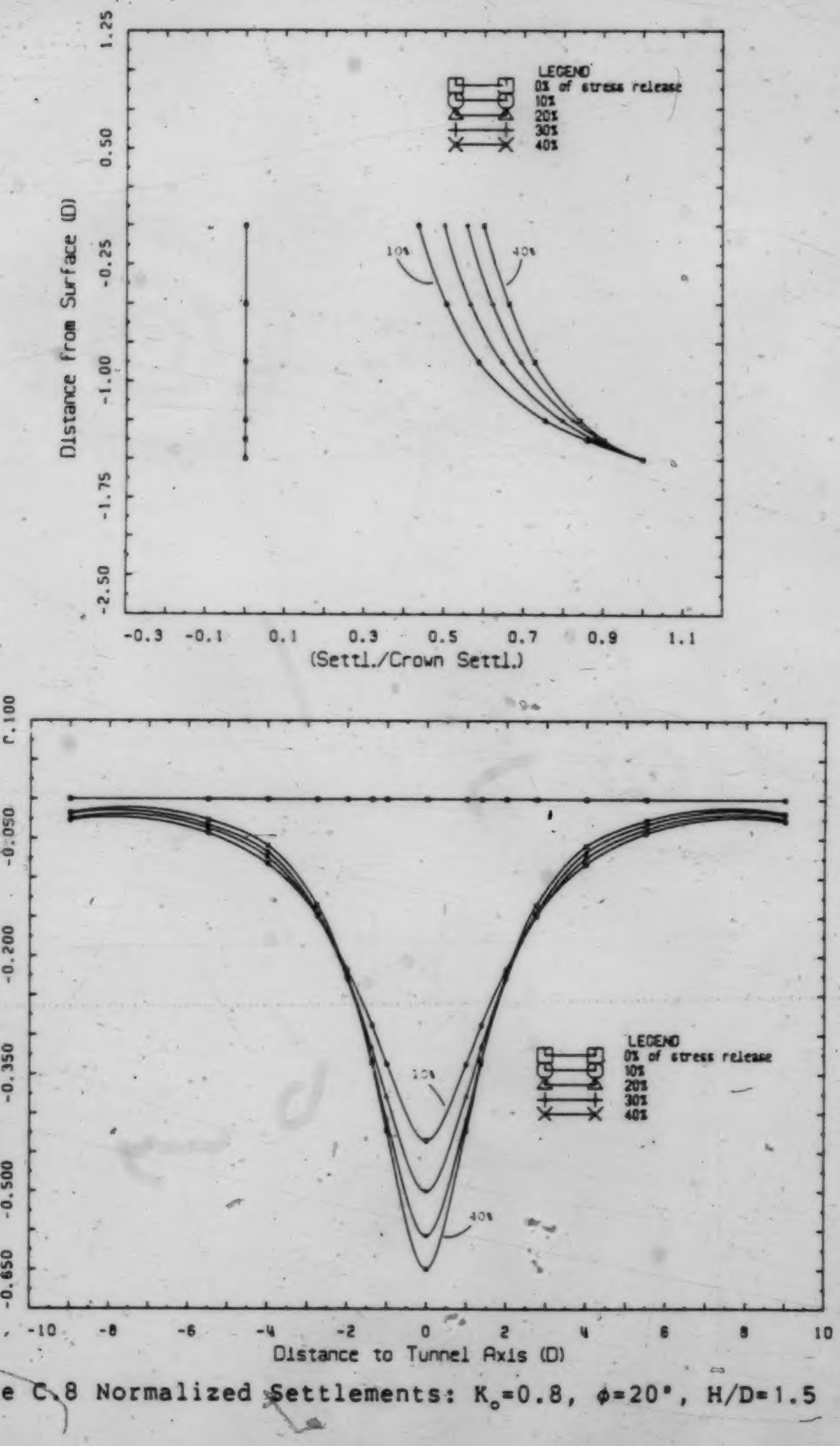

Figure C.8 Normalized Settlements: K_o=0.8, ϕ=20°, H/D=1.5

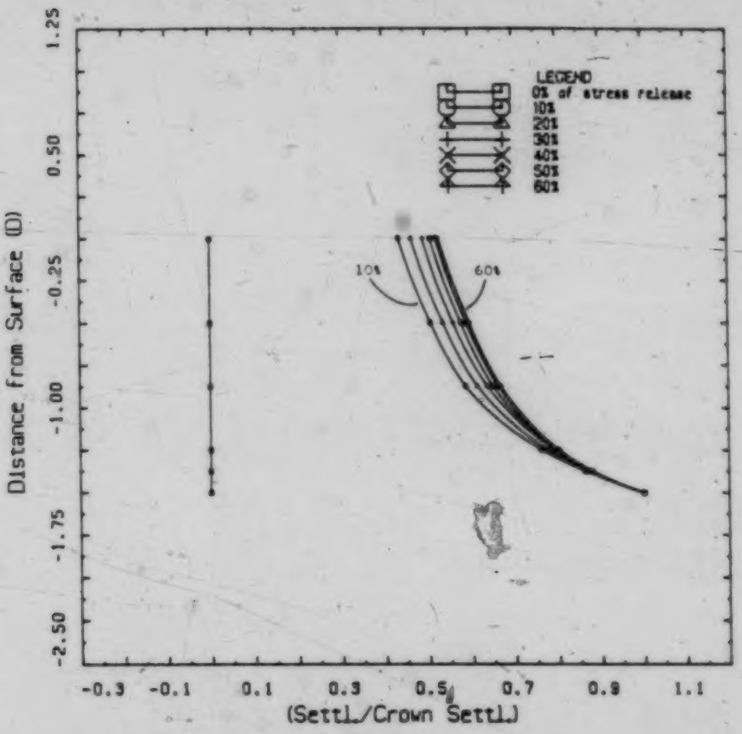

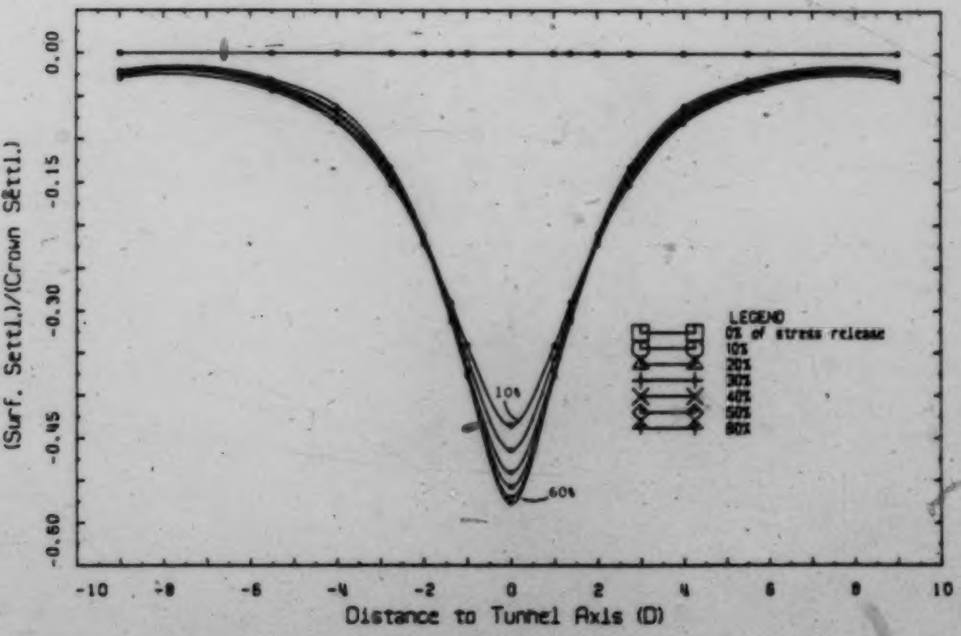

Figure C.9 Normalized Settlements: K_o=0.8, ϕ=30°, H/D=1.5

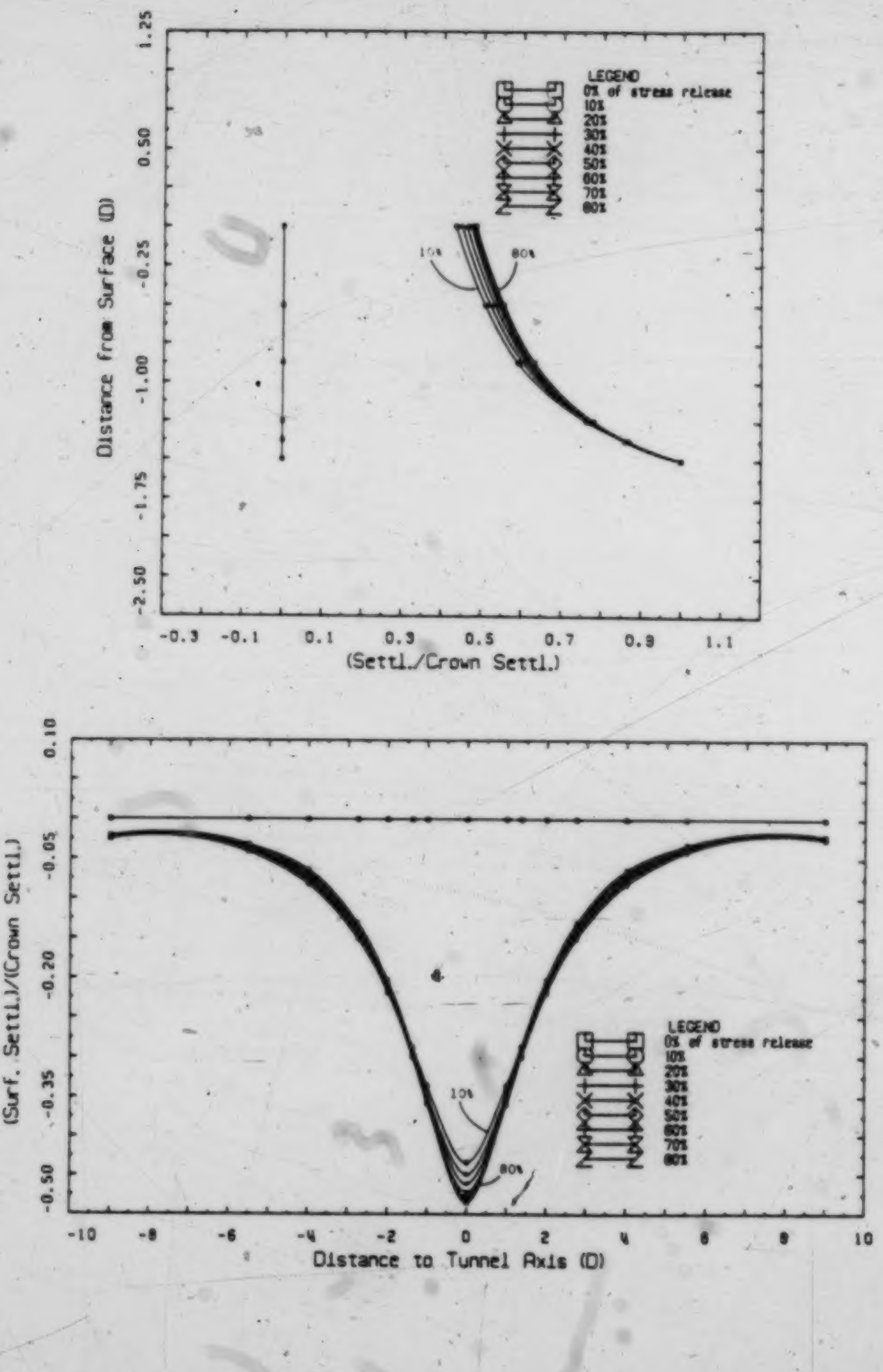

Figure C.10 Normalized Settlements: K_o=0.8, ϕ=40°, H/D=1.5

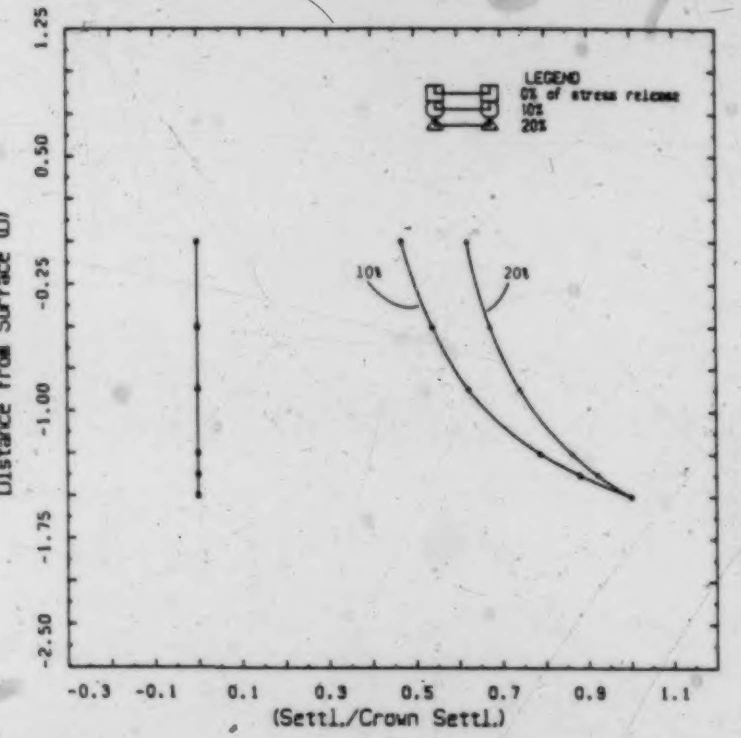

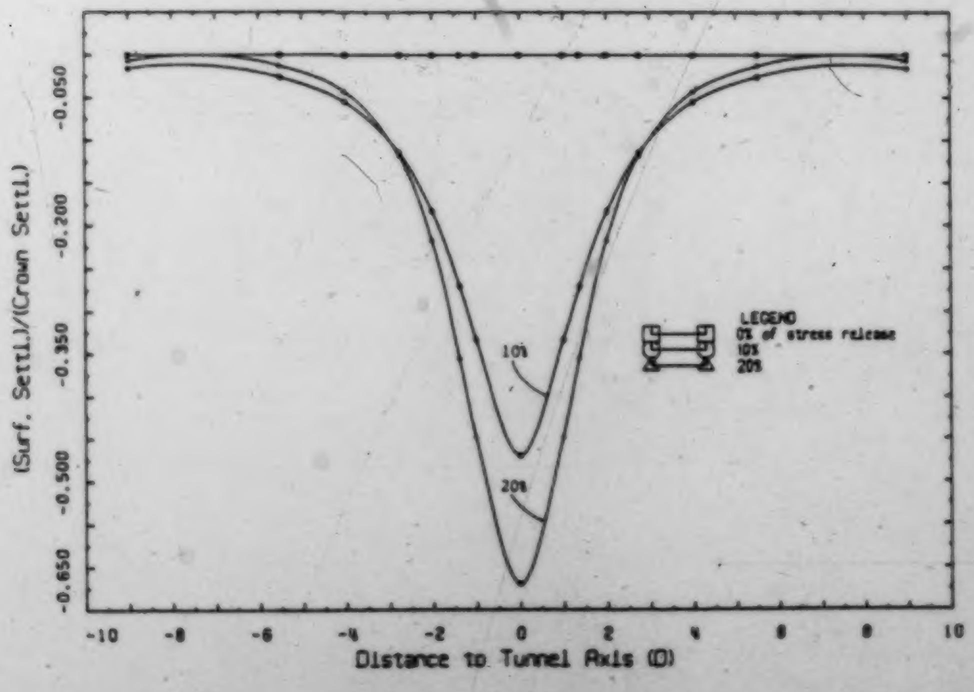

Figure C.11 Normalized Settlements: K_o=0.6, ϕ=20°, H/D=1.5

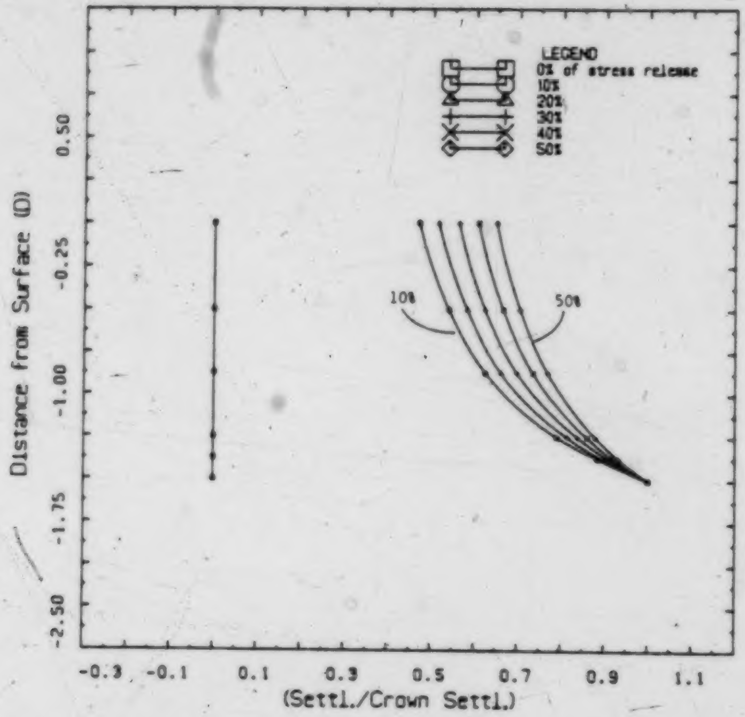

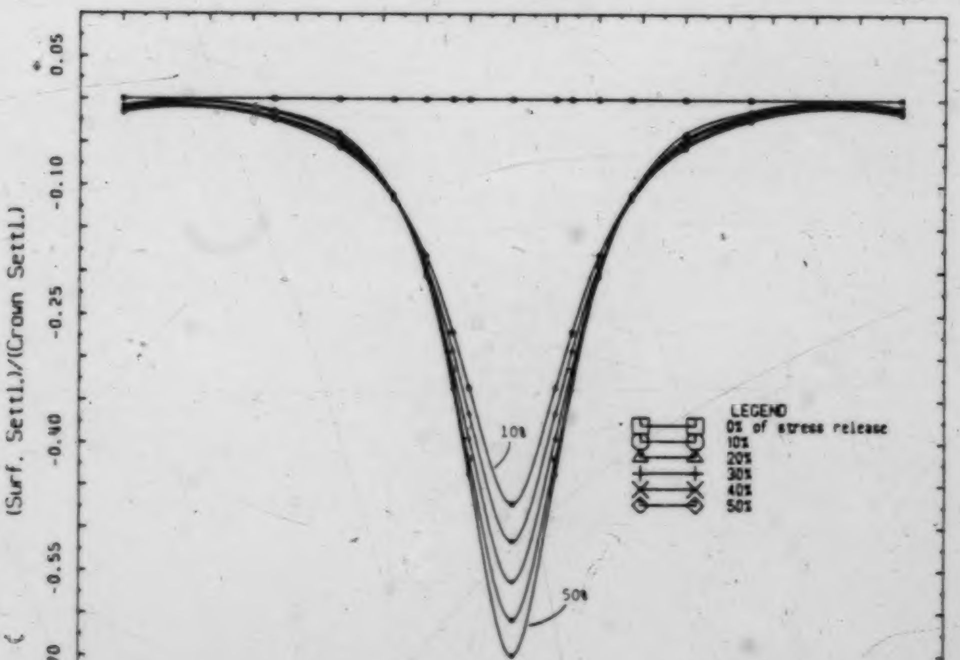

Figure C.12 Normalized Settlements: K_o=0.6, ϕ=30°, H/D=1.5

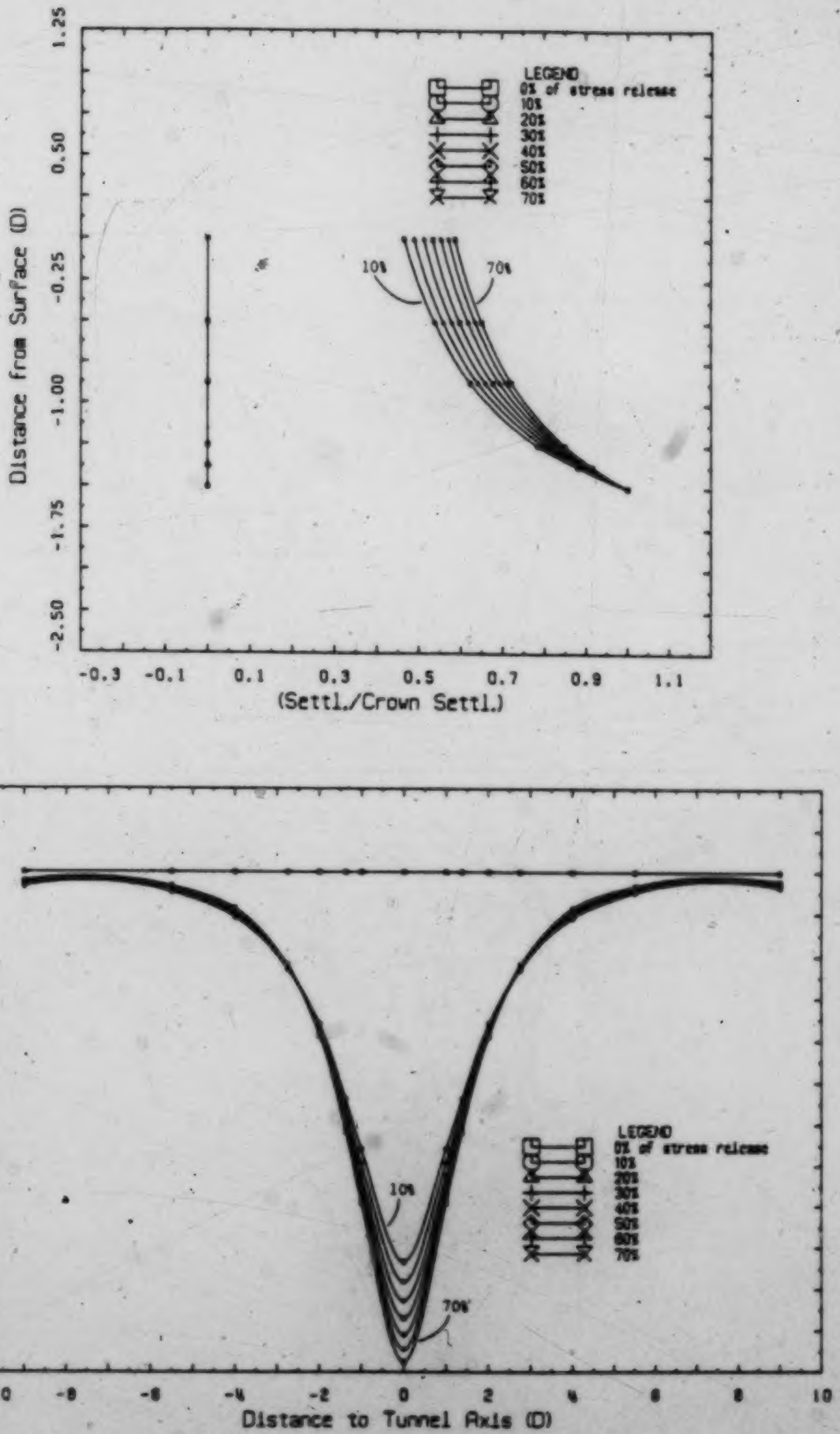

Figure C.13 Normalized Settlements: K_o=0.6, ϕ=40°, H/D=1.5

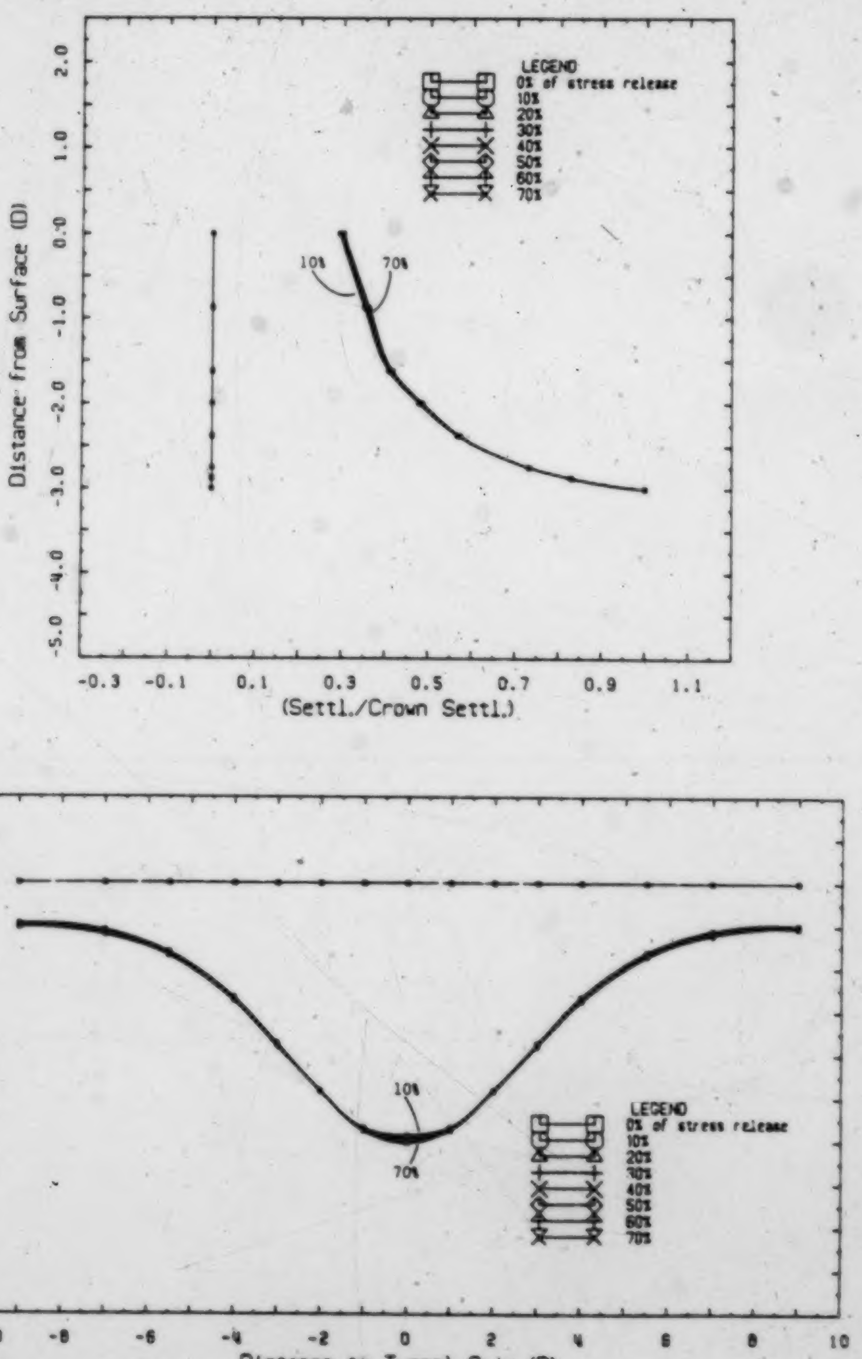

Figure C.14 Normalized Settlements: $K_o=1$, $c_u/\gamma D=2.5$, $H/D=3$

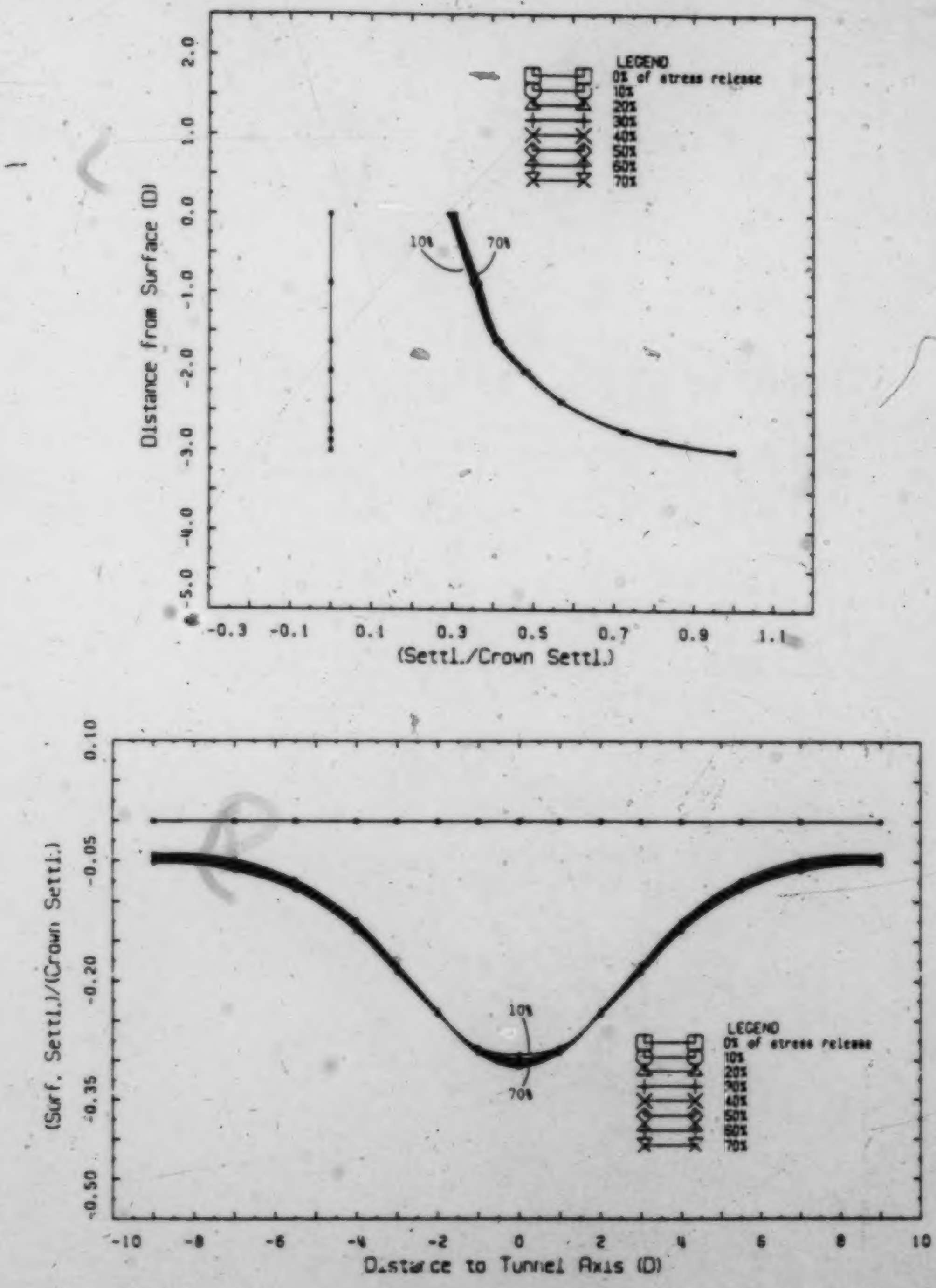

Figure C.15 Normalized Settlements: $K_o=1$, $c_u/\gamma D=1.25$, $H/D=3$

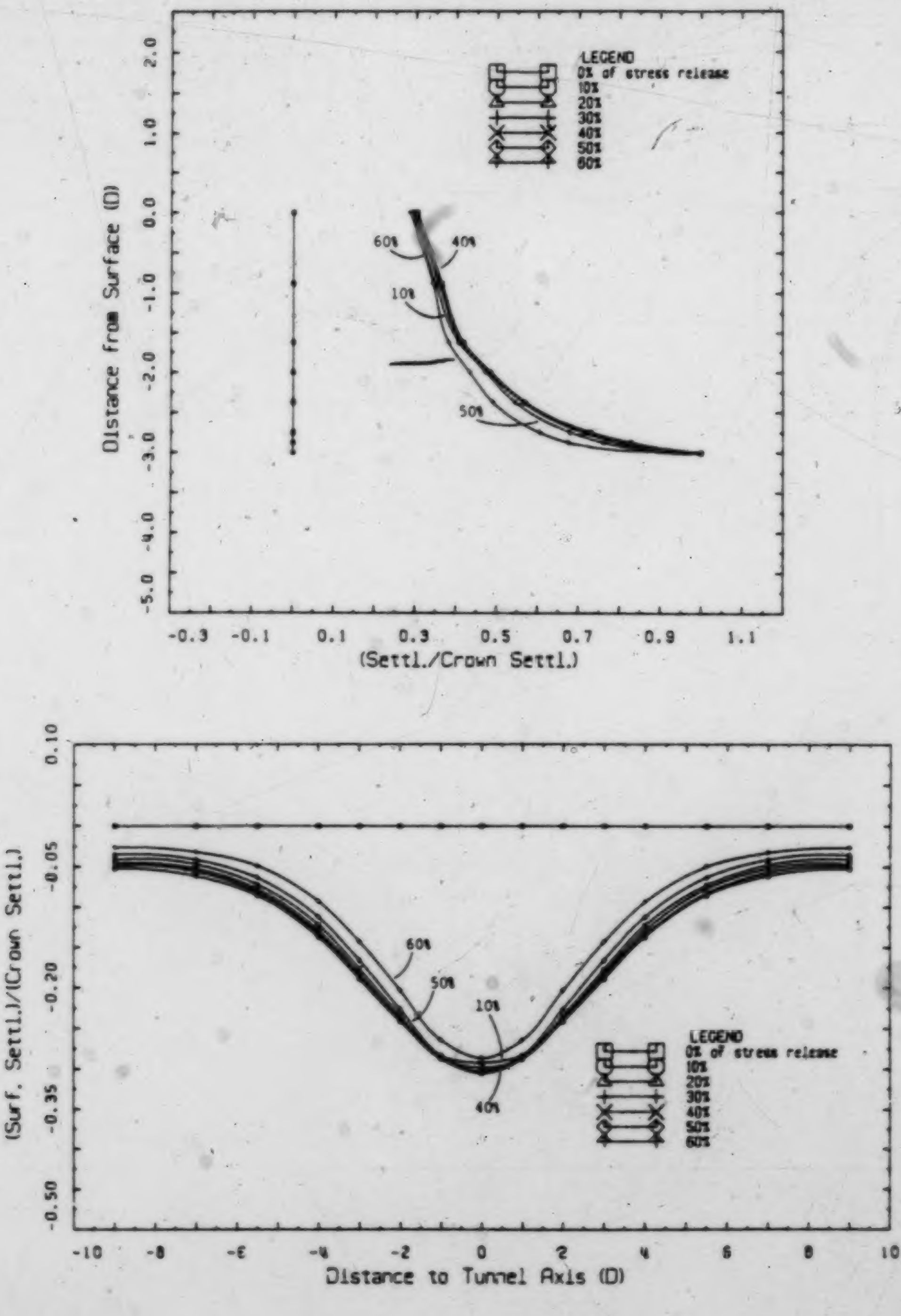

Figure C.16 Normalized Settlements: $K_o=1$, $c_u/\gamma D=0.625$, $H/D=3$

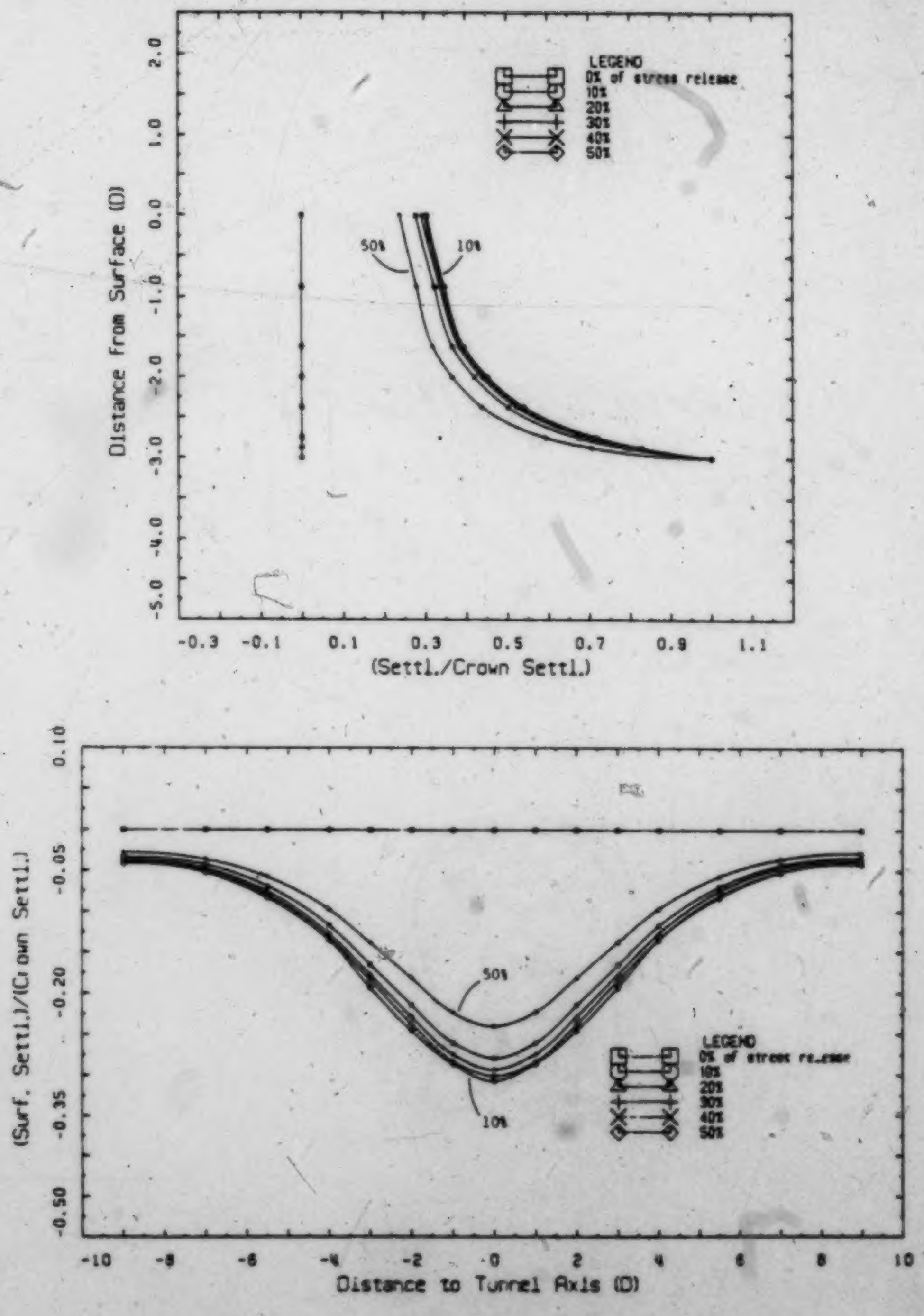

Figure C.17 Normalized Settlements: $K_o=1$, $\phi=20°$, $H/D=3$

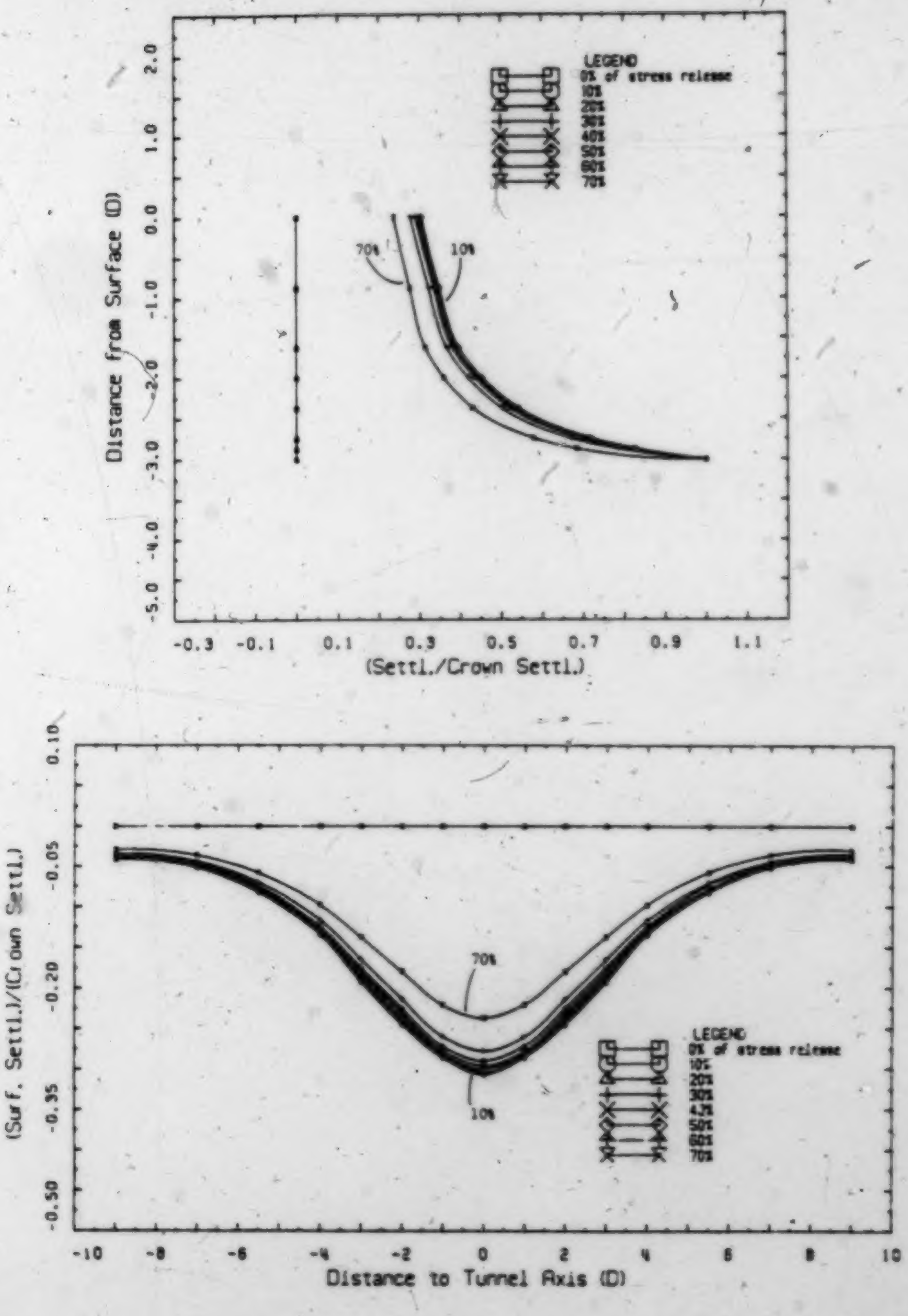

Figure C.18 Normalized Settlements: $K_o=1$, $\phi=30°$, $H/D=3$

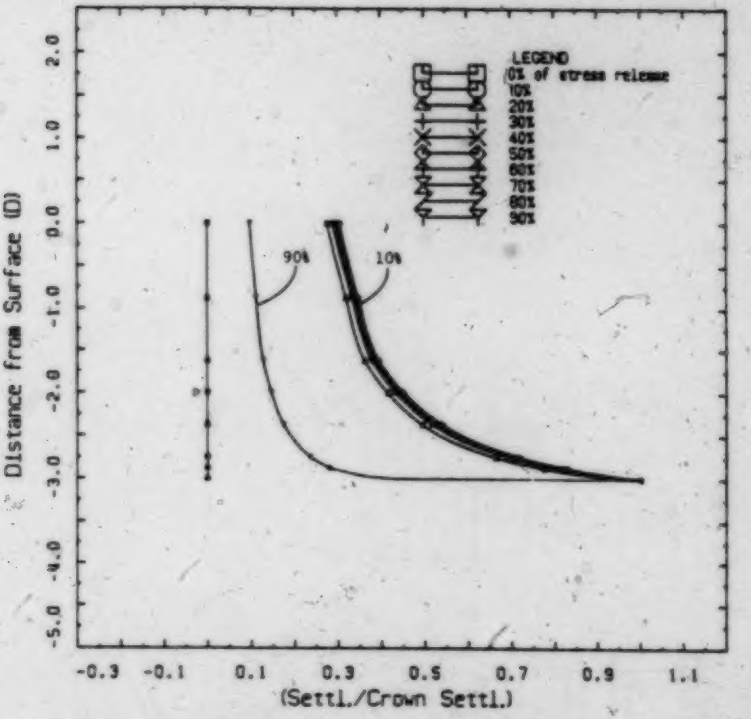

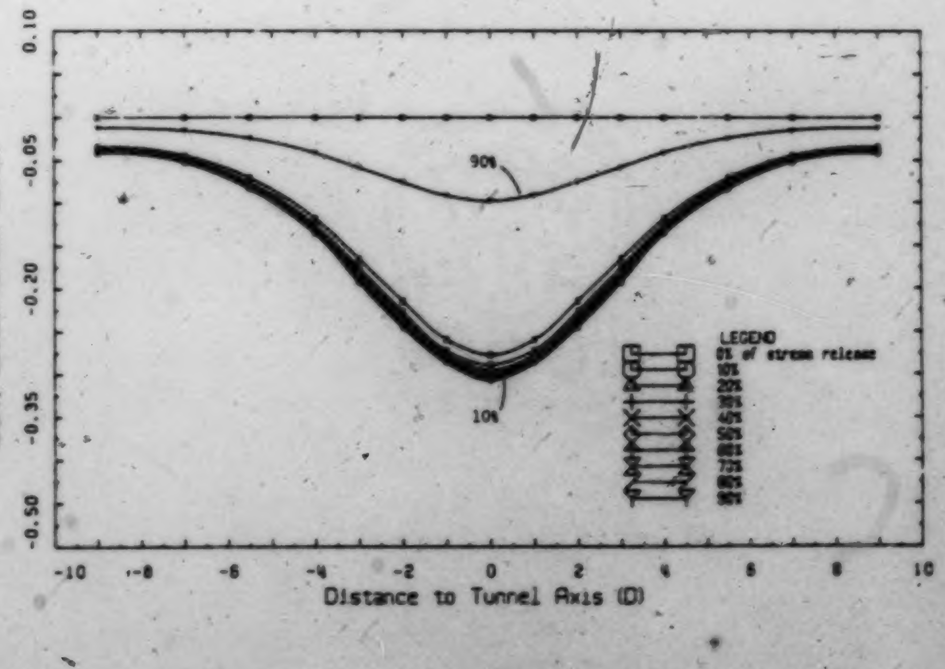

Figure C.19 Normalized Settlements: K_o=1, ϕ=40°, H/D=3

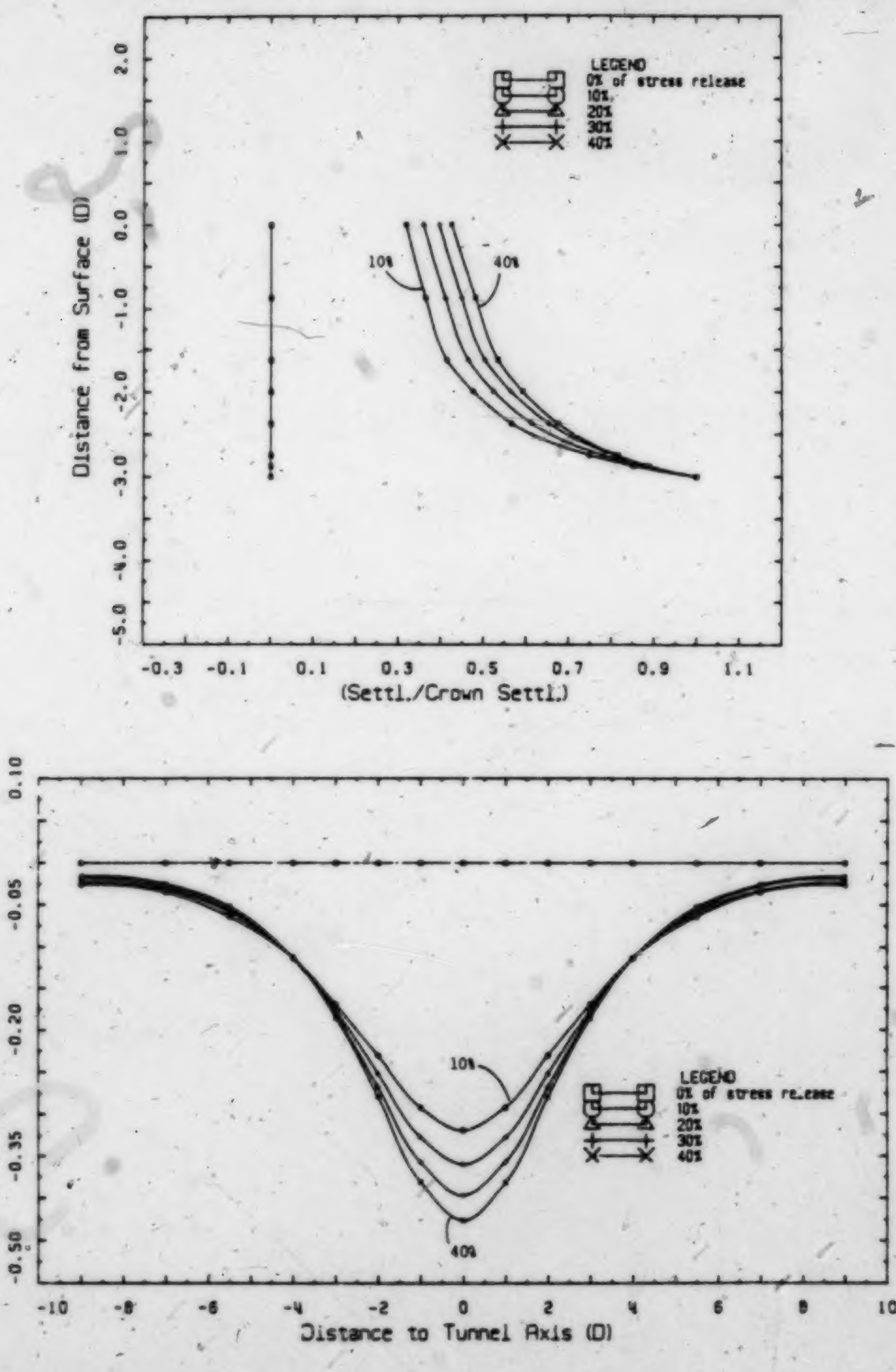

Figure C.20 Normalized Settlements: $K_o=0.8$, $\phi=20°$, $H/D=3$

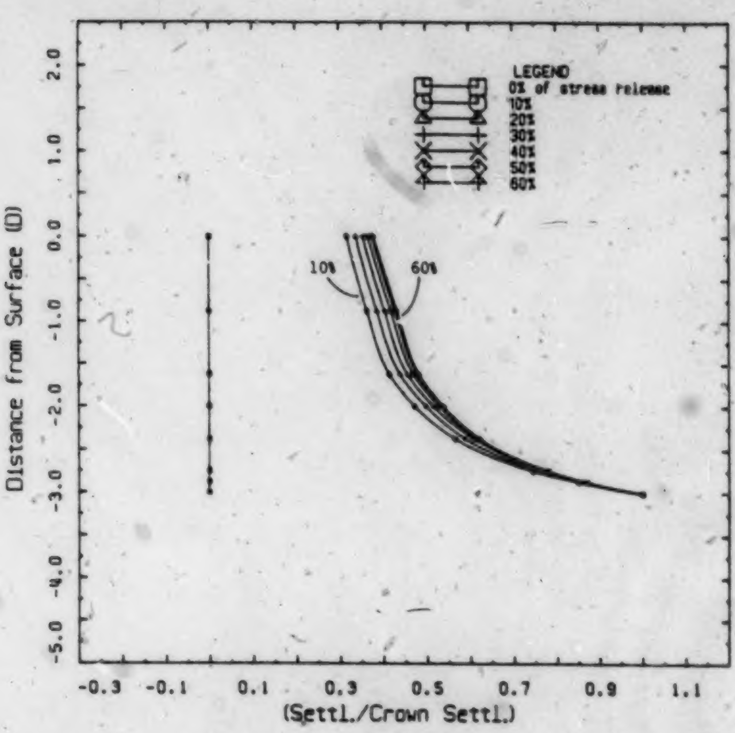

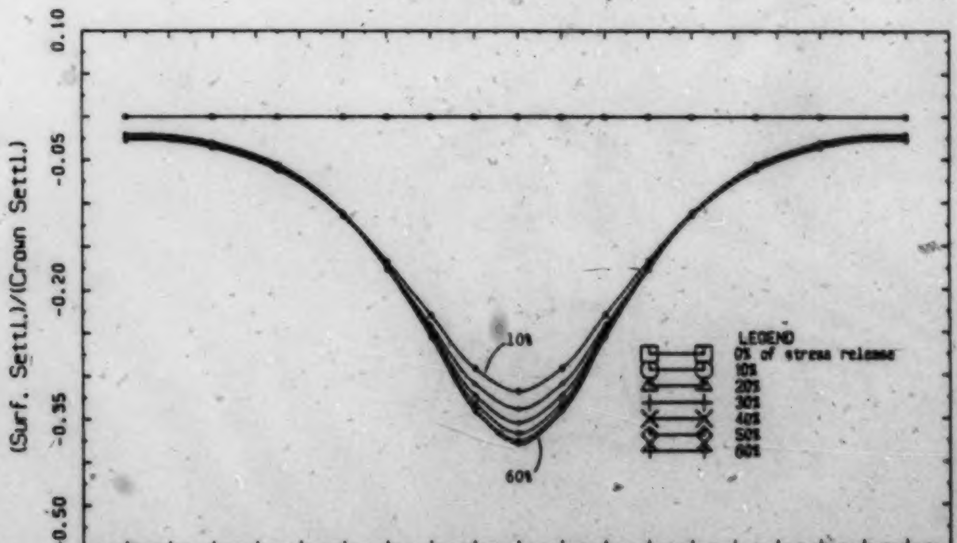

Figure C.21 Normalized Settlements: K_o=0.8, ϕ=30°, H/D=3

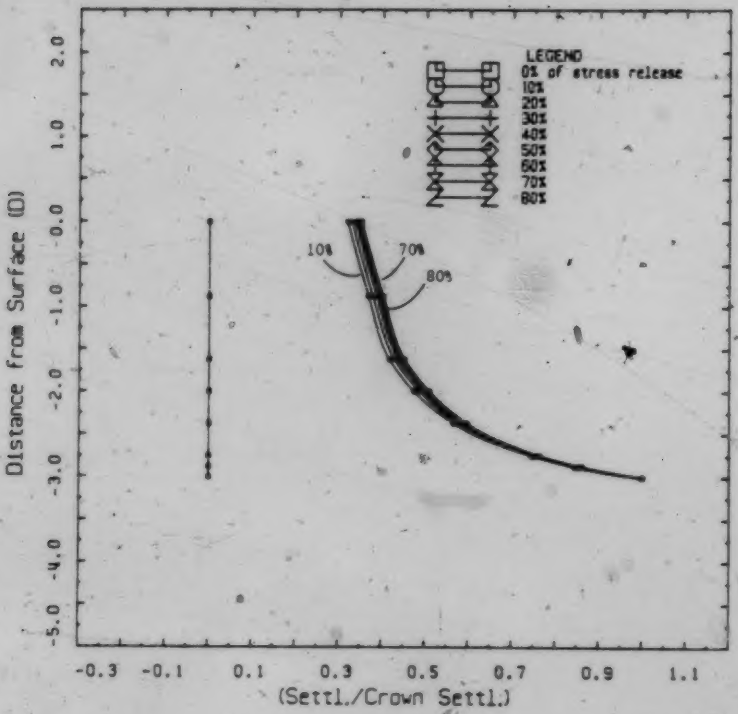

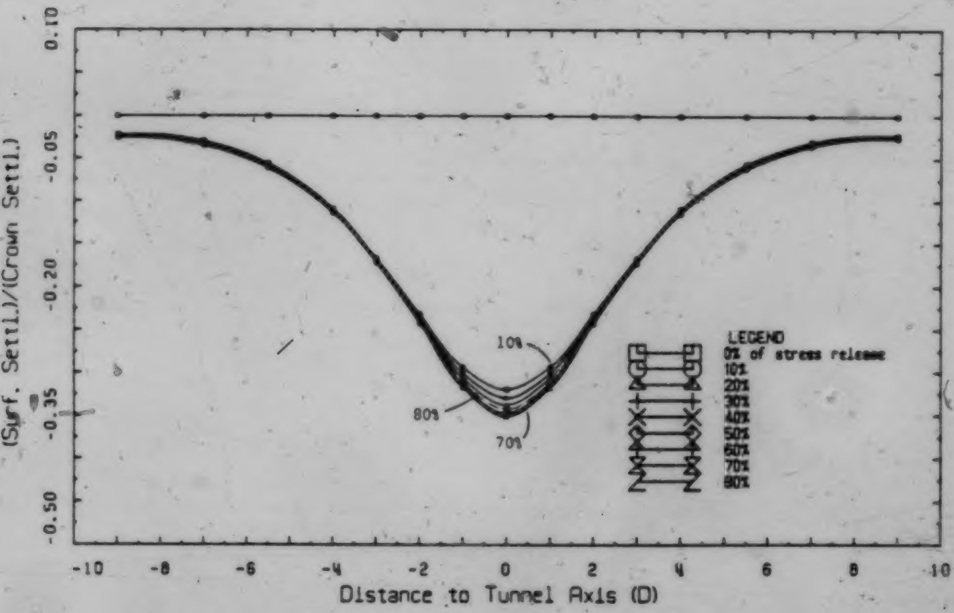

Figure C.22 Normalized Settlements: K_o=0.8, ϕ=40°, H/D=3

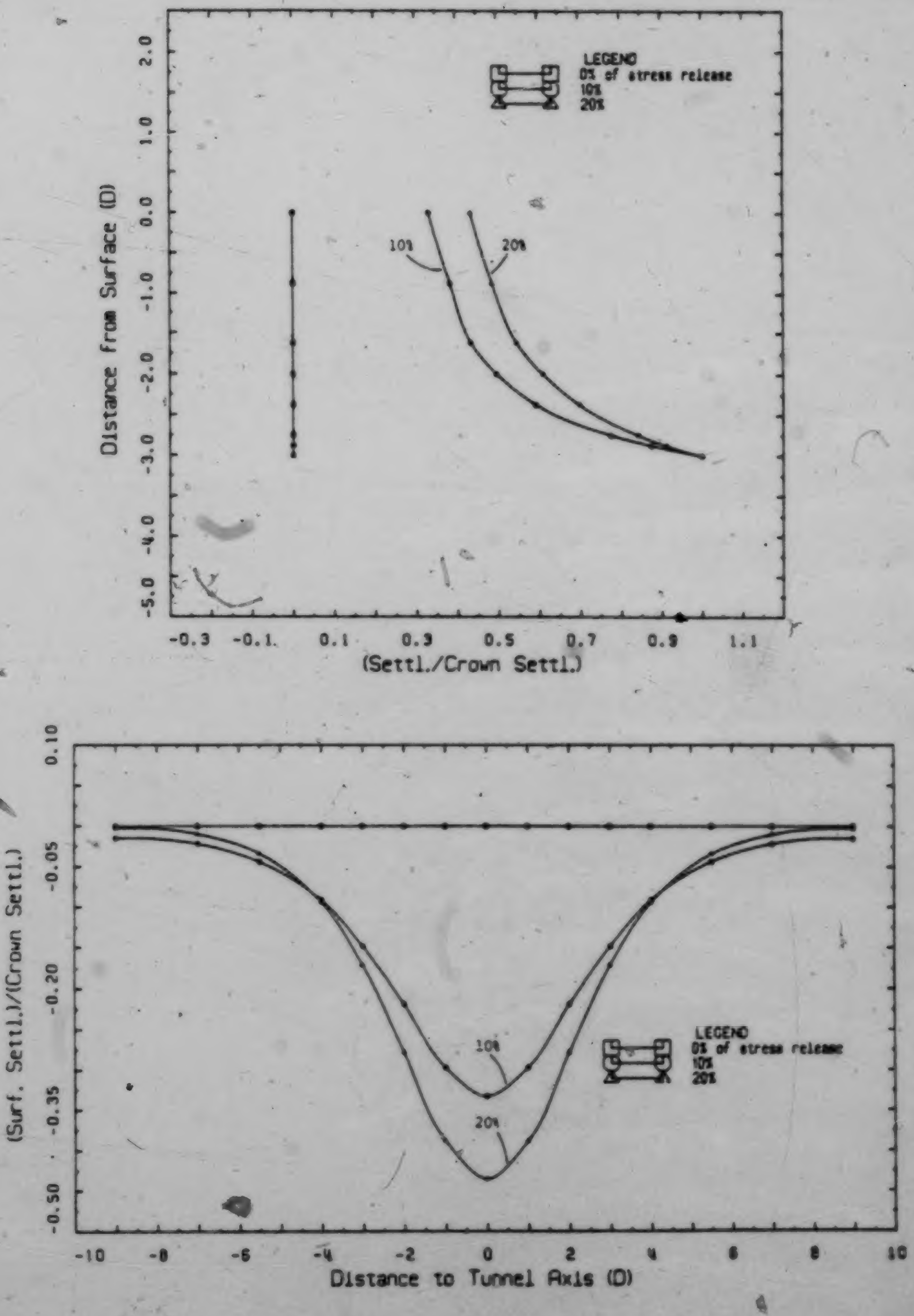

Figure C.23 Normalized Settlements: K_o=0.6, ϕ=20°, H/D=3

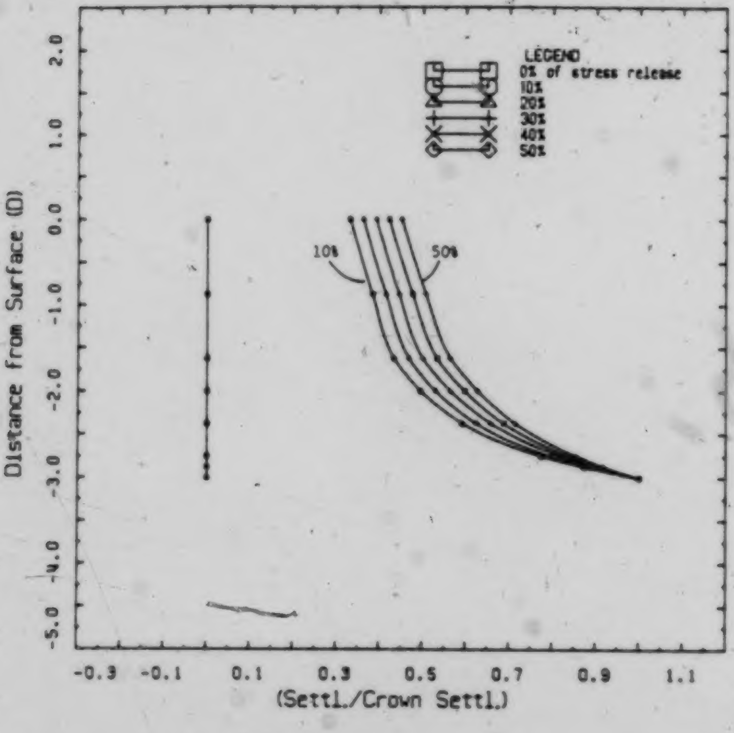

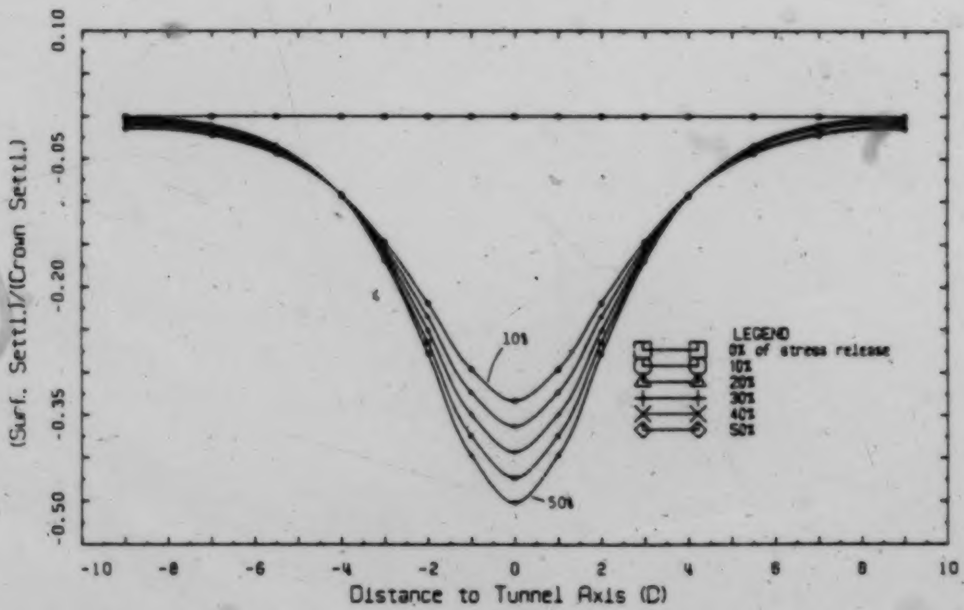

Figure C.24 Normalized Settlements: K_o=0.6, ϕ=30°, H/D=3

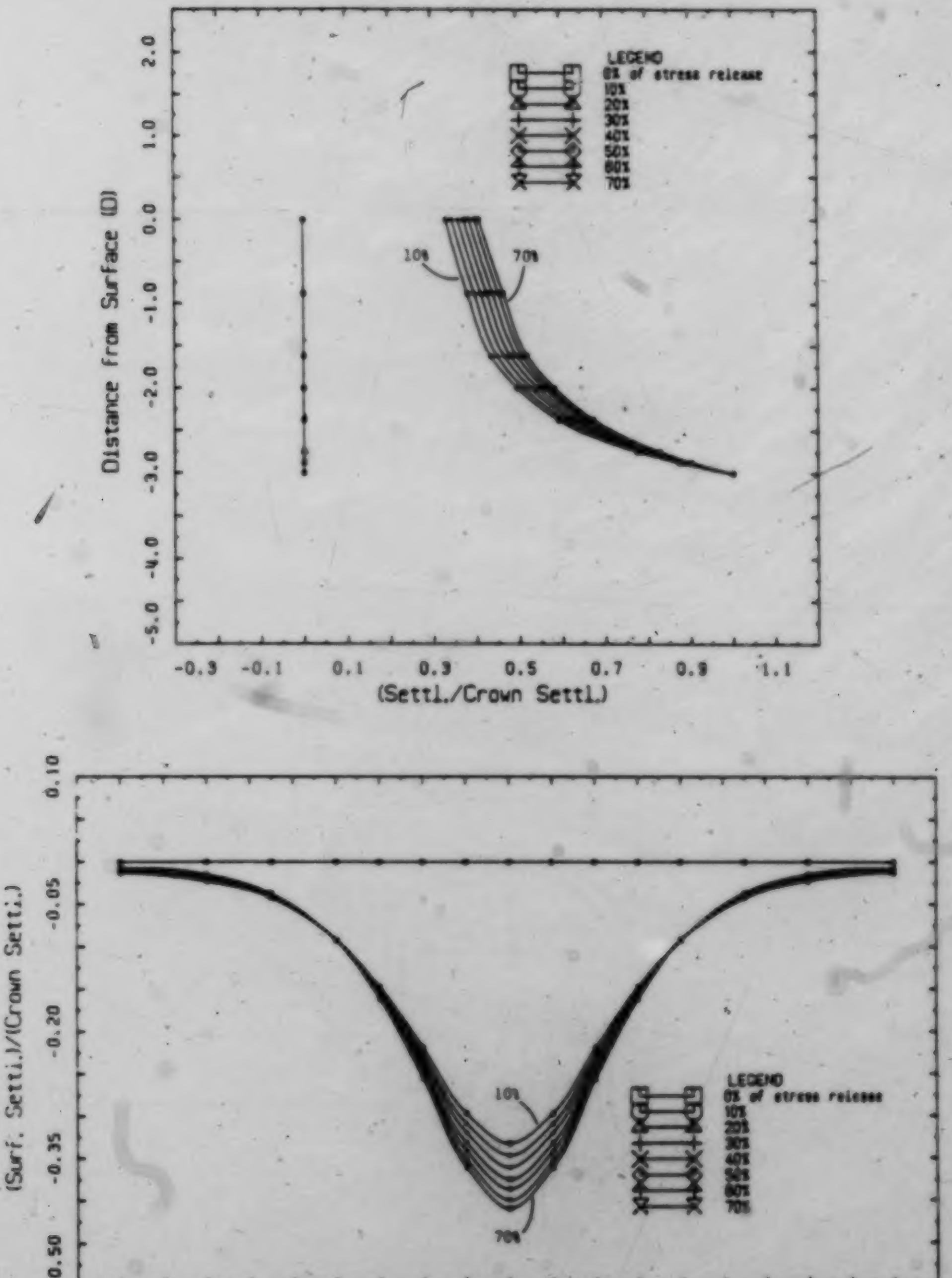

Figure C.25 Normalized Settlements: K_o=0.6, ϕ=40°, H/D=3

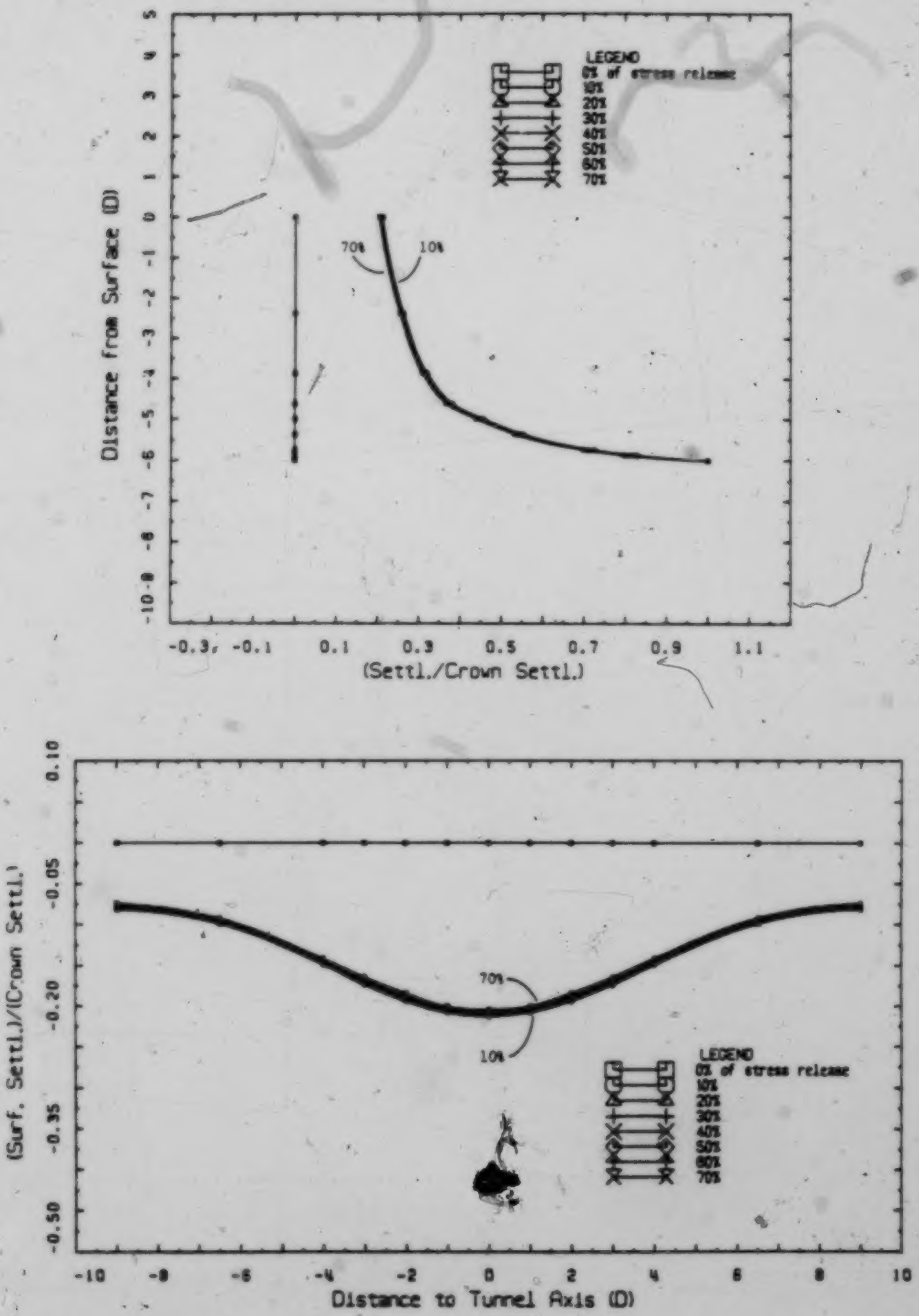

Figure C.26 Normalized Settlements: $K_o=1$, $c_u/\gamma D=2.5$, $H/D=6$

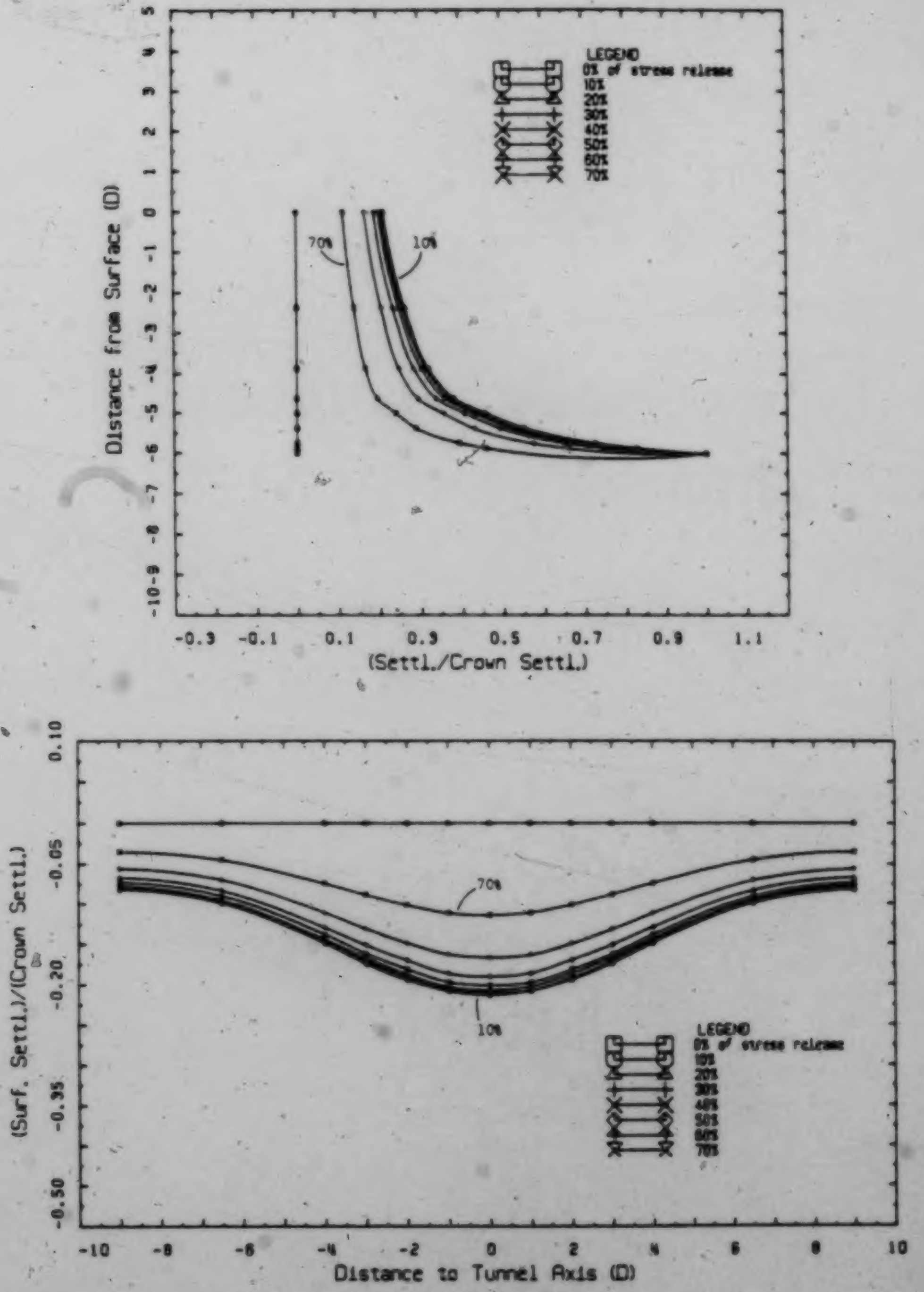

Figure C.27 Normalized Settlements: $K_o=1$, $c_u/\gamma D=1.25$, $H/D=6$

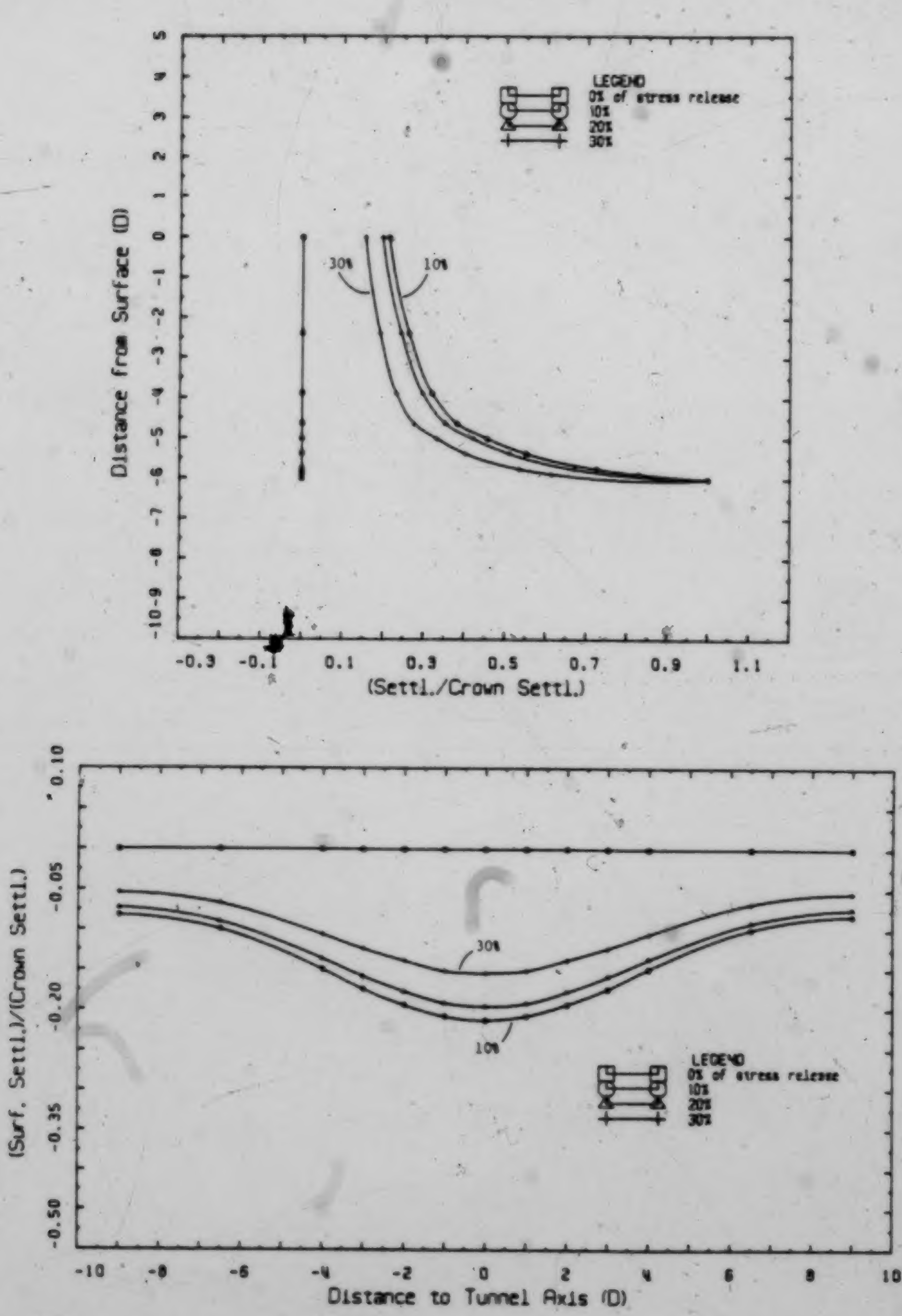

Figure C.28 Normalized Settlements: K_o=1, $c_u/\gamma D$=0.625, H/D=6

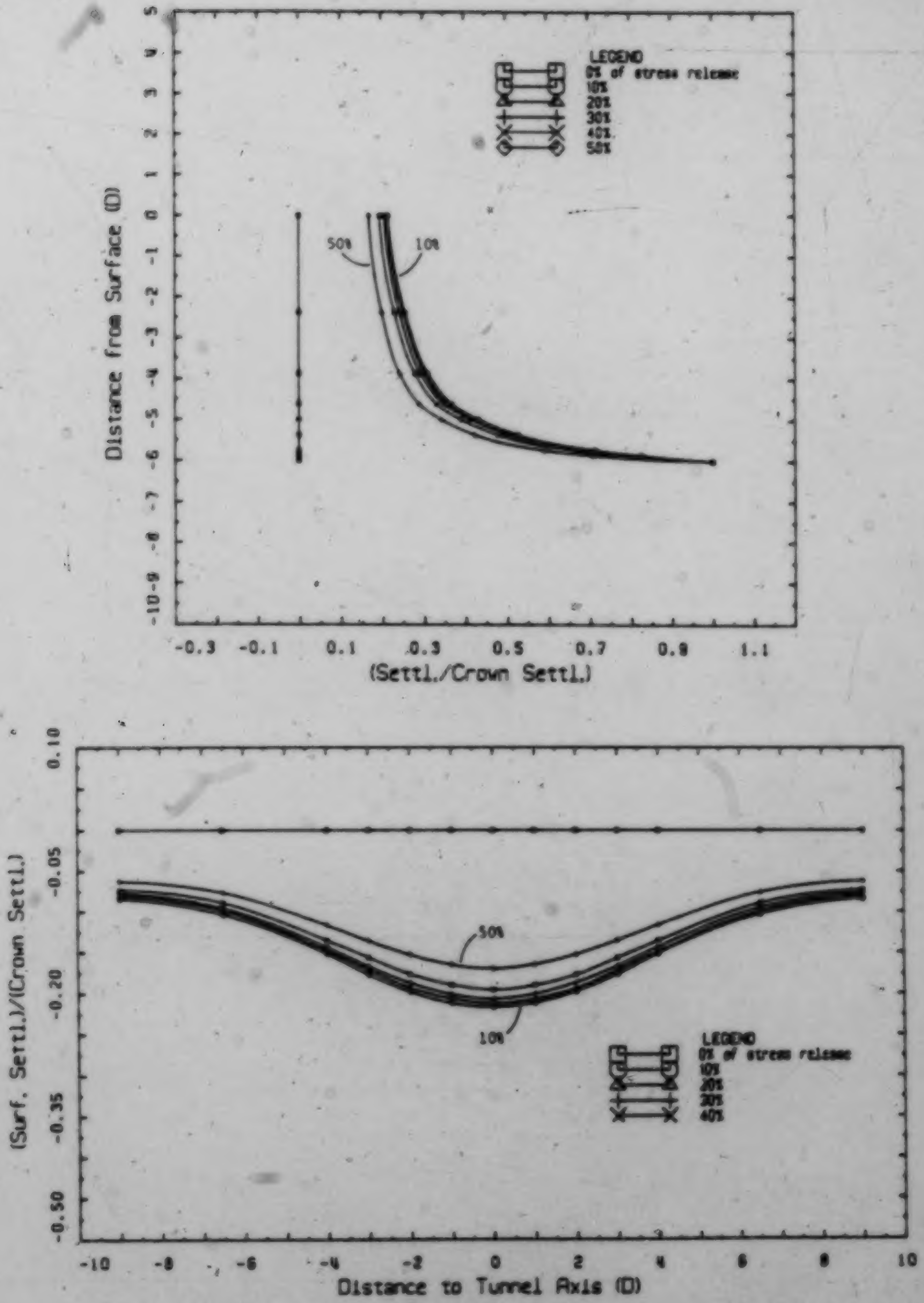

Figure C.29 Normalized Settlements: K_o=1, ϕ=20°, H/D=6

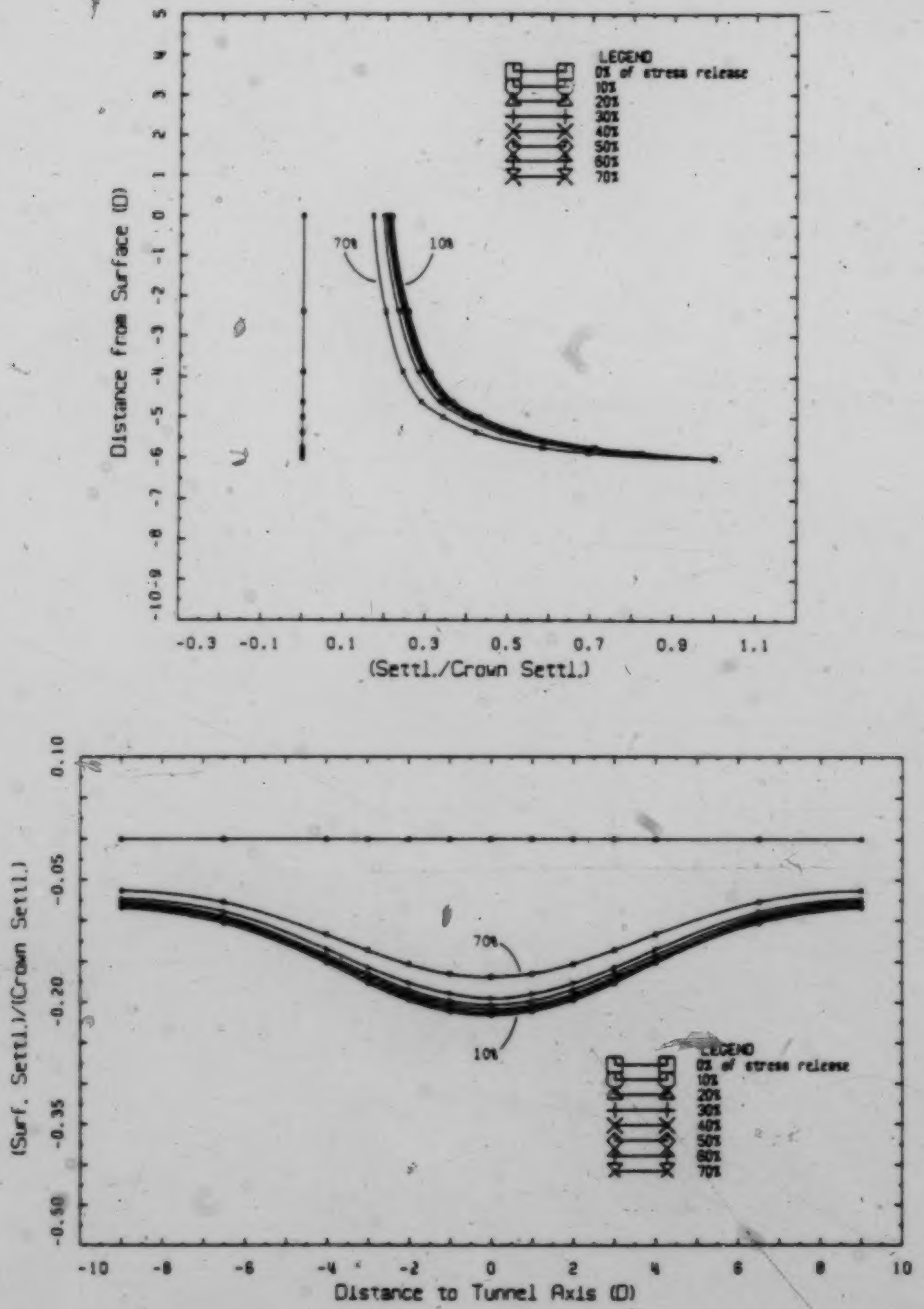

Figure C.30 Normalized Settlements: $K_o=1$, $\phi=30°$, H/D=6

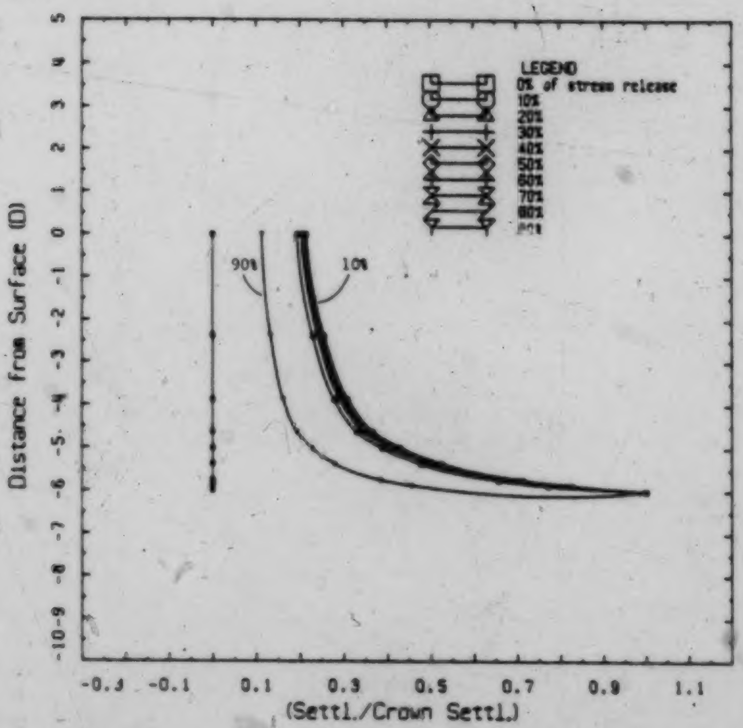

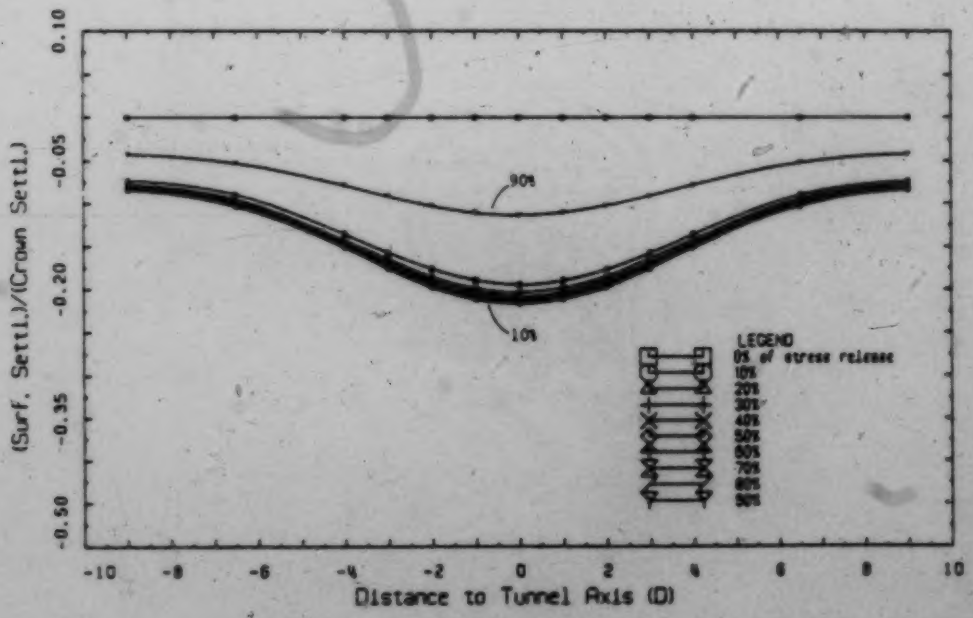

Figure C.31 Normalized Settlements: K_o=1, ϕ=40°, H/D=6

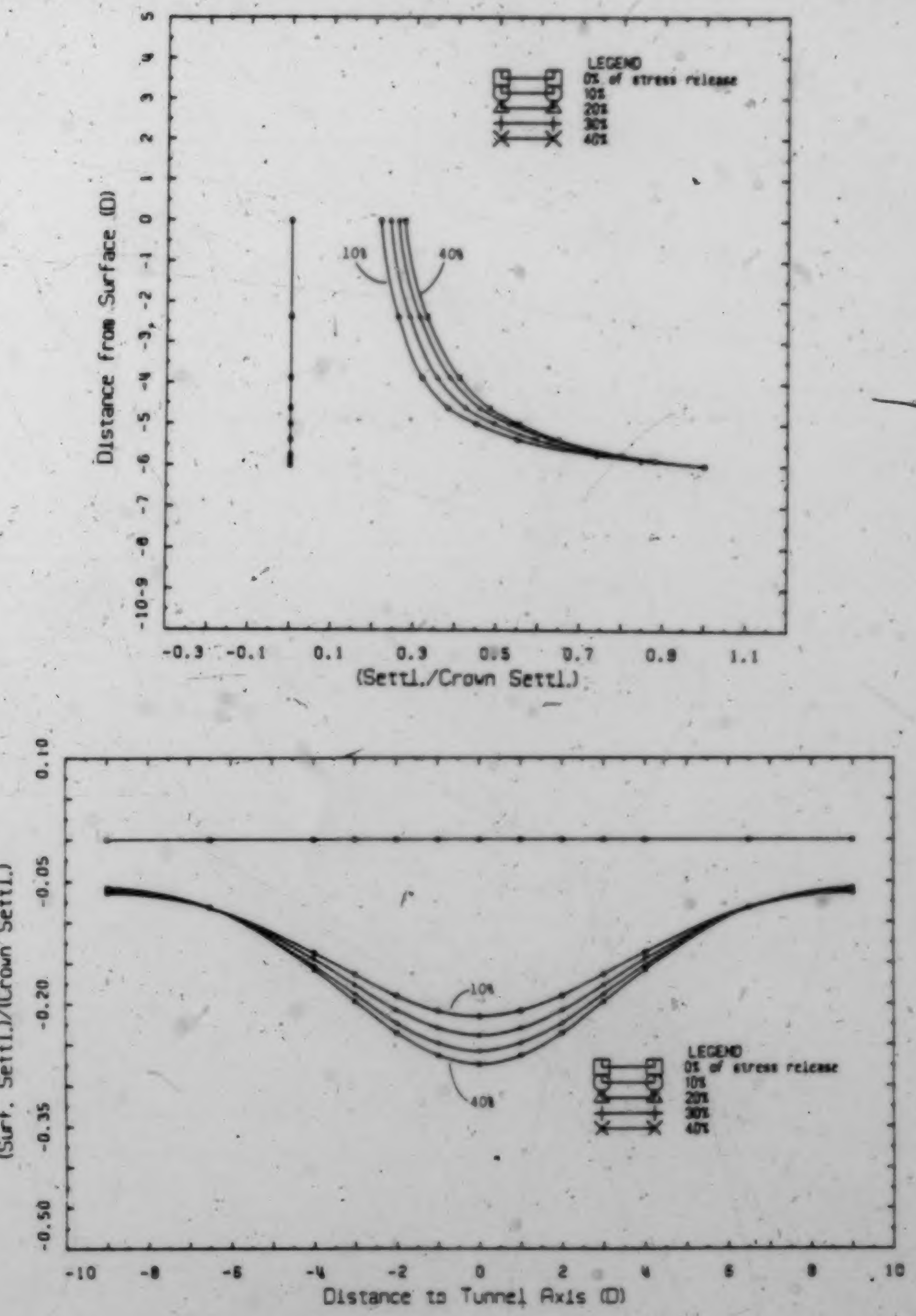

Figure C.32 Normalized Settlements: K_o=0.8, ϕ=20°, H/D=6

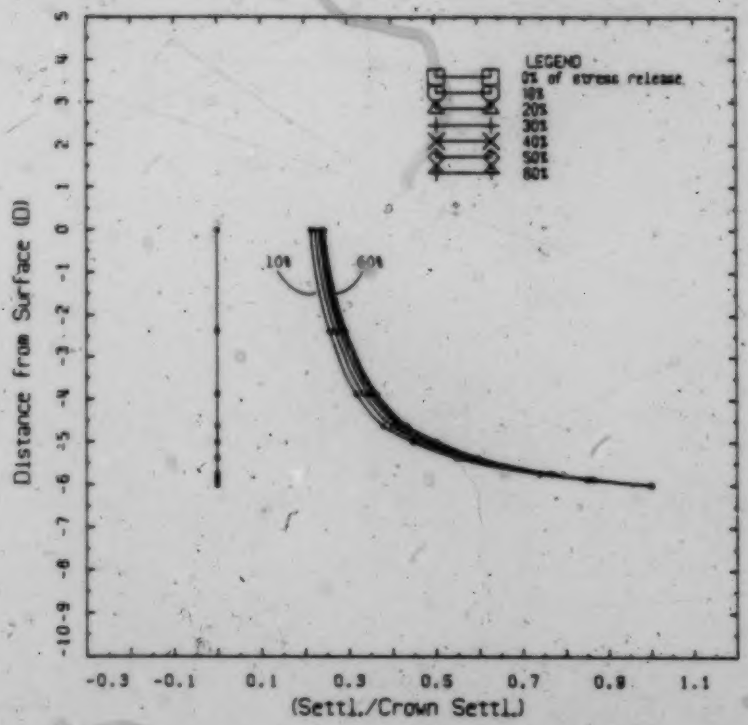

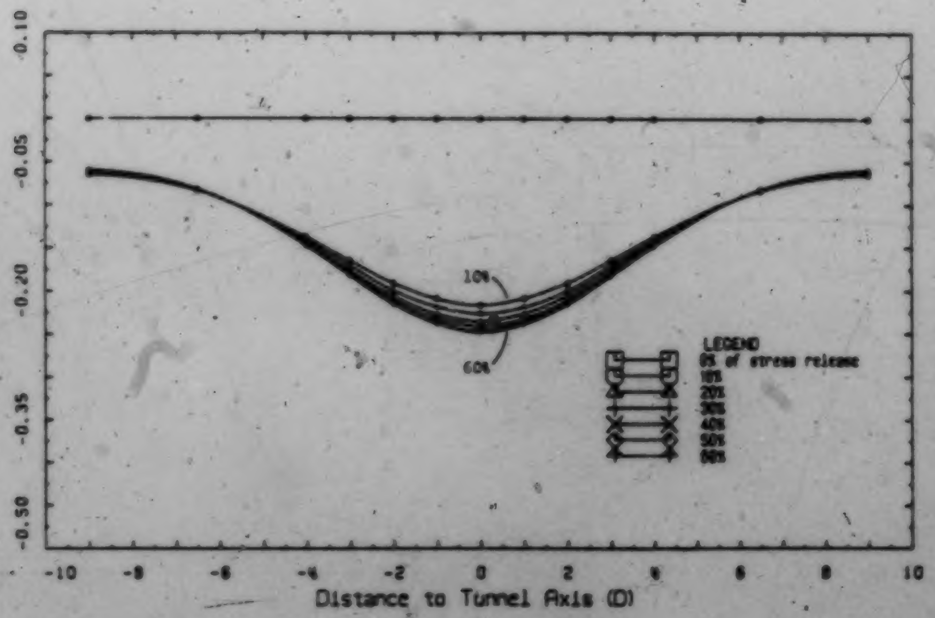

Figure C.33 Normalized Settlements: K_o=0.8, ϕ=30°, H/D=6

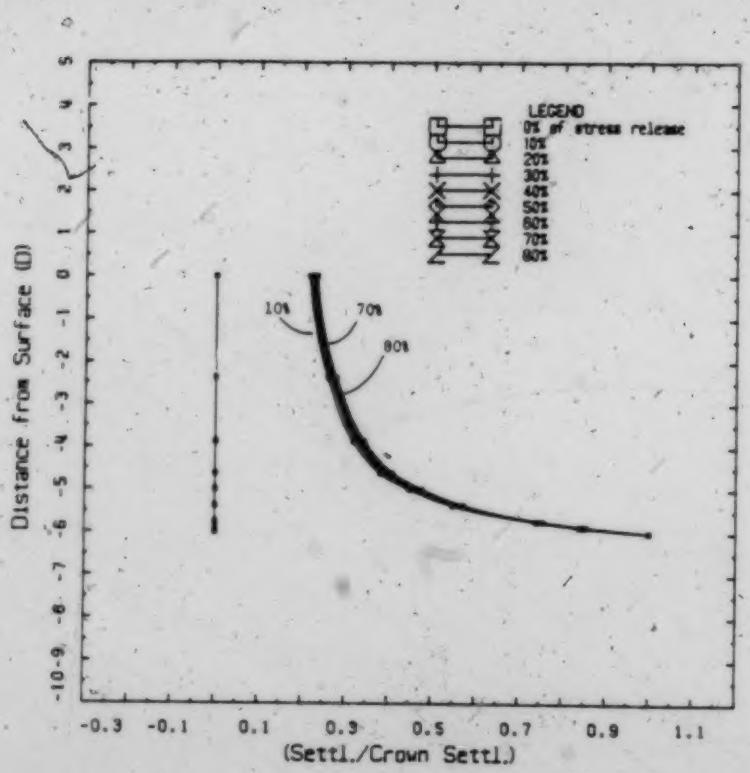

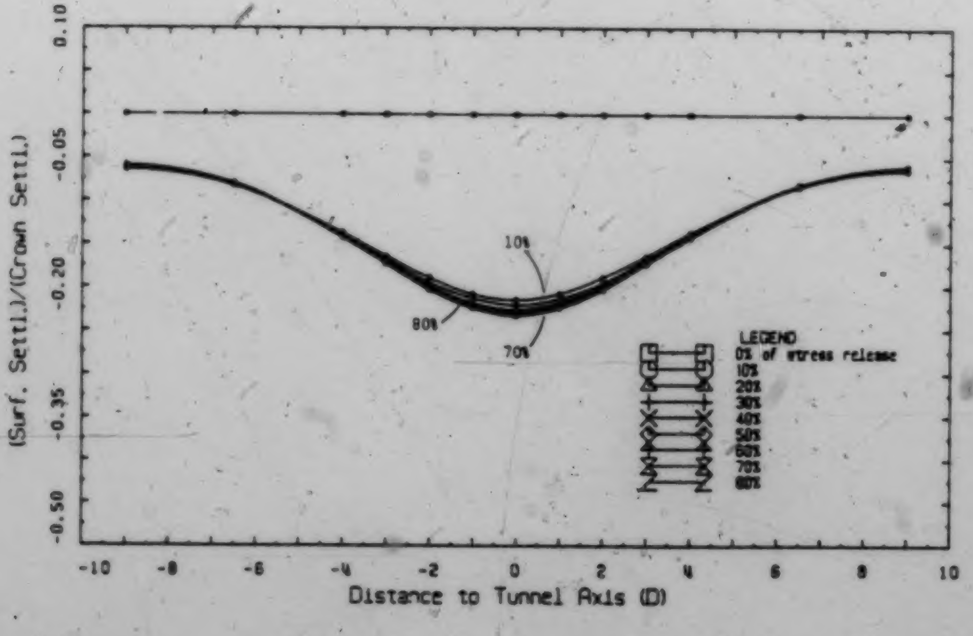

Figure C.34 Normalized Settlements: K_o=0.8, ϕ=40°, H/D=6

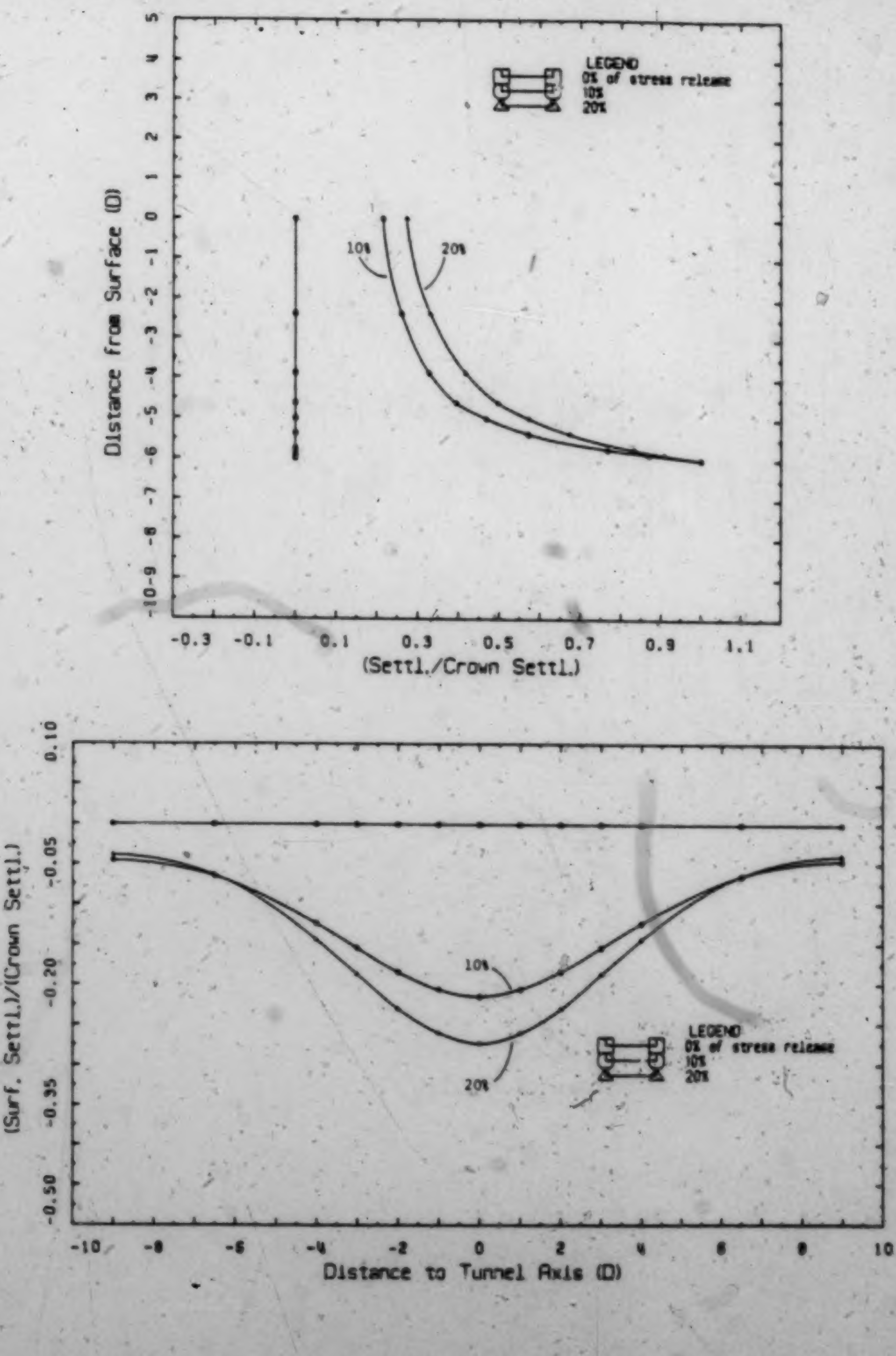

Figure C.35 Normalized Settlements: K_o=0.6, ϕ=20°, H/D=6

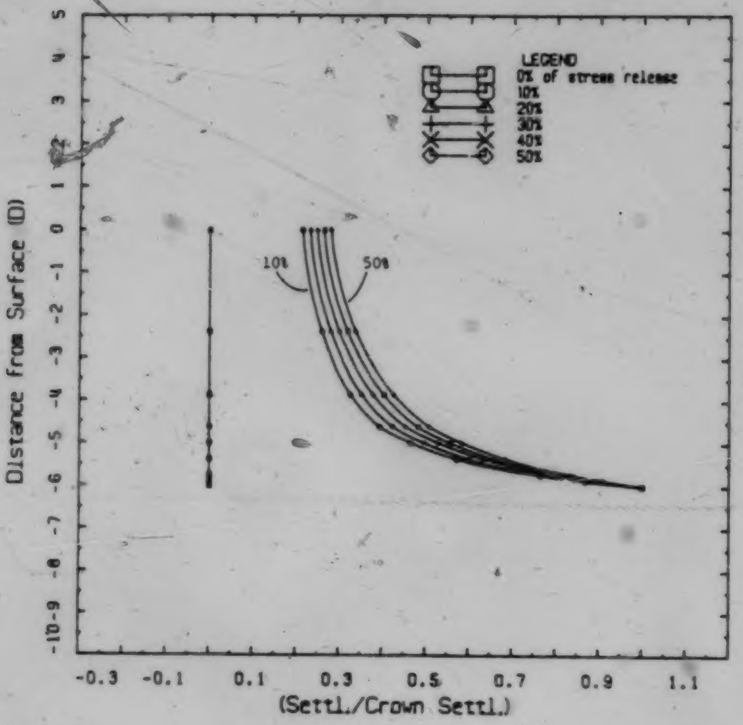

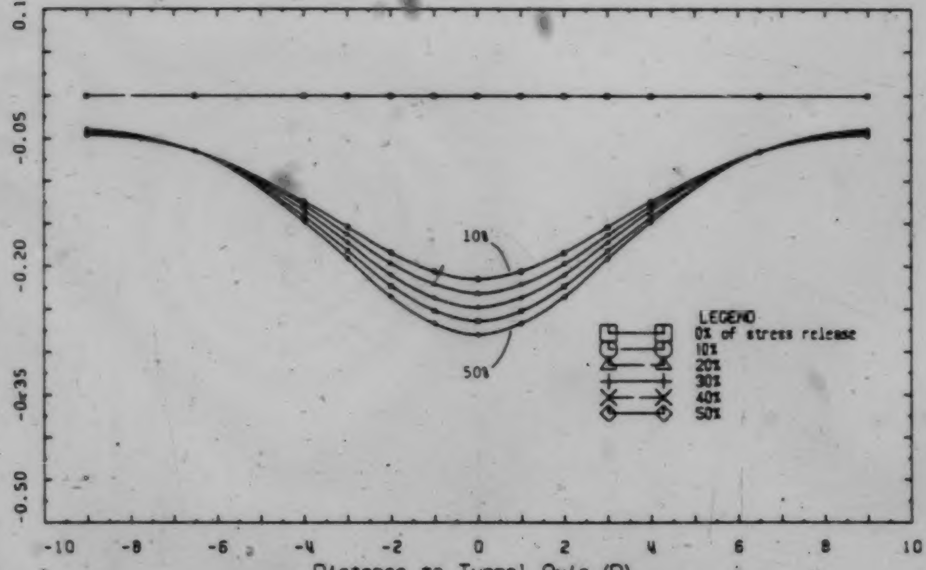

Figure C.36 Normalized Settlements: K_o=0.6, ϕ=30°, H/D=6

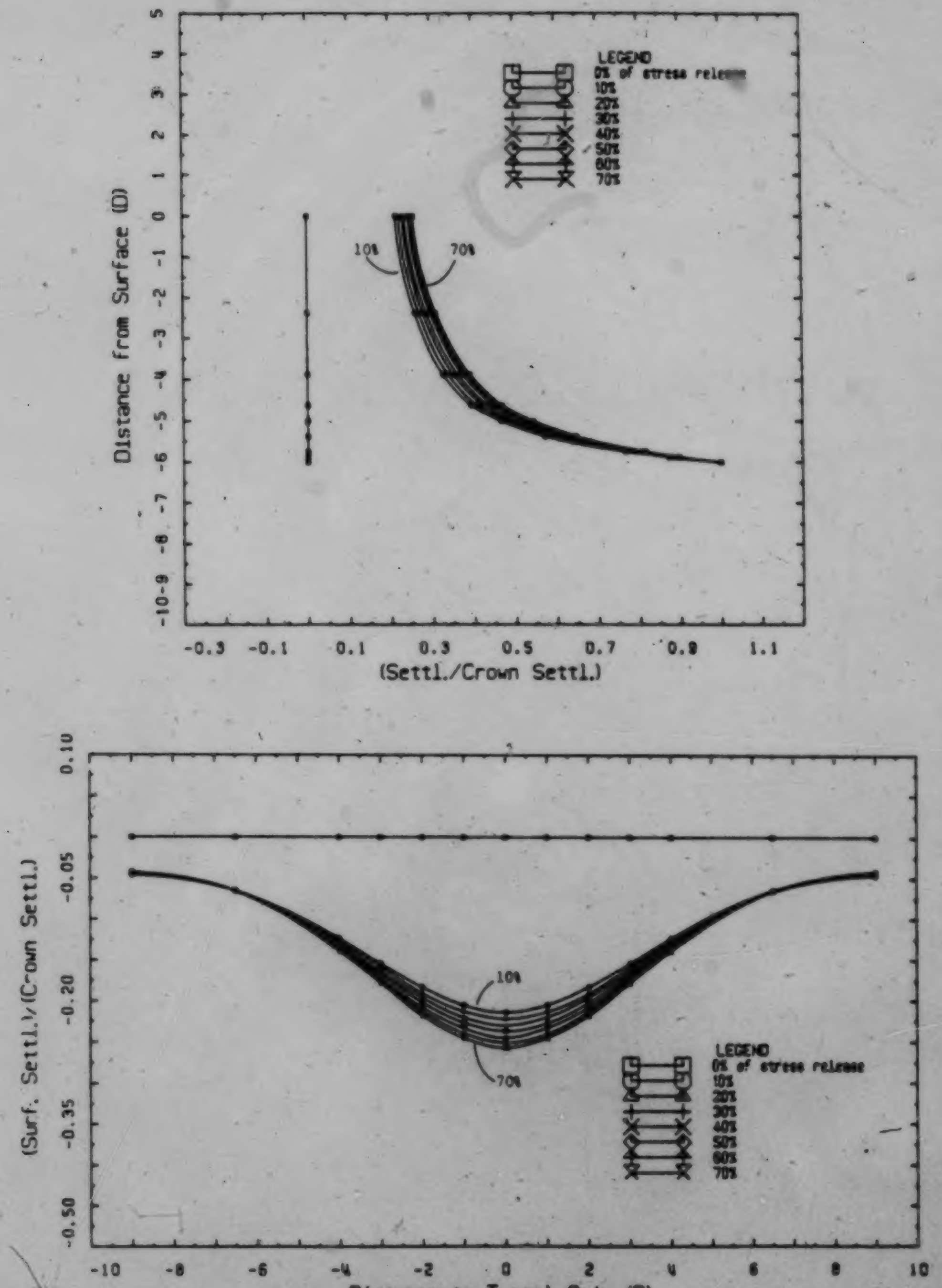

Figure C.37 Normalized Settlements: K_o=0.6, ϕ=40°, H/D=6

APPENDIX D - TWICE NORMALIZED GROUND REACTION CURVES

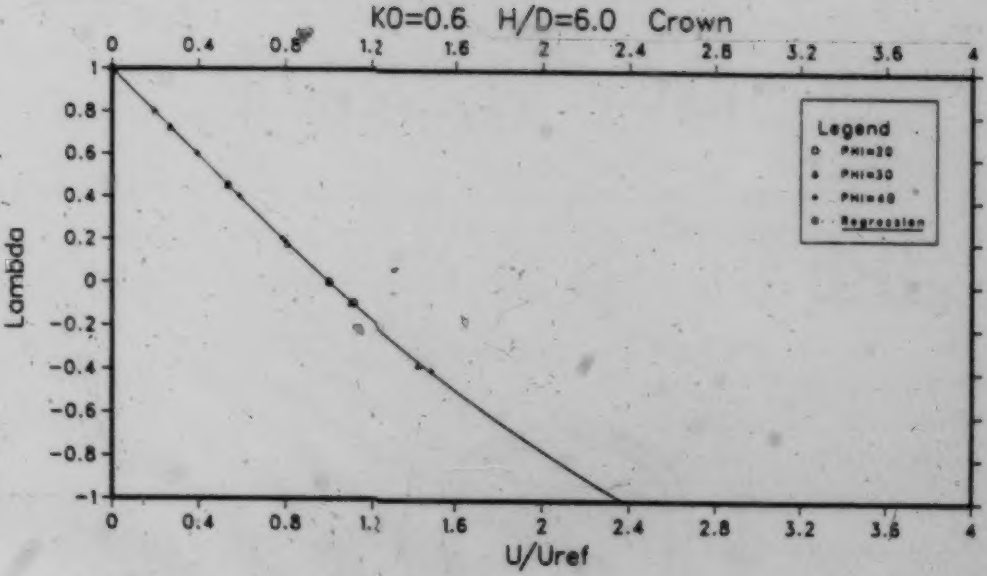

Figure D.1 NNGRC for Crown, K_o= 0.6, H/D=6

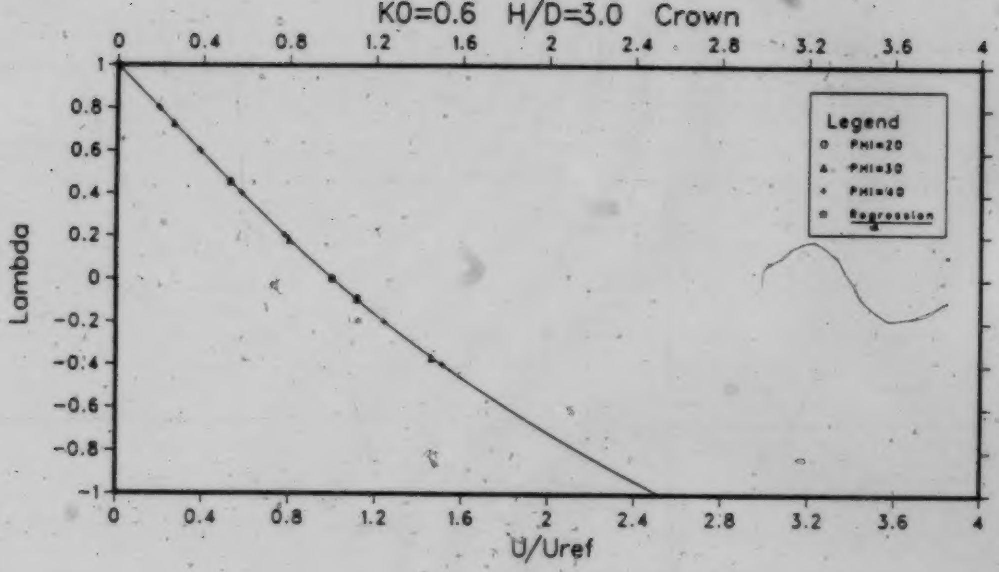

Figure D.2 NNGRC for Crown, K_o= 0.6, H/D=3

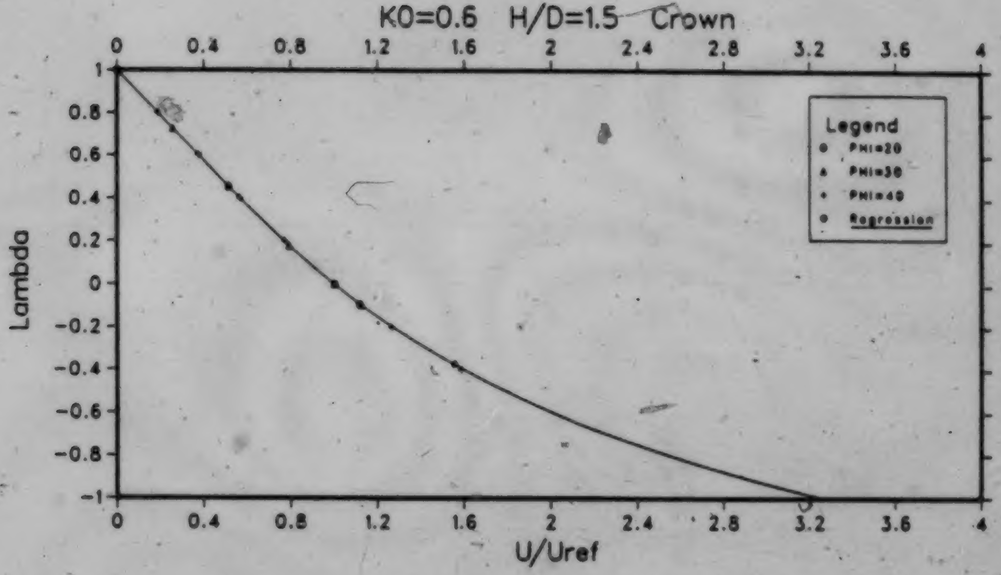

Figure D.3 NNGRC for Crown, K_o= 0.6, H/D=1.5

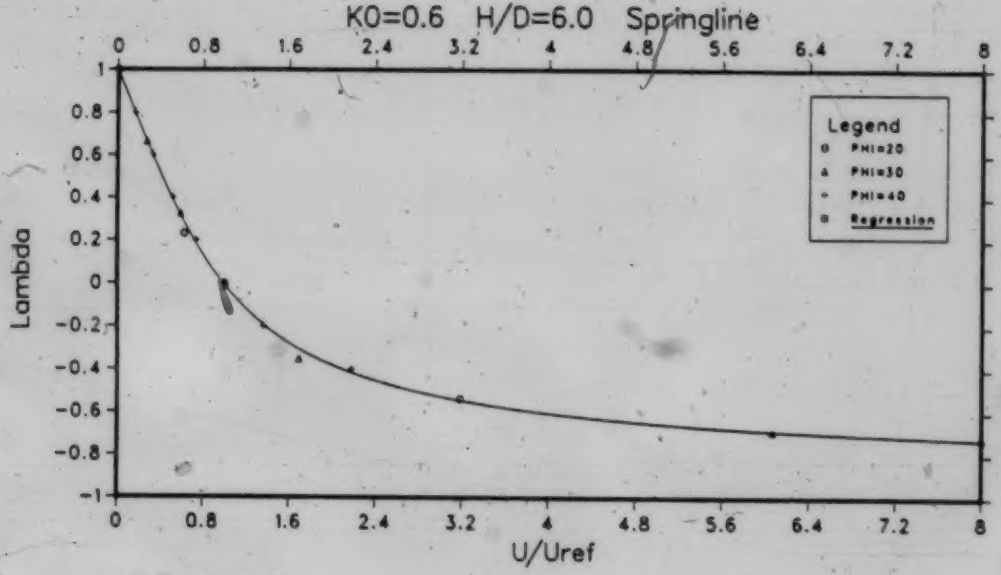

Figure D.4 NNGRC for Springline, K_o= 0.6, H/D=6

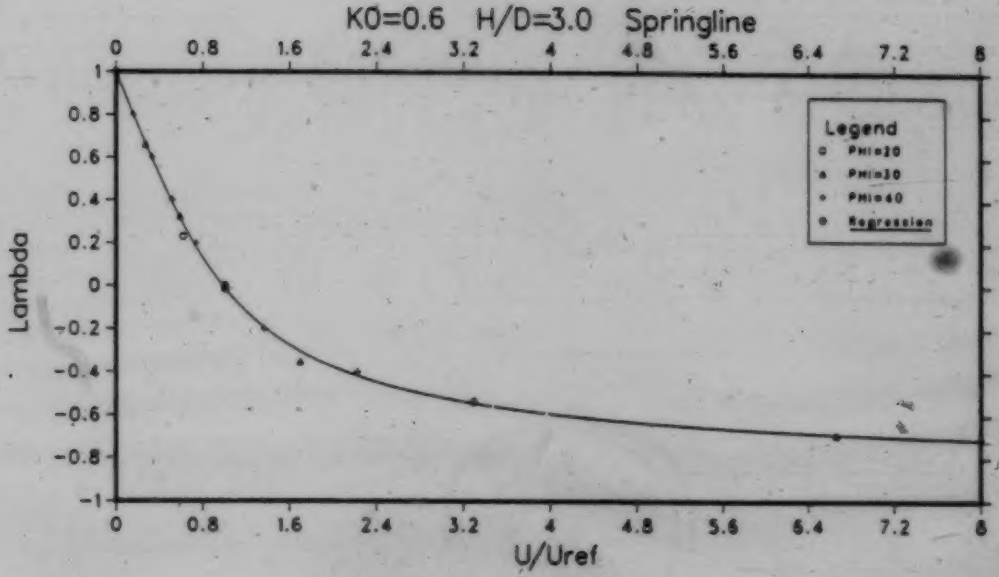

Figure D.5 NNGRC for Springline, K_o= 0.6, H/D=3

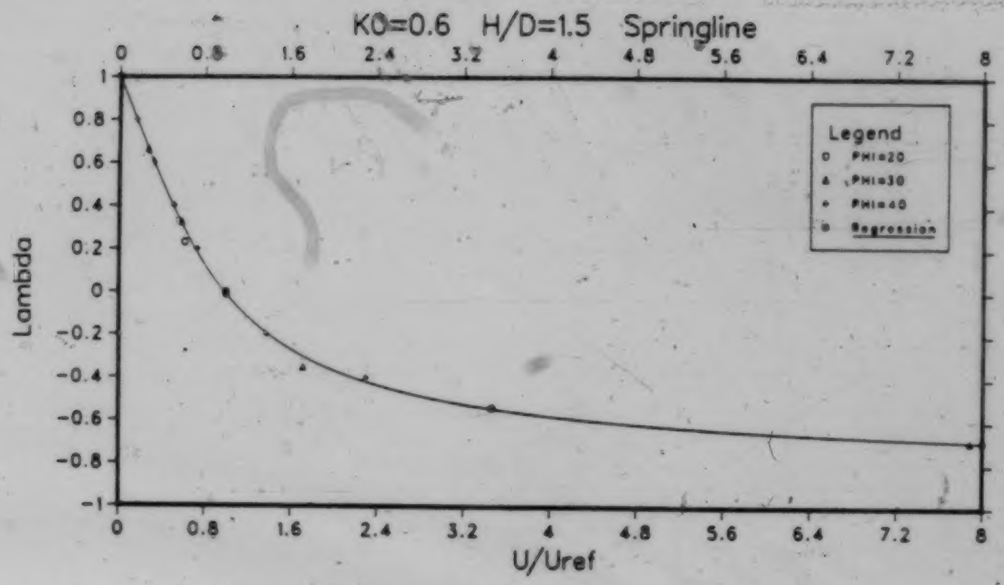

Figure D.6 NNGPC for Springline, K_o= 0.6, H/D=1.5

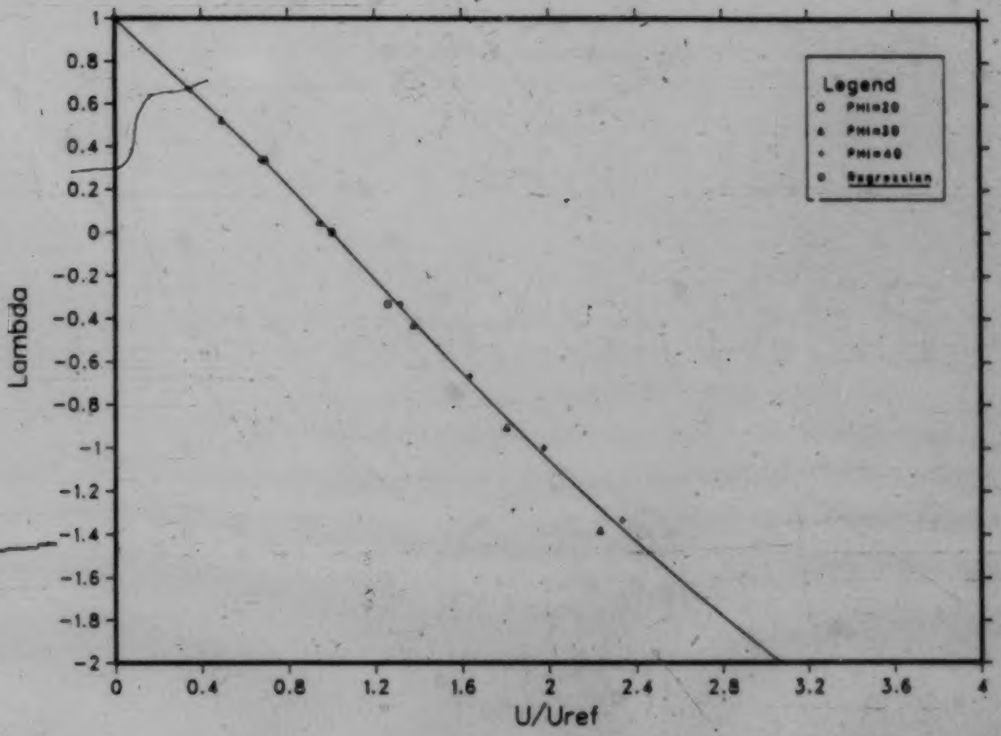

Figure D.7 NNGRC for Floor, K_o= 0.6, H/D=6

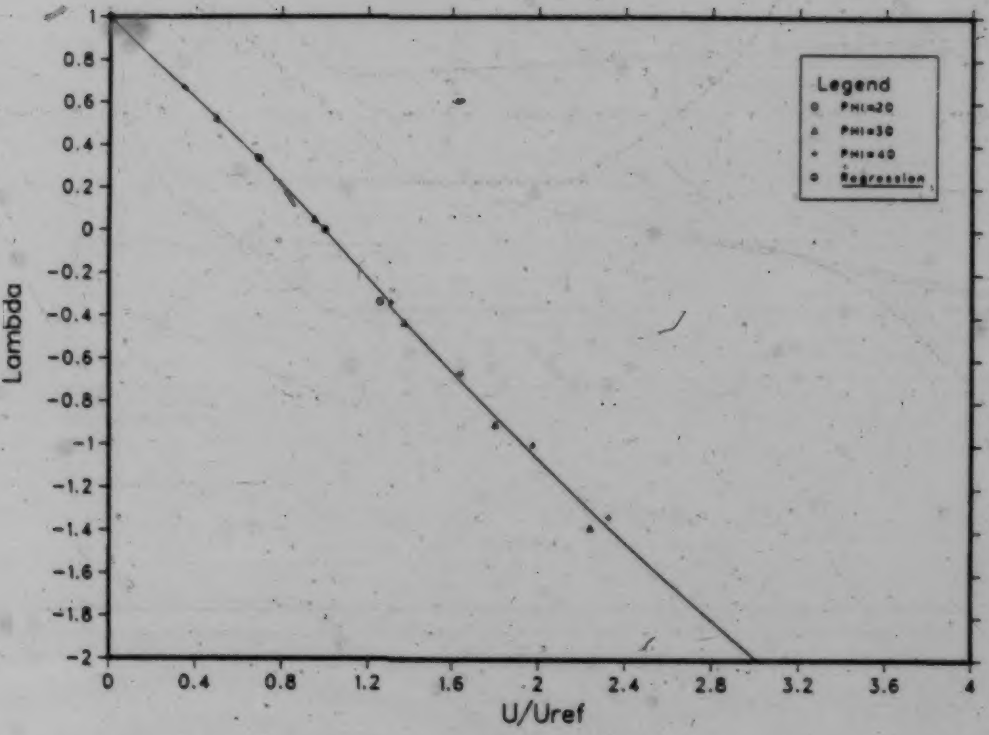

Figure D.8 NNGRC for Floor, K_o= 0.6, H/D=3

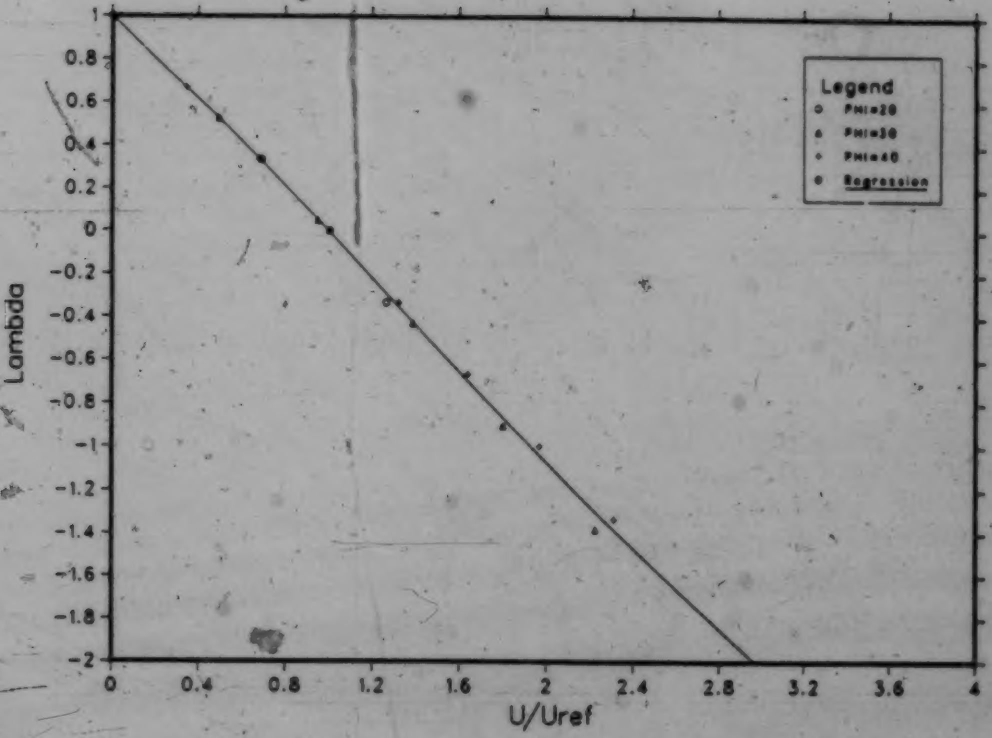

Figure D.9 NNGRC for Floor, K_o= 0.6, H/D=1.5

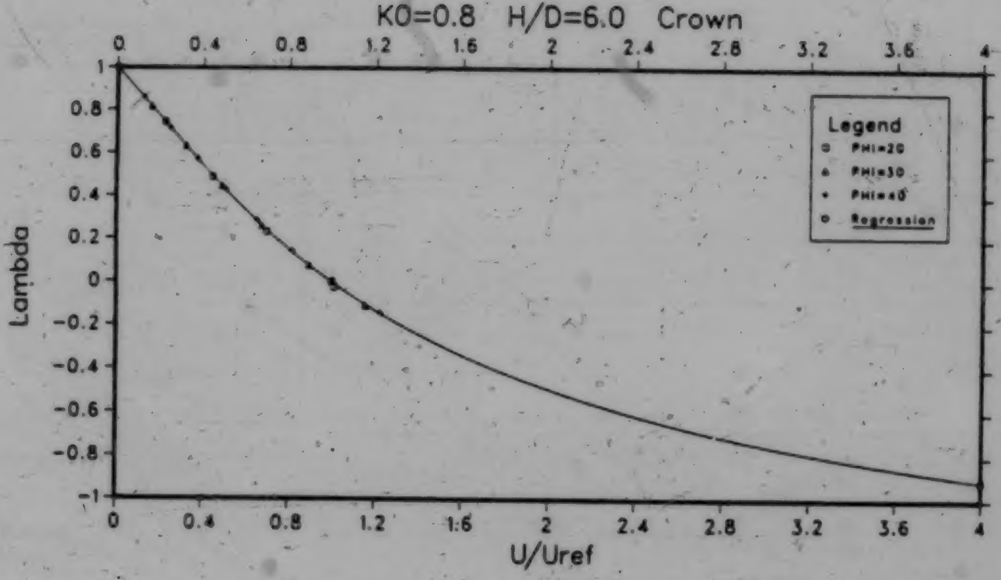

Figure D.10 NNGRC for Crown, K_o= 0.8, H/D=6

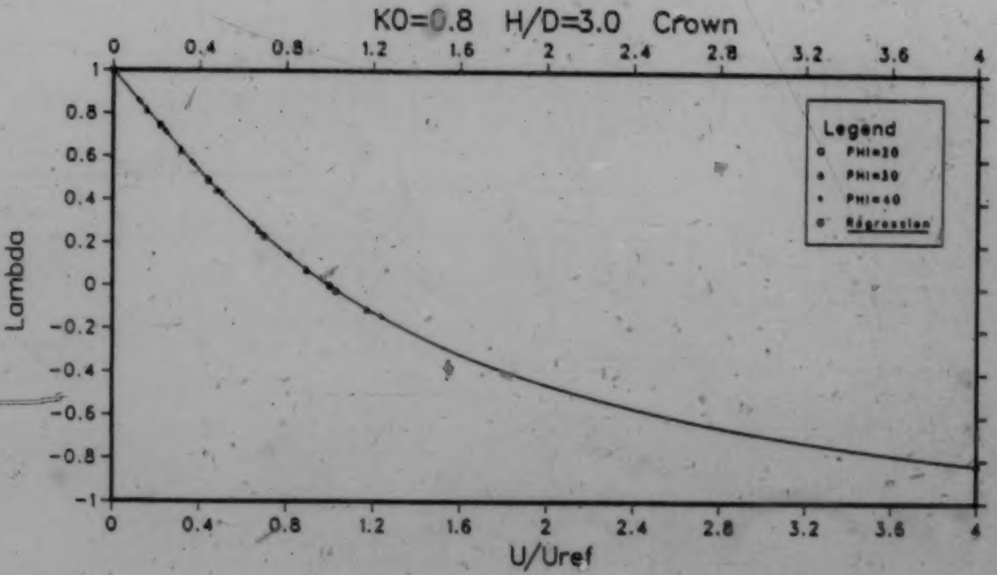

Figure D.11 NNGRC for Crown, K_o= 0.8, H/D=3

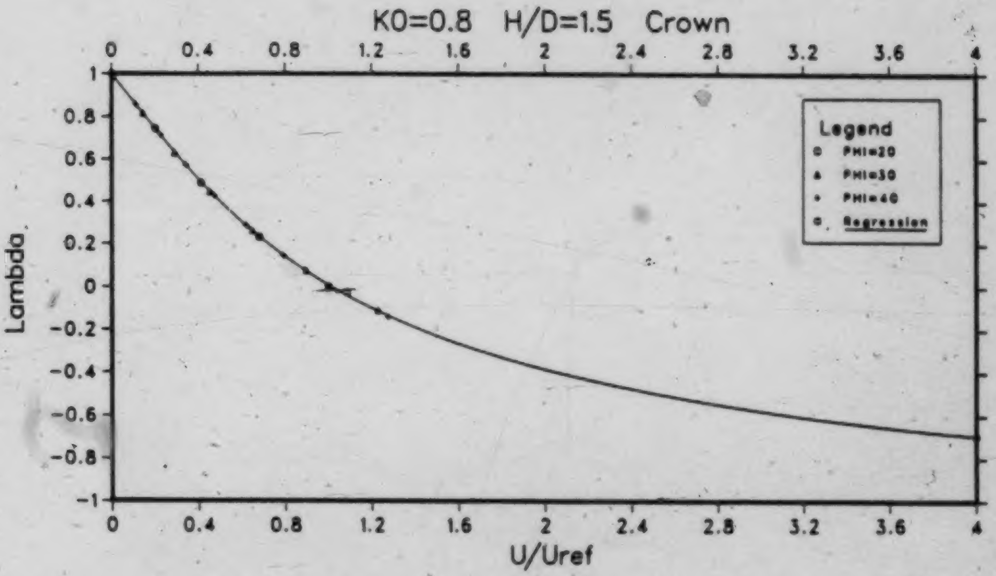

Figure D.12 NNGRC for Crown, K_o= 0.8, H/D=1.5

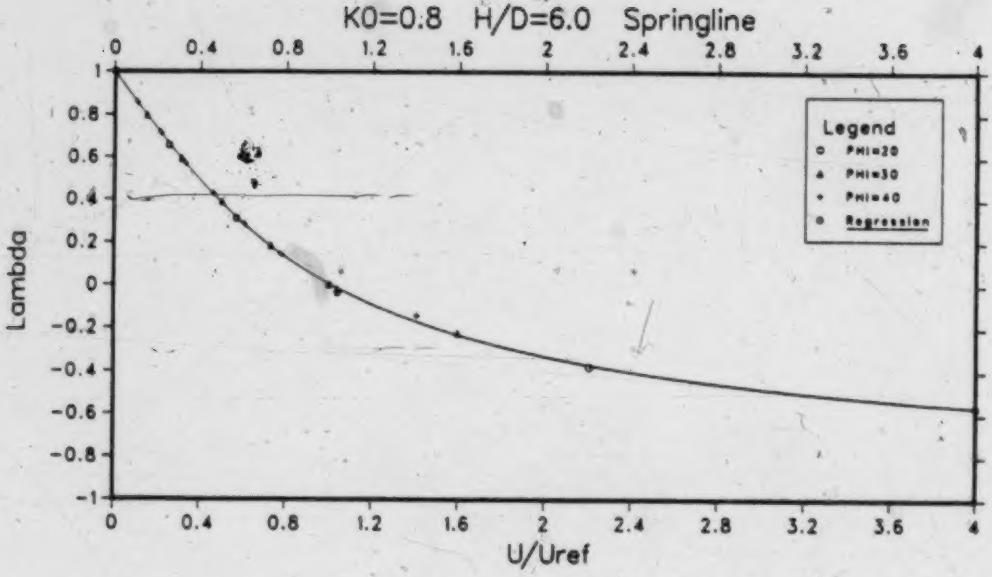

Figure D.13 NNGRC for Springline, K_o= 0.8, H/D=6

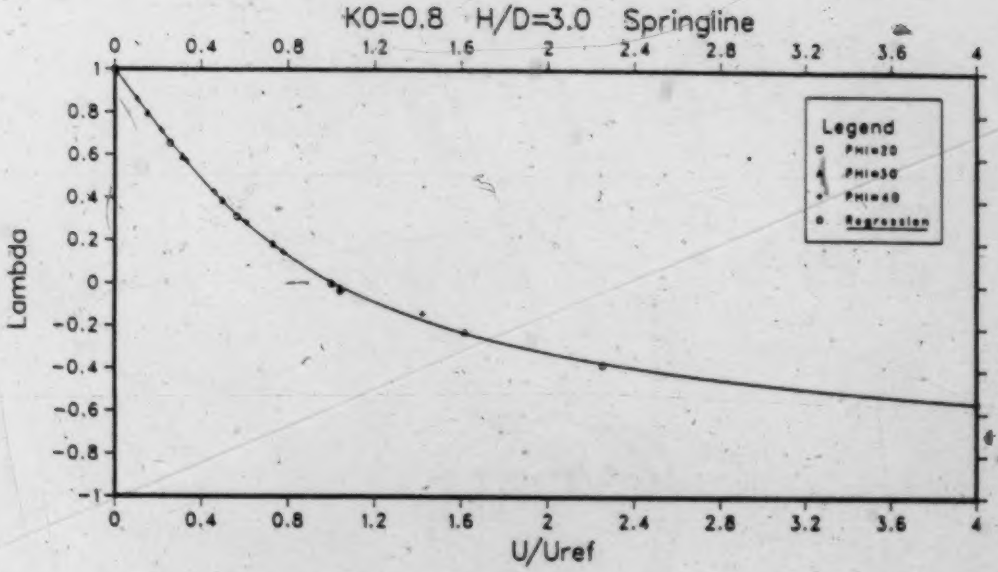

Figure D. 14 NNGRC for Springline, K_o= 0.8, H/D=3

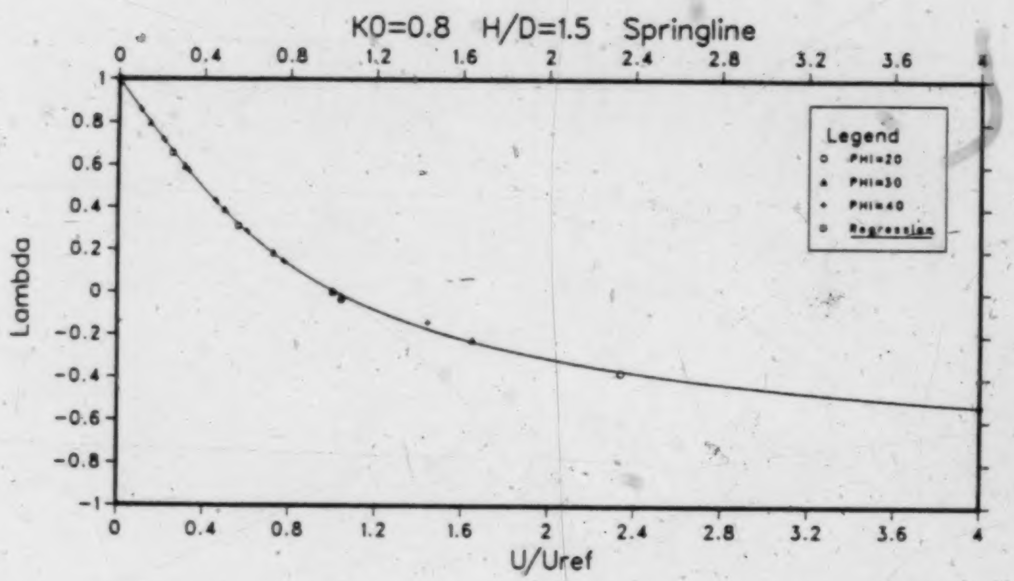

Figure D.15 NNGRC for Springline, K_o= 0.8, H/D=1.5

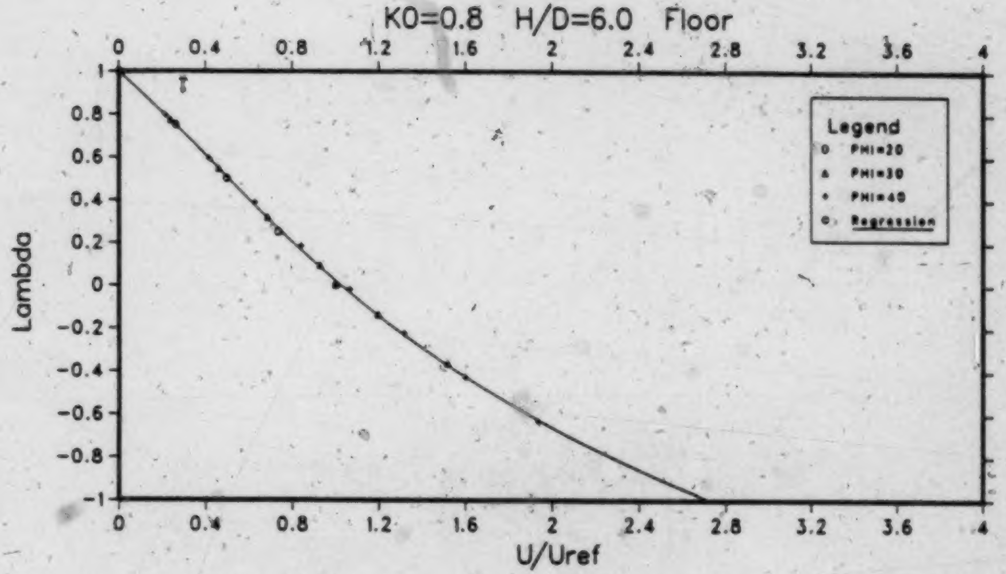

Figure D.16 NNGRC for Floor, K_o= 0.8, H/D=6

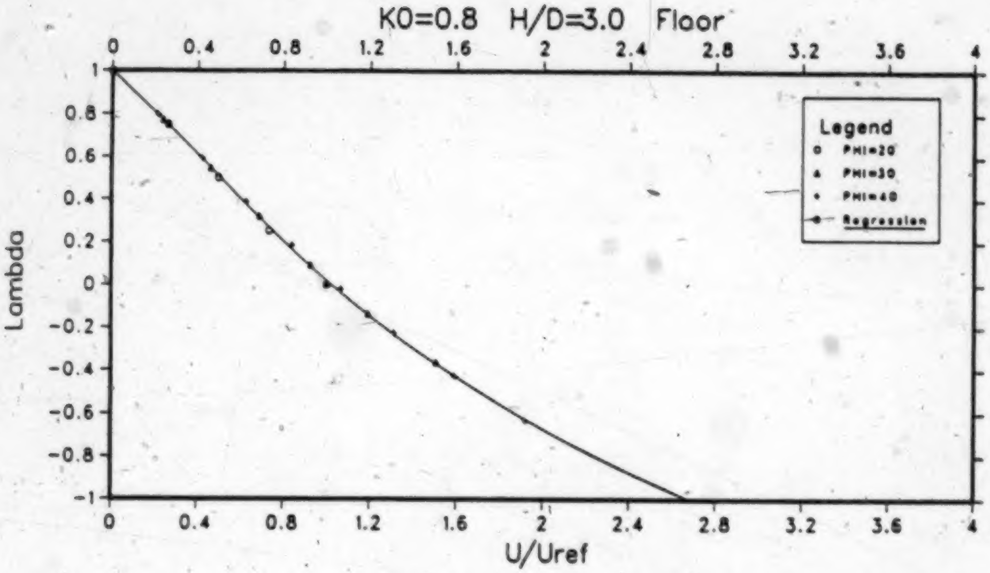

Figure D.17 NNGRC for Floor, K_o= 0.8, H/D=3

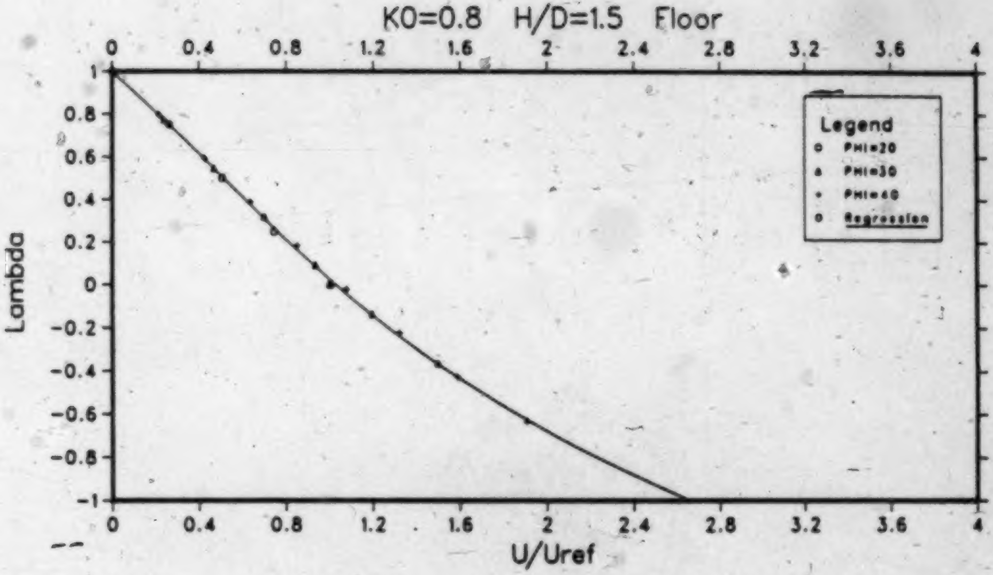

Figure D.18 NNGRC for Floor, K_o= 0.8, H/D=1.5

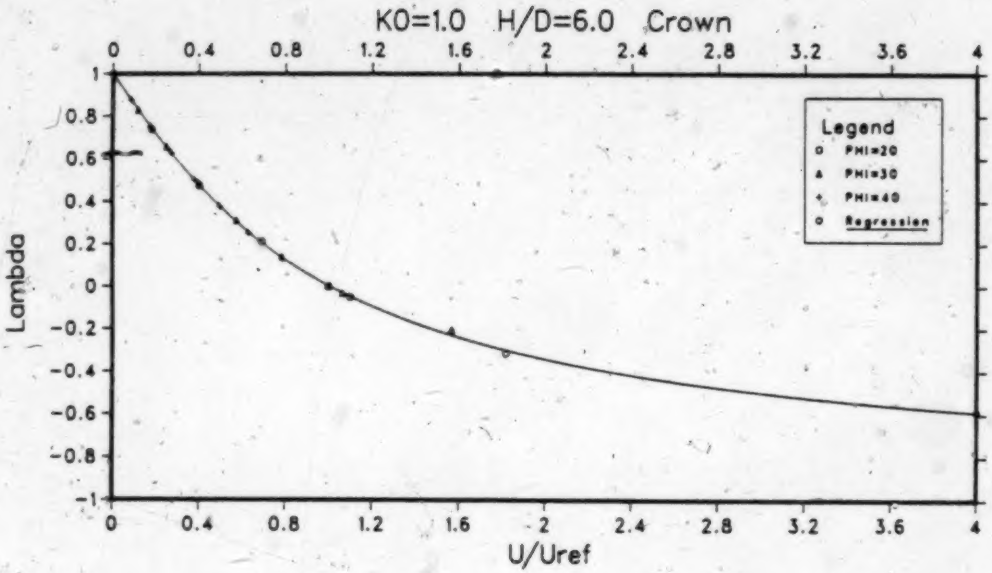

Figure D.19 NNGRC for Crown, K_o= 1.0, H/D=6

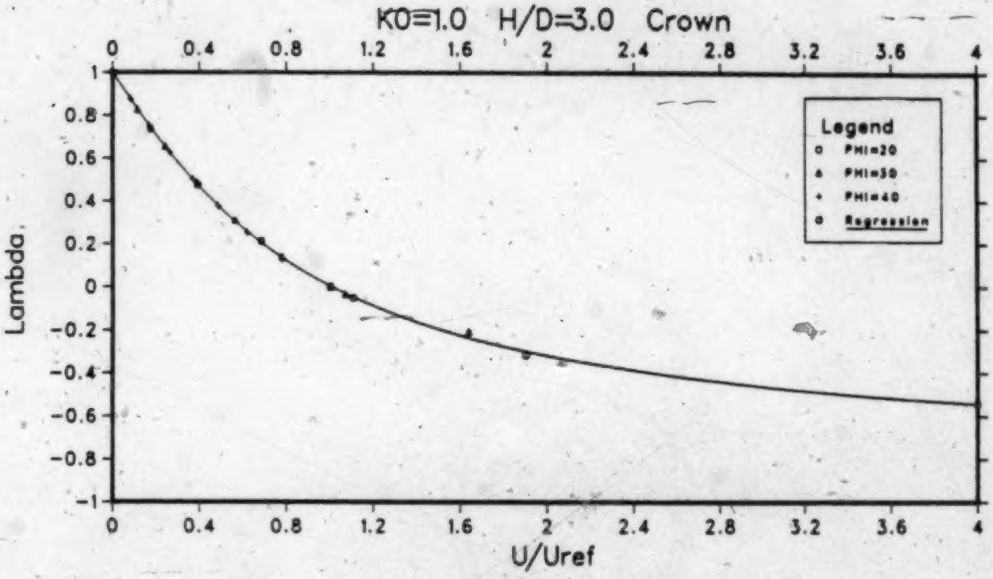

Figure D.20 NNGRC for Crown, K_o= 1.0, H/D=3

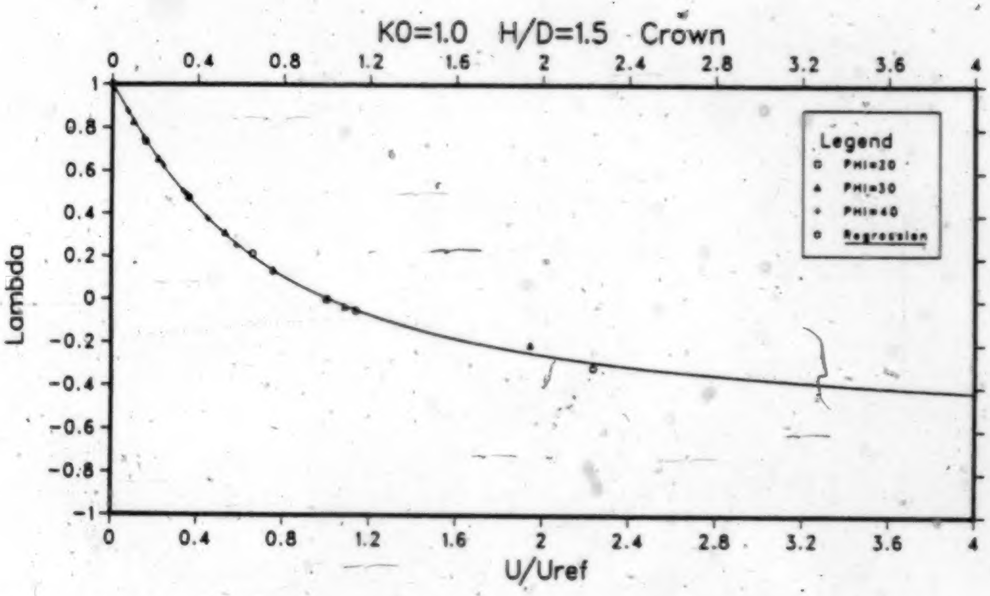

Figure D.21 NNGRC for Crown, K_o= 1.0, H/D=1.5

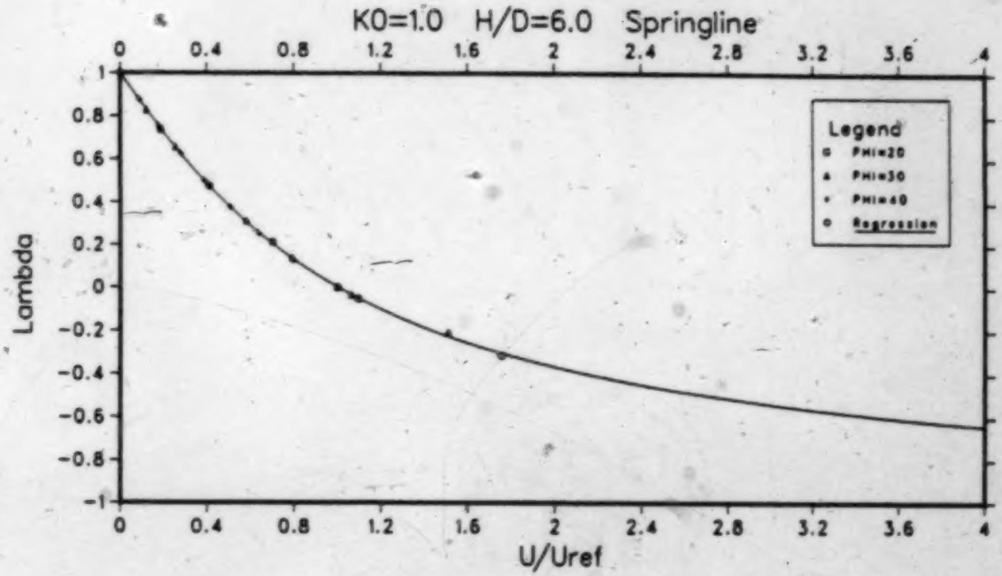

Figure D.22 NNGRC for Springline, K_o= 1.0, H/D=6

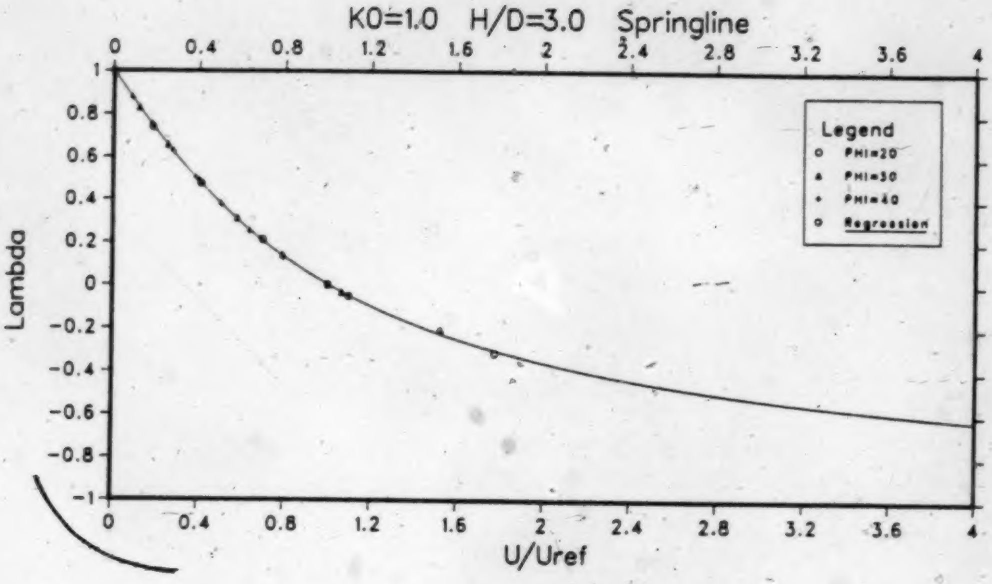

Figure D.23 NNGRC for Springline, K_o= 1.0, H/D=3

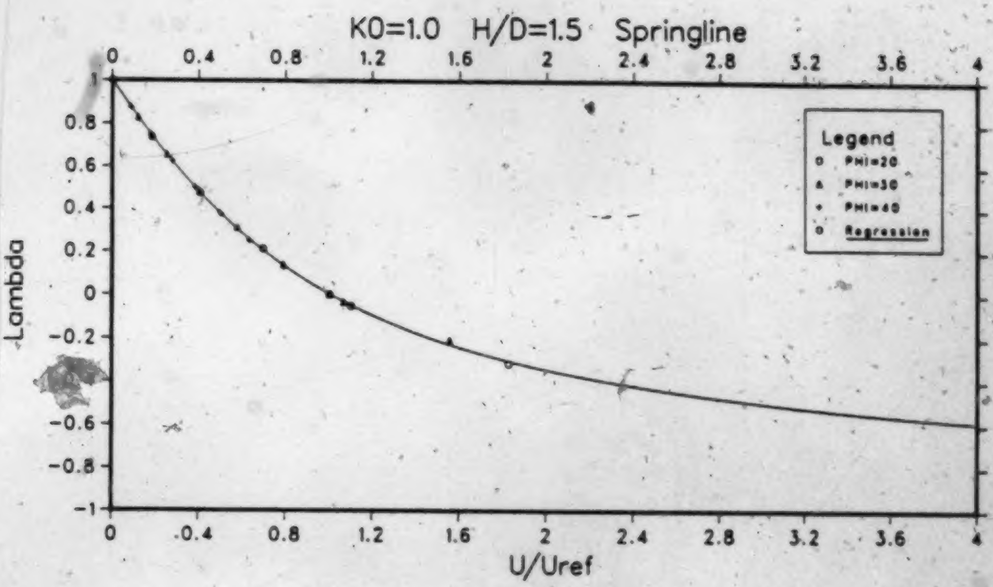

Figure D.24 NNGRC for Springline, K_o= 1.0, H/D=1.5

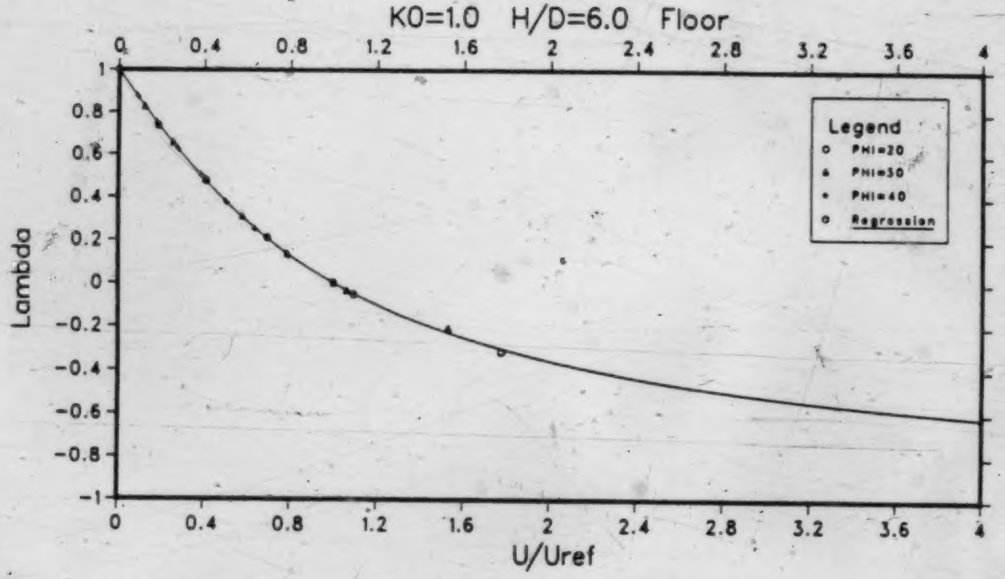

Figure D.25 NNGRC for Floor, K_o= 1.0, H/D=6

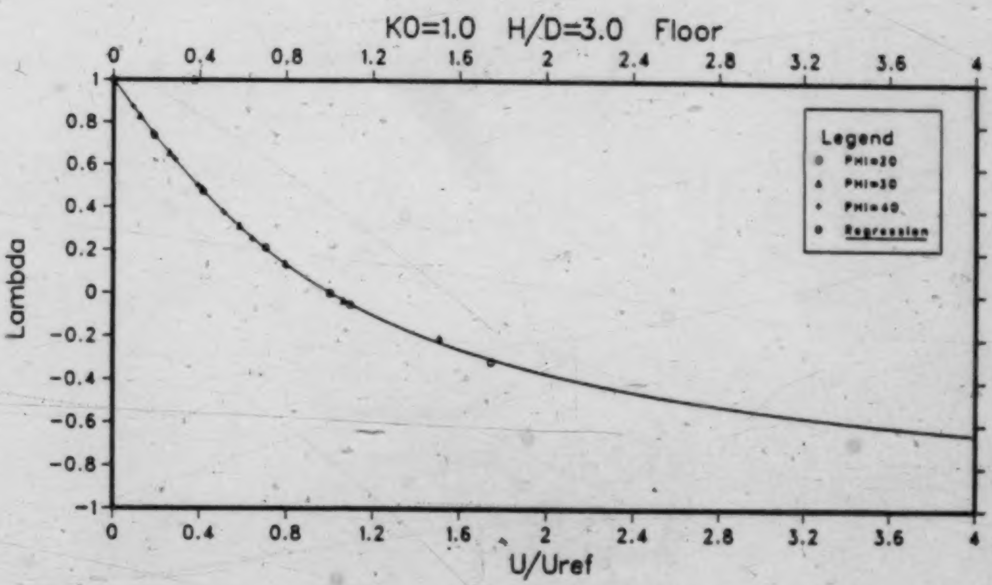

Figure D.26 NNGRC for Floor, K_o= 1.0, H/D=3

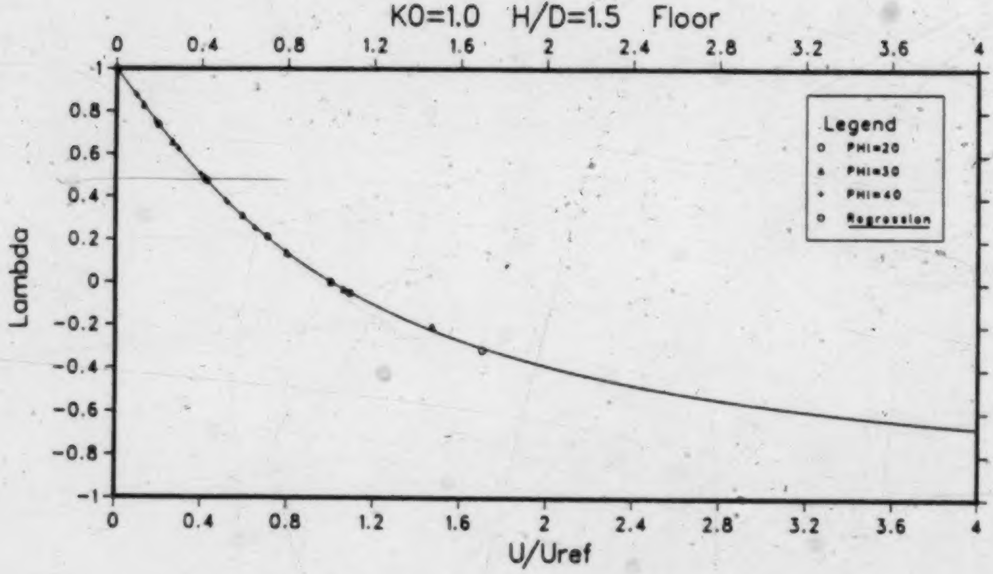

Figure D.27 NNGRC for Floor, K_o= 1.0, H/D=1.5